SHOUT
SHARE
IT

MRL

Volume 187 Number 1

THE BIOLOGICAL BULLETIN

Marine Biological Laboratory/
Woods Hole Oceanographic Institution
Library

AUG [illegible] 1994

[illegible]

AUGUST, 1994

Published by the Marine Biological Laboratory

THE
BIOLOGICAL BULLETIN

PUBLISHED BY
THE MARINE BIOLOGICAL LABORATORY

Associate Editors

PETER A. V. ANDERSON, The Whitney Laboratory, University of Florida
WILLIAM D. COHEN, Hunter College, City University of New York
DAVID EPEL, Hopkins Marine Station, Stanford University
J. MALCOLM SHICK, University of Maine, Orono

Editorial Board

THOMAS H. DIETZ, Louisiana State University
DAPHNE GAIL FAUTIN, University of Kansas
WILLIAM F. GILLY, Hopkins Marine Station, Stanford University
ROGER T. HANLON, Marine Biomedical Institute, University of Texas Medical Branch
CHARLES B. METZ, University of Miami
K. RANGA RAO, University of West Florida
BARUCH RINKEVICH, Israel Oceanographic & Limnological Research Ltd.
RICHARD STRATHMANN, Friday Harbor Laboratories, University of Washington
STEVEN VOGEL, Duke University
SARAH ANN WOODIN, University of South Carolina

Editor: MICHAEL J. GREENBERG, The Whitney Laboratory, University of Florida
Managing Editor: PAMELA L. CLAPP, Marine Biological Laboratory

AUGUST, 1994

Printed and Issued by
LANCASTER PRESS, Inc.
3575 HEMPLAND ROAD
LANCASTER, PA

THE BIOLOGICAL BULLETIN

THE BIOLOGICAL BULLETIN is published six times a year by the Marine Biological Laboratory, MBL Street, Woods Hole, Massachusetts 02543.

Subscriptions and similar matter should be addressed to Subscription Manager, THE BIOLOGICAL BULLETIN, Marine Biological Laboratory, Woods Hole, Massachusetts 02543. Single numbers, $37.50. Subscription per volume (three issues), $90.00 ($180.00 per year for six issues).

Communications relative to manuscripts should be sent to Michael J. Greenberg, Editor-in-Chief, or Pamela L. Clapp, Managing Editor, at the Marine Biological Laboratory, Woods Hole, Massachusetts 02543. Telephone: (508) 548-3705, ext. 428. FAX: 508-540-6902. E-mail: pclapp@hoh.mbl.edu.

POSTMASTER: Send address changes to THE BIOLOGICAL BULLETIN, Marine Biological Laboratory,
Woods Hole, MA 02543.

Copyright © 1994, by the Marine Biological Laboratory

Second-class postage paid at Woods Hole, MA, and additional mailing offices.
ISSN 0006-3185

INSTRUCTIONS TO AUTHORS

The Biological Bulletin accepts outstanding original research reports of general interest to biologists throughout the world. Papers are usually of intermediate length (10–40 manuscript pages). A limited number of solicited review papers may be accepted after formal review. A paper will usually appear within four months after its acceptance.

Very short, especially topical papers (less than 9 manuscript pages including tables, figures, and bibliography) will be published in a separate section entitled "Research Notes." A Research Note in *The Biological Bulletin* follows the format of similar notes in *Nature*. It should open with a summary paragraph of 150 to 200 words comprising the introduction and the conclusions. The rest of the text should continue on without subheadings, and there should be no more than 30 references. References should be referred to in the text by number, and listed in the Literature Cited section in the order that they appear in the text. Unlike references in *Nature*, references in the Research Notes section should conform in punctuation and arrangement to the style of recent issues of *The Biological Bulletin*. Materials and Methods should be incorporated into appropriate figure legends. See the article by Lohmann *et al.* (October 1990, Vol. **179**: 214–218) for sample style. A Research Note will usually appear within two months after its acceptance.

The Editorial Board requests that regular manuscripts conform to the requirements set below; those manuscripts that do not conform will be returned to authors for correction before review.

1. ***Manuscripts.*** Manuscripts, including figures, should be submitted in triplicate. (Xerox copies of photographs are not acceptable for review purposes.) The submission letter accompanying the manuscript should include a telephone number, a FAX number, and (if possible) an E-mail address for the corresponding author. The original manuscript must be typed in no smaller than 12 pitch or 10 point, using double spacing (*including* figure legends, footnotes, bibliography, etc.) on one side of 16- or 20-lb. bond paper, 8½ by 11 inches. Please, no right justification. Manuscripts should be proofread carefully and errors corrected legibly in black ink. Pages should be numbered consecutively. Margins on all sides should be at least 1 inch (2.5 cm). Manuscripts should conform to the *Council of Biology Editors Style Manual*, 5th Edition (Council of Biology Editors, 1983) and to American spelling. Unusual abbreviations should be kept to a minimum and should be spelled out on first reference as well as defined in a footnote on the title page. Manuscripts should be divided into the following components: Title page, Abstract (of no more than 200 words), Introduction, Materials and Methods, Results, Discussion, Acknowledgments, Literature Cited, Tables, and Figure Legends. In addition, authors should supply a list of words and phrases under which the article should be indexed.

2. ***Title page.*** The title page consists of a condensed title or running head of no more than 35 letters and spaces, the manuscript title, authors' names and appropriate addresses, and footnotes listing present addresses, acknowledgments or contribution numbers, and explanation of unusual abbreviations.

3. ***Figures.*** The dimensions of the printed page, 7 by 9 inches, should be kept in mind in preparing figures for publication. We recommend that figures be about 1½ times the linear dimensions of the final printing desired, and that the ratio of the largest to the smallest letter or number and of the thickest to the thinnest line not exceed 1:1.5. Explanatory matter generally should be included in legends, although axes should always be identified on the illustration itself. Figures should be prepared for reproduction as either line cuts or halftones. Figures to be reproduced as line cuts should be unmounted glossy photographic reproductions or drawn in black ink on white paper, good-quality tracing cloth or plastic, or blue-lined coordinate paper. Those to be reproduced as halftones should be mounted on board, with both designating numbers or letters and scale bars affixed directly to the figures. All figures should be numbered in consecutive order, with no distinction between text and plate figures. The author's name and an arrow indicating orientation should appear on the reverse side of all figures.

4. ***Tables, footnotes, figure legends, etc.*** Authors should follow the style in a recent issue of *The Biological Bulletin* in preparing table headings, figure legends, and the like. Because of the high cost of setting tabular material in type, authors are asked to limit such material as much as possible. Tables, with their headings and footnotes, should be typed on separate sheets,

numbered with consecutive Roman numerals, and placed after the Literature Cited. Figure legends should contain enough information to make the figure intelligible separate from the text. Legends should be typed double spaced, with consecutive Arabic numbers, on a separate sheet at the end of the paper. Footnotes should be limited to authors' current addresses, acknowledgments or contribution numbers, and explanation of unusual abbreviations. All such footnotes should appear on the title page. Footnotes are not normally permitted in the body of the text.

5. ***Literature cited.*** In the text, literature should be cited by the Harvard system, with papers by more than two authors cited as Jones *et al.*, 1980. Personal communications and material in preparation or in press should be cited in the text only, with author's initials and institutions, unless the material has been formally accepted and a volume number can be supplied. The list of references following the text should be headed Literature Cited, and must be typed double spaced on separate pages, conforming in punctuation and arrangement to the style of recent issues of *The Biological Bulletin.* Citations should include complete titles and inclusive pagination. Journal abbreviations should normally follow those of the U. S. A. Standards Institute (USASI), as adopted by BIOLOGICAL ABSTRACTS and CHEMICAL ABSTRACTS, with the minor differences set out below. The most generally useful list of biological journal titles is that published each year by BIOLOGICAL ABSTRACTS (BIOSIS List of Serials; the most recent issue). Foreign authors, and others who are accustomed to using THE WORLD LIST OF SCIENTIFIC PERIODICALS, may find a booklet published by the Biological Council of the U.K. (obtainable from the Institute of Biology, 41 Queen's Gate, London, S.W.7, England, U.K.) useful, since it sets out the WORLD LIST abbreviations for most biological journals with notes of the USASI abbreviations where these differ. CHEMICAL ABSTRACTS publishes quarterly supplements of additional abbreviations. The following points of reference style for THE BIOLOGICAL BULLETIN differ from USASI (or modified WORLD LIST) usage:

A. Journal abbreviations, and book titles, all underlined (for *italics*)

B. All components of abbreviations with initial capitals (not as European usage in WORLD LIST *e.g., J. Cell. Comp. Physiol.* NOT *J. cell. comp. Physiol.*)

C. *All* abbreviated components must be followed by a period, whole word components *must not* (*i.e., J. Cancer Res.*)

D. Space between all components (*e.g., J. Cell. Comp. Physiol.*, not *J.Cell.Comp.Physiol.*)

E. Unusual words in journal titles should be spelled out in full, rather than employing new abbreviations invented by the author. For example, use *Rit Vísindafjélags Islendinga* without abbreviation.

F. All single word journal titles in full (*e.g., Veliger, Ecology, Brain*).

G. The order of abbreviated components should be the same as the word order of the complete title (*i.e., Proc.* and *Trans.* placed where they appear, not transposed as in some BIOLOGICAL ABSTRACTS listings).

H. A few well-known international journals in their preferred forms rather than WORLD LIST or USASI usage (*e.g., Nature, Science, Evolution* NOT *Nature, Lond., Science, N.Y.; Evolution, Lancaster, Pa.*)

6. ***Reprints, page proofs, and charges.*** Authors receive their first 100 reprints (without covers) free of charge. Additional reprints may be ordered at time of publication and normally will be delivered about two to three months after the issue date. Authors (or delegates for foreign authors) will receive page proofs of articles shortly before publication. They will be charged the current cost of printers' time for corrections to these (other than corrections of printers' or editors' errors). Other than these charges for authors' alterations, *The Biological Bulletin* does not have page charges.

Reference: *Biol. Bull.* **187:** 1–7. (August, 1994)

Physiological Parameters Affecting the Chemosensory Response of *Tetrahymena*

UFFE KOPPELHUS[1], PER HELLUNG-LARSEN[2], AND VAGN LEICK

Institute of Medical Biochemistry and Genetics, Department B, The Panum Institute,
University of Copenhagen, Blegdamsvej 3, 2200 Copenhagen N, Denmark

Abstract. We have investigated the significance of a number of physiological parameters in the preparation of cells for experiments on chemokinesis in *Tetrahymena.* The study comprises (1) growth state of the cells, (2) composition of the starvation medium, (3) concentration of cells during starvation, (4) oxygen saturation of the starvation medium, (5) temperature during starvation, and (6) starvation period. By controlling the physiological state of the cells, we significantly improved the reproducibility of the results obtained in assays for chemokinesis in *Tetrahymena.* In short, cells optimal for chemokinesis at an assay temperature of 28°C should be starved from the exponential growth phase in a concentration below 2×10^5 cells ml^{-1} for 10–20 h. The surface-to-volume ratio of the starvation medium—water or Hepes buffer—should be about 5 cm^{-1} (or more) to ensure more than 95% oxygen saturation of the starvation medium. Maximal chemosensory responses were obtained if the cells were starved at 21°C. The chemokinetic potential of the cells decreased significantly, as did the levels of the ratio of ATP to ADP, if cells were starved at higher temperatures. A tentative correlation between the ATP level in the cells and the chemosensory potential of the cells has been found. We suggest that chemokinesis is a constant quality of *Tetrahymena,* because we found no sign that prolonged starvation or other changes applied to the cells produced an up-regulation of the chemosensory response. Apparently, starvation is obligatory only to remove the growth medium (which is itself a very potent attractant), thereby making the cells sensitive to the chemoattractants.

Introduction

Chemosensory responses to chemical attractants and repellants are a phenomenon of importance in most cells. Among the ciliate protozoa, chemokinesis has been much studied in genera such as *Paramecium, Blepharisma,* and *Tetrahymena* (Van Houten *et al.,* 1981; Leick and Hellung-Larsen, 1992). *Tetrahymena* exhibits positive chemokinesis towards certain peptide hormones and cytokines that also induce positive chemokinesis in specific animal cell types such as leucocytes, muscle cells, and dermal fibroblasts (see review by Leick and Hellung-Larsen, 1992). Furthermore, *Tetrahymena* is a useful model cell for electrophysiological investigations of chemoreception (Ueda and Kobatake, 1977, Tanabe *et al.,* 1980).

Various bioassays for chemokinesis have been applied to *Tetrahymena,* but the results have not been consistent, and day-to-day variations have been reported in many studies (Almagor *et al.,* 1981; Levandowsky *et al.,* 1984; Hellung-Larsen *et al.,* 1986; Leick *et al.,* 1990). We understood that the chemosensory sensitivity of the cells must be dependent on their physiological conditions, but the relationship was obscure.

Tetrahymena is readily obtainable in axenic cultures, and the physiological parameters characterizing populations of dividing and nondividing *Tetrahymena* have recently been described (Hellung-Larsen *et al.,* 1993). We therefore used such cells in a systematic examination of starvation and assay conditions. We have elucidated the relative importance of the physiological parameters involved in the preparation of cells for experiments on chemokinesis in *Tetrahymena.* Furthermore, we have tested a number of physiological conditions not previously controlled in this kind of experiment. Our conclusions about the chemosensory behavior of *Tetrahymena* may be applicable to other organisms.

Received 2 September 1993; accepted 27 May 1994.

[1] Present address: The Danish Cancer Society, Department of Virus and Cancer, Gustav Wieds Vej 10, DK-8000 Aarhus, Denmark.

[2] Author to whom correspondence should be addressed.

Materials and Methods

Cell cultures

Tetrahymena thermophila strain B7 was grown axenically in PY medium: 0.75% proteose peptone (Difco), 0.75% yeast extract (Difco), 1.5% glucose, 1 mM $MgSO_4$, 50 μM $CaCl_2$, and 100 μM ferric citrate. The PY medium was diluted to ⅓ in water prior to use. Fifty-milliliter cultures of B7 cells were grown at 35°C in 500-ml Fernbach flasks. The cultures were kept unshaken to avoid cell division stress (Hellung-Larsen and Lyhne, 1992). Cells in exponential growth phase were used to inoculate the cultures to a concentration of about 10^4 cells ml^{-1}. Transfer to starvation medium was performed after 16–20 h at a cell density of about 8×10^5 cells ml^{-1} (late exponential growth phase) or 40–50 h at a cell density of approximately 1.3×10^6 cells ml^{-1} (early stationary phase). For starvation, the cells were collected by centrifugation at $500 \times g$ for 3 min and then gently resuspended in the applied starvation medium (10 mM Hepes or deionized water). After starvation, the cells were used in the assay without further handling (resupension, dilution, etc.). All materials and media involved in the growth and starvation of the cells were sterilized by pressure sterilization (2 atm, 120°C, 30 min). Cell concentration and cell volumes were estimated with the aid of a Coulter Multisizer, as previously described (Hellung-Larsen and Andersen, 1989).

Oxygen tension

O_2 tension was measured by use of a microelectrode (WTW, Weilheim, Germany) or an acid-base analyzer (Radiometer ABL 30, Copenhagen) and expressed in percentage of maximum saturation in distilled water at 21°C.

ATP and ADP determinations

The ribonucleotides were analyzed by the high-performance liquid chromatography (HPLC) technique. A neutralized cellular PCA extract (100–200 μl) was applied to a strong anion exchange column (Partisil-10 SAX, 2 mm $\phi \times 200$ mm, Whatmann, Clifton, NJ). The column was eluted for 11 min with 0.005 M KH_2PO_4, pH 5.5, followed by a gradient for 14 min to 0.25 M KH_2PO_4 pH 4.5; an isocratic period was allowed for 10 min, and the column was re-equilibrated with the starting buffer before a new sample was added. The absorbancy at 254 nm was recorded, and the peaks were automatically integrated. Further details of the procedure are described elsewhere (Klenow and Ostergård, 1988). All PCA extractions were performed in duplicate and the standard error of the obtained pool sizes of ribonucleotides was less than 5%.

Swimming speed

Swimming speeds were determined in the laboratory of Professor Donat-P. Häder, Friedrich-Alexander Universität, Erlangen, Germany. About 2 ml of cell suspension was gently pumped into a circular vertical observation chamber positioned on a microscope, and the cell movement was recorded by a CCD video camera (LDH 600, Philips, Hamburg). A computerized analysis of swimming speeds was performed (Häder and Lebert, 1985). Each estimation was based on 2000 tracks or more, and the standard deviations were less than 10%.

Capillary assay

A capillary technique with single glass capillaries was used. Heparinized glass capillaries (75 mm long, inner diameter 1.1–1.2 mm) were filled with test solution, and one end of the capillary was sealed with wax. The capillary was placed horizontally through a sealed hole into the jar containing the cell suspension, and the open end of the capillary was brought in contact with the cell suspension. The assays were incubated for 45 min at 28°C. All experiments were carried out in quintuplicate. After incubation, the number of cells accumulated in the capillaries was determined by microscopic counting. Each capillary was emptied into a small test tube and 2 μl of an 0.2% aqueous solution of crystal violet was added to each sample. Subsequently, cells from 2×1.8 μl of each sample were counted in a hemacytometer. The cell concentrations in the capillaries are expressed as a percentage of the cell concentration (of the cell suspension) used in the particular assay.

Experimental setup

The basic experimental design is shown schematically in Figure 1. Exponentially growing cells or cells grown to the early stationary phase were transferred to starvation medium at a concentration of exactly 5×10^4 cells ml^{-1}. The cell suspension was divided into aliquots as follows: 50 ml in each of four 500-ml Fernbach flasks (a); 80 ml in each of four 250-ml Ehrlenmeyer flasks (b); 80 ml in each of four 100-ml Ehrlenmeyer flasks (c); and finally, four 100-ml Ehrlenmeyer flasks filled to the top with the cell suspension (d).

The surface-to-volume ratios (S/V) were calculated to be 4.8 cm^{-1} (a), 0.6 cm^{-1} (b), 0.2 cm^{-1} (c), and 0.03 cm^{-1} (d). As indicated in Figure 1, one of each "starvation system" was incubated for starvation at 15°, 21°, 28°, and 35°C. The chemosensory response and a number of physiological parameters were determined after 16 h of starvation (16 h was chosen because initial experiments had revealed this period of starvation to be optimal; nevertheless, we reinvestigated the importance of starvation and starvation period once the other variables were investigated, as described in the Results section titled *Starvation period*). The whole experiment was performed four times; a representative experiment is shown in Table I.

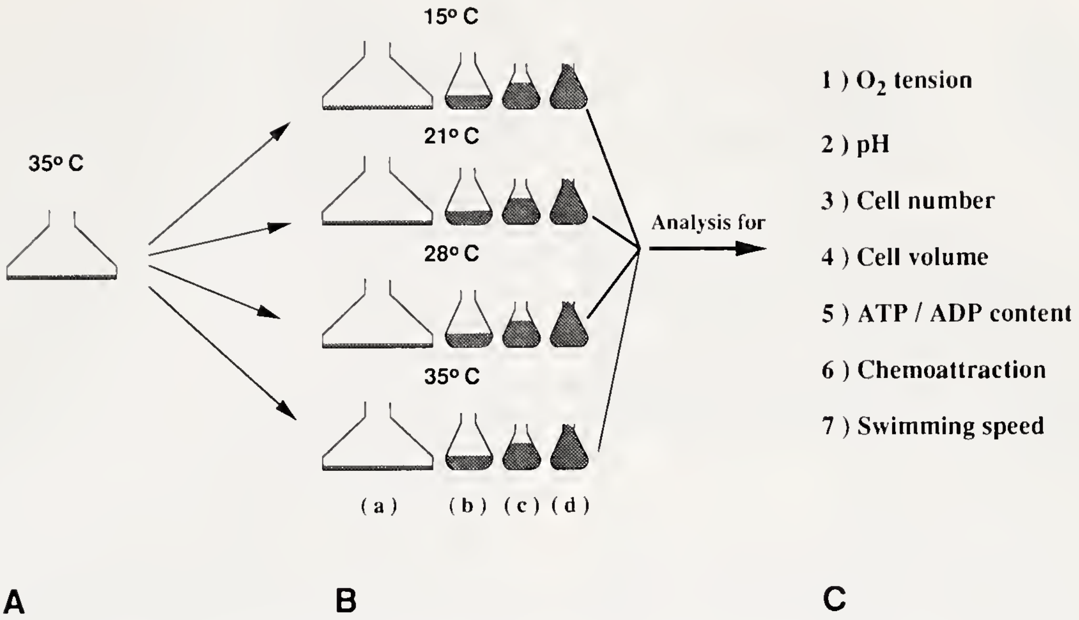

Figure 1. The experimental setup giving rise to different oxygen tensions (a, b, c, d). Cells grown at 35°C in Fernbach flasks (A) were transferred to starvation at a cell concentration of 5×10^4 cells ml^{-1}. Initially, Hepes-KOH buffer, pH = 7.4, was used as the starvation medium. The cell suspension was divided into the following aliquots: 50 ml in each of four 500-ml Fernbach flasks (a), 80 ml in each of four 250-ml Ehrlenmeyer flasks (b), 80 ml in each of four 100-ml Ehrlenmeyer flasks (c), and four 100-ml Ehrlenmeyer flasks filled to the top with the cell suspension (d). As indicated in (B), the cells were incubated in the starvation medium at 15°, 21°, 28°, and 35°C, respectively. The chemoattraction and a number of physiological parameters were determined after 16 h of starvation (C). The results of a representative experiment are summarized in Table I.

For the quantitative analysis of the chemosensory response of the cells, we used a capillary assay as illustrated in Figure 2. Proteose peptone (PP) in a concentration of 1 mg ml^{-1} was used as the attractant. All cell suspensions were maintained at 28°C for half an hour before the start of the assay. The assays were incubated for 45 min at 28°C. The assay temperature was chosen in accordance with earlier findings (Leick *et al.*, 1990). Recent studies have confirmed that the optimal temperature for chemokinesis in *Tetrahymena thermophila* is about 28°C (Koppelhus *et al.*, 1994). Five assays testing the effect of proteose peptone and five control assays were performed simultaneously. The mean values are listed in Table I and the standard deviations were calculated and listed for some selected measurements.

Results

We investigated the influence of the following physiological parameters in the preparation of *Tetrahymena* cells for experiments on chemosensory behavior: (1) growth state of the cells, (2) composition of the starvation medium, (3) cell number during starvation, (4) oxygen saturation of the starvation medium, (5) temperature during starvation, and (6) starvation period.

Influence of growth state of the cells

In the experiment summarized in Table I, cells were starved from exponential growth phase. Essentially identical results were obtained whether cells were starved from the late exponential growth phase or the stationary phase. As indicated in Table I, the cell concentration increased during starvation. We found that cells starved from logarithmic growth phase give rise to an increase in cell concentration of 10–30%, whereas cells starved from late logarithmic growth phase or stationary growth phase give rise to only a small, if any, increase in cell concentration. These findings indicate that cells at some stage of division will complete the initiated division even after transfer to the starvation medium.

Influence of starvation medium

We assumed that the pH of the medium would be affected if the starvation medium had no buffer capacity. Initially, we used 10 m*M* Hepes-KOH, pH 7.4 (Hepes) for the starvation medium because we recently found that long-term starved cells survive better in Hepes than in 10 m*M* Tris-HCl, pH 7.4 (Tris) (Hellung-Larsen *et al.*, 1993). As shown in Table I, pH was 7.4 after starvation

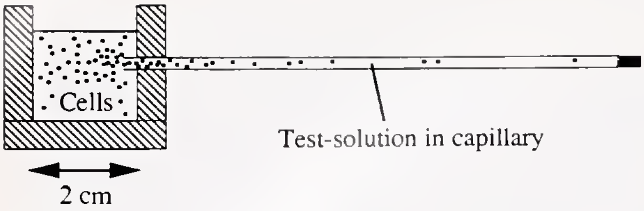

Figure 2. A schematic presentation of the capillary assay. Proteose peptone (PP) in a concentration of 1 mg ml^{-1} was placed in the capillary and one end of the capillary was sealed with wax. The capillary was then placed horizontally through a sealed hole into the jar containing 2.5 ml of cell suspension, and the open end of the capillary was brought in contact with the cell suspension. Incubation was usually for 45 min at 28°C, and the assays were scored by microscopic determination of the cell concentration in the capillary. Parallel assays containing only the solvent were performed as controls.

in Hepes. The minor decrease in pH observed in the most hypoxic cell suspensions was probably due to accumulation of lactic acid. When Hepes is used as starvation medium, it must also be used as diluent in the assays because we found that cells starved in Hepes swam more slowly than cells starved in deionized water (results not shown). This effect is probably due to the presence of K^+ in the buffer. K^+, as well as other cations, is known to influence the swimming speed of ciliate protozoa (Nakaoka *et al.*, 1983). To minimize kinetic effects of cations in the starvation medium, we attempted to starve cells in deionized water. Surprisingly, water proved to be an excellent starvation medium, and the chemosensory sensitivity of the cells was even higher than that observed using Hepes or Tris for starvation. Furthermore, the pH in cell suspensions starved in deionized water did not decrease if the O_2 tension was kept above 60% (results not shown).

Influence of the cell concentration during starvation

To illuminate the significance of the cell concentration during starvation, we starved cells at concentrations of 2.5×10^4, 5.0×10^4, 10×10^4, 20×10^4, and 40×10^4 cells ml^{-1}. The cells were starved at 21°C and S/V's were 4.8 cm^{-1}.

Cell suspensions of 2.5×10^4, 5.0×10^4, 10×10^4, and 20×10^4 cells ml^{-1} revealed 100% saturation of O_2 after starvation, whereas the saturation of O_2 decreased to 91% in the cell suspension of 40×10^4 cells ml^{-1}. In the cell suspensions having 100% saturation of O_2, we found that the chemosensory sensitivity toward PP was unaffected by the concentration of cells during starvation, as the responses were almost identical (SD less than 5%). Studies in another assay—the improved two-phase assay—revealed that sensitivity towards weak attractants such as certain amino acids was optimal if cells were starved at a concentration not exceeding 2×10^5 cells ml^{-1} (Koppelhus *et al.*, 1994).

Influence of temperature during starvation

As indicated in Table 1, the responses toward PP were significantly higher when cells were starved at 15° or 21°C than when cells were starved at 28° or 35°C. In contrast, the background level in the assay was highest when cells were starved at the highest temperatures. The ATP/ADP ratio decreased when the temperature was increased during starvation. The ATP pools of cells starved for 16 h were 1–4 nmol 10^{-6} cells. In comparison, the ATP pools of exponentially growing cells were about 20 nmol 10^{-6} cells (results not shown). The temperature of starvation also influenced the volume of the cells: the cells became smaller as a function of increasing temperature during starvation. At the smallest S/V, the cell volume decreased even more. Because of the indirect electronic volume determination applied, all cell suspensions were examined microscopically to confirm the qualitative conclusions. Microscopic examination revealed that the anoxic cells were somewhat flattened, and the divergence in cell volume compared to cells starved at the same temperature might be due to the osmotic state of the cells.

Influence of oxygen saturation of the starvation medium

The results in Table 1 reveal the precise dependence of oxygen saturation on the S/V of the starvation medium. The saturation of oxygen was essentially 100% if cells were starved under conditions in which S/V was equal to 4.8 cm^{-1}.

Suspensions having S/V equal to 0.6 cm^{-1} became more or less hypoxic during starvation, whereas the cells in suspensions having S/V equal to 0.03 cm^{-1} became strongly hypoxic (anoxic) during the period of starvation, which in turn killed the cells. The survivors in these cell suspensions had highly irregular swimming patterns. Disregarding the strongly hypoxic cell suspensions (*i.e.*, the (d) suspensions), we found that the lower the O_2 tension of the cell suspension, the greater the responses toward PP. The background level also increased in relation to lower O_2 tension of the cell suspension, but in general the background level did not increase in direct proportion to the response toward PP; as a result, signal-to-noise ratios were augmented (Table 1).

We found no significant differences in swimming speed of cells between cultures starved into self-induced hypoxia and suspensions that maintained full oxygen saturation during starvation. The swimming speeds were between 0.4 and 0.5 mm s^{-1} regardless of the oxygen saturation of the starvation medium. This also seems to indicate that there is no direct relationship between the ATP pools of the cells and their ability to maintain their swimming speed. For comparison, the swimming speeds of exponentially growing cells in culture are between 0.5 and 0.6 mm s^{-1} (Hellung-Larsen *et al.*, 1993).

Table I

Different physiological parameters, including chemosensory response, of Tetrahymena *starved under different conditions*

Temperature during starvation (°C)	Surface/volume ratio of starvation medium (cm^{-1})	O_2 tension of medium after starvation (%)	pH in medium after starvation (%)	Cell conc. after starvation (cells ml^{-1})	Cell volume after starvation (μm^3)	ATP/ADP (nmol 10^{-6} cells)	Capillary containing 1 mg PP ml^{-1} (signal) (% of original cell concentration)	Capillary containing no attractant (noise) (% of original cell concentration)	Signal/noise ratio
15	4.80 (a)	100	7.4	55,000	3500	3.2/0.8	96 ± 4	11 ± 2	9
	0.60 (b)	99	7.4	52,000	3500	ND	98 ± 4	8 ± 3	12
	0.20 (c)	42	7.4	55,000	3500	ND	143 ± 12	8 ± 3	18
	0.03 (d)	9	7.2	47,000	3300	ND	41 ± 8	5 ± 1	8
21	4.80 (a)	100	7.4	62,000	3000	2.4/0.5	99 ± 6	11 ± 2	9
	0.60 (b)	96	7.4	62,000	3000	2.3/0.4	128 ± 6	11 ± 2	12
	0.20 (c)	42	7.4	61,000	3000	2.3/0.6	165 ± 10	14 ± 1	12
	0.03 (d)	8	7.2	28,000	2500	0.4/2.3	62 ± 9	2 ± 1	31
28	4.80 (a)	100	7.4	64,000	2500	1.6/0.3	51 ± 5	12 ± 2	4
	0.60 (b)	95	7.4	62,000	2500	ND	74 ± 6	12 ± 3	6
	0.20 (c)	40	7.3	63,000	2500	ND	95 ± 7	14 ± 1	7
	0.03 (d)	8	7.1	20,000	2000	ND	15 ± 2	0 ± 0	—
35	4.80 (a)	98	7.4	63,000	1800	1.2/0.4	42 ± 4	15 ± 1	3
	0.60 (b)	84	7.4	63,000	1800	ND	63 ± 4	17 ± 5	4
	0.20 (c)	35	7.2	63,000	1800	ND	79 ± 6	17 ± 2	5
	0.03 (d)	8	7.0	13,000	1000	ND	5 ± 1	0 ± 0	—

Exponentially growing cells were starved at a concentration of 5×10^4 cells ml^{-1}. The cells were starved at different temperatures and at different S/V ratios (*cf.* Fig. 1). After starvation for 16 h, the O_2 tension, pH, cell concentration, cell volume, ATP/ADP, and chemosensory response were measured. The assays on chemokinesis were performed in quintuplicate, and mean values ±SD are given. ND = not determined.

Starvation period

Previous studies have suggested that starvation of *Tetrahymena* cells was necessary to obtain a chemosensory response (Levandowsky *et al.*, 1984). To investigate the chemoattraction of the nonstarved cells, we used deionized water to dilute a suspension of exponentially growing cells from a concentration of 6×10^5 cells ml^{-1} to a concentration of 5×10^4 cells ml^{-1}. Subsequently, we tested these nonstarved cells in the capillary assay and found a response toward PP of 85% and a background level of only 1%. These lower values of accumulation in comparison with cells starved for 16 h may be due to a competitive chemoattractive effect from the leftover growth medium within the cell suspension—the growth medium is itself a potent chemoattractant because of its PP content. This was further confirmed (results not shown) by the fact that addition of growth medium (or PP) to suspensions of starved cells suppressed the accumulation of cells in the assay according to the concentration of the added medium (or PP).

In another experiment, cells were starved at 5×10^4 cells ml^{-1} at 21°C in deionized water with an S/V of 4.8 cm^{-1}, and aliquots of the cell suspension were tested in the capillary assay after starvation for 1 day (16 h), 3 days, 5 days, and 7 days. The responses toward PP (1 mg/ml) were found to be 100 ± 7%, 92 ± 4%, 71 ± 5%, and 59 ± 2%, respectively. The accumulations in the respective control assays were 11 ± 2%, 9 ± 2%, 5 ± 1%, and 4 ± 1%. That is, the accumulation in the assays (both with and without PP) gradually decreased as the starvation of the cells proceeded. This effect may be a simple consequence of the gradual decrease in swimming speed known to take place during starvation (Hellung-Larsen *et al.*, 1993).

Discussion

The main purpose of this study was to determine the optimal physiological conditions for chemoattraction studies with *Tetrahymena*. The data obtained suggest that the cells should be starved for about 16 h at about 21°C, and that the surface-to-volume ratio of the cell suspension should be no less than 4.8 cm^{-1}. Furthermore, the cells should be starved at a concentration below 2×10^5 cells ml^{-1}. Deionized water proved to be a suitable starvation medium. Subsequent studies have revealed that cells starved in this way are indeed suitable for the detection of even weak attractants such as certain amino acids and peptides (Koppelhus *et al.*, 1994).

We did not find the increase in swimming speed observed by Nelsen and Debault (1978) in response to starvation. Some explanation for this discrepancy may be that Nelsen and Debault used "Dryls medium" containing 2 m*M* of $CaCl_2$ for the starvation medium. $CaCl_2$ at this concentration is known to hyperpolarize the cells, making them swim faster and more smoothly (Machemer, 1989).

Jauker and coworkers found a rate of decrease in ATP pools in *Tetrahymena* of 1–3 nmol h^{-1} after cells were transferred to starvation at room temperature (Jauker *et al.*, 1986). Our results seem to confirm these findings. Furthermore, the ATP decrease during starvation seems to be closely correlated to the applied temperature. When using cells starved at 21°, 28°, and 35°C, we found an interesting correlation between the ATP pools of the cells and their chemosensory responses. Higher levels of ATP gave better chemosensory responses than did low levels. The correlation is not straightforward, however, because cells starved at 15°C had similar chemosensory responses to cells starved at 21°C, even though they have larger pools of ATP.

We suggest that the nonoptimal responses obtained using nonstarved cells are due to a competitive effect of chemoattractants within the cell suspension. It might be preferable if cells were deprived of growth medium without any period of starvation (and consecutive loss of ATP). This might be done by applying an electric field to a cell culture and separating the cells from the medium by means of galvanotaxis.

We found no obvious sign of an up-regulation of the chemosensory response after prolonged starvation. This seems to indicate that the ability for chemosensory behavior in *Tetrahymena* is a constant quality of the cells and that starvation is obligatory only to remove the growth medium, which is a very potent chemoattractant. Furthermore, a certain period of starvation seems necessary for the cells to overcome the stress (ciliary damage, etc.) of being centrifuged. Without the possibility of completely separating growing cells from their medium in a manner that does not affect the cells, it seems impossible to further investigate the importance of short-term starvation on the chemosensory response of the cells.

The augmented responses observed when hypoxic cell suspensions were assayed suggest that *Tetrahymena* may exhibit a positive aerotactic behavior. Aerotactic responses are observed in a number of protozoa and bacteria and may be of vital importance in the survival of motile microorganisms (see review by Levandowsky and Hauser, 1978).

The results presented in Table I demonstrate that signal-to-noise ratios can be misleading as a quantitative measurement of the chemosensory response; thus, they must be considered inadequate if the cell material is not strictly standardized and controlled. Identical cells should be used in assays for the comparison of attractants.

Considering the capillary assay used for this study, we found that even with optimal cell material, the assay should be performed in at least quintuplicate to ensure statistical significance. This makes it difficult to test more than a few samples at a time. For the purpose of testing a large number of samples, we have developed a sensitive and easy-to-perform spectrophotometric assay, which is described in the accompanying paper (Koppelhus *et al.*, 1994).

Acknowledgments

Excellent technical assistance was delivered by Inger Lyhne. Use of facilities for swimming speed estimations in the laboratory of Professor Donat-P. Häder is gratefully acknowledged. We thank Dr. Overgaard-Hansen for help with the nucleotide determinations. The work was supported by grants from Dir. Henriksens fond, The Carlsberg Foundations, Novo's Foundations, and the Danish Medical Research Council.

Literature Cited

Almagor, M., A. Ron, and J. Bar-Tana. 1981. Chemotaxis in *Tetrahymena thermophila. Cell Motil.* **1:** 261–268.

Häder, D.-P., and M. Lebert. 1985. Real time computercontrolled tracking of motile microorganisms. *Photochem. Photobiol.* **42:** 509–514.

Hellung-Larsen, P., and I. Lyhne. 1992. Effect of shaking on growth of diluted cultures of *Tetrahymena. J. Protozool.* **39** (2): 345–349.

Hellung-Larsen, P., V. Leick, and N. Tommerup. 1986. Chemoattraction in *Tetrahymena:* on the role of chemokinesis. *Biol. Bull.* **170:** 357–367.

Hellung-Larsen, P., V. Leick, and N. Tommerup. 1986. Chemoattraction in *Tetrahymena.* on the role of chemokinesis. *Biol. Bull.* **170:** 357–367.

Hellung-Larsen, P., I. Lyhne, A. P. Andersen, and U. Koppelhus. 1993. Characteristics of dividing and non-dividing *Tetrahymena* cells at different physiological states. *Eur. J. Protistol.* **29:** 182–190.

Jauker, F., S. Lades, and T. Nowack. 1986. The energy budget of *Tetrahymena* and the material fluxes into and out of the adenylate pool. *Exp. Cell Res.* **166:** 161–170.

Klenow, H., and E. Ostergaard. 1988. Adenosine induction of rapid catabolism of adenine ribonucleotides and independent elevation of ATP content in quiescent mouse fibroblasts. *J. Cell. Phys.* **137:** 565–570.

Koppelhus, U., P. Hellung-Larsen, and V. Leick. 1994. An improved quantitative assay for chemokinesis in *Tetrahymena. Biol. Bull.* **187:** 8–15.

Leick, V., and P. Hellung-Larsen. 1992. Chemosensory behaviour of *Tetrahymena. Bioessays* **14(1):** 466–469.

Leick, V., K. Frederiksen, I. Lyhne, and P. Hellung-Larsen. 1990. A paper membrane filter assay for ciliate chemoattraction. *Anal. Biochem.* **184:** 63–66.

Levandowsky, M., T. Cheng, A. Kehr, J. Kim, L. Gardner, L. Silvern, L. Tsang, G. Lai, C. Chung, and E. Prakash. 1984. Chemosensory responses to amino acids and certain amines by the ciliate *Tetrahymena.* a flat capillary assay. *Biol. Bull.* **167:** 322–330.

Levandowsky, M., and D. C. R. Hauser. 1978. Chemosensory responses of swimming algae and protozoa. *Int. Rev. Cytol.* **53:** 145–210.

Machemer, H. 1989. Cellular behavior modulated by ions: electrophysiological implications. *J. Protozool.* **36:** 463–487.

Nakaoka, Y., T. Oka, K. Serizawa, H. Toyotama, and F. Oosawa. 1983. Acceleration of *Paramecium* swimming velocity is effected by various cations. *Cell Struct. Func.* **8:** 77–84.

Nelsen, E. M., and L. E. Debault. 1978. Transformation in *Tetrahymena pyriformis:* description of an inducible phenotype. *J. Protozool.* **25(1):** 113–119.

Tanabe, H., K. Kurihara, and Y. Kobatake. 1980. Changes in membrane potential and membrane fluidity in *Tetrahymena* in association with chemoreception of hydrophobic stimuli: fluorescence studies. *Biochemistry* **19:** 5339–5344.

Ueda, T., and Y. Kobatake. 1977. Hydrophobicity of biosurfaces as shown by chemoreceptive thresholds in *Tetrahymena, Physarum* and *Nitella. J. Membrane Biol.* **34:** 351–368.

Van Houten, J., D. C. R. Hauser, and M. Levandowsky. 1981. Pp. 67–124 in *Biochemistry and Physiology of Protozoa,* Vol. 4, M. Levandowsky and S. H. Hutner, eds. Academic Press, New York.

Reference: *Biol Bull.* **187**: 8–15. (August, 1994)

An Improved Quantitative Assay for Chemokinesis in *Tetrahymena*

UFFE KOPPELHUS[1], PER HELLUNG-LARSEN[2], AND VAGN LEICK

Institute of Medical Biochemistry and Genetics, Department B, The Panum Institute, University of Copenhagen, Blegdamsvej 3, 2200 Copenhagen N, Denmark

Abstract. This paper presents a quantitative and sensitive assay for the measurement of chemosensory behavior in *Tetrahymena.* The two-phase assay is easy to perform in large quantities, so a variety of compounds can be screened under comparable conditions. A suspension of 2×10^5 cells ml^{-1} (the upper phase) is starved for 20–40 h and then gently placed on top of a 5% solution of Metrizamide (the lower phase) in a disposable microcuvette. The optical density of the lower phase is monitored at 600 nm with an automated spectrophotometer at selected time points. Optimum sensitivity of the assay is achieved when the cells slowly but continuously enter the lower phase, so that about 5% of them will be in the lower phase within 30 min. Optimal chemosensory responses occurred in *Tetrahymena thermophila* at about 25°C. The response was delayed at 15°C and markedly reduced at 35°C. The data suggest three bases for quantifying the response in the assay: (1) initial slope of the absorbance *versus* time; (2) final maximal absorbance within the time period of measurement; and (3) signal-to-noise ratio (S/N) at a fixed time. We have quantified—in terms of S/N—the chemosensory responses in *Tetrahymena* for the following compounds: β-endorphin, fibroblast growth factor, insulin, and platelet-derived growth factor (PDGF); these substances were active in nanomolar concentrations, and the maximal S/N was between 3 and 5.1. Acetylcholine was active only in millimolar concentrations; maximal S/N was 4.1 at 1 m*M*. Glutamic acid, glutamine, glycine, isoleucine, leucine, methionine, phenylalanine, proline, serine, threonine, tryptophan, and valine were active in millimolar concentrations, with S/N between 1.5 and 2.5. We found S/N equal to 9.6 for a mixture of amino acids (1 m*M* of each amino acid). Furthermore, if PDGF was added to the mixture of amino acids, the S/N increased to 11.3. Proteose peptone at a concentration of 1 mg ml^{-1} produced a strong response, with S/N equal to 17.5. The assay is also suitable for the detection and quantification of repellents. We found that 20 m*M* KCl, 1 m*M* 4-nitroaniline (4-NA), and 100 μ*M* 2,4-dinitroaniline (2,4 DNA) each almost completely prevented the cells from migrating into the lower phase. The minimum concentrations of significant repellent effect using these substances were 500 μ*M*, 1 μ*M*, and 50 n*M*, respectively.

Introduction

Several assays have been proposed for the measurement of chemokinesis in *Tetrahymena,* including capillary assays (Almagor *et al.,* 1981; Leick and Helle, 1983; Levandowsky *et al.,* 1984), modified Zigmond chambers (Leick, 1988; Hellung-Larsen *et al.,* 1990), field assays (Hellung-Larsen *et al.,* 1986), and a membrane filter assay (Leick *et al.,* 1990). A common feature has been the time-consuming and labor-intensive setup of the assays, involving large volumes of cell suspension and microscopical or electronic counting of the cells. None of the assays have been useful for testing more than a few samples at a time, so precise and direct comparisons of many samples at the same time have been difficult to perform. Because of its chemosensory sensitivity to certain anilines and phenols, *Tetrahymena* has been proposed as a test organism in the screening of industrial aquatic pollutants (Berk *et al.,* 1990; Pauli and Berger, 1992). Therefore, a sensitive and easy-to-perform assay for chemokinesis in *Tetrahymena* will increase the usefulness of this organism in the area of aquatic ecotoxicology.

To make a detailed examination and comparison of the kinetics of the chemosensory response of *Tetrahymena*

Received 2 September 1993; accepted 27 May 1994.

[1] Present address: The Danish Cancer Society, Department of Virus and Cancer, Gustav Wieds Vej 10, DK-8000 Aarhus, Denmark.

[2] Author to whom correspondence should be addressed.

at different experimental conditions, an assay that produces precise time-response curves must be established. Indeed, none of the existing assays yielded more than a few points of the time-response curve of the chemosensory response of *Tetrahymena*.

Recently we found that control of the physiological state of the cells improved the reproducibility and sensitivity of a capillary assay for chemokinesis in *Tetrahymena* (Koppelhus *et al.*, 1994). Encouraged by these results, we have reinvestigated the two-phase assay that was introduced in 1986 as a semiquantitative method (Hellung-Larsen *et al.*, 1986). A quantitative assay with high sensitivity was then developed as described here.

Materials and Methods

Cell cultures

Tetrahymena thermophila strain B7 was grown axenically in PY medium: 0.75% proteose peptone (Difco), 0.75% yeast extract (Difco), 1.5% glucose, 1 m*M* $MgSO_4$, 50 μM $CaCl_2$, and 100 μM ferric citrate. The PY medium was diluted with water to ⅓ prior to use. Fifty-milliliter cultures of B7 cells were grown at 35°C in 500-ml Fernbach flasks. The cultures were left unagitated to avoid cell division stress (Hellung-Larsen and Lyhne, 1992). Cells in exponential growth phase were used to inoculate the cultures to a concentration of about 10^4 cells ml^{-1}.

Transfer to starvation was done after 16–20 h at a cell density of about 8×10^5 cells ml^{-1} (late exponential growth phase) or 40–50 h at a cell density of approximately 1.3×10^6 cells ml^{-1} (early stationary phase). For starvation, the cells were collected by centrifugation at $500 \times g$ for 3 min and then gently resuspended in deionized water to a cell concentration of approximately 1.5×10^5 cells ml^{-1}. The cells were starved at 21°C in 500-ml Fernbach flasks containing, at a maximum, 50 ml of cell suspension each. This ensured a constant maximal oxygen saturation of the suspensions of starving cells (Koppelhus *et al.*, 1994).

Cell concentration and cell volumes were determined with the aid of a Coulter Multisizer, as previously described (Hellung-Larsen and Andersen, 1989).

Chemoattraction assays

Capillary assay. A capillary technique with single glass capillaries was used. Heparinized glass capillaries (75 mm long, inner diameter 1.1–1.2 mm) were filled with test solution, and one end of the capillary was sealed with wax. The capillary was then placed horizontally through a sealed hole into the jar containing the cell suspension, and the open end of the capillary was brought in contact with the cell suspension. Incubation was usually for 45 min at 28°C. After incubation, the number of cells accumulated in the capillary was determined by microscopical counting in a hemacytometer. All experiments were carried out in series of five identical assays and five parallel control assays.

Two-phase assay. The chemoattractant was dissolved in 2–5% (w/v) metrizamide (2-[3-acetamido-5-N-methyl-acetamido-2,4,6-triiodo benzamido]-2-deoxyglucose) in deionized water and 1 ml was placed—as the lower phase—in a disposable plastic cuvette (Plastibrand, Germany, Cat. No. 759015). A 1.5-ml suspension of starved cells was then carefully layered on top of the metrizamide solution and the optical density (OD_{600}) of the metrizamide phase was monitored automatically every 2 min in a thermostated recording spectrophotometer (Shimadzu UV-160), where six cuvettes could be monitored in parallel. Assays were performed at 28°C, unless otherwise stated. The assay procedure is shown schematically in Figure 1.

The response at a given time was calculated as

$$\frac{OD_{600} \text{ of the lower phase}}{1.5 \times (OD_{600} \text{ of the original cell suspension used})} \times 100\%$$

The 100% response corresponds to the theoretical situation in which all cells from the upper phase (1.5 ml original cell suspension) are equally distributed throughout the lower phase (1 ml of metrizamide), thus giving rise to an optical density 1.5 times that of the cell suspension.

We found that the OD_{600} of an aqueous cell suspension is linearly proportional to the concentration of cells, when cells are equally distributed throughout the suspension (Figure 2). In the assay, we found that cells—when present in the lower phase—in fact tend to be equally distributed within the phase. This is in accordance with the observations reported earlier (Hellung-Larsen *et al.*, 1986). The OD_{600} of 5% metrizamide was equal to the OD_{600} of water.

Chemicals

Acetylcholine, amino acids, bovine serum albumin (BSA), β-endorphin, met-enkephalin, fibroblast growth factor (FGF), oxytocin, and vassopressin were purchased from Sigma. Metrizamide was obtained from NycoMed Pharma A/S or Sigma. Platelet-derived growth factor (PDGF; B/B) was purchased from Boehringer. Insulin (human recombinant) was delivered from Novo Nordisk, Denmark.

All stock solutions were prepared in deionized water, except for platelet-derived growth factor, which was prepared in an aqueous stock solution containing 0.1% BSA (w/v). For the experiment testing single amino acids, 30 m*M* stock solutions of each were prepared in a 10 m*M* TRIS/HCl buffer (TRIS) at pH = 7.4 and—if necessary—pH was adjusted to 7.4 with additional TRIS. The control

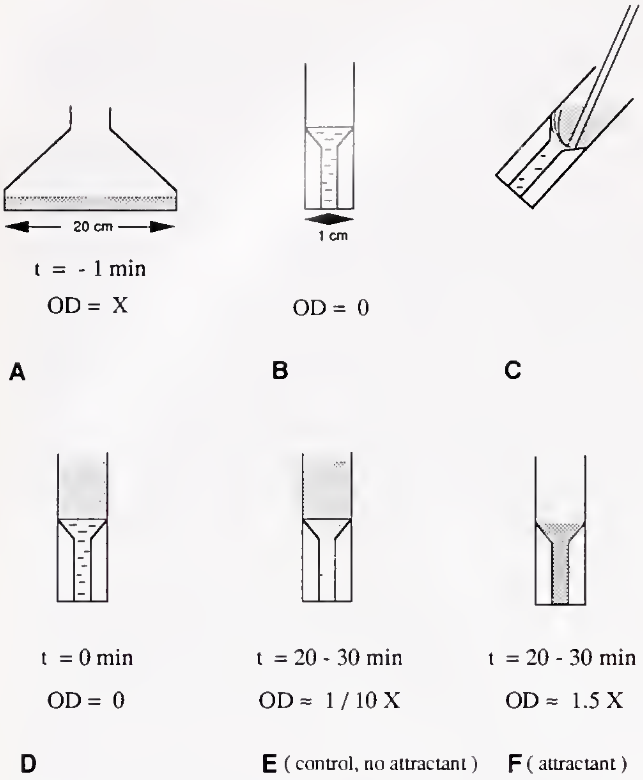

Figure 1. Schematic representation of the quantitative two-phase assay. Cells starved in a 500-ml Fernbach flask at a concentration of 1–2 × 10^5 cells ml^{-1} at a temperature of 21 °C for 20–40 h are used. OD_{600} of the cell suspension was measured just before the experiment, using the solution of metrizamide as reference. In this example, OD of the cell suspension equals X (A). One milliliter of the metrizamide solution is filled into the microcuvettes and each cuvette is blanked (B). Using a pasteur pipette and a steady fingertip, 1.5 ml of the cell suspension is carefully layered on top of the metrizamide (C). Immediately after the cells are applied, the optical density of the lower phase should still be zero (D). After 20–30 min, the OD of the lower phase containing 1 mg proteose peptone ml^{-1} will increase to about 1.5 X, implying that virtually all cells are now present in the lower phase (F). In the control cuvette, the OD is only slightly increased—to about 1/10 X (E).

assays in these experiments contained TRIS at the appropriate concentration.

The mixture of amino acids was prepared in a stock solution composed of 10 m*M* of each of the amino acids found in a synthetic medium proposed for growth of *Tetrahymena* (Rasmussen and Modeweg-Hansen, 1973). These are DL-alanine, L-arginine, L-asparagine, L-glutamate, L-glutamine, glycine, L-histidine, L-isoleucine, L-leucine, L-lysine, DL-methionine, DL-phenylalanine, L-proline, DL-serine, DL-threonine, L-tryptophan, and DL-valine. The amino acid mixture was adjusted to pH = 7.4 by the addition of NaOH.

Results

In the experiment shown in Figure 3, cells from late exponential growth phase were starved at a concentration of 1.6 × 10^5 cells ml^{-1}, and assays were performed after 2, 16, 40, and 64 h of starvation using no attractant (controls) or proteose peptone (PP) as attractant in a concentration of 1 mg ml^{-1}. The responses to PP were significant at all four periods of starvation, whereas the background levels (control) exhibited great variation (Fig. 3).

No significant response to amino acids and hormones could be detected after 2 h of starvation. After 16 h of starvation, sensitivity to hormones and amino acids could be observed. However, these responses were often difficult to detect and quantify because of high and unstable background levels in the controls. After 40 h of starvation, the cells were still sensitive to weak attractants and, at the same time, the background levels in the controls became lowered and more stable, thus making the assay more reproducible. In general, it proved to be true that after a certain period of starvation, the background level became low while the sensitivity of the assay was still high. In this (optimal) situation, cells slowly—but continuously—enter the lower phase in the control assay (Fig. 3C). After 64 h of starvation, the sensitivity to weak attractants was markedly decreased, and after 88 h of starvation only response toward PP could be detected. Responses to PP were observed even after 192 h of starvation.

The size of the background level and thus the sensitivity of the assay could be manipulated by the concentration of the metrizamide in the lower phase. This was true only at 40 h of starvation. Attempts to suppress the background levels at 16 h of starvation by increasing the concentration of metrizamide to as much as 20% were not successful. Similarly, increased sensitivity of the assay could not be established by lowering the concentration of metrizamide after 64 h of starvation.

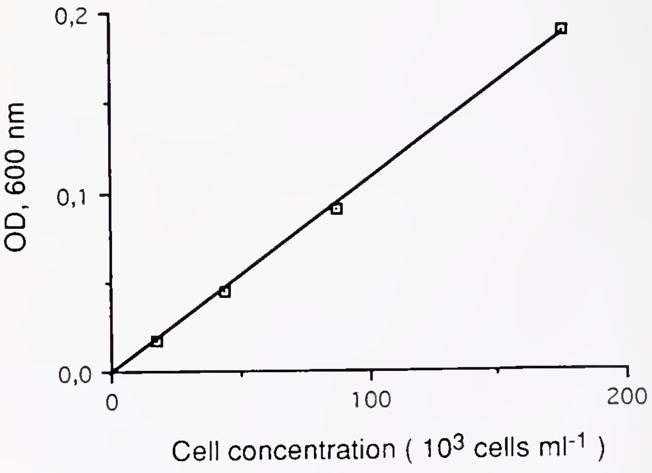

Figure 2. The relationship between OD_{600} and cell number in an aqueous suspension. Careful stirring ensured equal distribution of the cells throughout the suspension.

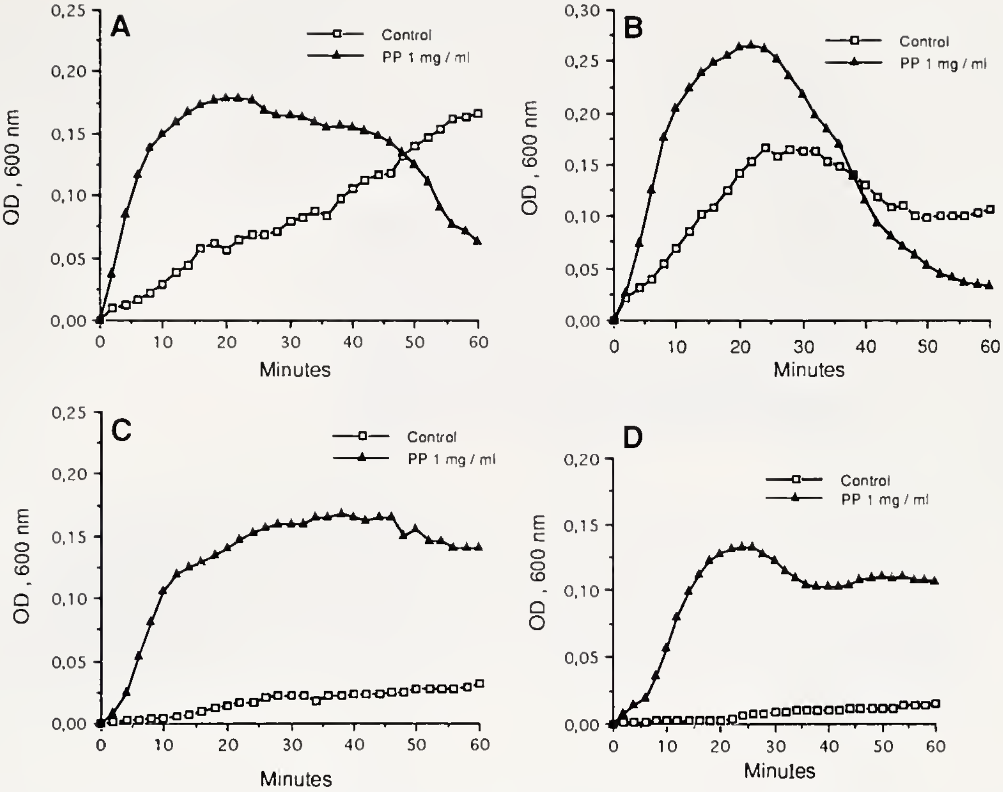

Figure 3. Time-response curves after 2 h (A), 16 h (B), 40 h (C), and 64 h (D) of starvation. The ODs of the cell suspension were 0.19, 0.20, 0.13, and 0.12, respectively, and the maximum ODs in response to PP at a concentration of 1 mg ml^{-1} (▲) were 0.18 (20 min), 0.27 (22 min), 0.17 (38 min), and 0.13 (24 min), respectively. That is, the maximum absolute responses to protease peptone (PP) were 63, 92, 85, and 77%, respectively. The background—control with no attractant (□)—was drastically reduced after 40 h of starvation in comparison to the background obtained after a shorter period of starvation. The assay was sensitive to weak attractants only between 16 and 64 h of starvation, and the most distinguishable and reproducible quantitative determinations were obtained using cells starved for 40 h.

Cells with maximal sensitivity could be obtained within a shorter period of starvation if cells were grown to the early stationary phase before they were transferred to starvation medium. Thus, the results shown in Figure 4 and Table 1 are from experiments using early stationary phase cells starved for 24 h.

The time-response curves offer three approaches for quantitative analysis: (1) initial slope of the absorbance *versus* time, (2) final maximal absorbance within the time period of measurement, and (3) signal-to-noise ratio (S/N) at a fixed time—*i.e.*, S/N = 1, no chemokinesis; S/N < 1, negative chemokinesis; S/N > 1, positive chemokinesis.

In the experiments shown in Figure 4 and Table 1, we tested a variety of animal peptide hormones, some of which have previously been found to work as chemoattractants for *Tetrahymena.* Table 1 lists the S/N's obtained after 24 min; Figure 4 shows representative time-response curves for a number of attractants tested. Obviously, β-endorphin, FGF, insulin, and PDGF all are good attractants in nanomolar concentrations, whereas oxytocin and vassopressin were not found to be attractants at all. Met-enkephalin induced a significant response, but only in micromolar concentrations; maximum S/N = 3.7 at 200 μM. Acetylcholine was a strong attractant in a way similar to the hormones, but was active only in millimolar concentrations; maximal S/N = 4.1 at 1 mM concentration.

PDGF was the most potent attractant of the peptide hormones tested. PDGF was kept in a stock solution of 300 nM containing 0.1% BSA. Maximum S/N of PDGF was 5.1 at a concentration of 3 nM. At this PDGF concentration, the concentration of BSA was 10 μg ml^{-1}. Although BSA at a concentration of 10 μg ml^{-1}, by itself, did not induce any chemoattraction, the effect of PDGF in the BSA solution might still be due to a synergistic or cooperative effect of the two compounds. However, earlier results obtained with PDGF

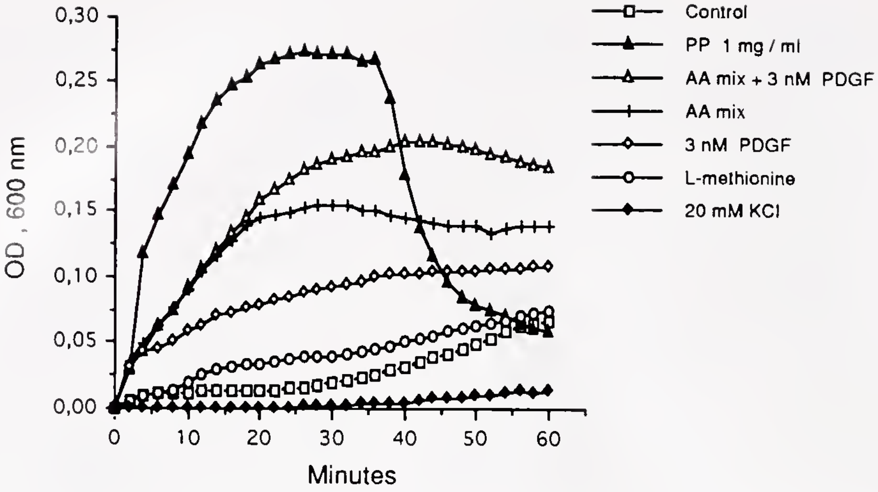

Figure 4. Effect of different attractants and one repellant. OD of the lower phase was monitored every second minute. PP, protease peptone; AA mix, mixture of amino acids (1 m*M* of each); PGDF, platelet-derived growth factor. The plots illustrate the chemosensory responses obtained using PP at a concentration of 1 mg ml^{-1} (▲), AA mix in combination with 3 n*M* PDGF (△), AA mix (+), 3 n*M* PDGF (◇), 5 m*M* L-methionine (○), and 20 m*M* KCl (◆), respectively. OD of the cell suspension used was 0.207. Cuvettes containing no attractant were tested as controls (□). The data shown represent only some of the data in the experiment.

tested in a neutralized HAc-solution seem to indicate that PDGF is itself a very potent chemoattractant to *Tetrahymena* (Hellung-Larsen *et al.*, 1986).

Insulin induced the maximal response at a concentration of 170 n*M*. However, 1.7 μ*M* insulin had a repellant effect (S/N = 0.1). Such a dramatic change of effect due to a 10-fold rise in concentration has not been observed for any other peptide attractant. All compounds tested were prepared in stock solution just before the experiment (except for the PDGF solution, which had been stored for approximately 1 year at −20°C). Initial screening revealed that β-endorphin had an atypical loss of activity after only a short storage (2–3 days) in aqueous solution at 0°C.

The hormones tested in this experiment were also examined in a capillary assay, and similar results were obtained (results not shown). Furthermore, experiments using the capillary method revealed that α-endorphin was also active as an attractant in nanomolar concentrations.

We also tested the 17 amino acids present in Holz-defined medium. The amino acids were screened twice at a concentration of 5 m*M*. Glutamic acid, glutamine, glycine, isoleucine, leucine, methionine, phenylalanine, proline, serine, threonine, tryptophan, and valine were all positive, with S/N's between 1.5 and 2.5 (results not shown).

We found S/N equal to 9.6 for a mixture of the 17 amino acids (1 m*M* of each amino acid). Furthermore, when PDGF was added to the mixture of amino acids (AA mix) the S/N increased to 11.3. The relatively high molarity of the AA mix did not seem to affect either the viability or the swimming of the cells applied in these assays. This was determined by microscopical analysis of cells taken from both the lower and the upper phases of such assays.

Using S/N values, a hierarchy of chemoattracting potentials of the various compounds can be listed: PP ≫ AA mix + PDGF > AA mix > single hormones > single amino acids > control > repellants. A similar order results if the initial slopes of the time-response curves are considered. However, the initial slopes using AA mix or AA mix + PDGF are virtually identical (Fig. 4), indicating that differences can be resolved when measuring S/N values rather than initial slopes. A similar conclusion is drawn when comparing different concentrations of the same attractant. Thus, PP in concentrations of 1, 0.5, and 0.1 mg ml^{-1} gave rise to nearly identical initial slopes, but the maximum responses in these experiments were not similar (Fig. 5).

When a repellant was present in the lower phase, cells were prevented from entering this phase. We found that 20 m*M* KCl, 1 m*M* 4-nitroaniline, and 100 μ*M* 2,4-dinitroaniline each almost completely prevented the cells from migrating into the lower phase. This was true even if PP (in any concentration) was present in the lower phase in combination with the repellant (results not shown). The sensitivity of the assay to repellents is independent of the starvation period of the cells. That is, any (detectable) background level in the assay will be suppressed when a repellant is present therein.

Table I

Chemoattractant activity of peptides and amino acids in the two-phase assay

Compound	Conc. (w/v)	Molarity	S/N at 24 min after setup
Control (no attractant)	—	—	1.0 ± 0.3 (10)
Platelet-derived growth factor	1 μg/ml (BSA 100 μg/ml)	30 nM	1.4
	100 ng/ml (BSA 10 μg/ml)	3 nM	5.1 ± 0.6 (4)
	10 ng/ml (BSA 1 μg/ml)	300 pM	2.1
Bovine serum albumin	100 μg/ml	—	1.3
	10 μg/ml	—	1.0
	1 μg/ml	—	1.2
Insulin	10 μg/ml	1.7 μM	0.1
	1 μg/ml	170 nM	4.7 ± 0.8 (4)
	100 ng/ml	17 nM	2.3
Fibroblast growth factor	1 μg/ml	75 nM	4.0 ± 0.4 (10)
	100 ng/ml	750 pM	1.0
β-endorphin	250 ng/ml	70 nM	1.8
	25 ng/ml	7 nM	3.0 ± 0.4 (4)
	2.5 ng/ml	700 pM	1.6
Met-enkephalin	100 μg/ml	200 μM	3.7 ± 0.5 (4)
	10 μg/ml	20 μM	2.1
	1 μg/ml	2 μM	1.0
Acetylcholine	1.8 mg/ml	10 mM	3.7
	180 μg/ml	1 mM	4.1 ± 0.6 (4)
	18 μg/ml	100 μM	1.1
Oxytocin	10 μg/ml	10 μM	0.8
	1 μg/ml	1 μM	0.8
	100 ng/ml	100 nM	1.0
	10 ng/ml	10 nM	1.0
	1 ng/ml	1 nM	1.0
Vassopressin	10 μg/ml	9 μM	0.8
	1 μg/ml	900 nM	1.0
	100 ng/ml	90 nM	1.0
	10 ng/ml	9 nM	0.9
	1 ng/ml	900 μM	1.0
Amino acid mixture (AA mix)	(5.0 mM of each)	115 mM	7.8
	(1.0 mM of each)	23 mM	9.6 ± 0.5 (4)
	(200 μM of each)	460 μM	5.1
AA mix +			
Platelet-derived growth factor	(1.0 mM of each) + 100 ng/ml (BSA 10 μg/ml)	23 mM + 3 nM	11.3 ± 0.7 (4)
Proteose peptone	1 mg/ml	—	17.5 ± 1.4 (4)

Signal/noise ratios (S/N) at 24 min of assaying are listed. Some determinations were performed in quadruplicate and are given as mean values of S/N ± standard deviation. All results presented originate from the same culture of starved cells. That is, all assays were performed within 6 h. Corresponding time-response curves of the experiment are shown in Figure 4. BSA = bovine serum albumin.

As previously stated, all experiment were performed at 28°C (Leick *et al.*, 1990). However, we reinvestigated the effect of temperature on the chemokinesis of *Tetrahymena* by performing experiments at 15°, 25°, and 35°C. Parallel assays were performed in three spectrophotometers with thermostats set to 15°, 25°, and 35°C, respectively. The responses were strongest at 25°C, delayed at 15°C, and markedly reduced at 35°C (Fig. 6). This was true for any concentration of PP, thus confirming that the optimal temperature for chemokinesis in *Tetrahymena thermophila* is about 25°C.

Discussion

In this paper, we have described a number of parameters for carying out the two-phase assay for chemokinesis in *Tetrahymena.* The sensitivity of the assay depends upon the period of starvation. Maximum reproducibility and sensitivity is reached within 20–40 h of starvation. It seems that during starvation the cells gradually lose their ability to pass the water-metrizamide interphase unless stimulated with chemoattractant. The reason for this phenomenon is not known. The results may suggest that *Tetra-*

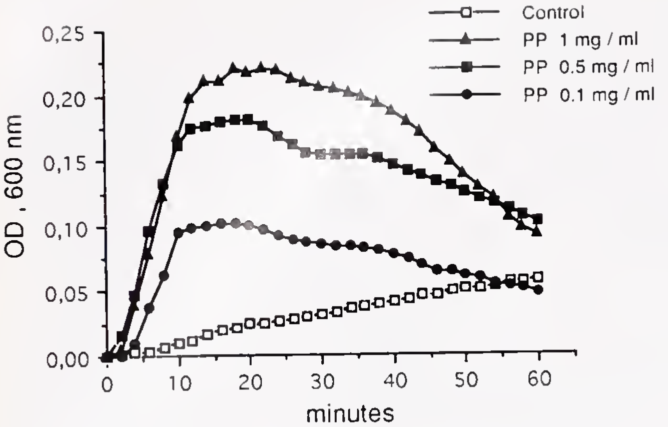

Figure 5. Effect of proteose peptone (PP) in different concentrations. PP was tested in final concentration of 0.1 mg ml^{-1} (●), 0.5 mg ml^{-1} (■), and 1 mg ml^{-1} (▲). Cuvettes containing no attractant were tested as controls (☐).

hymena, during starvation, undergoes a progressive decrease in cellular density, which in turn may affect the ability of the cells to enter the metrizamide phase. The metrizamide phase itself is known to reduce the swimming speed of the cells slightly (Hellung-Larsen *et al.*, 1986). The progressive decrease in swimming speed and cell volume known to take place during starvation might also offer some explanation of the observed phenomenon (Hellung-Larsen *et al.*, 1993).

During continued starvation, sensitivity to most attractants is gradually lost according to the relative strengths of the chemoattractants. It is remarkable, however, that sensitivity to PP was never lost. In addition to being a chemoattractant, PP is known to increase the swimming speed of the cells (Hellung-Larsen *et al.*, 1986). The stimulation by PP of the swimming speed may in part explain the strong chemosensory responses induced by this chemoattractant.

The results confirm that amino acids and peptides are chemoattractants for *Tetrahymena*. The responses to a mixture of amino acids were strong in comparison to the responses obtained using single amino acids. This additive effect may indicate a mechanism in which the amino acids work through specific receptors. Specific receptors may also explain the additive effect seen when AA mix + PDGF are tested in the assay.

We have confirmed the chemoattractive effect of PDGF, FGF, β-endorphin, and acetylcholine shown earlier (Tsang and Levandowsky, 1983; Andersen *et al.*, 1984; Leick and Hellung-Larsen, 1985; Hellung-Larsen *et al.*, 1986; O'Neill *et al.*, 1988). Furthermore, we have demonstrated a similar effect of insulin.

The fine adjustment of the starvation period necessary for optimal sensitivity towards attractants is not needed when testing repellants. Therefore, the assay might also be useful as a standard screening procedure in aquatic toxicology, because *Tetrahymena* is repelled from industrial pollutants such as anilines, phenols, and naphthalenes (Berk *et al.*, 1990; Pauli and Berger, 1992). Screening for repulsive effect of pollutants could be carried out in the two-phase assay as a competition assay with PP as the attractant.

The two-phase assay, in its present form, provides a sensitive and easy-to-perform spectrophotometric assay for chemokinesis in *Tetrahymena*. We infer that the assay could also be useful for testing chemokinesis in other ciliates and perhaps some flagellates. Such an approach will

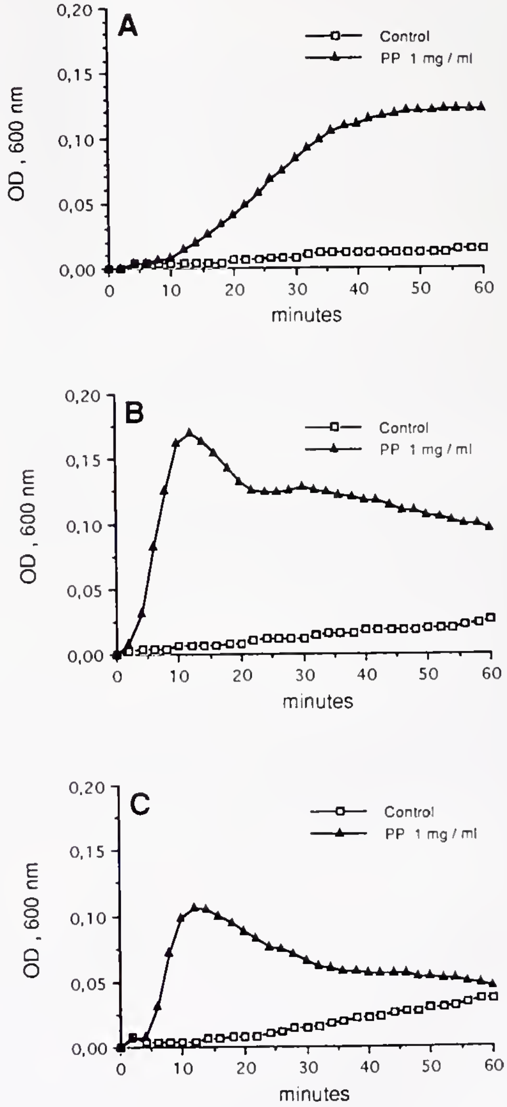

Figure 6. Effect of temperature on the chemosensory behavior of *Tetrahymena thermophila*. Parallel assays were performed at 15°C (A), 25°C (B), and 35°C (C) using no attractant (☐) or protease peptone (PP) at a concentration of 1 mg ml^{-1} in the assay (▲). OD of the cell suspension used was 0.15.

need proper adjustment of the metrizamide concentration in the lower phase and of the conditions for the starvation of the organism being tested.

Acknowledgments

The work was supported by grants from Dir. Henriksens fond, The Carlsberg Foundation, Novo's Foundation, and the Danish Medical Research Council.

Literature Cited

Almagor, M., A. Ron, and J. Bar-Tana. 1981. Chemotaxis in *Tetrahymena thermophila. Cell Motil.* **1:** 261–268.

Andersen, H. A., H. Flodgaard, H. Klenow, and V. Leick. 1984. Platelet-derived growth factor stimulates chemotaxis and nucleic acid synthesis in the protozoan *Tetrahymena. Biochim. Biophys. Acta* **782:** 437–440.

Berk, S. G., B. A. Mills, K. C. Stewart, R. S. Ting, and R. O. Roberts. 1990. Reversal of phenol and naphthalene effects on ciliate chemoattraction. *Bull. Environ. Contam. Toxicol.* **44:** 181–188.

Hellung-Larsen, P., and A. P. Andersen. 1989. Cell volume and dry weight of cultured *Tetrahymena. J. Cell Sci.* **92:** 319–324.

Hellung-Larsen, P., and I. Lyhne. 1992. Effect of shaking on growth of diluted cultures of *Tetrahymena. J. Protozool.* **39**(2): 345–349.

Hellung-Larsen, P., V. Leick, and N. Tommerup. 1986. Chemoattraction in *Tetrahymena:* on the role of chemokinesis. *Biol. Bull.* **170:** 357–367.

Hellung-Larsen, P., V. Leick, N. Tommerup, and D. Kronborg. 1990. Chemotaxis in *Tetrahymena. Eur. J. Protistol.* **25:** 229–233.

Hellung-Larsen, P., I. Lyhne, A. P. Andersen, and U. Koppelhus. 1993. Characteristics of dividing and non-dividing *Tetrahymena* cells at different physiological states. *Eur. J. Protistol.* **29:** 182–190.

Koppelhus, U., P. Hellung-Larsen, and V. Leick. 1994. Physiological parameters affecting the chemosensory response of *Tetrahymena. Biol. Bull.* **187:** 1–7.

Leick, V. 1988. Gliding *Tetrahymena thermophila.* oriented chemokinesis in a ciliate. *Eur. J. Protistol.* **23:** 354–360.

Leick, V., and J. Helle. 1983. A quantitative assay for ciliate chemotaxis. *Anal. Biochem.* **135:** 466–469.

Leick, V., and P. Hellung-Larsen. 1985. Chemosensory responses in *Tetrahymena:* the involvement of peptides and other signal substances. *J. Protozool.* **32(3):** 550–553.

Leick, V., K. Frederiksen, I. Lyhne, and P. Hellung-Larsen. 1990. A paper membrane filter assay for ciliate chemoattraction. *Anal. Biochem.* **184:** 63–66.

Levandowsky, M., T. Cheng, A. Kehr, J. Kim, L. Gardner, L. Silvern, L. Tsang, G. Lai, C. Chung, and E. Prakash. 1984. Chemosensory responses to amino acids and certain amines by the ciliate *Tetrahymena:* a flat capillary assay. *Biol. Bull.* **167:** 322–330.

O'Neill, J. B., C. B. Pert, C. C. Smith, W. J. Higgins, and B. Zipser. 1988. Identification and characterization of the opiate receptor in the ciliated protozoan, *Tetrahymena. Brain Research* **450:** 303–315.

Pauli, W., and S. Berger. 1992. Chemosensory and electrophysiological responses in toxicity assessment. Investigations with a ciliated protozoan. *Bull. Environ. Contam. Toxicol.* **49** (6): 892–899.

Rasmussen, L., and L. Modeweg-Hansen. 1973. Cell multiplication in *Tetrahymena* cultures after addition of particulate matter. *J. Cell Sci.* **12(1):** 275–286.

Tsang, L., and M. Levandowsky. 1983. Cholinergic chemosensory response of *Tetrahymena. J. Protozool.* **30,** 13 A (Abstract).

Reference: *Biol. Bull.* **187:** 16–22. (August, 1994)

Muscle and Nerve Terminal Fine Structure of a Primitive Crustacean, the Cephalocarid *Hutchinsoniella macracantha*

A. T. READ[1], R. R. HESSLER[2], AND C. K. GOVIND[1,*]

[1]*Life Sciences Division, Scarborough College, University of Toronto, 1265 Military Trail, Scarborough, Ontario, Canada M1C-1A4, and* [2]*Scripps Institution of Oceanography, University of California, La Jolla, California 92093-0202*

Abstract. Abdominal muscles of the cephalocarid *Hutchinsoniella macracantha* resemble the striated muscle fibers of other crustaceans, having regularly aligned sarcomeres that average 5 μm in length; thick, wavy Z-lines; and orbits of eight thin filaments surrounding a thick filament. However, unlike most crustacean muscle fibers, the cephalocarid muscle fibers are not subdivided into myofibrils by elaboration of the longitudinally oriented sarcoplasmic reticulum. Consequently, elements of the transverse tubule and sarcoplasmic reticulum in the form of triads occur scattered over the entire fiber. Motor innervation is by means of scattered nerve terminals, populated with round synaptic vesicles, indicative of excitatory axons. By lacking myofibrils, the cephalocarid and ostracod muscle represents a much simpler condition than the myofibril-rich muscles of the other crustacean classes and signifies a primitive condition in its resemblance to the onycophoran muscle.

Introduction

Members of the class Cephalocarida are the most primitive living crustaceans, on the basis of comparative studies of the external morphology, skeletomusculature, larval development, and behavior of the best-known species, *Hutchinsoniella macracantha* (Sanders, 1957, 1963; Hessler, 1964, 1992; Hessler and Newman, 1975). Studies of the nervous (Elofsson and Hessler, 1990, 1991, 1992) and digestive (Elofsson *et al.*, 1992) systems reveal fundamental apomorphies that indicate an ancient split from the rest of the Crustacea. Thus although cephalocarids can tell little about the interrelationships within Crustacea, they may tell much about the roots of the crustacean radiation. For this reason, it is important to know as much as we can about the anatomy of this small taxon.

The gross anatomy of the musculature of *H. macracantha* has been analyzed in detail (Hessler, 1964), but its fine structure has never been described. This is the subject of the present study. We focus on the abdominal musculature because of its simplicity.

The cephalocarid body is composed of cephalon, thorax, and abdomen. The cephalon and thorax are dorsoventrally compressed and bear appendages. As a result, the musculature of these tagmata is complicated. The abdomen is virtually a limbless, articulated cylinder capable of strong flexion in all directions; only the telson bears a terminal caudal furca. Hence the organization of the muscles in the abdomen is much simpler than that of the thorax, consisting of paired sheaths of dorsal and ventral longitudinal muscles that line the exoskeleton and insert upon it at the anterior end of each segment (Hessler, 1964).

Materials and Methods

Adults of *Hutchinsoniella macracantha* were collected from the silt-clay bottom of Buzzards Bay near Woods Hole, Massachusetts, and prepared for electron microscopy. The tiny elongate animals (about 3 mm) were cut transversely into two or three pieces and fixed for 1–2 h in 3% glutaraldehyde and 0.7 *M* NaCl in 0.1 *M* sodium cacodylate buffer (pH 7.4). After a brief rinse

---

Received 9 November 1993; accepted 19 May 1994.

* Author to whom correspondence should be addressed.

in buffer, the tissue was postfixed in 2% osmium tetroxide for 1 h, washed in buffer, dehydrated in ethanol, cleared in propylene oxide, and embedded in plastic. Thin (80–100 nm) sections were obtained with a diamond knife, mounted on formvar-coated single-slot grids, and stained with uranyl acetate and lead citrate. The tissue was examined with a Siemens 102 or Zeiss 9A electron microscope. The abdominal musculature from five animals was examined.

Results

Muscle

The muscle bundle in each segment is made up of a single layer of roughly elliptical fibers (Fig. 1A). Each fiber is defined by a distinct sarcolemma and is tightly packed with myofilaments. Mitochondria are found along the periphery of the fiber and are not seen within the body of the fiber amongst the myofilaments. Also along the periphery of the muscle sheath are muscle nuclei and motor nerve terminals. Individual fibers have numerous folds and invaginations of the sarolemmal membrane along their length, and this gives them a complex outline typical of crustacean muscle (Atwood, 1973).

The myofilaments are arranged into distinct sarcomeres defined by adjacent Z-lines that enclose I-bands on either side of a central A-band (Fig. 1C). The Z-lines are thick and wavy and somewhat regularly aligned, as are the sarcomeres. Measurements of individual sarcomeres from three animals revealed a range of 3.6 to 7.9 μm and a mean (SD) value of 5.1 μm (± 0.95, $n = 45$). To ensure that these differences are not due to differences in overlap of thick and thin filaments, individual A-bands were measured because these are less subject to change. The A-bands showed a trend similar to that of the sarcomeres, with a range of 3.2 to 4.8 μm and a mean (SD) value of 3.7 μm (± 0.38, $n = 45$). In cross-sectional view (Fig. 1B), the thick filament has an orbit of 6–10 thin filaments, for a mean (SD) of 8.3 (± 1.1, $n = 87$).

The tubule system in these cephalocarid muscles consists of the transverse tubules (t-tubules), which invaginate from the sarcolemma at the level of the I-band and Z-line, with branches in the A-band region forming part of a triad (Fig. 2A). The other system of tubules, *viz.*, the sarcoplasmic reticulum, is relatively simple, consisting of one or two longitudinally running tubules (Fig. 1C). Where these are juxtaposed on either side of the longitudinal elements of the t-tubule, a triad arrangement of tubules is seen in cross-section (Fig. 1B). Triads are restricted to the A-band region, where they occur scattered over the entire fiber (Fig. 3). The sarcoplasmic reticulum therefore does not form an elaborate network of tubules that subdivides the muscle fiber into myofibrils. Indeed, the absence of myofibrils is the most striking feature of the cephalocarid muscle fiber (Figs. 3, 4A).

Neuromuscular terminals

Motor innervation to the muscle group usually consists of a cluster of nerve terminals along the periphery of the muscle (Fig. 1A). These nerve terminals are located adjacent to the myofilaments on small islands of the muscle granular sarcoplasm that have relatively few tubules (Fig. 2B). The motor nerve terminals are characteristically populated with clear synaptic vesicles and make synaptic contact with the muscle granular sarcoplasm. At these synaptic contacts the membranes are densely stained and a dense body is found on the presynaptic membrane, denoting an active site for transmitter release. Mitochondria are seen in these terminals, but dense-core vesicles are not. The clear synaptic vesicles surveyed in more than 50 nerve terminals in five separate animals are spherical, suggesting that these are excitatory terminals because with aldehyde fixation the synaptic vesicles assume a characteristic shape—spherical for excitatory and elliptical for inhibitory axons (Tisdale and Nakajima, 1976).

Discussion

Muscle

The fine structure of the abdominal muscles of the cephalocarid *H. macracantha* is typical of crustacean striated muscle in that the myofilaments are highly organized in the transverse plane into sarcomeres (Atwood, 1973; Govind and Atwood, 1982). Also typical of the abdominal muscle in tailed decapods such as crayfish and lobsters is the differentiation into fast and slow fibers based on sarcomere length; short (2–4 μm) sarcomeres denoting fast fibers and long (>4 μm) sarcomeres denoting slow fibers. Fast and slow fibers occur in separate muscles in the abdomen of crayfish and lobsters and are used respectively for fast (escape) and slow (postural) movements. The cephalocarid abdominal muscle has sarcomeres of 5 μm, suggesting a slow fiber type; this is in keeping with the relatively slow movements of the abdomen. However, in this initial study of cephalocarid muscles, we cannot rule out the existence of fast type fibers with short sarcomeres in the abdomen.

Cephalocarid muscle deviates significantly from the general crustacean type in its lack of myofibrils. In the cephalocarids the muscle fiber remains as a single unit (which is punctuated with triads) (Fig. 4A), whereas in

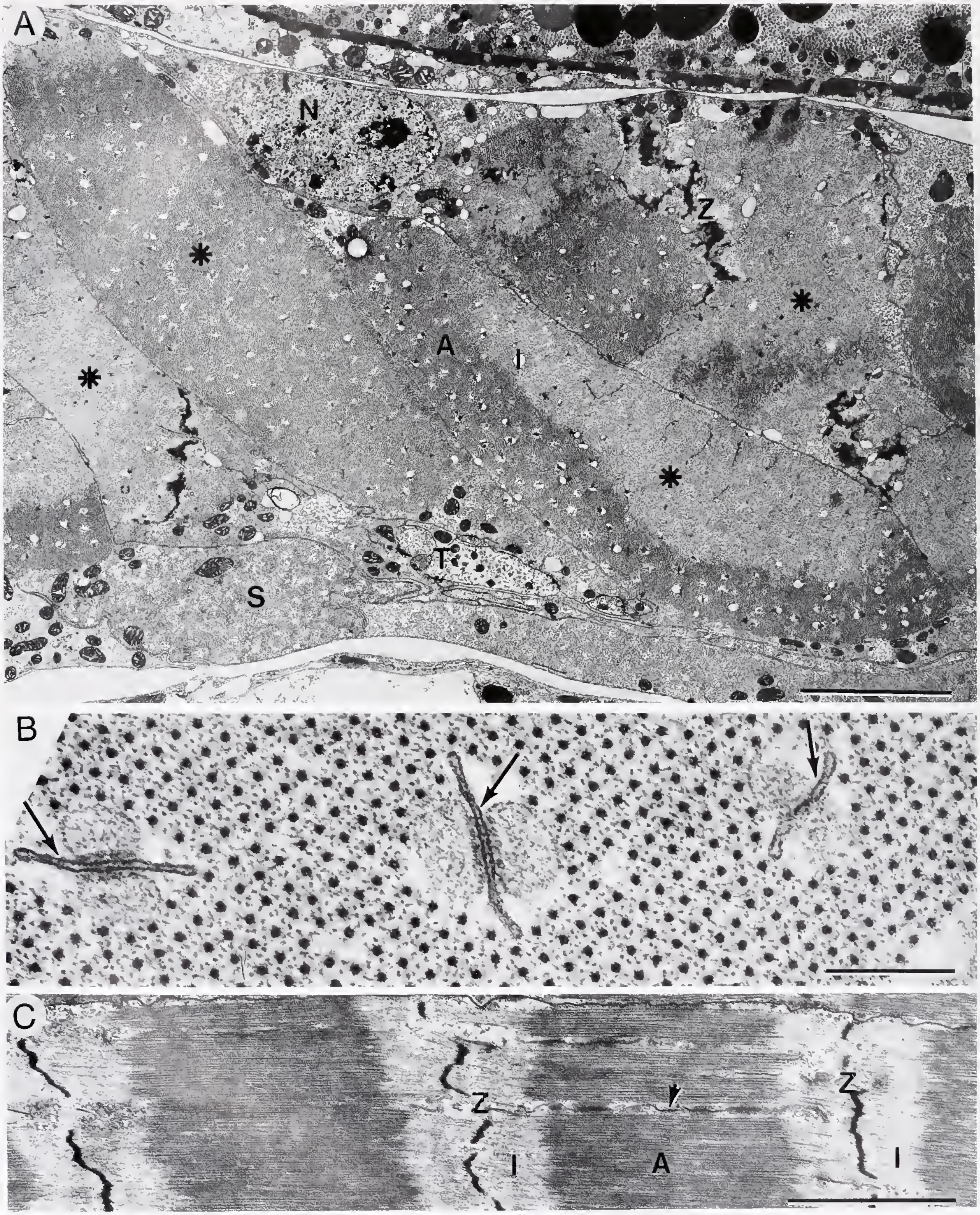
A
N
Z
*
*
A
I
*
*
T
S
B
C
Z
Z
I
A
I

most other crustaceans it is subdivided into numerous myofibrils (Fig. 4B, C) by elaboration of the sarcoplasmic reticulum, which forms an enveloping collar around each myofibril. In essence, these myofibrils functionally subdivide a single muscle fiber and permit a much finer control of its contraction. In the absence of myofibrils, such fine control may not accrue to the cephalocarid muscle, although the widespread distribution and high density of triads in the cephalocarid muscle fiber would ensure that no area of the fiber is far from these elements that couple excitation to contraction.

The only other known crustacean species in which the muscle fibers are also not subdivided into myofibrils by the sarcoplasmic reticulum is the ostracod *Cypridopsis vidua* (Fahrenbach, 1964) (Fig. 4A). Muscles of the appendages consist of single fibers that are the equivalent of single fibrils. Triads consisting of two elements of the sarcoplasmic reticulum and one of the t-tubule are usually scattered throughout these single fibers, although more complex associations, with three to nine elements of the sarcoplasmic reticulum, are also found. The latter associations denote a more elaborate development of the sarcoplasmic reticulum in the form of several layers of tubules. In comparison, the cephalocarid muscle with its triad denoting two tubules of the sarcoplasmic reticulum represents a less elaborate and much simpler system.

Muscle fibers in other known crustacean species are subdivided into myofibrils by a fenestrated collar of sarcoplasmic reticulum (Fig. 4C). At discrete locations around this collar are elements of the t-tubule giving rise to diads or triads. This type of organization is seen amongst all species examined in the class Malacostraca and these encompass stomatopods (*Hemisquilla:* McNeill *et al.,* 1972), amphipods (*Gammarus:* pers. obs.), and decapods (crabs, crayfish, and lobster: reviewed by Atwood, 1973). Amongst the other classes of crustacea, namely, Branchiopoda, Cephalocarida, Maxillopoda, Ostracoda, and Remipedia, only the last named has not been examined for its muscle fine structure. In Maxillopoda, myofibrils are seen in the barnacle *Balanus nubilus* (subclass Cirripedia) (Hoyle *et al.,* 1973) and in the copepod *Macrocyclops albidus* (subclass Copepoda) (Fahrenbach, 1963). In the latter case, diads and triads are found not only around the periphery of the myofibril (perifibrillar location) but also within the myofibril itself (intrafibrillar location) (Fig. 4B). In the class Branchiopoda, myofibrils—although poorly defined—are seen in *Daphnia,* with diads and triads restricted to the periphery of the myofibrils (pers. obs.). As mentioned above, only the ostracods and cephalocarids have muscles that lack myofibrils.

This brief comparative survey demonstrates a range of conditions from a relatively simple system of tubules of sarcoplasmic reticulum to a complex system that subdivides a muscle fiber into myofibrils. Triads found scattered over the entire muscle fiber in the case of the simple condition are restricted to the periphery of the myofibril in the more complex condition. Accordingly, ostracod and cephalocarid muscles with scattered triads (Fig. 4A) represent an early stage; copepod muscle represents an intermediate stage, with triads located both within the myofibril and along its periphery (Fig. 4B); and cirripeds, branchiopods, and malacostracans represent a more advanced stage, with the triads restricted to the periphery of the myofibrils (Fig. 4C).

While the lack of myofibrils represents a simple condition in the striated muscle organization of cephalocarids, does it also signify a primitive condition? Comparison with an outgroup such as the Onychophora throws light on this question. Muscle fibers in the onycophoran *Peripatus dominicae* are not subdivided into myofibrils, although the fiber is populated with many tubule systems, including sarcoplasmic reticulum and t-tubules (Hoyle and Williams, 1980). As a result, diads and triads occur scattered over the muscle fiber as in the cephalocarid muscle. Based on the view that the onychophorans predate the crustaceans, the lack of myofibrils may be construed as a primitive feature.

Neuromuscular terminals

The fine structure of motor nerve terminals in the abdominal muscles of the cephalocarid is similar to that seen in the decapods (Govind and Atwood, 1982). However, although both excitatory and inhibitory motor nerve terminals are readily seen in the abdominal muscles of

---

Figure 1. A. Cross-section of the cephalocarid ventral abdominal longitudinal muscle showing a single layer of fibers (asterisks) cut at various planes, such as through the A-band (A), I-band (I), and Z-line (Z). Muscle nuclei (N) and mitochondria are restricted to the edge of the band, and the muscle fibers lack myofibrils. Nerve terminals (T) are located amongst muscle granular sarcoplasm (S). B. Cross-section showing thick and thin filaments and triads (arrows) composed of a long, narrow t-tubule element flanked on either side by cisternae of the sarcoplasmic reticulum. C. Longitudinal section showing well-defined sarcomeres between adjacent Z-lines (Z), on either side of which are I-bands (I) enclosing a central A-band (A). Elements of sarcoplasmic reticulum are seen as longitudinal tubules (arrowhead). Magnifications: ×5400 (A), ×96,000 (B), ×10,300 (C). Scale bars: 5 μm (A), 0.25 μm (B), 3 μm (C).

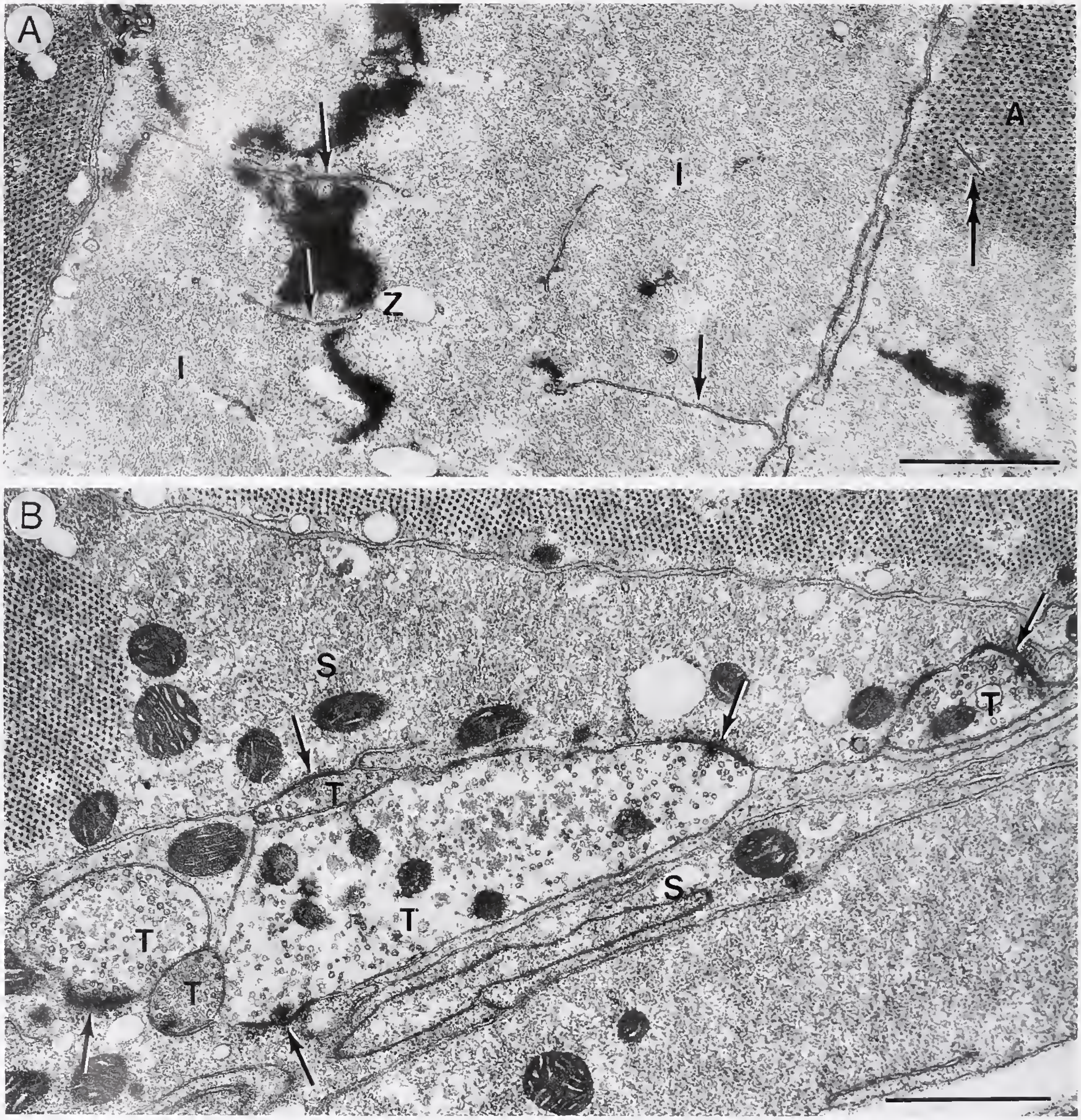

Figure 2. A. Cross-section of a ventral abdominal muscle through the A-band, I-band (I), and Z-line (Z) showing t-tubules through the I-band, Z-line (arrows), and the A-band (double arrow) where it forms part of a triad. B. Cross-section showing five variously sized profiles of nerve terminals (T) embedded in muscle granular sarcoplasm (S). Terminals are recognized by aggregations of clear synaptic vesicles that are spherical in shape. Synaptic contacts (arrows) are recognized by dense staining of regularly aligned presynaptic and postsynaptic membranes. At some of these contacts the presynaptic side has a dense body representing an active zone. Magnification: ×27,000. Scale bars: 1 μm.

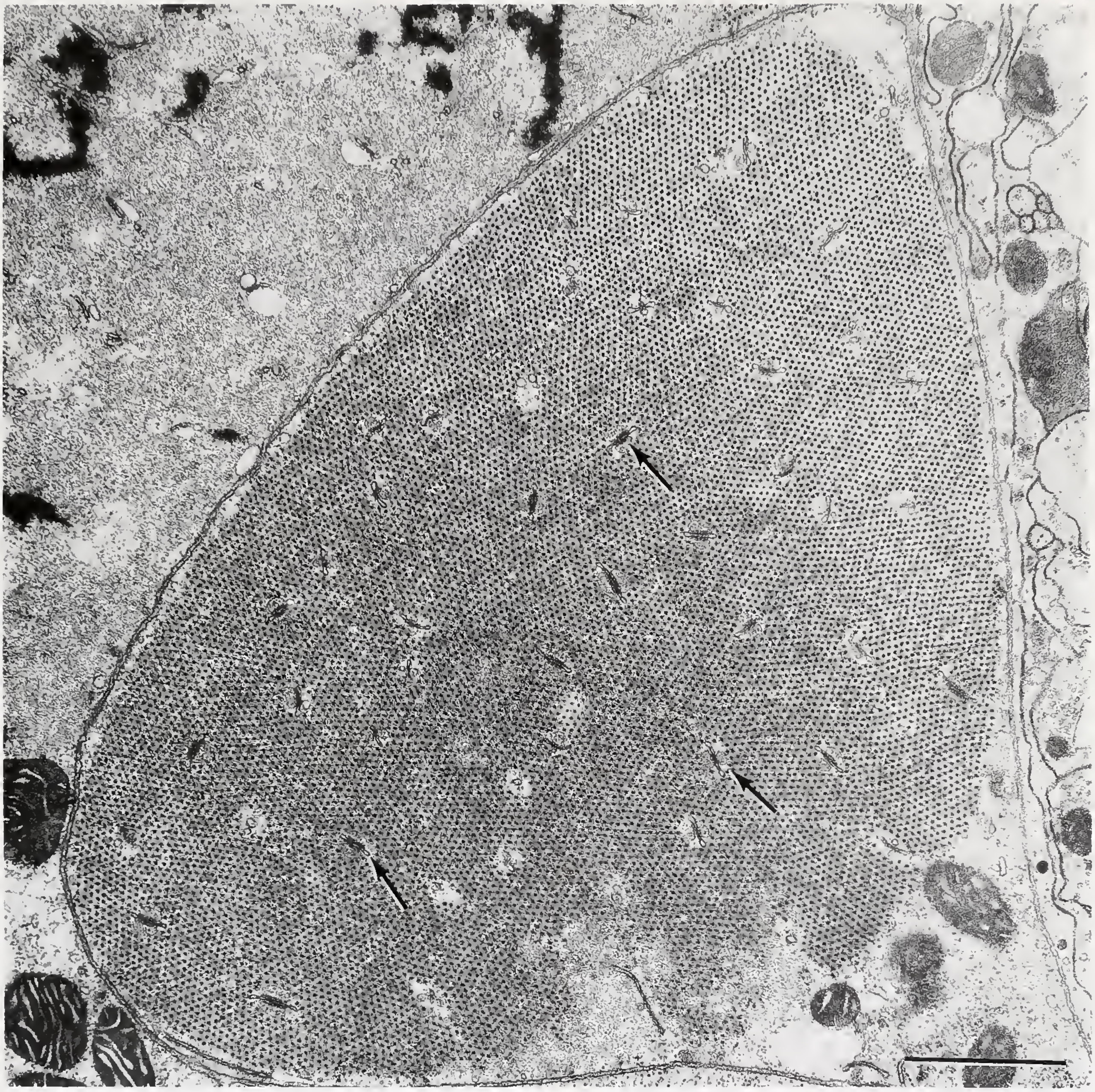

Figure 3. Cross-section of a single ventral abdominal muscle fiber through the A-band region packed with myofilaments and numerous scattered triads (arrows), but not subdivided into myofibrils. Note peripherally located mitochondria. Magnification: ×27,000. Scale bar: 1 μm.

tailed decapods such as crayfish and lobsters, the cephalocarid abdominal muscles displayed terminals with round synaptic vesicles, suggesting only excitatory motor innervation. Such a conclusion, although tentative, is in keeping with the relatively simple organization of the abdominal muscles that generate largely flexion-type movements and occur as a sheath lining the abdominal cylinder.

Simplicity in the neuromuscular terminals of the cephalocarid abdomen is also seen in the minimal elaboration of the surrounding muscle granular sarcoplasm. Thus synaptic contacts with the muscle membrane are made very close to the myofilaments, with little intervening sarcoplasm. In contrast, neuromuscular synaptic contacts occur on a highly elaborated sarcoplasmic reticulum amongst the decapods (Atwood, 1976; Govind and Atwood, 1982), reflecting a more extensive repertoire of movements than that of the cephalocarids.

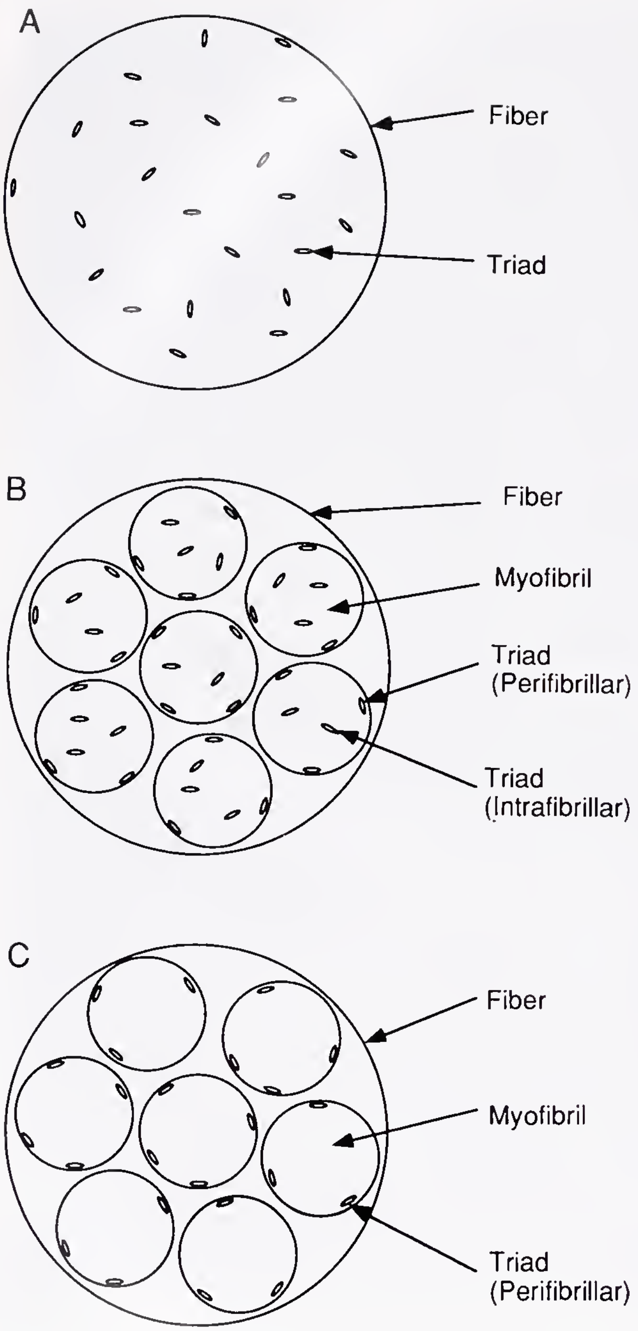

Figure 4. Stylized cross-sectional views of single muscle fibers amongst crustaceans, showing distribution of triads and subdivision into myofibrils. A. Single fiber not subdivided into myofibrils and with scattered triads as in the ostracod *Cypridopsis vidua* (Fahrenbach, 1964) and the cephalocarid *Hutchinsoniella macracantha* (present report). B. Single fiber subdivided into myofibrils by longitudinally running sarcoplasmic reticulum and with triads located along the periphery of the myofibril (perifibrillar location) as well as within the myofibril (intrafibrillar location), as in the copepod *Macrocyclops albidus* (Fahrenbach, 1963). C. Single fiber subdivided into myofibrils by sarcoplasmic reticulum and with triads located along the periphery of the myofibril (perifibrillar location), as in the majority of crustaceans, including stomatopods, amphipods, and decapods.

Acknowledgments

We are indebted to Arthur Humes for facilitating this study and to Joanne Pearce and two anonymous reviewers for a critical reading of the manuscript. Financial support was provided by the Natural Sciences and Engineering Research Council of Canada to C.K.G. and by the U.M. EgenFicka Fund to R.R.H.

Literature Cited

Atwood, H. L. 1973. An attempt to account for the diversity of crustacean muscle. *Am. Zool.* **13:** 357–378.

Atwood, H. L. 1976. Organization and synaptic physiology of crustacean neuromuscular systems. *Prog. Neurobiol.* **7:** 291–391.

Elofsson, R., and R. R. Hessler. 1990. Central nervous system of *Hutchinsoniella macracantha* (Cephalocarida). *J. Crust. Biol.* **10:** 423–439.

Elofsson, R., and R. R. Hessler. 1991. Sensory morphology in the antennae of the cephalocarid *Hutchinsoniella macracantha. J. Crust. Biol.* **11:** 345–355.

Elofsson, R., and R. R. Hessler. 1992. Monoaminergic and peptidergic neurons in the nervous system of *Hutchinsoniella macracantha* (Cephalocarida). *J. Crust. Biol.* **12:** 531–536.

Elofsson, R., R. R. Hessler, and A. Y. Hessler. 1992. Digestive system of the cephalocarid *Hutchinsoniella macracantha. J. Crust. Biol.* **12:** 571–591.

Fahrenbach, W. H. 1963. The sarcoplasmic reticulum of striated muscle of a cyclopoid copepod. *J. Cell. Biol.* **17:** 629–640.

Fahrenbach, W. H. 1964. A new configuration of the sarcoplasmic reticulum. *J. Cell. Biol.* **22:** 477–481.

Govind, C. K., and H. L. Atwood. 1982. Organization of neuromuscular systems. Pp. 63–103 in *The Biology of Crustacea, Vol. 3, Neurobiology: Structure and Function.* H. L. Atwood and D. C. Sandeman, eds. Academic Press, New York.

Hessler, R. R. 1964. The Cephalocarida: comparative skeletomusculature. *Mem. Conn. Acad. Arts Sci.* **16:** 1–97.

Hessler, R. R. 1992. Reflections on the phylogenetic position of the Cephalocarida. *Acta Zool.* **73:** 315–316.

Hessler, R. R., and W. A. Newman. 1975. A trilobitomorph origin for the Crustacea. *Fossils Strata* **4:** 437–459.

Hoyle, G., and M. Williams. 1980. The musculature of *Peripatus* and its innervation. *Phil. Trans. Roy. Soc. Lond. B* **288:** 481–510.

Hoyle, G., P. A. McNeill, and A. J. Selverston. 1973. Ultrastructure of barnacle giant muscle fibers. *J. Cell. Biol.* **56:** 74–91.

McNeill, P., M. Burrows, and G. Hoyle. 1972. Fine structure of muscles controlling the strike of the mantis shrimp, *Hemisquilla. J. Exp. Zool.* **179:** 395–416.

Sanders, H. L. 1957. The Cephalocarida and crustacean phylogeny. *Syst. Zool.* **16:** 112–129.

Sanders, H. L. 1963. The Cephalocarida: functional morphology, larval development and comparative external anatomy. *Mem. Conn. Acad. Arts Sci.* **15:** 1–80.

Tisdale, A. D., and Y. Nakajima. 1976. Fine structure of synaptic vesicles in two types of nerve terminals in crayfish stretch receptor organ: influence of fixation methods. *J. Comp. Neurol.* **165:** 369–386.

Reference: *Biol. Bull.* **187**: 23–34. (August, 1994)

Fertilization Between Closely Related Sea Urchins Is Blocked by Incompatibilities During Sperm-Egg Attachment and Early Stages of Fusion

EDWARD C. METZ[1], ROBERT E. KANE[2], HIROKO YANAGIMACHI[3], AND
STEPHEN R. PALUMBI[1]

University of Hawaii, [1]Department of Zoology and [3]Department of Anatomy, Honolulu, Hawaii 96822, and [2]Pacific Biomedical Research Center, Honolulu, Hawaii 96813

Abstract. Closely related sea urchin species in the genus *Echinometra* from Hawaii and Guam have strong species-specificity of fertilization. Crosses between the two species found in Hawaii, *E. mathaei* and *E. oblonga*, were compared in order to determine which steps of gamete interaction are responsible for fertilization barriers. The acrosome reaction, attachment of sperm to eggs, and fusion of sperm and egg membranes were measured in crosses between species and compared to within-species controls. In all crosses, eggs induced the acrosome reaction in 50–100% of sperm within 20 s. However, eggs bound about 3–5 times fewer heterospecific than conspecific sperm. In addition, electrical continuity between heterospecific gametes was achieved rarely under conditions that allowed conspecific gametes to achieve it readily. Only two sperm-egg fusion events were recorded in more than 80 min of heterospecific sperm interaction on 22 eggs. Accordingly, species-specific fertilization in these urchins results firstly from reduced attachment of the heterospecific sperm acrosomal process to the egg vitelline layer, and secondly from inability of attached heterospecific sperm to develop continuity with the egg plasma membrane. At both of these steps, incompatibilities are reciprocal. Thus a barrier to gene flow is mediated by molecular interactions during a specific part of the fertilization process, as the sperm acrosomal surface and the egg vitelline layer contact each other. Recognition molecules mediating these steps of fertilization may be capable of relatively rapid change, leading to species-specificity of fertilization.

Introduction

The relationship between the evolution of reproductive isolation and species formation is complex and differs among taxonomic groups (Mayr, 1963; Donoghue, 1985; Carson, 1987; Kaneshiro and Boake, 1987; Templeton, 1989). Species are genetically distinct, yet they may sometimes be reproductively compatible. Although reproductive barriers do not always define species boundaries, populations of organisms that do become intrinsically reproductively isolated will usually evolve independently. Thus knowledge of the evolution of species-specificity at genetic loci involved directly in mate recognition could contribute to an understanding of biological diversification. Many studies have focused on aspects of species-specific premating recognition that partition gene pools. In most cases, recognition involves complex neurophysiological processes (see review by Boake, 1991), and the genetic basis of these processes remains obscure. In a few cases, recent work directly implicates specific genes involved in mate recognition behavior in maintaining reproductive isolation between species (*e.g.*, Wheeler *et al.*, 1991, reviewed by Coyne, 1992).

Species-specific fertilization is a type of mate recognition that is amenable to study because it involves direct interaction of recognition molecules on the surfaces of just two cell types, the sperm and the egg. Species-specific fertilization is particularly important in many different types of free-spawning organisms like sea urchins, which have relatively simple premating behavior prior to the

Received 1 March 1994; accepted 1 June 1994.

interaction of gametes. Incompatibilities between gametes from different species cause premating reproductive isolation and create barriers to gene flow (O'Rand, 1988; Minor *et al.*, 1989; Lessios and Cunningham, 1990; Vacquier *et al.*, 1990; Palumbi and Metz, 1991; Metz *et al.*, 1991). Although broad-scale allopatric models of speciation have been applied to marine organisms including sea urchins (Mayr, 1954), many examples are coming to light of closely related and cryptic marine species that have differentiated without obvious geographical barriers (reviewed by Knowlton, 1993). Rapidly evolving specificity in mate recognition processes, including gamete interaction, may be important in generating intrinsic reproductive isolation between populations and facilitating diversification of marine organisms (reviewed by Palumbi, 1992). An understanding of how species-specificity can arise in the fertilization process may contribute to an understanding of speciation.

We have focused a study of fertilization on closely related urchin species in the genus *Echinometra* that have developed strong reciprocal gamete incompatibilities. In these urchins, the specificity of fertilization contributes substantially to maintenance of reproductive isolation between species. Indo-Pacific species in the genus *Echinometra* are among the most closely related sea urchins known. These urchins are abundant in mixed populations, and they contain gonads with mature gametes over broadly overlapping seasons (Kelso, 1970; Uehara and Shingaki, 1985; S.R.P., unpublished data). They show only slight ecological or morphological differentiation (Kelso, 1970; Uehara and Shingaki, 1985) and are similar enough to have been previously classified as different morphs of a single species (Mortensen, 1943). Measurements of genetic relationships indicate that the species are distinct from one another and probably differentiated from a common ancestor during the Pleistocene (Palumbi and Metz, 1991). Within that time, species-specificity of fertilization has arisen, making many of the possible crosses between these urchins incompatible (Kelso, 1970; Branham, 1972; Uehara *et al.*, 1990; Palumbi and Metz, 1991). In previous studies of gamete compatibility between Hawaiian *Echinometra* species, we found that only a small percentage of the eggs in reciprocal test crosses between these species typically become fertilized (Palumbi and Metz, 1991). Here we have extended cross-fertilization measurements to include a third species, referred to as 'type A' (Uehara and Shingaki, 1985), from Guam. Like the two species found in Hawaii (*E. mathaei* and *E. oblonga*), the two species found in Guam (*E. mathaei* and *Echinometra* type 'A') have strong reciprocal barriers to fertilization.

Fertilization depends on successful completion of a series of steps involving interactions between gametes; incompatibilities at these steps could prevent fertilization and provide the basis of species-specific fertilization (Lillie, 1919). These steps involve recognition and binding of surface molecules on sperm and eggs (for review see Metz and Monroy, 1985; Schatten and Schatten, 1989; Foltz and Lennarz, 1993). After conspecific sperm approach the sea urchin egg, four major steps of gamete interaction occur: (1) components of the egg jelly induce the sperm acrosome reaction (Trimmer and Vacquier, 1986); (2) sperm and egg attach as a result of interaction of the sperm protein bindin and its egg surface receptor (Minor *et al.*, 1989; Foltz and Lennarz, 1993); (3) molecular interactions of the attached acrosomal and vitelline surfaces bring gamete plasma membranes together; and (4) the membranes fuse, creating continuity between the gametes (Whitaker *et al.*, 1989; Chambers, 1989; Foltz and Lennarz, 1993).

Specificity of fertilization in crosses between several genera of urchins has been shown to result mainly from "primary gamete binding," the attachment of the sperm acrosomal process to the egg vitelline layer, visualized by electron microscopy (Summers and Hylander, 1975). We used electron microscopy to quantify the acrosome reaction and sperm-egg attachment in crosses of Hawaiian *Echinometra* species. In addition, we examined the species-specificity of events that occur after sperm-egg attachment and lead to gamete fusion. Fusion of the sea urchin sperm and egg plasma membranes results in a rapid depolarization of the egg membrane (reviewed in Jaffe, 1986). When eggs are held at their resting transmembrane potential to prevent normal depolarization, temporary continuity between the sperm and egg creates transient currents across the egg membrane (Chambers, 1989; Whitaker *et al.*, 1989; Chambers and McCulloh, 1990). To assess the capability of sperm and egg plasma membranes to fuse, we measured the incidence of transmembrane currents in voltage-clamped eggs.

The step-by-step examination of gamete interactions between Hawaiian *E. mathaei* and *E. oblonga* shows that reciprocal incompatibilities occur at the attachment step and in the interactions of attached gametes leading to membrane fusion. Comparison of these results with those reported from other crosses both within and between urchin genera suggests that when gamete incompatibility arises between species, these steps of fertilization are most likely to be involved.

Materials and Methods

Urchins and gametes

Echinometra mathaei and *E. oblonga* (*sensu* Edmondson, 1946), were collected from mixed populations at Kapapa Island in Kaneohe Bay, Oahu, Hawaii, and maintained in seawater tables at the Kewalo Marine Laboratory. Urchins of *Echinometra* species type 'A' (*sensu* Uehara and Shingaki, 1985) were shipped by air from Guam. Shedding of gametes was induced by injection of 0.5 *M* KCl into the coelomic cavity. Eggs were collected by inverting female urchins in dishes of seawater. Undiluted sperm was collected at the gonopores. Filtered (0.45 μm) seawater was used for washing and diluting gametes.

Measurement of cross-fertilization

Gametes were obtained from two males and two females of each of three species of *Echinometra* (*E. mathaei*, *E. oblonga*, and *Echinometra* type 'A'). The 36 possible crosses between these individuals were made as follows. Sperm concentrations were normalized by dilution with seawater to give an optical density reading of 0.5 in a spectrophotometer set at 340 nm. Eggs were washed twice by gentle centrifugation through seawater. A 20-μl volume of settled eggs was mixed with 200 μl of sperm suspension in a 1.5-ml microcentrifuge tube. Counts showed that these gamete mixtures contained about 300 sperm per egg (sperm were counted with the aid of a hemacytometer). Two replicate tubes were prepared for each cross. All crosses were performed with highly motile sperm within 2 h of induced spawning. After 10 min of gamete interaction, 50 μl of 5% glutaraldehyde in seawater was added to fix gametes in one tube; the other tube was fixed after 3 h of gamete interaction. Presence or absence of the fertilization envelope in the 10-min samples and presence or absence of cell division in the 3-h samples was recorded for all eggs in a haphazard succession of fields of view at 100× magnification under a light microscope, until at least 200 eggs had been examined for each sample.

Test crosses between *Echinometra* type 'A' and *E. mathaei* were also performed on sympatric urchins in Guam. In these crosses, percent fertilization was measured under conditions similar to those described above, for four to five different pairs of urchins in each direction.

Electron microscopy of Hawaiian Echinometra *Crosses*

For electron microscopy, each gamete mixture used for the crosses was composed of an approximately equal mixture of gametes from four individual urchins. Accordingly, in each cross the gamete interaction levels of 16 individual crosses were measured. This method will sample the cumulative results of all crosses between pooled individuals. Thus, if certain individual urchin pairs have high cross-fertilizability, estimates of the amounts of acrosome reaction and gamete attachment might be elevated compared to those from the average cross between one male and one female. Accordingly, our measurements can be considered to overestimate rather than underestimate the successful completion of each step of fertilization. This approach will be less likely to underestimate the potential for gene flow between species at the population level.

Eggs were washed twice by gentle centrifugation through seawater, and 200-μl aliquots of the egg pellet from four females were mixed to make a pooled sample of eggs for each species. Likewise, a pooled sperm sample was made for each species by mixing 10 μl of undiluted sperm from each of four individuals with 10 ml of seawater. Sperm concentrations were normalized by adding seawater to give an optical density reading of 1.0 at 340 nm. Each of the four possible crosses between the two pooled sperm samples and the two pooled egg samples was made as follows. A 3-ml volume of sperm suspension was added to 0.25 ml of packed eggs and inverted repeatedly to mix. Counts showed that these gamete mixtures contained about 1000 sperm per egg (sperm were counted with the aid of a hemacytometer). Sperm appeared highly motile when all crosses were made. The two interspecific crosses were made before the two intraspecific crosses. After 20 s of gamete interaction, the sample was fixed for 1 h at room temperature by mixing thoroughly with an equal volume of freshly prepared 5% glutaraldehyde in seawater. Glutaraldehyde fixes the jelly coat surrounding the egg and the sperm embedded in it, as well as the sperm bound to the egg surface. Unused pooled eggs were fixed in 1% glutaraldehyde in seawater as negative controls. No fertilization envelopes were seen in these control samples. The samples were postfixed with 1% OsO_4, block-stained with uranyl acetate, and processed for transmission electron microscopy.

Thin sections of gametes from the crosses were examined by electron microscopy at 10,000× magnification. Each sample was searched for sperm in which the tip appeared in longitudinal section near the egg surface. For convenience, a sperm was considered to be near the egg surface if the tip was within 5 μm of the egg surface. Sperm that have approached the egg surface this closely have presumably had an opportunity to interact with the egg jelly and undergo the acrosome reaction. Any sperm within 5 μm of the egg surface was counted if it had either a clearly visible acrosomal vesicle or an acrosomal process. Any sperm connected at the acrosomal process to the egg surface by densely staining material was considered to be attached. Each sperm tip found was scored as unreacted, acrosome reacted but unattached, or attached. For each sample cross, at least 35 sperm tips were scored.

This experiment was repeated as described above, using different individual urchins as the source of gametes. In the second experiment, the electron microscopy samples were fixed after 40 s of gamete interaction instead of 20 s. Because the experiment was repeated, a total of 32 urchin pairs were surveyed for each of the four possible crosses between the two species.

Although other methods for measurement of gamete interaction have been described (*e.g.*, Vacquier and Payne, 1973), examination of gamete interaction in the electron microscope allows the relative amounts of sperm undergoing different steps of fertilization to be visualized and measured within the same samples. For each egg sample, a *G*-test of independence (Sokal and Rohlf, 1981, pp. 735–738) was used to test the null hypothesis that the number of sperm completing each of the two steps (acrosome reaction and attachment) is independent of whether the sperm are conspecific or heterospecific (Figure 2).

Electrophysiological recordings of Hawaiian Echinometra *crosses*

Electrophysiological measurements were performed as previously described (Kane, 1990), with the following modifications. Microelectrodes filled with 0.5 *M* K_2SO_4, 20 m*M* NaDl, and 0.5 m*M* potassium citrate (Lynn and Chambers, 1984) had resistances of 20–30 mΩ. The bath electrode was Ag-AgCl with a seawater agar bridge. Electrical measurements and voltage clamping utilized an Axoclamp-2A amplifier with membrane potential and current displayed on a digital oscilloscope. The input of the sample-and-hold amplifier (monitor output) was continuously observed on another oscilloscope while the gain and phase of the clamp was adjusted. Eggs were impaled by means of a short (20 ms) oscillation induced by an increase in the negative capacitance. Only impaled eggs requiring less than 0.10 nA of current to maintain a transmembrane potential of −80 mV were used. Single-electrode voltage clamping (Wilson and Goldner, 1975; Finkel and Redman, 1984) was done at a switching frequency of 2 kHz and filtered at 200 Hz.

Undiluted "dry" sperm were stored on ice and diluted in seawater 2–3 min before use. Eggs were dejellied by vortexing them gently in 0.55 *M* NaCl, 0.01 *M* KCl, and 5 m*M* Tris pH 8.3. Dejellied eggs were placed in plastic petri dishes pretreated with 0.001% protamine sulfate to allow adhesion (Steinhardt *et al.*, 1971). As a positive control for fertilization, two to four dejellied eggs from the other *Echinometra* species were added to the dish near the egg to be impaled. The egg was then impaled and voltage clamped near the resting potential at −75 mV.

First, the heterospecific sperm were added to the impaled egg. A 2-μl volume of dry sperm from a heterospecific male was diluted into 40 ml of seawater and vigorously pipetted to mix. In some cases, 1 μl of dry sperm from each of four heterospecific males was diluted into 40 ml of seawater. In separate experiments, sperm concentration was increased fourfold; 8 μl of dry sperm was diluted into 20 ml of seawater. Transmembrane potential and current were recorded while 10-μl aliquots of sperm were added near the impaled egg. The same volume of sperm was added at intervals of about 1 min for 3–5 min. The impaled egg was observed under the microscope to verify that heterospecific sperm had arrived at the egg surface and that heterospecific gamete interaction occurred for several minutes. The time at which the positive control eggs (from the same species as the sperm) had elevated fertilization envelopes was noted. After an additional 1–3 min—to ensure that the impaled egg had been exposed to heterospecific sperm for long enough to undergo an electrical response—conspecific sperm were added to the impaled egg. A 2-μl volume of dry sperm from a conspecific male was diluted into 40 ml of seawater and added to the impaled egg in 10-μl aliquots about every 1–2 min for 2–5 min. The amount of conspecific sperm delivered to the dish never exceeded the amount of heterospecific sperm.

For each of the two *Echinometra* species, electrophysiological data were recorded for 11 eggs (one to three eggs from six to seven female urchins). Some of these eggs were treated with sperm from one heterospecific male at a time; the other eggs were treated with mixtures of sperm from four heterospecific males. Overall, we surveyed heterospecific crosses between 18 pairs of urchins for *E. mathaei* eggs, and 16 pairs for *E. oblonga* eggs.

Results

Cross-fertilizability of three species of Echinometra

Of the six possible crosses between *E. mathaei* and *E. oblonga* from Hawaii and *Echinometra* type 'A' (Uehara and Shingaki, 1985) from Guam, all but one were incompatible (Figure 1). Measurements of percent fertilization envelopes after 10 min were similar to measurements of percent dividing zygotes after 3 h. The mean of the 12 within-species crosses was 98% eggs with fertilization envelopes. Under these conditions, the mean fertilizability between *E. mathaei* and *E. oblonga* was 3% and the mean fertilizability between *E. mathaei* from Hawaii and *Echinometra* type 'A' from Guam was 1%. Low cross-fertilizability was also found in a separate set of crosses between sympatric *Echinometra* type 'A' and *E. mathaei* individuals from Guam. For these experiments, the mean and standard deviation of four to five crosses in both directions was 5 ± 6.5% (range <1%–20%). Accordingly, the sympatric species pairs found on Hawaii and on Guam are both reciprocally reproductively isolated at fertilization.

Substantial fertilization occurred in one of the crosses between allopatric populations of urchins. Sperm of *Echinometra* type 'A' from Guam were capable of fertilizing eggs of *E. oblonga* from Hawaii (Fig. 1). In this direction, fertilizability of eggs from different individual urchins was variable; cross-fertilization was 14–27% of eggs from one of the two *E. oblonga* females we tested and 95–97% in the other. This preliminary evidence of vari-

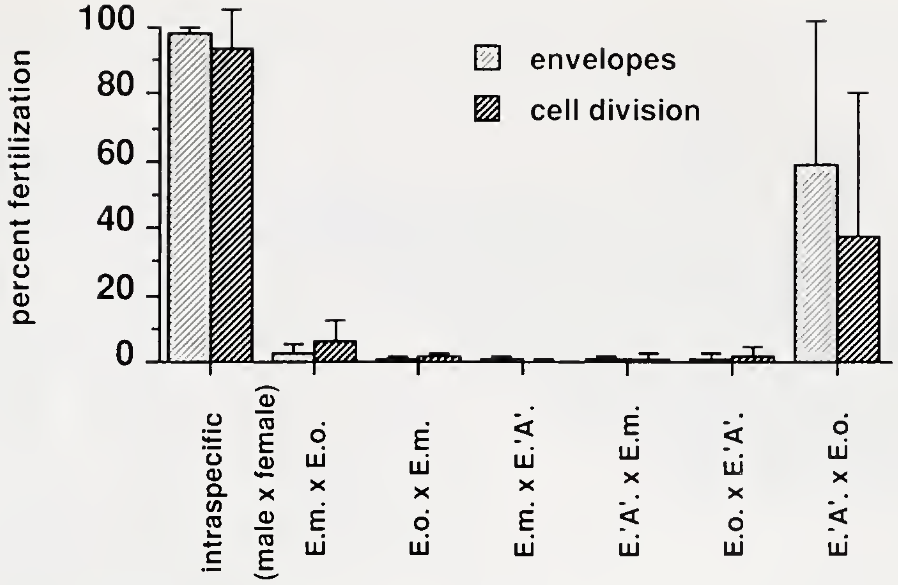

Figure 1. Cross-fertilization between *Echinometra mathaei* and *E. oblonga* from Hawaii and *Echinometra* species 'A' (Uehara and Shingaki, 1985) from Guam. All possible crosses between two males and two females of each species were made in duplicate with standardized gamete concentrations. For each heterospecific cross, the bars indicate the mean and standard error of four different crosses. Results of all 12 of the within-species crosses are shown together by the bars marked intraspecific. For each cross, the male is indicated first. E. m.: *E. mathaei;* E. o.: *E. oblonga;* E. 'A'.:*Echinometra* species 'A'.

ation in cross-fertilizability warrants further investigation. Although cross-fertilization between the two Hawaiian *Echinometra* species typically remains low even at high sperm concentrations (Palumbi and Metz, 1991), cross-fertilization between these allopatric urchins may depend more directly on sperm concentration.

Our results agree with results of a set of crosses made by Uehara *et al.* (1990) between *Echinometra* species in Okinawa. The Okinawan urchin phenotypically similar to Hawaiian *E. oblonga* is referred to as *Echinometra* type 'D'; comparisons of morphology and cross-fertilization are under way for these allopatric urchins (T. Uehara, pers. comm.). *E. oblonga* from Hawaii and *Echinometra* type 'D' from Okinawa showed low cross-fertilization with *E. mathaei* (Fig. 1, Uehara *et al.*, 1990), although more *Echinometra* type 'D' eggs than *E. oblonga* eggs may be fertilized by *E. mathaei* sperm. Substantial percentages of eggs from *E. oblonga* or *Echinometra* type 'D' were fertilized by sperm from *Echinometra* type 'A', whereas in both cases the reciprocal crosses were strongly blocked (Fig. 1, Uehara *et al.*, 1990). Finally, *E. mathaei* and *Echinometra* type 'A' were reciprocally incompatible in Okinawa (Uehara *et al.*, 1990), just as in our results for Guam and between Hawaii and Guam. Thus, in general, the patterns of fertilization between species appear to be similar both from crosses of sympatric urchins from different locations and for crosses between sympatric and allopatric populations of urchins.

Gamete interaction of Hawaiian Echinometra *species*

In all crosses between *Echinometra* species, sperm rapidly became embedded in the egg jelly. Electron microscopy revealed that in both heterospecific and conspecific crosses, sperm had arrived to within 5 μm of the egg vitelline layer within 20 s. Qualitatively, no differences were observed in the abundance of sperm at the egg surface in the different crosses.

More than 95% of sperm were acrosome-reacted within 20 s in three of the four possible crosses between the two Hawaiian *Echinometra* species (Fig. 2). A significantly reduced proportion of *E. mathaei* sperm approaching *E. oblonga* eggs underwent the acrosome reaction ($p < 0.005$, *G*-test of independence), indicating that in one direction there is specificity of the acrosome reaction. In this cross, the number of sperm acrosome-reacted at 40 s (72%) was higher than the number of sperm acrosome-reacted at 20 s (57%), suggesting a relatively slow rate of induction of the acrosome reaction compared to the other crosses.

In agreement with previous electron microscopy studies of sea urchin sperm, the acrosomal process of *Echinometra* sperm appeared to be coated with a densely staining granular substance, presumably including the protein bindin (Moy and Vacquier, 1979, Nishioka *et al.*, 1990). Sperm that had attached to the egg were connected to the vitelline layer by a continuous layer of this densely staining material (Fig. 3). Sperm in the process of fusing with eggs

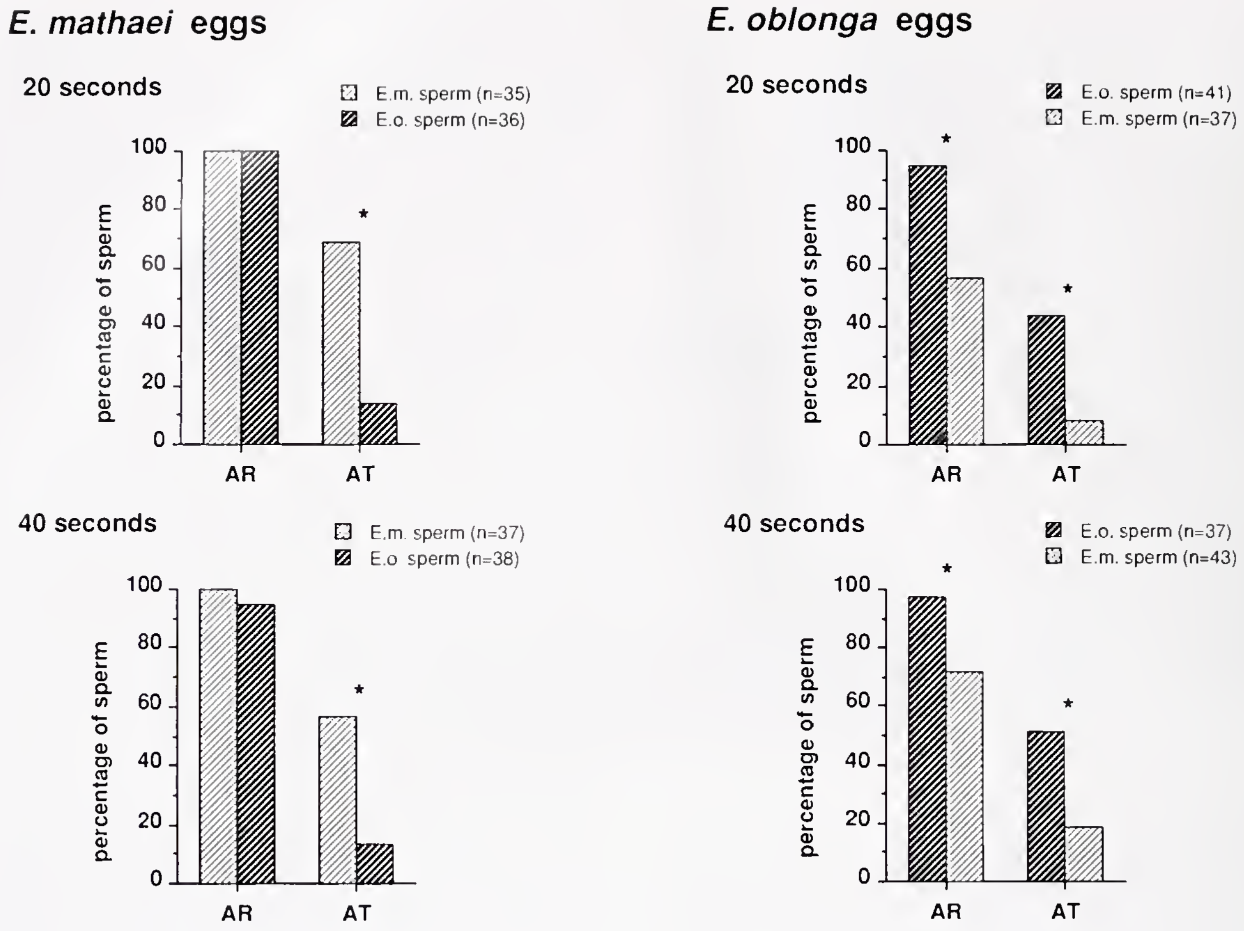

Figure 2. Measurements of gamete interaction in crosses between two *Echinometra* species. For eggs of each species, the percentages of conspecific and heterospecific sperm that underwent the acrosome reaction and became attached are shown for two experiments in which gamete interaction was allowed to occur for 20 s and 40 s, respectively. Different urchins were used in the two experiments. For each cross, the number of sperm, *n*, that were found in longitudinal section at the tip, within 5 μm of the egg surface, is indicated. AR: percentage of the *n* sperm that had undergone the acrosome reaction; AT: percentage of the *n* sperm that were attached to the egg vitelline layer by densely staining material; E. m.: *E. mathaei;* E. o.: *E. oblonga.*

For each egg sample, a *G*-test of independence (Sokal and Rohlf, 1981) was used to test the null hypothesis that the number of sperm completing each of the two steps (acrosome reaction and attachment) is independent of whether the sperm are conspecific or heterospecific. In comparisons marked with asterisks, the null hypothesis can be rejected. *:$p < 0.005$.

were observed in a few cases in the intraspecific crosses, but were not observed in any of the interspecific crosses.

In all cases, conspecific sperm demonstrated a significantly greater ability to attach to eggs than did heterospecific sperm ($p < 0.005$, *G*-test of independence). *E. mathaei* eggs bound 4.3–4.9 times more conspecific than heterospecific sperm; *E. oblonga* eggs bound 2.8–5.4 times more conspecific sperm than heterospecific sperm (Fig. 2). In each case, gamete interaction for the longer period resulted in relatively more heterospecific sperm becoming attached, suggesting that heterospecific sperm may attach at a slower rate than conspecific sperm.

Transient electrical continuity

After addition of heterospecific sperm to voltage-clamped eggs, about 3–10 sperm appeared to be in contact with each egg in the focal plane around the egg circumference. (Approximately 15–20 were seen when the sperm suspension added was fourfold more concentrated.) The total number of sperm contacting the egg was presumably several times higher. These heterospecific sperm appeared to be adhering to the surface of the dejellied egg; beating of flagella caused them to rotate around a contact point at their tip. In all cases, the positive control eggs (dejellied eggs from the same species as the sperm) had elevated

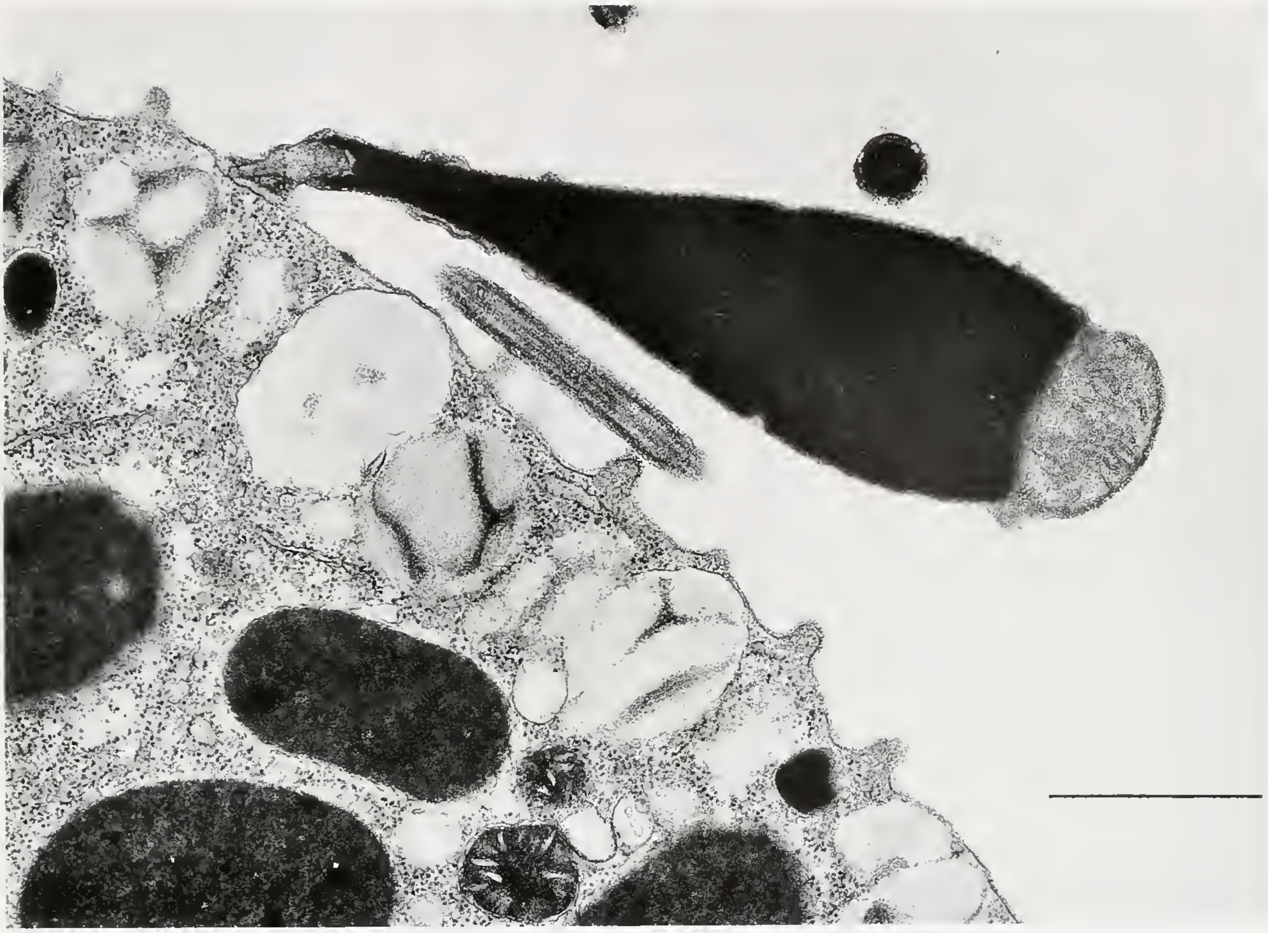

Figure 3. Electron micrograph of *Echinometra oblonga* sperm on *E. mathaei* egg fixed after 40 s of gamete interaction. Some heterospecific sperm-egg attachment occurs, but only rarely leads to gamete fusion. The acrosome is attached to the egg vitelline layer by densely staining acrosomal material, presumably bindin. (Bar = 1 μm.)

fertilization envelopes within 2–3 min, demonstrating that the heterospecific sperm were capable of fertilization.

Recordings totaling more than 80 min of heterospecific gamete interaction were taken from 22 eggs prior to addition of conspecific sperm; heterospecific sperm were allowed to interact for 2–6 min with each voltage-clamped egg. In spite of this opportunity for attachment and fusion, only two heterospecific transient current events occurred, both when *E. oblonga* eggs were exposed to concentrated *E. mathaei* sperm (Table I). For 20 out of 22 eggs, no electrical transients were observed for heterospecific sperm.

At an average of 30 s (range: 10–70 s) after addition of conspecific sperm near to voltage-clamped eggs, transient currents of 0.25–0.75 nA began to occur (Table I and Fig. 4). Under the conditions used for these experiments, the average number of transient current events per minute was similar in the two species: 1.9 for conspecific sperm on *E. mathaei* eggs and 1.4 for conspecific sperm on *E. oblonga* eggs. Occasionally, fusion with more than one conspecific sperm simultaneously was indicated by larger currents (Chambers and McCulloh, 1990). In most cases, the impaled eggs were then capable of undergoing a normal fertilization depolarization and elevation of the fertilization envelope when the voltage clamp was removed. The two heterospecific fusion events we recorded produced currents similar in magnitude and duration to those produced by conspecific fusion events.

Comparison of the two heterospecific crosses between Hawaiian *Echinometra* species shows that *E. oblonga* eggs appear to accept slightly more heterospecific fertilization (Fig. 1), heterospecific sperm attachment (Fig. 2), and heterospecific fusion (Table I), than *E. mathaei* eggs. However, the overall pattern in these urchins is strong reciprocal species-specificity of fertilization caused by

Table I

Incidence of transient currents in voltage-clamped eggs exposed first to heterospecific sperm and then to conspecific sperm

			Heterospecific sperm		Conspecific sperm		
Trial #	Female[1]	# males[2]	Time (s)[3]	Transients[4]	Time (s)[5]	Transients[6]	Fertilization[7]
E. mathaei eggs							
1	a	4	200	0	170	3	+
2	a	4	184	0	125	6	+
3	b	4	184	0	155	3	+
4	b	4	205	0	105	4	+
5	c	1	220	0	80	3	+
6	c	1	140	0	165	5	+
7	d	4	200	0	160	6	+
8	d	4	180	0	105	4	+
9	e	1 conc.	240	0	400	11	
10	f	4 conc.	295	0	145	7	
11	f	4 conc.	160	0	115	4	+
E. oblonga eggs							
1	a	1	225	0	145	4	+
2	b	1	275	0	130	3	+
3	b	1	185	0	95	2	+
4	b	1	180	0	130	4	+
5	c	4	275	0	95	3	+
6	c	4	195	0	135	3	+
7	d	4	200	0	85	3	+
8	d	4	225	0	90	3	+
9	e	1 conc.	380	0	300	5	
10	f	1 conc.	305	1	210	3	+
11	g	4 conc.	275	1	125	2	

[1] Each female from which eggs were obtained is designated by a different letter.

[2] Number of heterospecific males from which sperm was obtained; *conc.*: fourfold more concentrated sperm.

[3] Time in seconds of heterospecific gamete interaction before addition of conspecific sperm.

[4] Number of transient currents occurring prior to addition of conspecific sperm.

[5] Time in seconds between addition of conspecific sperm and removal of voltage clamp.

[6] Number of transients occurring after addition of conspecific sperm.

[7] After removal of the voltage clamp, normal fertilization depolarization and elevation of the fertilization envelope is indicated by a '+'.

strong reciprocal species-specificity of interactions as gametes attach and begin to fuse.

Discussion

Species-specificity of Echinometra *fertilization*

Of the many studies on sea urchin fertilization, few have examined species-specific fertilization step by step in crosses between congeners. Crosses of *Strongylocentrotus purpuratus* and *S. franciscanus* showed species-specificity of the sperm-egg attachment step but no specificity prior to attachment (reviewed in Minor *et al.*, 1989, 1991). Indo-Pacific *Echinometra* species are about 4–5 times more closely related than these *Strongylocentrotus* congeners (Palumbi and Metz, 1991) and provide a view of species-specific fertilization at a time much nearer the time of species formation. Barriers to fertilization have evolved in all but one of the six possible crosses between the three species of *Echinometra* found on Hawaii and Guam (Fig. 1), suggesting that gamete incompatibilities are a common feature of these urchins in spite of their close relationship. We have examined the steps of fertilization in crosses between Hawaiian *Echinometra* species in order to determine which ones are species-specific.

Step 1: Sperm activation. For successful fertilization to occur, sperm must first undergo a complex physiological activation induced by components of egg jelly—this allows them to find the egg and penetrate the jelly (reviewed in Ward and Kopf, 1993). Specificity of these events is generally moderate; only distantly related urchins are incompatible. For example, the egg-jelly peptide speract can activate sperm from different genera of urchins (Trimmer and Vacquier, 1986; Garbers, 1989; Ward and Kopf, 1993). In crosses of *Strongylocentrotus,* these events are also not species-specific (Minor *et al.,* 1991). Likewise, in crosses of Hawaiian *Echinometra,* large numbers of het-

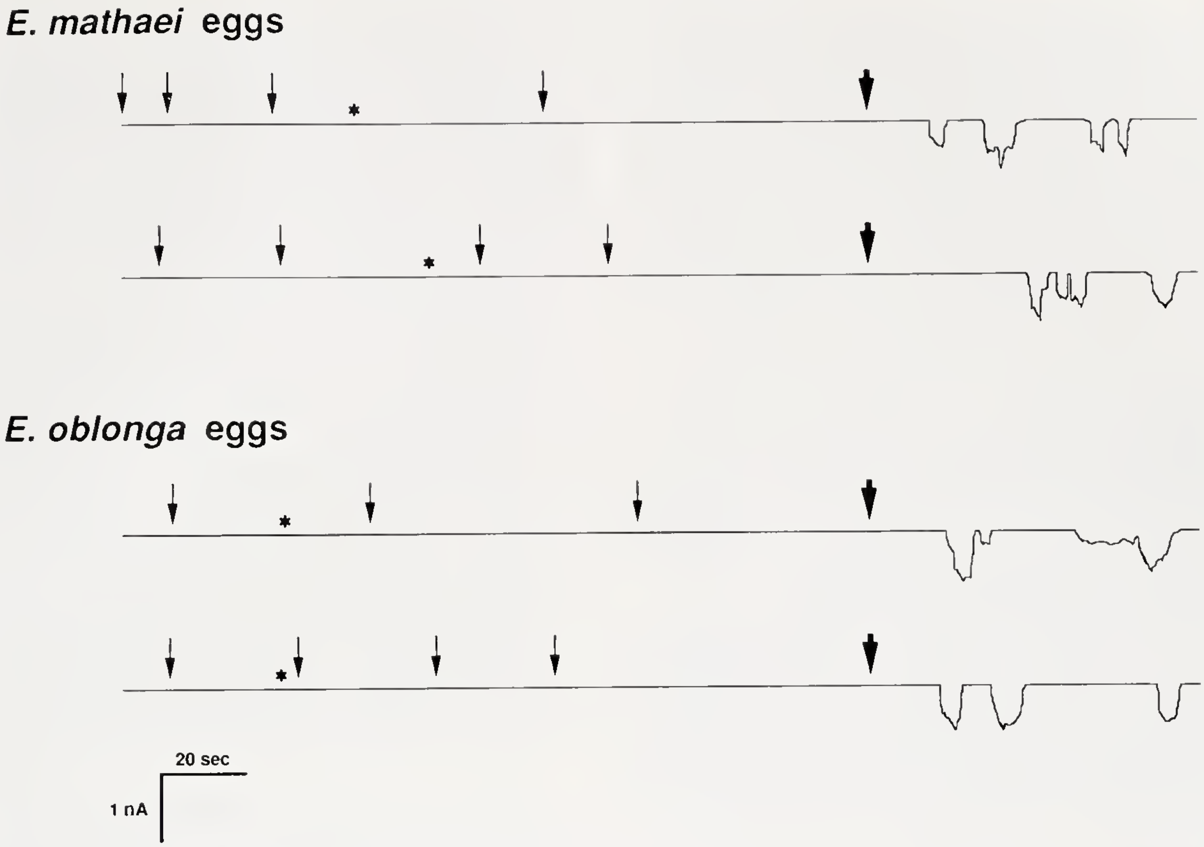

Figure 4. Portions of recordings of transmembrane current of *Echinometra* eggs voltage-clamped at approximately −75 mV. Small arrows indicate times of addition of aliquots of heterospecific sperm. Large arrow indicates time of addition of an equal aliquot of conspecific sperm. For clarity, the recordings have been aligned at the time of addition of conspecific sperm; the times of heterospecific gamete interaction are somewhat longer than is shown. The asterisk indicates the time at which all control eggs had elevated fertilization envelopes. Transient currents of approximately −0.5 nA occurring after addition of conspecific sperm indicate temporary electrical continuity between egg and sperm. In each of these trials, the voltage clamp was released, after which the impaled egg underwent normal fertilization depolarization and elevation of the fertilization envelope.

erospecific sperm rapidly arrive at the egg plasma membrane, suggesting that activation is readily achieved.

Step 2: Acrosome reaction. Although the acrosome reaction step is blocked in some crosses between divergent urchins (Segall and Lennarz, 1981), this step is typically not strongly and reciprocally species-specific. The acrosome reaction is not blocked in crosses between *Strongylocentrotus purpuratus* and *S. franciscanus* (reviewed in Minor *et al.*, 1989, 1991). In addition, the acrosome reaction has been shown to occur normally in most of the possible crosses between urchins from four different genera of Caribbean urchins, including *Echinometra lucunter,* and was not reciprocally blocked between any pair of these species (Summers and Hylander, 1975).

In Hawaiian *Echinometra* crosses, asymmetry was observed in the acrosome reaction step; in all crosses, however, more than half of the sperm approaching the egg surface underwent the acrosome reaction within 20 s. This degree of reaction is too high to account for the observation that only a small percentage of the eggs in both heterospecific crosses typically elevate fertilization envelopes. Even though induction of the acrosome reaction is measurably different depending on the direction of the cross, this step is not an effective barrier to cross-fertilization. The gamete interaction steps primarily responsible for preventing interspecific fertilization in both directions occur after the induction of the acrosome reaction.

Step 3: Sperm-egg attachment. In contrast to the preceding steps of gamete interaction, the attachment of sperm to the vitelline layer of eggs is species-specific in many urchin crosses (Summers and Hylander, 1975, 1976; Minor *et al.*, 1991). We found a similar pattern in crosses of the closely related Hawaiian *Echinometra* species, in which eggs bound severalfold fewer heterospecific sperm than conspecific sperm (Fig. 2). These results agree with our previous counts of sperm attachment to dejellied eggs (Palumbi and Metz, 1991). It might be expected that heterospecific sperm would fertilize one-third to one-fifth of the eggs fertilizable by conspecific sperm, because the results show that eggs will bind approximately one-third to one-fifth as many heterospecific sperm as conspecific sperm. Typically, however, only a much smaller proportion of eggs in heterologous crosses eventually become fertilized. This indicates that sperm-egg attachment is not the only barrier to cross-fertilization in *Echinometra*. Under certain conditions, sperm from *Strongylocentrotus purpuratus* will attach to the vitelline layer of eggs from the highly divergent urchin *Arbacia punctulata*, yet only a small proportion of the eggs fertilize (Glabe *et al.*, 1981). On the basis of these observations, Glabe *et al.* suggested that in heterospecific crosses, bound sperm may not always be capable of penetrating the vitelline layer and developing continuity with the egg plasma membrane.

Step 4: Interactions of attached gametes and sperm-egg fusion. The best-known indicator of sperm-egg fusion is the fertilization envelope. However, elevation of the fertilization envelope is a complex process that normally occurs only after the egg has undergone a series of changes induced by fusion with the sperm (reviewed in Jaffe, 1986; Kay and Shapiro, 1985); hence it is an indicator of *completed* gamete fusion. By contrast, the earliest stages of the gamete fusion process are indicated by transmembrane electrical changes during interaction of the attached sperm and egg (Chambers, 1989; Whitaker *et al.*, 1989; Chambers and McCulloh, 1990). It is not yet known whether complete fusion of the sperm and egg plasma membranes is required for the sperm to influence the egg transmembrane potential. It is clear, however, that if plasma membranes have fused, then electrical continuity must exist between the gametes. Eggs held at the resting potential by voltage clamping are prevented from undergoing the normal depolarization that accompanies gamete fusion; instead, transient fusion of a sperm creates a transient transmembrane current (Chambers, 1989). We measured the incidence of these transient currents in voltage-clamped eggs to directly compare the ability of conspecific and heterospecific sperm to initiate the process of fusion. In reciprocal heterospecific crosses of Hawaiian *Echinometra* species, sperm were typically incapable of developing temporary electrical continuity with the egg. Thus species-specificity resides in the interactions of the sperm acrosomal surface and the egg vitelline layer that bring the plasma membranes together and allow fusion to occur.

Levels of reproductive isolation

Species-specific gamete interactions contribute directly to reproductive isolation between sea urchin species. In some cases, however, sympatric congeneric sea urchins fertilize readily in one or both directions of hybrid crosses (Shearer *et al.*, 1913; Strathmann, 1981; Lessios and Cunningham, 1990; Uehara *et al.*, 1990). When barriers are not present at fertilization, other types of reproductive isolation—including habitat segregation, timing of spawning, and postmating incompatibilities—are likely to be involved in maintaining distinctions between marine species (see review by Knowlton, 1993).

Hybrid sterility and inviability are important aspects of postmating reproductive isolation in *Drosophila* and other organisms (reviewed by Coyne and Orr, 1989; Coyne, 1992). However, because of difficulties rearing sea urchins, little is known about postmating isolating mechanisms in this group. In Hawaii, the existence of rare morphologically intermediate urchins suggests that viable and fertile hybrids may result from interspecific crosses between *E. mathaei* and *E. oblonga* in nature (Kelso, 1970; Palumbi and Metz, 1991). Although the strength of postmating isolation remains unclear, the strong gamete incompatibilities that have evolved act first during reproduction and are probably most important in maintaining barriers to gene flow in present populations.

Mechanisms of gamete incompatibility

In the genus *Strongylocentrotus*, the sperm acrosomal protein bindin has been shown to species-specifically attach the sperm to a receptor on the egg vitelline layer (Vacquier and Moy, 1977; Glabe and Vacquier, 1977; Minor *et al.*, 1989, 1991; Lopez *et al.*, 1993; Foltz *et al.*, 1993; Foltz and Lennarz, 1993). In addition to its responsibility for attaching gametes, the bindin-receptor interaction is also likely to have a role in setting up plasma membrane fusion (Glabe, 1985; Foltz and Lennarz, 1993). The steps of fertilization that involve bindin correspond to the steps that are reciprocally species-specific in closely related *Echinometra* congeners.

Bindin and its receptor could contribute in two ways to the reciprocal barrier to fertilization between Hawaiian *Echinometra* species. First, heterospecific bindin might not be properly recognized by the receptor on the egg vitelline layer, resulting in the reduced gamete attachment that we observe. Second, mismatched heterologous bindin-receptor complexes that occasionally succeed in attaching gametes might not be capable of undergoing subsequent molecular interactions associated with membrane fusion. This could result in the barrier to the formation of continuity of the sperm and egg plasma membranes that we observe. Other recognition molecules are probably also involved in the barrier to interspecific fertilization, especially during the complex process of gamete fusion (Whitaker *et al.*, 1989; Foltz and Lennarz, 1993).

Which fertilization steps are evolutionarily labile?

Species-specific fertilization arises as gamete recognition molecules differentiate, so recognition molecules that have the most freedom to vary within populations over time are likely to be the ones that first develop species-specificity. In sea urchins, different steps of fertilization are not equally likely to become blocked between species. The responses of the sperm to egg jelly, including the acrosome reaction, are often not strongly and reciprocally species-specific, except in crosses between divergent species (Summers and Hylander, 1975; Minor *et al.*, 1991). Components of egg jelly, including a fucose sulfate glycoconjugate and sperm-activating peptides, operate together to initiate the acrosome reaction (reviewed in Ward and Kopf, 1993). In addition, these molecules initiate ionic movements across the sperm membrane and cAMP-dependent protein kinase activity in sperm associated with sperm activation (reviewed in Trimmer and Vacquier, 1986; Ward and Kopf, 1993). Multiple functions (and in the case of the fucose sulfate glycoconjugate, a complex biosynthetic pathway), are likely to create constraints on the variability of the egg jelly components. Constraints such as these could prevent rapid differentiation of species-specificity.

The attachment and fusion steps of sea urchin fertilization, which are most often species-specific, are likely to be mediated by molecules that have more freedom to differentiate. Reciprocally incompatible attachment and fusion suggest that two complementary recognition molecules, such as bindin and its receptor, both differentiate between species. In *Strongylocentrotus* bindin and its receptor, protein-protein recognition involving direct binding of polypeptides expressed on the two gametes has been found. Unmodified bindin polypeptide attaches to the egg surface (Lopez *et al.*, 1993), and conversely, a region of the receptor polypeptide binds to bindin particles (Foltz *et al.*, 1993). In addition, treatment of eggs with a peptide derived from bindin can inhibit fertilization, presumably by binding to the receptor (Minor *et al.*, 1993). All of these effects are species-specific and support the view that recognition and binding result primarily from interactions of polypeptide domains. As species differentiate, genetic changes could act directly on the amino acid sequence of recognition domains in proteins expressed on sperm and eggs. Changes in the surface proteins of both the male and the female gametes would likely be required for differentiation of recognition. Constraints on such changes may be substantial, but would be lessened if they were uncoupled from other functional constraints of cell physiology. Accordingly, recognition domains of proteins might be susceptible to relatively rapid differentiation, and gamete interaction steps mediated by this type of recognition might reasonably be the first to evolve reciprocal species-specificity and premating reproductive isolation.

Reciprocal gamete incompatibility between recently diverged *Echinometra* species occurs during the stages of fertilization in which bindin and its receptor play a major role. We recently obtained the nucleotide sequences of bindin genes from these urchins and found that they are substantially differentiated (E. C. Metz and S. R. Palumbi, in preparation). Further studies of the Indo-Pacific *Echinometra* species group may aid our understanding of how gamete recognition evolves and contributes to differentiation of species.

Acknowledgments

This paper is dedicated to the memory of Bob Kane, who helped complete these experiments shortly before his death on 2 April 1993. As a guiding force behind the Kewalo Marine Laboratory for 25 years, and as a friend, Bob had touched us all.

We thank T. Uehara and R. Richmond for shipments of urchins from Guam. We also thank M. Hadfield, A. Hofmann, K. Kaneshiro, M. McCartney, A. Taylor, T. Uehara, and R. Yanagimachi for discussions. O. McMillan and S. Romano provided helpful comments on the manuscript. Supported by NSF Predoctoral Fellowship and University of Hawaii Foundation Edmondson Fellowship to E. C. M. and by NSF Grants to S. R. P.

Literature Cited

Boake, C. R. B. 1991. Coevolution of senders and receivers of sexual signals: genetic coupling and genetic correlations. *Trends Ecol. Evol.* **6:** 225–227.

Branham, J. M. 1972. Comparative fertility of gametes from six species of sea urchins. *Biol. Bull.* **142:** 385–396.

Carson, H. L. 1987. The genetic system, the deme, and the origin of species. *Ann. Rev. Genet.* **21:** 405–423.

Chambers, E. L. 1989. Fertilization in voltage-clamped sea urchin eggs. Pp. 1–18 in *Mechanisms of Egg Activation*, R. Nuccitelli, G. N. Cherr, and W. H. Clark, eds. Plenum Press, New York.

Chambers, E. L., and D. H. McCulloh. 1990. Excitation, activation and sperm entry in voltage-clamped sea urchin eggs. *J. Reprod. Fert., Suppl.* **42:** 117–132.

Coyne, J. A. 1992. Genetics and speciation. *Nature* **355:** 511–515.

Coyne, J. A., and H. A. Orr. 1989. Two rules of speciation. Pp. 180–207 in *Speciation and Its Consequences*, D. Otte and J. A. Endler, eds. Sinauer, Sunderland, MA.

Donoghue, M. J. 1985. A critique of the biological species concept and recommendations for a phylogenetic alternative. *The Bryologist* **88:** 172–181.

Edmondson, C. H. 1946. *Reef and Shore Fauna of Hawaii.* 2nd ed. B. P. Bishop Museum Press, Honolulu.

Finkel, A. S., and S. J. Redman. 1984. Theory and operation of a single microelectrode voltage clamp. *J. Neurosci. Methods.* **11:** 101–127.

Foltz, K. R., and W. J. Lennarz. 1993. The molecular basis of sea urchin gamete interactions at the egg plasma membrane. *Dev. Biol.* **158:** 46–61.

Foltz, K. R., J. S. Partin, and W. J. Lennarz. 1993. Sea urchin egg receptor for sperm: sequence similarity of binding domain and hsp70. *Science* **259:** 1421–1425.

Garbers, D. L. 1989. The regulation of the spermatozoan function by the egg. Pp. 3–19 in *The Molecular Biology of Fertilization,* H. Schatten and G. Schatten, eds. Academic Press, San Diego.

Glabe, C. G. 1985. Interaction of the sperm adhesive protein, bindin, with phospholipid vesicles. II. Bindin induces the fusion of mixed phase vesicles that contain phosphatidylcholine and phosphatidylserine *in vitro. J. Cell Biol.* **100:** 800–806.

Glabe, C. G., and V. D. Vacquier. 1977. Species-specific agglutination of eggs by bindin isolated from sea urchin sperm. *Nature* **267:** 822–824.

Glabe, C. G., M. Buchalter, and W. J. Lennarz. 1981. Studies on the interactions of sperm with the surface of the sea urchin egg. *Dev Biol.* **84:** 397–406.

Jaffe, L. A. 1986. Electrical regulation of sperm-egg fusion. *Ann. Rev. Physiol.* **48:** 191–200.

Kane, R. E. 1990. Membrane conductance patterns during fertilization are sperm dependent in two sea urchin species. *Dev. Biol.* **141:** 330–343.

Kaneshiro, K. Y., and C. R. B. Boake. 1987. Sexual selection and speciation: issues raised by Hawaiian *Drosophila. Trends Ecol. Evol.* **2:** 207–212.

Kay, E. S., and B. M. Shapiro. 1985. The formation of the fertilization membrane of the sea urchin egg. Pp. 45–80 in *Biology of Fertilization,* C. B. Metz and A. Monroy, eds. Academic Press, New York.

Kelso, D. 1970. A comparative morphological and ecological study of two species of sea urchins, genus *Echinometra,* in Hawaii. Ph. D. Dissertation, Department of Zoology, University of Hawaii, Honolulu.

Knowlton, N. 1993. Sibling species in the sea. *Ann. Rev Ecol. Syst.* **24:** 189–216.

Lessios, H. A., and C. W. Cunningham. 1990. Gametic incompatibility between species of the sea urchin *Echinometra* on the two sides of the isthmus of Panama. *Evolution* **44:** 933–941.

Lillie, F. R. 1919. *Problems of Fertilization.* University of Chicago Press, Chicago.

Lopez, A., S. J. Miraglia, and C. G. Glabe. 1993. Structure/function analysis of the sea urchin sperm adhesive protein bindin. *Dev. Biol.* **156:** 24–33.

Lynn, J. W., and E. L. Chambers. 1984. Voltage clamp studies of fertilization in sea urchin eggs. I. Effect of clamped membrane potential on sperm entry, activation, and development. *Dev. Biol.* **102:** 98–109.

Mayr, E. 1954. Geographic speciation in tropical echinoids. *Evolution* **8:** 1–18.

Mayr, E. 1963. *Animal Species and Evolution.* Harvard University Press, Cambridge.

Metz, C. B., and A. Monroy, eds. 1985. *Biology of Fertilization.* Academic Press, New York.

Metz, E. C., H. Yanagimachi, and S. R. Palumbi. 1991. Gamete compatibility and reproductive isolation of closely related Indo-Pacific sea urchins, genus *Echinometra.* Pp. 131–137 in *Biology of Echinodermata,* T. Yanagisawa, I. Yasumasu, C. Oguro, N. Suzuki, and T. Motokawa, eds. A. A. Balkema, Rotterdam.

Minor, J. E., B. Gao, and E. Davidson. 1989. The molecular biology of bindin. Pp. 73–88 in *The Molecular Biology of Fertilization,* H. Schatten and G. Schatten, eds. Academic Press, San Diego.

Minor, J. E., D. R. Fromson, R. J. Britten, and E. H. Davidson. 1991. Comparison of the bindin proteins of *Strongylocentrotus franciscanus, S. purpuratus,* and *Lytechinus variegatus:* sequences involved in the species specificity of fertilization. *Mol. Biol. Evol.* **8:** 781–795.

Minor, J. E., R. J. Britten, and E. H. Davidson. 1993. Species-specific inhibition of fertilization by a peptide derived from the sperm protein bindin. *Mol. Biol. Cell.* **4:** 375–387.

Mortensen, T. 1943. *Monograph of the Echinoidea: Camarodonta.* C. A. Reitzel, Copenhagen.

Moy, G. W., and V. D. Vacquier. 1979. Immunoperoxidase localization of bindin during adhesion of sperm to sea urchin eggs. *Curr. Top. Dev. Biol.* **13:** 31–44.

Nishioka, D. R., R. A. Ward, D. Poccia, C. Kostacos, and J. E. Minor. 1990. Localization of bindin expression during sea urchin spermatogenesis. *Mol. Reprod. Dev.* **27:** 181–190.

O'Rand, M. G. 1988. Sperm-egg recognition and barriers to interspecies fertilization. *Gamete Res.* **19:** 315–328.

Palumbi, S. R. 1992. Marine speciation on a small planet. *Trends Ecol. Evol.* **7:** 114–118.

Palumbi, S. R., and E. C. Metz. 1991. Strong reproductive isolation between closely related tropical sea urchins (genus *Echinometra*). *Mol Biol. Evol.* **8:** 227–239.

Schatten, H., and G. Schatten, eds. 1989. *The Molecular Biology of Fertilization.* Academic Press, San Diego.

Segall, G. K., and W. J. Lennarz. 1981. Jelly coat and induction of the acrosome reaction in echinoid sperm. *Dev. Biol.* **86:** 87–93.

Shearer, De Morgan, and Fuchs. 1913. On the experimental hybridization of echinoids. *Phil. Trans. R. Soc, London.* **204:** 255–362.

Sokal, R. R., and F. J. Rohlf. 1981. *Biometry.* 2nd ed. W. H. Freeman, New York.

Steinhardt, R. A., L. Lundin, and D. Mazia. 1971. Bioelectric responses of the echinoderm egg to fertilization. *Proc. Natl. Acad. Sci. U. S. A* **68:** 2426–2430.

Strathmann, R. R. 1981. On the barriers to hybridization between *Strongylocentrotus droebachiensis* and *S. pallidus. J. Exp. Mar. Biol. Ecol.* **55:** 39–47.

Summers, R. G., and B. L. Hylander. 1975. Species-specificity of acrosome reaction and primary gamete binding in echinoids. *Exp. Cell Res.* **96:** 63–68.

Summers, R. G., and B. L. Hylander. 1976. Primary gamete binding. *Exp. Cell Res.* **100:** 190–194.

Templeton, A. R. 1989. The meaning of species and speciation: a genetic perspective. Pp. 3–27 in *Speciation and Its Consequences,* D. Otte and J. A. Endler, eds. Sinauer, Sunderland, MA.

Trimmer, J. S., and V. D. Vacquier. 1986. Activation of sea urchin gametes. *Annu Rev. Cell Biol.* **2:** 1–26.

Uehara, T., and M. Shingaki. 1985. Taxonomic studies in the sea urchin genus *Echinometra,* from Okinawa and Hawaii. *Zool. Sci.* **2:** 1009.

Uehara, T., H. Asakura, and Y. Arakaki. 1990. Fertilization blockage and hybridization among species of sea urchins. Pp. 305–310 in *Advances in Invertebrate Reproduction,* V. M. Hoshi and O. Yamashita, eds. Elsevier Science Publishers, Amsterdam.

Vacquier, V. D., and J. E. Payne. 1973. Methods for quantitating sea urchin sperm-egg binding. *Exp. Cell Res.* **82:** 227–235.

Vacquier, V. D., and G. W. Moy. 1977. Isolation of bindin: the protein responsible for adhesion of sperm to sea urchin eggs. *Proc. Natl. Acad Sci. U. S. A.* **74:** 2456–2460.

Vacquier, V. D., K. R. Carner, and C. D. Stout. 1990. Species-specific sequences of abalone lysin, the sperm protein that creates a hole in the egg envelope. *Proc. Natl. Acad Sci. U. S. A* **87:** 5792–5796.

Ward, C. R., and G. S. Kopf. 1993. Molecular events mediating sperm activation. *Dev. Biol.* **158:** 9–34.

Wheeler, D. A., C. P. Kyriacou, M. L. Greenacre, Q. Yu, J. E. Rutila, M. Rosbash, and J. C. Hall. 1991. Molecular transfer of a species-specific behavior from *Drosophila simulans* to *Drosophila melanogaster. Science* **251:** 1082–1085.

Whitaker, M., K. Swann, and I. Crossley. 1989. What happens during the latent period at fertilization? Pp. 157–171 in *Mechanisms of Egg Activation,* R. Nuccitelli, G. N. Cherr, and W. H. Clark, eds. Plenum Press, New York.

Wilson, W. A., and M. M. Goldner. 1975. Voltage clamping with a single microelectrode. *J Neurobiol.* **6:** 411–422.

Reference: *Biol. Bull.* **187:** 35–47. (August, 1994)

The Role of Podial Secretions in Adhesion in Two Species of Sea Stars (Echinodermata)

PATRICK FLAMMANG[1,*], STEPHANE DEMEULENAERE[1], AND MICHEL JANGOUX[1,2]

[1]*Laboratoire de Biologie marine, Université de Mons-Hainaut, 19 ave. Maistriau, B-7000 Mons, Belgium, and* [2]*Laboratoire de Biologie marine (C.P. 160/15), Université Libre de Bruxelles, 50 ave. F.D. Roosevelt, B-1050 Bruxelles, Belgium*

Abstract. Individuals of *Asterias rubens* and *Marthasterias glacialis* use their podia in locomotion, anchorage, and feeding. Each podium consists of a stem with a disk at its tip. The stem allows the podium to lengthen, flex, and retract, and the disk allows the podium to adhere to the substratum. Adhesion of sea star podia seems to rely on the epidermal secretions of the disk and not on a mechanical sucker-like operation. The disk epidermis is made up of five cell types: nonciliated secretory cells (NCS cells) of two different types (NCS1 and NCS2), both containing granules that are at least partly mucopolysaccharidic in composition; ciliated secretory cells (CS cells) containing small granules of unknown content; nonsecretory ciliated cells (NCS cells); and support cells. The epidermal cells of the podial disk are presumably functioning as a duo-gland adhesive system that is involved in an adhesive/de-adhesive process. The following model is presented. Adhesive secretions are produced by NCS1 and NCS2 cells (both of them have extruded some of their secretory granules in attached podia). These secretions constitute a layer of adhesive material between the podium and the substratum, this layer being the footprint left by the podium after it has become detached from the substratum. De-adhesion, on the other hand, would be due to CS cell secretions. All these secretions would be controlled by stimuli perceived by the two types of ciliated cells (receptor cells), which presumably interact with the secretory cells *via* the nerve plexus.

Introduction

Marine organisms have developed a wide range of mechanisms allowing them to attach to a substrate or to handle it (Nachtigall, 1974). Among these mechanisms, one can distinguish between mechanical attachments (with, for example, hooks or suckers) and chemical attachments (with adhesive substances). The way the former operate is generally obvious, whereas the functioning of the latter remains enigmatic.

Asteroid podia are traditionally viewed as suckered organs in which adhesion is partly due to suction (mechanical attachment) and partly to adhesives (chemical attachment) (Smith, 1937; Nichols, 1966). According to Paine (1926), about half of the adhesive force of the podia comes from suction and half from adhesive secretions. However, there is no agreement on this ratio. Some authors argue that the part of the percentage allotted to adhesive secretions has been underestimated (Thomas and Hermans, 1985); others believe that suction has been overlooked (Smith, 1991).

As far as the chemical mechanism is concerned, Hermans (1983) proposed that all echinoderm podia possess duo-gland adhesive systems enclosing two types of secretory cells (*viz.*, cells releasing an adhesive secretion and cells releasing a de-adhesive secretion) that are involved in the attachment to the substratum. But McKenzie (1988) concluded that morphological observations supporting such adhesive systems are rare and that more ultrastructural studies of echinoderm podia are needed.

This work, continuing an extended comparative ultrastructural study of echinoderm podia, describes the locomotory podial disk in two species of asteriid asteroids, *Asterias rubens* and *Marthasterias glacialis.* The study deals with the attachment mechanism of the podia on the substrate (mechanical *versus* chemical). It focuses especially on the epidermal secretory cells and their possible participation in a duo-glandular model of adhesion.

Received 18 August 1993; accepted 23 May 1994.

* Research Assistant, National Fund for Scientific Research (Belgium).

Materials and Methods

Individuals of *Asterias rubens* Linné, 1758, were collected intertidally in Audresselles (Pas-de-Calais, France) in November 1991; individuals of *Marthasterias glacialis* (Linné, 1758) were collected by scuba diving in Brest harbor (Brittany, France) in November 1990. Individuals of both species were transported to the marine biology laboratory of the University of Mons where they were kept in a marine aquarium with closed circulation (13°C, 33‰ salinity) and fed with mussels (*Mytilus edulis* Linné, 1758).

Light microscopy

Podia were cut off individuals that had previously been anesthetized with propylene phenoxetol (0.1% in seawater). The podia were fixed in Bouin's fluid, embedded in paraplast, and cut into 7 μm thick sections. The sections were stained with Masson's trichrome and Mayer's hemalum coupled with phloxine and light green. Alcian blue (pH 2.6) and the periodic acid-Schiff (PAS) techniques were used in the detection of mucopolysaccharides, and mercuric bromophenol blue and Danielli's technique in the detection of proteins (Ganter and Jollès, 1969–1970).

Scanning electron microscopy (SEM)

Podia were fixed in Bouin's fluid for 24 h. They were dehydrated in graded ethanol, dried by the critical point method (with CO_2 as transition fluid), mounted on aluminum stubs, coated with gold in a sputter coater, and observed with a JEOL JSM-6100 scanning electron microscope.

Footprints were prepared as follows. Podia were allowed to adhere firmly to clean glass coverslips. After the podia had detached themselves, the coverslips were soaked in Bouin's fluid and prepared for SEM by critical-point drying.

Transmission electron microscopy (TEM)

Two sets of podia were investigated: unattached podia that did not adhere to any substratum and attached podia that adhered to hardened Spurr blocks. Because podia do not adhere to clean Spurr blocks, the blocks had been placed in seawater for 4–5 days to allow the formation of a primary film. (The primary film is a moderately negative layer, consisting of adsorbed macromolecules and bacteria, that coats all marine surfaces; Characklis, 1981.) The unattached podia were fixed in 3% glutaraldehyde in cacodylate buffer (0.1 *M*, pH 7.8) for 3 h at 4°C, rinsed in cacodylate buffer, and postfixed for 1 h in 1% osmium tetroxide in the same buffer. The attached podia were fixed according to the same protocol as the unattached podia but with the addition of 0.05% ruthenium red to both the primary fixative and the postfixative (Luft, 1971). This technique allows better preservation of extracellular acid mucopolysaccharides as well as their labeling. After a final wash in buffer, both sets of podia were dehydrated in graded ethanol and embedded in Spurr. Ultrathin sections (40–70 nm) were cut with an LKB III ultramicrotome equipped with a diamond knife. They were stained with uranyl acetate and lead citrate and observed with a Zeiss EM 10 transmission electron microscope.

Results

External morphology of the podia

The locomotory podia of both *Asterias rubens* and *Marthasterias glacialis* are arranged in four longitudinal rows on the oral surface of the arms. In a specimen of *A. rubens* with arms about 5 cm long, a podium at the middle of the arm is about 1 mm in diameter and 10 mm in length when protracted. These measurements, in a specimen of *M. glacialis* of about 10-cm arm length, are 1.5 mm and 20 mm, respectively. Each podium consists of an extensible cylindrical stem topped by a somewhat wider flat disk (Figs. 1, 2).

The surface of the disk is sprinkled with uniformly distributed cilia and pores (Fig. 3). In both species, there are about 10 cilia/100 μm^2 and about 4 times as many pores. The cilia are about 1 μm long (Fig. 4). The pores measure about 600 nm in diameter in *A. rubens* (Fig. 5), but only about 450 nm in *M. glacialis* (Fig. 4). Secretory material extruded through the pores was clearly visible on some podia (Fig. 5).

Histology and cytology of the podial disk

The disk consists of four tissue layers that are, from the inside to the outside, a mesothelium, a connective tissue layer, a nerve plexus, and an epidermis covered by a cuticle (Figs. 6, 7).

Disk inner tissues. The inner tissues of the disk in the two species are very similar structurally, and the following description applies to both of them.

The mesothelium surrounds the ambulacral lumen. It is a pseudostratified epithelium comprising three cell types: adluminal cells, glandular cells, and myoepithelial cells; all of them contact the underlying basal lamina. Adluminal cells line the ambulacral cavity. These are T-shaped monociliated cells with a long vibratile cilium (Fig. 8) surrounded by a ring of about 10 microvilli. Glandular cells occur singly among the adluminal cells. Their cytoplasm is filled with membrane-bound, electron-dense secretory granules whose diameter varies between 0.7 and 1.5 μm (Fig. 9). Adluminal cells are bound together and to glandular cells by junctional complexes consisting of an apical zonula adher-

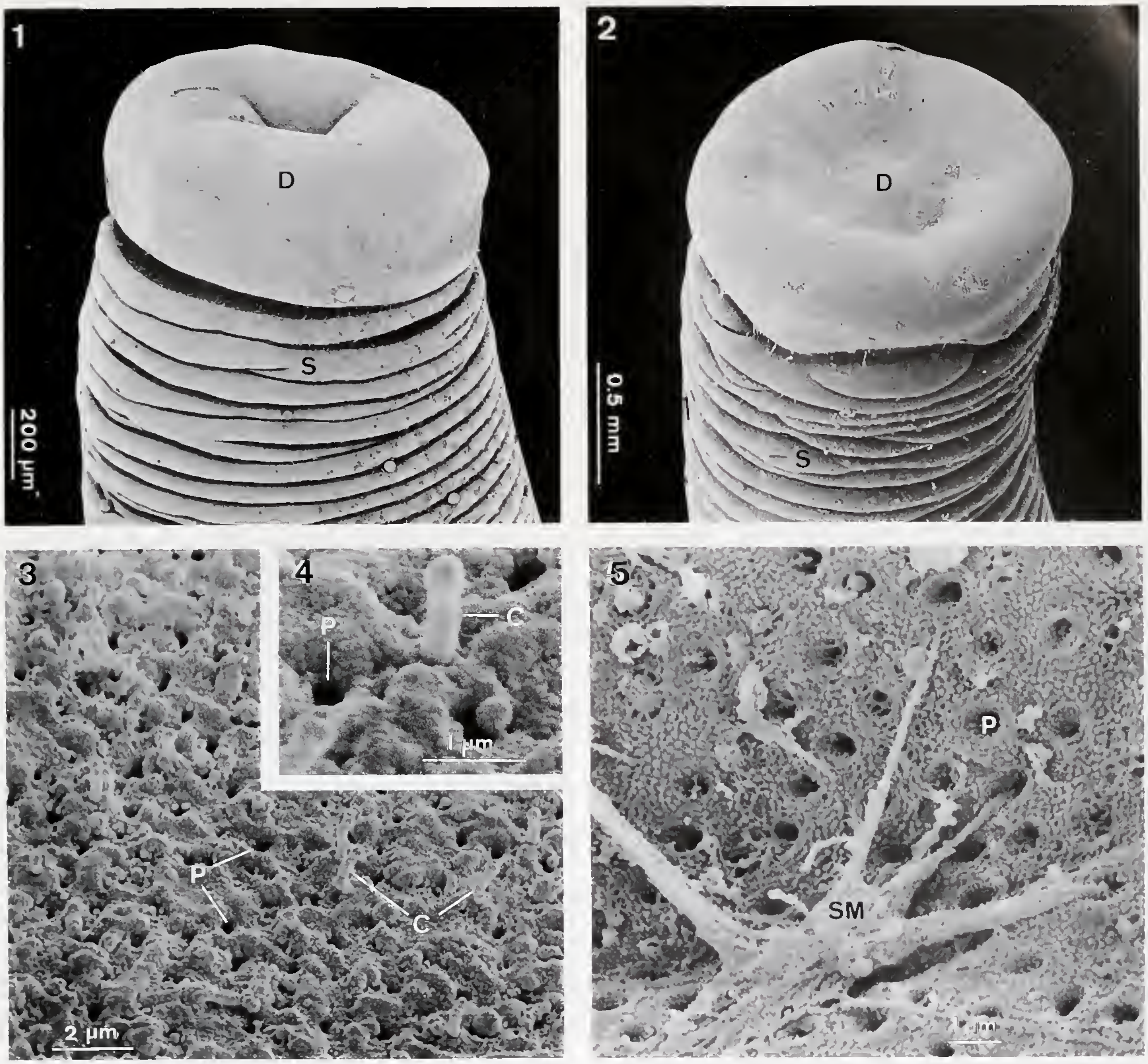

Figures 1–5. Outer aspect of the locomotory podia in *Asterias rubens* and *Marthasterias glacialis*. C, cilium; D, disk; P, pore; S, stem; SM, secretory material.

Figure 1. Podium (*A. rubens*).

Figure 2. Podium (*M. glacialis*).

Figure 3. Disk surface (*M. glacialis*).

Figure 4. Detailed view of cilia and pores (*M. glacialis*).

Figure 5. Disk surface with secretory material (*A. rubens*).

ens and a subapical septate desmosome. Both types of cells send basal processes that pass between myoepithelial cells before contacting the basal lamina. Myoepithelial cells are located below the cell bodies of the adluminal and glandular cells. They contain a bundle of myofilaments (Fig. 8) associated with numerous mitochondria and are bound together by regularly spaced desmosome-like junctions. The myoepithelial cells are arranged to form the muscle systems of the podia (that is, the retractor, the levator, and the radial systems; see Smith, 1947, for a detailed description of these systems in *A. rubens*). Intermingled with myoepithelial cells are slender cell processes (cell bodies have never been observed in the mesothelium) whose cytoplasm is filled with electron-dense membrane-bound granules (about 200 nm in diameter). These cells are similar to the

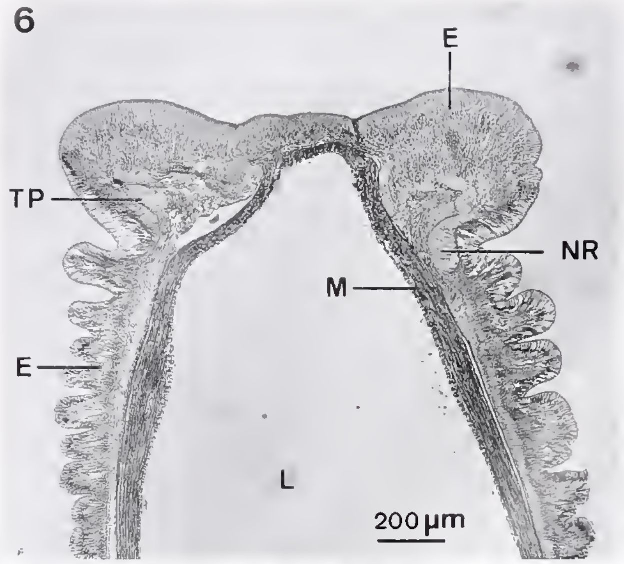
6
E
TP
NR
M
E
L
200 µm

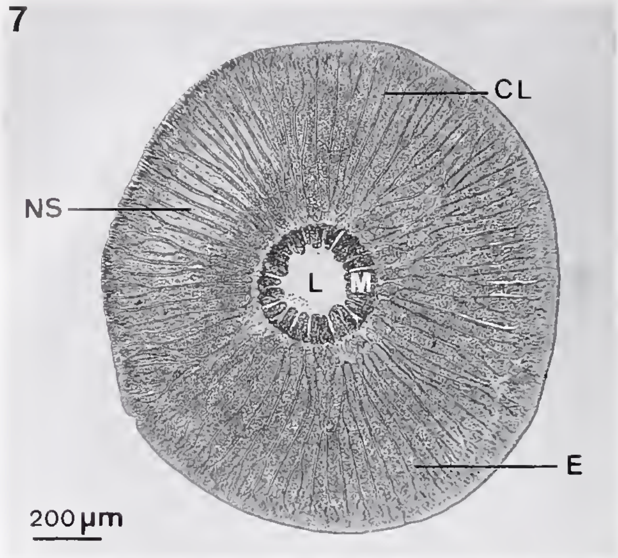
7
CL
NS
L
M
E
200 µm

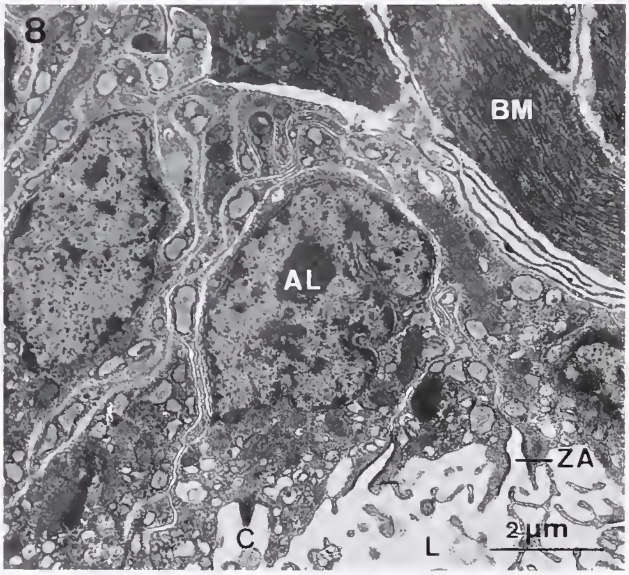
8
BM
AL
ZA
C
L
2 µm

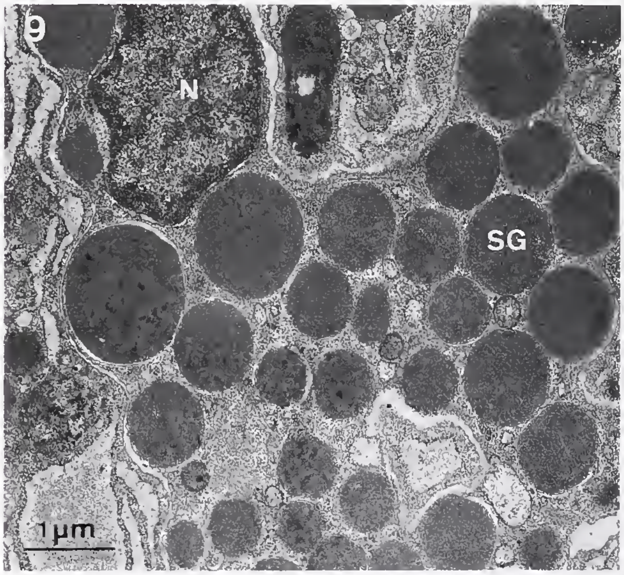
9
N
SG
1 µm

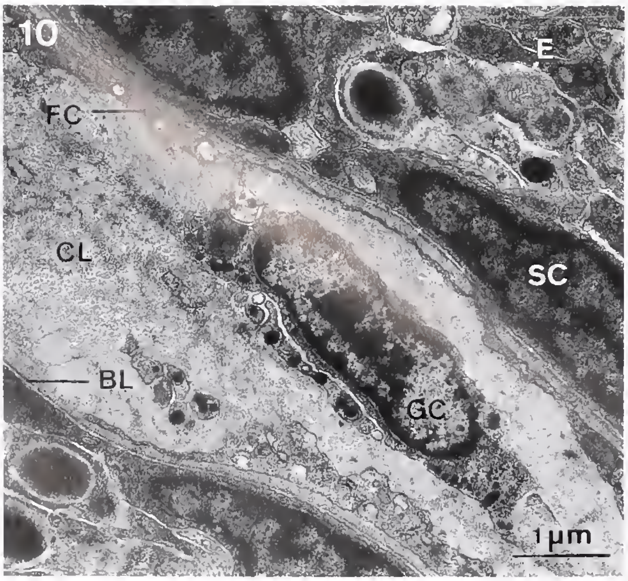
10
E
FC
CL
SC
BL
GC
1 µm

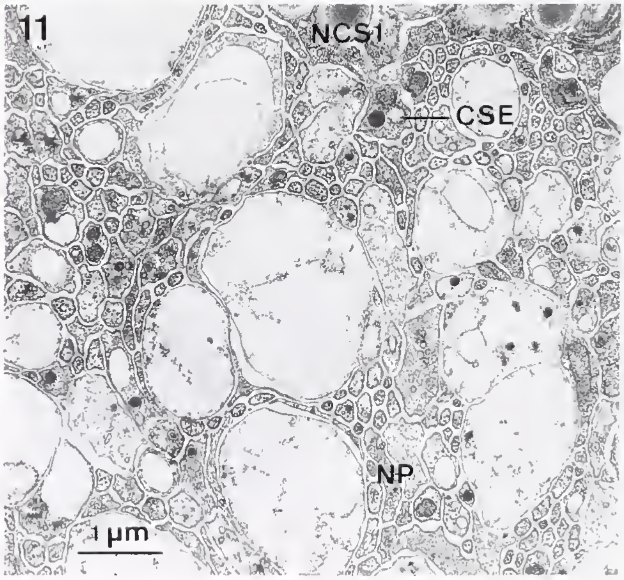
11
NCS1
CSE
NP
1 µm

granulocytes described by Wood and Cavey (1981) in the podial mesothelium of the asteroid *Stylasterias forreri*.

The connective tissue layer, which occupies most of the volume of the disk, is made of an amorphous ground substance that encloses collagen fibers and elongated cells with an electron-dense cytoplasm, which may be fibrocytes. Granulocytes resembling those in the mesothelium are also present (Fig. 10); they contain many electron-dense, spherical to ellipsoidal granules, 100 to 250 nm in diameter. The connective tissue layer consists mainly of a circular structure—the terminal plate—that underlies and supports the whole disk (Fig. 6). The center of the plate is much thinner than its margin, which forms a thickened rim continuous, proximally, with the cylindrical connective tissue sheath of the stem. Distally, the surface of the terminal plate is drawn out into a series of radial laminae that thrust into the epidermis of the disk (Fig. 7). Within these laminae, collagen fibers are arranged longitudinally (Fig. 10). A few micrometers before reaching the apical surface of the podium, the distal edge of each lamina divides into numerous collagen-rich sheets that insinuate between the epidermal cells and attach apically to the support cells of the epidermis.

The nervous tissue of the disk consists chiefly of two components. First, at the base of the disk, the nerve plexus of the stem is thickened to form the nerve ring (Fig. 6). It comprises nerve cell bodies as well as numerous neurites that contain mitochondria, microtubules, and clear or dense-core vesicles. Second, the nerve ring gives off radial branches that extend over the proximal surface of the terminal plate, where they run between the radial connective laminae. The radial nerve strands are made up of neurites that run mainly in a plane parallel to the apical surface of the podium (Fig. 11). Small bundles of neurites may also be observed between the basal parts of the epidermal secretory cells.

Disk epidermis. In both *A. rubens* and *M. glacialis*, the disk epidermis is made up of five cell types: nonciliated secretory cells (NCS cells) of two different types (NCS1 and NCS2); ciliated secretory cells (CS cells); nonsecretory ciliated cells (NSC cells); and support cells (Figs. 12–15). All of these cells are connected apically by junctional complexes made up of a distal zonula adherens and a proximal septate desmosome. In the epidermis, support cells are the most numerous and form a supportive mesh-

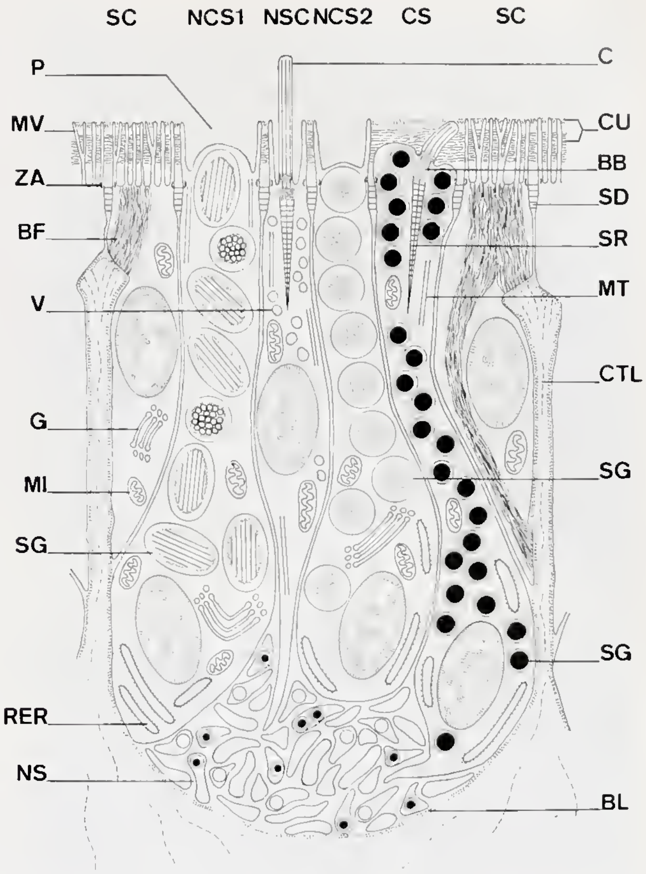

Figure 12. Reconstruction of a transverse section through a radial epidermal strip located between two adjacent connective tissue laminae (not to scale). BB, basal body; BF, bundle of filaments; BL, basal lamina; C, cilium; CS, ciliated secretory cell; CTL, connective tissue lamina; CU, cuticle; G, Golgi zone; MI, mitochondrion; MT, microtubule; MV, microvillus; NCS1, type 1 nonciliated secretory cell; NCS2, type 2 nonciliated secretory cell; NS, nerve strand; NSC, nonsecretory ciliated cell; P, pore; RER, rough endoplasmic reticulum cisternae; SC, support cell; SD, septate desmosome; SG, secretory granule; SR, striated rootlet; V, vesicle; ZA, zonula adherens.

Figures 6–11. Fine structure of the disk of locomotory podia of *Asterias rubens* and *Marthasterias glacialis*. AL, adluminal cell; BL, basal lamina; BM, bundle of myofilaments; C, cilium; CL, connective tissue lamina; CSE, ciliated secretory cell tapered basal end; E, epidermis; FC, fibrocyte-like cell; GC, granulocyte; L, ambulacral lumen; M, mesothelium; N, nucleus; NCS1, type 1 nonciliated secretory cell; NP, nerve processes; NR, nerve ring; NS, nerve strand; SC, support cell; SG, secretory granule; TP, terminal plate; ZA, zonula adherens.

Figure 6. Longitudinal section through the disk (*M. glacialis*).
Figure 7. Transverse section through the disk (*M. glacialis*).
Figure 8. Longitudinal section through the mesothelium (*M. glacialis*).
Figure 9. Glandular cell of the mesothelium (*A. rubens*).
Figure 10. Transverse section through a connective tissue lamina (*M. glacialis*).
Figure 11. Disk nerve strand (*M. glacialis*).

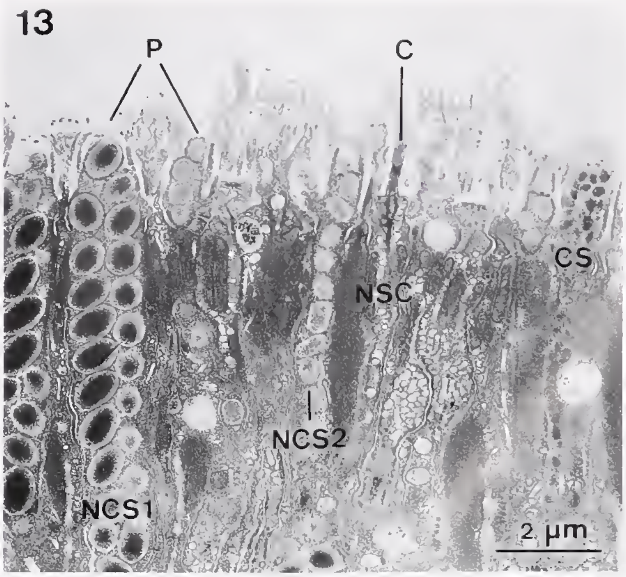
13
P
C
CS
NSC
NCS2
NCS1
2 μm

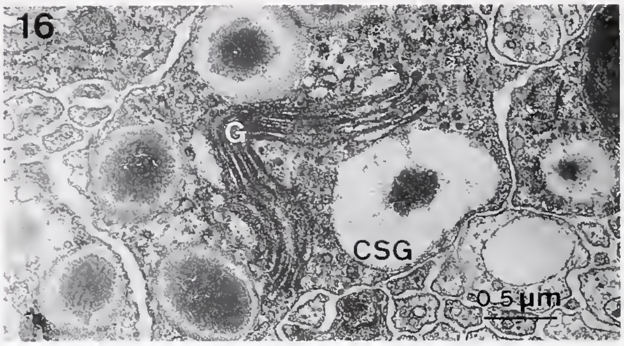
16
G
CSG
0.5 μm

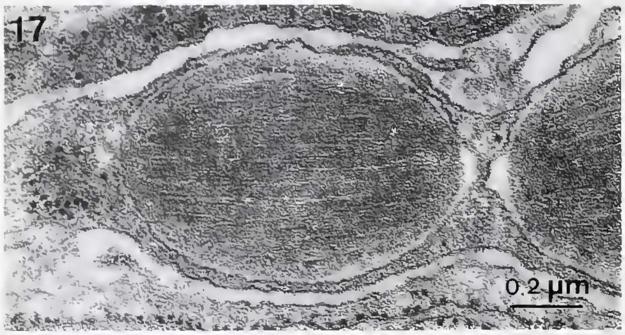
17
0.2 μm

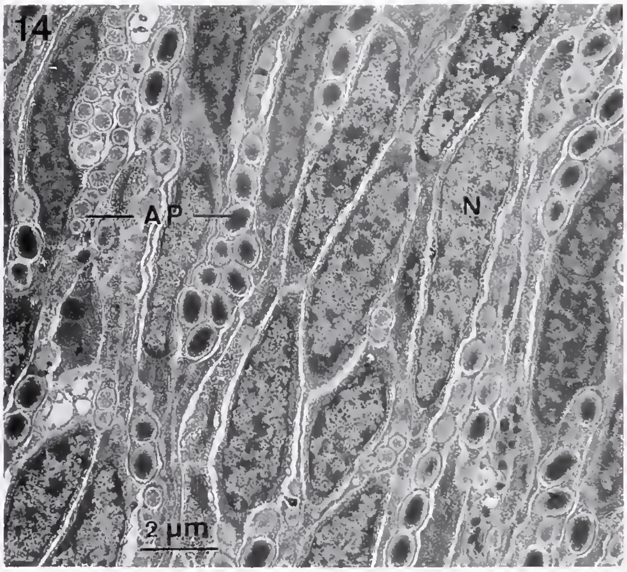
14
AP
N
2 μm

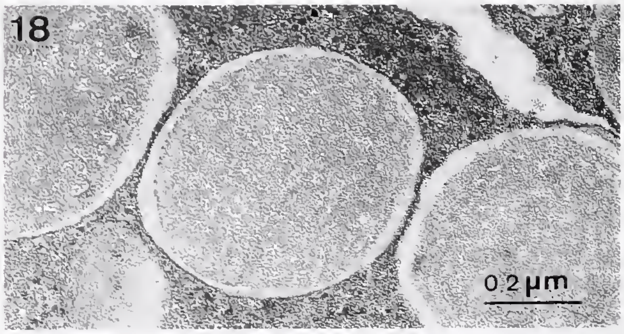
18
0.2 μm

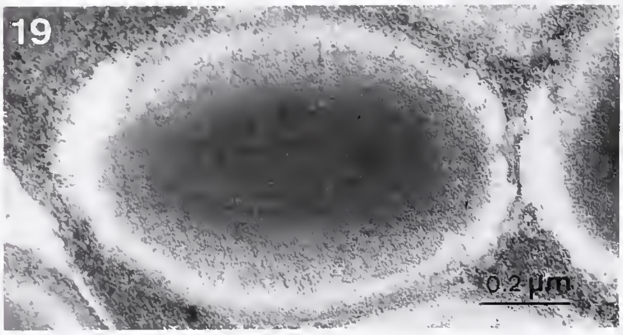
19
0.2 μm

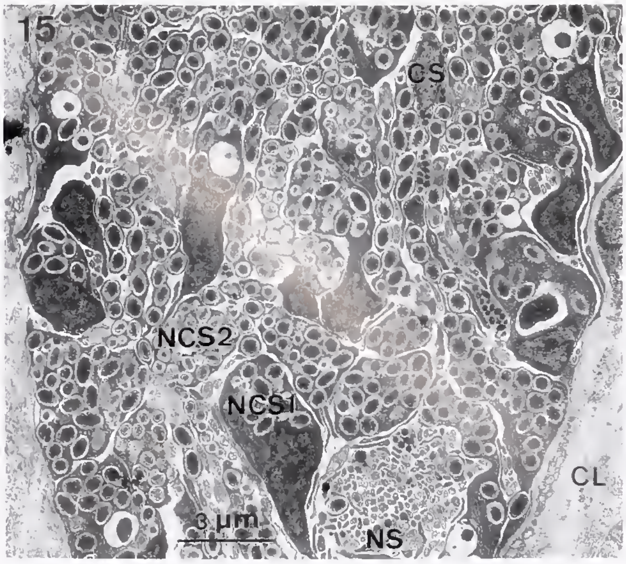
15
CS
NCS2
NCS1
CL
3 μm
NS

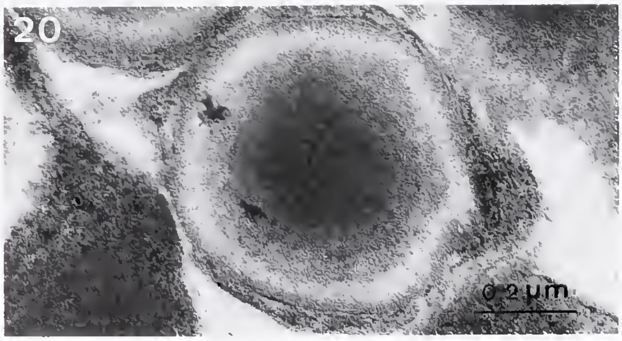
20
0.2 μm

work in which the other cell types are homogeneously distributed; the relative proportion of NCS1, NCS2, CS, and NSC cells is, respectively, 4:4:1:2.

Nonciliated secretory cells (NCS1 and NCS2 cells) are about 250 μm long and flask-shaped. Their enlarged cell bodies are located basally, at the bottom of the grooves made up by adjacent connective laminae and close to the radial nerve strands (Figs. 12, 15). Each cell body sends out a long apical process that reaches the apex of the podium (Figs. 12–14). The cytoplasm of both the cell body and the apical process is filled with densely packed membrane-bound secretory granules. In both NCS1 and NCS2 cells, the material enclosed in these secretory granules stains with alcian blue pH 2.6. The cytoplasm of the cell body also contains a well-developed Golgi apparatus, mitochondria, and cisternae of rough endoplasmic reticulum (RER) that are sometimes distended and filled with amorphous material (Fig. 16, 21). Developing secretory granules are closely associated with Golgi membranes and RER cisternae, suggesting that these organelles are involved in the synthesis of the contents of the granules. Besides secretory granules, the cytoplasm of the apical process contains longitudinally arranged peripheral microtubules. At the end of the apical processes, the granules are extruded through a duct delimited by a ring of microvilli and opening onto the disk surface as a cuticular pore (Figs. 12, 13). These pores correspond to those observed on SEM pictures of the disk surface (Figs. 3, 5).

The secretory granules of NCS1 cells are ellipsoids about 1 μm long and 0.6 μm in diameter (Figs. 17–20). They have a complex ultrastructure. Most of their volume is occupied by a bundle of parallel rods about 30 nm in diameter. These rods are somewhat more numerous in the granules of *A. rubens* (about 180, Fig. 18) than in those of *M. glacialis* (about 120, Fig. 20). In the latter, the rods appear to be embedded in material that is more electron-dense. Each bundle of rods is surrounded by a ring of the same density as the rods and separated from the granule membrane by a clear belt. The secretory granules of NCS2 cells are spherical in *A. rubens* (about 550 nm in diameter, Fig. 21) and slightly ellipsoidal in *M. glacialis* (about 500 nm in length and 300 nm in diameter, Fig. 22). They contain electron-lucent, finely granular material surrounded by a clear belt. In *M. glacialis,* some of these granules have an inner core that is more electron-dense (Fig. 22).

Ciliated secretory cells (CS cells) have the same shape and size as NCS cells. They possess an enlarged nucleus-containing cell body and a long and narrow apical process that ends with a bulge just beneath the cuticle (Figs. 12, 13, 23). The entire cytoplasm of the cell (basal part, process, and bulge) is filled with membrane-bound secretory granules. These granules are spherical in *A. rubens,* 300–450 nm in diameter (Fig. 24). They enclose an electron-dense homogeneous material surrounded by a thin, clear belt. In *M. glacialis,* the granules are spherical to ellipsoidal, 250–300 nm in diameter (Fig. 23). They contain an electron-dense fibrillar core surrounded by a less dense ring. The cytoplasm contains many mitochondria and RER cisternae. The apex of the CS cells is devoid of microvilli but bears a subcuticular cilium with a striated rootlet (Fig. 23). The very basal part of the cell is tapered and thrusts into the radial nerve strand (Figs. 11, 12).

Nonsecretory ciliated cells (NSC cells) are narrow and have a centrally located nucleus (Figs. 12, 13). Their cytoplasm includes mitochondria, small, clear vesicles of various shapes and sizes, and longitudinally arranged microtubules (Fig. 25). Their characteristic feature is a single short cilium (about 3 μm long) whose apex protrudes into the outer medium. The cilium has a regular 9 × 2 + 2 arrangement of microtubules and possesses a striated rootlet. It is surrounded by a ring of nine microvilli. These cilia are visible on SEM pictures of the disk surface (Fig. 3). NSC cells, like CS cells, terminate within the radial nerve strands.

Support cells have a centrally located nucleus (Figs. 12, 14). Their cytoplasm contains mitochondria and some clear vacuoles. Their apical surface bears numerous microvilli, and their base contacts the basal lamina of the epidermis either on the bottom of the grooves formed by adjacent connective laminae (thus traversing the radial nerve strands) or on the laminae themselves. One longitudinal bundle of intermediate filaments traverses the cell and joins its apical and basal membranes (Figs. 12, 25).

Figures 13–20. Fine structure of the disk epidermis of locomotory podia of *Asterias rubens* and *Marthasterias glacialis.* AP, NCS cell upper process; C, cilium; CS, ciliated secretory cell; CL, connective tissue lamina; CSG, condensing secretory granule; G, Golgi zone; N, nucleus; NCS1, type 1 nonciliated secretory cell; NCS2, type 2 nonciliated secretory cell; N, nucleus; NS, nerve strand; NSC, nonsecretory ciliated cell; P, pore.

Figures 13–15. Longitudinal sections through the disk epidermis (apex, mid part, and basal part; respectively) (*M glacialis*).

Figure 16. Nucleus-containing basal part of a type 1 nonciliated secretory cell (NCS1 cell) (*M. glacialis*).

Figures 17, 18. NCS1 cell secretory granules in *A rubens* (longitudinal and transverse section, respectively).

Figures 19, 20. NCS1 cell secretory granules in *M. glacialis* (longitudinal and transverse section, respectively).

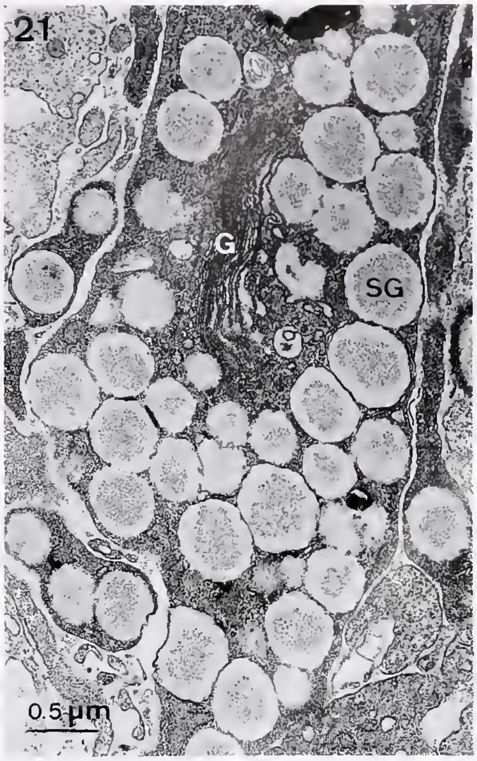

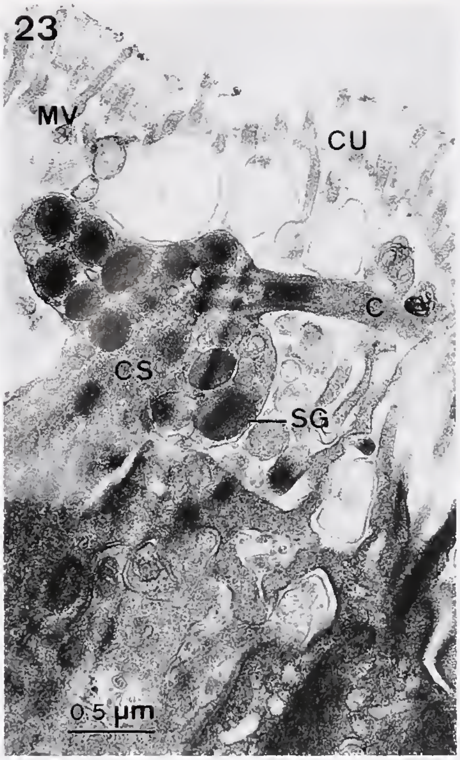

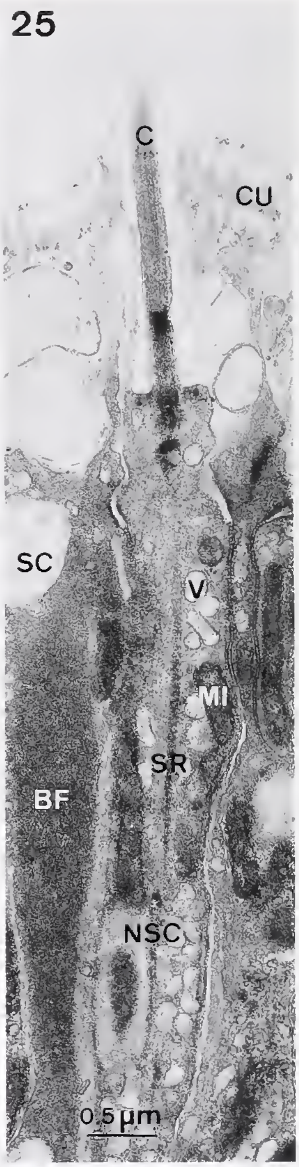

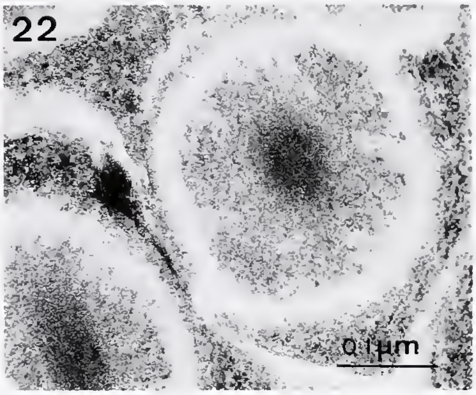

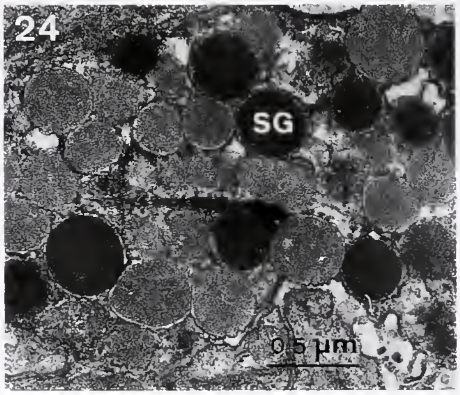

Figures 21–25. Fine structure of the disk epidermis of locomotory podia of *Asterias rubens* and *Marthasterias glacialis.* BF, bundle of filaments; C, cilium; CS, ciliated secretory cell; CU, cuticle; G, Golgi zone; MI, mitochondrion; MV, microvilli; NSC, nonsecretory ciliated cell; SC, support cell; SG, secretory granule; SR, striated rootlet; V, vesicle.

Figure 21. Nucleus-containing basal part of a type 2 nonciliated secretory cell (NCS 2 cell) (*A. rubens*).

Figure 22. NCS2 cell secretory granule (*M. glacialis*).

Figure 23. Apical bulge of a ciliated secretory cell (CS cell) (*M. glacialis*).

Figure 24. CS cell secretory granules (*A. rubens*).

Figure 25. Apex of a nonsecretory ciliated cell (*M. glacialis*).

A few micrometers before reaching the disk surface, support cells enlarge, forming an attachment area for the collagen fibers of the connective tissue sheets.

A two-layered cuticle covers the epidermal cells of the disk (Figs. 12, 23, 30). The cuticle is traversed by the epidermal cell microvilli and by the tips of the cilia of NSC cells, and is regularly interrupted by the secretory pores of NCS cells. It consists of an internal filamentous layer (about 600 nm thick in *A. rubens* and 350 nm in *M. glacialis*) and an external granular layer (about 200 nm thick in *A. rubens* and 100 nm in *M. glacialis*). The external layer is strongly labeled with ruthenium red, showing that it bears many negatively charged sites (Luft, 1971). The cuticle is separated from the epidermis by a subcuticular space that is wider in *M. glacialis* than in *A. rubens.*

Footprints and attached podia

The footprints left by the podia of both *A. rubens* and *M. glacialis* have the same shape and the same diameter as the podial disks (Fig. 26). Almost the whole surface of the print consists of adhesive material, except for some small areas that lack it (*i.e.*, one central circular zone and a few radial or concentric narrow stripes). Other footprints, less numerous, are completely full of adhesive material. Three different aspects of the adhesive material can be recognized; these may occur together in the same footprint and probably represent three successive stages in the accumulation of adhesive during the secretion process. In the first stage, the adhesive material has the shape of a network with a mesh of about 3 μm (Fig. 27). The second stage is characterized by the addition of secretory material that gives the footprint a felt-like appearance (Fig. 28). In the third stage, the adhesive material becomes still thicker, forming a homogeneous layer that completely covers the glass substratum (Fig. 29).

Smaller prints (Fig. 30) observed on the edges of the coverslips correspond to podia that adhered by the margin of their disk. The adhesive strength produced by these podia was equivalent to that of podia attached by their entire disk.

Electron micrographs of attached podia of *A. rubens* and *M. glacialis* reveal secretory material forming an adhesive layer between the podium and the substratum (Fig. 31)—more exactly, between the cuticle and the thin primary film covering the Spurr block. (The film stains heavily with ruthenium red, demonstrating that it bears many negatively charged sites; Luft, 1971). The material of the adhesive layer is a compact fibrillar matrix (Fig. 31). It binds ruthenium red, though the labeling is weaker than on both the primary film and the external layer of the cuticle.

The adhesive material clearly arises from the two types of nonciliated secretory cells (NCS1 and NCS2 cells; Figs. 30–33). The material enclosed in their most apical secretory granules (the outermost few, ranging from 1 up to 10 in some NCS1 cells) appears to swell, losing its usual aspect (Fig. 32). The apical cell membrane and the membranes of the secretory granules vanish, and the granule content is extruded through the cuticular pores (Fig. 33) in the space between the podium and the substratum, forming the adhesive layer.

As for the CS cells, they have the same morphology in attached and unattached podia (Fig. 34); *i.e.*, they do not appear to have extruded any of their secretory granules.

Discussion

Individuals of *Asterias rubens* and *Marthasterias glacialis* use their podia in locomotion and anchorage, and to open the bivalve mollusks on which they feed (Lawrence, 1987). These podia consist of a cylindrical stem topped by a specialized disk. The stem and the disk together form a functional unit: the stem allows the podium to lengthen, flex, and retract—through the action of the podial retractor muscle on the ambulacral fluid—and the disk allows it to adhere to the substratum.

Podial adhesion: mechanical versus chemical attachment

The disk has the classical tissue stratification of echinoderm podia; that is, from the inside to the outside, a mesothelium, a connective tissue layer, a nerve plexus, and an epidermis (Kawaguti, 1964; Florey and Cahill, 1977; Wood and Cavey, 1981).

In the mesothelium, myoepithelial cells arrange to form three muscle systems: the retractor, the levator, and the radial systems. The levator and the radial muscle systems have been implicated in a sucker-like mechanical operation of the disk; the former providing the suction and the latter releasing it (Smith, 1947).

Suction has often been regarded as the primary means of podial adhesion in seastars. Paine (1926), who studied the podia of *Asterias vulgaris*, concluded that 56% of podial attachment would be contributed by suction and the rest by adhesive secretions. Recently, Smith (1991) reevaluated the adhesive strength of suckers in water and suggested that suction may have been underestimated in the adhesive organs of several invertebrates, including sea stars. On the other hand, Thomas and Hermans (1985) found that podia of the sea star *Leptasterias hexactis* adhered very strongly to a fine-meshed, stainless steel plankton screen that precluded the podia from using suction. These workers concluded that, although sea star podia may use suction, it is a secondary adjunct to the adhesion established by secretions.

Data presented in this report support this second hypothesis: first, many epidermal secretory cells cover the entire apical surface of the disk; second, the footprints are completely (or almost completely) full of adhesive material; and third, podia may adhere strongly with only the margin of their disk (leaving crescent-shaped footprints). These complementary features argue for an adhesive process principally mediated by secretion. In this event, the musculature of the disk would act to modify the apical surface of the disk, molding it exactly to that of the substratum. However, suction cannot be ruled out altogether; *i.e.*, the muscular equipment in the podial disk can certainly develop suction sufficient to reinforce adhesion (Smith, 1991).

Comparison with other echinoderms

The disk epidermis consists of five cell types: two types of nonciliated secretory cells containing granules whose

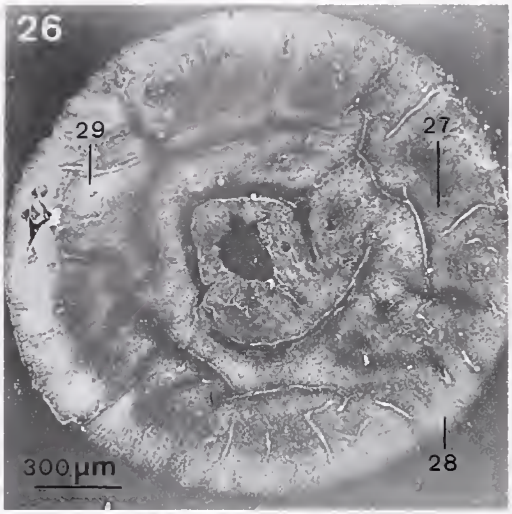
26
29
27
28
300 µm

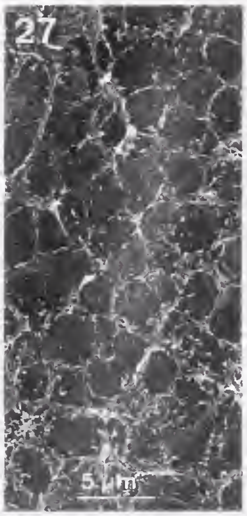
27
5 µm

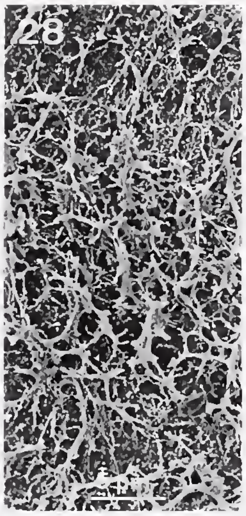
28

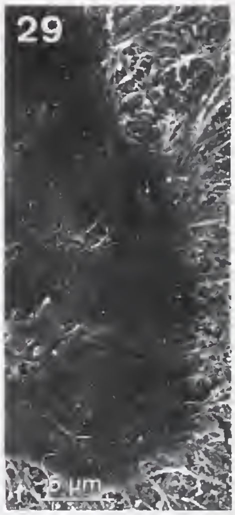
29
5 µm

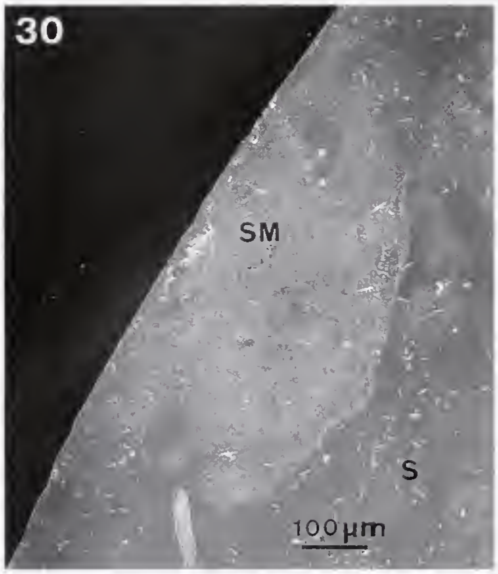
30
SM
S
100 µm

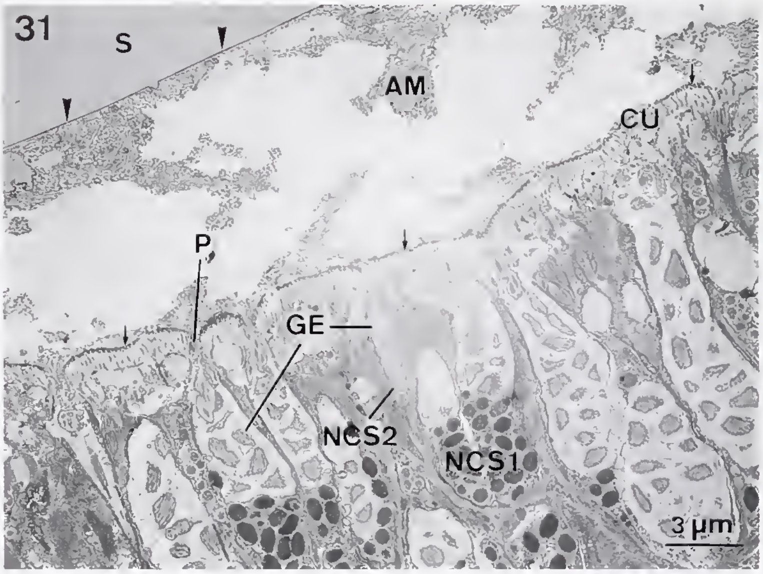
31
S
AM
CU
P
GE
NCS2
NCS1
3 µm

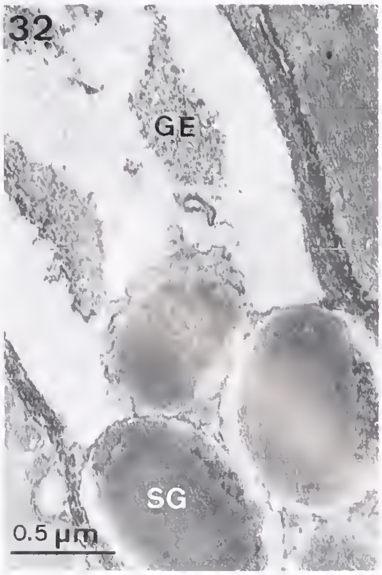
32
GE
SG
0.5 µm

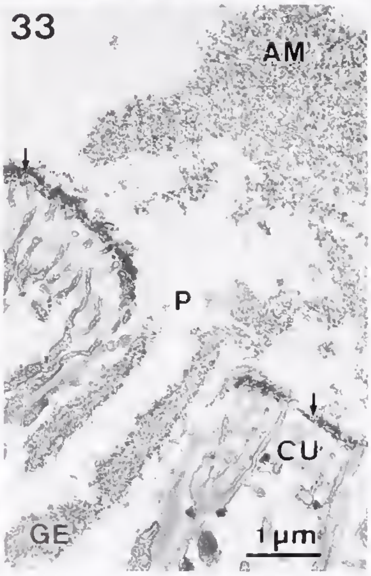
33
AM
P
CU
GE
1 µm

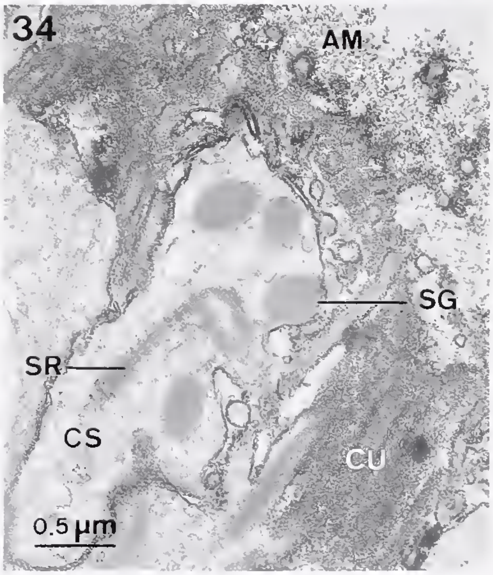
34
AM
SG
SR
CS
CU
0.5 µm

content is at least partly mucopolysaccharidic (NCS1 and NCS2 cells); ciliated secretory cells containing granules of unknown content (CS cells); nonsecretory ciliated cells (NSC cells); and support cells. The cilia of CS cells are subcuticular, whereas those of the NSC cells, although also short and rigid, traverse the cuticle and protrude into the outer medium. All of these cells are closely associated with well-developed nerve strands.

In both species, the two types of NCS cells occurring in the disk epidermis resemble each other morphologically; moreover, the tinctorial affinities of their secretory granules are also similar. This resemblance probably misled earlier students of asteroid podia, for they described only the NCS1 cells and failed to recognize the NCS2 cells (Harrison and Philpott, 1966; Souza Santos and Silva Sasso, 1968; McKenzie, 1988); only Chaet (1965) described the two types of NCS cells in the disk epidermis of *Asterias forbesi*. The NCS cells of *A. rubens* and *M. glacialis* are typical "apical duct" cells (according to the terminology of Flammang and Jangoux, 1992); *i.e.*, their secretory granules are extruded through a duct that is walled by microvilli and opens as a pore onto the secretory surface. Such cells have already been observed in the podia of paxillosid asteroids, which end not with a disk, but with a conical tip (Engster and Brown, 1972); in ophiuroid podia (Ball and Jangoux, 1990); and in the locomotory podia of several holothuroid species (Harrison, 1968; Flammang and Jangoux, 1992). In the podia of all these species, NCS cells are thought to be adhesive in function.

Both ciliated secretory cells (CS cells) and nonsecretory ciliated cells (NSC cells) terminate within the nerve strands. This, together with the fact that they both bear a short and rigid cilium, is indicative of their nervous origin and sensory function. In addition, CS cells are filled with secretory granules and, therefore, may be considered neurosecretory-like. Ciliated cells morphologically similar to these two cell types occur in the podial adhesive areas of most echinoderm species.

CS cells are remarkably similar in all echinoderm species whose podia have been examined. In all cases they contain small electron-dense granules and often present a subcuticular cilium (Engster and Brown, 1972; McKenzie, 1987; Ball and Jangoux, 1990; Flammang *et al.*, 1991; Flammang and Jangoux, 1992, 1993). CS cells of *A. rubens* and *M. glacialis* are, however, peculiar because they possess a large apical bulge instead of the more common granule-filled, microvillar-like cell processes (Flammang *et al.*, 1991; Flammang and Jangoux, 1993); and also because of the large size of their granules. Some workers have considered CS cells to be de-adhesive, although the way in which they fulfill this function remains obscure. Ball and Jangoux (1990) proposed that CS cell secretions could act as neurotransmitters controlling or terminating the release of the adhesive secretion. On the other hand, Flammang and Jangoux (1993) suggested that their granule content would be released into the outer medium, acting directly as a de-adhesive.

NSC cells are monociliated; their cilium traverses the cuticle and protrudes into the outer medium. These cells, like CS cells, are almost identical in the podia of all echinoderm species studied so far (Engster and Brown, 1972; Burke, 1980; McKenzie, 1987; Ball and Jangoux, 1990; Flammang *et al.*, 1991; Flammang and Jangoux, 1992, 1993).

Comparison with other taxa

Many marine benthic organisms are equipped with particular secretory organs that allow them to adhere to the substratum. Three forms of adhesion may be distinguished: (1) loose adhesion involving mucus and permitting simultaneous adhesion and movement along the substratum (*e.g.*, the foot secretions of some mollusks); (2) permanent adhesion involving the secretion of a cement (*e.g.*, the attachment of barnacles on rocks); and (3) temporary adhesion allowing an organism to attach strongly but momentarily to the substratum (Tyler, 1988).

Among the adhesive organs of marine invertebrates, duo-gland organs, enclosing two types of secretory cells (*viz.*, cells releasing an adhesive secretion and cells releasing a de-adhesive secretion) and involved in temporary attachment, are morphologically the closest to echinoderm podial adhesive systems. These duo-gland adhesive organs are very frequently found in small invertebrates inhabiting

---

Figures 26–34. Footprints and attached podia of *Asterias rubens* and *Marthasterias glacialis*. Arrowheads indicate the primary film; arrows indicate the external layer of the cuticle. AM, adhesive material; CS, ciliated secretory cell; CU, cuticle; GE, granules in the process of extrusion; NCS1, type 1 nonciliated secretory cell; NCS2, type 2 nonciliated secretory cell; P, pore; S, substratum; SG, secretory granule; SM, secretory material; SR, striated rootlet.

Figure 26. Footprint of *M. glacialis*.

Figures 27–29. The three aspects of the secretory material (*M. glacialis*).

Figure 30. Crescent-shaped footprint left by the margin of a podium of *A. rubens* on the edge of a coverslip.

Figure 31. Attached podium of *A. rubens*.

Figures 32, 33. Apical part and secretory pore, respectively, of a NCS1 cell (*A. rubens*).

Figure 34. Ciliated secretory cell (*M. glacialis*).

the interstitial environment—for example, in Turbellaria (Tyler, 1976); in Gastrotricha (Tyler and Rieger, 1980); in Nematoda (Adams and Tyler, 1980); and in Polychaeta (Gelder and Tyler, 1986). In every species studied, the adhesive organs contain two types of closely associated secretory cells. Cells of the first type are specialized epidermal cells similar to echinoderm NCS cells, and they release an adhesive material. Cells of the second type are derived from sensory nerve cells and resemble echinoderm CS cells; they are de-adhesive in function. They release their secretory granules through a pore adjoining the secretory pore of the adhesive cell.

A duo-gland adhesive system has also been described, recently, in the captacula (*i.e.*, the food-collecting tentacles) of scaphopod mollusks (Byrum and Ruppert, 1994), still widening the distribution range of this adhesive system in marine invertebrates. In the species examined, *Graptacme calamus*, the secretory cells look strikingly similar to echinoderm NCS and CS cells.

A model for the adhesive mechanism of sea star podia

Epidermal cells of the podial disk of *A. rubens* and *M. glacialis* are presumably involved in adhesion and de-adhesion and function as a duo-gland adhesive system, as proposed by Hermans (1983). In the functional model we propose, adhesive and de-adhesive secretions are produced by NCS and CS cells, respectively.

We consider the two types of NCS cells to be adhesive because they are the only secretory cells having extruded some of their secretory granules in attached podia. Moreover, these cells have been suggested to be adhesive in every podium so far studied. Their secretions form the adhesive layer joining the podium to the substratum; this layer remains on the substratum as a footprint after the podium has become detached.

The de-adhesion would be due to the material enclosed in the granules of CS cells. Indeed, there must be a detachment mechanism that is under control of the animal and allows the podia to easily become detached from the substratum. The CS cells are the best candidates for this function. In *A. rubens* and *M. glacialis*, the way their secretions are exocytosed is enigmatic; but, by analogy with echinoid CS cells, we believe that their secretory granules are extruded and act at the surface of the disk. This de-adhesive material would also prevent particles from accumulating on the adhesive surface of the disk.

All of these secretions are presumably controlled by stimulation of the two types of ciliated cells (receptor cells), which then interact with the secretory cells by means of the nerve strands. Because the cuticle-protruding cilia of NSC cells are the first to contact the substratum, it is likely that they trigger NCS cell secretion. On the other hand, the release of secretory granules by the CS cells would be induced by a stimulation of their subcuticular cilia.

The significance of two types of adhesive cells in the podial disk epidermis of both *A. rubens* and *M. glacialis* is obscure. Furthermore, asteroid podia are not exceptions: ophiuroid podia also have two types of adhesive cells (Ball and Jangoux, 1990), as do holothuroid locomotory podia (Flammang and Jangoux, 1992); and in non-echinoderm invertebrates, the co-occurrence of two types of adhesive cells has been reported in a species of turbellarians (Ehlers, 1989). Maybe the two secretions combine to form a special type of adhesive secretion. Another possibility is that one type of adhesive cell is used only in locomotion on horizontal substrata, whereas both types are necessary during locomotion on vertical substrata or for anchorage, when a stronger adhesive bond is required.

Tyler (1988) suggested that most adhesives in marine organisms involve an association of protein and glycans. In both *A. rubens* and *M. glacialis*, the adhesive secretion is probably a polysaccharide-protein complex, with the main component being an acid mucopolysaccharide (positive reaction of NCS cells with alcian blue pH 2.6, ruthenium red labeling of the adhesive layer between podia and substratum). We failed to detect proteins, but Perpeet and Jangoux (1973) found a protein component in NCS cell secretory granules of *A. rubens*. This adhesive material could link the negatively charged cuticle, through divalent cations, to the negatively charged primary film. Such a mode of adhesion has already been described in bacteria (Corpe, 1974; Marshall, 1974) and diatoms (Cooksey, 1981), and has been proposed in several turbellarians and archiannelids (Martin, 1978). This notion is, however, contrary to the model that Thomas and Hermans (1985) proposed for asteroid podia, in which acid mucopolysaccharides are considered to be de-adhesive in function. In the two species studied in this work, the composition of the de-adhesive secretion remains unknown, as it does in all marine invertebrates (Tyler, 1988).

Acknowledgments

We thank Professor P. Lassere for providing facilities at the Observatoire Océanologique de Roscoff (Brittany, France); Professor J. A. Heuson-Stiennon for the use of the transmission electron microscope; and E. Bricourt for technical assistance. Work was supported by FRFC contract number 2.4549.91. Contribution of the "Centre Interuniversitaire de Biologie Marine" (CIBIM).

Literature Cited

Adams, P. J. M., and S. Tyler. 1980. Hopping locomotion in a nematode: functional anatomy of the caudal gland apparatus of *Theristus caudasaliens* sp. n. *J. Morphol.* **164:** 265–285.

Ball, B., and M. Jangoux. 1990. Ultrastructure of the tube foot sensory-secretory complex in *Ophiocomina nigra* (Echinodermata, Ophiuroidea). *Zoomorphology* **109:** 201–209.

Burke, R. D. 1980. Podial sensory receptors and the induction of metamorphosis in echinoids. *J. Exp. Mar. Biol. Ecol.* **47:** 223–234.

Byrum, C. A., and E. E. Ruppert. 1994. The ultrastructure and functional morphology of a captaculum in *Graptacme calamus* (Mollusca, Scaphopoda). *Acta Zool. (Stockh.)* **75:** 37–46.

Chaet, A. B. 1965. Invertebrate adhering surfaces: secretions of the starfish, *Asterias forbesi*, and the coelenterate, *Hydra pirardi*. *Ann. N. Y. Acad. Sci.* **118:** 921–929.

Characklis, W. G. 1981. Fouling biofilm development: a process analysis. *Biotechnol. Bioeng.* **23:** 1923–1960.

Cooksey, K. E. 1981. Requirement for calcium in adhesion of a fouling diatom to glass. *Appl. Environ. Microbiol.* **41:** 1378–1382.

Corpe, W. A. 1974. Microfouling: the role of primary film forming marine bacteria. Pp 598–609 in *Fouling Biology: Proc. 3rd. Int. Cong. on Marine Corrosion and Fouling*, R. F. Acker, B. F. Brown, J. R. DePalma, and W. P. Iverson, eds. Northwestern University Press, Evanston, IL.

Ehlers, U. 1989. Duo-gland adhesive systems of *Schizochilus caecus* L'Hardy (Platyhelminthes, Kalyptorhynchia). *Microfauna Mar.* **5:** 243–260.

Engster, M. S., and S. C. Brown. 1972. Histology and ultrastructure of the tube foot epithelium in the phanerozonian starfish, *Astropecten*. *Tissue Cell* **4:** 503–518.

Flammang, P., and M. Jangoux. 1992. Functional morphology of the locomotory podia of *Holothuria forskali* (Echinodermata, Holothuroida). *Zoomorphology* **111:** 167–178.

Flammang, P., and M. Jangoux. 1993. Functional morphology of coronal and peristomeal podia in *Sphaerechinus granularis* (Echinodermata, Echinoida). *Zoomorphology* **113:** 47–60.

Flammang, P., C. De Ridder, and M. Jangoux. 1991. Ultrastructure of the penicillate podia of the spatangoid echinoid *Echinocardium cordatum* (Echinodermata) with special emphasis on the epidermal sensory-secretory complexes. *Acta Zool. (Stockh.)* **72:** 151–158.

Florey, E., and M. A. Cahill. 1977. Ultrastructure of sea urchin tube feet. Evidence for connective tissue involvement in motor control. *Cell Tissue Res.* **177:** 195–214.

Ganter, P., and G. Jollès. 1969–1970. *Histochimie normale et pathologique*, Vols. 1, 2. Gauthiers-Villars, Paris.

Gelder, S. R., and S. Tyler. 1986. Anatomical and cytochemical studies on the adhesive organs of the ectosymbiont *Histriobdella homari* (Annelida: Polychaeta). *Trans. Am. Microsc. Soc.* **105:** 348–356.

Harrison, G. 1968. Subcellular particles in echinoderm tube feet. II. Class Holothuroidea. *J. Ultrastruct. Res.* **23:** 124–133.

Harrison, G., and D. Philpott. 1966. Subcellular particles in echinoderm tube feet. I. Class Asteroidea. *J. Ultrastruct. Res.* **16:** 537–547.

Hermans, C. O. 1983. The duo-gland adhesive system. *Oceanogr. Mar. Biol. Ann. Rev.* **21:** 281–339.

Kawaguti, S. 1964. Electron microscopic structure of the podial wall of an echinoid with special references to the nerve plexus and the muscle. *Biol. J. Okayama Univ.* **10:** 1–12.

Lawrence, J. M. 1987. *A Functional Biology of Echinoderms.* Croom Helm, London.

Luft, J. H. 1971. Ruthenium red and violet. II. Fine structural localization in animal tissues. *Anat. Rec.* **171:** 369–416.

Marshall, K. C. 1974. Mechanism of adhesion of marine bacteria to surfaces. Pp 625–632 in *Fouling Biology: Proc. 3rd. Int. Cong. on Marine Corrosion and Fouling*, R. F. Acker, B. F. Brown, J. R. DePalma, and W. P. Iverson, eds. Northwestern University Press, Evanston, IL.

Martin, G. G. 1978. Ciliary gliding in lower invertebrates. *Zoomorphologie* **91:** 249–261.

McKenzie, J. D. 1987. The ultrastructure of the tentacles of eleven species of dendrochirote holothurians studied with special reference to surface coats and papillae. *Cell Tissue Res.* **248:** 187–199.

McKenzie, J. D. 1988. The ultrastructure of tube foot epidermal cells and secretions: their relationship to the duo-glandular hypothesis and the phylogeny of the echinoderm classes. Pp 287–298 in *Echinoderm Phylogeny and Evolutionary Biology*, C. R. C. Paul and A. B. Smith, eds. Clarendon Press, Oxford.

Nachtigall, V. 1974. *Biological Mechanisms of Attachment. The Comparative Morphology and Bioengineering of Organs for Linkage, Suction, and Adhesion* Springer-Verlag, Berlin.

Nichols, D. 1966. Functional morphology of the water-vascular system. Pp 219–240 in *Physiology of Echinodermata*, R. A. Boolootian, ed. Interscience Publishers, New York.

Paine, V. L. 1926. Adhesion of the tube feet in starfishes. *J. Exp. Zool.* **45:** 361–366.

Perpeet, C., and M. Jangoux. 1973. Contribution à l'étude des pieds et des ampoules ambulacraires d'*Asterias rubens* (Echinodermata, Asteroidea). *Forma Functio* **6:** 191–209.

Smith, A. M. 1991. Negative pressure generated by octopus suckers: a study of the tensile strength of water in nature. *J. Exp. Biol.* **157:** 257–271.

Smith, J. E. 1937. The structure and function of the tube feet in certain echinoderms. *J Mar Biol. Ass. U K.* **22:** 345–357.

Smith, J. E. 1947. The activities of the tube feet of *Asterias rubens* L. I. The mechanics of movement and of posture. *Quart. J. Microsc. Sci.* **88:** 1–14.

Souza Santos, H., and W. Silva Sasso. 1968. Morphological and histochemical studies on the secretory glands of starfish tube feet. *Acta Anat.* **69:** 41–51.

Thomas, L. A., and C. O. Hermans. 1985. Adhesive interactions between the tube feet of a starfish, *Leptasterias hexactis*, and substrata. *Biol. Bull.* **169:** 675–688.

Tyler, S. 1976. Comparative ultrastructure of adhesive systems in the Turbellaria. *Zoomorphologie* **84:** 1–76.

Tyler, S. 1988. The role of function in determination of homology and convergence—examples from invertebrate adhesive organs. *Fortschr Zool.* **36:** 331–347.

Tyler, S., and G. E. Rieger. 1980. Adhesive organs of the Gastrotricha. I. Duo-gland organs. *Zoomorphologie* **95:** 1–15.

Wood, R. L., and M. J. Cavey. 1981. Ultrastructure of the coelomic lining in the podium of the starfish *Stylasterias forreri*. *Cell Tissue Res.* **218:** 449–473.

Reference: *Biol. Bull.* **187:** 48–54. (August, 1994)

Glutamate Immunoreactivity in Non-neuronal Cells of the Sea Anemone *Metridium senile*

MICHEL ANCTIL* AND JEAN-PASCAL CARETTE

Département de sciences biologiques and Centre de recherche en sciences neurologiques, Université de Montréal, Case postale 6128, Succ. Centre-Ville, Montréal, Québec, Canada H3C 3J7

Abstract. The distribution of glutamate in the tentacles and oral disk of the sea anemone *Metridium senile* was investigated by wholemount immunohistochemistry with the use of a monoclonal antibody raised against the derivatization product γ-L-glutamyl-L-glutamic acid. Immunoreactivity was localized in one class of tentacle nematocysts and on their associated threads. These nematocysts were concentrated at the distal end of tentacles, none being found at the base of tentacles or in the oral disk. Muscle end-feet of epitheliomuscular cells also stained in the longitudinal muscle of tentacle ectoderm. In contrast, immunostaining in the oral disk was confined to ectodermal granule-containing cells overlying the radial muscle. These results support a role for glutamate as an osmolyte precursor in nematocysts but provide little clue as to the functional significance of this amino acid in muscle and gland cells.

Introduction

Glutamate has been identified as an excitatory neurotransmitter in the vertebrate central nervous system (CNS) (Fonnum, 1984; Monaghan *et al.*, 1989) as well as in invertebrates (Duce, 1988; Leake and Walker, 1980). It is established as the excitatory neuromuscular transmitter in arthropods (Usherwood, 1980). Among lower invertebrates, glutamate has been localized by immunohistochemistry in a small population of leech CNS neurons that may be associated with feeding behavior as well as with initiation of swimming (Brodfuehrer and Cohen, 1990, 1992). Glutamate also appears to act as an excitatory neuromuscular transmitter in the flatworm *Hymenolepis diminuta*, and glutamate immunoreactivity has been detected in the longitudinal nerve cord of this species (Webb, 1988; Webb and Eklove, 1989). Thus glutamate appears to be broadly distributed and evolutionarily conserved in the nervous systems of invertebrates.

Because cnidarians are considered to be modern representatives of the earliest organisms known to possess a nervous system (Bullock and Horridge, 1965; Anderson, 1990; Mackie, 1990), it is of interest to know whether amino acid transmitters such as glutamate play a neurotransmitter role in this group. Neuropeptides of the FMRFamide family were identified and localized to neurons in species from all three cnidarian classes: Hydrozoa, Scyphozoa, and Anthozoa (Grimmelikhuijzen *et al.*, 1992, for review; Anderson *et al.*, 1992). Similarly, conventional transmitters such as monoamines were detected in various cnidarians (Carlberg and Rosengren, 1985; De Waele *et al.*, 1987; Chung *et al.*, 1989; Pani and Anctil, 1994), and monoamine-containing neurons were visualized by immunohistochemistry in the anthozoan *Renilla koellikeri* (Umbriaco *et al.*, 1990; Anctil, 1990) and the hydrozoan *Hydra* (Carlberg, 1992; Carlberg and Anctil, 1993, for review). Amino acids, in contrast, have attracted less attention, except recently when taurine was reported to act electrophysiologically as a neurotransmitter on, and to be present within neurons of, the ectodermal motor nervenet of the jellyfish *Cyanea capillata* (Anderson and Trapido-Rosenthal, 1990; Carlberg *et al.*, 1993).

Carlyle (1974) reported that glutamic acid reversibly depressed electrically stimulated contractions of oral margin/sphincter muscle preparations in the sea anemone *Actinia equina*, an effect shown to be pharmacologically specific. McFarlane *et al.* (1990) confirmed this glutamate response on sphincter muscle preparations of the sea anemones *Calliactis parasitica* and *Tealia felina*. Furthermore, Carlyle (1974) produced biochemical evidence for the presence of large amounts of releasable glutamic acid

Received 28 February 1994; accepted 25 May 1994.

*To whom correspondence should be addressed.

in the oral margin of *A. equina.* Taken together, these observations suggest a possible transmitter role for glutamic acid in sea anemones.

An important criterion for validating glutamate as a neurotransmitter substance requires that glutamate be localized within neurons. The present immunocytochemical study was undertaken in an attempt to provide such evidence in the sea anemone *Metridium senile* and to search for a cellular substrate for the above-mentioned modulatory action of glutamate. Using a monoclonal antibody raised against a derivatized glutamate dipeptide, we visualized immunoreactive ectodermal cells, but not neuronal cells, in the tentacles and oral disk of this species.

Materials and Methods

Specimens of the sea anemone *Metridium senile* were obtained from Pacific Bio-Marine Laboratories (Venice, CA) and Marinus Inc. (Long Beach, CA). They were maintained for several months in recirculated and filtered artificial seawater (ASW) at 12–14°C. The animals were starved for at least 2 days before they were anesthetized by gradually replacing the seawater in which they were immersed with a 1:1 mixture of 0.37 *M* $MgCl_2$ and ASW. Several body regions were excised, although the tentacles and oral disk were investigated in the greatest detail.

The immunocytochemical procedure is based on the use of a monoclonal antibody characterized by Madl *et al.* (1986). The antibody, purchased from INCSTAR, was raised in mouse against the dipeptide γ-L-glutamyl-L-glutamic acid (γ-Glu-Glu) conjugated to keyhole limpet hemocyanin *via* glutaraldehyde-borohydride. To convert endogenous glutamate to γ-Glu-Glu, tissues were first immersed in 5% carbodiimide [(1-ethyl-3-dimethylaminopropyl)carbodiimide] (Sigma) freshly made in 0.1 *M* phosphate-buffered saline (PBS, adjusted with NaCl to seawater osmolarity) for 10–25 min at pH 7.2 and 4°C. This was immediately followed by a fixation with 4% glutaraldehyde in PBS for 80 min at pH 7.2 and 4°C. Tissues were rinsed three times in PBS under these conditions over a period of 12–48 h.

Most of the tentacle and oral disk tissues were then processed directly for wholemount immunocytochemistry. Some column and pedal tissue blocks were immersed in a graded series of sucrose (up to 30%) in PBS and embedded in O.C.T. compound (Miles Laboratories). The latter were frozen by immersion in isopentane chilled with dry ice. For tissue sectioning, 15-μm sections were prepared using a Hacker-Bright cryotome and deposited on gelatin-chromalum-coated sections.

For immunocytochemistry of either wholemount preparations or sections, tissues were first incubated in 0.1% H_2O_2 for 10 min to remove endogenous peroxidases, then blocked in 10% normal goat serum diluted in PBS-TX (0.3% Triton-X-100 in PBS) for 20 min. After tissues were rinsed in PBS (3 × 5 min), they were incubated in the primary antibody diluted 1:750 in PBS-TX for 16–24 h at 4°C. After rinsing as above, tissues were incubated for 12–24 h at 4°C in a goat anti-mouse, peroxidase-labeled secondary antibody, diluted 1:100 in PBS-TX. Tissues were rinsed (3 × 5 min) in 0.9% NaCl in 0.05 *M* Tris at pH 7.6, then reacted with 0.5% 3,3′-diaminobenzidine tetrahydrochloride (DAB, Sigma) and 0.01% H_2O_2 in NaCl/Tris buffer for 10–25 min. Sections were mounted in Aquamount (BDH) and wholemounts in glycerol:PBS (3:1).

As a control procedure for the immunostaining, the primary or secondary antibody was omitted on a few tentacle and oral disk preparations from all 13 animals processed in this study. In addition, some wholemounts from four animals were incubated in the primary antibody (diluted 1:750) preadsorbed overnight at 4°C with 1 mg/ml each of γ-Glu-Glu, *N*-acetyl-L-glutamic acid (*N*-Ac-Glu), L-aspartyl-L-glutamic acid (Asp-Glu) or L-glutamic acid (all from Sigma), after centrifugation for 5 min at 14,000 × *g* and retention of the supernatant.

Results

Detection of glutamate immunoreactivity

The following observations are based on wholemount preparations from 11 animals as immunostaining in sections was less well preserved or added no information beyond that available in wholemounts. Three types of immunoreactive elements were detected: ectodermal nematocysts in tentacles (Figs. 1–4), ectodermal muscle cells in tentacles (Fig. 5), and ectodermal granule-containing cells of the oral disk (Figs. 6–7). Only the last type was not detected in all animals examined, being present in oral disk preparations of six animals. No immunostaining was detected in the column and pedal disk of the specimens.

There was no detectable staining in preparations in which the primary or secondary antibody was omitted from the protocol or the primary antibody was preadsorbed with γ-Glu-Glu (Fig. 4). Preparations fixed with glutaraldehyde without prior treatment with carbodiimide also failed to stain. Preadsorption of antibody with *N*-Ac-Glu or Asp-Glu resulted in tentacles with a staining pattern similar to that obtained with untreated antibody, except that the maximum nematocyst staining as seen in Figure 1 was never observed. Preadsorption of antibody with glutamic acid resulted in a staining reaction that was indistinguishable from that associated with untreated antibody.

Nematocyst immunostaining

The most readily observed immunostaining was associated with tentacle nematocysts and their released fila-

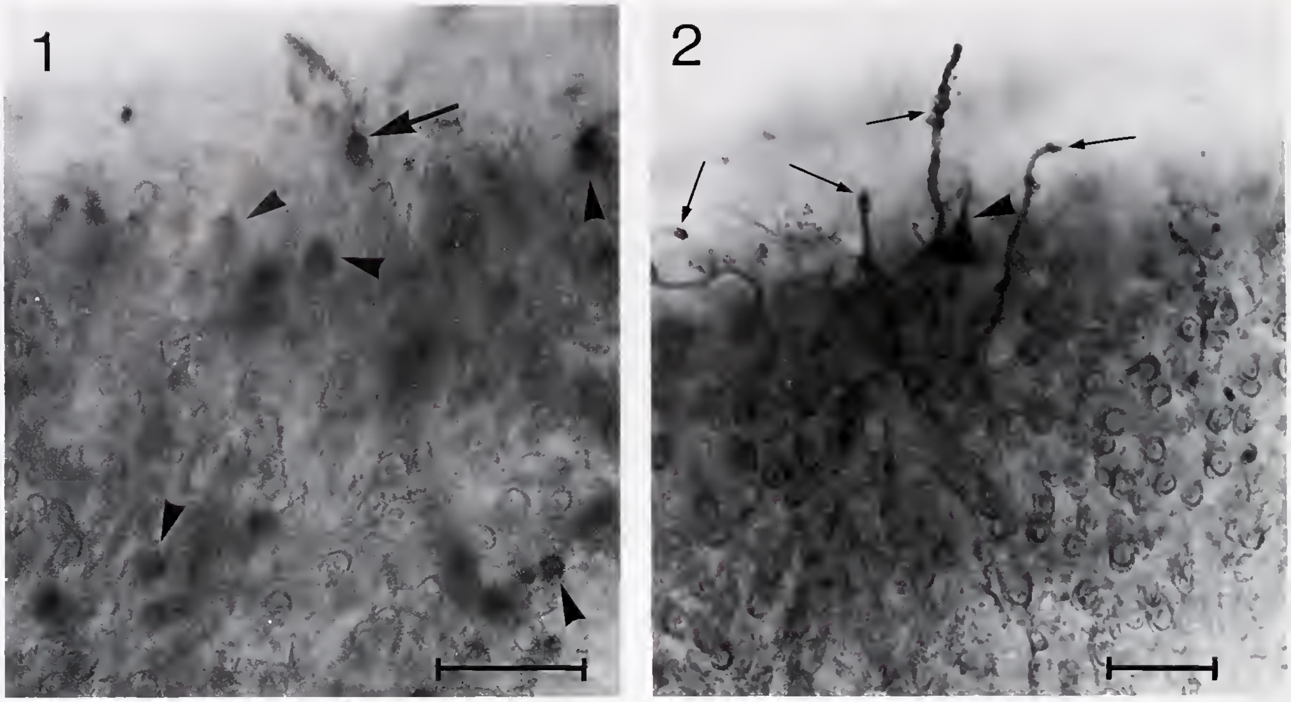

Figures 1, 2. Glutamate immunoreactive elements of tentacle nematocysts (wholemounts). Scale bars = 25 μm.

Figure 1. Stained nematocyst capsules. Note several stained, noneverted capsules (arrowheads) as well as capsule with everted thread that is heavily stained at its apex (arrow). Note also that most of the nematocyst capsules did not stain.

Figure 2. Stained everted threads showing tapering shaft (arrowhead) and decorated threads (arrows) reflecting their coiled or twisted state and the presence of spines.

ments (Figs. 1, 2). Nematocyst immunoreactivity was invariably concentrated distally on the tentacles on both their oral and aboral sides. Although all animals tested with the primary antibody displayed positive immunoreactive responses, the intensity of staining and number of stained elements varied substantially, even between tentacles from the same animal. From the tip of the tentacles, there was a more or less gradual decline in the number and intensity of the immunostained elements, until little or no staining was detected in the proximal two-thirds or half of the tentacle (Fig. 3).

Only a relatively small proportion of discharged or undischarged nematocysts present in the stained areas were immunoreactive, and in those nematocysts staining was mainly associated with the capsule wall (Fig. 1). There was an ascending gradient of staining intensity from the base to the distal end of the capsule where the shaft is anchored (Fig. 1). The nematocytes in which these capsules lie showed no staining reaction. The immunoreactive capsules seemed to belong to a single morphological type measuring 15–20 μm by 3–4 μm. This corresponds roughly to the microbasic b-mastigophore of ordinary tentacles as described in this species by Westfall (1965).

Many of the immunoreactive capsules displayed everted shafts and threads that stained also (Fig. 2). When these elements were completely uncoiled, reaching a length of up to 80 μm, it was possible to observe a shaft, 2 μm in diameter, emerging from the capsule and gradually tapering to a thread of 1 μm in diameter. This is also diagnostic of the microbasic b-mastigophore (Westfall, 1965; Mariscal, 1974). The strong staining reaction at the tip of some ordinary tentacles (Fig. 3) was in fact due to a meshwork of such immunoreactive shafts and threads that covers the surface of the ectoderm. These discharged filaments appear variously decorated, reflecting the extent to which they are coiled, folded, or endowed with spines. Staining seemed to be localized on the surface of the filaments (Fig. 2). Reduction of both stained nematocyst capsules and stained discharged filaments accounts for the lack of immunostaining in the proximal part of the tentacles.

Ectodermal muscle cell immunostaining

This staining reaction appears as a more or less continuous layer of processes, 2–4 μm in depth, at the base

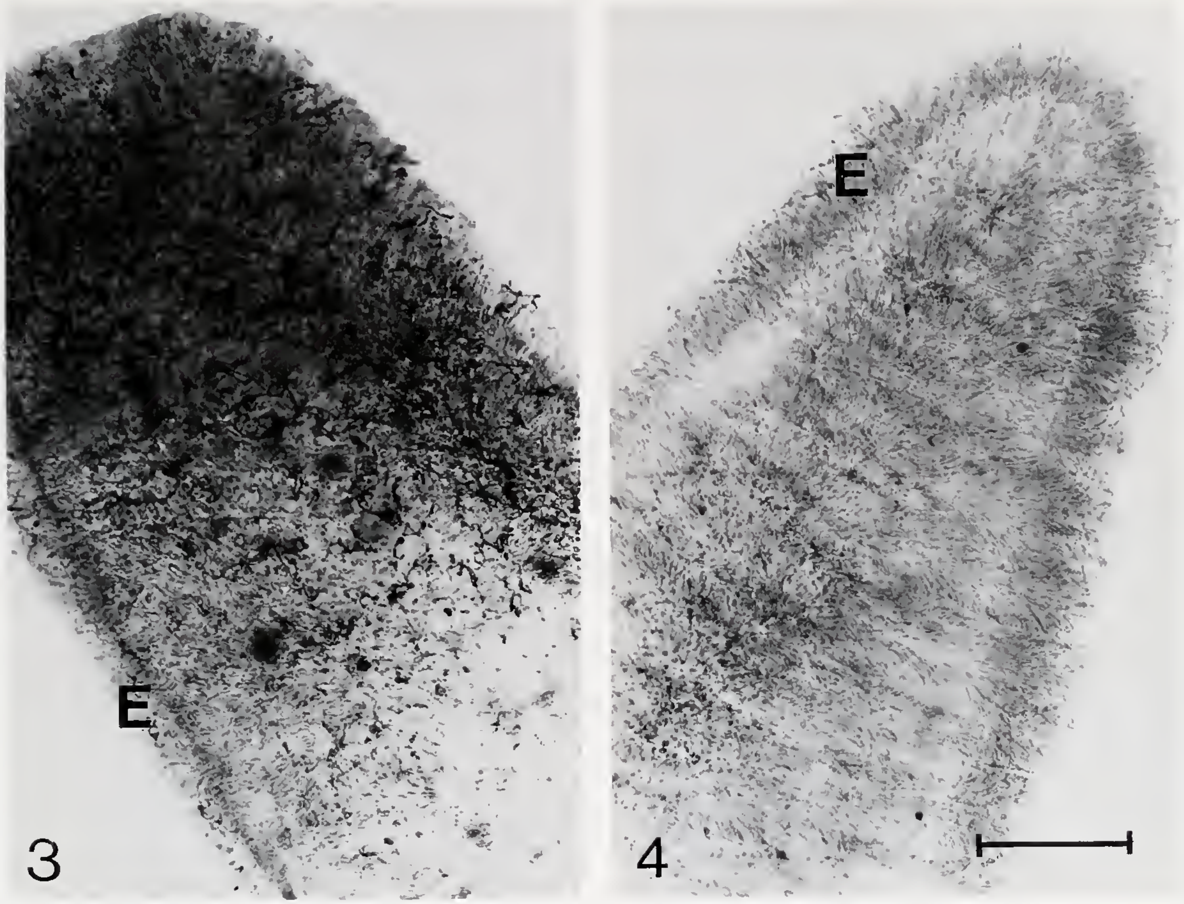

Figures 3, 4. Glutamate immunoreactivity in nematocysts of a tentacle (Fig. 3) and its absence in another (control) tentacle (Fig. 4) from the same specimen of *Metridium senile* (wholemounts). E, ectoderm.

Figure 3. Density of stained nematocysts diminishes from distal tip toward the base of the tentacle.

Figure 4. Tentacle was treated with primary antibody preabsorbed with γ-Glu-Glu; no staining was detected. Scale bar = 100 μm.

of the ectoderm (Fig. 5). Many such processes have a twisted or folded appearance (Fig. 5), presumably as a result of buckling in the tentacle. They seem to correspond to the layer of muscle feet of the musculoepithelial cells of the longitudinal musculature, associated cell bodies showing no clear evidence of staining (Fig. 5). Staining was present on both oral and aboral sides of the tentacles and usually extended from the base of the tentacles to within a short distance (0.1–0.3 mm) of their tip.

Ectodermal granule-containing cells

The third immunoreactive site was localized in the ectoderm of the oral disk proximal to the base of the tentacles (Fig. 6). The immunoreactivity was associated with pear-shaped cells (9 μm in perikaryon length) tapering to a single axon-like process and filled with large granules, 1–2 μm in diameter (Figs. 6, 7). There was no clear evidence that the granules themselves had stained. The processes were up to 40 μm in length and approximately parallel. The stained granular cells were distributed over the radial muscle in that area. The radial muscle itself was not stained.

Discussion

Our observations demonstrate the presence of glutamate immunoreactivity in the tentacles and oral disk of *M. senile,* in agreement with Carlyle's (1974) biochemical detection of large amounts of glutamic acid in the oral margin of the sea anemone *A. equina.* The lack of specificity of induced glutamate release from oral margin/sphincter preparations stopped Carlyle (1974) short of proposing a neurotransmitter role for this amino acid in this species; instead he proposed that "nematocysts and mucus-secreting cells may be potential sources of release" (Carlyle, 1974). Our results give credence to the latter view, because glutamate immunostaining was associated

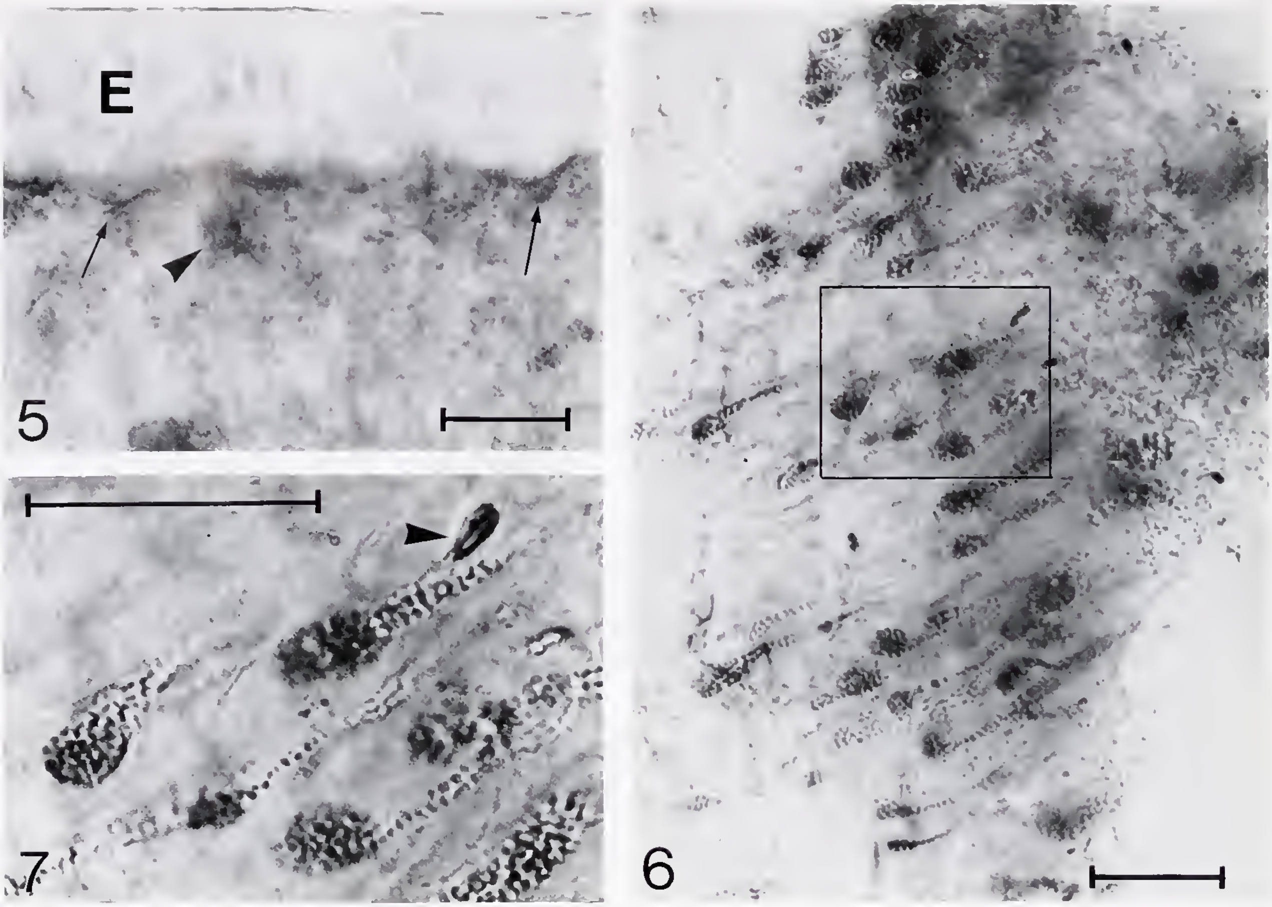

Figures 5–7. Glutamate immunoreactive cells in the ectoderm of tentacles and in the oral disk (wholemounts). Scale bars = 25 μm.

Figure 5. Layer of stained muscle feet of longitudinal muscle at the base of the ectoderm (E) in tentacle. Note out-of-focus cell body of musculoepithelial cell (arrowhead) as well as evidence of buckling (arrows). The apparent position of the cell body below the ectoderm is an artifact caused by tilting at the edge of the tentacle.

Figures 6–7. Low-power (Fig. 6) and high-power (Fig. 7) views of a field of granule-containing cells in the oral disk. Rectangle in Figure 6 delimits enlarged area shown in Figure 7. The dark background in Figure 6 represents the position of underlying radial muscle fields. Note parallel orientation of cell processes. Note also in Figure 7 that the granular texture of these cells is apparent in both cell bodies and processes. Arrowhead in Figure 7 indicates a nematocyst.

only with non-neuronal cells of *M. senile*, among which nematocysts and granular cells figure prominently.

Specificity of the immunostaining

Control procedures indicated that the observed immunostaining represents specific antibody binding to γ-Glu-Glu. The absence of effect or small effect of preadsorption tests with glutamate, *N*-Ac-Glu, and Asp-Glu on immunostaining in our preparations is largely consistent with the results of corresponding tests elsewhere (Madl *et al.*, 1986). Moreover, the absence of immunostaining in preparations fixed without carbodiimide all but excludes the presence of endogenous γ-Glu-Glu in the tissues.

Nematocyst immunostaining

Reports of large amounts of polymeric γ-glutamic acids in cnidarian nematocysts, including sea anemones (Weber, 1990, 1991), may appear to account for the nematocyst staining described in this study. However, such is apparently not the case, because omission of the carbodiimide treatment eliminated nematocyst immunostaining. In addition, staining was intense only in the periphery of the distal part of the capsule interior, not in the core (matrix) of the nematocysts where the polymers are expected to be concentrated (Weber, 1991). Thus nematocyst immunoreactivity in *M. senile* may represent a pool of free glutamate either recruited in the polymerization process or resulting from enzymatic hydrolysis of already-formed polymers (Weber, 1994). This immunostaining lends some indirect support to Weber's hypothesis that such polymers act as substrate for generating high osmotic pressures inside the nematocyst capsule, thus providing an intrinsic force for nematocyst discharge (Weber, 1989, 1991).

The question arises as to why only one category of nematocysts displayed immunostaining when polymeric γ-glutamic acids were reported also in other categories of nematocysts (Weber, 1991). One possibility is that other nematocyst classes may contain less of these polymers, therefore less free glutamate, than the microbasic b-mastigophores identified in this study. If these nematocysts concentrate such polymers more than the other kinds do, then one may expect that they discharge their thread more readily, owing to a greater buildup of osmotic pressure, than do the other kinds. This appears to be the case, because microbasic b-mastigophores are known to be easily discharged in *Metridium* (Westfall, 1965).

Our results show that the released shaft and thread of these nematocysts were stained, but that staining seemed to be associated only with their external surface. Such a staining pattern may have resulted from adhesion of the immunoreactive material in the nematocyst capsule on the filaments. A means of fortuitous non-neuronal release of glutamate—of the kind suggested by Carlyle (1974)—is thus provided, and one must use particular caution in interpreting studies of amino acid release in such animals. Whether the putative glutamate sticking on the filaments has any role associated with nematocyst discharge remains to be explored. Another unresolved matter is whether the uneven spatial distribution of stained nematocysts on tentacles represents an intrinsic arrangement of microbasic b-mastigophores conferring some functional specificity or reflects merely the skewed distribution of a subpopulation of these nematocysts.

Ectodermal cell immunostaining

Glutamate immunostaining in ectodermal muscle and granular cells is an unexpected finding. To our knowledge this is the first time that a putative neuroactive substance has been immunohistochemically localized in this type of muscle cell. In contrast, ectodermal gland cells of tentacles of the jellyfish *Cyanea lamarcki* were reported to show serotonin immunoreactivity (Elofsson and Carlberg, 1989), and dopamine-immunoreactive granule-containing cells strikingly similar in morphology to those of the present study were described by Carlberg (1992) in tentacles and peristomium of *Hydra attenuata*. The latter and the granular cells identified in our study are not epidermal mucous cells because their processes are directed inward, not toward the external surface as in mucous cells. Cells with similar morphology, size, and granule content were demonstrated by scanning electron microscopy in oral tentacles of the cerianthid *Ceriantheopsis americanus* ("gland cells" of Fig. 9 in Fautin and Mariscal, 1991). Thus these may be secretory cells, with glutamate as a putative secretory product serving some paracrine role. Because the distribution of these cells coincides with that of radial muscle fields in the oral disk, it is possible that this muscle layer constitutes one of the functional targets of the cell secretions.

Glutamate has been identified as a feeding stimulant in the sea anemones *Actinia equina* (Steiner, 1957) and *Calliactis parasitica* (McFarlane, 1975) by eliciting mouth opening. Combined with its relaxing effect on the sphincter muscle (Carlyle, 1974), a prerequisite for mouth opening (McFarlane, 1970), these responses would suggest that glutamate is involved in the coordination of feeding in sea anemones, although our study failed to find evidence of glutamate-immunoreactive cells in the vicinity of the sphincter muscle itself. Other prefeeding responses include expansion of the radial muscle in the oral disk and extension of the tentacles, both associated with activity in an ectodermal slow conducting system, possibly a nervenet (McFarlane, 1970; Lawn, 1975; McFarlane *et al.*, 1993). Although ectodermal muscle feet in *Metridium* tentacles apparently contain free glutamate, it is not clear how this glutamate is involved in these feeding responses.

In this study we have provided immunohistochemical evidence that, in the sea anemone *Metridium*, the amino acid glutamate or a related substance is stored only in non-neuronal cells; in contrast, in the scyphozoan jellyfish *Cyanea*, similar evidence suggests that another amino acid, taurine, is present only in neurons (Carlberg *et al.*, 1993). This disparity suggests that profoundly different paths of cellular commitment for processing amino acid transmitters may be expressed among cnidarian species.

Acknowledgments

This study was funded by grant OGP0006447 from the Natural Sciences and Engineering Research Council of Canada to M.A.

Literature Cited

Anctil, M. 1990. The antiquity of monoaminergic neurotransmitters. Pp. 141–155 in *Evolution of the First Nervous Systems*, P.A.V. Anderson, ed. Plenum Press, New York.

Anderson, P. A. V. (ed.). 1990. *Evolution of the First Nervous Systems*. Plenum Press, New York.

Anderson, P. A. V., and H. G. Trapido-Rosenthal. 1990. Electrophysiological evidence that a taurine-like amino acid is the neurotransmitter at a fast excitatory synapse. *Soc. Neurosci. Abstr.* **16:** 1185.

Anderson, P. A. V., A. Moosler, and C. J. P. Grimmelikhuijzen. 1992. The presence and distribution of Antho-RFamide-like material in scyphomedusae. *Cell Tissue Res.* **267:** 67–74.

Brodfuehrer, P. D., and A. H. Cohen. 1990. Initiation of swimming activity in the medicinal leech by glutamate, quisqualate, and kainate. *J. Exp. Biol* **154:** 567–572.

Brodfuehrer, P. D., and A. H. Cohen. 1992. Glutamate-like immunoreactivity in the leech central nervous system. *Histochemistry* **97:** 511–516.

Bullock, T. H., and G. A. Horridge. 1965. *Structure and Function in the Nervous Systems of Invertebrates.* Vol. 1. W. H. Freeman, San Francisco.

Carlberg, M. 1992. Localization of dopamine in the freshwater hydrozoan *Hydra attenuata. Cell Tissue Res.* **270:** 601–607.

Carlberg, M., and M. Anctil. 1993. Minireview: biogenic amines in coelenterates. *Comp. Biochem. Physiol.* **106C:** 1–9.

Carlberg, M., and E. Rosengren. 1985. Biochemical basis of adrenergic neurotransmission in coelenterates. *J Comp. Physiol.* **B155:** 251–255.

Carlberg, M., K. Alfredsson, S.-O. Nielsen, and P. A. V. Anderson. 1993. Taurine-like immunoreactivity in the motor nerve net of the jellyfish *Cyanea capillata. Soc. Neurosci. Abstr.* **19:** 490.

Carlyle, R. F. 1974. The occurrence in and actions of amino acids on isolated supra-oral sphincter preparations of the sea anemone *Actinia equina. J. Physiol. (Lond.)* **236:** 635–652.

Chung, J. M., A. N. Spencer, and K. H. Gahm. 1989. Dopamine in tissues of the hydrozoan jellyfish *Polyorchis penicillatus* revealed by HPLC and GC/MS. *J Comp. Physiol.* **B159:** 173–181.

De Waele, J.-P., M. Anctil, and M. Carlberg. 1987. Biogenic catecholamines in the cnidarian *Renilla köllikeri:* radioenzymatic and chromatographic detection. *Can. J. Zool.* **65:** 2458–2465.

Duce, I. R. 1988. Glutamate. Pp. 42–89 in *Comparative Invertebrate Neurochemistry,* G. G. Lunt and R. W. Olsen, eds. Cornell University Press, Ithaca, NY.

Elofsson, R., and M. Carlberg. 1989. Gland cells in the tentacles of the jellyfish *Cyanea lamarcki* reactive with an antibody against 5-hydroxytryptamine. *Cell Tissue Res.* **255:** 419–422.

Fautin, D. G., and R. N. Mariscal. 1991. Cnidaria: Anthozoa. Pp. 267–358 in *Microscopic Anatomy of Invertebrates, Vol. 2: Placozoa, Porifera, Cnidaria, and Ctenophora,* F. W. Harrison and J. A. Westfall, eds. Wiley-Liss, New York.

Fonnum, F. 1984. Glutamate: a neurotransmitter in mammalian brain. *J. Neurochem.* **42:** 1–11.

Grimmelikhuijzen, C. J. P., K. Carstensen, D. Darmer, A. Moosler, H.-P. Nothacker, R. K. Reinscheid, C. Schmutzler, and H. Vollert. 1992. Coelenterate neuropeptides: structure, action and biosynthesis. *Amer. Zool.* **32:** 1–13.

Lawn, I. D. 1975. An electrophysiological analysis of chemoreception in the sea anemone *Tealia felina. J. Exp. Biol.* **63:** 525–536.

Leake, L. D., and R. J. Walker. 1980. *Invertebrate Neuropharmacology.* Blackie, Glasgow and London.

Mackie, G. O. 1990. The elementary nervous system revisited. *Amer. Zool.* **30:** 907–920.

Madl, J. E., A. A. Larson, and A. J. Beitz. 1986. Monoclonal antibody specific for carbodiimide-fixed glutamate: immunocytochemical localization in the rat CNS. *J. Histochem. Cytochem.* **34:** 317–326.

Mariscal, R. N. 1974. Nematocysts. Pp. 129–178 in *Coelenterate Biology: Reviews and New Perspectives,* L. Muscatine and H. M. Lenhoff, eds. Academic Press, New York.

McFarlane, I. D. 1970. Control of preparatory feeding behaviour in the sea anemone *Tealia felina. J. Exp. Biol.* **53:** 211–220.

McFarlane, I. D. 1975. Control of mouth opening and pharynx protrusion during feeding in the sea anemone *Calliactis parasitica. J. Exp. Biol.* **63:** 615–626.

McFarlane, I. D., D. Graff, and C. J. P. Grimmelikhuijzen. 1990. Evolution of conducting systems and neurotransmitters in the Anthozoa. Pp. 111–127 in *Evolution of the First Nervous Systems,* P. A. V. Anderson, ed. Plenum Press, New York.

McFarlane, I. D., D. Hudman, H.-P. Nothacker, and C. J. P. Grimmelikhuijzen. 1993. The expansion behaviour of sea anemones may be coordinated by two inhibitory neuropeptides, Antho-KAamide and Antho-RIamide. *Proc. R. Soc. Lond.* **B253:** 183–188.

Monaghan, D. J., R. J. Bridges, and C. W. Cotman. 1989. The excitatory amino acid receptors: their classes, pharmacology, and distinct properties in the function of the central nervous system. *Annu. Rev. Pharmacol. Toxicol.* **29:** 365–402.

Pani, A. K., and M. Anctil. 1994. Quantitative survey of biogenic monoamines, their precursors and metabolites in the coelenterate *Renilla koellikeri. Biogen. Amines* **10:** 161–180.

Steiner, G. 1957. Uber die chemische Nahrungswahl von *Actinia equina* (L.). *Naturwissenschaften* **44:** 70–71.

Umbriaco, D., M. Anctil, and L. Descarries. 1990. Serotonin-immunoreactive neurons in the cnidarian *Renilla koellikeri. J Comp. Neurol.* **291:** 167–178.

Usherwood, P. N. R. 1980. Neuromuscular transmitter receptors of insect muscle. Pp. 141–153 in *Receptors for Neurotransmitters. Hormones and Pheromones in Insects,* D. B. Sattelle, L. M. Hall, and J. G. Hildebrand, eds. Elsevier/North-Holland, Amsterdam.

Webb, R. A. 1988. Release of exogenously supplied [^{3}H] glutamate and endogenous glutamate from tissue slices of the cestode *Hymenolepis diminuta. Can. J. Physiol. Pharmacol.* **66:** 889–894.

Webb, R. A., and H. Eklove. 1989. Demonstration of intense glutamate-like immunoreactivity in the longitudinal nerve cords of the cestode *Hymenolepis diminuta Parasitol Res.* **75:** 545–548.

Weber, J. 1989. Nematocysts (stinging capsules of Cnidaria) as Donnan-potential-dominated osmotic systems. *Eur. J. Biochem.* **184:** 465–476.

Weber, J. 1990. Poly(γ-glutamic acid)s are the major constituents of nematocysts in *Hydra* (Hydrozoa, Cnidaria). *J. Biol. Chem.* **265:** 9664–9669.

Weber, J. 1991. A novel kind of polyanions as principal components of cnidarian nematocysts. *Comp. Biochem. Physiol.* **98A:** 285–291.

Weber, J. 1994. The metabolism of poly(γ-glutamic acid)s of nematocysts in *Hydra vulgaris:* detection of two distinct hydrolytic enzymes in endoderm and in nematocysts. *Comp. Biochem. Physiol.* **107B:** 21–32.

Westfall, J. A. 1965. Nematocysts of the sea anemone *Metridium. Amer. Zool.* **5:** 377–393.

Reference: *Biol. Bull.* **187:** 55–63. (August, 1994)

Quantification of L-Dopa and Dopamine in Squid Ink: Implications for Chemoreception

MARY T. LUCERO[1], HERALDO FARRINGTON[2], AND WILLIAM F. GILLY[2]

[1]*University of Utah, Department of Physiology, 410 Chipeta Way, Salt Lake City, Utah 84108, and*
[2]*Stanford University, Hopkins Marine Station, Pacific Grove, California 93950*

Abstract. Squid ink is an alarm substance that both confuses predators and alerts conspecifics to the presence of danger. Although the ejection of ink is a powerful visual stimulus, studies also indicate a chemical component to the signal. Squid ink is composed mainly of melanin pigments, but the nonpigmented portion of the ink contains the enzymes and precursors of melanin synthesis. Our previous behavioral studies showed that squid olfactory organs detect L-dopa, a key chemical in melanogenesis. Squid olfactory neurons also respond to dopamine, a biogenic amine not previously described in squid ink. We performed HPLC on ink taken from the ink sacs of adult *Loligo opalescens.* The ink was conjugated with orthophthaldialdehyde (OPA) and injected into the HPLC, and amine-containing compounds were detected fluorometrically. Standard curves constructed for L-dopa and dopamine allowed quantitation from individual ink sacs. We found that L-dopa was present in undiluted ink at a mean concentration of 1.15 m*M* and was significantly greater than the mean dopamine concentration of 0.19 m*M*. These values are greater than those at which both compounds are effective in behavioral and electrophysiological experiments. In addition we found that an unidentified antioxidant in the ink may prevent rapid oxidation of L-dopa and dopamine following dilution in seawater.

Introduction

Inking by cephalopods has long been recognized as an adaptive response to predation and physical threat. The ink clouds produced by these animals allow for retreat from a threatening situation and leave behind either a diffuse "smoke screen" or a compacted, long-lasting decoy that serves as an effective visual distraction for predators. Ink may also contain compounds that interfere with a predator's chemosensory abilities, although the behavioral evidence is largely anecdotal (Fox, 1976; MacGinitie and MacGinitie, 1968). In support of these ideas, Prota *et al.* (1981) found a high specific activity of tyrosinase in cephalopod ink and suggested that the *in situ* oxidation, by this enzyme, of phenols in the ink to quinones may be a source of the hypothesized chemical messengers.

In addition to affecting predators, ink clouds may also alert conspecifics to danger, especially within the dense schools of many squid species. Furthermore, the warning signal is likely to be chemical as well as visual because the visual component would be of limited usefulness at night or in the dark ocean depths. In this respect, ink would play a pheromonal role, because its release and detection could provide a basis for intraspecies communication. Indeed, local application of diluted squid ink to the olfactory organ of restrained squid caused strong escape jetting responses (Gilly and Lucero, 1992). In addition, 1-3, 4-dihydroxyphenylalanine (L-dopa), a colorless compound found in cuttlefish ink (Jimbow *et al.*, 1984), elicited escape responses in the absence of other metabolites of melanogenesis including tyrosinase, phenols, or quinones. Therefore, without ruling out effects of the other metabolites, initial behavioral experiments implicated L-dopa as a potential chemical cue (Gilly and Lucero, 1992). L-dopa is an intermediate, not only in the synthesis of melanin and related pigments, but also of dopamine and other neurotransmitters (Waite, 1992). Thus, preliminary physiological studies were performed and showed that diluted squid ink, L-dopa, and dopamine all inhibited spontaneous firing in primary sensory neurons isolated from squid olfactory organs (Lucero *et al.*, 1992).

Because L-dopa and dopamine both mimic the effects of squid ink on primary sensory neurons, we postulate

Received 9 November 1993; accepted 6 June 1994.

that ejected ink functions as a warning signal, and that the two metabolites are effector molecules. Neither substance, however, has ever been identified in squid ink. Therefore, we used high pressure liquid chromatography (HPLC) to identify and quantify L-dopa and dopamine in the ink from individual ink sacs. We report here that squid ink contains free L-dopa and dopamine in concentrations sufficient to produce physiological effects. Moreover, the ink also appears to contain an antioxidant that retards the rapid oxidation of these compounds in seawater.

Materials and Methods

HPLC apparatus and fluorescence detection

Chromatography was performed with two Waters pumps connected to a Waters Model 720 System Controller programmed to generate a dual-solvent, stepped-elution profile. Peaks were detected by a Fluoro-Tec digital filter fluorometer with an excitation wavelength of 320 nm and an emission wavelength of 450 nm. Peak areas were integrated by a Waters Data Module. Separation of ortho-phthaldialdehyde (OPA)-derivatized primary amines was performed on an Ultrasphere 3-μm Octadecasilane (ODS) column of 75 mm length and 4.5 mm internal diameter (Jaeckle and Manahan, 1989; Manahan, 1989).

A combination of aqueous and nonaqueous solvents was used to create an elution profile with a total run time of 23 min. The aqueous solution (solvent A) contained 150 mm sodium acetate (pH 7.2), 9.5% methanol, and 0.5% tetrahydrofuran (THF). The nonaqueous solution (solvent B) was 100% methanol.

A modified stepped-elution profile was developed that allowed for the clear separation and signal integration of L-dopa and dopamine at a flow rate of 1.8 ml/min. The time course for solvent B was as follows: constant 10% from 0 to 1 min, linear increase to 20% from 1 to 4 min, constant 20% from 4 to 9 min, linear increase to 50% from 9 to 13.5 min, constant 50% from 13.5 to 19 min, linear increase to 90% from 19 to 21 min, linear decrease to 10% from 21 to 23 min. At 23 min, the initial conditions were reattained and the column was ready for the next injection. The elution times for L-dopa and dopamine under these conditions were 7.82 ± 0.08 (SD; $n = 19$) and 13.25 ± 0.08 min (SD; $n = 18$), respectively.

Electrochemical detection

An additional HPLC column and detection method was used to verify results obtained with the OPA method. HPLC separation of diluted squid ink was performed on a C-18 reverse phase column (Rainin) in phosphate-buffered mobile phase consisting of monosodium phosphate ($Na\text{-}H_2PO_4$), 50 mM; ethylenediaminetetraacetic acid (EDTA), 200 μM; and heptane sulfonic acid, 1.2 mM; pH 3.6. Biogenic amines in the ink were detected electrochemically with an ESA Coulochem (Model 5100A; 5021 conditioning cell; 5011 analytical cell) in the reductive mode (Gomez-Nino *et al.*, 1990).

Standards and standard curves for fluorescence detection

Because of their low solubility and rapid oxidation, 50 μm L-dopa and dopamine standards were made up in a solution of 10 mm ascorbic acid and 150 mm sodium acetate (pH 10). As an added measure to prevent oxidation during preparation, all solutions were bubbled with N_2 gas, placed on ice, and used within 6 h.

All samples were filtered (0.2 μm Millipore) prior to derivatization, which was carried out by adding 25% OPA by volume to the injection sample. The derivatized samples were then vortexed briefly and centrifuged (14,000 × *g*) for 1 min. Volumes of supernatant, ranging from 20 μl to 400 μl, were injected for analysis within 3 min of derivatization. An example of HPLC traces obtained for 100-μl injections of 50 μm L-dopa and dopamine is shown in Fig. 3A. Chemicals were obtained from Sigma (St. Louis, MO) and were HPLC grade or ACS reagent grade.

Standard curves (data not shown) were established over the range of injections that produced the best integrated peaks. The L-dopa curve was based on 19 injections with injection volumes corresponding to L-dopa amounts ranging from 0.5 to 5.0 nanomoles. The dopamine curve was based on 18 injections with the lower limit of detection at 1.25 nanomoles. Each curve was estimated by linear regression, and the r^2 values were 0.999 and 0.986 for L-dopa and dopamine, respectively.

Standards for electrochemical detection

The standards used for electrochemical detection were made fresh daily in 1 *N* perchloric acid (PCA) and included L-dopa, dopamine, dihydroxyphenyl acetic acid (DOPAC), and 3,4-dihydroxybenzylamine (DHBA). DOPAC is a catabolite of dopamine that occurs naturally in squid ink. DHBA was added, as an internal control, at the time of extraction of ink samples being prepared for electrochemical detection (see below). Electrochemical detection of these four standards is exemplified in Figures 2A (50 ng each) and 2B (100 pg each). Standards were run and calibrated at two different gain settings so that the L-dopa and dopamine peaks from ink could each be integrated at optimal sensitivities.

Extraction and preparation of squid ink for fluorescence detection

Live specimens of adult *Loligo opalescens* were collected in Monterey Bay, California. Squid were decapitated, ink sacs were removed by dissection, and whole ink was manually recovered.

An intact ink sac was placed on a sheet of Parafilm, and the ink duct was transected about 5 mm anterior to its emergence from the sac. A small glass rod was then used to gently express the ink onto the Parafilm. Simultaneously, one end of a sterile 10-μl microcapillary tube was introduced into the emerging ink and allowed to fill halfway by capillary action. Several tubes were necessary to collect the ink from a single sac. Nitrogen gas was used to blow the ink out of the tubes and into a preweighed Eppendorf vial that contained 1 ml of 150 m*M* sodium acetate and 10 m*M* ascorbic acid. The vial was immediately reweighed and put on ice. This procedure allowed us to rapidly collect and weigh most of the ink within an ink sac and simultaneously to dilute it into a solution containing an antioxidant, thereby minimizing the risk of oxidation. Only ink collections yielding more than 15 mg of ink from a single squid were used in the quantitative analysis of L-dopa and dopamine.

The vial containing diluted ink was centrifuged (14,000 × *g*) for 10 min at 4°C. The ink supernatant was removed and centrifuged in 0.2 μm filter tubes for 45 s. The filtered ink supernatant was conjugated with OPA in the same manner as described for the dopamine and L-dopa standards above.

Preparation of ink for electrochemical detection

In experiments where the electrochemical detection method was used, the ink sac was blotted dry and placed between a fold of parafilm with the ink duct extending into the collection tube. The parafilm was gently pressed, and drops of ink fell directly into an iced 1.5-ml tube containing 0.5 ml of the acetate/ascorbate buffer and 50 μg/ml DHBA. After 6 samples were collected, the tubes were vortexed for 30 s and immediately frozen on dry ice for shipment from Monterey, California, to Salt Lake City, Utah. Samples were kept frozen at −70°C for 3 days, quickly thawed, vortexed briefly, and run through alumina silica columns (Gomez-Nino *et al.*, 1990). L-dopa and catecholamines in the ink sample were eluted from the alumina column with 1 *N* PCA and stored at 4°C for 1–4 days. The alumina procedure was necessary to remove ascorbic acid from the ink because, as a reducing agent, ascorbic acid interferes with the oxidation-reduction reaction used in electrochemical detection (Gomez-Nino *et al.*, 1990).

Quantification of L-dopa and dopamine in ink by fluorescence detection

Several different volumes of a given sample were injected into the HPLC so that a range of well-integrated peaks could be obtained. The first injection volume for each ink sample was 100 μl, and the size of the resultant peaks guided the selection of the next injection volume. Whenever possible, replicates were injected at one particular volume to establish a measure of injection error. The standard curves for dopamine and L-dopa were used to transform the integrated peak areas from each analysis of ink into nanomolar quantities that were then corrected for injection volume and dilution to obtain millimolar concentrations that refer back to the original ink sample.

Quantification of L-dopa and dopamine in ink by electrochemical detection

Standards containing known amounts of L-dopa, dopamine, DHBA, and DOPAC were separated on the HPLC, and peaks were integrated and calibrated according to the known amount in the standard. The Waters Data Module was programmed to integrate and quantify peaks from ink samples having the same retention times as the standards. The amounts of biogenic amines in each ink sample were corrected for oxidative loss through the alumina column by a factor of 3.13 relative to the internal standard (DHBA). We were unable, however, to correct for the loss that probably occurred between the time the samples were thawed and run on alumina columns and the time of their injection into the HPLC.

Results

Identification of L-dopa and dopamine in squid ink

Two methods were used to identify the HPLC peaks corresponding to L-dopa and dopamine in the ink. One was to compare the profile and elution times of the peak with those of the standards, and the second was to 'spike' the ink by adding 4 nanomoles of L-dopa and dopamine to the ink sample. The HPLC trace of fresh ink from a single ink sac diluted with the antioxidant ascorbic acid is shown in Figure 1A. Several small unidentified peaks precede and follow the large L-dopa peak. The sizes of these smaller peaks in ink samples from different squid varied, as did the size of the dopamine peak.

Addition of L-dopa and dopamine to the ink is shown in Figure 1B. The areas of the L-dopa and dopamine peaks were dramatically increased without affecting the overall shapes or elution times of any of the other peaks in the sample. Thus, the L-dopa peak in ink had an average elution time of 8.08 ± 0.15 min (SD, $n = 47$), and the dopamine elution time averaged 13.49 ± 0.26 min (SD, $n = 41$). These values were very close to the elution times for the L-dopa and dopamine as cited above. Similarly, when preparations of ink and standards were run on the reverse phase C18 column and detected electrochemically, the ink samples had peaks that eluted at the same time as the standards. In Figures 2A and C, the gain of the

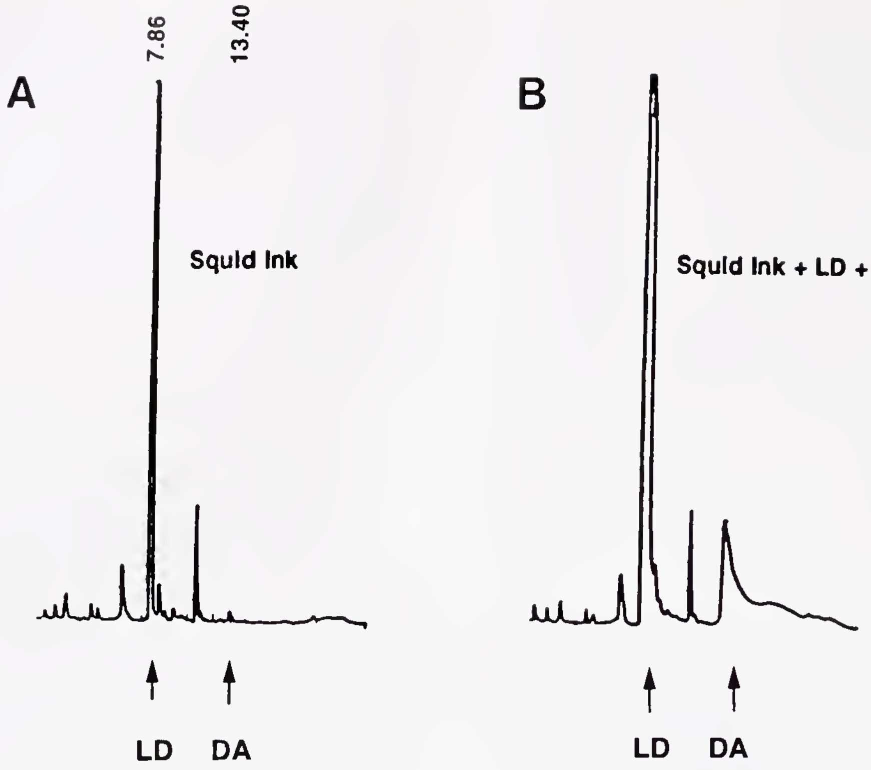

Figure 1. Primary amines were identified in squid ink by 'spiking' with L-dopa (LD) and dopamine (DA). (A) The HPLC trace obtained by injecting 50 μl of diluted squid ink conjugated with OPA (as described in the Methods) shows a prominent L-dopa peak at 7.86 min and a small dopamine peak at 13.4 min. (B) 50 μl of a 'spiking' cocktail containing 250 μl of diluted squid ink, 25 μl of L-dopa, and 25 μl of dopamine was injected into the HPLC to positively identify the L-dopa and dopamine peaks. Both peaks increased in area with little change in elution time.

electrochemical detector was set to 100, and an L-dopa peak can be seen at 4.72 min in both the standard and in the ink. The peaks for dopamine and DOPAC in ink are not resolvable at this gain setting, but a bump at 16–17 min is discernible. With the gain setting turned up to 9900, the dopamine and DOPAC peaks in the same sample of ink are clearly resolved (Fig. 2D), but the L-dopa peak (4.74 min) is now saturating. As mentioned in the Methods, 50 μg/ml DHBA was added to the ink as an internal standard and appears as the large saturating peak in Figures 2C and 2D at 10.37 and 10.34 min respectively.

Several amino acids and neurotransmitters were run as controls, either with fluorescence or electrochemical detection methods, to test whether their elution times differed from those of L-dopa and dopamine. None of the substances tested (aspartate, glutamate, arginine, tyrosine, taurine, phenylalanine, ammonia, ammonium, octopamine, histamine, and norepinephrine) overlapped with the L-dopa or dopamine peaks, but the retention times of some of the amino acids and amines were similar to those of other peaks in the ink sample, suggesting that these substances may also be present in ink.

Quantitative analysis

After correcting for the injection volume and dilution of the ink, the mean concentrations of L-dopa and dopamine were obtained for each ink sac analyzed by the fluorescence method (Table I). The number of injection volumes for a given ink sac (n) is less for dopamine than L-dopa, because several of the injection volumes used to obtain an L-dopa peak contained less than the minimum detectable amount of dopamine (1.25 nanomoles). Integration of the dopamine peaks in such profiles was deemed unreliable, and the resulting values were not used for further analysis.

The concentration of L-dopa in all of the ink sacs analyzed with the fluorescence detector averaged 1.15 ± 0.56 mM ($n = 10$), and the dopamine concentration averaged 0.19 ± 0.07 mM ($n = 9$). The highest values for each substance, approximately twice the means, were found in ink sac G. The coefficient of variation (CV), or percent error, in measuring the L-dopa and dopamine in individual ink samples by fluorescence detection averaged 3% (CV = SD/mean × 100%). This

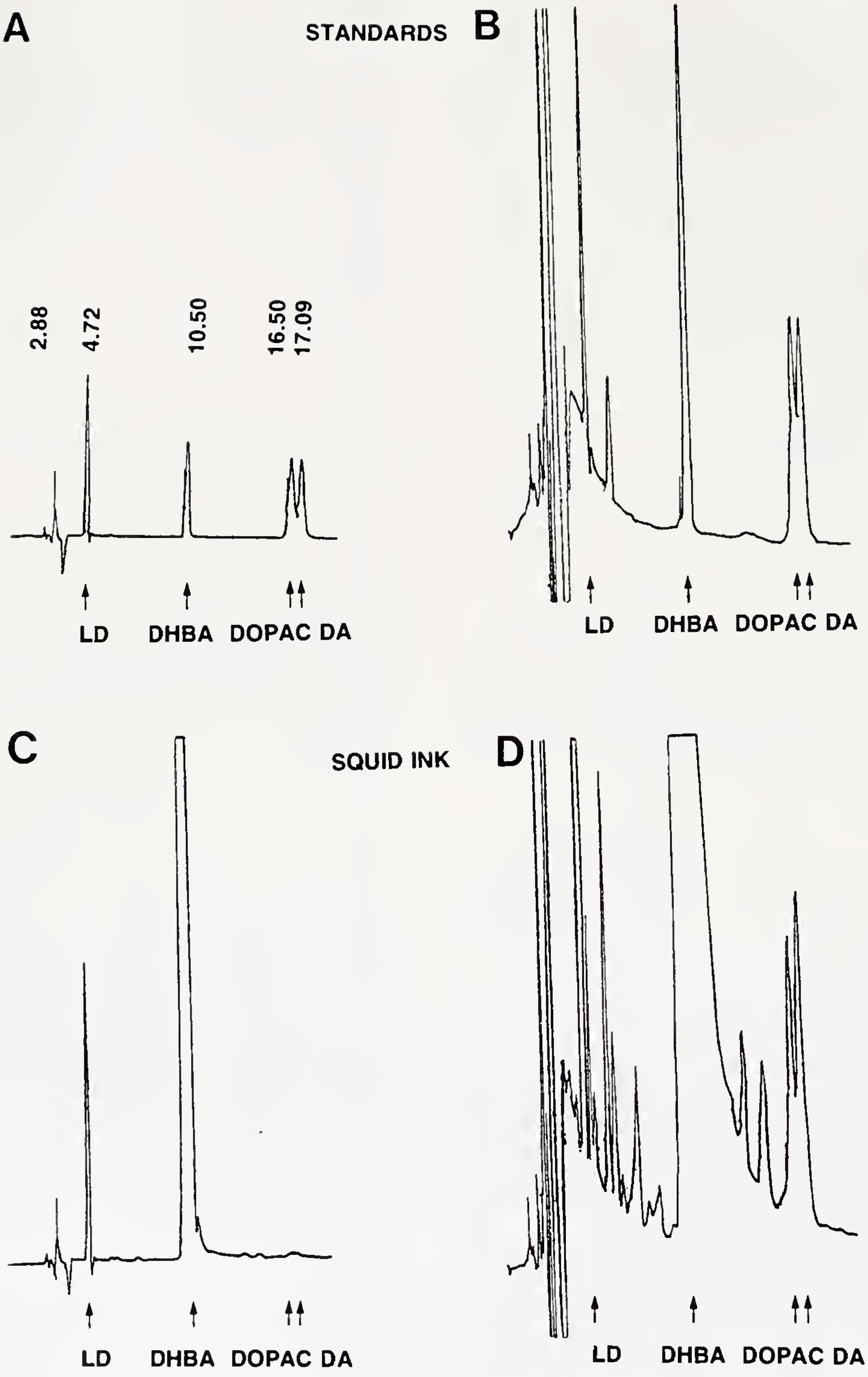

Figure 2. Electrochemical detection verifies the presence of L-dopa (LD) and dopamine (DA) in squid ink. (A) The HPLC trace of a 10 μl injection of standard solution containing 500 pg/μl each of DA, DOPAC (dihydroxyphenyl acetic acid), DHBA (3,4-dihydroxybenzylamine), and LD was obtained at a gain setting of 100. (B) The standard solution was diluted to a concentration of 10 pg/μl and the 10-μl injection is shown at a gain setting of 9900. The initial peaks at about 2 min in all traces represent the solvent front reaching the detector. (C) The HPLC trace of 20 μl of squid ink prepared for electrochemical detection (see Methods) recorded at the same gain as in (A) shows a large L-dopa peak at 4.72 min and a saturating DHBA peak at 10.37 min. The small DOPAC and dopamine peaks were not integrated. (D) The HPLC trace of 10 μl of squid ink from the same sample as in (C) recorded at a gain of 9900, shows that, although multiple peaks are visible at this sensitivity, the L-dopa, dopamine, DHBA, and DOPAC peaks are easily recognized.

Table I

Concentrations of L-dopa and dopamine for ink from individual ink sacks

	L-Dopa					Dopamine				
Ink sac	Mean conc. (mM)	(±)	SD	CV (%)	n	Mean conc (mM)	(±)	SD	CV (%)	n
A	0.812		0.034	4.2	7	—		—	—	—
B	0.598		0.035	5.8	5	0.183		—	—	1
C	0.615		0.022	3.6	6	0.081		0.003	3.7	2
E	1.967		0.098	5.0	5	0.249		0.002	0.8	2
F	1.557		0.054	3.5	3	0.160		0.006	3.7	2
G	2.001		0.062	3.1	3	0.268		0.006	2.2	2
H	1.513		0.022	1.4	4	0.249		0.004	1.6	2
I	0.339		0.004	1.2	4	0.083		0.000	0.5	2
J*	0.967		0.015	1.5	2	0.168		—	—	1
K*	1.092		0.097	8.9	2	0.248		0.001	0.4	2

	Mean of Mean Conc. (mM)	(±)	SD	CV (%)	n
L-Dopa	1.146		0.556	48.5	10
Dopamine	0.188		0.067	35.9	9

Aliquots of diluted ink from 9 ink sacs were analyzed by HPLC and quantified using the appropriate standard curve and correcting for injection volume and dilution; n = number of injections at various volumes.

* Ink was diluted and frozen for 3 weeks at −70°C before HPLC analysis.

value was similar to the CV measured for dopamine and L-dopa when constructing each standard curve, suggesting that the measurements of ink samples from a given ink sac are at least as accurate as the measurements made from stock solutions.

Much higher variability existed between ink sacs, the CV being 49% for L-dopa and 36% for dopamine. But this variation does not appear to be random, because the highest values for both L-dopa and dopamine, about twice that of the means, were found in ink sac G; and the lowest values were found in ink sac I. The concentrations of L-dopa and dopamine found in ink sac I (L-dopa, 339 μM; dopamine, 83 μM) are similar to those found in one ink sample by using the electrochemical detection method (318 μM and 25 μM respectively). The average concentrations, measured with the electrochemical detection method, of L-dopa and dopamine in ink were 162.8 ± 90.2 μM (n = 6) and 12.0 ± 7.0 μM (n = 6), respectively. Presumably, these slightly lower concentrations reflect slow oxidation of the ink before analysis (see Methods and below). The CV for measurements within an ink sample was higher than with the fluorescence method at 7%. As with fluorescence detection, there was a large degree of variability between ink samples (CV for L-dopa = 55%; dopamine/DOPAC = 58%).

Oxidation experiments

One possible explanation for the high variability between ink samples is that different amounts of oxidation of L-dopa and dopamine occurred during the preparative steps leading to HPLC analysis. To explore this idea, we studied the stability of biogenic amines, in stock solutions and in ink, that were diluted directly into sterile filtered seawater (0.2 μm Millipore filter), with and without the antioxidant, ascorbic acid.

First, Figure 3A shows the HPLC traces for control injections of 100 μl of 50 μM stock solutions of L-dopa and dopamine plus 10 mM ascorbic acid, at time zero and after 10.5 h at room temperature. There was only a 4% decrease in the amount of L-dopa and an 18% decrease in dopamine, indicating that ascorbic acid prevented oxidation of the stock solutions.

Second, stock solutions of L-dopa and dopamine (50 μM) were made up in sterile filtered seawater without ascorbic acid. At time zero (Fig 3Ba), a 200-μl injection of sample resulted in highly attenuated peaks for both L-dopa (82% reduction) and dopamine (52% reduction), relative to control data in Figure 3A. After 68 min, neither L-dopa nor dopamine were detectable, and both compounds thus appeared to be completely oxidized (Fig. 3Bb).

In contrast to the rapid and complete oxidation of L-dopa and dopamine stock solutions in seawater, dilution of squid ink into sterile filtered seawater decreased L-dopa by 15% and dopamine by only 1% (relative to time zero values), after 93 min at room temperature, including 25 min of gassing with oxygen (Fig. 3C). These results suggest that squid ink contains an antioxidant that protects L-dopa and dopamine from rapid oxidation. Moreover, the large variation in the amounts of L-dopa and dopamine among different ink sacs is not likely to be due to oxidation during ink collection or preparation for fluorescence analysis. In contrast, running samples through the alumina column for electrochemical detection (see Methods) will remove reducing agents from the ink. This difference in ink preparation may account for the lower average concentrations of L-dopa and dopamine found by electrochemical detection.

Discussion

This work represents the first quantitation of catecholamines in ink obtained from individual squid ink sacs and the first identification of dopamine in cephalopod ink. Although L-dopa has previously been identified in cuttlefish ink (Jimbow *et al.*, 1984), the reported units do not allow quantification of the concentration present in the native ink. Based on the measurements reported in the present study, the average concentrations of L-dopa and dopamine in squid ink are greater than those nec-

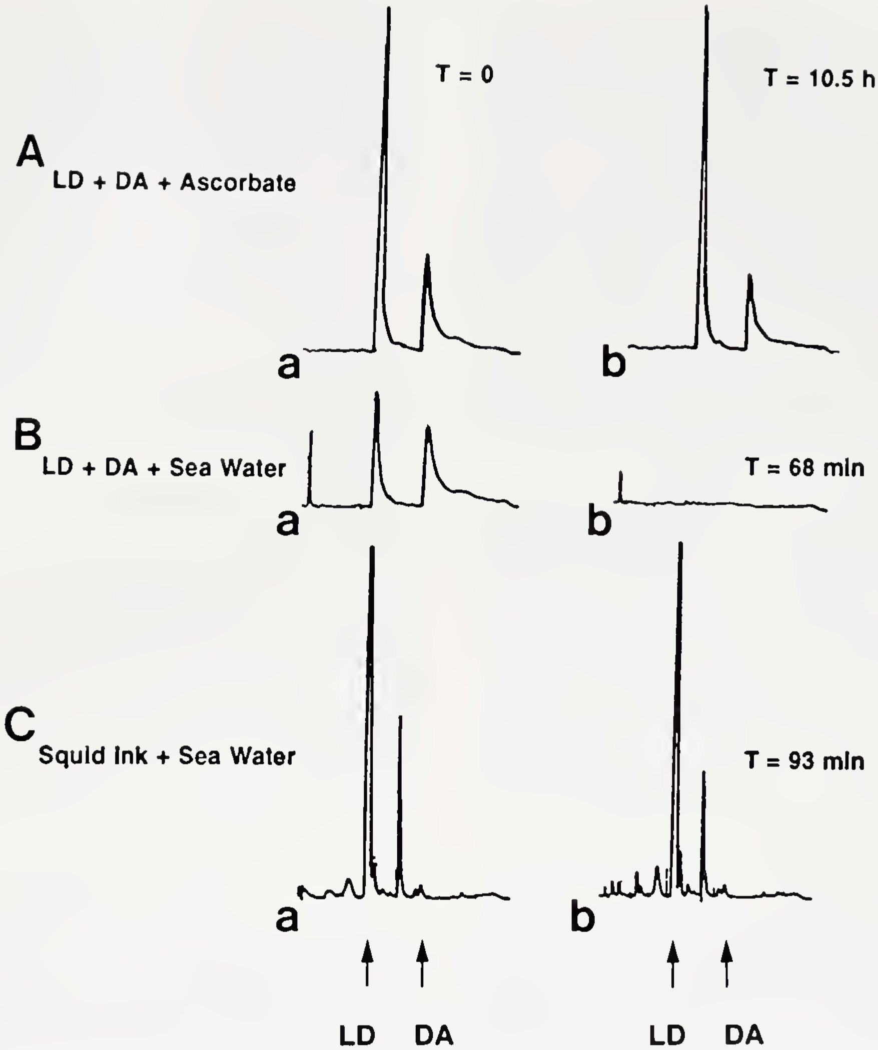

Figure 3. HPLC traces reveal that L-dopa (LD) and dopamine (DA) are stable in squid ink and in the presence of ascorbic acid, but oxidize rapidly in filtered seawater. (A) 100 μl of 50 μ*M* L-dopa and dopamine in Na-acetate buffer containing 10 m*M* ascorbic acid was injected into the HPLC at time zero (a) and after 10.5 h at room temperature (b). (B) HPLC traces show rapid oxidation of 200 μl of 50 μ*M* L-dopa and dopamine in seawater at time zero (a) and after 68 min at room temperature (b). The small sharp peak with an elution time of 0.6 min was assumed to be an oxidation product or contaminant and was not further characterized. (C) Squid ink diluted directly into seawater and injected into the HPLC at time zero (a) shows very little oxidation of L-dopa and dopamine after 93 min at room temperature, despite gassing for 25 min with O_2 (b).

essary to elicit behavioral (Gilly and Lucero, 1992) and physiological (Lucero *et al.*, 1992) responses and are therefore physiologically significant. Our work thus supports the idea that ink is an alarm substance and that products of melanin synthesis (L-dopa and dopamine) are present in the ink at levels that provide chemical signals to other squid. In addition, the levels of these biogenic amines vary considerably among individual ink sacs, and this variability is not due to differential oxidation of the ink during handling or to errors in measurement. Finally, we present preliminary evidence that a natural antioxidant that stabilizes these chemical messengers in seawater may be present in ink.

Both fluorescence and electrochemical detection methods were employed, after HPLC separation, to identify and quantify L-dopa and dopamine in squid ink. Both methods showed peaks in the ink that eluted at the same times and with the same characteristic shapes as L-dopa and dopamine standards. With fluorescence detection, the average concentrations for L-dopa were 1.15 ± 0.56 m*M* (n = 10), and for dopamine were 188 ± 67 μ*M* (n = 9). L-dopa concentrations were also obtained by electrochemical detection that were as high as the lowest levels measured with the fluorescence (ink sac I), and the maximum dopamine concentration measured electrochemically was about 3 time lower than the lowest value found with fluorescence. But oxidation experiments with standards (Fig. 3A) showed that, over a period of 10.5 h in the presence of 10 m*M* ascorbic acid, dopamine oxidized more rapidly than L-dopa. Thus, the reduced concentrations of both compounds measured electrochemically probably reflect oxidation that occurs after the removal of antioxidants with the alumina silica column. Similarly, slow differential oxidation of L-dopa, dopamine, and DHBA may have occurred during handling, shipment, and storage of the ink that cannot be corrected for by the known amount of DHBA degradation.

The concentrations of L-dopa and dopamine measured with the fluorescence detector are higher than those needed to elicit chemosensitive behavioral responses from intact animals (Gilly and Lucero, 1992) or electrophysiological responses from sensory neurons isolated from the squid olfactory organ (Lucero *et al.*, 1992). Exact quantitative comparisons are difficult because the dilution associated with pressure ejection from a small pipette is uncertain. Published experiments have revealed that squid can detect a 1:20 dilution of the ink (Gilly and Lucero, 1992), suggesting that the detection of chemical stimuli by squid is quite sensitive.

Thus, even when ejected ink is diluted into seawater, these compounds will still be detectable by a squid, at least for a short time. The lifetime of this chemical alarm signal would presumably depend on the extent to which dopamine or L-dopa remain bound to the mucus-like components of the ink that are responsible for holding the ink mass together in compacted form. A valuable approach to the biological relevance of our findings will be to employ electrochemical probe analysis of natural ink plumes to measure the temporal and spatial characteristics of the dopaminergic signal in ejected ink (Moore and Atema, 1988; Moore *et al.*, 1989).

The concentrations of L-dopa and dopamine varied greatly among ink sacs, but the ink sac with the highest concentration of L-dopa also had the highest dopamine concentration, suggesting a metabolic linkage. This is not surprising given that dopamine is synthesized from L-dopa through the action of dopa decarboxylase (Stryer, 1981).

The variability in catecholamine concentration among ink sacs seems not to be due to rapid oxidation, because the data shown in Figure 3 indicate that L-dopa and dopamine oxidize much more slowly in diluted ink than do standards added to filtered seawater. One source of ink antioxidant may be the melanin pigments. Recent studies suggest that, although melanins are assumed to be remarkably stable, those synthesized from L-dopa are capable of self-oxidation under biologically relevant conditions (Aime and Fasano, 1990; Crescenzi *et al.*, 1993). This reductive capacity of melanin pigments has led to the suggestion that, in living systems, melanin plays a role in removing H_2O_2 (Aime and Fasano, 1990). Although the melanin pigments could be stabilizing L-dopa and dopamine in squid ink by preventing oxidation, another antioxidant may also exist, because the experiments in Figure 3 were run on ink from which the majority of melanin pigments had been physically removed by centrifugation and filtration. Perhaps, in addition to the melanin, an antioxidant such as ascorbic acid is released with the ink. In any case, the variability among ink sacs is not due to rapid oxidation and may depend on the length of time that the ink was stored in the ink sac. We did not attempt to record the inking history of the squid used in these experiments, but some squid inked upon capture and others did not.

In summary, these experiments show that squid ink contains high concentrations of L-dopa and dopamine. This study supports earlier findings that these biogenic amines are behaviorally (Gilly and Lucero, 1992) and physiologically (Lucero *et al.*, 1992) relevant olfactory stimuli. Further work will be necessary to identify the antioxidant in the ink, determine the source of variability between animals, and characterize the chemical message in a natural ink plume.

Acknowledgments

The authors thank Dr. Randy Alberte and Dr. Sal Fidone for their generosity in allowing us the use of the HPLC equipment and gratefully acknowledge the invaluable assistance of Dr. Richard Zimmerman and Dr. Bruce Dinger. We also thank Dr. Jia Chen for running the alumina silica columns and Taylor Liu for obtaining live squid. We appreciate Jimmy Lucero's efforts both in maintaining the squid and in directing their dissection. Finally, we are grateful to the fishing community of Monterey Bay for providing us access to live squid. This work was funded by Office of Naval Research Grant N00014-89-J-1744.

Literature Cited

Aime, S. and M. Fasano. 1990. Solid-state ^{13}C NMR characterization of melanin free acids from biosynthetic and natural melanins. *Gazz. Chim. Ital.* **120:** 663–665.

Crescenzi, O., M. d'Ischia, A. Napolitano, and G. Prota. 1993. The alleged stability of dopa-melanins revisited. *Gazz. Chim. Ital.* **123:** 241–242.

Fox, D. L. 1976. *Animal Biochromes and Structural Colors.* University of California Press, Berkeley. Pp. 215–240.

Gilly, W. F., and M. T. Lucero. 1992. Behavioral responses to chemical stimulation of the olfactory organ in the squid *Loligo opalescens*. *J. Exp. Biol.* **162:** 209–229.

Gomez-Nino, A., B. Dinger, C. Gonzalez, and S. J. Fidone. 1990. Differential stimulus coupling to dopamine and norepinephrine stores in rabbit carotid body type I cells. *Brain Res.* **525:** 160–164.

Jaeckle, W. B., and D. T. Manahan. 1989. Amino acid uptake and metabolism by larvae of the marine worm *Urechis caupo* (Echiura) a new species in anexic culture. *Biol. Bull.* **176:** 317–322.

Jimbow, K., Y. Miyake, K. Homma, K. Yasuda, Y. Izumi, A. Tsutsumi, and S. Ito. 1984. Characterization of melanogenesis and morphogenesis of melanosomes by physicochemical properties of melanin and melanosomes in malignant melanoma. *Cancer Res.* **44:** 1128–1134.

Lucero, M. T., F. T. Horrigan, and W. F. Gilly. 1992. Electrical responses to chemical stimulation of squid olfactory receptor cells. *J. Exp. Biol.* **162:** 231–249.

MacGinitie, G., and N. MacGinitie. 1968. *Natural History of Marine Animals,* 2nd ed. McGraw-Hill, New York. Pp. 395–397.

Manahan, D. T. 1989. Amino acid fluxes to and from seawater in axenic veliger larvae of a bivalve (*Crassostrea gigas*). *Mar. Ecol. Prog. Ser* **53(3):** 247–255.

Moore, P., and J. Atema. 1988. A model of a temporal filter in chemoreception to extract directional information from a turbulent odor plume. *Biol. Bull.* **174:** 355–363.

Moore, P. A., G. A. Gerhardt, and J. Atema. 1989. High resolution spatio-temporal analysis of aquatic chemical signals using microelectrochemical electrodes. *Chem. Senses* **14:** 829–840.

Prota, G., J. P. Ortonne, C. Voulot, C. Khatchadourian, G. Nardi, and A. Palumbo. 1981. Occurrence and properties of tyrosinase in the ejected ink of cephalopods. *Comp. Biochem. Physiol.* **68B:** 415–419.

Stryer, L. 1981. *Biochemistry,* 2nd ed. W. H. Freeman and Company, San Francisco. Pp. 895–896.

Waite, J. H. 1992. The DOPA ephemera: a recurrent motif in invertebrates. *Biol. Bull.* **183:** 178–184.

Reference: *Biol. Bull.* **187**: 64–75. (August, 1994)

Electric Organ Discharge and Electrosensory Reafference in Skates

JOHN G. NEW

Marine Biological Laboratory, Woods Hole, Massachusetts 02543, and Department of Biology and The Parmly Hearing Institute, Loyola University of Chicago, Chicago, Illinois 60626

Abstract. Skates possess bilateral electric organs that produce intermittent, weak discharges of relatively long duration compared to the discharges of other weakly electric fish. They, like all elasmobranchs, also have an electrosensory system capable of detecting weak, low-frequency electric fields. Several studies have suggested that the discharge is used in some type of social communication. This study measured the strength and nature of the response of the skate electrosensory system to electric organ discharge.

Electric organ discharge (EOD) was elicited *via* electrical stimulation of the medullary command nucleus in two species of skates. The temporal structure and power spectra of the EODs demonstrated that they should be effective stimuli for the skate electrosensory system. The responses of electrosensory afferent fibers in the anterior lateral line nerve (ALLN) to EODs were variable depending upon the location and orientation of the receptor. The responses of most ALLN fibers were very weak compared to the strong reafference produced by the skate's ventilatory activity. Unlike the common-mode ventilatory reafference, EOD reafference was variable in terms of excitation or inhibition, depending upon receptor orientation. Despite the low signal-to-noise ratio observed in ALLN responses to EODs, it is likely that EODs serve as a communicative signal over moderate distances.

Introduction

Marine elasmobranchs of the skate family (Rajidae) possess electric organs that generate a weak electric organ discharge (EOD) (for reviews of electric organs see Grundfest and Bennett, 1961; Bennett, 1971; Bass, 1986). Although the existence of these organs has been known since the last century (Stark, 1844; Ewart 1888a, b, 1892), the behavioral function of these organs has yet to be conclusively determined. Owing to its small amplitude (Bennett, 1971; Bratton and Ayres, 1987), the EOD of the skate is unlikely to be used in prey capture, unlike the discharge of the larger and more powerful electric organ found in rays of the genus *Torpedo*. Furthermore, unlike the nonhomologous electric organs of freshwater teleost fishes (notably the gymnotids and mormyrids), the skate electric organ is only intermittently active and is more variable in amplitude and temporal discharge pattern (Bennett, 1971; Bratton and Ayres, 1987). Although an intra- or interspecific communicative function for this discharge has been suggested (Mikhailenko, 1971; Mortenson and Whitaker, 1973; Bratton and Ayres, 1987), the precise role of such communication in the skate's ethogram remains to be conclusively determined.

The electric organs of the skate are spindle-shaped structures that extend bilaterally along the length of the longitudinal axis of the tail (Stark, 1844; Ewart, 1888a; Sanderson and Gotch, 1888) (Fig. 1). The organ consists of approximately 8,000–10,000 cup- or disk-shaped electrocytes arranged anteroposteriorly in series (Ewart, 1892; Brock *et al.*, 1953; D. M. Koester, Univ. of New England, pers. comm.). Each electrocyte develops a weak potential when depolarized by the innervating nerve fibers (Bennett, 1971). Previous studies have demonstrated that the electric organ discharge of various skate species is of variable amplitude and duration, but generally consists of a monophasic, head-negative wave of 60–500 ms duration (Bennett, 1971; Bratton and Ayres, 1987). The electrocytes themselves are not electrically excitable overall, although the posterior face of the cup-shaped electrocytes possesses an electrically excitable component that involves a delayed rectification (Bennett, 1971). Electrocytes in the skate electric organ are innervated by motor neurons in the

Received 15 July 1993; accepted 19 May 1994.

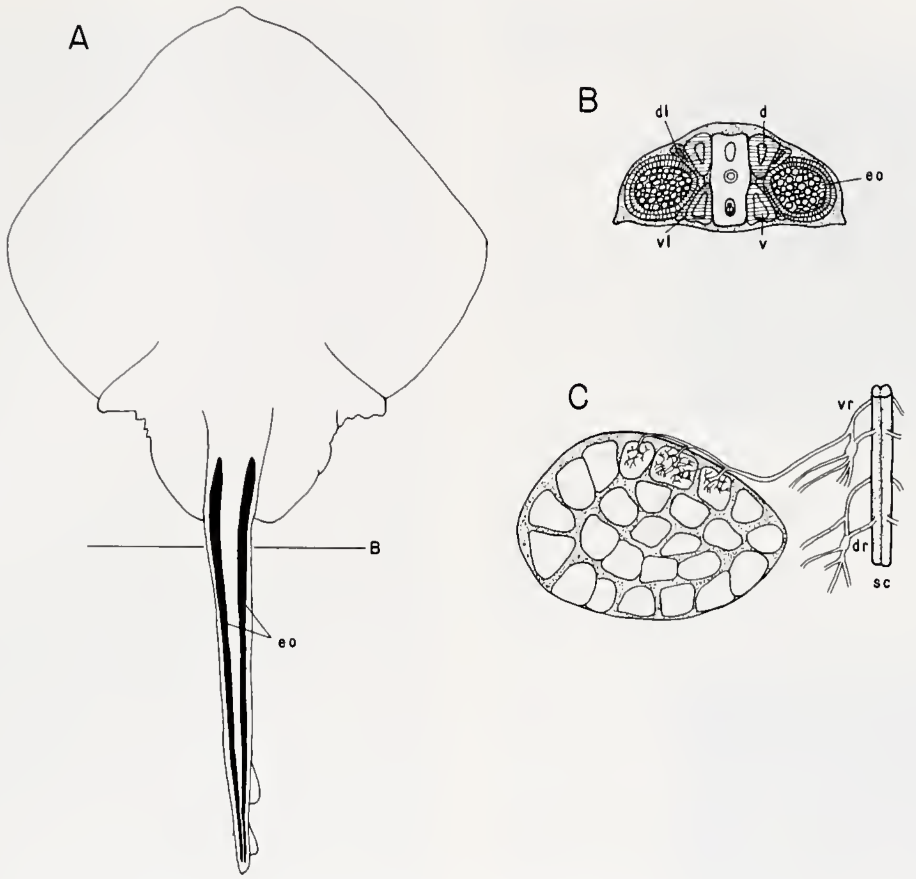

Figure 1. Location and innervation of the electric organs in *Raja.* (A) Location of electric organs (in black) in the tail of *Raja.* (B) Transverse section through the tail of *Raja* at the level indicated in A, showing the electric organs, muscles, and vertebral column. (C) Innervation of electrocytes by spinal electromotor nerves. (Modified from Ewart, 1892; and Bratton and Ayers, 1987.) Abbreviations: d, dorsal muscle group of epaxial musculature; dl, dorsolateral muscle group of epaxial musculature; dr, dorsal root of spinal nerve; eo, electric organ; sc, spinal cord; v, ventral muscle group of hypaxial musculature; vl, ventrolateral muscle group of hypaxial musculature; vr, ventral root of spinal nerve.

ventral spinal cord (Koester, 1987; Baron *et al.,* 1992), which in turn are believed to receive direct descending input from an electric organ command nucleus (EOCN) located in the basal midline of the medulla (Albe-Fessard and Szabo, 1955; Szabo, 1955, 1961). The location and nature of any higher level descending projections to the EOCN are unknown, although reflexive EODs in response to tactile stimulation can still be elicited in skates following ablation of the telencephalon or the cerebellum (Albe-Fessard and Szabo, 1955).

Skates, like other elasmobranchs, also possess an electrosensory system capable of detecting the very weak electric fields produced by physicochemical and biological phenomena in aquatic environments (for reviews, see Bodznick and Boord, 1986; Kalmijn, 1988). The electrosensory receptor organs, the ampullae of Lorenzini, are innervated by fibers of the anterior lateral line nerve (ALLN), which project to and terminate within the first-order electrosensory nucleus of the medulla, the dorsal octavolateralis nucleus (DON). The ampullae themselves consist of a long tubelike canal that terminates internally in a bulbous alveolus and externally through a pore in the epidermal surface (for reviews of ampullary electroreceptor structure and function, see Murray, 1974; Bennett and Clusin, 1978; Sejnowski and Yodlowski, 1982; Bodznick and Boord, 1986). The apical membranes of the receptor cells themselves are embedded in the base of the alveolus and connected to the walls of the alveolus by tight junctions. The walls of the alveolus and canals have a high electrical resistance, and the internal lumen of the ampulla is filled with a highly conductive, K^+-rich, jelly-like matrix (Murray and Potts, 1961). The ampulla thus functions as an insulated core conductor, and the receptor cells measure the voltage drop across the length of the ampulla; *i.e.,* the receptors measure the potential difference between the internal lumen, which is isopotential with the external environment at the epidermal pore, and the internal field gradient established within the animal by the low skin resistance and high conductivity of the internal tissues.

The electrosensory system of elasmobranchs is extremely sensitive; the behavioral threshold for responses to dipole sources is less than 5 nV/cm (Murray, 1974; Kalmijn, 1982). The electrosensory system is most sensitive to low-frequency electric fields, from near direct current (DC) (<0.01 Hz) to approximately 10–15 Hz (Montgomery, 1984a; New, 1990; Tricas and New, unpub. obs.). Behavioral studies have demonstrated that the electrosensory system is used in directing prey-catching behavior; elasmobranchs will strike at electrical sources that mimic the bioelectric fields produced by living organisms in water (Kalmijn, 1971, 1982). Other studies suggest that elasmobranchs may also use their electrosense to detect electric fields induced by movement relative to the earth's magnetic field (Kalmijn, 1978). Additionally, recent experiments in a mating population of stingrays (which lack an electric organ) demonstrated that males search for and locate females hidden beneath a sand substrate by detecting the weak ventilatory potentials produced by the females (T. Tricas, Florida Inst. Tech., pers. comm.). The ability of male stingrays to detect the very weak signals of females (approximately 5 μV intensity at 1 cm from the spiracle) at a distance (about 1 m) suggests that the electric organ in skates may serve a useful purpose in social communication (Mikhailenko, 1971).

The purpose of this study is to characterize the EOD and examine the responses of the skate electrosensory system to discharge of the animal's own electric organ, with specific regard to the usefulness of this organ in signaling other skates and to the nature and amount of reafference it produces. Previous studies have indicated that the ventilatory potentials produced by elasmobranchs are a significant source of electrosensory reafference (Montgomery, 1984a; New and Bodznick, 1990; Bodznick and Montgomery, 1992; Bodznick *et al.*, 1992). This internally generated reafference modulates the activity of electroreceptors by changing the voltage at the internal face of the apical membrane of the receptor cells. These internal potentials thus provide a source of common-phase reafference; all receptors are excited or inhibited in phase with one another regardless of receptor orientation or position on the body surface. Whether the electric organ discharge of the skate also constitutes a significant source of internal reafference, *via* a similar low-resistance internal pathway, is also investigated in this study.

Materials and Methods

Specimens of little skate, *Raja erinacea* (n = 18), and winter skate, *Raja ocellata* (n = 2), were collected by otter trawl in the vicinity of Woods Hole and the Elizabeth Islands, Massachusetts. The specific identity of individual skates was determined by counting the teeth series in each jaw (Bigelow and Schroeder, 1953). The animals were held in temperature-controlled (16°C) running seawater tanks prior to experimentation.

Individual skates were anesthetized in approximately 0.025% tricaine methanesulfonate (MS-222) and the dorsal aspect of the brain and anterior lateral line nerve (ALLN) exposed. In some cases, the thoracic spinal cord, the rostral and caudal poles of the electric organ, or all three, were exposed at one or two locations for implantation of stimulating electrodes. The animal was decerebrated by a complete transection of the diencephalon and caudal telencephalon at the level of the optic chiasm. The animal was then placed in an acrylic holder designed to hold the animal immobilized during the experiment. Immobilizing drugs such as curare were not employed in this study because they block synaptic transmission at the spinal motor nerve–electric organ electrocyte junction. The holder was positioned in an acrylic tank (61 cm × 12.5 cm × 45.5 cm), and cooled (12°C), recirculated, aerated seawater was passed over the gills by means of an oral tube to ensure an adequate supply of oxygen. A small pulse of fast green dye was injected into the oral tube to ensure that water was passing over the gills and not back out of the mouth or spiracle.

The discharges of the electric organ were measured through Ag-AgCl wire electrodes bilaterally or unilaterally implanted subcutaneously at about the level of the rostral and caudal poles of the electric organ in the tail. The discharges were amplified and recorded on tape with an instrumentation recorder (Vetter, Model B) for subsequent analysis. The spread and orientation of the internal and external fields generated by discharge of the electric organ were measured directly by electrodes either in the seawater bath or implanted in the ampullary clusters within the body of the skate (see below). External fields were measured using an Ag-AgCl wire electrode positioned at various locations around the animal's body in the seawater bath. A reference electrode was positioned at some distance (approximately 25 cm) from the animal. Both electrodes were connected to a Grass P-15 differential preamplifier, filtered between 0.3 Hz and 1.0 kHz (time constant >150 ms), and measured directly on an oscilloscope. Internal potentials were measured by implanting an insulated Ag-AgCl tipped wire electrode into the subdermal clusters of ampullary alveoli in which the electroreceptors are located. The recording electrodes were introduced through a fine hypodermic needle inserted through the skin at a point on the animal above the water line in the tank and then withdrawn. The reference electrode was then positioned at various locations around the skate's body to measure the voltage drop across the length of the receptors (in a manner similar to the voltage measured by the receptors). The potential difference between recording (internal) and reference (external) electrodes was amplified by a Grass P-15 preamplifier and measured on an oscilloscope.

The activity of individual ALLN fibers was recorded by means of glass micropipette electrodes filled with 2 *M* NaCl saturated with fast green dye and with input impedances of 12–20 megohms. Responses of ALLN fibers were recorded directly from the nerve, near the ALLN ganglion. Electrosensory ALLN fibers were initially identified by their responses to a uniform electric field oriented along the longitudinal axis of the tank between two carbon rod electrodes connected to a Grass Instruments S-88 stimulator. The field stimulus consisted of DC-step pulses of approximately 100 μV/cm amplitude and 700 ms duration. The intensity of the field was measured directly in the tank by means of two Ag-AgCl wire electrodes positioned 10 cm apart and parallel with the orientation of the field. The threshold receptive fields of the individual ALLN fibers were subsequently identified with a hand-positioned local dipole source consisting of two 2.0-mm (o.d.) glass tubes filled with 2% agar in seawater and connected to a Grass Instruments S-88 stimulator *via* Ag-AgCl wire electrodes. The initial intensity of the local DC-step field, measured directly at one of the poles, was <50 μV, and the average distance between the poles of the local dipole was 4.0 cm. Upon encountering ampullary pores responding to local electric field stimuli, the stimulus was systematically decreased to identify as nearly as possible the threshold receptive field of the recorded ALLN fiber. In this study, the threshold receptive field is defined as the location of the epidermal pore of the ampullary electroreceptor, but in actuality the "receptive field" of the electroreceptor is the distance between the pore and the electroreceptor cells within the internal alveoli across which the voltage drop is measured. Action potentials recorded from ALLN fibers were transformed into digital logic pulses through a WPI window discriminator and stored as peristimulus time histograms on a Tracor Northern signal analyzer. Additionally, spike activity and electric organ discharges were in some cases recorded as analog signals on a Vetter Model B reel-to-reel instrumentation tape recorder. Electric organ discharges recorded in this manner were converted to digital signals, and the power spectra of the signals were analyzed using a Zenith 286 microcomputer and ASYSTANT PLUS (Keithley Metrabyte) analytical software. Aliased frequencies represented in the generated power spectra were removed by software filtering.

Electric organ discharges (EODs) were elicited in skates by several different techniques. The methods employed included stimulation of the thoracic spinal cord either by insertion of a concentric bipolar stimulating electrode or *via* two monopolar stimulating electrodes located several centimeters distant from each other along the longitudinal axis of the cord. Alternatively, monopolar stimulating electrodes were placed at the rostral and caudal pores of the electric organ. Finally, EODs could be elicited through stimulation of the medullary electric organ command nucleus (EOCN) by means of an implanted concentric bi-

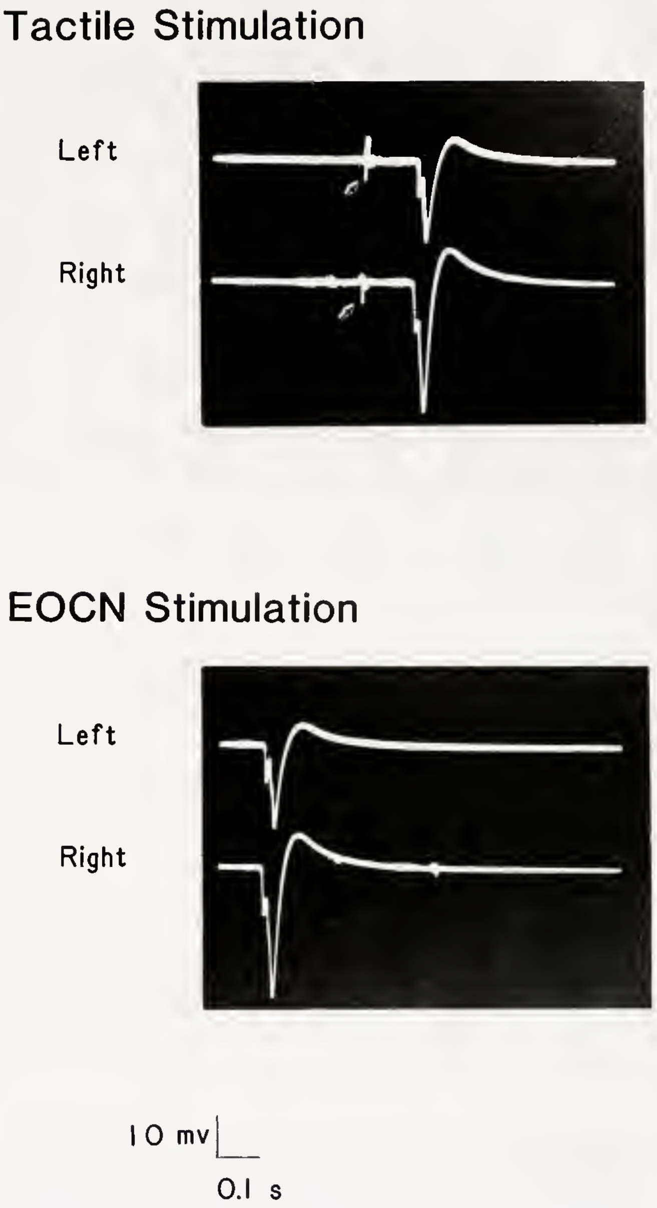

Figure 2. Electric organ discharges (EODs) measured simultaneously in right and left electric organs. Upper photo: EODs elicited by tactile stimulation (gentle tap of dorsal surface). Arrows indicate electromyograms of spinal reflexive withdrawal of pelvic fins following delivery of tactile stimulus. Lower photo: EODs recorded in the same animal by electric pulse train stimulation of the medullary electric organ command nucleus (EOCN). Stimulus delivery was 10 ms following initiation of the oscilloscope sweep.

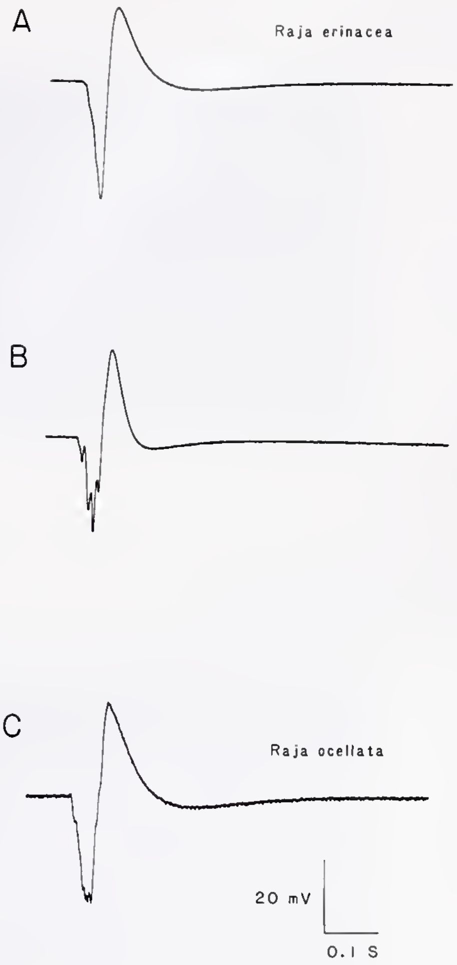

Figure 3. Electric organ discharges recorded from *Raja erinacea* (A, B) and *Raja ocellata* (C). The traces in (B) and (C) exhibit the multiple small peaks seen in many EODs evoked by both tactile and command nucleus stimulation.

polar electrode. In those cases in which the latter method of stimulation was employed, the trigeminal nerves were bilaterally transected to reduce movement caused by volume conduction of electrical current from the stimulating electrode to the nuclei of the branchiomeric motor column. Stimuli consisted of single DC step pulses or, more commonly, brief trains of pulses (3–5 pulses/train). The duration of the stimulus pulses was 0.5 ms, pulse amplitude 3–12 V; the pulse rate of the trains varied from 50–400 Hz, depending upon location; and the train duration was 40–70 ms.

Results

Electric organ discharges

Discharges of the electric organ (EODs) in the skate could be elicited by stimulation of the spinal cord, the electric organ, or the electric organ command nucleus; however, only the last method was found to be consistently reliable. Stimulation of the spinal cord with either a single concentric bipolar electrode or two monopolar electrodes placed at locations several centimeters distant from each other along the longitudinal axis of the cord was only occasionally successful in eliciting repeatable EODs, despite numerous repositionings of the stimulating electrode or electrode pairs. Neither single pulse stimuli nor trains of pulses up to 400 Hz elicited consistent EODs, despite the fact that they repeatedly and consistently elicited large motor neuron responses, as indicated by movement and electromyograms (EMGs) recorded *via* the subcutaneous electrodes planted in the tail. Similarly, concentric bipolar or paired monopolar electrodes implanted in the electric organ itself were only occasionally successful in eliciting EODs, presumably by means of the excitation of the presynaptic elements of the neural–electric organ junction.

Stimulation of the electric organ command nucleus (EOCN) was the most reliable method for eliciting consistent and repeatable EODs. Brief (50 ms) trains of 0.5-ms pulses delivered at 40–75 Hz and 3–5 V intensity were found to be sufficient stimuli. These were much lower frequencies and intensities (up to 15V and 500 Hz) than were required to occasionally elicit EODs by spinal cord or electric organ stimulation. The threshold of the EOD response to stimulation of the EOCN was dependent upon the location of the stimulating electrode; optimum results were found within an approximately 3-mm length of the basal medulla at the level of entry of the facial (VII) nerve.

The electric organ discharges recorded following stimulation of the EOCN were strongly similar in amplitude, duration, and waveform to those elicited by tactile stimulation (gently brushing or tapping the dorsal surface of the animal) and to the occasionally recorded spontaneous EODs generated by the animal (Fig. 2). Discharges in all cases were bilateral (both organs discharged) and synchronous, although occasionally an asymmetry in amplitude of the discharge was observed between the right and left electric organs. Such asymmetries occurred following both EOCN stimulation and tactile stimuli and persisted in multiple trials.

When measured across the rostrocaudal length of the electric organ by implanted subcutaneous electrodes, the EOD of both *R. erinacea* and *R. ocellata* consists primarily of a large peak that is negative with respect to the rostral pole of the organ, followed in most cases by a shallower and longer lasting positive component (Fig. 3). The mean amplitude of the negative peak for all waves recorded was −27.9 mV (SEM 2.58, $n = 35$), and the mean duration of the negative peak was 53.5 ms (SEM 2.16). The mean amplitude of the positive component of the EOD waveform was +11.12 mV (SEM 2.16, $n = 33$) and the mean duration was 192.35 ms (13.6 SEM). In both spontaneous EODs and those elicited by tactile or electrical stimulation,

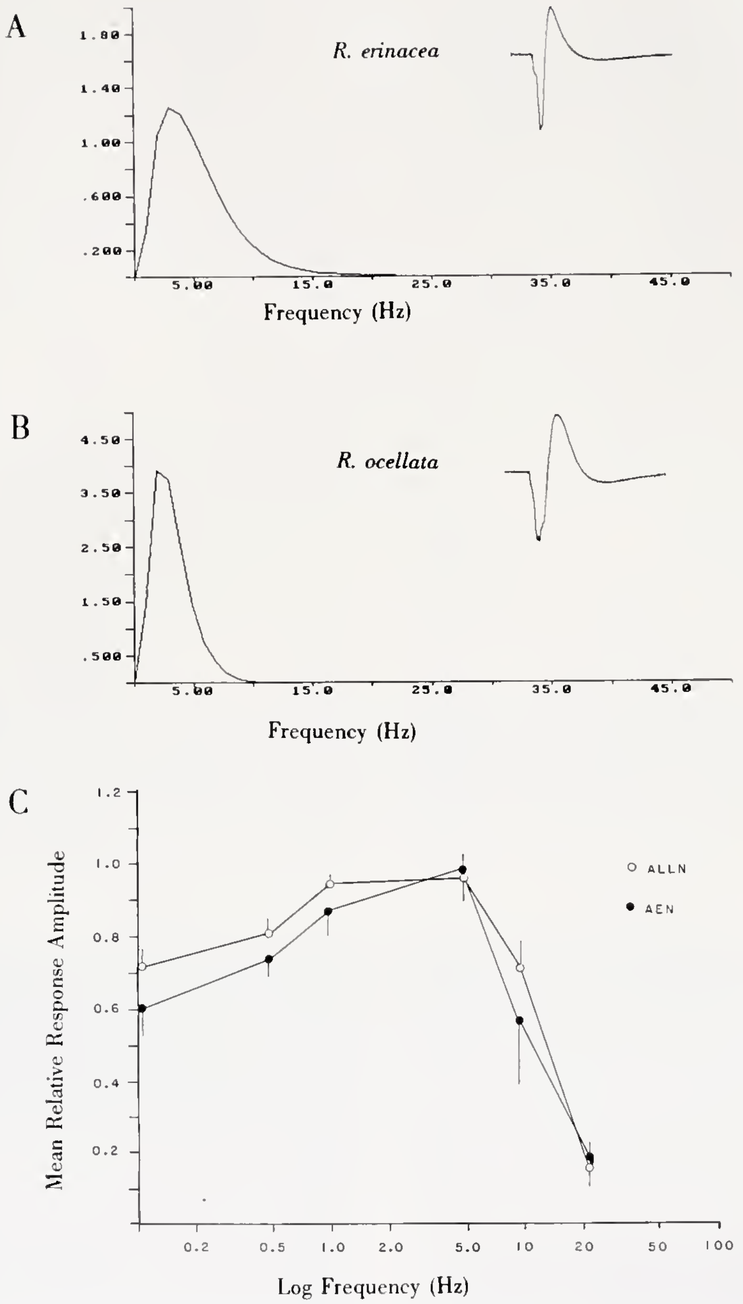

Figure 4. Power spectra of electric organ discharges recorded from *Raja erinacea* (A) and *Raja ocellata* (B) compared with frequency response curves generated for anterior lateral line nerve (ALLN) electrosensory afferent fibers and medullary ascending electrosensory neurons (AENs) (C). Bottom graph modified from New (1990).

there were frequently one or several small, sharp, positive peaks superimposed upon the slower negative wave (Fig. 3B). However, the shape of the waveform appeared to be very consistent for a specific individual, showing only minor variations, if any, between spontaneous and elicited EODs. The mean latency of the EOD of *R. erinacea* following EOCN stimulation was 89.4 ms (SEM 2.7, n = 26). The latency of EODs elicited by tactile stimulation was considerably longer than the responses of muscles that appeared to be involved in spinal reflexes, such as the pelvic fin withdrawal reflex. Figure 2 illustrates an EOD elicited by lightly tapping the animal's dorsal surface. The EMG recorded as the animal withdrew its pelvic fins can be observed at a considerably shorter latency (90 ms)

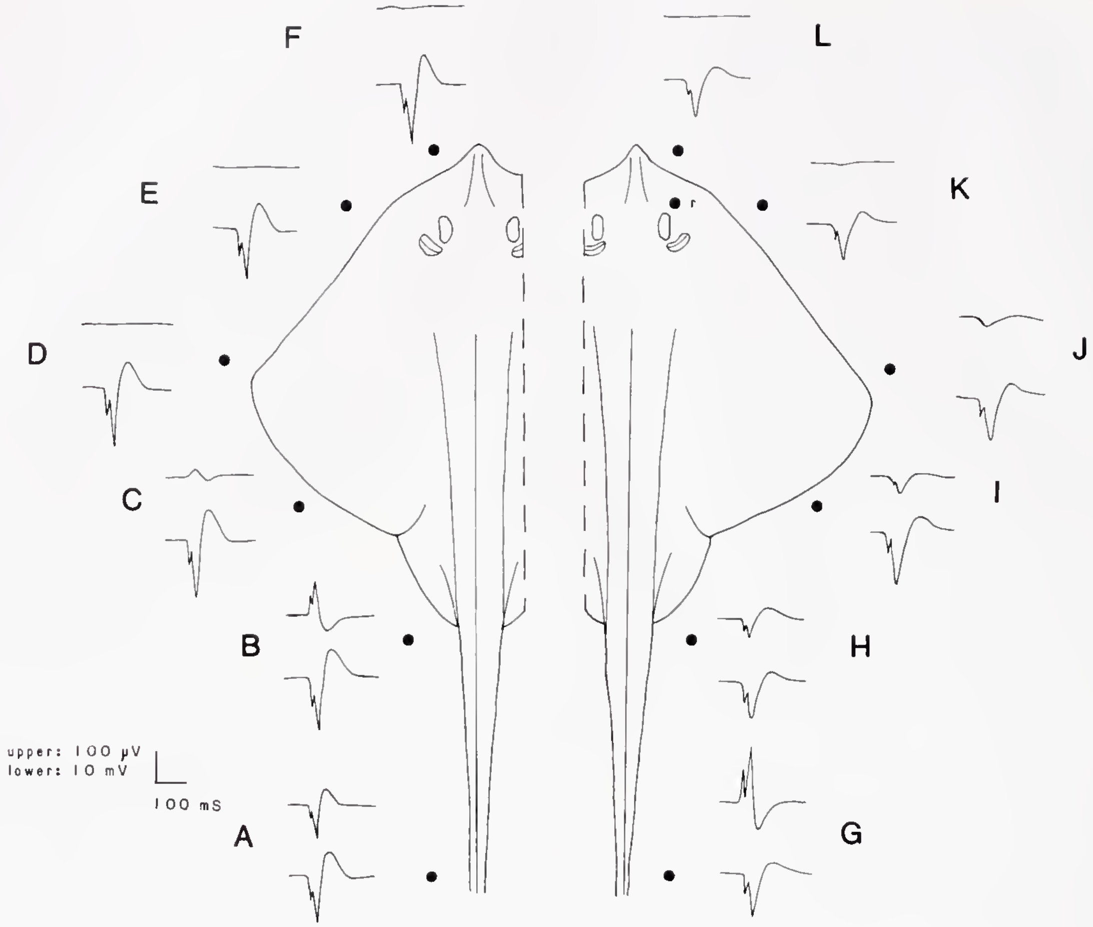

Figure 5. Field strength of the electric organ discharge elicited by EOCN stimulation measured around the body of the skate. Each pair of traces represents the field measured locally at the point indicated by the dot associated with each letter (top trace) and the EOD measured subcutaneously along the length of the electric organ (bottom trace). In traces A–F, the recording electrode was placed at the indicated locations and the reference electrode at a distant location. In traces G–L, the recording electrode was implanted in the ampullary tissues at the location marked "r" and the reference electrode at the positions indicated around the perimeter of the animal. In the latter examples, the voltage measured approximated the voltage drop along the length of the ampullary electroreceptors so oriented.

than the elicited EOD (235 ms), suggesting that somatosensory information must first ascend, presumably at least to medullary levels, rather than eliciting an EOD *via* a direct spinal reflex pathway to the electric organ motor neurons in the spinal cord.

The EODs of mature male and female specimens of *R. erinacea* and *R. ocellata* were recorded on tape and digitized for frequency composition analysis. The power spectra obtained from EODs of all specimens indicate that the majority of the power in the EOD signal is in a single range of frequencies between less than 1.0 Hz and 10–15 Hz, with the peak of the power spectra between 1.8 and 3.0 Hz (Fig. 4). Although the number of *R. ocellata* used in this study was too small for statistical analysis ($n = 2$), the mean duration and amplitude of the EOD of *R. ocellata* were within the range of those observed for *R. erinacea* (mean duration, negative peak = 50 ms, mean amplitude = −35 mV), and there appeared to be little difference in either the EOD waveform or power spectra between the two species.

The spread of the EOD around and through the skate was measured with external and internally implanted electrodes (Fig. 5). The externally measured field created by the EOD reverses its polarity across the length of the electric organ and diminishes sharply with increasing distance around the surface of the animal from the rostral terminus of the organ, diminishing to less than millivolt intensity at the rostral end of the skate's body (Fig. 5A–F). The amplitude of the externally measured EOD at the rostral terminus of the organ, at a lateral distance of 1 cm from the tail, was 180 µV peak to peak. At a distance of 4.6 cm from the rostral tip of the electric organ along

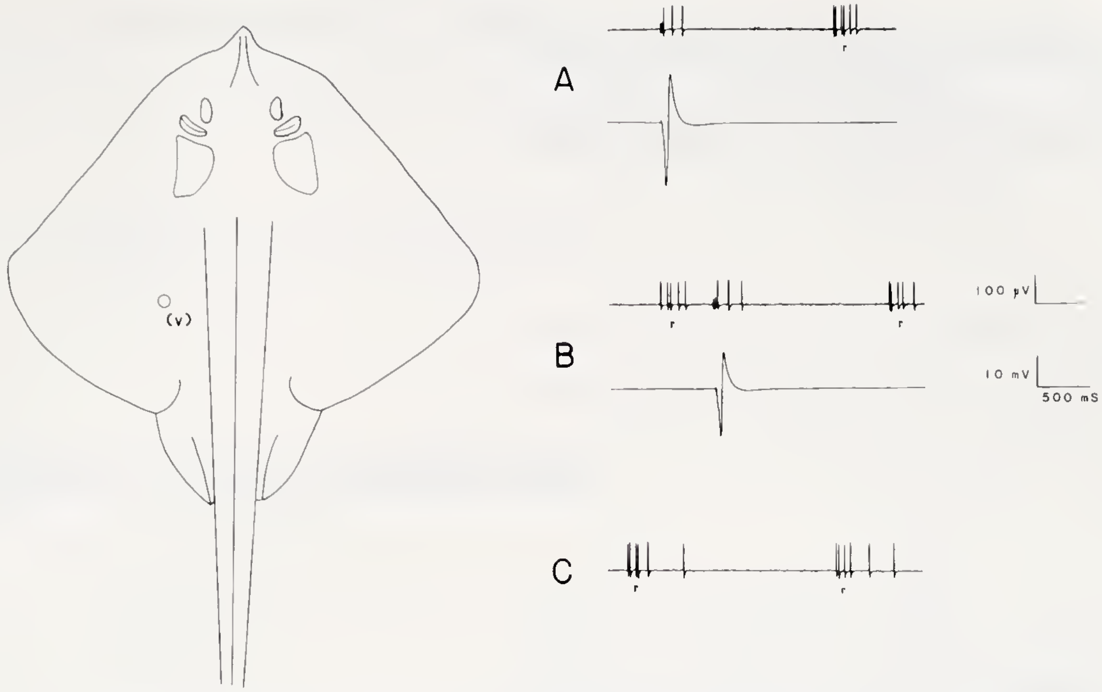

Figure 6. Responses of a single electrosensory ALLN afferent fiber to an elicited EOD. The location of the epidermal pore of the ampullary electroreceptor innervated by this particular afferent is shown at the location marked "(v)" (the pore was located upon the ventral surface of the skate). The small series of waves immediately preceding the EOD-invoked reafferent burst is a stimulus artifact of the train pulse delivered to the EOCN. The bursts of activity indicated with the letter "r" indicate reafferent activity caused by the animal's ventilation.

the pectoral disk, the amplitude had decreased to 50 μV, and at 8.7 cm (at the widest diameter of the pectoral disk) the peak-to-peak amplitude had decreased to less than 5 μV. A recording electrode was subsequently implanted inside the animal in the region of the superficial ophthalmic ampullary cluster. The EOD thus measured as the difference across the skin of the skate (*i.e.*, across the length of the receptors) was similar to the externally measured field in amplitude and decrease in amplitude with distance from the electric organ, but the polarity of the recorded discharge was reversed (Fig. 5G–L). The latter results indicate that the electric organ discharge does not generate a significantly strong internal field contrary to that generated during the animal's ventilatory activity.

Responses of electrosensory ALLN afferent fibers

A total of 32 individual ALLN fibers with identified ampullae were recorded in this study. The responses of electrosensory ALLN fibers innervating different ampullary electroreceptors displayed considerable variability, depending upon the location of the ampullary pore. Ampullary organs opening through caudally directed canals to pores located upon the caudal surface of the pectoral fin showed the greatest responses (Figs. 6, 7). The maximal instantaneous frequency of the action potential response recorded from these afferents was approximately 12 spikes/second. Ampullary organs with more rostrally located pores showed responses with a much lower signal-to-noise ratio (Fig. 8). The responses of the most rostrally located and directed organs (the majority of ampullary electroreceptors in the skate) showed very weak responses to electric organ discharges, or no detectable response above the normal resting activity of the ALLN fiber.

Additionally, the temporal pattern of the measurable responses of identified electrosensory ALLN afferents varied depending upon the location and orientation of the ampullary organ canal and epidermal pore. Generally, fibers innervating the most caudally oriented and located ampullary organs responded with a brief burst of action potentials during the positive-going phase of the EOD (Fig. 7). The response pattern for units innervating more-rostral ampullary organs is less clear owing to the low signal-to-noise ratio of the response and the ongoing activity of the fiber. However, several of these neurons demonstrated a response that was out of phase with the more caudal units, *i.e.*, an inhibition of activity associated with the EOD. In no case was the response of electrosensory ALLN fibers to discharge of the electric organ as robust as the response of these same units to the potentials gen-

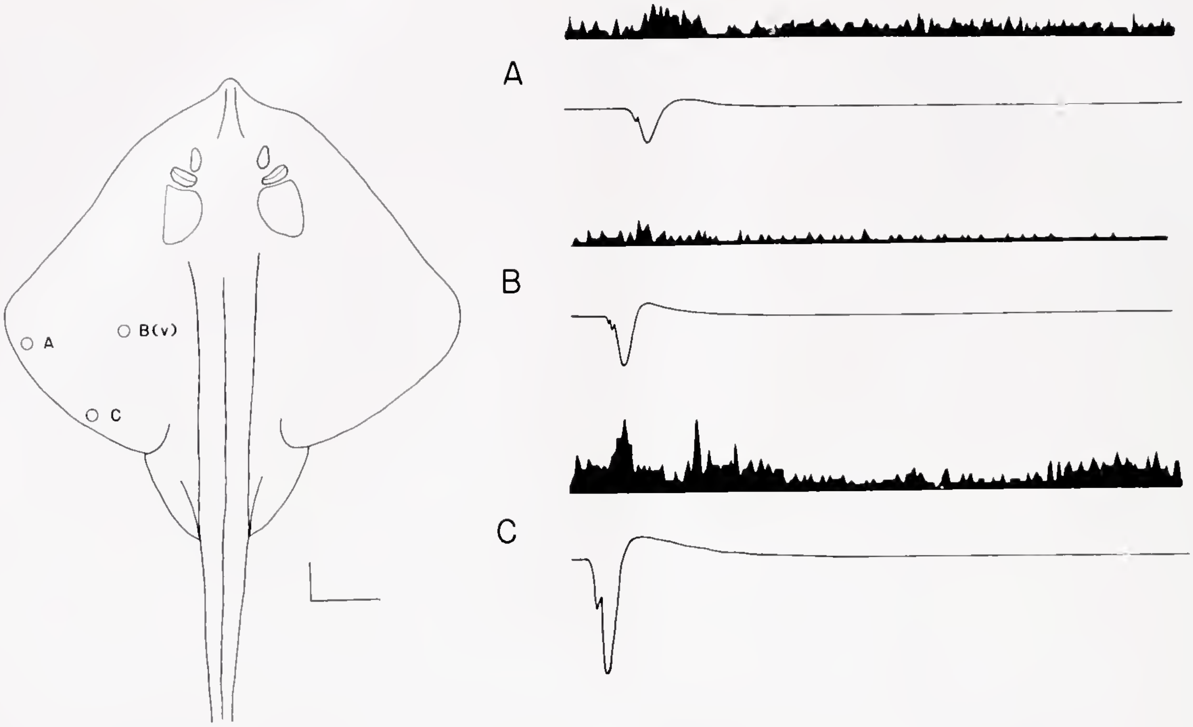

Figure 7. Peristimulus time histograms (PSTHs) of EOD-invoked reafference in three ALLN electrosensory afferent fibers innervating caudally oriented ampullary receptors. The ampullary pores of the receptors are indicated by the open circles; "v" indicates a pore on the ventral surface of the pectoral disk. The horizontal time scale equals 100 ms; the vertical scale indicates instantaneous frequencies of 17.5 spikes/s (A, B) and 7.5 spikes/s (C).

erated by the animal's ventilatory activity (Fig. 6). The maximal spike rate of the responses to respiratory potentials in ALLN fibers approached 91 spikes/second.

Discussion

Reafference produced as a result of motor activity plays an important role in the activity and organization of nervous systems. Ventilatory activity in skates produces a strong reafference, driving the electrosensory ALLN afferents through approximately 63% of their dynamic range (New and Bodznick, 1990). Reafference of this intensity may well interfere with the animal's ability to detect externally generated fields of interest to the animal. In the central nervous system of elasmobranchs, electrosensory reafference produced by ventilatory activity (gilling) is reduced through a common-mode rejection mechanism based upon commissural and unilateral local circuit neurons in the first-order medullary nucleus (Montgomery, 1984b; New and Bodznick, 1990; Bodznick and Montgomery, 1992). Unlike the common-mode reafference produced by ventilation, in which all fibers are excited and inhibited in phase together, the response of electrosensory ALLN afferents to the EOD is highly variable among fibers innervating different ampullary receptors, both in the intensity of the response and in the temporal pattern. Invariably, the reafference produced by discharge of the electric organ is much weaker than that generated by ventilation; the maximal response of the most caudally directed ampullary organs drives the fibers through less than 10% of their dynamic range. Indeed, for most of the electroreceptors, which are located in the rostral third of the pectoral disk, the responses of innervating ALLN fibers to the EOD are difficult to detect against the ongoing activity of the nerve.

The variability in intensity and temporal pattern of ALLN fiber responses indicates that the reafference produced by electric organ discharge is fundamentally different from that produced when the animal ventilates. Respiratory potentials are produced by the modulation of DC potentials generated by the different electrical properties of various body surfaces in contact with the surrounding seawater, particularly ion-exchange surfaces. Potentials thus produced are probably modulated by changes in the resistance of the current pathway caused by the opening and closing of mouth and gill slits during ventilation (Kalmijn, 1988; Bodznick *et al.*, 1992). These potentials modulate the activity of ampullary organs by changing the voltage at the *internal* surface of the apical

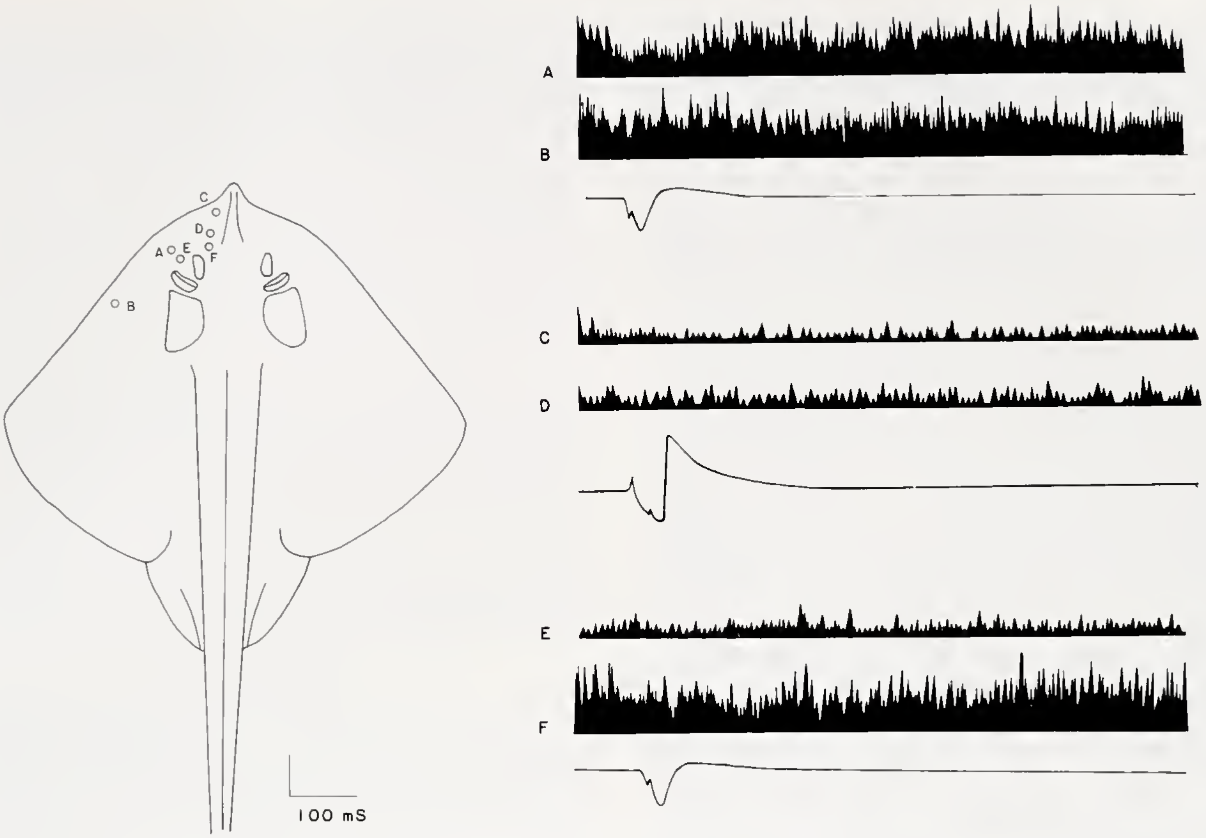

Figure 8. Peristimulus time histograms (PSTHs) of EOD-invoked reafference in ALLN electrosensory afferent fibers innervating rostrally located ampullary receptors. The ampullary pores of the receptors are indicated by the open circles; the pores were located on either the dorsal or ventral surface of the pectoral disk. The horizontal time scale equals 100 ms; the vertical scale indicates instantaneous frequencies of 20.0 spikes/s (A, B, F) and 17.1 spikes/s (C, D, E).

membrane of the receptor cells by means of current flow through a low-resistance pathway in the visceral tissues of the skate. All receptor cells are thus modulated in phase together from the inside, regardless of the orientation of the receptor's canal or the location of the ampullary pore on the surface of the body. Such is clearly not the case for reafference produced by the EOD.

The variability of the responses of ALLN fibers to EOD reafference suggests that the EOD spreads over the outside and inside of the animal and modulates the activity of ampullary electroreceptors differentially depending upon receptor location and orientation with respect to the generated external electric field. The experiments measuring the shape and intensity of the field generated by the EOD support this view. When measured with respect to a distant (approximately 25 cm) reference electrode, the strength of the field drops off rapidly with increasing distance from the electric organ, possibly dropping off to below the detectable range of elasmobranch electroreceptors within several body lengths. When the recording electrode is implanted within the tissues of the ampullary cluster, and the voltage drop along the length of the receptor is measured by moving the reference electrode to various locations around the animal's epidermis, a similar decrease in voltage with distance from the electric organ was observed, although the polarity of the recorded EOD was reversed. These results indicate that the EOD does not modulate the activity of electroreceptors internally, as do the potentials produced during ventilation, but rather through an external and internal spread of the EOD over the surface and through the tissues of the animal. It is possible that the electric organs are insulated from the low-resistance tissues of the viscera by the surrounding layers of muscle and connective tissue sheathing of the EOD in the skate's tail.

Although it is difficult to discern the responses of many individual electrosensory ALLN fibers to the EOD against the ongoing activity of the fiber, the peaks of the EOD power spectrum fall within the bandwidth to which ampullary electroreceptors are most sensitive (1–5 Hz) and suggest that the EOD should be an effective stimulus at short ranges. Although the signal-to-noise ratio of primary afferent fiber responses to EOD appears to be low when compared to that generated by ventilation, these fibers have a high, steady rate of resting activity and, in these experiments, are being strongly modulated by the fish's ventilatory potentials. Physiological studies in *Raja* and in other elasmobranchs have shown that the ascending electrosensory neurons (AENs) in the first-order medullary nucleus have a substantially higher signal-to-noise ratio for weak external fields. This higher ratio is the result of a low resting activity and the presence of central mechanisms for the suppression of ventilatory reafferent interference (Montgomery, 1984b; New and Bodznick, 1990; Bodznick and Montgomery, 1992). Furthermore, it has been demonstrated in elasmobranchs and other electroreceptive fish that behavioral thresholds for electric field detection are substantially lower than those measured physiologically, particularly at the level of the hindbrain. Thus, the responses of central neurons to electric organ discharges, produced as reafference or by another skate, may be substantially greater than those recorded in the ALLN fibers. Indeed the ability of male stingrays to detect the very much smaller respiratory potentials of female conspecifics at considerable distances (up to 1 m) (T. Tricas, Florida Inst. Tech., in prep., cited with permission) argues that the electric organ discharges of skates may be effective signals at considerable distances.

Although several studies have examined the production in different circumstances of electric organ discharges in skates, no behavioral studies have conclusively demonstrated a behavioral role for the EOD. Mikhailenko (1971) presented limited evidence that EODs may play a role in social communication by demonstrating seasonal variations in EOD structure. From these data he suggested a relationship between EOD changes and seasonal reproductive cycles. Mortenson and Whitaker (1973) reported that the frequency of electric organ discharge was greater from pairs of skates swimming together than for skates held singly; these authors also noted an increased frequency of discharge during the dark portion of the light: dark cycle. Bratton and Ayers (1987) observed that skates produced EODs in response to presentation of tactile or electric field stimuli and also when physically encountering other skates. All of these studies strongly suggest a social communication function for the EOD, but the lack of any overt behavior typically associated with discharge of the electric organ makes it difficult to define a contextual behavioral role for these discharges. The temporal structure and power spectra of the EODs of male and female *Raja erinacea* and *Raja ocellata* recorded in this study were very similar, which would seem to preclude gender or species identification by EOD identification. The results of this study differ somewhat from those of Mortenson and Whitaker (1973) and Bratton and Ayers (1987), in that the time course of EODs recorded from the two specimens of *R. ocellata* was very similar to that recorded from *R. erinacea*. Such a difference may be related to the method by which EODs were elicited in this study (electrical stimulation of the EOCN in a decerebrate animal), although EODs evoked by tactile stimulation were invariably very close to those elicited by EOCN stimulation. Alternatively, seasonal variation in the structure of the EODs of *R. ocellata* or the low number of specimens used in this study may account for the observed discrepancy, because variability in the EOD of *R. ocellata* has been observed in other studies (Bratton *et al.*, 1993). Studies in other fishes with weak electric organs have demonstrated that both the pattern of the EOD and the sensitivity of the electrosensory system can be modified by increased androgen secretion associated with sexual maturity (Meyer and Zakon, 1982; Meyer, 1983; Zakon and Meyer, 1983; Bass and Hopkins, 1984). However, changes in the EOD structure and receptor sensitivity have not been tested for in the reproductive cycles of skates.

Acknowledgments

This work was supported by the generosity of the Grass Foundation through a Grass Foundation Fellowship in Neurophysiology. Additional support was provided by an NIH NRSA postdoctoral fellowship. The author thanks Drs. S. L. Coombs, D. M. Koester, T. C. Tricas, T. H. Bullock, and an anonymous reviewer for critical comments and advice in the preparation of the manuscript.

Literature Cited

Albe-Fessard, D., and T. Szabo. 1955. Localisation du centre reflexe de la decharge electrique chez le Raie. *C R Seances Soc. Biol.* **149:** 459–452.

Baron, V. D., L. S. Sokolova, and N. A. Mikhailenko. 1992. Identification of spinal electromotoneurons in the ray, *Raja clavata* (Rajidae). *Neuroscience* **48(2):** 397–403.

Bass, A. H. 1986. Electric organs revisited. Pp. 13–70 in *Electroreception*, T. H. Bullock and W. Heiligenberg, eds. Wiley, New York.

Bass, A. H., and C. D. Hopkins. 1984. Shifts in frequency tuning in androgen-treated mormyrid fishes. *J. Comp. Physiol.* **155:** 713–724.

Bennett, M. V. L. 1971. Electric organs. Pp. 347–49 in *Fish Physiology, Vol. 5*, W. S. Hoar and D. J. Randall, eds. Academic Press, New York.

Bennett, M. V. L., and W. T. Clusin. 1978. Physiology of the ampulla of Lorenzini, the electroreceptor of elasmobranchs. Pp. 483–506 in *Sensory Biology of Sharks, Skates and Rays*, E. S. Hodgson and R. F. Mathewson, eds. Office of Naval Res., Arlington, VA.

Bigelow, H. B., and W. C. Schroeder. 1953. *Fishes of the Gulf of Maine.* U.S. Govt. Printing Office, Washington, DC.

Bodznick, D., and R. L. Boord. 1986. Electroreception in chondrichthyes. Pp. 225–256 in *Electroreception*, T. H. Bullock and W. Heiligenberg, eds. Wiley, New York.

Bodznick, D., and J. C. Montgomery. 1992. Suppression of ventilatory reafference in the elasmobranch electrosensory system: Medullary neuron receptive fields support a common mode rejection system. *J. Exp. Biol.* **171:** 127–137.

Bodznick, D., J. C. Montgomery, and D. J. Bradley. 1992. Suppression of common mode signals within the electrosensory system of the little skate, *Raja erinacea. J. Exp. Biol.* **171:** 107–125.

Bratton, B. O., and J. L. Ayers. 1987. Observations on the electric organ discharge of two skate species (Chondrichthyes: Rajidae) and its relationship to behavior. *Env. Biol. Fishes* **20(4):** 241–254.

Bratton, B. O., A. Christiano, N. McClennan, M. Murray, E. O'Neill, and K. Ritzen. 1993. The electric organ discharge of the skate (Rajidae): waveform, occurrence and behavior relationships. *Soc. Neurosci. Abstr.* **19:** 374.

Brock, L. G., R. M. Eccles, and R. D. Keynes. 1953. The discharge of individual electroplates in *Raja clavata J. Physiol.* (Lond.) **122:** 4–6P.

Ewart, J. C. 1888a. The electric organ of the skate. *Philos. Trans. Roy. Soc. Lond. B* **179:** 399–420.

Ewart, J. C. 1888b. The electric organ of the skate: the electric organ of *Raia radiata Philos. Trans. Roy. Soc. Lond. B* **179:** 539–552.

Ewart, J. C. 1892. The electric organ of the skate: observations on the structure, relations, progressive development, and growth of the electric organ of the skate. *Philos. Trans. Roy. Soc. Lond. B* **183:** 389–420.

Grundfest, H., and M. V. L. Bennett. 1961. Studies on the morphology and electrophysiology of electric organs: I. Electrophysiology of marine electric fishes. Pp. 57–105 in *Bioelectrogenesis*, C. Chagas and A. P. de Carvalho, eds. Elsevier, New York.

Kalmijn, A. J. 1971. The electric sense of sharks, skates and rays. *J. Exp. Biol.* **55:** 371–383.

Kalmijn, A. J. 1978. Electric and magnetic sensory world of sharks, skates and rays. Pp. 507–528 in *Sensory Biology of Sharks, Skates and Rays*, E. S. Hodgson and R. F. Mathewson, eds. Office of Naval Res., Arlington, VA.

Kalmijn, A. J. 1982. Electric and magnetic field detection in elasmobranch fishes. *Science* **218:** 916–918.

Kalmijn, A. J. 1988. Detection of weak electric fields. Pp. 507–528 in *Sensory Biology of Aquatic Animals*, J. Atema, R. R. Fay, A. N. Popper, and W. N. Tavolga, eds. Springer-Verlag, New York.

Koester, D. M. 1987. Identification of the electromotoneurons innervating the electric organ of skates. *Am. Zool.* **27(4):** 105.

Meyer, J. H. 1983. Steroid influences upon the discharge frequency of a weakly electric fish. *J. Comp. Physiol.* **153:** 29–38.

Meyer, J. H., and H. H. Zakon. 1982. Androgens alter the tuning of electroreceptors. *Science* **217:** 535–537.

Mikhailenko, N. A. 1971. Biological significance and dynamics of electrical discharges in weak electric fishes of the Black Sea. *Zool. Zh.* **50:** 1347–1352 (in Russian).

Montgomery, J. C. 1984a. Frequency response characteristics of primary and secondary neurons in the electrosensory systems of the thornback ray. *Comp. Biochem. Physiol.* **79A:** 189–195.

Montgomery, J. C. 1984b. Noise cancellation in the electrosensory system of the thornback ray; common mode rejection of input produced by the animal's own ventilatory movement. *J. Comp. Physiol.* **155A:** 103–111.

Mortenson, F. J., and R. H. Whitaker. 1973. Electric discharge in free-swimming female winter skates (*Raja ocellata*). *Am. Zool.* **13:** 1266.

Murray, R. W. 1974. The ampullae of Lorenzini. Pp. 125–145 in *Handbook of Sensory Physiology, Vol. III/3*, A. Fessard, ed. Springer-Verlag, New York.

Murray, R. W., and T. W. Potts. 1961. The composition of the endolymph and other body fluids of elasmobranchs. *Comp. Biochem. Physiol.* **2:** 65–75.

New, J. G. 1990. Medullary electrosensory processing in the skate. I. Response characteristics of neurons in the dorsal octavolateralis nucleus. *J Comp. Physiol.* **167A:** 285–294.

New, J. G., and D. Bodznick. 1990. Medullary electrosensory processing in the skate. II. Suppression of self-generated electrosensory interference during respiration. *J. Comp. Physiol.* **167A:** 295–307.

Sanderson, J. B., and F. Gotch. 1888. On the electric organ of the skate. *J. Physiol. (Lond.)* **9:** 137–166.

Sejnowski, T. J., and M. L. Yodlowski. 1982. A freeze fracture study of the skate electroreceptors. *J. Neurocytol.* **11:** 897–912.

Stark, D. 1844. On the existence of an electrical apparatus in the flapper skate and other rays. *Edinb. Roy. Soc. Proc.* **2:** 1844–1845.

Szabo, T. 1955. Quelques precisions sur lay noyau de commande centrale de la decharge electrique chez la Raie (*Raja clavata*). *J. Physiol. (Paris)* **47:** 283–285 (in French).

Szabo, T. 1961. Anatomo-physiologie des centres nerveux specificiques de quelques organes electriques. Pp. 185–201 in *Bioelectrogenesis*, C. Chagas and A. P. de Carvalho, eds. Elsevier, New York.

Zakon, H. H., and J. H. Meyer. 1983. Plasticity of electroreceptor tuning in the weakly electric fish *Sternopygus dariensis. J. Comp. Physiol.* **153:** 477–487.

Reference: *Biol. Bull.* **187:** 76–83. (August, 1994)

Osmoregulation in *Dreissena polymorpha:* the Importance of Na, Cl, K, and Particularly Mg

THOMAS H. DIETZ, DIONDI LESSARD, HAROLD SILVERMAN, AND JOHN W. LYNN

Department of Zoology and Physiology, Louisiana State University, Baton Rouge, Louisiana 70803

Abstract. Zebra mussels (*Dreissena polymorpha*) are unusual in that they cannot survive in Mg-deficient water. Analysis of blood samples from mussels obtained in the field indicated a Mg concentration of 1.5–2.0 m*M* immediately after animal collection. However, Mg concentration in the blood decreased rapidly when the mussels were transferred to Mg-free artificial pondwater (PW); the $t_{1/2}$ was 24 h. Blood Mg decreased to the limits of detection within 2 weeks, and the time to 50% mortality was about 17 days in Mg-free PW. When Mg-depleted specimens of *D. polymorpha* were returned to PW containing Mg, the net flux was 3 μmol Mg (g dry tissue · h)$^{-1}$, and blood Mg concentration was restored within a day to 0.4–0.6 m*M*. Mussels depleted of Mg did not survive beyond 51 days. When mussels were acclimated to K-free pondwater (containing Mg), their osmoregulatory ability was impaired, and the total solute of the blood dropped from 30–36 to 21–24 mosm, with blood Na and Cl concentrations declining 30–50%. This ion-depleted condition was reversed within 45 h upon return of K to the pondwater bathing medium. *D. polymorpha* individuals were unable to survive beyond 5 days in deionized water and required minimal concentrations of Na, Cl, K, and Mg for prolonged storage (>51 days) under laboratory conditions. Mussels survived Ca-deficient solutions for more than 51 days, presumably because they were able to mobilize Ca from internal stores (shell) to maintain blood calcium at 1 m*M*.

Introduction

In previous studies, we demonstrated that the tolerance of *Dreissena polymorpha* (zebra mussel) to elevated ion concentrations was notably lower than that of other freshwater bivalves (Horohov *et al.*, 1992). Krogh (1939) reported that although 3 days of salt depletion were required to stimulate Cl uptake in *Dreissena,* it took weeks to stimulate ion uptake in unionids. More recent studies have demonstrated that exposure of *D. polymorpha* to deionized water (DW) causes small mussels to begin dying within days, and all die within 30 days (Nichols, 1993; Ram and Walker, 1993). This inability to tolerate "pure" water is unusual for a freshwater animal; other freshwater bivalves (corbiculids, mytilids, unionids) will survive for months in DW with no mortality (Krogh, 1939; McCorkle and Dietz, 1980; Scheide and Dietz, 1982; Deaton *et al.*, 1989). The addition of either 0.5 m*M* NaCl or 0.5 m*M* $MgSO_4$ promotes short-term survival of zebra mussels compared to animals maintained in DW, and it was suggested that the absence of solute (<1 mosm) was more critical than any specific ion requirement (Ram and Walker, 1993).

Although magnesium transport has been studied extensively in many cells and tissues (Flatman, 1991; Beyenbach *et al.*, 1993) and recently in the freshwater carp (van der Velden *et al.*, 1991), the importance of Mg in the physiology of freshwater bivalves has not been reported. We have observed that survival of freshwater dreissenids in Mg-free pondwater (PW) is density dependent. For example, zebra mussels isolated in individual containers containing Mg-free PW or maintained in small groups (fewer than 20 animals in a liter of Mg-free PW) showed substantial mortality when the experiment lasted longer than 2–3 weeks (pers. obs.). Yet *D. polymorpha* maintained at high density (>100 mussels/l) in the same Mg-free PW suffered virtually no mortality over the same interval. Only when we stored animals longer than 2 months, unfed, in Mg-free PW did we observe some mortality in these mussels (Horohov *et al.*, 1992). Recently, an analysis of the chemical composition of lakes showed that zebra mussels were absent from lakes having low

Received 28 February 1994; accepted 1 June 1994.

concentrations of Ca (<0.5 m*M*); these lakes are also low in Mg (<0.1 m*M*) (Ramcharan *et al.*, 1992).

This is the first report demonstrating that a freshwater bivalve, *D. polymorpha*, has an absolute requirement for external Mg for survival. In addition, K, an ion identified as toxic to freshwater bivalves in concentrations above 0.3–0.5 m*M* (McMahon, 1991), is required in low concentrations for zebra mussels to maintain Na and Cl balance.

Materials and Methods

Animals

Specimens of *Dreissena polymorpha* were collected from Lake Erie at the mouth of the Raisin River in Michigan and used for most of this study. In addition, some mussels were collected from the Mississippi River near Baton Rouge, as noted in the text. Animals were acclimated to an artificial pondwater (PW) normally used for freshwater bivalves (0.5 m*M* NaCl, 0.2 m*M* $NaHCO_3$, 0.05 m*M* KCl, 0.4 m*M* $CaCl_2$) but containing 0.2 m*M* magnesium sulfate. The amount of Mg present in fresh water is extremely variable, but many rivers and other bodies of water tend to have a Ca:Mg ratio of 2:1, and we have selected this relationship for the artificial PW used for zebra mussels (Withers, 1992). Mussels were stored unfed in aerated PW at 22 ± 2°C and survived for months at this temperature with little mortality. For longer maintenance, mussels were held in PW at 16 ± 1°C and subsequently transferred to room temperature 5–7 days before use. We selected larger specimens for study (1.5–3 cm length) with dry tissue masses (excluding the shell) of 15–80 mg.

To prevent contamination of local water systems with mussels or veliger larvae, mussel tissue was excised from the shell and dried to constant weight at 95°C before being discarded. In addition, all acclimation water and animal containers were treated with 1% chlorine bleach for 24 h before being discarded.

Blood analysis

Blood was collected by heart puncture and centrifuged (14,000 $g \cdot$ min) before use (Fyhn and Costlow, 1975). We routinely collected blood volumes (>150 μl) equal to 10–20% of animal wet weight. Several animals were dissected to determine landmarks that would ensure pericardial puncture and prevent the collection of stomach fluid. Evidence of contamination included visible particulate material, the green color of algae, and premature freezing of the blood sample in the osmometer.

Total solute in the blood was determined by freezing point depression. Sodium and potassium concentrations were determined by emission flame photometry. Calcium and magnesium were diluted in $LaCl_2$ and assayed by atomic absorption spectroscopy. Chloride was determined by electrometric titration. Although the bicarbonate concentrations were not routinely measured, we have estimated the concentration previously (see Horohov *et al.*, 1992). These analytical methods ensured complete ionization and maximum estimates of element concentrations. The difference between the total solute and the sum of the measured ions was identified as "other" and is assumed to be mostly bicarbonate.

Ion net flux

Previously described methods (Graves and Dietz, 1982) were used to calculate net ion flux (J_n) from the change in ion concentration in the bathing medium. For flux studies, we chose animals that were attached (to the substrate or to each other) by byssal threads, and detached them by cutting the threads to avoid injuring the animals. The mussels were rinsed in DW for about 30 min and transferred to small beakers containing the appropriate bathing solution. Bath samples were collected at specific intervals, and J_n was calculated from the change in ion concentration in the bathing medium. Net ion flux was expressed as μmol (g dry tissue · h)$^{-1}$.

Survival in ion deficient solutions

To characterize the sensitivity of *D. polymorpha* to ions in the bathing medium, we transferred groups of 20 animals into either 1 l of DW or 1-l solutions of the 31 permutations of the salts present in PW (see Table III). During the study the shells of six animals were accidentally damaged, so these specimens were eliminated from the study. The solutions, covered to minimize evaporation, were continuously aerated and replaced on alternate days. The animals were examined regularly: gaping animals were touched with forceps to stimulate valve closure; unresponsive specimens were touched in the area of the siphons. If there were no valve or tissue responses, the animal was considered dead. Dead animals were removed from the container, the time noted, and the water changed. The time required to reach 50% mortality (LT_{50}) in each solution was derived from the probit model (Finney, 1971). Mortality rates were curvilinear, and the cumulative mortality was assigned a probability (probit) ranging from 0 to 1 at each point when an animal died. The LT_{50} was calculated from the linear regression of the logarithm of time and cumulative mortality:

$$\text{probit (\%dead)} = A + B\,(\text{log time, } h)$$

The time of death of the last animal in the test solution was reported as the time to 100% sample mortality (SM_{100}). Animals in 10 of the solutions, including the PW controls, had little or no mortality, and the experiment

Table I

Blood ion composition in Dreissena polymorpha *collected from the Mississippi River and transferred to Mg-free artificial pondwater (PW)*

Days in Mg-free PW	mosm (solute)	Concentration (m*M*)					
		Na	Ca	Mg*	K	Cl	Other
0	42 ± 0 (8)	17.4 ± 0.1 (8)	4.9 ± 0.2^a (8)	1.50 ± 0.20^a (8)	0.4 ± 0.0 (8)	16.9 ± 0.5^b (8)	1.0 ± 0.4^b (8)
2	42 ± 2 (4)	17.7 ± 0.4 (6)	3.6 ± 0.1^b (6)	0.33 ± 0.02^b (6)	0.5 ± 0.0 (6)	19.3 ± 0.4^a (6)	1.5 ± 0.8^b (4)
9	41 ± 1 (7)	17.2 ± 0.2 (7)	3.3 ± 0.3^b (7)	0.13 ± 0.01^c (7)	0.4 ± 0.0 (7)	14.3 ± 0.5^c (7)	5.7 ± 0.4^a (7)
15	42 ± 1 (8)	17.8 ± 0.6 (8)	5.4 ± 0.2^a (8)	0.07 ± 0.01^d (8)	0.5 ± 0.0 (8)	14.0 ± 0.6^c (8)	4.1 ± 0.6^a (8)

Means ± SEM with number of animals in parentheses. Total solute was rounded to 2 significant figures. "Other" represents the difference between the total solute and the sum of the measured ions. Values with different letters are significantly different (a > b > c > d) according to the Tukey-Kramer Multiple Comparison test ($P < 0.05$).

* Data were transformed by natural logarithm for analysis.

was terminated when only these groups of animals remained. Blood was collected from seven survivors from each of these 10 solutions. The remaining survivors from the K-deficient solutions were transferred into PW. The animals were allowed 45 h in which to replete missing ions, and blood samples were then collected. All animals survived the transfer to PW.

Statistical analysis

Data are expressed as means ± 1 standard error; the number of animals is in parentheses. To analyze the effects of PW ions on mussel blood composition, the data were analyzed by ANOVA, and if significant differences between means were found, we used the Tukey's Studentized Range test or, if the sample sizes were unequal, the Tukey-Kramer modification. Differences were considered significant if $P < 0.05$. Ion concentrations that were significantly different in the different treatments were assigned a letter, with "a" denoting the highest values. Bartlett's test for homogeneity of variance was used to determine whether there were significant differences in the standard deviations among groups, and the appropriate data sets were transformed by natural logarithm.

Results

Blood composition

The blood ion concentration in *D. polymorpha* was rather variable, depending on the source of the animals. Animals sampled at the time of their collection from the mouth of the Raisin River in Michigan (20°C) had a blood total solute of 50 ± 1 (8) mosm and a Mg concentration of 2.06 ± 0.12 m*M*. Zebra mussels collected from the Mississippi River near Baton Rouge (25°C) had significantly lower total solute of 42 ± 0 (6) mosm ($P < 0.01$) and [Mg] of 1.50 ± 0.20 m*M* ($P < 0.02$). The lower Mississippi River approximates what Withers (1992) classified as an "average" river in terms of ion concentrations (in m*M*: 0.9 Na, 0.8 Ca, 0.4 Mg, 0.17 K, 0.55 Cl, 0.5 SO_4, 2.7 unidentified). The composition of the blood from animals collected in Michigan was similar to, but significantly higher in total solute than, that found in freshly collected animals from the Mississippi River. Water temperature, however, differed by 5°C between the two locations. After 1–2 weeks acclimation to artificial PW, the blood composition of animals from Michigan and Louisiana tended to become indistinguishable; total solute of the blood stabilized at about 40–45 mosm, with Mg usually about 0.4–0.6 m*M*.

Mg depletion and repletion

Transferring zebra mussels directly from the Mississippi River into Mg-free PW resulted in a significant exponential decline ($r = 0.93$, $n = 27$) in blood [Mg] with a $t_{1/2}$ of about 1 day (Table I):

$$\text{Blood [Mg]} = 1.5 \text{ m}M\, e^{-(0.73 \cdot \text{days of Mg depletion})}$$

The total solute, [Na], and [K] did not change over a 2-week interval, but [Cl] decreased significantly and "other" (presumably HCO_3) was elevated (see Horohov *et al.*, 1992). Blood [Ca] initially declined during Mg-free PW acclimation but increased significantly with severe Mg depletion. Similar results have been obtained with mussels from Lake Erie (data not shown).

Transferring Mg-depleted zebra mussels to PW containing variable concentrations of Mg resulted in a rapid uptake of Mg that appeared to be maximal when the external concentration was between 0.1 and 0.2 m*M* Mg

(Table II). Following the 6-h net flux study, the animals were left in the solution overnight (17 h). Subsequent sampling showed that the Mg concentration in the blood of these mussels had been restored to levels comparable to those in animals continually maintained in PW (compare Tables II and IV). Also, the total solute in these animals was significantly elevated, primarily because of a modest elevation in the concentrations of both Na and Cl. The sum of the change in Na and Cl concentration accounted for 10 of the 13 mosm total solute increase. The negative value for "other" in the Mg-depleted animals was not significantly different from zero. However, we occasionally calculated the sum of the measured ions as slightly exceeding the total solute for some animals; thus our Ca values may be inflated due to complete Ca ionization (even of bound Ca) produced by the analytic procedures. A separate group of 20 zebra mussels acclimated to PW containing 0.05 m*M* $MgSO_4$ survived more than 60 days with only one death.

Selective ion depletion

Several salts constitute the artificial pondwater, and we examined the influence of each on the survival of zebra mussels. Mussels were maintained in solutions to which salts were added singly or in combination at the concentration present in PW. The LT_{50} and SM_{100} were determined, and the total numbers of animals that died are presented in Table III. All solutions deficient in Na, Cl, and Mg were lethal, and a minimal concentration of these ions was required for a 51-day survival. Mussels in DW or solutions deficient in Na did not survive a week. Survival was extended (LT_{50} = 2 weeks) in solutions containing only Na salts, but if Ca was present the LT_{50} was reduced. Magnesium by itself and in all combinations of salts with [Na] less than 0.2 m*M* did not promote survival beyond an LT_{50} of about 30 days. But the combination of 0.2 m*M* $NaHCO_3$, 0.05 m*M* KCl, and 0.2 m*M* $MgSO_4$ allowed the animals to survive for 51 days and, based on the apparently normal (51-day) blood composition, probably indefinitely (Table IV). A solution with $CaCl_2$ and $MgSO_4$ as the only solutes was among the more toxic combinations; but the addition of Na extended survival substantially. These data suggest that both the Ca:Mg ratio and the level of Na are critical to zebra mussel survival.

Prolonged storage of *D. polymorpha* in PW without feeding reduced total solute in the blood in PW controls to 30–35 mosm. Ion concentrations in blood samples taken from animals that survived the 51-day differential ion combination study are shown in Table IV. Magnesium, Na, and Cl were required for the 51-day survival, but if K was absent the measured blood ion concentrations were significantly lower than those found in PW. Most of the animals in K-deficient media survived and were attached by byssal threads, but all had significantly reduced total solute and significantly lower blood K, Na, and Cl concentrations—perhaps reduced to near the survival limit for these mussels. Animals in Ca-deficient solutions had significantly depressed blood [Ca] but elevated [Mg], suggesting a reciprocal relationship between these two ions.

Repletion of blood ions in K-depleted mussels

When the K-depleted mussels were returned to complete PW for 45 h of recovery, the missing ions were rapidly reaccumulated and the ion concentrations were restored to near normal (Table V, compare with Table IV).

Table II

Net Mg flux (over 6 h) and blood ion composition in Mg-depleted Dreissena polymorpha *17 h after reaccumulating ions from pondwater (PW) containing Mg*

Treatment	$^{Mg}J_{net}$ µmol (g · h)$^{-1}$	mosm (Total)	Concentration (m*M*)					
			Na	Ca	Mg*	K	Cl	Other
PW (0 m*M* Mg)	0 ± 0^b (5)	37 ± 3^b (5)	15.0 ± 2.0 (4)	5.2 ± 0.4 (5)	0.02 ± 0.02^c (5)	0.4 ± 0.1 (4)	17.9 ± 1.4 (4)	−1.0 ± 0.9 (4)
PW (0.05 m*M* Mg)	1.2 ± 0.2^b (5)	45 ± 2^b (5)	19.0 ± 1.0 (5)	3.8 ± 0.7 (5)	0.15 ± 0.03^{b,c} (5)	0.4 ± 0.0 (5)	20.6 ± 1.2 (5)	1.5 ± 1.0 (5)
PW (0.1 m*M* Mg)	3.8 ± 0.8^a (5)	48 ± 3^a (5)	17.2 ± 3.0 (3)	3.9 ± 0.7 (5)	0.20 ± 0.03^b (5)	0.3 ± 0.1 (3)	21.2 ± 1.8 (4)	2.3 ± 1.4 (3)
PW (0.2 m*M* Mg)	3.2 ± 0.4^a (5)	50 ± 2^a (5)	20.3 ± 1.1 (5)	3.6 ± 0.4 (5)	0.50 ± 0.9^a (5)	0.4 ± 0.0 (5)	22.4 ± 1.1 (4)	2.2 ± 1.1 (4)

Means ± SEM with number of samples in parentheses. Total solute was rounded to 2 significant figures. Values with different letters are significantly different (a > b > c) with the Tukey-Kramer Multiple Comparison test ($P < 0.05$).

* Data were transformed by natural logarithm for analysis.

Table III

Lethal time for 50% (LT) and 100% sample mortality (SM) of zebra mussels in solutions of single salts or mixtures of salts at pondwater (PW) ion concentrations

Ions	Days		
	LT_{50}	SM_{100}	*n* died
Distilled water	3.9	4.9	20
$MgSO_4$	1.5	3.9	20
KCl	1.7	3.9	20
$CaCl_2$	1.8	3.9	20
$NaHCO_3$	14.1	22.9	19*
NaCl	15.2	35.4	20
$CaCl_2$, $MgSO_4$	1.7	4.0	20
KCl, $CaCl_2$	2.5	3.9	20
KCl, $MgSO_4$	4.2	6.9	20
$NaHCO_3$, $CaCl_2$	6.9	12.0	20
NaCl, $CaCl_2$	12.4	37.3	20
NaCl, KCl	21.2	43.4	20
$NaHCO_3$, KCl	26.4	44.3	17*
$NaHCO_3$, NaCl	28.4	50.3	20
$NaHCO_3$, $MgSO_4$	29.8	48.8	20
NaCl, $MgSO_4$	—	>51	0
KCl, $CaCl_2$, $MgSO_4$	1.4	4.0	20
KCl, $NaHCO_3$, $CaCl_2$	13.1	17.9	20
NaCl, $NaHCO_3$, $CaCl_2$	14.9	23.8	20
NaCl, KCl, $CaCl_2$	16.9	44.8	20
NaCl, KCl, $NaHCO_3$	28.6	44.3	20
$NaHCO_3$, $CaCl_2$, $MgSO_4$	29.6	44.3	20
$NaHCO_3$, KCl, $MgSO_4$	—	>51	1
NaCl, KCl, $MgSO_4$	—	>51	1
NaCl, $NaHCO_3$, $MgSO_4$	—	>51	0
NaCl, $CaCl_2$, $MgSO_4$	—	>51	1
NaCl, KCl, $NaHCO_3$, $CaCl_2$ (Mg-free PW)	16.9	31.3	20
NaCl, KCl, $CaCl_2$, $MgSO_4$	—	>51	2
NaCl, KCl, $NaHCO_3$, $MgSO_4$	—	>51	3
KCl, $NaHCO_3$, $CaCl_2$, $MgSO_4$	—	>51	0
NaCl, $NaHCO_3$, $CaCl_2$, $MgSO_4$	—	>51	2
NaCl, KCl, $NaHCO_3$, $CaCl_2$, $MgSO_4$ (PW)	—	>51	1

PW = 0.5 m*M* NaCl, 0.05 m*M* KCl, 0.2 m*M* $NaHCO_3$, 0.4 m*M* $CaCl_2$, 0.2 m*M* $MgSO_4$.

* Less than 20 because some animals were accidentally damaged and were removed from the test.

The K balance was critical to the ability of the zebra mussel to maintain Na and Cl homeostasis. With the restoration of Ca in the PW, the blood Ca:Mg ratio returned to normal (Ca > Mg) as a result of both an elevation in the blood [Ca] and a decline in [Mg]. We have repeated the ion tolerance study using Mg-depleted mussels acclimated to PW. These animals were exposed to combinations of PW salts that excluded Mg. We observed a similar qualitative pattern of survival times, and no animal survived beyond 52 days (data not shown). The animals with the longest SM_{100} (52 days) were in the NaCl, KCl solution and the NaCl, KCl, and $NaHCO_3$ solution (LT_{50} 21 and 31 days, respectively), whereas mussels in deionized water had an LT_{50} of 2.3 days.

Discussion

Unionids and corbiculids can be maintained in the laboratory in Mg-free pondwater or deionized water for months. These two groups invaded fresh water separately, with the corbiculids being more recent (Pleistocene), and there are significant differences in their physiologic processes (Dietz, 1979; McMahon, 1991). The dreissenids represent a third independent (Pleistocene) invasion of fresh water (McMahon, 1991), and *Dreissena polymorpha* exhibits remarkably complex ion requirements not observed in other freshwater bivalves. Zebra mussels lose 50% of their blood [Mg] in one day when placed in Mg-deficient solutions. Apparently these animals are similar to fish in that reabsorption of Mg from the ultrafiltrate entering the kidney is limited; thus, urinary loss of Mg is substantial (Beyenbach *et al.*, 1993). In addition, the mantle or gill epithelia of zebra mussel may have a high passive permeability to Mg, contributing to the loss of this ion. Although the initial loss of Mg is remarkably rapid, a mechanism with a limited ability to reduce the rate of loss of Mg appears to become operational with prolonged depletion. With a $t_{1/2}$ of 1 day for the loss of Mg from the blood, the Mg should be unmeasurable within 7 half-lives, yet nearly 2 weeks were required for blood [Mg] to drop to zero (i.e., below detection limits).

Although the *D. polymorpha* individuals we tested experienced a high rate of Mg loss, their transport system rapidly took up Mg from PW (0.1–0.2 m*M* Mg). This transport system restored the blood Mg concentration in less than a day when Mg-depleted mussels were returned to solutions containing Mg. Moreover, they survived for more than 60 days with little mortality in PW containing 0.05 m*M* $MgSO_4$. The ^{28}Mg isotope is not currently available in the United States, so we have not measured the unidirectional flux. In carp, Mg is transported into the animal from fresh water by epithelial Mg transport, but intestinal uptake from dietary sources is required to maintain Mg balance (van der Velden *et al.*, 1991). Although dietary Mg may allow *D. polymorpha* to maintain blood [Mg] above 1 m*M*, unfed PW-acclimated mussels had blood [Mg] between 0.4 and 0.6 m*M*. In addition, all zebra mussels in Ca-deficient media containing 0.2 m*M* $MgSO_4$ had a blood [Mg] above 1 m*M*.

When minimal concentrations of Mg, Na, Cl, and K were in the bathing solution, *D. polymorpha* had blood solute levels near the low end of the normal range (>30 mosm) for bivalves. However, members of this species could not survive salt depletion in deionized water or selective depletion of any of the four critical ions for more than a short period (this study; Nichols, 1993; Ram and

Table IV

Blood ion concentration in Dreissena polymorpha *surviving 51 days in pondwater (PW) and solutions deficient in salts present in artificial PW*

Incubation medium	mosm (Total)	Concentration (m*M*) Na	Ca	Mg	K	Cl	Other
PW, day 0	38 ± 1^{a}	15.6 ± 0.7^{a}	3.3 ± 0.1^{a}	0.4 ± 0.0^{c}	0.4 ± 0.0^{b}	16.0 ± 0.5^{a}	2.3 ± 0.5
PW, day 51	$33 \pm 1^{a,b,c}$	$13.2 \pm 0.2^{a,b,c}$	$1.8 \pm 0.1^{c,d}$	0.6 ± 0.0^{c}	$0.5 \pm 0.0^{a,b}$	$14.3 \pm 0.8^{a,b}$	2.2 ± 0.4
NaCl, KCl, $NaHCO_3$, $MgSO_4$	$36 \pm 1^{a,b}$	16.1 ± 1.0^{a}	1.0 ± 0.2^{e}	$1.3 \pm 0.1^{a,b}$	0.6 ± 0.0^{a}	$14.2 \pm 0.7^{a,b}$	3.1 ± 1.0
NaCl, KCl, $CaCl_2$, $MgSO_4$	$35 \pm 2^{a,b,c}$	15.7 ± 1.0^{a}	$1.7 \pm 0.2^{c,d}$	0.5 ± 0.0^{c}	0.5 ± 0.0^{a}	$15.3 \pm 0.9^{a,b}$	1.6 ± 0.3
$NaHCO_3$, KCl, $CaCl_2$, $MgSO_4$	$31 \pm 1^{b,c}$	$11.1 \pm 0.6^{c,d,e}$	$2.4 \pm 0.2^{b,c}$	0.7 ± 0.1^{c}	$0.5 \pm 0.0^{a,b}$	$14.1 \pm 0.4^{a,b}$	2.5 ± 0.6
NaCl, $NaHCO_3$, $CaCl_2$, $MgSO_4$	21 ± 1^{d}	6.3 ± 0.9^{f}	2.5 ± 0.1^{b}	0.6 ± 0.1^{c}	0.1 ± 0.0^{c}	7.7 ± 0.9^{d}	3.4 ± 0.8
NaCl, KCl, $MgSO_4$	$34 \pm 1^{a,b,c}$	$14.4 \pm 0.4^{a,b}$	1.0 ± 0.1^{e}	1.2 ± 0.1^{b}	0.5 ± 0.0^{a}	$14.3 \pm 0.6^{a,b}$	2.8 ± 0.5
$NaHCO_3$, KCl, $MgSO_4$	30 ± 1^{c}	$12.0 \pm 0.8^{b,c,d}$	$1.2 \pm 0.1^{d,e}$	$1.5 \pm 0.1^{a,b}$	$0.5 \pm 0.0^{a,b}$	$12.4 \pm 0.5^{b,c}$	2.6 ± 0.3
NaCl, $CaCl_2$, $MgSO_4$	23 ± 1^{d}	$8.4 \pm 0.5^{e,f}$	$2.3 \pm 0.2^{b,c}$	0.6 ± 0.0^{c}	0.1 ± 0.0^{c}	$9.7 \pm 0.6^{c,d}$	1.8 ± 0.4
NaCl, $NaHCO_3$, $MgSO_4$	24 ± 2^{d}	$8.3 \pm 0.7^{e,f}$	$1.2 \pm 0.1^{d,e}$	1.8 ± 0.1^{a}	0.1 ± 0.0^{c}	$9.1 \pm 1.0^{c,d}$	3.2 ± 0.5
NaCl, $MgSO_4$	24 ± 1^{d}	$8.9 \pm 0.5^{d,e,f}$	$1.3 \pm 0.2^{d,e}$	1.2 ± 0.2^{b}	0.1 ± 0.0^{c}	8.6 ± 0.8^{d}	3.5 ± 0.7

Means ± SEM ($n = 7$). Total solute was rounded to 2 significant figures. PW = 0.5 m*M* NaCl, 0.05 m*M* KCl, 0.2 m*M* $NaHCO_3$, 0.4 m*M* $CaCl_2$, 0.2 m*M* $MgSO_4$. Means with different letters are significantly different (a > b > c > d > e > f) according to the Tukey Studentized Range test, $P < 0.05$.

Walker, 1993; Vinogradov *et al.*, 1993). The zebra mussel requirement for specific ions and "threshold" ion concentrations in the bathing medium is in contrast with the tolerance shown by other freshwater bivalves for prolonged salt depletion or selective ion depletion (Krogh, 1939; Murphy and Dietz, 1976; McCorkle and Dietz, 1980; Scheide and Dietz, 1982; Deaton *et al.*, 1989). The PW used in our laboratory for these earlier bivalve studies was Mg-free. The bivalves used in these previous studies have mechanisms that reduce the loss of ions by decreasing ion efflux as well as by increasing the influx of the ions independently of exogenous Mg.

Shell growth in zebra mussels and other freshwater bivalves requires Ca in the environment. Calcium mobilization from the reservoir in the shell allows bivalves to survive in Ca-deficient solutions. The endogenous sources of calcium were sufficient to maintain zebra mussel blood [Ca] at about 1 m*M* in Ca-free solutions. In contrast, ion depletion or other physiological challenges result in elevated blood [Ca] in other bivalves (Scheide and Dietz, 1982; Deaton *et al.*, 1989; Byrne *et al.*, 1991). However, with the mobilization of Ca and presumably CO_3 from the shell, limited amounts of HCO_3 ("other," in data tables) were retained in the blood of *D. polymorpha.*

The rather low blood bicarbonate concentration found in zebra mussels is similar to that in the Canadian unionid *Anodonta grandis simpsoniana* (Byrne and McMahon, 1991). In contrast, HCO_3 is substituted for Cl in the blood of other bivalves (Byrne *et al.*, 1991; Scheide and Dietz, 1982; Deaton *et al.*, 1989). Indeed, blood [HCO_3] of sev-

Table V

Blood ion concentration in Dreissena polymorpha *allowed to reaccumulate ions from pondwater (PW) for 45 h after surviving 51 days in PW or solutions containing Mg but deficient in K and one or more other ions*

Original incubation medium	*n*	mosm (Total)	Concentration (m*M*) Na	Ca	Mg	K	Cl	Other
PW, day 0	7	$38 \pm 1^{a,b}$	$15.6 \pm 0.7^{a,b}$	3.3 ± 0.1^{a}	0.4 ± 0.0^{b}	0.4 ± 0.0	16.0 ± 0.5	2.4 ± 0.5
PW, day 51	7	33 ± 1^{b}	13.2 ± 0.2^{b}	$1.8 \pm 0.1^{b,c}$	0.6 ± 0.0^{b}	0.5 ± 0.0	14.3 ± 0.8	2.2 ± 0.4
NaCl, $NaHCO_3$, $CaCl_2$, $MgSO_4$	4	$34 \pm 1^{a,b}$	$14.8 \pm 0.5^{a,b}$	$1.6 \pm 0.1^{b,c}$	$0.6 \pm 0.0^{a,b}$	0.4 ± 0.0	12.7 ± 1.6	4.4 ± 1.3
NaCl, $CaCl_2$, $MgSO_4$	5	38 ± 1^{a}	16.8 ± 0.5^{a}	2.3 ± 0.4^{b}	$0.7 \pm 0.0^{a,b}$	0.4 ± 0.0	13.2 ± 1.5	4.7 ± 0.6
NaCl, $NaHCO_3$, $MgSO_4$	4	$34 \pm 2^{a,b}$	$14.4 \pm 1.7^{a,b}$	1.4 ± 0.1^{c}	0.9 ± 0.2^{a}	0.4 ± 0.0	15.0 ± 1.0	2.0 ± 0.3
NaCl, $MgSO_4$	5	$36 \pm 1^{a,b}$	$14.6 \pm 0.7^{a,b}$	$1.9 \pm 0.2^{b,c}$	0.9 ± 0.1^{a}	0.4 ± 0.1	14.8 ± 0.8	3.4 ± 1.0

Means ± SEM, total solute was rounded to 2 significant figures. PW = 0.5 m*M* NaCl, 0.05 m*M* KCl, 0.2 m*M* $NaHCO_3$, 0.4 m*M* $CaCl_2$, 0.2 m*M* $MgSO_4$. The PW controls are the same values listed in Table IV. Values with different letters are significantly different (a > b > c) according to Tukey's Studentized Range test, $P < 0.05$.

eral PW-acclimated unionids is equal to or exceeds [Cl] (Dietz, 1979). One of the better single salts for extending survival of zebra mussels (LT_{50} = 2 weeks) was $NaHCO_3$, and the survival was doubled (LT_{50} = 4 weeks) with the addition of any ion but Ca.

Half of the animals exposed to calcium-containing solutions without Mg did not survive 2.5 weeks (maximum $LT_{50} < 17$ days). Apparently the presence of exogenous and endogenous Ca, in the absence of exogenous Mg, resulted in an unfavorable Ca:Mg balance, leading to death. We do not know which functions critical for survival are impaired by Mg deficiency, but candidates range from disruption of epithelial cell junctions to elevation of membrane ion permeability (both factors aggravating ion losses), or Ca interference with Mg-requiring enzymes. Deaton and Greenberg (1991) noted a good correlation between the osmoregulatory ability of bivalves and their capacity to mobilize calcium. They suggested that the ability to regulate membrane permeability to ions was intimately linked to calcium balance, especially the ability to elevate blood [Ca]. Blood [Ca] in *D. polymorpha* was regulated at relatively low concentrations under the conditions we studied, and our data seem to fit Deaton and Greenberg's hypothesis. Yet the role and importance of blood bicarbonate in bivalve osmoregulation is not being considered in this hypothesis and suggests an area meriting further study.

The two salts promoting the longest survival in the ion permutation experiments were NaCl and $MgSO_4$. It is unlikely, on the basis of the substantial loss of blood solutes observed, that the animals would have survived much beyond the study period (51 days) in this minimal salt mixture.

Blood Na and Cl balance could not be maintained following exposure of zebra mussels to solutions deficient in K. The loss of K from the blood and cells probably disrupted the electrochemical gradient required for Na and Cl transport. The [K] tolerance range of zebra mussels is exceptionally narrow. Potassium concentrations above 0.3–0.5 m*M* in PW are lethal to *D. polymorpha* and other freshwater bivalves, yet, unlike other freshwater mussels, zebra mussels cannot survive without K while being stored unfed in the laboratory (Dietz and Byrne, 1990; Fisher *et al.*, 1991; McMahon, 1991; Horohov *et al.*, 1992; Ram and Walker, 1993; Vinogradov *et al.*, 1993). Fed bivalves may survive a year in the laboratory, in part because of the food supplement, but starvation is not a significant short-term problem, because unfed zebra mussels will survive for over 6 months when maintained in Mg-PW. When zebra mussels are fed, the K content of the algal cells and the culture medium used to raise the algae must be monitored. If, during feeding, the K concentration in the bathing medium is elevated above the tolerated level, the zebra mussels will be killed by the excess K, not by too much food.

The ambient level of calcium is an important predictor of zebra mussel presence and has a positive correlation with population density in a variety of lakes that have been modeled (Ramcharan *et al.*, 1992). In contrast, [Mg] displays no relationship with mussel occurrence or abundance. The minimum amount of Mg present in lakes with sufficient Ca to support a high zebra mussel population is 0.1 m*M*, and with low zebra mussel density the minimum amount of Mg is 0.03 m*M*. The 0.03 m*M* Mg concentration is likely to be near the threshold for zebra mussel survival. Sprung (1987) also noted significantly more abnormal embryonic development when *D. polymorpha* was raised in 0.04 m*M* Mg. But since, in zebra mussels, the Mg requirement seems to be for threshold amounts, there is no correlation with mussel population density over a range of Mg concentrations.

According to the model of Ramcharan *et al.* (1992), the Mississippi River ion concentrations are well above the threshold for the factors contributing to zebra mussel populations of high density. Indeed, we observed that both the adult zebra mussels and some larvae survived the summer of 1993 in the Mississippi River, even though temperatures were above 27°C for nearly 3 months. The predictive models developed by Ramcharan *et al.* (1992) suggest that the Mississippi River can support high densities of zebra mussels.

The unique sensitivity of zebra mussels to environmental ion composition may explain some of the variability that has been reported in the survival and blood ion concentrations. Even though zebra mussels are normally found in water with moderate to high calcium concentrations, they will survive low environmental [Ca] providing the bathing fluid contains Mg in minimal amounts. Although zebra mussels have an absolute requirement for Mg in the water, they can be held for months in nominally Mg-free PW if they are stored in high density (>100/l). The Mg lost by one mussel will accumulate in the medium and be available for uptake by adjacent animals. Even the "weaker" animals suffering the greatest Mg loss would survive for weeks if the composition of the ion mixture in the bathing water were adequate.

D. polymorpha represents one of several independent invasions of fresh water, and these mussels have evolved many physiological processes that are in common with other freshwater bivalves (Dietz, 1979; Deaton *et al.*, 1989; Deaton and Greenberg, 1991; McMahon, 1991; Horohov *et al.*, 1992). However, zebra mussel ion transport rates are among the highest found in freshwater mussels and reflect the recent evolution from brackish-water ancestors (Horohov *et al.*, 1992). For survival in fresh water, the ionic uptake rate must be in balance with ionic loss (renal and extrarenal). Of the freshwater bivalves studied, zebra mussels are least capable of tolerating ion losses associated with salt-depletion conditions imposed by deionized water. Zebra mussels require minimal concentrations of ions (Mg, Na, K, Cl) in their environment for long-term (>50 days) survival. Thus, zebra mussels are the most stenohaline (both low and high salinity) freshwater bivalves that have been studied. Unlike other freshwater bivalves, *D. polymorpha* apparently has not evolved sufficient mechanisms to allow survival in the most dilute of freshwater environments.

Acknowledgments

We thank Drs. Robert McMahon and Roger Byrne for providing the zebra mussels collected from Lake Erie and for their many suggestions and comments. T. R. LeBlanc provided valuable assistance in collecting mussels from the Mississippi River at DOW Chemical, Plaquemine, LA. We also thank S. J. Nichols for many hours of discussion and the use of the USFWS facilities in Ann Arbor, MI. Julie Cherry and Janice Horohov provided technical assistance. D. L. participated with support from a Howard Hughes Medical Institute undergraduate science initiative grant to LSU. This research was supported, in part, by the LSU Center for Energy Studies grant 91-01-11 continuation and NSF grant DCB90-17461.

Literature Cited

Beyenbach, K. W., C. A. Freire, R. K. Kinne II, and E. Kinne-Saffran. 1993. Epithelial transport of magnesium in the kidney of fish. *Miner. Electrolyte Metab.* **19:** 241–249.

Byrne, R. A., and B. R. McMahon. 1991. Acid-base and ionic regulation, during and following emersion, in the freshwater bivalve, *Anodonta grandis simpsoniana* (Bivalvia: Unionidae). *Biol. Bull.* **181:** 289–297.

Byrne, R. A., B. N. Shipman, N. J. Smatresk, T. H. Dietz, and R. F. McMahon. 1991. Acid-base balance during prolonged emergence in the freshwater bivalve, *Corbicula fluminea. Physiol. Zool.* **64:** 748–766.

Deaton, L. E., and M. J. Greenberg. 1991. The adaptation of bivalve molluscs to oligohaline and freshwater: phylogentic and physiological aspects. *Malacol. Rev.* **24:** 1–18.

Deaton, L. E., J. G. S. Derby, N. Subhedar, and M. J. Greenberg. 1989. Osmoregulation and salinity tolerance in two species of bivalve mollusc: *Limnoperna fortunei* and *Mytilopsis leucophaeta. J. Exp. Mar. Biol. Ecol.* **133:** 67–79.

Dietz, T. H. 1979. Uptake of sodium and chloride by freshwater mussels. *Can. J. Zool.* **57:** 156–160.

Dietz, T. H., and R. A. Byrne. 1990. Potassium and rubidium uptake in freshwater mussels. *J. Exp. Biol.* **150:** 395–405.

Finney, D. J. 1991. *Probit Analysis.* Cambridge Univ. Press, Cambridge.

Fisher, S. W., P. Stromberg, K. A., Bruner, and L. D. Boulet. 1991. Molluscicidal activity of potassium to the zebra mussel, *Dreissena polymorpha:* toxicity and mode of action. *Aquatic Toxicol.* **20:** 219–234.

Flatman, P. W. 1991. Mechanisms of magnesium transport. *Ann. Rev. Physiol.* **53:** 259–271.

Fyhn, H. J., and J. D. Costlow. 1975. Anaerobic sampling of body fluids in bivalve molluscs. *Comp. Biochem. Physiol.* **52A:** 265–268.

Graves, S. Y., and T. H. Dietz. 1982. Cyclic AMP stimulation and prostaglandin inhibition of Na transport in freshwater mussels. *Comp. Biochem. Physiol.* **71A:** 65–70.

Horohov, J., H. Silverman, J. W. Lynn, and T. H. Dietz. 1992. Ion transport in the freshwater zebra mussel, *Dreissena polymorpha. Biol. Bull.* **183:** 297–303.

Krogh, A. 1939. *Osmotic Regulation in Aquatic Animals.* Cambridge University Press, Cambridge.

McCorkle, S., and T. H. Dietz. 1980. Sodium transport in the freshwater Asiatic clam, *Corbicula fluminea. Biol. Bull.* **159:** 325–336.

McMahon, R. F. 1991. Mollusca: Bivalvia. Pp. 315–399 in *Ecology and Classification of North American Freshwater Invertebrates,* J. H. Thorp and A. P. Covich, eds. Academic Press, San Diego.

Murphy, W. A., and T. H. Dietz. 1976. The effects of salt depletion on blood and tissue ion concentrations in the freshwater mussel, *Ligumia subrostrata* (Say). *J. Comp. Physiol.* **108:** 233–242.

Nichols, S. J. 1993. Maintenance of the zebra mussel (*Dreissena polymorpha*) under laboratory conditions. Pp. 733–747 in *Zebra Mussels, Biology, Impacts and Control,* T. F. Nalepa and D. W. Schloesser, eds. Lewis, London.

Ram, J. L., and J. U. Walker. 1993. Effects of deionized water on viability of the zebra mussel, *Dreissena polymorpha. Comp. Biochem. Physiol.* **105C:** 409–414.

Ramcharan, C. W., D. K. Padilla, and S. I. Dodson. 1992. Models to predict occurrence and density of the zebra mussel, *Dreissena polymorpha. Can. J. Fish. Aquat. Sci.* **49:** 2611–2620.

Scheide, J. I., and T. H. Dietz. 1982. The effects of independent sodium and chloride depletion on ion balance in freshwater mussels. *Can. J. Zool.* **60:** 1676–1682.

Sprung, M. 1987. Ecological requirements of developing *Dreissena polymorpha* eggs. *Arch. Hydrobiol.* **79:** 69–86.

van der Velden, J. A., Z. I. Kolar, G. Flik, P. Polak, J. J. M. de Goeij, and S. E. Wendelaar Bonga. 1991. Magnesium transport between carp and water studied with $^{28}Mg^{2+}$ as radiotracer. *Appl. Radiat. Isot.* **42:** 347–352.

Vinogradov, G. A., N. F. Smirnova, V. A. Sokolov, and A. A. Bruznitsky. 1993. Influence of chemical composition of the water on the mollusk *Dreissena polymorpha.* Pp. 273–293 in *Zebra Mussels, Biology, Impacts and Control,* T. F. Nalepa and D. W. Schloesser, eds. Lewis, London.

Withers, P. C. 1992. *Comparative Animal Physiology.* Saunders, New York.

Reference: *Biol. Bull.* **187:** 84–98. (August, 1994)

Oxygen Consumption Rates and Metabolic Enzyme Activities of Oceanic California Medusae in Relation to Body Size and Habitat Depth

ERIK V. THUESEN[1] AND JAMES J. CHILDRESS

Oceanic Biology Group, Marine Science Institute, University of California, Santa Barbara, California 93106

Abstract. Oxygen consumption rates were measured in 14 species of hydromedusae and 5 species of bathypelagic coronate scyphomedusae. Analysis of all individuals of all species of medusae showed the familiar pattern of decreasing specific oxygen consumption rate with increasing wet weight of animals. Citrate synthase (CS), lactate dehydrogenase (LDH), malate dehydrogenase (MDH), and pyruvate kinase (PK) activities were measured in more than 30 species of medusae. Octopine dehydrogenase, strombine dehydrogenase, and alanopine dehydrogenase were not detected in either hydromedusae or scyphomedusae. The allometric scaling phenomenon of decreasing activity in larger individuals was observed in Krebs cycle enzyme activities. LDH activities, on the other hand, increased with increasing wet weight. Most medusae were aerobically poised, with higher CS activities than LDH activities. However, several meso- and bathypelagic medusae, including the coronate scyphozoans *Periphylla periphylla* and *Nausithoë rubra*, were anaerobically poised, possibly as a mechanism to assist in vertical migrations at low oxygen concentrations in the oxygen minimum layer. There is poor correlation between CS activities and oxygen consumption rates in these medusae when compared to previously investigated animals. To account for this poor correlation, we propose the hypothesis that medusan CS at the periphery of the maximum diffusion distance may be oxygen-limited and does not function at the normal *in vivo* rate. For pelagic medusae, there is no apparent decline in metabolic rate and metabolic potential, as determined by enzymatic activity, with increasing depth of occurrence, beyond the declines caused by the decrease in temperature with depth. These patterns are in contrast to the rapid declines in metabolic rates and metabolic potentials with depth that have been observed for pelagic fishes and crustaceans. Deep-living medusae have metabolic rates of a magnitude similar to those of bathypelagic fishes and crustaceans.

Introduction

Previous studies on the metabolic rates of medusae have been mainly restricted to the more common near-shore species (*e.g.*, Arai, 1986; Larson, 1987b, and references cited therein). The few physiological and biochemical investigations on deep-living gelatinous organisms include measurements of the *in situ* respiration of the bathypelagic scyphomedusa *Poralia rufescens* (Smith, 1982); the metabolic rates of the midwater ctenophore *Bathocyroe fosteri* (Youngbluth *et al.*, 1988); and the oxygen consumption rate of the gelatinous pelagic holothuroid *Scotoanassa* sp. from the benthic boundary layer off southern California (Childress *et al.*, 1989). In addition, we recently measured the respiratory rates and enzyme activities of the gelatinous polychaete *Poeobius meseres* and some other deep-sea worms and chaetognaths (Thuesen and Childress, 1993a, b).

One method of estimating aerobic metabolic rates from enzymatic activities involves measurement of the activity of the electron transport system (ETS) (Båmstedt, 1980; Mayzaud, 1986; Packard, 1979; Packard *et al.*, 1975; Packard *et al.*, 1988). This method has been applied to various types of zooplankton, including three species of epipelagic hydromedusae by King and Packard (1975). They observed lower metabolic potentials (ETS activities) in relation to oxygen consumption for medusae than for other zooplankton. There are no previous studies on the metabolic enzyme activities of medusae.

Received 14 September 1993; accepted 6 June 1994.

[1] Present address: The Evergreen State College, Olympia, Washington 98505.

Many investigators have observed large declines in the metabolic rates of pelagic fishes and crustaceans with increasing habitat depth (Childress and Thuesen, 1992). The oxygen consumption and nitrogen excretion rates of pelagic crustaceans and the metabolic rates and metabolic potentials, as estimated by enzyme activities, of pelagic fishes, decline rapidly with increasing depth of occurrence (Childress, 1971, 1975; Childress and Somero, 1979; Cowles *et al.*, 1991; Ikeda, 1988; Quetin *et al.*, 1980; Sullivan and Somero, 1980; Torres *et al.*, 1979; Torres and Somero, 1988). Protein contents of pelagic crustaceans and fishes also decline as a function of depth of occurrence, but to a much lesser extent than metabolic rates and enzymatic activities (Bailey and Robison, 1986; Childress and Nygaard, 1973, 1974; Childress *et al.*, 1990b; Stickney and Torres, 1989). Differences in temperature, pressure, chemical composition, or size have been estimated to account for only a small fraction of the declines in metabolic rates of these organisms. The corresponding proportional decline of enzyme activities in fish white muscle indicates that the decline in metabolic rate is laid down at the subcellular level (Childress and Somero, 1979; Siebenaller and Yancey, 1984; Somero and Childress, 1980; Sullivan and Somero, 1980; Torres and Somero, 1988).

The visual interactions hypothesis has been proposed to account for the widely observed metabolic declines with habitat depths in pelagic crustaceans and fishes. It suggests that animals that use visual interactions in predator-prey relationships have high metabolic rates to maintain the robust bodies needed to react rapidly over the appreciable distances in which visual interactions take place in high light environments; whereas animals that live in environments where visual interactions are much more limited in distance due to low light levels, or that do not have image-forming eyes, have experienced reduced selection for locomotory capabilities and hence have lower metabolic rates compared to their visual counterparts (Childress and Mickel, 1985; Childress *et al.*, 1980; Childress *et al.*, 1990a). One test of the visual interactions hypothesis is to examine the metabolic characteristics of nonvisual pelagic animals with regard to increasing habitat depth. The visual interactions hypothesis suggests that bathypelagic nonvisual organisms would have metabolic rates similar to their epipelagic counterparts. We have tested this hypothesis by examining the metabolic rates and enzyme activities of California chaetognaths in relation to depths of occurrence, and our observations support the predictions of the visual interactions hypothesis (Thuesen and Childress, 1993a). Meso- and bathypelagic chaetognaths have oxygen consumption rates and enzyme activities comparable to epipelagic species when measured at the same temperature.

Herein we examine the predictions of the visual interactions hypothesis when applied to pelagic medusae—another group of pelagic organisms that do not have image-forming eyes. Gelatinous organisms are important components of pelagic ecosystems, and yet they have historically been overlooked or underestimated in studies on marine ecosystems. In the last decade, the quantitative importance of medusae, ctenophores, salps, and other gelatinous animals in the flow of energy through pelagic ecosystems has been recognized (Alldredge, 1984; Longhurst, 1985). This study is a broad comparison of the metabolic rates and potentials of oceanic hydromedusae and scyphomedusae living at depths down to 2 km. We examined enzyme activities and metabolic rates in relation to wet weight to determine the influence of body size on these parameters; we also looked at the metabolic poise of the medusae in this study by comparing anaerobic and aerobic metabolic potentials.

Materials and Methods

Collection of medusae

Our primary collecting gear was an opening-closing Mother Tucker trawl with a 10-m^2 mouth fitted with a closing 30-l insulated cod end (Childress *et al.*, 1978). The cod end prevented heat shock to animals living below the thermocline and injury due to turbulence while the net was being brought to the surface. Epipelagic medusae were occasionally captured by 200-m wire-out oblique tows of a 1-m ring net. Collections were carried out on the RV *Point Sur* in the San Clemente Basin during September 1988 and in an area about 160 km west of Point Conception, California (123°E, 34°50′ N) in July 1991, and on cruises of the RV *New Horizon* off Point Conception in June 1990 and February and June 1991. The ship speed was kept very low (0.5–1 kn) to decrease turbulence and abrasion in the net and reduce the number of animals collected in the cod end, thereby maximizing the condition of the gelatinous organisms. Animals were transferred to 5°C seawater upon recovery, quickly identified to species, and either held for measurements of metabolic rate or frozen in liquid nitrogen for later analyses of enzyme activity in the laboratory. Every effort was made to select animals with empty manubria and to remove commensal or epizoic organisms.

In addition to these collections, some animals were obtained with the sampling pumps and collecting devices of the Monterey Bay Aquarium Research Institute's ROV *Ventana* in Monterey Canyon in August 1990. Neritic, demersal, and epiphytic medusae were occasionally hand-collected in the Santa Barbara Channel by scuba divers over the course of this study.

The demersal hydrozoan *Polyorchis penicillatus* and the epipelagic hydrozoan *Leukartiara octona* were maintained in a planktonkreisel with an abundant supply of crustaceans, primarily *Holmesimysis costata*, as food for up to 48 h after capture. They were then held without food for 24 h until their manubria were empty, before being frozen for enzyme activity investigations. Selected individuals of *L. octona* were acclimated to a colder temperature, 5°C, in a planktonkreisel for 1 week under the same food conditions and then used for respiration experiments.

Some specimens that were originally frozen in liquid nitrogen were stored up to 6 months in a −80°C freezer without detectable loss of enzyme activities. Animals collected by meter net and remotely operated vehicle, without thermal protection, were used only for enzyme assay investigations.

The report on the hydromedusae of the Indian and Pacific Oceans by Kramp (1968), Russell's treatises on Atlantic medusae (Russell, 1953, 1970) and the numerous references cited therein were indispensable in our identification of medusae to species.

Metabolic rate measurement

Oxygen consumption measurements on animals that were recovered in excellent condition were carried out either on board ship or in the laboratory. Our previous experiments on the effect of hydrostatic pressure on two bathypelagic hydromedusae, *Crossota rufobrunnea* and *Aegina citrea,* showed no significant differences in metabolic rates measured at 1 and 101 atm (Childress and Thuesen, 1993). Therefore, all metabolic rates were measured at atmospheric pressure. Oxygen consumption rates were measured in two ways, depending on the size of the animal. Larger animals were transferred to water-jacketed respiration chambers of appropriate size containing 5°C filtered seawater with antibiotics (0.20-μm membrane filter; 25 mg l^{-1} each of streptomycin and penicillin) and equipped with small stirring pumps consisting of a magnetic stirring bar enclosed within a discrete plastic chamber. This mechanism allowed for gentle mixing of water and provided sufficient flow for the Clarke-type oxygen electrodes (Mickel *et al.*, 1983) without damage to the animal. Smaller animals were transferred to glass syringes used as miniature respiration chambers (Thuesen and Childress, 1993a). The syringes with filled with filtered seawater containing antibiotics as above and incubated at 5°C. Periodically, a gas-tight syringe was used to withdraw water samples from the incubation syringe through a three-way valve, and the new incubation volume was noted. Before the sample was withdrawn, syringes were turned end-over-end several times to mix the incubation medium. Oxygen and carbon dioxide content of the water was measured with a gas chromatograph (Childress *et al.*, 1984).

Oxygen consumption rates of hydromedusae from the Santa Barbara Channel, *Vallentinia adherens, Eirene mollis,* and *Leukartiara octona,* were measured at 15°C following the latter method. The oxygen consumption rates of acclimated *L. octona* were measured at 5°C. Oxygen consumption rates at 10°C of *Periphylla periphylla* and *Colobenema sericeum* were measured with oxygen electrodes.

Control syringes of filtered seawater containing the antibiotic mixture but without animals were run simultaneously. After removal of the animals, syringe and respirometer experiments were periodically left to continue as controls to check for bacterial contamination. If present, background respiration was subtracted from animal respiration. Background respiration was always undetectable at 5°C. After experiments at sea, animals were weighed using a shipboard motion-compensated precision balance system (Childress and Mickel, 1980). In the laboratory, animals were weighed on an analytical balance. All specimens used in oxygen consumption experiments were later frozen in liquid nitrogen for spectrophotometric analysis of enzyme activities.

Biochemical analysis

The following enzymes were screened to select appropriate indicators of aerobic and anaerobic metabolic potential: citrate synthase (CS, E.C. 4.1.3.7), malate dehydrogenase (MDH, E.C. 1.1.1.37), lactate dehydrogenase (LDH, E.C. 1.1.1.27), pyruvate kinase (PK, E.C. 2.7.1.40), octopine dehydrogenase (E.C. 1.5.1.11), alanopine dehydrogenase (E.C. 1.5.1.17), and strombine dehydrogenase (E.C. 1.5.1.?). Although we assayed for these enzymes in a variety of medusae, our study focused on CS and LDH as two enzymes representative of metabolic potential. CS is an important regulatory enzyme and functions in the first step of the citric acid cycle. MDH plays a variety of roles in intermediary metabolism and is important in the citric acid cycle. These enzymes serve as indicators of aerobic metabolic potential. LDH is the terminal enzyme in glycolysis, and PK is the regulatory enzyme that supplies pyruvate for LDH in the second-to-last step in glycolysis. These two enzymes are excellent indicators of glycolytic potential and contribute to both aerobic and anaerobic metabolic pathways. Because we did not assay the various opine dehydrogenase in all the species in this study, it could be that one or more of these enzymes are better indicators than LDH of anaerobic potential in some species. CS, MDH, LDH, and PK activities in fish muscle have all been found to correlate well with oxygen consumption rates (Childress and Somero, 1979; Somero and Childress, 1990; Sullivan and Somero, 1980; Torres and Somero, 1988).

Whole animals were weighed on a Mettler analytical balance while they were still frozen and were homogenized at a very low dilution (from 1:1 to 1:9 parts weight/volume in 0.01 *M* Tris homogenization buffer, pH 7.5, at 10°C) in Duall hand-held glass homogenizers kept on ice. Low dilutions were used to detect the low enzyme activities present in medusan homogenates. Very large animals were subsampled by removing a wedge-shaped piece of the whole animal for homogenization. Aliquots of homogenate were transferred to microfuge tubes and centrifuged at 6600 × *g* for 5 min at 5°C. Unlike the enzyme activities of fish muscle, activities in whole-animal homogenates decreased by 20–40% after 4 h standing on ice. Therefore, all assays were performed within 1 h of homogenization, using a Shimadzu UV160U spectrophotometer equipped with a water-jacketed cuvette holder. The subumbrellar, or swimming, muscle of some of the larger species of medusae was readily excised. For these species, the enzyme activities in these muscles were also measured. Small amounts of sample supernatant (10, 25, or 50 μl) were used for assays. To estimate maximum metabolic potential, measurements of enzyme activity were made in 1-ml quartz cuvettes at 20°C under nonlimiting conditions and followed procedures essentially the same as those described previously (Childress and Somero, 1979; Somero and Childress, 1980). Enzyme activities are expressed as units (micromoles substrate converted to product per min) per gram wet weight of animal.

CS activity was measured in a medium containing 50 m*M* imidazole/HCl buffer (pH 7.8 at 20°C), 0.5 m*M* oxaloacetate, 0.1 m*M* acetyl-CoA, 0.1 m*M* 5,5-dithiobis (2-nitrobenzoic acid) (DTNB), and 1.5 m*M* $MgCl_2$. The increase in absorbance at 412 nm due to the reaction of the reduced coenzyme A generated by the enzymatic reaction with DTNB was recorded. Background activity before the addition of homogenate supernatant was recorded, and this background rate was then subtracted from the overall rate after the assay reaction was initiated by addition of the oxaloacetate. Background activity was subtracted from total activity to calculate the enzyme activity of the sample. MDH activity measurements were performed in a medium containing 100 m*M* Tris/HCl buffer (pH 8.1 at 20°C), 20 m*M* $MgCl_2$, 0.4 m*M* oxaloacetate, and 150 μ*M* NADH. LDH activity was measured in a medium containing 80 m*M* Tris/HCl buffer (pH 7.2 at 20°C), 2 m*M* sodium pyruvate, 150 μ*M* NADH, and 100 m*M* KCl. PK activity was measured in a medium containing 50 m*M* imidazole/HCl buffer (pH 7.8 at 20°C), 100 m*M* KCl, 10 m*M* $MgSO_4$, 0.1 m*M* fructose-bisphosphate, 1.0 m*M* phosphoenolpyruvate, 5.0 m*M* ADP, 150 μ*M* NADH and excess LDH activity (rabbit muscle LDH, Sigma Chemical Co.). The assay reactions of MDH, LDH, and PK were started by addition of the sample supernatant, and the decrease in absorbance at 340 nm due to NADH oxidation was recorded.

Lactate concentration in tentacle and swimming muscle tissue of *Periphylla periphylla* and *Aegina citrea* was measured at sea. Frozen tissue was homogenized in 0.1 *M* perchloric acid, neutralized to a pH of 10 with KOH, and centrifuged at 6600 × *g* for 10 min. Lactate concentrations in the supernatant were measured enzymatically using L-lactic acid assay reagents (Boehringer-Mannheim).

Statistical analysis

All statistical analyses were performed with Statview II or SuperANOVA (Abacus Concepts, Inc., Berkeley, CA). Simple linear regressions, multiple regressions, Kendall nonparametric rank correlations, and analysis of covariance (ANCOVA) were used to explore the relationships among the parameters that were measured in this study. Simple linear regressions were used to describe the relationships between various variables, including relationships between weight-specific citrate synthase activity and weight-specific metabolic rates. Regressions of total (not standardized by weight) CS activities *versus* total oxygen consumption rates were not used. Although this statistical methodology has been used in previous studies on zooplankton physiology, it essentially regresses body mass on the *y*-axis with body mass on the *x*-axis, and it thereby results in higher values of correlation coefficients and apparent statistical significance when compared with a slope of zero. It does not, however, test the relationship between enzyme activity and oxygen consumption rate independent of body size. All rates of oxygen consumption and enzyme activity referred to in this study are weight-specific. All the regressions in this study were carried out on ln-transformed data to improve linearity.

Oxygen consumption rates and enzyme activities of medusae were evaluated in relation to wet mass of the animals, and scaling coefficients from the allometric equation $y = aM^b$ were derived, where M is the wet weight of the animal, b is the scaling coefficient, and a is a constant for the species at a given temperature (Schmidt-Nielsen, 1983). Mean values of specific oxygen consumption rates and the enzyme activities of whole-animal homogenates for each species were used in comparisons with crustacean and fish data from the same region (metabolic rate data on pelagic crustaceans [Childress, 1975] and enzyme activities of fishes [Childress and Somero, 1979; Wells and Childress, unpublished]) using ANCOVA to test whether the slopes of the various relationships between minimum depth of occurrence (MDO) and enzyme activity were significantly different. The Kendall rank correlation was used to test for significant relationships between MDO and the biochemical-physiological parameters without any assumptions of form or linearity of the relationships and to find correlations between the biochemical and physiological data. Since these tests are performed on data from within a single region that has a consistent relationship between temperature and depth, no correction for temperature difference is necessary. MDO in a given region is defined as that depth below which 90% of the population usually can be found (Childress, 1975). A depth of 10 m was taken as the MDO for animals living at 10 m or shallower to avoid distortions in regressions of ln-transformed data. Medusan MDOs are based on our personal observations using the opening-closing Mother Tucker trawl and published bathymetric distributions of medusae off southern California (Alvariño, 1967). When we did not have sufficient data to evaluate MDO for a given species, the shallowest capture depth was used. This was only done for the rarer species of medusae, which were uncommonly captured in trawls. Minimum capture depths for *Tiaranna rotunda*, *Euphysora gigantea*, and *Neoturris fontata* are 650, 350, and 650 m, respectively. The epiphytic medusa *V. adherens* was excluded from depth comparisons of pelagic species.

Wet mass was used as the size measurement, because this parameter is the physiologically significant one that determines constraints on animal locomotion, behavior, etc. Other measurements, such as dry weight or protein content, used as indicators of size can lead to misinterpretations concerning the biology and ecology of the whole organism. The significance of using various parameters of body size in this regard has been discussed previously (Childress, 1977; Childress and Somero, 1979).

Results

Oxygen consumption measurement

Many species of medusae were collected in excellent condition by using the large insulated cod end. These included four undescribed species of Trachymedusae: *Pantachogon* sp. A (*cf. P. haekeli*), *Vampyrocrossota childressi* (Thuesen, 1993), *Tetrorchis* sp. A (distinct from *T. erythrogaster*), and an orange and pink rhopalonematid, *Crossota* sp. A. Very large and fragile animals, such as *Solmissus incisa*, could not be collected in sufficiently healthy condition for oxygen consumption rate measurements; however, smaller fragile animals, such as species of the Halicreatidae, were often collected with tentacles more than several body-heights in length and with intact swimming bells. These animals were still swimming after 24 h in the incubation syringes. Coronate medusae, rhopalonematids, and other robust animals were caught in pristine condition and could be maintained alive and swimming for several days in 20-l buckets in a 5°C refrigerator. Oxygen consumption rates were measured on 14 hydrozoans and 5 species of coronate scyphozoan medusae: mean rates are presented in Table I. Oxygen consumption rates of three species of medusae were measured at two temperatures, and the Q_{10} for *Leukartiara octona* and the estimated Q_{10} values for *Colobenema sericeum* and *Periphylla periphylla* are 3.5, 4.8, and 2.6, respectively.

Analysis of all individuals of all species of medusae showed the familiar pattern of decreasing oxygen consumption rate with increasing wet weight of animals at both 5° and 15°C (Fig. 1). Scyphozoans analyzed as a separate group also showed a highly significant relationship between size and metabolic rate ($b = -0.26$; F test for regression coefficient, $P < 0.01$, 95% CI: ±0.17). However, among the hydrozoan medusae there was a less significant effect of size on metabolic rate ($b = -0.13$; F test for regression coefficient, $P = 0.07$, 90% CI: ±0.11). Although analysis of most species over a large enough size range with a sufficient number of individuals to determine species-specific scaling patterns was not possible, it was undertaken for *Aegina citrea*, *Crossota rufobrunnea*, and *Periphylla periphylla*. A significant size-metabolism relationship was found only for *C. rufobrunnea*, which had a scaling coefficient of −0.31 (F test for regression coefficient, $P = 0.02$; 95% CI: ±0.25).

Enzyme activity

Citrate synthase, lactate dehydrogenase, pyruvate kinase, or malate dehydrogenase activities were measured on more than 150 individuals of 32 species of medusae (Table II). LDH and CS activities were measured in isolated swimming muscle of large medusae: *Pelagia colorata*, *Atolla wyvillei*, *Periphylla periphylla*, and *Solmissus incisa* (Table II). We could not detect octopine dehydrogenase in any species tested (whole-animal homogenates of *Pelagia colorata*, *Aurelia aurita*, an unidentified epipelagic hydromedusan, *Crossota rufobrunnea*, *Crossota alba*, *Haliscera conica*, *Haliscera bigelowi*, or isolated muscle of *P. colorata* and *P. periphylla*). We also could not detect either alanopine dehydrogenase or strombine dehydrogenase in any species tested (whole-animal homogenates of *C. rufobrunnea*, *C. alba*, *H. conica*, *and H. bigelowi* or isolated muscle of *P. periphylla*).

The highest CS activities were measured in the epiphytic medusa *Vallentinia adherens*. The highest LDH activities were measured in *P. periphylla*. Citrate synthase and LDH activities in *S. incisa* were lower than could be detected, but both these enzymes were measured at low levels in isolated swimming bell muscle. Citrate synthase could not be detected in whole-animal homogenates or in isolated coronal muscle of *A. wyvillei* and *A. vanhoeffeni*, although the coronate medusae of other genera had readily measurable CS activities. CS activity was higher than LDH activity in many of the species, although LDH activities were higher than CS activities in *A. citrea*, *H. maasi*, *Ptychogena lactea*, and the coronate scyphozoans *A. vanhoeffeni*, *A. wyvillei*, *P. periphylla*, and *Nausithoë rubra*. PK and MDH activities were usually higher with respect to their corresponding LDH and CS activities in the few species for which these enzymes were investigated; how-

Table I

Metabolic rates of medusae collected off California

Class Order Family Genus and species	Wet weight range (g)	T (°C)	Oxygen consumption (mean ± SE) (μmol O_2 g^{-1} h^{-1})	Number of specimens
Hydrozoa				
Leptomedusae				
Eirenidae				
Eirene mollis	0.1262–0.3896	15.0	0.783 ± 0.144	3
Anthomedusae				
Pandeidae				
Leukartiara octona	0.0629–0.3411	5.0	0.410 ± 0.091	3
	0.0322–0.9685	15.0	1.429 ± 0.223	5
Limnomedusae				
Olindiadidae				
Vallentinia adherens	0.0129–0.0536	15.0	1.932 ± 0.478	5
Trachymedusae				
Halicreatidae				
Botrynema brucei	1.3299	5.0	0.140	1
Haliscera bigelowi	0.191–1.1677	5.0	0.128 ± 0.030	5
Halitrephes maasi	13.070–27.386	5.0	0.046 ± 0.006	4
Rhopalonematidae				
Colobenema sericeum	2.4368–7.3620	5.0	0.091 ± 0.030	2
	5.858	10.0	0.199	1
Crossota alba	0.3180–0.8793	5.0	0.332 ± 0.128	3
Crossota rufobrunnea	0.062–1.08	5.0	0.154 ± 0.024	11
Crossota sp. A	0.1286–0.1445	5.0	0.168 ± 0.070	2
Pantachogon sp. A	0.3690–0.7157	5.0	0.259 ± 0.017	2
Tetrorchis erythrogaster	0.3987–0.4751	5.0	0.117	2
Vampyrocrossota childressi	0.2871–0.4127	5.0	0.140 ± 0.023	2
Narcomedusae				
Aeginidae				
Aegina citrea	0.3658–9.760	5.0	0.185 ± 0.037	11
Scyphozoa				
Coronatae				
Atollidae				
Atolla vanhoeffeni	0.6029	5.0	0.201	1
Atolla wyvillei	0.2192–17.22	5.0	0.134 ± 0.044	5
Nausithoidae				
Nausithoë rubra	0.5354–13.030	5.0	0.219 ± 0.048	2
Periphyllinidae				
Paraphyllina ransoni	0.1866–0.3453	5.0	0.333 ± 0.104	2
Periphyllidae				
Periphylla periphylla	2.7598–42.39	5.0	0.094 ± 0.017	8
	22.93	10.0	0.152	1

ever, PK was lower than LDH in the two coronates *A. wyvillei* and *P. periphylla*. We detected lactate in *P. periphylla* tentacle and coronal muscle at concentrations of 1.65 (SE = 0.45; $n = 6$) and 0.89 (SE = 0.28; $n = 6$) μmol g^{-1}, respectively. No lactate was detected in either velum tissue ($n = 4$) or tentacle tissue ($n = 4$) of *Aegina citrea*.

The common allometric scaling phenomenon of decreasing activity in larger individuals was observed in Krebs cycle enzyme activities (Fig. 2; Table III). LDH activities, on the other hand, increased with increasing wet weight (Fig. 3; Table III). The slopes of these regressions were different from zero at the 95% significance level. Nonsignificant negative scaling was observed for PK activities. Sufficient numbers of individuals of several species were analyzed to calculate species-specific scaling patterns, and the slopes of these regressions were usually not significantly different from zero over the size range studied. Significant allometric scaling relationships are presented in Table III.

Weight-specific CS activities were significantly correlated with weight-specific oxygen consumption rates at both 5 and 15°C (Fig. 4, *F* test for regression coefficient,

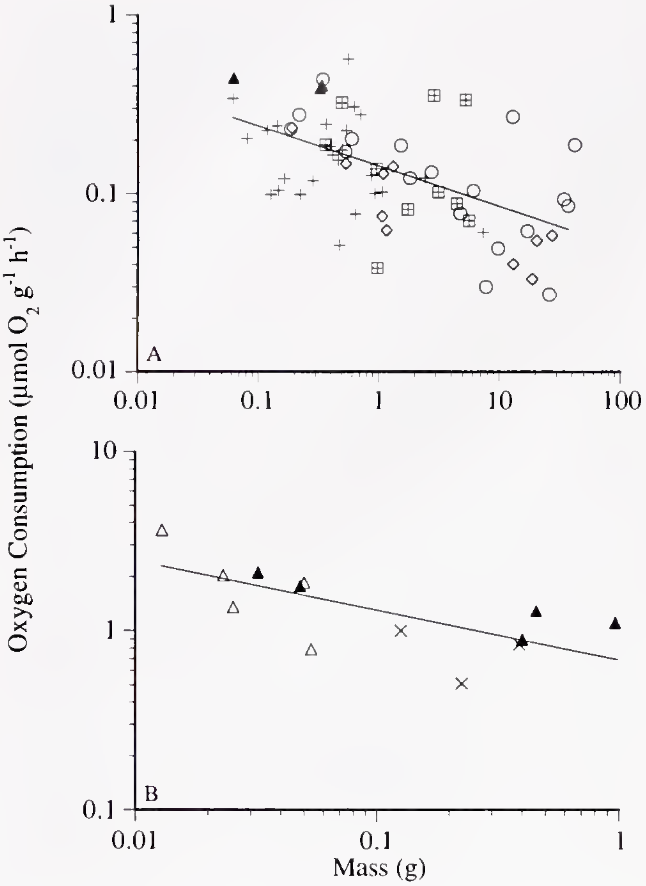

Figure 1. Oxygen consumption rates at 5°C (A) and 15°C (B) of California medusae as a function of their wet weight. The slope of the regression line for 5°C experiments is $y = 0.141\ x^{-0.22}$; $R = 0.45$. The slope of the regression line for 15°C experiments is $y = 0.712\ x^{-0.26}$; $R = 0.77$. Symbols for animals are as follows: Narcomedusae (⊞), Halicreatidae (^), Rhopalonematidae (+), Coronate scyphomedusae (○), *Vallentinia adherens* (△), Leptomedusae (×), *Leukartiara octona* (▲).

$P < 0.05$ for both regressions). Correlation coefficients were significant, $P < 0.05$ for both regressions, with $R = 0.31$ and 0.63 in the 5 and 15°C analyses, respectively.

Respiratory rate and enzyme activity in relation to depth of occurrence

No significant decline in metabolic rate or enzyme activity can be ascribed to minimum depth of occurrence in pelagic medusae (Figs. 5 and 6). The slopes of these regressions are not different from zero at the 95% significance level.

The slopes of the regressions describing the variation in metabolic rates and enzyme activities with depth are not statistically different from zero; however, they are significantly different from those for other groups that show significant declines in metabolic rates and enzyme activities with depth of occurrence. The pattern of change in medusan oxygen consumption rate with depth is significantly different from that observed for pelagic crustaceans (ANCOVA, $P < 0.02$; Fig. 5). The variation in CS activities with depth of occurrence in medusae (both with and without *V. adherens* data) is significantly different from the observed decrease in CS activity for pelagic fishes (ANCOVA, $P < 0.02$; Fig. 6A). The variation in LDH activities with depth in pelagic medusae is significantly different from that observed for pelagic fishes (ANCOVA, $P < 0.004$; Fig. 6B). Kendall's nonparametric test of rank correlation failed to show any significant correlation of mean medusan metabolic rate or enzyme activity with minimum depth of occurrence.

Discussion

Variability

Using an elaborate respirometer and a painstaking method of chemical analysis to determine oxygen and carbon dioxide content, Vernon (1895) was the first to measure the oxygen consumption rates of medusae. He observed considerable variability and, for the scyphozoan *Rhizostoma pulmo*, noted "distinct differences in the respiratory activity of different individual medusae" that could not be explained by size effects. Other investigators have also shown high variability in metabolic rate measurements of gelatinous animals (*e.g.*, Biggs, 1977; Larson, 1987b). One explanation may be that the nutritional status of the organism is reflected in metabolic rate measurements. Medusae undergo rapid periods of growth with high food concentration; furthermore, they "degrow" during periods of starvation and decrease in size to resemble a miniature adult (Hamner and Jenssen, 1974). Arai (1986) manipulated the nutritional status of the hydrozoan *Aequorea victoria* and observed higher metabolic rates in animals that had been starved for 3 days. She concluded that this was not due to behavioral changes and was unable to explain her findings. Other investigators have shown that nutritional status can be reflected in the enzyme activities of some organisms within days to weeks (Båmstedt, 1980; Clarke *et al.*, 1992; Clarke and Walsh, 1993; Lowery *et al.*, 1987; Roche-Mayzaud *et al.*, 1991). It is unknown how quickly enzyme activities in medusae are influenced by nutritional status.

Our investigation of enzymatic scaling in the demersal jellyfish *Polyorchis penicillatus* used individuals that were handled differently than other animals in this study, and the results of these experiments are less variable than results for the other species investigated. These *Polyorchis* had been kept in a planktonkreisel for up to 24 h with high concentrations of food. Perhaps the more uniform nutritional status of these individuals reduced the variability of their enzyme activity.

Table II

Enzyme activities of California medusae measured at 20°C

Class Family Genus and species	Minimum* depth (m)	Wet weight range (g)	Enzymatic activity (mean ± SE, number of specimens)			MDH (units g^{-1})
			CS (units g^{-1})	LDH (units g^{-1})	PK (units g^{-1})	
Hydrozoa						
Polyorchidae						
Polyorchis penicillatus	10	0.079–14.690	0.238 ± 0.029, 11	0.172 ± 0.016, 11	0.216 ± 0.019, 3	0.939 ± 0.019, 3
Campanulariidae						
Phialidium lomae	10	0.010	0.118, 1	0.003, 1	n.a.	n.a.
Laodiceidae						
Ptychogena lactea	200	6.281	0.0004, 1	0.0230, 1	n.a.	n.a.
Eirenidae						
Eirene mollis	10	0.126–0.390	0.174 ± 0.056, 3	0.010 ± 0.005, 3	n.a.	n.a.
Pandeidae						
Leukartiara octona	10	0.008–0.054	0.402 ± 0.019, 3	0.020 ± 0.005, 3	n.a.	n.a.
Eutimidae						
Tima sp. A	100	0.2149	0.028, 1	0.004, 1	n.a.	n.a.
Olindiadidae						
Vallentinia adherens	10	0.008–0.054	3.563 ± 0.86, 6	0.057 ± 0.008, 6	n.a.	n.a.
Halicreatidae						
Botrynema brucei	600	1.299	0.002, 1	0.002, 1	n.a.	n.a.
Halicreas minimum	700	2.740–3.405	0.006, 1	n.d.	0.012, 1	0.005, 1
Haliscera bigelowi	800	0.191–1.641	n.d.	0.028 ± 0.009, 6	n.a.	n.a.
Haliscera conica	400	1.928	0.0007, 1	n.d.	n.a.	n.a.
Haliscera racovitzae	700	0.328–1.167	0.007,1	0.018 ± 0.007, 2	0.191 ± 0.013, 4	0.201 ± 0.047, 2
Halitrephes maasi	500	18.764–27.386	0.004 ± 0.001, 2	0.017 ± 0.005, 2	n.a.	n.a.
Rhopalonematidae						
Colobenema sericeum	300	2.437–9.319	0.124 ± 0.016, 3	0.031 ± 0.014	n.a.	n.a.
Crossota alba	100	0.296–0.879	0.179 ± 0.018, 6	0.008 ± 0.004, 6	n.a.	n.a.
Crossota rufobrunnea	500	0.062–1.080	0.147 ± 0.013, 13	0.011 ± 0.007, 13	0.145 ± 0.024, 4	0.578 ± 0.432, 4
Crossota sp. A	1100	0.1286–2.7281	0.038 ± 0.005, 4	0.006 ± 0.004, 3	n.a.	n.a.
Pantachogon sp. A	800	0.216–0.716	0.108 ± 0.012, 6	0.022 ± 0.004, 5	0.262 ± 0.053, 4	0.915 ± 0.131, 4
Tetrorchis erythrogaster	600	0.263–0.475	0.044 ± 0.019, 5	0.005 ± 0.001, 5	n.a.	n.a.
Tetrorchis sp. A	800	1.425	0.070,1	0.0007,1	n.a.	n.a.
Vampyrocrossota childressi	750	0.286–0.417	0.065 ± 0.011, 3	0.001 ± 0.0003, 3	n.a.	n.a.
Aeginidae						
Aegina citrea	800	0.366–9.760	0.043 ± 0.007, 11	0.085 ± 0.015, 11	0.285 ± 0.080, 4	0.624 ± 0.084, 4
Aegina sp. A	1000	6.602–17.440	0.003 ± 0.001, 2	0.001, 1	n.a.	n.a.
Cuninidae						
Solmissus incisa	1200	91.704	n.d.	n.d.	0.004, 1	0.009, 1
S incisa (isolated swimming bell muscle)		93.5	0.007	0.003	n.a.	n.a.
Solmissus marshalli	10	5.015–17.292	0.006 ± 0.0, 2	0.028 ± 0.005, 2	n.a.	n.a.
Scyphozoa						
Atollidae						
Atolla vanhoeffeni	450	0.451–0.603	n.d.	0.318 ± 0.053, 3	n.a.	n.a.
Atolla wyvillei	500	0.219–71.050	n.d.	0.243 ± 0.055, 7	0.158 ± 0.008, 4	0.768 ± 0.208, 3
A wyvillei (isolated coronal muscle)		71.05	n.d.	2.750	n.a.	n.a.
Nausithoidae						
Nausithoë rubra	1100	0.535–13.030	0.003 ± 0.001, 2	0.064 ± 0.028, 2	n.a.	n.a.
Periphyllinidae						
Paraphyllina ransoni	800	0.187–124.70	0.124 ± 0.044, 4	0.195 ± 0.088, 6	n.a.	n.a.
Periphyllidae						
Periphylla periphylla	650	2.204–36.05	0.017 ± 0.003, 5	1.711 ± 0.552, 5	1.112 ± 0.202, 3	0.669 ± 0.144, 2
P. periphylla (isolated coronal muscle)		20.0	0.215	5.659	n.a.	n.a.
Pelagiidae						
Pelagia colorata	10	3750.0–6800.0	0.225 ± 0.014, 2	0.015 ± 0.002, 2	n.a.	n.a.
P colorata (isolated subumbrellar muscle)		6800.0	n.a.	5.08	n.a.	n.a.
Ulmaridae						
Aurelia aurita	10	98.4	0.019, 1	n.a.	n.a.	n.a.

CS: citrate synthase; LDH: lactate dehydrogenase; PK: pyruvate kinase; MDH: malate dehydrogenase; Units are micromoles substrate converted to product per minute. n.d.: not detected; n.a.; not assayed.

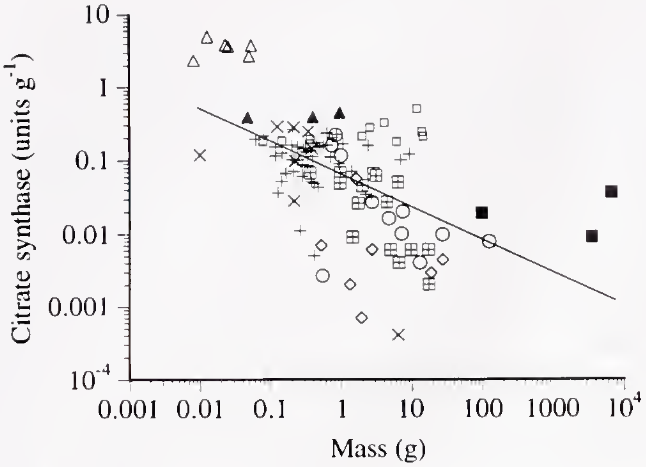

Figure 2. Citrate synthase activity as a function of wet weight for California medusae. The slope of the regression line is $y = 0.066x^{-0.44}$; $R = 0.67$. Symbols for medusae are given in Figure 1, and also include *Polyorchis penicillatus* (☐) and other scyphomedusae (■).

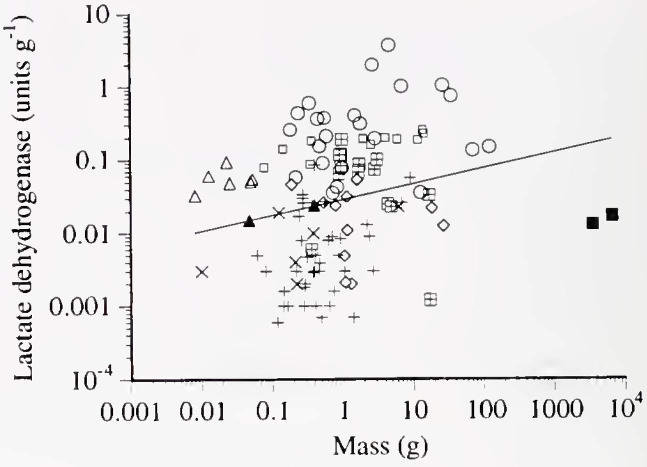

Figure 3. Lactate dehydrogenase activity as a function of wet weight for California medusae. Symbols for medusae are given in Figures 1 and 2. The slope of the regression line is $y = 0.027x^{0.22}$; $R = 0.08$.

This investigation included one species of "benthic" medusa: *Vallentinia adherens*. In contrast to the pelagic lifestyle of most medusae, *V. adherens* lives attached to kelp fronds and is exposed to much movement and water turbulence as it maintains itself near shore. We interpret the high CS activities in *V. adherens* as an indication of a metabolically robust animal that is adapted to life in such a high-energy environment. Thus, we believe that the interspecific variability of enzyme activities in the medusae investigated in this study indicates different physiological adaptations to their environments. For example, *Pelagia colorata* and *Periphylla periphylla* have LDH activities in swimming muscle comparable to those of the skeletal muscle of some of the deeper-living teleost fish, and most likely are active swimmers. Some of the species that have very low metabolic potentials are probably sit-and-wait predators maintaining their position in the water column with only periodic contractions of the swimming bell. Laterally flattened, or disk-shaped, medusae have lower CS activities than dorsoventrally elongated medusae, indicating that more hydrodynamic forms have higher metabolic potentials (for example, compare the more streamlined Rhopalonematidae with the Halicreatidae in Table II).

Enzymes

Some invertebrates use one or more amino acids as the terminal acceptor in glycolysis (Hochachka and Somero,

Table III

Allometric scaling relationships of enzymatic activities of pelagic medusae from California

Group	Enzyme	Enzymatic activity g^{-1} wet weight (y) as a function of total body wet weight (M), $y = aM^b$		
		a	b (±95% C.I., n)	$P<$
All medusae	CS	0.064	−0.43 (0.13, 102)	0.001
	LDH	0.027	0.22 (0.17, 112)	0.02
	MDH	0.434	−0.51 (0.39, 22)	0.02
All hydrozoans	CS	0.054	−0.37 (0.19, 82)	0.001
	LDH	0.015	0.45 (0.24, 81)	0.001
Rhopalonematidae	LDH	0.006	0.40 (0.37, 38)	0.04
Crossota alba	CS	0.236	0.47 (0.36, 6)	0.03
Polyorchis penicillatus	CS	0.213	0.10 (0.09*, 11)	0.08
	LDH	0.149	0.16 (0.09, 11)	0.01

Only regressions with slopes significantly different from zero are presented.
* 90% confidence interval.

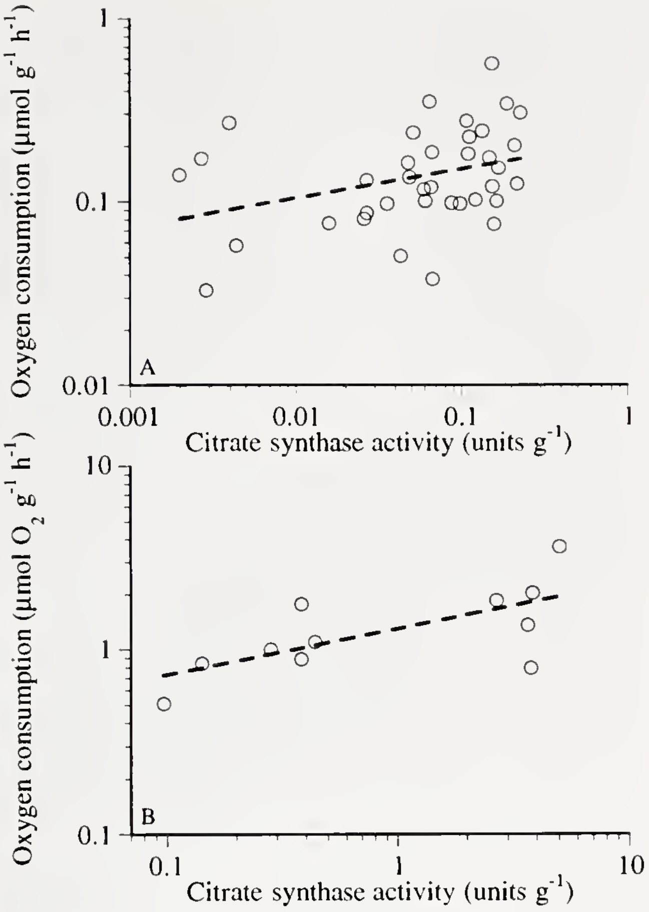

Figure 4. Relationships between citrate synthase activities and oxygen consumption rates measured at 5°C (A) and 15°C (B). The slope of the regression line for the 5°C data is $y = 0.216x^{0.16}$; $R = 0.31$. The slope of the regression line for the 15°C data is $y = 1.291x^{0.25}$; $R = 0.63$.

1984; Livingstone, 1991); these include some Cnidaria such as sea anemones (Walsh, 1981; Ellington; 1982). Although the biochemistry of glycolysis has been elaborated in several anthozoans (Livingstone, 1991; Shick, 1991), there are no previous reports on the enzyme biochemistry of scyphomedusae and hydromedusae. Our failure to detect octopine dehydrogenase, alanopine dehydrogenase, and strombine dehydrogenase in several species of scyphomedusae and hydromedusae suggests that these enzymes are either not present or not important in glycolysis in these cnidarians. The lactate levels we measured in *Periphylla periphylla* muscle (~1 µmol g^{-1}) are relatively high (*cf.* white muscle of rainbow trout at ~5 µmol g^{-1}; Milligan and Girard, 1993). Considering the low LDH activities of *Aegina citrea* compared with *P. periphylla* (Table II), it is not surprising that we were unable to detect lactate in *A. citrea*—the quantities of lactate in our *P. periphylla* samples were already in the lower range of accurate detectability. It is possible that some of the other medusae that we did not assay for -opine dehydrogenases do in fact have significant -opineDH activity. Furthermore, we have not assayed for the enzymes of other known anaerobic pathways or their endproducts (*e.g.*, succinate, propionate), and our limited data on cytosolic MDH do not allow us to assess its role in medusan anaerobic metabolism. Future studies on the evolution of glycolytic pathways in Cnidaria clearly should include specimens from the Scyphozoa, Hydrozoa, and Cubozoa.

The metabolic poise of most of the medusae studied seems to be aerobic, as CS activities were higher than corresponding LDH activities. The most notable exceptions are the meso- and bathypelagic coronate medusae. Several explanations are possible for the evolution of higher glycolytic potentials in these medusae. Coronates are apparently active predators (Larson, 1979) and may need an anaerobic energy supply during periods of active swimming in search of prey. Mills and Vogt (1984) found that epipelagic hydromedusae do not use ionic regulation as a buoyancy aid in vertical migrations. They proposed that these medusae must rely solely on swimming for diel vertical migrations. Although we did not find that the epipelagic hydromedusae in our study were anaerobically poised, they are likely using LDH for sustained bouts of swimming. Coronate medusae are also vertical migrators (Alvariño, 1967), and they may need an anaerobic energy supply if they are constantly swimming during periods of ascent and descent through the water column. Furthermore, as these organisms move through the water column, they spend considerable time in water of low oxygen concentration, the oxygen minimum layer (Wyrtki, 1962,

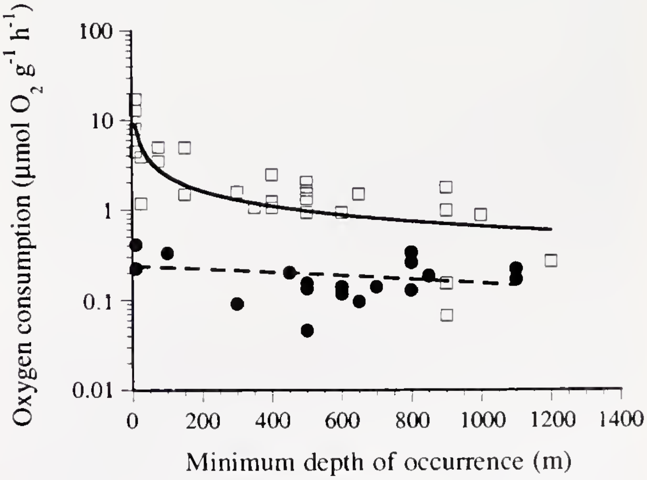

Figure 5. Metabolic rates of California medusae (●) as a function of minimum depth of occurrence (Table I) compared to pelagic crustacean data (□) from the same region. The slope of the regression line for medusan data is not significantly different from zero. The slope of the regression line for the crustacean data is $y = 32.819x^{-0.57}$; $R = 0.81$ (Childress, 1975). Results of ANCOVA show that the regressions of the two groups are significantly different from one another, $P < 0.02$.

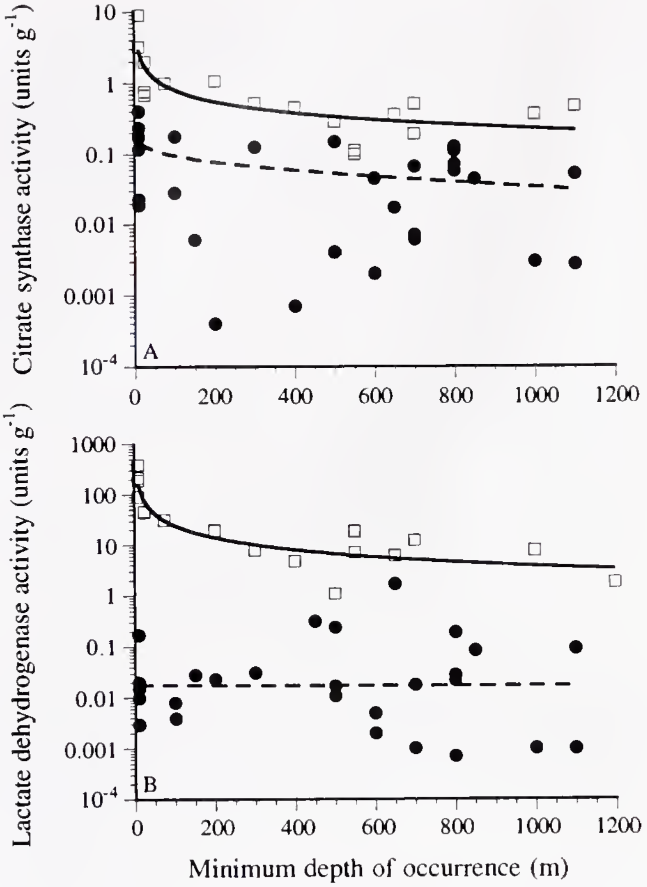

Figure 6. (A) Citrate synthase activities of California medusae (●) as a function of minimum depth of occurrence (Table II) compared to pelagic fish data (☐) from the same region. The slope of the regression line for medusan data is not significantly different from zero. The slope of the regression line for the fish data is $y = 10.355x^{-0.56}$; $R = 0.77$ (Childress and Somero, 1979; Wells and Childress, unpub.). Results of ANCOVA show that the regressions of the two groups are significantly different from one another, $P < 0.02$. (B) Lactate dehydrogenase activities of California medusae (●) as a function of minimum depth of occurrence (Table II) compared to pelagic fish data (☐) from the same region. The slope of the regression line for medusan data is not significantly different from zero. The slope of the regression line for the fish data is $y = 1000.5x^{-0.81}$; $R = 0.84$ (Childress and Somero, 1979). Results of ANCOVA show that the regressions of the two groups are significantly different from one another, $P < 0.01$.

1967). If they cannot supply their metabolic needs aerobically while in the oxygen minimum layer, they would need an anaerobic energy source for survival.

Comparison of our previous results on CS activity and oxygen consumption rate correlations in pelagic worms (Thuesen and Childress, 1993a, b) and fishes (Childress and Somero, 1979) with the present data on medusae shows that medusae have lower rates of oxygen consumption in relation to CS activities than do the other groups. That is, medusae have more CS relative to their oxygen consumption rates than do polychaetes, nemerteans, chaetognaths, and fishes. King and Packard (1975) found that the ratio of ETS activity to oxygen consumption was significantly higher in epipelagic hydrozoans than in the "non-medusoid zooplankton" they studied. Furthermore, the relation between oxygen consumption and CS activity in the medusae in the present study was not directly proportional, because increasing increments in CS are correlated with proportionately much smaller increases in oxygen consumption rates. The increase in CS activity is directly proportional to the increase in oxygen consumption rate in pelagic polychaetes and fishes (Thuesen and Childress, 1993b; Childress and Somero, 1979). Our data also show the following relationship in correlation coefficients: R (0.94) in pelagic polychaetes and nemerteans > R (0.58) in chaetognaths > R (0.31) in medusae. We propose that in animals such as medusae, which lack mechanisms for transport of oxygen within their bodies, the diffusion of oxygen may limit the effectiveness of oxygen supply to mitochondria while the inherent properties of the mitochondria and associated enzymes may remain the same as in other groups. Therefore, the mitochondrial aerobic metabolism realized *in vivo* would be limited by the supply of oxygen in these animals. The suggestion that the mitochondrial metabolism is limited by oxygen diffusion to the mitochondria is supported by our preliminary findings that these medusae generally show a dependent pattern of metabolism when exposed to lower oxygen concentrations. In such a situation, the synthesis of "excess" metabolic enzymes or mitochondria may be an important mechanism to maximize the use of the available oxygen.

The existence of oxygen-limited aerobic enzymes would account for the high ratios of CS or ETS activities to oxygen consumption rates and also partially explain the low correlation we found between medusan enzyme activities and oxygen consumption rates. A similar situation may exist in sea anemones (Shick, 1991). High-shore individuals of the intertidal anemone *Anthopleura elegantissima* have higher cytochrome *c* oxidase activities and greater numbers of mitochondria than low-shore individuals; however, the mass-specific oxygen consumption rates are lower in the high-shore individuals. Therefore, although enzyme activities measured at V_{max} may correlate well with oxygen consumption rates in animals such as crustaceans and fishes, which have evolved efficient oxygen uptake and transport systems, this method is evidently not a good one for predicting the metabolic rates of some gelatinous organisms.

This interpretation of our results does not agree with the physiological hypothesis of symmorphosis, which states that the structural designs of organisms are quantitatively matched to functional demands (Weibel *et al.*, 1991). The symmorphosis hypothesis predicts that the quantity and efficiency of aerobic enzymes should be matched with oxygen supply. Although enzyme activities and oxygen supply may be in balance in mammals, which have well-developed circulatory systems, oxygen diffusion and enzyme activities may not be in balance in medusae, which rely on direct diffusion from the environment to supply mitochondria with oxygen, if mitochondria at the periphery of diffusion distance are oxygen-limited.

Furthermore, different body tissues have different metabolic potentials and oxygen diffusion characteristics, and the contribution of muscle, gonads, mesoglea, *etc.*, to whole-organism respiration will be different, depending on the proportion of these tissues in each individual. In *Aurelia aurita*, different tissues can grow and degrow at different rates depending on animal size and nutritional state (Hamner and Jenssen, 1974). This implies that animals of identical body mass could have different proportions of metabolically active tissue, and could explain some of the variation observed in weight-specific metabolic relationships. For example, if mesoglea, a relatively metabolically inactive tissue, degrows first (de Beer and Huxley, 1924), the result would be an increase in mass-specific oxygen consumption with starvation. This could explain some of the variation observed in weight-specific metabolic relationships, as well as the observations, discussed earlier, made by Arai (1986) on the effects of starvation on the hydrozoan *Aequorea victoria*.

Scaling

Previous observations on the intraspecific metabolic scaling of gelatinous animals have found small or nonsignificant effects of size on oxygen consumption rate (*e.g.*, Kremer *et al.*, 1986; Larson, 1987b; Vernon, 1895). We have observed very little species-specific scaling, possibly because of variation in nutritional condition and tissue growth, as discussed above. However, it would appear that medusae do exhibit an overall trend toward lower specific metabolic rates in larger animals.

Our results also indicate that glycolytic potentials are elevated in larger medusae. This could indicate an increase in muscle mass relative to body mass or an increase in LDH activity per gram of muscle tissue. One study on the coastal scyphomedusa *Stomolophus meleagris* from the Gulf of Mexico has shown that in this species, unlike most other aquatic animals, transport costs do not continue to decline with size in larger animals, although they do decline with increasing body mass in smaller specimens (Larson, 1987a). This could result in larger medusae having elevated LDH activities to maintain their swimming performance. Another explanation may be that higher LDH activities in larger medusae are a consequence of greater oxygen diffusion distances, as discussed above for CS activities. Some fish show positive scaling of glycolytic enzymes, and this has been interpreted as an adaptation for size-independent acceleration used during predator-prey interactions (Childress and Somero, 1990; Somero and Childress, 1980, 1990). We do not think that this is the cause of the scaling pattern we observed, because medusae are poor accelerators. Larson (1987a) found little acceleration ability in *S. meleagris* and observed negative scaling of pulsation rate ($b = -0.12$). He concluded that medusae are cost-efficient swimmers because their proportionally small amounts of metabolically active tissue result in low energy usage. The general trends of negative scaling of aerobic metabolism and positive scaling of glycolytic potential with size may be common physiological phenomena in medusae.

Minimum depth of occurrence

No significant change in metabolic rates or metabolic potentials, as determined by enzymatic activities of the medusae, can be attributed to depth of occurrence. These results are in contrast to the patterns of metabolic rates seen in fishes and crustaceans, and they support the visual interactions hypothesis, because nonvisual animals would not be expected to show a metabolic decline with depth *per se* if the driving selective force behind the adaptation was the light regime of the environment. These results, along with the results of a previous study on chaetognaths (Thuesen and Childress, 1993a), confirm the differences between visually orienting and nonvisually orienting pelagic animals in their patterns of metabolic rate with increasing habitat depth.

According to the visual interactions hypothesis, reduced reliance on vision decreases selection for locomotory abilities; the locomotory ability of the bathypelagic mysid *Gnathophausia ingens* has been shown to be reduced compared to those of shallower-living crustaceans (Cowles and Childress, 1988). We predict that a comparison of morphologically similar medusae would not show lower locomotory abilities in bathypelagic species; many deeper-living species are in fact very robust. Investigations of benthic organisms do not show depth-related metabolic declines other than those that can be explained by the effects of temperature and size (Childress *et al.*, 1990a; Shirayama, 1992). These findings are in agreement with the visual interactions hypothesis, because little change in behavior with depth would be expected in animals that use the bottom substrate for concealment.

The other hypothesis that has been proposed to account for the widely observed decline in metabolic rates of pelagic animals—the food limitation hypothesis—suggests that animals living in a relatively food-poor environment have evolved lower metabolic rates as a way of conserving energy (Childress, 1971; Smith and Hessler, 1974). If food availability were a contributing factor in the evolution of metabolic rates, one could expect that the animals in regions of low productivity would have evolved lower metabolic rates than similar animals in highly productive environments. Contrary to this prediction, several studies have found pelagic crustaceans living in regions of different food availability to have similar metabolic rates (see review in Childress and Thuesen, 1992). Food limitation may be less of a problem for deep-living medusae, because potential prey organisms are so energy rich in comparison to medusan predators (Thuesen and Childress, unpub. data).

Another obvious variable with increasing depth is the increase in hydrostatic pressure. In a separate study, we tested the effects of pressure on the metabolic rates of *Aegina citrea, Crossota rufobrunnea,* three species of Chaetognatha, and a mesopelagic polychaete worm, *Poeobius meseres* (Childress and Thuesen, 1993). We observed no significant differences in metabolic rates measured at 1 atm and 101 atm ($\approx$1000 m) in any of these animals. Most previous studies have also found that the metabolic rates of mesopelagic and bathypelagic organisms show little change due to hydrostatic pressure when measured within the range of their normal habitat pressures (Belman, 1978; Quetin and Childress, 1976; Smith and Teal, 1973; Teal and Carey, 1967; Torres and Childress, 1983).

The high values of Q_{10} for oxygen consumption rate that we measured could have been influenced by increased activity at higher temperature. Although Mangum *et al.* (1972) observed similarly high Q_{10} values of oxygen consumption rates and bell pulsation rates for nonacclimated polyps of *Aurelia aurita* and *Chrysaora quinquecirrha,* they observed lower values of Q_{10} in medusae of *Cyanea capillata* acclimated for 3 days at each temperature. Vertically migrating medusae such *Colobenema sericeum* and *Periphylla periphylla* (estimated Q_{10} values of 4.8 and 2.6, respectively, in our study) could be expected to experience rapid changes in temperature on a regular basis, and our Q_{10} data indicate that they are not insensitive to such temperature changes or that their activity is stimulated by increased temperature. Therefore, the only physical parameters expected to contribute to differences in the metabolic rates of nonvisually orienting pelagic animals are those due to differences in water temperatures and oxygen concentrations.

Although deep-living gelatinous organisms are able to exploit the energy resources of lipid-rich vertically migrating crustaceans and have evolved life histories and energy-use strategies in response, their metabolic rates reflect no obvious selective pressure related to depth of occurrence. The absence of a depth-related decline in medusan metabolism means that the metabolic rates of deep-sea medusae approach those of deep-sea fishes and crustaceans, and therefore, medusae play a more important role than previously expected in the carbon flux of mesopelagic and bathypelagic environments.

Acknowledgments

We give our sincere thanks to K. L. Smith for inviting us to participate on research cruises off Point Conception (NSF grant OCE-8922620) and to A. L. Alldredge, A. N. Kuris, J. M. Shick, and G. N. Somero for constructive comments on the manuscript. We are grateful to B. H. Robison of MBARI and the captains, crews, and scientists aboard the research vessels *New Horizon, Point Sur,* and *Point Lobos* with the ROV *Ventana* for their assistance at sea. We thank C. E. Mills and S. H. D. Haddock for informative discussion concerning mesopelagic medusae, and R. E. Kochevar, J. F. Moeller, D. R. Oros and M. E. Wells for their assistance at sea, in the laboratory, or both. S. Anderson, J. McCullagh, and S. H. D. Haddock helped supply nearshore medusae. Research was supported by NSF grants OCE-8500237 and OCE-9115551 to J. J. Childress, and by a California Sea Grant Fellowship to E. V. Thuesen through NOAA, National Sea Grant College Program, Department of Commerce, under grant number NA89AA-D-SG138, project number USDC EG-10-8B, through the California Sea Grant College, and in part by the California State Resources Agency. The United States Government is authorized to reproduce and distribute this paper for governmental purposes.

Literature Cited

Alldredge, A. L. 1984. The quantitative significance of gelatinous zooplankton as pelagic consumers. Pp. 407–433 in *Flows of Energy and Materials in Marine Ecosystems.* M. J. R. Fasham, ed. Plenum, New York.

Alvariño, A. 1967. Bathymetric distribution of Chaetognatha, Siphonophorae, Medusae, and Ctenophorae off San Diego, California. *Pac. Sci* **21:** 474–485.

Arai, M. N. 1986. Oxygen consumption of fed and starved *Aequorea victoria* (Murbach and Shearer, 1902) (Hydromedusae). *Physiol. Zool.* **59:** 188–193.

Bailey, T. G., and B. H. Robison. 1986. Food availability as a selective factor on the chemical composition of midwater fishes in the eastern North Pacific. *Mar. Biol.* **91:** 131–141.

Båmstedt, U. 1980. ETS activity as an estimator of respiratory rate of zooplankton populations, the significance of variations in environmental factors. *J. Exp. Mar. Biol. Ecol.* **42:** 267–283.

Belman, B. 1978. Respiration and the effects of pressure on the mesopelagic vertically migrating squid *Histioteuthis heteropsis. Limnol. Oceanogr.* **23:** 735–739.

Biggs, D. C. 1977. Respiration and ammonium excretion by open ocean gelatinous zooplankton. *Limnol. Oceanogr.* **22:** 108–117.

Childress, J. J. 1971. Respiratory rate and depth of occurrence of midwater animals. *Limnol. Oceanogr.* **16:** 104–106.

Childress, J. J. 1975. The respiratory rates of midwater crustaceans as a function of depth occurrence and relation to the oxygen minimum layer off Southern California. *Comp. Biochem. Physiol.* **50A:** 787–799.

Childress, J. J. 1977. Physiological approaches to the biology of midwater crustaceans. Pp. 301–324 in *Oceanic Sound Scattering*

Prediction. N. R. Andersen and B. J. Zahuranec, eds. Plenum Press, New York.

Childress, J. J., and T. J. Mickel. 1980. A motion compensated shipboard precision balance system. *Deep-Sea Res.* **27A:** 965–970.

Childress, J. J., and T. J. Mickel. 1985. Metabolic rates of animals from the hydrothermal vents and other deep-sea habitats. *Bull. Biol. Soc. Wash.* **6:** 249–260.

Childress, J. J., and M. H. Nygaard. 1973. The chemical composition of midwater fishes as a function of depth of occurrence off Southern California. *Deep-Sea Res.* **20:** 1093–1109.

Childress, J. J., and M. H. Nygaard. 1974. The chemical composition and relative buoyancy of midwater crustaceans as a function of depth off Southern California. *Mar. Biol.* **27:** 225–238.

Childress, J. J., and G. N. Somero. 1979. Depth related enzymic activities in muscle, brain and heart of deep-living pelagic marine teleosts. *Mar. Biol.* **52:** 273–283.

Childress, J. J., and G. N. Somero. 1990. Metabolic scaling: a new perspective based on scaling of glycolytic enzyme activities. *Am. Zool.* **30:** 161–173.

Childress, J. J., and E. V. Thuesen. 1992. Metabolic potential of deep-sea animals: regional and global scales. Pp. 217–236 in *Deep-Sea Food Chains and the Global Carbon Cycle.* G. Rowe and V. Pariente, eds. Kluwer Academic Publishers, Dordrecht, The Netherlands.

Childress, J. J., and E. V. Thuesen. 1993. Effects of hydrostatic pressure on the metabolic rates of six species of deep-sea gelatinous zooplankton. *Limnol. Oceanogr.* **38:** 665–670.

Childress, J. J., A. T. Barnes, L. B. Quetin, and B. H. Robison. 1978. Thermally protecting cod ends for recovery of living deep-sea animals. *Deep-Sea Res.* **25:** 419–422.

Childress, J. J., S. M. Taylor, G. M. Cailliet, and M. H. Price. 1980. Patterns of growth, energy utilization and reproduction in some meso- and bathypelagic fishes off Southern California. *Mar. Biol.* **61:** 27–40.

Childress, J. J., A. J. Arp, and C. R. Fisher Jr. 1984. Metabolic and blood characteristics of the hydrothermal vent tube worm. *Riftia pachyptila. Mar. Biol.* **83:** 109–124.

Childress, J. J., D. L. Gluck, R. S. Carney, and M. M. Gowing. 1989. Biomass distribution and oxygen consumption in a deep-sea benthic boundary layer dominated by gelatinous organisms. *Limnol. Oceanog.* **34:** 915–932.

Childress, J. J., D. L. Cowles, J. A. Favuzzi, and T. J. Mickel. 1990a. Metabolic rates of benthic deep-sea decapod crustaceans decline with increasing depth primarily due to the decline in temperature. *Deep-Sea Res.* **37:** 929–949.

Childress, J. J., M. H. Price, J. A. Favuzzi, and D. L. Cowles. 1990b. The chemical composition of midwater fishes as a function of depth of occurrence off the Hawaiian Islands: food availability as a selective factor? *Mar. Biol.* **105:** 235–246.

Clarke, M. E., and P. J. Walsh. 1993. Effect of nutritional status on citrate synthase activity in *Acartia tonsa* and *Temora longicornis. Limnol. Oceanogr.* **38:** 414–418.

Clarke, M. E., C. Calvi, M. Domeier, M. Edmonds, and P. J. Walsh. 1992. Effects of nutrition and temperature on metabolic enzyme activities in larval and juvenile red drum, *Sciaenops ocellatus,* and lane snapper, *Lutjanus synagris. Mar. Biol.* **112:** 31–36.

Cowles, D. L., and J. J. Childress. 1988. Swimming speed and oxygen consumption in the bathypelagic mysid *Gnathophausia ingens. Biol. Bull.* **175:** 111–121.

Cowles, D. L., J. J. Childress, and M. E. Wells. 1991. Metabolic rates of midwater crustaceans as a function of depth of occurrence off the Hawaiian Islands: food availability as a selective factor? *Mar. Biol.* **110:** 75–83.

de Beer, G. R., and J. S. Huxley. 1924. Studies in dedifferentiation. V. Dedifferentiation and reduction in *Aurelia. Quart. J. Microscop. Sci.* **68:** 471–479.

Ellington, W. R. 1982. Metabolic responses of the sea anemone *Bunodosoma cavernata* (Bosc) to declining oxygen tensions and anoxia. *Physiol. Zool.* **55:** 240–249.

Hamner, W. M., and R. M. Jenssen. 1974. Growth, degrowth, and irreversible cell differentiation in *Aurelia aurita. Am. Zool.* **14:** 833–849.

Hochachka, P. W., and G. N. Somero. 1984. *Biochemical Adaptation.* Princeton University Press, Princeton, 537 pp.

Ikeda, T. 1988. Metabolism and chemical composition of crustaceans from the Antarctic mesopelagic zone. *Deep-Sea Res.* **35:** 1991–2002.

King, F. D., and T. T. Packard. 1975. Respiration and the activity of the respiratory electron transport system in marine zooplankton. *Limnol. Oceanogr.* **20:** 849–854.

Kramp, P. L. 1968. The hydromedusae of the Pacific and Indian Oceans. *"Dana"-Rep.* No. **72:** 1–200.

Kremer, P., M. P. Canino, and R. W. Gilmer. 1986. Metabolism of epipelagic tropical ctenophores. *Mar. Biol.* **90:** 403–412.

Larson, R. J. 1979. Feeding in coronate medusae (Class Scyphozoa. Order Coronatae). *Mar. Behav. Physiol.* **6:** 123–129.

Larson, R. J. 1987a. Costs of transport for the scyphomedusa *Stomolophus meleagris* L. Agassiz. *Can. J. Zool.* **65:** 2690–2695.

Larson, R. J. 1987b. Respiration and carbon turnover rates of medusae from the NE Pacific. *Comp. Biochem. Physiol.* **87A:** 93–100.

Livingstone, D. R. 1991. Origins and evolution of pathways of anaerobic metabolism in the animal kingdom. *Am. Zool.* **31:** 522–534.

Longhurst, A. R. 1985. The structure and evolution of plankton communities. *Prog. Oceanog.* **15:** 1–35.

Lowery, M. S., S. J. Roberts, and G. N. Somero. 1987. Effects of starvation on the activities and localization of glycolytic enzymes in the white muscle of the barred sand bass *Paralabrax nebulifer. Physiol. Zool.* **60:** 538–547.

Mangum, C. P., M. J. Oakes, and J. M. Shick. 1972. Rate-temperature responses in scyphozoan medusae and polyps. *Mar. Biol.* **15:** 298–303.

Mayzaud, P. 1986. Enzymatic measurements of metabolic processes concerned with respiration and ammonia excretion. Pp. 226–259 in *The Biological Chemistry of Copepods.* E. D. S. Corner and S. C. M. O'Hara, eds. Oxford University Press, Oxford.

Mickel, T. J., L. B. Quetin, and J. J. Childress. 1983. Construction of a polarographic oxygen sensor in the laboratory. Pp. 81–89 in *Polarographic Oxygen Sensors.* E. Gnaiger and H. Forstner, eds. Springer-Verlag, Berlin.

Milligan, C. L., and S. S. Girard. 1993. Lactate metabolism in rainbow trout. *J. Exp. Biol.* **180:** 175–193.

Mills, C. E., and R. G. Vogt. 1984. Evidence that ion regulation in hydromedusae and ctenophores does not facilitate vertical migration. *Biol. Bull.* **166:** 216–227.

Packard, T. T. 1979. Respiration and respiratory electron transport activity in plankton from the Northwest African upwelling area. *J. Mar. Res.* **37:** 711–742.

Packard, T. T., A. H. Devol, and F. D. King. 1975. The effect of temperature on the respiratory electron transport system in marine plankton. *Deep-Sea Res.* **22:** 237–249.

Packard, T. T., M. Denis, M. Rodier, and P. Garfield. 1988. Deep-ocean metabolic CO_2 production: calculation from ETS activity. *Deep-Sea Res.* **35:** 371–382.

Quetin, L. B., and J. J. Childress. 1976. Respiratory adaptations of *Pleuroncodes planipes* Stimpson to its environment off Baja California. *Mar. Biol.* **38:** 327–334.

Quetin, L. B., R. M. Ross, and K. Uchio. 1980. Metabolic characteristics of midwater zooplankton. Ammonia excretion, O:N ratio and the effect of starvation. *Mar. Biol.* **59:** 201–209.

Roche-Mayzaud, O., P. Mayzaud, and D. C. Biggs. 1991. Medium-term acclimation of feeding and of digestive and metabolic enzyme activity in the neritic copepod *Acartia clausi.* I. Evidence from laboratory experiments. *Mar. Ecol Prog. Ser.* **69:** 25–40.

Russell, F. S. 1953. *The Medusae of the British Isles.* Cambridge University Press. Cambridge. 530 pp.

Russell, F. S. 1970. *The Medusae of the British Isles. II Pelagic Scyphozoa with a Supplement to the First Volume on Hydromedusae.* Cambridge University Press, Cambridge. 284 pp.

Schmidt-Nielsen, K. 1983. *Animal Physiology: Adaptation and Environment.* Cambridge University Press, Cambridge. 619 pp.

Shick, J. M. 1991. *A Functional Biology of Sea Anemones.* Chapman & Hall, London. 369 pp.

Shirayama, Y. 1992. Respiration rates of bathyal meiobenthos collected using a deep-sea submersible *SHINKAI 2000. Deep-Sea Res.* **39:** 781–788.

Siebenaller, J. F., and P. H. Yancey. 1984. Protein composition of white skeletal muscle from mesopelagic fishes having different water and protein contents. *Mar. Biol.* **78:** 129–137.

Smith, K. L., Jr. 1982. Zooplankton of a benthic boundary layer: *in situ* rates of oxygen consumption and ammonium excretion. *Limnol. Oceanogr.* **27:** 461–471.

Smith, K. L., Jr., and R. R. Hessler. 1974. Respiration of benthopelagic fishes: *in situ* measurements at 1230 meters. *Science* **184:** 72–73.

Smith, K. L., Jr., and J. M. Teal. 1973. Temperature and pressure effects on respiration of thecosomatous pteropods. *Deep-Sea Res.* **20:** 853–858.

Somero, G. N., and J. J. Childress. 1980. A violation of the metabolism-size scaling paradigm: activities of glycolytic enzymes in muscle increase in larger-size fish. *Physiol. Zool.* **53:** 322–337.

Somero, G. N., and J. J. Childress. 1990. Scaling of ATP-supplying enzymes, myofibrillar proteins and buffering capacity in fish muscle: relationship to locomotory habit. *J. Exp. Biol.* **149:** 319–333.

Stickney, D. G., and J. J. Torres. 1989. Proximate composition and energy content of mesopelagic fishes from the eastern Gulf of Mexico. *Mar. Biol.* **103:** 13–24.

Sullivan, K. M., and G. N. Somero. 1980. Enzyme activities of fish skeletal muscle and brain as influenced by depth of occurrence and habits of feeding and locomotion. *Mar Biol.* **60:** 91–99.

Teal, J. M., and F. G. Carey. 1967. Effects of pressure and temperature on the respiration of euphausiids. *Deep-Sea Res.* **14:** 725–733.

Thuesen, E. V. 1993. *Vampyrocrossota childressi,* a new genus and species of black medusa from the bathypelagic zone off California (Cnidaria: Trachymedusae: Rhopalonematidae). *Proc. Biol. Soc. Wash.* **106:** 190–194.

Thuesen, E. V., and J. J. Childress. 1993a. Enzymatic activities and metabolic rates of pelagic chaetognaths: lack of depth-related declines. *Limnol. Oceanogr.* **38:** 935–948.

Thuesen, E. V., and J. J. Childress. 1993b. Metabolic rates, enzyme activities and chemical compositions of some deep-sea pelagic worms, particularly *Nectonemertes mirabilis* (Nemertea; Hoplonemertinea) and *Poeobius meseres* (Annelida; Polychaeta). *Deep-Sea Res.* **40:** 937–951.

Torres, J. J., and J. J. Childress. 1983. The relationship of oxygen consumption to swimming speed in *Euphausia pacifica* I. The effects of temperature and pressure. *Mar. Biol.* **74:** 79–86.

Torres, J. J., and G. N. Somero. 1988. Metabolism, enzymic activities and cold adaptation in Antarctic mesopelagic fishes. *Mar. Biol.* **98:** 169–180.

Torres, J. J., B. W. Belman, and J. J. Childress. 1979. Oxygen consumption rates of midwater fishes as a function of depth of occurrence. *Deep-Sea Res.* **26A:** 185–197.

Vernon, H. M. 1895. The respiratory exchange of the lower marine invertebrates. *J. Physiol. (London)* **19:** 18–70.

Walsh, P. W. 1981. Purification and characterization of two allozymic forms of octopine dehydrogenase from California populations of *Metridium senile. J. Comp. Physiol.* **143:** 213–222.

Weibel, E. R., C. R. Taylor, and H. Hoppeler. 1991. The concept of symmorphosis: a testable hypothesis of structure-function relationship. *Proc. Natl. Acad Sci. U.S.A.* **88:** 10357–10361.

Wyrtki, K. 1962. The oxygen minima in relation to ocean circulation. *Deep-Sea Res.* **9:** 11–23.

Wyrtki, K. 1967. Circulation and water masses in the eastern equatorial Pacific Ocean. *Int. J. Oceanol. Limnol.* **1:** 117–147.

Youngbluth, M. J., P. Kremer, T. G. Bailey, and C. A. Jacoby. 1988. Chemical composition, metabolic rates and feeding behavior of the midwater ctenophore *Bathocyroe fosteri. Mar. Biol.* **98:** 87–94.

Reference: *Biol. Bull.* **187:** 99–111. (August, 1994)

Protogynous Sex Change in the Intertidal Isopod *Gnorimosphaeroma oregonense* (Crustacea: Isopoda)

HEATHER J. BROOK[1], TIMOTHY A. RAWLINGS[2], AND RONALD W. DAVIES[1,*]

Bamfield Marine Station, Bamfield, British Columbia, Canada, V0R 1B0, and [1]Department of Biological Sciences, University of Calgary, Calgary, Alberta, Canada T2N 1N4, and [2]University of Alberta, Edmonton, Alberta, Canada T6G 2G9

Abstract. In Crustacea, the dominant pattern of sequential hermaphroditism is protandry (sex change from male to female). Here we provide the first evidence from external morphology and population structure that *Gnorimosphaeroma oregonense*, an abundant, sexually dimorphic intertidal isopod, undergoes protogynous (female to male) sex change. In the field, 31% of females had rudimentary penes, suggesting sex change, and laboratory growth experiments confirmed that females produced one brood of juveniles, then passed through a variable number of molts as immature males before becoming sexually mature males. Contrary to reports for other protogynous Crustacea, this study suggests that in *G. oregonense* sex change is not socially mediated, although it may be facultative, because a large percentage of laboratory-reared juvenile isopods developed directly into males. Potential adaptive explanations for protogyny are discussed in relation to protandry—the more common strategy in Crustacea.

Introduction

Although sex change occurs in only a small percentage of species, protandry (change from male to female) and protogyny (change from female to male) have been documented in a diverse assemblage of plant and animal taxa (Ghiselin, 1969; Policansky, 1982). However, either protandry or protogyny tends to predominate among closely related species. In the Crustacea, sex change is predominantly protandrous: 82% of the 60 sequentially hermaphroditic species listed in Table I undergo sex change from male to female. Protandry has been reported in the classes Cirripedia; Copepoda; and within the Malacostraca in nine families of Decapoda, two families of Amphipoda, and four families of Isopoda (Table I). Protogyny has been reported in five tanaidacean and four isopod species (Table I); thus both protandry and protogyny have likely developed independently several times in the Crustacea. Protandry can be advantageous when female fecundity increases with age or size but male mating success remains independent of size (Warner, 1975; Warner, 1988). Conversely, protogyny may arise when small males are prevented from mating with females by larger males, making it advantageous to become male only when a competitive larger size is reached (Warner, 1988).

The Isopoda is the only crustacean order in which both protandrous and protogynous species occur (Table I), giving the opportunity to compare closely related species exhibiting both forms of sequential hermaphroditism. In marine isopods, protogynous sex change appears, based on a limited number of species examined (Table I), to be restricted to free-living forms (Legrand and Juchalt, 1963; Burbanck and Burbanck, 1974; Buss and Iverson, 1981); whereas protandry occurs primarily within the parasitic suborders Epicarida and Flabellifera (Family Cymothoidae; Brusca, 1981).

In this study we examine sex change in the free-living marine isopod *Gnorimosphaeroma oregonense* Dana 1852, a common inhabitant of protected rocky intertidal shores ranging from Alaska to northern California (Hoestlandt, 1973). Although this species has been the subject of numerous physiological (Riegel, 1959a,b;

Received 31 July 1993; accepted 31 May 1994.

[*] Author to whom correspondence should be addressed: Dr. R. W. Davies, Department of Biological Sciences, University of Calgary, Calgary, Alberta, Canada T2N 1N4.

Table 1

Summary of the occurrence of protandrous and protogynous sex change within the Crustacea

Taxa[1]	Reference	Type of sex change Protandry	Protogyny
Class Malacostraca			
Subclass Eucarida			
O. Decapoda			
S.O. Pleocyemata			
I.O. Caridea			
Alpheidae			
Athanas kominatoenis	Suzuki, 1970	X	
Atyidae			
Paratya curvirostris	Carpenter, 1978	X	
Atya bisulcata	Carpenter, 1978	X	
A. serrata	Carpenter, 1978	X	
Caridina richtersi	Carpenter, 1978	X	
Axiidae			
Calocaris macandreae	Buchanan, 1963	X	
Campylonotidae			
Campylonotus rathbuni	Yaldwyn, 1966	X	
C. semistriatus	Yaldwyn, 1966	X	
C. capensis	Torti and Boschi, 1973	X	
C. vagans	Torti and Boschi, 1973	X	
Processidae			
Processa edulis	Nöel, 1973	X	
Hippolytidae			
Lysmata seticaudata	Dohrn, 1950	X	
L. nilita	Dohrn and Holthuis, 1950	X	
Chorismus antarcticus	Yaldwyn, 1966	X	
Hippolyte inermis	Veuille *et al.*, 1963	X	
Thor manningi	Bauer, 1986	X	
Pandalidae			
Pandalopsis dispar	Butler, 1964	X	
Pandalus borealis	Butler, 1964	X	
P. danae	Butler, 1964	X	
P. goniurus	Butler, 1964	X	
P. hypsinotus	Butler, 1964	X	
P. jordani	Butler, 1964	X	
P. montagui tridens	Butler, 1964	X	
P. stenolepis	Butler, 1964	X	
P. montagui	Allen, 1963	X	
P. kessleri	Aoto, 1952	X	
Crangonidae			
Argis dentata	Fréchette *et al.*, 1970	X	
Crangon crangon	Boddeke, 1968	X	
C. franciscorum	Gavio (pers. comm.)	X	
I.O. Anomura			
Hippidae			
Emerita analoga	Barnes and Wenner, 1968	X	
E. asiatica	Subramoniam, 1981	X	
S.O. Dendrobranchiata			
Solenoceridae			
Solenocera membranacea	Heergaard, 1967	X	
Subclass Peracarida			
O. Isopoda			
S.O. Anthuridea			
Anthuridae			
Cyanthura carinata	Legrand and Juchault, 1963		X
C. polita	Burbanck and Burbanck, 1974		X
C. profunda	Kensley, 1982		X

Table I. (*Continued*)

Taxa[1]	Reference	Type of sex change	
		Protandry	Protogyny
S.O. Flabellifera			
Sphaeromatidae			
Paraleptosphaeroma glynni	Buss and Iverson, 1981		X
Gnorimosphaeroma luteum	Brook (pers. obs.)		X
G. oregonense	Brook *et al.* (this paper)		X
Cymothoidae			
Emetha audouinii	Montalenti, 1941	X	
Anilocra physodes	Montalenti, 1941	X	
A. frontalis	Legrand and Juchault, 1970	X	
Philoscia elongata	Arcangeli, 1925	X	
Nerocila californica	Brusca, 1978	X	
S.O. Epicaridea			
Hemioniscidae			
Hemioniscus balani	Kozloff, 1987	X	
Liriopsidea			
Liriopsis pygmaea	Kozloff, 1987	X	
Cryptoniscidae	Charniaux-Cotton, 1960	X	
Bopyridae			
Munidion pleuroncodis	Markham, 1975	X	
S.O. Oniscoidea			
Oniscidea			
Rhyscotus ortonedae	Jackson, 1928	X	
O. Amphipoda			
S.O. Gammaridea			
Lysianassidae			
Acontiostoma marionis	Lowry and Stoddart, 1986	X	
A. tuberculata	Lowry and Stoddart, 1986	X	
Stomacontion pungapunga	Lowry and Stoddart, 1986	X	
Scolopostoma prionoplax	Lowry and Stoddart, 1986	X	
Ocosingo borlus	Lowry and Stoddart, 1986	X	
O. fenwicki	Lowry and Stoddart, 1986	X	
Stegocephalidae			
Stegocephalus inflatus	Steele, 1967	X	
O. Tanaidacea			
Heterotanais oerstedi	Bückle-Ramirez, 1965		X
Hageria rapax	Modlin and Harris, 1989		X
Leptochelia neapolitana	Ishimaru, 1984		X
L. dubia	Highsmith, 1983		X
L. forresti	Stoner, 1986		X
Class Copepoda			
O. Calanoida			
Calanidae	Fleminger, 1985	X	
Class Cirripedia			
O. Ascothoracica			
Synagoga sandersi	Newman, 1974	X	
Gorgonolaureus muzikae	Grygier, 1981	X	

[1] Taxonomy based on Kozloff (1987). O = order; S.O. = suborder; I.O. = infra-order.

Standing and Beatty, 1977), behavioral (Rees, 1975; Rawlings, 1994), and morphological studies (Hoestlandt, 1973, 1975), there are no records of its reproductive biology or mating system. To examine sex change in *G. oregonense*, we conducted a field census to determine the age and sexual structure of a population and whether social groupings occur. Mature females were raised in the laboratory to observe possible sex changes following hatching of a brood, and juvenile isopods were raised in the presence of adults of each sex to explore the potential for social mediation of sex determination.

Materials and Methods

Field survey

In September 1992, the population structure of *Gnorimosphaeroma oregonense* was examined in a low intertidal channel connecting the mainland to a small piece of land isolated at high tide in Grappler Inlet (48°49′ N, 125°07′ W), Bamfield, British Columbia, Canada. The substrata consisted of a dense covering of clam shells and barnacle- and mussel-covered rocks overlying a fine, silty mud (Rawlings, 1989). A transect was established parallel to the shoreline at a tidal height of 1.6 m above Canadian chart datum, and 10 quadrats (625 cm^2) were placed at 2-m intervals along the transect. All rocks and shells above the mud layer (approximately 7 cm deep) were collected from each quadrat, placed in plastic bags, and within 24 h washed with fresh water and sieved and sorted for isopods.

The isopods were immediately fixed in 70% ethanol and categorized to reproductive stage: juveniles (JUV), with no apparent sexual structures; receptive females, with small, nonfunctional oostegites and with (RFP) or without (RF) penes; mature females, with marsupium of large overlapping oostegites with or without embryos in the marsupium and with (MFP) or without (MF) penes; immature males (IM), with nonfunctional penes and lacking appendix masculina and ciliary tufts on the third and fourth pereopods; and mature males (MM), with functional penes and having appendix masculina and ciliary tufts upon the third and fourth pereopods. Individual body length (from the anterior tip of the cephalon to the posterior tip of the pleotelson) and, when present, penis length (base to the tip of the longest penis) were measured.

Examination of field aggregations. Preliminary field observations indicated that *G. oregonense* was often present in small aggregations arbitrarily defined as a group of more than five individuals within a 36-cm^2 quadrat, under rocks and in barnacle tests. In November 1992, a quadrat was placed over each of 10 aggregations; all the isopods were removed and immediately fixed in 70% ethanol for subsequent measurement and sexing in the laboratory.

Variation in female fecundity with body size. In November 1992, to examine the relationship between fecundity and body size, several randomly selected quadrats were collected (as in the field survey), brought to the laboratory, washed, and sorted for *G. oregonense.* The first 50 mature ovigerous females were fixed in 70% ethanol, measured (body length), and dissected to count brooded embryos.

Laboratory experiments

Culture of receptive and mature females. To monitor changes in external morphology before, during, and after brooding, 20 receptive females in precopula with mature males (guarded) and 20 mature females (not guarded) were collected in July 1992. Each guarded female was checked for the presence of small oostegites (*i.e.*, confirmed to be receptive) and thus represented the female morphology prior to brooding. Mature females were more developmentally advanced, with a functional marsupium containing embryos at various stages of development. Receptive females (with accompanying males) and mature females were cultured in mesh-paneled vials (35-ml vial, 2.5 cm in diameter, with a 4- × 5-cm window of 300-μm Nytex screen). Five vials, containing either receptive females (and accompanying males) or mature females, were randomly allocated to each of eight culture dishes (four replicates per female type) containing 200 ml of filtered (1 μm) seawater and were incubated at 17°C. Within a vial, each isopod was supplied *ad libitum* with the intertidal alga *Ulva fenestrata* for food. Seawater was changed at intervals of 3–4 days, at which time molts were collected and preserved in 5% formalin. When exuviae were observed, the body length of each isopod was measured, and any changes in external morphology were noted.

Sex ratio of developing juveniles. In October 1992, two simultaneous experiments were conducted to investigate the effect of the presence of mature males and mature females on the sexual development of juvenile *G. oregonense.* The effect of adult males was examined by adding either 0, 1, or 5 mature male isopods to a culture dish (500-ml dish containing 250 ml seawater) with 10 developing juveniles (five replicate dishes/treatment) at 17°C. To ensure that juvenile isopods were reproductively immature, only individuals with a body length of 3–4 mm and no external evidence of reproductive structures were used. The isopods were provided *ad libitum Ulva fenestrata* and clean clam shells for substratum. Seawater was changed every 3–4 days, at which time mortality was noted and, if necessary, mature males were replaced. To ensure that all surviving juveniles had the same length of exposure time to adults, dead juveniles were not replaced.

To examine the effect of mature females on the reproductive development of juveniles, the same procedures were followed, but the density of female rather than male *G. oregonense* was manipulated.

Scanning electron microscopy

To observe and compare reproductive structures of male and female *G. oregonense*, individuals were fixed for scanning electron microscopy. Specimens were anesthetized (in three parts seawater to one part carbonated water) and refrigerated at 4°C for 1 h. When relaxed, they were fixed in 2.5% glutaraldehyde for 2 h, washed for 30 min in distilled water, and postfixed in 1% osmium tetroxide for 1 h. After fixation, the specimens were dehydrated for 30 min at each dilution in an ethanol series (30%, 50%, 70%, 95%, and 100% ethanol in distilled water), critical-point dried in carbon dioxide (31°C, 1100 psi), sputter coated with gold for 10 min, and photographed using a Jeol JSM-35 scanning electron microscope.

Results

Field survey

Examination of field aggregations. Gnorimosphaeroma oregonense was patchily distributed among the shell debris and barnacle- and mussel-covered rocks in Grappler Inlet. In September 1992, densities varied from 80 to 13,136 individuals per square meter. Because two of the ten samples were extremely large ($n = 642$ and 821), eight samples were fully analyzed for population structure and the two large samples were subsampled by randomly mixing the isopods in 1 l of water and removing a fraction of the volume from the agitated solution (Wrona *et al.*, 1982). Of the 329 individuals examined, 78% were juveniles, 15% females (mature and receptive), and 7% males (Fig. 1). The operational sex ratio (mature males to receptive females) was 1:1.

Marked sexual dimorphism was evident among male and female *G. oregonense* (Fig. 1; Table II). Mean body length differed significantly among females and males (ANOVA; $F = 307.94$, $P < 0.0001$). Receptive females (RFP and RF) were significantly smaller than mature females, and mature females with penes (MFP) were not different in body length from mature females without penes (MF) (Table II). There was very little overlap in size range between mature females and mature males (Fig. 1).

Penes were present on all males, on 30% of mature females ($n = 80$), and on 11% of receptive females ($n = 38$) sampled in September 1992. All mature females ($n = 40$) collected in November 1992 had small penes. No other differences in body morphology were evident.

Penis length was related to sex and reproductive maturity. Mature females ($n = 35$) had penes that were significantly smaller (0.07 ± 0.005 mm) than penes of immature males ($n = 16$; 0.12 ± 0.015 mm) and mature males ($n = 48$; 0.45 ± 0.009 mm) (Kruskal-Wallis: $H = 75.17$, $P < 0.001$) (Figs. 2 and 3). Penis morphology also differed among reproductive stages. The penes of mature males were not only longer, but also had a pore or sphincter on the distal tip (Fig. 4) that was not present on penes of immature males or receptive and mature females.

Field aggregations of *G. oregonense* varied in number from 6 to 36 individuals and consisted primarily of juveniles and immature males (Fig. 5A). The presence of receptive and mature females was strongly correlated ($P < 0.001$) with the presence of mature males (Fig. 5B; $Y = 3.088X + 0.265$, $r^2 = 0.757$, $n = 10$, where Y is the number of mature males, and X is the number of receptive and mature females), suggesting that males and females were aggregating socially.

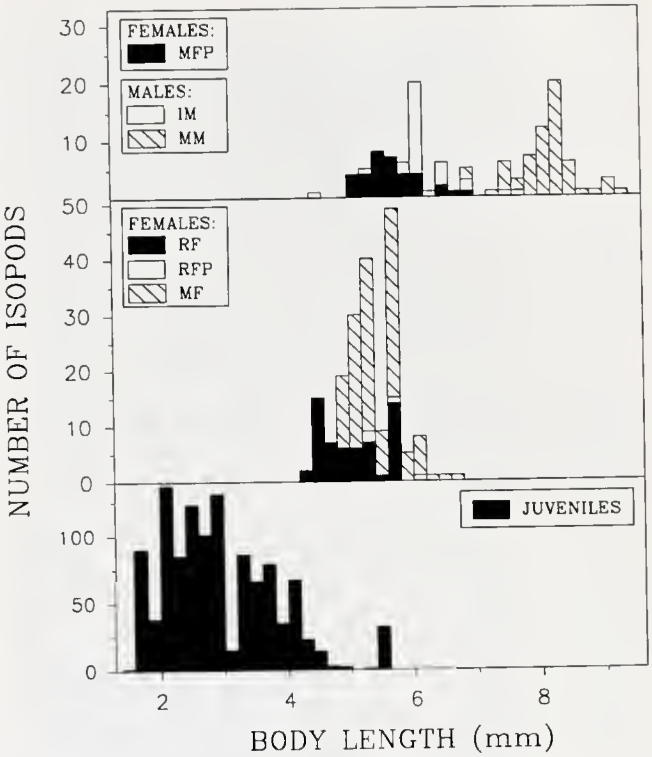

Figure 1. Size-frequency histogram of the body lengths of *Gnorimosphaeroma oregonense* collected from Grappler Inlet, September 1992. The population is classified into seven reproductive categories based on external morphology: juveniles (JUV)—no obvious sexual features; receptive females—small oostegites, no penes (RF) or with penes (RFP); mature females (MF)—large overlapping oostegites, no penes; mature females (MFP)—with penes; immature males (IM)—with penes, no oostegites; and mature males (MM)—penes, ciliary tufts on the third and fourth pereopods, and paired appendix masculina.

Variation in female fecundity with body size. Brood size in mature females varied from 13 to 42 and was associated with differences in female body size. Embryo number was positively correlated with female body length (Fig. 6; $Y = 17.69X - 66.90$, $r^2 = 0.67$, $n = 49$; where Y is the number of embryos, and X is the body length in millimeters).

Laboratory experiments (see below) showed no evidence of repeat brooding, indicating that *G. oregonense* broods only one clutch of embryos. Field collections provide corroborative evidence for a single brood, because there was no evidence of a bimodal frequency distribution of receptive or mature females suggestive of repeat brooding (Fig. 1).

Laboratory experiments

Culture of receptive females. Of the 20 females, 19 were securely guarded by mature males and had small ooste-

Table II

Differences in mean (±standard deviation) body length (mm) among reproductive stages of Gnorimosphaeroma oregonense *collected from Grapper Inlet, September 1992*

Sex/Stage	Sample size (*n*)	Body length[1]
Receptive females	37	4.98 ± 0.38^a
Mature females (no penes)	51	5.61 ± 0.42^b
Mature females (penes)	31	5.72 ± 0.44^b
Immature males	19	6.21 ± 0.72^c
Mature males	50	8.14 ± 0.45^d

[1] Body lengths of reproductive stages with the same superscript are not significantly different ($P > 0.05$) from one another (ANOVA, *a posteriori* Tukey test).

ANOVA: between sex/stage	df	MS	Error MS	*F*-ratio	*P*
	4	65.998	0.214	307.943	<0.0001

gites; the remaining female was mature and was removed from the experiment. Because only isopods with small oostegites occur in precopula, or are securely grasped by mature males, they were defined as receptive. Receptive females continued to be guarded by their males, female dorsum against the male venter, until the biphasic female reproductive molt was complete 1 to 13 days after collection. A biphasic molt was observed in all molts for juveniles, females, and males. The reproductive molt consisted of two phases, with the posterior portion of the female molting first, followed, within 24 h, by the anterior portion. Copulation was observed on one occasion following the first phase of the biphasic molt and was presumed to occur at this stage in all other pairs. Additionally, in all cases, mature males abandoned their females following the second half of the biphasic molt, suggesting that copulation had occurred.

The molt from the receptive to the mature female form was accompanied by an increase in body length and the formation of a functional marsupium (Fig. 7A, B). Most males (n = 16, 80%) died shortly (10–30 days) after copulation, and some female mortality occurred during brooding (n = 6, 31%) and later development (n = 4, 21%). Embryos became visible in the marsupium 1 to 3 days after completion of the anterior molt and developed at 17°C to hatchlings (mancas) in 8 to 10 weeks. No females molted during this brooding period (Fig. 7B). After the hatching of juveniles from the marsupium (days 100–120) (Fig. 7), all females molted to the immature male form, with the loss of oostegites and further development of penes. Females without penes already present (n = 2, 10%) developed them at this molt. Over the next 60 days (days 120–180), 90% of surviving females (n = 10) underwent a second molt, increasing in size but remaining in the immature male form. After 225 days, eight (42%) individuals molted to the mature male form with long penes, ciliary tufts on the third and fourth pereopods, and paired appendix masculina.

Culture of mature females. Brooding females demonstrated a pattern of morphological change similar to that of receptive females, although molting was less synchronous (Fig. 8A, B). During the first 90 days in the laboratory, all surviving brooding females (n = 17, 85%) released their broods, molted, and underwent a concomitant increase in size (Fig. 8B). These females usually molted within 3 to 4 weeks after juveniles hatched from the marsupium. Of these 17 females, 16 molted into immature males and 1 molted directly into a mature male. By day 70, two of the immature males also molted to the mature male form.

During the next 100 days in the laboratory, all surviving immature males molted a second time, but retained their immature male form (Fig. 8A, B). After 160 days, four of the surviving immature males (n = 13) molted to the mature male form (Fig. 8A, B), and two individuals (15% of survivors) molted for a third time as immature males, but died shortly thereafter. Consequently, after 200 days in the laboratory, seven of the surviving 14 brooding female isopods showed direct evidence of sex change.

There was considerable variation among females in the number of molts taken to become a mature male (Fig. 9). One mature female molted directly into a mature male, others took two or three molts (Fig. 8), and some remained

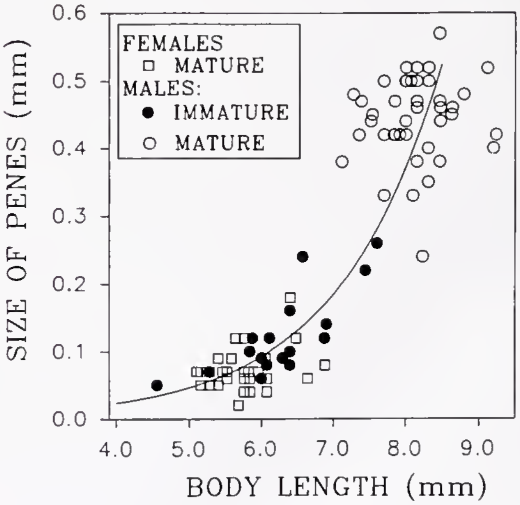

Figure 2. Relationship between penis length and body length for mature receptive and mature female (n = 33), immature male (n = 17), and mature male (n = 47) *Gnorimosphaeroma oregonense* collected from Grappler Inlet, September 1992. Penis length varied with body size according to the relationship $Y = 0.0014 \times 10^{0.301X}$, $r^2 = 0.82$.

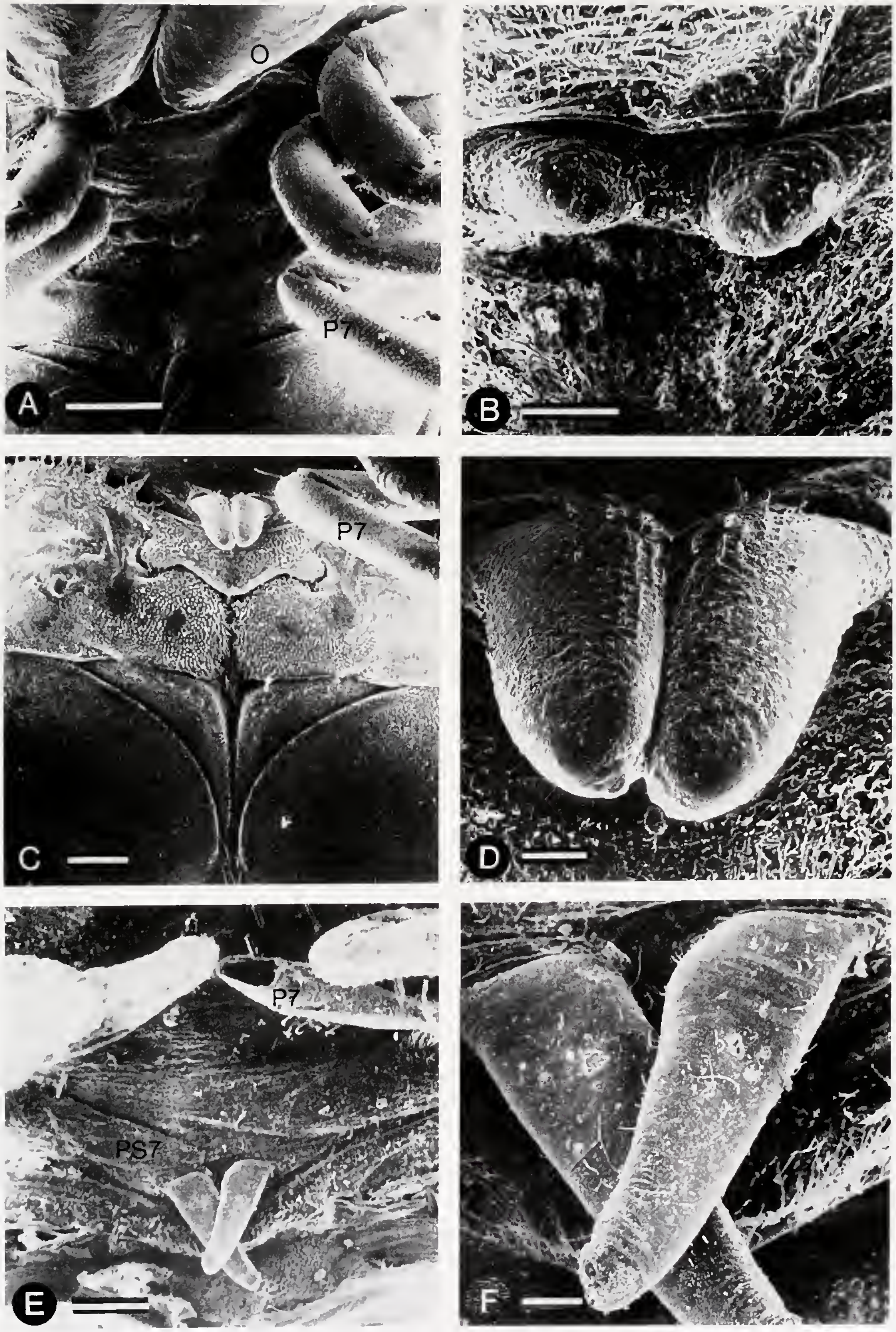

Figure 3. Scanning electron micrographs illustrating the development of penes on mature female (A, B), immature male (C, D), and mature male (E, F) *Gnorimosphaeroma oregonense*. For each reproductive stage, a low-magnification (A, C, E; scale bar = 0.30 mm) and high-magnification view (B, D, F; scale bar = 0.06 mm) of the paired penes are shown. Large oostegites and developing penes are shown in the mature female (A). O, oostegite arising from the 4th pereopod; P7, 7th pereopod; PS7, 7th pereonal segment.

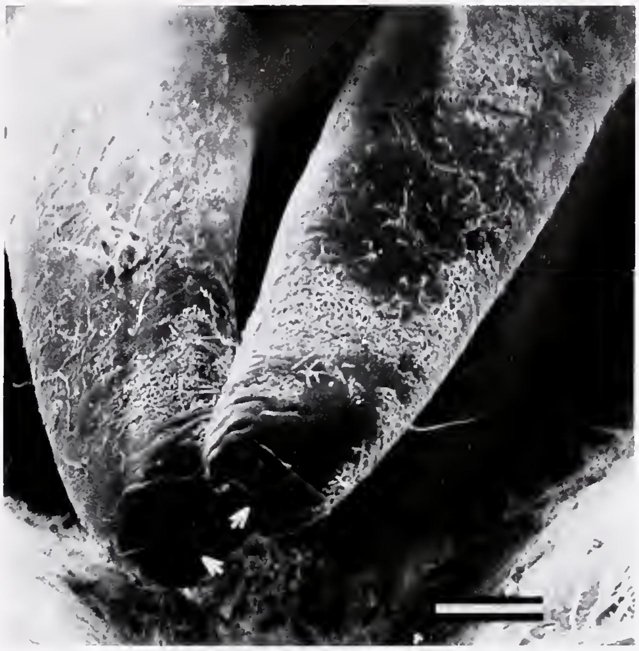

Figure 4. Scanning electron micrograph of the paired penes, with openings of the duct at the distal ends, of a mature male *Gnorimosphaeroma oregonense* (scale bar = 0.06 mm).

in the immature form after three molts. In the September 1992 field census, a few smaller males were present, similar in size to the one-molt mature males, suggesting that molt number varies in the field as well as in the laboratory. This variability was not associated with female size at brooding or with the precocial development of penes.

Sex ratio of developing juveniles. The sex ratio of developing juveniles was unaffected by the presence of mature male and mature female *G. oregonense* (Fig. 10). Due to the high mortality (50–51%) of juveniles over the course of the 52-day culture period in both experiments, replicates within a treatment were pooled for statistical analysis. The presence of adult males ($X_{0.05,4}{}^2 = 1.207$, $P > 0.80$) or brooding females ($X_{0.05,4}{}^2 = 1.590$, $P > 0.80$) had no significant effect on the sexual development of juveniles.

The results of these experiments showed that not all *G. oregonense* are protogynous. Although a large percentage of individuals could not be sexed at the end of the culture period, 63.3 ± 3.7% ($n = 126$) of juveniles developed into immature males, with penes and no oostegites. In contrast, only 8.2 ± 3.4% ($n = 16$) developed into receptive females. The remaining juveniles ($n = 57$) had not matured to a stage exhibiting external reproductive structures before the experiment was terminated. Immature males that were isolated and maintained in plastic vials after the end of the experiment continued to develop to the mature male form, and none became females.

Discussion

The results of this study provide direct evidence of protogynous sex change within the isopod *Gnorimosphaeroma oregonense*. Field surveys showed sexual size di-

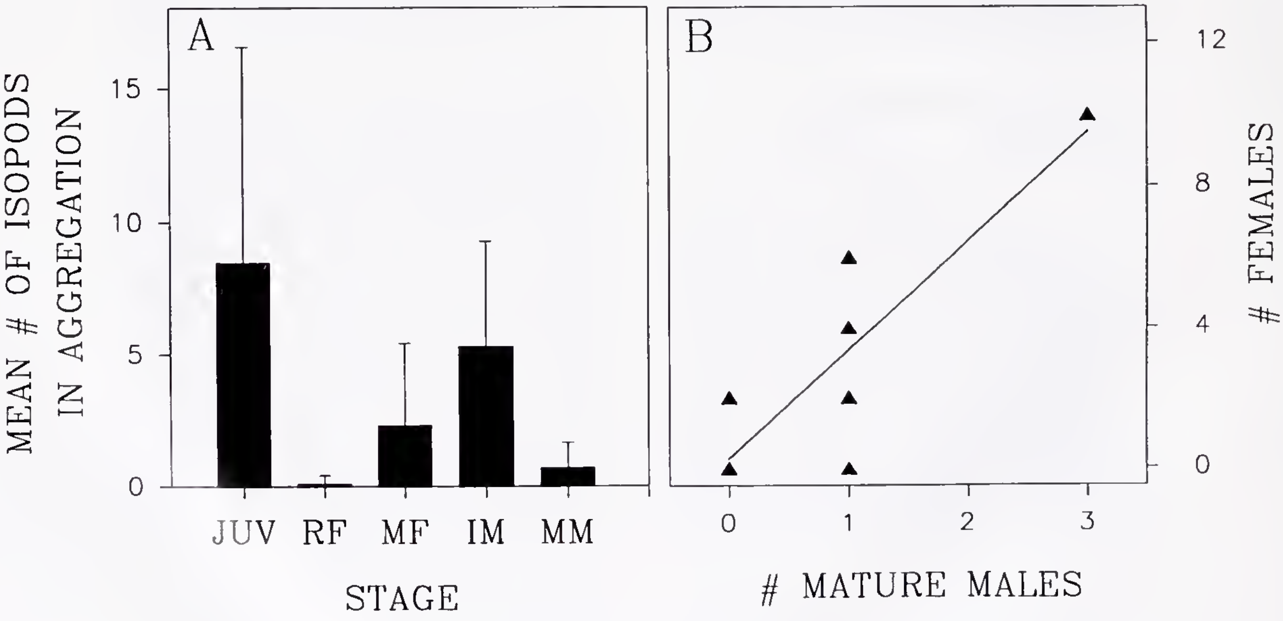

Figure 5. Number of individuals present in aggregations of *Gnorimosphaeroma oregonense* sampled from beneath rocks in Grappler Inlet, November 1992. (A) Mean number of isopods (+ standard deviation) of each stage in aggregations ($n = 10$); (B) relationship between the number of receptive and mature females (RF, RFP, MF, and MFP inclusive) and the number of mature males (MM) in aggregations ($Y = 3.088X + 0.265$; $r^2 = 0.75$, $n = 10$).

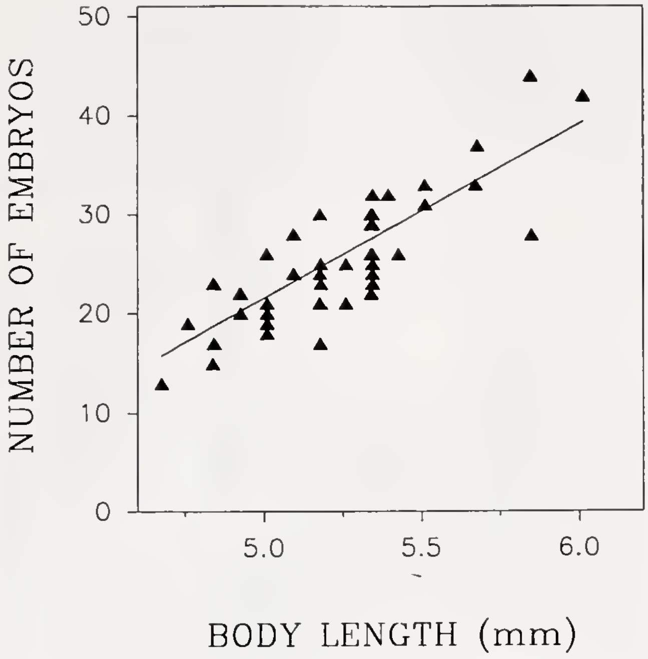

Figure 6. Fecundity of *Gnorimosphaeroma oregonense* collected from Grappler Inlet, November 1992 ($Y = 17.69X - 66.90$, $r^2 = 0.67$, $n = 49$). Females carrying embryos at all stages of development are included.

morphism, with males larger than females, and the presence of male and female characteristics within individual *G. oregonense.* Laboratory experiments showed that, following brood release, females either molt directly into mature males or pass through an immature male phase to become mature males, corroborating that *G. oregonense* is protogynous.

Selection favoring protogyny

Although a number of other crustaceans are reported to be protogynous (Table I), little is known about the reproductive biology and life-history characteristics associated with protogyny in this group. The isopod *Cyanthura carinata* and the tanaid *Hargeria rapax* are the only protogynous species in which the reproductive cycle and population dynamics have been thoroughly examined (Bamber, 1985; Modlin and Harris, 1989; Kneib, 1992). Within the tanaidaceans, protogyny appears to be associated with three life-history features: (1) low mobility of females, (2) low abundance of males due to high mortality, and (3) intense competition among males for access to females (Highsmith, 1983). Ghiselin (1969) proposed that sequential hermaphroditism will be favored by selection when the relative reproductive success of a male or female differs with size or age. Based on Ghiselin's size advantage model (1969), protogyny should be favored in species in which male reproductive success is dependent on large body size, increased experience, or female mate choice (Warner, 1975; Warner, 1988).

Precopulatory mate guarding in *G. oregonense* may be a primary selective force favoring protogyny. In many isopod species, males actively guard females in a precopulatory embrace (Wilson, 1991). Sexual dimorphism and precopula have been associated with protogyny in *G. oregonense, G. luteum* (Brook, personal observation), *Cyanthura carinata* (Bamber, 1985), and *Paraleptosphaeroma glynni* (Buss and Iverson, 1981). Active precopula has also been reported in gonochoristic species such as *Asellus aquaticus* (Manning, 1975, 1980), *A. meridianus* (Steel, 1961), *Jaera italica* and *J. nordmanni* (Veuille, 1980). Larger males may guard females or a resource more effectively or be able to remove a female from a smaller competitor, giving a higher reproductive success to larger males than to smaller ones (Ridley and Thompson, 1979; Ridley, 1983; Warner, 1988). Although the *G. oregonense* population sampled had more mature males than receptive females (Table II), all receptive fe-

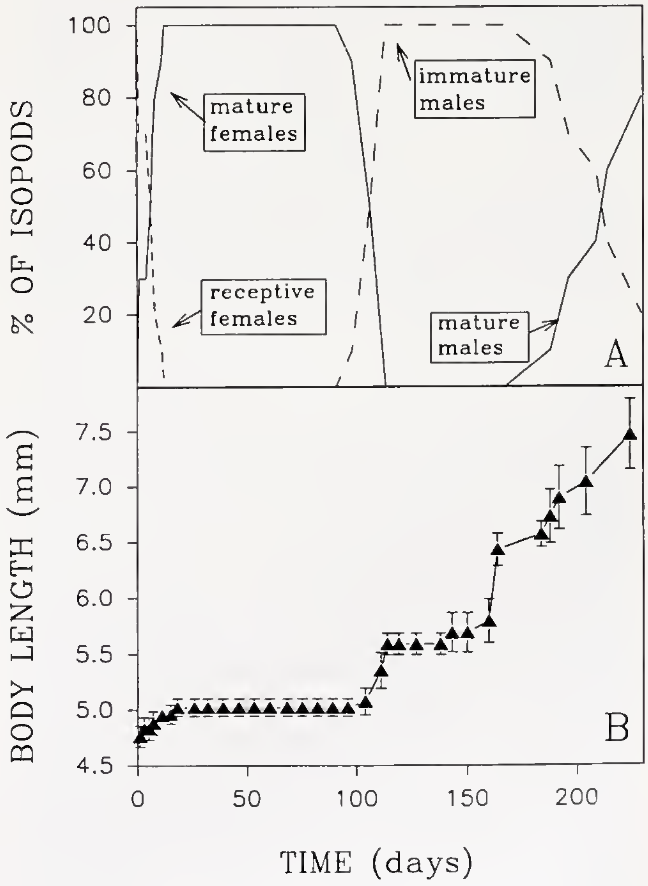

Figure 7. Changes in the external morphology of receptive female *Gnorimosphaeroma oregonense* that survived 225 days in the laboratory or that molted to the terminal mature male stage. (A) Percentage of isopods ($n = 10$) at each reproductive stage; (B) mean body length (±SE) of these individuals, for each observation interval.

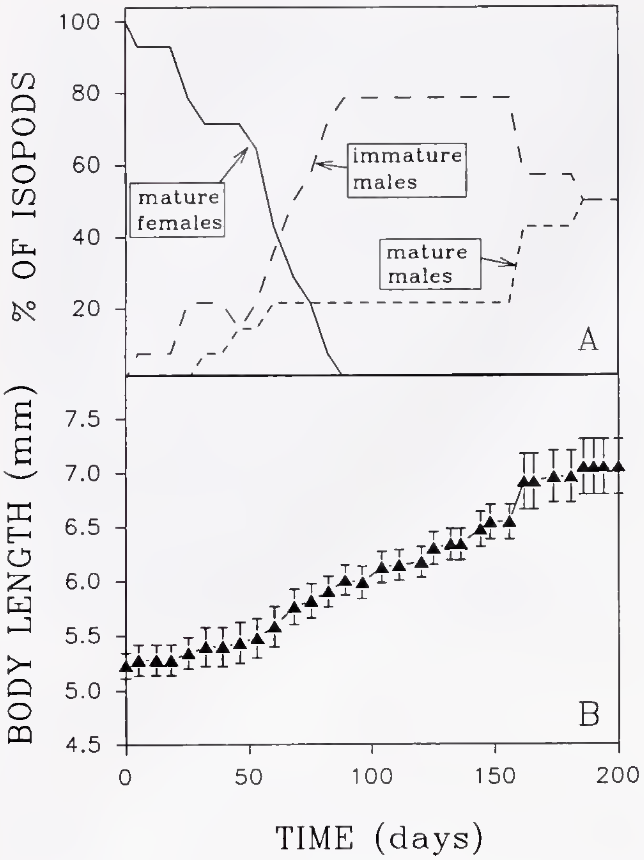

Figure 8. Changes in the external morphology of mature female *Gnorimosphaeroma oregonense* that survived 200 days in the laboratory or that molted to the terminal mature male stage. (A) Percentage of isopods ($n = 14$) at each reproductive stage; (B) mean body length (±SE) of these individuals, for each observation interval.

males are not necessarily nearing the reproductive molt. The operational sex ratio may thus be skewed towards males, further increasing male-male competition for females that are nearing the reproductive molt, as well as selection for larger male size.

Active precopulatory guarding has not been observed in protandrous isopods. Precopulatory behavior may involve the passive attachment of the dwarf male onto the larger female, as seen in the parasitic epicarids (Wilson, 1991). There is no evidence, however, that this excludes other males from mating with females in these species. In the protandrous hippolytid shrimp *Thor manningi* (Bauer, 1986), available evidence suggests that male reproductive success may be independent of size. Although larger males are more frequently paired with females in the partially protandrous shrimp *Athanas kominatoensis* (Nakashima, 1987), some small males do successfully mate with females. Female fecundity increases with body size, and thus a small male will increase its reproductive output. In both protandrous and protogynous crustaceans, female fecundity is usually positively correlated with body size (Charnov, 1979; Bauer, 1986; Nakashima, 1987; Bamber, 1985; Buss and Iverson, 1981; Kneib, 1992; this study). It appears, therefore, that the advantage gained by larger males in the protogynous crustacean mating system overrides the selective force of increased female fecundity with increased female body size.

Socially and environmentally mediated protogynous sex change

Protogynous sex change has been suggested to be socially mediated in the tanaids *Leptochelia dubia, Hargeria rapax,* and *Heterotanais oerstedi* and in the isopod *Paraleptosphaeroma glynni* (Highsmith, 1983; Modlin and Harris, 1989; Bückle-Ramirez, 1965, as cited in Gardiner, 1975; Buss and Iverson, 1981). In all these studies, protogynous sex change occurred (though not exclusively) when adult males were absent (Modlin and Harris, 1989). In our study, the presence of adult male and female *G. oregonense* had no significant effect on the sexual development of juveniles. Also, laboratory-cultured females changed sex to either the immature or mature male form, regardless of whether mature males were present. The absence of socially mediated sex change is less surprising if, as suspected, female *G. or-*

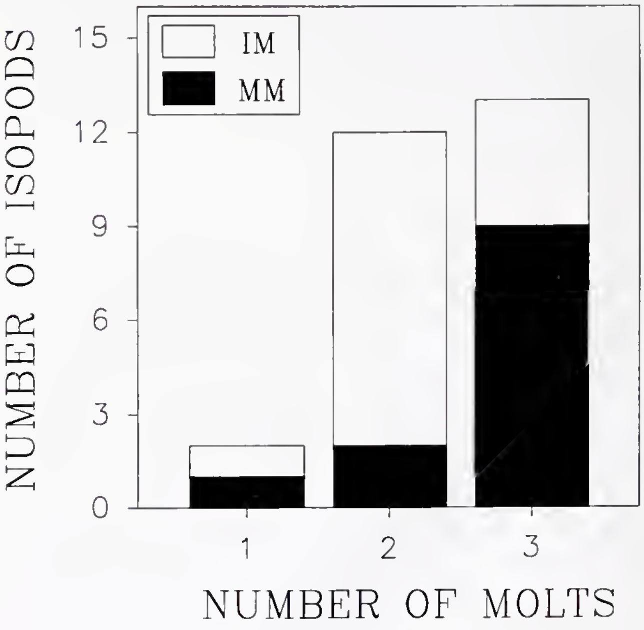

Figure 9. Number of molts required by mature female *Gnorimosphaeroma oregonense* to develop into mature males over 210 days in the laboratory. Solid bars refer to isopods that molted to the mature male (MM) condition over this time period. Hollow bars refer to individuals that underwent a variable number of molts as immature males (IM), but had not molted to the mature male form by the end of the experiment.

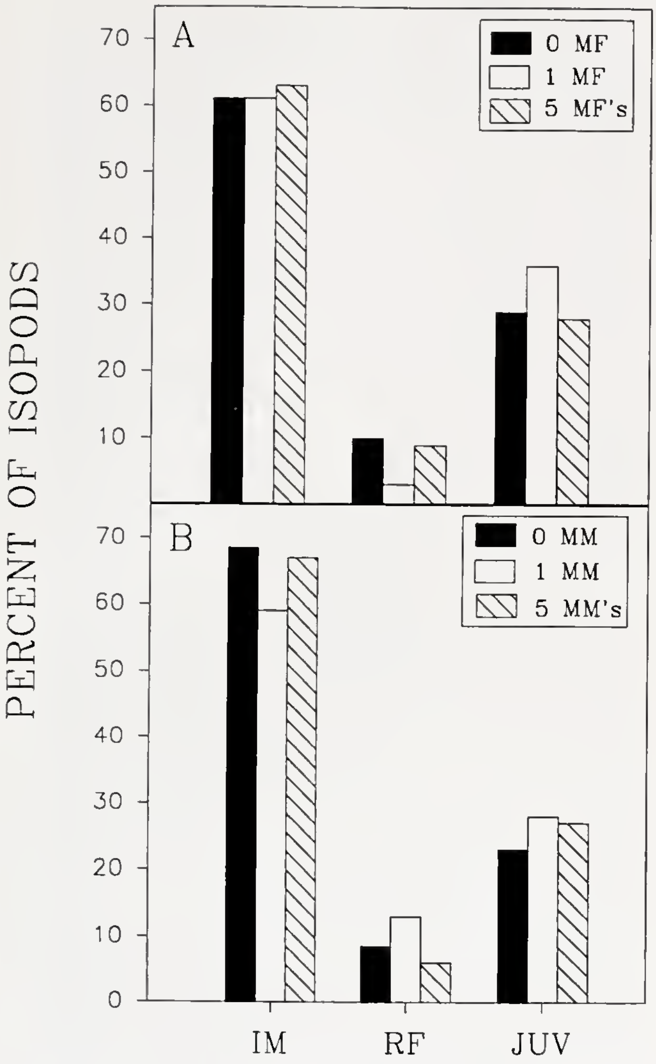

Figure 10. Percentage of juvenile isopods that developed into males or females or remained as juvenile *Gnorimosphaeroma oregonense*, after exposure to three different densities of (A) mature females (MF) (0, 1, or 5 females) or (B) mature males (MM) (0, 1, or 5 males) for 52 days. IM = immature males, RF = receptive females, JUV = juveniles.

egonense brood only one clutch of embryos. In that case, reproductive success could be increased only if a female changed sex to a male and contributed to the gene pool as both female and male. Because males may be able to inseminate multiple females in the time required for a female to brood a single clutch, sequential hermaphroditism is clearly potentially advantageous.

Unlike other protogynous isopod species, *G. oregonense* exhibited plasticity in the number of molts required for a female to undergo sex change. Buss and Iverson (1981) reported that the isopod *Paraleptosphaeroma glynni* could molt from a mature female to a mature male in one molt. The plasticity in *G. oregonense* may be adaptive—allowing an individual to optimize the timing of maturity, perhaps in response to the presence or absence of other adult males. Additionally, mature males are in their terminal molt and have a short life expectancy; therefore, plasticity of development may provide a means to optimize reproductive success. In the protandrous shrimp *Pandalus jordani*, individuals alter the age at which they change sex in response to year-to-year variations in population structure (Charnov, 1978).

Not all *G. oregonense* juveniles are protogynous: only a small percentage of juveniles developed into females in the laboratory. As in other protogynous crustaceans, some individuals first develop to breeding females and later change to reproducing males (termed secondary males); whereas others (termed primary males) remain as males, lacking any female characters, throughout their lives (Highsmith, 1983; Bamber, 1985; Stoner, 1986; this study). It appears that *Paraleptosphaeroma glynni* may be completely protogynous, because no small males were found in the field population (Buss and Iverson, 1981). In some species of protandrous caridean shrimp, all individuals undergo sex change. Other species show varying degrees of sex change, with some individuals changing sex and others remaining strictly female (primary females) throughout their lives (Bauer, 1986). The selective advantages associated with the difference between primary and secondary males or females have not been determined.

Although the sex of juveniles could possibly be determined very early in development, it is more likely to be controlled by environmental factors such as temperature or photoperiod or perhaps by the presence of immature males rather than adult females or males. Seasonal patterns in the occurrence of protogyny have been documented in the isopod *Cyanthura carinata* (Legrand and Juchault, 1963) and in the tanaid *Heterotanais oerstedi* (Bückle-Ramirez, 1965, as cited in Gardiner, 1975). The influence of environmental (epigenetic) factors such as temperature, photoperiod, and parasitism on the sex determination of Crustacea has been observed in isopods, amphipods, and copepods (Ginsberger-Vogel and Charniaux-Cotton, 1982; Juchault and Mocquard, 1989). Sex change has also been experimentally induced by androgenic gland grafting and removal in some malacostracans that are not hermaphroditic in nature (Charniaux-Cotton, 1975).

Although life-history theory predicts that protandry or protogyny should occur in many crustaceans (*e.g.*, many amphipods are sexually dimorphic and exhibit precopulatory guarding behavior; Ridley, 1983), protogynous sex change has not been reported. Perhaps the incurred costs of sex change in these and other gonochoristic crustacean species outweigh the benefits associated with increased reproductive output.

Acknowledgments

We thank Drs. L. D. Smith and D. Renfrew, D. Lello, K. Durante, L. Gosselin, and D. E. C. Smith for their helpful comments and suggestions in reviewing this manuscript; we also thank two anonymous reviewers for useful comments, suggestions, and criticisms. Dr. P.-Y. Qian provided technical assistance with specimen fixation, and Dr. C. L. Singla assisted with the scanning electron microscopy conducted at the University of Victoria. This research was supported by NSERC operating grants to R. W. Davies and A. R. Palmer.

Literature Cited

Allen, J. A. 1963. Observations on the biology of *Pandalus montagui* (Crustacea, Decapoda). *J. Mar. Biol. Assoc. U.K.* **43:** 665–682.

Aoto, T. 1952. Sexual phases in the prawn, *Pandalus kessleri* Czerniavski, with special reference to the reversal of sex. *J. Fac. Sci. Hokkaido Univ. Ser. VI, Zool.* **11:** 1–20.

Arcangeli, A. 1925. Ermafroditismo e partenogenesi negli ispodi terrestri. *Monogr. Zool. Ital.* **36:** 105–122.

Bamber, R. N. 1985. The autecology of *Cyanthura carinata* (Crustacea: Isopoda) in a cooling water discharge lagoon. *J. Mar. Biol. Assoc. U.K.* **65:** 181–194.

Barnes, N. B., and A. M. Wenner. 1968. Seasonal variation in the sand crab *Emerita analoga* (Decapoda, Hippidae) in the Santa Barbara area of California. *Limnol. Oceanogr.* **13:** 465–476.

Bauer, R. T. 1986. Sex change and life history pattern in the shrimp *Thor manningi* (Decapoda: Caridea): a novel case of partial protandric hermaphroditism. *Biol. Bull.* **170:** 11–31.

Boddeke, R. 1968. Sexual cycle and growth of the brown shrimp (*Crangon crangon* L.). *Neth. J. Zool.* **18:** 427 (Abstr.).

Brusca, R. C. 1978. Studies on the cymothoid fish symbionts of the eastern Pacific (Isopoda, Cymothoidae). I. Biology of *Nerocila californica*. *Crustaceana* **34:** 141–154.

Brusca, R. C. 1981. A monograph on the Isopoda Cymothoidae (Crustacea) of the eastern Pacific. *Zool. J. Linn. Soc.* **73:** 117–199.

Buchanan, J. B. 1963. The biology of *Calocaris macandreae* (Crustacea: Thalassinidea). *J. Mar. Biol. Assoc. U.K.* **43:** 729–748.

Bückle-Ramirez, L. F. 1965. Untershuchungen uber die Biologie von *Heterotanais oerstedi* Kröyer (Crustacea, Tanaidacea). *Z. Morphol. Oekol. Tiere* **55:** 714–782.

Burbanck, M. P., and W. D. Burbanck. 1974. Sex reversal of female *Cyanthura polita* (Stimpson, 1855) (Isopoda, Anthuridae). *Crustaceana* **26:** 110–112.

Buss, L. W., and E. W. Iverson. 1981. A new genus and species of Sphaeromatidae (Crustacea; Isopoda) with experiments and observations on its reproductive biology, interspecific interactions and color polymorphisms. *Postilla* **184:** 1–3.

Butler, T. H. 1964. Growth, reproduction and distribution of pandalid shrimps in British Columbia. *J. Fish. Res. Board Can.* **21:** 1403–1452.

Carpenter, A. 1978. Protandry in the freshwater shrimp, *Paratya curvirostris* (Heller, 1862) (Decapoda: Atyidae) with a review of the phenomenon and its significance in the Decapoda. *J. R. Soc. N. Z.* **3:** 343–358.

Charniaux-Cotton, H. 1960. Sex determination. Pp. 411–447 in *The Physiology of Crustacea*. Vol. 1, T. H. Waterman, ed. Academic Press, New York.

Charniaux-Cotton, H. 1975. Hermaphroditism and gynandromorphism in Malacostracan Crustacea. Pp. 91–105 in *Intersexuality in the Animal Kingdom*. R. Reinboth, ed. Springer-Verlag, Berlin.

Charnov, E. L. 1978. Sex ratio: adaptive response to population fluctuations in Pandalid shrimp. *Science* **200:** 204–206.

Charnov, E. L. 1979. Natural selection and sex change in Pandalid shrimp: test of a life-history theory. *Am. Nat.* **113:** 715–734.

Dohrn, P. F. R. 1950. Studi sulla *Lysmata seticaudata* Risso (Hippolytidae). *Pubbl. Stn. Zool. Napoli* **22:** 257–272.

Dohrn, P. F. R., and L. B. Holthuis. 1950. *Lysmata nilita*, a new species of prawn (Crustacea: Decapoda) from the western Mediterranean. *Pubbl. Stn. Zool. Napoli* **22:** 339–347.

Fleminger, A. 1985. Dimorphism and possible sex change in copepods of the family Calanidae. *Mar. Biol. (Berl.)* **88:** 273–294.

Fréchette, J., G. W. Corrivault, and R. Couture. 1970. Hermaphroditisme protérandrique chez une crevette de la famille des Cranoidés, *Argis dentata* Rathbun. *Nat. Can.* **97:** 805–822.

Gardiner, L. F. 1975. The systematics, postmarsupial development, and ecology of the deep-sea family Neotanaidae (Crustacea: Tanaidacea). *Smithson. Contrib. Zool.* **170:** 1–265.

Ghiselin, M. T. 1969. The evolution of hermaphroditism among animals. *Q. Rev. Biol.* **44:** 189–208.

Ginsberg-Vogel, T., and H. Charniaux-Cotton. 1982. Sex determination. Pp. 257–281 in *The Biology of Crustacea*, Vol. 2, D. E. Bliss, ed. Academic Press, New York.

Grygier, M. J. 1981. *Gorgonolaureus muzikae* sp. nov. (Crustacea: Ascothoracida) parasitic on a Hawaiian gorgonian, with special reference to its protandric hermaphroditism. *J. Nat. Hist.* **15:** 1019–1045.

Heergaard, P. 1967. On behavior, sex-ratio and growth of *Solenocera membranacea* (Risso) (Decapoda, Penaeidae). *Crustaceana* **13:** 227–237.

Highsmith, R. C. 1983. Sex reversal and fighting behavior: coevolved phenomena in a tanaid crustacean. *Ecology* **64:** 719–726.

Hoestlandt, H. 1973. Étude systématique et génétique de trois espèces pacifiques nord-américains du genre *Gnorimosphaeroma* Menzies (Isopodes Flabellifères). I. Considérations générales et systématique. *Arch. Zool. Exp. Gen.* **114:** 349–395.

Hoestlandt, H. 1975. Étude systématique et génétique de trois espèces pacifiques nord-américains du genre *Gnorimosphaeroma* Menzies (Isopodes Flabellifères). II. Génétique du polychromatisme et populations. *Arch. Zool. Exp. Gen.* **116:** 521–548.

Ishimaru, S. 1984. Sexual dimorphism and protogynous hermaphroditism in *Leptochelia neapolitana* (Tanaidacea, Paratanaidae). *Zool. Sci. (Tokyo)* **1:** 997 (Abstract).

Jackson, H. G. 1928. Hermaphroditism in *Rhyscotus*, a terrestrial isopod. *Quart. J. Microsc. Sci.* **71:** 527–539.

Juchault, P., and J.-P. Mocquard. 1989. Effect de l'inoculation d'une bacterie endocellulaire feminisante sur la croissance et la reproduction des femelles du Crustacé Onicsoi de *Armadillidium vulgare* (Latr.). Consequences possibles sur l'evolution des populations. *Crustaceana* **56:** 83–92.

Kensley, B. 1982. Deep-water Atlantic Anthuridea (Crustacea: Isopoda). *Smithson. Contrib. Zool.* **346:** 1–51.

Kneib, R. T. 1992. Population dynamics of the tanaid *Hargeria rapax* (Crustacea: Peracarida) in a tidal marsh. *Mar. Biol.* **113:** 437–445.

Kozloff, E. N. 1987. *Marine Invertebrates of the Pacific Northwest* University of Washington Press, Seattle.

Legrand, J. J., and P. Juchault. 1963. Mise en évidence d'un hermaphrodisme protogynique fonctionnel chez l'Isopode Anthuride *Cyanthura carinata* (Kroyer) et étude du mecanisme de l'inversion sexuelle. *C R Acad. Sci. Paris* **256:** 2931–2933.

Legrand, J. J., and P. Juchault. 1970. Controle de la sexualité chez les crustacés isopodes gonochoriques et hermaphrodites. *Bull. Soc. Zool. Fr.* **95:** 551–563.

Lowry, J. K., and H. E. Stoddart. 1986. Protandrous hermaphrodites among the Lysianassoid Amphipoda. *J. Crustacean Biol.* **6:** 742–748.

Manning, J. T. 1975. Male discrimination and investment in *Asellus aquaticus* and *A. meridianus* Racovitza (Crustacea: Isopoda). *Behaviour* **55:** 1–14.

Manning, J. T. 1980. Sex ratio and optimal male time investment strategies in *Asellus aquaticus* (L.) and *A. meridianus* Racovitza. *Behaviour* **74:** 264–273.

Markham, J. C. 1975. Biological results of the University of Miami deep sea expeditions. Part 113. A review of the biopyrid isopod genus *Munidion,* parasitic on galatheid crabs in the Atlantic and Pacific. *Bull. Mar. Sci.* **25:** 422–441.

Modlin, R. F., and P. A. Harris. 1989. Observations on the natural history and experiments on the reproductive strategy of *Hageria rapax* (Tanaidacea). *J. Crustacean Biol.* **9:** 578–586.

Montalenti, G. 1941. Studi sull' ermafroditismo dei cimotoidi—I. *Emetha audouinii* (M. Edw.) e *Anilocra physodes* (L.). *Pubbl. Stn. Zool. Napoli* **18:** 337–394.

Nakashima, Y. 1987. Reproductive strategies in a partially protandrous shrimp *Athanas kominatoensis* (Decapoda: Alpheidae): Sex change as the best of a bad situation for subordinates. *J. Ethol.* **5:** 145–159.

Newman, W. A. 1974. Two new deep-sea Cirripedia (Ascothoracica and Acrothoracica) from the Atlantic. *J. Mar. Biol. Assoc. U.K.* **54:** 437–456.

Noël, P. 1973. Cycle biologique et inversion sexuelle du crustacé décapode Natantia *Processa edulis. Cah. Biol. Mar.* **14:** 217–227.

Policansky, D. 1982. Sex change in plants and animals. *Ann. Rev. Ecol. Syst.* **13:** 471–495.

Rawlings, T. A. 1989. Functional morphology of egg capsules in a marine gastropod *Nucella emarginata.* M.Sc. Thesis. University of British Columbia, Vancouver.

Rawlings, T. A. 1994. Encapsulation of eggs by marine gastropods: effect of variation in capsule form on vulnerability of embryos to predation. *Evolution* (in press).

Rees, C. P. 1975. Competitive interactions and substratum preferences of two intertidal isopods. *Mar. Biol. (Berl.)* **30:** 21–25.

Ridley, M. 1983. *The Explanation of Organic Diversity. The Comparative Methods and Adaptations for Mating.* Clarendon Press, Oxford.

Ridley, M., and D. J. Thompson. 1979. Size and mating in *Asellus aquaticus* (Crustacea: Isopoda). *Z. Tierpsychol.* **51:** 380–397.

Riegel, J. A. 1959a. Some aspects of osmoregulation in two species of sphaeromid isopod Crustacea. *Biol. Bull.* **116:** 272–284.

Riegel, J. A. 1959b. A revision in the sphaeromid genus *Gnorimosphaeroma* Menzies (Crustacea: Isopoda) on the basis of morphological, physiological and ecological studies on two of its "subspecies." *Biol. Bull.* **117:** 151–162.

Standing, J. D., and D. D. Beatty. 1977. Humidity behaviour and reception in the sphaeromatid isopod *Gnorimosphaeroma oregonensis* (Dana). *Can. J. Zool.* **56:** 2004–2014.

Steel, E. A. 1961. Some observations on the life history of *Asellus aquaticus* (L.) and *Asellus meridianus* Racovitza (Crustacea: Isopoda). *Proc. Zool. Soc. Lond.* **137:** 71–87.

Steele, D. H. 1967. The life cycle of the marine amphipod *Stegocephalus inflatus* Kroyer in the Northwest Atlantic. *Can. J. Zool.* **45:** 623–628.

Stoner, A. W. 1986. Cohabitation on algal habitat islands by two hermaphroditic Tanaidacea (Crustacea: Peracarida). *J. Crustacean Biol.* **6:** 719–728.

Subramoniam, T. 1981. Protandric hermaphroditism in a mole crab, *Emerita asiatica* (Decapoda: Anomura). *Biol. Bull.* **160:** 161–174.

Suzuki, H. 1970. Taxonomic review of four alpheid shrimps belonging to the genus *Athanas* with reference to their sexual phenomena. *Sci. Rep. Yokohama Nat. Univ. Sect. II* **17:** 1–37.

Torti, M. R., and E. E. Boschi. 1973. Nuevos aportes al conocimiento de los crustaceos decapodos *Caridea* del genero *Campylonotus* Bate, 1888. *Physis Secc. A Oceanos Org.* **32:** 65–84.

Veuille, A. 1980. Sexual behaviour and evolution of sexual dimorphism in body size in *Jaera* (Isopoda Asellota). *Biol. J. Linn. Soc.* **13:** 89–100.

Veuille, A., J. Dax, and A.-M. Vouaux. 1963. Inversion sexuelle et parasitisme per *Bopyrina virbii* (Walz) chez la crevette *Hippolyte intermis* (Leach). *C. R. Acad. Sci. Paris* **256:** 790–791.

Warner, R. R. 1975. The adaptive significance of sequential hermaphroditism in animals. *Am. Nat.* **109:** 61–82.

Warner, R. R. 1988. Sex change and the size-advantage mode. *Trends Ecol. Evol.* **3:** 133–136.

Wilson, G. D. F. 1991. Functional morphology and evolution of isopod genitalia. Pp. 228–245 in *Crustacean Sexual Biology,* R. Bauer and J. Martin, eds. Columbia University Press, New York.

Wrona, F. J., J. M. Culp, and R. W. Davies. 1982. Macroinvertebrate subsampling: a simplified apparatus and approach. *Can. J. Fish Aquat. Sci.* **39:** 1051–1054.

Yaldwyn, J. C. 1966. Protandrous hermaphroditism in decapod prawns of the families Hippolytidae and Campylonotidae. *Nature* **209:** 1366.

Reference: *Biol. Bull.* **187**: 112–123. (August, 1994)

Small Size, Brooding, and Protandry in the Apodid Sea Cucumber *Leptosynapta clarki*

MARY A. SEWELL

Bamfield Marine Station, Bamfield, British Columbia, Canada V0R 1B0, and
Department of Zoology, University of Alberta, Edmonton, Alberta, Canada T6G 2E9

Abstract. The apodid sea cucumber *Leptosynapta clarki* exhibits the three commonly associated traits of small adult size (max. length 113 mm), brooding (intraovarian = viviparity), and hermaphroditism (protandric). Juvenile *L. clarki* are released from the ovary at a length of 1–2 mm in the early spring (April–May) and are reproductively active as males in the reproductive season (November) following their birth. In their second year, some individuals continue to reproduce as males, but others undergo protandric sex change to reproduce as females. Analysis of the relationship between size and sex revealed a "critical" size for sex change at a weight of 200–400 mg with a 1:1 sex ratio above 500 mg total weight. Transitional gonads with previtellogenic oocytes and mature spermatozoa were observed, suggesting that sex change is initiated prior to reproducing in the current reproductive season. A test of the allometric hypothesis on the association between small size and brooding found no evidence for scaling constraints on brood size in *L. clarki*. These allometric constraints may be avoided because of potentially low fertilization success and brooding within a distensible structure. The sequential hermaphroditism in *L. clarki* may additionally be a method to reduce inbreeding in a species with limited dispersal.

Introduction

Two characters of the adult have been associated with brooding in marine invertebrates: small size and the tendency towards hermaphroditism. Several hypotheses have been proposed to explain the association of small adult size with brooding. The energetic hypothesis of Chia (1974) suggested that the trend for lecithotrophy, brooding, or viviparity in small animals resulted from the lower energetic reserves for gamete production. Strathmann and Strathmann (1982) described three categories of hypotheses on the association of small adult size and brooding related to (1) dispersal, (2) adult longevity and recruitment, and (3) the allometry of structures associated with gamete production and brood care. These hypotheses are not mutually exclusive and no single one is entirely satisfactory (Strathmann and Strathmann, 1982). However, of these four hypotheses, the allometry hypothesis has received the most attention, primarily because it can be tested within a single species.

The allometry hypothesis predicts that brooding will not occur in large species, because of spatial limitations on brood size with increasing animal size (Heath, 1977; Strathmann and Strathmann, 1982). In numerical terms, fecundity is likely to increase with the cube of length, but the space for brooding may increase with a lower scaling constant, resulting in insufficient space for brooding the embryos. Although originally proposed for an external brooder (Strathmann and Strathmann, 1982), the allometry hypothesis has been tested by comparing the relationship between animal size, egg number, and number of brooded embryos in several marine invertebrates (Daly, 1972; Rutherford, 1973; Menge, 1974; Ockelmann and Muus, 1978; Rumrill, 1982; Strathmann *et al.,* 1984; Kabat, 1985; Gremare and Olive, 1986; McGrath and ÓFoighil, 1986; Russell and Huelsenbeck, 1989; Byrne, 1991; Brey and Hain, 1992; Hines, 1992; Hess, 1993).

Hermaphroditism, in which both male and female gametes are produced by a single individual in its lifetime, is common in marine invertebrates and is often associated with brooding (Ghiselin, 1969, 1974; but see Heller, 1993, for arguments against this association in gastropods). Ghiselin (1969, 1974) proposed three models for the evo-

Received 4 January 1994; accepted 25 May 1994.

Present address: Dept. of Biological Sciences, Simon Fraser University, Burnaby, B.C., Canada V5A 1S6.

Table I

Patterns of sex change and reproductive characters in the phylum Echinodermata

Species	Sex change	Brood[1]	Evidence for sex change[2]	Reference
Class Asteroidea				
Fromia ghardaqana	Protandric	N	H	Achituv and Delavault (1972)
Asterias forbesi	Protandric	N	L	Aldrich and Aldrich (1955)
Asterina gibbosa	Protandric	N	F^2, H	Bacci (1951)
	Protogynic	N	?	Bacci (1965)
	Protandric	N	H	Emson and Crump (1978)
Asterina pancerii	Protogynic	?	H	Cognetti (1954)
Patiriella exigua	Protandric	N	F^1, F^2	Byrne (1992)
Class Holothuroidea				
Holothuria atra	Protandric	N	F^1, F^2	Harriott (1982)
Labidoplax media	Protandric	?	F^1	Gotto and Gotto (1972)
Leptosynapta inhaerens	Protandric	N	F^1	Runnström (1927)
Leptosynapta clarki	Protandric	Y	H; F^1, F^2, H	Everingham (1961); Sewell (1991); herein
Class Ophiuroidea				
Ophiolepis kieri	Protandric	Y	F^1, F^2	Hendler (1979)
Amphiura stepanovii	Protandric	Y		Fedotov (1926)
Ophiocantha bidentata	Protandric	N	F^2, H	Tyler and Gage (1982)
Ophionereis olivacea	Protandric	Y	F^2, H	Byrne (1991)
Ophiothrix sp.	Protandric	Y	F^2	Schoppe and Holl (1994)

Species suspected of undergoing sex change: Brooder—*Pseudopsolus macquariensis* (Simpson, 1982); Nonbrooder—*Ophioplocus* (*Ophiceres*) *incipiens* (Mortensen, 1936); *Ophiothrix fragilis* (Gostan, 1956).

[1] Presence or absence of brooding based on review of Giese *et al.* (1991); Y = yes; N = no; ? = unknown.

[2] F = Field collections; F^1 = skewed sex ratio; F^2 = size/sex relationship; H = histology; L = laboratory observations.

lution of hermaphroditism. (1) The low-density model proposes that in sessile or slow-moving species, or in low-density populations, simultaneous hermaphroditism is advantageous because each contact of mature individuals can lead to reproduction (Tomlinson, 1966; Ghiselin, 1969). (2) The size-advantage model proposes that sequential hermaphroditism occurs when an individual can reproduce most efficiently as a member of one sex when small or young, but as a member of the other sex when it gets older and larger. Originally proposed by Ghiselin (1969), this has been extensively modeled (*e.g.*, Warner, 1975; Leigh *et al.*, 1976; Charnov, 1982, 1986; Iwasa, 1991). (3) The gene-dispersal model proposes that when motility is low, both the number and variety of potential mates are limited, and the genetic environment may be affected. Ghiselin (1969) discusses two particular effects: sequential hermaphroditism, which could reduce sibling crosses (Ghiselin, 1969), and simultaneous hermaphroditism, which could increase effective population size (Murray, 1964).

More recently, Heath (1977, 1979) predicted that if the space for brooding was limited and could hold fewer embryos than the individual could produce, then the remainder of reproductive resources could be reallocated towards male function as a simultaneous hermaphrodite. Data collected in *Asterina phylactica* were inconsistent with this hypothesis and led Strathmann *et al.* (1984) to propose that the correlation between brooding and simultaneous hermaphroditism was related to levels of inbreeding.

Although most brooding echinoderms are simultaneous hermaphrodites, recent research has suggested an association between brooding and sequential hermaphroditism within this phylum. In a comprehensive review of sex-changing species, Policansky (1982) cited evidence that 10 species of echinoderms change sex, the majority being protandric; two of these are brooders (Table I). Since that review, two protandric brooding ophiuroids (Byrne, 1991; Schoppe and Holl, 1994) and a protandric nonbrooding asteroid (Byrne, 1992) have been described (Table I). There are also reports of one brooding and two nonbrooding echinoderms that may change sex (Table I).

Leptosynapta clarki is a small (maximum length 113 mm), apodid sea cucumber found on the intertidal mudflats of Grappler Inlet, Bamfield, Vancouver Island, Canada. *L. clarki* has an annual reproductive cycle, brooding pentactulae in the ovary from November to April or May (Everingham, 1961; Sewell and Chia, 1994). Abundant sperm found in the ovaries of *L. clarki* sampled in False Bay, San Juan Island, Washington, in March or April (Everingham, 1961; Eckelbarger and Young, 1992) led Everingham to suggest that this species might be a protandric hermaphrodite. The present study confirms that *L. clarki* is protandric, describes the population consequences of that sex change, and examines the hypotheses for the association between small adult size and brooding in marine invertebrates.

Materials and Methods

Collections and size measurements

Specimens of *Leptosynapta clarki* were collected at two sites in Grappler Inlet, Bamfield, British Columbia (Site 1: 48°49′57″ N, 125°06′45″ W; Site 2: 48°50′ N, 125°06′36″ W). Site 1 is located on the northern side of Barge Bay and has a short intertidal area (*ca.* 20 m) and a high proportion of gravel in the substrate. Site 2 is a gentler sloping mudflat (intertidal area *ca.* 60 m) at the opposite end of the channel separating "No-name" Island from Vancouver Island proper (see Sewell and Chia, 1994, Fig. 1). This site has a finer sediment composition with little gravel and contains *L. clarki* of a larger size than Site 1 (mean total weight ± SD: Site 1: 307.8 ± 153.99 mg, $N = 720$; Site 2: 490.4 ± 268.80 mg, $N = 660$; Sewell and Chia, 1994). Both sites have extensive *Zostera* beds in the lower intertidal that extend into the shallow subtidal.

The sea cucumbers were collected on the mid-intertidal mudflats, either by using cores or by sweeping away the upper 5 cm of sediment to reveal the animals in their burrows; put in buckets with the surrounding mud; and transported to the laboratory. Adults were removed from the sediment with a 2- or 0.85-mm sieve. The remaining fraction was then sieved through a 0.25-mm sieve to remove juveniles. Sea cucumbers were kept in seawater until length and weight were determined.

Animals to be measured were placed in a 90-mm petri dish containing 2.5% $MgCl_2$ in seawater (w/v). Length was measured, in millimeters, from the anterior end of the calcareous ring to the posterior. Sea cucumbers less than 20 mm were measured on a dissecting microscope equipped with an eyepiece graticule calibrated against a stage micrometer. Larger sea cucumbers were gently held straight with tweezers and length was measured to the nearest millimeter with reference to a small plastic ruler under the petri dish. After measurement of length, the sea cucumber was placed on a tissue to remove external water and then weighed on a fine-scale balance to determine its total weight (TW) in milligrams.

Size-sex relationship

The relationship between size and sex in *L. clarki* was determined in July 1991 when the gonads were well developed (Sewell and Chia, 1994). After a specimen was weighed, its sex was determined by examining the color of the gonads through the semitransparent body wall. In July, females had yellow ovaries with large eggs (*ca.* 200 μm) and males had white testes (Sewell and Chia, 1994). Juvenile sea cucumbers or those with small gonads were dissected to verify sex identification.

The relationship between sea cucumber size and sex was determined by calculating the percentage of females in each weight or length class. For weights less than 800 mg the data were divided into 50-mg size classes. Few sea cucumbers were found above 800 mg, so the size class was increased to 100 mg. The final category was sea cucumbers with weights > 1300 mg. Sea cucumbers in this category ranged from 1412 to 1684 mg ($N = 4$), so are plotted as a single point at 1500 mg. Sea cucumber length was divided into 5-mm size classes until 100 mm; the three sea cucumbers with greater length (104, 108, 113 mm) are plotted as a single point at 110 mm. The total number of sea cucumbers sampled was 693 (454 males, 239 females).

The breeding sex ratio was determined from haphazard cores used in following the recruitment of *L. clarki* on the intertidal mudflats at Site 1 (Sewell, 1993a). Ten haphazardly thrown cores were taken on the mid-intertidal in Barge Bay (Sewell, 1993a), the animals removed by sieving, and the size and sex of each sea cucumber determined in four samples during the winter of 1990–1991 and the summer of 1991.

Gonadal changes

Sea cucumbers sampled during regular gonad index dissections in January and February 1990 and 1991 (Sewell and Chia, 1994) were used to determine the size of animals with transitional gonads (that is, animals in the process of changing from male to female). Sea cucumbers were collected from Sites 1 and 2 (Total $N = 240$) and weighed and dissected as described in Sewell and Chia (1994). The gonad in *L. clarki* consists of two separate tubules that join through the dorsal mesentery to a single gonoduct (Sewell and Chia, 1994). Both gonad tubules were dissected, placed on a glass slide (38 × 75 mm) with a small amount of seawater, and temporarily mounted with a coverslip (35 × 50 × 0.02 mm). The weight of the coverslip revealed details of the gonad, such as the presence of oocytes, without the need for histology. Of the 240 sea cucumbers dissected, 87 were females brooding pentactulae or undergoing resorption. Of the remaining 153 sea cucumbers, 75 had transitional gonads; these were divided into 50-mg size classes for analysis.

Histological descriptions of protandric sex change were obtained during a detailed study of reproduction in *L. clarki* (Sewell and Chia, 1994). Gonads were preserved in Bouin's fixative, stored in 70% ethanol, and embedded in Paraplast. Sections were cut at 7 μm, stained in hematoxylin and eosin, and photographed on a Zeiss photomicroscope.

Allometry of reproduction

The relationship between the size of the female and the number of unfertilized eggs was determined in late October 1989 and 1990 prior to the spawning period in November and December (Everingham, 1961; McEuen, 1986; Sewell and Chia, 1994). Sea cucumbers were collected from Sites 1 and 2 and sieved from the sediment as described above. After total weight (TW) was measured, a longitudinal incision was made from the base of the calcareous ring to the posterior, the coelomic water was drained from the body cavity, and the animal was reweighed to obtain its drained weight (DW) in milligrams. The gonad was dissected and temporarily mounted under a coverslip. Counts were made of the total number of mature eggs per gonad ($N = 2$ tubules) in 20 females at two sites in each year (Total $N = 80$ females).

The relationship between the size of the female and the number of fertilized eggs/embryos was examined in sea cucumbers in late November and early December 1989 and mid-November 1990. This was during the spawning period of *L. clarki* at Bamfield (Sewell and Chia, 1994) but before degeneration of unfertilized eggs or significant pentactulae mortality (Sewell, 1993a). Counts were made of the number of unfertilized eggs, early stage embryos, or pentactulae in each gonad for 50 females. The allometric relationship between female size and number of pentactulae was determined for those females that had early embryos or pentactulae present ($N = 28$).

The allometric relationship between size and number of eggs or pentactulae was tested using a Model II reduced major axis (RMA) regression. Ordinary least squares (OLS) regressions were calculated using Microsoft Excel Version 3.0. Because of the considerable error in measuring size in sea cucumbers (Sewell, 1990), OLS regression will underestimate the value of the slope (see McArdle, 1988; LaBarbera, 1989), and may suggest that scaling constraints exist when there are none (Hess, 1993). RMA regressions were performed on raw and natural log ($\log_e$) transformed data. Standard error (s^2) and asymmetric confidence intervals were attached to the slope of the RMA regression using the formulas in McArdle (1988).

If there are no constraints on brood size, the number of embryos brooded is assumed to scale with body size in the same way as the fecundity of broadcast spawning animals; *i.e.*, linearly with body weight or the cube of length (Strathmann and Strathmann, 1982). To test whether brood size was limited by scaling constraints, the slope of the RMA line was thus compared to the slope predicted by isometry ($b = 1$ for the relationship between $\log_e$ body weight and $\log_e$ number of pentactulae) using a Student's t test (Clarke, 1980; McArdle, 1988). A slope less than 1 in this relationship would indicate scaling constraints on brood size in larger sea cucumbers.

Results

Size-sex relationship

Leptosynapta clarki is a protandric hermaphrodite in which sex change occurs over a broad range of size (Fig. 1). Sea cucumbers in the smallest weight class (0–50 mg) are juveniles of the year (Sewell, 1993a) and are all male (Fig. 1A). The smallest females found weighed 77, 120, and 150 mg (21, 36, 30 mm in length, respectively; Fig. 1).

Sex change did not occur in a distinct weight class (Fig. 1A). Few females were found until 200–250 mg total weight (Fig. 1A). Between 200 and 400 mg there was an increasing percentage of females in each size class. This percentage stabilized at about 50%, at weights above 500 mg (Fig. 1A).

A similar increase in percent females was seen with increased sea cucumber length (Fig. 1B). No females were found until the 20–25 mm size class. The percentage of females increased between 25 and 45 mm, plateauing at 50%, above a length of about 50 mm (Fig. 1B).

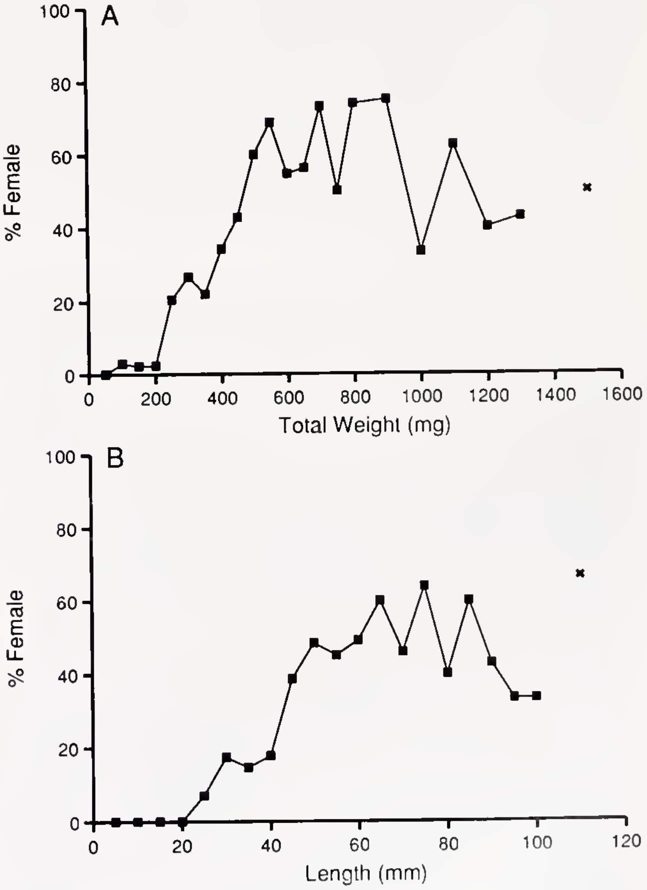

Figure 1. *Leptosynapta clarki.* Percent female sea cucumbers from Grappler Inlet, Bamfield, in size classes of (A) total weight (mg) and (B) length (mm). Point is plotted at upper limit of size class except for final category shown with (x); see details in text.

The presence of large numbers of small, but sexually active, males in the population strongly biases the sex ratio in *L. clarki* (Table II). In all samples the sex ratio was above 70% male, with a maximum of 88.5% male in August (Table II).

Gonadal changes

Most sea cucumbers with transitional gonads in January or February were in the 200–400 mg size range (Fig. 2). Sex change was, however, observed in some very large specimens (Fig. 2). The largest sea cucumber found with a transitional gonad weighed 855 mg (TW).

After spawning, the testes became thin and yellow, and shrank in length towards the gonad basis (Sewell and Chia, 1994). In protandric males, new oocytes were observed in fresh gonad tubules at the basal end adjacent to the gonad basis (Fig. 3A). Unspawned sperm were often present in the tubules with the new oocytes (Fig. 3B) and were active when exposed to seawater.

Histological examination of male gonads revealed that oocytes were present along the tubule wall in some mature testes (Fig. 3C). The testis lumen was packed with mature spermatozoa, whereas previtellogenic oocytes 10 to 20 μm in diameter were found along the tubule wall (Fig. 3C). After the spermatozoa were spawned, the oocytes continued to grow while the remnant spermatozoa were resorbed (Fig. 3D). Sex change must, therefore, be initiated prior to spawning in the current reproductive season.

Allometry of reproduction

Using raw and $\log_e$-transformed variables, reduced major axis (RMA) regressions were calculated between female size and number of eggs or pentactulae (Table III). In the period before spawning, female sea cucumbers show a positive significant relationship between weight (TW or DW) and egg number (Fig. 4, Table III). Regressions using natural log transformations of these variables are also significant, although there is a slight reduction of the r^2 in both cases (Table III). The allometric exponent of the $\log_e$-transformed egg number/drained weight relationship is 1.46, with 95% confidence intervals being 1.3–1.65 (Table III).

Table II

Breeding sex ratio of Leptosynapta clarki *at Site 1, Grappler Inlet*

Date	% Male	Sex Ratio (Male:Female)	*N*
7 December 1990	70.5	2.4:1	112
7 February 1991	85.3	5.8:1	143
15 July 1991	85.9	6.1:1	128
12 August 1991	88.5	7.7:1	96
Mean	82.6		
Std. Deviation	8.2		

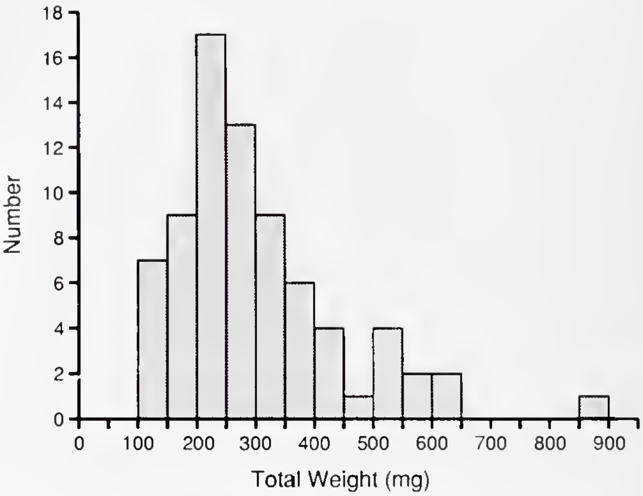

Figure 2. *Leptosynapta clarki.* Number of transitional gonads in each 50-mg total weight class during January and February 1990 and 1991. $N = 75$ sea cucumbers.

Lengths of the females used in the egg number/weight relationship were not recorded. These lengths were estimated using the OLS regression between total weight and length determined from the size/sex relationship described above (Length = 0.0595 (TW) + 20.519, $F = 2393.37$, df = 1,691, $p < 0.0001$, $r^2 = 0.776$). For this analysis, OLS regression is appropriate because the value for length is being estimated from the measurement of another variable (LaBarbera, 1989). A significant relationship was found between length and number of eggs in raw and natural log regressions, with an allometric exponent of 2.465 in the $\log_e$ transformation (Table III).

Weak relationships were found between female size and the number of pentactulae brooded (Table III). The only significant relationship was between drained weight and number of pentactulae in raw and $\log_e$-transformed data (Table III). Both regressions have low r^2 values (< 0.4, Table III). The allometric exponent of the $\log_e$-transformed regression was 1.84 (Table III). This slope is significantly greater than 1 ($T = 4.772$, df = 26, $p < 0.001$), indicating that fecundity is not proportionately smaller in larger sea cucumbers. In fact, larger females are producing disproportionately larger broods. This suggests that there are no scaling constraints on brood size in *L. clarki.*

Fertilization success in female *L. clarki* was variable. During the period sampled, 22 of the 50 females (44%) were unfertilized (0% fertilization). The remainder had percent fertilization ranging from 4.18–98.49% (mean ± SD = 47.74 ± 25.37%) with the mode at 40–50% fertilization (Fig. 5). There was no relationship between female weight and the percent fertilization (TW: $F = 0.193$, df = 1, 26, NS; DW: $F = 0.986$, df = 1, 26, NS).

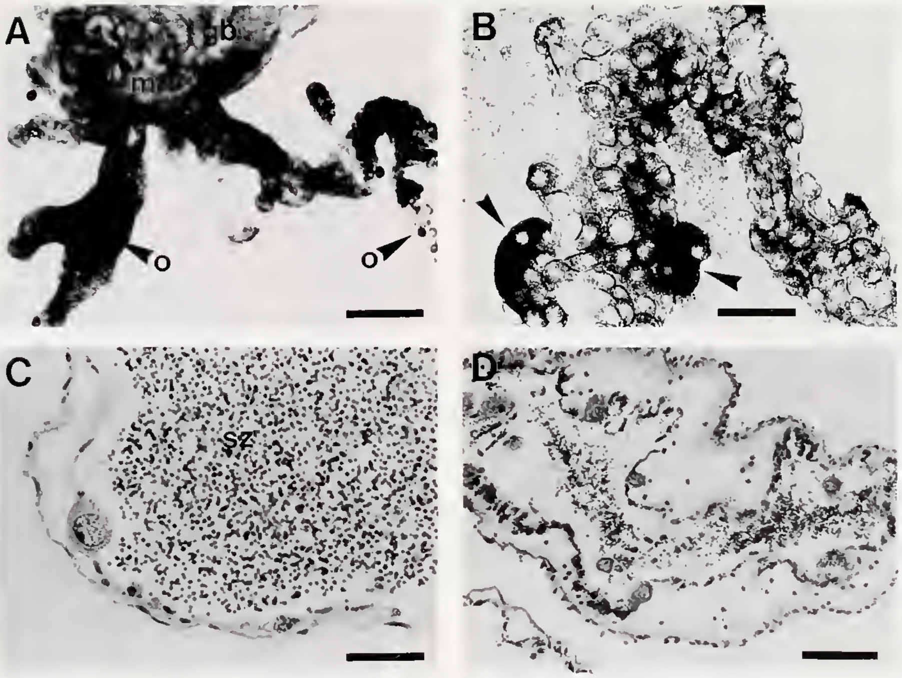

Figure 3. *Leptosynapta clarki.* Photomicrographs of transitional gonads. (A) Small resorbing testis in process of sex change. Almost the entire gonad is shown. Note the swollen gonad basis (gb) with madreporite (m), and small oocytes (o) in the tubules. Bar = 500 μm. (B) Transitional testis. Tubule contains numerous oocytes and remnant packets of sperm (arrow). Some sperm have broken from tubule onto base of slide. Bar = 200 μm. (C) Histological section of mature testis with spermatozoa (sz) in the lumen and early oocytes forming along the tubule wall. Section stained with hematoxylin/eosin. Bar = 25 μm. (D) Histological section of postspawned testis in transitional stage. Some remnant spermatozoa are seen in the lumen. Oocytes are present along the tubule wall. Bar = 50 μm.

Discussion

Protandry in Leptosynapta clarki

The histological and population information presented here confirms that *Leptosynapta clarki* is a protandric hermaphrodite and provides the first direct evidence of sex change within the class Holothuroidea. Two other holothurians in the order Apodida have been suggested to be protandric, though the evidence in both cases is somewhat circumstantial. *Leptosynapta inhaerens* was believed to be protandric because only 4 of 80 spawning specimens shed eggs (Runnström, 1927; cited in Hyman, 1955), and the lack of males in a sampled population of *Labidoplax media* led Gotto and Gotto (1972) to suggest that only very small and young specimens produce sperm.

There are few reports of sex change in the five remaining holothurian orders. Despite some anecdotal reports of protandry among dendrochirote holothurians (Smiley *et al.*, 1991), protandry has not been clearly demonstrated in any species. In aspidochirote holothurians, protandry is suggested in *Holothuria atra* on the basis of a change in the sex ratio with increased size (Harriott, 1982). However, sex change in *H. atra* is difficult to demonstrate because the species also reproduces asexually by binary fission and because the gonads regress after each spawning, making determination of the previous sex impossible (Harriott, 1982).

Sex allocation theory predicts that sex change should be an "all-or-nothing" response, with the animal or plant producing gametes of one sex until it is more profitable to produce gametes of the other sex, and then switching entirely to the latter (Charnov, 1982). Research on marine invertebrates has, however, shown a number of species that do not display an all-or-nothing response but have a 1:1 sex ratio above a certain size (*Patella argenvillei*—Branch, 1981; *Lottia gigantea*—Wright, 1989; *Patella kermadecensis*—Creese *et al.*, 1990; present study), or a wide size range or time over which sex change occurs (*Fromia ghardaqana*—Achituv and Delavault, 1972; *Crepidula fornicata*—Hoagland, 1978; *Ophionereis olivacea*—Byrne, 1991; *Coralliophila violacea*—Soong and Chen, 1991; *Patiriella exigua*—Byrne, 1992). The debate continues as to whether this is the result of a genetically programmed sex change, an environmental sex determination, or both.

One explanation applied in a number of marine invertebrates is that there are two sexual types within a species. Bacci (1951), who proposed this terminology in *Asterina gibbosa*, described one "race," or type, whose individuals (known as balanced hermaphrodites) change sex at a specific time in their existence. The other type contains two categories: unbalanced hermaphrodites, which change sex earlier or later, depending upon the individual, and true males and females, which remain one sex all their lives (Bacci, 1951). In the latter type, the presence of "true" males or females suggests a genetic predetermination for that sex. Evidence for predetermination is seen in *Bonellia viridis:* 10% of the larvae of this echiuran develop as males even if the "male determining factors" of a female proboscis are absent (Leutert, 1975). Similarly, in *Patella vulgata*, some individuals never change sex (Orton, 1928; Ballantine, 1961), and in *Lottia gigantea*, about 15% of the population change sex annually, regardless of environmental setting or age (Lindberg and Wright, 1985).

In *L. clarki*, all individuals start their reproductive lives as males (Sewell, 1991; Sewell and Chia, 1994; Sewell, 1993a); thus any "true sex" individuals (those that do not change sex during their lifetimes) in the population would be male. The rest of the population must be divided into those that change sex at some specific time, and those that change sex under the influence of some genetic or environmental factor. Male *L. clarki* may either delay sex change, as shown by the large size of some transitional males (Fig. 2), or have a labile sexuality that alternates between male and female. There is some circumstantial evidence that sex can be reversed from female to male (Sewell and Chia, 1994), and it is conceivable that sex may change more than once in the lifetime of a holothurian (Everingham, 1961; Harriott, 1982).

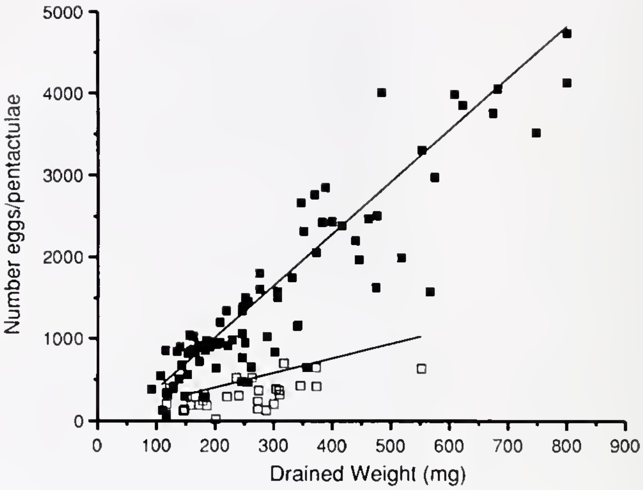

Figure 4. *Leptosynapta clarki*. Relationship between drained weight (mg) and number of eggs (filled squares) or pentactulae (open squares). RMA regressions:

Eggs: $y = 6.348x - 237.726$, $r^2 = 0.829$, $N = 80$.
Pentactulae: $y = 1.795x + 44.960$, $r^2 = 0.375$, $N = 28$.

The size-sex relationship presented here is a static data set that combines sea cucumbers of many ages within a size class (Fig. 1). Juveniles released from the mother in May 1990 were maintained in the laboratory for 1 year and used for measurements of growth (Sewell, 1993a). These individuals reproduced as males in November 1990 (Sewell, 1993a). When the growth experiment finished in May 1991, the surviving sea cucumbers were kept in the laboratory until the gonads had regrown after postspawning resorption (Sewell and Chia, 1994). In July 1991, eight animals of the surviving 78 had changed sex (unpub. data). These protandric sea cucumbers were above 185 mg TW,

Table III

Leptosynapta clarki: *Scaling constants for relationships between sea cucumber size and number of eggs or pentactulae*

Regression[1]	N	F[2]	r^2	ln(a)	b	$s^2\beta$	β lower	β upper
TW *vs* # eggs	80	168.94***	0.684	−12.300	3.637	0.038	3.206	4.127
DW *vs* # eggs	80	377.55***	0.829	−237.726	6.348	0.071	5.785	6.968
Length *vs* # eggs	80	168.94***	0.684	−1050.37	61.169	0.775	53.911	69.405
ln TW *vs* ln # eggs	80	161.69***	0.675	−0.010	1.416	9.5×10^{-3}	1.246	1.610
ln DW *vs* ln # eggs	80	205.89***	0.725	0.114	1.463	9.5×10^{-3}	1.300	1.646
ln Length *vs* ln # eggs	80	138.53***	0.640	−0.589	2.465	0.011	2.154	2.821
TW *vs* # pentactulae	28	0.143 NS	0.005					
DW *vs* # pentactulae	28	15.590***	0.375	44.960	1.795	0.055	1.312	2.456
Length *vs* # pentactulae	28	0.143 NS	0.005					
ln TW *vs* ln # pentactulae	28	0.184 NS	0.007					
ln DW *vs* ln # pentactulae	28	6.644**	0.204	1.069	1.835	0.063	1.289	2.611
ln Length *vs* ln # pentactulae	28	0.122 NS	0.005					

Relationships are determined from an RMA regression on raw or $\log_e$-transformed data. Formula for standard error ($s^2\beta$) and confidence intervals (β lower, β upper) on the RMA slope from McArdle (1988).

[1] TW = total weight (mg). DW = drained weight (mg).

[2] NS = nonsignificant; $^{**}p < 0.05$, $^{***}p < 0.001$.

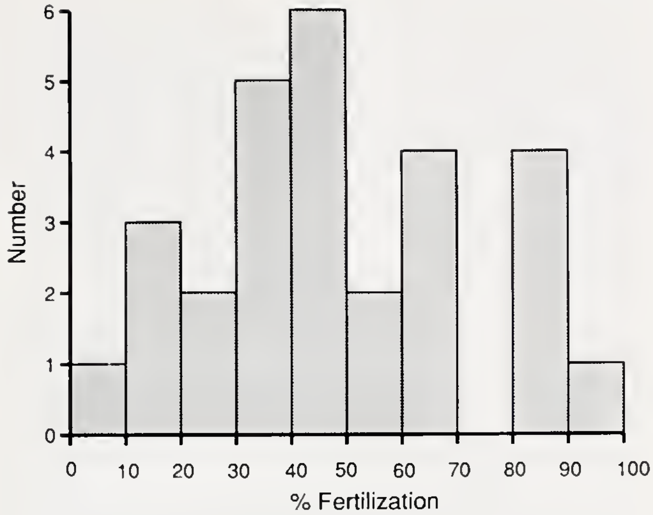

Figure 5. *Leptosynapta clarki.* Number of female sea cucumbers in each percent fertilization class during November and December 1989 and 1990. $N = 28$ females.

which is about the critical size of 200–250 mg determined from field collections. The other 70 individuals, although of the same age, were male or of undetermined sex. Seven of these 70 sea cucumbers were above 185 mg TW but had not changed sex. These results suggest, therefore, that size in combination with some environmental or genetic factor may be more important than age to the timing of sex change in *L. clarki.*

Brooding and small body size

Brooding is size-dependent in many marine invertebrates, and species with smaller adults protect their embryos to more advanced stages of development (see review by Strathmann, 1990). This trend has been noted in two families of holothurians, the Cucumaridae (Menge, 1975) and the Synaptidae (Strathmann, 1990). *L. clarki* conforms to these trends in being small (adult size maximum at Bamfield is 113 mm) and brooding pentactulae in the ovary (Everingham, 1961; McEuen, 1986; Sewell and Chia, 1994).

A test of the allometry hypothesis to explain the association of small adult size with brooding (Strathmann and Strathmann, 1982) in *L. clarki* did not show proportionately smaller broods in larger sea cucumbers. The slope of the relationship between $\log_e$ drained weight and $\log_e$ number of pentactulae was not less than 1, indicating no spatial constraints on brood size in larger *L. clarki.*

Constraints on brood size can also occur if the larger broods from larger adults develop more slowly or suffer higher mortality (Strathmann and Strathmann, 1982). In *L. clarki,* despite a trend for larger females to have a higher number of pentactulae, larger females or females with a high number of pentactulae do not show a higher degree of mortality (Sewell, 1993a). These results suggest that brood size is not constrained in larger *L. clarki* by either brood space or differential embryonic mortality.

Although the allometry hypothesis is intuitively appealing (Hess, 1993), the evidence for scaling constraints on brood size in marine invertebrates is remarkably poor. Studies that suggest that brood size is unconstrained by brood space include species of polychaetes (Daly, 1972; Gremare and Olive, 1986; Hess, 1993), bivalves (Ockelmann and Muus, 1978; Kabat, 1985; McGrath and ÓFoighil, 1986; Russell and Huelsenbeck, 1989; Brey and Hain, 1992), asteroids (Menge, 1974), ophiuroids (Rumrill, 1982; Byrne, 1991), holothuroids (Rutherford, 1973), and pinnotherid crabs (Hines, 1992). In fact, when the study on *Asterina phylactica* that provided the first empirical evidence for the hypothesis (Strathmann *et al.,* 1984) was reanalyzed with RMA regression, no scaling constraints on brooding were indicated (Hess, 1993).

One species that might show allometric constraints on brooding is the hermaphroditic, bursal-brooding *Axiognathus squamata* (Rumrill, 1982). In this species, the relationship between brood number and parental body size is significantly different from zero, but with a low slope (untransformed data $b = 0.57$; Rumrill, 1982). This indicates that smaller adults brood numbers of embryos nearly equivalent to those brooded by larger adults (Rumrill, 1982). However, in *Axiognathus squamata,* staggered oocyte maturation and brood release ensures that the production of oocytes never exceeds the capacity of the adult to brood the developing embryos (Rumrill, 1982). Therefore, the observed allometric constraint on brood size in this species may depend more upon the rate of oocyte maturation than on body size (Rumrill, 1982).

In *L. clarki,* sperm released externally enters the ovary through an as yet unknown means (Everingham, 1961; McEuen, 1987; Hess *et al.,* 1988; Sewell and Chia, 1994), but probably via the gonopore. Large amounts of sperm are available during the spawning season as a result of early reproduction, which skews the sex ratio dramatically towards males (Table II), and the production of large quantities of sperm by each male (Sewell and Chia, 1994). Although all males invest a similar proportion of energy in reproduction (about 5% of drained weight, Sewell and Chia, 1994), larger males will have larger volumes of sperm, which might result in higher fertilization success. However, even though sperm does not appear to be limiting because of high-density populations (at Bamfield, mean density = 169 per m^2; Sewell, 1993a), a skewed sex ratio, and large amounts of sperm per male, in some females fertilization is low or zero. There is also no evidence to suggest that larger females have a higher fertilization success. If fertilization is a constraint for *L. clarki* or other brooders, then limitations on brood size due to space or embryonic requirements for dissolved materials (Strathmann and Strathmann, 1982) may never be reached.

In brooding species where fertilization success is high (*e.g., Cucumaria pseudocurata*—Rutherford, 1973; *Ophioplocus esmarki*—Rumrill, 1982; *Ophionereis olivacea*—Byrne, 1991), allometric constraints on space may be avoided by brooding of embryos to a limited stage of development (Daly, 1972; Ockelmann and Muus, 1978), three-dimensional packing of embryos in the brood space (Kabat, 1985), sequential brooding throughout the reproductive season (Kabat, 1985; Hess, 1993), or brooding within a distensible structure (Hines, 1992; present study). In the latter case, the ability for the brood structure to expand to accommodate the number of fertilized eggs might ensure that, even when fertilization success is high, all the embryos can be brooded. In such cases, a test of the allometry hypothesis may be inappropriate because, in contrast to external brooders or species with a well-defined, solid brood space, there may not be a limit to brood space.

Alternative hypotheses to explain the association between small size and brooding—such as lower energetic reserves (Chia, 1974), dispersal, or recruitment (Strathmann and Strathmann, 1982)—cannot be considered in relation to brooding in *L. clarki* until there is comparative information on other sea cucumber species. Hess (1993) has recently suggested that the slower developmental rate of embryos in large brooders may be a factor in the evolution of brooding. This time-constraint hypothesis suggests that longer developmental times may be disadvantageous because the stage-specific mortality rate is experienced over a longer period of time, and the number of broods per unit time is reduced. In the development of this hypothesis, Hess assumes that embryonic mortality may be low and relatively unimportant in brooders, but this may not be true for all brooding species (Sewell, 1993a, b). If embryonic mortality is high, as in some female *L. clarki* (Sewell, 1993a, b), then the costs of a longer development in larger brooders will be even greater (H. Hess, pers. comm.).

Although the time-constraint hypothesis may be applicable to species that spawn more than once per season, alternative hypotheses will be needed to explain the association between small size and brooding in semelparous brooders or in individuals that produce only one brood per season (Hess, 1993). As the latter category includes many echinoderms in which the association between small size and brooding is particularly pronounced (see Strathmann, 1990), this emphasizes that no single hypothesis will be applicable in all taxa (Strathmann and Strathmann, 1982).

Brooding and hermaphroditism

The association between brooding and hermaphroditism has been noted in a variety of marine invertebrates (Ghiselin, 1969, 1974; Charnov, 1982; Strathmann and Strathmann, 1982), including asteroid, ophiuroid, and holothuroid echinoderms (Ghiselin, 1969, 1974). The fairly high incidence of protandry in ophiuroids and holothuroids was believed by Ghiselin (1969) to favor the gene-dispersal model for hermaphroditism.

In the gene-dispersal model, sequential hermaphroditism can act to prevent inbreeding due to fertilization between siblings, especially in forms with restricted gene flow (Ghiselin, 1969, 1974). For example, if all members of a clutch are males at the onset of sexual maturity and change into females simultaneously, then they are never able to mate with each other (Ghiselin, 1974). The observation that there is a higher incidence of sequential hermaphroditism in forms with restricted gene flow (species with no larvae or brooders) provides some support for the hypothesis (Ghiselin, 1974), though there is little direct evidence for reduced levels of inbreeding in sequential hermaphrodites (but see Hunt, 1993), and none for brooding species. Studies on the scale of genetic differentiation in *L. clarki* (Hess *et al.,* 1988) and the confirmation of protandry in the present study may provide direct evidence for this hypothesis in a brooding species.

In an electrophoretic study of three geographically separate *L. clarki* populations on San Juan Island, Washington, Hess *et al.* (1988) found no evidence for inbreeding: the two polymorphic loci studied did not show the reduced numbers of heterozygotes expected in inbred populations. The authors concluded that there was enough movement of either individuals or gametes within each population to allow random mating and maintain heterozygosity. Similar results were obtained by Hunt (1993) in the asteroid *Patiriella exigua,* which is protandric and oviposits direct-developing eggs on the undersides of intertidal boulders (Byrne, 1992). This species has no known method for dispersal, but showed no evidence of inbreeding (Hunt, 1993). In both cases, low dispersing and protandric species, one with direct development, the other a brooder, showed evidence for random mating within isolated local populations (Hess *et al.,* 1988; Hunt, 1993).

L. clarki juveniles released from the mother rapidly form shallow burrows, and dispersal—though rare—might occur by rafting, floating, swimming, or incidental dispersal as a result of water movement (Sewell, 1993a). The combination of occasional dispersal and sequential hermaphroditism might reduce levels of inbreeding in an *L. clarki* population. However, because growth rates in juvenile *L. clarki* are extremely variable (Sewell, 1993a) and protandry appears to be dependent upon the combined effects of size and environmental/genetic effects, it is unlikely that all siblings undergo a simultaneous sex change. Although *L. clarki* does show some evidence to support the gene-dispersal model for sequential hermaphroditism, further clarification is required to determine how far siblings disperse from one another; whether all, or only some, individuals in a clutch change sex at the same time; and if there is a reduction in inbreeding in the Bamfield population.

If we assume that sequential hermaphroditism is an advantageous strategy for *L. clarki,* the question to be answered is, Why is *L. clarki* protandric and not protogynic?

Juvenile sea cucumbers are released from the mother into the adult habitat in April or May (Sewell and Chia, in press; Sewell, 1993a). The transitional gonads with new eggs are, however, seen in sex-changing animals in January while these pentactulae were still being brooded. Therefore, if the sea cucumbers were to be reproductively active as females in their first year, they would need to start egg development while being brooded within the female. In addition, based on the regression line for drained weight *versus* number of eggs (Table III, Fig. 4), to produce any eggs at all a sea cucumber must weigh over 37 mg DW during late October. Although growth to sizes at which eggs could be produced is possible on the basis of laboratory measurements (Sewell, 1993a), the time required to produce mature eggs (10 months, Jan-Nov.; Sewell and Chia, 1994) might be a constraint to early reproduction as a female.

In terms of the size-advantage hypothesis, although there is clearly an increase in the number of eggs produced per female with size (Fig. 4), the potential for low fertilization (as number of eggs fertilized) in all females may reduce any advantage in large females. In addition, there is a strong relationship between testis weight and male size (unpub. data), so larger males are producing larger volumes of sperm. Until the mechanism of fertilization in *L. clarki* is determined, it is not known whether male size is important to an individual's fertilization success.

Future research

Leptosynapta is an ideal genus in which to conduct further research on the association of small size, hermaphroditism, and brooding in marine invertebrates. These sea cucumbers are of small to moderate size (Hyman, 1955; 12–30 cm maximum adult length [except for *L. minuta,* 1 cm]; McEuen, 1986); are characterized by burrowing habits (Hyman, 1955); and exhibit a wide range of reproductive strategies—from lecithotrophic broadcast spawners (*L. inhaerens, L. galliennei, L. girardii, L. tenuis*) to coelomic (*L. minuta*) and ovarian brooders (*i.e.,* viviparous species: *L. clarki, L. transgressor;* for references see Smiley *et al.,* 1991). Of these species, *L. clarki* and probably *L. inhaerens* are protandric, whereas *L. minuta* is reported to be hermaphroditic (Smiley *et al.,* 1991). Further comparative work on this genus would therefore be of considerable interest because it removes phylogenetic constraints from the consideration of life history questions relating small size, brooding, and hermaphroditism.

Acknowledgments

I thank my supervisor, F-S. Chia; thesis committee, J. Holmes, H. Clifford, J. Spence; and M. Byrne and H. Hess for comments on the manuscript. I am also grateful to D. Levitan for many thought-provoking discussions and E. Charnov for discussions on sex-change theory. Funds to support this research were provided by the Zoology Department, University of Alberta, a Sigurd Tveit Memorial Scholarship from Bamfield Marine Station to the author, and an NSERC Grant to F-S. Chia.

Literature Cited

Achituv, Y., and R. Delavault. 1972. Nouvelles recherches sur l'hermaphrodisme de *Fromia ghardaqana* Mrtsn (Échinoderme, Astéride). *Cah. Biol. Mar.* **13:** 433–442.

Aldrich, F. A., and M. M. Aldrich. 1955. Studies on the reproductive functional morphology of Asteroideans. I. Sex reversal in the common sea star, *Asterias forbesi* (Desor). *Not. Natl. Acad. Nat. Sci. Phila.* **276.** 2 pp.

Bacci, G. 1951. On two sexual races of *Asterina gibbosa* (Penn.). *Experientia* **7:** 31–33.

Bacci, G. 1965. *Sex Determination.* Pergamon Press, Oxford. 306 pp.

Ballantine, W. J. 1961. The population dynamics of *Patella vulgata* and other limpets. Ph.D. Thesis, Queen Mary College, London University. 236 pp.

Branch, G. M. 1981. The biology of limpets: physical factors, energy flow, and ecological interactions. *Oceanogr. Mar. Biol. Annu. Rev.* **19:** 235–380.

Brey, T., and S. Hain. 1992. Growth, reproduction and production of *Lissarca notorcadensis* (Bivalvia: Philobryidae) in the Weddell Sea, Antarctica. *Mar. Ecol Prog. Ser.* **82:** 219–226.

Byrne, M. 1991. Reproduction, development and population biology of the Caribbean ophiuroid *Ophionereis olivacea,* a protandric hermaphrodite that broods its young. *Mar. Biol.* **111:** 387–399.

Byrne, M. 1992. Reproduction of sympatric populations of *Patiriella gunnii, P. calcar* and *P. exigua* in New South Wales, asterinid seastars with direct development. *Mar. Biol.* **114:** 297–316.

Charnov, E. L. 1982. The theory of sex allocation. Monographs in Population Biology 18, Princeton University Press, Princeton. 355 pp.

Charnov, E. L. 1986. Size advantage may not always favor sex change. *J. Theor. Biol.* **119:** 283–285.

Chia, F. S. 1974. Classification and adaptive significance of developmental patterns in marine invertebrates. *Thalassia Jugosl.* **10:** 121–130.

Clarke, M. R. B. 1980. The reduced major axis of a bivariate sample. *Biometrika* **67:** 441–446.

Cognetti, G. 1954. La proteroginia in una popolazione di *Asterina pancerii* Gasco del Golfo di Napoli. *Boll. Zool.* **21:** 77–80.

Creese, R. G., D. R. Schiel, and M. J. Kingsford. 1990. Sex change in a giant endemic limpet, *Patella kermadecensis,* from the Kermadec Islands. *Mar. Biol.* **104:** 419–426.

Daly, J. M. 1972. The maturation and breeding biology of *Harmathoë imbricata* (Polychaeta: Polynoidae). *Mar. Biol.* **12:** 53–66.

Eckelbarger, K. J., and C. M. Young. 1992. Ovarian ultrastructure and vitellogenesis in ten species of shallow-water and bathyal sea cucumbers (Echinodermata: Holothuroidea). *J. Mar. Biol. Ass. U.K.* **72:** 759–781.

Emson, R. H., and R. G. Crump. 1978. Brooding in *Asterina gibbosa* Pennant. *Thalassia Jugosl.* **12:** 99–108.

Everingham, J. W. 1961. The intra-ovarian embryology of *Leptosynapta clarki.* Masters Thesis, University of Washington, Seattle. 70 pp.

Fedotov, D. M. 1926. Die morphologie der Euryalae. *Z. Wiss. Zool.* **127:** 403–528.

Ghiselin, M. T. 1969. The evolution of hermaphroditism among animals. *Quart. Rev. Biol.* **44:** 189–208.

Ghiselin, M. T. 1974. *The Economy of Nature and the Evolution of Sex.* University of California Press, Berkeley. 346 pp.

Giese, A. C., J. S. Pearse, and V. B. Pearse, eds. 1991. *Reproduction of Marine Invertebrates, Vol. VI, Echinoderms and Lophophorates.* The Boxwood Press, Pacific Grove, California. 808 pp.

Gostan, G. 1956. Cas d'hermaphroditisme chez *Ophiothrix fragilis* Abildgaard. *Bull. Soc. Zool. Fr.* **81:** 85–87.

Gotto, D. M., and R. V. Gotto. 1972. *Labidoplax media* Oestergren: A sea-cucumber new to British and Irish waters, with observational notes. *Ir. Nat. J.* **17:** 250–252.

Gremare, A., and P. J. W. Olive. 1986. A preliminary study of fecundity and reproductive effort in two polychaetous annelids with contrasting reproductive strategies. *Int. J. Invert. Reprod. Dev.* **9:** 1–16.

Harriott, V. 1982. Sexual and asexual reproduction of *Holothuria atra* Jaeger at Heron Island Reef, Great Barrier Reef. Pp. 53–66 in *Papers from the Echinoderm Confr., Sydney,* F. W. E. Rowe, ed. Mem. Aust. Mus. No. 16.

Heath, D. J. 1977. Simultaneous hermaphroditism; cost and benefit. *J. Theor. Biol.* **64:** 363–373.

Heath, D. J. 1979. Brooding and the evolution of hermaphroditism. *J. Theor. Biol.* **81:** 151–155.

Heller, J. 1993. Hermaphroditism in molluscs. *Biol. J. Linn. Soc.* **48:** 19–42.

Hendler, G. 1979. Sex-reversal and viviparity in *Ophiolepis kieri,* n. sp., with notes on viviparous brittlestars from the Caribbean (Echinodermata: Ophiuroidea). *Proc. Biol. Soc. Wash.* **92:** 783–795.

Hess, H. C. 1993. The evolution of parental care in brooding spirorbid polychaetes: the effects of scaling constraints. *Am. Nat.* **141:** 577–596.

Hess, H., B. Bingham, S. Cohen, R. K. Grosberg, W. Jefferson, and L. Walters. 1988. The scale of genetic differentiation in *Leptosynapta clarki* (Heding), an infaunal brooding holothuroid. *J. Exp. Mar. Biol. Ecol.* **122:** 187–194.

Hines, A. H. 1992. Constraint on reproductive output in brachyuran crabs: Pinnotherids test the rule. *Am. Zool.* **32:** 503–511.

Hoagland, K. E. 1978. Protandry and the evolution of environmentally-mediated sex change: a study of the Mollusca. *Malacologia* **17:** 365–391.

Hunt, A. 1993. Effects of contrasting patterns of larval dispersal on the genetic connectedness of local populations of two intertidal starfish, *Patiriella calcar* and *P. exigua. Mar. Ecol. Prog. Ser.* **92:** 179–186.

Hyman, L. H. 1955. *The Invertebrates: Echinodermata. The Coelomate Bilateria,* McGraw-Hill Book Company, New York. 763 pp.

Iwasa, Y. 1991. Sex change evolution and cost of reproduction. *Behav. Ecol.* **2:** 56–68.

Kabat, A. R. 1985. The allometry of brooding in *Transennella tantilla* (Gould) (Mollusca: Bivalvia). *J. Exp. Mar. Biol. Ecol.* **91:** 271–279.

LaBarbera, M. 1989. Analyzing body size as a factor in ecology and evolution. *Annu. Rev. Ecol. Syst.* **20:** 97–117.

Leigh, E. G., E. L. Charnov, and R. R. Warner. 1976. Sex ratio, sex change, and natural selection. *Proc. Natl. Acad. Sci. U.S.A.* **73:** 3656–3660.

Leutert, R. 1975. Sex-determination in *Bonellia.* Pp. 84–90 in *Intersexuality in the Animal Kingdom,* R. Reinboth, ed. Springer-Verlag, New York.

Lindberg, D. R., and W. G. Wright. 1985. Patterns of sex change of the protandric patellacean limpet *Lottia gigantea* (Mollusca: Gastropoda). *Veliger* **27:** 261–265.

McArdle, B. H. 1988. The structural relationship: regression in biology. *Can. J. Zool.* **66:** 2329–2339.

McEuen, F. S. 1986. The reproductive biology and development of twelve species of holothuroids from the San Juan Islands, Washington. Ph.D. Thesis, University of Alberta, Edmonton. 286 pp.

McEuen, F. S. 1987. Phylum Echinodermata, Class Holothuroidea. Pp. 574–596 in *Reproduction and Development of Marine Invertebrates of the Northern Pacific Coast,* M. F. Strathmann, ed. University of Washington Press, Seattle.

McGrath, D., and D. ÓFoighil. 1986. Population dynamics and reproduction of hermaphroditic *Lasaea rubra* (Montagu) (Bivalvia, Galeommatacea). *Ophelia* **25:** 209–219.

Menge, B. A. 1974. Effect of wave action and competition on brooding and reproductive effort in the seastar, *Leptasterias hexactis. Ecology* **55:** 84–93.

Menge, B. A. 1975. Brood or broadcast? The adaptive significance of different reproductive strategies in the two intertidal sea stars *Leptasterias hexactis* and *Pisaster ochraceus. Mar. Biol.* **31:** 87–100.

Mortensen, T. 1936. Echinoidea and Ophiuroidea. *Discovery Rep.* **12:** 199–348.

Murray, J. 1964. Multiple mating and effective population size in *Cepaea nemoralis. Evolution* **18:** 283–291.

Ockelmann, K. W., and K. Muus. 1978. The biology, ecology and behaviour of the bivalve *Mysella bidentata* (Montagu). *Ophelia* **17:** 1–93.

Orton, J. H. 1928. Observations on *Patella vulgata,* Pt. I. Sex phenomena, breeding and shell growth. *J. Mar. Biol. Ass. U.K.* **15:** 851–862.

Policansky, D. 1982. Sex change in plants and animals. *Annu. Rev. Ecol. Syst.* **13:** 471–495.

Rumrill, S. S. 1982. Contrasting reproductive patterns among ophiuroids (Echinodermata) from southern Monterey Bay, U.S.A. Masters Thesis, University of California, Santa Cruz. 260 pp.

Runnström, S. 1927. Über die Entwicklung von *Leptosynapta inhaerens* (O. Fr. Müller). *Bergens Mus. Årb.* **1927(1):** 1–80.

Russell, M. P., and J. P. Huelsenbeck. 1989. Seasonal variation in brood structure of *Transennella confusa* (Bivalvia: Veneridae). *Veliger* **32:** 288–295.

Rutherford, J. C. 1973. Reproduction, growth and mortality of the holothurian *Cucumaria pseudocurata. Mar. Biol.* **22:** 167–176.

Schoppe, S., and A. Holl. 1994. Reproduction of the Caribbean ophiuroid, *Ophiothrix* sp., a protandric hermaphrodite. In *Echinoderms through Time (Echinoderms Dijon),* B. David and A. Guille, eds. A. A. Balkema, Rotterdam. In press.

Sewell, M. A. 1990. Aspects of the ecology of *Stichopus mollis* (Echinodermata: Holothuroidea) in north-eastern New Zealand. *N.Z. J. Mar. Freshw. Res.* **24:** 97–103.

Sewell, M. A. 1991. Protandry in the sea cucumber *Leptosynapta* sp. *Am. Zool.* **31:** 104A.

Sewell, M. A. 1993a. Reproductive cycle, sex change, and mortality during brooding of a viviparous sea cucumber *Leptosynapta clarki.* Ph.D. Thesis, University of Alberta, Edmonton. 154 pp.

Sewell, M. A. 1993b. Mortality of pentactulae during intraovarian brooding in the sea cucumber *Leptosynapta clarki. Am. Zool.* **33:** 110A.

Sewell, M. A., and F-S. Chia. 1994. Reproduction of the intraovarian brooding apodid *Leptosynapta clarki* (Echinodermata: Holothuroidea) in British Columbia. *Mar. Biol.* In press.

Simpson, R. D. 1982. The reproduction of some echinoderms from Macquarie Island. Pp. 39–52 in *Papers from the Echinoderm Confr., Sydney,* F. W. E. Rowe, ed. Mem. Aust. Mus. No. 16.

Smiley, S., F. S. McEuen, C. Chaffee, and S. Krishnan. 1991. Echinodermata: Holothuroidea. Pp. 663–750 in *Reproduction of Marine Invertebrates, Volume VI, Echinoderms and Lophophorates,* A. C. Giese, J. S. Pearse, and V. B. Pearse, eds. The Boxwood Press, Pacific Grove, California.

Soong, K., and J-L. Chen. 1991. Population structure and sex-change in the coral-inhabiting snail *Coralliophila violacea* at Hsiao-Liuchiu, Taiwan. *Mar. Biol.* **111:** 81–86.

Strathmann, R. R. 1990. Why life histories evolve differently in the sea. *Am. Zool.* **30:** 197–207.

Strathmann, R. R., and M. F. Strathmann. 1982. The relationship between adult size and brooding in marine invertebrates. *Am. Nat.* **119:** 91–101.

Strathmann, R. R., M. F. Strathmann, and R. H. Emson. 1984. Does limited brood capacity link adult size, brooding, and simultaneous hermaphroditism? A test with the starfish *Asterina phylactica. Am. Nat.* **123:** 796–818.

Tomlinson, J. 1966. The advantages of hermaphroditism and parthenogenesis. *J. Theor. Biol.* **11:** 54–58.

Tyler, P. A., and J. D. Gage. 1982. The reproductive biology of *Ophiacantha bidentata* (Echinodermata: Ophiuroidea) from the Rockall Trough. *J. Mar. Biol. Ass. U.K.* **62:** 45–55.

Warner, R. R. 1975. The adaptive significance of sequential hermaphroditism in animals. *Am. Nat.* **109:** 61–82.

Wright, W. G. 1989. Intraspecific density mediates sex-change in the territorial patellacean limpet *Lottia gigantea. Mar. Biol.* **100:** 353–364.

Marine
Biological
Laboratory
Woods Hole
Massachusetts

Ninety-Sixth Report
for the Year 1993
One-Hundred and Fifth Year

Officers of the Corporation

Denis M. Robinson, *Honorary Chairman of the Board of Trustees*
Sheldon J. Segal, *Chairman of the Board of Trustees*
Robert E. Mainer, *Vice Chairman of the Board of Trustees*
James D. Ebert, *President of the Corporation*
John E. Burris, *Director and Chief Executive Officer*
Robert D. Manz, *Treasurer*
Neil Jacobs, *Clerk of the Corporation*

Contents

Report of the Director R1
Report of the Treasurer R5
Financial Statements R7
Report of the Librarian R17

Educational Programs

Summer Courses R20
Short Courses R23

Summer Research Programs

Principal Investigators R29
Other Research Personnel R30
Library Readers R32
Institutions Represented R33
Year-Round Research Programs R37
Honors R43
Board of Trustees and Committees R47
Laboratory Support Staff R50

Members of the Corporation

Life Members R52
Members R53
Associate Members R64
Certificate of Organization R67
Articles of Amendment R67
Bylaws R68

Report of the Director and Chief Executive Officer

1993 marked the 105th year of the Marine Biological Laboratory and my first full year as its Director and CEO. It was an exciting time, one filled with top-flight science, excellent educational opportunities, and infrastructure change.

Scientific Activities

The MBL's year-round research program continues to be a vigorous, diverse, and well-funded mix of scientific investigations.

The largest group of year-round scientists at the MBL are in the Ecosystems Center co-directed by Jerry Melillo and John Hobbie. This group conducts field, laboratory, and computer modeling studies in areas such as coastal zone management, river basin modeling, biogeochemical cycling in the Arctic of Alaska, and the preservation of biodiversity in tropical rain forests. Its work has been central to the prediction and modeling of global climate change, especially the impact of terrestrial ecosystems. Work at the Center has also been important at the local level where studies are under way on the environment around the present outfall pipe and its future site outside of Boston Harbor.

Cutting-edge research is under way at the Architectural Dynamics in Living Cells Program where Shinya Inoué, a recently elected member of the National Academy of Sciences, and his colleagues are probing the structure of living cells at high levels of resolution. Newly developed equipment and techniques continue to allow the investigators to probe even further into the fine structure of the cell.

In the Molecular Evolution Program, studies by Mitchell Sogin and others have further elucidated the evolution of parasites relative to the later emergence of their contemporary hosts. The human pathogens of *Giardia* and *Toxoplasma* have been particularly important organisms for the study of ribosomal RNA sequences as a means of learning more about the relatedness of organisms.

Lionel Jaffe and Andrew Miller, with the input of numerous colleagues, have been carefully investigating patterns of calcium distribution to learn more about its importance in cell development and other biological phenomena. The successful transfection of the cellular slime mold *Dictyostelium* with apoaequorin has produced a strain of mold that luminesces to reveal patterns of internal free calcium during development.

In the summer, the number of scientists at the Laboratory increases several fold to over 400. The quality and diversity of their research is impressive, as is the excitement they bring. In true MBL tradition, the community gathers to share scientific information in a variety of ways: through formal evening lectures, during brown bag lunches, and in passing in the halls and streets of the MBL campus.

The active scientific interchange that occurs led this past year, as in previous years, to many experiments to test ideas. A number of these were reported at the annual General Scientific Meetings. It is at this meeting that year-round and summer scientists gather to share the results of their recent investigations at the MBL. The topics at the Meetings ranged from calcium in development to gamete physiology and biochemistry to neurobiology to behavior to comparative physiology and estuarine ecology. This extraordinary mix of topics was presented by more than 50 investigators, students, and fellows. Of these presentations, 33 were written up, reviewed, and published as short reports in the October 1993 issue of *The Biological Bulletin.*

As in previous summers, the MBL awarded a number of research fellowships. This year 22 scientists, a record number, from around the world came to the Laboratory to study topics ranging from creating computer models of neural networks, to real-time visualizations of DNA replication in mammalian

Sam Sweezy

Sam Sweezy

nuclei, to understanding the roles of kinesin and other motor proteins in mitosis and organelle transport.

All of the scientists at the MBL have benefited from the recently completed Marine Resources Center. During 1993, the facility's state-of-the-art life support and recirculating seawater systems became fully operational, allowing many of the important marine model organisms to be maintained, as well as the initiation of culturing efforts.

Two organisms that are being cultured are the dwarf surf clam, *Mulinia lateralis,* and the bay scallop, *Aquipecten irradians. Mulinia* is becoming increasingly popular as a model for studying cell division, cell cycling, gamete metabolism, and fertilization. This tiny clam, which measures no larger than a small fingernail, is proving to be as reliable a model as the surf clam, *Spisula.* As surf clams become more difficult to obtain, genetically defined, cultured *Mulinia* may provide researchers with a viable alternative model system.

Hundreds of mature *Aquipecten* are being maintained in the mariculture room as part of a joint project with Taylor Seafood. These scallops have spawned tens of millions of scallops which have recently been moved into ponds where it is hoped that they will reach maturity and eventually find their way to dinner tables around the country. Several millions of the juveniles have also been seeded in public shellfishing areas to enhance local stocks.

In addition to culturing efforts such as these, a variety of other valuable animals are maintained in the MRC. For example, the dogfish shark can now be held year-round in the facility, providing researchers whose

Steve Rosenthal

Steve Rosenthal

work has implications for such diseases as cystic fibrosis and cancer with a constant supply of healthy research organisms. Leukemic *Mya* clams are now being used in studies on the effects of PCBs under controlled conditions. And scup are being used in the investigation of how varied temperatures affect muscle physiology, respiration, and contractility.

Educational Programs

The MBL's tradition of excellence in education continued in 1993. There were a record number of students and instructors participating in the most extensive course schedule ever to be offered at the Laboratory. Eighteen courses were held in 1993, covering the neurosciences, cellular and molecular biology, developmental biology, molecular evolution, microbiology, and information science, as well as training in a variety of specialized laboratory techniques. Of particular note was the Embryology course, which celebrated its 100th anniversary.

The courses continue to be extremely popular and competitive, with the Education Office receiving over 2700 inquiries leading to the selection of more than 400 students representing 268 institutions. Many of these students were able to come because of the extensive scholarship support offered by the Laboratory. The students were joined by 382 instructors and lecturers who make it possible for the MBL to offer an unmatched, individualized educational opportunity. Not only were students able to participate in the courses, but for the first time in recent years, funds were raised that specifically supported post-course research for a limited number of students. During the post-course experience the students were able to conduct independent research based on projects begun during the laboratory sessions of their courses.

Although the MBL summer courses are for graduate and postgraduate students, undergraduates have an opportunity to study at the Laboratory primarily in the Boston University Marine Program. BUMP has now grown to almost 70 undergraduates and graduates who are here mainly in the fall to take a wide variety of courses. The graduate students spend year-round taking courses and doing research under the five full-time Boston University faculty now in residence in Woods Hole.

Infrastructure

The MBL was the site of changes in both its governance and physical infrastructure in 1993. The governance changes voted in 1992 were implemented successfully at the February 1993 meeting of the MBL Board of Trustees. During 1993, three new Trustees were elected to the Board: Paul Marks, President and CEO of Memorial Sloan-Kettering Cancer Center; Philip Needleman, President of Searle Research and Development; and William Steere, Jr., Chairman and CEO of Pfizer, Inc. The first Science Council, chaired by George Langford, was elected by the Corporation at its August meeting.

Our physical plant received significant attention in 1993. Extensive renovations to the Lillie Research Building are nearing completion as I write; this project was supported in part by a grant from the National Science Foundation. We also completed construction of the Marine Resources Center's Collection Support Facility, which includes a diving support facility. Finally, the Brick Apartment Dormitory has been modernized and refitted with new plumbing, wiring, and storm windows.

An important part of any institutional growth is a positive funding situation. The MBL was most fortunate this year to receive several major gifts that increased our endowment by more than 20%. Foremost among these were gifts from Dr. Ellen Grass and the Grass Foundation and bequests from Anita Zorzoli and Harold Glassman. It was also particularly gratifying that the annual fund reached a new record of $272,000, a 15% increase over 1992's total.

Looking Ahead

1993 was a good year for the Marine Biological Laboratory, as recounted in the preceding outline of the many positive research and educational activities, as well as infrastructural and financial ones. In an era of austerity and general pessimism about science, it is gratifying to be able to provide such good news. Will I be able though to continue to provide such positive reports?

My sense is that things indeed will continue to improve. As the Laboratory confronts the changing patterns of both research and funding, its small size and unique status will continue to allow it to initiate and react quickly to new opportunities. Flexibility and a diverse funding base appear to me to be crucial traits of the MBL that will enable us to deal with change. Our educational and research programs fill a niche occupied by few, if any, other institutions. The loyalty and generosity of our Corporation members, as well as the friends of the Laboratory and long-time Foundation supporters, encourage optimism about the Laboratory's continuing to contribute to the life sciences and remaining an attractive place for the independent researcher who is searching for the freedom of the MBL research environment.

I look forward to seeing many of you in 1994, the 106th year in the long and distinguished history of the Marine Biological Laboratory.

—John E. Burris

Report of the Treasurer

A year ago, in reviewing the financial results for 1992, I reported that we had entered a period of transition, and had come through the initial phase of that transition in a modestly successful financial manner. I also reported that as we looked forward to 1993, we sensed a continuing and an improving financial stability.

I am happy to report that the 1993 financial results have continued the financial progress we witnessed in 1992, and have even exceeded our expectations. In 1993, we had the most successful financial operating results in the recent history of the MBL.

We finished the year with an excess of revenues over expenditures in the current unrestricted fund of $657,774. After mandatory transfers to fund debt principal of $67,339 and the procurement of equipment in the amount of $92,485, I am pleased to report that we funded a portion of our depreciation by transferring $494,490 to the renewals and replacement plant fund. For the Housing Auxiliary, the funding of the renewals and replacement fund was $184,490; more significantly, for the first time in my tenure as Treasurer, we were able to transfer $310,000 to the general operations renewal and replacement fund for use in future major capital repairs and improvements.

I cannot emphasize enough the importance of this modest but significant financial achievement by the MBL, for it fulfills a long-standing goal of the Trustees. Therefore, I report to you the first step in what we hope will be a continuing and annual outcome of future financial operations. To put things in perspective, it should be understood that this funding of depreciation is far less than the amount of $1,183,814 reported in the financial statements and also far less than the $750,000 on the urgent deferred maintenance and repair schedule, but it is a start and a record we can build on in the future.

Private gift giving at the MBL continues to improve, and in 1993 we experienced the best year in modern history from the standpoint of private gift giving, recording over $5.2 million dollars with almost 53% going into the endowment fund. Continuing the success of last year, our annual fund increased by 15%, reflecting a new sense of vitality and confidence in the community (Fig. 1).

The value of our endowment funds increased by 22%, most of which is attributed to private gift support, but also including over $900,000 of growth in the value of our money through portfolio appreciation (Figs. 2,3).

Other noteworthy financial information, not directly reflected in the financial statements, includes a four

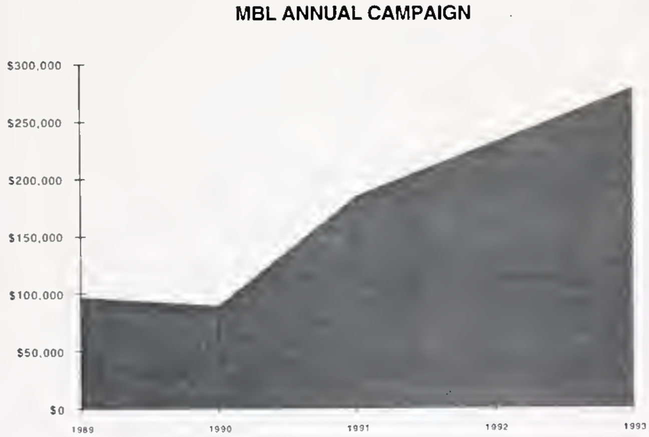

Figure 1

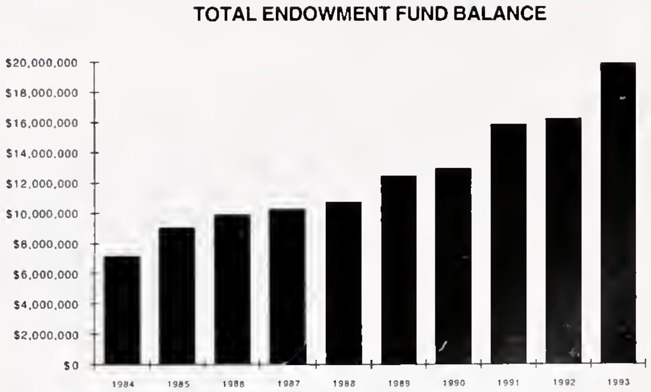

Figure 2

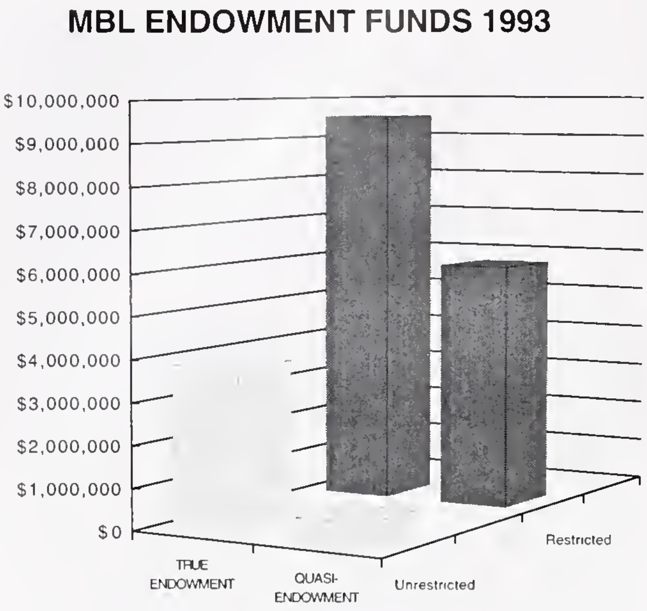

Figure 3

year overhead agreement at 51% with the Department of Health and Human Services, which should add a great deal of stability to our financial planning. In addition, we were able to obtain from the same organization approval to fund our post retirement health care liability through our fringe benefit rate.

The financial achievements of 1993 represent a stepping stone to the future. We must, however, intensify our efforts to improve the financial infrastructure and flexibility of the MBL. This can be achieved by increasing our endowment, as well as by increasing the size of our relatively small scientific support base. Only with increased financial resources will we be able to maintain and enhance the excellent research and educational opportunities offered by the Laboratory.

—Robert D. Manz

Coopers
&Lybrand

certified public accountants

REPORT OF INDEPENDENT ACCOUNTANTS

To the Board of Trustees of
Marine Biological Laboratory
Woods Hole, Massachusetts

We have audited the accompanying balance sheet of Marine Biological Laboratory as of December 31, 1993 and the related statement of support, revenues, expenses and changes in fund balances for the year then ended. We previously examined and reported upon the financial statements of the Laboratory for the year ended December 31, 1992, for which condensed statements are presented for comparative purposes only. These financial statements are the responsibility of the Laboratory's management. Our responsibility is to express an opinion on these financial statements based on our audit.

We conducted our audit in accordance with generally accepted auditing standards. Those standards require that we plan and perform the audit to obtain reasonable assurance about whether the financial statements are free of material misstatement. An audit includes examining, on a test basis, evidence supporting the amounts and disclosures in the financial statements. An audit also includes assessing the accounting principles used and significant estimates made by management, as well as evaluating the overall financial statement presentation. We believe that our audit provides a reasonable basis for our opinion.

In our opinion, the financial statements referred to above present fairly, in all material respects, the financial position of Marine Biological Laboratory at December 31, 1993, and its support, revenues, expenses and changes in fund balances for the year then ended in conformity with generally accepted accounting principles.

Our audit was conducted for the purpose of forming an opinion on the basic financial statements taken as a whole. The supplemental schedules of support, revenues, expenses and changes in fund balances for current funds (Schedule I), endowment funds (Schedule II) and plant funds (Schedule III) as of December 31, 1993 are presented for purposes of additional analysis and are not a required part of the basic financial statements. Such information has been subjected to the auditing procedures applied in the audit of the basic financial statements and, in our opinion, is fairly stated, in all material respects, in relation to the basic financial statements taken as a whole.

Coopers & Lybrand

Boston, Massachusetts
April 20, 1994

MARINE BIOLOGICAL LABORATORY

BALANCE SHEETS

December 31, 1993
(with comparative totals for 1992)

ASSETS	1993	1992
Cash	$ 580,165	$ 499,514
Restricted cash	9,354	6,667
Investments, at market (Note C)	2,048,483	1,628,270
Accounts receivable, net of allowance for doubtful accounts of $10,000 and $8,000	804,955	597,946
Receivables due for costs incurred on grants and contracts	906,011	625,857
Other assets	421,392	180,927
Total current assets	4,770,360	3,539,181
Restricted cash (Note E)	54,847	285,094
Investments, at market (Notes C and D)	21,636,024	18,236,843
Deposits with trustee (Note F)	492,852	1,492,410
Fixed assets (Note B):		
Land	689,661	689,660
Buildings	29,403,841	27,716,029
Equipment	3,120,483	3,024,613
Construction in progress	1,148,917	131,078
	34,362,902	31,561,380
Less accumulated depreciation	(11,884,268)	(10,707,699)
	22,478,634	20,853,681
Total assets	$49,432,717	$44,407,209

LIABILITIES AND FUND BALANCES	1993	1992
Current portion of long-term debt (Note F)	$ 69,010	$ 65,000
Accounts payable and accrued expenses	1,489,146	1,278,535
Deferred income	240,672	250,490
Total current liabilities	1,798,828	1,594,025
Accounts payable (Note E)	218,050	208,167
Annuities payable (Note B)	157,359	184,553
Long-term debt (Note F)	2,475,680	2,535,000
Deferred support (Note G)	3,796,864	3,518,263
Total long-term liabilities	6,647,953	6,445,983
Commitments (Note E)		
Total liabilities	8,446,781	8,040,008
Current unrestricted fund balances	32,097	12,857
Annuities fund balance	70,115	145,435
Endowment fund balances:		
Quasi-endowment unrestricted	595,694	548,061
Endowment, income for unrestricted purposes	3,876,604	3,765,379
Endowment, income for restricted purposes	9,547,900	6,337,988
Quasi-endowment restricted	5,907,490	5,629,395
Total endowment funds	19,927,688	16,280,823
Plant fund balances:		
Unrestricted	19,869,320	19,708,718
Repairs and replacement reserve	546,838	196,470
Restricted	539,878	22,898
Total plant funds	20,956,036	19,928,086
Total liabilities and fund balances	$49,432,717	$44,407,209

The accompanying notes are an integral part of the financial statements.

MARINE BIOLOGICAL LABORATORY

STATEMENT OF SUPPORT, REVENUES, EXPENSES AND CHANGES IN FUND BALANCES

for the year ended December 31, 1993
(with appropriate totals for 1992)

	Current Funds										
	Unrestricted					Endowment Funds		Plant Funds		1993	1992
	Operating Fund	Auxiliary Enterprises Fund	Total	Restricted Funds	Annuity Fund	Unrestricted	Restricted	Unrestricted	Restricted	Total All Funds	Total All Funds
SUPPORT AND REVENUES:											
Grant reimbursements of direct costs				$5,565,338						$ 5,565,338	$ 5,982,265
Grant for capital additions									$1,450,632	1,450,632	4,032,660
Recovery of indirect costs	$3,711,139		$3,711,139							3,711,139	3,530,621
Tuition				611,700						611,700	485,247
Fee for services	1,325,443	$1,993,746	3,319,189	162,115						3,481,304	3,274,931
Investment income	415,137		415,137	521,022	$ 1,208				31,362	968,729	927,910
	5,451,719	1,993,746	7,445,465	6,860,175	1,208				1,481,994	15,788,842	18,233,634
Gifts	572,556		572,556	1,845,424	12,598		$ 2,779,659		44,000	5,254,237	1,678,279
Change in deferred support	527,945		527,945	(806,546)						(278,601)	773,442
	1,100,501		1,100,501	1,038,878	12,598		2,779,659		44,000	4,975,636	2,451,721
Miscellaneous revenue	106,548		106,548	332,275					60,000	498,823	446,383
Total support and revenues	6,658,768	1,993,746	8,652,514	8,231,328	13,806		2,779,659		1,585,994	21,263,301	21,131,738
EXPENSES:											
Research				5,727,323						5,727,323	6,019,891
Instruction				1,538,190						1,538,190	1,526,154
Scholarships, fellowships and stipends				447,454						447,454	394,544
Services	1,962,483	1,611,963	3,574,446	381,849						3,956,295	3,892,623
Administration	2,412,999	157,293	2,570,292	6,820						2,577,112	2,761,753
Plant operations	1,850,002		1,850,002	111				$ 72,493		1,922,606	1,785,659
Depreciation								1,183,814		1,183,814	722,959
Other				248,238	15			—		248,253	246,981
Total expenses	6,225,484	1,769,256	7,994,740	8,349,985	15		—	1,256,307	—	17,601,047	17,350,564
Excess (deficit) of support and revenues over expenses	433,284	224,490	657,774	(118,657)	13,791		2,779,659	(1,256,307)	1,585,994	3,662,254	3,781,174
Net realized gain (loss) on investments				155,460	$(86,616)	$ 32,841	955,896			1,057,581	1,000,393
Net unrealized gain (loss) on investments				(58,026)	(2,495)	4,142	(44,721)			(101,100)	(936,136)
Total gain on investments				97,434	(89,111)	36,983	911,175		—	956,481	64,257
Transfers	(414,044)	(224,490)	(638,534)	21,223	—	10,650	(91,602)	1,767,277	(1,069,014)	—	—
Net change in fund balances	19,240	—	19,240	—	(75,320)	47,633	3,599,232	510,970	516,980	4,618,735	3,845,431
Fund balances, beginning of year	12,857	—	12,857	—	145,435	548,061	15,732,762	19,905,188	22,898	36,367,201	32,521,770
Fund balances, end of year	$ 32,097	—	$ 32,097	—	$ 70,115	$595,694	$19,331,994	$20,416,158	$539,878	$40,985,936	$36,367,201

The accompanying notes are an integral part of the financial statements.

Marine Biological Laboratory

Notes to Financial Statements

A. *Purpose of the Laboratory:*

The purpose of Marine Biological Laboratory (the "Laboratory") is to establish and maintain a laboratory or station for scientific study and investigations, and a school for instruction in biology and natural history.

B. *Significant Accounting Policies:*

Basis of Presentation—Fund Accounting

In order to ensure observance of limitations and restrictions placed on the use of resources available to the Laboratory, the accounts of the Laboratory are maintained in accordance with the principles of fund accounting. This is the procedure by which resources are classified into separate funds in accordance with specified activities or objectives. Separate accounts are maintained for each fund; however, in the accompanying financial statements, funds that have similar characteristics have been combined into fund groups. Accordingly, all financial transactions have been recorded and reported by fund group.

Externally restricted funds may only be utilized in accordance with the purposes established by the donor or grantor of such funds. However, the Laboratory has full control over the utilization of unrestricted funds. Restricted gifts, grants, and other restricted support are accounted for in the appropriate restricted funds. Restricted current funds are reported as revenue as the related costs are incurred (see Note G).

Endowment funds are subject to restrictions which require that the principal be invested in perpetuity. Related investment income is available for use for restricted or unrestricted purposes by the Laboratory depending on donor restrictions. Quasi-endowment funds have been established by the Laboratory for the same purposes as endowment funds; however, the principal of these funds may be expended for various restricted and unrestricted purposes at the direction of the Trustees.

Fixed Assets

Land, buildings and equipment purchased by the Laboratory are recorded at cost. Donated fixed assets are recorded at fair market value at the date of the gift. Depreciation is computed using the straight-line method, beginning the month after the asset is placed in service, over the asset's estimated useful life. Estimated useful lives are generally three to five years for equipment and 20 to 40 years for buildings and improvements. When assets are sold or retired, the cost and accumulated depreciation are removed from the accounts and any resulting gain or loss is included in income for the period.

Contracts and Grants

Revenues associated with contracts and grants are recognized in the statement of support, revenues, expenses and changes in fund balances as the related costs are incurred (see Note G). Reimbursement of indirect costs relating to government contracts and grants is based on negotiated indirect cost rates. Any over or underrecovery of indirect costs is recognized through future adjustments of indirect cost rates.

Investments

Investments purchased by the Laboratory are carried at market value. Money market securities are carried at cost plus accrued interest, which approximates market value. Donated investments are recorded at fair market value at the date of the gift. For determination of gain or loss upon disposal of investments, cost is determined based on the first-in, first-out method.

The Laboratory is the beneficiary of certain investments reported in the endowment funds which are held in trust by others. The Laboratory's continuing right to these funds is subject to review every 10 years by an independent committee. The market values of such investments are $4,873,242 and $4,743,257 at December 31, 1993 and 1992, respectively. The income on these investments totaled $226,702 and $219,050 in 1993 and 1992, respectively.

Investment Income and Distribution

The Laboratory follows the accrual basis of accounting except that investment income is recorded on a cash basis. The difference between such basis and the accrual basis does not have a material effect on the determination of investment income earned on a year-to-year basis.

Investment income includes income from a pooled investment account, which income is allocated to the participating funds on the market value unit basis (Note D).

Annuities Payable

Amounts due to donors in connection with gift annuities are determined based on remainder value calculations, as of December 31, 1993 with varied assumptions of rates of return and payout terms.

Reclassifications

Certain 1992 balances have been reclassified for comparative purposes. In 1993, the laboratory reclassified the revenues, expenses and fund balances related to annuity contracts from the current fund into a separate Annuity Fund.

Tax-Exempt Status

The Laboratory is exempt from federal income tax under Section 501(c)3 of the Internal Revenue Code.

C. *Investments:*

The following is a summary of the cost and market value of investments at December 31, 1992 and 1991:

	Market		*Cost*	
	1993	*1992*	*1993*	*1992*
Certificates of deposit	$ 48,483	$ 47,700	$ 48,483	$ 46,745
Money market securities	4,822,875	1,952,867	4,822,875	1,952,867
U.S. Government securities	—	1,788,066	—	1,771,308
Corporate fixed income	9,706,380	8,968,745	8,824,824	8,533,859
Common stocks	9,093,522	6,764,488	7,052,496	4,173,965
Real estate	13,247	343,247	13,247	343,247
Total investments	$23,684,507	$19,865,113	$20,761,925	$16,821,991

Investments by fund group and related portfolios for the years ended December 31, 1993 and 1992 are as follows:

	Market		*Cost*	
	1993	*1992*	*1993*	*1992*
Current Funds				
Certificates of deposit	$ 48,483	$ 47,700	$ 48,483	$ 46,745
Money market securities	2,000,000	1,400,000	2,000,000	1,400,000
Library funds	—	180,570	—	183,548
Total	2,048,483	1,628,270	2,048,483	1,630,293
Long-Term Funds				
Endowment and quasi-endowment				
General endowment trust fund	3,855,724	3,755,124	3,135,652	2,897,718
Library endowment trust fund	1,017,518	988,133	807,175	753,904
Ecosystem funds	4,829,277	4,507,857	4,029,966	3,756,446
Pooled funds	10,343,724	6,910,904	9,187,655	5,806,114
Instruction fund	1,378,838	1,731,578	1,339,557	1,634,269
Other Funds:				
State Street Annuity Fund	197,696	—	200,190	—
Real Estate	13,247	343,247	13,247	343,247
Total	21,636,024	18,236,843	18,713,442	15,191,698
Total investments	$23,684,507	$19,865,113	$20,761,925	$16,821,991

D. *Accounting for Pooled Investments:*

Certain endowment fund assets are pooled for investment purposes. Investment income from the pooled investment account is allocated on the market value unit basis, and each endowment fund subscribes to or disposes of units on the basis of the market value per unit at the beginning of the calendar quarter within which the transaction takes place. The unit participation of the funds at December 31, 1993 and 1992 is as follows:

	1993	*1992*
Quasi-endowment unrestricted	4,342	4,260
Quasi-endowment restricted	8,771	8,717
Endowment, income for restricted purposes	62,158	40,345
Endowment, income for unrestricted purposes	152	79
Total	75,423	53,401

Pooled investment activity on a per-unit basis was as follows:

	1993	*1992*
Unit value at beginning of year	$128.66	$128.42
Unit value at end of year	137.18	128.66
Increase in realized and unrealized appreciation	8.52	.24
Net income earned on pooled investments	4.52	5.71
Total return on pooled investments	$ 13.04	$ 5.95

E. *Deposits and Commitments for Construction Programs:*

As of December 31, 1993, the Laboratory has $492,852 in Deposit with Trustees for the renovations of laboratories. On December 31, 1993, the Laboratory was contractually obligated for approximately $579,463 of additional expenditures in connection with its current building program. The expenditures are covered by funding commitments.

F. *Long-Term Debt:*

Long-term debt at December 31, 1993 amounted to $2,544,690. The aggregate amount of principal due for each of the next five fiscal years and thereafter is as follows:

1994	$ 69,010
1995	79,010
1996	76,670
1997	80,000
1998	85,000
Thereafter	2,155,000
	2,544,690
Less current portion	69,010
Total	$2,475,680

In 1992, the Laboratory issued $1,100,000 Massachusetts Industrial Finance Authority (MIFA) Series 1992A Bonds and $1,500,000 MIFA Series 1992B. These bonds pay varying annual interest rates and Series 1992 A and B Bonds mature on December 1, 2012. The Series 1992 A and B Bonds are collateralized by a first mortgage on certain Laboratory property.

In compliance with the 1992 MIFA bond indentures, the Laboratory has on deposit with State Street Bank and Trust, as trustee for Series 1992 Bonds, investments for construction projects in the amount of $492,852.

Under the most restrictive covenant of long-term debt, the Laboratory's operating surplus (before transfers), interest, expense and transfers from the quasi-endowment for debt service must equal or exceed all debt service payments.

G. *Restricted Current Funds Deferred Support:*

The Laboratory defers revenue on current restricted funds until the related costs are incurred. Amounts received in excess of expenses are recorded as deferred support. The following summarizes the activity of the deferred support account:

	1993	*1992*
Balance at beginning of year	$3,518,263	$4,291,705
Additions:		
Gifts, endowment income and grants received	8,509,929	7,997,702
Net unrealized gains (losses)	(58,026)	(77,518)
Net realized gains	155,460	78,636
Transfers	21,223	—
Deductions:		
Funds expended under gifts and grants	8,349,985	8,722,851
Transfers	—	49,411
Balance at end of year	$3,796,864	$3,518,263

Deferred restricted gifts of $527,945 and $453,970 were expended in 1993 and 1992, respectively, for the support of indirect costs attributable to the Laboratory's instruction programs.

H. *Retirement Plan:*

The Laboratory participates in the defined contribution pension plan of TIAA-CREF (the "Plan"). The Plan is available to permanent employees that have completed two years of service. Under the Plan, the Laboratory contributes 10% of total compensation for each participant. Contributions amounted to $507,324 in 1993 and $502,215 in 1992.

I. *Pledges:*

As of December 31, 1993, the Laboratory has outstanding pledges of $420,948 of which $399,948 is restricted (unaudited). Pledges are not included in the financial statements since it is not practicable to estimate the net realizable value of such pledges. These pledges are scheduled to be paid over the next four years in the amounts of $315,248, $87,700, $12,000, and $7,000, respectively.

J. *Interfund Borrowings:*

Current unrestricted fund interfund borrowings at December 31 are as follows:

	1993	*1992*
Due from restricted education funds	$ 31,098	
Due to restricted endowment fund	(6,445)	$(118,755)
Due from (to) restricted quasi-endowment funds	125,000	(50)
Total	$149,653	$(118,805)

K. *Financial Accounting Standard No. 106:*

In December 1990, the Financial Accounting Standards Board (FASB) released Statement No. 106, "Employers' Accounting for Postretirement Benefits Other Than Pensions." This new standard requires employers to accrue, during the years that the employee renders the necessary service, the expected cost of benefits to be provided during retirement. On November 20, 1993, the Laboratory adopted Statement No. 106 for the year beginning January 1, 1994 and intends to record the accumulated benefit obligation of $1,588,000 over a twenty-year amortization period.

The Laboratory's policy is that all current retirees and certain eligible employees who retire prior to June 1, 1994 will continue to receive postretirement health benefits. The remaining current employees will continue to receive benefits; however, those benefits will be limited as defined by the Plan. Employees hired on or after January 1, 1995 will not be eligible to participate in the postretirement medical benefit plan.

SCHEDULE I

MARINE BIOLOGICAL LABORATORY

STATEMENT OF SUPPORT, REVENUES, EXPENSES AND CHANGES IN FUND BALANCES

CURRENT FUNDS

for the year ended December 31, 1993

	Current Unrestricted Funds				
	Operating Fund	*Auxiliary Enterprises Fund*	*Total*	*Current Restricted Fund*	*Total*
SUPPORT AND REVENUES:					
Grant reimbursements of direct costs				$5,565,338	$5,565,338
Recovery of indirect costs	$3,711,139		$3,711,139		3,711,139
Tuition				611,700	611,700
Fees for services:					
Dormitories		$1,077,547	1,077,547		1,077,547
Dining hall		916,199	916,199		916,199
Library	437,352		437,352		437,352
Biological Bulletin	235,993		235,993		235,993
Research services	423,760		423,760	162,115	585,875
Marine resources	228,338		228,338		228,338
Investment income	415,137		415,137	521,022	936,159
	5,451,719	1,993,746	7,445,465	6,860,175	14,305,640
Gifts	572,556		572,556	1,845,424	2,417,980
Change in deferred support	527,945		527,945	(806,546)	(278,601)
	1,100,501		1,100,501	1,038,878	2,139,379
Miscellaneous revenue	106,548		106,548	332,275	438,823
Total support and revenues	6,658,768	1,993,746	8,652,514	8,231,328	16,883,842
EXPENSES:					
Research				5,727,323	5,727,323
Instruction				1,538,190	1,538,190
Scholarships, fellowships and stipends				447,454	447,454
Services:					
Dormitories		829,274	829,274		829,274
Dining hall		782,689	782,689		782,689
Library	768,366		768,366	203,994	972,360
Biological Bulletin	185,744		185,744		185,744
Research services	560,961		560,961	168,836	729,797
Marine resources	447,412		447,412	9,019	456,431
Administration:					
Administration	2,066,297	157,293	2,223,590	6,820	2,230,410
Sponsored projects administration	346,702		346,702		346,702
Plant operations	1,850,002		1,850,002	111	1,850,113
Other				248,238	248,238
Total expenses	6,225,484	1,769,256	7,994,740	8,349,985	16,344,725
Excess of support and revenues over expenses	433,284	224,490	657,774	(118,657)	539,117
Net unrealized gain on investments				155,460	155,460
Net realized (loss) on investments				(58,026)	(58,026)
Net gain on investments				97,434	97,434
TRANSFERS AMONG FUNDS:					
Debt service	(27,339)	(40,000)	(67,339)		(67,339)
Acquisition of fixed assets	(92,485)	—	(92,485)		(92,485)
Repairs and replacement	(310,000)	(184,490)	(494,490)		(494,490)
Endowment transfer				325,000	325,000
Capitalization of income				(227,847)	(227,847)
Other	15,780		15,780	(75,930)	(60,150)
Total transfers among funds	(414,044)	(224,490)	(638,534)	21,223	(617,311)
Net change in fund balances	19,240		19,240		19,240
Fund balances, beginning of year	12,857		12,857		12,857
Fund balances, end of year	$ 32,097		$ 32,097		$ 32,097

SCHEDULE II

MARINE BIOLOGICAL LABORATORY

STATEMENT OF SUPPORT, REVENUES, EXPENSES AND CHANGES IN FUND BALANCES

ENDOWMENT FUNDS

for the year ended December 31, 1993

	Unrestricted	*Restricted*				
	Quasi-Endowment	*Income for Unrestricted Purposes*	*Income for Restricted Purposes*	*Quasi-Endowment*	*Total Restricted*	*Total*
SUPPORT AND REVENUES:						
Gifts		$ 10,000	$2,769,509	$ 150	$ 2,779,659	$ 2,779,659
Total support and revenues		10,000	2,769,509	150	2,779,659	2,779,659
Net realized gain on investments	$ 32,841	238,531	389,749	327,616	955,896	988,737
Net unrealized gain (loss) on investments	4,142	(137,306)	34,453	58,132	(44,721)	(40,579)
Net gain (loss) on investments	36,983	101,225	424,202	385,748	911,175	948,158
TRANSFERS AMONG FUNDS:						
Capitalization of income	10,650			217,197	217,197	227,847
Endowment transfers				(325,000)	(325,000)	(325,000)
Other transfers			16,201	—	16,201	16,201
Total transfers among funds	10,650		16,201	(107,803)	(91,602)	(80,952)
Net change in fund balances	47,633	111,225	3,209,912	278,095	3,599,232	3,646,865
Fund balances, beginning of year	548,061	3,765,379	6,337,988	5,629,395	15,732,762	16,280,823
Fund balances, end of year	$ 595,694	$ 3,876,604	$ 9,547,900	$ 5,907,490	$19,331,994	$19,927,688

SCHEDULE III

MARINE BIOLOGICAL LABORATORY

STATEMENT OF SUPPORT, REVENUES, EXPENSES AND CHANGES IN FUND BALANCES

PLANT FUNDS

for the year ended December 31, 1993

	Unrestricted				
	Unrestricted	*Repairs and Replacements Reserve*	*Total Unrestricted*	*Restricted*	*Total*
SUPPORT AND REVENUES:					
Grant for capital additions				$1,450,632	$ 1,450,632
Gifts				44,000	44,000
Investment income				31,362	31,362
Other revenue				60,000	60,000
Total support and revenues				1,585,994	1,585,994
EXPENSES:					
Depreciation	$ 1,183,814		$ 1,183,814		1,183,814
Plant operations		$ 72,493	72,493		72,493
Total expenses	1,183,814	72,493	1,256,307		1,256,307
Excess (deficit) of support and revenues over expenses	(1,183,814)	(72,493)	(1,256,307)	1,585,994	329,687
TRANSFERS AMONG FUNDS:					
Debt service	67,339		67,339		67,339
Acquisition of fixed assets	92,484		92,484		92,484
Capital additions	1,184,593		1,184,593	(1,069,014)	115,579
Repairs and replacements		494,490	494,490		494,490
Other transfers		(71,629)	(71,629)		(71,629)
Total transfers among funds	1,344,416	422,861	1,767,277	(1,069,014)	698,263
Net change in fund balances	160,602	350,368	510,970	516,980	1,027,950
Fund balances, beginning of year	19,708,718	196,470	19,905,188	22,898	19,928,086
Fund balances, end of year	$19,869,320	$ 546,838	$20,416,158	$ 539,878	$20,956,036

Report of the Librarian

The Library

In 1993 the MBL/WHOI Library moved towards greater inter-office cooperation. This effort was evident through our improved services, policies, budgets, planning and collections.

The journal collection

The journal cancellation process conducted in 1993 reflected the planning and cooperative efforts undertaken by staff and scientists throughout all the Woods Hole institutions. To get a profile of current use patterns, the Library staff conducted an overview of reading room materials being copied by and for WHOI, MBL, USGS, and NMFS patrons.

After twice circulating a preliminary list of MBL-collected journals being considered for cancellation, 60 subscriptions were ultimately cancelled for 1994. Many of these journals will still be available as part of our reciprocal agreement with Brandeis University. Articles from the cancelled series can be requested for quick delivery through the Library's interlibrary loan service, and the tables of contents will be provided in the Bay Reading Room as they are published.

The book collection

The WHOI Research Librarian oversaw a project to collect and analyze areas of our monograph collection that need strengthening. In response to the analysis, the MBL/WHOI Library Joint Advisory Committee approved a new procedure to expand the monograph collection. The procedure involves assigning Library Coordinators from the departments and groups of our sponsoring institutions. These coordinators will provide a list of proposed acquisitions, and texts will be purchased from that list. Twelve departments were represented at the first meeting.

Library staff have evaluated, rearranged, labeled, expanded, and updated the Grass Reference Room collection. They have also added to the collection laboratory manuals, bibliographic material, general reference books, directories, writing and field guides, handbooks, dictionaries, guides to research and a much requested collection on Woods Hole and its scientific community. The Library also received books from the July 1993 Book Publishers Fair. Publishers from Oxford, Harvard, Yale University Press, AAUP, Sinauer, and Freeman continue to donate what amounts to 15 percent of the Library's collection.

The book recall is in its final stages. More than 5,000 books were returned to the Library for bar-coding, and have been entered into the electronic catalog.

The volunteers

The Library took advantage of strong community support, and, with the help of the MBL Associates, established a volunteer program. Volunteers have been willing and productive as they work in the book stacks, gather data, repair monographs and improve the operations of the Library. The Rare Book and Archive volunteers, Dr. and Mrs. Robert Huettner, mounted three major exhibits in the Lillie Lobby in the past year: *On the Street Where You Live*, *Voyeurs of Exploration*, and currently, *Women of Science at Woods Hole*. Garfield Arthur and Linda Landland continue their work in the Data Library at Clark with the ALVIN Video collections, and Roger Longley and Fred Pratt have made headway with the maps and charts collections. We are very grateful to the volunteers, all of whom donate their time unselfishly to the Library. We hope to continue this program in the future.

The archives, preservation, and rare books collection

The Library has many volumes that require restoration. A few volumes at a time are being selected for professional repair. For example, the Leuckart teaching charts—examples of outstanding biological illustration—have been photographed and stored in newly constructed cabinets. These charts are also being digitized for electronic distribution and use as a teaching tool.

As part of the computerization of our collection, we have been cataloging the obscure records of our rare books. More than half the collection can now be viewed on the public access terminals. Before long, the entire archival book collection will be available on the terminals.

Cataloging

The Library has a number of classic volumes on oceanographic expeditions and hydrographic cruises. This valuable collection has been cataloged and entered into our local database. To get a sense of the richness of this resource, one need go no further than the "A"'s, where one can find information on Arctic and Antarctic expeditions; Agassiz's cruises on the BLAKE; Albert I, Prince of Monaco's expeditions from 1889 to 1922; the Allan Hancock Atlantic Expeditions; and cruises of the ANTON DOHRN.

Cooperative relationships

The MBL/WHOI Library received part of a Boston Library Consortium (BLC) grant called *At Your Service: High speed delivery of text and graphic library resources.* Through the federal LSCA pilot project grant the cooperating libraries provide faster and higher-quality document transmission to BLC members, via the Internet and high speed/high resolution scanning workstations. Students, faculty, investigators, and staff of the academic institutions who have sophisticated information needs will find this resource particularly useful.

With the addition of the University of Massachusetts' four campus libraries, the BLC has increased its library membership to 14. The cooperative association of these academic and research libraries support resource sharing and service enhancement. A computerized Gateway information service facilitates access to research materials by providing a link to the catalogs and union lists of participating libraries, reciprocal interlibrary loan and document delivery, borrowing privileges and a card program that identifies patrons and allows them to register at consortium libraries.

The user-friendly electronic library

Scientists working in Woods Hole or across the globe may obtain the Library's electronic services throughout the year. The *User Friendly Electronic Library Services* handbook is a guide through the myriad of electronic services available from the Library. Researchers can access catalogs of other libraries and universities, perform literature searches in dozens of databases, keep up to date on the latest journal issues in our own stacks, view the tables-of-contents of a publication, and order documents to be faxed to a laboratory or office.

WHOI branch libraries

Bill Dunkle of the Data Library is developing a display that depicts the U.S. Navy's role in creating the American Oceanography Program. The Data Library is also developing a database for Lowering Summary Data for ANGUS, ARGO, and Jason. The information in this database will be available through an index for all lowerings carried out by these platforms.

In 1993, the Documents Library acquired more than 600 technical documents. One example, the ALVIN bibliography, contains more than 1,000 bibliographic records of the ALVIN dives, and has been mounted on a WHOI computer server. It can be accessed through the Internet library called Gopher. The Documents Library also started an outreach program to explain the new electronic services.

Gifts and donations

The Library used a grant from the Bay Foundation to expand electronic access to indices mounted on the network. This gift provided 10 additional databases in the areas of ecology fisheries and water resource management. The Library also established book funds in 1993 in memory of Dr. Kimball Atwood, Dr. Allyn Vine and Dr. Henry Stommel. Dr. Thomas Brock donated to the Library a research collection of microbiology monographs.

The Information Systems Division

The Information Systems Division (ISD) managed electronic support for Library systems. ISD implemented new "friendlier" Internet tools such as Gopher and Mosaic, and established policies on the use of the network. To ensure physical and electronic security, ISD initiated new policies that limited access to our resources. ISD installed more than 100 new network connections this year, including connections in the Whitman research labs as well as the renovated space in Lillie. ISD expanded its instructional classes, and began outreach to local Falmouth hospital staff and the general community. ISD also taught introductory courses in Medical Informatics to more than 400 students in 1993.

Library leadership

Last year, the joint MBL/WHOI Trustees' Library Planning Committee gave a report to both institutions. Trustees unanimously agreed on the goals of the Library, stating: the primary mission of the MBL/WHOI Library is to provide, in a collaborative and collegial environment, access to the best available information essential to scientific research and teaching at the two institutions.

Other professionals in the community meet their needs through contractual agreements. They recommend three developmental priorities:

- A provision in the Library's budget for Library leadership, informatics expertise and fund-raising capacity.
- Renovations of the Library space in Lillie to restrict access, improve lighting, reduce the risk of fire, install fire alarm systems, climate control, and repave the building envelope.
- Preserving deteriorating volumes that should remain in the collections.

Dr. David Stonehill finished his mission at the MBL/WHOI Library this past February. After his three-year stay here, with sponsorship from the Mellon grant, Dr. Stonehill went on to another leadership role at Miami University in Ohio. Carol Winn, the Research Librarian at WHOI, retired in June, 1994. Catherine Norton, the new Head Librarian, holds a joint appointment from both MBL and WHOI. Happily, this important transition for the Library and its staff has been a smooth one.

—Catherine Norton

Peter Sutter

Educational Programs

Summer Courses

Biology of Parasitism

(June 13–August 14)

Director
John Boothroyd, Stanford University School of Medicine

Associate Director
Richard Komuniecki, University of Toledo

Course Faculty
Richard Davis, San Francisco State University
Jean-Francois Dubremetz, INSERM
Fred Finkelman, USUHS, Herbert School of Medicine
Patricia Johnson, University of California, Los Angeles
Richard Locksley, University of California, San Francisco
Suzanne Morris, Uniformed Services University of the Health Service
Steven L. Reiner, University of California, San Francisco
Joe Urban, USDA

Instructor
Peter Hotez, Yale University

Teaching Assistants
Peter Bradley, University of California, Los Angeles
Emilio Duran, University of Toledo
Melissa A. Perregaux, Yale University School of Medicine
Martine Soete, INSERM
Jacinto Villanueva, San Francisco State University
Keith Wilson, Stanford University School of Medicine

Course Assistants
Michele Klingbeil, University of Toledo
Kersten Moorehead, San Francisco State University
Sally Riddles, University of Toledo

Students
Niklas Ahlborg, Stockholm University
Lisa M. Barthel, Northwestern University
Paul Bloch, Danish Bilharziasis Laboratory
Marcelo R. S. Briones, Escola Paulista de Medicina
Fidel de la Cruz Hernández, CINVESTAV-IPN Mexico
Wolfgang H. Hoffmann, University of Tübingen
David A. Horn, Rockefeller University
Jorge A. Huete-Perez, University of Sao Paulo-Ribeirao Preto
Catharine E. Johnson, Johns Hopkins University School of Medicine
Maxine F. Kellman, VA-MD Regional College of Veterinary Medicine
Johannes CH. Koeller, University of Munich
Fatima SM. Noronha, Universidad Federal de Minas Gerais
Claudia M. Ochatt, INGEBI
Levi L. Omara, University of Calgary
Simon Paul, Rockefeller University
Barbara Rick, Zoologisches Institute der Universität Bonn
Paul M. Selzer, Universität Tubingen
Tim T. Stedman, Virginia Commonwealth University
Jan Tachezy, Charles University
James Tang, University of Queensland

Embryology *(June 18–July 30)*

Directors
Eric H. Davidson, California Institute of Technology
Michael Levine, University of California, San Diego
David McClay, Duke University

Course Faculty
Marianne Bronner-Fraser, University of California, Irvine
Andrew R. Cameron, California Institute of Technology
Scott E. Fraser, California Institute of Technology
Janet Heasman, The Wellcome/CRC Institute
Alexander D. Johnson, University of California, San Francisco
Randall Moon, University of Washington
Noriyuki Satoh, Kyoto University
Paul Sternberg, California Institute of Technology
Christopher Wylie, The Wellcome/CRC Institute

Teaching Assistants
Helen Chamberlin, California Institute of Technology
Akiro Hikosaka, Address unknown
Carole LaBonne, Harvard University
Lynn McGrew, Address unknown
Jeffrey Miller, Duke University
Jannette Rusch, Address unknown
Mark Selleck, Address unknown
Colin Sharpe, Cambridge University
John Shih, California Institute of Technology
Robert W. Zeller, California Institute of Technology

Administrator
Jane Rigg, California Institute of Technology

Course Assistant
Aaron Sloboda, Skidmore College

Course Coordinator
Linda Huffer, Marine Biological Laboratory

Students

Kristine B. Artinger, University of California, Irvine
Clare VH. Baker, Wellcome/CRC Institute
Elizabeth M. Callery, University of Toronto
Matthew J. Cockerill, Imperial Cancer Research Fund
Robbert J. Créton, University of Utrecht
Lance A. Davidson, University of California, Berkeley
David S. Fashena, University of Oregon
Silvia C. Finnemann, Freie Universität Berlin
Giulio Ghersi, Universität di Palermo
Sunita Gupta, SUNY, Stony Brook
Yohko Hatada, University of Oxford
Paul G. Hodor, Carnegie Mellon University
Gabrielle Kardon, Duke University
Evelyn F. Keller, Massachusetts Institute of Technology
Karel F. Liem, Jr., Columbia University
Malcolm P. O. Logan, National Institute for Medical Research
Denise K. Lokhorst, Harvard Medical School
Edwin M. Munro, University of Washington
Cyrus Papan, Universität zu Köln
Kathleen I. Pinson, University of Michigan Medical School
Christopher S. Rose, Harvard University
Hyla C. Sweet, University of Texas, Austin
Winston E. Thompson, University of Medicine & Dentistry of New Jersey
Katherine Woo, California Institute of Technology

Microbial Diversity (*June 13–July 29*)

Directors

John Breznak, Michigan State University
Martin Dworkin, University of Minnesota

Teaching Assistants

Andreas Brune, Michigan State University
Jared Leadbetter, Michigan State University
Joerg Overmann, University of British Columbia
Anjelica Seitz, University of Connecticut

Course Coordinator

Richard M. Behmlander, University of Minnesota

Laboratory Assistant

Jessica L. Breznak

Students

Dianne M. Ahmann, Massachusetts Institute of Technology
Carol C. Barford, Harvard University
Alain Brauman, Centre ORSTOM
Tsute Chen, University of Massachusetts
Paul G. Egland, University of Iowa
Eric Frings, University of Bonn
Lee E. Hughes, University of North Texas
Jill A. Kreiling, West Virginia University
Eva S. Lindström, Uppsala University
Magdalena Martinez-Canamero, University of Medicine and Dentistry of New Jersey
Margret I. Moré, Cornell University
Gerard Muyzer, Max-Planck-Institute For Marine Microbiology
Guadalupe V. Nevárez-Moorillon, University of North Texas
Diana E. Northup, University of New Mexico
Clifford A. Ochs, University of Mississippi
Rafael F. Rosenzweig, University of Idaho
Maria R. Uria-Nickelsen, University of Connecticut
Minoru Wada, University of Tokyo
Tom Wakeford, King's College
Ann E. West, University of Colorado, Boulder

Neural Systems & Behavior (*June 13–August 6*)

Directors

Ronald L. Calabrese, Emory University
Martha Constantine-Paton, Yale University

Course Faculty

Robert Douglas, University of British Columbia
William Kristan, University of California, San Diego
Christine Li, Boston University
Shawn Lockery, University of Oregon
Christine Rose, University of Kaiserslautern
Martin Shankland, Harvard Medical School
James Weimann, Stanford University

Instructors

Alexander Borst, Max Planck Institute fur Biologische Kybernetik
Holly Cline, University of Iowa
Patsy Dickinson, Bowdoin College
Cole Gilbert, Cornell University
Richard Levine, University of Arizona
Eduardo Macagno, Columbia University
Robert Malinow, University of Iowa
Pierre Meyrand, University of Bordeaux
Michael Nusbaum, University of Alabama, Birmingham
Mu-Ming Poo, Columbia University
Leslie Stevens, Albert Einstein College of Medicine
Janis Weeks, University of Oregon
Anegla Wenning, Universitat Konstanz

Scholars-in-Residence

Susan McConnell, Stanford University
Richard G. M. Morris, University of Edinburgh

Teaching Assistants

Yang Dan, Columbia University
Douglas Falls, Harvard Medical School
Jurgen Haag, Max-Planck-Institut für Biologische Kybernetik
Neal Hessler, Address unknown
William Lemon, University of Arizona
Andrea Novicki, University of Oregon
Glen Prusky, Address unknown
David Sandstrom, Address unknown
Aneil Shirke, University of Iowa
Thomas White, Harvard Medical School
Laura Wolszon, Columbia University
James Q. Zheng, Columbia University

Course Coordinator

Leslie D. Herman, Vanderbilt University

Course Assistant

Kyle C. Kennon

Students

Marlene Bartos, Technische Universität München
John M. Beggs, Yale University
Cynthia J. Gill, University of Virginia
Joshua I. Gold, Stanford University School of Medicine
Roberto B. Gonzales, University of Texas, San Antonio
Sally K. Guthrie, University of Michigan
Jon M. Karpilow, University of Wisconsin, Madison
Madelyne Kraft, City College
Rafael Levi, Hebrew University of Jerusalem
Christina R. McKittrick, Rockefeller University
William L. Miller, University of California, Davis
Constance T. Moore, University of Nebraska Medical Center
Farzan Nadim, Boston University
Oystein H. Olsen, University of Glasgow
Craig M. Powell, Baylor College of Medicine
Janine M. Simmons, UCLA School of Medicine
Laura C. Sisola, University of Minnesota
Johanna E. Speksnijder, Hubrecht Laboratory
Adam F. Strassberg, California Technological Institute
Masanori Takahashi, Osaka University Medical School

Neurobiology *(June 13–August 14)*

Directors

Irwin Levitan, Brandeis University
Leonard Kaczmarek, Yale University School of Medicine

Course Faculty

Hana Asmussen, University of Virginia Medical School
Gary Banker, University of Virginia
Arlene Chiu, Beckman Research Institute of the City of Hope
Judith Drazba, National Institutes of Health/NINDS
Keith Elmslie, Case Western Reserve University
Richard Horn, Jefferson Medical College
Stephen Jones, Case Western Reserve University
Bechara Kachar, National Institutes of Health/NINDS
Richard Kramer, Columbia University
Diane Lipscombe, Brown University
John Marshall, Yale University School of Medicine
Sally Moody, The George Washington University
Angus Nairn, The Rockefeller University
Marina Picciotto, The Pasteur Institute
Thomas Reese, National Institutes of Health
Peter Reinhart, Duke University Medical Center
Talvinder Sihra, University of Dundee
Carolyn Smith, National Institutes of Health
Donald Wigston, Emory University School of Medicine

Instructor

Laura M. Roman, Yale University

Course Assistant

Ethan Treistman, University of North Carolina, Chapel Hill

Students

Cynthia Church, University of Colorado
Allen J. Ebens, Howard Hughes Medical Institute
James E. Galagan, University of Miami
Kathryn J. Greene, Case Western Reserve University
Barbara D. Hettinger-Smith, Oregon State University
Richard J. Kollmar, University of Wisconsin, Madison
C. J. Malanga, West Virginia University School of Medicine
Hidemi Misawa, Tokyo Metropolitan Institute for Neuroscience
Heidi Scrable, University of Cincinnati College of Medicine
Orian Shirihai, Technion-Israel Institute of Technology
Deborah L. Sodickson, Harvard Medical School
Kristina Wietasch, Harvard Medical School

Physiology *(June 12–July 24)*

Director

Thomas Pollard, Johns Hopkins Medical School

Course Faculty

William Busa, Johns Hopkins University
Laura Davis, Howard Hughes Medical Institute
Michael Mendelsohn, New England Medical Center
Andrew Murray, University of California
Robert Palazzo, University of Kansas
Edward Salmon, University of North Carolina
Roger D. Sloboda, Dartmouth College
Cynthia Stauffacher, Purdue University
Ray Stephens, Marine Biological Laboratory and Boston University
Murray Stewart, Medical Research Council
Edwin Taylor, University of Chicago
Ron Vale, University of California, San Francisco
Katherine L. Wilson, Johns Hopkins University School of Medicine

Instructor

Margaret A. Titus, Duke University Medical Center

Teaching Assistants

Linda Ferrans, Johns Hopkins University
Holly Goodson, Stanford University Medical School
Richard Karas, New England Medical Center/Tufts University
Karen King, Florida State University
C. Lawrence Martin, Purdue University
Jeremy Minshull
Sarah O'Neill, Tufts University
Laura Romberg
Robert Skibbens, University of North Carolina
Jackie Vogel, University of Kansas
Yan Zhu

Course Assistants

Daniel Pollard
Katie Pollard, Pomona College
Michael Salmon, Pitzer College

Students

Katherine M. Armstrong, Stanford Medical School
Mary Lynn Benka, Oregon State University
Sharon A. Beresford, SUNY, Stony Brook
David J. Carroll, University of Connecticut Health Center
Jung-Ren Chen, University of Miami School of Medicine
Tehyen Chu, SUNY, Stony Brook
Signe R. Erickson, Georgia Institute of Technology
Diane E. Frank, University of Wisconsin-Madison

Scott B. Herrick, University of California, Riverside
Raquell M. Holmes, Tufts University
Stanley J. P. Iyadurai, University of Minnesota
Michelle R. Johnson, Howard University
Keith G. Kozminski, Yale University
Dmitri Krylov, Oregon State University
Annette K. Lewis, Washington University School of Medicine
Helen J. McBride, University of Utah Medical School
Joseph H. McCarty, University of California, Santa Barbara
Susan B. McLeskey, Duke University
William A. Mohler, Stanford University
Roland D. Mullins, University of Kentucky
Steven H. Myster, University of Minnesota
Kristine D. Novak, Duke University
Thandi M. Onami, Scripps Institution of Oceanography
Katsushige Sato, Tokyo Medical and Dental University School of Medicine
Sara J. Sawyer, University of California, Los Angeles
Robert H. Scannevin, SUNY, Stony Brook
Hans-Joerg Schaeffer, University of Virginia
Suzaynn F. Schick, University of California, San Francisco
Wenying Shou, Pomona College
Diana M. Toivola, Abo Akademi University
Barbara H. Toomey, Hopkins Marine Station
Alexander J. A. Travis, University of Pennsylvania Medical Center
Jian Wang, University of Washington
Anne K. Warner, Dartmouth College
Clare M. Waterman-Storer, University of Pennsylvania Veterinary School
Cheng Zhu, Georgia Institute of Technology

Short Courses

Advances in Mariculture (May 16-29)

Director
Roger Hanlon, Marine Biomedical Institute

Course Manager
Philip Alatalo, Woods Hole Oceanographic Institution

Course Faculty
Bob Anderson, Bigelow Laboratories for Ocean Sciences
Joe Ayers, Northeastern University
Dave Bengston, University of Rhode Island
Patricia Bubukis, Mystic Marinelife Aquarium
Robert Bullis, Marine Biological Laboratory
Tom Chen, University of Maryland
Elizabeth Clarke, University of Miami
Jack Costello, Providence College
Scott Gallager, Woods Hole Oceanographic Institution
Alan Kuzirian, Marine Biological Laboratory
Jim Lester, University of Houston, Clear Lake
Donal Manahan, University of Southern California
Judy McDowell, Woods Hole Oceanographic Institution
Mike Rice, University of Rhode Island
Steve Spotte, University of Connecticut
Steve Ward, U.S. Fish and Wildlife Service

Students
Daniel Abed-Navandi, University of Vienna
Charles M. Chester, University of New Hampshire
Hyacinth A. Fields, CERMES
Philippe Grosjean, CREC Station Marine
George R. Harbison, Woods Hole Oceanographic Institution
Lisa C. Hendrickson, National Marine Fisheries Service
Kris G. Kosteretz, University of Wisconsin, Milwaukee
Craig Lithgow, Beals Island Regional Shellfish Hatchery
Bill Mebane, Marine Biological Laboratory
Geoffrey F. Sampson, New England Bioassay
Craig A. Weedon, Maryland Department of Natural Resources

Analytical & Quantitative Light Microscopy (May 15-21)

Directors
Greenfield Sluder, Worcester Foundation for Experimental Biology
David E. Wolf, Worcester Foundation for Experimental Biology

Course Faculty, Lecturers, and Staff
William B. Amos, Medical Research Council
Stephen Block, Rowland Institute for Science
Richard Cardullo, University of California, Riverside
Jeff Gelles, Brandeis University
Jeff Guild, Cornell University
Shinya Inoué, Marine Biological Laboratory
Aaron Lewis, Hebrew University—Givat Ram
Leslie Loew, University of Connecticut, Farmington
Christine McKinnon, Worcester Foundation for Experimental Biology
Frederick Miller, Worcester Foundation for Experimental Biology
Edward D. Salmon, University of North Carolina, Chapel Hill
Kenneth R. Spring, National Institutes of Health
Elizabeth Thompson, Worcester Foundation for Experimental Biology
YuLi Wang, Worcester Foundation for Experimental Biology
Watt Webb, Cornell University
Chris Xu, Cornell University

Students
Nelson R. Barton, Harvard University
Robert L. Becker, Jr., Armed Forces Institute of Pathology
David A. Begg, University of Alberta
Tatiana B. Dvornikova, University of California, Irvine
Hong Gao, LSU Medical Center, Shreveport
Jesper L. Gromada, University of Copenhagen
David A. Hessinger, Loma Linda University
Steve G. Hilliard, University of Georgia
Jan H. Hoh, Maurice E. Müller Institute at the Biocenter
Pawel J. Jastreboff, University of Maryland, Baltimore
Nanna K. Jorgensen, University of Copenhagen
Ronald J. Korthuis, LSU Medical Center
Kajedan Z. Kraszewski, Yale University School of Medicine
Damien P. Kuffler, University of Puerto Rico
Marjana Martinic, University of Virginia Medical School
Heinrich J. G. Matthies, Harvard University
Guang Mei, Marine Biological Laboratory
Ramkumar K. Moorthy, Scanalytics/CSPI
Jeffrey H. Price, University of California, San Diego
Noah Sciaky, National Institutes of Health/NICHD
Randi B. Silver, Cornell University Medical College

Robert M. Simmons, University of London
Robert H. Snyder, Pennsylvania State University
Josef M. Steenbergen, Indiana University School of Medicine
Linda A. Thomas, National Institutes of Health
Shigeo Yoshino, Massachusetts Institute of Technology

Cellular and Molecular Neurobiology and Development of the Leech (August 8–28)

Directors
Pierre Drapeau, McGill University
David Weisblat, University of California, Berkeley

Course Faculty
Shirley Bissen, University of Missouri
Susannah Blackshaw, University of Glasgow
Francisco Fernandez de Miguel, UNA Mexico
Jorgen Johansen, Iowa State University
Kenneth Muller, University of Miami
John Nicholls, University of Basel
Martin Shankland, Harvard Medical School
Lidia Szczupak, University of California, San Diego

Guest Lecturer
Ronald Calabrese, Emory University

Lecturers
W. Otto Friesen, University of Virginia
William Kristan, Jr., University of California, San Diego
Eduardo Macagno, Columbia University

Students
Blake D. Anson, University of Oregon
Gerald W. M. Bothe, Columbia University
Marco Bove, Bioelectronics Laboratory
Ashley E. Bruce, Harvard Medical School
Silvina A. Fratantoni, Instituto de Biologia Celular
Dorit Parnas, The Hebrew University
David R. Reese, Montreal General Hospital
Carolina Salvador, Albert Einstein College of Medicine
Leonard A. Stein, SUNY, Stony Brook
Zoltán M. Varga, Biocenter of Basel University
Jamie L. Weiss, Iowa State University
Jane Williams, University of Glasgow

DNA Methodology Workshops (August 2–7 and August 9–14)

Director
Robert Farrell, Exon-Intron, Inc.

Course Faculty
Greg Hale, Exon-Intron, Inc.
Greg Leppert, Exon-Intron, Inc.
Charlie Vaslet, Brown University

Students
Susan E. Aach, U.S. Geological Survey
Pamela L. Arnofsky, Northeastern University
Donald C. Chang, Hong Kong University of Science & Technology
Howard A. Chansky, University of Washington
Doni J. Clark, Beckman Instruments, Inc.
Kimberlee E. Fish, Children's Hospital
George M. Langford, Marine Biological Laboratory
Ming-Chou Lee, Beckman Institute
James K. Min, University of Pennsylvania
Raymond N. Sambrotto, Columbia University
Amy R. Simon, New England Medical Center, Tufts University
Deepak Srivastava, Children's Hospital
Ruci Vergidis, Thunder Bay Regional Cancer Centre
Brian T. Williamson, Eco Science

History of Biology (August 1–11)

Directors
Garland Allen, Washington University
John Beatty, University of Minnesota
Jane Maienschein, Arizona State University

Course Faculty
Mark B. Adams, University of Pennsylvania
Eric Juengst, National Center for Human Genetics Research
Evelyn Fox Keller, Massachusetts Institute of Technology
Barbara Kimmelman, Freelance
Susan Lindee, University of Pennsylvania
Martin Natowicz, Shriver Center
Dorothy Nelkin, New York University
Diane Paul, University of Massachusetts, Boston
Robert Proctor, Pennsylvania State University
Keith Wailoo, University of North Carolina

Visiting Lecturer
Bernardino Fantini, University of Geneva

Students
Lois M. Banta, Haverford College
John S. Ceccatti, Conceptual Foundations of Science
Kathy J. Cooke, California Institute of Technology
Sharon J. Durfy, University of Washington
Kenneth L. Garver, West Pennsylvania Hospital, University of Pittsburgh
Betty L. Garver, Freelance
Christiane Groeben, Statione Zoologica-Anton Dohrn
Jennifer L. Gunn, University of Pennsylvania
Elizabeth A. Hanson, University of Pennsylvania
Youngran Jo, IHPST, Victoria College
Stephanie H. Kenen, University of California, Berkeley
Eric D. Kupferberg, Massachusetts Institute of Technology
Catharina Landström, University of Göteborg
Maureen A. McCormick, West Virginia University
Sylvia W. McGrath, Stephen F. Austin State University
Ronald J. Overmann, National Science Foundation
Karen A. Rader, Indiana University
Robert G. Resta, Swedish Hospital Medical Center
Clark T. Sawin, Veterans Administration Medical Center
Carmen J. Schifellite, York University
Judith Johns Schloegel, Indiana University
Jessica J. Shubow, Brown University
Susan B. Spath, University of California
Karen-Sue Taussig, Johns Hopkins University
Tracy L. Teslow, University of Chicago

David A. Valone, California Institute of Technology
Todd A. Waldman, Johns Hopkins Medical School
Nadine M. Weidman, Cornell University
Janey H. Youngblom, California State University, Stanislaus

Medical Informatics (June 2–8)

Director

Homer R. Warner, University of Utah School of Medicine

Course Faculty

Paul Clayton, Columbia Presbyterian Medical Center
Peter J. Haug, University of Utah School of Medicine
Donald D. A. B. Lindberg, National Library of Medicine
David J. Lipman, Biotechnical Information
Daniel R. Masys, Listerhill Center for Biomedical Communications
Carol Newton, University of California School of Medicine
Rick Rodgers, National Library of Medicine
Robert V. Sideli, Center for Medical Informatics

Lab Coordinator

Sylvia Jessen, University of Utah School of Medicine

Course Assistant

Andy Kogelnik, Emory University School of Medicine

Students

James L. Bingham, University of Kansas Medical Center
Kevin J. Black, Washington University School of Medicine
Gerald J. Cason, University of Arkansas for Medical Sciences
David A. Chernin, Harvard School of Dental Medicine
Keith W. Cogdill, University of Illinois, Chicago
Diana J. Cunningham, Medical Sciences Library
Robert H. Dolin, Kaiser-Permanente
Edward M. Dzierzak, Marshall University
Paul A. Farber, Temple University
Ann R. Fingar, Ohio University
Valerie Florance, Welch Medical Library
Roger J. Guard, SIU School of Medicine
Christopher L. Hatch, National Cancer Institute
Deborah A. Jankowski, Michigan State University
Irene P. Kaplan, Albany College of Pharmacy
Ross S. Kazer, United Family Health Center
Karen E. Larsen, Rochester Methodist Hospital
Steven Lipson, Hebrew Home of Greater Washington
Phillip D. Long, SUNY Health Science Center
John P. Mordes, University of Massachusetts Medical School
Narayan H. Nayak, Kaiser Foundation Hospital
Charles J. Okstein, Maricopa Medical Center
Grace I. Paterson, Dalhousie University
Kathleen F. Ryan, Hahnemann Hospital
Thomas S. Scanlon, Naval Hospital
Jeremy C. Shellhase, University of Pittsburgh
Andrew M. Sherrington, Medical Research Council of Canada
Dennis R. Sinar, East Carolina University
Mark-Allen Taylor, Temple University School of Medicine
Donald E. Wheeler, University of Texas Southwestern Medical Center

Methods in Computational Neuroscience (August 3–31)

Directors

David Kleinfeld, AT&T Bell Laboratories
David W. Tank, AT&T Bell Laboratories

Course Faculty

Joseph Atick, Rockefeller University
Mark F. Bear, Brown University
William Bialek, NEC Research Institute
Rodney James Douglas, MRC
Bard Ermentrout, University of Pittsburgh
William N. Frost, University of Texas Medical School
Apostolos P. Georgopoulos, VA Medical Center
Charles Gray, Salk Institute
John J. Hopfield, California Institute of Technology
Christof Koch, California Institute of Technology
Nancy Kopell, Boston University
Stephen M. Kosslyn, Harvard University
Jeff W. Lichtman, Washington University
John E. Lisman, Brandeis University
Rodolfo R. Llinás, New York University Medical Center
Eve E. Marder, Brandeis University
John H. R. Maunsell, University of Rochester
David A. McCormick, Yale University School of Medicine
Bruce L. McNaughton, University of Arizona
Kenneth D. Miller, California Institute of Technology
John Rinzel, National Institutes of Health
David A. Robinson, Johns Hopkins University
Idan Segev, Hebrew University
H. Sebastian Seung, AT&T Bell Laboratories
Arthur Sherman, National Institutes of Health
Karen Sigvardt, University of California, Davis
Haim Sompolinsky, Hebrew University
Michael Stryker, University of California Medical Center
Roger Traub, IBM Corporation

Lab Instructors

David Berkowitz, Yale University Medical School
David Golomb, National Institutes of Health
Michael Hines, Duke University Medical Center
Roderick Jensen, Texas A&M University
Terrance Kovacs, AT&T Bell Laboratories
Rafael Yuste, AT&T Bell Laboratories

Students

Maria E. Andreu, Universdad de Alicante
Naama Barkai, Hebrew University
Victoria Booth, Northwestern University
Brian W. Colder, University of California, Los Angeles
Yang Dan, Columbia University
Chandan Dasgupta, Indian Institute of Science
Didier A. Depireux, University of Montreal
Patricia M. Di Lorenzo, State University of New York, Binghamton
Andrew A. Hill, University of Massachusetts, Amherst
Lindsay B. Hough, Albany Medical College
Michael Hucka, University of Michigan
Adam L. Jacobs, University of California, Berkeley
Robert A. Jacobs, University of Rochester
Shan Jiang, Brown University

Jürgen Klingauf, Max-Planck-Institut für Biophysikalische Chemie
Kevin E. Martin, University of North Carolina, Chapel Hill
Mayank R. Mehta, Hebrew University of Jerusalem
Partha P. Mitra, Harvard University
Chris L. Passaglia, Syracuse University
Richard D. Rabbitt, Washington University
Moshe Rapp, The Hebrew University
Thorsteinn S. Rögnvaldsson, Lunds Universitet
Jesper N. Tegnér, Karolinska Institutet
John A. White, University of Iowa

Microinjection Techniques (May 25–June 21)

Director
Robert B. Silver, Cornell University

Course Faculty
Suzanne Chandler, Cornell University
Karen Kindle, Cornell University
Douglas Kline, Kent State University
Patricia Wadsworth, University of Massachusetts

Course Assistant
Elizabeth Allen, Cornell University

Students
Moira K. Behan-Martin, SERC Daresbury Laboratory
Andrew S. Belmont, University of Illinois, Champaign-Urbana
Nancy L. Bossert, Duke University Medical Center
Carlos Collin, NINDS, National Institutes of Health
Teresa M. Dunn, SUNY, Stony Brook
Daniel C. Flynn, West Virginia University
Stephen L. Frawley, Oregon Health Sciences University
Masahiko Fujinaga, Anesthesiology Service
Ursula E. Glück, Weizmann Institute of Science
Ming-Ta Hsu, Institute of Biomedical Sciences
Bruce E. Magun, Oregon Health Science University
Merle Mizell, Tulane University
Nancy S. Rafferty, Marine Biological Laboratory
Barnard B. Rees, Stanford University
Mary Ann Sens, Medical University of South Carolina
David I. Soybel, Brigham & Women's Hospital
Jan M. Spitsbergen, Cornell University
Fedora Sutton, South Dakota State University
Richard Yanagihara, National Institutes of Health

Workshop on Molecular Evolution (August 8–20)

Director
Mitchell L. Sogin, Marine Biological Laboratory

Course Faculty
Patrick Argos, European Molecular Biology Laboratory
Dan Davison, University of Houston
Michael Donoghue, Harvard University
Joseph Felsenstein, University of Washington
Walter Fitch, University of California, Irvine
Jotun Hein, Institute for Biological Sciences
Martin Kreitman, University of Chicago
Laura Landweber, Harvard University
David Maddison, University of Arizona
Roger Milkman, University of Iowa
Gary Olsen, University of Illinois
James Ostell, National Library of Medicine
Margaret Riley, Yale University
Monica Riley, Marine Biological Laboratory
James Shapiro, University of Chicago
Terry Speed, University of California, Berkeley
David Swofford, Smithsonian Institution
Bruce Walsh, University of Arizona
Liz Zimmer, Smithsonian Institution

Teaching Assistants
Doug Eernisse, University of Michigan
Steve Thompson, Washington State University, Pullman

Course Consultant
Brendan Reilly, Software Editing Corporation

Course Assistant
Scott Price

Students
Jonathan H. Badger, University of Illinois, Urbana-Champaign
J. William O. Ballard, University of Chicago
Jonas L. O. Blomberg, University of Lund
Michael Boshart, Max-Planck-Institut für Biochemie
Eugenia S. Boulygina, University of Minnesota
Ian A. Boussy, Loyola University of Chicago
Steven M. Carr, Memorial University of Newfoundland
Lisa A. Castlebury, University of Illinois, Urbana-Champaign
Edward S. Chen, University of Houston
Michael I. Cherry, South Africa Museum
Soowon Cho, University of Maryland
Cynthia S. Cohen, Hopkins Marine Station
Joseph A. Cook, University of Alaska Museum
Catherine L. Craig, Yale University
Elisa Cupolillo, Harvard Medical School
Niels Daugbjerg, University of Copenhagen
Lidia L. Demchyshyn, Clark Institute of Psychiatry
Sergio F. dosReis, University of California, Berkeley
Nicole Dubilier, Harvard University
Richard W. Eberle, National Science Foundation
Suzanne Edmands, University of California, Santa Cruz
Karol S. Elias, USD/ARS
Andrea Gargas, Smithsonian Institution
Clarke E. Garry, University of Wisconsin, River Falls
Brandon S. Gaut, North Carolina State University
Jennifer M. Gleason, Yale University
Terry A. J. Hedderson, Louisiana State University
Victoria C. Hollowell, Columbia College
Patrick J. Keeling, Dalhousie University
Dilip S. Kittur, Johns Hopkins Medical Institutions
Marcia C. Lara, University of California, Berkeley
Dolena R. Ledee, Ohio State University
Tim G. Littlejohn, University of Montreal
Jose V. Lopez, NCI-FCRDC
Wojciech Makalowski, University of Montreal
Dmitri A. Maslov, University of California, Los Angeles
Monica Medina, RSMAS
Diogo Meyer, Universidade de Sao Paulo

Alison E. Murray, Tiburon Center for Environmental Studies
Michele K. Nishiguchi, University of California, Santa Cruz
Dimitri M. Odorico, James Cook University of North Queensland
Cristian Orrego, San Francisco State University
Christopher L. Parkinson, University of Louisville
Christian W. Pitulle, University of Houston
David D. Pollock, Stanford University
Thomas O. Powers, University of Nebraska, Lincoln
Kathleen M. Pryer, Duke University
Jonathan P. Rast, All Children's Hospital
Steve A. Rehner, ARS, USDA, SBML
Sandra L. Romano, Kewalo Marine Lab/PBRC
Elaine Rumbak, The Natural History Museum
Jack W. Sites, Brigham Young University
Yan Song, Johns Hopkins University
Diane R. Stothard, Ohio State University
Ying Tan, Yale University
George Tzertzinis, Harvard University
Mary A. Voytek, University of California
Elizabeth R. Waters, University of Arizona
James L. Wee, Loyola University
Jennifer J. Wernegreen, Yale University
Dawn M. Wesson, Centers for Disease Control

Optical Microscopy (October 20–28)

Director
Colin S. Izzard, State University of New York, Albany

Course Faculty
Steven M. Block, Rowland Institute for Science
Gary R. Bright, Case Western Reserve University
Fredric S. Fay, University of Massachusetts Medical School
Kevin Fogarty, University of Massachusetts Medical School
Robert Hard, State University of New York, Buffalo
Shinya Inoué, Marine Biological Laboratory
Ernst Keller, Carl Zeiss, Inc.
Greta M. Lee, University of North Carolina
John M. Murray, University of Pennsylvania
Kenneth R. Spring, National Institutes of Health

Central Microscopy Coordinator
Louis Kerr, Marine Biological Laboratory

Course Associates
Gerald Rupp, State University of New York, Buffalo
Elizabeth Welnhofer, State University of New York, Albany
Joseph A. DePasquale, New York State Department of Health

Lab Manager
Linda Huffer, Marine Biological Laboratory

Students
Shawn L. Anderson, University of Virginia
Mikhail L. Borin, University of Maryland, Baltimore
Mary B. Boyle, University of Texas Medical Branch
David K. Brauer, EERC/ARS/USDA
Michael Cammer, Albert Einstein College of Medicine
Mark A. Chamberlin, Pioneer Hi-Bred International
Nancy Connelly, Schering Plough Research Institute
Eugene V. Golanov, Cornell Medical College
Shelley Halpain, University of Virginia Health Sciences Center
James J. Hartman, University of California, San Francisco
Ajaykvmar R. Jain, Omega Optical Inc.
Tatiana A. Kassessinoff, National Institutes of Health
Martha R. Kirby, National Institutes of Health
Larry G. Moss, New England Medical Center
Roland H. O. Nitschke, National Institutes of Health
Pamela M. Pasciak, Bristol Myers Squibb Company
Giovanni Pauletti, UCLA School of Medicine
Douglas J. Pon, Merck Frosst Centre for Therapeutic Research
Anne M. Sydor, Harvard University
Keith Taylor, State University of New York, Buffalo
Peter W. Tsao, Dupont-Merck Pharmaceutical Company
William P. Van De Merwe, Uniformed Services University of the Health Sciences
Joanne H. Whallon, Michigan State University
Lloyd M. Williams, Hunter College

Pathogenesis of Neuroimmunologic Diseases (August 15–27)

Directors
J. Murdoch Ritchie, Yale University School of Medicine
Byron Waksman, New York and Harvard Universities

Course Faculty
Vahi E. Amassian, State University of New York, Brooklyn
Stanley H. Appel, Baylor College of Medicine
Barry G. W. Arnason, University of Chicago
Etty Benveniste, University of Alabama, Birmingham
Joel A. Black, VA Medical Center and Yale University
Ivan Bodis-Wollner, University of Nebraska Medical Center
Celia F. Brosnan, Albert Einstein College of Medicine
Ian Nicholas Crispe, Yale School of Medicine
Judah A. Denburg, McMaster Medical Center
Susan D. Denburg, McMaster Medical School
Daniel B. Drackman, Johns Hopkins School of Medicine
Andrew G. Engel, Mayo Clinic
David C. Felten, University of Rochester School of Medicine
Diane E. Griffin, Johns Hopkins School of Medicine
David A. Hafler, Brigham & Women's Hospital of Harvard Medical School
Stephen L. Hauser, University of California School of Medicine
William F. Hickey, Dartmouth-Hitchcock Medical Center
Gilla Kaplan, The Rockefeller University
Jeffrey Kocsis, VA Medical Center and Yale University
Norman Latov, College of Physicians and Surgeons of Columbia University
Cathy G. McAllister, University of Pittsburgh
Robert B. Nussenblatt, National Eye Institute, NIH
Jerome B. Posner, Memorial Sloan-Kettering Cancer Center
Donald L. Price, Johns Hopkins University
Richard W. Price, University of Minnesota Health Center
James W. Prichard, Yale University Medical School
Anthony T. Reder, University of Chicago
Jack Rosenbluth, New York University Medical Center
Benjamin F. Roy, Albany Medical Center
Clifford B. Saper, Beth Israel Hospital
Randolph B. Schiffer, Strong Memorial Hospital
Bhagwan T. Shahani, University of Illinois, Chicago
Moon L. Shin, University of Maryland, Baltimore
Raymond A. Sobel, Stanford University Medical Center

- Michele Solimena, Yale University Medical School
- J. Wayne Streilein, University of Miami School of Medicine
- Howard L. Weiner, Brigham & Women's Hospital of Harvard Medical School
- Jerry S. Wolinsky, University of Texas Health Science Center at Houston
- Scott Zamvil, Brigham & Women's Hospital
- Susan Zolla-Pazner, New York University Medical Center

Students

- Donald W. Ayres, Sioux City Neurology Neurosurgery
- Jeffrey P. Blount, University of Minnesota
- Gerhard A. Brandl, Max-Planck-Institut für Psychiatrie
- Nora A. R. Fernandez Liguori, Hospital Tornu-Bueno Aires
- Alison J. Gatrill, University of Cambridge
- Maira Gironi, Hospital Sau Raffaela
- Norbert Goebels, Max-Planck-Institute für Psychiatrie
- Daniel Gonzalez-Dunia, Institut Pasteur
- Maria Isabel S. Leite, Hospital Geral Santo Antonio
- Margarita I. Manescau, Laboratorio de Neuroquimica
- Clyde E. Markowitz, Columbia Presbyterian Medical Center
- Deborah S. Rames, Texas A&M University
- Adrienne Riethmüller, University of Tübingen
- Pradeep K. Sahota, University of Missouri Hospitals & Clinics
- Boris Sakic, McMaster University
- Virginia J. Sanders, University of California, Los Angeles
- Lisa M. Schrott, University of Colorado Health Sciences Center
- Gary G. Schwartz, University of Pittsburgh School of Medicine
- Pradip K. Toshniwal, Private practice
- Raymond D. Voltz, Max-Planck-Institut für Psychiatrie
- Emmanuelle L. Waubant, University of California, San Francisco
- Mauro Zaffaroni, Centro Studi Sclerosi Multipla
- Andrew W. Zimmerman, East Tennessee Children's Hospital
- Einat Zisman, The Weizmann Institute of Science

Summer Research

Principal Investigators

Adamo, Shelley A., Cornell University
Alkon, Daniel L., National Institutes of Health
Armstrong, Clay, University of Pennsylvania
Armstrong, Peter B., University of California, Davis
Arnold, John M., University of Hawaii, Manoa
Augustine, George J., Duke University Medical Center

Baker, Robert, New York University Medical Center
Barlow, Jr., Robert B., Syracuse University Institute for Sensory Research
Bearer, Elaine, Brown University
Beauge, Luis, Instituto M. y M. Ferreyra, Argentina
Belanger, Jim H., University of Arizona, Arizona Research Laboratories
Bennett, Michael V. L., Albert Einstein College of Medicine
Bestor, Timothy, Harvard Medical School
Bloom, George S., The University of Texas Southwestern Medical Center at Dallas
Bodznick, David, Wesleyan University
Borgese, Thomas A., Lehman College, CUNY
Borst, David, Illinois State University
Boyer, Barbara C., Union College
Brady, Scott T., The University of Texas Southwestern Medical Center at Dallas
Brown, Joel, Albert Einstein College of Medicine
Burdick, Carolyn J., Brooklyn College, CUNY
Burger, Max M., Friedrich Miescher Institut, Switzerland

Chaet, A. B., University of West Florida
Chang, Donald C., Hong Kong University of Science & Technology, Hong Kong
Chappell, Richard L., Hunter College, CUNY
Charlton, Milton, University of Toronto, Canada
Clay, John, National Institutes of Health
Cline, Hollis, University of Iowa
Cohen, William D., Hunter College, CUNY
Cook, Heather, University of Toronto, Canada
Cooperstein, Sherwin J., The University of Connecticut Health Center
Crutcher, Keith A., University of Cincinnati

D'Avanzo, Charlene, Hampshire College
Dawson, Timothy C., University of Kansas
Demarest, Jeffery R., University of Arkansas
DeWeer, Paul, University of Pennsylvania School of Medicine
Di Polo, Reinaldo, IVIC, Venezuela
Dowling, John E., Harvard University

Eckberg, William R., Howard University
El Manira, Abdel, Karolinska Institutet for Neurophysiology, Sweden
Eliot, Lise, Baylor College of Medicine

Fischer, Gabriele, Konstanz, Germany
Fishman, Harvey M., The University of Texas Medical Branch at Galveston
Flucher, Bernhard, National Institutes of Health, NINDS

Gadsby, David, The Rockefeller University
Gainer, Harold, National Institutes of Health
Galione, Antony, Oxford University, UK
Garcia-Blanco, Mariano A., Duke University Medical Center
Garrick, Rita Anne, Fordham University College at Lincoln Center
Gelfand, Vladimir, University of Illinois at Urbana-Champaign
Gesteland, Robert C., University of Cincinnati College of Medicine
Giuditta, Antonio, University of Naples, Italy
Gold, Albert M., University of Medicine and Dentistry of New Jersey
Goldman, Robert D., Northwestern University Medical School
Gould, Robert, New York State Inst. Basic Research in Develop. Disabilities
Gramoll, Siglunde, Emory University
Grillner, Sten, Karolinska Institute, Sweden
Gyoeva, Fatima, Russian Academy of Sciences, Institute of Protein Research

Haimo, Leah, University of California, Riverside
Halvorson, Harlyn O., University of Massachusetts, Dartmouth
Heins, Susanne, Maurice E. Muller-Institut, Germany
Highstein, Steven M., Washington University School of Medicine
Hill, Susan D., Michigan State University
Holz IV, George G., Harvard Medical School, Massachusetts General Hospital
Hoskin, Francis C. G., Illinois Institute of Technology
Humphreys, Tom, University of Hawaii

Ip, Wallace, University of Cincinnati College of Medicine

Johnston, Daniel, Baylor College of Medicine
Josephson, Robert K., University of California, Irvine
Kaneshiro, Edna, University of Cincinnati
Kaplan, Ilene M., Union College
Khan, Shahid, Albert Einstein College of Medicine/National Institutes of Health
Koide, Samuel S., Population Council
Kremer, James N., University of Southern California
Kuhns, William, The Hospital for Sick Children, Canada
Kumar, Ajit, George Washington University School of Medicine
Kuznetsov, Sergei, Moscow State University, Russia

Landowne, David, University of Miami
Lane, Mary C., University of California
Langford, George, Dartmouth College
Laufer, Hans, The University of Connecticut
Lemon, William C., University of Arizona
Lester, Roger, Univ. of Arkansas Medical Sciences

Levin, Jack, Univ. of California School of Medicine, San Francisco
Lin, Shien-Fong, Vanderbilt University
Lisman, John, Brandeis University
Llinás, Rodolfo R., New York University Medical Center

Makarenko, Vladimir I., Russian Academy of Sciences, Russia
Malchow, Robert Paul, University of Illinois at Chicago College of Medicine
Metuzals, Janis, University of Ottawa, Canada
Miyakawa, Hiroyoshi, Yamagata University School of Medicine

Nasi, Enrico, Boston University School of Medicine
Nelson, Leonard, Medical College of Ohio
Nigg, Erich A., Swiss Institute for Exp. Cancer Research, Switzerland

Obaid, Ana Lia, University of Pennsylvania School of Medicine
Olson, Andrew, University of Pennsylvania
Oosawa, Fumio, Aichi Institute of Technology, Japan

Palazzo, Robert E., University of Kansas
Pant, Harish, National Institutes of Health, NINDS
Pastor-Loro, Angel Manuel, University of Seville, Spain
Pierson, Elisabeth, University of Siena, Italy

Qian, Haohua, Harvard University
Quigley, James P., State University of New York, Stony Brook

Rakowski, Robert F., University of Health Sciences/The Chicago Medical School
Ratner, Nancy, University of Cincinnati
Reese, Thomas S., National Institutes of Health, NINDS
Rieder, Conly L., Wadsworth Center for Labs and Research
Ripps, Harris, University of Illinois College of Medicine
Rome, Lawrence, University of Pennsylvania
Ross, William, New York Medical College
Ruderman, Joan V., Harvard Medical School
Russell, John M., Medical College of Pennsylvania
Ryckebusch, Sylvie, California Institute of Technology

Salzberg, Brian M., University of Pennsylvania School of Medicine
Scholey, Jonathan, University of California, Davis
Segal, Sheldon, The Population Council
Sheetz, Michael P., Duke University Medical Center
Shimizu, Takashi, National Institutes of Bioscience & Human Technology, Japan
Silver, Robert B., Cornell University, New York State College of Veterinary Medicine
Sloboda, Roger D., Dartmouth College
Sperelakis, Nicholas, University of Cincinnati College of Medicine
Standart, Nancy, University of Cambridge, UK
Steinacker, Antoinette, Puerto Rico Medical Sciences Campus
Swenson, Katherine I., Duke University Medical Center

Telzer, Bruce, Pomona College
Trinkaus, John P., Yale University
Troll, Walter, New York University Medical Center
Tytell, Michael, Bowman Gray School of Medicine of Wake Forest University

Ueno, Hiroshi, Osaka Medical College, Japan

Vilim, Ferdinand S., Columbia University, NYSPI
Vogel, Steven S., National Institutes of Health

Wahl, Philip, Royal Danish School of Pharmacy
Wang, Samuel S. H., Stanford University/Hopkins Marine Station
Wangh, Lawrence J., Brandeis University
Weiss, Dieter, University of Rostock
Wright, Jonathan, McMaster University, Canada

Yoshioka, Tohru, Waseda University, Japan

Zigman, Seymour, University of Rochester School of Medicine & Dentistry
Zottoli, Steven J., Williams College
Zuazaga de Ortiz, Conchita, University of Puerto Rico

Other Research Personnel

Abbas, Rashida, Vanderbilt University
Abraham, Vivek C., Franklin & Marshall College
Ahl, Jonna, University of Hartford
Almazan, Guillermina, McGill University, Canada
Altamirano, Anibal A., Medical College of Pennsylvania
Andrews, Brian, NIH
Armstrong, Clara F., University of Pennsylvania

Baldridge, William, McMaster University, Canada
Bence, Kendra K., University of Connecticut Health Center
Benech, Juan Claudio, Instituto de Investigaciounes Biologicas Clemente Estable, Uruguay
Betz, Heinrich, Max-Planck-Institut für Hirnforschung, Germany
Breitwieser, Gerda E., Johns Hopkins School of Medicine
Browning, Curtis L., University of West Florida
Burgess, David R., University of Pittsburgh
Burns, Marie E., Duke University
Burpee, Dianne, Illinois State University
Busquets, Xavier F., Friedrich-Miescher Institut, Switzerland

Cheng, Peter, National Institutes of Health
Chludzinski, John, National Institutes of Health, NIH
Cohen, Darien, Dartmouth College
Cohen, Ricky, McGill University, Canada
Collin, Carlos, National Institutes of Health
Collins, Glynnis, University of Southern California
Crispino, Marianna, University of Naples, Italy

De Berberian, Graciela Elso, Instituto M. y M. Ferreyra, Argentina
de Menil, Ben, Hunter College, CUNY
DeBello, William M., Duke University
Devlin, C. Leah, Pennsylvania State University
Drazba, Judith, National Institutes of Health, NINDS
Dube, François, Hopkins Marine Station, Stanford University

Gallant, Paul, National Institutes of Health, NINDS
Gerosa, Daniela, Friedrich Miescher-Institut, Switzerland
Gilland, Edwin, New York University Medical Center
Goldman, Anne E., Northwestern University Medical School
Gomez, Froylan, University of Pennsylvania
Gomez, Maria, Boston University School of Medicine
Grant, Philip, National Institutes of Health
Guillfoyle, Kerry Jo., Hampshire College

Hammar, Kasia, National Institutes of Health, NINDS
Hammes, Michelle, Hampshire College
Hershko, Avram, Technion-Israel Institute of Technology, Israel
Herzog, Erik, Syracuse University

Hessler, Neal, University of Iowa
Holmgren, Miguel, University of Health Sciences/Chicago Medical School
Huerta, Julio, Hunter College, CUNY
Huerta, Patricia, Brandeis University
Hunt, ames M., Duke University

Ito, Etsuro, National Institutes of Health, NINDS
Ito, Ken-Ichi, Yamagata University, Japan

Johnson, Donald, Lehman College
Juneja, Renu, Population Council
Jung, Jeanie, Brandeis University

Kaech, Stefanie, National Institutes of Health, NINDS
Kaplan, Barry B., Western Psychiatric Institute and Clinic
Kelly, Mary, Syracuse University
Kezuka, Hiroaki, Hitachi Ltd., Japan
Khodakhah, Kamran, University of Pennsylvania
Khuon, Sayta, Northwestern University
Kirino, Yutaka, Kyushu University, Japan
Kouchi, Takeshi, Waseda University, Japan
Koyano, Takeshi, University of Pennsylvania School of Medicine
Krasovitsky, Vadim, Illinois State University
Krause, Todd, University of Texas
Kudo, Yoshihisa, Mitsubishi Kasei Inst. Life Sciences, Japan

Ladurner, Peter, University of Innsbruck, Austria
Lasser-Ross, Nechama, New York Medical College
Levin, Francine, University of California School of Medicine
Lim, Jong, New York University Medical Center
Lorenzoni, Patrizia, Friedrich Miescher-Institut, Switzerland
Lu, Jin, University of Texas Medical Branch
Lu, Pin, Hong Kong University of Science & Technology, Hong Kong

Mair, Gunnar, University of Innsbruck, Austria
Malinow, Robert, University of Iowa
McPhie, Donna, National Institutes of Health
Mensinger, Allen F., Vanderbilt University
Minkoff, Charles G., Duke University Medical Center
Miyaguchi, Katsuyuki, National Institutes of Health, NINDS
Miyakawa, Atsuo, Hamamatsu University School of Medicine, Japan
Momose-Sato, Yoko, Tokyo Medical and Dental University School of Medicine, Japan
Monterrubio, Jose, University of Puerto Rico
Moreira, Jorge, National Institutes of Health, NINDS
Morgan, James L. M., University of Arkansas
Morita, Mitsuhiro, Japan Tobacco, Japan
Murthy, Rajan, Massachusetts Institute of Technology

Nelson, Mark, University of Illinois

O'Neill, Peggy, Illinois State University
Ogielski, Andrew, Parallel Computing & Algorithum Research Group
Oka, Kotaro, Fujitsu Laboratories, Ltd., Japan
Olds, James L., National Institutes of Health

Parmentier, Patricia, Albert Einstein College of Medicine
Paulin, Michael, University of Otago, New Zealand
Perez, Reynaldo, University of Puerto Rico
Pethig, Ronald, University of Wales, UK
Powers, Maureen, Vanderbilt University

Radominska, Anna, University of Arkansas Medical Sciences
Rayos, Nancy, Hunter College, CUNY
Reese, Barbara, National Institutes of Health, NINDS
Regehr, Wade, University of Pennsylvania
Reiter, Dietmar, University of Innsbruck, Austria
Rence, Kendra K., University of Connecticut Health Center
Ross, Lawrence, Hunter College, CUNY
Rusciano, Dario, Friedrich Miescher-Institut, Switzerland

Sakakibara, Manabu, Tokai University, Japan
Salvenmoser, Willibald, Universitat Innsbruck, Austria
Sanchez, Ivelisse, Hunter College, CUNY
Sanger, Jean M., University of Pennsylvania
Sanger, Joseph, University of Pennsylvania
Sardet, C., Centre National de la Recherche Scientifique, France
Sawin, Hemant, Emory University
Schneggenburger, Ralf, Universitat des Saarlandes, Germany
Shafi, Nadeem Iqbal, National Institutes of Health, LTPB, NICHD
Sheller, Rebecca, University of Texas
Short, Lisa, Howard University
Srimal, Subita, Bangalore Genei (P) Ltd., India
Stokes, Darrell R., Emory University
Sudakin, Valery, Israel Institute Technology, Israel
Sugimori, Mutsuyuki, New York University Medical Center
Swank, Doug, University of Pennsylvania

Takac, Peter, Institute of Experimental Phytopathology and Entomology, Slovak Republic
Takagi, Hiroshi, Waseda University, Japan
Takahashi, Megumi, Waseda University, Japan
Takeshita, Tomoko, Waseda University, Japan
Takimizu, Hideyuki, Waseda University, Japan
Terasaki, Mark, National Institutes of Health, NINDS
Thompson, Winston, University of Medicine and Dentistry of New Jersey
Todora, Michael, University of Texas, Austin
Tokumaru, Hiroshi, Kyushu University, Japan
Treat, Susan, University of Arkansas Medical Sciences
Tsukimura, Brian, Illinois State University

Valdes, Lexia M., Barry University
Van Egeraat, Jan, University of Amsterdam, The Netherlands
Vogel, Jackie, University of Kansas

Wang, Sam, Duke Medical Center
Warner, Anne, Dartmouth College
Weiler, Reto, University of Oldenburg, Germany
Wellington, Melanie, Duke University Medical Center
Wikswo, John P., Vanderbilt University
Wirtz, Karel, State University of Utrecht, The Netherlands
Witte, Sonia, University of Iowa

Xou, Dong-Jing, University of Iowa

Yang, Ling-Sheng, The Population Council
Ye, Jane, Dartmouth College

Zakevicius, Jane M., University of Illinois at Chicago College of Medicine
Zheng, Xin, Albert Einstein College of Medicine
Zigman, Bunnie Rose, University of Rochester School of Medicine & Dentistry
Zukin, R. Suzanne, Albert Einstein College of Medicine

Library Readers

Abbott, Jane, Marine Research, Inc.
Alkon, Daniel L., National Institutes of Health
Allen, Nina S., Wake Forest University
Anderson, Everett, Harvard Medical School
Ayvazian, Suzanne, University of Western Australia

Babitsky, Steven, Kistin, Babitsky, Falmouth, MA
Baccetti, Baccio, Institute of General Biology
Benjamin, Thomas, Harvard Medical School
Bernhard, Jeffrey, University of Massachusetts

Candelas, Graciela, University of Puerto Rico
Cariello, Lucio, Stazione Zoologica, Naples
Carriere, Rita, McGill University
Chambers, Edward, University of Miami
Clark, Arnold, Woods Hole, MA
Cobb, Jewel P., California State University
Cohen, Leonard, American Health Foundation
Cohen, Seymour, Woods Hole, MA
Collier, Marjorie M., St. Peters College
Copeland, Eugene, Woods Hole, MA

D'Alessio, Giuseppe, University of Naples
Duncan, Thomas, Nichols College

Epstein, Herman, Woods Hole, MA
Escalona de Motta, Gladys, San Juan, Puerto Rico

Federici, Celine, New York, New York
Frantz, John D., Carnegie Institution

Gabriel, Mordecai, Brooklyn College
German, James, New York Blood Center
Ghislain, Nicaise, University of Nice
Gilbert, Daniel L., National Institutes of Health
Goldfarb, Ronald, Pittsburgh Cancer Institute
Goward, Samuel, University of Maryland
Grossman, Al, NYU Medical Center
Gruner, John A., Cephalon Inc.
Guttenplan, Joseph, NYU Dental Center

Hall, Valerie, Nantucket, MA
Harrington, J.P., University of Southern Alabama
Herskovits, T., Fordham University
Hines, Michael, Duke University Medical Center
Hundert, Edward, Harvard Medical School

Ilan, Joseph, Case Western Reserve University
Ilan, Judith, Case Western Reserve University
Inoue, Sadayuki, McGill University

Jacobson, Allan, University of Massachusetts Medical School

Kaltenbach, Jane, Mount Holyoke College
Kaminer, Benjamin, Boston University
Kelly, Robert E., University of Illinois
King, Kenneth, Falmouth, MA
Karlin, Arthur, Columbia University
Klemow, Kenneth, Wilkes University
Kramer, Fred R., Public Health Research Institute, New York
Kravitz, Edward, Harvard Medical School

Laderman, Aimlee, Yale University
Levy, R. Galatzer, Institute for Psychoanalysis
Leighton, Joseph, Peralta Cancer Research Institute
Linck, Richard W., University of Minnesota
Lorand, Laszlo, Northwestern University

Masland, Richard, Massachusetts General Hospital
Mauzerall, David, Rockefeller University
McCleskey, Ed, Washington University
Mizell, Merle, Tulane University
Moore, John W., Duke Medical Center
Mooseker, Mark, Yale University
Morrell, Frank, Rush Medical College
Morrell, Leyla, Rush Medical College

Narahashi, Toshio, Northwestern University
Nickerson, Peter, SUNY, Buffalo

Olins, Ada, University of Tennessee
Olins, Donald E., University of Tennessee

Pappas, George, University of Illinois
Person, Philip, Flushing, New York
Pierce, Sidney K., University of Maryland
Prusch, Robert, Gonzaga University

Rao, T.S.S., Dona paula, Goa India
Rabinowitz, M., MBL, Harvard Medical School
Reynolds, George T., Princeton University
Rickles, Frederick, University of Connecticut Health Center
Roennenberg, Til, University of Munich
Rose, Birgit, University of Miami School of Medicine
Roth, Lorraine, Brookline, MA

Schippers, Jay, no affiliation listed
Sears, James R., University of Massachusetts, Dartmouth
Shepro, David, Boston University
Shriftman, M.S., Health Services, New York
Shepard, Frank, Woods Hole Database
Sonnenblick, Ben, Rutgers University
Spector, Abraham, Columbia University
Spiegel, Melvin, Dartmouth College
Spiegel, Evelyn, Dartmouth College
Spirin, Alexander, Russian Academy of Sciences
Starr-Shriftman, Health Services, New York
Stephenson, W., Earlham College
Stuart, Ann, University of North Carolina
Sweet, Frederick, Washington University School of Medicine
Sundquist, Eric, U.S. Geological Survey
Sydlik, Mary A., Westfield State College

Tilney, Louis, University of Pennsylvania
Trager, William, The Rockefeller University
Treistman, Steven, University of Massachusetts Medical Center
Tweedell, K., University of Notre Dame
Tykocinski, Mark L., Case Western Reserve University

Van Holde, K., Oregon State University

Warren, Leonard, Wistar Institute
Webb, Marguerite, Woods Hole, MA
Weidner, Earl, Louisiana State University
Weissmann, Gerald, NYU Medical Center
Wittenberg, B., Albert Einstein University
Wittenberg, J., Albert Einstein University
Wilbur, Charles, Colorado State University
Wolken, Jerome, Carnegie Mellon University
Woods Hole Research Center, Woods Hole, MA

Domestic Institutions Represented

A-M Systems
AT&T Laboratories
Alabama, University of, at Birmingham
Albany College of Pharmacy
Albany Medical College
Albert Einstein College of Medicine
American Bionetics, Inc.
American Psychological Association
Ames Laboratory
Analytical Luminescence Laboratory
Applied Biosystems
Arizona Research Laboratory
Arizona, University of
Arizona, University of, School of Medicine
Armed Forces Institute of Pathology
Astro-Med, Inc.
Axon Instruments, Inc.

Bates College
Barry College
Baruch College of City University of New York
Baylor College of Medicine
Beals Island Regional Shellfish Hatchery
Beckman Instruments, Inc.
Becton Dickinson IS
Belmont Abbey College
Bethesda Research Labs
Bio-Rad Laboratories
Bodega Marine Station
Boston Biomedical Research Institute
Boston Children's Hospital
Boston University
Boston University School of Medicine
Boston VA/Tufts Medical School
Bowling Green State University
Brandeis University
Brigham & Women's Hospital
Brigham Young University
Brinkmann Instruments, Inc.
Brookhaven National Laboratory
Brooklyn College of City University of New York
Brown University
Bryn Mawr College
BTX
Bunton Instrument Company, Inc.

California Institute of Technology
California State University, Stanislaus
California, University of, Berkeley
California, University of, Davis
California, University of, Irvine
California, University of, Los Angeles
California, University of, Riverside
California, University of, San Diego
California, University of, San Francisco
California, University of, Santa Barbara
California, University of, Santa Cruz
Cambridge Instruments
Cambridge Technology
Case Western Reserve University
Case Western Reserve University School of Medicine
Carnegie Institute of Washington
Carnegie-Mellon University
Case Western Reserve University
Cell Robotics
Center for Bioengineering/University of Washington
Center for Great Lakes Studies
Center for Marine Science Research
Center for Neurobiology and Behavior
Centers for Disease Control
Chicago Medical School
Chicago, University of
Children's Hospital and Harvard Medical School
Chronical of Higher Education, The
Ciba Corning Diagnostics Corp.
Cincinnati, University of
City College of New York
City University of New York
City University of New York, Lehman College
City University of New York Medical School
Clark University
Cleveland Veterans Affairs Medical College
Codonics
Colgate University
Colorado College
Colorado State University
Colorado, University of, Boulder
Colorado, University of, Health Sciences Center
Columbia University
Columbia University College of Physicians and Surgeons
Connecticut, University of
Connecticut, University of, Health Center
Cornell Medical College
Cornell Medical School
Cornell University
Cornell University, N.Y. State College of Veterinary Medicine
Costar Corporation
Coy Corporation
Crimson Camera Technical Sales

Dage MTI, Inc.
Dana-Farber Cancer Institute
Dartmouth College
Dawson Company
Delaware Diamond Knives, Inc.
Delaware, University of
Diamond General Corporation
Digital Equipment Corporation
DNA Star
Drew University
Drummond Scientific
Duke University
Duke University Medical School

E. I. duPont de Nemours & Co., (Inc.)
East Tennessee State University
Eastman Kodak Company
Eco Science Corp.
E.G.&G. Instruments
Emory University
Emory University School of Medicine
Eppendorf, Inc.
Ericomp, Inc.
Exon-Intron, Inc.

FDA-Bethesda
Finnegan, Henderson, Farabow Law Firm
Fisher Scientific
Florida State University
Florida, University of
Flow Laboratories
John Fluke Manufacturing Company

Galileo Electro-Optics Corporation
General Scanning, Inc.
General Valve Corporation
George Mason University
George Washington University
Georgetown University Medical School
Georgia Institute of Technology
Georgia, University of
Gerontonlogy Research Institute
GIBCO/BRL Life Technologies, Inc.
Gilson Medical Electronics, Inc.
Gonzaga University
Gould, Inc.
Grass Instrument Company

Hacker Instruments, Inc.
Frederick Haer & Company
Hahnemann Medical College
Hahnemann University
Hamamatsu Photonic Systems
Hampshire College
Harbor-University of California Los Angeles Medical Center
Harvard Medical School
Harvard University
Hawaii, University of
Health Sciences, University of
Health Sciences, University of,/Chicago Medical School
Hebrew Home of Greater Washington
HHMI, Johns Hopkins Medical School
HHMI, Massachusetts General Hospital
Hitachi
Hoefer Scientific
Holy Cross College
Honeywell Corporation
Hopkins Marine Station
Houston, University of
Howard Hughes Medical Institute
Howard University
Hutchinson Cancer Research Center
Hunter College

Hunter College and City University of New York Graduate Center

I.B.M.-T.J. Watson Research Center
IBI
ICN Radiochemicals (Division of ICN Biomedicals, Inc.)
ICRF
Idaho, University of
Illinois Natural History Survey
Illinois State University
Illinois, University of
Illinois, University of, Urbana-Champaign
Indec Systems Corporation
Inovision Corporation
Indiana University
Indiana University School of Medicine
Institute for Basic Research
Institute for Basic Research in Developmental Disabilities
Institute of Neuroscience
Intelligenetics
International Equipment Company
INUS Systems, Inc.
Iowa State University
Iowa, University of
ISCO, Inc.

James Cook University
JEOL
Johns Hopkins Hospital
Johns Hopkins Medical Institute
Johns Hopkins University
Johns Hopkins University School of Medicine
Jouan, Inc.

Kansas, University of
Kent State University
Kentucky, University of
Kentucky, University of, Medical School
Kinetic Systems
KinTek Instruments
Kipp & Zonen
Kodak Research Laboratory
David Kopf Instruments
Kramer Scientific Corporation

Lab Line Instruments, Inc.
Lab Products
Laser Science
Lehman College of City University of New York
Leica, Inc.
Lindberg Enterprises
Living State Physics Group, Vanderbilt University
Los Alamos National Laboratories
Louisiana State University
Louisiana State University Medical Center, Shreveport
Loyola University
Ludlum Measurements, Inc.

Marine Biological Laboratory
Marine Biomedical Institute, Galveston
Marquette University
Maryland, University of
Maryland, University of, Baltimore
Maryland, University of, Center of Marine Biotechnology
Maryland, University of, Eastern Shore
Maryland, University of, School of Medicine
Massachusetts General Hospital
Massachusetts Institute of Technology
Massachusetts, University of
Massachusetts, University of, Amherst
Massachusetts, University of, Boston
Massachusetts, University of, Medical Center
Massachusetts, University of, Medical School
Mayo Clinic
Medical College of Georgia
Medical College of Ohio
Medical Systems Corporation
Medical University of South Carolina
Meiji Techno America
Memorial Sloan Kettering Cancer Center
Merck & Company
Merck, Sharp & Dohme Research Laboratory, New Jersey
Meridian Instruments
Miami, University of
Miami, University of, School of Medicine
Michigan State University
Michigan State University, Center for Microbial Ecology
Michigan Technological University
Michigan, University of
Michigan, University of, Ann Arbor
Micro Video Instruments
Miles Inc., Diagnostics Division
Millipore Corporation
Minnesota, University of
Missouri-Columbia, University of
MJ Research
Molecular Dynamics
Molecular Probes
Moravian College
Mount Holyoke College
Mt. Sinai School of Medicine
Murray State University

NACVIS Systems
Narischige USA, Inc.
NEC Research Institute
NIH/NIDDK/MDB
National Cancer Institute
National Heart, Lung and Blood Institute
National Institutes of Health
National Institutes of Health/NCI
National Institutes of Health/NHLBI
National Institutes of Health/NICHD
National Institutes of Health/NINDS
National Institutes of Health/NIEHS
National Institutes of Health/NIDDK
National Institutes of Mental Health/NIH
National Jewish Center for Immunology & Respiratory Medicine
National Marine Fisheries Service/Univ. Maryland Eastern Shore
National Multiple Sclerosis Society
National Science Foundation
Naval Hospital, San Diego
Naval Medical Research Institute
Naval Research Laboratory
Nebraska, University of
Neslab Instruments, Inc.
Neuro Data Instrument Corporation
Neurological Institute, New York
Neurometabolic Disorders Foundation
New Brunswick Scientific Company, Inc.
New England Bioassay, Inc.
New England Medical Center
New Hampshire, University of
New Jersey Medical School
New Jersey Medical School and Fordham University
New Mexico, University of, School of Medicine Cancer Center
New York Medical College
New York State Department of Health
New York State Institute for Basic Research
New York University
New York University Medical Center
New York University School of Medicine
Newport Corporation
Nikon, Inc.
Noran Instruments
North Carolina State University
North Carolina, University of, Chapel Hill
North Dakota University
North Texas, University of
Northfield Mount Hermon School
Northeastern University
Northwestern University
Northwestern University Medical School

Oberlin College
Office of Naval Research
Ohio State College
Ohio State University
Oklahoma State University
Oklahoma, University of
Olympus Corporation
Omega Optical Inc.
Opti-Quip
Oregon Health Sciences University
Oregon State University
Oregon, University of
Oregon, University of, Institute of Neuroscience
Owl Scientific

Panasonic Communications and Systems Company
Parmley Hearing Institute, Loyola University of Chicago
Pennsylvania State University

Pennsylvania, University of
Pennsylvania, University of, School of Medicine
Perceptics Corporation
Perkin-Elmer Corporation
Pharmacia, Inc.
Photometrics, Ltd.
Photonic Microscopy, Inc.
Photon Technology International
Physitemp Instruments, Inc.
Pioneer Hi-Bred International
Pittsburgh, University of
Pittsburgh, University of, Medical School
Polaroid Corporation
Pomona College
Ponce School of Medicine
Portland State University
Presbyterian University Hospital
Princeton Instruments, Inc.
Princeton University
Puget Sound, University of

R & M Biometrics, Inc.
Radiomatic Instruments & Chemical Company, Inc.
Reed College
Research Precision Instruments
RMC
Robbins Scientific
Roche Institute of Molecular Biology
Rochester, University of
Rochester, University of, School of Medicine
Rochester, University of, School of Medicine & Dentistry
Rockefeller University, The
Rockefeller University, Howard Hughes Medical Institute
Rowland Institute for Science
RSMAS, University of Miami
Rutgers University

Salk Institute
San Diego Instruments
San Francisco General Hospital
San Francisco State University
Sarastro, Inc.
Savant Instruments, Inc.
Scientific Systems
Scanalytic/CSPI
Scientific Systems
Scott and White Clinic
Scripps Clinic and Research Foundation
Scripps Institute of Oceanography
Sequoia Turner
SERC-Daresbury Laboratory
Shandon-Lipshaw
Shimadzu Scientific Instruments, Inc.
Silicon Graphics, Inc.
Sinauer Associates
Sioux City Neurology Neurosurgery
SLMOAminco
Smithsonian Institution
Society of Polymer Science
Solomat
Sony Medical Electronics
South Carolina, University of
Southern California, University of
Southern California Kaiser Permanente
St. Mary-of-the-Woods College
Stanford University
Stanford University Medical Center
State University of New York
State University of New York, Albany
State University of New York, Binghamton
State University of New York, Buffalo
State University of New York Health Science Center, Brooklyn
State University of New York, Purchase
State University of New York, Stony Brook
State University of New York, Syracuse
Stephen F. Austin State University
Stoelting Company
Stratagene
Strong Memorial Hospital
Sun Microsystems
Supercomputing Research Center, Applications Research
Sutter Instrument Company
Swarthmore College
Swedish Medical Center, Seattle
Swift Instruments
Syracuse University

Technical Manufacturing Corporation
Technical Products International, Inc.
Technical Video, Ltd.
Temple University
Texas A&M University
Texas Christian University
Texas Tech. University
Texas, University of, Austin
Texas, University of, Health Science Center, Houston
Texas, University of, Medical Branch-Galveston
Texas, University of, Medical School
Thomas Jefferson University Hospital
Tissue Engineering, Inc.
Tremont Research Institute
Tufts University
Tufts University School of Medicine
Tufts University School of Veterinary Medicine
Tulane University
Turner Designs

Union College
United States Department of Agriculture
United States Food & Drug Administration
Universal Imaging Corporation
University Hospitals of Cleveland
University Press of Kansas
Ursinus College
USDA/ARS/SRRC
Utah, University of

Vanderbilt University
Vassar College
Vaytek, Inc.
Veterans Affairs Medical Center
VA/MD Regional College of Veterinary Medicine
Video Scope International, Ltd.
Virginia Commonwealth University
Virginia, University of
Virginia, University of, School of Medicine
Vital Images

Wake Forest University
Wake Forest University/Bowman Gray Medical School
Warner Instrument Corporation
Washington, University of
Washington University Medical School
Washington, University of, St. Louis
Washington University School of Medicine
Waters Chromatography Division
Welch Library, Johns Hopkins University
Wesleyan University
West Florida, University of
West Pennsylvania Hospital
West Virginia University
Wheaton College
Whitehead Institute
Wild Leitz USA, Inc.
Williams College
Wisconsin, University of
Wisconsin, University of, River Falls
Wisconsin, University of, Madison
Woods Hole Oceanographic Institution
Worcester Foundation for Experimental Biology
Worcester Polytechnic Institute

Xybion Corporation

Yale University
Yale University School of Medicine

Carl Zeiss, Inc.

Foreign Institutions Represented

AA Bogomoletz Institute of Physiology, Russia
Abo Akademi University, Finland
Academy of Sciences, Institute of Cytology, Russia
Alberta, University of, Canada
Auckland, University of, New Zealand

Basel, University of, Switzerland
Belgrade, University of, Yugoslavia
Bernhard Nocht Institut fur Tropenmedizin, Germany
Bergen, University of, Norway
Bielefeld, University of, Germany
Biozentrum, Basel, Switzerland

Bonn, University of, Germany
Botanisches Institut, Germany
British Columbia, University of, Canada
British Museum of Natural History, United Kingdom
Brussels, University of, Belgium

Calgary, University of, Canada
Cambridge, University of, United Kingdom
CAS in Marine Biology-Portonovo, India
Catania, University of, Italy
Centrol Studi Sclerosi Multipla
Center for Research & Advanced Studies-IPN, Mexico
CERMES, University of West Indies
Charles University, Prague
Chiba University, Japan
Chiba University School of Medicine, Japan
Chile, University of, C.E.C.S., Chile
CINEVESTA V-IPN, Mexico City, Mexico
Clarke Institute, University of Toronto, Canada
Cologne, University of, Germany
Concordia University, Canada
Cooperative Oxford Laboratory, United Kingdom
Copenhagen, University of, Denmark
Curtin, John, School of Medical Research, Australia
Cyprus Institute of Neurology & Genetics, Cyprus

Dalhousie University, Canada
Dalhousie University Medical School, Canada
Danish Bilharziasis Laboratory, Denmark
Dublin City University, Ireland

Fac. de Ciencias Universidad de Chile, Chile
Federal University of Pernambuco, Brazil
Federal University, Rio de Janeiro, Brazil
FIDIA Research Laboratories, Italy
Freie Universitat, Berlin, Germany
Friedrich Miescher Institut, Switzerland

Gene Center, Munich, Germany
Glasgow University, Scotland
Goteborg, University of
Goettingen, University of, Germany
Granada, University of, Spain
GSF-Forschungszentrum, Germany

H. San Raffaele, Milan, Italy
Hamamatsu Photonics, KK, Japan
Hebrew University, Israel
Helsinki, University of, Finland
Herlev University Hospital, Denmark
Hong Kong University, Hong Kong
Hospital Santo Antonio, Portugal
Hospital Tornú, Buenes Aires, Argentina

Imperial College of Science & Technology, United Kingdom
Indian Institute of Science, India
INGEBI-CONICET
Institut für Tropenmedizin Tubingen, Germany
Institute for Biological Research, Yugoslavia
Institute of Histology & Embryology, Austria
Institut Pasteur, France
Institute for Developmental Biology, Germany
Institute for Tropical Medicine, Hamburg, Germany
Instituto M.y.M. Ferreyra, Argentina
Instituto Oswaldo Cruz, Brazil
I.V.I.C., Venezuela

Katholieke Universiteit-Leuven, Belgium
Kobe University, Japan
Koln, University of, Germany
Konstanz, University of, Germany

Life Sciences Institute, Israel
London School of Hygiene & Tropical Medicine, United Kingdom
London School of Hygiene, Brazil
London, University of, Egham, United Kingdom
Ludwig Institute for Cancer Research, United Kingdom
Lund, University of, Sweden

Max-Planck-Institut-für-Biophysikalische Chemie, Nikolausberg, Germany
Max Planck Institute
Max-Planck-Institut-für-Biologie, Germany
Max-Planck-Institut-für-Biologische Kybernetick, Germany
Max-Planck-Institut-für-Entwicklungsbiologie, Germany
Manitoba Institute of Cell Biology, Canada
McGill University, Canada
McMaster University, Canada
Medical Research Council, Canada
Medical Research Council, United Kingdom
Medical Research Council, Laboratory of Molecular Biology, United Kingdom
Memorial University of Newfoundland
Merck Frosst Inc.
Milan, University of, Italy
Montreal Chest Hospital Centre, Canada
Montreal Neurological Institute, Canada
Montreal, University of, Canada
Moscow State University, Russia
Mueller Institute, University of Basel, Switzerland
Munich, University of, Germany

Naples, University of, Italy
Naples Zoological Station, Italy
Nottingham, University of, England, United Kingdom
National Institute for Medical Research, United Kingdom
National Research Center for Biotechnology, Germany
Nobelinstitute for Neurophysiology, Sweden

Ocean Research Institute, University of Tokyo, Japan
Osnabruch, University of, Germany
Ottawa, University of, Canada
Oxford University, United Kingdom

Philipps-Universitat, Germany
Philipps-Universitat, Marburg, Germany
Pisa, University of, Italy

Queens College, United Kingdom
Queens University, Canada
Queensland, University of, Australia

Ruhr-University of Bochun, Germany

Sao Paolo School of Medicine, University of, Brazil
St. Andrews University, Scotland
Seoul National University, Korea
Sienna, University of, Italy
Simon Bolivar, University of, Venezuela
Simon Fraser University, Canada
Southampton, University of, United Kingdom
State University of Utrecht, The Netherlands
Stazione Zoologica, Italy
Stockholm, University of, Sweden
Swiss Federal Institute, Switzerland
Swiss Federal Institute of Technology, Switzerland

Technische Universitat, Munchen, Germany
Technion, Israel
Tokyo, University of, Japan
Tokyo Medical and Dental University, Japan
Tokyo Metropolitan Institute for Neuroscience, Japan
Toronto, University of, Canada
Tubingen, University of, Germany
TNO Medical Biological Laboratory, The Netherlands

Umea, University of, Sweden
Ulm, University of, Germany
University College, London, United Kingdom
Universita di Palermo, Italy
University Hospital of Basel, Switzerland
Uppsala University, Sweden
Utrecht, University of, The Netherlands

Vienna, University of, Austria
Vrije Universiteit Brussels, Belgium

Waseda University, Japan
Weizmann Institute of Science, Israel
Wellcome Research Laboratories, United Kingdom
Western Ontario, University of, Canada
Wolfson College, United Kingdom

Yamagata University School of Medicine, Japan
Yoido St. Mary's Hospital, Korea

Zimbabwe, University of, Zimbabwe
Z.L.F. Kantonsspital, Basel, Switzerland

Lynne Layman

Year-Round Research Programs

Architectural Dynamics in Living Cells Program

Established in 1992, this program focuses on architectural dynamics in living cells—the timely and coordinated assembly and disassembly of macromolecular structures essential for the proper functioning, division, motility, and differentiation of cells; the spatial and temporal organization of these structures; and their physiological and genetic control. The program is also devoted to the development and application of powerful new imaging and manipulation devices that permit such studies directly in living cells and functional cell-free extracts. The Architectural Dynamics in Living Cells Program promotes interdisciplinary research and consists of resident core investigators and a cadre of adjunct members.

Resident Core Investigators

Inoué, Shinya, Distinguished Scientist
Mei, Guang, Research Associate
Oldenbourg, Rudolf, Associate Scientist
Stemmer, Andreas, Visiting Assistant Scientist

Staff

Knudson, Robert, Instrument Development Engineer
Leighton, Jane, Executive Assistant

Boston University Marine Program

Faculty

Atema, Jelle, Professor of Biology, Director
Dionne, Vincent, Professor of Biology
Humes, Arthur G., Professor of Biology Emeritus
Tamm, Sidney L., Professor of Biology
Valiela, Ivan, Professor of Biology
Voigt, Rainer, Research Associate Professor

Staff

Hahn, Dorothy, Senior Administrative Secretary
Kean, Kristen, Program Assistant
Schillizzi, Cynthia, Program Manager

Visiting Faculty and Investigators

D'Avanzo, Charlene, Hampshire College
DiLorenzo, Patricia, SUNY, Binghamton
Dubin, Adrienne, Visiting Research Scientist
Gunderson, John, Tennessee Technological University
Kaufman, Les, New England Aquarium
Kremer, James, USC
Levine, Joe, Boston Science Communications
Lobel, Phillip, Associate Scientist, WHOI
Mulsow, Sandor, Bedford Institute of Oceanography
Rietsma, Carol, SUNY, New Paltz
Rosenbaum, Joel, Yale University
Sardet, Christian, Villefranche Zoological Station
Simmons, William, Visiting Lecturer, Boston University
Trouslard, Robert, Institut National Agronamique, Paris
Ward, Nathalie, Center for Coastal Studies

Research Staff

Basil, Jennifer, Postdoctoral Investigator
Bierzychudek, Ann, Visiting Research Assistant
Breithaupt, Thomas, Postdoctoral Investigator
Collins, Glynnis, Visiting Research Assistant
Eisthen, Heather, Postdoctoral Investigator
Foreman, Kenneth, Postdoctoral Investigator
Gerardo, Hortense, Postdoctoral Investigator
Grasso, Frank, Postdoctoral Investigator
McConnell, Joanne, Postdoctoral Investigator
Pinedo, Susana, Visiting Investigator
Soucy, Lori, Research Assistant
Seely, Brad, Visiting Research Assistant
Tamm, Signhild, Senior Research Associate

Graduate Students

Anderson, John
Barak, Jeri
Batjakas, Ioannis
Bloom, David
Bryden, Cynthia
Burns, Maura
Bushman, Paul
Dale, Jonathan

Eisenegger, Felice
Farley, Lynda
Fricke, Julie
Gomez, George
Han, Tina
Hersh, Douglas
Joy, Jennifer
Karavanich, Christy
La Duca, Nathalia
LaMontagne, Michael
Landmesser, Shari
LaRocca, Beth
Larsen, David
Lowe, Brian
Loynes, Janet
Ma, Diana
Manglapus, Glen
McClelland, James
Millard, Jennifer
Mosiach, Simon
O'Brien, Todd
Phipps, Derek
Portnoy, John
Rubenstein, Belinda
Schlezinger, David
Tamse, Armando
Thomassen, Lori
Usup, Gires
White, David

Summer Undergraduate Interns

Bayha, Keith
Bello, Roberto
Duran, Robert
Evans, Chloë
Faulstich, Emily
Flowers, Alissa
Gribble, Kristin
Hauxwell, Jennifer
Judge, Bryan
Kaplan, Liat
Lin, Winchee
Lowrance, Courtney
Richards, Timothy
Terry, Joseph
Tolley, Krystal
Williams, Semanthia

Undergraduate Students, Fall 1993

Agudelo, Sylvia
Arnell, Harry
Barth, Colleen
Berg, Heather
Brown, Julie
Burns, Jennifer
Carnes, Denise
Carroll, Mark
Colby, William
Darras, Todd
Davis, Travis
Director, Syril
Dunlavey, Eric
Economakis, Alistair
Ellison, Rob
Fowler, Brandi
Geer, Tom
Goldsboro
Grady Erinn
Gregoire, Judith
Griffin, Sean
Gunderson, Troy
Highestad, Richard
Holeva, Tom
Howard, Corinne
Hunt, Ritchie
Iocco, Linda
Jehn, Christopher
Kapoor, Tina
Kim, Hea Jin
Kitson, Mark
Koonce, Lea
Kooy, Liz
Landers, Thomas
Leonard, Ann
Lowrance, Courtney
Machelor, Eva
McCullough, Michelle
Monti, Jill
Muehe, Melanie
Patel, Druhvesh
Pothier, Bryan
Raines, Jason
Sheehan, Daniel
Sugarman, Casey
Townsend, Jessica
Tsutsui, Neil
Vincent, Lara
Voparil, Ian
Washburn, Erika
Wennemer, Heidi
York, Randall

Laboratory of Jelle Atema

Organisms use chemical signals as their main channel of information about the environment. These signals are transported in the marine environment by turbulent currents, viscous flow, and molecular diffusion. Receptor cells extract signals through various filtering processes. Currently, the lobster with its exquisite sense of taste and smell, is our major model to study the signal filtering capabilities of the whole animal and its narrowly tuned receptor cells. Research focuses on food signals and pheromones used in courtship and dominance, neurophysiology of receptor cells, behavior guided or modulated by chemical signals, computational models of odor plumes and neural filters, and underwater robotics.

Laboratory of Vincent Dionne

Odors are powerful stimuli. They can focus the attention, elicit behaviors (or misbehaviors), and even resurrect forgotten memories. These actions are directed by the central nervous system, but they depend upon the initial transduction of chemical signals by olfactory receptor neurons in the nasal passages. The processes that underlie odor transduction are far more diverse than once thought, involving hundreds of receptor molecules, several different second messengers, and various types of membrane ion channels. Using electrophysiological and molecular approaches, our research examines how these cellular components produce odor detection, identification, and discrimination. The studies are conducted on aquatic salamanders using amino acids and other soluble chemical stimuli which they perceive as odors.

Laboratory of Arthur G. Humes

Research interests include systematics, development, host specificity, and geographical distribution of copepods associated with marine invertebrates. Current research is on taxonomic studies of copepods from invertebrates in the tropical Indo-Pacific area, and poecilostomatoid and siphonostomatoid copepods from deep-sea hydrothermal vents and cold seeps.

Laboratory of Sidney Tamm

Marine model systems offer unique experimental advantages for solving basic problems in cell biology and physiology. In particular, comb jellies (ctenophores), important members of the marine zooplankton, possess the largest cilia and smooth muscles in nature, a simple nervous system, and interesting feeding and locomotory behaviors. We use ctenophores to investigate the mechanism of ciliary movement and ciliary coordination, the neural and ionic control of cilia (particularly stimulus-evoked intraciliary calcium transients and distribution of ciliary calcium channels), geotaxis and mechanosensory transduction by motile cilia statocyst, structure and function of smooth muscle, double-modality sensory receptors and the cytoskeleton, and evolution of neurotransmitters, and a new type of reversible cell-cell adhesion that closes the mouth of *Beroë,* a voracious predator of other ctenophores. In addition, we use a termite protozoan with a continuously rotating head to investigate novel types of cell motility, the fluid nature of cell membranes, and remarkable prokaryotic-eukaryotic motility symbioses.

Laboratory of Ivan Valiela

Our major research activity involves the Waquoit Bay Land Margin Ecosystems Research Project. This work examines how human activity in coastal watersheds (including landscape use and urbanization) increases nutrient loading to groundwater and streams. Nutrients in groundwater are transported to the sea, and, after biogeochemical transformation, enter coastal waters. There, increased nutrients bring about a series of changes. The Waquoit Bay LMER is designed to help understand and model the coupling of land use and consequences to receiving waters, to study the processes involved, and to assess consequences and opportunities for coastal management.

A second long-term research topic is the structure and function of salt marsh ecosystems, including the processes of predation, herbivory, decomposition, and nutrient cycles.

Calcium Patterning Program

This laboratory investigates the role played by calcium ions in a wide range of fundamental cell processes: in developing eggs, in differentiated tissues, and in cell extracts. This is possible through the use of aequorin, a bioluminescent protein complex. Aequorin can either be microinjected into cells or transgenically expressed without disturbing function or development. The pattern of luminescence that is emitted by an aequorin-loaded cell reveals changing patterns and levels of free calcium within the cell (or its progeny). Photons are collected and correlated with dynamic cellular events by an imaging system developed in our laboratory. This technique has some substantial advantages over other methods of imaging intracellular calcium and as a result supports an extensive collaborative research effort. The laboratory is currently studying cytokinesis in frog and fish eggs; cell cycle control in sea urchin and surf clam eggs; polarity expression in frog eggs; tip growth in pollen tubes; injury and degeneration in neurons; mechanisms of fertilization in sea urchins; differentiation in slime molds; and calcium release in cell extracts from frog eggs. The laboratory is supported by the NSF to both pursue biological questions and to develop the aequorin-based imaging technique.

Staff

Miller, Andrew L., Assistant Scientist
Karplus, Eric, Design Engineer
Jaffe, Lionel F., Senior Scientist
Fischer, Gabriele, Graduate Student

Visiting Investigators

Abraham, Vivek, C., Franklin and Marshal College
Browne, Carole, Wake Forest University
Creton, Robert, University of Utrecht, The Netherlands
Cubitt, Andrew, C., UCSD
Denegre, Jim, University of California, Irvine
Eckberg, Bill, Howard University
Febvre, Jean, Villefranche-sur-mer, France
Febvre-Chevalier, Colette, Villefranche-sur-mer, France
Fechter, Larry, University of Oklahoma
Fishman, Harvey M., University of Texas Medical Branch.
Fluck, Richard, A., Franklin and Marshal College
Galione, Antony, Oxford University, UK
Kinney, Greg, A., Northwestern University Medical School
Pierson, Elizabeth, University of Siena, Italy
Rossi, David, J., Northwestern University Medical School
Sardet, Christian, Villefranche-sur-Mer, France
Short, Lisa, Howard University
Speksnijder, Johanna, E., Hubrecht Laboratory, The Netherlands
Tobias, Martha, Columbia University
Todora, Michael, University of Texas Medical Branch
Wilding, Martin, University College London, UK

The Ecosystems Center

The Center was established in 1975 to promote research and education in ecosystems ecology. Twelve senior scientific staff and 43 research assistants and support staff study the terrestrial and aquatic ecology of a wide variety of ecosystems ranging from Brazil (carbon cycling and trace gas emissions from tropical forests and pastures) to the Alaskan Arctic (long-term studies of the response of tundra, lake, and stream biota to change) to the Harvard Forest (long-term studies of the effects of disturbance in forest ecosystems) to Massachusetts Bay (rates of denitrification). Many projects, such as those dealing with sulfur transformations in lakes and nitrogen cycling in the forest floor, investigate the movements of nutrients and make use of the Center's mass spectrometry laboratory (directed by Brian Fry) to measure the stable isotopes of carbon, nitrogen, and sulfur. The research results are applied wherever possible to questions of the successful management of the natural resources of the earth. In addition, the ecological expertise of the staff is made available to public affairs groups and government agencies who deal with such problems in acid rain, ground water contamination, and possible carbon dioxide-caused climate change.

Staff

Hobbie, John E., Co-Director
Melillo, Jerry M., Co-Director
Bahr, Michele
Castro, Mark
Castro, Nancy Mathews
Catricala, Chris
Deegan, Linda
Donovan, Suzanne
Dornblaser, Mark
Downs, Martha
Drummey, Todd
Dugan, Deirdre
Fry, Brian
Garritt, Robert
Giblin, Anne
Giehtbrock, David
Golden, Heidi
Griffin, Elisabeth
Helfrich, John
Hopkinson, Charles
Hullar, Meredith
Jesse, Martha
Jones, David
Kicklighter, David
Kwiatkowski, Bonnie
Laundre, James
McGuire, A. David
Monahan, Jean
Murray, Georgia
Nadelhoffer, Knute
Newkirk, Kathleen
Nolin, Amy
O'Hara, Patricia
Peterson, Bruce
Rastetter, Edward
Redmond, Leslie
Regan, Kathleen
Repert, Deborah
Ricca, Andrea
Scanlon, Deborah
Seifert, Mary Ann
Shaver, Gaius
Steudler, Paul
Tholke, Kristin
Tucker, Jane

Postdoctorals

McKane, Robert
Neill, Christopher
Johnson, Loretta
Vallino, Joseph

Visiting Scholars

Norrman, Bosse

Consultants

Bowles, Francis
Bowles, Margaret
Schwarzman, Elisabeth
Thomson, Lee

Laboratory for Marine Animal Health

The laboratory provides diagnostic, consultative research, and educational services to the institutions and scientists of the Woods Hole community concerned with marine animal health. Diseases of wild, captive, and cultured animals are investigated.

Staff

Abt, Donald A., Director and The Robert R. Marshak Term Professor of Aquatic Animal Medicine and Pathology, School of Veterinary Medicine, University of Pennsylvania
Bullis, Robert A., Research Assistant Professor of Microbiology, University of Pennsylvania
Leibovitz, Louis, Director Emeritus
McCafferty, Michelle, Histology Technician, University of Pennsylvania
Moniz, Priscilla C., Secretary
Smolowitz, Roxanna M., Research Associate in Pathology, University of Pennsylvania
Wadman, Elizabeth A., Microbiology Technician, University of Pennsylvania

Laboratory of Aquatic Biomedicine

This laboratory investigates leukemias of soft shell clams. Monoclonal antibodies developed by this laboratory and techniques in molecular biology are used to investigate the differences between normal and leukemic cells and their ontogeny. The impact of pollutants on leukemogenesis is currently being studied with an emphasis on regional superfund sites.

Staff

Reinisch, Carol L., Investigator, MBL, and Chairperson Department of Comparative Medicine, Tufts University School of Veterinary Medicine
Rosenfield, Jonah, Laboratory Assistant

Laboratory of Cell Biochemistry

This laboratory uses cell and molecular biological methods to study the regulation of gene expression in marine fish. Current emphasis is on gene products involved in hepatic heme biosynthesis and utilization. These processes are affected by hormonal, nutritional, and pharmacological agents as well as xenobiotics, and carcinogens. In addition, free heme is a feedback regulator of its biosynthesis. The principal site at which these agents act to control the rate of heme production is 5-aminolevulinate synthase (ALS), the first enzyme of the pathway. However, it has not been possible to define the mechanisms that lead to enzyme induction or repression. Marine fish are attractive for that purpose because they have similar regulatory features for heme biosynthesis but lack some of the hepatic processes that have confounded studies in mammals. Evidence to date strongly indicates that expression of fish ALS is regulated at a posttranscriptional stage. Cloned cDNAs have been isolated for both the housekeeping and erythroid forms of ALS, and the sequence of the e-type cDNA encodes an iron regulatory element that controls the rate of mRNA translation. It is expected that these studies of the fish ALS system will give new insights into the control of heme biosynthesis in vertebrate organisms, including man. Primary cultures of fish hepatocytes provide the experimental material for this work, and an additional interest of this laboratory is in establishing these cell cultures as a nonmammalian model for biomedical research.

Staff

Cornell, Neal W., Senior Scientist
Bruning, Grace, Research Assistant
Pianka, Karen, Research Assistant
Rosenfield, Jonah, Laboratory Assistant

Visiting Scientist

Fox, T. O., Harvard Medical School

Laboratory of Shinya Inoué

Study of the molecular mechanism and control of mitosis, cell division, cell motility, and cell morphogenesis, with emphasis on biophysical studies made directly on single living cells, especially developing eggs in marine invertebrates. Development of biophysical instrumentation and methodology, such as polarization optical and video microscopy and digital image processing techniques, and exploration of their underlying theory are an integral part of the laboratory's effort.

Staff

Inoué, Shinya, Distinguished Scientist
Knudson, Robert, Instrument Development Engineer
Leighton, Jane, Executive Assistant
Mei, Guang, Research Associate
Stemmer, Andreas, Visiting Assistant Scientist
Woodward, Bertha M., Laboratory Manager

Visiting investigators

Bajer, Andrew, University of Oregon
Burgos, Mario, Universidad Nacional de Cuyo-Conicet
Febvre, Colette, Station Zoologique, Villefranche-sur-Mer, France
Febvre, Jean, Station Zoologique, Villefranche-sur-Mer, France
Sardet, Christian, Station Zoologique, Villefranche-sur-Mer, France

Laboratory of Alan M. Kuzirian

Research in this laboratory explores the functional morphology and ultrastructure of various organ systems present in opisthobranch mollusks. The program includes mariculture of the nudibranch, *Hermissenda crassicornis,* with emphasis on developing reliable culture methods for rearing and maintaining this animal as a research resource. Studies include optimization of adult and larval nutrition, control of facultative pathogens and disease, development of morphologic criteria for staging larvae and juveniles, and metamorphic induction. Morphologic studies stress the ontogeny of neural and sensory structures, and neurochemicals associated with the photic and vestibular systems which have been used as models systems in learning and memory studies.

Concurrent with these studies is the development of a new technique to obtain and reconstruct serial block face images (SBFI) of epoxy-embedded or cryoprepared tissues sectioned or freeze-fractured/freeze-etched inside an SEM by an *in situ* miniature ultramicrotome.

Collaborative research includes histochemical investigations on strontium's role in initiating calcification in molluscan embryos (shell and statoliths), as well as immunocytochemical labelling of cell-surface and secretory product antigens using monoclonal and polyclonal antibodies on *Hermissenda* sensory and neurosecretory neurons *in situ,* and in cell culture.

Additional collaborative research includes DNA fingerprinting of *Hermissenda* using RAPD-PCR techniques in preparation for genetic strain development, as well as chemical ecological studies of the roles natural products play in larval metamorphosis and predator-prey recognition and defense mechanisms. Systematic and taxonomic studies of nudibranch mollusks are also of interest.

Staff

Kuzirian, Alan M., Associate Scientist
Tamse, Catherine T., Research Assistant

Visiting Investigators

Avila, Conxita, Postdoctoral Associate, Centre d'Estudis Avançats de Blanes, Blanes, Spain
Chikarmane, Hemant, Assistant Scientist, MBL
Leighton, Stephen B., Biomed. Engineering/Instrumen. Branch, NCRR-NIH

Laboratory of Rudolf Oldenbourg

We study physical optics relevant to microscopic imaging and develop advanced instrumentation in light microscopy for the study of structural dynamics in cells and cell components. The current focus of this new laboratory is the development of a novel polarized light microscope that combines polarization optics with new electro-optical components, video, and digital image processing for a fast analysis of specimen anisotropies over the entire viewing field at the highest resolution of the light microscope. Biological mechanisms to be explored with this new instrument range from the emergence and functional role of filamentous structures in living cells, to the generation of ordered domains in liquid crystals and polymer solutions. The laboratory currently investigates the distribution and dynamics of spindle microtubules directly in living cells (fertilized sea urchin eggs and newt lung cells).

Staff

Oldenbourg, Rudolf, Associate Scientist
Mei, Guang, Research Associate
Knudson, Robert, Instrumentation Engineer

Laboratory of Nancy Rafferty

This laboratory investigates the role of the lens cytoskeleton and its associated proteins in the maintenance of lens shape, in lens accommodation and development of cataract when the cytoskeleton is disrupted. Studies include an assessment of the role of cytosolic free calcium on homeostasis of the lens cytoskeleton, the localization of various cytoskeletal proteins in lens epithelium, and determination of the relative amounts of soluble actin to filamentous actin in lens cells during aging. Most of these studies employ an elasmobranch fish and rabbit model using primary cultures of lens epithelium and electron and immunofluorescence microscopy.

Staff

Rafferty, Nancy S., Scientist, Northwestern University
Rafferty, Keen A., Research Associate

Laboratory of Monica Riley

Research in this laboratory focuses on the molecular evolution and gene expression in the bacterium *Escherichia coli.* In a collaborative effort, a database containing information on the intermediary metabolism and biochemical pathways of *E. coli* is being developed. When completed, this database is expected to contain information on each metabolic reaction, the enzyme, the reactants, products, cofactors, activators, inhibitors, kinetics, equilibrium constants, binding constants, etc.

Related research is on the evolution of the *E. coli* DNA and organization of the genes in the chromosome. Comparative nucleotide and amino acid sequence data provide information on the evolutionary relationships of *E. coli* genes to other genes in the *E. coli* genome and to homologous genes in related bacteria.

Staff

Riley, Monica, Senior Scientist
Pellegrino-Toole, Alida, Research Assistant

Laboratory of Sensory Physiology

Since 1973, The Laboratory has conducted research on various aspects of vision. Current investigations focus on structural, functional, and evolutionary questions concerning visual pigments. The chemical basis of color vision is investigated principally with light-microscope-based absorption spectroscopy. In collaboration with other laboratories, we study gene sequences and evolutionary aspects of visual pigments aimed at revealing the molecular mechanisms responsible for spectral tuning.

Staff

Harosi, Ferenc I., Associate Scientist, MBL, and Boston University School of Medicine

Visiting Investigators

Hawryshyn, Craig W., University of Victoria, Canada
Schmitt, Ellen A., and Dowling, John E., Harvard University
Kelly, Mary E., and Barlow, Robert B. Jr., Syracuse University
Solessio, Eduardo, and Engbretson, Gustaf, Syracuse University

Laboratory of Osamu Shimomura

Various biochemical mechanisms involved in the bioluminescence of different luminous organisms are investigated. Based on the results obtained in this laboratory, various improved forms of bioluminescent probes are designed and produced for the measurements of intracellular free calcium and superoxide anion.

Staff

Shimomura, Osamu, Senior Scientist, MBL, and Boston University School of Medicine
Shimomura, Akemi, Research Assistant

Laboratory of Raquel Sussman

We investigate the molecular mechanism of DNA damage-inducible functions in *E. coli.* Present studies deal with novel genes that affect radiation-induced mutagenesis and analysis of RecA functions. In addition, we have been developing techniques for genomic mapping and collaborating in the isolation of neuronal genes in squid.

Staff

Sussman, Raquel, Associate Scientist

Visiting Investigators

Wangh, Larry, Brandeis University
Berberian, Graciela, Instituto de Investigacion Medica, Cordoba, Argentina

Molecular Evolution Program

The major research effort of this laboratory is the structure analysis of ribosomal RNAs. Similarities between small subunit ribosomal RNA sequences are used to infer the evolutionary history of eukaryotic microorganisms and to design molecular probes for studies in marine ecology.

Staff

Sogin, Mitchell L., Director and Senior Scientist
Gunderson, John, Research Associate
Hinkle, Greg, Postdoctoral Fellow
Leipe, Detlev, Postdoctoral Fellow
Morrison, Hillary, Postdoctoral Fellow
Silberman, Jeffrey, Postdoctoral Fellow

National Vibrating Probe Facility

The past year has seen a pronounced shift in interest from the Facility's tool of long standing, the vibrating probe, to the recently developed ion-selective probe. Twenty-four off-campus investigators have visited the Facility this past year, and nearly all of them have exploited the unique qualities of this newly invented electrophysiological technique. Studies have ranged from measuring calcium flux across growing pollen tubes, through developmental currents and pancreatic beta cell transmembrane ion flux, to monitoring free-radical attacks on cultured neurons. The forthcoming year promises further developments of magnesium-selective probes and the first animal experiments with the ground-breaking BioKelvin probe.

Staff

Jaffe, Lionel F., Director Emeritus
Smith, Peter J. S., Director
McLaughlin, Jane A., Research Assistant
Sanger, Richard H., Senior Electronics Technician
Shipley, Alan M., Research Associate

Sabbatical Visitors

Kunkel, Joseph, University of Massachusetts, Amherst
Ryan, James, Hobart and William Smith College

Visiting Investigators

Allen, Nina, Wake Forest
Baikie, Iain, Aberdeen, U.K.
Fishman, Harvey, Texas A & M University
Hill, Susan, Michigan State
Kaczmarek, Leonard, Yale University
Knox, Ronnie, Yale University
Leech, Colin, Harvard University and Massachusetts General Hospital
Marcus, Daniel, Omaha, NB
Nagel, Wolfram, Munich, Germany
Pierson, Elisabeth, Siena, Italy
Shepherd, Dave, Southampton, U.K.
Tytell, Mike, Wake Forest
Wright, Jonathan, McMaster University

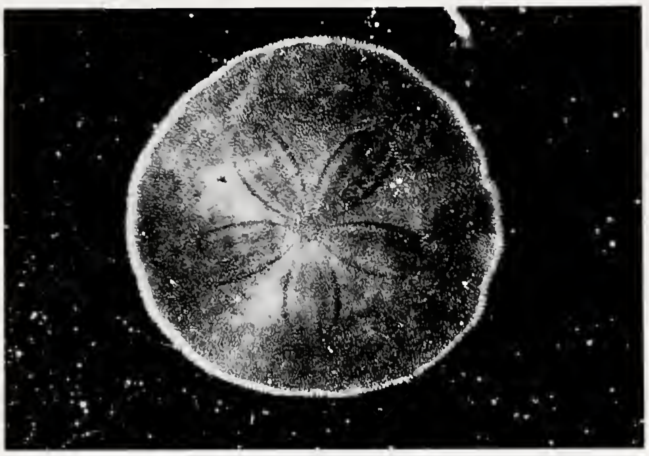

Honors

Friday Evening Lectures

Hans Moravec, Robotics Institute, Carnegie Mellon University, June 25, "*The Age of Mind*"

Juergen Tautz, Theodor-Boveri-Institut der Universitaet, July 2, "*Aircraft Detectors, Combination Locks, and Trap Triggers: Functional Diversity in Insect Mechanosensory Hairs*"

Bruce M. Alberts, President, National Academy of Sciences, July 9, "*The Centrosome: Organizer of the Cytoplasm in the Early* Drosophila *Embryo*"

Sten Grillner, Karolinska Institutet, Forbes Lectures July 15 and 16, "*Cellular Mechanisms Used to Control Timing in a Pattern-Generating Network*" and "*How Does the Lamprey Nervous System Make the Lamprey Swim? Integration Between the Networks Controlling Locomotion and Equilibrium*"

Norman R. Pace, Indiana University, July 23, "*Seeing the Unseen: Opening the Door Onto the Natural Microbial World*"

Shirley Tilghman, Princeton University, July 30, "*Parental Imprinting in the Mouse*"

J. Michael Bishop, University of California, San Francisco, August 6, "*Wayward Cells: The Genesis of Human Cancer*"

Gene E. Likens, Mary Flagler Carey Arboretum, August 13, "*Human-Accelerated Environmental Change: An Ecologist's View*"

Arnold J. Levine, Princeton University, August 20, "*Genes Involved in Inherited and Spontaneous Human Cancer: The p-53-mdm-2 Suppressor Gene*"

Fellowships and Scholarships

In 1993, the MBL awarded research fellowships amounting to $131,076 to 22 scientists from around the world who investigated topics ranging from creating computer models of neural networks, to real-time visualization of DNA replication in mammalian nuclei, to studying kinesin and motor proteins in mitosis and organelle transport. The MBL's educational and training program attracted more than 400 students who participated in the most extensive course schedule yet offered at the Laboratory. Scholarship awards totalling $104,098 helped to underwrite this important program.

Donors who made a gift to the Fellowship and Scholarship Program during 1993 are noted below in bold letters. The 1993 recipients of the awards are listed below in italics along with their institutions.

MBL Research Fellowships Awarded in 1993:

ROBERT DAY ALLEN FELLOWSHIP FUND
Drs. Jean and Joseph Sanger
Fatima K. Gyoeva, Russian Academy of Sciences

FREDERIK B. BANG FELLOWSHIP FUND
Mrs. Betsy G. Bang
Nancy Standard, University of Cambridge

JOHN O. CRANE FELLOWSHIP FUND
Hollis Cline, University of Iowa

DAN FUND
Drs. Joseph and Jean Sanger, Mrs. Eleanor Steinbach

FRIES FELLOWSHIP
the Estate of Anna B. Fries

M.G.F. FUORTES FELLOWSHIP FUND
Siglunde Gramoll, Emory University

GRASS ENDOWMENT FUND
Mrs. Ellen R. Grass, Grass Foundation
Jim H. Belanger, University of Arizona
Heather Cook, University of Toronto
Lise Eliot, Baylor College of Medicine
William C. Lemon, University of Arizona
Abdel El Manira, Karolinska Institutet for Neurophysiology
Andrew Olson, University of Pennsylvania
Angel Manuel Pastor-Loro, University of Sevilla

Haohua Quian, Harvard University
Sylvia Ryckebusch, California Institute of Technology
Ferdinand Sven Vilim, Columbia University
Philip Wahl, Royal Danish School of Pharmacy
Samuel Sheng-Hung Wang, Hopkins Marine Station, Stanford University

LAKIAN RESEARCH FELLOWSHIPS

Lakian Foundation
Timothy Bestor, Harvard Medical School
Jonathan M. Scholey, University of California, Davis

LAKIAN POST-DOCTORAL SCHOLAR

Lakian Foundation
Joseph Vallino, Scripps Institution of Oceanography

JAMES S. McDONNELL FOUNDATION FELLOWSHIP

Vladimir I. Makarenko, Russian Academy of Sciences, Institute of Mathematic Problems of Biology

JAMES A. AND FAITH MILLER FELLOWSHIP FUND

Mary Constance Lane, University of California, Berkeley

NIKON INC. FELLOW

Nikon, Inc.
Vladimir I. Gelfand, University of California, San Francisco

EVELYN AND MELVIN SPIEGEL FELLOWSHIP

Drs. Joseph and Jean Sanger, Sprague Foundation, Inc.

H. B. STEINBACH FELLOWSHIP FUND

Mrs. H. Burr Steinbach
Jonathan Wright, McMaster University

MBL Steps Toward Independence (STEPS) FELLOWSHIP FUND

Dr. Shinya Inoué, Dr. J. P. Trinkaus
Hollis Cline, University of Iowa
Jeffery R. Demarest, University of Arkansas
Siglunde Gramoll, Emory University
Fatima K. Gyoeva, Russian Academy of Sciences
Sergei A. Kuznetsov, Moscow State University
Elisabeth Pierson, University of Siena
Takashi Shimizu, National Institute of Bioscience & Human Technology
Nancy Standard, University of Cambridge
Jonathan Wright, McMaster University

HORACE W. STUNKARD FELLOWSHIP FUND

the Estate of Horace W. Stunkard
Hollis Cline, University of Iowa

MBL Research Fellowships and Scholarships Awarded in 1993 (Combined funds):

BERNARD DAVIS FELLOWSHIPS AND SCHOLARSHIPS

Dr. Porter W. Anderson, Jr.
Alain Brauman, Centre ORSTOM
Gabriele Fischer, University of Konstanz
Eric Frings, University of Bonn
Lee Hughes, University of North Texas
Shahid Khan, Albert Einstein College of Medicine
Jill Kreiling, West Virginia University
Eva Lindstrom, Uppsala University
Magdalena Martinez-Caname, University of Medicine and Dentistry of New Jersey
Margret Moré, Cornell University
Clifford Ochs, University of Mississippi

FRANK R. LILLIE FELLOWSHIP AND SCHOLARSHIP FUND

Malcolm Logan, National Institute for Medical Research
Steven Myster, University of Minnesota
Clifford Ochs, University of Mississippi
Fumio Oosawa, Aichi Institute of Technology
Rafael Rosenzweig, University of Idaho

WILLIAM TOWNSEND PORTER FELLOWSHIP AND SCHOLARSHIP FUND

Sharon Beresford, SUNY, Stony Brook
Timothy C. Dawson, University of Kansas
Roberto Gonzales, University of Texas, San Antonio
Raquell Holmes, Tufts University
Michelle Johnson, Howard University
Maxine Kellman, VA-MD Regional College of Veterinary Medicine
Winston Thompson, University of Medicine and Dentistry of New Jersey

HERBERT W. RAND FELLOWSHIP AND SCHOLARSHIP FUND

Bernhard E. Flucher, National Institutes of Health
Antony Galione, Oxford University
Hiroyoshi Miyakawa, Yamagata University School of Medicine
Farzan Nadim, Boston University
Erich A Nigg, Swiss Institute for Experimental Cancer Research

MBL Scholarships Awarded in 1993:

AMERICAN SOCIETY FOR CELL BIOLOGY SCHOLARSHIPS

American Society for Cell Biology
Sharon Beresford, SUNY, Stony Brook
Roberto Gonzales, University of Texas, San Antonio
Raquell Holmes, Tufts University
Michelle Johnson, Howard University
Maxine Kellman, VA-MD Regional College of Veterinary Medicine
Thandi Onami, Scripps Institution of Oceanography
Winston Thompson, University of Medicine and Dentistry of New Jersey

BIOLOGY CLUB OF THE CITY OF NEW YORK SCHOLARSHIP FUND

Madelyne Kraft, City College

FATHER ARSENIUS BOYER SCHOLARSHIP FUND

Joshua Gold, Stanford University School of Medicine

C. LALOR BURDICK SCHOLARSHIP FUND

Christina McKittrick, Rockefeller University

GARY N. CALKINS SCHOLARSHIP FUND

Tim Stedman, Virginia Commonwealth University

FRANCES S. CLAFF SCHOLARSHIP FUND

Giulio Ghersi, Universitá di Palermo

EDWIN GRANT CONKLIN SCHOLARSHIP FUND

Tim Stedman, Virginia Commonwealth University
Adam Strassberg, California Technological Institute

LUCRETIA CROCKER SCHOLARSHIP FUND

Farzan Nadim, Boston University
Oystein Olsen, University of Glasgow

WILLIAM F. AND IRENE C. DILLER SCHOLARSHIP FUND

Joshua Gold, Stanford University School of Medicine
Steven Myster, University of Minnesota

CASWELL GRAVE SCHOLARSHIP FUND

Jorge Huete-Perez, University of San Paulo-Ribeirao Preto
Malcolm Logan, National Institute for Medical Research

ALINE D. GROSS SCHOLARSHIP FUND

Mr. and Mrs. Alfred Weisberg
Gabrielle Kardon, Duke University

WILLIAM RANDOLPH HEARST EDUCATIONAL ENDOWMENT SCHOLARSHIPS

Clare Baker, Wellcome/CRC Institute
Elizabeth Callery, University of Toronto
Gabrielle Kardon, Duke University

HOWARD HUGHES MEDICAL INSTITUTE EDUCATIONAL PROGRAM SCHOLARSHIP FUNDING

Sharon Beresford, SUNY, Stony Brook
Roberto Gonzales, University of Texas, San Antonio
Raquell Holmes, Tufts University
Michelle Johnson, Howard University
Dmitri Krylov, Oregon State University
Farzan Nadim, Boston University
Thandi Onami, Scripps Institution of Oceanography
Janine Simmons, University of California, Los Angeles, School of Medicine
Johanna Speksnijder, Hubrecht Laboratory
Winston Thompson, University of Medicine and Dentistry of New Jersey
Anne Warner, Dartmouth College
Clare Waterman-Storer, University of Pennsylvania Veterinary School
Cheng Zhu, Georgia Institute of Technology

MERKEL H. JACOBS SCHOLARSHIP FUND

Marlene Bartos, Technische Universität München

ARTHUR KLORFEIN SCHOLARSHIP FUND

Marlene Bartos, Technische Universität München
Heidi Scrable, University of Cincinnati College of Medicine
Orian Shirihai, Technion-Israel Institute of Technology
Deborah Sodickson, Harvard Medical School
Kristina Wietasch, Harvard Medical School

JACQUES LOEB FOUNDERS' SCHOLARSHIP FUND

Christina McKittrick, Rockefeller University

JOHN D. AND CATHERINE T. MacARTHUR FOUNDATION SCHOLARSHIPS

Niklas Ahlborg, Stockholm University
Lisa Barthel, Northwestern University
Paul Bloch, Danish Bilharziasis Laboratory
Marcelo Briones, Escola Paulista de Medicine
Fidel de la Cruz Hernandez, CINVESTAV-IPN Mexico
Wolfgang Hoffmann, University of Tübingen
David Horn, Rockefeller University
Jorge Huete-Perez, University of San Paulo-Ribeirao Preto
Catharine Johnson, John Hopkins College of Veterinary Medicine
Maxine Kellman, VA-MD Regional College of Veterinary Medicine
Johannes Koeller, University of Munich
Fatima Noronha, Universidad Federal de Minas Gerais
Levi Omara, INGEBI
Simon Paul, Rockefeller University
Barbara Rick, Zoologisches Institute der Universität Bonn
Paul Selzer, Universität Tubingen
Tim Stedman, Virginia Commonwealth University
Jan Tachezy, Charles University
James Tang, University of Queensland

S. O. MAST MEMORIAL FUND SCHOLARSHIPS

Craig Powell, Baylor College of Medicine
Orian Shirihai, Technion-Israel Institute of Technology

ALLEN R. MEMHARD MEMORIAL FUND SCHOLARSHIPS

Constance Moore, University of Nebraska Medical Center

MICHIGAN STATE UNIVERSITY CENTER FOR MICROBIAL ECOLOGY SCHOLARSHIP

Maria Uria-Nickelsen, University of Connecticut

ALBERTO MONROY FOUNDATION SCHOLARSHIP

Giulio Ghersi, Universitá di Palmero

JAMES S. MOUNTAIN MEMORIAL FUND, INC. SCHOLARSHIPS

Dr. Isabel Mountain
Katherine Armstrong, Stanford Medical School
Diane Frank, University of Wisconsin-Madison
Keith Kozminski, Yale University
Thandi Onami, Scripps Institution of Oceanography
Alexander Travis, University of Pennsylvania Medical Center

PLANETARY BIOLOGY INSTITUTE SCHOLARSHIPS

Tsute Chen, University of Massachusetts
Lee Hughes, University of North Texas

MOSHE SHILO MEMORIAL SCHOLARSHIP FUND

Dr. Silke Bernhard, Dr. and Mrs. Bernard D. Davis, B. DeRothschild Foundation, Dr. Edward Goldberg, Prof. Gerhard Gottschalk, Dr. E. Peter Greenberg, Dr. and Mrs. Harlyn O. Halvorson, Israel Academy of Sciences and Humanities, Dr. Wolfgang Krumbein, Dr. and Mrs. Laszlo Lorand, Dr. Joel Mandelstam, Dr. Richard Mateles, Mrs. David Shemin, Mrs. Miriam Shilo, Dr. Melvin I. Simon

SOCIETY FOR DEVELOPMENTAL BIOLOGY SCHOLARSHIPS

Kristine Artinger, University of California, Irvine
Sunita Gupta, SUNY, Stony Brook
Karel Liem, Jr., Columbia University
Hyla Sweet, University of Texas, Austin

SOCIETY FOR GENERAL PHYSIOLOGY SCHOLARSHIPS

Cheng Zhu, Georgia Institute of Technology

MARJORIE W. STETTEN SCHOLARSHIP FUND

Craig Powell, Baylor College of Medicine

WILLIAM MORTON WHEELER FAMILY FOUNDERS' SCHOLARSHIPS

Richard Kollmar, University of Wisconsin-Madison
Orian Shirihai, Technion-Israel Institute of Technology

CARL ZEISS, INC. SCHOLARSHIPS

Carl Zeiss, Inc.
William Miller, University of California, Davis
Claudia Ochatt, INGEBI
Wenying Shou, Pomona College

Post-Course Research Support:

UNIVERSAL IMAGING CORPORATION

Sharon Beresford, SUNY, Stony Brook
Robbert Créton, University of Utrecht
Alex Travis, University of Pennsylvania Medical Center

CARL ZEISS, INC.

Jill Kreiling, West Virginia University
Stanley Jones Iyadurai, University of Minnesota
Heidi Scrable, University of Cincinnati College of Medicine

Board of Trustees and Committees

Corporation Officers and Trustees

Chairman of the Board of Trustees, Sheldon J.Segal, The Population Council, New York, NY
Vice Chairman of the Board of Trustees, Robert E. Mainer, The Boston Company, Boston, MA
President of the Corporation, James D. Ebert, Johns Hopkins University, Baltimore, MD
Director and Chief Executive Officer, John E. Burris, Marine Biological Laboratory, Woods Hole, MA*
Chair of the Science Council, Dr. George M. Langford, Dartmouth College, Hanover, NH*
Treasurer, Robert D. Manz, Helmer & Associates, Waltham, MA*
Clerk of the Corporation, Neil Jacobs, Hale and Dorr, Boston, MA

Class of 1997

Frederick Bay, The Bay Foundation, New York, NY
Martha W. Cox, Nantucket, MA
Mary J. Greer, Cambridge, MA
Thomas D. Pollard, John Hopkins Medical School, Baltimore, MD
William C. Steere, Jr., Pfizer Inc., New York, NY
Gerald Weissmann, New York University School of Medicine, New York, NY

Class of 1996

Norman Bernstein, Diane and Norman Bernstein Foundation, Washington, DC
Alexander W. Clowes, University of Washington School of Medicine, Seattle, WA
Eric H. Davidson, California Institute of Technology, Pasadena, CA
Robert D. Goldman, Northwestern University Medical School, Chicago, IL
Paul A. Marks, Memorial Sloan-Kettering Cancer Center, New York, NY
Irving W. Rabb, University Place at Harvard Square, Cambridge, MA

Class of 1995

Robert E. Mainer, The Boston Company, Boston, MA
Neil Jacobs, Hale and Dorr, Boston, MA
Mary-Ellen Cunningham, Grosse Pointe Farms, MI
Edward A. Kravitz, Harvard Medical School, Boston, MA
Philip Needleman, Searle Research & Development, Skokie, IL

Class of 1994

William L. Brown, Weston, MA
Franklin M. Loew, Tufts University School of Veterinary Medicine, North Grafton, MA
Joan V. Ruderman, Harvard University School of Medicine, Boston, MA
Henry H. Schmidek, Marion, MA
Sheldon J. Segal, The Population Council, New York, NY

Honorary Trustees

Honorary Chairman of the Board of Trustees, Denis M. Robinson, Key Biscayne, FL
William T. Golden, New York, NY
Ellen R. Grass, The Grass Foundation, Quincy, MA

Emeriti

Edward A. Adelberg, Yale University, New Haven, CT
John B. Buck, Sykesville, MD
Seymour S. Cohen, Woods Hole, MA
Arthur L. Colwin, Key Biscayne, FL
D. Eugene Copeland, Marine Biological Laboratory, Woods Hole, MA
Sears Crowell, Indiana University, Bloomington, IN
Alexander T. Daignault, Boston, MA
Teru Hayashi, Woods Hole, MA
Ruth Hubbard, Cambridge, MA
Lewis Kleinholz, Reed College, Portland, OR
Maurice E. Krahl, Tucson, AZ
Charles B. Metz, Miami, FL
Keith R. Porter, University of Pennsylvania, Philadelphia, PA
C. Ladd Prosser, University of Illinois, Urbana, IL
S. Meryl Rose, Waquoit, MA
W. D. Russell-Hunter, Syracuse University, Syracuse, NY
John W. Saunders, Jr., Waquoit, MA
Mary Sears, Woods Hole, MA
David Shepro, Boston University, Boston, MA
Homer P. Smith, Woods Hole, MA
D. Thomas Trigg, Wellesley, MA
Walter S. Vincent, Woods Hole, MA
George Wald, Cambridge, MA

* *Ex officio*

Executive Committee of the Board of Trustees

Sheldon J. Segal, Chairman
Frederick Bay, 1997
William Brown, 1994
John E. Burris*
Mary-Ellen Cunningham, 1995
Robert D. Goldman, 1996
George Langford*
Robert E. Mainer, Vice-Chairman
Robert Manz*
Thomas D. Pollard, 1997
Gerald Weissmann, 1997

Trustee Committees

Development

Mary-Ellen Cunningham, Chair
Robert Barlow
Fred Bay
Martha Cox
James Ebert
Neil Jacobs
Franklin Loew
Henry Schmidek
William Speck
William Steere

Facilities and Capital Equipment

Robert Goldman, Chairman
Jelle Atema
Alfred Chaet
Franklin Loew
Jerry Melillo
Joan Ruderman
Robert Silver

Finance and Investment

Robert Mainer, Chairman
Norman Bernstein
William Brown
Alexander Clowes
Eric Davidson
Donald DeHart
Neil Jacobs
Werner Lowenstein
Robert Manz
Irving Rabb
Thomas Trigg

Long-Range Planning

Fred Bay, Co-Chair
Thomas Pollard, Co-Chair
Eric Davidson
John Dowling
Gerald Fischbach
Robert Goldman
Mary Greer
George Langford
Robert Manz
Philip Needleman
Joan Ruderman
Henry Schmidek

Nominating

Gerald Weissmann, Chairman
Alexander Clowes
Martha Cox
Mary-Ellen Cunningham
Mary Greer
George Langford
Philip Needleman
Thomas Pollard
Sheldon Segal
William Steere

Corporation Standing Committees

Buildings & Grounds

Alfred B. Chaet, Chairman
Barbara Boyer
Lawrence B. Cohen
Richard D. Cutler*
William Eckberg
Ferenc Harosi
Lionel Jaffe
Thomas Meedel
Kenyon Tweedel

Fellowships

Thoru Pederson, Chairman
Martha Constantine-Paton
Pamela M. Ghetti*
Ann Giblin
George M. Langford
José Lemos
Eduardo Macagno
Carol L. Reinisch

Housing, Food Service, and Child Care

Thomas S. Reese, Chairman
Elaine Bearer
Donald C. Chang
Milton Charlton
Richard Cutler*
Robert Gould
Stephen Highstein
LouAnn King*
Joan Ruderman
Darrell R. Stokes

Instruction

Ed Kravitz, Chairman
George Augustine
Rachel Fink
Tom Fox
Susan Hill
Ron Hoy
Hans Laufer
Jean Monahan*
Robert B. Silver
David Stonehill*
Kathryn Swenson
John Waterbury

MBL/WHOI Library Joint Advisory

David Shepro, Chairman, MBL
Werner Deuser, WHOI
Henry Dick, WHOI
Kevin Friedland, NMFS
John Hobbie, MBL
David Stonehill*
Page Valentine, USGS
Gerald Weissmann, MBL

Marine Resources

Robert Goldman, Chairman
Donald Abt
William Cohen
Richard Cutler*
Ed Enos*
Alan Kuzirian*
Toshio Narahashi
George Pappas
Roger Sloboda

* *Ex officio*

Melvin Spiegel
Antoinette Steinacher

Research Services

Peter Armstrong, Chairman
Neal Cornell
Richard Cutler*
Barbara Ehrlich
Kenneth Foreman
Joseph Ilan
Aimlee Laderman
Jack Levin
Andrew Mattox*
Robert Palazzo
James Quigley
Peter J.S. Smith
Paul Steudler
Mark Tykocinski

Research Space

Hans, Laufer, Chairman
Paul DeWeer
David Landowne
Eduardo Macagno
Andrew Mattox*
Jerry Melillo
Robert Silver
Steven Treistman
Ivan Valiela
Richard Vallee

* *Ex officio*

Laboratory Support Staff*

Biological Bulletin

Clapp, Pamela L., Managing Editor
- Gibson, Victoria R.
- Liles, Beth R.
- McCaffrey, Karen

Controller's Office

Speer, John W., Controller

Accounting Services
- Afonso, Janis E.
- Binda, Ellen F.
- Campbell, Ruth B.
- Davis, Doris C.
- Ghetti, Pamela M.
- Gilmore, Mary F.
- Hobbs, Roger W., Jr.
- Poravas, Maria

Chem Room
- Schorer, Timothy M.
- Shepherd, Denise M.

Purchasing
- Hall, Lionel E., Jr.
- Shepherd, Denise M.

Director's Office

Burris, John E., Director and CEO
- Burrhus, I. Elaine
- Catania, Didia
- Kaufmann, Sandra J.
- Nelson, Mary F.

External Affairs

Carotenuto, Frank C., Director
- Aspinwall, Duncan P.
- Berthel, Dorothy
- Faxon, Wendy P.
- Lessard, Kelley J.
- Nelson, Mary F.

Associates Program
- Armstrong, Ellen P., Liaison
- Brown, M. Kathryn S.
- DiIorio, Anne E.

Communications Office
- Clapp, Pamela L., Director
- Liles, Beth R.
- Moorhouse, Laura A.

Housing

King, LouAnn D., Conference Center and Housing Manager
- Johnson, Frances N.

Telephone Office
- Baker, Ida M.
- Geggatt, Agnes L.
- Ridley, Alberta W.

Human Resources

Goux, Susan P., Manager
- Donovan, Marcia H.

MBL/WHOI Library

Stonehill, David L., Director, MBL/WHOI Library Center
- Ashmore, Judith A.
- Costa, Marguerite E.
- Mirra, Anthony J.
- Monahan, A. Jean
- Nelson, Heidi
- Pratson, Patricia G.
- deVeer, Joseph M.
- Zuwallack, Ronald

Copy Service Center
- Mountford, Rebecca J., Supervisor
- Barry, Maureen
- Jesse, Martha V.
- Mancini, Mary
- Ridley, Sherie
- Tebeau, Christopher

Information Systems Division
- Norton, Catherine N., Director
- Hamre, Lynne
- Remsen, David
- Renna, Denis J.
- Space, David B.
- Tollios, Constantine D.

Safety Services

Mattox, Andrew H., Safety Officer

Apparatus
- Barnes, Franklin D.
- Haskins, William A.
- Martin, Lowell V.
- Nichols, Francis H., Jr.

Shipping and Receiving
- Collins, Paul J.
- Geggatt, Richard E.
- Illgen, Robert F.
- Luther, Herbert

Services, Projects, and Facilities

Cutler, Richard D., Manager
- Enos, Joyce B.
- Kurland, Charles I.

Building Services and Grounds
- Hayes, Joseph N., Superintendent
- Allen, Wayne D.
- Anderson, Lewis B.
- Barnes, Susan M.
- Beaudoin, Helen
- Boucher, Richard L.
- Collins, Paul J.
- Conlin, Henry P.
- Dorris, John J.
- Dutra, Roger S., Jr.
- Gibbons, Roberto G.
- Gonsalves, Walter W., Jr.
- Krajewski, Viola I.
- Lynch, Henry L.

---

* *Including persons who joined or left the staff during 1993.*

Mancini, Mary
McNamara, Noreen
Rattacasa, Frank D.
Serrano, Robert A.

Plant Operations and Maintenance

Fleet, Barry M., Superintendent
Lehy, Donald B., Superintendent
Blunt, Hugh F.
Bourgoin, Lee E.
Carini, Robert J.
Fish, David L., Jr.
Fuglister, C. Kurt
Gonsalves, Paul J.
Gonsalves, Walter W., Jr.
Hathaway, Peter J.
Justason, C. Scott
Lochhead, William M.
Lunn, Alan G.
McAdams, Herbert M. III
Mills, Stephen A.
Olive, Charles W., Jr.
Schoepf, Claude
Sexton, Andrew
deVeer, Robert L.

Instrument Development Lab

Knudson, Robert A.

Machine Shop

Sylvia, Frank E.

Marine Resources Center

Enos, Edward G., Jr., Superintendent
Boucher, Richard L.
Cipoletta, Charles D.
Fisher, H. Thomas, Jr.
Moniz, Priscilla C.
Monteiro, Dana
Sullivan, Daniel A.
Tassinari, Eugene

MRC Life Support System

Mebane, William N., Systems Operator
Hanley, Janice S.

Photolab

Golder, Linda M.
Golder, Robert J.

Sponsored Programs

Garrick, Leslie D., Administrator
Chrysler, Dorianne
Huffer, Linda
Kaufmann, Sandra J.
Lynch, Kathleen F.
Price, F. Carol

Electron Microscopy Lab

Kerr, Louis M.

Temporary Employees

Carroll, James R.
Kaufmann, Sandra J.
Kehoe, Elizabeth D.
Laurençot, Colette
Luther, Herbert

Summer Support Staff

Adams, Virginia A.
Albers, Catherine
Andrews, Ethan
Andrews, Mark
Antonangeli, Donald, Jr.
Baldic, David P.
Balmer, Ethan
Baptiste, Michael
Biega, Cara M.
Broadhurst, Jennifer
Cadwalader, George, Jr.
Callahan, Ann M.
Cameron, Lisa A.
Capobianco, James A.
Cardoza, Laurie A.
Carroll, James R.
Chappell, Carol L.
Crabb, Andrew H.
Cutler, Laura
DeLinks, Elizabeth
Diachun, Peter
Farley, Lynda G.
Furie, Eric A.
Halfant, Jennie A.
Hogg, Brian N.
Horne, Joseph M.
Just, Thomas
Kan, Rebecca J.
Kelty, Ruth A.
Kessler, Anne P.
Kessler, Toby J.
Kilpatrick, Brian
Langford, Joy C.
Lovell, Lynne
Luther, Jonathan A.
Mancini, Rhonda A.
Masino, Mark A.
McDonald, Brian
McNeill, Jeffrey
Michael, Samuel A.
Muncher, David A.
Murray, Raymond J.
Nelson, Beth
O'Connor, John E.
O'Connor, Patricia M.
Pant, Alok C.
Pennington, Susan M.
Philibotte, James A.
Rakowski, Cara E.
Reese, Caroline S.
Regan, John F.
Richmond, Hazel E.
Rickles, Jason D.
Rugh, Douglas E.
Schmidek, Alexandra
Schou, Carolyn A.
Smith, Kelli M.
Sonnabend, Aaron P.
Stephen, Michael J.
Stradley, Douglas W.
Stukey, Jetly
Tamm, Ingrid J.
Thompson, Nuala
Torres, Sophie J.
Ulbrich, Ciona
Varao, John
Walsh, Jamie T.
Welenc, Karen
Wetzel, Ernest D.

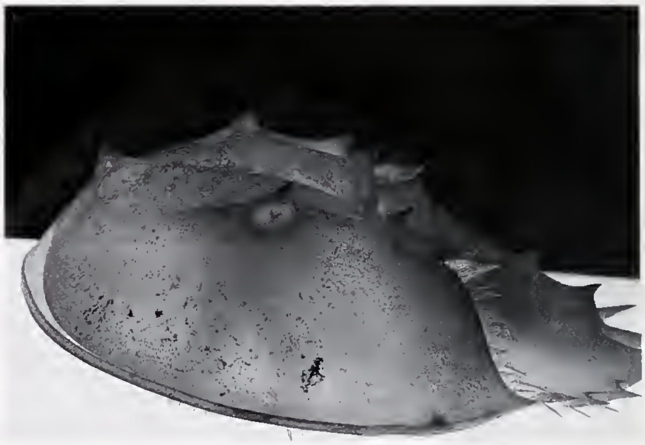

Members of the Corporation*

Life Members

Adelberg, Edward A., Provost's Office, Yale University, 115 Hall of Graduate Studies, New Haven, CT 06520
Amatniek, Ernest, 4797 Boston Post Road, Pelham Manor, NY 10803

Bang, Betsy G., 76 F.R. Lillie Road, Woods Hole, MA 02543
Bartlett, James H., Department of Physics, University of Alabama, Box 870324, Tuscaloosa, AL 35487-0324
Bernheimer, Alan W., Department of Microbiology, New York University Medical Center, 550 First Ave., New York, NY 10016
Bertholf, Lloyd M., Westminster Village #2114, 2025 E. Lincoln St., Bloomington, IL 61701-5995
Bridgman, A. Josephine, 913 Wesley Woods Towers, 1825 Clifton Rd., NE, Atlanta, GA 30329
Buck, John B., 7200 Third Ave., #C020, Sykesville, MD 21784
Burbanck, Madeline P., Box 15134, Atlanta, GA 30333
Burbanck, William D., Box 15134, Atlanta, GA 30333

Carlson, Francis D., Johns Hopkins University, Biophysics Department, Jenkins Hall, N. Charles Street, Baltimore, MD 21218
Clark, Arnold M., 53 Wilson Rd., Woods Hole, MA 02543
Cohen, Seymour S., 10 Carrot Hill Rd., Woods Hole, MA 02543-1206
Colwin, Arthur L., 320 Woodcrest Rd., Key Biscayne, FL 33149
Colwin, Laura Hunter, 320 Woodcrest, Key Biscayne, FL 33149
Copeland, D. E., 41 Fern Lane, Woods Hole, MA 02543
Corliss, John O., P. O. Box 53008, Albuquerque, NM 87153
Costello, Helen M., Carolina Meadows, Villa 137, Chapel Hill, NC 27514
Crouse, Helen, Address unknown

Dudley, Patricia L., Department of Biological Sciences, Barnard College, Columbia University, 3009 Broadway, New York, NY 10027

Edwards, Charles, 2244 Harbour Court Drive, Longboat Key, FL 34228
Erulkar, Solomon D., 318 Kent Road, Bala Cynwyd, PA 19004

Failla, Patricia M., 2149 Loblolly Lane, Johns Island, SC 29455
Ferguson, James K. W., 56 Clarkehaven St., Thornhill, Ontario L4J 2B4 Canada

Glusman, Murray, 50 E. 72nd St., New York, NY 10021
Goldman, David, 63 Loop Rd., Falmouth, MA 02540
Graham, Herbert, 36 Wilson Rd., Woods Hole, MA 02543
Green, James W., 409 Grant Ave., Highland Park, NJ 08904

Hamburger, Viktor, Department of Biology, Washington University, St. Louis, MO 63130
Hamilton, Howard L., Department of Biology, University of Virginia, 238 Gilmer Hall, Charlottesville, VA 22901
Harding, Clifford V., Jr., 54 Two Ponds Road, Falmouth, MA 02540
Haschemeyer, Audrey E. V., 21 Glendon Road, Woods Hole, MA 02543
Hauschka, Theodore S., FD1, Box 781, Damariscotta, ME 04543
Hisaw, F. L., 5925 SW Plymouth Drive, Corvallis, OR 97330
Hubbard, Ruth, 21 Lakeview Avenue, Cambridge, MA 02138
Humes, Arthur G., Boston University Marine Program, Marine Biological Laboratory, Woods Hole, MA 02543
Hurwitz, Charles, Veterans Administration Hospital, Basic Science Research Laboratory, Albany, NY 12208

Karush, Fred, Department of Microbiology, University of Pennsylvania School of Medicine, Philadelphia, PA 19104-6076
Kille, Frank R., 1111 S. Lakemont Ave. #444, Winter Park, FL 32792 (deceased)
Kingsbury, John M., Department of Plant Biology, Cornell University, Plant Science Building, Ithaca, NY 14853
Kleinholz, Lewis, Department of Biology, Reed College, 3203 SE Woodstock Blvd., Portland, OR 97202

Laderman, Ezra, Yale University, School of Music, New Haven, CT 06520
Lauffer, Max A., Address unknown
LeFevre, Paul G., 15 Agassiz Road, Woods Hole, MA 02543
Levine, Rachmiel, 2024 Canyon Rd., Arcadia, CA 91006
Lochhead, John H., 49 Woodlawn Rd., London SW6 6PS, England, UK
Loewus, Frank A., Washington State University, Institute of Biological Chemistry, Pullman, WA 99164
Loftfield, Robert B., Department of Biochemistry, University of New Mexico School of Medicine, Albuquerque, NM 87131

Magruder, Samuel R., 270 Cedar Lane, Paducah, KY 42001
Malkiel, Saul, Allergic Diseases, Inc., 130 Lincoln St., Worcester, MA 01609

---

* Including action of the 1993 Annual Meeting.

Martin, Lowell V., 10 Buzzards Bay Avenue, Woods Hole, MA 02543
Mathews, Rita W., Box 131, Southfield, MA 01259
Miller, James A., 307 Shorewood Drive, E. Falmouth, MA 02536 (deceased)
Moore, John A., Department of Biology, University of California, Riverside, CA 92521
Moscona, Arthur A., University of Chicago, Department of Molecular Genetics and Cell Biology, 920 East 58th Street, Chicago, IL 60637
Mullins, Lorin J., University of Maryland School of Medicine, Department of Biophysics, Baltimore, MD 21201 (deceased)
Musacchia, Xavier J., P.O. Box 5054, Della Vista, AR 72714-0054

Nasatir, Maimon, P. O. Box 379, Ojai, CA 93024-0379

Pollister, A. W., 8 Euclid Ave., Belle Mead, NJ 08502
Prosser, C. Ladd, Department of Physiology, Burrill Hall 524, University of Illinois, Urbana, IL 61801
Prytz, Margaret McDonald, Address unknown

Ratner, Sarah, Department of Biochemistry, Public Health Research Institute, 455 First Ave., New York, NY 10016
Renn, Charles E., Address unknown
Reynolds, George, Department of Physics, Princeton University, Jadwin Hall, Princeton, NJ 08544
Rice, Robert V., 30 Burnham Dr., Falmouth, MA 02540
Richards, A. Glenn, 942 Cromwell Ave., St. Paul, MN 55114
Rockstein, Morris, 600 Biltmore Way, Apt. 805, Coral Gables, FL 33134
Ronkin, Raphael R., 3212 McKinley St., NW, Washington, DC 20015-1635
Rose, S. Meryl, 32 Crosby Ln., E. Falmouth, MA 02536

Sanders, Howard, Woods Hole Oceanographic Institution, Woods Hole, MA 02543
Sato, Hidemi, Faculty of Social Science, Nagano University, Shiminogo, Ueda, Nagano 386-12, Japan
Saz, Arthur K, Georgetown University Medical School, Department of Immunology, Washington, DC 20007
Scharrer, Berta, Department of Anatomy, Albert Einstein College of Medicine, 1300 Morris Park Avenue, Bronx, NY 10461
Schlesinger, R. Walter, University of Medicine and Dentistry of New Jersey, Department of Molecular Genetics and Microbiology, Robert Wood Johnson Medical School, Piscataway, NJ 08854-5635
Schmitt, F. O., Room 16-512, Massachusetts Institute of Technology, Cambridge, MA 02139
Scott, Allan C., 1 Nudd St., Waterville, ME 04901
Silverstein, Arthur M., The Johns Hopkins Hospital, Johns Hopkins University, Institute of the History of Medicine, 1900 E. Monument Street, Baltimore, MD 21205
Smith, Homer P., 8 Quissett Ave., Woods Hole, MA 02543
Smith, Paul F., P. O. Box 264, Woods Hole, MA 02543
Sonnenblick, B. P., 515A Heritage Hill Village, Southbury, CT 06488
Steinhardt, Jacinto, 1508 Spruce St., Berkeley, CA 94709
Stephens, Grover C., Department of Ecology & Evolutionary Biology, School of Biological Sciences, University of California, Irvine, CA 92717

Taylor, Robert E., 20 Harbor Hill Rd., Woods Hole, MA 02543
Trager, William, The Rockefeller University, 1230 York Ave., New York, NY 10021-6399

Villee, Claude A., Harvard Medical School, Carol L. Countway Library, 25 Shattuck Street, Boston, MA 02115
Vincent, Walter S., 16 F.R. Lillie Rd., Woods Hole, MA 02543

Wald, George, 21 Lakeview Ave., Cambridge, MA 02138
Waterman, T. H., Yale University, 210 OML Biology Department, Box 6666, New Haven, CT 06511
Wiercinski, Floyd J., 21 Glenview Road, Glenview, IL 60025
Wigley, Roland L., 35 Wilson Rd., Woods Hole, MA 02543
Wilber, Charles G., Department of Biology, Forensic Science Lab, Colorado State University, Fort Collins, CO 80523

Zinn, Donald J., Department of Zoology, University of Rhode Island, Kingston, RI 02881
Zweifach, Benjamin W., 8811 Nottingham Place, La Jolla, CA 92037

Members

Abt, Donald A., Marine Biological Laboratory, Laboratory for Marine Animal Health, Woods Hole, MA 02543
Acheson, George H., 25 Quissett Ave., Woods Hole, MA 02543
Adams, James A., Florida A & M University, Department of Biology, Tallahasee, FL 32307-0077
Adelman, William J., Jr., 160 Locust St., Falmouth, MA 02540
Afzelius, Bjorn, Address unknown
Alberte, Randall S., Department of Molecular Genetics and Cell Biology, University of Chicago, 1103 E. 57th Street, Chicago, IL 60637
Alkon, Daniel, 9000 Rockville Pike, 36-4A21, Bethesda, MD 20892
Allen, Garland E., Department of Biology, Washington University, Box 1137, One Brookings Drive, St. Louis, MO 63130-4899
Allen, Nina S., Department of Biology, Wake Forest University, Box 7325, Winston-Salem, NC 27109
Anderson, Everett, Department Cell Biology, Harvard Medical School, 25 Shattuck St., Boston, MA 02115
Anderson, J. M., 110 Roat St., Ithaca, NY 14850
Anderson, Porter W., Department of Pediatrics, University of Rochester Medical Center, Box 690, 601 Elmwood Ave., Rochester, NY 14642
Armett-Kibel, Christine, Dean of Science Faculty, University of Massachusetts, Boston, MA 02125
Armstrong, Clay M., Department of Physiology, University of Pennsylvania Medical School, 8701 Richards Bldg., Philadelphia, PA 19104-6085
Armstrong, Peter B., Section of Molecular/Cellular Biology, University of California, Davis, CA 95616-8755
Arnold, John M., Pacific Biomedical Research Center, 209A Snyder Hall, University of Hawaii, Honolulu, HI 96822-2233
Arnold, William A., 102 Balsam Rd., Oak Ridge, TN 37830
Ashton, Robert W., Esq., Bay Foundation, 18th Floor, 99 Wall St., New York, NY 10005
Atema, Jelle, Boston University Marine Program, Marine Biological Laboratory, Woods Hole, MA 02543
Augustine Jr., George J., Department of Neurobiology, Duke University Medical Center, PO Box 3209, Durham, NC 27710
Ayers, Donald E., 4607 1/2 MacArthur Blvd., NW #B, Washington, DC 20007-2533

Baccetti, Baccio, Institute of Zoology, University of Siena, 53100 Siena, Italy
Baker, Robert G., Department of Physiology and Biophysics, New York University Medical Center, 550 First Ave., New York, NY 10016
Baldwin, Thomas O., Department of Biochemistry and Biophysics, Texas A&M University, College Station, TX 77843
Barlow, Robert B., Jr., Institute for Sensory Research, Syracuse University, Merrill Lane, Syracuse, NY 13244-5290
Barry, Daniel T., 2415 Fairwind Dr., Houston, TX 77062-4756

Barry, Susan R., Mount Holyoke College, Dept. of Biological Sciences, So. Hadley, MA 01075
Bartell, Clelmer K., 2000 Lake Shore Drive, New Orleans, LA 70122
Bass, Andrew H., Seely Mudd Hall, Department of Neurobiology, Cornell University, Ithaca, NY 14853
Battelle, Barbara-Anne, Whitney Laboratory, University of Florida, 9505 Ocean Shore Blvd., St. Augustine, FL 32086
Bauer, G. Eric, Department of Anatomy, University of Minnesota, Minneapolis, MN 55455 (dropped)
Bay, Frederick, Bay Foundation, 99 Wall St., 18th Fl., New York, NY 10005
Baylor, Edward R., P. O. Box 93, Woods Hole, MA 02543 (deceased)
Baylor, Martha B., P. O. Box 93, Woods Hole, MA 02543
Bearer, Elaine L., Division of Biology & Medicine, Department of Pathology, Brown University, Box G, Providence, RI 02912
Beauge, Luis Alberto, Department of Biophysics, Instituto M.y.M. Ferreyra, Casilla de Correo 389, 5000 Cordoba, Argentina
Beck, Lyle V., 2455 Tamarack Trail, Apt. 8, Bloomington, IN 47408
Begenisich, Ted, Department of Physiology, University of Rochester, Medical Center, Box 642, 601 Elmwood Ave., Rochester, NY 14642
Begg, David A., Department of Anatomy & Cell Biology, University of Alberta, Edmonton, Alberta T6G 2H7, Canada
Bell, Eugene, 305 Commonwealth Avenue, Boston, MA 02115
Benjamin, Thomas L., Harvard Medical School, Pathology, D2-230, 200 Longwood Avenue, Boston, MA 02115
Bennett, M. V. L., Albert Einstein College of Medicine, Department of Neuroscience, 1410 Pelham Pkwy. S., Bronx, NY 10461
Bennett, Miriam F., Department of Biology, Colby College, Waterville, ME 04901
Berg, Carl J., Jr., P. O. Box 769, Kilauea, Kauai, HI 96754-0769
Berlin, Suzanne T., 5 Highland St., Gloucester, MA 01930
Berne, Robert M., Department of Physiology, University of Virginia, School of Medicine, Box 116, MR4, Charlottesville, VA 22908
Bernstein, Norman, Diane and Norman Bernstein Foundation, Inc., 5301 Wisconsin Ave., #600, Washington, DC 20015-2015
Bezanilla, Francisco, Department of Physiology, University of California, Los Angeles, CA 90024
Biggers, John D., Department of Physiology, Harvard Medical School, Boston, MA 02115
Bishop, Stephen H., Department of Zoology, Iowa State University, Ames, IA 50010
Blaustein, Mordecai P., Department of Physiology, School of Medicine, University of Maryland, 655 W. Baltimore Street, Baltimore, MD 21201
Bloom, George S., Department of Cell Biology and Neuroscience, The University of Texas Southwestern Medical Center, 5223 Harry Hines Blvd., Dallas, TX 75235-9039
Bloom, Kerry S., Department of Biology, University of North Carolina, 623 Fordham Hall, Chapel Hill, NC 27516
Bodznick, David A., Department of Biology, Wesleyan University, Lawn Avenue, Middletown, CT 06457
Boettiger, Edward G., 29 Juniper Point, Woods Hole, MA 02543
Boolootian, Richard A., Science Software Systems, Inc., 3576 Woodcliff Rd., Sherman Oaks, CA 91403
Borgese, Thomas A., Department of Biology, Lehman College, CUNY, Bedford Park Blvd., West, Bronx, NY 10468
Borisy, Gary G., Laboratory of Molecular Biology, University of Wisconsin, Madison, WI 53706
Borst, David W., Jr., Department of Biological Sciences, Illinois State University, Normal, IL 61790-4120
Bosch, Herman F., Box 617, Woods Hole, MA 02543
Bowles, Francis P., P. O. Box 674, Woods Hole, MA 02543
Boyer, Barbara C., Department of Biology, Union College, Schenectady, NY 12308
Brandhorst, Bruce P., Department of Biological Sciences, Simon Fraser University, Barnaby, BC V5A 156, Canada
Brinley, F. J., Neurological Disorders Program, NINCDS, NIH, 812 Federal Building, Bethesda, MD 20892
Brown, Joel E., Albert Einstein College of Medicine, 506 Kennedy Center, 1400 Pelham Parkway, Bronx, NY 10461 (resigned)
Brown, Stephen C., Department of Biological Sciences, SUNY, Albany, NY 12222
Brown, William L., Retired Chairman, Bank of Boston, 100 Federal St. 01-23-11, Boston, MA 02106-2016
Browne, Carole L., Department of Biology, Wake Forest University, Winston-Salem, NC 27109
Browne, Robert A., Department of Biology, Wake Forest University, Box 7325, Winston-Salem, NC 27109
Bryant, Shirley H., Department of Pharmacology and Cell Biophysics, ML 575, University of Cincinnati, Cincinnati, OH 45267
Bucklin, Anne C., University of New Hampshire, Ocean Process Analysis Lab, 142 Morse Hall, Durham, NH 03824
Bullis, Robert A., Marine Biological Laboratory, LMAH, Woods Hole, MA 02543
Burd, Gail Deerin, Department of Molecular and Cell Biology, Life Sciences South, Rm 444, University of Arizona, Tucson, AZ 85721
Burdick, Carolyn J., Department of Biology, Brooklyn College, 2900 Bedford Avenue, Brooklyn, NY 11210
Burger, Max, Freidrich Miesner Institut Bau 1060 Postfach 2543, Basel 4002, Switzerland
Burgos, Mario, IHEM Medical School, UNC Conicet, Casilla de Correo 56, 5500 Mendoza, Argentina
Burky, Albert, Department of Biology, University of Dayton, Dayton, OH 45469
Burris, John E., Marine Biological Laboratory, Woods Hole, MA 02543
Burstyn, Harold L., Morrison Law Firm, The Morrison Building, 145 North Fifth Avenue, Mt. Vernon, NY 10550
Bursztajn, Sherry, Harvard Medical School, Mailman Research Center, 115 Mill St., Belmont, MA 02178
Busa, William, Department of Biology, Johns Hopkins University, 3400 N. Charles St., Baltimore, MD 21218

Calabrese, Ronald L., Department of Biology, Emory University, 1555 Pierce Drive, Atlanta, GA 30322
Callaway, Joseph C., Department of Physiology, New York Medical College, Basic Sciences Bldg., Valhalla, NY 10595
Calvin, Katherine Graubard, University of Washington, Department of Zoology, NJ-15, Seattle, WA 98195
Cameron, Andrew, Department of Biology, California Institute of Technology, Pasadena, CA 91125
Campbell, Richard H., Bang-Campbell Associates, Box 402, Eel Pond Place, Woods Hole, MA 02543
Candelas, Graciela C., Department of Biology, University of Puerto Rico, PO Box 23360, San Juan, PR 00931-3360
Carew, Thomas J., Department of Psychology, Yale University, P. O. Box 11A, Yale Station, New Haven, CT 06520
Cariello, Lucio, Biochemistry Department, Stazione Zoologica, Villa Comunale, 80121 Naples, Italy
Carriere, Rita M., Department of Anatomy and Cell Biology, Box 5, SUNY Health Science Center, 450 Clarkson Ave., Brooklyn, NY 11203 (resigned)
Case, James, University of California, Associate Vice Chancellor of Research, Santa Barbara, CA 93106
Cassidy, Rev. J. D., Providence College, Priory of St. Thomas Aquinas, Providence, RI 02918
Cavanaugh, Colleen M., Harvard University, Biological Laboratories, 16 Divinity Ave., Cambridge, MA 02138

Cebra, John J., Department of Biology, Leidy Labs, G-6, University of Pennsylvania, Philadelphia, PA 19174

Chaet, Alfred B., University of West Florida, Department of Cell & Molecular Biology, 11000 University Parkway, Pensacola, FL 32514

Chambers, Edward L., Department of Physiology and Biophysics, University of Miami, School of Medicine, P. O. Box 016430, Miami, FL 33101

Chang, Donald C., Hong Kong University of Science & Technology, Department of Biology, Clear Water Bay, Kowloon, Hong Kong

Chappell, Richard L., Department of Biological Sciences, Hunter College, Box 210, 695 Park Ave., New York, NY 10021

Chen, Thomas T., Center for Marine Biotechnology, University of Maryland, 600 E. Lombard St., Baltimore, MD 21202

Chikarmane, Hemant M., Marine Biological Laboratory, Woods Hole, MA 02543

Child, Frank M., III, Department of Biology, Trinity College, Hartford, CT 06106

Chisholm, Rex L., Department of Cell Biology, Northwestern University Medical School, Chicago, IL 60611

Citkowitz, Elena, 410 Livingston St., New Haven, CT 06511

Clark, Eloise E., Vice President, Bowling Green State University, Bowling Green, OH 43403

Clark, Hays, 26 Deer Park Drive, Greenwich, CT 06830

Clark, James M., 210 Emerald Lane, Palm Beach, FL 33480

Clark, Wallis H., Jr., 5400 NW 39th Ave., T170, Gainesville, FL 32606

Claude, Philippa, University of Wisconsin, Primate Center, 1223 Capital Court, Madison, WI 53715

Clay, John R., Laboratory of Biophysics, NIH, 36/2C02, Bethesda, MD 20892

Clowes, Alexander W., Department of Surgery RF-25, University of Washington School of Medicine, Seattle, WA 98195

Clutter, Mary, Office of the Director, Room 518, National Science Foundation, Washington, DC 20550

Cobb, Jewel Plummer, California State University, 5151 State University Drive, Los Angeles, CA 90032-8500

Cohen, Carolyn, Rosenstiel Basic Medical Sciences Research Center, Brandeis University, Waltham, MA 02254

Cohen, Lawrence B., Department of Physiology, Yale University School of Medicine, 333 Cedar Street, New Haven, CT 06510-8026

Cohen, Maynard, Department of Neurological Sciences, Rush Medical College, 600 South Paulina, Chicago, IL 60612

Cohen, Rochelle S., Department of Anatomy, University of Illinois, 808 W. Wood Street, Chicago, IL 60612

Cohen, William D., Department of Biological Sciences, Hunter College, 695 Park Ave., Box 79, New York, NY 10021

Coleman, Annette W., Division of Biology and Medicine, Brown University, Providence, RI 01912

Collier, Jack R., Department of Biology, Brooklyn College, Bedford & Avenue H, Brooklyn, NY 11210

Collier, Marjorie McCann, Biology Department, Saint Peter's College, 2641 Kennedy Boulevard, Jersey City, NJ 07306

Collin, Carlos, National Institutes of Health, Laboratory of Adaptive Systems, Bldg. 36, B308, Bethesda, MD 20892

Cook, Joseph A., The Edna McConnell Clark Foundation, 250 Park Ave., New York, NY 10177-0026

Cooperstein, S. J., University of Connecticut School of Medicine, Department of Anatomy, Farmington Ave., Farmington, CT 06032

Cornell, Neal W., Marine Biological Laboratory, Woods Hole, MA 02543

Cornwall, Melvin C., Jr., Department of Physiology L714, Boston University School of Medicine, 80 E. Concord St., Boston, MA 02118

Corson, David Wesley, Jr., 516 Rice Hope Dr., Mt. Pleasant, SC 29464-9296

Corwin, Jeffrey T., Department of Otolaryngology, University of Virginia Medical Center, Box 430, Charlottesville, VA 22908

Costello, Walter J., Department of Zoology Z/BS, College of Medicine, Ohio University, Athens, OH 45701

Couch, Ernest F., Department of Biology, Texas Christian University, Fort Worth, TX 76129

Crane, Sylvia E., 438 Wendover Drive, Princeton, NJ 08540

Cremer-Bartels, Gertrud, Universitats Augenklinik, 44 Munster, Germany

Crow, Terry J., Department of Neurobiology and Anatomy, University of Texas Medical School, Houston, TX 77225

Crowell, Sears, Department of Biology, Indiana University, Bloomington, IN 47405

Crowther, Robert, Department of Biology, University of New Brunswick, BS 45111, Fredericton, NB, Canada E3B 6E1

Cunningham, Mary-Ellen, 62 Cloverly Road, Grosse Pointe Farms, MI 48236

Currier, David L., P. O. Box 2476, Vineyard Haven, MA 02568

Cutler, Richard, Marine Biological Laboratory, Woods Hole, MA 02543

D'Alessio, Giuseppe, Department of Organic & Biological Chemistry, University of Naples, Via Mezzocannone 16, Naples, Italy 80134

D'Avanzo, Charlene, Department of Natural Science, Hampshire College, Amherst, MA 01002

Daignault, Alexander T., 29 Quisset Harbor Rd., Falmouth, MA 02540

Dan, Katsuma, Tokyo Metropolitan Union, 1-1 Minami-Osawa, Hachioji City 192-03, Tokyo, Japan

David, John R., Tropical Public Health, Harvard School of Public Health, 665 Huntington Ave., Boston, MA 02115

Davidson, Eric H., Division of Biology, 156-29, California Institute of Technology, 1201 E. California Blvd., Pasadena, CA 91125

Davis, Joel P., P.O. Box 208, Brooksville, ME 04617

Daw, Nigel W., 5 Old Pawson Rd., Branford, CT 06405

Deegan, Linda A., The Ecosystems Center, Marine Biological Laboratory, Woods Hole, MA 02543

DeGroof, Robert C., 145 Water Crest Dr., Doylestown, PA 18901

DeHaan, Robert L., Department of Anatomy and Cell Biology, Emory University School of Medicine, Atlanta, GA 30322

DeLanney, Louis E., The Parkinson's Institute, 1170 Morse Avenue, Sunnyvale, CA 94089

Denkla, Marth B., Kennedy-Krieger Institute, Johns Hopkins School of Medicine, 707 North Broadway, Baltimore, MD 21205

Dentler, William L., Department of Physiology & Cell Biology, University of Kansas, 4011 Haworth Hall, Lawrence, KS 66044

DePhillips, Henry A., Jr., Department of Chemistry, Trinity College, 300 Summit Street, Hartford, CT 06106

DeSimone, Douglas W., Department of Anatomy and Cell Biology, Box 439, Health Sciences Center, University of Virginia, Charlottesville, VA 22908

DeToledo-Morrell, Leyla, Rush-Presbyterian-St. Lukes Medical Center, 1653 West Congress Parkway, Chicago, IL 60612

Dettbarn, Wolf-Dietrich, Department of Pharmacology, School of Medicine, Vanderbilt University, Nashville, TN 37232

De Weer, Paul J., Department of Physiology, University of Pennsylvania School of Medicine, Philadelphia, PA 19104-6085

Dixon, Keith E., School of Biological Sciences, Flinders University, Bedford Park, 5042, South Australia, Australia

Dowling, John E., The Biological Laboratories, Harvard University, 16 Divinity St., Cambridge, MA 02138

DuBois, Arthur Brooks, John B. Pierce Foundation Laboratory, 290 Congress Ave., New Haven, CT 06519

Duncan, Thomas K., Department of Environmental Sciences, Nichols College, Dudley, MA 01571
Dunham, Philip B., Department of Biology, Syracuse University, Syracuse, NY 13244
Dunlap, Kathleen, Department of Physiology, Tufts University Medical School, Boston, MA 02111
Dunlap, Paul V., Department of Biology, Woods Hole Oceanographic Institution, Redfield 316, Woods Hole, MA 02543
Dworkin, Martin, Department of Microbiology, University of Minnesota, 1460 Mayo Bldg., Box 196 UMHC, Minneapolis, MN 55455-0312

Ebert, James D., Department of Biology, The Johns Hopkins University, Homewood, Baltimore, MD 21218
Eckberg, William R., Howard University, Department of Zoology, P.O. Box 887, Admin. Bldg., Washington, DC 20059
Edds, Kenneth T., R&D Systems, Inc., Hematology Division, 614 McKinley Place, NE, Minneapolis, MN 55413
Eder, Howard A., Albert Einstein College of Medicine, 1300 Morris Park Ave., Bronx, NY 10461
Edstrom, Joan, 2515 Milton Hills Dr., Charlottesville, VA 22901
Egyud, Laszlo G., 18 Skyview, Newton, MA 02150
Ehrlich, Barbara E., Division of Cardiology, University of Connecticut School of Medicine, 263 Farmington Avenue, Farmington, CT 06030
Eisen, Arthur Z., Division of Dermatology, Washington University, St. Louis, MO 63110
Eisen, Herman N., Massachusetts Institute of Technology, Center for Cancer Research, E17-128, 77 Massachusetts Ave., Cambridge, MA 02139
Elder, Hugh Young, Institute of Physiology, University of Glasgow, Glasgow, Scotland G12 8QQ
Elliott, Gerald F., The Open University Research Unit, Foxcombe Hall, Berkeley Rd., Boars Hill, Oxford, England OX1 5HR
Englund, Paul T., Department of Biological Chemistry, Johns Hopkins University, Baltimore, MD 21205
Epel, David, Hopkins Marine Station, Pacific Grove, CA 93950
Epstein, Herman T., 18 Lawrence Farm Road, Woods Hole, MA 02543
Epstein, Ray L., 30 Coonamessett Circle, Hatchville, MA 02536

Farb, David H., Department of Pharmacology L603, Boston University School of Medicine, 80 E. Concord St., Boston, MA 02118
Farmanfarmaian, A., Department of Biological Sciences, Nelson Biological Laboratory, Rutgers University, POB 1059, Piscataway, NJ 08855
Fein, Alan, Department of Physiology, University of Connecticut Health Center, Farmington, CT 06032 (resigned)
Feinman, Richard D., Box 8, Department of Biochemistry, SUNY Health Science Center, 450 Clarkson Avenue, Brooklyn, NY 11203
Feldman, Susan C., Department of Anatomy, University of Medicine and Dentistry of New Jersey, New Jersey Medical School, 100 Bergen St., Newark, NJ 07103
Fessenden, Jane, 225 Lakeview Ave., Falmouth, MA 02540
Festoff, Barry W., Neurology Service (127), Veterans Administration Medical Center, 4801 Linwood Blvd., Kansas City, MO 64128
Fink, Rachel D., Department of Biological Sciences, Clapp Laboratory, Mount Holyoke College, South Hadley, MA 01075
Finkelstein, Alan, Albert Einstein College of Medicine, 1300 Morris Park Ave., Bronx, NY 10461
Fischbach, Gerald, Department of Neurobiology, Harvard Medical School, 220 Longwood Ave., Boston, MA 02115
Fishman, Harvey M., Department of Physiology and Biophysics, University of Texas Medical Branch, 301 Univ. Blvd., Galveston, TX 77555-0641
Flanagan, Dennis, 12 Gay St., New York, NY 10014
Fluck, Richard Allen, Department of Biology, Franklin & Marshall College, Box 3003, Lancaster, PA 17604-3003
Foreman, K. H., Boston University Marine Program, Marine Biological Laboratory, Woods Hole, MA 02543
Fox, Thomas Oren, Division of Medical Sciences, Harvard Medical School, 260 Longwood Ave., Boston, MA 02115
Franzini-Armstrong, Clara, School of Medicine, University of Pennsylvania, 330 S. 46th Street, Philadelphia, PA 19143
Frazier, Donald T., Department of Physiology and Biophysics, University of Kentucky Medical Center, Lexington, KY 40536
French, Robert J., Health Sciences Center, University of Calgary, Calgary, Alberta, T2N 4N1, Canada
Friedler, Gladys, Boston University School of Medicine, 80 East Concord Street, Boston, MA 02118
Fry, Brian, Marine Biological Laboratory, Woods Hole, MA 02543
Fulton, Chandler M., Department of Biology, Brandeis University, Waltham, MA 02254
Furshpan, Edwin J., Department of Neurophysiology, Harvard Medical School, 220 Longwood Ave., Boston, MA 02115
Futrelle, Robert P., College of Computer Science, Northeastern University, 360 Huntington Avenue, Boston, MA 02115

Gabriel, Mordecai, Department of Biology, Brooklyn College, 2900 Bedford Ave., Brooklyn, NY 11210
Gadsby, David C., Laboratory of Cardiac Physiology, The Rockefeller University, 1230 York Avenue, New York, NY 10021-6399
Gainer, Harold, Lab of Functional Neurochemistry, NIH, Bldg. 36, Room 4D-20, Bethesda, MD 20892
Galatzer-Levy, Robert M., 180 N. Michigan Avenue, Chicago, IL 60601
Gall, Joseph G., Carnegie Institution, 115 West University Parkway, Baltimore, MD 21210
Gallant, Paul E., NIH, Bldg. 36, Rm. 2A-29, Bethesda, MD 20892 (resigned)
Garber, Sarah S., Department of Physiology, Medical College of Pennsylvania, 2900 Queen Ln., Philadelphia, PA 19129
Gascoyne, Peter, Box 85E, University of Texas, M. D. Anderson Hospital and Tumor Institute, 6723 Bertner Avenue, Box 85E, Houston, TX 77030
Gelperin, Alan, Department of Biophysics, AT&T Bell Labs, Room 1C464, 600 Mountain Avenue, Murray Hill, NJ 07974
German, James L., III, Lab of Human Genetics, The New York Blood Center, 310 East 67th St., New York, NY 10021
Gibbs, Martin, Institute for Photobiology of Cells and Organelles, Brandeis University, Waltham, MA 02254
Giblin, Anne E., Ecosystems Center, Marine Biological Laboratory, Woods Hole, MA 02543
Gibson, A. Jane, Department of Biochemistry, Cornell University, Ithaca, NY 14850
Gifford, Prosser, 540 N Street, SW, S-903, Washington, DC 20024
Gilbert, Daniel L., Clinical Neuroscience Branch, NIH/NINDS, Bldg. 36, Room 5A09A, Bethesda, MD 20892
Giudice, Giovanni, Dipartimento di Biologia Cellulare e Dello Sviluppo, I-90123, Via Archirafi 22, Universita di Palermo, Palermo, Italy
Giuditta, Antonio, Department of General Physiology, University of Naples, Via Mezzocannone 8, Naples, Italy 80134
Glynn, Paul, 2770 Beechwood Blvd., Pittsburgh, PA 15217
Golden, William T., American Museum of Natural History, 40 Wall St., Room 4201, New York, NY 10005

Goldman, Robert D., Department of Cell, Molecular and Structural Biology, Northwestern University, 303 E. Chicago Ave., Chicago, IL 60611

Goldsmith, Paul K., NIH, Bldg. 10, Room 9C-101, Bethesda, MD 20892

Goldsmith, Timothy H., Department of Biology, Yale University, New Haven, CT 06510

Goldstein, Moise H., Jr., ECE Department, Barton Hall, Johns Hopkins University, Baltimore, MD 21218

Goodman, Lesley Jean, Department of Biological Sciences, Queen Mary College, Mile End Road, London, E1 4NS, England, UK

Gould, Robert Michael, Institute for Basic Research in Developmental Disabilities, 1050 Forest Hill Rd., Staten Island, NY 10314

Gould, Stephen J., Museum of Comparative Zoology, Agassiz Museum, Harvard University, Cambridge, MA 02138

Govind, C. K., Life Sciences Division, Scarborough College, 1265 Military Trail, West Hill, Ontario, M1C 1A4, Canada

Grace, Dick, Doreen Grace Fund, The Brain Center, Seanest Drive, Promontory Pt., New Seabury, MA 02649

Graf, Werner, Rockefeller University, 1230 York Ave., New York, NY 10021

Grant, Philip, 2939 Van Ness Street, N.W., Apt. 302, Washington, DC 20008

Grass, Ellen R., The Grass Foundation, 77 Reservoir Rd., Quincy, MA 02170

Grassle, Judith, Institute of Marine & Coastal Studies, Rutgers University, Box 231, New Brunswick, NJ 08903

Greenberg, Everett Peter, Department of Microbiology, College of Medicine, University of Iowa, Iowa City, IA 52242

Greenberg, Michael J., Whitney Laboratory, University of Florida, 9505 Ocean Shore Blvd., St. Augustine, FL 32086-8623

Greer, Mary J., 16 Hillside Ave., Cambridge, MA 02140

Griffin, Donald R., Concord Field Station, Harvard University, Old Causeway Road, Bedford, MA 01730

Gross, Paul R., Center for Advanced Studies, University of Virginia, 444 Cabell Hall, Charlottesville, VA 22903

Grossman, Albert, New York University Medical Center, 550 First Ave., New York, NY 10016

Grossman, Lawrence, Department of Biochemistry, Johns Hopkins University, 615 North Wolfe Street, Baltimore, MD 21205

Gruner, John, Cephalon, Inc., 145 Brandywine Parkway, W. Chester, PA 19380-4245

Gunning, A. Robert, P. O. Box 165, Falmouth, MA 02541

Gwilliam, G. P., Department of Biology, Reed College, Portland, OR 97202

Haimo, Leah, Department of Biology, University of California, Riverside, CA 92521

Hall, Linda M., Department of Biochemistry and Pharmacology, SUNY, 317 Hochstetter, Buffalo, NY 14260

Hall, Zack W., Department of Physiology, University of California, San Francisco, CA 94143

Halvorson, Harlyn O., 26 Fay Road, P.O. Box 81, Woods Hole, MA 02543

Hamlett, Nancy V., Department of Biology, Harvey Mudd College, 301 E. 12th St., Claremont, CA 91711

Haneji, Tatsuji, Kyushu Dental College, Department of Anatomy, 2-6-1, Manazuru, Kokurakita-Ku, Kitakyushu 803, Japan

Hanlon, Roger T., University of Texas Medical Branch, Marine Biomedical Institute, 200 University Boulevard, Galveston, TX 77550-2772

Hanna, Robert B., Department of Environmental Science and Forestry, SUNY, Syracuse, NY 13210

Harosi, Ferenc I., Laboratory of Sensory Physiology, Marine Biological Laboratory, Woods Hole, MA 02543

Harrigan, June F., 7415 Makaa Place, Honolulu, HI 96825

Harrington, Glenn W., Weber State University, Department of Microbiology, Ogden, UT 84408

Hastings, J. W., The Biological Laboratories, Harvard University, 16 Divinity Street, Cambridge, MA 02138

Hayashi, Teru, 7105 SW 112 Place, Miami, FL 33173

Haydon-Baillie, Wensley G., Porton Int., 2 Lowndes Place, London, SW1X 8DD, England, UK

Hayes, Raymond L., Jr., Department of Anatomy, Howard University, College of Medicine, 520 W St., NW, Washington, DC 20059

Hepler, Peter K., Department of Botany, University of Massachusetts, Amherst, MA 01003

Herndon, Walter R., University of Tennessee, Department of Botany, Knoxville, TN 37996-1100

Herskovits, Theodore T., Department of Chemistry, Fordham University, John Mulcahy Hall, Room 638, Bronx, NY 10458

Hiatt, Howard H., Department of Medicine, Brigham and Women's Hospital, 75 Francis Street, Boston, MA 02115

Highstein, Stephen M., Department of Otolaryngology, Box 8115, Washington University School of Medicine, St. Louis, MO 63110

Hildebrand, John G., Arizona Research Laboratories, Division of Neurobiology, 603 Gould-Simpson Science Building, University of Arizona, Tucson, AZ 85721

Hill, Richard W., Department of Zoology, Michigan State University, E. Lansing, MI 48824

Hill, Susan D., Department of Zoology, Michigan State University, E. Lansing, MI 48824

Hillis, Llewellya, Smithsonian Tropical Research Institute, Unit 0948 APO-AA, Miami, FL 34002-0948

Hillman, Peter, Department of Biology, Life Sciences & Neurobiology, Hebrew University, Jerusalem 91904, Israel

Hinegardner, Ralph T., Division of Natural Sciences, University of California, Santa Cruz, CA 95064

Hines, Michael, Department of Neurobiology, Duke University Medical Center, Box 3209, Durham, NC 27710

Hinsch, Gertrude, W., Department of Biology, University of South Florida, Tampa, FL 33620

Hobbie, John E., Ecosystems Center, Marine Biological Laboratory, Woods Hole, MA 02543

Hodge, Alan J., 3843 Mt. Blackburn Ave., San Diego, CA 92111

Hoffman, Joseph, Department of Physiology, School of Medicine, Yale University, New Haven, CT 06515

Hollyfield, Joe G., Baylor School of Medicine, Texas Medical Center, Houston, TX 77030

Holtzman, Eric, Department of Biological Sciences, Columbia University, New York, NY 10027 (deceased)

Holz, IV, George G, Massachusetts General Hospital, Laboratory of Molecular Endocrinology, Wellman 320, 50 Blossom St., Boston, MA 02114

Hopkinson, Charles S., Jr., Ecosystems Center, Marine Biological Laboratory, Woods Hole, MA 02543

Hoskin, Francis C. G., Illinois Institute of Technology, Department of Biology, Chicago, IL 60616

Houghton, Richard A., III, Woods Hole Research Center, P. O. Box 296, Woods Hole, MA 02543 (resigned)

Hoy, Ronald R., Section of Neurobiology and Behavior, Cornell University, Ithaca, NY 14853

Hufnagel-Zackroff, Linda A., Department of Microbiology, University of Rhode Island, Kingston, RI 02881

Hummon, William D., Department of Zoology and Biomedical Science, Ohio University, Athens, OH 45701

Humphreys, Susie H., Food and Drug Administration, HFS-156 Switzer, 200 C Street, SW, Washington, DC 20204-0001

Humphreys, Tom D., University of Hawaii, Kewalo Marine Lab, 41 Ahui St., Honolulu, HI 96813

Hunt, Richard T., ICRF, Clare Hall Laboratories, South Mimms Potter's Bar, Herb EN6-3LD, England
Hunter, Robert D., Department of Biological Sciences, Oakland University, Rochester, MI 48309-4401
Hunter, W. Bruce, Box 321, Lincoln Center, MA 01773 (resigned)
Huxley, Hugh E., Department of Biology, Rosenstiel Center, Brandeis University, Waltham, MA 02154
Hynes, Thomas J., Jr., Meredith and Grew, Inc., 160 Federal Street, Boston, MA 02110-1701

Ilan, Joseph, Department of Developmental Genetics and Anatomy, Case Western Reserve University School of Medicine, Cleveland, OH 44106
Ingoglia, Nicholas, Department of Physiology, New Jersey Medical School, 100 Bergen St., Newark, NJ 07103
Inoué, Saduyki, Department of Anatomy, McGill University Cancer Centre, 3640 University St., Montreal, PQ H3A 2B2, Canada
Inoué, Shinya, Marine Biological Laboratory, Woods Hole, MA 02543
Isselbacher, Kurt J., Massachusetts General Hospital, Boston, MA 02114
Issidorides, Marietta, R., Department of Psychiatry, University of Athens, Monis Petraki 8, Athens, 140 Greece
Izzard, Colin S., Department of Biological Sciences, SUNY, 1400 Washington Ave., Albany, NY 12222

Jacobs, Neil, Hale & Dorr, 60 State St., Boston, MA 02109
Jaffe, Lionel, Marine Biological Laboratory, Woods Hole, MA 02543
Jannasch, Holger W., Department of Biology, Woods Hole Oceanographic Institution, Woods Hole, MA 02543
Jeffery, William R., Bodega Marine Laboratory, University of California, Box 247, Bodega Bay, CA 94923
Johnston, Daniel, Division of Neuroscience, Baylor College of Medicine, 1 Baylor Plaza, Houston, TX 77030
Josephson, Robert K., Department of Psychobiology, University of California, Irvine, CA 92717

Kaczmarek, Leonard K., Department of Pharmacology, Yale University School of Medicine, 333 Cedar St., New Haven, CT 06520
Kaley, Gabor, Department of Physiology, Basic Sciences Building, New York Medical College, Valhalla, NY 10595
Kaltenbach, Jane, Department of Biological Sciences, Mount Holyoke College, South Hadley, MA 01075
Kaminer, Benjamin, Department of Physiology, School of Medicine, Boston University, 80 East Concord St., Boston, MA 02118
Kaneshiro, Edna S., Department of Biological Sciences, University of Cincinnati, JL 006, Cincinnati, OH 45221-0006
Kao, Chien-yuan, Department of Pharmacology, Box 29, SUNY, Downstate Medical Center, 450 Clarkson Avenue, Brooklyn, NY 11203
Kaplan, Ehud, Department of Biophysics, The Rockefeller University, 1230 York Ave., New York, NY 10024
Karakashian, Stephen J., Apt. 16-F, 165 West 91st St., New York, NY 10024
Karlin, Arthur, Department of Biochemistry, Columbia University, 630 West 168th St., New York, NY 10032
Katz, George M., Fundamental and Experimental Research Labs, Merck Sharp and Dohme, P. O. Box 2000, Rahway, NJ 07065
Kelley, Darcy Brisbane, Columbia University, Department of Biological Sciences, 1018 Fairchild, New York, NY 10032
Kelly, Robert E., Department of Anatomy, University of Illinois, P. O. Box 6998, Chicago, IL 60680
Kemp, Norman E., Department of Biology, University of Michigan, Ann Arbor, MI 48109
Kendall, John P., Faneuil Hall Associates, 176 Federal Street, 2nd Floor, Boston, MA 02110
Kendall, Richard E., 26 Green Harbor Road, East Falmouth, MA 02536
Kerr, Louis M., Marine Biological Laboratory, Woods Hole, MA 02543
Keynan, Alexander, Laboratory for Developmental and Molecular Biology, Department of Biochemistry, Hebrew University of Jerusalem, Givat-Ram, Jerusalem, Israel
Khan, Shahid M. M., Department of Anatomy & Structural Biology, Albert Einstein College of Medicine, 1300 Morris Park Ave., Bronx, NY 10461
Kiehart, Daniel P., Department of Cellular Biology, Duke Medical Center, Box 3709, 307 Nanaline Duke Bldg., Durham, NC 27710
Kirk, Mark D., Division of Biological Sciences, University of Missouri, Columbia, MO 65211
Klotz, Irving M., Department of Chemistry, Northwestern University, Evanston, IL 60201
Knudson, Robert A., Marine Biological Laboratory, Instrument Development Lab, Woods Hole, MA 02543
Koide, Samuel S., Population Council, The Rockefeller University, 1230 York Avenue, New York, NY 10021
Kornberg, Sir Hans, The Master's Lodge, Christ's College, Cambridge CB2 3BU, England, UK
Kosower, Edward M., address unknown
Krahl, M. E., 2783 W. Casas Circle, Tucson, AZ 85741
Krane, Stephen M., Arthritis Unit, Massachusetts General Hospital, Fruit Street, Boston, MA 02114
Krauss, Robert, FASEB, 9650 Rockville Pike, Bethesda, MD 20814
Kravitz, Edward A., Department of Neurobiology, Harvard Medical School, 220 Longwood Ave., Boston, MA 02115
Kriebel, Mahlon E., Department of Physiology, SUNY Health Science Center, Syracuse, NY 13210
Kristan, William B., Jr., Department of Biology B-022, University of California San Diego, La Jolla, CA 92093
Kropinski, Andrew M. B., Department of Microbiology/Immunology, Queen's University, Kingston, Ontario K7L 3N6, Canada
Kuhns, William J., Hospital for Sick Children, Department of Biochemistry Research, Toronto, Ontario M5G 1X8, Canada
Kusano, Kiyoshi, NIH, Bldg. 36, Room 4D-20, Bethesda, MD 20892
Kuzirian, Alan M., Marine Biological Laboratory, Woods Hole, MA 02543

Laderman, Aimlee, Yale University School of Forestry and Environmental Studies, 370 Prospect, New Haven, CT 06511
LaMarche, Paul H., Eastern Maine Medical Center, 489 State St., Bangor, ME 04401
Landis, Dennis M. D., Department of Developmental Genetics and Anatomy, Case Western Reserve University School of Medicine, Cleveland, OH 44106
Landowne, David, Department of Physiology, P. O. Box 016430, University of Miami School of Medicine, Miami, FL 33101
Langford, George M., Department of Biological Sciences, Dartmouth College, 6044 Gilman Laboratory, Hanover, NH 03755
Lasser-Ross, Nechama, Department of Physiology, New York Medical College, Valhalla, NY 10595
Laster, Leonard, University of Massachusetts Medical School, 55 Lake Avenue, North, Worcester, MA 01655
Laufer, Hans, Department of Biological Science, Molecular and Cell Biology, Group U-125, University of Connecticut, Storrs, CT 06269-3125
Lazarow, Paul B., Department of Cell Biology and Anatomy, Mount Sinai Medical School, Box 1007, 5th Avenue & 100th Street, New York, NY 10021

Lazarus, Maurice, Federated Department Stores, Inc., Sears Cresent, City Hall Plaza, Boston, MA 02108
Leadbetter, Edward R., Department of Molecular and Cell Biology, U-131, University of Connecticut, Storrs, CT 06268
Lederberg, Joshua, The Rockefeller University, 1230 York Ave., New York, NY 10021
Lee, John J., Department of Biology, City College of CUNY, Convent Ave. and 138th St., New York, NY 10031
Lehy, Donald B., 35 Willow Field Dr., N. Falmouth, MA 02556
Leibovitz, Louis, 3 Kettle Hole Road, Falmouth, MA 02540
Leighton, Joseph, 2324 Lakeshore Avenue, #2, Oakland, CA 94606
Leighton, Stephen, NIH, Bldg. 13 3W13, Bethesda, MD 20892
Leinwand, Leslie Ann, Department of Microbiology and Immunology, Albert Einstein College of Medicine, 1300 Morris Park Ave., Bronx, NY 10461
Lerman, Sidney, Eye Research Lab, Room 41, New York Medical College, 100 Grasslands Ave., Valhalla, NY 10595
Lerner, Aaron B., Department of Dermatology, PO Box 3333, Yale University, School of Medicine, New Haven, CT 06510
Lester, Henry A., Division of Biology, California Institute of Technology, 156-29, Pasadena, CA 91125
Levin, Jack, Veterans Administration Medical Center, 113A, 4150 Clement St., San Francisco, CA 94121
Levine, Richard B., ARL, Division of Neurobiology, University of Arizona, 611 Gould-Simpson Bldg., Tucson, AZ 85721
Levinthal, Francoise, 435 Riverside Dr., New York, NY 10025
Levitan, Herbert, National Science Foundation, 4201 Wilson Boulevard, Room 835, Arlington, VA 22230
Levitan, Irwin B., Center for Complex Systems, Brandeis University, Waltham, MA 02254
Linck, Richard W., Department of Cell Biology and Neuroanatomy, University of Minnesota, 321 Church Street, S. E., Minneapolis, MN 55455
Lipicky, Raymond J., Department of Cardio-Renal/Drug Prod. Div., FDA, Rm. 16B-45, 5600 Fishers Lane, Rockville, MD 20857
Lisman, John E., Department of Biology, Brandeis University, Waltham, MA 02254
Liuzzi, Anthony, 320 Beacon St., Boston, MA 02116
Llinás, Rodolfo R., Department of Physiology and Biophysics, New York University Medical Center, 550 First Ave., New York, NY 10016
Loew, Franklin M., Tufts University School of Veterinary Medicine, 200 Westboro Rd., N. Grafton, MA 01536-1895
Loewenstein, Birgit R., Department of Physiology and Biophysics, R-430, University of Miami School of Medicine, Miami, FL 33101
Loewenstein, Werner R., Department of Physiology and Biophysics, University of Miami, P. O. Box 016430, Miami, FL 33101
London, Irving M., Massachusetts Institute of Technology, Harvard-MIT Division, E-25-551, Cambridge, MA 02139
Longo, Frank J., Department of Anatomy, University of Iowa, Iowa City, IA 52442
Lorand, Laszlo, Northwestern University Medical School, CMS Biology, Searle 4-555, 303 East Chicago, Chicago, IL 60611-3008
Luckenbill-Edds, Louise, 155 Columbia Ave., Athens, OH 45701

Macagno, Eduardo R., 1003B Fairchild, Department of Biosciences, Columbia University, New York, NY 10027
MacNichol, E. F., Jr., Department of Physiology, Boston University School of Medicine, 80 E. Concord St., Boston, MA 02118
Maglott-Duffield, Donna R., American Type Culture Collection, 12301 Parklawn Drive, Rockville, MD 20852-1776
Maienschein, Jane Ann, Department of Philosophy, Arizona State University, Tempe, AZ 85287-2004
Mainer, Robert, The Boston Company, One Boston Place, OBP-15-D, Boston, MA 02108
Malbon, Craig Curtis, Department of Pharmacology, Health Sciences Center, SUNY, Stony Brook, NY 11794-8651
Manalis, Richard S., Department of Biological Sciences, Indiana University—Purdue University at Fort Wayne, 2101 Coliseum Blvd., E., Fort Wayne, IN 46805
Mangum, Charlotte P., Department of Biology, College of William and Mary, Williamsburg, VA 23187-8795
Manz, Robert D., Helmer and Associates, Suite 1310, 950 Winter St., Walthan, MA 02154
Margulis, Lynn, Botany Department, University of Massachusetts, Morrill Science Center, Amherst, MA 01003
Marinucci, Andrew C., 102 Nancy Drive, Mercerville, NJ 08619
Marsh, Julian B., Department of Biochemistry and Physiology, Medical College of Pennsylvania, 3300 Henry Ave., Philadelphia, PA 19129
Martinez, Jr., Joe L., Department of Psychology, University of California, Berkeley, 3210 Tolman Hall, Berkeley, CA 94720
Martinez-Palomo, Adolfo, Seccion de Patologia Experimental, Cinvesav-ipn, 07000 Mexico, D.F. A.P., 140740, Mexico
Maser, Morton, Woods Hole Education Assoc., P. O. Box EM, Woods Hole, MA 02543
Mastroianni, Luigi, Jr., Department of Obstetrics and Gynecology, Hospital of the University of Pennsylvania, 106 Dulles, 3400 Spruce Street, Philadelphia, PA 19104-4283
Matteson, Donald R., Department of Biophysics, University of Maryland School of Medicine, 660 West Redwood Street, Baltimore, MD 21201
Mautner, Henry G., Department of Biochemistry, Tufts University School of Medicine, 136 Harrison Ave., Boston, MA 02111
Mauzerall, David, The Rockefeller University, 1230 York Ave., New York, NY 10021
McCann, Frances, Department of Physiology, Dartmouth Medical School, Hanover, NH 03755
McLaughlin, Jane A., Marine Biological Laboratory, Woods Hole, MA 02543
McMahon, Robert F., Department of Biology, Box 19498, University of Texas, Arlington, TX 76019
Meedel, Thomas, Biology Department, Rhode Island College, 600 Mt. Pleasant Ave., Providence, RI 02908
Meinertzhagen, Ian A., Department of Psychology, Life Sciences Center, Dalhousie University, Halifax, Nova Scotia B3H 4J1, Canada
Meiss, Dennis E., Immunodiagnostic Laboratories, 488 McCormick St., San Leandro, CA 94577
Melillo, Jerry M., Ecosystems Center, Marine Biological Laboratory, Woods Hole, MA 02543
Mellon, DeForest, Jr., Department of Biology, Gilmer Hall, University of Virginia, Charlottesville, VA 22903
Mellon, Richard P., P. O. Box 187, Laughlintown, PA 15655
Mendelsohn, Michael E., Cardiovascular Division, Harvard Medical School, 75 Francis Street, Boston, MA 02115
Metuzals, Janis, Department of Pathology, University of Ottawa, 451 Smythe Road, Ottawa, Ontario K1H 8M5, Canada
Metz, Charles B., 7220 SW 124th St., Miami, FL 33156
Miledi, Ricardo, Department of Psychobiology, University of California, Irvine, CA 92717
Milkman, Roger, Department of Biology, University of Iowa, Iowa City, IA 52242
Miller, Andrew L., Marine Biological Laboratory, Woods Hole, MA 02543
Mills, Robert, 10315 44th Avenue, W 12 H Street, Bradenton, FL 33507-1535
Misevic, Gradimir, Department of Research, University Hospital of Basel, Mebelstrasse 20, CH-4031, Basel, Switzerland

Mitchell, Ralph, DAS, Harvard University, 29 Oxford Street, Cambridge, MA 02138

Miyakawa, Hiroyoshi, Tokyo University of Pharmacy, Department of Molecular Bioscience, 1432-1 Horinouchi, Hachiouji, Tokyo 192-03, Japan

Miyamoto, David M., Department of Biology, Drew University, Madison, NJ 07940

Mizell, Merle, Department of Cell & Molecular Biology, Tulane University, New Orleans, LA 70118

Moore, John W., Department of Neurobiology, Box 3209, Duke University Medical Center, Durham, NC 27710

Moore, Lee E., Department of Physiology and Biophysics, University of Texas Medical Branch, Galveston, TX 77550

Morin, James G., Department of Biology, University of California, Los Angeles, CA 90024

Morrell, Frank, Department of Neurological Science, Rush Medical Center, 1653 W. Congress Parkway, Chicago, IL 60612

Morse, Patricia M., University of Washington Marine Labs, 620 University Rd., Friday Harbor, WA 98250

Morse, Stephen Scott, The Rockefeller University, 1230 York Ave., Box 120, New York, NY 10021-6399

Mote, Michael I., Department of Biology, Temple University, Philadelphia, PA 19122

Mountain, Isabel, Arleigh Burke Pavilion, 1739 Kirby Road, McLean, VA 22101

Muller, Kenneth J., Department of Physiology and Biophysics, University of Miami School of Medicine, Miami, FL 33101

Murray, Andrew W., Department of Physiology, University of California, Box 0444, 513 Parnassus Ave., San Francisco, CA 94143-0444

Murray, Sandra Ann, Department of Neurology, Anatomy and Cell Science, University of Pittsburgh School of Medicine, Pittsburgh, PA 15261

Nabrit, S. M., 686 Beckwith St., SW, Atlanta, GA 30314

Nadelhoffer, Knute, Marine Biological Laboratory, Ecosystems Center, Woods Hole, MA 02543

Naka, Ken-ichi, 2-9-2 Tatsumi Higashi, Okazaki, Japan 444

Nakajima, Shigehiro, Department of Pharmacology and Cell Biology, University of Illinois College of Medicine at Chicago, 835 S. Wolcott Ave., Chicago, IL 60612

Nakajima, Yasuko, Department of Anatomy and Cell Biology, University of Illinois College of Medicine at Chicago, M/C 512, Chicago, IL 60612

Narahashi, Toshio, Department of Pharmacology, Northwestern University Medical School, 303 East Chicago Ave., Chicago, IL 60611

Nasi, Enrico, Department of Physiology, Boston University School of Medicine, R-406, 80 E. Concord St., Boston, MA 02118

Nealson, Kenneth H., Great Lakes Research Center, University of Milwaukee, 600 E. Greenfield Ave., Milwaukee, WI 53204

Nelson, Leonard, Department of Physiology, CS10008, Medical College of Ohio, Toledo, OH 43699

Nelson, Margaret C., Section of Neurobiology and Behavior, Cornell University, Ithaca, NY 14850

Nicholls, John G., Biocenter, Klingelbergstrasse 70, Basel 4056, Switzerland

Nickerson, Peter A., Department of Pathology, SUNY, Buffalo, NY 14214

Nicosia, Santo V., Department of Pathology, University of South Florida, College of Medicine, Box 11, 12901 North 30th St., Tampa, FL 33612

Noe, Bryan D., Department of Anatomy and Cell Biology, Emory University School of Medicine, Atlanta, GA 30322

Northcutt, R. Glenn, University of California, San Diego, Neuroscience 0201, 9500 Gilman Drive, La Jolla, CA 92093-0201

Norton, Catherine N., Marine Biological Laboratory, Woods Hole, MA 02543

Nusbaum, Michael P., Neurobiology Research Center, University of Alabama, Birmingham, 1719 6th Ave. S., CIRC-545, Birmingham, AL 35294-0021

O'Herron, Jonathan, Jonathan & Shirley O'Herron Foundation, One Rockefeller Plaza, New York, NY 10020

O'Melia, Anne F., 16 Evergreen Lane, Chappaqua, New York 10514

Obaid, Ana Lia, Department of Neuroscience, University of Pennsylvania School of Medicine, 234 Stemmler Hall, Philadelphia, PA 19104-6074

Ohki, Shinpei, Department of Biophysical Sciences, SUNY at Buffalo, 224 Cary Hall, Buffalo, NY 14214

Oldenbourg, Rudolf, Marine Biological Laboratory, Woods Hole, MA 02543

Olds, James L., NIH, 9/1W125, Bldg. 9, Bethesda, MD 20892

Olins, Ada L., University of Tennessee-Oak Ridge, Graduate School of Biomedical Sciences, Biology Division ORNL, P. O. Box 2009, Oak Ridge, TN 37831-8077

Olins, Donald E., University of Tennessee-Oak Ridge, Graduate School of Biomedical Sciences, Biology Division ORNL, P. O. Box 2009, Oak Ridge, TN 37831-8077

Oschman, James L., 31 Whittier Street, Dover, NH 03820

Palazzo, Robert E., Department of Physiology & Cell Biology, Haworth Hall, University of Kansas, Lawrence, KS 66045

Palmer, John D., Department of Zoology, University of Massachusetts, Amherst, MA 01003

Palti, Yoram, Rappaport Institution, Technion, POB 9697, Haifa, 31096 Israel

Pant, Harish C., NINCDS/NIH, Laboratory of Neurochemistry, Bldg. 36, Room 4D-20, Bethesda, MD 20892

Pappas, George D., Department of Anatomy, College of Medicine, University of Illinois, 808 South Wolcott St., Chicago, IL 60612

Pardee, Arthur B., Dana-Farber Cancer Institute, D810, 44 Binney Street, Boston, MA 02115

Pardy, Roosevelt L., School of Life Sciences, University of Nebraska, Lincoln, NE 68588

Parmentier, James L., 175 S. Great Road, Lincoln, MA 01773-4112

Passano, Leonard M., Department of Zoology, Birge Hall, University of Wisconsin, Madison, WI 53706

Pearlman, Alan L., Cell Biology, Box 8228, School of Medicine, Washington University, St. Louis, MO 63110

Pederson, Thoru, Worcester Foundation for Experimental Biology, Shrewsbury, MA 01545

Perkins, C. D., 400 Hilltop Terrace, Alexandria, VA 22301

Person, Philip, 137-87 75th Road, Flushing, NY 11367

Peterson, Bruce J., Marine Biological Laboratory, Ecosystems Center, Woods Hole, MA 02543

Pethig, Ronald, School of Electronic Engineering Science, University College of N. Wales, Dean St., Bangor, Gwynedd, LL57 1UT, UK

Pfohl, Ronald J., Department of Zoology, Miami University, Oxford, OH 45056

Pierce, Sidney K., Jr., Department of Zoology, University of Maryland, College Park, MD 20742

Poindexter, Jeanne S., Barnard College, Columbia University, 3009 Broadway, New York, NY 10027-6598

Pollard, Harvey B., NIH, NIDDKD, Lab of Cell Biology & Genetics, Bldg. 8, Rm. 401, Bethesda, MD 20892

Pollard, Thomas D., Department of Cell Biology and Anatomy, Johns Hopkins University, 725 North Wolfe St., Baltimore, MD 21205

Porter, Beverly H., 5542 Windysun Ct., Columbia, MD 21045

Porter, Keith R., Department of Biology, Leidy Laboratories, Rm. 303, University of Pennsylvania, Philadelphia, PA 19104-6018

Porter, Mary E., Department of Cell Biology and Neurology, University of Minnesota, 4-147 Jackson Hall, Minneapolis, MN 55455

Potter, David, Department of Neurobiology, Harvard Medical School, 25 Shattuck St., Boston, MA 02115

Potts, William T., Department of Biology, University of Lancaster, Lancaster, England, UK

Powers, Dennis A., Hopkins Marine Station, Stanford University, Pacific Grove, CA 93950

Powers, Maureen K., Department of Psychology, 301 Arts & Science Psych Building, Vanderbilt University, Nashville, TN 37240

Pratt, Melanie M., Department of Anatomy and Cell Biology, University of Miami School of Medicine (R124), P. O. Box 016960, Miami, FL 33101

Prendergast, Robert A., Wilmer Institute, Johns Hopkins Hospital, 601 N. Broadway, Baltimore, MD 21287-9142

Presley, Phillip H., Carl Zeiss, Inc., 1 Zeiss Drive, Thornwood, NY 10594

Price, Carl A., Waksman Institute of Microbiology, Rutgers University, P. O. Box 759, Piscataway, NJ 08854

Prior, David J., Department of Biological Sciences, NAU Box 5640, Northern Arizona University, Flagstaff, AZ 86011

Prusch, Robert D., Department of Life Sciences, Gonzaga University, Spokane, WA 99258

Purves, Dale, Department of Neurobiology, Duke University Medical Center, Box 3209, 1011 Bryan Research Building, Durham, NC 27710

Quigley, James, Department of Pathology, SUNY Health Science Center, BHS Tower 9, Rm. 140, Stony Brook, NY 11794-8691

Rabb, Irving W., University Place at Harvard Square, 124 Mt. Auburn St., Suite 200, Cambridge, MA 02138

Rabin, Harvey, DuPont Merck Pharmaceutical, R&D Division, Exp. Station 328/358, Wilmington, DE 19880

Rabinowitz, Michael B., Marine Biological Laboratory, Woods Hole, MA 02543

Rafferty, Nancy S., Marine Biological Laboratory, Woods Hole, MA 02543

Rakowski, Robert F., Department of Physiology and Biophysics, UHS/The Chicago Medical School, 3333 Greenbay Rd., N. Chicago, IL 60064

Ramon, Fidel, CINVESTAV, Depto Fisiologia, Apto Postal 14-740, Mexico, D.F., 07000

Ranzi, Silvio, Sez Zoologia Sc Nat, Dip di Biologia, Via Coloria 26, 20133, Milano, Italy

Rastetter, Edward B., Ecosystems Center, Marine Biological Laboratory, Woods Hole, MA 02543

Rebhun, Lionel I., Department of Biology, Gilmer Hall 43, University of Virginia, Charlottesville, VA 22901

Reddan, John R., Department of Biological Sciences, Oakland University, Rochester, MI 48309-4401

Reese, Barbara F., NINCDS/NIH, Bldg. 36, Room 3B26, 9000 Rockville Pike, Bethesda, MD 20892

Reese, Thomas S., NINCDS/NIH, Bldg. 36, Room 2A27, 9000 Rockville Pike, Bethesda, MD 20892

Reinisch, Carol L., Department of Comparative Medicine, Tufts University School of Veterinary Medicine, 200 Westboro Rd., Bldg. 20, North Grafton, MA 01536

Rich, Alexander, Department of Biology 16-735, Massachusetts Institute of Technology, Cambridge, MA 02139

Rickles, Frederick R., Center for Disease Control, MS-D02, 1600 Clifton Road, NE, Atlanta, GA 30333

Riley, Monica, Marine Biological Laboratory, Woods Hole, MA 02543

Ripps, Harris, Department of Ophthalmology, University of Illinois, 1855 W. Taylor Street, Chicago, IL 60611

Ritchie, Murdoch, Department of Pharmacology, Yale University School of Medicine, 333 Cedar St., New Haven, CT 06510

Robinson, Denis M., 200 Ocean Lane Drive #908, Key Biscayne, FL 33149

Rome, Lawrence C., Department of Biology, University of Pennsylvania, Philadelphia, PA 19104

Rosenbaum, Joel L., Department of Biology, 310 Kline Biology Tower, Yale University, New Haven, CT 06520

Rosenbluth, Jack, Department of Physiology, New York University School of Medicine, 550 First Ave., New York, NY 10016

Rosenbluth, Raja, Simon Fraser University, Institute of Molecular Biology and Biochemistry, Burnaby, BC, Canada, V5A 1S6

Roslansky, John, Box 208, 26 Bar Neck Road, Woods Hole, MA 02543

Roslansky, Priscilla F., 57 Buzzards Bay Ave., Woods Hole, MA 02543

Ross, William N., Department of Physiology, New York Medical College, Valhalla, NY 10595

Roth, Jay S., 18 Millfield Street, P. O. Box 285, Woods Hole, MA 02543

Rowland, Lewis P., Neurological Institute, 710 West 168th St., New York, NY 10032

Ruderman, Joan V., Department of Anatomy and Cell Biology, Harvard University School of Medicine, 220 Longwood Ave., Boston, MA 02115

Rushforth, Norman B., Department of Biology, Case Western Reserve University, Cleveland, OH 44106

Russell-Hunter, W. D., Department of Biology, Lyman Hall 012, Syracuse University, Syracuse, NY 13244

Saffo, Mary Beth, Institute of Marine Sciences, 272 Applied Sciences, University of California, Santa Cruz, CA 95064

Sager, Ruth, Dana Farber Cancer Institute, 44 Binney St., Boston, MA 02115

Sagi, Amir, Department of Life Sciences, Ben-Gurion University of the Negev, P.O. Box 653, Bee-Sheva, Israel, 84105

Salama, Guy, Department of Physiology, University of Pittsburgh, Pittsburgh, PA 15261

Salmon, Edward D., Department of Biology, Wilson Hall, CB3280, University of North Carolina, Chapel Hill, NC 27599

Salzberg, Brian M., Department of Neuroscience, University of Pennsylvania, 234 Stemmler Hall, Philadelphia, PA 19104-6074

Sanger, Jean M., Department of Anatomy, School of Medicine, University of Pennsylvania, 36th and Hamilton Walk, Philadelphia, PA 19104-6058

Sanger, Joseph, Department of Anatomy, School of Medicine, University of Pennsylvania, 36th and Hamilton Walk, B-13, Philadelphia, PA 19104-6058

Saunders, John W., Jr., P. O. Box 381, Waquoit Station, Waquoit, MA 02536

Schachman, Howard K., Department of Molecular Biology, University of California, 229 Stanley Hall #3206, Berkeley, CA 94720-3206

Schatten, Gerald P., Integrated Microscopy Facility for Biomedical Research, University of Wisconsin, 1117 W. Johnson St., Madison, WI 53706

Schatten, Heide, Department of Zoology, University of Wisconsin, Madison, WI 53706

Schiff, Jerome A., Institute for Photobiology of Cells and Organelles, Brandeis University, Waltham, MA 02254

Schmeer, Arline C., Mercenene Cancer Institute, 1073 Racebrook Road, Woodbridge, CT 06525

Schmidek, Henry H., Department of Neurosurgery, St. Luke's Hospital, 102 Page St., New Bedford, MA 02740

Schnapp, Bruce J., Department of Cellular & Molecular Physiology, Harvard Medical School, 25 Shattuck St., Boston, MA 02115

Schuel, Herbert, Department of Anatomical Sciences, SUNY, Buffalo, Buffalo, NY 14214

Schwartz, James H., Center for Neurobiology and Behavior, New York State Psychiatric Institute—Research Annex, 722 W. 168th St., 7th Floor, New York, NY 10032

Schweitzer, A. Nicola, School of Medicine, Section of Immunobiology, Yale University, New Haven, CT 06510

Scofield, Virginia Lee, Department of Microbiology and Immunology, UCLA School of Medicine, Los Angeles, CA 90024

Sears, Mary, P. O. Box 152, Woods Hole, MA 02543

Segal, Sheldon J., The Population Council, One Dag Hammarskjold Plaza, New York, NY 10036

Selman, Kelly, Department of Anatomy and Cell Biology, Box 100235, College of Medicine, University of Florida, Gainesville, FL 32601

Shanklin, Douglas R., Department of Pathology, Room 576, University of Tennessee College of Medicine, 800 Madison Avenue, Memphis, TN 38117

Shashoua, Victor E., Ralph Lowell Labs, Harvard Medical School, McLean Hospital, 115 Mill St., Belmont, MA 02178

Shaver, Gaius R., Ecosystems Center, Marine Biological Laboratory, Woods Hole, MA 02543

Shaver, John R., Department of Zoology, Michigan State University, East Lansing, MI 48824

Sheetz, Michael P., Department of Cell Biology, Duke University Medical Center, Box 3709, 385 Nanaline Duke Bldg., Durham, NC 27710

Shepard, David C., P. O. Box 44, Woods Hole, MA 02543

Shepro, David, Department of Microvascular Research, Boston University, 5 Cummington St., Boston, MA 02215

Sheridan, William F., Biology Department, University of North Dakota, Box 8238, University Station, Grand Forks, ND 58202-8238

Sherman, I. W., Department of Biology, University of California, Riverside, CA 92521

Shimomura, Osamu, Marine Biological Laboratory, Woods Hole, MA 02543

Shipley, Alan M., Marine Biological Laboratory, Woods Hole, MA 02543

Siegel, Irwin M., Department of Ophthalmology, New York University Medical Center, 550 First Avenue, New York, NY 10016

Siegelman, Harold W., Department of Biology, Brookhaven National Laboratory, Upton, NY 11973 (deceased)

Silver, Robert B., Department of Physiology, Cornell University, 822 Veterinary Research Tower, Ithaca, NY 14853-6401

Siwicki, Kathleen K., Biology Department, Swarthmore College, 500 College Ave., Swarthmore, PA 19081

Sjodin, Raymond A., Department of Biophysics, University of Maryland, Baltimore, MD 21201

Skinner, Dorothy M., Oak Ridge National Laboratory, P. O. Box 2009, Biology Division, Oak Ridge, TN 37831

Sloboda, Roger D., Department of Biological Sciences, 306 Gilman, Dartmouth College, Hanover, NH 03755

Sluder, Greenfield, Worcester Foundation for Experimental Biology, 222 Maple Ave., Shrewsbury, MA 01545

Smith, Peter J. S., Marine Biological Laboratory, Woods Hole, MA 02543

Smith, Ralph I., Department of Integrative Biology, University of California, Berkeley, CA 94720 (deceased)

Smith, Stephen J., Department of Molecular & Cellular Physiology, Beckman Center, Stanford University School of Medicine, Stanford, CA 94305-5426

Smolowitz, Roxanne M., Laboratory of Marine Animal Health, Marine Biological Laboratory, Woods Hole, MA 02543

Sogin, Mitchell, Marine Biological Laboratory, Woods Hole, MA 02543

Sorenson, Martha M., Cidade Universitaria-RFRJ, Department de Bioquimica-ICB/CCS, Rio de Janeiro, RJ 21910, Brasil

Speck, William T., Columbia Presbyterian Medical Center, 161 Ft. Washington Avenue, New York, NY 10032

Spector, Abraham, Department of Ophthalmology, Columbia University, 630 West 168th Street, New York, NY 10032

Speer, John W., Marine Biological Laboratory, Woods Hole, MA 02543

Speksnijder, Johanna E., University of Groningen, Department of Genetics, Kerklaan 30, 9751 NN Haren, The Netherlands

Sperelakis, Nicholas, Department of Physiology & Biophysics, University of Cincinnati, 231 Bethesda Ave., Cincinnati, OH 45267-0576

Spiegel, Evelyn, Department of Biological Sciences, Dartmouth College, 204 Gilman, Hanover, NH 03755

Spiegel, Melvin, Department of Biological Sciences, Dartmouth College, 204 Gilman, Hanover, NH 03755

Spray, David C., Albert Einstein College of Medicine, Department of Neurosciences, 1300 Morris Park Avenue, Bronx, NY 10461

Steele, John Hyslop, Woods Hole Oceanographic Institution, Woods Hole, MA 02543

Steinacker, Antoinette, Dept. of Otolaryngology, Washington University, School of Medicine, Box 8115, 4566 Scott Avenue, St. Louis, MO 63110

Steinberg, Malcolm, Princeton University, Department of Molecular Biology, M-18 Moffett Laboratory, Princeton, NJ 08544-1014

Stemmer, Andreas C., Marine Biological Laboratory, Woods Hole, MA 02543

Stetten, Jane Lazarow, 4701 Willard Ave., Apt. 1413, Chevy Chase, MD 20815-4635

Steudler, Paul A., Ecosystems Center, Marine Biological Laboratory, Woods Hole, MA 02543

Stokes, Darrell R., Emory University, Department of Biology, 1510 Clifton Rd., NE, Atlanta, GA 30322-1100

Stommel, Elijah W., P.O. Box 31, E. Thetford, VT 05043

Stracher, Alfred, Department of Biochemistry, SUNY Health Science Center, 450 Clarkson Ave., Brooklyn, NY 11203

Strehler, Bernard L., 2310 North Laguna Circle Dr., Agoura, CA 91301-2884

Strumwasser, Felix, USUHS, Department of Psychiatry, 4301 Jones Bridge Rd., Bethesda, MD 20814-4799

Stuart, Ann E., Department of Physiology, Medical Sciences Research Bldg. 206H, University of North Carolina, Chapel Hill, NC 27599-7545

Sugden, Donata O., University of Wisconsin, Department of Neurophysiology, 281 Medical Science Building, Madison, WI 53706

Sugimori, Mutsuyuki, Department of Physiology and Biophysics, New York University Medical Center, 550 First Avenue, New York, NY 10016

Summers, William C., Huxley College of Environmental Studies, Western Washington University, Bellingham, WA 98225

Suprenant, Kathy A., Department of Physiology and Cell Biology, 4010 Haworth Hall, University of Kansas, Lawrence, KS 66045

Sussman, Maurice, 72 Carey Lane, Falmouth, MA 02540

Sussman, Raquel B., Marine Biological Laboratory, Woods Hole, MA 02543

Sweet, Frederick, Department of OB & GYN, Box 8064, Washington University School of Medicine, 499 South Euclid, St. Louis, MO 63110
Swenson, Katherine I., Duke University Medical Center, Section of Cell Growth, Regulation, and Oncogenesis, P.O. Box 3682, Durham, NC 27710
Sydlik, Mary Anne, Department of Biology, Westfield State College, Westfield, MA 01086
Szent-Györgyi, Andrew, Department of Biology, Brandeis University, Bassine 244, 415 South Street, Waltham, MA 02254
Szent-Gyorgyi, Gwen P., Marine Biological Laboratory, Woods Hole, MA 02543
Szuts, Ete Z., 12 Hamlin Ave., Falmouth, MA 02540-2820

Tabares, Lucia, AVDA, Department of Physiology, Sanchez, Pizjuan 4, 411009 Seville, Spain
Tamm, Sidney L., Boston University Marine Program, Marine Biological Laboratory, Woods Hole, MA 02543 (reinstated)
Tanzer, Marvin L., University of Connecticut School of Dental Medicine, Department of Biostructure and Function, Farmington, CT 06030-3705
Tasaki, Ichiji, Laboratory of Neurobiology, NIMH/NIH, Bldg. 36, Rm. 2B-16, Bethesda, MD 20892
Taylor, Douglass L., Center for Fluorescence Research, Carnegie Mellon University, 4400 Fifth Avenue, Pittsburgh, PA 15213
Teal, John M., Department of Biology, Woods Hole Oceanographic Institution, Woods Hole, MA 02543
Telfer, William H., Department of Biology, University of Pennsylvania, Philadelphia, PA 19104
Telzer, Bruce, Pomona College, Department of Biology, Thille Building, 175 W. 6th Street, Claremont, CA 91711
Thorndike, W. Nicholas, Wellington Management Company, 200 State St., Boston, MA 02109
Townsel, James G., Department of Physiology, Meharry Medical College, Nashville, TN 37208
Travis, David M., 223 Newell Road, Holden, MA 01520-1442
Treistman, Steven N., University of Massachusetts Medical Center, Department of Pharmacology, 55 Lake Avenue North, Worcester, MA 01655
Trigg, D. Thomas, One Federal Street, 9th Floor, Boston, MA 02211
Trinkaus, J. P., Department of Biology, Yale University, New Haven, CT 06511
Troll, Walter, Department of Environmental Medicine, College of Medicine, New York University, New York, NY 10016
Troxler, Robert F., Department of Biochemistry, School of Medicine, Boston University, 80 East Concord St., Boston, MA 02118
Tucker, Edward B., Department of Natural Sciences, Baruch College, CUNY, 17 Lexington Ave., New York, NY 10010
Turner, Ruth D., Mollusk Department, Museum of Comparative Zoology, Harvard University, Cambridge, MA 02138
Tweedell, Kenyon S., Department of Biological Sciences, University of Notre Dame, Notre Dame, IN 46656
Tykocinski, Mark L., Institute of Pathology, Case Western Reserve University, 2085 Adelbert Rd., Cleveland, OH 44106
Tytell, Michael, Department of Anatomy, Bowman Gray School of Medicine, Wake Forest University, Winston-Salem, NC 27103

Ueno, Hiroshi, Kyoto University, Faculty of Agriculture, Department of Agricultural Chemistry, Sakyo, Kyoto 606, Japan

Valiela, Ivan, Boston University Marine Program, Marine Biological Laboratory, Woods Hole, MA 02543
Vallee, Richard, Cell Biology Group, Worcester Foundation for Experimental Biology, Shrewsbury, MA 01545
Valois, John, Marine Biological Laboratory, Woods Hole, MA 02543
Van Holde, Kensal, Department of Biochemistry and Biophysics, Oregon State University, Corvallis, OR 97331-6503
Vogel, Steven S., LTPB/NICHD, Bldg. 10, Rm. 6C205, Bethesda, MD 20892

Waksman, Byron, Foundation for Microbiology, 300 East 54th St., #5K, New York, NY 10022
Wall, Betty, 9 George St., Woods Hole, MA 02543
Wallace, Robin A., Whitney Laboratory, 9505 Ocean Shore Blvd., St. Augustine, FL 32086
Wang, Ching Chung, Department of Pharmaceutical Chemistry, University of California, San Francisco, CA 94143
Wang, Hsien-yu, Department of Biochemistry, National Defense Medical Center, Taipei, Taiwan, Republic of China
Wangh, Lawrence J., Department of Biology, Brandeis University, 415 South St., Waltham, MA 02254
Warner, Robert C., Department of Molecular Biology and Biochemistry, University of California, Irvine, CA 92717
Warren, Kenneth S., Maxwell Communications Corp., 866 Third Avenue, New York, NY 10022
Warren, Leonard, Wistar Institute, 36th and Spruce Streets, Philadelphia, PA 19104
Waterbury, John B., Department of Biology, Woods Hole Oceanographic Institution, Woods Hole, MA 02543
Watson, Stanley, Associates of Cape Cod, Inc., P. O. Box 224, Woods Hole, MA 02543
Waxman, Stephen G., Department of Neurology, P.O. Box 208018, Yale School of Medicine, 333 Cedar Street, New Haven, CT 06510
Webb, H. Marguerite, Marine Biological Laboratory, Woods Hole, MA 02543
Weber, Annemarie, Department of Biochemistry and Biophysics, School of Medicine, University of Pennsylvania, Philadelphia, PA 19066
Weidner, Earl, Department of Zoology and Physiology, Louisiana State University, Baton Rouge, LA 70803
Weiss, Dieter G., Institut fur Zoologie, Technische Universitat Munchen, 8046 Garching, FRG
Weiss, Leon P., Department of Animal Biology, School of Veterinary Medicine, University of Pennsylvania, Philadelphia, PA 19104
Weissmann, Gerald, New York University Medical Center, 550 First Avenue, New York, NY 10016
Werman, Robert, Neurobiology Unit, The Hebrew University, Jerusalem, Israel
Westerfield, R. Monte, The Institute of Neuroscience, University of Oregon, Eugene, OR 97403
Whittaker, J. Richard, Department of Biology, Bag Service #45111, University of New Brunswick, Fredericton, NB E3B 6E1, Canada
Wichterman, Ralph, 31 Buzzards Bay Avenue, Woods Hole, MA 02543
Wilson, Darcy B., San Diego Regional Cancer Center, 3099 Science Park Road, San Diego, CA 92121
Wilson, T. Hastings, Department of Physiology, Harvard Medical School, Boston, MA 02115
Witkovsky, Paul, Department of Ophthalmology, New York University Medical Center, 550 First Ave., New York, NY 10016
Wittenberg, Beatrice, Department of Physiology & Biophysics, Albert Einstein College of Medicine, 1300 Morris Park Ave., Bronx, NY 10461
Wittenberg, Jonathan B., Department of Physiology and Biophysics, Albert Einstein College, 1300 Morris Park Ave., Bronx, NY 01461
Wolken, Jerome J., Department of Biological Sciences, Carnegie Mellon University, 440 Fifth Ave., Pittsburgh, PA 15213
Wonderlin, William F., Department of Pharmacology & Toxicology, West Virginia University, Morgantown, WV 26506
Worden, Mary Kate, Department of Neurobiology, Harvard Medical School, 220 Longwood Ave., Boston, MA 02115

Worgul, Basil V., Department of Ophthalmology, Columbia University, 630 West 168th St., New York, NY 10032

Wu, Chau Hsiung, Department of Pharmacology, Northwestern University Medical School, Chicago, IL 60611

Wyttenbach, Charles R., Department of Physiology and Cell Biology, University of Kansas, Lawrence, KS 66045

Yashphe, Jacob, Hebrew University, Hadassah Medical School, Jerusalem, Israel, 91010 (resigned)

Yeh, Jay Z., Department of Pharmacology, Northwestern University Medical School, Chicago, IL 60611

Zigman, Seymour, University of Rochester Medical School, Box 314, 601 Elmwood Avenue, Rochester, NY 14642

Zimmerberg, Joshua J., NIH, Bldg. 12A, Room 2007, Bethesda, MD 20892

Zottoli, Steven J., Department of Biology, Williams College, Williamstown, MA 01267

Zucker, Robert S., Neurobiology Division, Department of Molecular and Cellular Biology, University of California, Berkeley, CA 94720

Zukin, Ruth Suzanne, Department of Neuroscience, Albert Einstein College of Medicine, 1410 Pelham Parkway South, Bronx, NY 10461

MBL Associates

Executive Board

Megan Jones, President
Mary Ulbrich, Vice President
Deborah G. Senft, Treasurer
Pucky Roslansky, Secretary
Alfred F. Borg
Jennie P. Brown
Julie Child
Elaine Pear Cohen, Arts Chair
Hanna Hastings
Doris B. Hiatt
Ruth Ann Laster, Membership Chair
Evelyn Laufer
Barbara Little
Robert Livingstone
Luigi Mastroianni
Nella McElroy
Jack Pearce
Robert Reynolds
Ted Rowan
Barbara Wheeler

Sustaining Associate

George Frederick Jewett Foundation
Mr. and Mrs. Richard P. Mellon
Mr. Jonathan O'Herron
Plymouth Savings Bank

Supporting Associate

Ms. Frances B. Bator
Benthos, Inc.
Mr. James M. Clark
Mr. and Mrs. LeRoy Clark, Jr.
Dr. and Mrs. Alexander W. Clowes
Mrs. Margaret Clowes
Mr. and Mrs. Ian D. W. Cramer
Dr. and Mrs. James D. Ebert
Mr. and Mrs. David Fausch
Mrs. Mary Jewett Gaiser
Dr. and Mrs. Prosser Gifford
Mr. and Mrs. William H. Greer, Jr.
Dr. and Mrs. Howard H. Hiatt
Mr. and Mrs. William K. Mackey
Miss Anne Camille Maher
Drs. Elaine P. and Luigi Mastroianni, Jr.
Dr. and Mrs. J. Wister Meigs
Drs. Matthew & Jeanne Meselson
Mr. and Mrs. David Palmer
Drs. Christina and John Tochko
Mr. and Mrs. Frank L. Nickerson
Ms. Linda Sallop and Mr. Michael Fenlon
Mr. and Mrs. John E. Sawyer

Dual Membership

Mr. and Mrs. David C. Ahearn
Mr. and Mrs. Douglas F. Allison
Dr. and Mrs. Richard Armstrong
Dr. and Mrs. Samuel C. Armstrong
Mr. and Mrs. Henry Ashworth
Mr. and Mrs. Duncan P. Aspinwall
Mr. and Mrs. Donald R. Aukamp
Mr. and Mrs. David Bakalar
Mr. and Mrs. William L. Banks
Mr. and Mrs. R. Channing Barlow
Dr. and Mrs. Robert B. Barlow, Jr.
Mr. and Mrs. Richard T. Baum
Dr. and Mrs. Robert M. Berne
Drs. Alan and Harriet Bernheimer
Mr. and Mrs. Robert O. Bigelow
Dr. and Mrs. Edward G. Boettiger
Dr. and Mrs. Alfred F. Borg
Dr. and Mrs. Thomas A. Borgese
Dr. and Mrs. Francis P. Bowles
Dr. and Mrs. Mark J. Brauer
Dr. and Mrs. Thornton Brown
Dr. and Mrs. John B. Buck
Dr. and Mrs. John E. Burris
Mrs. Barbara Burwell
Mr. and Mrs. Winslow G. Carlton
Dr. and Mrs. Frank M. Child, III
Dr. and Mrs. Arnold M. Clark
Dr. and Mrs. Neal W. Cornell
Mr. and Mrs. David L. Crabb
Mr. and Mrs. Melvin C. Crane
Mr. and Mrs. Thomas S. Crane
Mr. and Mrs. Norman Cross
Mr. and Mrs. Alexander T. Daignault
Mr. and Mrs. Bruce G. Daniels
Mr. and Mrs. Joel P. Davis
Dr. and Mrs. Clyde J. Dawe
Mr. and Mrs. David L. Donovan
Mr. and Mrs. Charles E. Drummey
Mr. and Mrs. William P. Dugan
Mr. A. Felix DuPont, Jr.
Dr. and Mrs. James J. Ferguson, Jr.
Dr. and Mrs. Gerald Fischbach
Mr. and Mrs. Frederick S. Fisher, III
Mr. and Mrs. Howard G. Freeman
Mr. and Mrs. Leonard D. Friedman
Dr. and Mrs. Robert A. Frosch
Dr. and Mrs. Mordecai L. Gabriel
Mr. and Mrs. Robert S. Gilette
Dr. and Mrs. Phyllis Goldstein
Mr. and Mrs. Charles Goodwin
Mr. and Mrs. John Grassle
Dr. and Mrs. B. Herold Griffith
Dr. Antoine F.O. Hadamard
Dr. and Mrs. Harlyn O. Halvorson
Mr. and Mrs. Robert B. Harrington
Dr. and Mrs. J. Woodland Hastings
Mr. and Mrs. Gray G. Hayward
Dr. and Mrs. John E. Hobbie
Mr. and Mrs. Lon Hocker
Dr. and Mrs. Stuart Hodge
Drs. Francis C. G. Hoskin and Elizabeth M. Farnham
Dr. and Mrs. Robert J. Huettner
Mr. and Mrs. Raymond L. Jewett
Mr. and Mrs. DeWitt C. Jones, III
Dr. and Mrs. Benjamin Kaminer
Mr. and Mrs. Richard E. Kendall
Dr. Peter N. Kivy
Mr. and Mrs. A. Sidney Knowles
Dr. and Mrs. Leonard Laster
Dr. and Mrs. Hans Laufer
Mr. William Lawrence
Dr. and Mrs. Berton J. Leach
Mr. and Mrs. A. Dix Leeson
Dr. and Mrs. Rachmiel Levine
Mr. and Mrs. Donald W. Light
Mr. and Mrs. James E. Lloyd
Mrs. Ermine W. Lovell
Mr. and Mrs. B. Glenn MacNary
Mr. and Mrs. Bernard Manuel
Mr. and Mrs. Joseph C. Martyna
Mr. and Mrs. Appleton Mason
Mr. and Mrs. Frank J. Mather, III
Mr. and Mrs. James W. Mavor, Jr.
Mr. and Mrs. Arthur V. Meigs
Dr. and Mrs. Jerry M. Melillo
Dr. and Mrs. Charles B. Metz
Mr. and Mrs. Richard Meyers
Dr. and Mrs. Merle Mizell
Dr. and Mrs. Charles H. Montgomery
Mr. and Mrs. Bassett K. Morse
Mr. and Mrs. Richard S. Morse, Jr.

Mr. and Mrs. Clifford T. O'Connell
Dr. and Mrs. George D. Pappas
Mr. and Mrs. Robert Parkinson
Dr. and Mrs. John B. Pearce
Mr. and Mrs. John B. Peri
Dr. and Mrs. Courtland D. Perkins
Dr. and Mrs. Philip Person
Mr. and Mrs. Frederick S. Peters
Mr. and Mrs. E. Joel Peterson
Mr. and Mrs. George H. Plough
Dr. and Mrs. Aubrey Pothier, Jr.
Drs. Frank and Billie Press
Mr. Allan Ray Putnam
Mr. and Mrs. William A. Putnam
Mr. and Mrs. Robert M. Reynolds
Drs. Virginia and George Reynolds
Dr. and Mrs. Renato A. Ricca
Mr. and Mrs. Harold Righter
Mr. and Mrs. John Ripple
Ms. Jean Roberts
Drs. John and Priscilla F. Roslansky
Drs. Ruth Sager and Arthur B. Pardee
Mr. Harold B. Sears
Mr. John Seder and Ms. Frances Plough
Dr. and Mrs. Sheldon J. Segal
Drs. Cecily C. Selby and James S. Coles
Dr. and Mrs. Douglas R. Shanklin
Mr. and Mrs. Robert W. Sharp
Dr. and Mrs. David Shepro
Mr. and Mrs. Jonathan O. Simonds
Drs. Frederick and Marguerite Smith
Mr. and Mrs. Homer P. Smith
Mr. and Mrs. Heinz Specht
Drs. Melvin and Evelyn Spiegel
Dr. and Mrs. William K. Stephenson
Mr. and Mrs. Gerard L. Swope
Mr. and Mrs. Gordon F. Todd
Mr. and Mrs. D. Thomas Trigg
Dr. and Mrs. Walter Troll
Mr. and Mrs. Volker Ulbrich
Mr. and Mrs. John Valois
Mr. and Mrs. Samuel Vincent
Dr. Walter S. Vincent and Ms. Dore Butler
Mr. and Mrs. Henry Walter
Dr. Henry Warren and Ms. Cornelia Brown
Mr. and Mrs. Alfred Weisberg
Dr. and Mrs. Gerald Weissman
Dr. and Mrs. Paul S. Wheeler
Mr. and Mrs. Leslie J. Wilson
Mr. and Mrs. Wolfe Wolfinsohn
Mr. and Mrs. Bruce Zimmerli
Dr. and Mrs. Donald J. Zinn

Individual Member

Drs. James and Helene Anderson
Mrs. Marion S. Adelberg
Mr. Henry Albers
Dr. Nina S. Allen
Dr. Edwin J. Andrews
Mr. Ambrose Anoruo
Mrs. Kimball C. Atwood, III
Mr. Everett E. Bagley
Mrs. Elizabeth E. Ballantine
Mrs. Betsy G. Bang
Mr. John E. Barnes
Dr. Michael V. L. Bennett
Mr. and Mrs. C. John Berg
Dr. Harriet P. Bernheimer
Ms. Carol L. Bissonnette
Dr. Thomas P. Bleck
Mr. Robert D. Boche
Mrs. Julie Boettiger
Mr. and Mrs. Thomas C. Bolton
Mr. Theodore A. Bonn
Mr. Anthony Briana
Mrs. Jennie P. Brown
Mrs. Thomas A. Brown
Dr. Robert H. Broyles
Dr. Alan H. Burghauser
Mrs. Beatrice F. Buxton
Mr. Bruce E. Buxton
Mrs. David Campbell
Dr. Francis D. Carlson
Mr. Frank C. Carotenuto
Dr. Robert H. Carrier
Mrs. Patricia A. Case
Mrs. Shirley R. Chaet
Mrs. Christie L. Chapman
Dr. Sallie Chisholm
Dr. Peter L. Clark
Mrs. Roberta Clark
Ms. Ann P. Cleary
Mrs. Octavia C. Clement
Dr. Laurence P. Cloud
Mr. Allen W. Clowes
Dr. Jewel Plummer Cobb
Mrs. Elaine Pear Cohen
Prof. D. Eugene Copeland
Dr. Helen M. Costello
Dr. Vincent Cowling
Ms. Charlotte E. Cross
Ms. Dorothy Crossley
Miss Helen Crossley
Mrs. Villa B. Crowell
Dr. Morton Davidson
Dr. Marie A. DiBerardino
Ms. Suzanne Droban
Mr. and Mrs. Charles E. Eastman
Dr. and Ms. Frank Egloff
Mr. Raymond Eliott
Dr. Arthur J. Esswein
Mr. Gordon C. Estabrooks
Mr. John W. Folino, Jr.
Mr. Lewis W. Francis, Jr.
Dr. Krystyna Frenkel
Dr. James H. Fribourgh
Dr. John J. Funkhouser
Mrs. Paul M. Fye
Miss Eleanor Garfield
Dr. Sydney Gellis
Dr. James L. German, III
Mr. Charles Gifford
Mrs. Rebeckah D. Glazebrook
Mr. Gary Glenn
Mr. Michael P. Goldring
Mrs. Rose Grant
Mrs. Edith T. Grosch
Mrs. Mona Gross
Mrs. Barbara Grossman
Dr. Harry O. Haakonsen
Mr. Peter A. Hall
Mrs. Valerie A. Hall
Ms. Mary Elizabeth Hamstrom
Mrs. Janet M. Harvey
Dr. Robert R. Haubrich
Dr. David S. Hays
Mrs. Jane M. Hersey
Dr. Barbara Hichar
Mrs. Bertha V. Hill
Mrs. Eleanor M. Hirschfield
Mrs. Helen Hodosh
Mrs. Mary Jean Howard
Ms. Susan A. Huettner
Mrs. Pauline J. Hyde
Miss Elizabeth B. Jackson
Ms. Mary D. Janney
Mrs. Barbara W. Jones
Mr. Frederick S. Jones, II
Dr. and Mrs. Edwin P. Jordan
Dr. Harry S. Kahn
Mrs. Joan T. Kanwisher
Mrs. Sally Karush
Mrs. Marcella Katz
Mrs. Patricia E. Keoughan
Mrs. Jessie Keosian
Dr. Ben Korgen
Mr. Ezra Laderman
Ms. Rebecca Lash
Mr. and Mrs. F. Arthur Le Blond
Dr. Michael T. Leahy
Dr. Marian E. LeFevre
Dr. Mortimer Levitz
Mr. Lennart Lindberg
Mr. Timothy Lindner
Mrs. Barbara C. Little
Mr. Robert Livingstone, Jr.
Mrs. Sarah Loessel
Miss Doris L. Low
Mrs. Margaret M. Macleish
Ms. Chris Magee
Mrs. Annemarie E. Mahler
Dr. and Mrs. Philip B. Maples
Dr. Julian B. Marsh
Mrs. Miriam J. Mauzerall
Mrs. Nella W. McElroy
Dr. Suzanne I. McGee
Mr. Paul McGonigle
Dr. Susan Gerbi McIlwain
Ms. Mary W. McKoan
Mr. John J. McMahon
Ms. Cornelia McMurtrie
Dr. Martin Mendelson
Mr. Mentor Metaxas
Dr. Daniel G. Miller
Mrs. Margaret A. Mills-Michael
Mrs. Florence E. Mixer
Mrs. Anna Monroy
Mrs. Mary E. Montgomery
Dr. M. Patricia Morse
Mrs. Eleanor M. Nace
Mr. Paul F. Nace, Jr.
Mr. John E. Naugle
Mr. William G. Neall
Dr. Leonard Nelson
Dr. Pamela Nelson

Mr. Thomas O'Neil
Dr. Renee Bennett O'Sullivan
Dr. Janice S. Olszowka
Dr. Karen J. Ott
Mrs. Malcolm S. Park
Miss Carolyn L. Parmenter
Dr. Charles Parmenter
Ms. Joan Pearlman
Dr. Judith Pederson
Mrs. Claudia R. Pendergast
Ms. Joyce S. Pendery
Mr. Raymond W. Peterson
Mr. Richard F. Petty
Dr. and Mrs. Anthony Pires
Dr. Keith R. Porter
Mrs. F. Carol Price
Mr. John S. Price
Dr. C. Ladd Prosser
Mr. Fernando Quezada
Mrs. Julia S. Rankin
Dr. Samuel O. Raymond
Ms. A. Kathy Regis
Mr. John Riina
Dr. Monica Riley
Mrs. Lola E. Robertson
Dr. Denis M. Robinson
Ms. Hilde Rosenthal
Mrs. Atholie K. Rosett
Ms. Virginia F. Ross
Dr. Don Rowe
Mr. Francis C. Ryder
Dr. John W. Saunders, Jr.
Mrs. Ruth L. Saz
Dr. Edward K. Scheer
Dr. R. Walter Schlesinger
Mr. Peter J. Schwamb
Mrs. Elsie M. Scott
Mrs. Deborah G. Senft
Mrs. Harriet S. Shapiro
Dr. John R. Shaver
Dr. Charlotte Shemin
Dr. James Sidie
Mr. Bertram R. Silver
Mr. Daniel M. Singer
Mrs. Virginia B. Sinnott
Mrs. Diana M. Smith
Mrs. Perle Sonnenblick
Dr. William T. Speck
Mrs. M. Evelyn Steele
Dr. Robert E. Steele
Mrs. Eleanor Steinbach
Mrs. Judith G. Stetson
Ms. Gail Stetten
Mrs. Jane Lazarow Stetten
Dr. Dorothy A. Stracher
Mr. Robert Stump
Mr. Albert H. Swain
Mrs. Marjorie P. Swope
Mr. George H. Taber
Mr. James K. Taylor
Mr. Emil D. Tietje, Jr.
Mrs. Linda L. Timmins
Mrs. Ida Trager
Miss Natalie Trousof
Ms. Ciona Ulbrich
Ms. Diane Ursone
Mrs. Alice H. Van Buren
Mrs. Barbara Van Holde
Mrs. Alice M. Veeder
Dr. Claude A. Villee, Jr.
Dr. Dorothy Villee
Mr. Arthur D. Voorhis
Mrs. Joyce Waksman
Mrs. Eve Warren
Mr. John T. Weeks
Ms. Lillian Wendorff
Dr. Gary Wessel
Dr. William M. Wheeler
Mrs. Barbara Whitehead
Mr. Geoffrey G. Whitney, Jr.
Mrs. Joan Wickersham
Mrs. Clare M. Wilber
Dr. T. Hastings Wilson
Dr. William M. Winn
Ms. Nancy Woitkoski
Mrs. Elizabeth S. Yntema
Dr. Sumner Zacks
Mr. Kenneth H. Zimble

MBL Associates Gift Shop Volunteers

Marion Adelberg
Barbara Atwood
Pat Barlow
Harriet Bernheimer
Gloria Borgese
Jennie Brown
Kitty Brown
Elizabeth Buck
Mary Buckley
Shirley Chaet
Vera Clark
Peggy Clowes
Jewel Cobb
Villa Crowell
Janet Daniels
Betsy Daugnault
Fran Eastman
Alma Ebert
Margaret German
Violet Gifford
Becky Glazebrook
Rose Grant
Eddie Grosch
Barbara Grossman
Jean Halvorson
Pat Hancock
Helen Hodosh
Polly Hyde
Sally Karush
Bucky Ketchum
Barbara Little
Sally Loessel
Winnie Mackey
Miriam Mauzerall
Mary Mavor
Florence Mixer
Lorraine Mizell
Eleanor Nace
Bertha Person
Julie Rankin
Jean Ripps
Lilyan Sauders
Cynthia Smith
Louise Specht
Susie Steinbach
Peg Talcot
Eleanor Troll
Natalie Trousof
Mary Ulbrich
Barbara Van Holde
Alice Veeder
Dorothy Villie
Clare Wilber

MBL Summer Tour Guides

Betsy Bang
John Buck
Sears Crowell
Teru Hayashi
Julie Rankin
Lola Robertson
Mary Ulbrich
Donald Zinn
Margery Zinn

Certificate of Organization
Articles of Amendment
Bylaws

Certificate of Organization

(On File in the Office of the Secretary of the Commonwealth)

No. 3170

We, Alpheus Hyatt, President, William Stanford Stevens, Treasurer, and William T. Sedgwick, Edward G. Gardiner, Susan Mims and Charles Sedgwick Minot being a majority of the Trustees of the Marine Biological Laboratory in compliance with the requirements of the fourth section of chapter one hundred and fifteen of the Public Statutes do hereby certify that the following is a true copy of the agreement of association to constitute said Corporation, with the names of the subscribers thereto:

We, whose names are hereto subscribed, do, by this agreement, associate ourselves with the intention to constitute a Corporation according to the provisions of the one hundred and fifteenth chapter of the Public Statutes of the Commonwealth of Massachusetts, and the Acts in amendment thereof and in addition thereto.

The name by which the Corporation shall be known is
THE MARINE BIOLOGICAL LABORATORY.

The purpose for which the Corporation is constituted is to establish and maintain a laboratory or station for scientific study and investigations, and a school for instruction in biology and natural history.
The place within which the Corporation is established or located is the city of Boston within said Commonwealth.
The amount of its capital stock is none.
In Witness Whereof, we have hereunto set our hands, this twenty seventh day of February in the year eighteen hundred and eighty-eight, Alpheus Hyatt, Samuel Mills, William T. Sedgwick, Edward G. Gardiner, Charles Sedgwick Minot, William G. Farlow, William Stanford Stevens, Anna D. Phillips, Susan Mims, B. H. Van Vleck.
That the first meeting of the subscribers to said agreement was held on the thirteenth day of March in the year eighteen hundred and eighty-eight.
In Witness Whereof, we have hereunto signed our names, this thirteenth day of March in the year eighteen hundred and eighty-eight, Alpheus Hyatt, President, William Stanford Stevens, Treasurer, Edward G. Gardiner, William T. Sedgwick, Susan Mims, Charles Sedgwick Minot.
(Approved on March 20, 1988 as follows:
I hereby certify that it appears upon an examination of the within written certificate and the records of the corporation duly submitted to my inspection, that the requirements of sections one, two and three of chapter one hundred and fifteen, and sections eighteen, twenty and twenty-one of chapter one hundred and six, of the Public Statutes, have been complied with and I hereby approve said certificate this twentieth day of March A.D. eighteen hundred and eighty-eight.

Charles Endicott
Commissioner of Corporations)

Articles of Amendment

(On File in the Office of the Secretary of the Commonwealth)

We, James D. Ebert, President, and David Shepro, Clerk of the Marine Biological Laboratory, located at Woods Hole, Massachusetts 02543, do hereby certify that the following amendment to the Articles of Organization of the Corporation was duly adopted at a meeting held on August 15, 1975, as adjourned to August 29, 1975, by vote of 444 members, being at least two-thirds of its members legally qualified to vote in the meeting of the corporation:

Voted: That the Certificate of Organization of this corporation be and it hereby is amended by the addition of the following provisions:
"No Officer, Trustee or Corporate Member of the corporation shall be personally liable for the payment or satisfaction of any obligation or liabilities incurred as a result of, or otherwise in connection with, any commitments, agreements, activities or affairs of the corporation.
"Except as otherwise specifically provided by the Bylaws of the corporation, meetings of the Corporate Members of the corporation may be held anywhere in the United States.
"The Trustees of the corporation may make, amend or repeal the Bylaws of the corporation in whole or in part, except with respect to any provisions thereof which shall by law, this Certificate or the bylaws of the corporation, require action by the Corporate Members."

The foregoing amendment will become effective when these articles of amendment are filed in accordance with Chapter 180, Section 7 of the General Laws unless these articles specify, in accordance with the vote adopting the amendment, a later effective date not more than thirty days after such filing, in which event the amendment will become effective on such later date.

In Witness whereof and Under the Penalties of Perjury, we have hereto signed our names this 2nd day of September, in the year 1975, James D. Ebert, President; David Shepro, Clerk.
(Approved on October 24, 1975, as follows:
I hereby approve the within articles of amendment and, the filing fee in the amount of $10 having been paid, said articles are deemed to have been filed with me this 24th day of October, 1975.

Paul Guzzi
Secretary of the Commonwealth)

Bylaws

(Revised August 7, 1992 and December 10, 1992)

ARTICLE I—THE CORPORATION

A. *Name and Purpose.* The name of the Corporation shall be The Marine Biological Laboratory. The Corporation's purpose shall be to establish and maintain a laboratory or station for scientific study and investigation and a school for instruction in biology and natural history.

B. *Nondiscrimination* The Corporation shall not discriminate on the basis of age, religion, color, race, national or ethnic origin, sex or sexual preference in its policies on employment and administration or in its educational and other programs.

ARTICLE II—MEMBERSHIP

A. *Members.* The Members of the Corporation ("Members") shall consist of persons elected by the Board of Trustees (the "Board"), upon such terms and conditions and in accordance with such procedures, not inconsistent with law or these Bylaws, as may be determined by the Board. At any regular or special meeting of the Board, the Board may elect new Members. Members shall have no voting or other rights with respect to the Corporation or its activities except as specified in these Bylaws, and any Member may vote at any meeting of the Members in person only and not by proxy. Members shall serve until their death or resignation unless earlier removed with or without cause by the affirmative vote of two-thirds of the Trustees then in office. Any Member who has retired from his or her home institution may, upon written request to the Corporation, be designated a Life Member. Life Members shall not have the right to vote and shall not be assessed for dues.

B. *Meetings.* The annual meeting of the Members shall be held on the Friday following the first Tuesday in August of each year, at the Laboratory of the Corporation in Woods Hole, Massachusetts, at 9:30 a.m. The Chairperson of the Board shall preside at meetings of the Corporation. If no annual meeting is held in accordance with the foregoing provision, a special meeting may be held in lieu thereof with the same effect as the annual meeting, and in such case all references in these Bylaws, except in this Article II.B., to the annual meeting of the Members shall be deemed to refer to such special meeting. Members shall transact business as may properly come before the meeting. Special meetings of the Members may be called by the Chairperson or the Trustees, and shall be called by the Clerk, or in the case of the death, absence, incapacity or refusal by the Clerk, by any other officer, upon written application of Members representing at least ten percent of the smallest quorum of Members required for a vote upon any matter at the annual meeting of the Members, to be held at such time and place as may be designated.

C. *Quorum.* One hundred (100) Members shall constitute a quorum at any meeting. Except as otherwise required by law or these Bylaws, the affirmative vote of a majority of the Members voting in person at a meeting attended by a quorum shall constitute action on behalf of the Members.

D. *Notice of Meetings* Notice of any annual meeting or special meeting of Members, if necessary, shall be given by the Clerk by mailing notice of the time and place and purpose of such meeting at least 15 days before such meeting to each Member at his or her address as shown on the records of the Corporation.

E. *Wavier of Notice.* Whenever notice of a meeting is required to be given a Member, under any provision of the Articles or Organization or Bylaws of the Corporation, a written waiver thereof, executed before or after the Meeting by such Member, or his or her duly authorized attorney, shall be deemed equivalent to such notice.

F. *Adjournments.* Any meeting of the Members may be adjourned to any other time and place by the vote of a majority of those Members present at the meeting, whether or not such Members constitute a quorum, or by any officer entitled to preside at or to act as Clerk of such meeting, if no Member is present or represented. It shall not be necessary to notify any Members of any adjournment unless no Member is present or represented at the meeting which is adjourned, in which case, notice of the adjournment shall be given in accordance with Article II.D. Any business which could have been transacted at any meeting of the Members as originally called may be transacted at an adjournment thereof.

ARTICLE III—ASSOCIATES OF THE CORPORATION

Associates of the Corporation. The Associates of the Marine Biological Laboratory shall be an unincorporated group of persons (including associations and corporations) interested in the Laboratory and shall be organized and operated under the general supervision and authority of the Trustees. The Associates of the Marine Biological Laboratory shall have no voting rights.

ARTICLE IV—BOARD OF TRUSTEES

A. *Powers.* The Board of Trustees shall have the control and management of the affairs of the Corporation. The Trustees shall elect a Chairperson of the Board who shall serve until his or her successor is elected and qualified. They shall annually elect a President of the Corporation. They shall annually elect a Vice Chairperson of the Board who shall be Vice Chairperson of the meetings of the Corporation. They shall annually elect a Treasurer. They shall annually elect a Clerk, who shall be a resident of Massachusetts. They shall elect Trustees-at-Large as specified in this Article IV. They shall appoint a Director of the Laboratory for a term not to exceed five years, provided the term shall not exceed one year if the candidate has attained the age of 65 years prior to the date of the appointment. They shall choose such other officers and agents as they shall think best. They may fix the compensation of all officers and agents of the Corporation and may remove them at any time. They may fill vacancies occurring in any of the offices. The Board shall have the power to choose an Executive Committee from their own number as provided in Article V, and to delegate to such Committee such of their own powers as they may deem expedient in addition to those powers conferred by Article V. They shall, from time to time, elect Members to the Corporation upon such terms and conditions as they shall have determined, not inconsistent with law or these Bylaws.

B. *Composition and Election*

(1) The Board shall include 24 Trustees elected by the Board as provided below:

(a) At least six Trustees ("Corporate Trustees") shall be Members who are scientists, and the other Trustees ("Trustees-at-Large") shall be individuals who need not be Members or otherwise affiliated with the Corporation.

(b) The 24 elected Trustees shall be divided into four classes of six Trustees each, with one class to be elected each year to serve for a term of four years, and with each such class to include at least one Corporate Trustee. Such classes of Trustees shall be designated by the year of expiration of their respective terms.

(2) The Board shall also include the Chief Executive Officer, Treasurer and the Chairperson of the Science Council, who shall be *ex officio* voting members of the Board.

(3) Although Members or Trustees may recommend individuals for nomination as Trustees, nominations for Trustee elections shall be made by the Nominating Committee in its sole discretion. The Board may also elect Trustees who have not been nominated by the Nominating Committee.

C. *Eligibility.* A Corporate Trustee or a Trustee-at-Large who has been elected to an initial four-year term or remaining portion thereof, of which he/she has served at least two years, shall be eligible for re-election to a second four-year term, but shall be ineligible for re-election to any subsequent term until one year has elapsed after he/she has last served as a Trustee.

D. *Removal.* Any Trustee may be removed from office at any time with or without cause, by vote of a majority of the Members entitled to vote in the election of Trustees; or for cause, by vote of two-thirds of the Trustees then in office. A Trustee may be removed for cause only if notice of such action shall have been given to all of the Trustees or Members entitled to vote, as the case may be, prior to the meeting at which such action is to be taken and if the Trustee to be so removed shall have been given reasonable notice and opportunity to be heard before the body proposing to remove him or her.

E. *Vacancies* Any vacancy in the Board may be filled by vote of a majority of the remaining Trustees present at a meeting of Trustees at which a quorum is present. Any vacancy in the Board resulting from the resignation or removal of a Corporate Trustee shall be filled by a Member who is a scientist.

F. *Meetings* Meetings of the Board shall be held from time to time, not less frequently than twice annually, as determined by the Board. Special meetings of Trustees may be called by the Chairperson, or by any seven Trustees, to be held at such time and place as may be designated. The Chairperson of the Board, when present, shall preside over all meetings of the Trustees. Written notice shall be sent to a Trustee's usual or last known place of residence at least two weeks before the meeting. Notice of a meeting need not be given to any Trustee if a written waiver of notice executed by such Trustee before or after the meeting is filed with the records of the meeting, or if such Trustee shall attend the meeting without protesting prior thereto or at its commencement the lack of notice given to him or her.

G. *Quorum and Action by Trustees.* A majority of all Trustees then in office shall constitute a quorum. Any meeting of Trustees may be adjourned by vote of a majority of Trustees present, whether or not a quorum is present, and the meeting may be held as adjourned without further notice. When a quorum is present at any meeting of the Trustees, a majority of the Trustees present and voting (excluding abstentions) shall decide any question, including the election of officers, unless otherwise required by law, the Articles of Organization or these Bylaws.

H. *Transfers of Interests in Land* There shall be no transfer of title nor long-term lease of real property held by the Corporation without prior approval of not less than two-thirds of the Trustees. Such real property transactions shall be finally acted upon at a meeting of the Board only if presented and discussed at a prior meeting of the Board. Either meeting may be a special meeting and no less than four weeks shall elapse between the two meetings. Any property acquired by the Corporation after December 1, 1989 may be sold, any mortgage or pledge of real property (regardless of when acquired) to secure borrowings by the Corporation may be granted, and any transfer of title or interest in real property pursuant to the foreclosure or endorsement of any such mortgage or pledge of real property may be effected by any holder of a mortgage or pledge of real property of the Corporation, with the prior approval of not less than two-thirds of the Trustees (other than any Trustee or Trustees with a direct or indirect financial interest in the transaction being considered for approval) who are present at a regular or special meeting of the Board at which there is a quorum.

ARTICLE V—COMMITTEES

A. *Executive Committee.* There shall be an Executive Committee of the Board of Trustees which shall consist of not more than eleven (11) Trustees, including *ex officio* Trustees, elected by the Board.

The Chairperson of the Board shall act as Chairperson of the Executive Committee and the Vice Chairperson as Vice Chairperson. The Executive Committee shall meet at such times and places and upon such notice and appoint such subcommittees as the Committee shall determine.

The Executive Committee shall have and may exercise all the powers of the Board during the intervals between meetings of the Board except those powers specifically withheld, from time to time, by vote of the Board or by law. The Executive Committee may also appoint such committees, including persons who are not Trustees, as it may, from time to time, approve to make recommendations with respect to matters to be acted upon by the Executive Committee or the Board.

The Executive Committee shall keep appropriate minutes of its meetings, which shall be reported to the Board. Any actions taken by the Executive Committee shall also be reported to the Board.

B. *Nominating Committee.* There shall be a Nominating Committee which shall consist of not fewer than four nor more than six Trustees appointed by the Board in a manner which shall reflect the balance between Corporate Trustees and Trustees-at-Large on the Board. The Nominating Committee shall nominate persons for election as Corporate Trustees and Trustees-at-Large, Chairperson of the Board, Vice Chairperson of the Board, President, Treasurer, Clerk, Director of the Laboratory and such other officers, if any, as needed, in accordance with the requirements of these Bylaws. The Nominating Committee shall also be responsible for overseeing the training of new Trustees. The Chairperson of the Board of Trustees shall appoint the Chairperson of the Nominating Committee. The Chairperson of the Science Council shall be an *ex officio* voting member of the Nominating Committee.

C. *Science Council.* There shall be a Science Council (the "Council") which shall consist of Members of the Corporation elected to the Council by vote of the Members of the Corporation, and which shall advise the Board with respect to matters concerning the Corporation's mission, its scientific and instructional endeavors, and the appointment and promotions of persons or committees with responsibility for matters requiring scientific expertise. Unless otherwise approved by a majority of the members of the Council, the Chairperson of the Council shall be elected annually by the Council. The chief executive officer of the Corporation shall be an *ex officio* voting member of the Council.

D. *Board of Overseers.* There shall be a Board of Overseers which shall consist of not fewer than five nor more than eight scientists who have expertise concerning matters with which the Corporation is involved. Members of the Board of Overseers may or may not be Members of the Corporation and may be appointed by the Board of Trustees on the basis of recommendations submitted from scientists and scientific organizations or societies. The Board of Overseers shall be available to review and offer recommendations to the officers, Trustees and Science Council regarding scientific activities conducted or proposed by the Corporation and shall meet from time to time, not less frequently than annually, as determined by the Board of Trustees.

E. *Board Committees Generally.* The Trustees may elect or appoint one or more other committees (including, but not limited to, an Investment Committee, a Development Committee, an Audit Committee, a Facilities and Capital Equipment Committee and a Long-Range Planning Committee) and may delegate to any such committee or committees any or all of their powers, except those which by law, the Articles of Organization or these Bylaws the Trustees are prohibited from delegating; provided that any committee to which the powers of the Trustees are delegated shall consist solely of Trustees. The members of any such committee shall have such tenure and duties as the Trustees shall determine. The Investment Committee, which shall oversee the management of the Corporation's endowment funds and marketable securities shall include as *ex officio* members, the Chairperson of the Board, the Treasurer and the Chairperson of the Audit Committee, together with such Trustees as may be required for not less than two-thirds of the Investment Committee to consist of Trustees. Except as otherwise provided by these Bylaws or determined by the Trustees, any such committee may make rules for the conduct of its business, but, unless otherwise provided by the Trustees or in such rules, its business shall be conducted as nearly as possible in the same manner as is provided by these Bylaws for the Trustees.

F. *Actions Without a Meeting.* Any action required or permitted to be taken at any meeting of the Executive Committee or any other committee elected by the Trustees may be taken without a meeting if all members of such committees consent to the action in writing and such written consents are filed with the records of meetings. Members of the Executive Committee or any other committee elected by the Trustees may also participate in any meeting by means of a telephone conference call, or otherwise take action in such a manner as may, from time to time, be permitted by law.

G. *Manual of Procedures.* The Board of Trustees, on the recommendation of the Executive Committee, shall establish guidelines and modifications thereof to be recorded in a Manual of Procedures. Guidelines shall establish procedures for: (1) Nomination and election of members of the Corporation, Board of Trustees and Executive Committee; (2) Election of Officers; (3) Formation and Function of Standing Committees.

ARTICLE VI—OFFICERS

A. *Enumeration.* The officers of the Corporation shall consist of a President, a Treasurer and a Clerk, and such other officers having the powers of President, Treasurer and Clerk as the Board may determine, and a Director of the Laboratory. The Corporation may have such other officers and assistant officers as the Board may determine, including (without limitation) a Chairperson of the Board, Vice Chairperson and one or more Vice Presidents, Assistant Treasurers or Assistant Clerks. Any two or more offices may be held by the same person. The Chairperson and Vice Chairperson of the Board shall be elected by and from the Trustees, but other officers of the Corporation need not be Trustees or Members. If required by the Trustees, any officer shall give the Corporation a bond for the faithful performance of his or her duties in such amount and with such surety or sureties as shall be satisfactory to the Trustees.

B. *Tenure.* Except as otherwise provided by law, by the Articles of Organization or by these Bylaws, the President, Treasurer, and all other officers shall hold office until the first meeting of the Board following the annual meeting of Members and thereafter, until his or her successor is chosen and qualified.

C. *Resignation.* Any officer may resign by delivering his or her written resignation to the Corporation at its principal office or to the President or Clerk and such resignation shall be effective upon receipt unless it is specified to be effective at some other time or upon the happening of some other event.

D. *Removal.* The Board may remove any officer with or without cause by a vote of a majority of the entire number of Trustees then in office, at a meeting of the Board called for that purpose and for which notice of the purpose thereof has been given, provided that an officer may be removed for cause only after having an opportunity to be heard by the Board at a meeting of the Board at which a quorum is personally present and voting.

E. *Vacancy.* A vacancy in any office may be filled for the unexpired balance of the term by vote of a majority of the Trustees present at any meeting of Trustees at which a quorum is present or by written consent of all of the Trustees, if less than a quorum of Trustees shall remain in office.

F. *Chairperson.* The Chairperson shall have such powers and duties as may be determined by the Board and, unless otherwise determined by the Board, shall serve in that capacity for a term coterminous with his or her term as Trustee.

G. *Vice Chairperson.* The Vice Chairperson shall perform the duties and exercise the powers of the Chairperson in the absence or disability of the Chairperson, and shall perform such other duties and possess such other powers as may be determined by the Board. Unless otherwise determined by the Board, the Vice Chairperson shall serve for a one-year term.

H. *Director.* The Director shall be the chief operating officer and, unless otherwise voted by the Trustees, the chief executive officer of the Corporation. The Director shall, subject to the direction of the Trustees, have general supervision of the Laboratory and control of the business of the Corporation. At the annual meeting, the

Director shall submit a report of the operations of the Corporation for such year and a statement of its affairs, and shall, from time to time, report to the Board all matters within his or her knowledge which the interests of the Corporation may require to be brought to its notice.

I. *Deputy Director.* The Deputy Director, if any, or if there shall be more than one, the Deputy Directors in the order determined by the Trustees, shall, in the absence or disability of the Director, perform the duties and exercise the powers of the Director and shall perform such other duties and shall have such other powers as the Trustees may, from time to time, prescribe.

J. *President.* The President shall have the powers and duties as may be vested in him or her by the Board.

K. *Treasurer and Assistant Treasurer.* The Treasurer shall, subject to the direction of the Trustees, have general charge of the financial affairs of the Corporation, including its long-range financial planning, and shall cause to be kept accurate books of account. The Treasurer shall prepare a yearly report on the financial status of the Corporation to be delivered at the annual meeting. The Treasurer shall also prepare or oversee all filings required by the Commonwealth of Massachusetts, the Internal Revenue Service, or other Federal and State Agencies. The account of the Treasurer shall be audited annually by a certified public accountant.

The Assistant Treasurer, if any, or if there shall be more than one, the Assistant Treasurers in the order determined by the Trustees, shall, in the absence or disability of the Treasurer, perform the duties and exercise the powers of the Treasurer, shall perform such other duties and shall have such other powers as the Trustees may, from time to time, prescribe.

L. *Clerk and Assistant Clerk.* The Clerk shall be a resident of the Commonwealth of Massachusetts, unless the Corporation has designated a resident agent in the manner provided by law. The minutes or records of all meetings of the Trustees and Members shall be kept by the Clerk who shall record, upon the record books of the Corporation, minutes of the proceedings at such meetings. He or she shall have custody of the record books of the Corporation and shall have such other powers and shall perform such other duties as the Trustees may, from time to time, prescribe.

The Assistant Clerk, if any, or if there shall be more than one, the Assistant Clerks in the order determined by the Trustees, shall, in the absence or disability of the Clerk, perform the duties and exercise the powers of the Clerk and shall perform such other duties and shall have such other powers as the Trustees may, from time to time, prescribe.

In the absence of the Clerk and an Assistant Clerk from any meeting, a temporary Clerk shall be appointed at the meeting.

M. *Other Powers and Duties.* Each officer shall have in addition to the duties and powers specifically set forth in these Bylaws, such duties and powers as are customarily incident to his or her office, and such duties and powers as the Trustees may, from time to time, designate.

ARTICLE VII—AMENDMENTS

These Bylaws may be amended by the affirmative vote of the Members at any meeting, provided that notice of the substance of the proposed amendment is stated in the notice of such meeting. As authorized by the Articles of Organization, the Trustees, by a majority of their number then in office, may also make, amend or repeal these Bylaws, in whole or in part, except with respect to (a) the provisions of these Bylaws governing (i) the removal of Trustees and (ii) the amendment of these Bylaws and (b) any provisions of these Bylaws which by law, the Articles of Organization or these Bylaws, requires action by the Members.

No later than the time of giving notice of meeting of Members next following the making, amending or repealing by the Trustees of any Bylaw, notice thereof stating the substance of such change shall be given to all Members entitled to vote on amending the Bylaws.

Any Bylaw adopted by the Trustees may be amended or repealed by the Members entitled to vote on amending the Bylaws.

ARTICLE VIII—INDEMNITY

Except as otherwise provided below, the Corporation shall, to the extent legally permissible, indemnify each person who is, or shall have been, a Trustee, director or officer of the Corporation or who is serving, or shall have served at the request of the Corporation as a Trustee, director or officer of another organization in which the Corporation directly or indirectly has any interest as a shareholder, creditor or otherwise, against all liabilities and expenses (including judgments, fines, penalties, and reasonable attorneys' fees and all amounts paid, other than to the Corporation or such other organization, in compromise or settlement) imposed upon or incurred by any such person in connection with, or arising out of, the defense or disposition of any action, suit or other proceeding, whether civil or criminal, in which he or she may be a defendant or with which he or she may be threatened or otherwise involved, directly or indirectly, by reason of his or her being or having been such a Trustee, director or officer.

The Corporation shall provide no indemnification with respect to any matter as to which any such Trustee, director or officer shall be finally adjudicated in such action, suit or proceeding not to have acted in good faith in the reasonable belief that his or her action was in the best interests of the Corporation. The Corporation shall provide no indemnification with respect to any matter settled or comprised unless such matter shall have been approved as in the best interests of the Corporation, after notice that indemnification is involved, by (i) a disinterested majority of the Board of the Executive Committee, or (ii) a majority of the Members.

Indemnification may include payment by the Corporation of expenses in defending a civil or criminal action or proceeding in advance of the final disposition of such action or proceeding upon receipt of an undertaking by the person indemnified to repay such payment if it is ultimately determined that such person is not entitled to indemnification under the provisions of this Article VIII, or under any applicable law.

As used in the Article VIII, the terms "Trustee," "director," and "officer" include their respective heirs, executors, administrators and legal representatives, and an "interested" Trustee, director or officer is one against whom in such capacity the proceeding in question or another proceeding on the same or similar grounds is then pending.

To assure indemnification under this Article VIII of all persons who are determined by the Corporation or otherwise to be or to have been "fiduciaries" of any employee benefits plan of the Corporation which may exist, from time to time, this Article VIII shall be interpreted as follows: (i) "another organization" shall be deemed to include such an employee benefit plan, including without limitation, any plan of the Corporation which is governed by the Act of Congress entitled "Employee Retirement Income Security Act of 1974," as amended, from time to time, ("ERISA"); (ii) "Trustee" shall be deemed to include any person requested by the Corporation to serve as such for an employee benefit plan where the performance by such person of his or her duties to the Corporation also imposes duties on, or otherwise involves services by, such person to the plan or participants or beneficiaries of the plan; (iii) "fines" shall be deemed to include any excise tax plan pursuant to ERISA; and (iv) actions taken or omitted by a person with respect to an employee benefit plan in the performance of such person's duties for a purpose reasonably believed by such person to be in the interest of the participants and beneficiaries of the plan shall be deemed to be for a purpose which is in the best interests of the Corporation.

The right of indemnification provided in this Article VIII shall not be exclusive of or affect any other rights to which any Trustee, director or officer may be entitled under any agreement, statute, vote of Members or otherwise. The Corporation's obligation to provide indemnification under this Article VIII shall be offset to the extent of any other source of indemnification of any otherwise applicable insurance coverage under a policy maintained by the Corporation or any other person. Nothing contained in the Article shall affect any rights to which employees and corporate personnel other than Trustees, directors or officers may be entitled by contract, by vote of the Board or of the Executive Committee or otherwise.

ARTICLE IX—DISSOLUTION

The consent of every Trustee shall be necessary to effect a dissolution of the Marine Biological Laboratory. In case of dissolution, the property shall be disposed of in such a manner and upon such terms as shall be determined by the affirmative vote of two-thirds of the Trustees then in office in accordance with the laws of the Commonwealth of Massachusetts.

ARTICLE X—MISCELLANEOUS PROVISIONS

A. *Fiscal Year.* Except as otherwise determined by the Trustees, the fiscal year of the Corporation shall end on December 31st of each year.

B. *Seal.* Unless otherwise determined by the Trustees, the Corporation may have a seal in such form as the Trustees may determine, from time to time.

C. *Execution of Instruments.* All checks, deeds, leases, transfers, contracts, bonds, notes and other obligations authorized to be executed by an officer of the Corporation in its behalf shall be signed by the Director or the Treasurer except as the Trustees may generally or in particular cases otherwise determine. A certificate by the Clerk or an Assistant Clerk, or a temporary Clerk, as to any action taken by the Members, Board of Trustees or any officer or representative of the Corporation shall as to all persons who rely thereon in good faith be conclusive evidence of such action.

D. *Corporate Records.* The original, or attested copies, of the Articles of Organization, Bylaws and records of all meetings of the Members shall be kept in Massachusetts at the principal office of the Corporation, or at an office of the Corporation's Clerk or resident agent. Said copies and records need not all be kept in the same office. They shall be available at all reasonable times for inspection by any Member for any proper purpose, but not to secure a list of Members for a purpose other than in the interest of the applicant, as a Member, relative to the affairs of the Corporation.

E. *Articles of Organization.* All references in these Bylaws to the Articles of Organization shall be deemed to refer to the Articles of Organization of the Corporation, as amended and in effect, from time to time.

F. *Transactions with Interested Parties.* In the absence of fraud, no contract or other transaction between this Corporation and any other corporation or any firm, association, partnership or person shall be affected or invalidated by the fact that any Trustee or officer of this Corporation is pecuniarily or otherwise interested in or is a director, member or officer of such other corporation or of such firm, association or partnership or in a party to or is pecuniarily or otherwise interested in such contract or other transaction or is in any way connected with any person or person, firm, association, partnership, or corporation pecuniarily or otherwise interested therein; provided that the fact that he or she individually or as a director, member or officer of such corporation, firm, association or partnership in such a party or is so interested shall be disclosed to or shall have been known by the Board of Trustees or a majority of such Members thereof as shall be present at a meeting of the Board of Trustees at which action upon any such contract or transaction shall be taken; any Trustee may be counted in determining the existence of a quorum and may vote at any meeting of the Board of Trustees for the purpose of authorizing any such contract or transaction with like force and effect as if he/she were not so interested, or were not a director, member or officer of such other corporation, firm, association or partnership, provided that any vote with respect to such contract or transaction must be adopted by a majority of the Trustees then in office who have no interest in such contract or transaction.

CONTENTS

CELL BIOLOGY

Koppelhus, Uffe, Per Hellung-Larsen, and Vagn Leick
Physiological parameters affecting the chemosensory response of *Tetrahymena* 1

Koppelhus, Uffe, Per Hellung-Larsen, and Vagn Leick
An improved quantitative assay for chemokinesis in *Tetrahymena* 8

Read, A. T., R. R. Hessler, and C. K. Govind
Muscle and nerve terminal fine structure of a primitive crustacean, the cephalocarid *Hutchinsoniella macracantha* 16

ECOLOGY AND EVOLUTION

Metz, Edward C., Robert E. Kane, Hiroko Yanagimachi, and Stephen R. Palumbi
Fertilization between closely related sea urchins is blocked by incompatibilities during sperm-egg attachment and early stages of fusion 23

FUNCTIONAL MORPHOLOGY

Flammang, Patrick, Stephane DeMeulenaere, and Michel Jangoux
The role of podial secretions in adhesion in two species of sea stars (Echinodermata) 35

NEUROBIOLOGY AND BEHAVIOR

Anctil, Michel, and Jean-Pascal Carette
Glutamate immunoreactivity in non-neuronal cells of the sea anemone *Metridium senile* 48

Lucero, Mary T., Heraldo Farrington, and William F. Gilly
Quantification of L-dopa and dopamine in squid ink: implications for chemoreception 55

New, John G.
Electric organ discharge and electrosensory reafference in skates 64

PHYSIOLOGY

Dietz, Thomas H., Diondi Lessard, Harold Silverman, and John W. Lynn
Osmoregulation in *Dreissena polymorpha:* the importance of Na, Cl, K, and particularly Mg 76

Thuesen, Erik V., and James J. Childress
Oxygen consumption rates and metabolic enzyme activities of oceanic California medusae in relation to body size and habitat depth 84

SEX CHANGE IN INVERTEBRATES

Brook, Heather J., Timothy A. Rawlings, and Ronald W. Davies
Protogynous sex change in the intertidal isopod *Gnorimosphaeroma oregonense* (Crustacea: Isopoda) 99

Sewell, Mary A.
Small size, brooding, and protandry in the apodid sea cucumber *Leptosynapta clarki* 112

Annual Report of the Marine Biological Laboratory R1

Volume 187 Number 2

THE BIOLOGICAL BULLETIN

OCTOBER, 1994

Published by the Marine Biological Laboratory

AEK 7312

THE
BIOLOGICAL BULLETIN

PUBLISHED BY
THE MARINE BIOLOGICAL LABORATORY

[illegible] Inst.
NOV 17 1994
Woods Hole, MA 02543

Associate Editors

PETER A. V. ANDERSON, The Whitney Laboratory, University of Florida
WILLIAM D. COHEN, Hunter College, City University of New York
DAVID EPEL, Hopkins Marine Station, Stanford University
J. MALCOLM SHICK, University of Maine, Orono

Editorial Board

THOMAS H. DIETZ, Louisiana State University
DAPHNE GAIL FAUTIN, University of Kansas
WILLIAM F. GILLY, Hopkins Marine Station, Stanford University
ROGER T. HANLON, Marine Biomedical Institute, University of Texas Medical Branch
CHARLES B. METZ, University of Miami
K. RANGA RAO, University of West Florida
BARUCH RINKEVICH, Israel Oceanographic & Limnological Research Ltd.
RICHARD STRATHMANN, Friday Harbor Laboratories, University of Washington
STEVEN VOGEL, Duke University
SARAH ANN WOODIN, University of South Carolina

Editor: MICHAEL J. GREENBERG, The Whitney Laboratory, University of Florida
Managing Editor: PAMELA L. CLAPP, Marine Biological Laboratory

OCTOBER, 1994

Printed and Issued by
LANCASTER PRESS, Inc.
3575 HEMPLAND ROAD
LANCASTER, PA

THE BIOLOGICAL BULLETIN

THE BIOLOGICAL BULLETIN is published six times a year by the Marine Biological Laboratory, MBL Street, Woods Hole, Massachusetts 02543.

Subscriptions and similar matter should be addressed to Subscription Manager, THE BIOLOGICAL BULLETIN, Marine Biological Laboratory, Woods Hole, Massachusetts 02543. Single numbers, $37.50. Subscription per volume (three issues), $90.00 ($180.00 per year for six issues).

Communications relative to manuscripts should be sent to Michael J. Greenberg, Editor-in-Chief, or Pamela L. Clapp, Managing Editor, at the Marine Biological Laboratory, Woods Hole, Massachusetts 02543. Telephone: (508) 548-3705, ext. 428. FAX: 508-540-6902. E-mail: pclapp@hoh.mbl.edu.

POSTMASTER: Send address changes to THE BIOLOGICAL BULLETIN, Marine Biological Laboratory,
Woods Hole, MA 02543.

Copyright © 1994, by the Marine Biological Laboratory

Second-class postage paid at Woods Hole, MA, and additional mailing offices.
ISSN 0006-3185

INSTRUCTIONS TO AUTHORS

The Biological Bulletin accepts outstanding original research reports of general interest to biologists throughout the world. Papers are usually of intermediate length (10–40 manuscript pages). A limited number of solicited review papers may be accepted after formal review. A paper will usually appear within four months after its acceptance.

Very short, especially topical papers (less than 9 manuscript pages including tables, figures, and bibliography) will be published in a separate section entitled "Research Notes." A Research Note in *The Biological Bulletin* follows the format of similar notes in *Nature*. It should open with a summary paragraph of 150 to 200 words comprising the introduction and the conclusions. The rest of the text should continue on without subheadings, and there should be no more than 30 references. References should be referred to in the text by number, and listed in the Literature Cited section in the order that they appear in the text. Unlike references in *Nature*, references in the Research Notes section should conform in punctuation and arrangement to the style of recent issues of *The Biological Bulletin*. Materials and Methods should be incorporated into appropriate figure legends. See the article by Lohmann *et al.* (October 1990, Vol. **179:** 214–218) for sample style. A Research Note will usually appear within two months after its acceptance.

The Editorial Board requests that regular manuscripts conform to the requirements set below; those manuscripts that do not conform will be returned to authors for correction before review.

1. ***Manuscripts.*** Manuscripts, including figures, should be submitted in triplicate. (Xerox copies of photographs are not acceptable for review purposes.) The submission letter accompanying the manuscript should include a telephone number, a FAX number, and (if possible) an E-mail address for the corresponding author. The original manuscript must be typed in no smaller than 12 pitch or 10 point, using double spacing (*including* figure legends, footnotes, bibliography, etc.) on one side of 16- or 20-lb. bond paper, 8½ by 11 inches. Please, no right justification. Manuscripts should be proofread carefully and errors corrected legibly in black ink. Pages should be numbered consecutively. Margins on all sides should be at least 1 inch (2.5 cm). Manuscripts should conform to the *Council of Biology Editors Style Manual*, 5th Edition (Council of Biology Editors, 1983) and to American spelling. Unusual abbreviations should be kept to a minimum and should be spelled out on first reference as well as defined in a footnote on the title page. Manuscripts should be divided into the following components: Title page, Abstract (of no more than 200 words), Introduction, Materials and Methods, Results, Discussion, Acknowledgments, Literature Cited, Tables, and Figure Legends. In addition, authors should supply a list of words and phrases under which the article should be indexed.

2. ***Title page.*** The title page consists of a condensed title or running head of no more than 35 letters and spaces, the manuscript title, authors' names and appropriate addresses, and footnotes listing present addresses, acknowledgments or contribution numbers, and explanation of unusual abbreviations.

3. ***Figures.*** The dimensions of the printed page, 7 by 9 inches, should be kept in mind in preparing figures for publication. We recommend that figures be about 1½ times the linear dimensions of the final printing desired, and that the ratio of the largest to the smallest letter or number and of the thickest to the thinnest line not exceed 1:1.5. Explanatory matter generally should be included in legends, although axes should always be identified on the illustration itself. Figures should be prepared for reproduction as either line cuts or halftones. Figures to be reproduced as line cuts should be unmounted glossy photographic reproductions or drawn in black ink on white paper, good-quality tracing cloth or plastic, or blue-lined coordinate paper. Those to be reproduced as halftones should be mounted on board, with both designating numbers or letters and scale bars affixed directly to the figures. All figures should be numbered in consecutive order, with no distinction between text and plate figures. The author's name and an arrow indicating orientation should appear on the reverse side of all figures.

4. ***Tables, footnotes, figure legends, etc.*** Authors should follow the style in a recent issue of *The Biological Bulletin* in preparing table headings, figure legends, and the like. Because of the high cost of setting tabular material in type, authors are asked to limit such material as much as possible. Tables, with their headings and footnotes, should be typed on separate sheets, numbered with consecutive Roman numerals, and placed after

the Literature Cited. Figure legends should contain enough information to make the figure intelligible separate from the text. Legends should be typed double spaced, with consecutive Arabic numbers, on a separate sheet at the end of the paper. Footnotes should be limited to authors' current addresses, acknowledgments or contribution numbers, and explanation of unusual abbreviations. All such footnotes should appear on the title page. Footnotes are not normally permitted in the body of the text.

5. ***Literature cited.*** In the text, literature should be cited by the Harvard system, with papers by more than two authors cited as Jones *et al.*, 1980. Personal communications and material in preparation or in press should be cited in the text only, with author's initials and institutions, unless the material has been formally accepted and a volume number can be supplied. The list of references following the text should be headed Literature Cited, and must be typed double spaced on separate pages, conforming in punctuation and arrangement to the style of recent issues of *The Biological Bulletin.* Citations should include complete titles and inclusive pagination. Journal abbreviations should normally follow those of the U. S. A. Standards Institute (USASI), as adopted by BIOLOGICAL ABSTRACTS and CHEMICAL ABSTRACTS, with the minor differences set out below. The most generally useful list of biological journal titles is that published each year by BIOLOGICAL ABSTRACTS (BIOSIS List of Serials; the most recent issue). Foreign authors, and others who are accustomed to using THE WORLD LIST OF SCIENTIFIC PERIODICALS, may find a booklet published by the Biological Council of the U.K. (obtainable from the Institute of Biology, 41 Queen's Gate, London, S.W.7, England, U.K.) useful, since it sets out the WORLD LIST abbreviations for most biological journals with notes of the USASI abbreviations where these differ. CHEMICAL ABSTRACTS publishes quarterly supplements of additional abbreviations. The following points of reference style for THE BIOLOGICAL BULLETIN differ from USASI (or modified WORLD LIST) usage:

A. Journal abbreviations, and book titles, all underlined (for *italics*)

B. All components of abbreviations with initial capitals (not as European usage in WORLD LIST *e.g., J. Cell. Comp. Physiol.* NOT *J. cell. comp. Physiol.*)

C. *All* abbreviated components must be followed by a period, whole word components *must not* (*i.e., J. Cancer Res.*)

D. Space between all components (*e.g., J. Cell. Comp. Physiol.*, not *J.Cell.Comp.Physiol.*)

E. Unusual words in journal titles should be spelled out in full, rather than employing new abbreviations invented by the author. For example, use *Rit Vísindafjélags Islendinga* without abbreviation.

F. All single word journal titles in full (*e.g., Veliger, Ecology, Brain*).

G. The order of abbreviated components should be the same as the word order of the complete title (*i.e., Proc.* and *Trans.* placed where they appear, not transposed as in some BIOLOGICAL ABSTRACTS listings).

H. A few well-known international journals in their preferred forms rather than WORLD LIST or USASI usage (*e.g., Nature, Science, Evolution* NOT *Nature, Lond., Science, N.Y.; Evolution, Lancaster, Pa.*)

6. ***Reprints, page proofs, and charges.*** Authors receive their first 100 reprints (without covers) free of charge. Additional reprints may be ordered at time of publication and normally will be delivered about two to three months after the issue date. Authors (or delegates for foreign authors) will receive page proofs of articles shortly before publication. They will be charged the current cost of printers' time for corrections to these (other than corrections of printers' or editors' errors). Other than these charges for authors' alterations, *The Biological Bulletin* does not have page charges.

Reference: *Biol. Bull.* **187:** 125–131. (October, 1994)

A Tribute to Professor Katsuma Dan on His 90th Birthday

Professor Katsuma Dan at the Misaki Marine Biological Station Centennial Celebration, 1987.

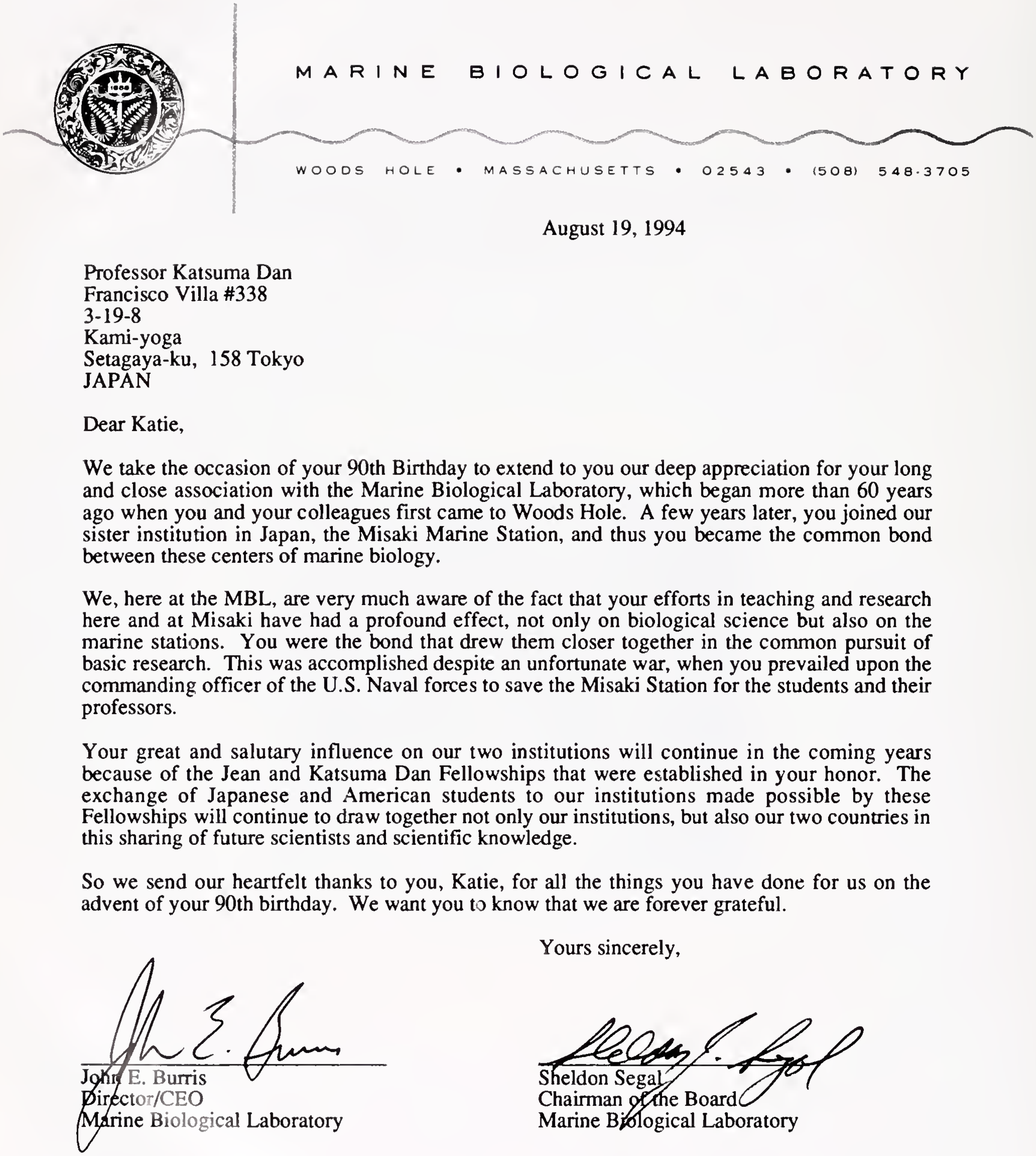

MARINE BIOLOGICAL LABORATORY

WOODS HOLE • MASSACHUSETTS • 02543 • (508) 548-3705

August 19, 1994

Professor Katsuma Dan
Francisco Villa #338
3-19-8
Kami-yoga
Setagaya-ku, 158 Tokyo
JAPAN

Dear Katie,

We take the occasion of your 90th Birthday to extend to you our deep appreciation for your long and close association with the Marine Biological Laboratory, which began more than 60 years ago when you and your colleagues first came to Woods Hole. A few years later, you joined our sister institution in Japan, the Misaki Marine Station, and thus you became the common bond between these centers of marine biology.

We, here at the MBL, are very much aware of the fact that your efforts in teaching and research here and at Misaki have had a profound effect, not only on biological science but also on the marine stations. You were the bond that drew them closer together in the common pursuit of basic research. This was accomplished despite an unfortunate war, when you prevailed upon the commanding officer of the U.S. Naval forces to save the Misaki Station for the students and their professors.

Your great and salutary influence on our two institutions will continue in the coming years because of the Jean and Katsuma Dan Fellowships that were established in your honor. The exchange of Japanese and American students to our institutions made possible by these Fellowships will continue to draw together not only our institutions, but also our two countries in this sharing of future scientists and scientific knowledge.

So we send our heartfelt thanks to you, Katie, for all the things you have done for us on the advent of your 90th birthday. We want you to know that we are forever grateful.

Yours sincerely,

John E. Burris
Director/CEO
Marine Biological Laboratory

Sheldon Segal
Chairman of the Board
Marine Biological Laboratory

MARINE BIOLOGICAL LABORATORY

WOODS HOLE MASSACHUSETTS 02543 (508) 548-3705

October, 1994

Professor Katsuma Dan
Francisca Villa #338
3-19-8
Kami-yoga
Setagaya-ku, 158 Tokyo
JAPAN

Dear Katie,

In ten short months, 50 years will have passed since your hand-written message prompted American forces to return the Misaki Lab to the biology students of Japan. Who but you could have imagined that your plea, brush-stroked on wrapping paper, would have led to such reasonable action by an occupation force?

After the War, you and Jean nursed me back to health in your Nagai home, and then sustained me with scholarship. It was the start of a new life for Kayo and Endo-san and myself when we finally all reassembled in your and Jean's second floor laboratory overlooking Abura-tsubo Bay.

After Jean successfully negotiated with the U.S. armed forces to return the land that had been taken from local farmers by the Japanese military, you brought her back into the lab. There, using the same phase contrast microscope that she had brought to you after her first trip back to the States, Jean subsequently discovered the acrosomal reaction. By then she had arranged a fellowship for me to do my graduate work at Princeton. That allowed me to visit Woods Hole and the MBL, where I met Dan Mazia, Don Costello, Suzie and Burr Steinbach, L. V. Heilbrunn, Doc Chambers, Marion Osterhout, and Jim Graham, all of whom I'd heard so much about from you and Jean.

I remember so much from our days together: Your first class at Musashi, for instance, where, perched on the lectern you surprised us by asking "Now, what shall we talk about today?" You challenged three rascals in our lab session (Tsuruta, Tamiya, and me) to "figure out how impulse is transmitted along Lillie's passivated iron wire model of nerve conduction." I remember as if it were yesterday the exciting discussion and experiments that we designed to distinguish between a chemical and electrical signal that propagated the wave of brown nitrous oxide along the wire. I remember, too, sneaking out to snip off some of the iron cable that wrapped around the old telephone pole in front of the school.

Then there was our first field trip to Misaki where you showed us a meter-long chain of *Salpa* floating in the Pacific at the edge of the Kuroshio; *Euplectella* hosting its shrimp at the floor of Abura-tsubo Bay; the *Comantus* that spawned in unison on cue from the moon and tide; the long train of hermaphroditic sea slugs crawling up the slippery docking ramp; and, of course, the many tide-pool creatures hiding beneath the rocks.

It was into one of these same tide pools that the Empress nearly slipped when she, the very young Crown Prince, and the Emperor were enjoying the new-found freedom during their first trip to Misaki after he was released from being worshipped as deity. For their visit you suggested that I demonstrate the twinkling birefringence of biocrystalline spicules in swimming sea urchin plutei. I assembled my first Shinya-scope, with string and wooden blocks onto a cast-off machine gun base, in preparation for that demonstration. The assembly held together well for the demonstration, and I understand that it also served Kayo and your own needs for a number of years after I had left for Princeton.

I remember well those years between Musashi and the end of the war. That evening at your house in Kudan when we tried, during an air-raid blackout, to repeat W. J. Schmidt's observation of spindle birefringence. Your being punished at Tokyo University for accepting me as your student. And my naiveté in not having the faintest idea that the space carved out for me among the big jars of pickled fish in the basement was the zoology department's revenge against you for daring to take on a graduate student.

As you say, those were challenging yet happy days for us. I wonder: if it hadn't been for the experience of having had to make do, of having—one way or another—to carve out our tools and ideas with our own hands and imagination, would I have been able to lead as full a life as I have? Do today's students suffer from having too much of a good thing?

Clearly, it wasn't just having to make do that helped my scientific career. In addition to friendship and encouragement, you and Jean showed me that seemingly insurmountable hurdles can indeed be overcome. Your example must have, if only subconsciously, provided me with an almost stubborn optimism. And now, just short of half a century later, I find myself working at the MBL as the senior resident scientist.

Today Sylvia and I send you our warmest greetings for your 90th birthday. We are always grateful for your generous warm friendship, and look forward to many more happy occasions that we can share together.

Most affectionately,
Shinya

DR. SHINYA INOUE
40 Shore Street
Falmouth, MA 02540
USA

References:

Dan, K. 1987. "Uni toh kataru." (Dialogue with sea urchin.) Gakkai Shuppan Center, Tokyo.
Inoué, Shinya. 1988. The Living Spindle. *Zoological Science* 5: 529–538.

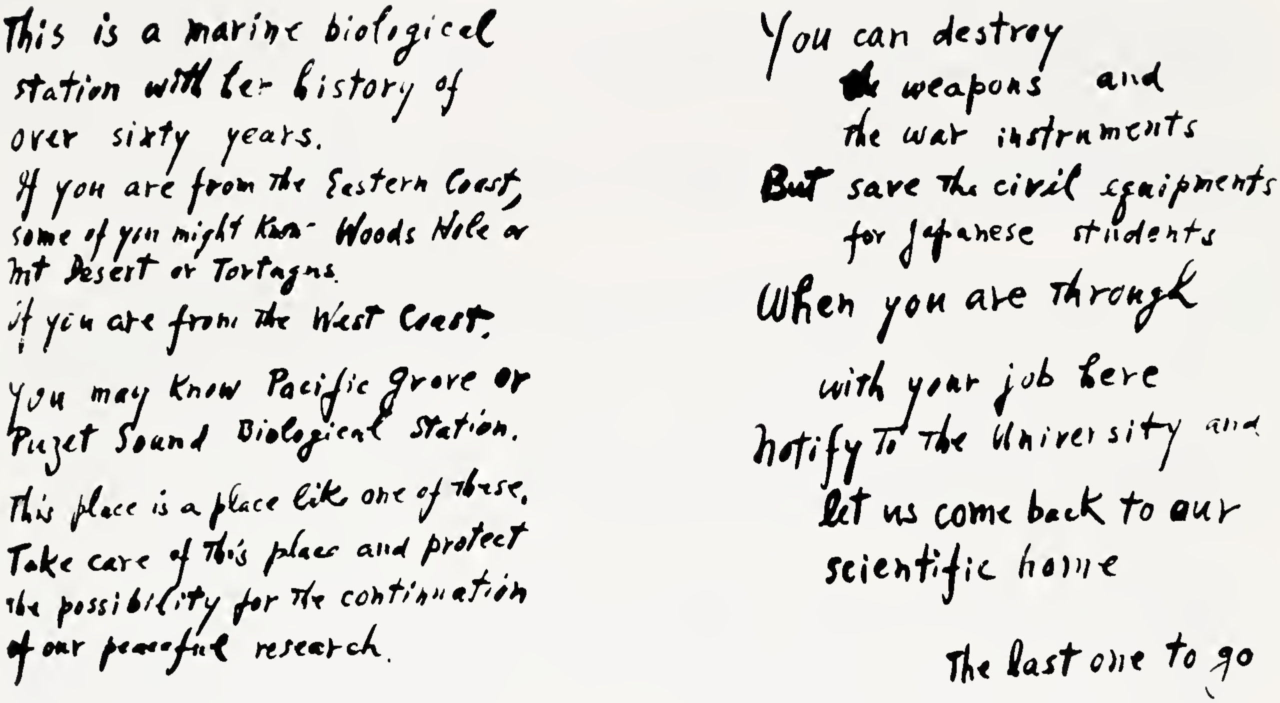

This is a marine biological
station with her history of
over sixty years.
If you are from the Eastern Coast,
some of you might know Woods Hole or
Mt Desert or Tortugas.
If you are from the West Coast,
you may know Pacific Grove or
Puget Sound Biological Station.
This place is a place like one of these.
Take care of this place and protect
the possibility for the continuation
of our peaceful research.

You can destroy
the weapons and
the war instruments
But save the civil equipments
for Japanese students
When you are through
with your job here
notify to the University and
let us come back to our
scientific home

The last one to go

THIS NOTICE WAS FOUND POSTED ON THE DOOR OF THE UNIVERSITY OF TOKYO MARINE BIOLOGICAL STATION LOCATED AT A MIDGET SUBMARINE BASE, MOROISO KO, JAPAN, ON SEPTEMBER 2, 1945, BY UNITS OF U. S. SUBMARINE SQUADRON TWENTY.

Jan. 16th, 1946

Dear Don:

Hello Don! No matter how many years I havn't written to you, still I have to start in the usual way. How are you? One day toward the end of last year, Lieutenant Coe dropped in, bringing your message. He came all the way from Tokyo in a jeep and must be quite tired, for he didn't stay long. But we gathered enough information about you and we were quite happy.

We got another friend here. Can you guss who it is? Edwin Helwig. But since he has been away from home for three years, the informations we can get through him are slightly stale. ....

In the last four years, we simply had lots of things. But ducking under bombs was not so bad. Rather it was a great excitement. Hide and seek at the expense of your life cann't help being exciting. There was, however, an awful side to it too.

During first three years of the war, our everyday life was not fundamentally affected and we could work regularly. Then, in January, a year ago from now, the Japanese navy took over the station and changed it to a temporary submarine base. As a result, the laboratory moved to a near-by village. Although, we succeeded in getting a wooden building built, we had a hard time to install sea-water pumps and so forth. When the war was over, the American troops occupied the station, for the reason that the Japanese navy had been there. When American officers came there for the first time to take over the place, I went there. It was a funny experience. On one side of a long table, three American officers were sitting and on the opposite side two Japanese navy officers and I were sitting. They served beer and canned asparagus with tomato ketchup. This slightly cute menu made me smile. But, oh boy, the both sides were pretty much excited. I am sure they were really scared of each other. They yelled whatever they wanted to say at the top of their voice but never listened to the other side. And an interpreter translated off and on, paying no attention whether it made sense or not. I was partly absorbed in watching the chaos and partly in the asparagus and was still partly absorbing the beer. Neither side understood the other. But to start with neither side knew what they were going to say. Toward the end, I was loudly laughing which nobody noticed. Somehow the meeting came to end. So I started to work. I stuck to a major and explained to him that this building originally belonged to the University etc., etc. In ten minutes, he began to see the situation. As soon as I saw the sign of dawning in his chaotic mind, I ran back to the building, wrote a psoter asking soldiers to take good care of the place because it is a research institute, pasted it on the wall and took leave from the back door leaving the noisy bunch there. There was no way to know what influence the poster excerted on the American soldiers who came there. But to my greatest surprise, in a copy of over-sea edition of Time issued in the beginning of December, I came across my own words all printed. Moreover, it had a title "Appeal to Gothe".

....

From Katsuma

Katsuma Dan and the Quiet Revolution[1]

His many friends and admirers throughout the world may, at first thought, find my characterization of Katsuma Dan as a revolutionary more than a little disquieting. Yet, in truth, he, along with a small band of like-minded innovators, fomented a profound change in our thinking about the mechanisms of development.

Today students of development everywhere focus their attention on surface interactions of cells, on the nature of signals, of cell receptors, of the role of ions, and of contractile proteins in differentiation and morphogenesis. However, our ability, indeed our willingness, to explore developmental mechanisms in this perspective have emerged slowly over several decades in contrast to the almost cataclysmic effects on developmental biology of the "quest for the organizer". It has been a quiet revolution.

It may be less apparent to younger readers, reared in the second messenger era, than to an older generation brought up to believe that cell-cell interactions require the exchange of "information" contained in large molecules, putatively nucleic acids, but Dan's career is a paradigm of independent thought—nourished by strong convictions, sustained by an accomplished wife and brought to fruition by his technical ingenuity.

Armed with his doctorate from the University of Pennsylvania in 1934, Dan returned to the Misaki Marine Station where he and his colleagues forged new trails in studies of the mechanisms of cell division and morphogenesis. His investigations of the mitotic apparatus, SH-protein fractions of the cytoplasm, and on the origin of form in the sea urchin embryo and larva, which span several decades, are all the more remarkable because they were accomplished first in the face of the gathering storm of World War II and later against the tide of the extraordinary advances generated by the one gene–one enzyme hypothesis, leading on the one hand to the emergence of molecular genetics and nucleic acid chemistry as focal fields of research, and, on the other, to diminishing opportunities for studying the behavior of cells and groups of cells. Happily, revolutionary discoveries neither die nor fade away. Today Dan's prescient contributions are fresh and meaningful.

How does one capture the essence of this incomparable scientist? One can speak of his courage and his indomitable spirit, of his leadership and capacity for persuasion, of his continuing impact on the world community of scholars. These attributes are important yet they scarcely begin to describe the rich tapestry that is Katsuma Dan. How does one describe a virtuoso: a Toscanini, a Titian, a Kawabata, a Dan? On an earlier occasion I quoted the words of Lao Tzu. They are especially appropriate here:

> "See simplicity in the complicated.
> Achieve greatness in small things"

Dan's accomplishments stem from a deep simplicity: it appears at times that he is able to talk with cells. Like other masters before him, Dan understands full well that cells do not yield their secrets unless they are asked the right questions.

Dan and I taught together in the Embryology Course at the Marine Biological Laboratory in the summer of 1962. He is a gifted teacher, luminous and intense, providing the vital ingredients in that long and delicate process by which the young mind attains the ability to make informed choices between alternatives. Teaching at the MBL is characterized by the most intimate interactions of teacher and student. In that setting Dan was a master, teaching by example, thereby emphasizing the importance of exercising critical judgment and the character to choose scientific tasks not for their ease but for their importance.

Dan bears his mastery with modesty. A quotation ascribed to Goethe possibly best captures his spirit: "Ultimately the reason I prefer to associate harmoniously with Nature is that she is always right and error can be only on my side".

James D. Ebert
Baltimore and Woods Hole
October 22, 1975

---

[1] Reprinted by permission of the author and *Development Growth & Differentiation*. Vol. **18**: i–ii.

Reference: *Biol. Bull.* **187**: 133–142. (October, 1994)

A Metamorphic Inducer in the Opisthobranch *Haminaea callidegenita:* Partial Purification and Biological Activity

GLENYS D. GIBSON[1] AND FU-SHIANG CHIA[2]

Zoology Department, University of Alberta, Edmonton, Alberta, Canada T6G 2E9

Abstract. Larvae of *Haminaea callidegenita* (Mollusca: Cephalaspidea) were induced to metamorphose by a compound found in the gelatinous matrix composing most of the egg mass. A functionally similar compound isolated from adult tissue also induced metamorphosis in *H. callidegenita* larvae. Opisthobranchs are frequently induced to metamorphose by a specific prey item or a substrate characteristic of the adult habitat, but this is the first known instance of metamorphosis occurring in response to a compound produced by adult conspecifics. The inducer was purified from egg mass jelly (EMJ) by high pressure liquid chromatography (HPLC) and was found to be smaller than 1000 Da, polar, non-proteinaceous, and very stable. We isolated a compound of identical activity from egg masses produced by four other opisthobranch species, suggesting that the same or chemically similar compounds are intrinsic to opisthobranch egg masses. However, only *H. callidegenita* larvae metamorphosed in response to EMJ. Competent larvae of five other mollusc species did not respond to the partially purified EMJ inducer but did respond to a specific substrate associated with each species. The presence of the inducer within the egg mass causes an unusual developmental pattern in *H. callidegenita,* a poecilogonous species that produces both swimming veliger and crawling juvenile offspring.

Introduction

Larvae of most benthic marine invertebrate species are induced to metamorphose by a cue, either chemical or physical, that identifies a specific habitat as suitable for juvenile or adult existence (reviewed by Pawlik, 1992). This cue, or metamorphic inducer, triggers a radical transformation of the morphology, physiology, ecology, and behavior of the larva to the juvenile stage. Chemical inducers are water-borne or tactile, and originate from conspecifics, prey species, or a characteristic micro- or macrobiotic substrate (bacterial film or an algal, invertebrate, or vertebrate species; see Pawlik, 1992). For example, most progress in the isolation of metamorphic inducers in opisthobranchs has involved two nudibranchs, both of which are induced to metamorphose by a highly specific adult prey species. Larvae of *Phestilla sibogae* metamorphose in response to a small, water-soluble molecule derived from the coral *Porites* (Hadfield, 1977; Hadfield and Scheuer, 1985), and those of *Eubranchus doriae* respond to a small, polar compound with glucosidic residues originating from the hydroid *Kirchenpaueria* (Bahamondes-Rojas, 1988; Bahamondes-Rojas and Dherbomez, 1990). Despite many attempts to purify metamorphic inducers in marine invertebrates in general, such inducers have been identified for only a few species and include a variety of chemical groups (see review by Pawlik, 1992; also Kitamura *et al.*, 1993).

The opisthobranch *Haminaea callidegenita* (*Haminaea* = *Haminoea* [*cf.* Giannuzzi-Savelli and Gentry, 1990]) is induced to metamorphose by a compound found in the gelatinous layers composing most of the egg mass (Gibson and Chia, 1989a). An unusual life history results in which half the siblings per egg mass metamorphose in response to egg mass jelly (EMJ; the metamorphic inducer) to hatch as crawling juveniles. The other half hatch as swimming veligers and, during a two-week planktonic period, gradually become competent to metamorphose in response to EMJ as well as to other substrates indicative of a juvenile

Received 31 May 1994; accepted 4 August 1994.

[1] Present Address: Scripps Institution of Oceanography, Marine Life Research Group, 9500 Gilman Drive, La Jolla, CA 92093-0218.

[2] Present Address: Hong Kong Institute of Science and Technology, Clear Water Bay, Kowloon, Hong Kong.

food source (Gibson, 1993). Only EMJ induces intracapsular metamorphosis; veligers do not become sensitive to the other substrates until after hatching (Gibson and Chia, 1989a). The ecological consequence of this developmental pattern is that each parent simultaneously produces both dispersive (lecithotrophic veliger) and nondispersive (juvenile) offspring. Hatchling type depends on the presence of EMJ before hatching and the time at which metamorphic competence occurs (before or after hatching).

In this paper, we characterize the metamorphic inducer found in EMJ and describe purification techniques. The inducer was smaller than 1000 Da in molecular weight, polar, and stable to temperature and acid. We also describe the ecological distribution of the EMJ inducer that influences its activity. A functionally similar compound was extracted from adult *H. callidegenita* tissue as well as from the egg masses of other opisthobranch species. Metamorphic inducing activity of EMJ was specific to *H. callidegenita* larvae. We have focused on intracapsular metamorphosis only, because this is the basis for poecilogony in this species; substrates that induce metamorphosis after hatching are described elsewhere (Gibson, 1993).

Materials and Methods

Culture and bioassay procedures

Haminaea callidegenita were collected at Padilla Bay or Spencer Spit and maintained after collection at the University of Washington, Friday Harbor Laboratories, all in Washington State. Egg masses used in these assays were collected either in the field or within 24 h of natural spawning by animals maintained in the laboratory. Culture techniques for adults are described elsewhere (Gibson, 1993). Gastrulae were separated from the sausage-shaped egg mass by removing the jelly layers composing most of the mass because this jelly is known to induce metamorphosis within the egg mass (Gibson and Chia, 1989a). EMJ was removed from developing embryos with fine forceps, then the embryos were rinsed in 1-μm filtered seawater (fSW). Embryos were still contained by an embryonic capsule. Unlike the egg masses of other opisthobranchs, *H. callidegenita* egg masses fall apart easily and all traces of EMJ can be removed. Embryos were cultured in 100 ml of fSW at 17°C, and cultures were cleaned twice weekly. Hatching, defined as the escape of larvae or juveniles from the capsule, began about 14 days after spawning. In intact egg masses, hatchlings must also crawl through the jelly matrix; thus hatching takes slightly longer in intact masses (4–5 days; Gibson, 1993) than in separated capsules (maximum of 2–3 days).

About 10 days after oviposition, encapsulated larvae were placed in cultures containing potential metamorphic inducers. Cultures were maintained in tissue culture plates (Falcon Wells) containing 1 to 2 ml of fSW and a single inducer (defined below) at 17°C. About 15 to 20 larvae were placed in each well, depending on the size of the egg mass used and the number of wells required for the assay. At 24-h intervals, new hatchlings were counted and removed under a Wild M-5 microscope. Hatchlings were removed daily so that estimates would not include post-hatching metamorphosis (either spontaneous or in response to the tested inducer), which begins within 3 days of hatching (Gibson, 1993). Hatchlings were immediately scored as veligers or juveniles. Veligers were identified by the presence of an intact, ciliated velum and were either swimming or, less frequently, crawling. Individuals identified as metamorphosed juveniles had lost the velar cilia and the velar lobes had been resorbed (in many cephalaspideans, the shell is retained through the adult stage). Additional morphological changes (shell growth, elongation of the foot, acquisition of feeding structures and onset of feeding) occur within 2–3 days after hatching (Gibson and Chia, 1989a). The percentage of juveniles hatching in each well was determined for each day of the hatching period and is generally presented as a cumulative percent for each clutch by the end of the hatching period. Data are presented as the mean (± standard error) percentage of intracapsular metamorphosis occurring per treatment; data were arcsin transformed before further statistical analysis. Sample size refers to the number of egg masses (= number of clutches) used. Subgroups of larvae from each mass were simultaneously tested for each treatment per assay to allow an inter-clutch comparison of metamorphic rates. This comparison was necessary because larvae from different clutches are known to show variable rates of intracapsular metamorphosis (ranging from 4–100% in intact egg masses) arising from a genetically determined time of metamorphic competence (Gibson, 1993).

All assays contained two standard controls: (1) separated embryos cultured in fSW to determine the percentage of siblings per clutch undergoing spontaneous metamorphosis in absence of inducer; and (2) embryos cultured with untreated EMJ (about 1 mm^3 per well) to determine the proportion of embryos per mass competent to metamorphose during the assay period. Antibiotics were added to culture water to prevent degradation of EMJ or jelly extract (40 mg/l each of streptomycin sulfate and penicillin G).

Characterization and purification of the metamorphic inducer in egg mass jelly

EMJ was collected, drained of seawater, and stored frozen at either −9 or −60°C. About 1 mm^3 of untreated or experimentally treated EMJ (wet volume) was added to the indicated assay. In all cases, EMJ was thawed and thoroughly rinsed, first in distilled water and then in fSW, to remove any residual contaminants of each treatment.

The general stability of the metamorphic inducer in EMJ was determined by boiling (100°C, 20 min) or by lyophilizing (−46°C, 24 h) manually homogenized EMJ. Stability of inducer in the presence of acid was determined by acidifying an aqueous EMJ homogenate with acetic acid (0.1 *M*, 2 h). EMJ was also treated with one of two nonspecific proteases to determine if the inducer was proteinaceous. Proteinase K (final concentration 0.1 mg/ml) was added to 5 ml EMJ for 90 min at 18–20°C. Protease XIV from *Streptomyces griseus* (Sigma P-5147; final concentration 1 mg/ml) was added to 20 ml EMJ in 20 ml fSW at 17–20°C for 12 h, with continual mixing.

The molecular weight of the inducer was estimated with Amicon diaflo ultrafilters. We used a methanol (MeOH) EMJ extract, rather than EMJ pieces, in this bioassay to prevent clogging of the ultrafilters with the large mucoproteins composing much of the gelatinous matrix. Lyophilized EMJ (15 ml wet volume) was twice extracted (1 h each) with 25 ml MeOH. The combined extract was centrifuged (3000 rpm, 5 min.), the supernatant lyophilized, resuspended in distilled water, then filtered through both 5000 Da (Amicon YM5) and 1000 Da (Amicon YM2) ultrafilters (flow rates of 1 ml/2.5 min.). All solutions were lyophilized and resuspended in 30 ml fSW. Bioactivity was tested at several stages: (1) MeOH residue resuspended in distilled water before centrifugation; (2) distilled water suspension before filtration; (3) filtrates; and (4) residue from both YM5 and YM2 filters.

The inducer was isolated from EMJ by sequentially extracting the jelly with organic solvents of increasing polarity (20 ml each), including hexane, diethyl ether, 1:1 diethyl ether: methanol, methanol, and distilled water (Pawlik, 1986). Solvent was added to lyophilized EMJ (10 ml wet volume) and sonicated for 1 min, followed by extraction for 1 h with continual gentle agitation. Solvents were filtered, dried, resuspended in fSW, and added to each Falcon well (2-ml aliquots). Individual solvents were also tested (in absence of EMJ) for potential effects by evaporating an equivalent volume of solvent and resuspending any possible residue in fSW (*cf.* Pennington and Hadfield, 1989).

The metamorphic inducer was partitioned from the active fraction (MeOH extract) with HPLC (Spectra-Physics) using two buffer systems (gradient and isocratic). Bioactivity was determined for both crude MeOH extract (50 μl resuspended in 2 ml fSW) and HPLC fractions pooled over 2-min intervals (corresponding to 50 μl crude extract/2 ml fSW). Lyophilized EMJ was extracted with hexane to remove nonpolar compounds; eluant was discarded and EMJ dried. Residual EMJ was extracted with absolute MeOH as described above. The centrifuged MeOH extract was injected (100 μl) onto an Alltech RPC18 column (25 cm × 4.6 mm, 10 μm particle size) and partitioned on a buffer gradient from 100% methanol to 100% water over 30 min. Fractions were collected at 1-min intervals. All fractions were tested for inductive activity regardless of the presence of a visible peak (UV-vis detector set at 254 nm). Solvent was evaporated, the residue was resuspended in fSW, and the resuspension was added to Falcon wells and assayed as outlined above. Two fractions were found to contain activity (min 9–10, 17–18). To determine if both peaks represent the same or similar compounds, fractions containing the first peak of activity (min 9–10) were collected for three runs (300 μl original crude extract), concentrated in absolute MeOH, and repartitioned at the same gradient conditions. Fractions were collected and assayed as described above. In the final step of the purification procedure, the two active peaks (min 9–10, 17–18) were collected for three runs (300 μl crude extract), pooled, dissolved in MeOH, and subsequently reinjected through the same column under isocratic buffer conditions (absolute MeOH). Fractions were collected at intervals corresponding to visible peaks (at 254 nm) on the chromatograph, and both peaks and inter-peak intervals were assayed as outlined above.

Biological distribution of the metamorphic inducer

We examined specific tissues of adult *Haminaea callidegenita* for inductive activity. Tissues investigated were parapodial lobes, anterior and posterior mucous glands of the female reproductive system, gametolytic sac, and digestive gland. Tissue samples from three adults were combined, then extracted with MeOH and assayed as outlined above.

EMJ of four additional opisthobranch species was tested for ability to induce metamorphosis in *H. callidegenita* veligers. EMJ assayed for inductive potential came from the following opisthobranchs: *H. callidegenita; H. vesicula*, a sympatric congener that is morphologically and ecologically similar; *Melanochlamys diomedea*, a cephalaspidean found in the same habitat; *Alderia modesta*, an ascoglossan found in association with the zanthophyte *Vaucheria* sp. located in the high intertidal zone of the same bays as *H. callidegenita;* and *Onchidoris bilamellata*, a nudibranch found in rocky intertidal zones in association with barnacles. We tested both pieces of EMJ as well as a MeOH jelly extract for inductive potential on *H. callidegenita* larvae. Egg masses of the first three species were collected from False Bay and *Onchidoris* egg masses were collected at Friday Harbor Laboratories, both on San Juan Island, Washington State.

The metamorphic inducer found in *H. callidegenita* EMJ was tested on five other species of mollusc: the four opisthobranchs mentioned above (*H. vesicula, Melanochlamys diomedea, Alderia modesta, Onchidoris bilamellata*) and the oyster *Crassostrea gigas*. Planktotrophic veligers of all five species were cultured as by Kempf and

Willows (1977), except that antibiotics were not used and larvae were supplied with a 1:1:1 mixture of *Isochrysis galbana*, *Pavlova lutheri*, and *Rhodomonas* sp. as food. Larvae were identified as metamorphically competent when the propodium was well developed and the mantle was retracted from the shell (Bickell, 1978). These larvae were placed in 100-ml jars (*n* = 10 larvae/jar) containing fSW and one of the following substrates: EMJ (pieces of jelly or a MeOH extract); a metamorphosis-inducing substrate associated with that species; or 19 mmol K^+ in fSW. The latter two treatments were used to ensure that tested veligers were metamorphically competent. Metamorphosis-inducing substrates included diatoms and adult mucus for *H. vesicula* (Gibson and Chia, 1989b), sand containing nematodes for *Melanochlamys* (Gibson, pers. obs.), the alga *Vaucheria* for *Alderia* (Seeleman, 1933), the barnacle *Chthamalus dalli* for *Onchidoris* (Chia and Koss, 1988), and adult shell for *Crassostrea* (Crisp, 1967). All substrates were freshly collected from the adult habitat of each species. Competence was also determined using seawater containing excess potassium (19 mmol K^+), which is known to induce metamorphosis in several phyla of marine invertebrate (Yool *et al.*, 1986; Todd *et al.*, 1991). Percent metamorphosis was determined after 48 h.

EMJ from masses containing embryos of different developmental stages was assayed for inductive activity to test for effects of egg mass age. EMJ was separated and pooled from five egg masses at each of the following stages: gastrula; early veliger (showing cephalopedal rudiment); mid-veliger (statocysts visible, growth of larval shell complete); late veliger (eyes and heart well developed); and posthatch (all hatching was completed). EMJ was assayed as described above. Data were analyzed with a one-way ANOVA using the Scheffé procedure for unplanned comparisons among treatments (Day and Quinn, 1989).

Results

Characterization and isolation of the metamorphic inducer from egg mass jelly

Haminaea callidegenita larvae were induced to metamorphose within the embryonic capsule by egg mass jelly. Embryos cultured in the presence of EMJ metamorphosed within the embryonic capsule (X ± SE 52.68 ± 4.49% juveniles were released at hatching, *n* = 24 cultures) at rates expected of intact egg masses (61.32 ± 1.41% juveniles, *n* = 288 egg masses). Most embryos cultured in the absence of EMJ hatched as swimming veligers (2.12 ± 1.22% juveniles, *n* = 24 cultures of 15–20 larvae each). In assays involving pieces of EMJ, jelly was in the culture water but not necessarily in contact with developing embryos, indicating that the inducer is a water-soluble compound.

Inducer activity of EMJ was not destroyed by boiling (49% intracapsular metamorphosis was induced; Table I), lyophilizing (56%), or acidifying (46%) the jelly. Rates of intracapsular metamorphosis in these treatments were similar to rates observed in larvae cultured with untreated EMJ in the same experiment (67% intracapsular metamorphosis occurred; Table I). The metamorphic inducer passed through ultrafilters of both 5000 (46% metamorphosis) and 1000 molecular weight cutoff (36%; Table II), indicating that the inducer is less than 1000 Da in molecular weight. Activity was somewhat lower in treatments containing ultrafiltrate than in those with untreated EMJ (71%), but activity appeared to have been lost during extraction before filtration took place (the resuspended extract induced only 31% metamorphosis; Table II). Inductive potential was also unaffected by the action of two general proteases. EMJ treated with proteinase K induced 45% intracapsular metamorphosis, and 43% occurred in response to untreated EMJ (in absence of proteinase; Table III). Results were similar when EMJ was treated with pronase XIV, with 53% metamorphosis occurring in response to pronase-treated EMJ and 54% occurring in response to untreated EMJ (Table III).

The only organic solvent to extract significant amounts of inducer from EMJ was methanol (46% intracapsular metamorphosis; Table IV). Some inducer was retained by the EMJ, as evidenced by subsequent extraction of inducer with distilled water and the small amount of activity remaining in the EMJ after extraction (Table IV). The MeOH extract showed peak absorbance at 254 and a smaller peak at 303 nm, as well as a peak corresponding to the absorbance maximum for pure MeOH at 205 nm. Metamorphosis was not induced by potential residues left after evaporation of any of the organic solvents used in these extractions (Table IV). Spontaneous metamorphosis (in seawater only, and in absence of known cue) occurred in 2% of veligers tested, whereas 68% intracapsular meta-

Table I

Characteristics of the metamorphic inducer found in Haminaea callidegenita *egg mass jelly*

Treatment	*n*	% Metamorphosis
Seawater	11	5.36 ± 6.50
EMJ	11	67.36 ± 6.39
EMJ (100°C)	9	49.11 ± 8.29
EMJ (Lyophilized)	11	56.55 ± 4.36
EMJ (+ 0.1M H^+)	8	46.75 ± 8.74

Data are the mean (± standard error) percentage of intracapsular metamorphosis that occurred in response to EMJ or EMJ treated as indicated. Data from two controls are also listed, including rates of metamorphosis occurring in seawater (spontaneous metamorphosis) and rates of metamorphosis in response to untreated EMJ. *n* = number of egg masses tested.

Table II

Molecular weight estimates for the metamorphic inducer found in Haminaea callidegenita *egg mass jelly*

Treatment	*n*	% Metamorphosis
Seawater	6	6.95 ± 3.27
EMJ	6	71.34 ± 1.85
Resuspended extract	6	31.02 ± 5.87
<5000 Da Filtrate	6	46.53 ± 7.97
<1000 Da Filtrate	6	36.45 ± 6.12

Data are the mean (± standard error) percentage of intracapsular metamorphosis that occurred in response to EMJ extract and extract filtrates, as indicated. Data from two controls are also listed and include rates of metamorphosis occurring in seawater and in response to untreated EMJ. *n* = number of egg masses tested.

morphosis occurred in response to untreated EMJ (Table IV).

The inducer was partitioned from an EMJ extract in methanol with HPLC over a gradient from absolute MeOH to absolute water. The inducer eluted at 9–10 min (at a buffer concentration of about 70% MeOH) and at 17–18 min (about 40% MeOH) after injection (Fig. 1A), with some spreading of activity around the first active peak. Fraction 9–10 induced slightly less intracapsular metamorphosis (60%) than did EMJ (70%) or the crude MeOH extract (93%). Fraction 17–18 induced metamorphosis at a much lower rate (32%; Fig. 1A). Rates of intracapsular metamorphosis in cultures containing most other HPLC fractions were similar to rates in embryos cultured in seawater only. Fraction 9–10 was collected and pooled over three runs, then re-eluted under the same conditions to determine if the inducer would separate into two fractions. Again, the inducer eluted at two intervals, the first appearing 7–8 min after injection (59.19 ± 3.04% intracapsular metamorphosis) and the second at 15–18 min (27.48 ± 4.23%). This suggests that the inducer either racemizes under polar conditions or degrades during the elution procedure. Degradation of the inducer is less likely because the crude extract retains high levels of activity for at least several weeks (9°C).

The combined active fractions (min 9–10, 17–18) were re-eluted under isocratic buffer conditions (absolute MeOH). This resulted in a single peak of inducer eluting 8 min after injection (peak E in Fig. 1B), as well as the partitioning of several contaminants. Peak E was accumulated over several runs and the solvent was evaporated. A very small amount of dry residue remained as a fine, white powder that reacted strongly with vanillin, indicating the presence of steroids, phenols, or fatty acids as functional groups; alternatively, the strength of the vanillin reaction may indicate the presence of a residual contaminant, such as a polar lipid that may be derived from the presence of eggs in the original egg mass extract. The inducer residue also had a slight reaction with ninhydrin, indicative of the presence of primary amines. To detect possible contaminants, the pure fraction was re-eluted with HPLC and each fraction scanned with a refractive-index detector to reveal the presence of all compounds, regardless of specific ultraviolet or visual absorbance. The result was a single sharp peak, suggesting that this fraction represents pure inducer, although the presence of a contaminant eluting precisely with the inducer can not be eliminated.

Biological distribution

A metamorphic inducer was present in methanol extracts of several adult tissues, with most activity occurring in extracts of the posterior mucous gland of the female reproductive tract (61% intracapsular metamorphosis occurred), digestive gland (49%), and parapodial lobes (56%; Fig. 2). All three extracts induced intracapsular metamorphosis at rates comparable to that induced by untreated EMJ (48%). Less activity was evident in extracts of the anterior mucous gland of the female reproductive tract. Extracts of the gametolytic sac showed no activity (Fig. 2).

EMJ produced by other opisthobranch species also induced high rates of intracapsular metamorphosis in

Table III

The effects of two general proteases on the metamorphic inducer found in Haminaea callidegenita *egg mass jelly*

Proteinase K			Pronase XIV		
Treatment	*n*	% Metamorphosis	Treatment	*n*	% Metamorphosis
Seawater	8	7.6 ± 1.65	Seawater	12	6.79 ± 2.93
Untreated EMJ	8	43.75 ± 3.78	Untreated EMJ	12	54.56 ± 5.13
Proteinase treated EMJ	8	45.13 ± 8.19	Pronase treated EMJ	12	53.47 ± 6.21

Data are the mean (± standard error) percentage of intracapsular metamorphosis that occurred in response to EMJ or EMJ incubated with protease. Data from two controls are also listed, including rates of metamorphosis occurring in seawater (spontaneous metamorphosis) and rates of metamorphosis in response to untreated EMJ. *n* = number of egg masses tested.

Table IV

Extraction of the metamorphic inducer found in Haminaea callidegenita *egg mass jelly using sequential solvents of increasing polarity*

A. EXTRACTS			B. SOLVENT ONLY		
Treatment	*n*	% Metamorphosis	Treatment	*n*	% Metamorphosis
Seawater	12	2.27 ± 3.4	—	—	—
EMJ	10	68.00 ± 4.74	—	—	—
EMJ Extracts:					
Hexane	9	7.07 ± 2.71	Hexane	4	0.88 ± 0.62
Ether	6	1.43 ± 1.12	Ether	4	2.90 ± 1.05
Ether:MeOH 1:1	6	3.47 ± 1.76	Ether: MeOH 1:1	4	3.24 ± 1.22
MeOH	6	46.00 ± 5.62	MeOH	4	3.93 ± 1.42
Water	6	12.70 ± 3.88	Water	4	1.93 ± 1.69
Extracted EMJ	6	16.6 ± 6.12	—	—	—

Data are the mean (± standard error) percentage of intracapsular metamorphosis that occurred in response to EMJ or EMJ extract (column A), or residue of evaporated solvent (column B). Data from two controls are also listed: rates of metamorphosis occurring in seawater (spontaneous metamorphosis), and rates of metamorphosis in response to untreated EMJ. *n* = number of egg masses tested.

Haminaea callidegenita veligers (solid bars; Fig. 3). A similar response was observed in *H. callidegenita* veligers treated with a methanol extract of EMJ produced by these species (hatched bars; Fig. 3), suggesting that the inducer present in the jelly of other species is chemically similar to that produced by *H. callidegenita* (*i.e.,* also a small, polar compound). However, EMJ did not induce metamorphosis in any of the other four opisthobranch species tested (*H. vesicula*, *Melanochlamys*, *Alderia*, and *Onchidoris*; Fig. 4). Larvae of these four species were competent to metamorphose, as indicated by their response to excess K^+ in seawater as well as to species-specific metamorphic inducers (Fig. 4; substrates described in the Methods). Although veligers of the oyster *Crassostrea gigas* did metamorphose in response to EMJ pieces, they did not respond to a MeOH extract of EMJ (Fig. 4). Oyster larvae are known to metamorphose in response to microbial film (Coon *et al.*, 1985); thus these larvae were probably responding to bacteria associated with the jelly rather than to the specific inducer known to affect *H. callidegenita* veligers.

There were no significant differences in inductive activity of EMJ of different ages (Fig. 5), indicating that activity of the metamorphic inducer found in EMJ was not influenced by the age of the jelly (one-way ANOVA, $p \gg 0.05$).

Discussion

Opisthobranchs are often considered to have highly specific metamorphic cues that are derived from specific prey species or characteristics of post-metamorphic habitats. This generalization originates from widespread laboratory observations of metamorphosis but is based on only a few orders of opisthobranchs (especially nudibranchs, but also some anaspideans and ascoglossans), and exceptions have been noted within each order (in nudibranchs—Hubbard, 1988; in anaspideans—Pawlik, 1989). Metamorphic cues for larvae belonging to other opisthobranch orders are not as well understood and in cephalaspideans are known for three species only: *Haminoea solitaria* (Harrigan and Alkon, 1978) and *H. vesicula* (Gibson and Chia, 1989b), both known to settle on microbial film; and *H. callidegenita*, which has a highly specific inducer before hatching (EMJ). After hatching, *H. callidegenita* gradually becomes sensitive to a variety of additional substrates associated with small juveniles in the field and probably indicative of a juvenile food source (including the seagrass *Zostera marina*, the filamentous green alga *Chaetomorpha linum*, and sea lettuce, *Ulva* sp.). *H. callidegenita* veligers will also metamorphose in response to EMJ after hatching as they become competent (Gibson, 1993); therefore, this inducer acts both intracapsularly and on dispersive larvae.

Within the egg mass, approximately 60% of the *H. callidegenita* embryos respond to the EMJ inducer and hatch as juveniles. The remainder are released as swimming veligers and do not become competent to metamorphose until after hatching (range is 1–14 days posthatching; Gibson, 1993), although all veligers from a clutch eventually metamorphose successfully. The ecological result of this hatching pattern is poecilogonous development (variable development within one species) whereby every parent produces two types of offspring: swimming, lecithotrophic veligers with a higher potential for dispersal, and crawling juveniles that may recruit directly into the parental population. The percentage of metamorphosis that occurs within the egg mass is genetically determined, and 100% intracapsular metamorphosis occurs in rare cases only (<3% in more than 800 egg masses examined; Gibson, 1993).

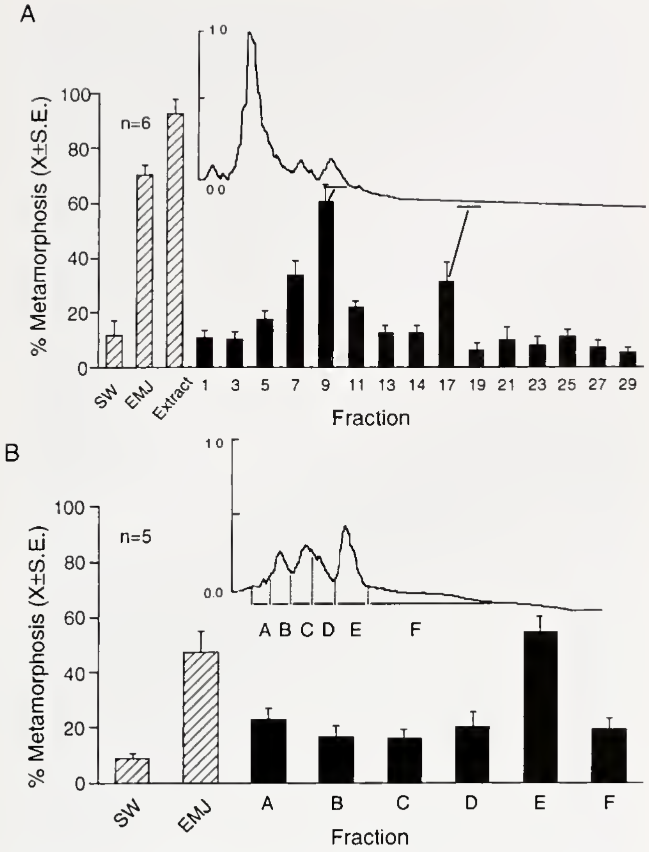

Figure 1. Isolation of metamorphic inducer with high performance liquid chromatography (HPLC). Data are the results of partitioning the inducer from a crude methanol extract with a buffer gradient from absolute methanol to absolute water (A) and partitioning the partially purified active fractions from A with an isocratic buffer system (absolute methanol) (B). In both A and B, the chromatograph indicates absorbance of each fraction as eluted from an RP-C18 column, detected at 254 nm, and the histogram gives results of the bioassay used to test the inductive potential of each fraction. In A, bioassay results are the percentage (mean ± standard error) of *Haminaea callidegenita* veligers that underwent intracapsular metamorphosis in response to seawater (SW), with untreated inducer (EMJ), with a crude EMJ extract (all in hatched bars), as well as with the indicated HPLC fractions (solid bars) pooled over 2-min intervals throughout a 30-min elution period. Peaks of activity are cross-referenced to the chromatograph. In B, results include the percentage of intracapsular metamorphosis occurring in response to standard controls (hatched bars) as well as in response to the fractions indicated in the chromatograph (solid bars). *n* = number of egg masses assayed.

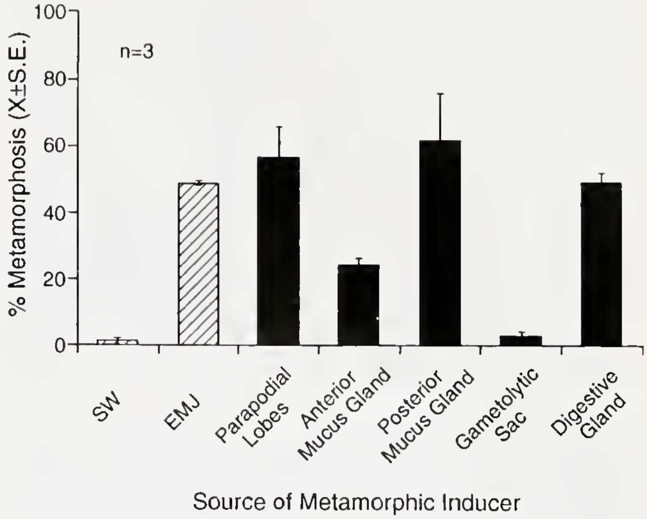

Figure 2. Activity of adult tissue as a metamorphic inducer. Data are the percentage of *Haminaea callidegenita* veligers that underwent intracapsular metamorphosis (mean ± standard error) in response to seawater (SW), untreated egg mass jelly (EMJ; both in hatched bars) as well as to a methanol extract of the indicated adult tissues (solid bars). *n* = number of egg masses assayed.

Isolation of the metamorphic inducer has been extensively studied in two species of opisthobranch, but in both cases the inducer has yet to be identified. Veligers of the nudibranch *Phestilla sibogae* are induced to metamorphose by a water-borne compound that is released from its prey, the hard coral *Porites* (Hadfield, 1977). This compound is small (200–500 Da) and stable to temperature and pH (Hadfield and Scheuer, 1985). The nudibranch *Eubranchus doriae* also metamorphoses in response to its prey species, the hydroid *Kirchenpaueria pinnata* (Bahamondes-Rojas, 1988). In this case, the inducer is water soluble and contains galactosidic residues. Metamorphosis of *E. doriae* is also induced by *cis*-isomers of various sugars (Bahamondes-Rojas and Dherbomez, 1990). The EMJ inducer that was active on *Haminaea*

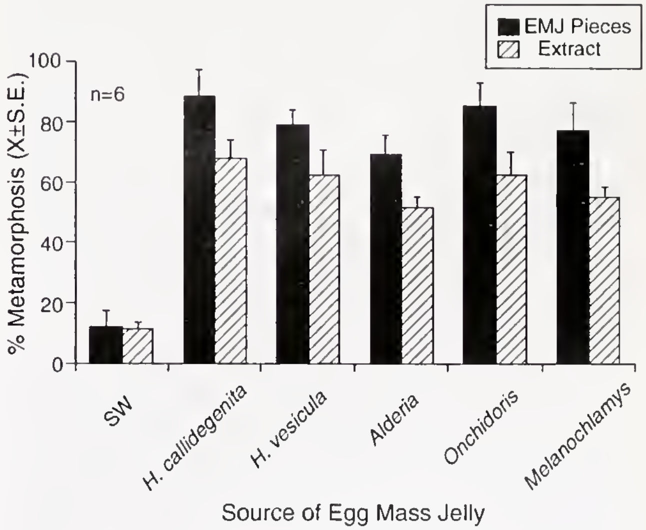

Figure 3. Metamorphic inducing activity of egg mass jelly (EMJ) produced by other opisthobranch species. Data are the percentage (mean ± standard error) of *Haminaea callidegenita* veligers undergoing intracapsular metamorphosis in response to seawater (SW), to EMJ pieces (solid bars), or to a methanol EMJ extract (hatched bars). Source of EMJ is indicated on the horizontal axis. *n* = number of *H. callidegenita* egg masses assayed.

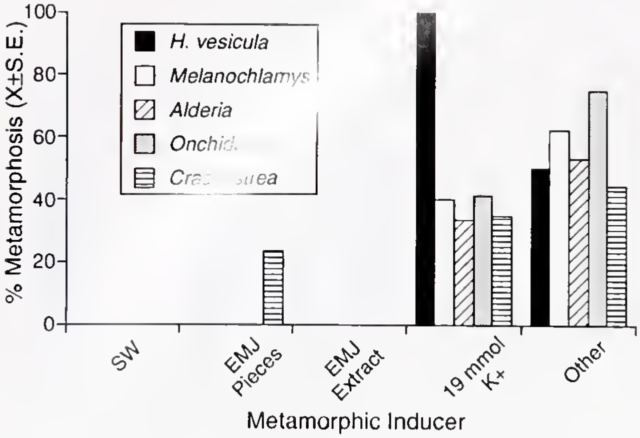

Figure 4. Specificity of egg mass jelly (EMJ) activity to *Haminaea callidegenita* Data are the percentage of metamorphosis in veligers of five mollusc species (identified in the legend) in response to seawater (SW), EMJ, a methanol jelly extract, 19 mmol K$^+$, and a natural substrate associated with metamorphosis in that species (identified in text).

callidegenita veligers was a polar (methanol- and water-soluble) compound that was smaller than 1000 Da in molecular weight, non-proteinaceous, and stable to temperature (−60° to 100°C) and acid. It is interesting that veligers of all three opisthobranchs metamorphose in response to inducers that are small, non-proteinaceous, water-soluble compounds; however, further comparisons are not possible until these inducers have been identified. Under field conditions, metamorphic cues that are water soluble may become highly dilute within a short distance from the inducer source (Hadfield and Scheuer, 1985). Dilution of the EMJ inducer would presumably not be a problem as the compound need only diffuse through the egg mass to be effective (less than a few millimeters). Active inducer is present in jelly throughout the 2-week encapsulated period (the period from oviposition to hatching), suggesting that it is not released as the gelatinous matrix degrades during hatching. It is possible that the inducer is bound to a nonsoluble component of the egg mass (such as the matrix) or if it diffuses from the egg mass, it is present in large enough quantities to allow expected rates of metamorphosis.

The metamorphic inducer found in egg mass jelly appears to be derived from the parent, because methanol extracts of adult tissue contain a functionally similar compound. This potentially similar compound was isolated from most adult tissues assayed, suggesting that it is not uniquely produced or sequestered in the mucous glands of the reproductive tract (the organs that produce the egg mass; Rudman, 1971) but rather is found throughout most of the adult. Larvae of many benthic marine invertebrates are induced to metamorphose by conspecifics, including barnacles (*e.g.*, Knight-Jones, 1953), bivalves (*e.g.*, Veitch and Hidu, 1971), polychaetes (*e.g.*, Knight-Jones, 1951; Jensen and Morse, 1984), echinoids (Highsmith, 1982; Burke, 1984), and others (see reviews by Burke, 1986; Pawlik, 1992). This process causes gregarious settlement of larvae, either in response to adults (*e.g.*, Knight-Jones, 1953; Burke, 1984) or newly metamorphosed juveniles (*e.g.*, Cole and Knight-Jones, 1949; Leitz and Lange, 1991). Many advantages have been associated with this pattern of settlement, including identification of a habitat that will support juvenile and adult survival (Jensen, 1989) and the proximity of potential mates (Crisp, 1979; Pennington, 1985). Intracapsular metamorphosis in *H. callidegenita* is obviously not gregarious settlement (offspring hatching as juveniles have not settled), but advantages associated with a conspecific cue remain the same, both at the level of individual larvae (EMJ would identify a suitable juvenile habitat as one containing a reproductively active population of *H. callidegenita*) and the population (induction of intracapsular metamorphosis by EMJ would ensure continuous recruitment to the parental population). EMJ induces metamorphosis in veligers throughout the metamorphic period (Gibson, 1993); therefore, it may have a role in inducing gregarious settlement of hatched veligers, including those from other populations. However, its functional importance may primarily involve intracapsular metamorphosis, because a hatched veliger is less likely to encounter EMJ than the other, more widespread substrates known to induce metamorphosis posthatching (*e.g.*, *Zostera marina*).

A functionally similar metamorphic inducer is also found in the egg masses of other opisthobranch species,

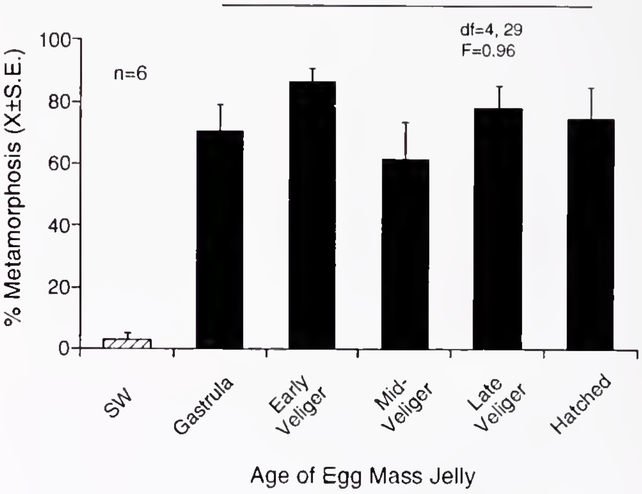

Figure 5. Effect of egg mass age on activity of the metamorphic inducer in egg mass jelly. Data are the percentage (mean ± standard error) of *Haminaea callidegenita* veligers that underwent intracapsular metamorphosis in response to seawater (SW) and egg mass jelly separated from egg masses at the stage indicated. The horizontal bar indicates that no significant differences were found among these groups (1-way ANOVA). *n* = number of egg masses assayed.

suggesting that this compound or group of similar compounds is intrinsic to the structure of these gelatinous egg masses. As such, production of the inducer, unlike the release of a more specific pheromone, would not require an additional expenditure of energy by the adult. Response of larvae to the inducer may be a consequence of opisthobranch veligers being sensitive to cues denoting a juvenile or adult food source. After hatching, juvenile *H. callidegenita* often graze diatoms and detritus from the surface of the egg mass and appear to ingest EMJ as well, before moving to nearby *Zostera* or *Chaetomorpha* (Gibson, pers. obs.)

Despite the fact that the inducing compound is not uniquely derived in *H. callidegenita,* its effects as a metamorphic inducer are restricted to this species. Competent veligers of five other molluscan species did not metamorphose in response to the metamorphic inducer in EMJ in a partially purified condition. This is not surprising for stenophagous species (in this study, *Onchidoris* and *Alderia* have restricted trophic requirements) as these larvae would be expected to metamorphose only on a highly specific substrate (Seeleman, 1933; Chia and Koss, 1988). *H. vesicula* coexists with *H. callidegenita* and adults of both species appear to have similar trophic requirements, but their larvae metamorphose in response to cues associated with more general characteristics of the habitat. Lack of response by these veligers to EMJ may reflect a higher probability of these long-lived veligers (4 weeks in *H. vesicula* and 6 weeks in *Melanochlamys;* Gibson, pers. obs.) contacting a more widespread cue than the less likely encounter with an egg mass after hatching. It would be interesting to test the EMJ inducer on opisthobranchs known to prey on the egg masses of other species, such as *Olea hanseensis* (Strathmann, 1987), which is also seasonally found in Padilla Bay (Gibson, pers. obs.).

The primary ecological effect of the presence of a metamorphic inducer in the egg mass is poecilogonous development: that is, by promoting intracapsular metamorphosis, this inducer allows for the release of both swimming veligers and crawl-away juveniles from each egg mass. Therefore, each parent produces dispersive propagules while simultaneously providing immediate recruits to the parental population. The second major factor shaping this developmental mode is variable intra-clutch time of competence, spanning both the hatching and posthatching larval periods (Gibson, 1993). The role of EMJ as an inductive substrate probably arose through a combination of two conditions: the nonspecific distribution of the chemical inducer (the inducer or a similar compound is found in adult tissue as well as in the egg masses of other opisthobranchs), and its role as a juvenile food source (possibly as a substrate from which to graze diatoms and detritus). To our knowledge, this is the first described example of larvae metamorphosing in response to a maternally derived egg mass, as well as the first description of an opisthobranch metamorphosing in response to conspecifics.

Acknowledgments

We thank Dennis Willows, Director, Friday Harbor Laboratories, for kindly providing us with laboratory facilities. We also thank the library at Friday Harbor Laboratories. R. Strathmann provided us with *Crassostrea* larvae. Doug Bulthius, Research Coordinator, Padilla Bay National Estuarine Research Reserve and Washington State Parks, Spencer Spit State Park, generously permitted us access to collection sites. This paper benefited from the comments of L. Barlow, P. Fankboner, J. Holmes, A. Kohn, A. Spencer, and two reviewers. Much thanks goes to R. Andersen for his advice on isolation protocols for marine natural products. This research was funded by an NSERC grant to FSC.

Literature Cited

Bickell, L. R. 1978. *Larval Development, Metamorphosis and Juvenile Feeding of* Doridella steinbergae *(Lance) (Opisthobranchia: Nudibranchia).* M. Sc. Thesis, University of Alberta, Edmonton, Alberta. 226 pp.

Bahamondes-Rojas, I. 1988. Induction de la métamorphose des larves d'*Eubranchus doriae* (Trinchèse, 1879), Mollusque, Nudibranche, par les substances provenant de l'espèce proie *Kirchenpaueria pinnata,* Hydozoaire, Cnidaire. *Vie Marine* **9:** 1–6.

Bahamondes-Rajas, I., and M. Dherbomez. 1990. Purification partielle des substances glycoconjuguées capable d'induire la métamorphose des larves compétentes d'*Eubranchus doriae* (Trinchèse, 1879), mollusque nudibranche. *J. Exp. Mar. Biol. Ecol.* **144:** 17–47.

Burke, R. D. 1984. Pheromonal control of metamorphosis in the Pacific sand dollar, *Dendraster excentricus. Science* **225:** 442–443.

Burke, R. D. 1986. Pheromones and the gregarious settlement of marine invertebrate larvae. *Bull. Mar. Sci.* **39:** 323–331.

Chia, F.-S., and R. Koss. 1988. Induction of settlement and metamorphosis of the veliger larvae of the nudibranch, *Onchidoris bilamellata. Int. J. Invert. Reprod. Dev.* **14:** 53–70.

Cole, H. A., and E. W. Knight-Jones. 1949. The settling behaviour of larvae of the European oyster *Ostrea edulis* L. and its influence on methods of cultivation and spat collection. *Fish. Invest. Minist. Agric. Fish. Food G. B. Ser. II* **17** (3): 1–39.

Coon, S. L., D. B. Bonar, and R. M. Weiner. 1985. Induction of settlement and metamorphosis of the Pacific oyster, *Crassostrea gigas* (Thunberg) by L-DOPA and catecholamines. *J. Exp. Mar. Biol. Ecol.* **94:** 211–221.

Crisp, D. J. 1967. Chemical factors inducing settlement in *Crassostrea virginica* (Gmelin). *J. Anim. Ecol.* **36:** 329–335.

Crisp, D. J. 1979. Dispersal and re-aggregation in sessile marine invertebrates, particularly barnacles. Pp. 319–327 in *Marine Organisms—Genetics, Ecology and Evolution.* G. Larwood and B. R. Rosen, eds. Volume II. Academic Press, London.

Day, R. W., and G. P. Quinn. 1989. Comparisons of treatments after an analysis of variance in ecology. *Ecol. Mongr.* **59**(4): 433–463.

Giannuzzi-Savelli, R., and A. Gentry. 1990. *Haminaea* Leach [1820] (Mollusca, Gastropoda): proposed conservation. *Bull. Zool. Nomencl.* **47**(4): 263–269.

Gibson, G. D. 1993. Developmental variability and the induction of metamorphosis in the opisthobranch mollusc *Haminaea callidegen-*

ita. Doctoral Dissertation, University of Alberta, Edmonton, Alberta, 137 pp.

Gibson, G. D., and F.-S. Chia. 1989a. Developmental variability (pelagic and benthic) in *Haminoea callidegenita* (Opisthobrancha: Cephalaspidea) is influenced by egg mass jelly. *Biol. Bull.* **176:** 103–110.

Gibson, G. D., and F.-S. Chia. 1989b. Embryology and larval development in *Haminoea vesicula* Gould (Opisthibranchia: Cephalaspidea). *Veliger* **32:** 409–412.

Hadfield, M. G. 1977. Chemical interactions in larval settling of a marine gastropod. Pp. 403–413 in *Marine Natural Products Chemistry,* D. J. Faulkner and W. H. Fenical, eds. Plenum Press, New York.

Hadfield, M. G., and D. Scheuer. 1985. Evidence for a soluble metamorphic inducer in *Phestilla:* ecological, chemical and biological data. *Bull. Mar. Sci.* **37:** 556–566.

Harrigan, J. F., and D. L. Alkon. 1978. Laboratory culture of *Haminoea solitaria* (Say, 1822) and *Elysia chlorotica* (Gould, 1870). *Veliger* **21:** 299–305.

Highsmith, R. C. 1982. Induced settlement and metamorphosis of sand dollar (*Dendraster excentricus*) larvae in predator-free sites: adult sand dollar beds. *Ecology* **63:** 329–337.

Hubbard, E. J. 1988. Larval growth and the induction of metamorphosis of a tropical sponge-eating nudibranch. *J. Moll. Stud.* **54:** 259–255.

Jensen, G. C. 1989. Gregarious settlement by megalopae of the porcelain crab *Petrolisthes cinctipes* (Randall) and *P. eriomerus* Stimpson. *J. Exp. Mar. Biol. Ecol.* **131:** 223–231.

Jensen, R. A., and D. E. Morse. 1984. Intraspecific facilitation of larval recruitment: gregarious settlement of the polychaete *Phragmatopoma californica* (Fewkes). *J. Exp. Mar. Biol. Ecol.* **83:** 107–126.

Kempf, S. C., and A. O. D. Willows. 1977. Laboratory culture of the nudibranch *Tritonia diomedea* Bergh (Tritoniidae: Opisthobranchia) and some aspects of its behavioral development. *J. Exp. Mar. Biol. Ecol.* **30:** 261–276.

Kitamura, H., S. Kitahara, and H. B. Koh. 1993. The induction of larval settlement and metamorphosis of two sea urchins, *Pseudocentrotus depressus* and *Anthocidaris crassispina,* by free fatty acids extracted from the coralline red alga *Corallina pilulifera. Mar. Biol.* **115:** 387–392.

Knight-Jones, E. W. 1951. Gregariousness and some other aspects of the settling behaviour of *Spirorbis. J. Mar. Biol. Assoc. U. K.* **30:** 201–222.

Knight-Jones, E. W. 1953. Laboratory experiments on gregariousness during settling in *Balanus balanoides* and other barnacles. *J. Exp. Biol.* **30:** 584–599.

Leitz, T., and R. G. Lange. 1991. A substance released by metamorphosing larvae and young polyps of *Hydractinia echinata* induces metamorphosis in conspecific larvae. *Roux's Arch. Dev. Biol.* **199:** 370–372.

Pawlik, J. R. 1986. Chemical induction of larval settlement and metamorphosis in the reef-building tube worm *Phragmatopoma californica* (Polychaeta: Sabellariidae). *Mar. Biol.* **91:** 59–68.

Pawlik, J. R. 1989. Larvae of the sea hare *Aplysia californica* settle and metamorphose on an assortment of macroalgal species. *Mar. Ecol. Prog. Ser.* **51:** 195–199.

Pawlik, J. R. 1992. Chemical ecology of the settlement of benthic marine invertebrates. *Oceanogr. Mar. Biol. Annu. Rev.* **30:** 273–335.

Pennington, T. 1985. The ecology of fertilization of echinoid eggs: the consequences of sperm dilution, adult aggregation, and synchronous spawning. *Biol. Bull.* **177:** 350–355.

Pennington, T., and M. G. Hadfield. 1989. Larvae of a nudibranch mollusc (*Phestilla sibogae*) metamorphose when exposed to common organic solvents. *Biol. Bull.* **169:** 417–430.

Rudman, W. B. 1971. On the opisthobranch genus *Haminoea* Turton and Kingston. *Pac. Sci.* **25:** 545–559.

Seeleman, U. 1933. Rearing experiments on the amphibian slug *Alderia modesta. Helgo. wiss. Meeresunters.* **15**(1): 128–134.

Strathmann, M. F. 1987. P. 281 in *Reproduction and Development of Marine Invertebrates of the Northern Pacific Coast: Data and Methods for the Study of Eggs, Embryos, and Larvae.* University of Washington Press, Seattle.

Todd, C. D., M. G. Bentley, and J. N. Havenhand. 1991. Larval metamorphosis of the opisthobranch mollusc *Adalaria proxima* (Gastropoda: Nudibranchia): the effects of choline and elevated potassium ion concentration. *J. Mar. Biol. Assoc. U. K.* **71:** 53–72.

Veitch, F. P., and H. Hidu. 1971. Gregarious setting in the American oyster *Crassostrea virginica* Gmelin I. Properties of a partially purified "setting factor." *Chesapeake Sci.* **12:** 173–178.

Yool, A. J., S. M. Grau, M. G. Hadfield, R. A. Jensen, D. A. Markell, and D. E. Morse. 1986. Excess potassium induces larval metamorphosis of marine invertebrate species. *Biol. Bull.* **170:** 255–266.

Reference: *Biol. Bull.* **187**: 143–155. (October, 1994)

Gamete Spawning and Fertilization in the Gymnolaemate Bryozoan *Membranipora membranacea*

M. H. TEMKIN

Department of Biological Sciences, University of Southern California, Los Angeles, California 90089-0371

Abstract. The simultaneously hermaphroditic zooids of *Membranipora membranacea* colonies spawn primary oocytes and spermatozeugmata (aggregates of 32 or 64 spermatozoa) into ambient seawater. Eggs are released through the intertentacular organ (ITO) whereas spermatozeugmata are spawned through the tips of the two distomedial tentacles. Fertilized eggs undergo planktotrophic development to form long-lived cyphonautes larvae. Examination of ovarian, coelomic, and spawned oocytes for sperm nuclei, using either Bisbenzimide H33342 or aceto-orcein staining, revealed that a single sperm fuses with primary oocytes during or shortly after ovulation. In *M. membranacea,* egg activation does not immediately follow sperm-egg fusion, but occurs after oocytes are spawned through the ITO. The period between sperm-egg fusion and egg activation may last up to four days. Once zygotes begin to develop, they follow an *Ascaris*-type of fertilization pattern (Wilson, 1925). Internal sperm-egg fusion does not preclude cross-fertilization in *M. membranacea,* because spawned spermatozeugmata enter maternal coeloms through ITOs after being drawn into lophophores. The ITO actively regulates the entrance of spermatozeugmata and the release of oocytes by the closure of the distal pore. The ITO does not act as a filter to prevent self-fertilization, so that the paternal colony may also function as the maternal colony. Self-fertilization may be reduced in *M. membranacea* via increasing sperm dispersal away from the paternal colony, which is accomplished by the bending of the distomedial tentacles such that they release spermatozeugmata into the exhalent feeding current of the colony.

Introduction

In 1966, Silén reported that external cross-fertilization occurred in two gymnolaemate bryozoan species, *Electra posidoniae* and *E. crustulenta.* This report contradicted the 100-year-old belief that internal self-fertilization is obligatory in this group of hermaphroditic invertebrates (Huxley, 1856; Prouho, 1892; Calvet, 1900; Pace, 1906; Bonnevie, 1907; Marcus, 1938, 1941; Silén, 1944; Correa, 1948; Mawatari, 1952). The two species that Silén (1966) examined have planktotrophic larvae and spawn primary oocytes through a secondary reproductive structure called an intertentacular organ (ITO). The ITO, which is present in several gymnolaemate genera (*e.g., Alcyonidium, Conopeum, Electra, Farella,* and *Membranipora*), forms at the base of the two distomedial tentacles and provides a conduit for oocytes from the maternal visceral coelom to the external seawater. For *E. posidoniae,* Silén reported that spawned sperm caught by lophophores of neighboring colonies became attached to the abfrontal sides of the tentacles. According to Silén, sperm detached from the tentacles and swarmed around oocytes emerging from the ITO. For *E. crustulenta,* Silén was unable to follow sperm, however he reported finding sperm inside the ITO. Silén concluded that fertilization in *E. posidoniae* and *E. crustulenta* is external to the maternal coelom, occurring while oocytes are in either the ITO or seawater. However, Silén did not actually observe sperm-egg fusion in either species of *Electra.*

Silén (1966) proposed that external cross-fertilization may be a general phenomenon among gymnolaemate bryozoans and not restricted to species that possess an ITO. This proposal appears to be supported by two facts. First, spawning of sperm is widespread among bryozoan species. Silén (1966, 1972) and Bullivant (1967) described sperm spawning in 13 gymnolaemate genera. In some

Received 20 July 1993; accepted 18 July 1994.

Present Address: Biology Department, St. Lawrence University, Canton, New York 13617.

Abbreviation: ITO—Intertentacular organ.

genera, such as *Schizoporella*, sperm are spawned through the tips of all the tentacles, whereas in other genera, such as *Electra* and *Membranipora*, sperm or tightly organized aggregates of 32 or 64 sperm (Fig. 1) called spermatozeugmata (Bonnevie, 1907; Franzén, 1956; Zimmer and Woollacott, 1974), are released through only the two distomedial tentacles. Both Silén (1966, 1972) and Bullivant (1967) suggested that in these species, spawned sperm may externally cross-fertilize eggs as they emerge from the ITO or as they are transferred to an external site for brooding. The second fact supporting Silén's proposal is that egg activation (*e.g.*, elevation of a fertilization envelope), which closely follows sperm-egg fusion in most animal species (*e.g.*, Longo, 1987; Epel, 1990), does not seem to occur in gymnolaemate oocytes until after they are spawned (*e.g.*, Prouho, 1892; Calvet, 1900; Silén, 1966; Reed, 1988, 1991).

To date no study has directly evaluated the proposal that gymnolaemate bryozoans use external cross-fertilization. The lack of such an evaluation is due to the fact that the fertilization process has never been completely described for any gymnolaemate species. I report here that the site of sperm-egg fusion in the planktotrophic species *Membranipora membranacea* is within the maternal coelom, whereas the site of egg activation is in the external seawater. In *M. membranacea*, sperm-egg fusion and egg activation may be temporally separated by as many as four days. Although sperm-egg fusion occurs inside the maternal zooid, cross-fertilization is still possible because spawned spermatozeugmata gain access to the maternal visceral coelom via the ITO.

Materials and Methods

Observations of gamete spawning and egg activation

Observations of gamete spawning and spermatozeugmata transfer were made using one-zooid-row preparations. To make these preparations, sexually reproductive *Membranipora membranacea* colonies growing on *Iridaea cordata* were collected from the surface waters at or near the Friday Harbor Laboratories, University of Washington, San Juan Island, Washington. Colonies encrusting this substrate had two advantages over colonies growing on brown macroalgae, such as *Nereocystis luetkeana*. First, *M. membranacea* population densities on *I. cordata* were low; consequently, colonies several centimeters in diameter were frequently found. Such large colonies often have areas in which the zooids form long, unbranching, and parallel rows. By cutting down alternating rows with a scalpel blade, portions of colonies were made into strips, one-zooid wide and several zooids long. Although zooids on either side of this row were destroyed, the zooids within the row continued to feed and spawn gametes. The second advantage in using *I. cordata* is that after this alga is cut, it secretes a minimal amount of mucus as compared to the brown macroalgae. After cutting the colony into strips, one-zooid rows were rinsed several times with seawater to remove debris and placed in small plastic petri dishes filled with unfiltered seawater. These petri dishes were kept in an incubator maintained at 15°C.

One-zooid rows were placed on their sides in petri dishes. A Zeiss RA 16 Research microscope fitted with a phototube and a Panasonic WV-BL204 black and white television camera was used to observe and record gamete spawning and spermatozeugmata transfer. Images were recorded using a Panasonic VHS video recorder. Selected images were transferred to 35-mm format by photographing frozen frames from a television monitor onto Plus-X panchromatic film.

Two sets of measurements were made using one-zooid-row preparations to determine the length of time for oocytes to be spawned and undergo egg activation. Video images were used to measure the lengths of time for oocytes to pass from the visceral coelom, through the ITO, and into the ambient seawater. For the second set of measurements, a Wild M5 dissecting microscope was used to follow oocytes produced by individuals in one-zooid-row preparations from the time they completed their entry into the ITO until they initiated egg activation. Egg activation was considered to begin when the fertilization envelope first started to elevate. Elapsed time was measured using a digital stop watch.

The ability of seawater to stimulate egg activation in *M. membranacea* oocytes was investigated by removing oocytes from maternal coeloms by dissection and rinsing them with seawater. Oocytes from several zooids were pooled and then distributed into two groups. In one group, oocytes were washed with three exchanges of 0.2 μm filtered seawater, while oocytes in the second group were washed with three exchanges of filtered seawater containing 0.1 mM disodium ethylenediamine tetraacetic acid (EDTA). The presence of 0.1 mM EDTA enhances the percentage of spawned oocytes that develop in the laboratory (Reed, 1987). Oocytes were used from adjacent sister zooids of the same colony for each trial. The number of oocytes that underwent egg activation and the number of activated oocytes that developed to a swimming gastrula stage were determined for each group.

Observations of fertilization

The events of fertilization were determined from the study of whole mount preparations of ovarian, coelomic, and recently spawned oocytes. Some colonies were fixed before ovaries and coelomic oocytes were removed from

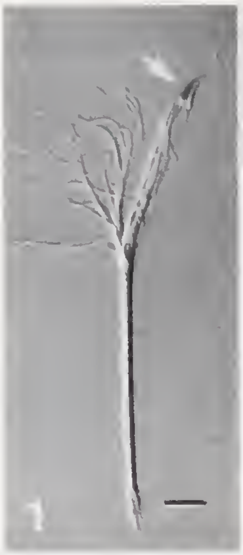

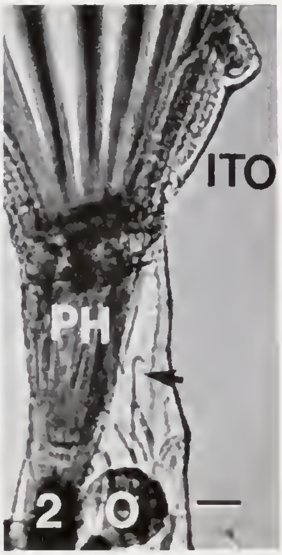

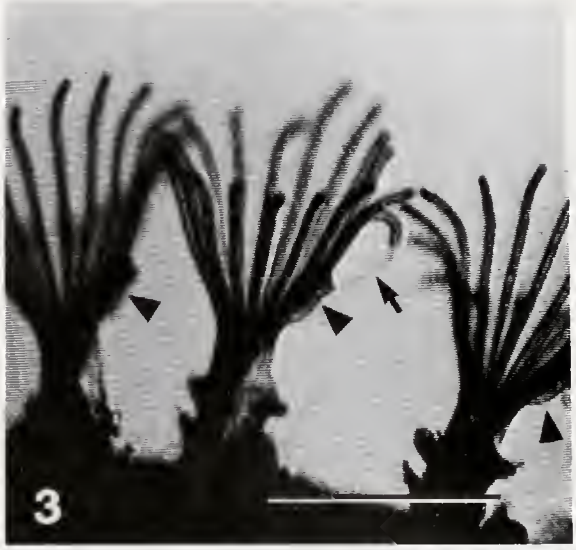

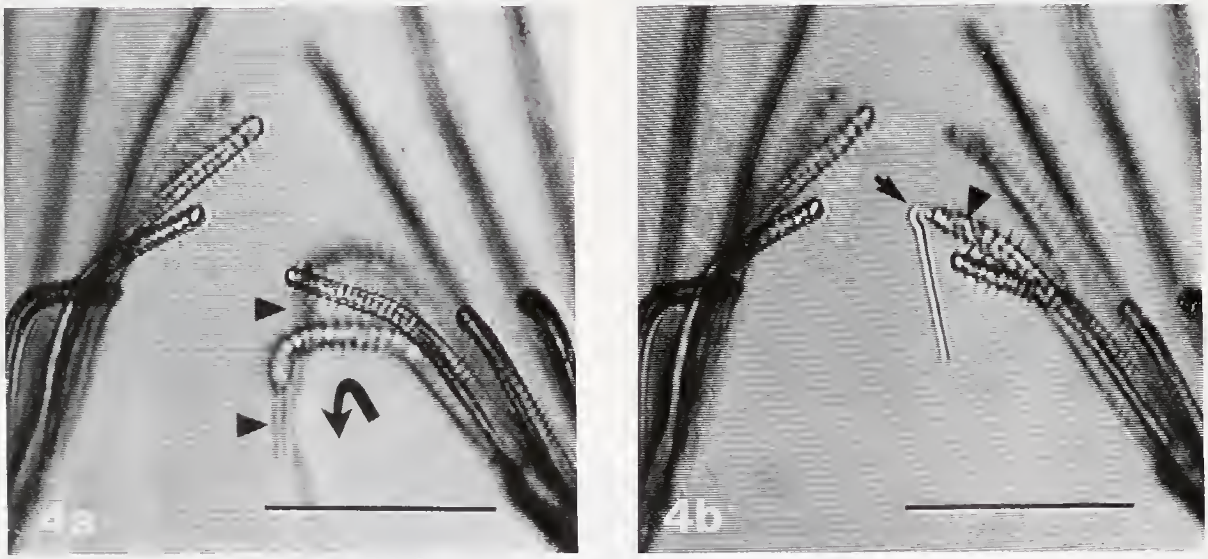

Figure 1. Differential interference contrast image of a partially disassociated spermatozeugma. The arrow indicates the head regions of spermatozoa that have remained joined. The tail region of the spermatozeugma has remained intact. Scale bar = 12 μm.

Figure 2. Video image of spermatozeugmata (arrow) and a primary oocyte (O) positioned between the pharynx (PH) and body wall of an extended polypide. The intertentacular organ (ITO) consists of a proximal and distal chamber. Scale bar = 50 μm.

Figure 3. A video image of three extended polypides protruding above the surface of a colony. All three lophophores possess an ITO (arrow heads). A spermatozeugma (arrow) is being spawned through one of the distomedial tentacles of the central lophophore. This tentacle is bent in an abfrontal direction so that the spermatozeugma is released into the exhalent flow of the feeding current passing beneath the canopy of tentacles. Scale bar = 360 μm.

Figure 4. Video images of spermatozeugmata being spawned tail ends first through the tips of the two distomedial tentacles. (a) The tightly bound tail portions of spermatozeugmata (arrow heads) are emerging from the tips of both tentacles. Arrow shows motion of tentacles bending in an abfrontal direction. (b) A spermatozeugma, which has been almost completely discharged, is bent downward at the flexible region (arrow) in the midpiece. The arrow head indicates the portion of the spermatozeugma that is still within the lumen of the tentacle pushing the spermatozeugma out. Scale bars = 150 μm.

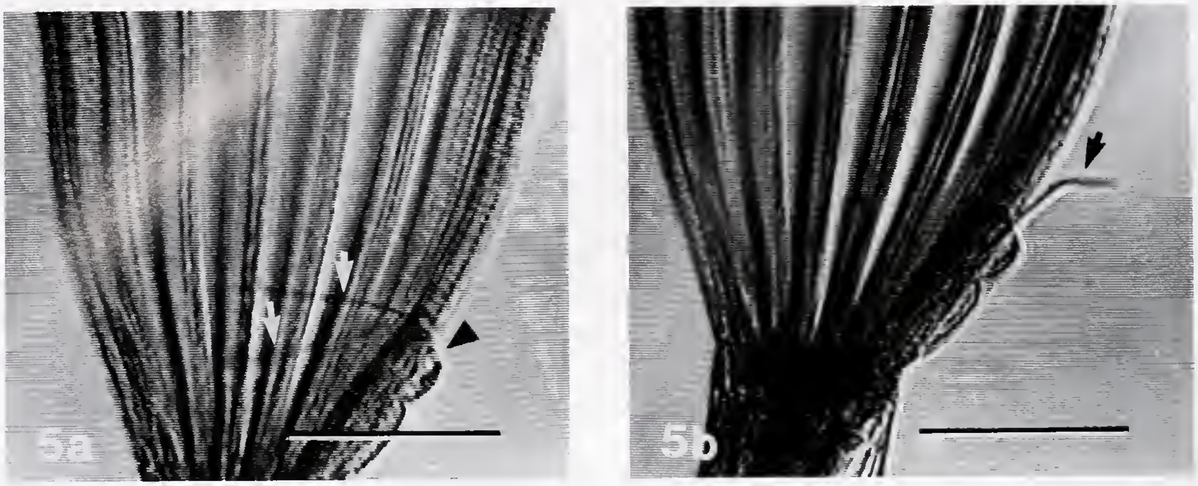

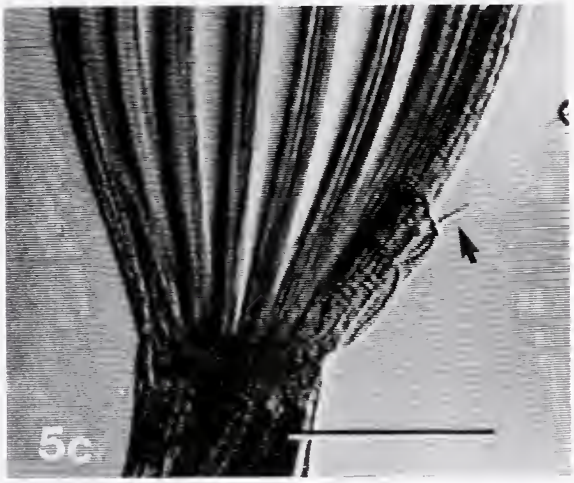

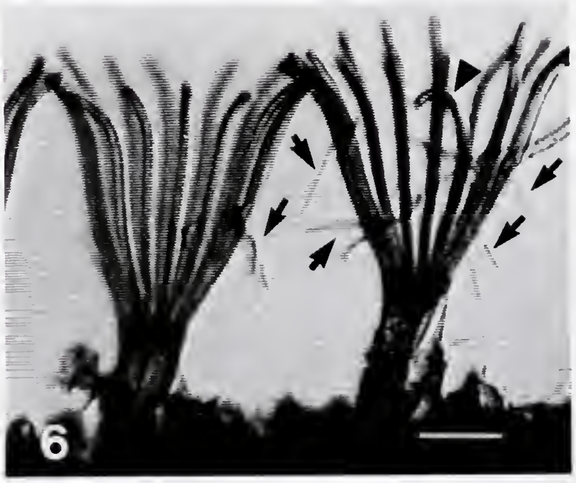

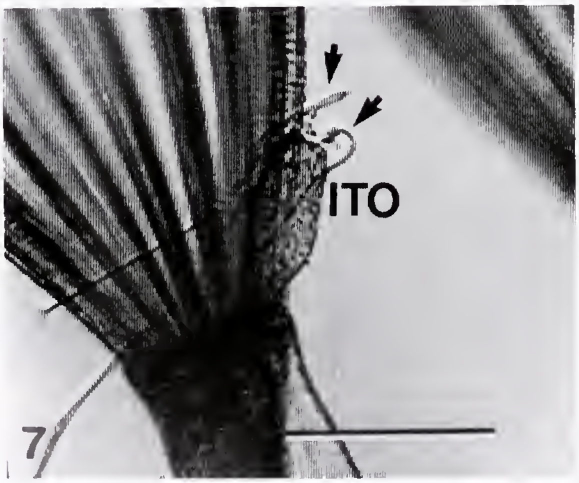

Figure 5. Video images of a spermatozeugma entering the ITO. (a) Two spermatozeugmata (arrows) within the lophophore are oriented so that their heads ends are positioned near the distal opening of the ITO (arrow head). The upper spermatozeugma has its head end inside of the ITO. (b) Thirty-five seconds later this spermatozeugma has been partially drawn into the ITO. The tail end of the spermatozeugma

zooids by dissection to prevent the occurrence of fertilization or activation events during these manipulations. Spawned oocytes were obtained by placing colonies in custard dishes containing 1.0 μm filtered seawater with 0.1 m*M* EDTA. Sexually active colonies transferred from 12–14°C to room temperature usually spawned oocytes within an hour.

Two stains were used in this study to visualize the nuclei within ovarian, coelomic, and spawned oocytes in order to (1) determine the stage and location of oocytes at sperm-egg fusion and (2) describe nuclear events during egg maturation, pronuclear migration, and syngamy. The DNA-specific fluorochrome bisbenzimide H33342 was used at 10 μg/ml by diluting a 100 μg/ml stock in 475 m*M* sodium chloride and 25 m*M* potassium chloride 1:10 with 0.2 μm filtered seawater. Two different staining protocols were followed. Ovaries and oocytes were either (1) fixed for 20 min in 4% formaldehyde buffered with seawater, rinsed thoroughly with 0.2 μm filtered seawater, stained for 5 min with bisbenzimide H33342 (10 μg/ml), and rinsed three times with 0.2 μm filtered seawater; or (2) stained for 10–30 min with bisbenzimide H33342 (10 μg/ml) and rinsed three times with 0.2 μm filtered seawater. Preparations stained with bisbenzimide were mounted for microscopy in 0.2 μm filtered seawater on glass slides with coverslips supported at their corners by plasticene clay "feet." Nuclei stained with bisbenzimide H33342 were visualized using a Zeiss epifluorescent microscope equipped with a 360 nm excitation filter, 395 nm dichroic filter, and 420 nm barrier filter. During prolonged observations, two 50% neutral density filters were placed in the light path to prevent photobleaching of the bisbenzimide fluorescence. Photomicrographs were taken with an Olympus OM-2S camera using 400 ASA Ektachrome slide film.

The second stain used was aceto-orcein. Materials were either (1) fixed for 30 min with 3:1 methanol-acetic acid, stained for 30 min with a 45% solution of aceto-orcein (Humanson, 1979), and rinsed in 20% acetic acid; or (2) fixed for 20 min in 4% formaldehyde buffered with 0.2 *M* phosphate, rinsed thoroughly with Millonig's phosphate buffer rinse (0.2 *M* phosphate, 0.15 *M* NaCl), fixed with 3:1 methanol-acetic acid for 60 min, stained with aceto-orcein for 60 min, and cleared in 30% acetic acid. Aceto-orcein stained preparations were mounted as described above, except that glycerol was used as a mounting medium. These preparations were preserved permanently by ringing the coverslip with nail polish. Materials stained with aceto-orcein were viewed using bright field microscopy, with a green filter (550 nm) inserted into the light path to enhance contrast. To further enhance contrast, differential interference contrast (DIC) microscopy was used in some instances. Photomicrographs were taken with an Olympus OM-2S camera using Panatomic-X film (ASA 32).

Results

Spawning and interzooidal transfer of spermatozeugmata

Membranipora membranacea zooids spawn spermatozeugmata through the two distomedial tentacles tail ends first into the exhalent feeding current of the colony. Prior to spawning, spermatozeugmata move freely within the visceral coelom (Fig. 2). Frequently, spermatozeugmata become situated between the body wall and the distomedial side of the pharynx, near the pore that connects the visceral and lophophoral coeloms. However, only those spermatozeugmata oriented with their tail ends toward the pore enter the lophophoral coelom of the distomedial tentacles. As spermatozeugmata move through the tentacles toward the terminal pores, the distomedial tentacles bend in an abfrontal direction (Figs. 3, 4). Consequently, spermatozeugmata emerge from the terminal pores of the tentacles tail ends first into the exhalant feeding current generated by the colony. Spermatozeugmata appear to be pushed through the tentacle lumen by an undulating movement of the midpiece region (Fig. 4b).

Spermatozeugmata in the water column become entrained in the feeding currents generated by *M. membranacea* colonies. Once drawn into lophophores, strong undulating movements of midpieces begin after spermatozeugmata contact the tentacles. These movements appear to allow some spermatozeugmata to remain within the lophophore long enough to find the distal opening to the ITO. For a spermatozeugma to enter an ITO it must be situated within the lophophore so that its head end emerges between the two distomedial tentacles and in close proximity to the distal pore of the ITO (Fig. 5a). If the head end of a spermatozeugma successfully enters the

Figure 5. (*Continued*) (arrow) is curved away from the lophophore because of the feeding current generated by the tentacles. (c) After 120 seconds, only the posterior portion of the spermatozeugma tail end (arrow) remains outside of the ITO. Scale bars = 100 μm.

Figure 6. Video image of two extended lophophores with attached spermatozeugmata (arrows) but lacking ITOs. One tentacle (arrow head) of the central lophophore is bent in a frontal direction, a movement often used in food capture. Scale bar = 100 μm.

Figure 7. Video image of an ITO (ITO) with a closed distal pore preventing the entrance of spermatozeugmata (arrows). Scale bar = 100 μm.

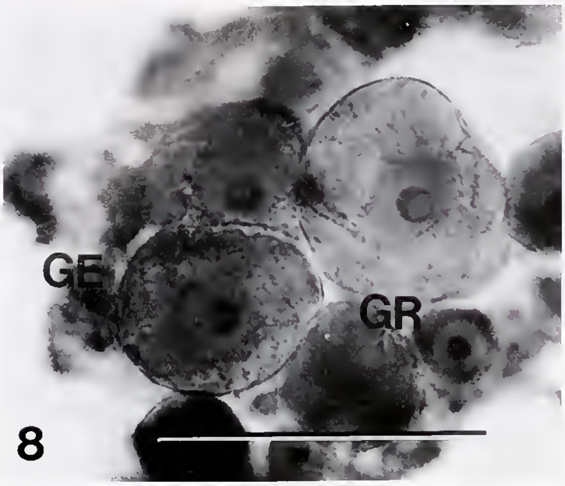

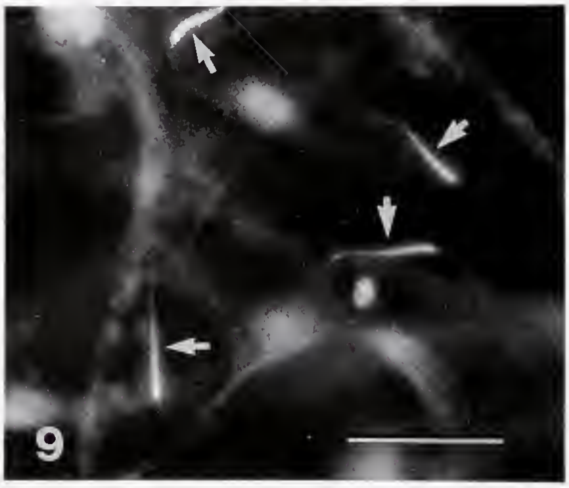

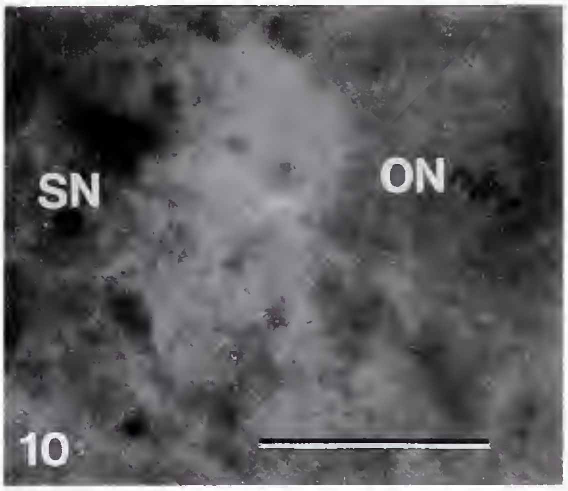

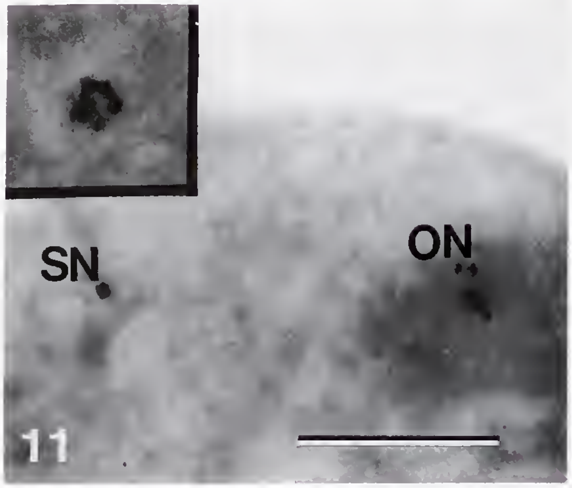

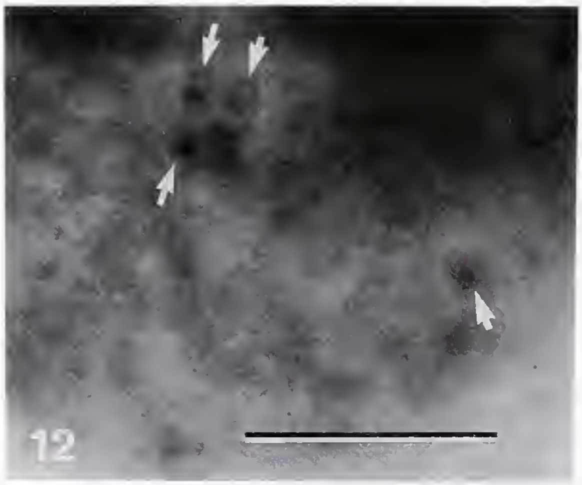

Figure 8. Aceto-orcein stained primary oocytes, containing only an oocyte nucleus as a germinal vesicle, within the growth (GR) and germinal (GE) zones of the ovary. Scale bar = 100 μm.

Figure 9. Single spermatozoa (arrows) present on the surface of follicle cells of an ovary stained with bisbenzimide H33342. Scale bar = 20 μm.

distal pore of the ITO, the undulating movement of the spermatozeugma stops and it is drawn into the ITO (Fig. 5b, c). Spermatozeugmata are drawn completely into ITOs within 2–3 min of first entering the distal pore. Although some of the spermatozeugmata that are drawn into lophophores are eaten, most are rejected as food particles. In several instances, spermatozeugmata became ensnared in the tentacles (Fig. 6). These ensnared spermatozeugmata were never observed to enter an ITO.

The ITO regulates the passage of spermatozeugmata from the external seawater into the ITO. Spermatozeugmata may be prevented from entering an ITO by the closure of the pore located in the distal end of the organ (Fig. 7). However, it is important to note that the ITO does not discriminate between spermatozeugmata produced by genetically identical zooids of the same colony and spermatozeugmata produced by zooids of other colonies. That is, when dishes contain zooids from only one colony, ITOs still permit spawned spermatozeugmata to enter maternal coeloms.

The location of sperm-egg fusion

A comparison of nuclei present in *M. membranacea* ovarian, coelomic, and recently spawned oocytes indicates that sperm fuse with primary oocytes during or shortly after ovulation. All ovarian oocytes contain only an oocyte nucleus, as either a germinal vesicle (Fig. 8) or a set of 12 chromosomes aligned on the first metaphase plate of meiosis, even though spermatozoa are found on the ovarian surface (Fig. 9). In contrast to those in the ovary, coelomic and recently spawned oocytes possess a second nucleus in addition to the oocyte chromosomes aligned on the first meiotic metaphase plate (Figs. 10, 11). This additional nucleus, whose chromatin is organized as chromosomes (Fig. 11), is a partially modified sperm nucleus as confirmed by observations of meiotic divisions and pronuclear migration (see below). Although the sperm nucleus is usually located close to the oolemma, it maintains no specific position with respect to the oocyte nucleus.

The percentage of *M. membranacea* oocytes that are fertilized is very high. For example, 98% of the 396 coelomic and spawned oocytes examined during this study contained a sperm nucleus. In eight instances, background staining may have prevented the observation of a sperm nucleus. On the other hand, the occurrence of polyspermy is low. Only one spawned oocyte possessed more than one sperm nucleus. This polyspermic oocyte contained at least 14 sperm nuclei. Even though the shape of these sperm nuclei was spherical, their chromatin was not always organized as chromosomes (Fig. 12).

Oocyte spawning and egg activation

The ITO mediates the release of oocytes into the ambient seawater (Fig. 13a–e). Oocytes are transferred from the visceral coelom into the ITO via the supraneural pore (Fig. 13a). This transfer takes an average of 42 ± 10 (SD) s ($n = 32$). During this transfer, oocytes are deformed as they pass through the supraneural pore (Fig. 13b). After being transferred into the ITO, oocytes are propelled toward the distal pore. Oocytes are usually retained within the ITO by the closure of the distal pore (Fig. 13b, c, d). The distal pore may close either before or after an oocyte enters the ITO. Oocytes spend an average of 44 ± 16 SD s ($n = 32$) in the ITO with the distal pore closed. Following the opening of the distal pore, it takes an average of 17 ± 8 SD s ($n = 32$) for an oocyte to emerge from the ITO (Fig. 13e). Thus, the total time for an oocyte to pass from the maternal coelom into the external seawater is 104 ± 23 SD s ($n = 32$), with an average of 61 ± 20 SD s ($n = 32$) spent within the ITO itself.

At the light microscope level, the two most dramatic morphological modifications of the oocyte during egg activation are a change in cell shape, from discoidal to spherical, and the elevation of a fertilization envelope (Fig. 14). These changes begin only after oocytes are spawned into seawater. The average time for oocytes to begin elevating a fertilization envelope after emerging from the ITO is 180 ± 68 SD s ($n = 16$). This is true even when oocytes are retained within an ITO for very long periods of time. For example, in one case, the distal sphincter muscle of an ITO remained closed, apparently to prevent the entrance of a spermatozeugma. By this action, two oocytes were restrained from leaving the ITO for more than 4 min, and during this time the oocytes did not change shape, elevate a fertilization envelope, or form polar bodies.

Oocytes are not stimulated to undergo egg activation when they are removed from the maternal coelom and

Figure 10. A coelomic oocyte in polar view stained with aceto-orcein, containing the chromosomes of the sperm nucleus (SN) and oocyte nucleus (ON). Scale bar = 25 μm.

Figure 11. A recently spawned oocyte without a fertilization envelope stained with aceto-orcein. The sperm nucleus (SN) is slightly out of focus. The oocyte nucleus (ON) is a set of chromosomes aligned on the first meiotic metaphase plate. Scale bar = 25 μm. Inset: Chromosomes of the sperm nucleus inside of a recently spawned oocyte.

Figure 12. Four of the fourteen partially modified sperm nuclei (arrows) from a polyspermic spawned oocyte. Scale bar = 20 μm.

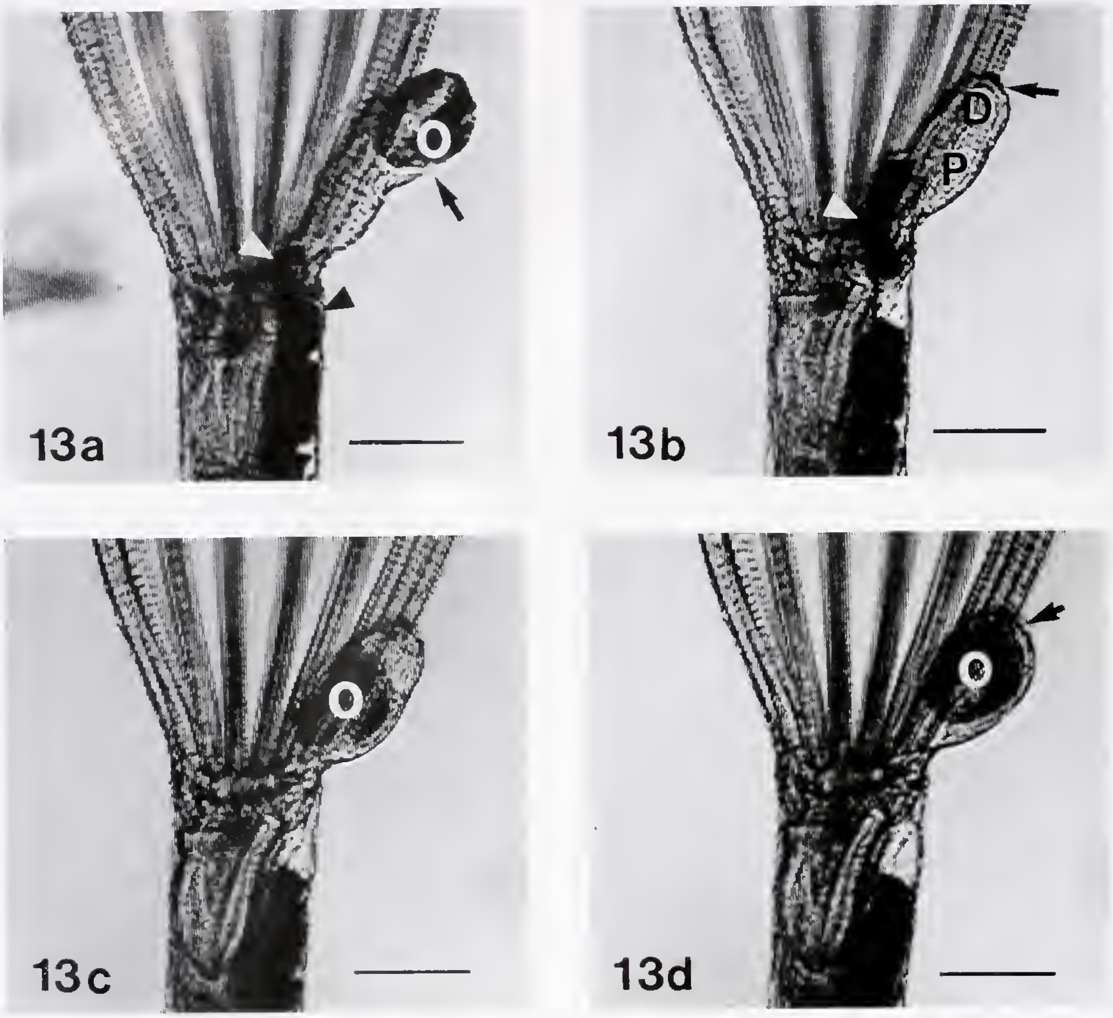

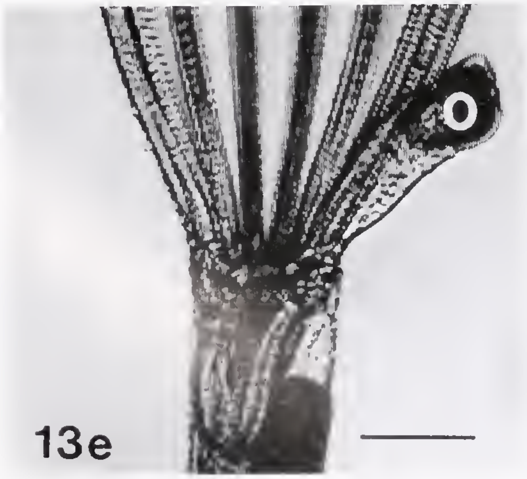

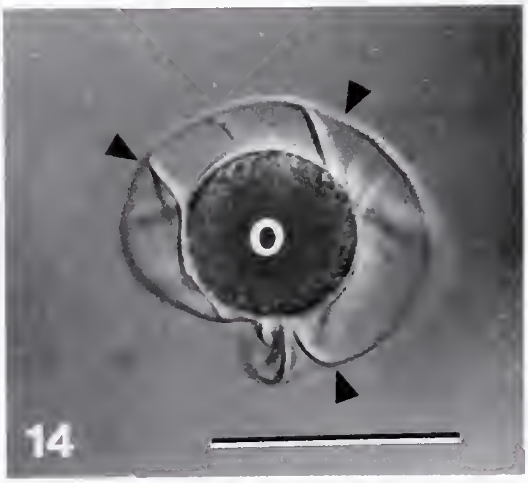

Figure 13. Video images of oocyte spawning in *Membranipora membranacea.* In (a) an oocyte (O) is almost completely discharged from the ITO and the distal pore (arrow) is opened widely. A second oocyte (black arrow head) is about to enter the ITO through the supraneural pore (white arrow head). To the right of the pharynx several other oocytes, which appear as opaque disks, are in line to be spawned (elapsed time = 0). In (b), the distal pore (arrow) of the ITO has closed, while the next oocyte to be spawned is moving

washed with filtered seawater. Only three (6.5%) of the 46 coelomic oocytes so treated formed a fertilization envelope, and none of these three activated oocytes developed. In contrast, 45 (98%) of the 46 oocytes dissected from maternal coeloms and rinsed with filtered seawater containing 0.1 m*M* EDTA underwent egg activation and developed to a swimming gastrula stage.

Egg maturation

The meiotic divisions of the oocyte nucleus begin following the elevation of the fertilization envelope and change in cell shape (Fig. 15). The plane of the meiotic metaphase plate of primary oocytes is parallel to the animal-vegetal axis (Fig. 10). Before the first meiotic division occurs, the meiotic spindle rotates 90° to position a centriole at the animal pole of the zygote. The maturation divisions in *M. membranacea* produce two polar bodies, the first of which does not divide again. Because egg maturation occurs after the elevation of the fertilization envelope, both polar bodies remain within the perivitelline space (Fig. 16).

Pronuclear formation and male pronuclear migration

Following the completion of the meiotic divisions, the chromatin of the female and male pronuclei begins to decondense (Fig. 16) and the male pronucleus starts to migrate toward the female pronucleus. The distance a male pronucleus traverses differs in each zygote, because the entry point of sperm is highly variable. It is not uncommon for a male pronucleus to migrate across the entire diameter of the spherical zygote (about 60 μm). During the migration period, the chromatin of both pronuclei continues to decondense, as indicated by the increasingly diffuse bisbenzimide staining (Fig. 17). After remaining in a highly decondensed state for approximately 20 min, the chromatin of the pronuclei begins to recondense. As this occurs, chromosomes become visible within each of the pronuclei (Fig. 18). By the end of the recondensation period, the pronuclei are ellipsoidal and the bisbenzimide fluorescence is intense (Fig. 19). When the migration of the male pronucleus is completed, the two pronuclei are adjacent to one another, but do not fuse to form a single zygote nucleus.

Syngamy and cleavage

Chromosomes from each pronucleus become aligned on the first mitotic metaphase plate independently of one another. Initially, chromosomes become apparent within each pronucleus. For the three zygotes in which these events were observed, it appears that the chromosomes of the female pronucleus begin to align on the metaphase plate slightly before those of the male pronucleus (Fig. 20). By the end of this phase of fertilization, the chromosomes from both pronuclei are aligned on the same mitotic metaphase plate in preparation for the first cleavage. At temperatures between 12 and 20°C, the first cleavage of zygotes occurs from 60 to 90 min after spawning.

Discussion

Since Silén (1966) first described the release of sperm by bryozoan zooids two questions have remained unanswered: (1) can spawned sperm enter maternal zooids and (2) are there aspects of sperm and egg spawning that influence whether zygotes are produced by self-fertilization or cross-fertilization? In *Membranipora membranacea,* spawned sperm may enter maternal zooids to fuse with oocytes within the visceral coelom. Spawned *M. membranacea* spermatozeugmata are captured by lophophores of feeding zooids in a manner that is similar to that described for *Electra posidoniae* (Silén, 1966). However, subsequent events may differ between the two species. In *E. posidoniae,* Silén (1966) reported that sperm, adhering to the abfrontal sides of tentacles, detached to swarm around oocytes emerging from the ITO. In *M. membranacea,* some spermatozeugmata become ensnared in the tentacles, but these spermatozeugmata do not detach from the tentacles in response to oocytes being spawned. Instead, spermatozeugmata drawn into *M. membranacea* lophophores swim vigorously trying to maintain a position within the lophophore in order to contact and enter ITOs. Silén (1966) reported the presence of sperm within the ITO of *E. crustulenta,* but did not observe how they entered the ITO. Spermatozeugmata of *M. membranacea* come into contact with ITOs through what appears to be a random search process, and may not be due to chemotaxis. The role of a sperm chemoattractant in directing

Figure 13. (*Continued*) from the visceral coelom through the supraneural pore (arrow head) into the proximal chamber (P) of the ITO. D denotes the distal chamber of the ITO (elapsed time = 42 s). In (c) the oocyte (O) that is inside the ITO is moving toward the distal pore which is closed (elapsed time = 65 s). In (d) the oocyte (O) is positioned just beneath the distal pore (arrow) of the ITO which remains closed. The closure of the distal pore prevented the release of the oocyte for 25 s after it reached this position (elapsed time = 95 s). In (e) the oocyte (O) is released from the ITO through the pore of the distal chamber (elapsed time = 124 s). Scale bars = 75 μm.

Figure 14. Differential interference contrast image of a spawned oocyte (O) that has an elevated fertilization envelope (arrow heads) and has become spherical. Scale bar = 60 μm.

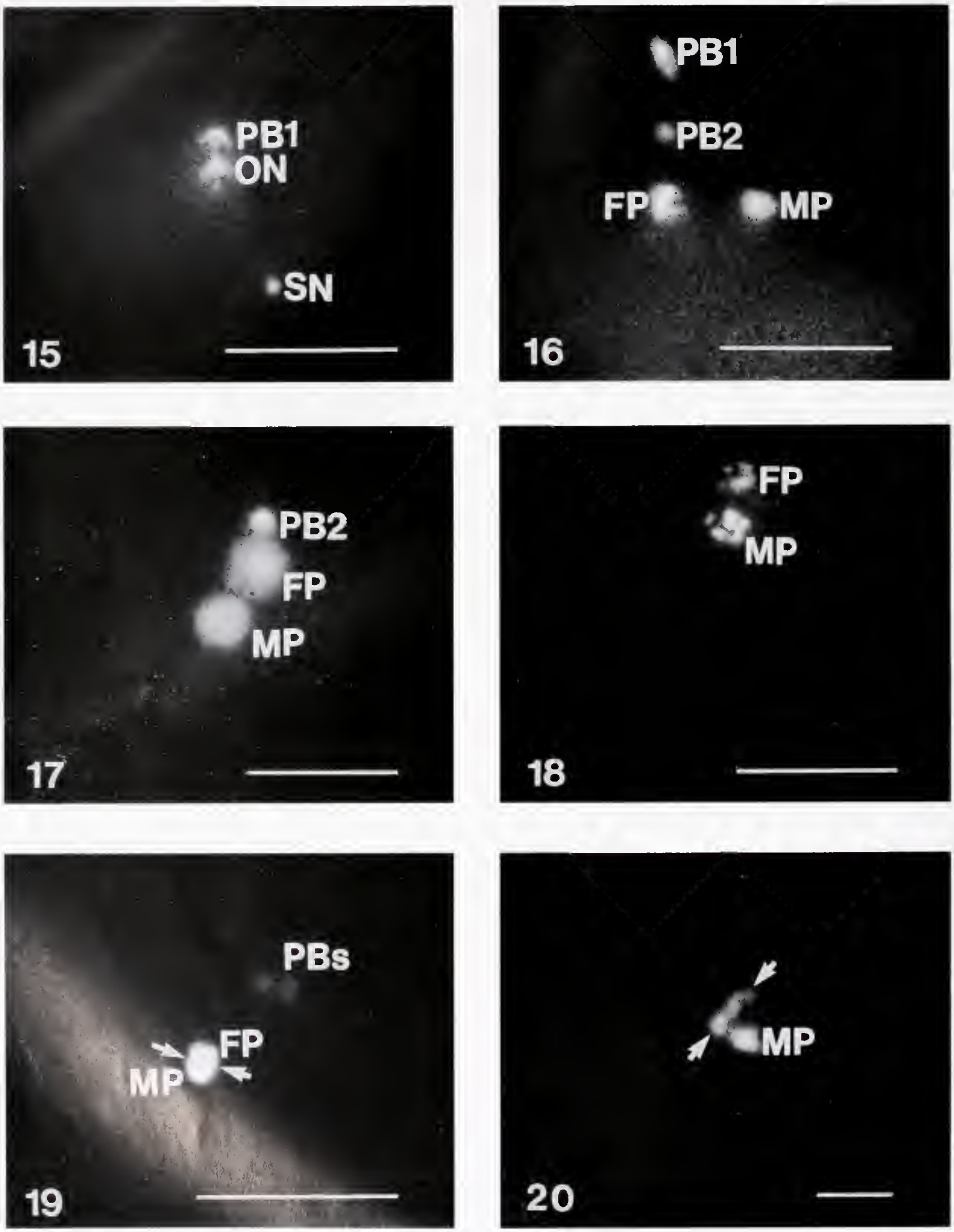
PB1
ON
SN
15
PB1
PB2
FP
MP
16
PB2
FP
MP
17
FP
MP
18
PBs
FP
MP
19
MP
20

Figures 15–20. Pronuclear formation and male pronucleus migration in *Membranipora membranacea* zygotes stained with bisbenzimide H33342.

Figure 15. A zygote at first meiotic anaphase shown in side view. The first polar body nucleus (PB1) is located at the animal pole. SN, sperm nucleus; ON, secondary oocyte nucleus. Scale bar = 25 μm.

spermatozeugmata to the ITO seems unlikely because water flow over the ITO is away from the lophophore. Nevertheless, a sperm chemoattractant may be important in directing the movement of spermatozeugmata after initial physical contact with the ITO and in directing sperm to oocytes after ovulation as in other metazoans (Miller, 1985). However, the presence of such chemoattractants in bryozoans is yet to be ascertained.

The release and capture of spermatozeugmata by *M. membranacea* zooids promotes cross-fertilization, but still allows self-fertilization to occur. The ITO in *M. membranacea* does not act as a filter to separate spermatozeugmata produced by genetically identical members of the same colony from those produced by zooids of other colonies. Consequently, both types of sperm cells may enter maternal coeloms to fuse with oocytes. Because *M. membranacea* is not self-sterile (Temkin, 1991), the potential for self-fertilization would increase if sperm did not disperse from paternal/maternal colonies. Silén (1966) suggested that releasing sperm through the tentacle tips would position sperm outside of the paternal zooid's feeding current. But, Silén did not take into account that releasing sperm in this manner might deliver sperm directly into the feeding currents or lophophores of neighboring sister zooids. *M. membranacea* may achieve greater sperm dispersal by bending the distomedial tentacles in an abfrontal direction to release spermatozeugmata into the exhalent flow of the colony's feeding current. In *M. membranacea,* the exhalent current flows out of chimneys or at the edge of colonies (Banta *et al.*, 1974; Lidgard, 1981), decreasing the chances that spermatozeugmata will be retained by the colony that produced them. In fact, electrophoretic studies of protein polymorphism in *M. membranacea* by Thorpe and Beardmore (1981) indicate that the allele frequencies of the few polymorphic loci that they observed were not significantly different from Hardy-Weinburg expections. Still, it is important to remember that *M. membranacea* spawns spermatozeugmata, aggregates of 32 or 64 sperm cells, and even a single spermatozeugma that enters a maternal zooid may have a significant effect on paternity, through either self-fertilization or cross-fertilization.

In *M. membranacea,* sperm-egg fusion is temporally separated from egg activation by the time between ovulation and spawning, a period that Hageman (1983) determined may last as long as four days. In most metazoans, sperm-egg interaction and membrane fusion almost immediately stimulate egg activation, a series of biochemical, physiological, and morphological changes in the egg cell that reinitiate the cell cycle and prevent polyspermy (*e.g.*, Longo, 1987; Epel, 1990). How egg activation is regulated in *M. membranacea* remains to be determined. The fact that egg activation does not begin until after oocytes are released into the ambient seawater indicates that some aspect of the spawning process allows egg activation to occur. However, it is not contact with seawater that initiates egg activation, because oocytes dissected from maternal coeloms and washed with seawater remain unactivated. Coelomic oocytes do have the potential to undergo egg activation as exposing them to 0.1 m*M* EDTA does permit egg activation and normal embryonic development to occur. The mechanism by which EDTA permits the initiation of egg activation in *M. membranacea* oocytes is unclear, and it is not known if EDTA affects oocytes in the same way as the natural stimulus. The low concentration of EDTA used in this study would not be expected to alter levels of Ca^{++} and Mg^{++} in seawater, which are in excess of 10 m*M*. The addition of 0.1 m*M* EDTA to seawater lowers the pH by 0.4 units (7.6 to 7.2), but a comparable decrease in pH alone does not cause *M. membranacea* coelomic oocytes to undergo egg activation (Temkin, unpub.). Two aspects of the spawning process that may affect egg activation are physical stress and exposure to ITO secretions. Oocytes become highly deformed as they pass through the supraneral pore, and this physical stress may initiate egg activation. Alternatively, the proximal chamber of the ITO is glandular (Hageman, 1981) and may secrete a factor that stimulates egg activation. The ITO actively retains *M. membranacea* oocytes for about 1 min. During this time, secretions of the ITO

Figure 16. A zygote shown in side view with the first (PB1) and second (PB2) polar bodies above the female pronucleus (FP) at the animal pole. The chromatin is beginning to decondense in both the female and male (MP) pronuclei. Scale bar = 25 μm.

Figure 17. A zygote viewed from the animal pole, in which the male pronucleus (MP) has migrated toward the female pronucleus (FP). The first polar body is positioned directly above the female pronucleus and thus cannot be seen in this picture. Second polar body nucleus, PB2. Scale bar = 25 μm.

Figure 18. A zygote shown in side view with the female pronucleus (FP) located near the animal pole. The chromosomes of the male (MP) and female pronuclei are apparent as the chromatin of each recondenses. Scale bar = 25 μm.

Figure 19. A zygote shown in polar view in which the male pronucleus (MP) is adjacent to the female pronucleus (FP). The arrows indicate the separation between the two pronuclei. The polar bodies (PBs) which are also fluorescing are out of focus. Scale bar = 25 μm.

Figure 20. In this zygote, the chromosomes of the female pronucleus (arrows) have become aligned on the first mitotic metaphase plate before those of the male pronucleus (MP). Scale bar = 10 μm.

may remove inhibitors from the surface of oocytes either chemically (*e.g.*, chelate) or enzymatically. Another possibility is that an ITO secretion may trigger egg activation through a receptor-ligand interaction. Further studies are required to determine if (1) sperm-egg interaction triggers egg activation, but some inhibitor prevents oocytes from responding to the stimulus until they are spawned or (2) some aspect of the spawning process replaces sperm-egg interaction as the inducer of egg activation.

A pattern of internal sperm-egg fusion and external egg activation may benefit *M. membranacea* zooids in two ways. First, internal sperm-egg fusion allows *M. membranacea* to fertilize nearly 100% of its eggs. This is achieved by maternal zooids capturing spawned spermatozeugmata and concentrating sperm and eggs within the maternal coelom instead of gamete interaction occurring in the water column where dilution factors may severely limit fertilization success (Pennington, 1985; Levitan, 1989; Levitan *et al.*, 1992). Second, the delay between sperm-egg fusion and egg activation allows the passage of pliable oocytes through a much smaller supraneural pore. In almost all species for which egg spawning has been observed, including *M. membranacea*, the passage through the supraneural pore requires oocytes to deform (for a review see Reed, 1991). The deformation may be extreme in species that brood their embryos and produce very large eggs. In these species, oocytes appear "thread-like" as they stream through the supraneural pore into brood chambers (*e.g.*, Silén, 1945; Reed, 1991). It is difficult to believe that once embryos begin to develop and form a hardened fertilization envelope they could undergo such a deformation. It is true that gymnolaemate bryozoan larvae are muscular and are capable of squeezing out of aperatures with slightly smaller diameters than themselves during their release, nevertheless, larvae cannot undergo the dramatic deformation that eggs do during spawning. If intracoelomic egg activation occurred in gymnolaemate bryozoans, it would seem likely that the maternal body wall would need to be ruptured for larvae to be released. Thus, the deformation of pliable oocytes during spawning may play an integral role in preserving the integrity of the maternal body wall and permitting, at the same time, formation of a large egg.

One consequence of extracoelomic egg activation in *M. membranacea* is the prevention of internal brooding. This raises important questions concerning the evolution of brooding patterns in gymnolaemate bryozoans. The majority of gymnolaemate bryozoans brood their embryos at one of four external sites: (1) attached to the external body wall, (2) in the tentacle sheath or vestibule, (3) in embryo sacs, or (4) in ovicells (Hyman, 1959; Ström, 1977; Reed, 1991). Brooding gymnolaemate bryozoan species are believed to have evolved from those that freely spawn their eggs into the ambient seawater such as *M. membranacea* (Jagërsten, 1972; Zimmer and Woollacott, 1977; Strathmann, 1978). It may be that as gymnolaemate species with a lecithotropic larva arose they were constrained from brooding internally by the requirement to spawn oocytes before egg activation could occur. Reports of intraovarian sperm-egg fusion for several species of brooding gymnolaemates (Marcus, 1938, 1941; Correa, 1948; Mawatari, 1952; and Dyrynda and King, 1983) suggest that internal sperm-egg fusion may be typical for gymnolaemate bryozoans. However, a complete evaluation of this proposal requires further study of sperm-egg fusion and egg activation in more brooding and non-brooding species.

In summary, this investigation provides the most complete description of the fertilization process for any gymnolaemate bryozoan to date. Except for the temporal separation between sperm-egg fusion and egg activation, *M. membranacea* has an *Ascaris*-type fertilization process. The *Ascaris*-type fertilization process is characterized by (1) overlap of late oogenic and early fertilization events and (2) syngamy at the onset of the first mitotic division of the zygote, without the fusion of male and female pronuclei to form a zygote nucleus (Wilson, 1925; Longo, 1987). The *Ascaris*-type fertilization process is typical of species in which sperm fuse with primary or secondary oocytes. In *M. membranacea*, primary oocytes arrested at first meiotic metaphase fuse with a single sperm cell during or shortly after ovulation, but do not undergo egg activation until they are spawned into the ambient seawater. Nevertheless, internal sperm-egg fusion in *M. membranacea* does not preclude the possibility for cross-fertilization because spawned spermatozeugmata may enter the maternal coelom through the ITO.

Acknowledgments

I thank Dr. Russel Zimmer, Dr. Anu Srinivasan, and Ms. Marianne DiMarco for reading the manuscript. Comments from three anonymous reviewers helped to improve the manuscript. I thank Dr. Richard Strathmann for allowing me to use his video equipment while at the Friday Harbor laboratories. This research was supported in part by funds provided by several NIH Biomedical Research Support Grants (BRSG SO7 RR07012-2) and a NSF Dissertation Improvement Grant (BSR-88-18512). This paper is dedicated to the memory of Dr. Christopher G. Reed.

Literature Cited

Banta, W. C., F. K. McKinney, and R. L. Zimmer. 1974. Bryozoan monticules: excurrent water outlets? *Science* **185:** 783–784.

Bonnevie, K. 1907. Untersuchungen über Keimzellen. II. Physiologische Polyspermie bei Bryozoen. *Jena Z. Naturwiss.* **42:** 567–598.

Bullivant, J. S. 1967. Release of sperm by Bryozoa. *Ophelia* **4:** 139–142.

Calvet, L. 1900. Contribution a l'histoire naturelle des Bryozoaires Ectoproctes marins. *Trav. Inst. Zool. Univ. Montpellier,* Ser. 2, **8:** 1–488.

Correa, D. D. 1948. A embryologia de *Bugula flabellata* (J. V. Thomson) (Bryozoa Ectoprocta). *Univ. São Paulo. Fac. Filos., Cienc. Let.* **13:** 7–71.

Dyrynda, P. E. J., and P. E. King. 1983. Gametogenesis in placental and non-placental ovicellate cheilostome Bryozoa. *J. Zool., Lond.* **200:** 471–492.

Epel, D. 1990. The initiation of development at fertilization. *Cell Differ. Dev.* **29:** 1–12.

Franzén, Å. 1956. On spermiogenesis, morphology of the spermatozoon, and biology of fertilization among invertebrates. *Zool. Bidr. Uppsala* **31:** 355–482.

Hageman, G. S. 1983. A fine structural analysis of ovarian morphology, oogenesis, and ovulation in the marine bryozoan *Membranipora serrilamella* (Cheilostomata, Anasca). Ph.D. Dissertation, University of Southern California, Los Angeles, CA. 487 pp.

Hageman, G. S. 1981. Accessory reproductive structures in *Membranipora serrilamella:* a fine structural study. P. 331 in *Recent and Fossil Bryozoa; Proceeding of the Fifth Conference of the International Bryozoology Association,* G. P. Larwood and C. Nielsen, eds. Olsen and Olsen, Fredensborg.

Humason, G. L. 1979. *Animal Tissue Techniques, 4th Edition.* W. H. Freeman and Company, San Francisco. 661 pp.

Huxley, T. H. 1856. Note on the reproductive organs of the cheilostome Polyzoa. *Q. J. Microsc. Sci.* **4:** 191–192.

Hyman, L. H. 1959. *The Invertebrates: Smaller Coelomate Groups, Chaetognatha, Hemichordata, Pogonophora, Phoronida, Ectoprocta, Brachiopoda, Sipunculida, the Coelomate Bilateria, Vol. 5.* McGraw-Hill, New York. 783 pp.

Jägersten, G. 1972. *Evolution of the Metazoan Life Cycle: A Comprehensive Theory.* Academic Press, New York. 282 pp.

Levitan, D. R. 1989. Density-dependent size regulation in *Diadema antillarum*—effects on fecundity and survivorship. *Ecology* **70:** 1414–1424.

Levitan, D. R., M. A. Sewell, and F. S. Chia. 1992. How distribution and abundance influence fertilization success in the sea urchin *Strongylocentrotus franciscanus. Ecology* **73:** 248–254.

Lidgard, S. 1981. Water flow, feeding, and colony form in an encrusting cheilostome. Pp. 135–142 in *Recent and Fossil Bryozoa. Proceeding of the Fifth Conference of the International Bryozoology Association.* G. P. Larwood and C. Nielsen, eds. Olsen and Olsen, Fredensborg.

Longo, F. J. 1987. *Fertilization.* Chapman and Hall, New York. 183 pp.

Marcus, E. 1938. Bryozoarios marinhos brasilieros II. *Univ. São Paulo, Fac. Filos., Cien. Let., Bol. Zool.* **2:** 1–196.

Marcus, E. 1941. Sobre Bryozoa de Brazil. *Univ. São Paulo, Fac. Filos., Cienc. Let., Bol. Zool.* **25:** 3–208.

Mawatari, S. 1952. On *Watersipora cucullata* (Busk) II. *Misc. Rep. Res. Inst. Nat. Resour. (Tokyo)* **28:** 17–27.

Miller, R. L. 1985. Sperm chemo-orientation in the Metazoa. Pp. 276–337 in *Biology of Fertilization, Vol. 2, Biology of the Sperm,* C. B. Metz and A. Monroy, eds. Academic Press Inc., Orlando.

Pace, R. M. 1906. On the early stages in the development of *Flustrella hispida* (Fabricius), and on the existence of a "yolk nucleus" in the egg of this form. *Q. J. Microsc. Sci. N.S.* **50:** 435–478.

Pennington, J. T. 1985. The ecology of fertilization of echinoid eggs: the consequence of sperm dilution, adult aggregation, and synchronous spawning. *Biol. Bull.* **169:** 417–430.

Prouho, H. 1892. Contribution a l'histoire des Bryozoaires. *Arch. Zool. Exp. Gén. ser. 2,* **10:** 557–656.

Reed, C. G. 1987. Phylum Bryozoa. Pp. 494–510 in *Reproduction and Development of Marine Invertebrates of the Northern Pacific Coast,* M. F. Strathmann, ed. University of Washington Press, Seattle.

Reed, C. G. 1988. The reproductive biology of the gymnolaemate bryozoan *Bowerbankia gracilis* (Ctenostomata: Vesiculariidea). *Ophelia* **29:** 1–23.

Reed, C. G. 1991. Bryozoa. Pp. 86–245 in *Reproduction of Marine Invertebrates, Vol. 6, Lophophorates and Echinoderms,* A. C. Giese, J. S. Pearse, and V. B. Pearse, eds., Boxwood press, Pacific Grove.

Silén, L. 1944. The anatomy of *Labiostomella gisleni* Silén (Bryozoa Protocheilostomata). *K. Sven. Vetenskaps. Akad. Handl.* **21:** 1–111.

Silén, L. 1945. The main features of the development of the ovum, embryo and ooecium in the ooeciferous Bryozoan Gymnolaemata. *Ark. Zool.* **35A:** 1–34.

Silén, L. 1966. On the fertilization problem in the gymnolaematous Bryozoa. *Ophelia* **3:** 113–140.

Silén, L. 1972. Fertilization in the Bryozoa. *Ophelia* **10:** 27–34.

Strathmann, R. R. 1978. The evolution and loss of feeding larval stages of marine invertebrates. *Evolution* **32:** 894–906.

Ström, R. 1977. Brooding patterns in bryozoans. Pp. 23–66 in *Biology of the Bryozoans,* R. M. Woollacott and R. L. Zimmer, eds. Academic Press, New York.

Temkin, M. H. 1991. Fertilization in the gymnolaemate Bryozoa. Ph.D. Dissertation, University of Southern California, Los Angeles, CA. 139 pp.

Thorpe, J. P., and J. A. Beardmore 1981. Genetic variation in natural populations of marine bryozoans. Pp. 263–272 in *Recent and Fossil Bryozoa: Proceedings of the Fifth Conference of the International Bryozoology Association,* G. P. Larwood and C. Nielsen, eds. Olsen and Olsen, Fredensborg.

Wilson, E. B. 1925. *The Cell in Development and Heredity.* Macmillan Co., New York. 1232 pp.

Zimmer, R. L., and R. M. Woollacott. 1974. Morphological and biochemical modifications of the spermatozoan mitochondria of *Membranipora* sp (Bryozoa). *J. Cell Biol.* **63:** 385a.

Zimmer, R. L., and R. M. Woollacott. 1977. Structure and classification of gymnolaemate larvae. Pp. 57–89 in *Biology of Bryozoans,* R. M. Woollacott and R. L. Zimmer, eds. Academic Press, New York.

Reference: *Biol. Bull.* **187:** 156–163. (October, 1994)

Locomotion in Developing *Artemia* Larvae: Mechanical Analysis of Antennal Propulsors Based on Large-Scale Physical Models

TERRI A. WILLIAMS*

Department of Zoology NJ-15, University of Washington, Seattle, Washington 98195

Abstract. A physical model of the swimming appendage (second antenna) of a larval *Artemia* was oscillated and translated through a tank of glycerine to determine how such a shape may be used to generate thrust at the intermediate Reynolds numbers at which it operates. Force on the model was measured by strain gauges and used to calculate coefficients of drag at a series of speeds and frequencies that represented flow regimes of different larval stages. Measured coefficients of drag (C_d) over this Reynolds number range (~ 1–10) suggest that an expression for a cylinder perpendicular to flow at intermediate Reynolds number ($C_d = 1 + 10\ Re^{-2/3}$) best represents the changes in drag coefficients for this geometry.

Unsteady forces were found to be a negligible portion of the force on the model in spite of a high ratio of frequency of oscillation to forward translational velocity (*i.e.*, Strouhal number).

Comparison of the thrust generated by the model with its fan of setae rigidly fixed *versus* passively flexing suggests that passive extension of setae can be influenced by relative limb and body speed.

Introduction

Animals that swim span an enormous range of sizes. This range is so great that the hydrodynamics that governs propulsion of the very small, slow swimmers and the large, fast swimmers are quite different. Small swimmers contend only with the viscosity of the fluid around them: flows are reversible, and shape does not greatly affect the pattern of flow. By contrast, large, fast swimmers use the inertial properties of fluids for propulsion: bodies are streamlined to reduce pressure drag, and propulsion is often achieved by accelerations of the surrounding fluid.

We understand the principles that determine these extreme cases because theoretical fluid dynamics provides solutions to the Navier-Stokes equations for these extremes: at the low end, inertial effects of the fluid are neglected; at the high end, viscous effects are neglected. But many organisms exist between these two extremes, and the flows they experience are a result of both fluid viscosity and fluid inertia. Planktonic animals are a good example of a whole category of organisms that inhabit this fluid regime. They include not only adults but also the larval stages of many animals.

Larvae are particularly interesting because, unlike their adult counterparts, they undergo changes in size and shape. This means that early in its life cycle an animal can be moving in a fluid regime dominated by viscosity and then, as it grows and develops, can experience flows that result from an increase in the importance of inertial effects. The brine shrimp, *Artemia*, provides such an example. Larvae swim actively from hatching until maturity. They are about 0.5 mm long when they hatch and swim at an average speed of 2 mm/s using only one pair of limbs. These limbs, the antennae, dominate propulsion during the first half of larval life and are gradually succeeded by a series of limbs that develop sequentially on the trunk. During part of the larval development of *Artemia*, the antennae increase in length from 0.25 mm to 0.50 mm, and the frequency of limb beat drops from 9.5 Hz to 8.0 Hz. Reynolds numbers of the limb based on limb length range from 1 to 9, and Strouhal numbers based on average body velocity drop from 8 to 3 (Table I). The antennae are used in a paddling mode of propulsion throughout this period of growth and change of form.

Received 4 June 1993; accepted 19 July 1994.

* Present address: Department of Anatomy, University of Vienna, Währingerstrasse 13, A-1090 Wien, Austria.

Table 1

Parameters used to model limb beat in selected larval stages, and forces measured on model limb

Stage	Antennal length (mm)	Freq. (Hz)	Body speed (mm s^{-1})	Re	St	Re model	St model	σ from eqn. 5	σ from eqn. 6	Drag-based force (N)	Unsteady force (N)
A) nauplius	0.24	9.5	1.8	1	8	2	5	0.16	0.14	5.7×10^{-2}	4.5×10^{-4}
B) limb bud	0.30	9.0	3.0	3	6	3	6	0.10	0.09	1.2×10^{-1}	1.3×10^{-3}
C) 4 trunk limbs	0.40	8.3	8.4	7	3	5	3	0.09	0.10	3.9×10^{-1}	3.5×10^{-3}
D) 7 trunk limbs	0.50	8.0	8.0	9	3	6	4	0.14	0.10	4.3×10^{-1}	4.8×10^{-3}

How does the balance of forces that determine movement change as the animal grows? Neither viscosity nor inertia dominate in determining the movements of *Artemia* larvae and other small crustaceans. Because both these effects must be accounted for, the Navier-Stokes equations of motion cannot be simplified to provide an analytical solution for force production. Existing models and measures of propulsion in small crustaceans import equations from engineering based on flow past geometric shapes at intermediate Reynolds numbers (*e.g.*, Morris *et al.*, 1985). I test the applicability of such equations by actual force measurements on a large-scale physical model of a larval *Artemia* antenna.

Because larvae are too small (~1 mm) for direct force measurements, I built a physical model of the limb which could both translate and oscillate through a tank of glycerin. For a series of larval stages, I preserved relevant fluid parameters based on kinematics measured from high-speed cine-photography and the morphology of the limbs. By mimicking the change in hydrodynamic regime these limbs experience during the development of *Artemia*, I estimated forces for a variety of stages and inspected how the growth of inertial effects influences force generation through development. In addition to assessing the overall importance of inertial effects, I tested the importance of unsteady or accelerational fluid forces in these high-frequency oscillating propulsors of developing larvae. These results are used in a theoretical model of rowing propulsion that can be directly compared to kinematic sequences of *Artemia* larvae taken with high-speed cine-photography (Williams, 1994).

Materials and Methods

Fluid forces and dynamic modeling

The force due to drag on an object moving through fluid at a constant velocity can be written:

$$\text{force} = 1/2\rho S(U)^2 C_d \qquad (1)$$

where ρ is the density of the fluid, S is the area of the object, U is the velocity of the object, and C_d is the coefficient of drag (defined below). This general expression applies to both viscous and inertia-dominated flow conditions. However, drag is generated differently in the two situations, and this will be reflected by the expression that defines the coefficient of drag, C_d. To determine an expression for C_d in the hydrodynamic regimes that the larvae experience, I measure drag directly on a large-scale physical model (see below) and calculate a value for C_d based on the average of the values calculated throughout a single stroke cycle of this model.

This expression for drag describes the force generated in a steady or time-invariant flow but, when inertial effects are important, an additional force may arise. This is the unsteady or added mass force that depends on the reaction of fluids to acceleration.

I assess the relative role of the unsteady forces in two ways. First, I compare thrust produced by the model with thrust predicted on the basis of steady and unsteady forces. I calculate this unsteady force, G, using:

$$G = \text{acceleration reaction} = \alpha\rho(V)dU/dt \qquad (2)$$

where α is the added-mass coefficient, a shape-dependent factor that is close to 1.0 (Daniel, 1984), V is the volume of the object, and U is its speed. I then compare the relative magnitudes of the steady and unsteady forces in the total force produced to gauge, theoretically, the importance of unsteady forces.

Second, I compare thrust produced by the model with a theoretical thrust calculated only on the basis of the angular position of the model as if it were oscillating without translating. If there are no unsteady effects, these two measures of thrust should be in phase; *i.e.*, the forces generated by translation and those generated by oscillation should add in a linear fashion.

Scaling of the model

I used two indices to mimic the hydrodynamic regime of a beating *Artemia* limb, Reynolds and Strouhal numbers. Both are dimensionless numbers that encapsulate certain features of the fluid environment.

The Reynolds number (Re) is defined as

$$Re = \rho \ell U_a/\mu \quad (3)$$

where ρ = fluid density, ℓ = some characteristic linear dimension of the object, in this case the length of the limb, U_a = average speed, and μ = viscosity of the fluid. For objects of the same geometry, equality of Reynolds number implies equality of the pattern of flow and equality of drag coefficients. My physical model can preserve these two features of an *Artemia* antenna, assuming that it represents the important features of antennal geometry.

However, the limbs oscillate. The Strouhal number (= reduced frequency parameter) is another dimensionless index that characterizes the flow. Conservation of this parameter implies conservation of the relative importance of fluid acceleration to steady flows. Strouhal number (St) is defined as

$$St = \omega \ell / U_b \quad (4)$$

where ω is the angular frequency of the limb, ℓ is the length of the limb, and U_b is the average velocity of the body.

I chose speeds and frequencies to drive the large-scale physical model of *Artemia* antenna that would approximate the combination of Re and St of the beating antenna at four selected larval stages. These are based on high-speed cine-photography and therefore do not account for stage-specific variation in larvae (see companion paper for discussion; Williams, 1994).

Measurement of force coefficients

Simple translation of the physical model (see below) yielded only a very limited range of speeds for direct measurements of drag coefficients. To evaluate the drag coefficients over a broader, more biologically relevant range, I calculated an average drag coefficient for the different trial runs (in which the model both translated and oscillated, see *Fluid forces and dynamic modeling,* above). The higher velocities resulting from the combined speed of translation and speed of oscillation yielded a broader range of Reynolds numbers. I compare the coefficient of drag calculated this way to two, different expressions for the coefficient of drag (C_d) of a cylinder perpendicular to flow: either

$$C_d = 24/Re \quad (5)$$

which expresses the low Reynolds number linear dependence of force on speed (Batchelor, 1967), or

$$C_d = 1 + 10(Re^{-2/3}) \quad (6)$$

which allows for the growth of pressure drag at intermediate Reynolds number situations, $1 < Re < 1 \times 10^5$ (White, 1974).

I also evaluated which expression for C_d better predicts the actual thrust produced by the model by comparing thrust predicted on the basis of either expression with measured thrust. I used the expression for standard deviation (Sokal and Rohlf, 1981), σ, as a measure of fit between the measured and predicted curves:

$$\sigma = [1/n \, \Sigma \, (t_c - t_m)^2]^{1/2} \quad (7)$$

where n is the number of points, t_c is the calculated thrust, and t_m is the measured thrust. See Williams (1994) for the details of calculating thrust.

The physical model and driving apparatus

A physical model of a limb that could be propelled within a tank of glycerin mimicked certain features of the active *Artemia* antennae. For the geometry of the model limb (*i.e.,* limb shape and setal spacing), I used direct tracings from film sequences of free-swimming animals (Williams, 1994). The model was constructed with casting resin. Thin brass cylinders formed a fixed fan that flexibly attached to the distal edge of the model (Fig. 1). This allowed the fan to flex during the recovery stroke; a raised lip in the cast itself anchored the fan in an extended position during the power stroke. Alternatively, the fan could be anchored in place so that it remained extended in both power and recovery strokes. This allowed comparison between a symmetrical and a passively asymmetrical stroke.

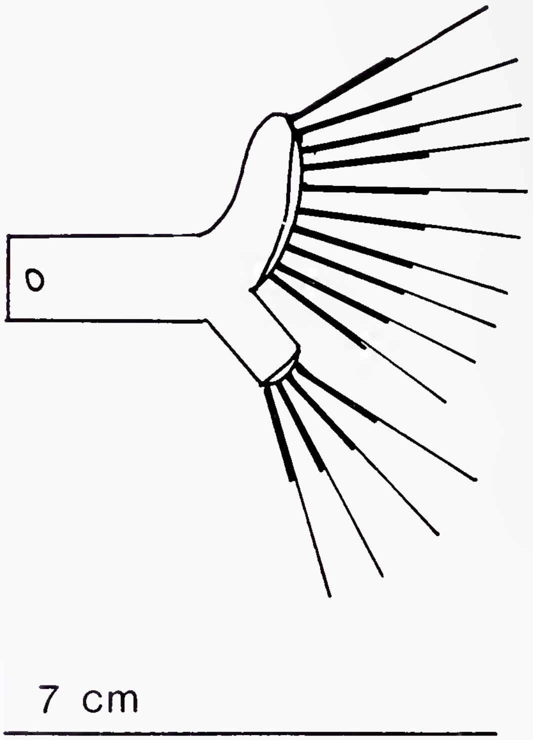

Figure 1. Cast resin model of *Artemia* larval antenna. Setal fan built of fine brass and tungsten wire.

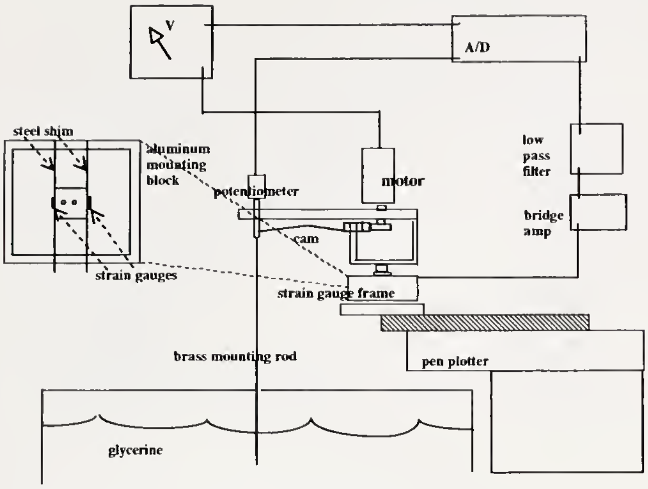

Figure 2. Apparatus used for measuring thrust of the model of *Artemia* larval antenna. The mounting carriage translates along an axis perpendicular to the plane of the page. The strain gauge frame is seen in planar view to the left of the diagram. (V = voltage; A/D = analog to digital.)

The model was attached to the end of a long, thin, brass rod that extended into a 50-gallon tank of glycerine (Fig. 2). The model rode in the middle of the tank approximately six model-lengths to the sides of the tank and seven to the bottom. The model limb could oscillate and translate independently at various speeds and frequencies. A modified pen plotter (Houston Instruments, Omnigraphic), controlled directly by a computer, translated the limb at speeds ranging from 1.2 cm s^{-1} to 6.0 cm s^{-1}. A rotating cam, driven by a small motor connected to the base of the brass rod, swung the limb in a 100° arc in an oscillating manner. A potentiometer documented the position of the model in the cycle. Frequencies ranged from 0.15 Hz to 0.55 Hz.

Two opposing 350-ohm semiconductor strain gauges (Entran), aligned perpendicular to the direction of thrust, measured displacement. I calibrated the force required to yield these displacements by hanging a series of small weights, 0.5–20 g, from the aluminum block between the two strain gauges (planar view of strain gauge frame: see Fig. 2, strain gauge frame). From this, I calculated a relationship between force and voltage. The response of the strain gauges was linear for the displacements I measured. The signal was amplified by a Gould bridge amplifier and filtered with a Krohn-Hite variable filter. Low-pass filtering with a 10-Hz cutoff removed the mechanical and other high-frequency noise caused by translating the model down the plotter. This cutoff introduced a slight phase shift (8°) in the signal at the high end of experimental frequencies. I corrected for the phase shift in computations of the phase between measured force and speed of the model.

The apparatus automatically repeated runs at each particular speed and frequency 100 times so that an average signal for thrust was obtained. In order to subtract drag of the brass rod from the experimental runs, I measured drag on the brass rod alone at the appropriate speeds.

Results

Average coefficients of drag calculated from thrust produced during trials in which the speed and frequency of the model is scaled to mimic four ontogenetic stages are plotted along with C_d predicted from equations 5 and 6 (Fig. 3). Average values for C_d follow almost exactly those predicted for a circular cylinder normal to flow at intermediate Reynolds numbers. In addition, values of the standard deviation, σ, between thrust produced by the model and thrust calculated on the basis of these two different expressions for C_d, confirm that, in three of four cases, the model generates thrust roughly as a cylinder at intermediate Reynolds numbers (Table I). The measured thrust per stroke of the model is compared in Figure 4 with thrust calculated on the basis of equation 6.

Two measures show the absence of unsteady forces on the model. First, in the calculation of thrust, the unsteady effects are two orders of magnitude lower than drag-based effects in all stages examined (Table I). Second, the time-course of thrust production can be predicted simply by the angular position of the model. Figure 5 compares thrust generated by the model with thrust calculated on the basis of angular position only. The difference between the measured thrust and such predicted thrust is simply due to the drag imposed by towing the model; there is no phase lag that would indicate unsteady effects. The difference is greater in the simulations of later stages where the towing speed is greater.

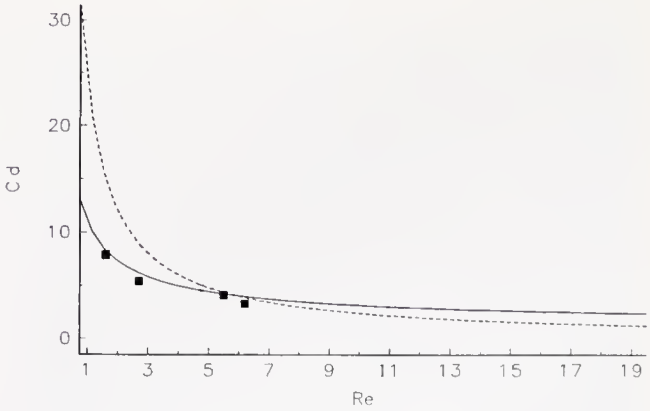

Figure 3. Relationship between drag coefficient (C_d) and Reynolds number (Re) for eqn. 5 (dotted line) and eqn. 6 (solid line). Filled squares represent the average C_d calculated from measured thrust of the model during different trials consisting of 100 runs each.

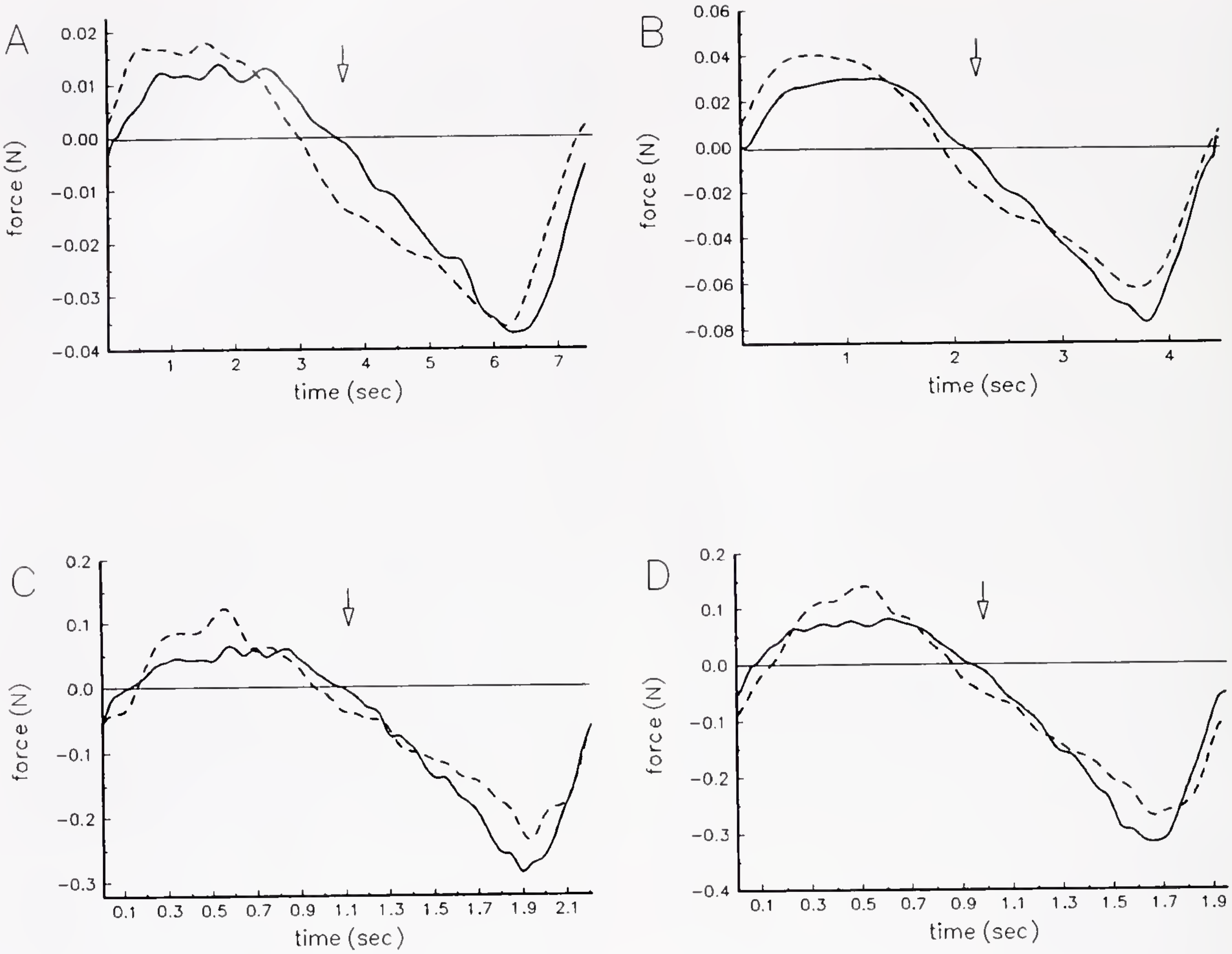

Figure 4. Comparison of thrust generated by the model (dotted lines) with thrust calculated on the basis of the same frequency and speed using eqn. 6 (solid lines). Each graph represents a single stroke of the model, although the force is averaged over all strokes during the 100 runs (and total stroke number depends on the frequency and speed). Arrows mark onset of recovery stroke. A–D correspond to the four successive larval stages the model mimics (see Table 1).

Figure 6 compares the symmetrical stroke of the model (where the fan of thin brass rods is unable to flex during the recovery stroke) with the asymmetrical stroke of the same frequency and speed (where the fan is free to flex during the recovery stroke and then opens passively during the course of the power stroke). Simulations with higher Strouhal numbers show similar patterns of thrust during the stroke. However, as the Strouhal numbers drop, the maximum thrust generated during the stroke is shifted later in the cycle, reflecting the later extension of the fan. This occurs because the model must overcome a relatively greater translational speed before it generates thrust. The result is a decrease in the relative thrust per cycle produced by the limb (as reflected by the difference between the areas under the two curves during the power stroke).

Discussion

Artemia larvae grow through a range of sizes and speeds that entail changes in the forces that determine their motions in the fluid. A physical model of the early larval propulsors, the antennae, shows that under the hydrodynamic regime experienced by the animals, these limbs generate force roughly as a cylinder at intermediate Reynolds numbers flows (eqn. 6). This empirically derived result is in agreement with a theoretical model of propulsion by copepod thoracic limbs which uses this equation to model copepod swimming by sequential movement of five pairs of appendages (Morris *et al.*, 1985).

In spite of the high frequency of the limb beat, unsteady forces are a negligible part of thrust production. Although unsteady forces are not always calculated as a source of

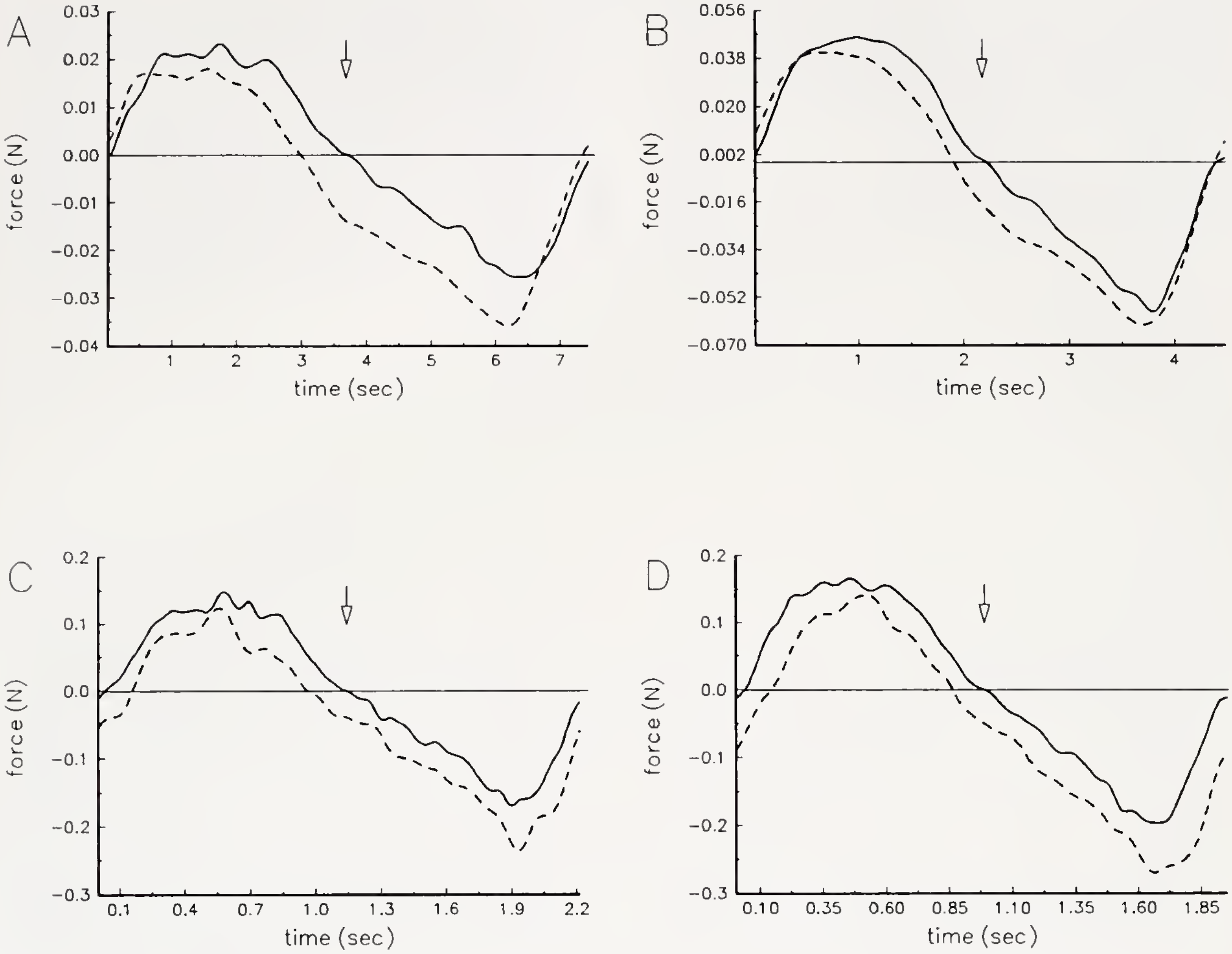

Figure 5. Comparison of thrust generated by the model (dotted lines) with thrust calculated only on the basis of the angular position of the model (solid lines). Each graph represents a single stroke of the model, although the force is averaged over all strokes during the 100 runs (and total stroke number depends on the frequency and speed). Arrows mark onset of recovery stroke. A–D correspond to the four successive larval stages the model mimics (see Table I). In C and D there is an offset due to greater translational speeds.

thrust on oscillatory propulsors (*e.g.*, Nachtigall, 1974), Blake (1985) has shown that they may produce as much as one-third of the thrust on the limbs of water boatmen, *Cenocorixa bifida*. The Reynolds number of these animals is about two orders of magnitude higher than those experienced by *Artemia* larvae modeled here (600 *vs.* 1–9), so it is not surprising that unsteady forces are correspondingly greater.

Although the model does not capture all of the details of the animal's limb kinematics, it does provide some generalizations about oscillating propulsion. In an overview of swimming in crustaceans, Hessler (1985) hypothesizes that setal structures on diverse swimming limbs may extend passively. Such passive extension is the case for the feeding setae of a filter-feeding shrimp (Fryer, 1977). This passive behavior may be possible only in some hydrodynamic regimes. At the intermediate Reynolds numbers modeled here, comparison of the thrust generated by the model at low and high Strouhal numbers suggests that an animal could use passively extending setae only if the speed of limb oscillation is high relative to the forward speed of the body—otherwise a passively extending system provides little thrust for propulsion. However, real setae are not accurately modeled by a metal wire fan. Typically, setal diameter varies from base to tip, and setal morphology is asymmetrical in the direction of power and recovery strokes. My results suggest that the influence of both setal material and morphology on passive behavior would be worth investigating, as these could influence the time-course of thrust production in real animals.

The kinematics of the model and the kinematics of an *Artemia* antenna differ in a significant way. *Artemia* an-

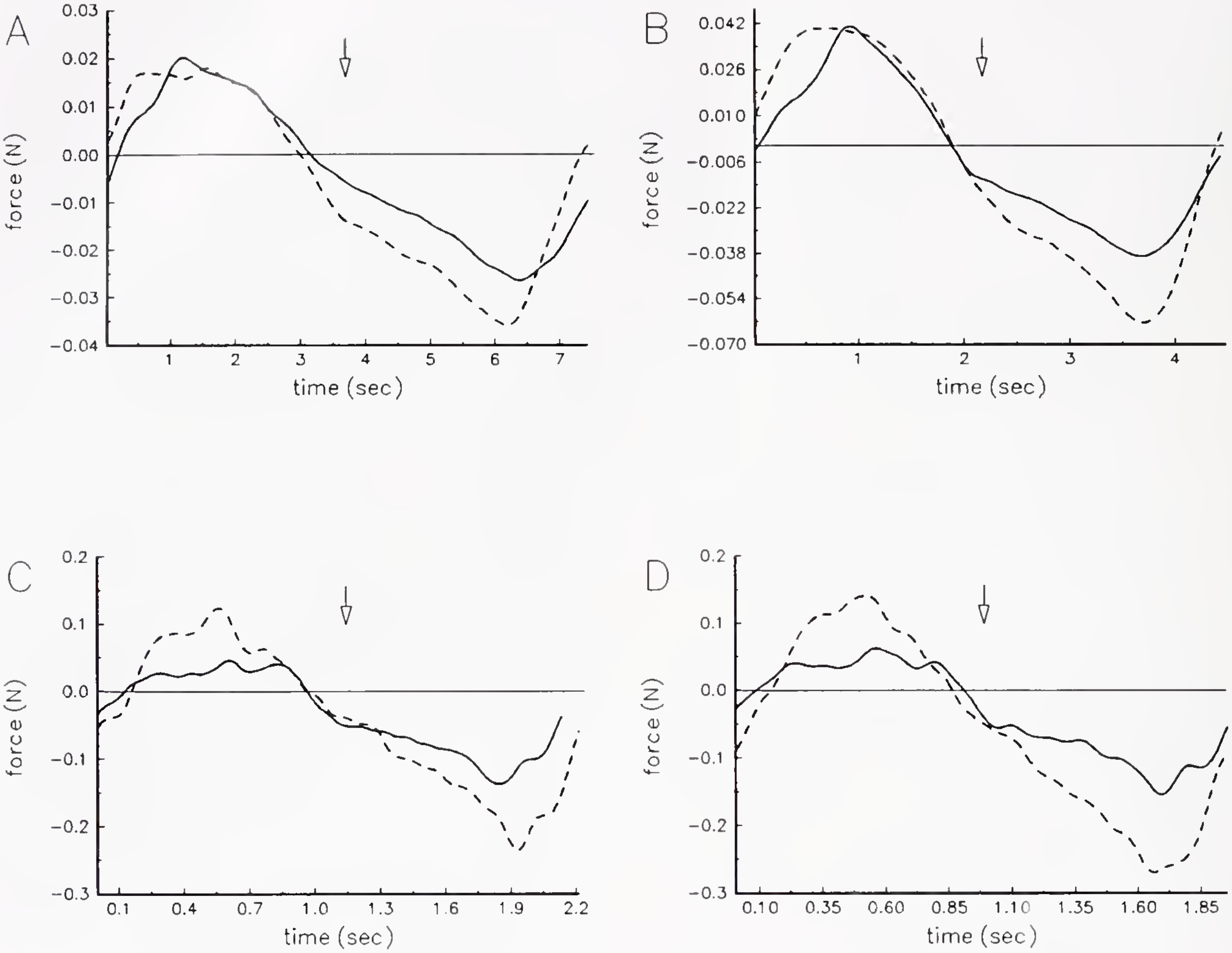

Figure 6. Thrust generated by the model when the stroke is symmetrical (dotted lines) compared with thrust generated when the stroke is asymmetrical (solid lines). Graphs represent a single stroke of the model, although the force is averaged over many strokes. Arrows mark onset of recovery stroke. A–D correspond to the four successive larval stages the model mimics (see Table I). Note that in later stages (C, D), the thrust generated during the power stroke is much smaller with an asymmetrical stroke than a symmetrical one.

tennae are linked to a freely moving body whose trajectory through the water changes as the animal develops: early stages swim in a highly pulsatile fashion; later stages do not (Williams, 1994). Therefore, unlike the model, the oscillation of the appendage is not simply coupled to a constant velocity, and the distribution of velocity along the length of the limb changes accordingly as the animal develops (Williams, 1994). Thus, the model does not provide direct information about the actual time-course of thrust production by an *Artemia* antenna during the stroke cycle. However, the force coefficient determined for the model does provide an *empirical* basis for determining drag produced by the antennal geometry moving in a fluid regime where both inertial and viscous effects determine flows. I use this empirically based force coefficient in a purely theoretical model in which I link thrust produced by a pair of appendages to resistive forces on the body and examine the mode of swimming that results (Williams, 1994).

Acknowledgments

I gratefully acknowledge grants from Sigma Xi, the Lerner-Grey fund for Marine Science, NSF grant DCB-8711654 to Tom Daniel, NSF grant BSR-8700523 to Alan Kohn. Tom Daniel, Joel Kingsolver, Alan Kohn, Garry Odell, and Dick Strathmann criticized this paper at various stages.

Literature Cited

Batchelor, G. K. 1967. *An Introduction to Fluid Mechanics.* Cambridge University Press, London. 615 pp.

Blake, R. W. 1986. Hydrodynamics of swimming in the water boatman, *Cenocorixa bifida. Can. J Zool.* **64:** 1606–1613.

Daniel, T. L. 1984. Unsteady aspects of aquatic locomotion. *Am. Zool.* **24:** 121–134.

Fryer, G. 1977. Studies on the functional morphology and ecology of the aytid prawns of Dominica. *Phil. Trans R. Soc. Lond. B* **279:** 57–129.

Hessler, R. R. 1985. Swimming in Crustacea. *Trans. Roy. Soc. Edin.* **76:** 115–122.

Morris, M. J., G. Gust, and J. J. Tores. 1985. Propulsion efficiency and cost of transport for copepods: a hydromechanical model of crustacean swimming. *Mar. Biol.* **86:** 283–295.

Nachtigall, W. 1974. Locomotion, mechanics, and hydrodynamics of swimming in aquatic insects. Pp. 381–432 in *Physiology of Insecta, Vol. 3,* M. Rockstein, ed. Academic Press, New York.

Sokal, R. R., and F. J. Rohlf. 1981. *Biometry, the Principles and Practice of Statistics in Biological Research.* W. H. Freeman, San Francisco. 859 pp.

White, F. M. 1974. *Viscous Fluid Flow.* McGraw-Hill, New York. 725 pp.

Williams, T. A. 1994. A model of rowing propulsion and the ontogeny of locomotion in *Artemia* larvae. *Biol. Bull.* **187:** 164–173.

Reference: *Biol. Bull.* **187:** 164–173. (October, 1994)

A Model of Rowing Propulsion and the Ontogeny of Locomotion in *Artemia* Larvae

TERRI A. WILLIAMS*

Department of Zoology NJ-15, University of Washington, Seattle, Washington 98195

Abstract. Newly hatched *Artemia* larvae use one pair of limbs to locomote. During development they gradually add additional limbs along the elongating trunk. As larvae grow, body length increases from about 0.4 mm to 4 mm, mean swimming speed increases from 1.8 mm s^{-1} to 9.9 mm s^{-1}, and frequency of antennal beat decreases from 9.5 to 6.7 Hz.

As new limbs are added, they become active in the metachronal rhythm of pre-existing limbs.

The body velocity oscillates as early larvae swim; later larvae swim without a cyclic acceleration and deceleration of the body. The change in the pattern of swimming is correlated with the addition of propulsors and a transition in the relative importance of viscous and inertial effects that determine the propulsion in subsequent stages. Reynolds number (based on body length) increases from 2 to 37.

A theoretical analysis of rowing propulsion at these intermediate Reynolds numbers shows that initial development of new limbs in *Artemia* larvae is unimportant for propulsion.

Rowing propulsion at the low Reynolds numbers is drag-based; as Reynolds number increases, inertial effects become more important, and unsteady forces on the body become significant in the balance between limb and body. A glide of the body develops at the end of the powerstroke, and relative limb velocity changes.

Introduction

Many animals span a broad range of sizes during the course of their complete life cycles. Animals that are active and motile during growth are subject to potentially large differences in the forces they experience during locomotion. Most studies of locomotion have focused on adults whose wings or fins are unlikely to undergo further changes in size or shape (*e.g.*, Wu *et al.*, 1974). Only rarely have comparisons included successive ontogenetic stages of a single species (*e.g.*, Katz and Gosline, 1992). I have analyzed swimming during the larval period in the crustacean *Artemia*. How does function develop in species with active larval forms having different morphologies and locomotory systems than the adults they will become? For animals that swim, ontogenetic changes in size and shape will influence the actual mechanisms by which they propel themselves. Viscous effects predominate in the swimming of very small organisms; inertial effects predominate in the swimming of very large organisms.

The developmental pattern of *Artemia* is unlike that in the more familiar arthropods that exhibit radical changes in body form from one molt to the next. These small crustaceans change gradually as they grow; *i.e.*, they are anamorphic developers. When they hatch, they swim with one pair of limbs, the second antennae (hereafter antennae). These limbs dominate propulsion during the first half of larval life and are gradually succeeded by a series of limbs that develop sequentially on the trunk. In contrast to an animal that radically changes its morphology between one molt and the next, an *Artemia* larva must coordinate new pairs of limbs with pre-existing ones (Fryer, 1983). The antennae and the trunk limbs are coordinated in a metachronal rhythm, while growth and the gradual acquisition of new limbs effectively reset the body trajectory and the relative motions of the limbs and body at each stage. How does locomotion change as an animal proceeds through the size and shape changes of ontogeny?

To explore changes in the mechanics of swimming in animals too small for direct measurement, I built a physical model of the limb to empirically determine force coefficients acting in flow regimes relevant to developing *Ar-*

Received 4 June 1993; accepted 19 July 1994.

* Present address: Department of Anatomy, University of Vienna, Währingerstrasse 13, A-1090 Wien, Austria.

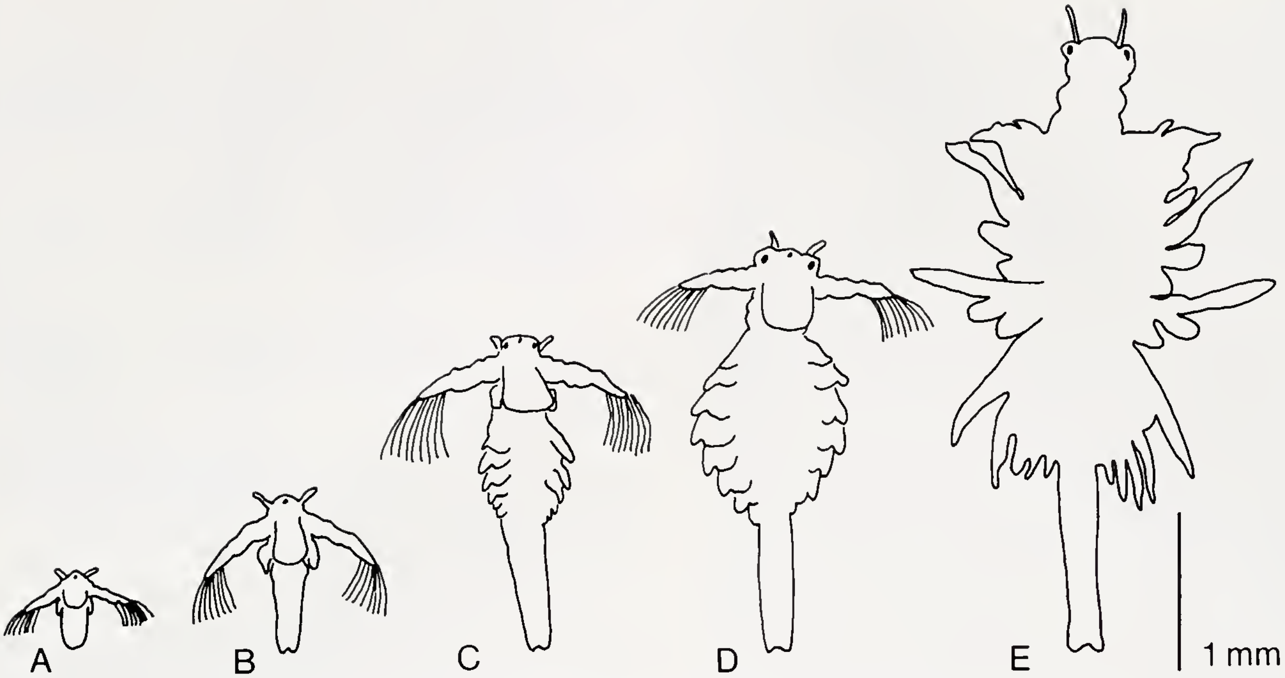

Figure 1. Selected stages to show the gradual development of *Artemia* larvae. (A) Nauplius. (B) Post-nauplius with rudiments of limbs developing on the trunk. (C) Larva with four active trunk limbs. (D) Larva with eight active trunk limbs. (E) Animal with 11 active trunk limbs.

temia larvae (Williams, 1994). Here I develop a theoretical model of swimming by antennal propulsion that incorporates those results. I predict the swimming movements of a body propelled only with a single pair of limbs by balancing the thrust produced by the limbs with forces on the body that resist motion. Because the larvae use only one pair of limbs upon hatching, I can compare body movements predicted by the model with actual movements of the larvae and thus evaluate the accuracy of the model. I then ignore the development of trunk limbs and ask, How would swimming change if the initial propulsive system were scaled up in exactly the same way the larvae grow? How would the antennae alone drive the body at later larval stages? Comparisons with actual later stage larvae allow me to dissect increases in size from changes in morphology. Does functional change correlate simply with morphological change? *e.g.*, how important are the additional trunk limbs in generating thrust?

Past studies of locomotion have been based on the assumption that thrust production by small rowing animals is purely drag-based (Nachtigall, 1980; Zaret and Kerfoot, 1980). Although *Artemia* hatchlings swim at fairly low Reynolds numbers, they grow through a size and speed range that includes fluid regimes in which inertia becomes important. Not only does drag scale differently at low and high Reynolds numbers, but also, at high Reynolds numbers, momentum can be transferred simply by the accelerations and decelerations of fluids (Daniel, 1984). I include both of these possible scale effects such that the model is free to reflect the different flow regimes that the larvae experience.

Materials and Methods

Animals

Artemia larvae grew at room temperature (~ 21°C) in an aerated brine solution of 35–40‰; the animals fed on varying diets of yeast and green algae. The number of molts was not crucial to my study, so I staged the larvae as follows: (1) newly hatched larva (nauplius)—the most oblate form with no differentiation of the trunk region, yolk still present; (2) larvae with visible limb buds—differentiation in the trunk region has led to visible protrusions of what will be limbs, and body is more elongate; (3) a series of larval stages identified by the number of actively beating trunk appendages present. This series of stages terminated with forms that have attained the adult complement of 11 pairs of trunk appendages and have lost the larval form of the second antennae (Fig. 1).

Filming

I filmed the larvae with a Locam high-speed movie camera running at 200 frames per second. The time between frames, 0.005 s., was accurate to ~5% as measured by the slippage of a timing marker made by the camera on the edge of the film. Either an Olympus BH microscope with transmitted illumination or a Wild M5 dissecting scope with fiber optic epi-illumination magnified the animals for filming. I tried to minimize wall effects by designing the filming chambers according to the formula, $y/\ell > 20/Re$, to calculate y, the shortest distance to the nearest wall (Vogel, 1981), where ℓ is some characteristic length. I chose body length. I used chambers: 22 × 22 × 5 mm and 22 × 22 × 8 mm. The animals tended to swim in a plane parallel to the bottom of the chamber and, therefore, to stay roughly in mid-chamber. However, since the animals were free-swimming, the actual sequences captured on film and digitized came from various locations within the chamber.

The obvious constraints of using high-speed cine-photography to film free-swimming animals prevented me from gathering data on many individuals from each stage. Results here are from measurements on individuals and reflect the clearest and most complete sequences. The results are limited because I cannot include variation, either individual or stage-specific, but they are supplemented by hours of viewing time that confirm the developmental trends I present. My description is supported by Barlow and Sleigh (1980), who report limb beat frequencies of 8–10 Hz in early stages and 6–7 Hz in later stages, and the same increase in both absolute and relative body length. Larvae do show variation in limb length, etc., at a given stage—due in part to rearing conditions—but this variation should not materially change the gross developmental trends reported here.

I digitized body motions from the films with a Bitpad digitizer. I chose sequences in which the animal remained in the plane of focus and digitized both the anterior- and posterior-most point on the body. The variability in measurements of body length ranged from a standard deviation of 0.01 mm in the smallest animal, to 0.05 mm in the largest. The distance between the two points provided a measure of body length, and the displacement of a single point in successive frames provided a measure of body velocity.

I quantified limb motions by digitizing the most proximal and distal points along the limb plus an arbitrary number of points along the edge of the limb. The collection of points from each frame defined a curve that could subsequently be fit with a small number of segments to calculate relative velocities along the limb. This procedure precluded the problem of trying to follow ill-defined landmarks on the limb from one frame to the next.

To quantify the asymmetry of stroke due to the curling of the antennae and the collapse of setae during the recovery stroke, I measured the projected area, S_a, of the limb perpendicular to the body axis at the 90° position during the power stroke and the recovery stroke and computed the ratio of the two areas.

Force balance for predicted body velocity

To predict the instantaneous motion of a body propelled by a single pair of limbs, I used a simple linear momentum balance (*e.g.*, Daniel and Webb, 1987) for the forces of the limbs and forces on the body.

I prescribe the variation of limb angle with respect to the long axis of the body, or angular position, θ, based on sinusoidal motion:

$$\theta(t) = \theta_o + (A/2)\,(1 - \cos(\omega t)); \qquad (1)$$

where A is the amplitude of limb beat and ω, the angular frequency, $= 2\pi f$, ($f =$ frequency), and θ_o is the starting angle (Fig. 2).

Limb speed at the tip of the limb is given by a linear combination of its angular frequency and the speed of the body (U_b). I assume flows parallel to the limb contribute negligibly to thrust. The normal component of limb velocity, U_a, is given by:

$$U_a = (-\ell d\theta/dt + U_b \sin\theta); \qquad (2)$$

where ℓ = length of the antenna and U_a depends on $-(\ell d\theta/dt)$ due to the convention of choosing forward body velocity as the positive direction (*i.e.*, thrust acts in the opposite direction).

I use this speed to calculate two types of forces that might arise from limb motion: the drag force and the unsteady, or added mass, force. I assume that the limb moves symmetrically about the axis perpendicular to the body and that only the component of flows parallel to the long axis of the body contribute to generating thrust.

The drag force of the limb, D_a, is proportional to the velocity normal to the limb and is perpendicular to the limb in direction:

$$D_a = 0.5\rho S_a(U_a)^2 C_{da}; \qquad (3)$$

where ρ is the density of the fluid, S_a is the projected surface area of the limb, and C_{da} is the coefficient of drag on the limb. The ratio of surface area on the power stroke to recovery stroke is 3.3:1.

For both C_{da} and C_{db}, the coefficient of drag on the body, I use $C_d = 1 + 10Re^{-2/3}$. I use this coefficient of

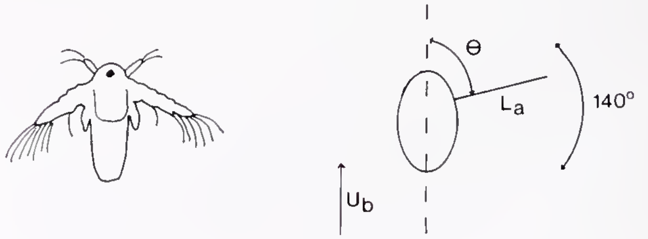

Figure 2. Forces on a pair of limbs are calculated on the basis of a prescribed sinusoidal motion. These are balanced by forces acting on a body to give instantaneous body velocity. U_b is body velocity, L_a is limb length, and θ is limb angle relative to the long axis of the body.

Table I

Morphological and kinematic parameters of selected larval stages and comparison to model predictions

	Measured values					Model predictions	
Stage	Body length (mm)	Antennal length (mm)	Freq. (Hz)	Average speed (mm s^{-1})	Reynolds number	Reynolds number (pred.)	Volume/stroke (normalized)
Nauplius	0.39	0.25	9.5	1.8	2	2	1.2×10^{-2}
Limb bud	0.77	0.5	9.1	4.4	5	9	1.8×10^{-2}
Limb bud	0.77	0.5	9.1	3.3	5	NA	NA
4 trunk limbs	1.79	0.6	8.3	8.4	14	17	4.3×10^{-2}
8 trunk limbs	2.58	0.6	6.7	8.1	20	NA	NA
11 trunk limbs	3.87	*	5.1	9.9	37	NA	NA

NA: Comparison not made.
* Metamorphosed into adult form.

drag because it most accurately mimics the behavior of a physical model of the limb tested under similar hydrodynamic conditions (Williams, 1994). The Reynolds number, $Re = \rho \ell U/\mu$, where ρ = fluid density, ℓ = some characteristic linear dimension of the object—in this case the length of the limb—U = average speed, and μ = viscosity of the fluid. To calculate C_{db}, I divide the expression for C_d at intermediate Reynolds numbers by 1.5 to account for the long axis of the body being parallel to flow instead of perpendicular to flow (Vogel, 1981). In this case, the characteristic length for Reynolds number calculations is body length.

I also account for any unsteady forces that arise in the fluid as a result of the acceleration of the fluid adjacent to the limb. Unsteady forces are proportional to the rate of change of the velocity of the limb; I assume the component parallel to the limb contributes negligibly to thrust. I define the acceleration of the limb:

$$dU_a/dt = (-\ell d^2\theta/dt^2 + dU_b/dt \sin \theta). \qquad (4)$$

The unsteady force on the limb, G_a becomes:

$$G_a = \alpha \rho V_a dU_a/dt; \qquad (5)$$

where α is the added mass coefficient, which I assume = 1 (Daniel, 1984), and V_a is the volume of the limb, which I assume to be cylindrical.

The sum of the drag and unsteady forces, (3) and (5), gives the total thrust produced by the limb:

$$F_a = 0.5\rho S_a(-\ell d\theta/dt + U_b \sin \theta)^2 C_{da} + \alpha \rho V_a(-\ell d^2\theta/dt^2 + dU_b/dt \sin \theta). \qquad (6)$$

This force is balanced by the two analogous forces on the body as well as by body inertia, and the total momentum balance becomes:

$$2[0.5\rho S_a U_a^2 C_{da} + \rho V_a dU_a/dt] = 0.5\rho S_b U_b C_{db} + 2\rho V_b dU_b/dt; \qquad (7)$$

where S_b = the surface area of the body and V_b = the volume of the body, which I assume to be a cylinder whose volume is calculated based on body length. Limb forces are multiplied by 2 to account for the pair of limbs.

I solve for U_b numerically using a fourth-order Runge-Kutta numerical scheme (Boyce and DiPrima, 1977); I wrote the computer code. For each larval stage simulated by the model, I input frequency of antennal beat (f), body length (ℓ_b), and antennal length (ℓ_a), all measured from high-speed films.

Results

Kinematics

What limbs are present and active as the larvae mature? Artemia hatches as a nauplius larva: the body is ovoid and bears three pairs of appendages (Fig. 1) that beat metachronally. But because the other two pairs of limbs are small relative to the antennae, the animal effectively swims with only the antennae. The antennae are approximately 0.3 mm long and project laterally from the body; they are cylindrical in cross-section and covered by a flexible cuticle. The distal part of the limb bifurcates and bears long setae that fan out in a plane perpendicular to the direction of forward swimming. This fan accounts for approximately 75% of the projected surface area of the limb and, as the limb oscillates in a rowing motion, it alternately opens and shuts.

As *Artemia* passes through successive larval stages, the body elongates 10-fold (from 0.39 mm to 4 mm; Table I), and limbs are added serially along the lengthening body (Fig. 1). These limbs gradually overtake the antennae in size. In contrast to the cylindrically shaped antennae that project laterally, the trunk limbs are flat, leaflike appendages that project ventrally from the body. These limbs grow gradually, with the anterior-most appendages developing first. At any given time there is a series of trunk limbs in progressive stages of maturity; the full development of each limb requires several molts. The antennae remain similar throughout larval development, although their length relative to body length decreases (Table I).

How does the body move at different stages? The average swimming velocity increases during development from roughly 2 mm s^{-1} to 10 mm s^{-1}. This increase in speed coupled with the increase in body length leads to a change in Reynolds number from 2 in the newly hatched larva to almost 40 in the last larval stage (Table I). The time-course of body motion changes even more strikingly. The young nauplius ratchets through the water at high frequency, each beat cycle yielding a discrete forward lurch and backward slip of the body. There is no glide in the nauplius: at the end of the power stroke, the body virtually stops moving (Fig. 3A). The effect is a visibly jerky mode of swimming due to the continuous oscillation of the body back and forth in the water.

Later, as the more complicated rhythms of the developing metachrony of the trunk limbs arise, the axial body movements, although still pulsatile, gradually become less so. As the initial trunk limbs develop, the body develops a glide past the end of the power stroke of the antennae. This glide grows in duration as more limbs develop and begin to beat (Fig. 3B). When four pairs of trunk appendages are beating, the larvae no longer experience any backward motion. The role of the antennae is still quite distinct: as in the earliest stages, the peak body velocity is midway during the power stroke of the antennae (0.03 s; Fig. 3C), indicating that the power stroke still produces the greatest thrust. With eight pairs of trunk limbs present, the body still oscillates in the water, but multiple limbs act simultaneously to propel the animal, so it is difficult to relate the movement of the body to the action of any single pair of limbs (Fig. 3D). After 11 pairs of trunk appendages are added, the larval form of the antenna is lost. The movement of the body at this stage is more or less smooth and nonoscillatory (Fig. 3E).

The movement of the limbs relative to surrounding fluid changes. The stereotyped stroke of the antennae relative to the body during larval development does not result in a stereotyped pattern of movement relative to the surrounding fluid. Figure 4 shows the velocity distribution relative to still water along the length of the antennae for two stages: a newly hatched larva and a larva with four actively beating trunk limbs. For a newly hatched larva, midway through the power stroke (first half of the graph, Fig. 4A), the velocity near the distal end of the appendage is actually lower than at the proximal end. This velocity distribution along the limb makes it appear as though the limb virtually pivots around a point near the distal part of the limb. In later stages, the distal portion of the antennae moves faster than the more proximal parts (Fig. 4B).

Model predictions

Comparison of larval body trajectories and predicted body trajectories. Although the model is based on thrust production by a single pair of limbs, it predicts some of the changes in body trajectory experienced by the morphologically complex larvae. Figure 5 shows the measured body velocity per limb beat cycle superimposed on body velocities predicted by the mathematical model for an animal similar to each stage in body and antennal lengths and limb beat frequency (Table I). The predicted body velocities mimic measured larval body velocities in certain important respects:

1. The model predicts a negative body velocity during the recovery stroke; this is large for early stages and decreases in later stages. The decrease in the degree of axial oscillations in swimming (*i.e.*, positive and negative body velocities associated with the power and recovery strokes) predicted by the model closely matches the movement of a larva with no active trunk limbs (Figs. 5A, B) and even that of a larva with four active trunk limbs (Fig. 5C). At the stage where eight trunk limbs are continuously and metachronally active, the animal swims more smoothly than the model—which is based on antennal rowing alone—predicts (Fig. 5D).
2. The negative velocity of the body, associated with the recovery stroke of the antennae, is delayed in successive larval stages. The model predicts this delay: in small animals the body slips backward with the onset of the recovery stroke halfway through the limb beat cycle; in larger animals a glide develops that carries the body forward beyond the onset of the recovery stroke.
3. During early larval stages, the magnitude of body velocity increases. The model also reproduces this trend (Fig. 5A–C).

Balance of forces. Figures 6A–C represent the balance of forces through the single cycle of limb motion that produced the predicted swimming trajectories in Figures 5A, B, C. The most striking change during development is the increase in the contribution of the unsteady forces on the body. Initially, the Reynolds number is low, ~2 (Table I), and the interaction of limb and body viscous drag forces largely determines the body velocity. In later stages, unsteady effects come into play. Unsteady forces on the body tend to resist changes in body velocity. At the onset of the power stroke, they resist acceleration of the body. These trends make the limb and body motions

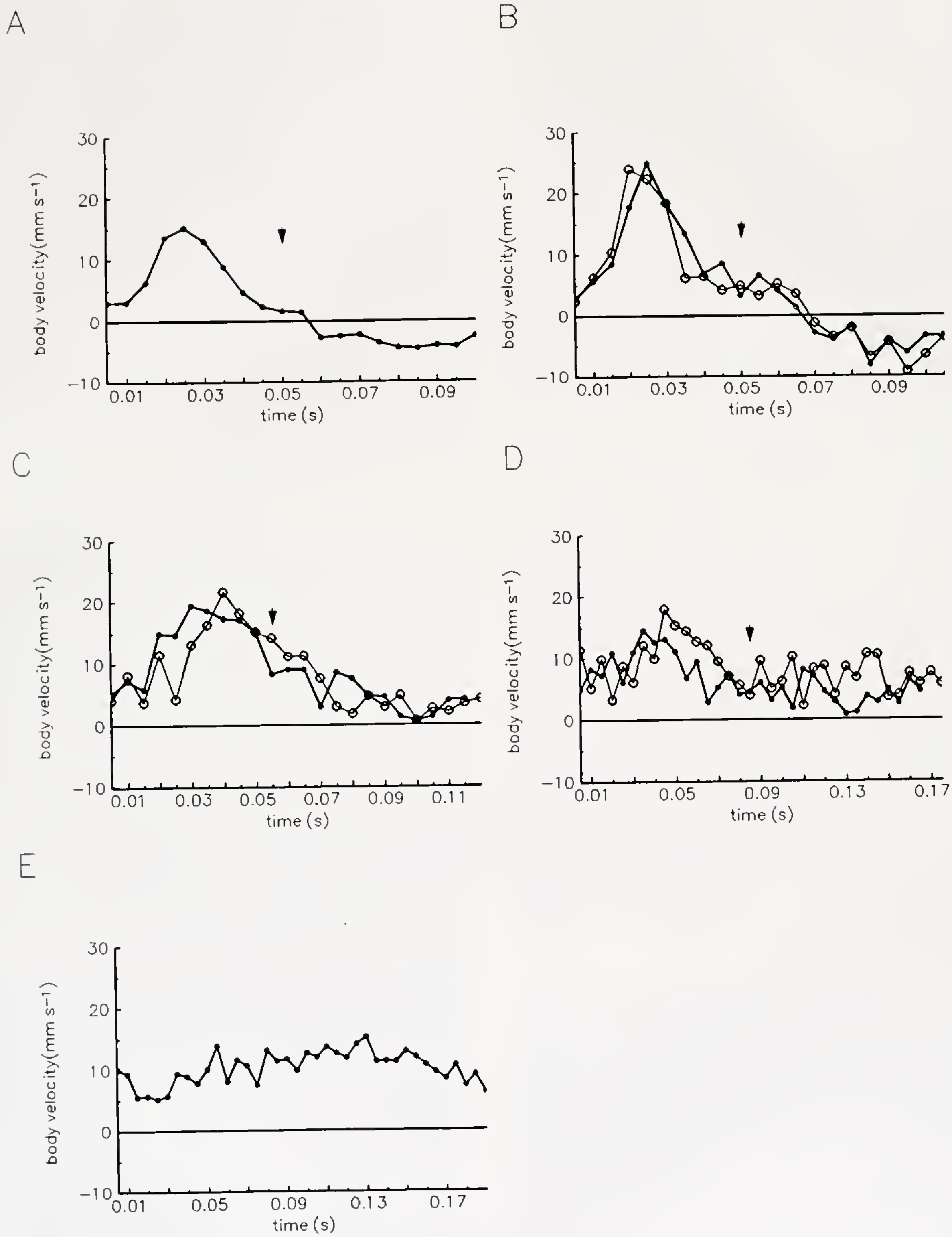

Figure 3. Body velocity of *Artemia* larvae (relative to still fluid) at different stages in larval development. Letters designate stages as indicated in Figure 1. Negative velocity represents backward movement of the body in the water. Arrows mark onset of recovery stroke. B–D illustrate two individuals each to give an idea of individual variation.

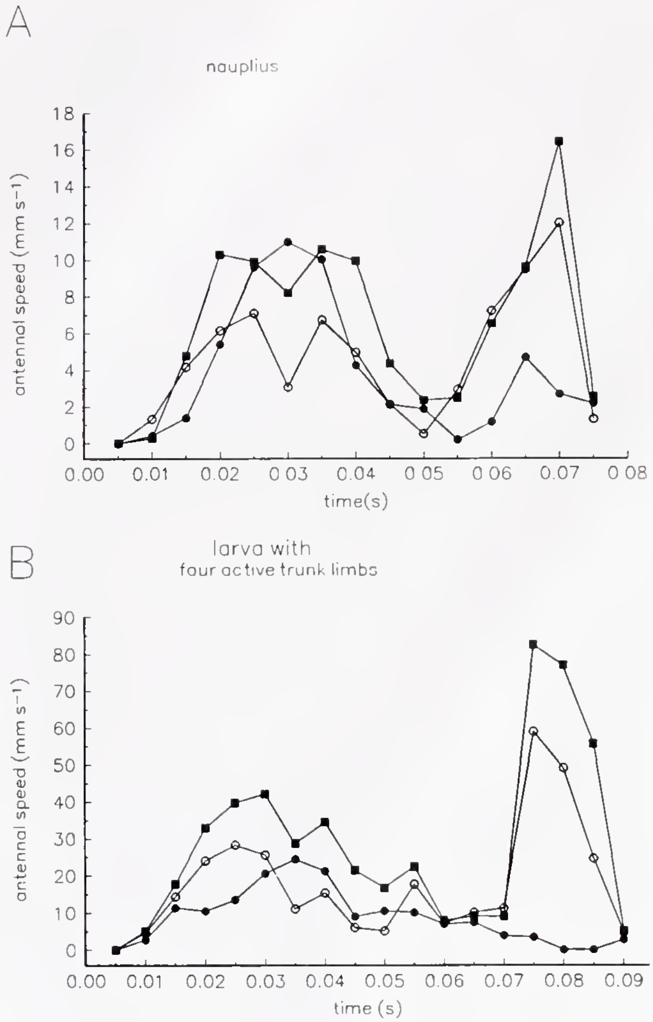

Figure 4. Typical velocity distribution of three points, from proximal to distal, along the antennae for a representative nauplius (A) and a larva with four active trunk limbs (B). Proximal point, filled circles; mid-point, open circles; distal point, filled squares. Both graphs begin at the onset of the power stroke and measure velocity relative to a fixed frame of reference.

out of phase; peak limb velocity precedes body velocity as thrust is required to overcome the unsteady forces on the body (Fig. 7). At the end of the power stroke, however, when the limb undergoes reversal, unsteady forces on the body resist deceleration and tend to carry the body forward even as the limb is generating negative thrust (Fig 6B). These unsteady forces increase in simulations of later stages, giving rise to an increased glide on the body (Fig 6C).

How do the propulsive limbs operate differently as the balance of forces changes? The change in the balance of forces during growth gives rise, not only to differences in body velocity during a cycle of limb beat, but also to differences in the movement of the propulsive limbs. As stated above, the growth of unsteady effects shifts the phases of peak limb motion relative to peak body motion. In addition, the velocity distribution along the limb, relative to still water, changes with the growth of unsteady effects. When limb and body movements are in phase, the distal part of the limb moves relatively little with respect to distant surrounding fluid as it swings in the power stroke (Fig. 7A). In contrast, with the shift in phase predicted for later stages, the limb sweeps a broad arc through the water. This change mimics the one in relative antennal velocity measured from high-speed films (Fig. 4A, B). To index the change in relative antennal velocity, I calculated the volume of space through which the distal one-third of the limb moves. To allow comparison between different stages, I normalized these volumes by dividing by the length of the limb cubed. In simulations of later stages, the limbs move through a proportionately greater volume than in earlier stages (Table I).

Discussion

Artemia develop from a small, rotund nauplius that ratchets along with one pair of oars to a multi-limbed adult that glides continuously through the water. As the animals approach the adult morphology by growing and adding limbs along the trunk, their average swimming speed increases and, more strikingly, the jerky swimming of the hatchling is transformed into the smooth gliding of the adult. The gradual change in swimming corresponds to the gradual addition of trunk limbs. But, as indicated by the increase in Reynolds number during development, this change in swimming also corresponds with a change in forces that determine movement. When *Artemia* hatch, viscous forces have a large role in the flows around the animal: abrupt reversals of the limb are manifest immediately as abrupt changes in body motions. As larvae grow, inertial effects become more important: the body is carried beyond the immediate movement of the limbs. A theoretical analysis of rowing locomotion shows that early changes in kinematics are purely a mechanical consequence of scaling and not tightly linked to the complex morphological changes the larvae undergo. The activity and coordination of trunk limbs appear unimportant for propulsion during early stages, even when four trunk limbs are actively beating.

This result depends on the fact that as inertial forces play an ever greater role in propulsion, unsteady forces on the body begin to develop. Unsteady effects are predicted to provide thrust for animals with oscillating limbs (Daniel, 1984). From kinematic analysis of successive stages of larval herring, Batty (1984) postulated that the change in undulatory swimming in later larval stages is due to increasing importance of inertial effects. Blake (1986) calculated that unsteady forces on the limbs of

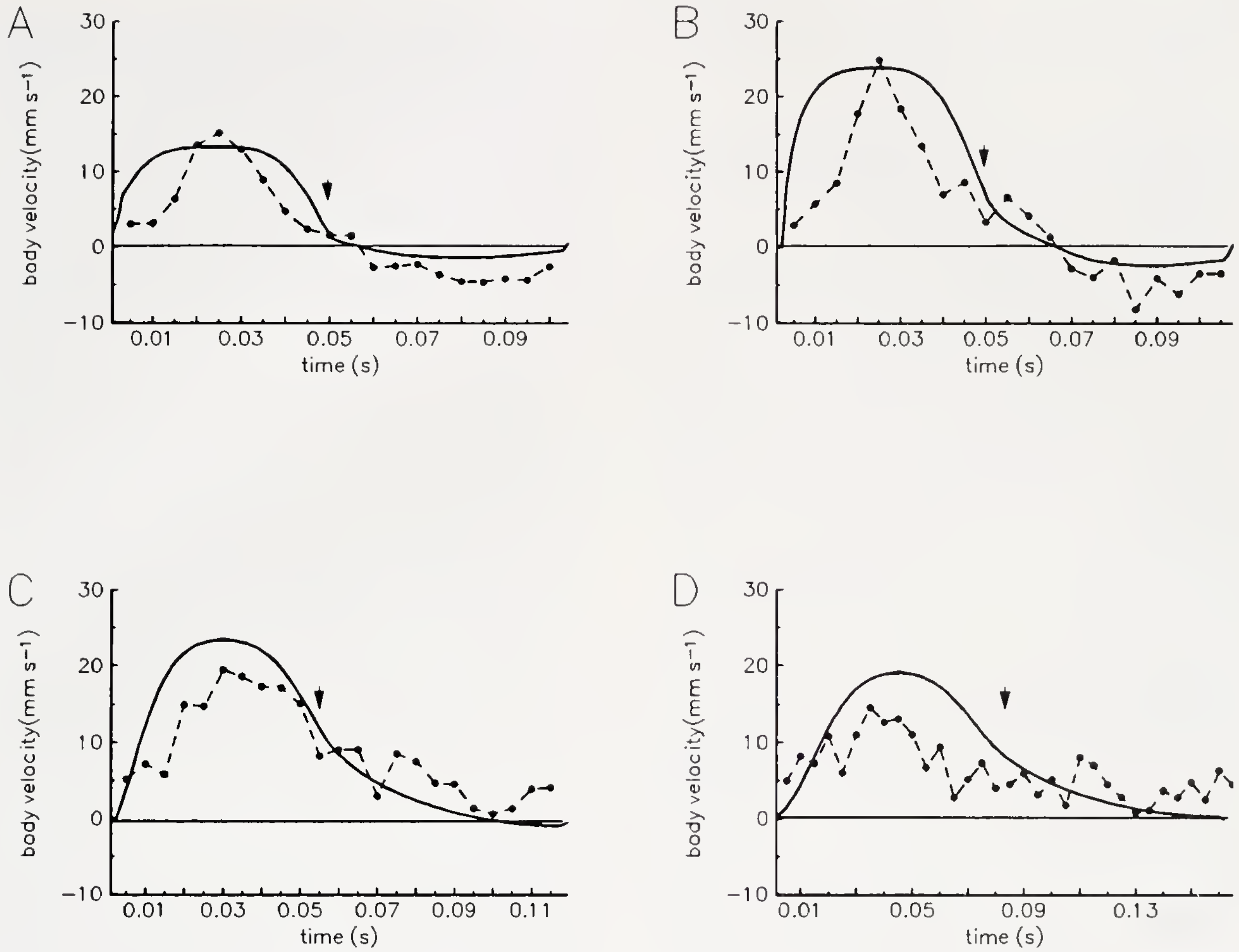

Figure 5. Measured body trajectory of *Artemia* larvae that are both growing and adding limbs, compared with the predicted velocity of an animal with a single pair of limbs but of the same dimensions and frequency as the developing larvae (see Table I). The solid lines illustrate body motion through one cycle of antennal motion for four different larval stages corresponding to A–D in Figure 3. The dotted lines represent body motion predicted by the model. Negative velocity indicates backward movement of the body relative to the fluid. Arrows mark onset of recovery stroke.

rowing water boatmen (Re = 800) could produce roughly one-third of the thrust during the power stroke. As a result of increases in larval size and speed, unsteady effects on the body grow and cause the balance between limb and body to shift. This shift results in a glide of the body at the end of the power stroke and a higher relative velocity at the tip of the limb. Unsteady forces calculated for the limb are negligible, a result corroborated by force measurements on a physical model of an antenna operating at similar Reynolds numbers (Williams, 1994).

Mechanical analyses of animals that paddle have typically dealt only with the adult form and have assumed forward, steady motion (*e.g.*, Blake, 1979; Nachtigall, 1980). Because it does not assume steady motion, but instead couples limb and body motion, the model is free to predict changes in the *time course* of swimming motion on the basis of changes in hydrodynamic regime. Interpretations of biologically relevant flows based on Reynolds numbers calculated from time-averaged swimming speeds may fail to recognize the potential importance of unsteady effects in animals that use reciprocating limbs. In this model, one system of oscillating limbs produces different swimming behaviors even over a narrow range of Reynolds numbers, 2–40.

The antennae that propel the hatchling remain present and grow as the animal grows, and they continue to move in a stereotyped manner. Because of their coupling to the body, they have a different velocity profile along their length as the force balance between limbs and body changes during larval development. This is likely to have consequences for the function of these limbs. Cheer and Koehl (1987) have shown theoretically that structures such

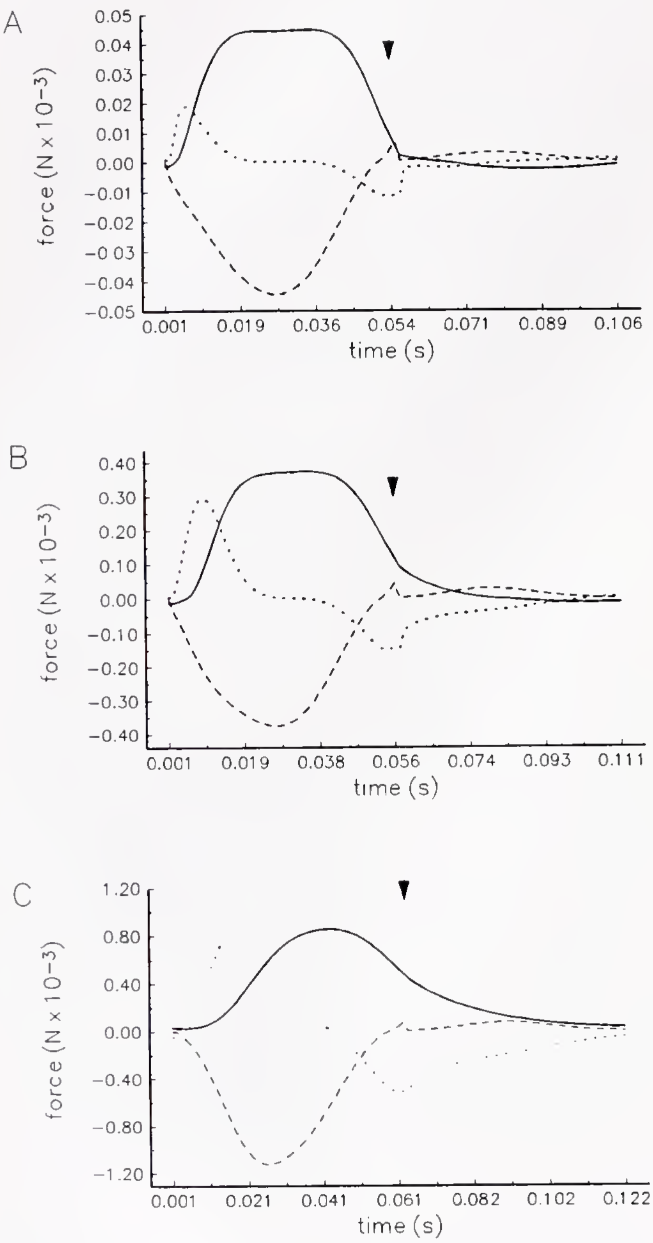

Figure 6. Balance of forces through one cycle of the antennal motion that gives rise to the body motions predicted in Figure 5A–C. By convention, positive thrust is in the direction opposite to forward body motion. Solid line = body drag; dashed line = thrust of limb; dotted line = unsteady force on the body. In C, the unsteady force on the body propels the body beyond the onset of the recovery stroke. (The calculated unsteady force on the limb was always 2 orders of magnitude lower than any other force and is omitted from the graphs.) Arrows mark onset of recovery stroke.

as setose limbs (*i.e.*, cylinders bearing other cylinders), will either allow fluid through the array or force it around, depending on the importance of viscous drag. Some copepods do not use a sweep net to feed, but individually handle fluid parcels surrounding a food item (Koehl, 1981). Other species use the same appendage and the same movements essentially as a filter. In spite of the stereotypic form and movement of the antennae of *Artemia* larvae, their movement relative to the surrounding fluid changes during development. This change in relative limb velocity agrees with a study by Barlow and Sleigh (1980), who postulate that early stages may be unable to capture food because of the relatively low fluid velocities at the distal end of their antennae. A similar conclusion is reached by Fryer (1983) for another anostracan, *Branchianecta ferox*.

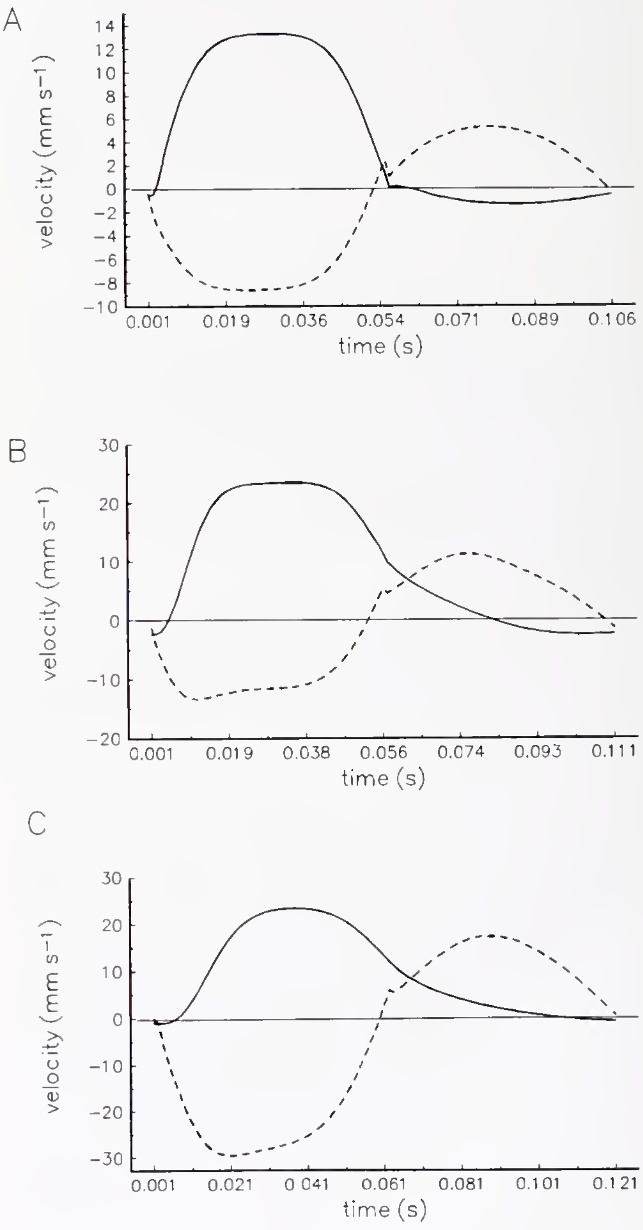

Figure 7. Relative limb and body motions corresponding to Figure 6A–C. Solid lines = body velocity; dotted lines = limb velocity. Positive velocity is in the direction of body motion.

He excludes the possibility that the distal setal fan on the larval antennae functions in feeding and postulates that this function is performed by a spine in a more proximal position on the limb. Levering or stepping through the water generally occurs in larvae that use a single pair of oars. This movement, which occurs in barnacle larvae (pers. obs.), limits our using tethered animals to study behaviors that depend on natural flow situations (*e.g.*, feeding; Moyse, 1984), even though such studies do isolate and help clarify other aspects of movement.

In insects, the aerodynamic and thermodynamic capabilities as measured by physical models scale differently with size: in small models, wings of a particular size function primarily in thermoregulation. In large models of the same relative wing length, the function of the wings is primarily aerodynamic (Kingsolver and Koehl, 1985). That analysis showed that function could simply change with size over the course of evolutionary time. This analysis of swimming in *Artemia* shows that changes in size, shape, and environment experienced by *single* individuals during larval development have consequences for the propulsive mechanisms used in swimming.

Artemia larvae pass through a series of morphological stages as they develop. Functional change may or may not correspond directly to morphological change; *e.g.*, I claim that activity of initial trunk limbs is unimportant in propulsion in *Artemia* larvae, although these limbs obviously propel later stages. Initially, these limbs could perform other roles not treated by this analysis, either mechanical (*e.g.*, stability), or nonmechanical. This model provides a mechanical analysis of swimming on the basis of the morphology of one larval stage in *Artemia*. A single pair of oscillating limbs generates body velocities that mimic the kinematic changes of an early period of development. These results illustrate how, at a particular stage in development, larval morphology engenders a range of behaviors by its very design.

Acknowledgments

I gratefully acknowledge grants from Sigma Xi, the Lerner-Grey fund for Marine Science, NSF grant DCB-8711654 to Tom Daniel, NSF grant BSR-8700523 to Alan Kohn. Tom Daniel, Joel Kingsolver, Alan Kohn, Garry Odell, Dick Strathmann, and Steve Wainwright criticized this paper at various stages.

Literature Cited

Barlow, D. I., and M. A. Sleigh. 1980. The propulsion and use of water currents for swimming and feeding in larval and adult *Artemia*. Pp. 61–73 in *The Brine Shrimp Artemia. Vol 1. Morphology, Genetics, Radiobiology, Toxicology*. G. Persoone, P. Sorgeloos, O. Roels, and E. Jaspers, eds. Universa Press, Wetteren, Belgium.

Batty, R. S. 1984. Development of swimming movements and musculature of larval herring (*Clupea harengus*). *J. Exp. Biol.* **37:** 129–153.

Blake, R. W. 1979. The mechanics of labriform locomotion. I. Labriform locomotion in the anglefish (*Pterophyllum eimekei*): an analysis of the power stroke. *J. Exp. Biol.* **82:** 255–271.

Blake, R. W. 1986. Hydrodynamics of swimming in the water boatman, *Cenocorixa bifida Can. J. Zool.* **64:** 1606–1613.

Boyce, E., and R. C. DiPrima. 1977. *Elementary Differential Equations.* John Wiley and Sons, New York. 512 pp.

Cheer, A. Y. L., and M. A. R. Koehl. 1987. Paddles and rakes: fluid flow through bristled appendages of small organisms. *J. Theor. Biol.* **129:** 17–39.

Daniel, T. L. 1984. Unsteady aspects of aquatic locomotion. *Am. Zool.* **24:** 121–134.

Daniel, T. L., and P. W. Webb. 1987. Physical determinants of locomotion. Pp. 343–369 in *Comparative Physiology: Life in Water and on Land*, P. Dejours, L. Bolis, C. R. Taylor, and E. R. Weibel, eds. Liviana Press, New York.

Fryer, G. 1983. Functional ontogenetic changes in *Branchinecta ferox. Phil. Trans R. Soc. Lond. B* **303:** 229–343.

Katz, S. L., and J. M. Gosline. 1992. Ontogenetic scaling and mechanical behavior of the tibia of the african desert locust (*Schistocerca gregaria*). *J. Exp. Biol.* **168:** 125–150.

Kingsolver, J. G., and M. A. R. Koehl. 1985. Aerodynamics, thermoregulation, and the evolution of insect wings: differential scaling and evolutionary change. *Evolution* **39:** 488–504.

Koehl, M. A. R. 1981. Feeding at low Reynolds number by copepods. *Lect. Math. Life Sci.* **14:** 89–117.

Moyse, J. 1984. Some observations on the swimming and feeding of the nauplius larvae of *Lepas pectinata* (Cirripedia: Crustacea). *Zool. J. Linn. Soc.* **80:** 323–336.

Nachtigall, W. 1980. Mechanics of swimming in water beetles. Pp. 107–124 in *Aspects of Animal Movement*. H. Y. Elder and E. R. Trueman, eds. Cambridge University Press, London.

Vogel, S. 1981. *Life in Moving Fluids.* Princeton University Press, Princeton. 352 pp.

Williams, T. A. 1994. Locomotion in developing *Artemia* larvae: mechanical analysis of antennal propulsors based on large-scale physical models. *Bio. Bull.* **187:** 156-163.

Wu, T. Y.-T., C. J. Brokaw, and C. Brennen. 1974. *Swimming and Flying in Nature.* Plenum Press, New York and London.

Zaret, R. E., and W. C. Kerfoot. 1980. The shape and swimming technique of *Bosmina longirostris. Limnol. Oceanogr.* **25:** 126–133.

Reference: *Biol. Bull.* **187:** 174–184. (October, 1994)

Transmitter-Specific Subsets of Sensory Elements in the Prosobranch Osphradium

L. P. NEZLIN[1], R. ELOFSSON[2], AND D. A. SAKHAROV[1]

[1]*Institute of Developmental Biology, Russian Academy of Sciences, Moscow, Russia, and*
[2]*Department of Zoology, University of Lund, Lund, Sweden*

Abstract. The osphradium is a putative chemosensory organ of aquatic molluscs. Previously, we identified two distinct types of primary sensory neurons in the osphradial ganglion of freshwater pulmonates, one immunoreactive to leucine-enkephalin (LEnk-ir) and another to FMRFamide (FMRFa-ir). In addition, NADPH diaphorase (NADPHd)-positive elements apparently producing nitric oxide (NO) were demonstrated in the organ. In the present study, prosobranch molluscs, which have retained the osphradial sensory neurons within the epithelium, were studied. Both types of peptidergic neurons, as well as NADPHd-positive cells, were found within the epithelium or in a basiepithelial position in the relatively simple osphradium of the mesogastropod *Littorina littorea* and in the complex, bipectinate osphradium of the neogastropod *Buccinum undatum*. Similar evidence was also obtained for another mesogastropod, *Ampullarius* sp. Transmitter-specific sensory cell types like those discovered in the osphradium are also present as single neuroepithelial cells in other organs of the mantle complex in prosobranchs and in the pelecypod *Anodonta cygnea*. We suggest that evolutionarily conservative, transmitter-specific types of epithelial and neuroepithelial sensory cells predated the osphradium, which developed as the site of their concentration while retaining characteristic subsets of sensory neurons.

Introduction

The osphradium is a molluscan sensory organ characteristic mainly of aquatic forms. Evidence suggesting its chemosensory function has been considered and summarized (Sokolov *et al.*, 1980; Croll, 1983; Haszprunar, 1985; Emery, 1992). The position and common structural features shared by osphradia of various molluscs indicate a homology of the organ across the phylum (Haszprunar 1985, 1987).

According to our previous findings in a freshwater pulmonate, *Lymnaea stagnalis,* two distinct types of osphradial sensory neurons can be distinguished immunocytochemically, one labeled with an antiserum against FMRFamide (FMRFa-ir), and another immunoreactive to an antiserum against leucine-enkephalin (LEnk-ir). Cell bodies of these primary sensory neurons are situated within the osphradial ganglion, and their distal processes penetrate the sensory epithelium. Other, nonsensory neurons within the ganglion contain neuroactive substances that were demonstrated immunocytochemically, with antisera against serotonin and methionine-enkephalin (MEnk-ir), and histochemically, with a procedure for NADPH diaphorase (NADPHd) (Elofsson *et al.*, 1993; Nezlin *et al.*, 1994).

Transmitter specificity is claimed to be a conservative feature of homologous nerve cells (Sakharov, 1970). We test this idea in a comparative study of immunocytochemically identified sensory cells: we ask whether nonpulmonate osphradia share common transmitter-specific neuron phenotypes with those of pulmonates. In addressing this question, we chose prosobranch molluscs for two reasons. First, unlike evolutionarily advanced pulmonates, most of the prosobranchs retain their osphradial sensory neurons in the supposed initial position—within the sensory epithelium of the organ (Haszprunar, 1985). Second, prosobranch osphradia demonstrate a wide range of complexity, ranging from a hardly noticeable structure in *Littorina littorea,* to a large, gill-like organ—the so-called

Received 12 November 1993; accepted 19 July 1994.

Abbreviations: FMRFa-ir, FMRFamide-like immunoreactive; LEnk-ir, leucine-enkephalin-like immunoreactive; MEnk-ir, methionine-enkephalin-like immunoreactive; NADPHd, NADPH diaphorase; NO, nitric oxide.

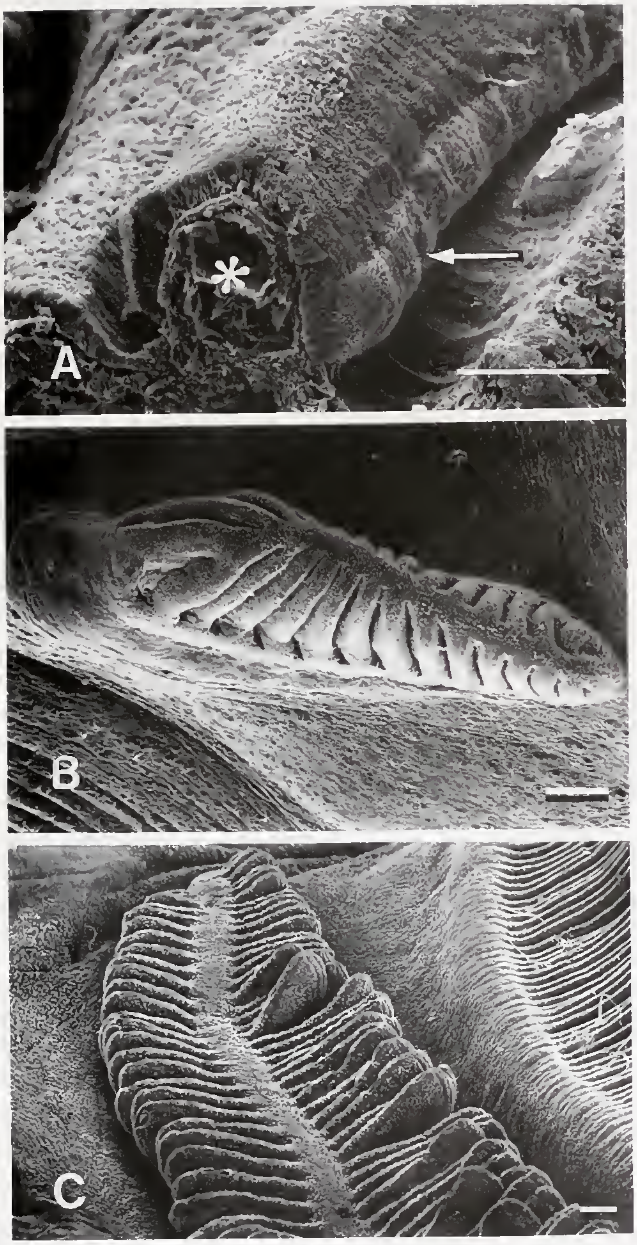

Figure 1. Scanning electron micrographs of the osphradium in the prosobranchs studied. A. *Littorina littorea.* A transverse section has been made through the osphradium. Asterisk labels the ganglion, and the arrow indicates the lateral ciliated zone of the ridge. B. *Ampullarius* sp. C. *Buccinum undatum.* Scale bars: A = 100 μm; B, C = 200 μm.

bipectinate osphradium—in *Buccinum undatum.* Our comparative study also included the morphologically peculiar organ of an ampullariid snail (Haszprunar, 1985) and the mantle epithelia surrounding the prosobranch osphradium as well as that of a pelecypod, the freshwater mussel *Anodonta cygnea,* which has a poorly developed osphradium.

Materials and Methods

Specimens of the periwinkle *Littorina littorea* (Prosobranchia, Mesogastropoda, Littorinoidea), 2–2.5 cm long, and the whelk *Buccinum undatum* (Prosobranchia, Neogastropoda, Buccinoidea), 7–9 cm long, were collected in the wild at the Kristineberg Marine Biological Station on the west coast of Sweden, and maintained in aquaria for about two weeks at about 10°C. Specimens of the freshwater snail *Ampullarius* sp. (Prosobranchia, Mesogastropoda, Viviparoidea) and the pelecypod *Anodonta cygnea* were from an aquarial culture. To dissect osphradia and surrounding tissues, animals were anesthetized in an isotonic solution of $MgCl_2$ for 20 min and then extracted from their shells.

Scanning electron microscopy

The osphradia were fixed in 2.5% glutaraldehyde (TAAB) in 0.05 *M* Na-cacodylate buffer, pH 7.3 (23 mg/ml NaCl were added for the marine species), for 2 h, and washed in the same buffer for 2 h. To remove mucus from the surface, the specimens were treated for 6 h with leech hyaluronidase (Sigma), 50–100 units/ml, in the same buffer. All steps were at room temperature. Finally, the specimens were dehydrated in an ethanol series, dryed in Balsers Union Critical Point Dryer, fixed to stubs, and coated with about 14 nm of gold in a Bio-Rad Polaron SEM Coating System. Observations and micrographs were made with a JEOL JSM-T330 electron microscope.

Immunolabeling

The dissected osphradia were fixed for 2 h at 4°C in 4% paraformaldehyde dissolved in 0.2 *M* (0.1 *M* for *Ampullarius*) Na-phosphate buffer solution (PBS), pH 7.4, washed overnight at 4°C in PBS, immersed for 1 h at 4°C in 20% sucrose in the same buffer, embedded in Tissue Tek (Miles), and frozen in liquid nitrogen. Serial sections were cut at a thickness of 20 μm with a Reichert-Jung Frigocut E 2800 cryostat and placed on chrome-alum/gelatin-coated glass slides. The slides were air-dried for 15 min, washed in PBS containing 0.25% Triton X-100 (TX), and treated at room temperature as follows:

1. Incubate for 30 min with 10% normal swine serum, diluted in PBS-TX containing 0.2% Bovine Serum Albumine (BSA, Sigma).
2. Wash in PBS-TX (3 × 20 min).
3. Incubate with primary antiserum, 1:1000, in PBS-TX-BSA (6 h).
4. Wash in PBS-TX (3 × 20 min).
5. Incubate with swine anti-rabbit immunoglobulins, 1:50, in PBS-TX-BSA (2 h).

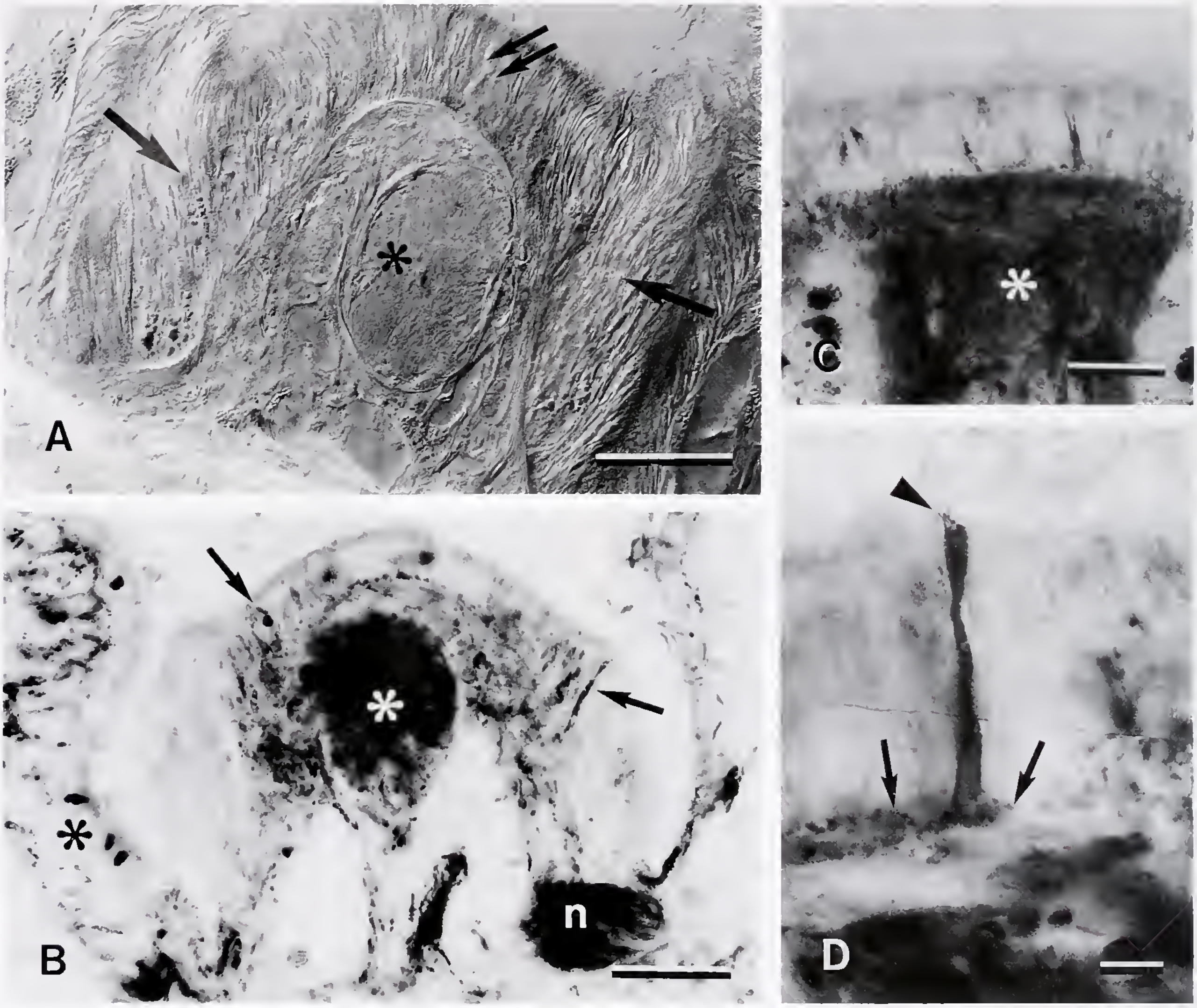

Figure 2. Transverse sections through the osphradium of *Littorina littorea.* (A) General view of an unstained specimen, interference contrast. Asterisk, the osphradial ganglion; arrows, lateral ciliated epithelium facing the groove; double arrow, the central epithelial zone. (B–D) FMRFa-ir elements, peroxidase labeling. (B) Section similar to A. White asterisk, the osphradial ganglion; black asterisk, non-specifically labeled cells in the epithelium; arrows, immunopositive epithelial cells; n, the osphradial nerve. (C) Central portion of the osphradium with immunopositive epithelial cells and intensive labeling in the ganglion (white asterisk). (D) Neuroepithelial cell in the central epithelial zone with two basal processes (arrows) and apical protrusions (arrowhead). Scale bars: A–C = 50 μm; D = 10 μm.

6. Wash in PBS-TX (3 × 20 min).
7. Incubate with peroxidase-anti-peroxidase complex, 1:100, in PBS-TX-BSA (2 h).
8. Wash in PBS-TX (3 × 20 min).
9. Wash in 0.1 *M* Tris-HCl buffer solution (TBS), pH 7.4 (2 × 15 min).
10. Incubate in 0.05% diaminobenzidine (DAB) in TBS (20 min).
11. Incubate in DAB with 0.01% H_2O_2 in TBS (20 min).
12. Wash in TBS (3 × 20 min).
13. Dehydrate in an ethanol series, and embed in Permount (Fisher Scientific).

After stage 3, some slides were treated as follows:

4. Wash in PBS (3 × 20 min).
5. Incubate with fluorescein-(FITC)-labeled swine anti-rabbit immunoglobulins, 1:50, in PBS-BSA (2 h).
6. Wash in PBS (3 × 20 min).
7. Embed in PBS-glycerol (1:1).

The slides were examined with a Leitz-Aristoplan Universal microscope. Epifluorescence equipment (excitation maximum 490 nm, emission barrier >515 nm) was used for FITC-labeled specimens. Polyclonal antisera raised against FMRFamide-, leucine-enkephalin-, and methionine-enkephalin-conjugates were purchased from Incstar (Stillwater, Minnesota). Controls included the omission of primary antibody, or its replacement with normal rabbit serum.

NADPH-diaphorase histochemistry

The osphradia were fixed in paraformaldehyde in PBS and sectioned as above. The slides were washed (2 × 15 min) in 0.05 *M* TBS (0.5 *M* for marine species), pH 8.0, at room temperature and treated according to a standard histochemical procedure. They were incubated in the darkness for 1 h, at room temperature or at 37°C, in TBS containing 0.8 mg/ml β-NADPH (Sigma), 0.4 mg/ml Nitro Blue Tetrazolium (BDH), and 0.2% TX-100. In the control solutions, β-NADPH was replaced with α-NADPH, Sigma, in the same concentration (Hope and Vincent, 1989). Then the slides were rinsed in TBS followed by distilled water, dehydrated through an ethanol series, and embedded in Entellan (Merck).

Results

In all three prosobranch species examined, the osphradium is situated in the mantle roof, at the base of the siphon, which means that it is exposed to the inhalant current of external water. Although the outer morphology varies considerably (Fig. 1A–C), the internal structures correspond to a great degree. The main constituents of the osphradium are an elongated axial cord of the nervous tissue, the osphradial ganglion, and a specialized epithelium containing several types of neuroepithelial cells (Crisp, 1973; Haszprunar, 1985). The organ also contains connective tissue, muscle fibers, and hemocoel. The ganglion is connected with the CNS via one or more branches of the supraintestinal nerve. In the epithelium, sensory (central), ciliated, and glandular zones can be recognized (Hyman, 1967).

The control preparations could be used to identify the background and unspecific staining of *Littorina* and *Buccinum* tissues by both immunocytochemical and histochemical methods. *Ampullaris*, however, is a special case (see below).

Littorina littorea

The osphradium is a relatively simple structure running alongside the left gill. Its form is that of a long ridge rising from the bottom of a groove (Fig. 1A, 2A, B). The central zone of the epithelium is at the top of the ridge, above the sausage-like osphradial ganglion. On each side of the ridge is a band of thickened epithelium identified as the ciliated zone (Crisp, 1973; Haszprunar, 1985) (Fig. 2A). Glandular zones have not been clearly indicated by earlier authors.

FMRFa-ir elements. Labeled cells were consistently seen both in the osphradial epithelium and in the ganglion (Fig. 2B). In the epithelium, they are represented by neuroepithelial cells (Fig. 2C) giving rise to a proximal neurite (Fig. 2D). The cells appear differently in various parts of the epithelium. In the central zone, they are oblong and terminate with a few short protrusions resembling reduced cilia (Fig. 2C, D). In the lateral ciliary zone, they are extremely thin and elongated (Fig. 2B, arrow). Proximal neurites extending from epithelial FMRFa-ir cells of the central zone could be traced into the basal plexus, which is connected to the osphradial ganglion. Within the ganglion, these afferent projections and processes of intrinsic FMRFa-ir neurons form a dense FMRFa-ir neuropile.

LEnk-ir elements. Neuroepithelial cells of this type show two distinct sites of localization in the osphradial epithelium. One is a narrow band of cells on top of the ridge. Within the epithelium, these multipolar LEnk-ir cells send fine processes in different directions (Fig. 3A). The other site is a band along the lateral sides of the ridge (Fig. 3B). In this case, the cell bodies are situated deep in the epithelium close to the base of the ridge and send long processes to the surface. Groups of similar basiepithelial LEnk-ir cells are consistently present in the wall of the groove and, more peripherally, in adjacent portions of the mantle wall (Fig. 3C). Fibers from LEnk-ir neuroepithelial cells concentrate mostly around and in the outer zone of the osphradial ganglion. The intrinsic neuronal population of the ganglion includes a small number of scattered LEnk-ir neurons.

MEnk-ir elements. These are absent from the osphradial epithelium. They appear as a fiber meshwork and, occasionally, as cell bodies under the epithelium and in the osphradial ganglion (Fig. 3D). In the mantle wall outside the osphradium, MEnk-ir elements are sometimes well developed, particularly in the connective tissue.

NADPHd-positive elements. The mantle epithelium on each side of, and adjacent to, the osphradium is thicker than that of the surrounding mantle wall and more closely resembles the osphradial epithelium. In this area of the mantle, a band of scattered cells stained with β-NADPH (Fig. 4A) lies close to the osphradium and just outside the groove. The cells are elongated and sometimes possess a thin distal process, but they are apparently devoid of a proximal, basal neurite. NADPHd-positive epithelial cells were otherwise absent from the mantle except for a narrow region of the so-called "mantle ridge," the outer edge of

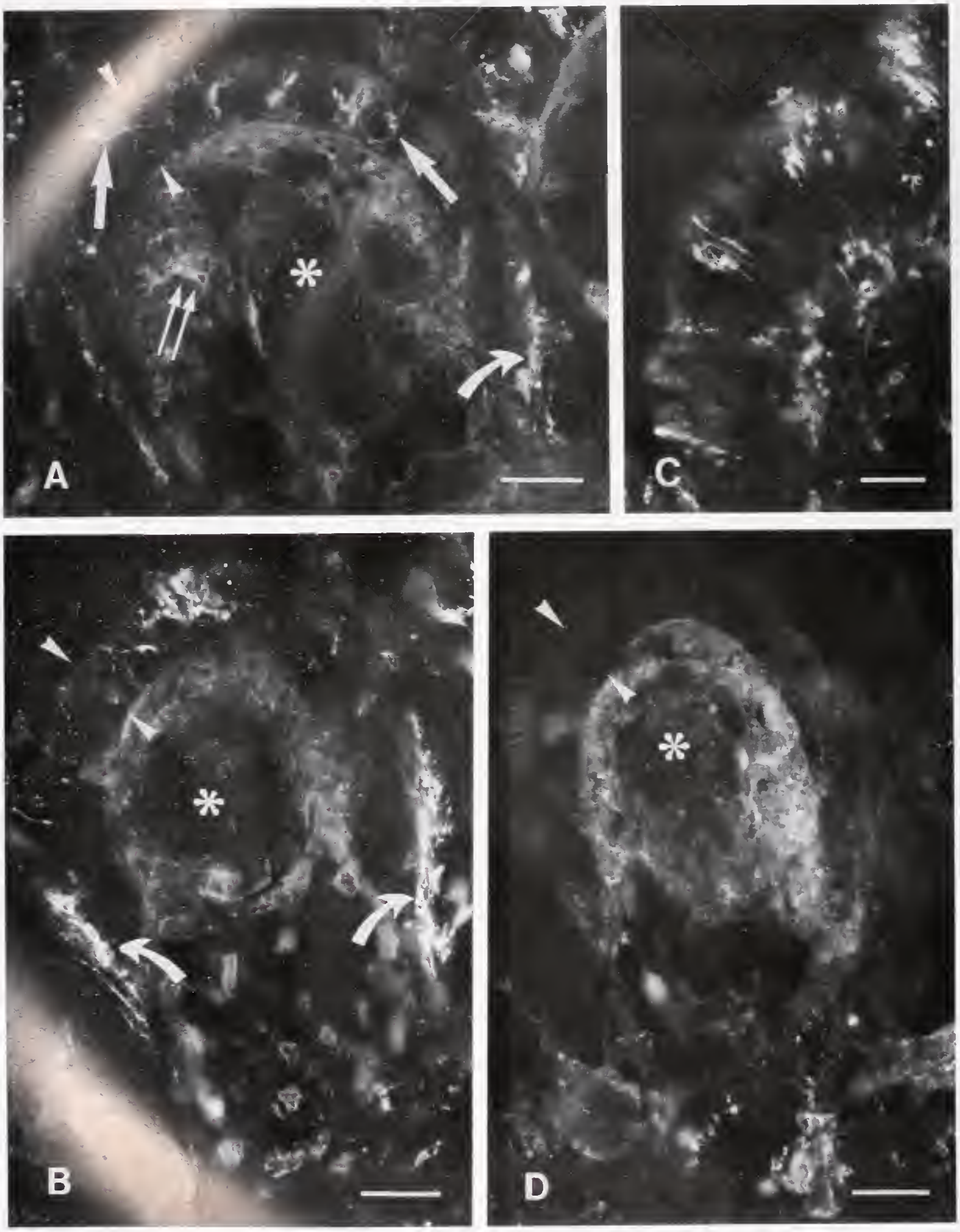

Figure 3. Enkephalin immunoreactivity in transverse sections of the osphradium of *Littorina littorea.* FITC-labeling. (A) LEnk-ir elements. Asterisk, the osphradial ganglion; arrowheads, the borders of the central epithelium; arrows, immunopositive neuroepithelial cells with branched processes; double arrow,

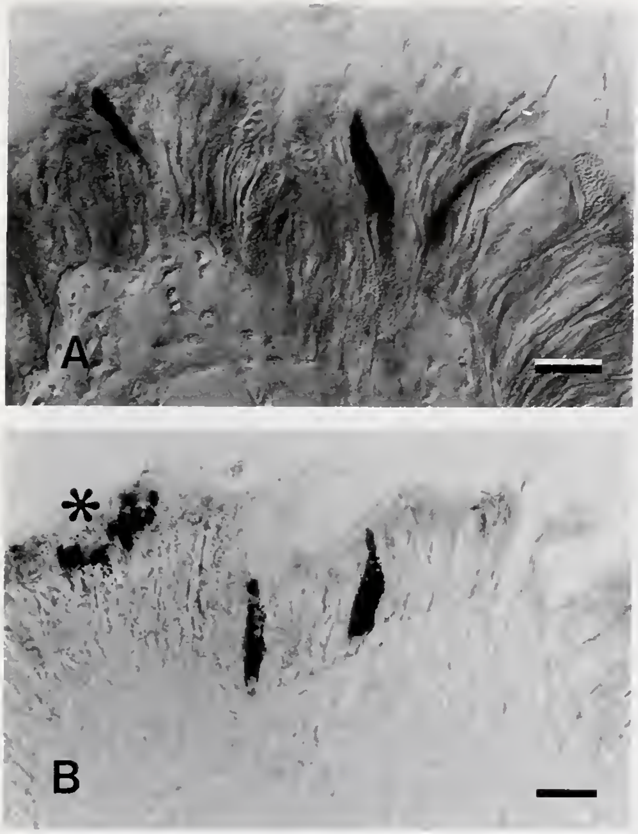

Figure 4. NADPHd-positive cells in the epithelium of the mantle wall adjacent to the osphradium (A) and of the mantle ridge (B) of *Littorina littorea* In A, the osphradial groove starts just to the right of stained cells. Asterisk in B indicates pigment granules in the epithelium. Scale bars = 10 μm.

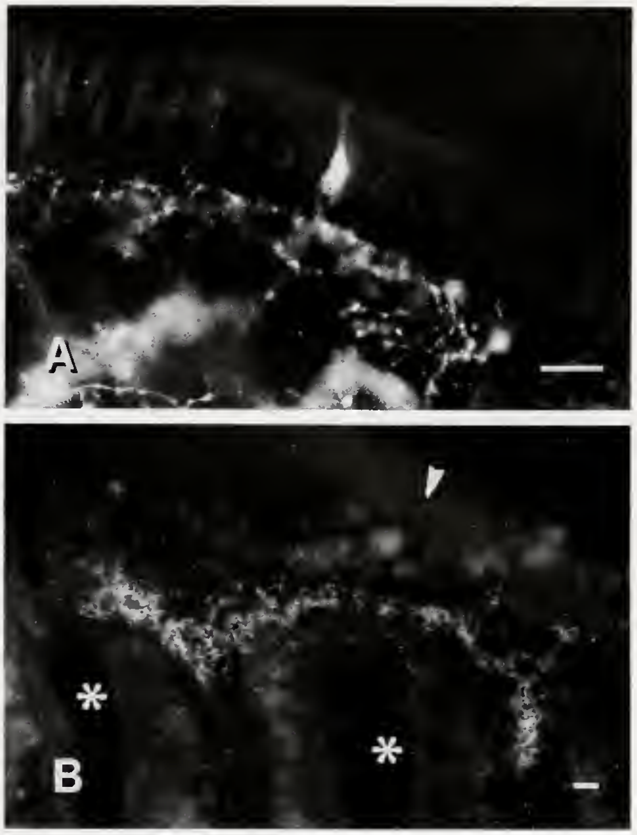

Figure 5. Immunoreactivity in a transverse section of the osphradium of *Ampullarius* sp., FITC-labeling. (A) FMRFa-ir cell body in the epithelium of the central zone with a dense plexus beneath. (B) LEnk-ir fibers in a horizontal section of the outer wall of the osphradial pockets (asterisks). Arrowhead, the outer boarder of the epithelium. Scale bars = 20 μm.

the mantle (Fig. 4B). In control preparations no staining was observed.

Ampullarius sp.

The osphradium of this mesogastropod is more complicated than that of *Littorina.* It is essentially a large oblong fold elevated over the mantle wall. A long, sausage-shaped ganglion is centrally located in the osphradium, and a broad lamella of the nervous tissue runs dorsally along the ganglion. Narrow pockets, perpendicular to the ganglion and aligned with each other on both sides (Fig. 1B), form a lamellar appearance in horizontal sections through the organ.

FMRFa-ir elements are abundant and have their cell bodies in the epithelium. Most of the cells are situated in the epithelium surrounding the ventral portion of the pocket. A smaller fraction is present in the central zone of the osphradial epithelium situated on the top of the organ (Fig. 5A).

LEnk-ir elements appear as very fine fibers in the epithelium of the outer ventral wall of the pockets (Fig. 5B). The cell bodies have a basiepithelial position and are also

---

Figure 3. (*Continued*) cell body in the ganglion; curved arrow, lateral band of immunopositive cells in the ciliated epithelium. (B) LEnk-ir elements. Curved arrows demonstrate two symmetrical lateral bands of immunopositive cells. White asterisk, the osphradial ganglion; arrowheads, the borders of the central epithelium. (C) LEnk-ir cells in the epithelium of the mantle wall adjacent to the osphradium. (D) MEnk-ir elements. White asterisk, the osphradial ganglion; arrowheads, the borders of central epithelium. Scale bars: A, B, D = 50 μm; C = 10 μm.

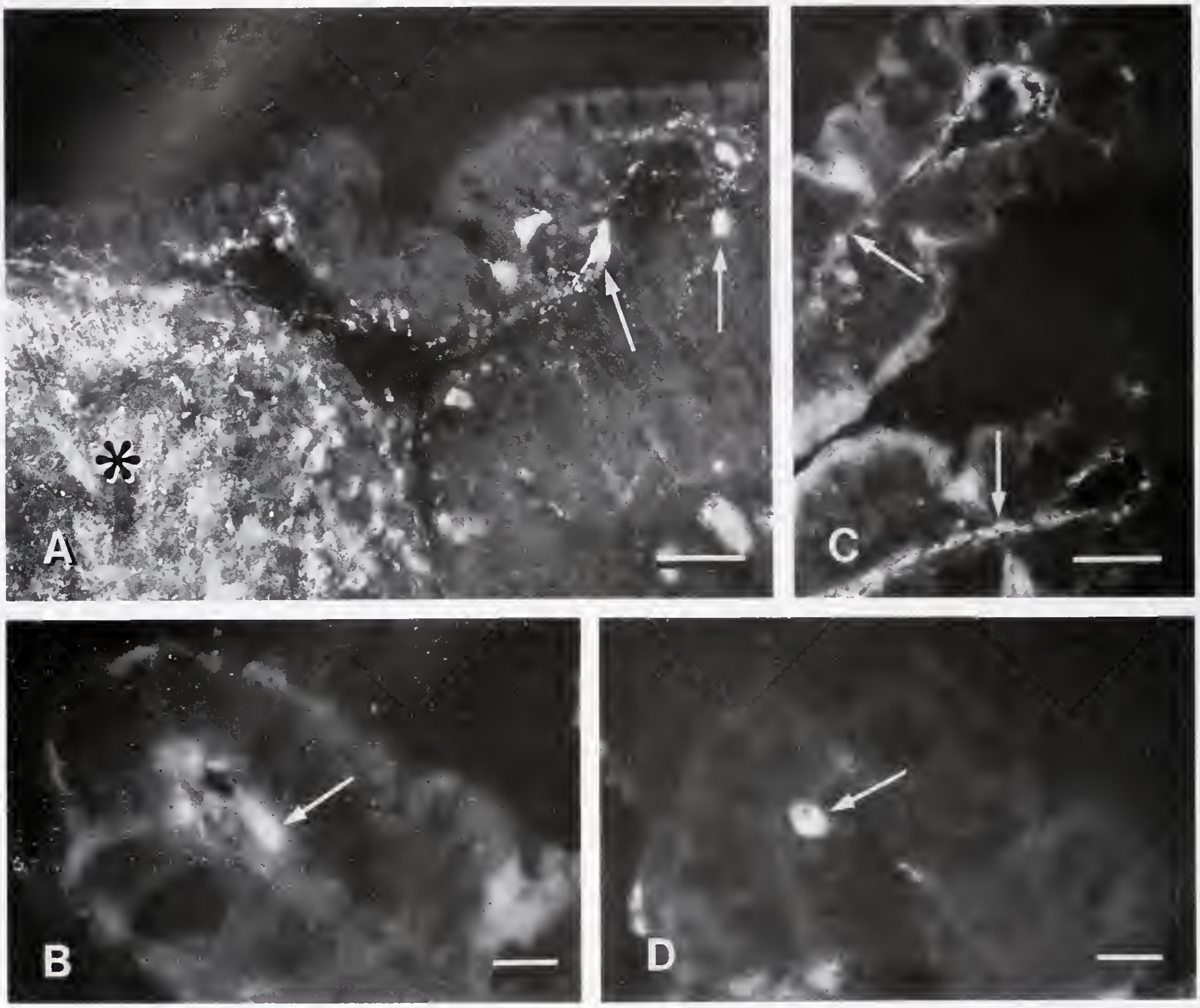

Figure 6. Immunoreactivity in the osphradium of *Buccinum undatum.* FITC-labeling. (A) FMRFa-ir elements in a transverse section of the osphradial ganglion (asterisk) and the medial part of the lamella; arrows, basiepithelial cells in the lamella. (B, C) LEnk-ir elements in a transverse section of the peripheral part of osphradial lamellae. Arrows: in B indicates the cell body; in C, immunopositive processes. (D) MEnk-ir elements in a transverse section of the peripheral part of the osphradial lamellae. Arrow shows a cell body. Scale bars: A, C = 50 μm; B, D = 20 μm.

placed a long distance away, probably close to the ventral surface of the ganglion.

MEnk-ir elements represented only by nerve fibers concentrate in small islets in the connective tissue of the organ.

NADPHd-positive elements are shown as an intensive staining of the outer portion of the osphradial epithelium, including the layer occupied by cilia. In addition, solitary nerve cell bodies and fibers in the ganglion were stained. With α-NADPH as a substrate, the entire osphradial epithelium was diffusely stained.

Buccinum undatum

Among Prosobranchia, neogastropods have the most sophisticated osphradium. Due to pectination, it resembles a gill. In the bipectinate osphradium of *B. undatum,* narrow folds called leaflets, or lamellae, extend laterally from a central core in a very regular fashion (Fig. 1C). Each lamella receives a branching nerve from the central, sausage-like ganglion. The whole structure is raised well above the epithelium of the mantle.

Figure 1C clearly shows the osphradial lamellae; they are narrow where they join the ganglion-containing central

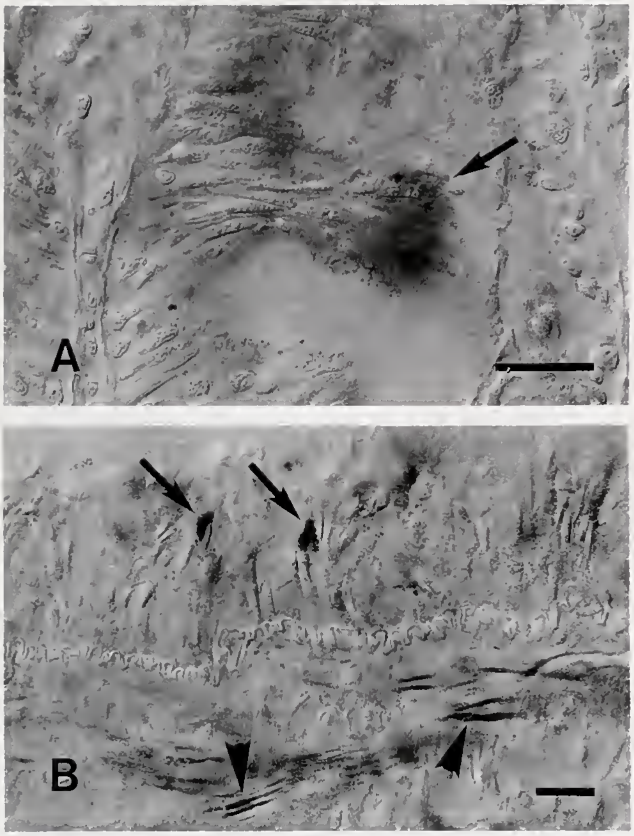

Figure 7. NADPHd-positive cells in the ciliated zone of the lamella (A) and in the mantle wall adjacent to the osphradium (B) of *Buccinum undatum*. Arrows indicate specific staining in apical portions of the epithelial cells; arrowheads, staining in muscle fibers. Scale bars = 20 μm.

core, and wide at the periphery. The glandular zone of the osphradial epithelium runs along the curved outer edge and is tube-like on a cross section (Fig. 6C). This peripheral tube is separated from the main portion of the lamella with a constriction. The ciliary zone is found adjacent to this constriction. The main portion of the lamella is described as a sensory type epithelium, the only type on the central core of the osphradium (Hyman, 1967; Crisp, 1973; Haszprunar, 1985).

FMRFa-ir elements are consistently found in the medio-apical portion of the sensory epithelium of the lamella. They are mostly represented by groups of relatively large, oval or round cells that have a fine distal process facing the mantle cavity and a basal neurite branching in the lamella. Cell bodies occupy a basiepithelial position in the lamella (Fig. 6A). The fibers do not enter the nerve that arises from the ganglion, but approach the ganglion separately. A second site of FMRFa-ir neuroepithelial cells (not represented in Fig. 6A), is found in the central zone of the epithelium covering the ganglion. Neurites of these randomly distributed cells project directly to the ganglion. The ganglion is very rich in intrinsic FMRFa-ir nerve cells and fibers.

LEnk-ir elements are concentrated in the lateral edges of the lamellae, *i.e.,* in the glandular zone that forms a loop approaching the basal part of the connective-tissue sheath of the ganglion. The LEnk-ir cell bodies are situated just beneath the outer cellular layer of the glandular zone (Fig. 6B, C). Their processes run in two directions. Some of them form a plexus underneath the cell bodies and approach the ganglion running inside the tube-like glandular zone itself. Others run to the ganglion directly, through the ciliated and sensory zones (Fig. 6C). At the periphery of the osphradial ganglion, LEnk-ir fibers form a loose meshwork. Further, there are a small number of LEnk-ir neurons within the ganglion.

MEnk-ir elements of this species are found in the glandular zone of the lamellae (Fig. 6D), as well as in the osphradial ganglion and its surroundings, and are similar to those reacting to antibodies against LEnk. Outside the osphradium, LEnk- and MEnk-ir nerve elements have different distribution patterns.

NADPHd-positive elements are found in the osphradium and concentrated in the ciliated zone of the lamellae, where apical portions of the epithelial cells are stained (Fig. 7A). There are also large, uniform-looking NADPHd-positive cells within the mantle epithelium in the vicinity of the osphradial lamella (Fig. 7B). A few muscle fibers of this particular region also show a positive reaction. No staining was detected after replacement of β-NADPH with α-NADPH.

Non-osphradial epithelia of the gill area

In all species examined, single FMRFa- and LEnk-ir neuroepithelial cells could be seen in the gill and mantle epithelium. Their number is markedly higher in the gill of the pelecypod *Anodonta cygnea* (Fig. 8A, B) than in those of the prosobranchs (Fig. 8C). LEnk-ir cells of these epithelia have a characteristic feature; a strongly immunoreactive layer in the apical part of the cell (Fig. 8B, C). They share this feature with LEnk-ir elements of the osphradial canal in the pulmonate *Lymnaea stagnalis* (Nezlin *et al.,* 1994).

Discussion

Our study has shown that transmitter-specific sensory cells are found in the osphradia of pulmonate and prosobranch molluscs. The FMRFa- and LEnk-ir sensory cells of the osphradium of *Lymnaea stagnalis* (Nezlin *et al.,* 1994) appear also in osphradia of various prosobranch species with different degree of complexity. Thus this work lends support to the idea that transmitter specificity can

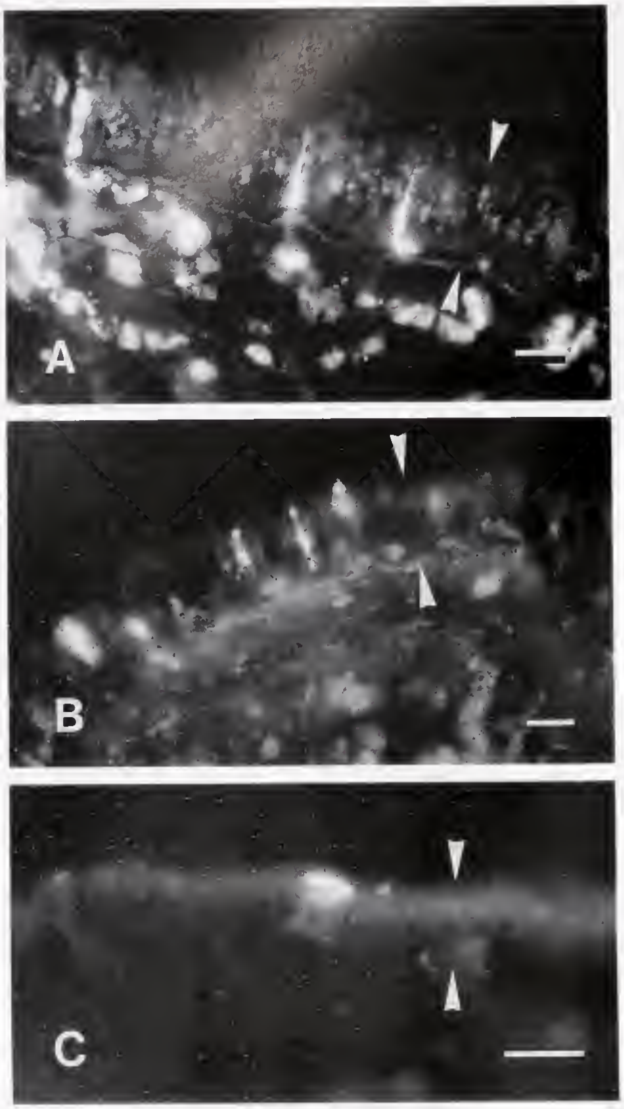

Figure 8. FMRFa-ir (A) and LEnk-ir (B) cells in the gill epithelium of *Anodonta cygnea,* and LEnk-ir (C) cell in the mantle epithelium of *Buccinum undatum.* FITC-labeling. Arrowheads label the borders of the epithelium. Scale bars = 20 μm.

be a conservative feature of homologous nerve cells (Sakharov, 1970).

In the simple osphradium of *Littorina,* all primary sensory neurons labeled with antisera to the two neuropeptides are neuroepithelial cells; that is, they are situated within the epithelium of the organ. This situation refers to the FMRFa-ir sensory cells in the osphradium of *Ampullarius* and *Buccinum,* and to some degree to the LEnk-ir sensory cells. In pulmonates, which are more recent gastropod molluscs, homologous primary sensory cells are true ganglionic neurons incorporated into the osphradial ganglion (Nezlin *et al.,* 1994). Similarly, two ultrastructurally different types of primary sensory neurons were demonstrated underneath the osphradial epithelium in the opisthobranch *Aplysia californica* (Theler *et al.,* 1987). The concentration of specific nerve elements in specific sites and the migration of neuroepithelial cells into central nervous structures are both widely recognized general trends of neural evolution. The sensory cells of the molluscan osphradia seemingly fit well into this model. But there are exceptions like the patellid limpets, which are considered primitive prosobranchs. The cell bodies of their osphradial sensory neurons are situated underneath the epithelium, as in the pulmonates (Haszprunar, 1985). Comparative studies of osphradia might help to elucidate the factors that govern the behavior of neuroepithelial cells, which sometimes migrate from their sites of origin and sometimes, on the contrary, firmly retain their epithelial position.

Reports reviewed by Haszprunar (1985) indicate that, at least in primitive prosobranchs, osphradia are activated by chemical signals from a potential sexual partner. Moreover, sexual arousal of gastropod molluscs is supposedly accompanied by an opioid-dependent suppression of noxious responsiveness and defense behavior (Leonard *et al.,* 1991). An enkephalin-like transmitter released from activated osphradial sensory elements might mediate chemical signals and integrate respective behavioral state.

As for FMRFa-ir sensory elements of the osphradium, they could contain a number of neuropeptides related to, and reactive with, antisera against FMRFamide (Greenberg and Price, 1992; Walker, 1992). At the same time, FMRFamide itself was shown to antagonize the behavioral effects of opioids in molluscs (Kavaliers *et al.,* 1985). We suggest that the two systems of peptidergic sensory neurons of the gastropod osphradium mediate signals inducing opposite behaviors.

Previous examination of the osphradial epithelium by electron microscopy revealed neuroepithelial sensory cells, not only in the central "sensory" zone of the earlier light microscopical investigations, but in the ciliated zone as well (Welsh and Storch, 1969; Crisp, 1973; Haszprunar, 1985). Our results, based on visualization of transmitter-specific elements and summarized in Figure 9, confirm previous conclusions that sensory cells may appear outside of the so-called sensory zone. They also allow us to suggest an extension of the sensory area to zones that are even more lateral to the relatively simple osphradium of *Littorina.* This might lead to a reconsideration of the boundaries of the osphradium to the surrounding mantle wall.

The results show that single FMRFa- and LEnk-ir epithelial cells similar to those occurring in the osphradium can be found in the epithelia covering other organs of the pallial (mantle) complex in prosobranch molluscs. In the

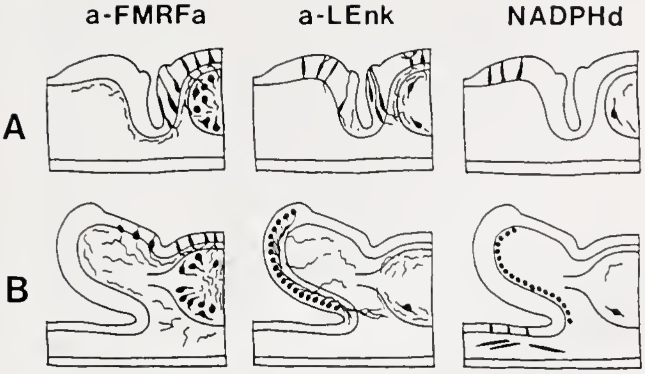

Figure 9. Schematic representation of FMRFa- and LEnk-immunoreactive and NADPHd-positive elements in the left half of the osphradia of *Littorina littorea* (A) and *Buccinum undatum* (B).

bivalve mollusc *Anodonta*, LEnk- and FMRFa-ir cells were found abundantly distributed in the gill epithelium. Correspondingly, bivalves have been described as having poorly differentiated osphradial sensory system (Sokolov and Zaitseva, 1982; Haszprunar, 1987). These findings lead us to speculate that the osphradium may have originated as a site of concentration of epithelial sensory elements that predated the organ itself. The degree of specialization might then have increased progressively during evolution. Note in this connection that, although no LEnk-ir cells were found in or below the epithelium, including the mantle epithelium, of pulmonate molluscs (Sakharov *et al.*, 1993), the concentration of LEnk-ir elements in their osphradial epithelium is extremely high (Nezlin *et al.*, 1994).

MEnk-ir cells were found in a similar position as the LEnk-ir cells only in the highly evolved osphradium of *Buccinum*. In all other prosobranch species, MEnk-ir cell bodies and fibers were distributed in a uniform manner within and around the ganglion. The sensory nature of these cells has not been established, but the involvement of additional sensory subsets of neurons in more sophisticated osphradia is suggested by this finding.

NO attracts wide attention as a novel signal molecule. A possible role for this intercellular messenger in olfactory signal processing has been recently discussed by Breer (1993) and Breer and Shepherd (1993). The osphradium of the pulmonate snail *Lymnaea stagnalis* appears to have been the first invertebrate structure wherein NADPHd-positive cells were demonstrated by a histochemical method and synthesis of NO was proved biochemically (Elofsson *et al.*, 1993). The extent to which this subpopulation of NADPHd-positive elements (the putative NO-producing elements) is present in prosobranch osphradia, and its possible involvement in invertebrate sensory systems, is part of our scientific program. Thus the finding that histochemically positive cells occur in the osphradial region and epithelium was included in this report.

Our results confirm that the dependence of β-NADPH is stereospecific. It was earlier shown by Hope and Vincent (1989) that β-NADPH and α-NADPH gave different staining patterns in the rat brain. Specifically, the alpha form did not stain brain blood vessels that are known to contain NADPH diaphorase related to the NO-synthase (Iadecola, 1993). In our material, no staining at all was obtained with α-NADPH in the osphradia of the two marine species examined, and seemingly nonspecific diffuse staining only was observed in that of *Ampullarius* sp. when α-NADPH was used.

With β-NADPH as a substrate, the NADPHd-positive cells were found in an area next to the osphradium proper in *Littorina* and *Buccinum* and, in addition, seem to be a part of the osphradial lamellae themselves of *Buccinum*. These findings are especially interesting in the case of ciliated NADPHd-positive cells of *Buccinum* in the context of recent results obtained on rat olfactory cilia. A selective inhibitor of NO formation has been shown to prevent completely an increase in cGMP production in response to high odor doses, indicating that, in the rat, NO generated in stimulated receptor cilia may activate guanylate cyclase in adjacent cells (Breer *et al.*, 1992). The NADPH-positive ciliated cells of the gastropod osphradium may provide an advantageous preparation for studying the underlying mechanisms.

Acknowledgments

The work was undertaken as part of a collaborative research project of the Department of Zoology of the University of Lund and the Institute of Developmental Biology of the Russian Academy of Sciences, Moscow, supported by a grant from the Royal Swedish Academy of Sciences to R.E. and D.S. Thanks are due to the Director and staff of the Kristineberg Marine Biological Station, Sweden, providing facilities for obtaining animals.

Literature Cited

Breer, H. 1993. Second messenger signalling in olfaction. Pp. 97–109 *The Molecular Basis of Smell and Taste Transduction.* Ciba Foundation Symp. **179.** John Wiley, Chichester.

Breer, H., and G. M. Shepherd. 1993. Implications of the NO/cGMP system for olfaction. *Trends Neurosci.* 16: 5–9.

Breer, H., T. Klemm, and I. Boekhoff. 1992. Nitric oxide mediated formation of cyclic GMP in the olfactory system. *NeuroReport* **3:** 1030–1032.

Crisp, M. 1973. Fine structure of some prosobranch osphradium. *Mar. Biol.* **22:** 231–240.

Croll, R. P. 1983. Gastropod chemoreception. *Biol. Rev.* **58:** 293–319.

Elofsson, R., M. Carlberg, L. Moroz, L. Nezlin, and D. Sakharov. 1993. Is nitric oxide (NO) produced by invertebrate neurons? *NeuroReport* **4:** 279–282.

Emery, D. G. 1992. Fine structure of olfactory epithelia of gastropod molluscs. *Microsc. Res. Tech.* **22:** 307–324.

Greenberg, M. J., and D. A. Price. 1992. Relationships among the FMRFamide-like peptides. *Progr. Brain Res.* **92:** 25–37.

Haszprunar, G. 1985. The fine morphology of the osphradial sense organs of the Mollusca. I. Gastropoda, Prosobranchia. *Phil. Trans. R. Soc. Lond* **B 307:** 457–496.

Haszprunar, G. 1987. The fine morphology of the osphradial sense organs of the Mollusca. III. Placophora and Bivalvia. *Phil. Trans. R. Soc. Lond* **B 315:** 37–61.

Hope, B. T., and S. R. Vincent. 1989. Histochemical characterization of neuronal NADPH-diaphorase. *J. Histochem. Cytochem.* **37:** 653–661.

Hyman, L. H. 1967. *The Invertebrates.* vol VI. McGraw-Hill Book Co. New York.

Iadecola, C. 1993. Regulation of the cerebral microcirculation during neural activity: Is nitric oxide the missing link? *Trends Neurosci.* **16:** 206–214.

Kavaliers, M., M. Hirst, and G. C. Teskey. 1985. The effects of opioid and FMRF-amide peptides on thermal behavior in the snail. *Neuropharmacology* **24:** 621–626.

Leonard, J. L., M. Martinez-Padron, J. P. Edstrom, and K. Lukowiak. 1991. Does altering identified gill motor neuron activity alter gill behavior in *Aplysia*? Pp. 30–37 in *Molluscan Neurobiology,* K. S. Kits *et al.*, eds. North-Holland, Amsterdam.

Nezlin, L., L. Moroz, R. Elofsson, and D. Sakharov. 1994. Immunolabeled neuroactive substances in the osphradium of the pond snail *Lymnaea stagnalis. Cell Tissue Res.* **275:** 269–275.

Sakharov, D. A. 1970. Cellular aspects of invertebrate neuropharmacology. *Ann. Rev. Pharmacol.* **10:** 335–352.

Sakharov, D., L. Nezlin, L. Moroz, and R. Elofsson. 1993. Patterns of enkephalin immunolabeling in the pulmonate snail *Cepaea nemoralis* and related molluscs. *Brain Res.* **620:** 114–121.

Sokolov, V. A., and O. V. Zaitseva. 1982. Osphradial chemoreceptors in lamellibranch molluscs *Unio pectorum* and *Anodonta cygnea. J. Evol. Biochem. Physiol.* **18:** 56–61.

Sokolov, V. A., N. N. Kamardin, O. V. Zaitseva, and T. P. Tsirulis. 1980. Osphradial sensory system of gastropod molluscs. Pp. 159–176 *Sensory Systems.* Nauka, Leningrad (in Russian).

Theler, J.-M., V. F. Castellucci, and A. J. Baertschi. 1987. Ultrastructure of the osphradium of *Aplysia californica. Cell Tissue Res.* **247:** 639–649.

Walker, R. J. 1992. Neuroactive peptides with an RFamide or Famide carboxyl terminal. *Comp. Biochem. Physiol.* **102C:** 213–222.

Welsch, U., and V. Storch. 1969. Uber das Osphradium der prosobranchen Schnecken *Buccinum undatum* (L.) und *Neptunea antiqua* (L.) *Z. Zellforsch.* **95:** 317–330.

Reference: *Biol. Bull.* **187:** 185–199. (October, 1994)

Characterization and Solubilization of the FMRFamide Receptor of Squid

GILBERT J. CHIN[1], KEMAL PAYZA[1], DAVID A. PRICE[2], MICHAEL J. GREENBERG[2], AND KAREN E. DOBLE[2]

[1]*Laboratory of Cellular and Molecular Neurophysiology, NICHD, Bethesda, Maryland 20892, and* [2]*The Whitney Laboratory, University of Florida, St. Augustine, Florida 32086*

Abstract. The optic lobe of squid (*Loligo pealei*) contains FMRFamide receptors that can bind an iodinated FMRFamide analog: [^{125}I]-desaminoTyr-Phe-norLeu-Arg-Phe-amide ([^{125}I]-daYFnLRFa). Radioligand binding assays revealed that squid FMRFamide receptors are specific, saturable, high affinity sites ($K_d = 0.15$ nM) densely concentrated in optic lobe membranes ($B_{max} = 237$ fmole/mg protein). The receptors appeared to be coupled to G_s because guanine nucleotides inhibit receptor binding and the stimulation of adenylate cyclase by FMRFamide is GTP-dependent. Both the binding and cyclase data showed that FMRFamide, but not FMRF-OH, interacts at FMRFamide receptors; thus the C-terminal Arg-Phe-amide is critical for binding. The high binding affinity of FMRFamide (0.4 nM IC_{50}) was specific for FMRFamide-like peptides. The structure-activity relations of many FMRFamide analogs were defined in detail and were nearly identical for both the membrane-bound and detergent-solubilized receptors. We also found that squid optic lobe contains FMRFamide-like reactivity as measured with both a radioimmunoassay and a radioreceptor assay. Moreover, we have sequenced a fragment of genomic DNA that encodes a FMRFamide precursor. Our findings in sum suggest that FMRFamide is a neurotransmitter in squid optic lobe, and that this tissue is a good source from which to purify FMRFamide receptors.

Introduction

The tetrapeptide FMRFamide (Phe-Met-Arg-Phe-NH_2) functions as a neurotransmitter in many invertebrates. Biochemical and molecular biological studies indicate that FMRFamide-related peptides constitute a large and diverse transphyletic peptide family (Price and Greenberg, 1989). A single species often contains more than one FMRFamide-related peptide; multiple FMRFamide-related peptides are encoded by a single mRNA in *Aplysia* (Taussig and Scheller, 1986), *Drosophila* (Schneider and Taghert, 1988), *Lymnaea* (Linacre *et al.*, 1990), and *Caenorhabditis* (Rosoff *et al.*, 1992). Acting through G-protein-regulated pathways, FMRFamide activates K^+ channels in *Aplysia* sensory neurons (Abrams *et al.*, 1984) and inhibits Ca^{2+} channels in *Helisoma* neurons (Man-Son-Hing *et al.*, 1989). The peptide also excites the heart in *Macrocallista* (Price and Greenberg, 1977), *Hirudo* (Kuhlman *et al.*, 1985), *Helix* (Payza, 1987), *Octopus* (Martin and Voigt, 1987; Voigt *et al.*, 1981), and *Sepia* (Kling and Jakobs, 1987). In addition to their diverse effects in invertebrates, FMRFamide-related peptides modulate opioid analgesia, tolerance, and dependence in rats

---

Received 10 January 1994; accepted 5 August 1994.

Reprint requests should be addressed to Dr. Gilbert J. Chin, AAAS/Science, 1333 H Street, N.W., Washington, DC 20005. Current address for Dr. Payza: ASTRA, Biotechnology Research Institute, 6100 Royalmount Ave, Montreal, Quebec, H4P 2R2 Canada.

Abbreviations: In addition to standard one- and three-letter abbreviations for amino acids, the following are used: the letter "a" at *C*-terminal ends of peptides signifies an amide; ac, acetyl; BSA, bovine serum albumin fraction V; cAMP, adenosine-3′,5′-cyclic monophosphate; CHAPS, 3-[(3-cholamidopropyl)-dimethylammonio]-1-propane sulfonic acid; CHAPSO, 3-[(3-cholamido-propyl)-dimethylammonio]-2-hydroxy-1-propane sulfonic acid; daY, desaminotyrosine; dNTPs, equimolar mixture of dATP, dGTP, dCTP, and dTTP; DTT, dithiothreitol; EDTA, disodium ethylenediamine tetraacetate; FMRFamide, Phe-Met-Arg-Phe-NH_2; Gpp[NH]p, guanylyl-imidodiphosphate; GTP[γ]S, guanosine-5′-*O*-(3-thiotriphosphate); HEPES, *N*-2-hydroxyethylpiperazine-*N*′-2-ethane sulfonic acid; IBMX, isobutylmethylxanthine; MES, 2-[*N*-morpholino]ethane sulfonic acid; PIPES, piperazine-*N*,*N*′-bis-2-ethane sulfonic acid; nL, norleucine; NS, nonspecific binding; PCR, polymerase chain reaction; PMSF, phenylmethylsulfonylfluoride; RIA, radioimmunoassay; SB, specific binding; SQM, squid optic lobe membranes; TB, total binding; TIC, L-1,2,3,4 tetrahydroisoquinoline-3-carboxylic acid.

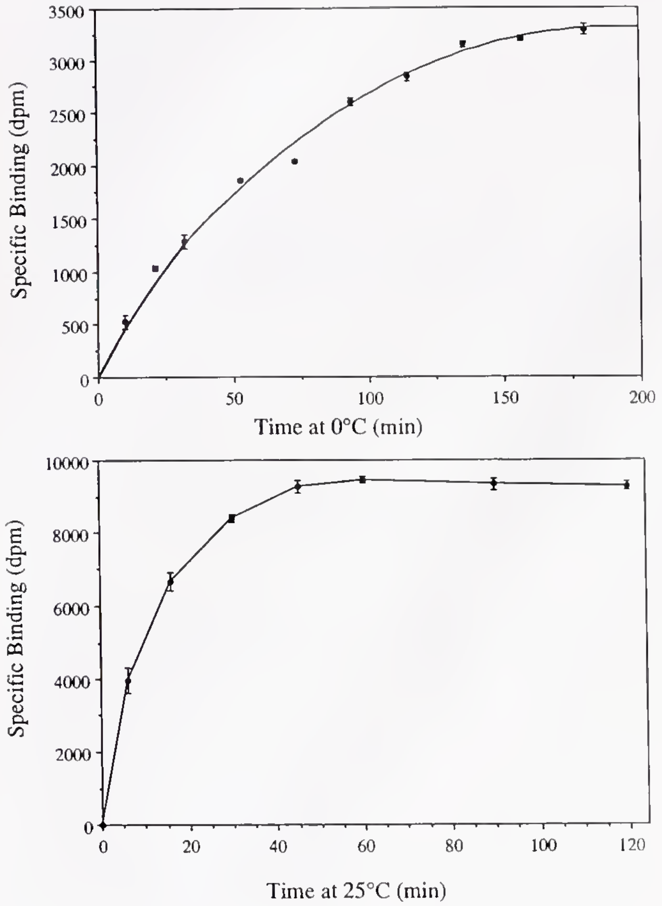

Figure 1. Time course of FMRFamide receptor binding in SQM. For the upper and lower figures respectively, [^{125}I]-daYFnLRFa (0.026 and 0.032 n*M*) was incubated with SQM (50 and 10 μg protein) at 0° and 25°C. The total and nonspecific binding were determined in triplicate in single experiments at the times indicated, and the specific binding (± SEM) is plotted against time.

(Lake *et al.*, 1991; Malin *et al.*, 1990a, b; Malin *et al.*, 1993; Tang *et al.*, 1984; Yang *et al.*, 1985); for reviews, see Raffa (1988) and Rothman (1992). The actions of FMRFamide and the mammalian FMRFamide-related peptide Neuropeptide FF (NPFF) appear to be mediated through binding to NPFF receptors in rats (Allard *et al.*, 1989; Payza *et al.*, 1993).

Despite numerous studies of the cellular effects of FMRFamide and related peptides, little is known about the receptors for these ligands. An *in vitro* radioligand binding assay was developed and used to characterize the receptor in *Helix* nervous tissue and heart (Payza, 1987; Payza *et al.*, 1989). These studies indicated that [^{125}I]-daYFnLRFa binds in a reversible, saturable, and specific manner to FMRFamide receptors of high (13 n*M*) and low (250 n*M*) affinity in *Helix* brain. This approach has been extended to include characterization of the rat spinal cord receptor for NPFF (Allard *et al.*, 1989; Payza and Yang, 1993). Nevertheless, purified FMRFamide receptor protein and sequence information are necessary to develop specific molecular probes with which to study receptor expression, distribution, and diversity. Thus, we sought to identify a source of molluscan nervous tissue in which FMRFamide receptors could be studied, and from which the receptors could be solubilized and eventually purified.

Here we describe the characterization, effector-coupling, and solubilization of FMRFamide receptors in the squid *Loligo pealei*. We also present evidence that FMRFamide is present in this species. *Loligo pealei* is used as our molluscan model system because squid nervous tissue is abundant and readily available, and because the relevance of FMRFamide in *Loligo* was demonstrated by its potentiation of transmitter release at the giant synapse (Cottrell *et al.*, 1989).

Materials and Methods

Materials

Frozen squid optic lobes were from Calamari, Inc. (Woods Hole, MA). The peptides FMRFa and acFnLRFa

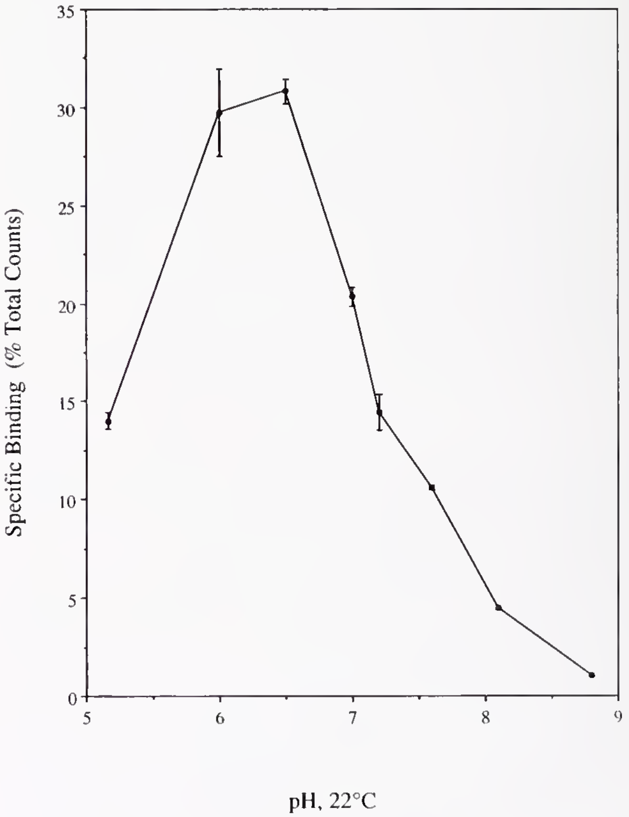

Figure 2. Dependence of FMRFamide receptor binding on pH. Squid optic lobe membranes were incubated with 0.014 n*M* [^{125}I]-daYFnLRFa in 80 m*M* Hepes/Tris buffered at the pH values indicated. After 2.5 h at 0°C, the total and nonspecific binding were determined in triplicate. The specific binding values were normalized to the total radioligand, and have been plotted against pH. Points are mean values (± SEM) from one experiment.

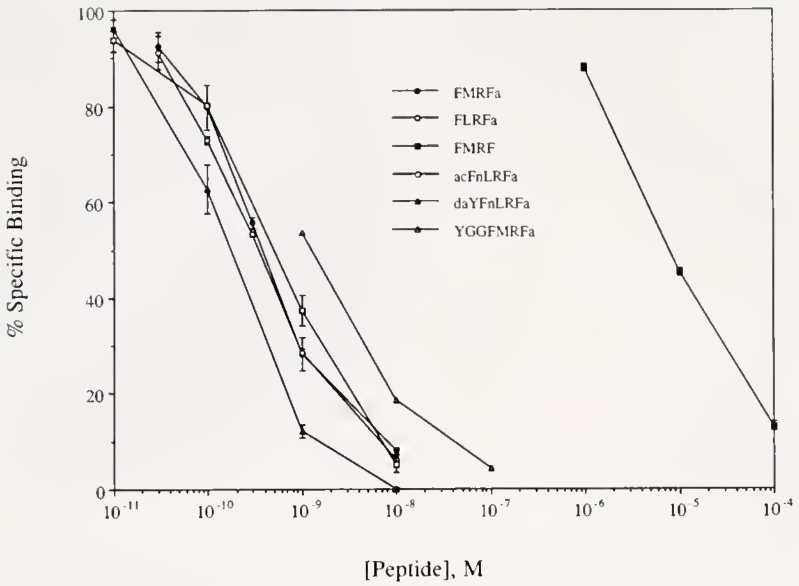

Figure 3. Specificity of FMRFamide receptor binding. The specific binding of 0.02 nM [^{125}I]-daYFnLRFa to SQM (50 μg protein) was determined after incubation for 2.5 h at 0°C in the presence of competing peptides at the concentrations indicated. The percentage of control specific binding has been plotted against peptide concentration. Points are means (± SEM) of triplicate determinations from single experiments, except for YGGFMRFa (duplicates from one experiment).

were from Sigma (St. Louis, MO). The YFMRFa was from Peninsula (Belmont, CA), and FnLRFa was from Cambridge Research Biochemicals (Cambridgeshire, England). The [D-F]MRFa, F[D-M]RFa, FM[D-R]Fa, and FMR[D-F]a were from Bachem (Torrance, CA). Except for daYFnLR[TIC]amide (which we made), the remaining peptides were synthesized by Dr. B. M. Dunn (University of Florida, Gainesville, FL), purified by reverse-phase HPLC, and quantitated by amino acid analysis. Aprotinin, creatine kinase, and nucleotides (Li$_4$)GTP[γ]S, (Li$_2$)GTP, (Li$_2$)GDP, and (Na$_2$)ATP were from Boehringer Mannheim (Indianapolis, IN). The (Li$_4$)Gpp[NH]p and (Na$_2$)GMP, isobutylmethylxanthine (IBMX), and digitonin were from Fluka (Ronkonkoma, NY). The CHAPS and CHAPSO were from Calbio-chem (La Jolla, CA). Bestatin was from Cambridge Research Biochemicals (Wilmington, DE).

Preparation of squid optic lobe membranes (SQM)

Squid optic lobes (12 per preparation, each ~0.15 g wet weight) were thawed and homogenized with 12 strokes of a motor-driven Potter-Elvehjem pestle in 24 ml homogenization buffer (50 m*M* Hepes-NaOH, pH 7.4, 150 m*M* NaCl, 5 mM 2-mercaptoethanol, 3 m*M* EDTA, 1 m*M* EGTA) containing 0.4 m*M* PMSF and 5 m*M* benzamidine. The homogenate was centrifuged at 3000 rpm (1,000 × *g*) for 10 min, and the pellet was rehomogenized in 24 ml homogenization buffer with inhibitors and recentrifuged. The two supernatants were combined, diluted to 200 ml with homogenization buffer, and centrifuged at 50,000 rpm (200,000 × *g*) for 30 min. This supernatant was discarded. The pellets were twice suspended in 200 ml of 20 mM Pipes-Tris (pH 6.5) and centrifuged. The final pellets were suspended in Pipes-Tris buffer to a protein concentration of 5–15 mg/ml, quick-frozen in dry ice, and stored at −20°C. Protein was measured as previously described (Chin and Goldman, 1992). These membranes retained most of their binding activity after freezing and thawing repeatedly.

Binding of [^{125}I]-daYFnLRFa to SQM

Squid optic lobe membranes (10–75 μg protein) were combined with the indicated concentrations (see figure legends) of mono-iodo [^{125}I]-daYFnLRFa, prepared and purified to 2200 Ci/mmole as before (Payza, 1987), in a total volume of 300 μl of 40 m*M* Pipes-Tris (pH 6.5), 1% BSA. Nonspecific binding was determined in the presence of 1–10 μM FMRFamide or acFnLRFa. Effects of test substances on radioligand binding were determined by including other peptides or nucleotides in the assay. The mixtures were incubated for the times and temperatures specified in the figure and table legends. The samples were then filtered through wet Whatman GF/B filters on a vacuum manifold, and the filters were washed four times with 4 ml of ice-cold Pipes buffer with 0.75% BSA. Radioactivity trapped on the filters was measured with a

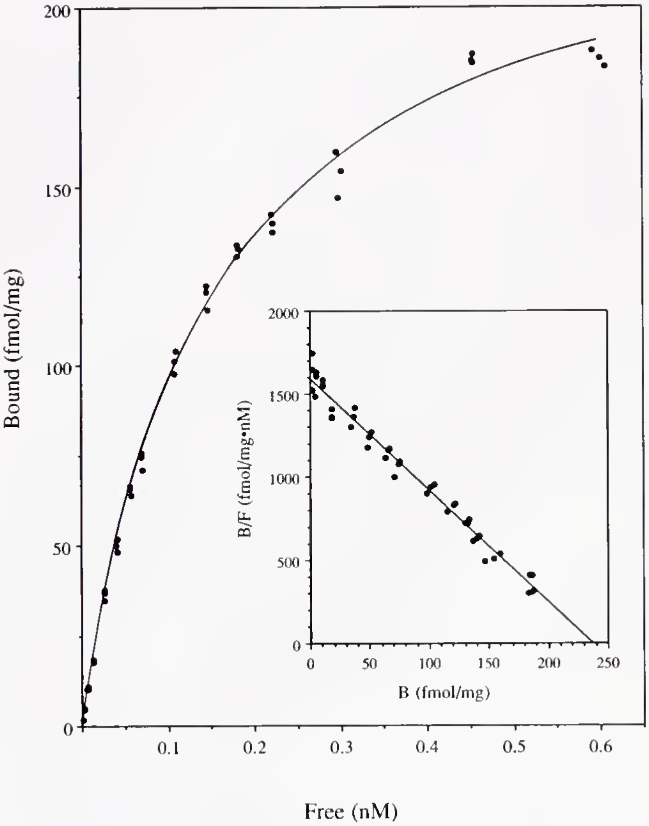

Figure 4. Saturation of specific [^{125}I]-daYFnLRFa binding to FMRFamide receptors. The specific binding of [^{125}I]-daYFnLRFa (0.002 to 0.7 n*M*) to SQM (58 μg protein) was determined after incubation for 2.5 h at 0°C. The specific binding values (fmole/mg protein) have been plotted against free radioligand concentration. Inset: Scatchard analysis of the specific binding data ($r^2 = 0.98$). Points are individual determinations from one experiment.

gamma counter, and specific binding (SB) was defined as the difference between total and nonspecific binding. The SB accounted for 68–82% of the total binding. The IC_{50} values for peptides were from plots of percent SB *versus* log [molar peptide]. Hill coefficients (n_H) were calculated from plots of log[%SB/(100−%SB)] *versus* log [molar peptide].

Binding of [^{125}I]-daYFnLRFa to solubilized SQM

Squid optic lobe membranes were incubated for 30 min on ice with various concentrations of CHAPS and then centrifuged at 43,000 rpm (100,000 × *g*) for 30 min. The standard protocol used in most of the experiments was 0.25% CHAPS and 1 mg/ml SQM protein. The supernatant was assayed for ligand binding activity in 40 m*M* Pipes-Tris (pH 7.0), 0.1% BSA, 1 m*M* DTT, 1 m*M* EDTA containing 10–50 p*M* [^{125}I]-daYFnLRFa. Samples (1–10 μg squid protein) were incubated in a final volume of 0.3 ml for 1.5–2.0 h at 23°C in the absence or presence of 10 μ*M* acFnLRFa. Then 0.75 ml of ice-cold 0.75% charcoal, 0.075% dextran, 20 m*M* Mes-Tris (pH 6.5), 0.02% NaN_3 was added, and the samples were mixed thoroughly. They were incubated on ice for 10–15 min to allow charcoal adsorption of free radioligand and were then centrifuged in a refrigerated microfuge (12,000 × *g*) for 2.5 min. Radioactivity in a 0.9 ml aliquot of the supernatant was measured. Under these conditions more than 95% of the unbound radioactivity was adsorbed to charcoal. Tracer integrity was determined by HPLC as before (Payza, 1987); degradation was less than 5%. Specific binding, assayed in triplicate, was linear with the amount of protein and was 5–10% of the total radioactivity added. The buffers MES, HEPES, and PIPES were equally effective in the charcoal solution.

Adenylate cyclase assays

Squid optic lobe membranes (5 μg protein) were combined with various test peptides in 300 or 400 μl of 50 m*M* Tris, 20 m*M* NaCl, 3 m*M* magnesium acetate, 500 μ*M* ATP, 1 m*M* IBMX, 50 μ*M* GTP, 20 m*M* creatine phosphate, 10 U creatine kinase, 100 μ*M* bestatin, 100 μ*M* PMSF, 15 μ*M* aprotionin, 1% BSA, pH 7.7. The pH 7.6 was chosen because the basal and acFnLRFa-stimulated cyclase were decreased by reductions of the assay pH towards the optimal binding pH of 6.5. The mixtures were incubated at 30°C for 10 min and the reactions terminated by boiling. The cAMP generated was acetylated and measured by RIA, in which an [^{125}I]-Tyr-cAMP analog was used with antiserum to cAMP (gift of Dr. David C. Klein, NICHD).

Identification of FMRFamide-like peptides in squid

Seven optic lobes (1.6 g) were homogenized in 40 ml of cold 1 *M* acetic acid with 0.02 *M* HCl. The homogenate was centrifuged at 48,000 × *g* for 10 min at 4°C, raised to pH 2.5, and applied to a C_{18} Sep-pak (Waters). The retained material was washed with 30 ml water and then eluted with 6 ml of 75% acetonitrile in 0.1% TFA (HPLC solvent B). The eluant was dried, resuspended in 2 ml methanol, and spun in a microfuge. The supernatant was dried and resuspended in 1 ml 0.1% TFA (HPLC solvent A). An aliquot (170 μl) was brought up to 15% B, microfuged again, and the supernatant was injected onto a C_4 HPLC column (Biorad) with a gradient of 15 to 30% B in 20 min at a flow of 1.5 ml/min. Aliquots of the 30-s fractions (some of which were pooled) were diluted 50-fold in 15 m*M* Pipes-Tris, pH 6.4, 0.3% BSA. In the radioimmunoassay (RIA), duplicate aliquots (20 μl) were combined with 300 μl of S253 antiserum (Price, 1983) at 1:20,000 final dilution, and 16,000 dpm of [^{125}I]-daYFnLRFa (0.01 n*M*). After incubation for 17 h at 4°C, each tube was vortexed with 1 ml cold ethanol and cen-

Table I

Inhibition of [^{125}I]-daYFnLRFa binding to SQM by FMRFamide analogs

Phe^1	% INH	Met^2	% INH	Arg^3	% INH	Phe^4	% INH
YMRFa	88.09	FIRFa	97.34	FMHFa	43.41	FMRMa	56.62
HMRFa	28.79	FFRFa	89.45	FMSFa	31.16	FMRIa	19.87
MMRFa	19.41	FLRFa	89.20	FMNFa	22.11	FMRVa	10.46
CMRFa	18.85	FVRFa	86.37	FMWFa	21.37	FMRHa	10.19
AMRFa	15.99	FYRFa	74.29	FMAFa	11.60	FMRAa	9.06
PMRFa	14.37	FWRFa	72.33	FMEFa	9.34	FMRTa	7.57
KMRFa	12.67	FCRFa	65.05	FMFFa	6.31	FMRDa	7.07
LMRFa	10.37	FTRFa	59.67	FMKFa	4.64	FMRLa	6.61
VMRFa	9.81	FHRFa	54.06	FMYFa	3.95	FMRPa	4.75
NMRFa	9.11	FQRFa	45.71	FMPFa	2.37	FMREa	3.68
EMRFa	9.09	FERFa	40.06	FMTFa	1.80	FMRKa	2.61
SMRFa	7.10	FPRFa	25.75	FMIFa	1.20	FMRYa	2.01
DMRFa	5.98	FDRFa	21.53	FMLFa	0.00	FMRRa	1.31
QMRFa	4.62	FRRFa	18.74	FMGFa	0.00	FMRNa	0.64
TMRFa	2.16	FSRFa	17.04	FMDFa	0.00	FMRQa	0.00
RMRFa	0.00	FGRFa	15.20	FMMFa	0.00	FMRGa	0.00
		FNRFa	12.74				
		FKRFa	11.04				

The specific binding of [^{125}I]-daYFnLRFa (0.05–0.06 nM) to SQM (15–50 μg protein) was determined in the presence of a high concentration (0.2 μM, 500 times the IC$_{50}$ of FMRFamide) of test peptide after incubation for 2.5 h at 0°C. The percent inhibition of control specific binding (mean, $n = 2$ or 3) has been displayed for each FMRFamide analog. Values below 50% indicate that the test peptide is more than 500-fold less potent than FMRFamide.

trifuged for 25 min at 4,800 × *g*. The supernatants were decanted and the radioligand binding to antiserum precipitated in the pellets was determined. The nonspecific binding was determined in the presence of 60 pmole FMRFamide; control specific binding (4980 dpm) accounted for 91% of the total binding. The inhibition of

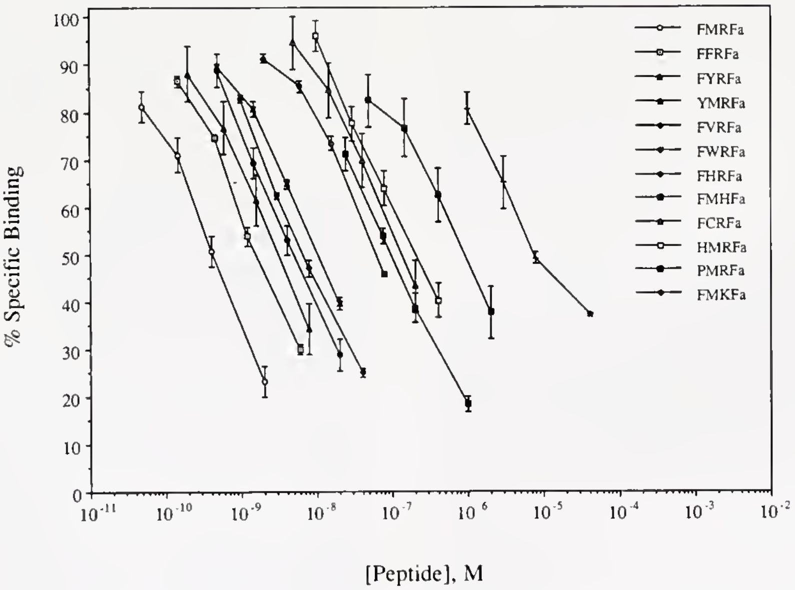

Figure 5. Structure-activity relations of peptide binding to FMRFamide receptors. The specific binding of 0.03 nM [^{125}I]-daYFnLRFa to SQM (30 μg protein) was determined after incubation for 2.5 h at 0°C in the presence of competing peptides at the concentrations indicated. The percent of control specific binding (mean ± SEM) has been plotted against peptide concentration. Results are from triplicate determinations of one experiment.

Table II

Potencies of peptides at membrane-bound and solubilized FMRFamide receptors

Peptide	IC_{50} (membrane)	IC_{50} (solubilized)
FMRFa	0.40	0.13
FLRFa	0.40	0.33
acFnLRFa	0.51	0.43
YGGFMRFa	1.0	0.50
FFRFa	1.4	0.55
FYRFa	2.8	0.60
YMRFa	5.0	1.7
FVRFa	6.2	3.0
FWRFa	10	2.0
FHRFa	55	6.5
FMHFa	85	100
FCRFa	120	25
HMRFa	200	50
FMKFa	7000	3000

Potencies of peptides (n*M*) in competing for [^{125}I]-daYFnLRFa binding to intact and CHAPS-solubilized SQM (with 0.03 and 0.06 n*M* radioligand respectively) were determined from displacement curves as described in the Methods.

specific binding by each sample was calculated and compared to a standard curve of FMRFamide (IC_{50} = 0.081 pmole). In the radioreceptor assay, duplicate aliquots (25 μl) were combined with 20 μg of SQM protein and 50,000 dpm [^{125}I]-daYFnLRFa (0.03 n*M*) in 300 μl of receptor binding buffer. Radioligand binding was determined after incubation for 1 h at 25°C; control-specific binding (5224 dpm) accounted for 82% of the total binding. The inhibition of specific binding was calculated, compared to a standard curve of FMRFamide (IC_{50} = 0.077 pmole), and the receptor-reactivity was plotted against elution time. The elution profiles of the FMRFamide immunoreactivty and receptor-reactivity were compared to the elution times of FMRFamide and FLRFa standards.

Identification of a FMRFamide precursor fragment in squid genomic DNA

A squid optic lobe was heated to 95°C for 10 min in 0.1 *M* NaOH. The mixture was spun in an Eppendorf centrifuge at 14,000 rpm, and 0.3 μl of the supernatant was used for PCR. The reaction mixture of 100 μl contained 200 μ*M* dNTPs, 4 U of Taq polymerase (Promega), and about 200 pmol of each primer:

Sense primer:

A C C

GAI AAG CGI TTC TTG AGG TTC GG

Anti-sense primer:

A T C A T

CAT GAA ICG TTT ICC GAA ICG CAT

The reaction mixture was covered with mineral oil and then subjected to 40 cycles of PCR under the following conditions: 94°C, 1 min; 50°C, 1 min; 72°C, 1 min. The PCR products were then cloned and sequenced.

Results

Identification of FMRFamide receptors in squid optic lobe

The presence of FMRFamide receptors in squid was examined by testing optic lobe membranes for specific binding of the FMRFamide receptor ligand [^{125}I]-daYFnLRFa. Incubation of SQM with [^{125}I]-daYFnLRFa resulted in a time-dependent increase in specific binding that attained equilibrium in 2.5 h at 0°C or 1 h at 25°C (Fig. 1). The degradation of radioligand at both temperatures was less than 10% as assayed by HPLC. The specific binding was maximal at pH 6–6.5 (Fig. 2) and was linearly dependent on the amount of membrane protein in the assay. The binding was specific for FMRFamide-related peptides (Fig. 3) and showed specificity for the C-terminal amide, since FMRF-OH (IC_{50} = 7 μ*M*) was over four orders of magnitude weaker than FMRFamide (IC_{50}

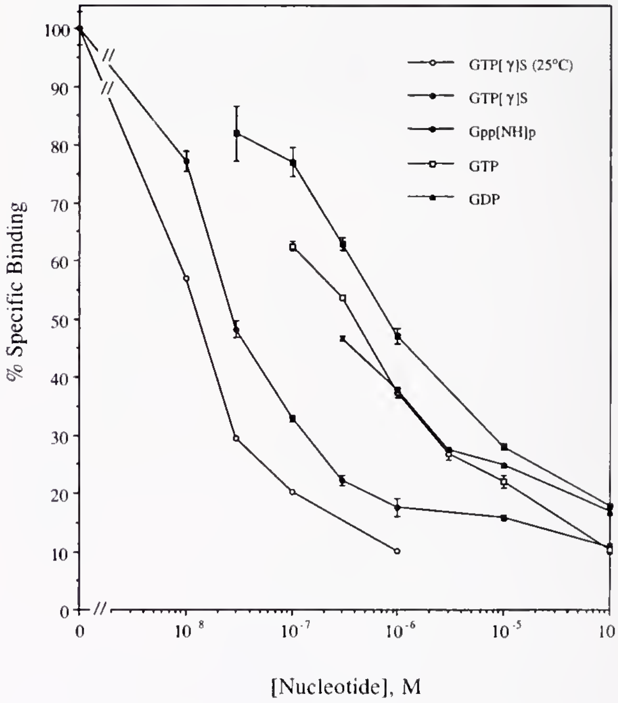

Figure 6. Nucleotide effects on FMRFamide receptor binding. The specific binding of [^{125}I]-daYFnLRFa (0.06 n*M*) to SQM (20 μg protein) was determined after incubation in triplicate for 2.5 h at 0°C in the presence of nucleotides at the concentrations indicated. An identical experiment was carried out in duplicate at 25°C for 1 h with GTP[γ]S. The percent of control specific binding (mean ± SEM) has been plotted against nucleotide concentration.

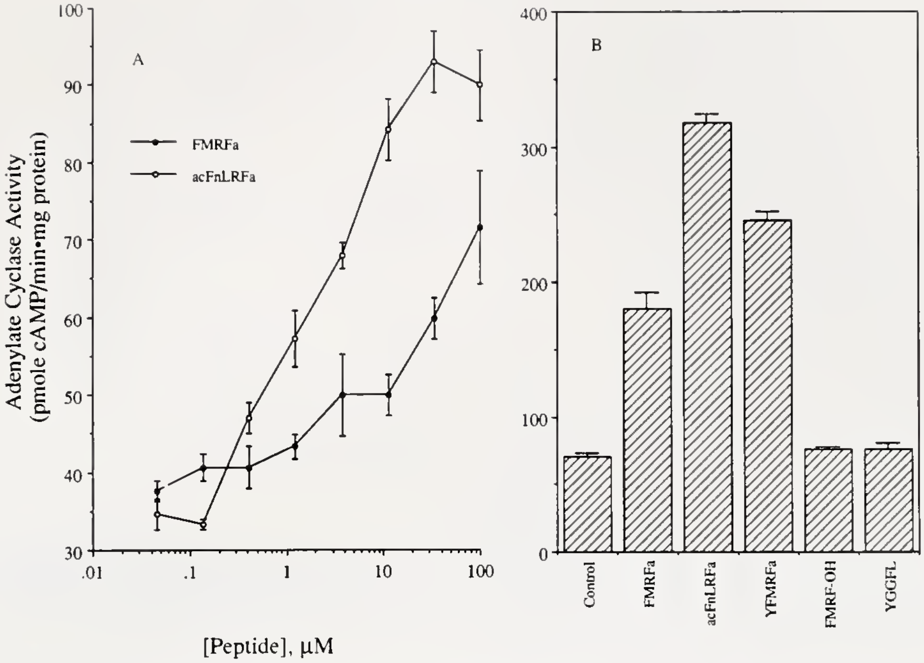

Figure 7. Stimulation of adenylate cyclase by FMRFamide-related peptides. The adenylate cyclase activity in SQM was measured in the presence of 0–100 μM peptides. (A) Dose-response curve for stimulation of adenylate cyclase by FMRFamide and acFnLRFa. (B) Effects on adenylate cyclase of peptides at 100 μM. Results are means (± SEM) of triplicate determinations from single experiments.

= 0.4 nM). The potency of FMRFamide was close to the 0.2 nM IC$_{50}$ of the most potent ligand, daYFnLRFa (Fig. 3). The binding was not displaced by the unrelated peptides cholecystokinin octapeptide and leucine-enkephalin. Scatchard analysis of [^{125}I]-daYFnLRFa binding revealed a single population of high-affinity binding sites, with a K$_d$ of 0.15 nM and B$_{max}$ of 237 fmole/mg protein (Fig. 4).

Characterization of FMRFamide receptors in squid

The structure-activity relations of FMRFamide receptor binding were examined by testing a series of FMRFamide analogs for displacement of specific [^{125}I]-daYFnLRFa binding to SQM. We first examined the stereospecificity of binding, and found that D-amino acid substitution drastically reduced the subnanomolar potency of FMRFamide: [D-F]MRFa had an IC$_{50}$ of 0.13 μM, F[D-M]RFa and FM[D-R]Fa both had IC$_{50}$ values of 1.3 μM, and FMR[D-F]a displaced only 28% of specific binding at the highest concentration tested (4 μM). We next screened a series of analogs, L-substituted at each of the four amino acid positions, and all at 0.2 μM, to determine whether any other structures can bind to FMRFamide receptors at a concentration 500 times the IC$_{50}$ of FMRFamide (Table I). The potencies for a selection of these FMRFamide analogs were then determined by generating displacement curves (Fig. 5) and calculating IC$_{50}$ values for each peptide (Table II). The Hill coefficients were determined for each peptide in Figure 5, and the values ranged from 0.65 to 0.92. We also found that a FMRFamide analog with L-1,2,3,4 tetrahydroisoquinoline-3-carboxylic acid (TIC) in place of the C-terminal Phe, daYFnLR[TIC]-amide displaced radioligand binding with a potent IC$_{50}$ of 0.39 nM (n_H = 0.87).

Coupling of FMRFamide receptors to G-proteins and adenylate cyclase

The coupling of FMRFamide receptors to G-proteins was examined by testing guanine nucleotides for inhibitory effects on specific [^{125}I]-daYFnLRFa binding to SQM. The nucleotides GTP, Gpp[NH]p, GTP[γ]S, and GDP inhibited FMRFamide receptor binding in a dose-dependent manner (Fig. 6). This effect was not observed with GMP or ATP. The inhibitory effect of GTP[γ]S at 25°C was about 2.5-fold more potent than at 0°C (Fig. 6), a finding consistent with a previous report (Aronstam and Narayanan, 1988). The coupling of FMRFamide receptors to adenylate cyclase was examined by testing FMRFamide for modulation of the enzyme activity in SQM. Production of cAMP from ATP by adenylate cyclase in SQM was stimulated in a dose-dependent manner by FMRFamide (Fig. 7A). The peptides acFnLRFa and

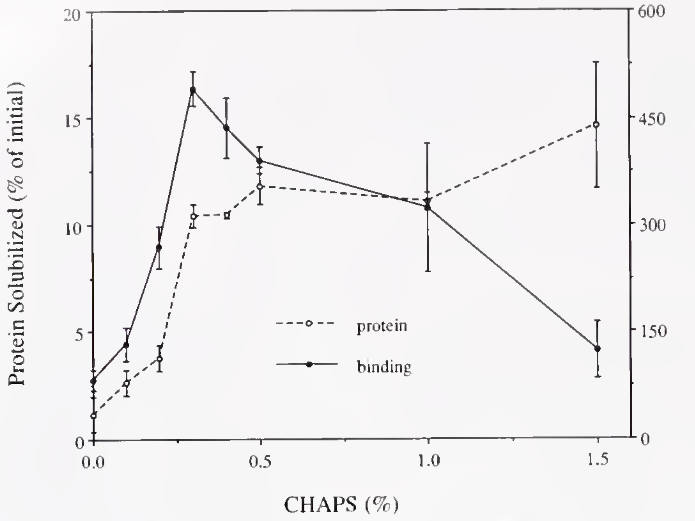

Figure 8. Solubilization of FMRFamide receptors from SQM. Membranes (1 mg/ml) were incubated with CHAPS on ice for 30 min, centrifuged at 100,000 × *g* for 30 min, and the supernatant was assayed for protein and specific binding in the presence of ~0.05 nM [^{125}I]-daYFnLRFa. Similar results were obtained in four independent experiments and at initial protein concentrations of 2, 5, and 10 mg/ml.

YFMRFa were more active than FMRFa, but FMRF-OH and Leu-enkephalin were without effect (Fig. 7B). If a G-protein participates in the activity of FMRFamide-stimulated adenylate cyclase, then GTP must be required, and this requirement was examined. In the presence of GTP (20 or 50 μM), 100 μM acFnLRFa produced a two-fold stimulation of adenylate cyclase, but in the absence of GTP it had no effect.

Solubilization of FMRFamide receptors

In exploratory studies, the following observations were made. Specific [^{125}I]-daYFnLRFa binding activity could be solubilized with digitonin (0.25–1.0%) over a broader range of detergent concentrations than with CHAPS, but the recoveries were not as high as those achieved with CHAPS. CHAPSO at 0.25% also solubilized specific binding activity. CHAPS solubilization was optimal at pH 6.5, whereas solubilized ligand binding activity was optimal at pH 7.0. Solubilization of ligand binding activity was reduced at high ionic strength (50% less in 0.15 M NaCl or KCl). The measurement of binding activity was much less sensitive to ionic strength but was significantly reduced by divalent cations (40% less in 5 mM $MgCl_2$ or $CaCl_2$). The CHAPS-solubilized preparation was stable for at least 6 h on ice, and stability was not affected by sucrose or glycerol. Protease inhibitors (PMSF, benzamidine, bestatin, bacitracin, leupeptin, aprotinin, pepstatin) did not consistently improve the recovery of binding activity when they were added either during the solubilization or during the binding incubation. Finally, both [^{125}I]-D-YFnLRFa and [^{125}I]-YGGFLRFa bound to the solubilized preparation with similarly high affinity and specificity but with more nonspecific binding as compared to [^{125}I]-daYFnLRFa.

In the experiments reported below and illustrated in the figures, the zwitterionic detergent CHAPS was used to solubilize the FMRFamide receptor from SQM. CHAPS concentrations in the neighborhood of the critical micelle concentration (about 0.4%) solubilized 10% of the total membrane protein (Fig. 8). The optimal solubilization of specific binding activity occurred in the range 0.25–0.5% CHAPS. The decrease of binding activity recovered at higher CHAPS concentrations probably was due to denaturation of the receptor as a consequence of its direct interaction with detergent or of delipidation. Alternatively, higher CHAPS concentrations might disrupt the association of the receptor and G-protein, causing a loss in receptor binding affinity.

Characterization of solubilized FMRFamide receptors

The time courses of association of radioligand with receptor and of dissociation of radioligand from receptor after addition of 1 μM unlabeled ligand are shown in Figure 9. Association under pseudo first-order conditions reached a plateau after 90–120 min incubation at room temperature; a semilogarithmic plot of the approach to equilibrium as a function of time (inset) yielded $k_{on} = 9.6 \times 10^7 M^{-1} min^{-1}$. Ligand dissociation was slow and yielded $k_{off} = 0.00894 min^{-1}$ for an equilibrium dissociation constant of 0.093 nM, which was slightly more potent (1.6-fold) than the K_d measured in unsolubilized SQM (0.15 nM). Scatchard analysis of specific binding as a

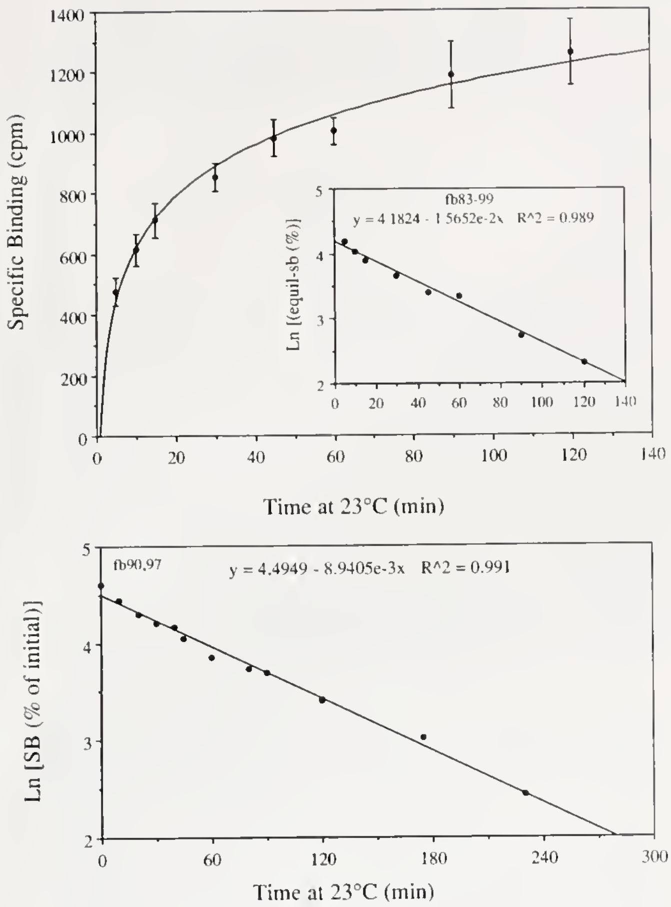

Figure 9. Association and dissociation of receptor and ligand. (A) Solubilized SQM was combined with 0.07 nM [^{125}I]-daYFnLRFa and assayed for specific binding as a function of time. The equilibrium value was estimated to be 1400 cpm from five independent experiments. The inset shows the relation of the difference between the actual and equilibrium values of binding as a function of time, under pseudo first-order conditions with [ligand]/[receptor] ~7. (B) Solubilized SQM was incubated with radioligand for 3 h, and then 1 μM acFnLRFamide was added. The amount of bound radioactivity remaining was determined as a function of time in two independent experiments. The initial value was taken as the amount bound just prior to addition of acFnLRFamide.

function of ligand concentration produced curved plots whether CHAPS or CHAPSO was employed to solubilize the receptors (Fig. 10). The curved Scatchard plots made it difficult to estimate precisely the affinity and yield of receptors from the solubilization step. Using a nonlinear curve-fitting program (JMP, SAS Institute, Cary, NC), we determined that the data could not be fit to a two-site model.

Binding to the solubilized receptors was sensitive to guanine nucleotides as for the membrane-bound receptors (Fig. 11). Again, GTP[γ]S was more potent than GTP, and ATP had no effect over the same range of concentrations. The IC$_{50}$s for GTP and GTP[γ]S were 0.17 μM and 0.028 μM, each about 200-fold more potent than observed with unsolubilized SQM. The complete inhibition by GTP and GTP[γ]S indicated that all of the active, solubilized receptors were complexed with G-proteins. These results are consistent with a GTP-induced decrease in the affinity of the receptor for ligand, because the charcoal adsorption assay does not detect interactions with $K_d > \sim 0.1\ \mu M$. Scatchard analysis in the presence of 0.17 μM GTP produced a curve, parallel to that shown in Figure 10, but shifted downward with an apparent loss of about half of the binding sites (not shown).

The binding specificity of the solubilized receptors was determined by displacement of the radioligand with other peptides. As shown in Figure 12, FMRFamide and acFnLRFa both had IC$_{50}$s < 1 nM, whereas the non-amidated FMRF had an IC$_{50}$ of 30 μM. Selected FMRFamide analogs (from a panel of 60 peptides) displayed intermediate IC$_{50}$s as shown in Table II, whereas the unrelated peptides leucine-enkephalin, methionine-enkephalinamide, somatostatin, and substance P (7–11) did not displace at concentrations up to 10 μM. The competition curves for displacement of radioligand from the solubilized receptor were similar in maximal displacement and steepness for many of the FMRFamide analogs tested, suggesting displacement from a single population of sites. Hill plots yielded coefficients of 0.52–0.86, indicating noninteracting binding sites. The log[IC$_{50}$] values determined for each peptide with the CHAPS-solubilized receptors

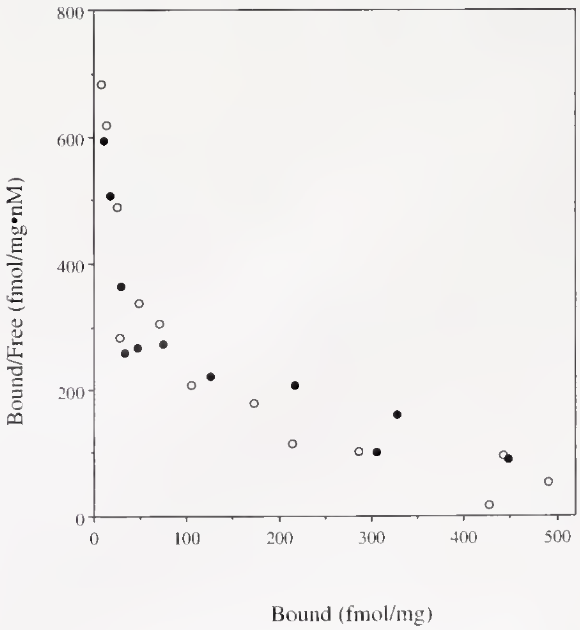

Figure 10. Scatchard plot of binding to solubilized receptors. The specific binding of increasing concentrations of [^{125}I]-daYFnLRFa to solubilized SQM was determined. The values of bound/free radioligand (fmole/mg protein · nM) have been plotted against bound radioligand. Results are from single experiments in which the receptors were solubilized with CHAPS (closed circles) or CHAPSO (open circles).

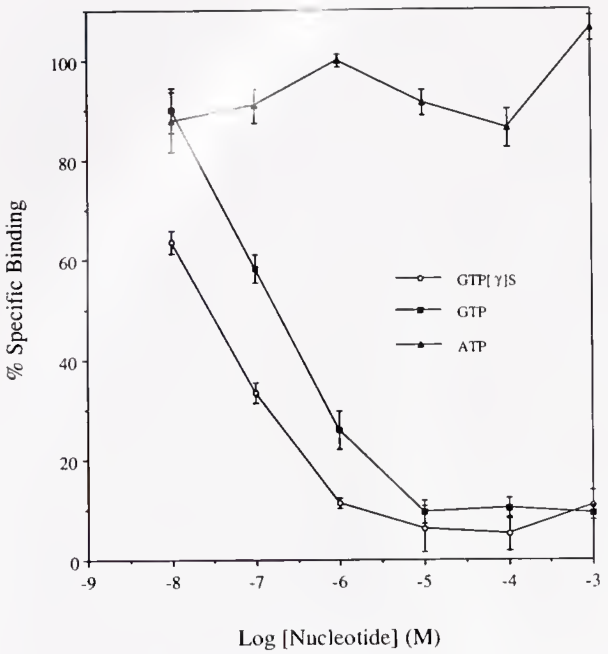

Figure 11. Nucleotide effects on solubilized receptors. The specific binding of 0.07 n*M* radioligand to solubilized SQM was determined in two independent experiments with the nucleotides GTP, GTP[γ]S and ATP. The percentage of control specific binding (mean ± SEM) has been plotted against nucleotide concentration.

were linearly related to those determined with the membrane-bound receptors, and the slope was unity (Fig. 13). This finding suggests that the binding specificities of the two preparations were nearly identical, and that CHAPS treatment had not altered the structure of the protein. Overall, solubilization improved displacement potency of the peptides tested by an average of half a log unit (threefold).

Identification of FMRFamide-like peptides in squid optic lobe

The demonstration of FMRFamide receptors in squid optic lobe suggests that FMRFamide itself should be detectable in this tissue. An acid extract of squid optic lobes was subjected to reverse-phase HPLC, and the fractionated eluant was analyzed both by radioimmunoassay (RIA) and by the radioreceptor assay described above. Some of the fractions were immunoreactive in the RIA with [^{125}I]-daYFnLRFa and anti-YGGFMRFamide antiserum S253 (Price, 1983). Most of the FMRFamide-immunoreactivity eluted in the positions of authentic FMRFamide and FLRFa (Fig. 14A). Moreover, the same HPLC fractions of the extract displaced [^{125}I]-daYFnLRFa from binding sites in squid optic lobe membranes; thus, the receptor-reactivity coeluted with the immunoreactivity in the positions of FMRFamide and FLRFa (Fig. 14B). The results of both assays were in close agreement that the amount of FMRFamide in the tissue (5.2–6.4 nmole/g wet weight) was about 13- to 14-fold that of FLRFa (0.36–0.51 nmole/g). An acetone extract of squid optic lobes was also subjected to reverse-phase HPLC on a C_{18} column, and the fractions were assayed with S253 antiserum and [^{125}I]-YGGFMRFamide. Again, some of the immunoreactivity

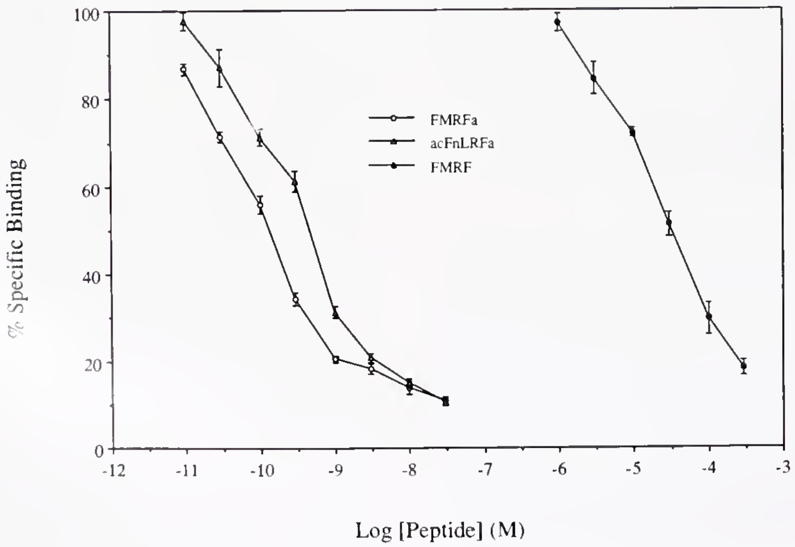

Figure 12. Binding specificity of solubilized receptors. The specific binding of 0.07 n*M* radioligand to solubilized SQM was determined in the presence of FMRFamide, acFnLRFamide, and the non-amidated FMRF at the indicated concentrations in many independent experiments. The percentage of control specific binding (mean ± SEM) has been plotted against peptide concentration.

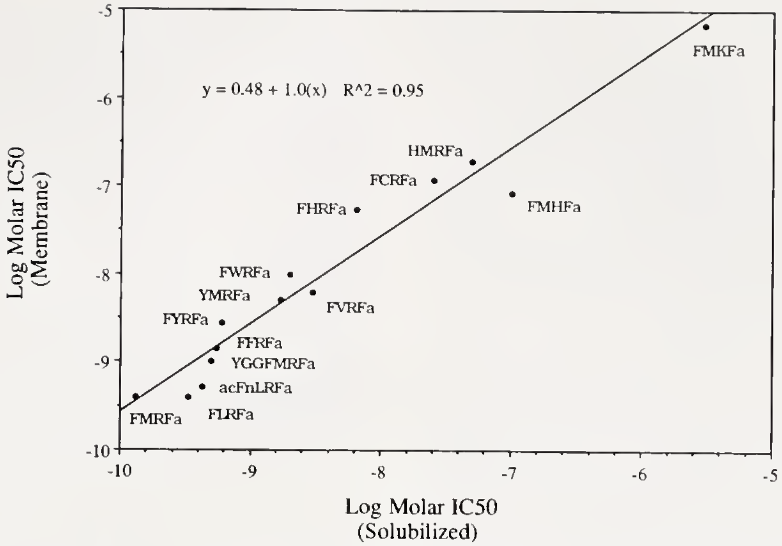

Figure 13. Comparison of the CHAPS-solubilized and membrane-bound FMRFamide receptors. FMRFamide analogs were tested for their ability to displace radioligand binding from CHAPS-solubilized and unsolubilized SQM, and their log (IC_{50}) values (from Table II) were plotted together. Results are compiled from many separate experiments.

eluted in the positions of authentic FMRFamide and FLRFa, and unidentified, later-eluting peaks were also detected by S253 antiserum (not shown).

Identification of a FMRFamide precursor fragment in squid genomic DNA

As demonstrated above, coelution in distinct parallel assays strongly indicates that FMRFamide and FLRFamide are present in squid optic lobes. Nevertheless, in the absence of information from either sequencing or mass spectrometry, these data are not unimpeachable. Moreover, although FMRFamide and FLRFamide have been chemically identified in every major class of molluscs (Price and Greenberg, 1989), including cephalopods (Martin and Voigt, 1987), this has never been done in any squid. Still, rather than identifying these particular peptides in yet another species of mollusc, we proceeded to clone and sequence part of a FMRFamide precursor from squid genomic DNA. Following the strategy described in the Methods, a fragment of the genome was amplified by PCR, then cloned and sequenced (Fig. 14C). This fragment encodes, between the primers, three copies of the peptide: Lys-Arg-Phe-Met-Arg-Phe-Gly-Arg, where the basic residues at the *C*- and *N*-terminals are cleavage sites, and the glycyl residue is the amidation site.

Discussion

FMRFamide receptors in squid

Our finding of specific, saturable [^{125}I]-daYFnLRFa binding to optic lobe membranes of *Loligo pealei* constitutes the first direct evidence of FMRFamide receptors in this tissue. The ability of [^{125}I]-daYFnLRFa to specifically label FMRFamide receptors in *Loligo* is consistent with the prior use of this radioligand in the land snail *Helix aspersa*, the main similarity between the receptors of the two molluscs being the low binding potency of FMRF-OH with respect to FMRFamide (Payza, 1987). These strict preferences for the amidated form of the peptide are consistent with the bioactivity of the peptides on the isolated *Helix* heart (Payza, 1987). Similarly, FMRFa, FLRFa, YGGFMRFa, and YGGFLRFa were cardioexcitatory on the isolated systemic heart of *Octopus vulgaris*, and these effects were specific for the *C*-terminal amide (Martin and Voigt, 1987; Voigt *et al.*, 1981). The main differences between the receptors of *Helix* and *Loligo* are that (1) in squid [^{125}I]-daYFnLRFa binds to a single population of binding sites, whereas in *Helix*, multiple sites were observed (Payza, 1987; Payza *et al.*, 1989); (2) the receptors in squid show a much higher affinity for FMRFamide; and (3) *N*-terminal extensions greatly improved the micromolar potency of FMRFamide at *Helix* receptors, but did not improve the already subnanomolar FMRFamide affinity at squid receptors; *i.e.*, the potencies of acFnLRFa and daYFnLRFa were similar to that of FMRFamide, and YGGFMRFa was 2.5-fold weaker. The pH optimum of binding was also more acidic in squid than in *Helix*.

Structure-activity relations of receptor binding

In contrast to the minor effects of the *N*-terminal extensions, the effects of single amino acid substitutions in

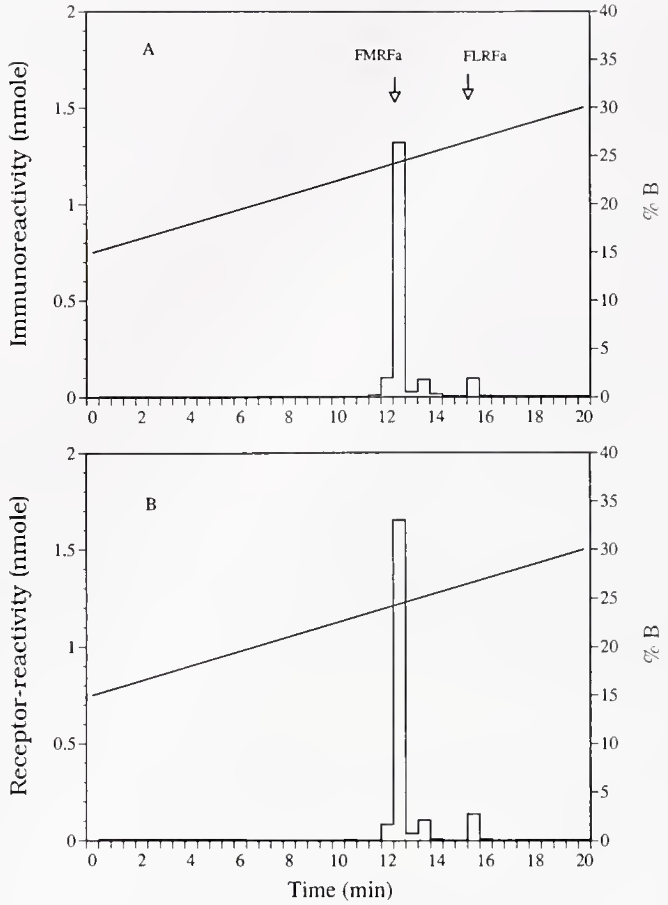

C

GAG	AAG	AGG	TTC	TTG	AGG	TTC	GGT	AAG	TCA	GAG	GAC	AAA	AGG	TTC	45
E	K	R	F	L	R	F	G	K	S	E	D	K	R	**F**	
ATG	AGA	TTT	GGC	CGA	GAC	CCC	AGC	GAT	GTT	GAA	GAT	GAA	TTG	GAA	90
M	**R**	**F**	**G**	R	D	P	S	D	V	E	D	E	L	E	
GAG	GAC	AAA	CGT	TTT	ATG	CGA	TTC	GGA	CGC	GGC	GCC	GAA	GAT	GAT	135
E	D	K	R	**F**	**M**	**R**	**F**	**G**	R	G	A	E	D	D	
GAG	GAA	GAA	GCC	GAG	AAG	AGA	TTT	ATG	AGA	TTT	GGA	CGT	GAC	CCC	180
E	E	E	A	E	K	R	**F**	**M**	**R**	**F**	**G**	R	D	P	
GAA	AAG	AAA	TTC	ATG	CGC	TTC	GGC	AAA	CGC	TTC	ATG				216
E	K	K	F	M	R	F	G	K	R	F	M				

FMRFamide ranged from no effect to the complete elimination of binding at 0.2 μM peptide. In the Phe^1 position, the least detrimental substitution was with Tyr; all other substitutions tested were not tolerated (*e.g.*, HMRFa and PMRFa had IC_{50}s of 0.2 and 1.0 μM, respectively). The Met^2 was the position most tolerant to substitution; FLRFa was equipotent with FMRFamide, and analogs containing aromatic residues were also active (see FFRFa, FYRFa, FWRFa). The Arg^3 could not be substituted with the positively charged Lys, but it could be replaced by His with a 200-fold loss in binding. The *C*-terminal Phe was extremely intolerant to substitution with almost any amino acid tested; the only exception was the rigid Phe analog, TIC. The potent binding of daYFnLR[TIC]amide suggests it should be a potent agonist or antagonist.

FMRFamide receptor coupling

Our results suggest that FMRFamide receptors in squid optic lobe are coupled to G_s. The specificity of the guanine nucleotide effect on FMRFamide receptor binding is consistent with GTP regulation of other G-protein-coupled receptors, such as receptors for opiates (Childers and Snyder, 1980) and the mammalian FMRFamide-related peptide Neuropeptide FF (Payza and Yang, 1993). Moreover, the stimulation of adenylate cyclase by FMRFamide in squid shows a requirement for GTP. Thus, squid FMRFa receptors appear to be members of the family of G-protein-coupled receptors, one of which (phospholipase *C*-coupled rhodopsin) has been cloned recently in squid (Hall *et al.*, 1991). The coupling of FMRFamide receptors in optic lobe of *Loligo* is in agreement with FMRFamide-stimulated cAMP production in *Mercenaria* heart (Higgins *et al.*, 1978), *Lampsilis* heart (Painter, 1983), and *Aplysia* gill (Weiss *et al.*, 1984). The low potency of FMRFamide receptor-stimulated adenylate cyclase in SQM is consistent with the observed inhibitory effect of GTP on receptor binding. The larger effects of acFnLRFa and YFMRFa relative to FMRFamide suggest that the *N*-terminally modified peptides may have higher efficacies at the receptor.

Solubilized FMRFamide receptors

The FMRFamide receptor in the squid shares with the family of G-protein-coupled receptors the characteristic that it can be solubilized by digitonin, CHAPS, and CHAPSO (all detergents containing the steroid skeleton), while still retaining the ability to bind ligands (Haga *et al.*, 1990). This family of receptors consists of integral membrane proteins of 40–50 kDa, with seven membrane-spanning regions and a ligand-binding pocket buried within the transmembrane domain of the protein (Dohlman *et al.*, 1987; Lismaa and Shine, 1992). In some instances, as with the FMRFamide receptor, solubilized receptors retain their association with the heterotrimeric G-proteins and display GTP-sensitive ligand affinity as in the intact cell (Berrie *et al.*, 1984; Knuhtsen *et al.*, 1988; Marie *et al.*, 1989; Gimpl *et al.*, 1990). The immunoprecipitation of somatostatin receptors has been reported with antibodies directed against G-proteins (He *et al.*, 1990; Law *et al.*, 1991), and this may provide a useful purification step for use with the FMRFamide receptor. In addition, the increased potency of guanine nucleotides observed in the solubilized preparation is consistent with recent reports of similar changes in the neuropeptide Y and somatostatin receptors (Marie *et al.*, 1989; Gimpl *et al.*, 1990).

The unsolubilized FMRFamide receptors appeared to be a single population of high affinity, non-interacting sites. After CHAPS-solubilization, the kinetic analysis of radioligand binding and the potencies of FMRFamide analogs in the displacement experiments suggest that high affinity binding is slightly enhanced by CHAPS treatment. The unchanged structure-activity relations of peptide binding suggest that the detergent did not adversely affect the ligand binding site, but the curvilinear Scatchard plot does indicate some heterogeneity. Considering also the Hill coefficients of 0.5–0.9 for the peptide analogs, we suggest that the solubilized preparation contains a mixture of receptors, some of which have been perturbed by detergent and show a decreased affinity for ligand. This heterogeneity would account for the nonlinear Scatchard

Figure 14. Identification of immunoreactive and receptor-reactive FMRFamide in squid optic lobe. (A) In one experiment a squid optic lobe extract was analyzed on a C_4 HPLC column as described in the Methods. The fractions were analyzed by RIA with S253 antiserum, and the FMRFamide immunoreactivity has been plotted against time. The peaks eluting in the positions of FMRFamide and FLRFa (indicated with arrows) inhibited 76 and 44% of specific binding in the assay, corresponding to 1.32 and 0.096 nmoles, respectively. (B) The fractions from the HPLC in A were analyzed by radioreceptor assay with squid optic lobe membranes and [^{125}I]-daYFnLRFa, and the FMRFamide receptor-reactivity has been plotted against time. The peaks eluting in the positions of FMRFamide and FLRFamide inhibited 82 and 54% of specific binding in the assay, corresponding to 1.65 and 0.14 nmoles, respectively. (C) A squid optic lobe was heated to 95°C for 10 min in 0.1 M NaOH. The mixture was spun in an Eppendorf centrifuge at 14,000 rpm, and 0.3 μl of the supernatant was used for PCR with the primers and conditions described in the Methods. The sequence of one of the cloned PCR products is shown.

plots and the Hill coefficients less than unity, and would also be consistent with the sub-nM IC_{50}s measured at low radioligand concentrations (conditions under which the highest affinity binding sites are primarily detected). At higher radioligand concentrations, as in the Scatchard analyses, the lower affinity sites are occupied and contribute to the observed values of specific binding. Since the membrane-bound receptor shows no sign of heterogeneity, it seems clear that solubilization is responsible for producing it. In that case, the optimal recovery of high affinity FMRFamide receptors from SQM will require the development of protective conditions to preserve high affinity binding. Once optimal conditions are achieved, the high affinity, specificity, and abundance of FMRFamide receptors in squid optic lobe suggest it is an ideal source from which to purify the receptors.

FMRFamide-like peptides in squid

We have clearly shown that FMRFamide and related peptides are present in squid optic lobe. First, HPLC peaks of FMRFamide-like reactivity that elute with synthetic FMRFamide and FLRFa have been detected both with a specific RIA and with a specific radioligand receptor assay. The concordance of these parallel assays already suggests strongly that squid optic lobes contain authentic FMRFamide and FLRFa. This conclusion is further reinforced by our detection, in genomic DNA prepared from optic lobe, of a gene encoding the FMRFamide precursor protein. Unidentified peaks of FMRFamide reactivity were also detected. One of these, eluting between FMRFamide and FLRFa, contained material that binds to both the FMRFamide antiserum and the receptor; later-eluting peaks from acetone extracts were also detected, but only by their immunoreactivity. Thus, other FMRFamide-like peptides probably occur in squid optic lobe. These findings are consistent with the notion, based on numerous observations, that FMRFamide, FLRFamide and various homologs, some *N*-terminally extended, occur in all molluscs (Price and Greenberg, 1989). More to the point, however, Martin and Voigt (1987) have identified FMRFamide, FLRFa, AFLRFa, and TFLRFa in the optic lobe of an octopodid cephalopod, *Octopus vulgaris*. Our identification of both FMRFamide-related peptides and FMRFamide receptors in squid optic lobes indicates that members of this peptide family function as neurotransmitters in this part of the central nervous system. Such a regulatory role for FMRFamide has been described for the squid giant synapse (Cottrell *et al.*, 1989), but further studies will be required to elucidate the functions of FMRFamide-like peptides in the optic lobe.

Acknowledgments

We thank our colleagues for helpful discussions, and James T. Russell for support and laboratory space. We also thank Joe DeGeorgis for the dissection and preservation of squid tissues. Support for peptide syntheses was provided by grant No. HL28440 to M.J.G. This is contribution No. 312 of the Tallahassee, Sopchoppy, and Gulf Coast Marine Biological Association. G.J.C. would like to dedicate this paper to Professor Guido Guidotti.

Literature Cited

Abrams, T. W., V. F. Castellucci, J. S. Camardo, E. R. Kandel, and P. E. Lloyd. 1984. Two endogenous neuropeptides modulate the gill and siphon withdrawal reflex in *Aplysia* by presynaptic facilitation involving cAMP-dependent closure of a serotonin-sensitive potassium channel. *Proc. Natl. Acad. Sci. USA* **81:** 7956–7960.

Allard, M., S. Geoffre, P. Legendre, J. D. Vincent, and G. Simonnet. 1989. Characterization of rat spinal cord receptors to FLFQPQRFamide, a mammalian morphine modulating peptide: a binding study. *Brain Res.* **500:** 169–176.

Aronstam, R. S., and T. K. Narayanan. 1988. Temperature effect on the detection of muscarinic receptor-G protein interactions in ligand binding assays. *Biochem. Pharmacol.* **37:** 1045–1049.

Berrie, C. P., N. J. Birdsall, E. C. Hulme, M. Keen, and J. M. Stockton. 1984. Solubilization and characterization of guanine nucleotide-sensitive muscarinic agonist binding sites from rat myocardium. *Br. J. Pharmacol.* **82:** 853–861.

Childers, S. R., and S. H. Snyder. 1980. Differential regulation by guanine nucleotides of opiate agonist and antagonist interactions. *J. Neurochem.* **34:** 583–93.

Chin, G. J., and S. A. Goldman. 1992. Purification of squid synaptic vesicles and characterization of the vesicle-associated proteins synaptobrevin and Rab3A. *Brain Res.* **571:** 89–96.

Cottrell, G. A., E. F. Stanley, M. Sugimori, J. W. Lin, and R. Llinas. 1989. Arterial perfusion of FMRFamide-related peptides potentiates transmission at the giant synapse of the squid. *Biol. Bull.* **177:** 322.

Dohlman, H. G., M. G. Caron, and R. J. Lefkowitz. 1987. A family of receptors coupled to guanine nucleotide regulatory proteins. *Biochemistry* **26:** 2657–2664.

Gimpl, G., R. Gerstberger, U. Mauss, K. N. Klotz, and R. E. Lang. 1990. Solubilization and characterization of active neuropeptide Y receptors from rabbit kidney. *J. Biol. Chem.* **265:** 18142–18147.

Haga, T., K. Haga, and E. C. Hulme. 1990. Solubilization, purification, and molecular characterization of receptors: principles and strategy. Pp. 1–50 in *Receptor Biochemistry: A Practical Approach*, E. C. Hulme, ed. Oxford University Press, New York.

Hall, M. D., M. A. Hoon, N. J. Ryba, J. D. Pottinger, J. N. Keen, H. R. Saibil, and J. B. Findlay. 1991. Molecular cloning and primary structure of squid (*Loligo forbesi*) rhodopsin, a phospholipase C-directed G-protein-linked receptor. *Biochem. J.* **274:** 35–40.

He, H. T., D. S. Rens, J. M. Martin, S. F. Law, S. Borislow, M. Woolkalis, D. Manning, and T. Reisine. 1990. Solubilization of active somatostatin receptors from rat brain. *Mol. Pharmacol.* **37:** 614–621.

Higgins, W. J., D. A. Price, and M. J. Greenberg. 1978. FMRFamide increases the adenylate cyclase activity and cylic AMP level of molluscan heart. *Eur. J. Pharmacol.* **48:** 425–430.

Kling, G., and P. M. Jakobs. 1987. Cephalopod myocardial receptors: pharmacological studies on the isolated heart of *Sepia officinalis* L. *Experientia* **43:** 511–525.

Knuhtsen, S., J. P. Esteve, B. Bernadet, N. Vaysse, and C. Susini. 1988. Molecular characterization of the solubilized receptor of somatostatin from rat pancreatic acinar membranes. *Biochem J.* **254:** 641–647.

Kuhlman, J. R., C. Li, and R. L. Calabrese. 1985. FMRF-amide-like substances in the leech. II. Bioactivity on the heartbeat system. *J. Neurosci.* **5:** 2310–2317.

Lake, J. R., M. V. Hammond, R. C. Shaddox, L. M. Hunsicker, H. Y. Yang, and D. H. Malin. 1991. IgG from neuropeptide FF antiserum reverses morphine tolerance in the rat. *Neurosci. Lett.* **132:** 29–32.

Law, S. F., D. Manning, and T. Reisine. 1991. Identification of the subunits of GTP-binding proteins coupled to somatostatin receptors. *J. Biol. Chem.* **266:** 17885–17897.

Linacre, A., E. Kellett, S. Saunders, K. Bright, P. R. Benjamin, and J. F. Burke. 1990. Cardioactive neuropeptide Phe-Met-Arg-Phe-NH_2 (FMRFamide) and novel related peptides are encoded in multiple copies by a single gene in the snail *Lymnaea stagnalis*. *J. Neurosci.* **10:** 412–419.

Lismaa, T. P., and J. Shine. 1992. G protein-coupled receptors. *Curr. Opin. Cell. Biol.* **4:** 195–202.

Malin, D. H., J. R. Lake, D. E. Fowler, M. V. Hammond, S. L. Brown, J. E. Leyva, P. E. Prasco, and T. M. Dougherty. 1990a. FMRF-NH_2-like mammalian peptide precipitates opiate-withdrawal syndrome in the rat. *Peptides* **11:** 277–280.

Malin, D. H., J. R. Lake, M. V. Hammond, D. E. Fowler, R. B. Rogillio, S. L. Brown, J. L. Sims, B. M. Leecraft, and H. Y. Yang. 1990b. FMRF-NH_2-like mammalian octapeptide: possible role in opiate dependence and abstinence. *Peptides* **11:** 969–972.

Malin, D. H., K. Payza, J. R. Lake, L. S. Corriere, T. M. Benson, D. A. Smith, R. K. Baugher, K. K. Ho, and K. Burgess. 1993. Enhanced antiopiate activity in peptidomimetics of FMRFamide containing Z-2,3-methanomethionine. *Peptides* **14:** 47–51.

Man-Son-Hing, H., M. J. Zoran, K. Lukowiak, and P. G. Haydon. 1989. A neuromodulator of synaptic transmission acts on the secretory apparatus as well as on ion channels. *Nature* **341:** 237–239.

Marie, J. C., P. Cotroneo, R. de Chasseval, and G. Rosselin. 1989. Solubilization of somatostatin receptors in hamster pancreatic beta cells. Characterization as a glycoprotein interacting with a GTP-binding protein. *Eur. J. Biochem.* **186:** 181–188.

Martin, R., and K. H. Voigt. 1987. The neurosecretory system of the octopus vena cava: a neurohemal organ. *Experientia* **43:** 537–543.

Painter, S. D. 1983. FMRFamide inhibition of a molluscan heart is accompanied by increases in cyclic AMP. *Neuropeptides* **3:** 19–28.

Payza, K. 1987. FMRFamide receptors in *Helix aspersa Peptides* **8:** 1065–1074.

Payza, K., and H.-Y. T. Yang. 1993. Modulation of neuropeptide FF receptors by guanine nucleotides and cations in membranes of rat brain and spinal cord. *J. Neurochem.* **60:** 1894–1899.

Payza, K., M. J. Greenberg, and D. A. Price. 1989. Further characterization of *Helix* FMRFamide receptors: kinetics, tissue distribution, and interactions with the endogenous heptapeptides. *Peptides* **10:** 657–661.

Payza K., C. A. Akar, and H.-Y. T. Yang. 1993. Neuropeptide FF receptors: structure-activity relationship and effect of morphine. *J. Pharmacol. Exp. Therap.* **267:** 88–94.

Price, D. A. 1983. FMRFamide: Assays and artifacts. Pp. 184–190 in *Molluscan Neuroendocrinology*, J. Lever and H. H. Boer, eds. North Holland Publishing Co., New York.

Price, D. A., and M. J. Greenberg. 1977. Structure of a molluscan cardioexcitatory neuropeptide. *Science* **197:** 670–671.

Price, D. A., and M. J. Greenberg. 1989. The hunting of the FaRPs: the distribution of FMRFamide-related peptides. *Biol. Bull.* **177:** 198–205.

Raffa, R. B. 1988. The actions of FMRFamide (Phe-Met-Arg-Phe-NH_2) and related peptides on mammals. *Peptides* **9:** 915–922.

Rosoff, M. L., T. R. Bürglin, and C. Li. 1992. Alternatively spliced transcripts of the flp-1 gene encode distinct FMRFamide-like peptides in *Caenorhabditis elegans*. *J Neurosci.* **12:** 2356–2361.

Rothman, R. B. 1992. A review of the role of anti-opioid peptides in morphine tolerance and dependence. *Synapse* **12:** 129–138.

Schneider, L. E., and P. H. Taghert. 1988. Isolation and characterization of a *Drosophila* gene that encodes multiple neuropeptides related to Phe-Met-Arg-Phe-NH_2 (FMRFamide). *Proc. Natl. Acad. Sci. USA* **85:** 1993–1997.

Tang, J., H.-Y. T. Yang, and E. Costa. 1984. Inhibition of spontaneous and opiate-modified nociception by an endogenous neuropeptide with Phe-Met-Arg-Phe-NH_2-like immunoreactivity. *Proc. Natl. Acad. Sci. USA* **81:** 5002–5005.

Taussig, R., and R. H. Scheller. 1986. The *Aplysia* FMRFamide gene encodes sequences related to mammalian brain peptides. *DNA* **5:** 453–461.

Voigt, K. H., C. Kiehling, D. Frösch, M. Schiebe, and R. Martin. 1981. Enkephalin-related peptides: direct action on the octopus heart. *Neurosci. Lett.* **27:** 25–30.

Weiss, S., J. I. Goldberg, K. S. Chohan, W. K. Stell, G. I. Drummond, and K. Lukowiak. 1984. Evidence for FMRF-amide as a neurotransmitter in the gill of *Aplysia californica*. *J. Neurosci.* **4:** 1994–2000.

Yang, H.-Y. T., W. Fratta, E. A. Majane, and E. Costa. 1985. Isolation, sequencing, synthesis, and pharmacological characterization of two brain neuropeptides that modulate the action of morphine. *Proc. Natl. Acad. Sci. USA* **82:** 7757–7761.

Reference: *Biol. Bull.* **187**: 200–207. (October, 1994)

Neurofilament-Like Immunoreactivity in the Sea Anemone *Condylactis gigantea* (Cnidaria: Anthozoa)

CHRISTIAN DELLACORTE[1]*, DON S. ANDERSON[2],
WILLIAM. O. McCLURE[1], AND D. LYNN KALINOSKI[3]

[1]*Department of Neurobiology, University of Southern California, Los Angeles, California 90089-2520;* [2]*School of Dentistry, University of Southern California, Los Angeles, California 90089;* [3]*Monell Chemical Senses Center, 3500 Market St., Philadelphia, Pennsylvania 19104*

Abstract. The neuronal cytoskeleton contains neurofilament proteins that serve as markers for nervous tissue in many species across phyla. Antiserum generated to mammalian neurofilaments was used for immunocytochemical staining of tissues in the sea anemone *Condylactis gigantea* (Cnidaria: Anthozoa). Specific staining, visible at the light and electron microscope levels, was found in the tissues of the tentacle. Proteins were extracted from the tissues and solubilized. SDS-polyacrylamide gel electrophoresis and Western blotting revealed two bands of MW_r 156 kD and 74 kD that reacted with antiserum generated to neurofilaments. The protein bands also bound a monoclonal antibody shown to react with a highly conserved epitope in many classes of intermediate filaments. These data suggest that the neurons of this anthozoan contain neurofilament-like proteins with molecular properties similar to those of mammalian neurons.

Introduction

Nervous systems probably evolved in animals related to members of present-day cnidarians. The nervous system in these primitive metazoans has been described as consisting of diffuse nets of sensory, motor, and neurosecretory cells that provide connections within the epithelial layers (Bullock and Horridge, 1965).

Neuronal cells and processes contain a filamentous framework that forms the cytoskeleton. Neurofilaments (NFs), a class of structures that express a head-rod-tail organization, belong to the family of intermediate filaments (IFs) and are major components of the neuronal cytoskeleton (Wang *et al.*, 1985; Steinert and Roop, 1988). The central helical rod domain has a hydrophobic backbone that causes aggregation of the subunits into coiled-coil 10-nm filamentous structures; this domain also contains an evolutionarily conserved region, a major feature found in identified IF proteins (Pruss *et al.*, 1981; Geisler and Weber, 1982; Hanukoglu and Fuchs, 1983; Steinert *et al.*, 1983). Besides playing a central role in the structural matrix of neurons, NFs are of particular interest because they may be determining factors in the development of the central nervous system.

The presence and location of these filaments have been visualized by various methods, including histological staining and immunocytochemistry (Phillips *et al.*, 1983; Lasek *et al.*, 1985). NFs have been isolated from many cell types (Cooke and Chase, 1971; Daniels and Huneeus, 1973; Brown *et al.*, 1976) and a variety of species (Lasek *et al.*, 1979; Moon *et al.*, 1981; Phillips *et al.*, 1983). Mammalian neurofilaments are composed of three polypeptides (the "triplet" proteins), with molecular weights of approximately 200 kD (NF-H), 160 kD (NF-M), and 70 kD (NF-L) (Kaufmann *et al.*, 1984; Scott *et al.*, 1985). Some non-mammalian species have triplet proteins that are homologous to those found in mammals. Others, however, have only a single high molecular weight subunit that is immunologically similar to both NF-H and NF-M (Shaw *et al.*, 1984; Shaw, 1991). In invertebrates, neurofilaments are even more variable than their vertebrate counterparts (Eagles *et al.*, 1981; Shaw, 1991; Szaro *et al.*, 1991; Way *et al.*, 1992).

The cytoskeletal components that form an early metazoan nervous system, such as the one found in members of the phylum Cnidaria, are not well-defined. We use im-

---

Received 22 October 1993; accepted 2 August 1994.

* Corresponding author's present address: Monell Chemical Senses Center, 3500 Market St., Philadelphia, PA 19104.

munocytochemical techniques, as well as protein isolation, light microscopy, and transmission electron microscopy (TEM), in our studies of the nervous system in these lower organisms. In this investigation, we focused on confirming the presence of neurofilament-like antigens in the tissues of the subtropical sea anemone *Condylactis gigantea* (Cnidaria: Anthozoa). Our studies suggest that neurons of this anthozoan contain neurofilament-like proteins with molecular properties similar to those of higher species.

Materials and Methods

Animals

Specimens of *Condylactis gigantea* were obtained from a supplier in Los Angeles, California, and kept in aerated, filtered, recirculating aquaria at 24°C in natural seawater from the Catalina Marine Science Center (Santa Catalina Island, California). Animals acquired from local suppliers in Philadelphia, Pennsylvania, were kept in aerated, filtered artificial seawater. All animals were maintained on a 12/12 photoperiod and fed *Artemia* nauplii, small pieces of squid, or both three times a week. Water was changed at two-week intervals.

Specimens were relaxed by immersion in seawater containing succinylcholine chloride (67 μg/ml, Sigma Chemical Co., St. Louis, Missouri). The tentacles of these relaxed animals were of about normal length, but the diameter was somewhat smaller than normal. They were clamped with a hemostat at the junction of the oral disk and excised.

Bodian silver stain

The Bodian silver stain method allows visualization of neural tissue in many species (Bodian, 1936; Gambetti *et al.*, 1981). Bodian silver stain was applied to tissue sections as described by Clark (1981) and to SDS polyacrylamide gels after electrophoresis of proteins as described by Gambetti *et al.* (1981).

Light microscopic immunocytochemistry

Excised tentacles were placed in 2% paraformaldehyde in phosphate buffered saline (PBS; 0.1 *M* sodium phosphate buffer, 0.9% NaCl), pH 6.5, for 2 h at room temperature and were postfixed in 2% paraformaldehyde in PBS, pH 11 (Berod *et al.*, 1981), for 8 h at 4°C. Samples were rinsed three times in PBS, pH 7.4, and cryoprotected by immersion for 12 h each in 10, 20, and 30% sucrose in PBS, pH 7.4, at 4°C. Tissue was placed in Tissue-Tek (Miles Inc., Elkhart, Indiana) and frozen in isopentane at liquid nitrogen temperatures. Twenty micrometer sections were made on a Microm 500 M Cryostat (Zeiss Inc., Thornwood, New York) at −20°C and thaw-mounted on slides.

Slides were placed in PBS for 20 min and endogenous peroxidases were inactivated with 0.3% hydrogen peroxide in PBS for 20 min. After being rinsed in three successive 15-min changes of PBS, the specimens were incubated for 1 h in PBS containing 0.3% Triton X-100 and 10% normal serum (Vector Laboratories, Burlingame, California), then placed in primary antiserum [polyclonal neurofilament 200 (NF 200, Chemicon International, Temecula, California, and Sigma Chemical Co., St. Louis, Missouri)] at a 1:20,000 dilution for 12 h at 4°C. Three 15-min rinses in PBS were followed by incubation with a biotinylated secondary antibody, several PBS rinses, and incubation with a preformed avidin/biotinylated horseradish peroxidase complex (Vector Laboratories, Burlingame, California) following the manufacturer's instructions. Tissues were rinsed two successive times for 10-min each in freshly made acetate/imidazole buffer (0.01 *M* imidazole, 0.05 *M* sodium acetate, pH 7.4) and transferred to a nickel chromagen [0.095 *M* nickel (II) sulfate, 0.05% DAB, 0.03% hydrogen peroxide] in acetate/imidazole buffer to develop.

Control procedures included deletion of secondary antibodies and replacement of the primary antiserum with normal serum.

Electron microscopic immunocytochemistry

Portions of tentacles were placed in 4.0% paraformaldehyde/0.5% glutaraldehyde in 0.1 *M* PBS, pH 6.5, for 1 h at room temperature and transferred to 4.0% paraformaldehyde/0.5% glutaraldehyde, pH 11, for 8 h at 4°C before washing in PBS, pH 7.4, and dehydration in a graded ethanol series. Samples were infiltrated and embedded in EM-BED-812 (Electron Microscopy Sciences, Ft. Washington, Pennsylvania) according to manufacturer's directions. Silver to gold sections were placed on nickel grids (Ted Pella Inc., Redding, California). Grids were floated on small amounts of reagent at room temperature as follows: (1) 1 h on 0.1 *M* PBS at pH 7.4; (2) 5 min on a saturated solution of sodium metaperiodate, followed by 1 h on several changes of PBS; (3) 1 h on 10% normal serum (Vector Laboratories, Burlingame, California); (4) three successive 30-min rinses on PBS; and (5) 2 h on antiserum to polyclonal NF 200 (Sigma Chemical Co., St. Louis, Missouri). Grids were rinsed on three successive changes of PBS and floated on a 1:40 dilution of gold-conjugated IgG (Janssen Life Sciences Products, Piscataway, New Jersey) for 1 h, followed by two successive 20-min distilled water rinses. Grids were postfixed for 15 min on a drop of 2% glutaraldehyde and poststained in lead citrate and uranyl acetate, followed by two successive 15-min rinses on distilled water. Specimens were examined and photographed in a JEOL 100CXII electron microscope (JEOL USA Inc., Peabody, Massachusetts).

Controls consisted of replacement of the primary antiserum with normal serum.

Isolation of neurofilament-like proteins

To demonstrate the existence of neurofilament-like components in the sea anemone *C. gigantea*, we isolated the constituent proteins. To minimize protein contamination, food was withheld from anemones for three days before extraction. Whole anemones were cleaned of debris and weighed. Specimens were chilled for 15 min at −70°C before being quickly chopped into 1-cm^3 pieces and placed in SEDTA (20 m*M* Na-ACES buffer, pH 7.4, 0.3 *M* sucrose, 2 m*M* EDTA) for 15 min with intermittent gentle hand agitation to remove mucus. Minced tissue was transferred to TME medium [10 m*M* tris(hydroxymethyl)-aminomethane (Tris) HCl, 3 m*M* $MgCl_2$, 2 m*M* K_2-ethylene glycol-bis(β-aminoethyl ether)-*N,N,N′,N′*-tetraacetic acid (EGTA), pH 8.2] and homogenized, with the aid of a Teflon-glass homogenizer, in the presence of protease inhibitors [10 μg/ml leupeptin, 76.8 n*M* aprotinin, 0.7 μM pepstatin, 0.83 m*M* benzamide, 0.23 m*M* phenylmethanesulfonyl fluoride (PMSF), and 1 m*M* iodoacetamide] at 4°C. The homogenate was centrifuged at 9000 × *g* (SS34 rotor) for 2 h at 0°C and the supernatant (S1) reserved. The pellet was successively washed four times in ice cold TME with a brief centrifugation after each wash at 9000 × *g* for 15 min at 0°C. Because of the difficulty encountered in solubilizing cytoskeletal components in Triton X-100 in early experiments, all subsequent procedures utilized sodium dodecyl sulfate (SDS). Pelleted material was resuspended in TME containing 2% SDS, homogenized in a Teflon-glass homogenizer, and centrifuged at 9000 × *g* for 2 h at 0°C. The supernatant (S2) was removed and stored at −70°C. The pellet (P2) was washed in TME and re-extracted in SDS. Any remaining insoluble material was removed by centrifugation at 9000 × *g* for 2 h at 0°C, and the supernatant (S3) was stored at −70°C. Protein content was determined by the method of Bradford (1976).

Control procedures consisted of extraction of rat brain as described above.

Absorption of the neurofilament-like extract

In several experiments, polyclonal NF 200 antibodies were absorbed with the washed resuspension of neurofilament-like protein (S2, above) from which the SDS had been removed (Suzuki and Terada, 1988) prior to use. The preparation, consisting of the extract of neurofilament-like proteins and the added antibodies, was placed at 4°C for 24 h with gentle stirring. The supernatant was decanted after centrifugation at 9500 × *g* for 2 h at 0°C and was used for immunostaining.

SDS-polyacrylamide gel electrophoresis and Western blotting

Proteins were electrophoresed in the presence of SDS on 12.5% and 4/20% gradient gels by the method of Laemmli (1970) and transferred to nitrocellulose sheets. Western blotting was performed by the method of Towbin *et al.* (1979). In brief, blots were processed through incubations with blocking solution (5% skim milk in 0.1 *M* PBS/0.1% Tween-20) for 12 h at 4°C, and immunostained with one of the following: (1) polyclonal anti-NF 200 at a 1:150 dilution of a 9.87 mg/ml stock solution (Sigma Chemical Co., St. Louis, Missouri); (2) monoclonal antibody generated to mouse NF 200 (phosphorylated and nonphosphorylated forms; Clone N52) at a 1:150 dilution of the stock solution (Sigma Chemical Co., St. Louis, Missouri); (3) monoclonal anti-microtubule-associated protein-2 (anti-MAP-2) at a 1:2000 dilution of a 2 mg/ml stock solution (clone AP20; Boehringer Mannheim Corp., Indianapolis, Indiana); (4) monoclonal anti-tau microtubule-associated protein (anti-tau) at a 1:100 dilution of the 1 mg/ml stock solution (clone Tau 1; Boehringer Mannheim Corp., Indianapolis, Indiana); or (5) undiluted hybridoma supernatant to an anti-IFA antibody (Antibody to Intermediate Filament Antigen; Pruss *et al.*, 1981) for 1 h at 4°C. Incubation was followed by biotinylated anti-rabbit or anti-mouse immunoglobulins and an avidin-horseradish peroxidase complex (Vector Laboratories, Burlingame, California) according to manufacturer's directions. Conjugates were visualized with a 4-chloro-1-naphthol/peroxidase substrate system (Kirkegaard & Perry, Gaithersburg, Maryland).

Results

Bodian silver stain

The Bodian method was originally developed to stain neural components and is known to stain NF proteins specifically. Bodian silver stain was applied to tissue sections and to SDS polyacrylamide gels after electrophoresis. Neither method produced a visible reaction product (not shown).

Light microscopic immunocytochemistry

Figure 1 shows a transverse section of anemone tentacle stained with polyclonal antiserum raised to NF 200. These antibodies exhibit wide species cross-reactivity (Chemicon International, Temecula, California, Sigma Chemical Co., St. Louis, Missouri). A large proportion of the nickel-enhanced immunoreactive product was localized to an area above the mesoglea known to contain a dense plexus

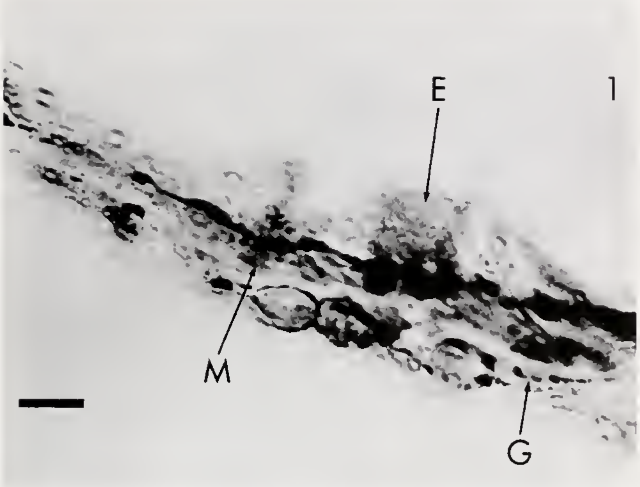

Figure 1. Light microscopy. Cross-section of a tentacle of *Condylactis gigantea* showing specific nickel-enhanced immunostain with polyclonal NF 200 antisera. The product is localized to an area above the muscle layer and mesoglea that contains the neural plexus. Reaction product is also seen in the gastrodermis. The scale bar is 10 μm. E, epidermis; M, mesoglea; G, gastrodermis.

of nerve cell bodies and processes (C. DellaCorte, C. Fulenwider, D. Hessinger, and W.O. McClure, manuscript in prep). Immunolocalization was also seen within the gastrodermis, central to symbiotic zooxanthellae. Absorption of the antibodies with an extract of *C. gigantea* neurofilament-like protein removed this reactivity. Replacement of the primary, specific antibody with normal serum, or deletion of the secondary antibody, also eliminated the appearance of product.

Electron microscopic immunocytochemistry

Immunocytochemical localization within the tissues of *C. gigantea* was examined further by electron microscopy. With the chosen protocol, we were able to preserve antigenicity. Cytoskeletal morphology could not be fully maintained, however. Immunogold labeling was predominately localized within the processes of the neural plexus (Fig. 2) above the layer of myocytes. Immunogold labeling displayed the same relative pattern in all cellular neural compartments considered. No appreciable number of gold particles were observed over non-neural tissues. The specificity of labeling was assessed with controls: sections adjacent to those immunolabeled with anti-NF 200 were reacted with normal serum. The control sections lacked the labeling described above, or showed only extremely sparse and randomly scattered distribution of gold particles, demonstrating low background. These observations provide additional evidence that the immunoreactive material is located in the neurons of *C. gigantea*.

Gel electrophoresis and Western blotting

To further demonstrate the existence of neurofilament-like proteins in this species, we probed Western blots of Triton-insoluble proteins with several specific immunological probes. Polyclonal NF 200 antiserum revealed two bands of apparent molecular weights 156,000 and 74,000 daltons (Fig. 3). A similar pattern (not shown) was found with a monoclonal antiserum known to react with an epitope present on both the phosphorylated and non-phosphorylated forms of the polypeptide in the tail domain of the NF-H subunit.

Western blots of Triton-insoluble material from *C. gigantea* were also probed with monoclonal antibodies to the microtubule-associated proteins, anti-MAP2 (Fig. 4) and anti-tau (Fig. 5), and with a monoclonal antibody (anti-IFA; Pruss *et al.*, 1981) known to bind to most of the defined major intermediate filament proteins. MAP2 isolated from rat brain consists of two major polypeptides (MAP2a and MAP2b) of similar molecular weights, approximately 275 kD, although proteolysis can result in a 35 kD domain and a major 240 kD domain (Vallee, 1980). Clear patterns of immunolabeling of the putative neurofilament bands (*i.e.*, 156,000 and 74,000 daltons) extracted from *C. gigantea* are evident in both blots probed with antibodies to MAP2 (Fig. 4) and tau (Fig. 5), as are the expected high molecular weight MAP2 protein band and the multiple 55 kD to 62 kD tau bands (Cleveland *et al.*, 1977a,b) present in the control tissues of the rat. In a similar fashion, the anti-IFA Western blot revealed two distinct bands of about 156 kD and 74 kD in the extract from the tissues of the sea anemone (Fig. 6).

Discussion

The presence of neurofilament-like proteins in the sea anemone *Condylactis gigantea* was investigated using

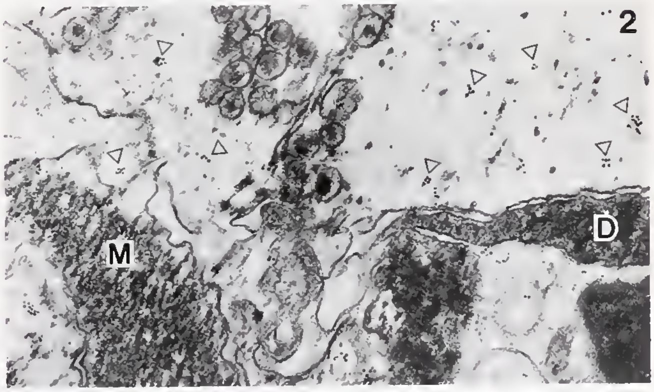

Figure 2. Transmission electron microscopy. Cross-section of a tentacle showing immuno-gold labeling of anti-NF 200 localized within the cytoplasm of the neural processes. Synaptic vesicles line a neuro-neuronal synapse. Reaction product (arrowheads) is seen within the neuronal processes. Magnification: 50,000×. M, muscle; D, desmocyte process.

3

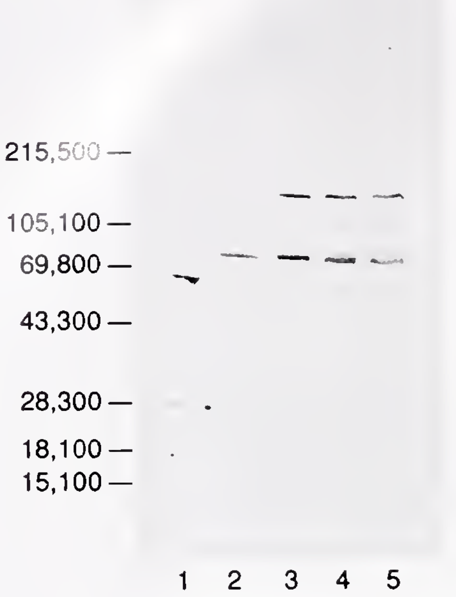

Figure 3. Western blotting. Proteins were separated on a 4/20% gradient gel and visualized with a polyclonal antibody directed against NF 200. Two bands of MW$_r$ 156 kD and 74 kD were specifically labeled in the extract from the sea anemone *Condylactis gigantea.* Lane 1: molecular weight standards (MW$_r$); Lane 2: anemone S2 fraction, 5.0 μg protein per lane; Lane 3: anemone S2 fraction, 9.5 μg protein per lane; Lane 4: anemone S2 fraction, 12.0 μg protein per lane; Lane 5: anemone S2 fraction, 15.0 μg protein per lane.

several methods, including Bodian stain which binds an acidic, glutamate-rich region in the carboxy terminal of NF-L, NF-M, and NF-H (Autilio-Gambetti *et al.,* 1981). This staining technique, used to identify neurofilament proteins in many species, did not produce positive results. But other data gathered during our study suggest that neurofilament-like proteins are present in *C. gigantea.*

A number of immunological studies have shown regional phylogenetic conservation of neurofilament proteins (Chiu *et al.,* 1980; Autilio-Gambetti *et al.,* 1981; Shaw *et al.,* 1984). Immunological staining of Western blots of Triton-insoluble proteins from *C. gigantea* revealed 156,000 and 74,000 dalton molecular weight bands that correspond to those seen in published electrophoretic profiles. Explaining the presence of a low molecular weight band when using monoclonal and polyclonal antisera to NF-H is problematic, however. Many polyclonal and monoclonal antibodies reportedly recognize epitopes shared by NF-H and NF-M (Lee *et al.,* 1987; Schmidt *et al.,* 1987). Cross-reactivity between these subunits and NF-L is less well-known, although there is a report of simultaneous immunodetection of all three NF subunits (Cochard and Paulin, 1984). The presence of these immunoreactive proteins suggests that polypeptide regions homologous to those found in other organisms are present in this species.

Immunological studies also reveal species-specific differences in the number and the molecular weight of neurofilament proteins. In birds and crocodilia, NF proteins appear to be directly homologous to the neurofilament triplet. Other reptiles express only a single high molecular weight subunit immunologically related to both NF-H and NF-M (Shaw *et al.,* 1984; Shaw, 1991). Studies in fish demonstrate between one and four (or more) major subunits (Phillips *et al.,* 1983; Lasek *et al.,* 1985; Dahl *et al.,* 1986). Neurofilaments in invertebrates, however, are more variable than their vertebrate counterparts. Two high molecular weight subunits, each about 160 kD, are found in the marine fan worm *Myxicola infundibulum* (Eagles *et al.,* 1981). Squid contain neurofilament subunits of 60, 200, and 500 kD (Roslansky *et al.,* 1980), although NF proteins with approximate weights of 60, 70, and 220 kD have recently been identified (Szaro *et al.,* 1991; Way *et al.,* 1992). *Aplysia* neurofilaments have apparent molecular weights of 60 kD and 65 kD. This nudibranch is the

4

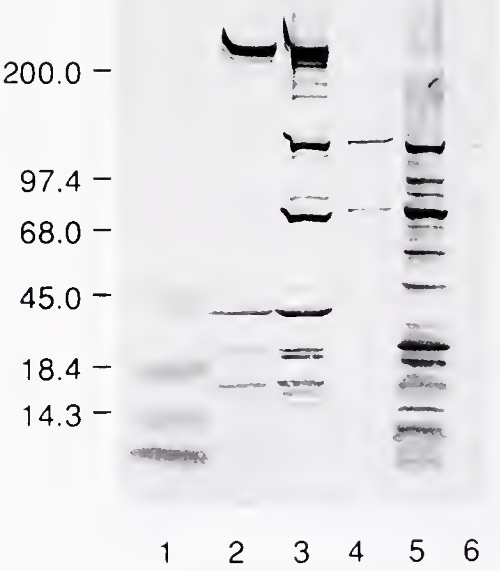

Figure 4. Western blotting. Proteins were separated on a 4/20% gradient gel and were immunoblotted with a monoclonal antibody generated to MAP2. In the protein fraction from *Condylactis gigantea,* two bands of approximate molecular weights 156 kD and 74 kD are found. Immunolocalization to protein fractions from control tissue show a large molecular weight subunit. A smaller, low molecular weight subunit, which may be due to proteolysis, is also present. Lane 1: molecular weight standards (MW$_r$); Lane 2: rat brain cytosolic fraction (S1), 15 μg protein per lane; Lane 3: rat brain membrane fraction (S2), 15 μg protein per lane; Lane 4: anemone S1 fraction, 10 μg protein per lane; Lane 5: anemone S2 fraction, 9.4 μg protein per lane; Lane 6: anemone S3 fraction, 10 μg protein per lane.

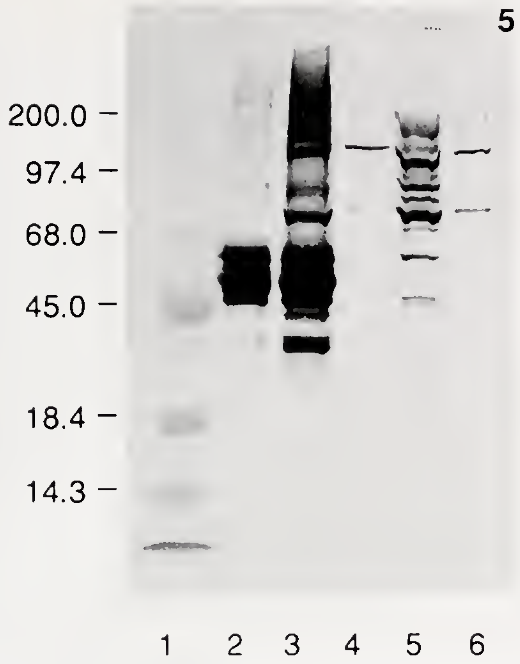

Figure 5. Western blotting. Proteins were separated on a 12.5% gel and bands visualized using monoclonal anti-tau antibody. Cross-reactivity with proteins of MW_r 156 kD and 74 kD extracted from *Condylactis gigantea* is seen. Immunoblotting of protein fractions from control tissue reveals a series of bands of MW_r 55 kD to 62 kD. Lane 1: molecular weight standards (MW_r); Lane 2: rat brain cytosolic fraction (S1), 15 μg protein per lane; Lane 3: rat brain membrane fraction (S2), 15 μg protein per lane; Lane 4: anemone S1 fraction, 10 μg protein per lane; Lane 5: anemone S2 fraction, 9.4 μg protein per lane; Lane 6: anemone S3 fraction, 10 μg protein per lane.

only species investigated to date that does not express a subunit with a molecular weight greater than 100 kD and whose NFs lack an affinity for Bodian stain (Lasek *et al.*, 1985). The presence of only two neurofilament-like proteins in *C. gigantea* may be a reflection of species-specificity.

More evidence for the presence of neurofilament-like epitopes was provided by absorption of the extract containing the neurofilament-like proteins with neurofilament antibodies and by immunoblotting with an antibody, anti-IFA, known to recognize a common antigenic determinant. In many species, anti-IFA has identified the presence of intermediate filaments, although immunoreactivity was not detected in the single species of Cnidaria investigated by others (Pruss *et al.*, 1981; Bartnik *et al.*, 1985; Shaw, 1991). Our immunoblot results with anti-IFA, however, suggest that *C. gigantea* does, in fact, contain the evolutionarily highly conserved epitope. Recognition of this sequence within the rod portion of the filament has, in many cases, been used to identify intermediate filaments (Shaw, 1991).

Microtubules are primary cytoskeletal elements that form polymers with neurofilaments in the nerve cells of many species (Wuerker and Palay, 1969; Hirokawa, 1982). These polymers contain a variety of microtubule-associated proteins (MAPs), including MAP2 and the closely related protein family, tau (Borisy *et al.*, 1975; Weingarten *et al.*, 1975; Cleveland *et al.*, 1977a,b). Antibodies generated to MAP2 and tau cross-react with neurofilament proteins (Kosik *et al.*, 1988; Shaw, 1991). Investigations suggest similarities in sequence and the presence of heavily phosphorylated regions as one explanation for the cross-reactive properties. Tau from rat brain contains four internal repeats consisting of a "Lys-Ser-Pro-Val" motif in the COOH-terminal domain similar to the numerous Lys-Ser-Pro (KSP) repeats found in neurofilament (Kanai *et al.*, 1989; Shaw, 1991. Sequences of MAP2 also demonstrate carboxy-terminal repeats that are highly homologous to those found in tau (Lewis *et al.*, 1988). In addition, some tau isoforms contain amino-terminus regions rich in proline and charged amino acid residues (Goedert *et al.*, 1991. The well-characterized Tau 1 antibody used in this study recognizes an amino terminus epitope located between Pro 189 and Gly 207. This sequence is suggested to be similar to the carboxy-terminus of NF-M (Kosik *et al.*, 1988; Goedert *et al.*, 1991). The antibody is not known to react, however, when Ser 199 and Ser 202 are phosphorylated (Riederer and Binder, 1994). The MAP2 an-

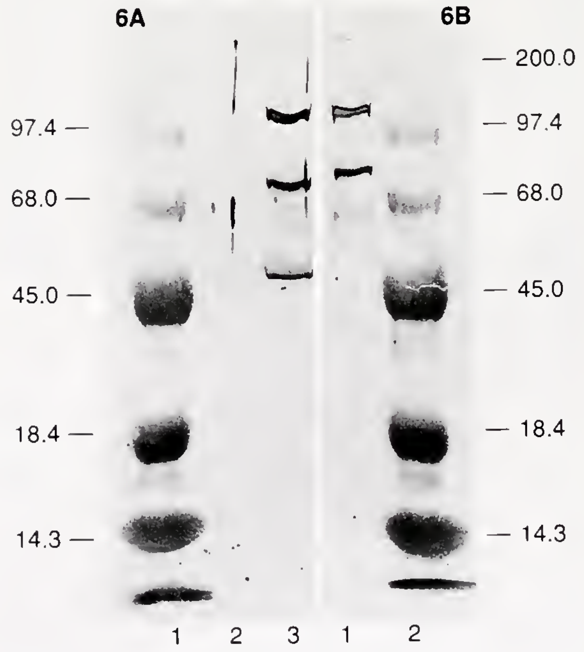

Figure 6. Western blotting. Proteins were electrophoresed on a 12.5% gel and reacted with anti-IFA, resulting in the visualization of two bands of MW_r 156 kD and 74 kD in the extract from *Condylactis gigantea*. **(A)** Lane 1: molecular weight standards (MW_r); Lane 2: rat brain cytosolic fraction (S1), 15 μg protein per lane; Lane 3: rat brain membrane fraction (S2), 15 μg protein per lane; **(B)** Lane 1: anemone S2 fraction, 9.4 μg protein per lane; Lane 2: molecular weight standards (MW_r).

tibody, clone AP20, has only recently been mapped to a carboxy terminus encompassing amino acids 997-1332 (L. Binder, pers. comm.), a region suggested to contain sequences closely related to those found in NF-H, NF-M, and tau proteins (Shaw, 1989). The presence of these conserved regions suggests evolutionary relationships and may account for the immunological similarity seen in a number of studies, including ours.

Considering the well-documented description of a diffuse nerve net in cnidarians, we were surprised to find little immunostaining throughout the epidermis and gastrodermis of the tentacle using anti-NF200. Most of the reaction product was localized within an epidermal neural plexus and, to a lesser extent, to components within the gastrodermis. This pattern was reversed when tissues were immunostained with a polyclonal antiserum generated to NF 150 (C. DellaCorte, unpub. ob.). Selective reactivity of the antisera (*i.e.*, immunodetection of specific subsets of neural components) was not expected but may be the result of several factors including cell size, cell type, presence or lack of post-translational modifications, or the cross-reactivity of the antisera. Many regions in mammalian nervous systems show strong NF staining for some neuronal cell types and partial or complete absence of immunoreactivity in others. This is particularly true for small neurons (Sharp *et al.*, 1982; Trojanowski *et al.*, 1986). In addition to other factors, the type and size of cells in the nervous system of *Condylactis gigantea* may affect the presence and the extent of immunoreactivity in this invertebrate.

The present data suggest that neurons in this anthozoan may contain proteins with molecular properties similar to those of higher species. Although various assumptions about these neurofilament-like proteins may be made, no definitive conclusions can yet be drawn. Knowledge of the primary structure of these early metazoan proteins will provide insight into the functional constraints of protein sequences during evolution.

Acknowledgments

We thank Dr. B. G. Szaro of the Department of Biological Sciences, State University of New York at Albany, for his very generous gift of antibody used in this study. C.D.C. also thanks Alicia Thompson of the University of Southern California's Center for Electron Microscopy and Microanalysis for her invaluable help. This work was supported by a Biomedical Research Support Grant from the University Park Campus of the University of Southern California, by a grant from the Los Angeles chapter of the ARCS (Achievement Rewards for College Scientists) Foundation through the Hancock Institute for Marine Studies at the University of Southern California and, in part, by NIH DG001228 to D.L.K.

Literature Cited

Autilio-Gambetti, L., M. E. Velasco, J. Sipple, and P. Gambetti. 1981. Immunochemical characterization of antisera to rat neurofilament subunits. *J. Neurochem.* **37:** 1260–1265.

Bartnik, E., M. Osborn, and K. Weber. 1985. Intermediate filaments in non-neuronal cells of invertebrates: isolation and biochemical characterization of intermediate filaments form the esophageal epithelium of the mollusk *Helix pomatia*. *J. Cell Biol.* **101:** 427–440.

Berod, A., B. K. Hartman, and J. F. Pujol. 1981. Importance of fixation in immunohistochemistry: Use of formaldehyde solutions at variable pH for the localization of tyrosine hydroxylase. *J. Histochem. Cytochem.* **29:** 844–885.

Bodian, D. 1936. A new method for staining nerve fibers and nerve endings in mounted paraffin sections. *Anat. Rec.* **65:** 89–97.

Borisy, G. G., J. M. Marcum, J. B. Olmstead, D. B. Murphy, and K. A. Johnson. 1975. Purification of tubulin and associated high molecular weight proteins from porcine brain and characterization of microtubule assembly in vitro. *Ann. NY Acad. Sci.* **253:** 107–132.

Bradford, M. M. 1976. A rapid and sensitive method for the quantitation of microgram quantities of protein utilizing the principle of protein-dye binding. *Anal. Biochem.* **72:** 248–254.

Brown, S., W. Levinson, and J. A. Spudich. 1976. Cytoskeletal elements of chick embryo fibroblasts revealed by detergent extraction. *J. Supramol. Struct.* **5:** 119–130.

Bullock, T. H., and G. A. Horridge, eds. 1965. Coelenterata and Ctenophora. Pp. 459–534 in *Structure and Function in the Nervous Systems of Invertebrates*, Vol I. W. H. Freeman Press, San Francisco.

Chiu, F. C., B. Korey, and W. T. Norton. 1980. Intermediate filaments from bovine, rat and human CNS: Mapping analyses of the major proteins. *J. Neurochem.* **34:** 1149–1159.

Clark, G. ed. 1981. Bodian's protargol method. Pp. 152–154 in *Staining Procedures*. Williams and Wilkins, Baltimore, MD.

Cleveland, D. W., S. Hwo, and M. W. Kirschner. 1977a. Purification of tau, a microtubule-associated protein that induces assembly of microtubules from purified tubulin. *J. Mol. Biol.* **116:** 207–225.

Cleveland, D. W., S. Hwo, and M. W. Kirschner. 1977b. Physical and chemical properties of purified tau factor and the role of tau in microtubule assembly. *J. Mol. Biol.* **116:** 227–247.

Cochard, P., and D. Paulin. 1984. Initial expression of neurofilament and vimentin in the central and peripheral nervous system of the mouse embryo in vivo. *J. Neurosci.* **4:** 2080–2094.

Cooke, P. H., and R. H. Chase. 1971. Potassium chloride insoluble myofilaments in vertebrate smooth muscle cells. *Exp. Cell Res.* **66:** 417–425.

Dahl, D., C. J. Crosby, and A. Bignami. 1986. Neurofilament proteins in fish: a study with monoclonal antibodies reacting with mammalian NF 150K and NF 200K. *J. Comp. Neurol.* **250:** 399–402.

Daniels, M. P., and F. C. Huneeus. 1973. Fine structural changes in neurons and nerve fibers associated with colchicine inhibition of nerve fiber formation in vitro. *J. Cell Biol.* **58:** 463–470.

Eagles, P. A. M., D. S. Gilbert, and A. Maggs. 1981. The location of phosphorylation sites and Ca^{2+}-dependent proteolytic cleavage sites on the major neurofilament polypeptides from *Myxicola infundibulum*. *Biochem. J.* **199:** 101–111.

Gambetti, P., L. Autilio-Gambetti, and S. Ch. Papasozomenos. 1981. Bodian's silver method stains neurofilament polypeptides. *Science* **213:** 1521–1522.

Geisler, N., and K. Weber. 1982. The amino acid sequence of chicken muscle desmin provides a common structural model for intermediate filament proteins. *EMBO J.* **1:** 1649–1656.

Goedert, M., R. A. Crowther, and C. C. Garner. 1991. Molecular characterization of microtubule-associated proteins tau and MAP2. *Trends Neurosci.* **5:** 193–199.

Hanukoglu, I., and E. V. Fuchs. 1983. The cDNA sequence of a type II cytoskeletal keratin reveals constant and variable structure domains among keratins. *Cell* **33:** 915–924.

Hirokawa, N. 1982. The crosslinker system between neurofilaments, microtubules and membranous organelles in frog axons revealed by quick freeze, freeze-fracture, deep-etching method. *J. Cell Biol.* **94:** 129–142.

Kanai, Y., R. Takemura, T. Ohshim, H. Mori, Y. Ihara, M. Yanagisawa, T. Masaki, and N. Hirokawa. 1989. Expression of multiple tau isoforms and microtubule bundle formation in fibroblasts transfected with a single tau cDNA. *J. Cell Biol.* **109:** 1173–1184.

Kaufmann, E., N. Geisler, and K. Weber. 1984. SDS-PAGE strongly overestimates the molecular masses of the neurofilament proteins. *FEBS Lett.* **170:** 81–84.

Kosik, K. S., L. D. Orecchio, L. Binder, J. Q. Trojanowski, V. M.-Y. Lee, and G. Lee. 1988. Epitopes that span the tau molecule are shared with paired helical filaments. *Neuron* **1:** 817–825.

Laemmli, U. K. 1970. Cleavage of structural proteins during assembly of the head of bacteriophage T4. *Nature* **227:** 680–685.

Lasek, R. J., N. Krishnan, and I. R. Kaiserman-Abramof. 1979. Identification of the subunit proteins of 10 nm neurofilaments isolated from axoplasm of Squid and *Myxicola* giant axons. *J. Cell Biol.* **82:** 336–346.

Lasek, R. J., L. Phillips, M. J. Katz, and L. Autilio-Gambetti. 1985. Function and evolution of neurofilament proteins. *Ann. N.Y. Acad. Sci.* **455:** 462–478.

Lee, V. M.-Y., M. J. Carden, W. W. Schlaepfer, and J. Q. Trojanoski. 1987. Monoclonal antibodies distinguish several differentially phosphorylated states of the two largest neurofilament subunits (NF-H and NF-M) and demonstrate their existence in the normal nervous system of adult rats. *J. Neurosci.* **7:** 3474–3488.

Lewis, S. A., D. Wang, and N. J. Cowan. 1988. Microtubule-associated protein MAP2 shares a tubulin-binding motif with tau protein. *Science* **242:** 936–939.

Moon, H. M., T. Wisniewski, P. Merz, J. De Martini, and H. M. Wisniewski. 1981. Partial purification of neurofilament subunits from bovine brains and studies on neurofilament assembly. *J. Cell Biol.* **89:** 560–567.

Phillips, L. L., L. Autilio-Gambetti, and R. J. Lasek. 1983. Bodian's silver method reveals molecular variation on the evolution of neurofilament proteins. *Brain Res.* **278:** 219–223.

Pruss, R. M., R. Mirsky, and M. C. Raff. 1981. All classes of intermediate filaments share a common antigenic determinant defined by a monoclonal antibody. *Cell* **27:** 419–428.

Riederer, B. M., and L. I. Binder. 1994. Differential distribution of tau proteins in developing cat cerebellum. *Brain Res. Bull.* **33:** 155–161.

Roslansky, P. F., A. Cornell-Bell, R. V. Rice, and W. J. Adelman. 1980. Polypeptide composition of squid neurofilaments. *Proc. Natl. Acad. Sci. USA* **77:** 404–408.

Schmidt, M. I., M. J. Carden, V. M.-Y. Lee, and J. Q. Trojanoski. 1987. Phosphate dependent and independent neurofilament epitopes on the axonal swellings of patients with motor neuron disease and controls. *Lab Invest* **56:** 282–294.

Scott, D., K. E. Smith, B. J. O'Brien, and K. J. Angelides. 1985. Characterization of mammalian neurofilament triplet proteins, subunit stoichiometry and morphology of native and reconstituted filaments. *J. Biol. Chem.* **260:** 10736–10747.

Sharp, G. A., G. Shaw, and K. Weber. 1982. Immunoelectronmicroscopical localization of the three neurofilament proteins along neurofilaments in cultured dorsal root ganglion cells. *Exp. Cell Res.* **137:** 403–413.

Shaw, G. 1989. Identification of previously unrecognized sequence motifs at the extreme carboxyterminus of the neurofilament subunit NF-M. *Biochem. Biophys. Res. Comm.* **162:** 294–299.

Shaw, G. 1991. Neurofilament proteins. Pp. 185–214 in *The Neuronal Cytoskeleton*, R. D. Burgoyne, ed. Wiley-Liss, Inc., New York.

Shaw, G., E. Debus, and K. Weber. 1984. The immunological relatedness of neurofilament proteins of higher vertebrates. *Eur. J. Cell Biol.* **34:** 130–138.

Steinert, P. M., R. H. Rice, D. R. Roop, B. L. Trus, and A. C. Steven. 1983. Complete amino acid sequence of a mouse epidermal keratin subunit and implications for the structure of intermediate filaments. *Nature* **302:** 794–800.

Steinert, P. M., and D. R. Roop. 1988. Molecular and cellular biology of intermediate filaments. *Annu. Rev. Biochem.* **57:** 593–625.

Suzuki, H., and T. Terada. 1988. Removal of dodecyl sulfate from protein solution. *Anal. Biochem.* **172:** 259–263.

Szaro, B. G., H. C. Pant, J. Way, and J. Battey. 1991. Squid low molecular weight neurofilament proteins are a novel class of neurofilament protein. *J. Biol. Chem.* **266:** 15035–15041.

Towbin, H., T. Staehelin, and J. Gordon. 1979. Electophoretic transfer of proteins from polyacrylamide gels to nitrocellulose sheets: procedure and some applications. *Proc. Natl. Acad. Sci. USA* **76:** 4350–4354.

Trojanowski, J. Q., N. Walkenstein, and V. M.-Y. Lee. 1986. Expression of neurofilament subunits in neurons of the central and peripheral nervous system; an immunohistochemical study with monoclonal antibodies. *J. Neurosci.* **6:** 650–660.

Vallee, R. B. 1980. Structure and phosphorylation of microtubule-associated protein 2 (MAP2). *Proc. Natl. Acad. Sci. USA* **77:** 3206–3210.

Wang, E., D. Fischman, R. K. H. Liem, and T-T. Sun. eds. 1985. *Intermediate Filaments. Ann. N.Y. Acad. Sci.* **455:** 1–832.

Way, J., M. R. Hellmich, H. Jaffe, G. Szaro, H. C. Pant, H. Gainer, and J. Battey. 1992. A high-molecular-weight squid neurofilament protein contains a lamin-like rod domain and a tail domain with Lys-Ser-Pro repeats. *Proc. Natl. Acad. Sci. USA* **89:** 6963–6967.

Weingarten, M. D., A. H. Lockwood, S. Hwo, and M. W. Kirschner. 1975. A protein factor essential for microtubule assembly. *Proc. Natl. Acad. Sci. USA* **72:** 1858–1862.

Wuerker, E. B., and S. L. Palay. 1969. Neurofilaments and microtubules in anterior horn cells of the rat. *Tissue Cell* **1:** 387–402.

Reference: *Biol. Bull.* **187:** 208–214. (October, 1994)

Homeoviscous Properties Implicated by the Interactive Effects of Pressure and Temperature on the Hydrothermal Vent Crab *Bythograea thermydron*

CHRIS N. AIRRIESS[1,*] AND JAMES J. CHILDRESS[2]

[1]*Department of Biological Sciences, University of Calgary, 2500 University Dr. N.W., Calgary, Alberta, T2N 1N4, Canada, and* [2]*Department of Biological Sciences and Marine Science Institute, University of California at Santa Barbara, Santa Barbara, California 93106*

Abstract. Specimens of the hydrothermal vent crab *Bythograea thermydron*, collected from 13° N on the East Pacific Rise, were exposed to pressures greater than those in their natural habitat over a range of temperatures to assess how increased hydrostatic pressure affects a species that requires high pressure to survive. We measured heart beat frequency and contraction waveform at pressures ranging from 28 MPa (normal environmental pressure for this species) to 62 MPa at 5°, 10°, and 20°C. At 5°C, increased hydrostatic pressure induced bradycardia or acardia in conjunction with marked disruption of the ventricular contraction waveform. The animals did not survive following decompression. The effects of increased pressure were less pronounced at 10°C and almost negligible at 20°C. Our results support previous findings at subambient pressures which suggest that the lipid bilayers of cell and organelle membranes are the primary sites affected by short-term pressure variation in deep-sea organisms. We also found evidence of an adaptive mechanism of pressure-temperature interaction in these animals from the eurythermic habitat of the hydrothermal vents.

Introduction

Hydrostatic pressure increases by one atmosphere (101.3 kPa) for each 10 m of depth in the ocean; thus, organisms living at greater depths experience greater pressures (Saunders and Fofonoff, 1976). Elevated pressures have been shown to have a variety of effects on biological systems, with the primary loci for effects being enzyme and membrane systems (Macdonald and Miller, 1976; Wann and Macdonald, 1980; Siebenaller and Somero, 1989; Somero, 1992). At the enzymatic level, pressure exerts an inhibitory effect when there is a volume increase associated with substrate binding or catalytic activity (Siebenaller and Somero, 1989; Somero, 1992). In membranes, the structure of the membrane is altered by the greater compressibility of lipid as compared to water and other membrane components (Macdonald and Miller, 1976).

Both enzyme and membrane adaptations have been found in deep-sea organisms. The enzymatic adaptations involve a reduction in the volume change that occurs in the enzymes of deep-sea organisms during catalysis. As a result, enzyme-substrate affinity and other catalytic properties of the enzymes of deeper-living species are more independent of pressure (Siebenaller and Somero, 1989; Somero, 1992). At the membrane level, the adaptations involve a shift in membrane lipid composition with increasing depth. This shift maintains optimal fluidity (homeoviscous adaptation) in the face of increasing pressure, which would tend to order the membrane lipids (Cossins and Macdonald, 1984, 1986, 1989; Cossins and Sinensky, 1986). The effects of homeoviscous adaptation are expected to be especially prominent in excitable tissues and, unlike those of enzymatic adaptation, to show profound interaction with temperature: lower temperatures ameliorate the effects of lower pressures and higher temperatures ameliorate the effects of higher pressures through their opposite effects on the fluidity of membrane lipids (Cossins and Macdonald, 1989). In addi-

---

Received 7 December 1993; accepted 18 July 1994.

[*] Present address: Laboratory of Molecular Signalling, Department of Zoology, University of Cambridge, Downing Street, Cambridge CB2 3EJ, UK.

tion, one would not expect homeoviscous adaptation to reduce the sensitivity to pressure, as is the case for enzymatic adaptations, but rather to shift the tolerated range of pressure in the same way that it does in temperature adaptation (Sinensky, 1974). There is some indication that the membranes of fishes living at depths greater than 2500 m have reduced compressibility (Behan *et al.*, 1992). Along with reducing the effects of pressure variation on membrane function, this adaptation would preserve the activity of membrane-associated enzymes which are critically dependent on the physical state of the membrane (Gibbs and Somero, 1989).

Although it is clear from the work cited above that both enzyme and membrane adaptations are found in deep-sea organisms, the evaluation of their relative importance must come from studies of the functioning of deep-sea animals. Much work on hydrostatic pressure effects has been concerned with the effects of elevated pressures on organisms that normally live at 1 atm. Other pressure studies have been concerned with species of fishes and crustaceans that live at depths of about 1000 m and have typically demonstrated mild responses to reduced pressure in conjunction with somewhat greater tolerance of elevated pressures (Belman and Gordon, 1979; Quetin and Childress, 1980). Recent studies that used pressure traps to recover specimens demonstrated that species living below 2000 m are dependent on elevated pressures (Macdonald and Gilchrist, 1980, 1982; Yayanos, 1981). Animals living at depths of about 2500 m around hydrothermal vents on the Galapagos Rift also require high pressure for long-term survival, although many can survive decompression to 1 atm if this is soon followed by recompression (Arp and Childress, 1981; Mickel and Childress, 1982a,b; Arp *et al.*, 1984). These animals are also uniquely suited to studies of pressure-temperature interactions because, unlike other deep-sea animals, they experience wide natural temperature ranges. Mickel and Childress (1982a) have demonstrated that when the vent crab *Bythograea thermydron* is exposed to pressures substantially lower than those of its natural habitat, heart rate is reduced and the EKG wave form becomes irregular. Furthermore, the onset of these effects was at higher pressures at higher temperatures and at lower pressures at lower temperatures, a result which the authors interpreted as evidence that membrane lipid properties are important in determining the pressure sensitivity of this species. This study did not, however, test for the effects of superambient pressures on this species, and no other such studies have been conducted on any deep-sea animal. The purpose of the present study was twofold: first, to determine at what pressures an elevation in pressure affects the functioning of a deep-sea animal that requires high pressure for survival; second, to examine the interactive effects of these elevated pressures with temperature.

Materials and Methods

Collection and maintenance

Baited traps deployed and retrieved by the Deep Submergence Vehicle *Alvin* were used to collect specimens of *B. thermydron*, of either sex, from the hydrothermal vent field at 13° N on the East Pacific Rise. Crabs were brought to the surface in insulated containers that kept temperature, but not pressure, relatively constant. Once at the surface, crabs were examined to obtain demographic data, then placed in steel vessels that were maintained at a pressure of 21 MPa (204 atm) and supplied with flowing seawater at approximately 8°C. Under such conditions, survival for more than 18 months has been reported (Mickel and Childress, 1982a).

Animal preparation

In preparation for experimental use, crabs were slowly depressurized, removed from the maintenance vessel, and transferred to a shallow glass container filled with ice-cold seawater. Instrumentation of the animals for impedance pneumography was accomplished as quickly as possible to minimize disturbance and hypobaric trauma.

To measure heart beat frequency, holes were drilled in the dorsal carapace on either side of the heart and two fine silver wires were inserted so that their ends just penetrated the pericardial sinus. To prevent bleeding and hold the wires in position, dental dam was placed over the wires and holes and fixed to the carapace with cyanoacrylate cement. Changes in impedance associated with ventricular contraction were detected by an impedance converter (UFI, model 2991) and recorded on a Gould two-channel pen recorder.

Although not reported as a part of this study, the frequency of scaphognathite beating was recorded as an indicator of the physiological state of the animals. Two impedance pneumography electrodes were affixed inside the exhalant channel of the right branchial chamber and impedance changes caused by movement of the scaphognathite were recorded as above.

Following preparation, crabs were placed without additional restraint in a 6-l stainless steel vessel (Autoclave Engineers) filled with aerated, filtered seawater. Experimental temperatures were maintained inside the pressure vessel by a water-jacket surrounding the chamber. A hand pump (Enerpac) connected *via* Hastelloy C tubing and Autoclave Engineers fittings was used to pressurize the vessel to 28 MPa (272 atm); pressure was monitored using a gauge on the pump. The entire system was rated to 69 MPa (680 atm) working pressure with a 4:1 safety factor.

Animals were allowed to recover at normal environmental pressure until the heart beat frequency stabilized and the scaphognathite began to alternate between periods of continuous beating and inactivity in the fashion typical of nonstressed decapod crustaceans (McMahon and Wilkens, 1972). Animals that did not regain typical, stable readings of heart and scaphognathite activity within 2 h of instrumentation were not used in subsequent experiments.

Experimental protocol

Once the crabs appeared to have recovered, the chart speed was increased to allow resolution of individual contractions of the ventricle. Heart beat frequency was obtained by counting the waveform peaks over a 30-s period. Ventricular contraction pattern was quantified by calculating the standard deviation of 10 successive interbeat intervals. Immediately after this control recording, the pressure inside the experimental chamber was increased from 28 to 31 MPa. The animals were allowed 10 min to adjust, then the chart speed was increased for determination of ventricular contraction frequency and pattern before the pressure was raised to 34 MPa. This protocol continued, with pressure increasing in 3-MPa steps, until the maximum pressure tested (62 MPa) was reached. After 30 min, the vessel pressure was gradually lowered to 28 MPa. Data were obtained 30 min after return to the original pressure, and the chamber was subsequently depressurized for removal of the crabs.

The effects of pressure and temperature on heart beat frequency and contraction pattern were estimated using analysis of variance with repeated measures (ANOVAR). ANOVARs significant at the 0.05 level were further analyzed using Tukey's HSD multiple-comparison test. In addition, Spearman rank correlation was used to determine the relationship between pressure and heart beat frequency at each temperature. All values are reported as the mean ± 1 SEM.

Results

Contraction frequency

The control heart beat frequency of crabs allowed to recover from the instrumentation procedure was positively correlated with experimental temperature ($r_s = 0.937$, $n = 15$, $P < 0.01$). The relationship between temperature and contraction frequency did not, however, remain constant as pressure within the experimental chamber increased (Fig. 1).

At 5°C, heart rate dropped 92% from its control value at 28 MPa to 3.3 ± 1.3 min^{-1} after 10 min at 62 MPa (Fig. 1). The negative correlation between contraction frequency and pressure was highly significant ($r_s = -0.940$, $n = 60$, $P < 0.01$). Heart beat frequency was significantly different from the control value at all pressures greater than 41 MPa at this temperature ($F = 72.05$, $P < 0.01$). Following 30 min of recovery at 28 MPa, heart rate was still markedly different from the pre-exposure value ($P < 0.01$; Table 1).

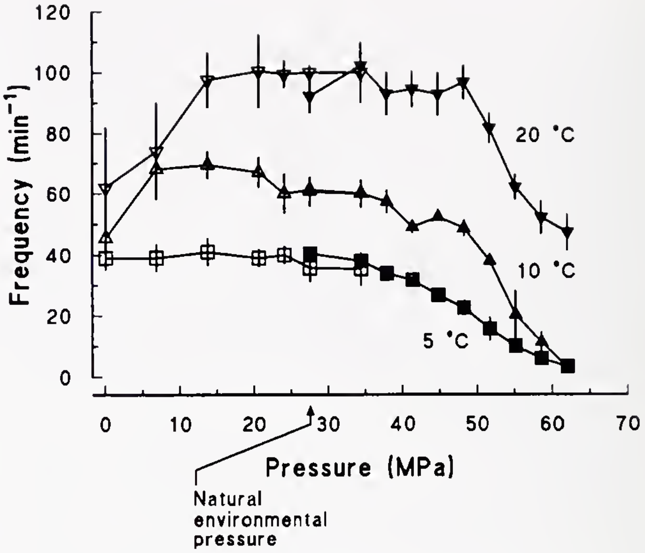

Figure 1. The effect of altered pressure on heart beat frequency in *Bythograea thermydron* at three temperatures. For comparison, the data of Mickel and Childress (1982a; open symbols) are presented along with those from the present study (solid symbols). The middle curve from the former study was obtained from experiments conducted at 12° rather than 10°C. At 5°C (■) the rate fell almost linearly to its minimum value as pressure was increased; however, contraction frequency was maintained until the pressure reached about 52 MPa in crabs tested at 10°C (▲). The heart rate of crabs tested at 20°C (▼) also remained constant at pressures below 52 MPa, but then declined less severely than in 10°C crabs. Generally, the decline in heart rate brought about by hypobaric exposure was ameliorated by lower temperatures, whereas high temperatures buffered the effects of hyperbaric exposure. Although the crabs used in these two studies were obtained from sites thousands of miles apart and the experimental techniques varied somewhat in detail, excellent agreement of the normobaric data supports the validity of combining the data sets. Spearman rank correlation coefficients (r_s) for heart rate and pressure (data from the present study) were calculated as: $r_s = -0.940$, $n = 60$, $P < 0.01$ at 5°C; $r_s = -0.923$, $n = 30$, $P < 0.01$ at 10°C; $r_s = -0.706$, $n = 60$, $P < 0.01$ at 20°C. Normal environmental pressure is about 28 MPa for this species. Data shown as mean ± 1 SEM.

The heart beat frequency of crabs tested at 10°C fell from 60.7 ± 4.8 to 3.0 ± 1.5 min^{-1} over the same pressure range as above (Fig. 1). The correlation between pressure and heart rate ($r_s = -0.923$, $n = 30$, $P < 0.01$) was also significant, but the difference between control and experimental contraction frequencies was significant only at pressures greater than 52 MPa ($F = 32.76$, $P < 0.05$). The bradycardia continued immediately after the return to normal environmental pressure ($P < 0.05$), but after 30 min of recovery the heart rate had rebounded and

Table I

Heart rate of Bythograea thermydron *before and after hyperbaric exposure (62 MPa) at three temperatures*

	f_H(min^{-1})	
Temperature (°C)	Control	Recovery
5 (6)	40.5 ± 0.8	15.2 ± 4.0*
10 (3)	60.7 ± 4.8	43.3 ± 13.0
20 (6)	92.2 ± 5.5	104.2 ± 9.6

Crabs were allowed 30 min after return to normal pressure before the recovery values were obtained. Values are shown as the mean ± 1 SEM; sample size in parentheses.

* Value significantly different from control ($P < 0.01$, ANOVAR).

was not significantly different from the control value (Table I).

At 20°C, the change in heart rate with increasing pressure was much less dramatic than at the lower temperatures. The rate decreased only 49%, reaching a minimum of 47.3 ± 5.9 min^{-1} at 62 MPa (Fig. 1). There was a significant correlation between heart beat frequency and pressure ($r_s = -0.706$, $n = 60$, $P < 0.01$), but significant changes from the control rate occurred only above 55 MPa ($F = 20.38$, $P < 0.01$). As soon as the pressure was lowered, heart beat frequency rebounded above pre-exposure values and remained elevated for at least 30 min (Table I).

Contraction pattern

The relationship between ventricular contraction pattern and experimental pressure was also dependent on temperature. Generally, the systolic spikes became less defined and the interbeat interval tended to vary more as pressure was increased. These effects were more pronounced at lower temperatures (Figs. 2, 3). Crabs tested at 5°C showed increased variability in ventricular contraction waveform at pressures as low as 34 MPa; variability continued to increase until about 55 MPa, when ventricular contractions became extremely sporadic or ceased. At 62 MPa, the standard deviation of the interbeat intervals increased significantly compared to the control value ($F = 20.14$, $P < 0.01$; Fig. 3). Following return to normal environmental pressure there was little increase in the uniformity of ventricular contraction and all crabs died within 1 h of decompression, suggesting that the effects of hyperbaric exposure are irreversible at this temperature.

At 10°C, the ventricular contraction pattern began to degenerate at pressures above 41 MPa (Fig. 2). The higher chart speed used at this temperature allows resolution of biphasic contraction peaks and ventricular fibrillation at pressures of 55 and 62 MPa, respectively. Variability of the interbeat interval also increased significantly ($F = 17.54$, $P < 0.01$) compared to the 28 MPa control (Fig. 3). After 30 min of recovery at 28 MPa, the ventricular contraction pattern became much more regular, although a diastolic notch not present in the control recording became evident (Fig. 2), and the standard deviation of the interbeat intervals was markedly reduced (Fig. 3). Crabs in this group were returned to normobaric holding vessels, but all died within 24 h of experimental use.

Above 55 MPa the interbeat interval of crabs tested at 20°C became increasingly variable (Fig. 3) and there was evidence of a systolic plateau in some animals (Fig. 2). However, all animals examined at this temperature maintained organized cardiac activity, and they regained their initial ventricular contraction pattern as soon as they were returned to normal environmental pressure. All animals in this group survived, apparently healthy, for at least 48 h after experimental use.

Discussion

During preparation at ambient sea-level pressure the crabs appeared healthy and responsive, although all showed the marked lack of coordination typical of this species when depressurized (Mickel and Childress, 1982a). Tolerance of repeated decompression for extended periods and survival at sea level at 5°C for up to 5 days have also been reported (Mickel and Childress, 1982a), suggesting that the short hypobaric exposure required for instrumentation of the crabs did not irreversibly affect their physiological state.

The relationship between temperature and heart beat frequency at the normal environmental pressure for *B. thermydron* is directly comparable to that observed in shallow-living invertebrates (deFur and Mangum, 1979). At higher pressures this relationship changed markedly, with heart rate first becoming more, then less dependent on temperature in the 5 to 10°C range. Between 10 and 20°C, the dependency of heart beat frequency on temperature remained more or less constant over the entire pressure range.

The effect of high hydrostatic pressure on membrane lipids is to decrease fluidity by increasing the order of the hydrophobic acyl chains within the membrane (Wann and Macdonald, 1980; Somero, 1992). This packing of the acyl chains may both change the ion permeability of the membrane and limit the diffusion of membrane proteins (Cossins and Macdonald, 1989). In addition, fusion of neurotransmitter vesicles with the postsynaptic terminal of nerve fibers may be disrupted (Wann and Macdonald, 1980), leading to failure of postsynaptic activation (see below). The combined tendencies of low temperature and high pressure to order membrane lipids may be countered

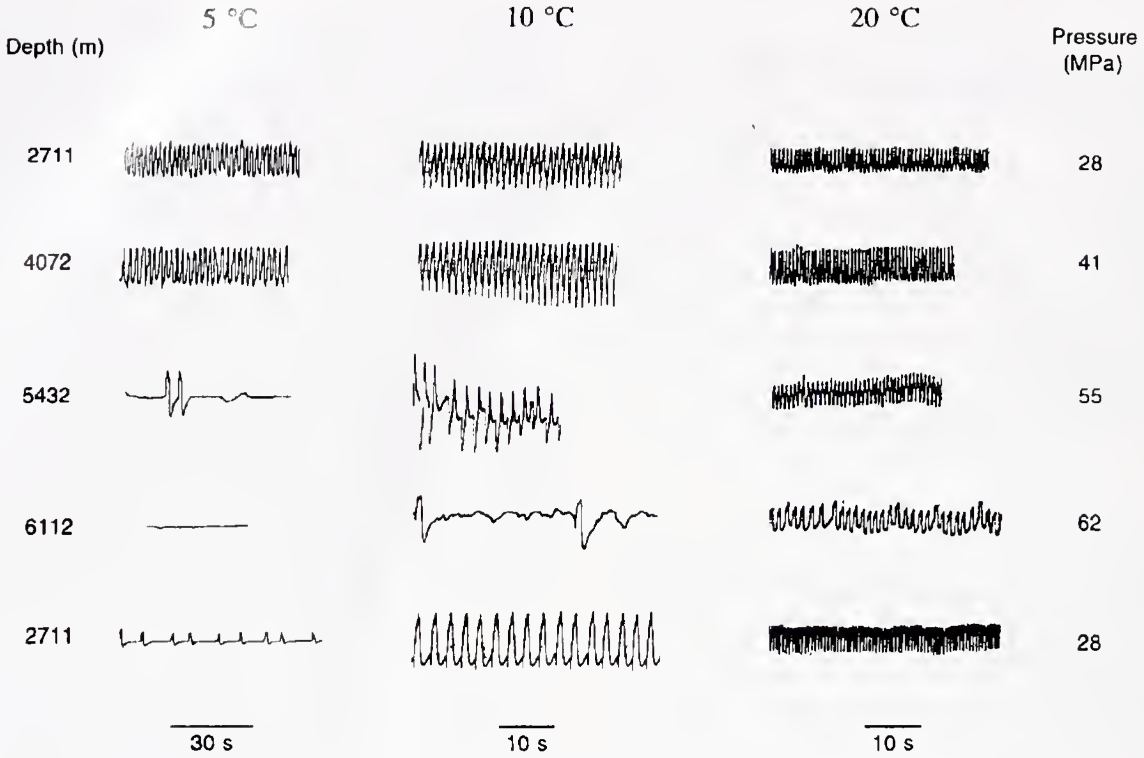

Figure 2. Chart records showing ventricular contraction in three individual *Bythograea thermydron* during progressive hyperbaric exposure at 5°, 10°, and 20°C. The 28 MPa records at the bottom of the illustration were obtained following 30 min of recovery at normal environmental pressure for this species. At 5°C, the contraction waveform became less distinct and interbeat variability increased with higher pressure. Total acardia occurred at pressures higher than 55 MPa, and contractions remained disorganized following return to normal pressure. Hyperbaric exposure was better tolerated in crabs tested at 10°C, but extra systolic spikes and ventricular fibrillation were evident at higher pressures. Recovery was more complete at this temperature than at 5°C, although the contraction frequency remained depressed. Compared to the other two experimental temperatures, the effects of increased pressure on contraction frequency and waveform at 20°C were minimal. After 30 min of recovery, the contraction pattern had returned to normal and the heart rate had rebounded above control values.

within the lifetime of an organism by increasing the ratio of unsaturated to saturated fatty acids composing the membrane bilayer (Cossins and Macdonald, 1989). In organisms living in the high pressure–high temperature environment of the hydrothermal vents, the effects of high pressure on membrane fluidity may be partially compensated, requiring a lower proportion of unsaturated membrane constituents to achieve optimal membrane viscosity.

The beat of the crustacean heart is neurogenic (Alexandrowicz, 1932), generated by burst discharges from the cardiac ganglion (CG) on its inner dorsal wall. The striated muscle of the myocardium is polyneuronally and polysynaptically innervated by processes from the large motor neurones of the CG (Alexandrowicz, 1932). This innervation, along with tight electrotonic coupling between individual muscle fibers, ensures rapid spread of excitation throughout the myocardium, resulting in strong, coordinated contraction of the ventricle with each burst from the CG (Kuramoto and Kuwasawa, 1980). The amplitude and duration of spontaneous burst discharges from these motoneurons may be modulated by output from the small pacemaker cells at the posterior of the ganglion (Hartline, 1967), although it has been suggested that fine control of burst characteristics is achieved by interaction between the large and small CG cells (Sullivan and Miller, 1984). In the gastropod *Helix*, increased hydrostatic pressure reduces the firing rate of postsynaptic cells (Wann *et al.*, 1979), possibly due to a reduction in excitatory junctional potential (ejp) amplitude arising from decreased neurotransmitter release at higher pressures. Although pacemaker cell burst frequencies may increase in response to increased pressure (Wann and Macdonald, 1980), there are several potential sites for postsynaptic failure between the pacemaker cells of the crustacean CG and the myocardium.

Mickel and Childress (1982a) showed that both the reduction in heart beat frequency and the degeneration of EKG organization brought about by decreasing pressure

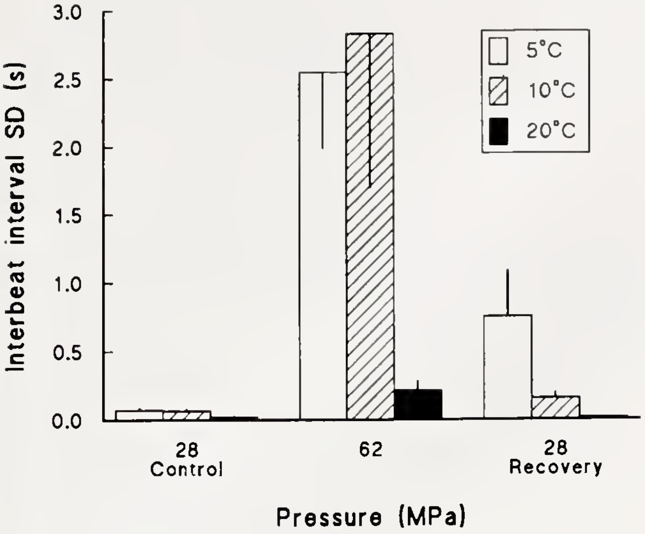

Figure 3. Average standard deviation of the intervals between 10 successive contractions of the ventricle of *Bythograea thermydron* before, during, and after hyperbaric exposure at 5°, 10°, and 20°C. Interbeat variability increased markedly in crabs exposed to 62 MPa pressure at both 5° and 10°C ($F = 20.14$, $P < 0.01$ and $F = 17.54$, $P < 0.01$, respectively); however, variability remained much higher after return to normal pressure in crabs tested at the lower temperature. The interbeat interval also increased significantly in response to hyperbaric exposure at 20°C ($F = 8.42$, $P < 0.01$), although the change was much less dramatic and recovery more complete than at 5° or 10°C. Error bars represent 1 SEM.

were less pronounced at lower temperatures. The change in heart rate accompanying decompression was, in fact, negligible at 5°C (Mickel and Childress, 1982a; Fig. 1). In contrast, the present study clearly demonstrates that higher temperatures reduce the severity of bradycardia resulting from hyperbaric exposure as well as limit the associated disorganization of the contraction waveform. If the primary effects of pressure variation on cardiac function were enzymatically mediated, then one would expect that temperature changes would have comparable effects on cardiac function under both hypo- and hyperbaric conditions. Conversely, if the system affected by pressure challenge is lipid-based, then a decrease in pressure (which decreases the viscosity of phospholipid membranes) would be compensated by a temperature reduction (causing an increase in membrane viscosity), whereas increased pressure would be counteracted by a temperature increase. The latter type of pressure-temperature interaction has now been shown to occur in response to both hypo- and hyperbaric exposure in *B. thermydron*, implicating a homeoviscous mechanism in which phospholipid membrane fluidity is affected by external pressure disturbance. Superfluous ventricular contraction spikes and prolonged plateaus suggest that disturbed membrane transport leads to the failure of neurotransmitter release and (or) myocardial excitation in the neuromuscular system of the heart.

The failure of crabs subjected to a pressure of 62 MPa at 5°C to recover fully from treatment suggests that disruption of the phospholipid membranes at this pressure-temperature combination is so complete as to be irreversible. The slower rate of recovery of crabs tested at 10°C and the complete recovery of animals in the 20°C group indicates that the higher temperatures precluded complete disruption of the membrane systems and further supports the involvement of membrane properties rather than enzyme kinetics in the observed cardiac responses to changes in pressure.

Shedding of proteins from cell membranes begins at pressures above 30 MPa (Deckmann *et al.*, 1985), and is another possible explanation for the irreversible effects of hyperbaric exposure observed in *B. thermydron*. Substantial release of integral membrane proteins occurs only at much higher pressures (about 100 MPa), however, and protein release is enhanced by higher temperatures (Deckmann *et al.*, 1985). These findings are in contrast to the present data, which show more deleterious effects of increased pressure at lower temperatures.

Despite the changes in heart beat frequency and ventricular contraction pattern associated with pressure variation in *B. thermydron*, this species shows remarkable tolerance toward pressure changes at all temperatures tested. At 5°C, the lowest temperature used in the present study, there were no significant differences in heart rate and no obvious changes in contraction pattern at pressures up to 41 MPa. Previous results from the same species at 5°C showed no significant pressure effect on heart rate between 0.1 and 34 MPa and disruption of the EKG waveform only at pressures less than 6.9 MPa (Mickel and Childress, 1982a), giving *B. thermydron* a tolerable pressure range of 6.9 to 41 MPa for apparently normal physiological function. At the higher temperatures tested, the pressure range for stable cardiac function is shifted toward higher pressures, but the magnitude of the tolerable range remains similar. The tolerance of *B. thermydron* for such broad ranges of pressure at any temperature implicates adaptations that decrease membrane compressibility and is consistent with both the prediction of Gibbs and Somero (1989) and the findings of Behan *et al.* (1992) that species found at greater depths show greater compensation for the effects of pressure. A reduction in membrane compressibility compared with shallower-living species would preserve the integrity and function of cell membranes and their associated proteins, making this deep-sea crab less susceptible to the deleterious effects of changes in environmental pressure.

Acknowledgments

The authors thank the captains and crews of R/V *John V. Vickers* and R/V *Atlantis II*, and the pilots of DSV

Alvin: without them these studies could not have been conducted. Special thanks are also due to Dr. G. Somero for his counsel on the effects of pressure on enzyme function, and L. Gorodezky for her assistance and support during the experimental portion of this work. Financial support was provided by NSF grants OCE-9012076 and OCE-9301374 as well as by NSERC and AHFMR fellowships to CNA.

Literature Cited

Alexandrowicz, J. S. 1932. The innervation of the heart of the Crustacea. I. Decapoda. *Q. J. Microsc. Sci.* **75:** 181–249.

Arp, A. J., and J. J. Childress. 1981. Blood function in the hydrothermal vent vestimentiferan tube worm. *Science* **213:** 342–344.

Arp, A. J., J. J. Childress, and C. R. Fisher Jr. 1984. Metabolic and blood gas transport characteristics of the hydrothermal vent bivalve. *Calyptogena magnifica. Physiol. Zool.* **57:** 648–662.

Behan, M. K., A. G. Macdonald, G. R. Jones, and A. R. Cossins. 1992. Homeoviscous adaptation under pressure: the pressure dependence of membrane order in brain myelin membranes of deep-sea fish. *Biochim. Biophys. Acta* **1103:** 317–323.

Belman, B. W., and M. S. Gordon. 1979. Comparative studies on the metabolism of shallow-water and deep-sea marine fishes. V. Effects of temperature and hydrostatic pressure on oxygen consumption in the mesopelagic zoarcid *Melanostigma pammelas. Mar. Biol.* **50:** 275–281.

Cossins, A. R., and A. G. Macdonald. 1984. Homeoviscous theory under pressure. II. The molecular order of membranes from deep-sea fish. *Biochim. Biophys. Acta* **776:** 144–150.

Cossins, A. R., and A. G. Macdonald. 1986. Homeoviscous adaptation under pressure. III. The fatty acid composition of liver mitochondrial phospholipids of deep-sea fish. *Biochim. Biophys. Acta* **860:** 325–335.

Cossins, A. R., and A. G. Macdonald. 1989. The adaptation of biological membranes to temperature and pressure: fish from deep and cold. *J. Bioenerg. Biomembr.* **21:** 115–135.

Cossins, A. R., and M. Sinensky. 1986. Adaptation of membranes to temperature, pressure, and exogenous lipids. Pp. 1–20 in *Physiology of Membrane Fluidity*, M. Shinitsky, ed. CRC Press, Boca Raton, FL.

Deckmann, M., R. Haimovitz, and M. Shinitzky. 1985. Selective release of integral proteins from human erythrocyte membranes by hydrostatic pressure. *Biochim. Biophys. Acta* **821:** 334–340.

deFur, P. L., and C. P. Mangum. 1979. The effects of environmental variables on the heart rates of invertebrates. *Comp. Biochem. Physiol.* **62A:** 28[illegible]294.

Gibbs, A., an[illegible] N. Somero. 1989. Pressure adaptation of Na$^+$/K$^+$-ATPase in [illegible] marine teleosts. *J. Exp. Biol.* **143:** 475–492.

Hartline, D. K. 1967. Impulse identification and axon mapping of the nine neurons in the cardiac ganglion of the lobster *Homarus americanus. J. Exp. Biol.* **47:** 327–340.

Kuramoto, T., and K. Kuwasawa. 1980. Ganglionic activation of the myocardium of the lobster, *Panulirus japonicus. J. Comp. Physiol. B* **139:** 67–76.

Macdonald, A. G., and I. Gilchrist. 1980. Effects of hydraulic decompression and compression on deep sea amphipods. *Comp. Biochem. Physiol.* **67A:** 149–153.

Macdonald, A. G., and I. Gilchrist. 1982. The pressure tolerance of deep sea amphipods collected at their high ambient pressure. *Comp. Biochem. Physiol.* **71A:** 349–352.

Macdonald, A. G., and K. W. Miller. 1976. Biological membranes at high hydrostatic pressure. Pp. 117–147 in *Biochemical and Biophysical Perspectives in Marine Biology*, D. C. Malins and J. R. Sargent, eds. Academic Press, New York.

McMahon, B. R., and J. L. Wilkens. 1972. Simultaneous apnoea and bradycardia in the lobster *Homarus americanus. Can. J. Zool.* **50:** 165–170.

Mickel, T. J., and J. J. Childress. 1982a. Effects of pressure and temperature on the EKG and heart rate of the hydrothermal vent crab *Bythograea thermydron* (Brachyura). *Biol. Bull.* **162:** 70–82.

Mickel, T. J., and J. J. Childress. 1982b. Effects of temperature, pressure, and oxygen concentration on the oxygen consumption rate of the hydrothermal vent crab *Bythograea thermydron* (Brachyura). *Physiol. Zool.* **55:** 199–207.

Quetin, L. B., and J. J. Childress. 1980. Observations on the swimming activity of two bathypelagic mysid species maintained at high hydrostatic pressures. *Deep-Sea Res.* **27:** 383–391.

Saunders, P. M., and N. P. Fofonoff. 1976. Conversion of pressure to depth in the ocean. *Deep-Sea Res.* **23:** 109–111.

Siebenaller, J. F., and G. N. Somero. 1989. Biochemical adaptation to the deep-sea. *Crit. Rev. Aquat. Sci.* **1:** 1–25.

Sinensky, M. 1974. Homeoviscous adaptation—a homeostatic process that regulates the viscosity of membrane lipids in *E. coli. Proc. Natl. Acad. Sci.* **76:** 522–525.

Somero, G. N. 1992. Biochemical ecology of deep-sea animals. *Experientia* **48:** 537–543.

Sullivan, R. E., and M. W. Miller. 1984. Dual effects of proctolin on the rhythmic burst activity of the cardiac ganglion. *J. Neurobiol.* **15:** 173–196.

Wann, K. T., and A. G. Macdonald. 1980. The effects of pressure on excitable cells. *Comp. Biochem. Physiol.* **66A:** 1–12.

Wann, K. T., A. G. Macdonald, and A. A. Harper. 1979. The effects of high hydrostatic pressure on the electrical characteristics of *Helix* neurons. *Comp. Biochem. Physiol.* **64A:** 149–159.

Yayanos, A. A. 1981. Reversible inactivation of deep-sea amphipods (*Paralicella capresca*) by a decompression from 601 bars to atmospheric pressure. *Comp. Biochem. Physiol.* **69A:** 563–565.

Reference: *Biol. Bull.* **187:** 215–222. (October, 1994)

Localization of the Chloroperoxidase of the Capitellid Polychaete *Notomastus lobatus*

K. S. YOON, Y. P. CHEN, C. R. LOVELL, D. E. LINCOLN,
L. W. KNAPP, AND S. A. WOODIN*

Department of Biological Sciences, University of South Carolina, Columbia, South Carolina 29208

Abstract. Antisera against the two constituent proteins of the chloroperoxidase enzyme of the capitellid polychaete *Notomastus lobatus* were used to identify and localize these polypeptides by immunoblotting and indirect immunofluorescence. Immunofluorescence staining showed the enzyme to be localized primarily in tissues of the tail region of the worm. Some reactivity was also observed in the epidermis of the mid-body, but none was seen in the head region. These immunofluorescence results were supported by immunoblotting experiments, which also showed that chloroperoxidase holoenzyme is localized in the tail. Immunological results were substantiated by the distribution of enzyme activity and the *in vivo* products of the chloroperoxidase, 4-bromophenol, 2,4-dibromophenol, and 2,4,6-tribromophenol. Chloroperoxidase is the principal enzyme involved in the production of bromoaromatics in *N. lobatus.* Localization of most of this enzyme in the tail region explains the detection of high levels of bromophenols in the tail, the most exposed portion of this head-down, deposit-feeding worm. This pattern of bromoaromatic distribution is consistent with the hypothesis that the worms produce these compounds as defensive chemicals against epifaunal predators.

Introduction

A variety of sediment-dwelling, soft-bodied marine invertebrates, including hemichordates and polychaetes, contain high levels of volatile brominated compounds, such as bromophenols, bromopyrroles, and bromobenzylalcohols (Woodin *et al.,* 1987; Woodin, 1991). These brominated compounds are also released by the worms into the sediments surrounding their burrows (King, 1986; Woodin *et al.,* 1987; Steward *et al.,* 1992). Many marine sediments support significant populations of infaunal worm species that produce volatile, malodorous, brominated aromatic compounds. Examples of such populations include the terebellid polychaete *Lanice conchileca* in the North Sea (Buhr, 1976; Weber and Ernst, 1978) and the hemichordate *Balanoglossus* in the southeastern United States (Peterson and Peterson, 1979).

High concentrations of bromophenols are found in the capitellid polychaete *Notomastus lobatus,* which is a head-down, sediment deposit feeder. Bromophenols can be produced through the activity of bromo- or chloroperoxidases; Ahern *et al.* (1980) had previously detected bromoperoxidase activity in the terebellid polychaete *Thelepus setosus.* Chen *et al.* (1991) purified and characterized a chloroperoxidase from *N. lobatus* and found that this enzyme has several unique properties. It is composed of two dissociable protein components, a flavoprotein and a heme protein, which associate in a 1:1 molar ratio to form holoenzyme. The flavoprotein is composed of four identical subunits (alpha) and contains flavin adenine dinucleotide (Chen *et al.,* 1991). The heme protein is a tetramer composed of two copies each of two nonidentical subunits (beta and gamma) and contains 1 mol of ferriheme per mol of protein. The *N. lobatus* chloroperoxidase thus has a subunit structure of $\alpha_4\beta_2\gamma_2$. Neither the flavoprotein nor the heme protein moiety alone has detectable chloroperoxidase activity, but they readily associate to form fully active enzyme. The chloroperoxidase of *N. lobatus* is capable of oxidizing Cl^-, Br^-, and I^-. It is the first haloperoxidase to be purified to homogeneity from a marine worm and the first haloperoxidase ever found

---

Received 9 November 1993; accepted 20 July 1994.

*Author to whom correspondence should be addressed.

Abbreviations: PBS, phosphate buffered saline; GC, gas chromatography.

to contain flavin. The enzyme can halogenate a wide variety of aromatic compounds and is the only detectable halogenating enzyme in *N. lobatus.* The enzyme is very abundant, constituting approximately 2% of soluble protein in *N. lobatus* crude extract. Using phenol and sodium bromide as substrates, it produces 4-bromophenol, 2,4-dibromophenol, and 2,4,6-tribromophenol, the compounds found in *N. lobatus* (Chen *et al.*, 1991). It is clear that this chloroperoxidase is responsible for the production of bromophenols in *N. lobatus* and that production of these toxic compounds is likely to be significant in both the ecology and physiology of this animal.

In a variety of terrestrial and marine plants as well as such sessile marine organisms as coelenterates and sponges, noxious compounds have been shown to have utility as antipredator and antifouling agents (Hay and Fenical, 1988). In at least some cases, these compounds show distinctive patterns of localization—for example, in sponge, in spherulous cells near excurrent canals (Thompson *et al.*, 1983); and in red alga, in outer cortical cells and trichoblast cells (Young *et al.*, 1980). In most, but not all cases (see Hashimoto *et al.*, 1991), the compounds have some autotoxicity properties and thus are encapsulated within vesicles apparently at the point of synthesis in the organism (Thompson *et al.*, 1983). King (1986) has hypothesized that compounds such as those produced by *Notomastus lobatus* are antimicrobial agents and act to reduce bacterial populations in the burrow lining. To be consistent with this hypothesis, the enzyme and its products should be localized in the epidermis over the entire body of the worm. In contrast, Woodin *et al.* (1987) suggested that these compounds are primarily antipredator compounds. For this hypothesis, the enzyme and its products are expected to be concentrated in the tail, which is the portion of the organism most exposed to surface predators (Powell, 1977). In this study, we used a combination of techniques, including immunohistochemistry and assays of enzyme identity and activity, to determine the distribution of the chloroperoxidase and its products in *N. lobatus.* This localization study complements a more direct test of the antipredator hypothesis; results of that test will be published elsewhere. The products of enzymes, particularly toxic and autotoxic compounds such as these, can have several simultaneous effects. Knowledge of localization and activity of the enzyme can help to discriminate among these, particularly in this case where the enzyme represents such a large percentage of the animal's soluble protein (2%).

Materials and Methods

Specimens of *Notomastus lobatus* were collected at low tide from Debidue flat, in the North Inlet estuary (Georgetown, South Carolina, USA, 33°20′ N, 79°10′ W). The worms were removed from the sediment and washed in seawater to remove external sediment. Three body regions were clearly visible from external features: the head, which lacked branchiae and was seemingly quite muscular; the mid-body, which had branchiae and was much less rigid; and the tail, which lacked branchiae and was sticky, translucent, and quite glandular in appearance. Intact worms were treated differently depending upon their planned use. Those to be used for immunochemistry were cut with a razor blade into 1-cm lengths of head, mid-body, and tail regions. Segments adjacent to the junctions between body regions were discarded. Each length was immediately placed into 10 volumes of Carnoy's fixative (95% absolute ethanol + 5% glacial acetic acid) on ice in the field and transported on ice to the University of South Carolina main campus. In the laboratory, the fixed body portions were transferred to −10°C and maintained for two days. Worms used for measurement of enzyme activity, quantification of enzyme, or extraction of enzyme were cut into head, mid-body, and tail regions, immediately frozen on dry ice, and transported on dry ice to the University of South Carolina main campus. In the laboratory, the worms were transferred to −70°C until used. Chen *et al.* (1991) found that *N. lobatus* can be stored in this manner for several months with little loss of chloroperoxidase activity.

The heme protein and flavoprotein moieties of the *Notomastus lobatus* chloroperoxidase were purified separately as described by Chen *et al.* (1991). Purity of each protein was checked by native polyacrylamide gel electrophoresis. Polyclonal antibodies to purified heme protein and flavoprotein moieties were raised separately in male New Zealand white rabbits. Purified proteins were dissolved in phosphate buffered saline (PBS, pH 7.4) at a concentration of 100 μg/ml and emulsified in Freund's complete adjuvant for the initial, subcutaneous injection. Subsequent injections of antigens were carried out using Freund's incomplete adjuvant. The antisera were tested for specificity by immunoblot analysis using purified heme protein and flavoprotein moieties, reconstituted chloroperoxidase formed by mixing the two subunits in a 1:1 molar ratio, and a crude extract of *N. lobatus.* The crude extract was prepared as described in Chen *et al.* (1991).

After fixation, the body regions to be examined by immunohistochemistry were passed through three changes of 100% ethanol and three changes of toluene for 10 min each and embedded in low-melting-point paraffin in reduced light. These methods were used because the compounds are volatile and the enzyme is sensitive to both temperature and light. The embedded tissue was sectioned to a thickness of 9 μm. Some sections were stained with hematoxylin and eosin for bright-field microscopy.

For indirect immunofluorescence microscopy, the paraffin was removed from the sections by treatment with toluene, and the sections were then rehydrated in a graded ethanol series (100, 100, 95, 85, and 70%) for 1 min each. Sections were blocked with 1% goat serum in PBS for 30 min at room temperature. Serially matched sections were incubated overnight at 4°C in a 1:100 dilution of rabbit anti-heme protein, or anti-flavoprotein serum, or a mixture of anti-heme protein and anti-flavoprotein (1:1) sera. The sections were rinsed in PBS three times for 5 min each and then incubated in diluted (1:50) second antibody (fluorescein-conjugated, goat anti-rabbit IgG (H&L) antibodies; ICN Immunobiologicals, Lisle, IL) at room temperature for 1 h. Sections were then rinsed in PBS three times for 5 min each and mounted in 10% glycerol. Sections treated with preimmune rabbit serum, blocked with goat serum, and then treated with second antibody were used as controls. Sections were examined at 16× on a Zeiss Universal microscope equipped for epifluorescence.

For determination of brominated aromatic compounds, each frozen body region (head, mid-body, or tail) was thawed to room temperature, immediately placed in HPLC-grade methanol, and refrigerated pending extraction. The body regions were then ground in ice-cold methanol and the homogenates centrifuged at 1000 × *g* for 15 min. To each supernatant a known amount of 2,6-dichlorophenol was added as an internal standard. Each supernatant was diluted initially with 10 volumes of acidified, saturated sodium chloride solution (pH 2.0) and extracted five times with 1 volume of HPLC-grade pentane. For each extraction the amount of pentane added was equal to the volume of the supernatant (typically 5 to 10 ml). The pentane fractions were pooled, concentrated, and analyzed by gas chromatography (GC) with a Varian Model 3300 equipped with a fused silica capillary column (15 m × 0.53 mm ID) coated with a 1.5-μm film of cross-linked SE-54 phase (DB-5, J & W Scientific, Folsom, CA), an electron capture detector, and an integrator. The brominated compounds were resolved with the aid of a temperature program (120° to 160°C at 10°C/min, 30 ml/min N_2 flow) and quantified with standard curves derived from known concentrations of reagent-grade bromophenols previously determined to be found in *N. lobatus* (4-bromophenol, 2,4-dibromophenol, and 2,4,6-tribromophenol; Chen *et al.*, 1991) as well as with standard curves for the internal standard, 2,6-dichlorophenol.

Frozen, dissected worm heads, mid bodies, and tails were separately thawed at room temperature, weighed (about 0.5 g dry weight), and washed several times with 50 m*M* sodium phosphate buffer, pH 4.1. Each body region was homogenized by hand grinding in an ice-cold mortar and pestle with 2 ml added cold phosphate buffer. The homogenates were centrifuged at 10,000 × *g* for 20 min, then loaded onto a Sephadex G-50 column (0.5 × 5 cm), pre-equilibrated with phosphate buffer. The proteins were eluted with 50 m*M* phosphate buffer. The products of chloroperoxidase activity in each body region were measured by GC. Known amounts of purified chloroperoxidase formed by adding purified heme protein and flavoprotein moieties in a 1:1 molar ratio were added to a reaction mixture containing 10 m*M* NaCl, 440 μM H_2O_2, and 50 m*M* phenol in 100 m*M* phosphate buffer, pH 5.0 (Chen *et al.*, 1991). Assay mixtures were incubated at room temperature for 30 min. The reaction mixture was extracted five times with 1 ml of pentane per extraction. The pentane fractions were then combined, concentrated, and analyzed by GC as described above. The presence and identities of the chlorophenols produced were confirmed using both gas chromatography and mass spectroscopy (Chen *et al.*, 1991). One unit of specific enzyme activity was defined as 1 μmol of product formed by 1 mg of protein per minute. Protein concentration was assayed by the method of Lowry *et al.* (1951), with bovine serum albumin as the standard.

For analysis by Western immunoblotting, native polyacrylamide gel electrophoresis was performed with a Bio-Rad Protean II gel electrophoresis system. The polypeptides were transferred electrophoretically to nitrocellulose membrane. The nitrocellulose membrane was immersed in a blocking solution containing 3% goat serum in PBS for 30 min prior to incubation overnight in the mixture of anti-heme protein and anti-flavoprotein sera (1:1000 dilution) at room temperature. The nitrocellulose membrane was washed in PBS and then incubated in a horseradish-peroxidase-conjugated goat anti-rabbit IgG (1:5000 dilution) (BioRad Laboratories, Richmond, CA) for 30 min at room temperature. The blot was rinsed twice with 0.05% Tween 20 for 5 min each and rinsed again in PBS for 5 min. Polypeptides from each region on the worm were visualized by reaction with hydrogen peroxide and 4-chloro-1-naphthol. Polypeptide bands were quantified using a Hewlett Packard Scanjet Plus.

To confirm its specificity, anti-heme protein serum was absorbed against purified heme protein from *N. lobatus* overnight at 4°C. Supernatant was collected after centrifugation of precipitated antibody-antigen complexes. Ten microliters of purified heme protein and 10 μl of fresh *N. lobatus* crude extract were spotted onto nitrocellulose membrane, allowed to dry at room temperature, then rinsed once with TBS (50 m*M* Tris HCl, 150 m*M* NaCl, pH 8.0). The nitrocellulose membranes were then soaked in blocking solution (5% (w/v) nonfat dry milk in TBS) for 30 min, washed twice for 5 min each with TBST (TBS + 0.05% (v/v) Tween-20), and rinsed again with TBS. The membranes were then reacted with the primary absorbed serum (diluted 1:1000 with TBS) or unabsorbed rabbit anti-heme serum for 1 h, washed twice for 5 min each with TBST, and rinsed with TBS. They were then reacted with horseradish peroxidase conjugated with goat anti-rabbit IgG (BioRad; diluted 1:1000 with TBS) for 1 h and then washed twice for 5 min each with TBST and rinsed with TBS. Polypeptides were visualized by reaction with hydrogen peroxide and 4-chloro-1-naphthol for 15 min.

Results

To determine the specificity of the antisera raised in rabbit against the purified heme protein and flavoprotein moieties of chloroperoxidase from *Notomastus lobatus,* we used the sera to probe Western blots containing purified heme protein complex, purified flavoprotein moiety, and whole-worm crude extracts. The anti-flavoprotein antiserum reacted only with the flavoprotein. The anti-heme protein serum reacted strongly with the purified heme protein, but not with the flavoprotein moiety. Each serum thus reacted only with its respective protein in the crude extract of *N. lobatus.* The anti-flavoprotein serum produced a band at a molecular weight consistent with the chloroperoxidase flavoprotein (120,000; Chen *et al.,* 1991) (Fig. 1: lane 4). The anti-heme protein serum produced a band at a molecular weight consistent with the chloroperoxidase heme protein (54,500; Chen *et al.,* 1991) (Fig. 1: lane 5). As expected, a mixture of anti-heme protein serum and anti-flavoprotein serum reacted with crude extract prepared from *N. lobatus* tail tissue produced two bands corresponding to the molecular weights of the heme protein and flavoprotein moieties (Fig. 1: lane 3). Bands consistent with heme protein were also seen in the head and mid-region extracts (Fig. 1: lanes 1 and 2 respectively). A small band consistent with the flavoprotein complex was seen in the mid-region extract, but none was seen in the head region extract (Fig. 1: lanes 2 and 1 respectively). The constituent proteins of the chloroperoxidase were thus easily detectable with the anti-heme protein and anti-flavoprotein sera.

To determine the histological location and regional distribution of the enzyme, tissue cross sections of head, mid-body, and tail regions were treated with a 1:1 mixture of heme protein and flavoprotein antisera. Positive immune staining was observed primarily in the tail and to a lesser extent in the mid-body (Figs. 2 and 3). The head region was completely negative in all sections.

Sections of tail region were treated with anti-heme protein or anti-flavoprotein serum, or a 1:1 mixture of the sera (Fig. 2A, B, C). In all cases, intense fluorescence labeling was observed in the muscles and with less intensity in the epidermis (Fig. 2B, C). Controls consisted of sections reacted with preimmune rabbit serum in PBS and then rinsed and incubated with second antibody (fluorescein-tagged goat anti-rabbit IgG serum). Control sections showed no nonspecific immunoreaction (Fig. 2D). The samples treated with anti-heme protein (Fig. 2A) or anti-flavoprotein sera (Fig. 2B) were very similar to each other and to the samples treated with the 1:1 serum mixture (Fig. 2C). In addition to the staining of muscle, gut epithelium in the tail was also intensely labeled by the antibody (Fig. 3A). These results show the presence of chloroperoxidase in the muscle, epidermis, and gut lining in the tail. We also observed minor fluorescence labeling in the epidermis of the mid-body. In contrast to the Western immunoblot data, no fluorescence labeling was seen in any of the sections of the head region treated with either anti-heme protein or anti-flavoprotein sera.

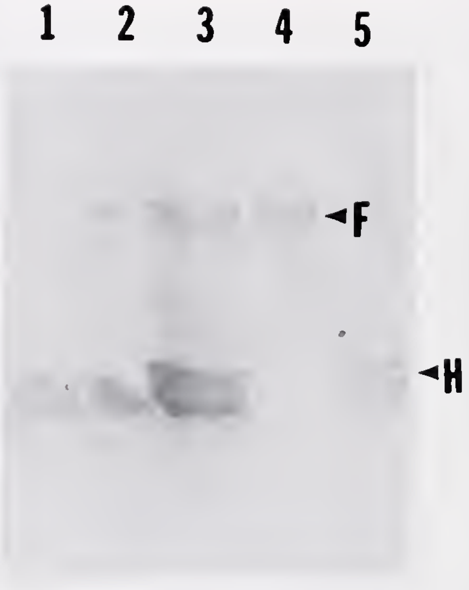

Figure 1. Western immunoblot of partially purified chloroperoxidase from *Notomastus lobatus,* reacted with a 1:1 ratio of heme protein and flavoprotein antisera. Lane 1: head region; Lane 2: mid-body; Lane 3: tail region; Lane 4: purified flavoprotein subunit of chloroperoxidase; Lane 5: purified heme protein subunit of chloroperoxidase.

As a second approach to confirmation of the immunocytochemical results on localization, we used Western immunoblotting to further examine the extracted enzyme moieties from each body region. Proteins transferred to nitrocellulose membranes were treated with the anti-heme protein and anti-flavoprotein antibodies, and the colored products of the reaction were quantified by scanning densitometry. Known amounts (Lowry *et al.,* 1951) of the purified flavoprotein and heme protein components were included as controls. As expected from the immunocytochemical results, the flavoprotein moiety was present in large quantities in the tail, but in much smaller quantities in the mid-body of the worm (Table I; Fig. 1). No

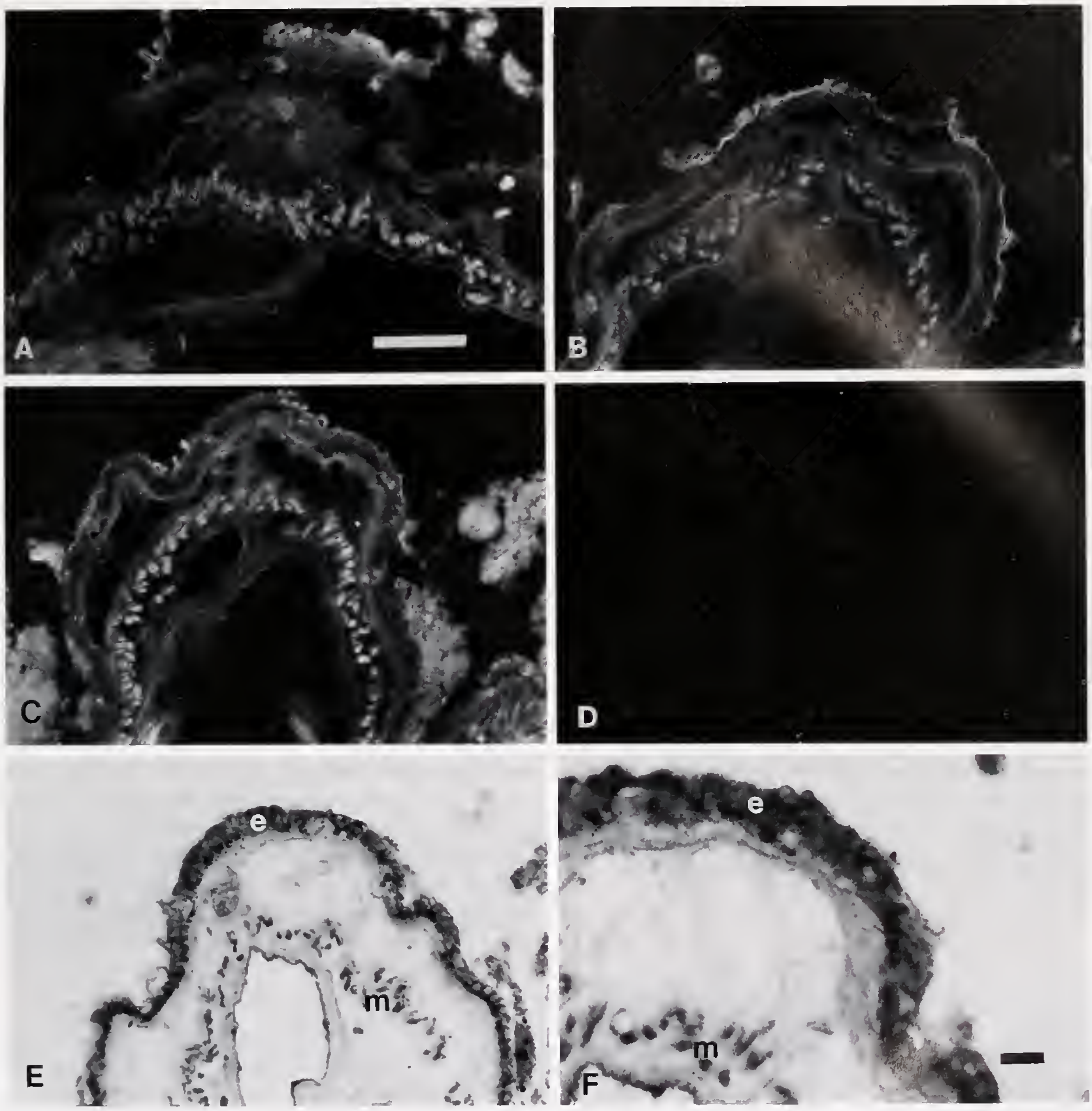

Figure 2. Immunofluorescence labeling of cross sections of the tail of *Notomastus lobatus.* Polyclonal antisera to heme protein and flavoprotein subunits of chloroperoxidase from *N lobatus* were used; binding was visualized by fluorescein-conjugated anti-rabbit antibody. Labeling with (A) heme protein antibody; (B) flavoprotein antibody; (C) 1:1 mixture of heme protein and flavoprotein antibodies; (D) preimmune rabbit serum. (E) Neighboring section stained with hemotoxylin and eosin and examined with light microscopy (m—muscle, e—epidermis). (F) Same section as in (E), at higher magnification (m—muscle, e—epidermis). Scale bar in A = 72 μm and applies to A–E. Scale bar in F = 36 μm.

flavoprotein moiety was detected in the head region. In contrast to the immunocytochemical results, heme protein was detected in all three body regions (Table I). This could be due to nonspecific activity of the antiserum or to the actual presence of heme protein in all three body regions. If the latter, then the heme protein may have another function in the head and mid-body of the worm, but it must be complexed in some way such that we did not detect it by immunocytochemistry (Knapp *et al.,* 1991). Tests for nonspecific activity of the anti-heme protein serum were negative. When anti-heme protein serum preabsorbed with the purified heme protein moiety was reacted with crude extract and pure heme protein, no reaction was seen with either the purified heme protein

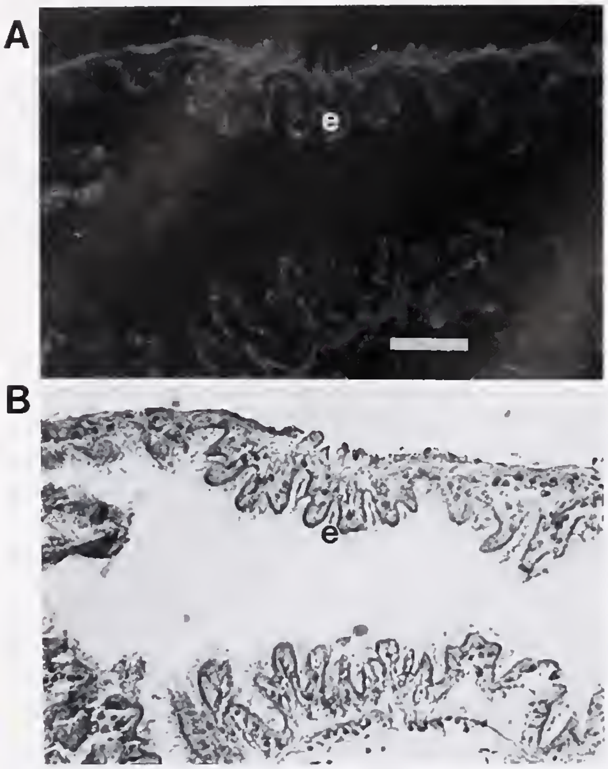

Figure 3. (A) Immunofluorescence labeling of gut epithelium (e) in cross sections of the tail of *Notomastus lobatus.* A mixture of polyclonal antibodies to the heme protein and flavoprotein subunits of chloroperoxidase was used; binding was visualized by FITC-conjugated anti-rabbit antibody. (B) Neighboring section stained with hemotoxylin and eosin and examined with light microscopy (e—gut epithelium). Scale bar = 72 μm.

moiety or with crude extract of *N. lobatus.* Anti-heme protein serum that had not been preabsorbed reacted strongly with both the purified heme protein moiety and the crude extract of *N. lobatus.*

Both flavin and heme moities are necessary for holoenzyme activity. To determine presence of holoenzyme per body region, the enzyme activity of the chloroperoxidase extracted from different regions of the body of *N. lobatus* was assayed by comparing the amount of halogenated product produced per milligram of protein. The product was assayed by GC. Since the worm naturally contains brominated aromatic products, assays for brominated products with crude extracts suffer from background contamination. The worm does not contain chlorinated aromatics, but its chloroperoxidase will catalyze the synthesis of these compounds *in vitro* (Chen *et al.*, 1991). Therefore, we used an enzyme reaction mixture including phenol and NaCl, which in the presence of enzyme produced 4-chlorophenol. This product was assayed by GC and its identity verified by mass spectroscopy. The highest enzyme activity was detected in extracts from the tail region, with much less in extracts from the mid-body and head regions (Table I). In addition, the amount of brominated aromatic compounds found in methanol extracts of each body region was measured by GC (Table I). The highest concentration of bromophenols was found in the tail, with a lower level in the mid-body (Table I) and only trace amounts in the head region.

Discussion

Chloroperoxidase and its products are localized primarily in the tail region of *Notomastus lobatus* (Table I). Immunohistochemistry revealed that the chloroperoxidase was located in muscle, epidermis, and gut lining of the tail region as well as to a lesser extent in the mid-body (Figs. 2 and 3). This corresponds closely with the data on the distribution of the natural brominated products of this chloroperoxidase (4-bromophenol, 2,4-dibromophenol, and 2,4,6-tribromophenol), which are also concentrated in the tail region (Table I). The tail region has 3.2 times more bromophenol than the mid-body and 75.2 times more than the head region (bromophenol expressed as micrograms per milligram of protein). In fact, so little bromophenol was detected in the head region that it may represent contamination of the external body surface with bromophenols released from the tail or the mid-body when the worm was collected. Regional distribution of enzyme activity was consistent with these results. The tail showed a very high level of activity, as measured by the ability of extracts to catalyze production of chlorophenol; the tail region had 29.5 times more activity than the mid-

Table I

Occurrence of chloroperoxidase and bromophenols in the three body regions of Notomastus lobatus plus activity of chloroperoxidase by body region

	Body Region		
	Head	Middle	Tail
Chloroperoxidase quantity[1] (OD · mm^2 band area)			
Heme-containing subunit	0.44	0.29	0.59
Flavin-containing subunit	0.0	0.07	0.23
Chloroperoxidase specific activity[2] (μmol substrate/mg crude extract protein/min)	0.20	0.06	1.86
Bromophenol compounds quantity (μg/mg protein)	5	117	376

[1] Determined by scanning densitometry of Western blot to nitrocellulose membrane.

[2] Measured as the ability of the enzyme to produce the product 4-chlorophenol.

body and 9.3 times more than the head region. The only data that appeared to be inconsistent with the conclusion that the chloroperoxidase was localized in the tail tissue were the data from Western blots. These data showed the heme protein moiety of the chloroperoxidase to be abundant in all body regions of the worm (Table I). However, the flavoprotein moiety either was not present (head) or was present in only trace amounts (mid-body). Since both proteins are required for chloroperoxidase activity, this strongly suggests that no functional chloroperoxidase enzyme existed in the head and only trace amounts in the mid-body of the worm (Table I). Thus, there is no inconsistency with respect to the absence of enzyme activity in regions other than the tail.

Localization of product (or products) and enzyme near the site of their expected use or release appears to be typical of many noxious chemicals in marine organisms (Young *et al.*, 1980; Thompson *et al.*, 1983; Hay and Fenical, 1988) as well as in terrestrial plants (Langenheim *et al.*, 1978). It also seems to be characteristic of organisms that do not synthesize their own noxious compounds but rather derive them from their foods (*e.g.*, gastropods: Jensen, 1984; Faulkner and Ghiselin, 1983; insects: Bowers and Puttick, 1986; Malcolm, 1991). Because many of the endogenously produced compounds probably have autotoxic properties, one would expect them to be synthesized at the site of sequestration and localized in a manner appropriate for their functional role (Hay and Fenical, 1988). Exceptions to this pattern are known: in some terrestrial plants, for example, alkaloids are synthesized at one location within the plant and then translocated to their site of utility (Hashimoto *et al.*, 1991). In the marine worm *N. lobatus*, it is clear that synthesis and storage of toxic bromophenols occur primarily in the tail region (Table I, Figs. 2 and 3).

Notomastus lobatus lives in sediments in a habitat that is intensively excavated by a variety of large digging predators such as rays, skates, and blue crabs (Peterson and Peterson, 1979). The predatory rays, for example, are capable of excavating to depths of more than 0.5 m in pursuit of prey (Orth, 1975). Methods of escape for sediment dwellers probably include life among partial structural refuges such as oyster reefs, rapid burrowing deep within the sediments, very rapid withdrawal into a very deep burrow, and distastefulness. *N. lobatus* is not a rapid burrower, nor does it withdraw rapidly into the deepest portions of its burrow. It lives in muds into which predators can readily dig. The localization of chloroperoxidase and its bromophenol products in the tail suggests that these compounds serve an antipredator function. If these compounds were primarily used as antimicrobial or antifouling compounds, as suggested by King (1986) and others, one would expect to see both the bromophenols and the chloroperoxidase evenly distributed across all three body regions in the epidermis; they are not (Table I; Figs. 2 and 3). The distribution of the bromophenols and the chloroperoxidase enzyme responsible for their production in *N. lobatus* is consistent with the hypothesis that they are used as antipredator compounds by this worm. *N. lobatus* lives head down, ensuring that the first portion of the body to be encountered by an epifaunal predator will be the tail, the region of the body containing the highest concentration of the brominated compounds and the highest activity of the chloroperoxidase enzyme (Table I). We surmise that encounters with the tail and its noxious brominated compounds reduce predatory pursuit. Feeding experiments that will more directly test this antipredator hypothesis are under way.

Acknowledgments

The authors thank the Trustees of the Belle W. Baruch Institute for Marine and Coastal Research for access to habitats and C. Steward for field assistance. D. S. Wethey provided useful comments on the manuscript. A. Jennings, N. Watabe, and D. Dunkelberger provided technical advice. This work was supported in part by NSF grant no. BSR-8906705 to S. A. Woodin, D. E. Lincoln, and C. R. Lovell.

Literature Cited

Ahern, T. J., G. G. Allan, and D. G. Medcalf. 1980. New bromoperoxidases of marine origin partial purification and characterization. *Biochim. Biophys. Acta* **616:** 329–339.

Bowers, M. D., and G. M. Puttick. 1986. The fate of ingested plant allelochemicals: iridoid glycosides and lepidopteran herbivores. *J. Chem. Ecol.* **12:** 169–178.

Buhr, K.-J. 1976. Suspension-feeding and assimilation efficiency in *Lanice conchilega* (Polychaeta). *Mar. Biol.* **38:** 373–383.

Chen, Y. P., D. E. Lincoln, S. A. Woodin, and C. R. Lovell. 1991. Purification and properties of a unique flavin-containing chloroperoxidase from the capitellid polychaete *Notomastus lobatus*. *J. Biol Chem* **266:** 23909–23915.

Faulkner, D. J., and M. T. Ghiselin. 1983. Chemical defense and evolutionary ecology of dorid nudibranchs and some other opisthobranch gastropods. *Mar. Ecol. Prog. Ser.* **13:** 295–301.

Hashimoto, R., A. Hayashi, Y. Amano, J. Kohno, H. Iwanari, S. Usuda, and Y. Yamada. 1991. Hyoscyamine 6β-hydrolase, an enzyme involved in tropane alkaloid biosynthesis, is localized at the pericycle of the root. *J. Biol. Chem.* **266:** 4648–4653.

Hay, M. E., and W. Fenical. 1988. Marine plant-herbivore interactions: the ecology of chemical defense. *Ann. Rev. Ecol. Syst.* **19:** 111–145.

Jensen, K. R. 1984. Defensive behavior and toxicity of ascoglossan opisthobranch *Mourgona germaineae* Marcus. *J. Chem. Ecol.* **10:** 475–486.

King, G. M. 1986. Inhibition of microbial activity in marine sediments by a bromophenol from a hemichordate. *Nature* **323:** 257–259.

Knapp, L. W., P. Linser, W. E. Carver, and R. H. Sawyer. 1991. Biochemical identification and immunological localization of two non-keratin polypeptides associated with the terminal differentiation of avian scales. *Cell Tissue Res.* **265:** 535–545.

Langenheim, J. H., W. H. Stubblebine, D. E. Lincoln, and C. E. Foster. 1978. Implications of variation in resin compositions among organs, tissues and populations in the tropical legume *Hymenaea*. *Biochem. Syst. Ecol.* **6:** 299–313.

Lowry, O. H., N. J. Rosebrough, A. L. Farr, and R. J. Randall. 1951. Protein measurements with the folin phenol reagent. *J. Biol. Chem.* **193:** 265–275.

Malcolm, S. B. 1991. Cardenolide-mediated interactions between plants and herbivores. Pp. 251–296 in *Herbivores. Their Interactions with Plant Secondary Metabolites*, Rosenthal, G. A., and M. R. Berenbaum, eds. Academic Press, San Diego.

Orth, R. J. 1975. Destruction of eelgrass, *Zostera marina*, by the cownose ray, *Rhinoptera bonasus*, in the Chesapeake Bay. *Chesapeake Sci.* **16:** 205–208.

Peterson, C. H., and N. M. Peterson. 1979. *The Ecology of Intertidal Flats of North Carolina: a Community Profile.* Fish and Wildlife Service, Office of Biological Services, Slidell, LA. FWS/OBS-79/39. 73 pp.

Powell, E. N. 1977. The relationship of the trace fossil *Gyrolithes* (= *Xenohelix*) to the family Capitellidae (Polychaeta). *J. Paleontol.* **51:** 5552–556.

Steward, C. C., J. Pinckney, Y. Piceno, and C. R. Lovell. 1992. Bacterial numbers and activity, microalgal biomass and productivity, and meiofaunal distribution in sediments naturally contaminated with biogenic bromophenols. *Mar. Ecol. Prog. Ser.* **90:** 61–71.

Thompson, J. E., K. D. Barrow, and D. J. Faulkner. 1983. Localization of two brominated metabolites, aerothionin and homoaerothionin, in spherulous cells of the marine sponge *Aplysina fistularis* (= *Verongia thiona*). *Acta Zool.* **64:** 199–210.

Weber, K., and W. Ernst. 1978. Occurrence of brominated phenols in the marine polychaete *Lanice conchilega*. *Naturwissenschaften* **65:** 262.

Woodin, S. A. 1991. Recruitment of infauna: positive or negative cues. *Am. Zool.* **31:** 797–807.

Woodin, S. A., M. D. Walla, and D. E. Lincoln. 1987. Occurrence of brominated compounds in soft-bottom benthic organisms. *J. Exp. Mar. Biol. Ecol.* **107:** 209–217.

Young, D. N., B. M. Howard, and W. Fenical. 1980. Subcellular localization of brominated secondary metabolites in the red alga *Laurencia snyderae*. *J. Phycol.* **16:** 182–185.

Reference: *Biol. Bull.* **187**: 223–292. (October, 1994)

Reports of Papers Presented at the General Scientific Meetings of the Marine Biological Laboratory

August 15 to 17, 1994

Program Chairs: Robert Paul Malchow, Peter J. S. Smith, and Anne E. Giblin

Special Editorial Board

Daniel Alkon
Nina Allen
Guillermo Alvarez
Ricardo Araneda
Clay Armstrong
Peter Armstrong
Jelle Atema
Conxita Avila
Robert Barlow
Michael Bennett
Joshua Berlin
David Bodznick
Robert Bullis
Richard Chappell
Larry Cohen
Carlos Collin
Neal Cornell
Vince Dionne
William Eckberg
Barbara Ehrlich
Harvey Fishman
Kenneth Foreman
James Galbraith
Maria Gomez del Pilar
Mark Hahn
Susan Douglas Hill
John Hobbie
Chuck Hopkinson
Tom Humphreys
Laurinda Jaffe
Lionel Jaffe
Daniel Johnston
Alan Kuzirian
Michael LaMontagne
William Lemon
Vladimir Makarenko
Guang Mei
Andrew Miller
Enrico Nasi
Rudolf Oldenbourg
Robert Palazzo
Haohua Qian
James Quigley
Robert Rakowski
Thomas Reese
Harris Ripps
Larry Rome
Edward Salmon
Rafael Sarda
Andrew Sharp
Erik Sobel
Abe Spector
Mark Terasaki
Kris Tholke
William Trager
Jane Tucker
Ivan Valiela
Joe Vallino
Rainer Voigt
Ebenezer Yamoah

Contents

Featured Articles: A Primitive Immune Defense System

Armstrong, Peter B., Sandra Misquith, Subita Srimal, Ralph Melchoir, and James P. Quigley
Identification of limulin as a major cytolytic protein in the plasma of the American horseshoe crab, *Limulus polyphemus* 227

Melchior, Ralph, James P. Quigley, and Peter B. Armstrong
Clearance of proteases from the circulation of the American horseshoe crab, *Limulus polyphemus:* a possible function for α_2-macroglobulin 228

Quigley, James, Sandra Misquith, Avadhesha Surolia, Subita Srimal, and Peter Armstrong
Preliminary investigation of the molecular basis for the functional differences between the two pentraxins limulin and C-reactive protein from the plasma of the American horseshoe crab, *Limulus polyphemus* 229

Cell Division, Cell Motility, and Development

Salmon, E. D., T. Inoué, A. Desai, and A. W. Murray
High resolution multimode digital imaging system for mitosis studies *in vivo* and *in vitro* 231

Inoué, Shinya, and Theodore D. Inoué
Through-focal and time-lapse stereoscopic images of dividing cells and developing embryos in DIC and polarization microscopy 232

Meng, C. L., and D. C. Chang
Study of calcium signaling in cell cleavage using confocal microscopy 234

Silver, Robert B.
Video light microscopic imaging of the calcium signal that initiates nuclear envelope breakdown in sand dollar (*Echinaracnius parma*) cells 235

Silver, Robert B., Anthony P. Reeves, Marcia Whitman, and Brian Kelley
Analysis of spatial and temporal patterns in the Ca^{2+} signal that signals nuclear envelope breakdown in sand dollar (*Echinaracnius parma*) cells 237

Henry, Jonathan Q., and Mark Q. Martindale
Inhibitory cell-cell interactions control development in the embryos of *Cerebratulus lacteus* 238

Miller, Brent, Amrit Chauhan, Lionel F. Jaffe, and Andrew L. Miller
Oscillations in free $[\mathrm{Ca}^{2+}]_i$ during early cell division cycles in *Xenopus laevis* embryos 239

Roegiers, Fabrice, Phong Tran, and Shinya Inoué
Mitosis, cleavage, and development of highly compressed sea urchin (*Lytechinus variegatus*) zygotes 240

Silver, Robert B., Jeb B. Oblak, Gwendolyn S. Jeun, Jenny J. Sung, and Timothy C. Dutta
Leukotriene B_4, an arachidonic acid metabolite, regulates intracellular free calcium release in eggs and mitotic cells of the sand dollar (*Echinaracnius parma*) 242

Tran, Phong T., Shinya Inoué, Edward D. Salmon, and Rudolf Oldenbourg
Muscle fine structure and microtubule birefringence measured with a new pol-scope 244

Comparative Biochemistry and Toxicology

Borgese, Thomas A., Sharon Bourke, Bernarda Frias, Donald Johnson, and John Harrington
Copper induced polymerization of hemoglobin from the ocean pout, *Macrozoarces americanus* 246

Zigman, Seymour, and Nancy S. Rafferty
Catalase activity in dogfish (*Mustelus canis*) ocular tissues 247

Heck, Diane E., Jeffrey D. Laskin, Seymour Zigman, and Walter Troll
N^{G}-monomethyl-L-arginine inhibits *Arbacia* fertilization and differentiation 248

Hoskin, Francis C. G., and John E. Walker
Enzymatic hydrolysis of Tetriso as a model for the detoxication of the neurotoxic agent VX 249

Tamse, Catherine T., Peter J. S. Smith, Amine Aloulou, Herman T. Epstein, and Alan M. Kuzirian
Lead toxicity in *Hermissenda crassicornis* embryos and cultured neurons 251

Comparative Biology

Avila, Conxita, Adel Arigue, Catherine T. Tamse, and Alan M. Kuzirian
Hermissenda crassicornis larvae metamorphose in the laboratory in response to artificial and natural inducers 252

Hill, Susan Douglas, Alan M. Shipley, and Peter J. S. Smith
Ionic fluxes during wound healing following segment amputation in sabellid fanworms 253

Sadusky, Terrie J., and Robert A. Bullis
Experimental disinfection of lobster eggs infected with *Leucothrix mucor* 254
Weidner, Earl, S. B. Manale, S. K. Halonen, and J. W. Lynn
Microsporidian spore invasion tubes as revealed by fluorescent probes 255

Neurobiology: Sensory Physiology and Neural Networks

Makarenko, Vladimir
Neural network with embedded oscillators ... 256
Lu, Jin, and Harvey M. Fishman
Operational properties of voltage-clamped electroreceptive ampullary organ excised from *Raja* 257
Fay, Richard R., Peggy L. Edds-Walton, and Stephen M. Highstein
Directional sensitivity of saccular afferents of the toadfish to linear acceleration at audio frequencies 258
Gomez, George, and Jelle Atema
Time course of recovery from adaptation by hydroxyproline-sensitive lobster olfactory receptor neurons 259
Passaglia, C. L., F. A. Dodge, and R. B. Barlow, Jr.
Visual responses in the brain of *Limulus* 260
Dodge, F. A., D. M. Porcello, S. A. Dodge, E. Kaplan, and R. B. Barlow, Jr.
Noise components in *Limulus* vision 261
Malchow, Robert Paul, Haohua Qian, Laura M. Haugh-Scheidt, and Harris Ripps
The effects of quinine and quinidine on isolated retinal horizontal cells 262
Qian, Haohua, Robert Paul Malchow, Richard L. Chappell, and Harris Ripps
The $GABA_A$ receptors of Müller (glial) cells in skate retina 263
Yamoah, Ebenezer, and Alan M. Kuzirian
Effects of GABA on outward currents in *Hermissenda* photoreceptors 265
Steinacker, Antoinette, and Conchita Zuazaga
Calcium and voltage sensitivity of potassium current activation in toadfish semicircular canal hair cells 267

Neurobiology: Calcium Regulation

Benech, Juan, Marianna Crispino, Jong Tai Chun, Barry B. Kaplan, and Antonio Giuditta
Protein synthesis in nerve endings from squid brain: modulation by calcium ions 269
Yamoah, Ebenezer, and Peter J. S. Smith
Second messenger modulation of steady-state calcium efflux in *Aplysia* bag cells 270
Kunkel, Joseph G., and Peter J. S. Smith
Three-dimensional calibration of the non-invasive ion probe, NVP_1, of steady ionic currents 271

Behavior

Basil, Jennifer, and Jelle Atema
Lobster orientation in turbulent odor plumes: simultaneous measurement of tracking behavior and temporal odor patterns 272
Leonard, Ann E., Rainer Voigt, and Jelle Atema
Lobster orientation in turbulent odor plumes: electrical recording of bilateral olfactory sampling (antennular "flicking") 273
Tyndale, Elizabeth, Conxita Avila, and Alan M. Kuzirian
Food detection and preferences of the nudibranch mollusc *Hermissenda crassicornis*: experiments in a Y-maze 274
Bushmann, Paul, and Jelle Atema
Aggression-reducing courtship signals in the lobster, *Homarus americanus* 275

Ecology: Impact of Nutrient Loading on Estuaries and Marshes

McDonnell, Kristin, Michelle Rudy, Ivan Valiela, and Kenneth Foreman
The effect of coastal land use on inorganic nutrient concentrations in groundwater entering estuaries of Waquoit Bay, Massachusetts 276
Ingram, Krista K., Charles S. Hopkinson, Katherine Bowman, Robert Garritt, and Joe Vallino
From watershed to estuary: assessment of nutrient loading, retention, and export from the Ipswich River Basin 277
Rudy, Michelle, Kristin McDonnell, Ivan Valiela, and Kenneth Foreman
Dissolved organic nitrogen in groundwater bordering estuaries of Waquoit Bay, Massachusetts: relations with watershed landscape mosaics ... 278
Horne, Ashton, James McClelland, and Ivan Valiela
The growth and consumption of macroalgae in estuaries: the role of invertebrate grazers along a nutrient gradient in Waquoit Bay, Massachusetts 279
Chalfoun, Anna, James McClelland, and Ivan Valiela
The effect of nutrient loading on the growth rate of two species of bivalves, *Mercenaria mercenaria* and *Mya arenaria*, in estuaries of Waquoit Bay, Massachusetts 281

Sardá, Rafael, Kenneth Foreman, and Ivan Valiela
Long-term changes of macroinfaunal assemblages in experimentally enriched salt marsh tidal creeks ... 282
Hurlbut, Peter, Charlene D'Avanzo, Deepti Sethi, and Kerry Guilfoyle
Effects of algal biomass on benthic nitrogen flux in nutrient-loaded estuaries of Waquoit Bay, Massachusetts ... 283

Ecology: Phytoplankton Dynamics

Boxhill, Jessica L., Lory Santiago Vásquez, Timothy R. Harrison, Kenneth Foreman, and James N. Kremer
Daily variation in phytoplankton production in two subestuaries of Waquoit Bay, Massachusetts ... 284
Santiago Vásquez, Lory Z., Jessica L. Boxhill, Timothy R. Harrison, James N. Kremer, and Kenneth Foreman
The effects of wind speed and direction on stratification and phytoplankton production in an estuary of Waquoit Bay, Massachusetts ... 285
Harrison, Timothy R., Jessica L. Boxhill, Lory Z. Santiago Vásquez, Kenneth Foreman, and James N. Kremer
Comparison of phytoplankton and ecosystem gross production in the Quashnet River, an estuary of Waquoit Bay, Massachusetts ... 287

Ecology: Sediment Processes

Monaghan, Eileen, and Anne E. Giblin
The effects of coupling between the oxic and anoxic layers of sediment on nutrient release to overlying water ... 288
Johnson, Rachel, Michael LaMontagne, and Ivan Valiela
Rate of denitrification in submerged salt marsh sediments ... 289
Zago, Cristina, and Anne E. Giblin
Analysis of acid volatile sulfide and metals to predict the toxicity of Boston Harbor sediments 290

ABSTRACTS

In addition to the work described here in Short Reports, the following papers were also presented at the meetings and are listed below. The abstracts of these papers are available from the Marine Biological Laboratory Archives.

Cubitt, Andrew B., Richard A. Firtel, Gabriele Fischer, Lionel F. Jaffe, Eric Karplus, and Andrew L. Miller
Patterns of free calcium in developing *Dictyostelium*

Gerardo, Hortense F., and Robert A. Bullis
Effects of different quarantine procedures on the mudpuppy, *Necturus maculosus*

Humphreys, Tom, Stephen E. Schauer, and Royce C. Lin
An examination of histocompatibility and immunogenetics in the red beard sponge, *Microciona prolifera*

Kuhns, William J., Max M. Burger, and Gradimir Misevic
Cellular retention of aggregation factor/adhesive proteoglycan accompanies loss of motility following sulfate restriction in *Microciona prolifera*, the marine sponge

Reference: *Biol. Bull.* **187**: 227–230. (October, 1994)

Introduction to Featured Articles: A Primitive Immune Defense System

Members of several invertebrate phyla have maximum lifespans that approach that of humans. A precondition for longevity is a highly effective immune defense system that operates to inactivate invasive pathogens. Invertebrates do not possess the well-studied antibody-based immune system, which is found only in the vertebrates. Our research has focused on immune defense proteins in the plasma of arthropods that show extreme evolutionary conservation. Two of these, the α_2-macroglobulins and the pentraxins, are present in modern representatives of vertebrates and arthropods, and thus must have originated in evolution prior to the great evolutionary divergence of the Pre-Cambrian that gave rise, finally, to the modern multicellular phyla. In these reports we show that the pentraxin, limulin, is the principal mediator of a plasma-based cytolytic system in Limulus polyphemus, *and that the α_2-macroglobulin of* Limulus *mediates the recognition and clearance of proteases from the circulation and serves as a regulator of the limulin-based cytolytic system. We suggest that the α_2-macroglobulins and the pentraxins are mediators of primitive immune defense systems that protect a diversity of animals from pathogenic attack.*

—Peter B. Armstrong and James P. Quigley
August, 1994

Reference: *Biol. Bull.* **187**: 227–228. (October, 1994)

Identification of Limulin as a Major Cytolytic Protein in the Plasma of the American Horseshoe Crab, *Limulus polyphemus*

Peter B. Armstrong (Department of Molecular and Cellular Biology, University of California, Davis, CA 95616-8755), Sandra Misquith, Subita Srimal, Ralph Melchior, and James P. Quigley

A major problem of comparative immunology is the identification and characterization of the internal defense systems that lyse foreign cells, such as bacteria and other microbial pathogens, that have gained entry into the body (1). Lysis must be selective to avoid collateral damage to the organism's own tissues. *Limulus* shows a potent cytolytic activity in the plasma that has been assayed by its ability to lyse sheep erythrocytes (2). In this report, we present evidence that the mediator of the cytolytic system of *Limulus* is the protein limulin, a sialic acid-binding lectin of the plasma. The sialic acid (SA)-binding lectins that have been found in the plasma of a variety of invertebrates (3) are poorly characterized in function. *Limulus* possesses several SA-binding lectins, of which limulin is the best described (4).

For the present studies, limulin was purified to homogeneity from the plasma of *Limulus* by sequential affinity chromatography on phosphorylethanolamine (PE)-agarose and fetuin-Sepharose, a sialic acid affinity resin. The binding of limulin both to PE and to sialic acid is Ca^{+2}-dependent. The following observations indicate that limulin is necessary for hemolysis by hemocyanin-depleted *Limulus* plasma. The lytic activity on sheep erythrocytes was Ca^{+2}-dependent and was abolished if the plasma was depleted in limulin, either by passage over PE-agarose or over fetuin-Sepharose. Hemolytic activity was restored to limulin-depleted plasma by the addition of purified limulin. Limulin is sufficient for hemolysis because purified limulin was hemolytic in a Ca^{+2}-dependent manner at 10 n*M* [assuming a molecular mass of 300 kDa (5)] in the absence of other plasma components. The hemolytic activity of purified limulin was dependent on its SA-recognition capabilities, because limulin-mediated hemolysis was abolished by desialylation of the target erythrocytes with *V. cholerae* neuraminidase, or by inclusion of 9 μM fetuin in the incubation medium, and was reduced 50% by 0.1 *M* N-acetyl neuraminic acid.

Limulin can be separated from the other SA-lectins in the plasma of *Limulus* by its unique ability to bind to PE-agarose. Although the other SA-lectins of *Limulus* plasma, which were isolated from the PE-agarose breakthrough fraction by their affinity to fetuin-Sepharose, agglutinated sheep erythrocytes, they showed no ability to lyse the cells when they were present at hemagglutination titers equivalent to those of active concentrations of limulin. Thus hemolysis is not produced by any and all SA-lectins.

Limulus α_2-macroglobulin (LAM), a second plasma protein with potential immune function, plays a regulatory role for limulin-mediated cytolysis. LAM that was activated by exposure to low molecular mass primary amines or to proteases reduced the cytolytic activities of purified limulin. This activity was not shown by unactivated LAM, but unactivated LAM could reverse the inhibitory activity of amine- and protease-activated LAM.

Identification of the cytolytic protein in the plasma of *Limulus* as the lectin limulin is an important advance in our understanding of the mechanisms of immunity in this animal. The recognition of foreign cells for subsequent cytolytic destruction probably depends on the presentation of sugars recognized by limulin on the surfaces of the foreign cells. Although several plasma lectins have been identified in a variety of animals, the functions of this class of proteins have been poorly characterized. To our knowledge, this is the first demonstration of a cytolytic function for a plasma lectin. The ability of LAM to regulate the activity of limulin is as yet not well characterized, but it may be important in the integration of the different components of the immune defense system of *Limulus.*

Supported by Grant No. MCB-9218460 from the National Science Foundation.

Literature Cited

1. **Canicatti, C. 1990.** *Experientia* **46:** 239–243.
2. **Armstrong, P. B., M. T. Armstrong, and J. P. Quigley. 1993.** *Mol. Immunol.* **30:** 929–934.
3. **Mandal, C., and C. Mandal. 1990.** *Experientia* **46:** 433–441.
4. **Kehoe, J. M., and R. K. Seide. 1986.** Pp. 345–358 in *Hemocytic and Humoral Immunity in Arthropods,* A. P. Gupta, ed. John Wiley & Sons, New York.
5. **Quigley, J. P., S. Misquith, A. Surolia, S. Srimal, and P. B. Armstrong. 1994.** *Biol. Bull.* **187:** 229–230.

Reference: *Biol. Bull.* **187:** 228–229. (October, 1994)

Clearance of Proteases from the Circulation of the American Horseshoe Crab, *Limulus polyphemus:* A Possible Function for α_2-Macroglobulin

Ralph Melchior (Department of Molecular and Cellular Biology, University of California, Davis, CA 95616-8755), James P. Quigley, and Peter B. Armstrong

The protease inhibitor α_2-macroglobulin (α_2M), which is found at high concentration in the plasma of vertebrates, arthropods, and molluscs (1), binds proteases by a unique process that begins with the proteolytic cleavage of α_2M and is completed when α_2M enfolds the target protease in a molecular cage (2). Only enzymatically active proteases can react with α_2M (2). The conformational change that results in protease entrapment also exposes a previously buried site in mammalian α_2M that is recognized by cell surface receptors of hepatocytes and macrophages (3, 4). An identical conformational change can be produced by reaction of α_2M with small primary amines such as methylamine (MA) (3). In mammals, protease- and MA-activated α_2M is then rapidly cleared from the plasma by a receptor-mediated endocytotic process (4).

α_2-Macroglobulin was purified from the plasma of *Limulus* as described previously (5). Trypsin was fluoresceinated with fluorescein-isothiocyanate (FITC) and was then purified on a benzamidine-Sepharose column. To search for a clearance process for proteases in *Limulus,* FITC-labeled proteins were introduced into the circulation by intracardiac injection. Blood samples were taken from the blood spaces of the leg joints. Blood

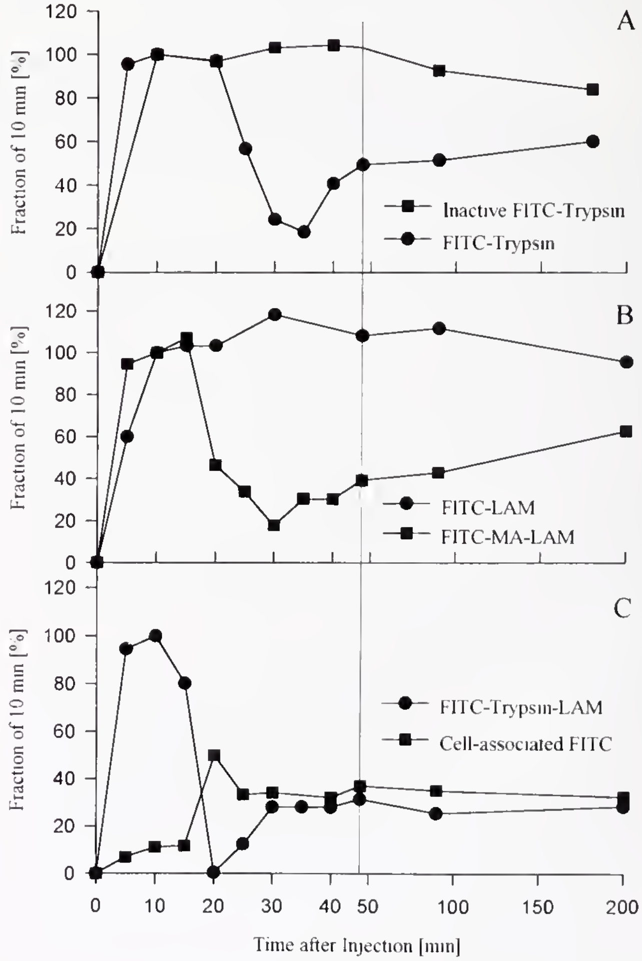

Figure 1. *Clearance from the plasma of* Limulus *of (A) fluorescein (FITC)-labeled samples of trypsin; (B) methylamine (MA)-reacted* Limulus *α_2-macroglobulin (LAM); and (C) trypsin-reacted LAM. Trypsin inactivated by prior reaction with phenylmethyl-sulfonyl fluoride (A) and native LAM (B) were not cleared from the circulation during the period of observation, whereas trypsin and activated LAM were cleared rapidly and efficiently (trypsin $t_{1/2}$ = 26 min; MA-LAM $t_{1/2}$ = 20 min; trypsin-LAM $t_{1/2}$ = 17 min). The fraction of the fluorescein label that was associated with the blood cells was maximal at the time that the label in the plasma was minimal (C).*

cells were removed by centrifugation, and the concentration of FITC-labeled proteins in the plasma was measured with a fluorometer. In addition, the blood cell-associated fluorescence was measured after cell lysis with sodium dodecyl sulfate.

An injected inert protein (FITC-hemocyanin) reached 90% mixing in the peripheral blood by 5 min, and a steady state concentration by 10 min after injection. These results were confirmed by angiography. There was no detectable clearance of the control protein, FITC-labeled hemocyanin, over a period of 180 min. FITC-labeled trypsin was cleared in a triphasic manner, with an initial lag period (10–20 min) and a rapid clearance period (20–30 min), followed by the reappearance of FITC in the circulation (45–90 min) (Fig. 1A). The clearance of trypsin requires its protease activity, because phenylmethyl sulfonyl fluoride-inactivated FITC-labeled trypsin was cleared only very slowly if at all ($t_{1/2} > 180$ min) (Fig. 1A). FITC-labeled, MA-reacted *Limulus*-α_2M (LAM) (Fig. 1B) and FITC-labeled, trypsin-reacted LAM (Fig. 1C) were cleared rapidly from the plasma of *Limulus*, whereas FITC-labeled native LAM persisted in excess of 400 min (Fig. 1B).

The blood cells of *Limulus* bound FITC-labeled, MA-reacted LAM and FITC-labeled, trypsin-reacted LAM. Forty percent of the cleared fluorescence was recovered from SDS-solubilized blood cells at 30 min. The peak of recovery from the blood cells coincided with the minimum of FITC-labeled protein in the plasma (Fig. 1C).

In summary, we have demonstrated the existence of a clearance pathway in *Limulus* that operates selectively on enzymatically active proteases. The *Limulus* homologue of α_2M appears to be capable of mediating this clearance, because protease- and MA-activated LAM were cleared with kinetics similar to those of introduced proteases. Native LAM was retained in the plasma and was not cleared. It appears that LAM is the only protease inhibitor in the plasma of *Limulus* (6). Several problems remain. We have not characterized the FITC-labeled material that reappeared in the plasma following clearance. Because this material passed through a molecular size exclusion of 10 kDa, it may consist of proteolyzed fragments of protein that result from its endocytosis and degradation by the blood cells. Also, we have not identified the cell surface receptor for activated LAM.

Supported by Grant No. MCB-9218460 from the National Science Foundation.

Literature Cited

1. **Armstrong, P. B., and J. P. Quigley. 1985.** Pp. 291–310 in *Immunology of Insects and Other Arthropods*, A. P. Gupta, ed. CRC Press, Boca Raton, FL.
2. **Starkey, P. M., and A. J. Barrett. 1977.** Pp. 663–680 in *Proteinases in Mammalian Cells and Tissues*, A. J. Barrett, ed. Elsevier/North Holland Biomedical Press, Amsterdam.
3. **Sottrup-Jensen, L. 1987.** Pp. 191–291 in *The Plasma Proteins, Structure, Function, and Genetic Control*, Vol 5, 2nd Ed., F. W. Putnam, ed. Academic Press, New York.
4. **Van Leuven, F. 1984.** *Mol. Cell. Biochem.* **58:** 121–128.
5. **Armstrong, P. B., W. F. Mangel, J. S. Wall, J. F. Hainfield, K. E. Van Holde, A. Ikai, and J. P. Quigley. 1991.** *J. Biol. Chem.* **266:** 2526–2530.
6. **Quigley, J. P., and P. B. Armstrong. 1983.** *J. Biol. Chem.* **258:** 7903–7906.

Reference: *Biol. Bull.* **187:** 229–230. (October, 1994)

Preliminary Investigation of the Molecular Basis for the Functional Differences Between the Two Pentraxins Limulin and C-Reactive Protein from the Plasma of the American Horseshoe Crab, *Limulus polyphemus*

James Quigley (Department of Pathology, Health Sciences Center, Tower 9, Room 140, State University of New York, Stony Brook, NY 11798-8691), Sandra Misquith, Avadhesha Surolia, Subita Srimal, and Peter Armstrong

The pentraxins are a family of plasma proteins that include C-reactive protein (CRP) and serum amyloid protein in mammals (1) and a family of pentraxins from the American horseshoe crab, *Limulus polyphemus* (2, 3). Both the mammalian and *Limulus* pentraxins bind pneumococcal C-polysaccharide in a Ca^{+2}-dependent manner. The pentraxins of the plasma of *Limulus* can be isolated by affinity chromatography on phosphoethanolamine (PE)-derivatized resins.

We have now shown that the *Limulus* pentraxins are composed of at least two proteins, a homologue of mammalian CRP and limulin, a lectin with recognition capabilities for sialic acid (SA) and 2 keto-3-deoxyoctonate (4). Although it was previously assumed that limulin and *Limulus* CRP were the same protein (*cf.*, 5), we have found them to be distinct but closely related proteins. Limulin was purified by sequential chromatographic isolation (in either order) on fetuin-Sepharose (an SA-resin) and PE-agarose. *Limulus* CRP was purified as the unbound fraction when the total PE-binding fraction was subsequently chromatographed on fetuin-Sepharose. Less than 1% of the PE-agarose-binding (pentraxin) fraction is limulin. Clearly limulin and *Limulus* CRP are closely related: both proteins bind to PE-affinity resins; both have the same native (~300 kDa—by size exclusion chromatography on Sephacryl S-300 HR resin) and subunit [~24–28 kDa—by SDS-polyacrylamide gel electrophoresis (PAGE)] molecular masses; and both have the same amino terminal peptide sequence (LEEGEGITSKV), and a polyclonal antiserum produced against purified *Limulus* CRP cross-reacts with limulin.

However, the two proteins do show important functional differences: limulin, but not *Limulus* CRP, binds to sialic acid, agglutinates sheep and rabbit erythrocytes, and lyses sheep erythrocytes (6, 7). In our attempts to discover the molecular basis for these significant functional differences between two closely related proteins, we have found that limulin and *Limulus* CRP show small but reproducible differences in the pattern of protein bands seen by SDS-PAGE. Before experimental proteolysis, both *Limulus* CRP and limulin show two closely spaced protein bands by SDS-PAGE (both with and without 2-mercaptoethanol), with the lower band staining more intensely for *Limulus* CRP and the upper staining more intensely for limulin (both Coomassie blue and silver staining). The two proteins differ in the extent of proteolytic fragmentation and the sizes of the peptide fragments generated by exposure to the proteases endoprotease Lys-C (from *P. aeruginosa*), endoprotease Glu-C (from *S. aureus*), and alkaline protease (from *B. licheniformis*). This suggests that, while the amino termini of limulin and *Limulus* CRP are identical, the two proteins may possess differences in amino acid sequence in the interiors of the polypeptide chains. There are multiple genes for the *Limulus* pentraxins, consistent with this possibility (2, 3). About 2.5–3.3% of the molecular mass of *Limulus* CRP and of limulin is neutral sugar (determined by the phenol-sulfuric acid method), but *Limulus* CRP is recognized by a mannose-binding lectin from *Artocarpus integrifolia*, indicating that its carbohydrate is of the polymannosyl type, whereas limulin fails to bind this lectin. These data are consistent with the possibility that limulin and *Limulus* CRP differ both in amino acid sequence and in glycosylation. Experiments are under way to determine which of these subtle structural differences in the two proteins are responsible for their distinctive functional properties.

This research was supported by Grant No MCB-9218460 from the National Science Foundation.

Literature Cited

1. **Tennent, G. A., and M. B. Pepys. 1994.** *Biochem. Soc. Trans.* **22:** 74–79.
2. **Nguyn, N. Y., A. Suzuki, S.-M. Cheng, G. Zon, and T.-Y. Liu. 1986.** *J. Biol. Chem.* **261:** 10450–10455.
3. **Nguyn, N. Y., A. Suzuki, R. A. Boykins, and T.-Y. Liu. 1986.** *J. Biol. Chem.* **261:** 10456–10465.
4. **Kehoe J. M., and R. K. Seide. 1986.** Pp. 345–358 in *Hemocytic and Humoral Immunity in Arthropods,* A. P. Gupta, ed. John Wiley & Sons, New York.
5. **Robey, F. A., and T.-Y. Liu. 1981.** *J. Biol. Chem.* **256:** 969–975.
6. **Armstrong, P. B., S. Misquith, S. Srimal, R. Melchior, and J. P. Quigley. 1994.** *Biol. Bull.* **187:** 227–228.
7. **Srimal, S., J. P. Quigley, and P. B. Armstrong. 1993.** *Biol. Bull.* **185:** 325.

Reference: *Biol. Bull.* **187**: 231–232. (October, 1994)

High Resolution Multimode Digital Imaging System for Mitosis Studies *In Vivo* and *In Vitro*

E. D. Salmon (Biology, Univ. of N. Carolina, Chapel Hill, NC), T. Inoué, A. Desai, and A. W. Murray

Many questions about the mechanisms of mitotic spindle assembly, chromosome movement, and chromosome segregation can be answered by quantitative measurements of digital images obtained from several optical modes. For example, epifluorescent detection of X-rhodamine-labeled tubulin reveals spindle microtubule organization, whereas DAPI or other DNA-binding dyes stain the chromosomes in live preparations where these structures are often invisible to phase or DIC methods (1–4). Photoactivated fluorophores bound to tubulin can be used to measure microtubule assembly dynamics in real time (1, 2), and other fluorescent probes can be used to track the dynamics of membranes, other organelles, or molecular complexes within the spindle (5). In transparent specimens, the movements of chromosomes and centrosomes can be recorded with transmitted light if phase contrast or DIC optics are employed (6), while polarization methods can reveal spindle fiber microtubule dynamics and provide a quantitative measure of microtubule assembly and orientation (6). In addition to real-time recording, a digital fluorescence microscope system can also provide 3-D structural detail from stacks of optical sections when the specimens are stained with specific molecular probes.

The high resolution, multimodal digital microscope system that we have constructed for our mitosis studies is diagrammed in Figure 1. Optical components of the Nikon FXA microscope stand were chosen to provide diffraction-limited resolution in transmitted and fluorescence modes for images projected onto a cooled charge coupled device (CCD) camera (Fig. 2C).

Cooled CCD cameras have several advantages for digital imaging over unintensified and intensified video detectors, including dynamic range, linearity, low noise, and little geometrical distortion. The Hamamatsu C4880 was chosen because it has two readout modes: a fast scan mode (up to 7 frames/s) which is useful for focusing, and a slow scan mode (12 bit/pixel, 500,000 bytes/s readout rate), which gives the most useful dynamic range (4000 grey levels above a noise floor of about 50 ± 10). The MetaMorph digital imaging system is programmed to control image acquisition from the CCD camera. We have found that the central area (300 × 300 pixels) of the 1000 × 1000 pixel detector provides sufficient resolution and field of view for our mitosis images while reducing the time required to process the digital images and the amount of digital storage required (180 KBytes/image).

An important criterion in our mitosis studies is that all the epi- and trans-illumination images be aligned and in focus at the same position on the CCD detector. This was accomplished with a single Chroma filter cube containing a multiple bandpass dichromatic mirror and emission filters designed for the DAPI (blue), fluorescein (green), and X-rhodamine (red) emission wavelengths. Excitation intensity and wavelength are selected by a MetalTek stepper motor controlled dual filter wheel, where one 8-position wheel holds a series of neutral density filters, and the other holds narrow bandpass filters for the different excitation wavelengths. Other filters and iris diaphragms in the epi- and trans-illumination paths are used to provide further manual control of illumination intensity and field of illumination (Fig. 1). Focus position along the z-axis is controlled by a Ludl stepper motor attached to the Nikon FXA fine focus.

The MetaMorph digital imaging system has programs and journal scripts that control for either time-lapse or z-axis stepping,

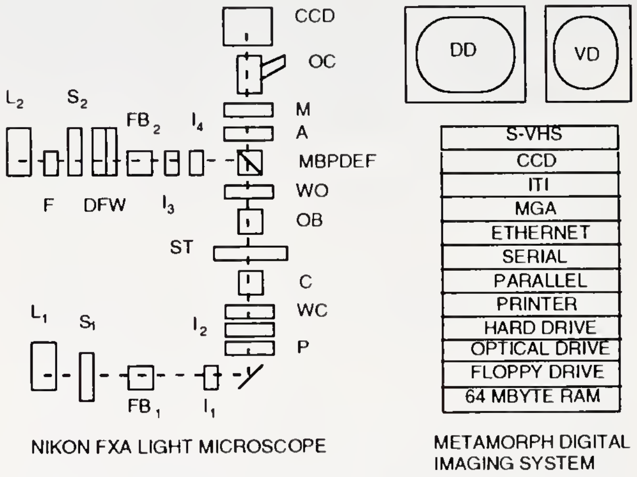

Figure 1. *Component parts are L1, 100 W quartz halogen lamp; S1, Uniblitz shutter (#225L2A1Z523398, Vincent Associates, Rochester, NY); FB1, FB2, manual filter changers for Nikon FXA stand; I_1, I_2, I_3, I_4 field and condenser iris diaphragms; P, AP, high transmission Nikon polaroid polarizer and removable analyzer; WC, WO, DIC Wollaston prisms; C, Nikon NA = 1.4 CON A, Achr-Apl condenser; ST, rotatable stage with focus position controlled by z-axis stepper motor (Mac2000, Ludl Electronic Products, LTD., Hawthorne, NY); OB, 20×/NA = .75 or 60×/NA = 1.4 Nikon objectives; MBPDEF, filter block with multiple bandpass dichromatic mirror and emission filter (#83101 and #83100, Chroma Technology Corp., Brattleboro, VT); L2, 100 W HBO Hg lamp; F, KG4 heat cut filter; S2, DFW, shutter and dual 8-position filter wheel (MetalTek, Raleigh, NC), one wheel containing neutral density filters (#FNQ011, Melles Griot, Irvine, CA), and the other a series of narrow bandpass excitation filters (#83360, #83490, #83570, Chroma Technology Corp.); M, optivar magnification changer, 1X-2X; OC, oculars; CCD, cooled CCD camera (#C4880, Hamamatsu Photonics, Bridgewater, NJ); DD, 1024 × 768 pixel, 20 inch digital graphics display monitor (#2082, Viewsonic); VD, RGB video display monitor (#PVM1271Q, Sony); MetaMorph digital imaging system (Universal Imaging Corp., West Chester, PA) using a 66 MHz, 486 processor, EISA bus, 64 MByte RAM memory, Imaging Technology AFG digital and video image processing card; Hamamatsu C4880 CCD controller card; Matrox MGA Ultima graphics display card, graphics display to S-VHS converter card (Hyperconverter, PC Video Conversion Corp., San Jose, CA), 1.4 MByte floppy drive, 580 MByte hard drive, Pinnacle Micro 650 MByte optical drive, Ethernet card, parallel port cards for controlling shutter S1 and driving laser printer; 8 serial port card for controlling MetalTek filter wheel, Ludl z-axis stepper, CCD camera, and OMDR.*

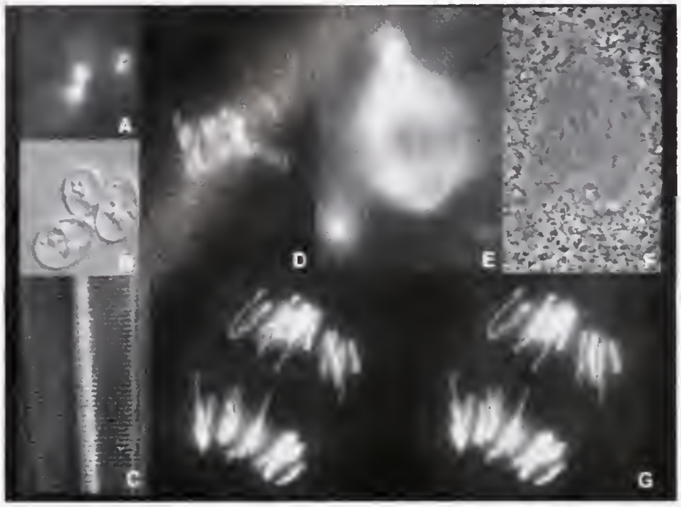

Figure 2. *Views of a living, dividing yeast (*Saccharomyces cerevisiae*) produced by (A) green fluorescent protein (7) bound to nuclear histones and (B) DIC*. (C) Image in DIC of the 0.24 μm spacing between rows of frustrual pores of the diatom* Amphipleura *illuminated with green light*. Images of a spindle undergoing anaphase in* Xenopus *cytoplasmic egg extracts: (D) DAPI stained chromosomes, (E) Rhodamine-tubulin labeled spindle and aster microtubules, and (F) phase contrast (Nikon 20X/NA = 0.75 Fluar Phase 3 objective). Stereo pair images (F) of DAPI stained chromosomes generated from a stack of 0.5 μm optical sections through a* Xenopus *spindle fixed in the extracts in mid-anaphase* (*, Nikon 60×/NA = 1.4 Plan Apo DIC objective and NA = 1.4 condenser illumination for DIC).*

shutters in the light paths, filter wheel positions, image size and acquisition from the CCD camera, and image storage into stacks identified by their mode of acquisition (DAPI, Xrhod, phase, DIC, etc.). Image stacks are initially stored within the 64 MBytes of RAM memory, then archived on the hard drive or the Pinnacle optical disk drive. MetaMorph also provides comprehensive functions for quantitative analysis of intensity and motion, multicolor overlays of different image stacks (*e.g.*, DAPI and rhodamine channels), and movie presentation, either on the high resolution graphics screen or by conversion of the digital images to video through a VGA to S-VHS video converter. Large stacks of images can also be converted to video for storage on an optical memory video disk recorder (Panasonic TQ2028 or TQ3038F).

Using this system we were able to obtain novel high resolution real-time images of yeast nuclear motion in the cell division cycle (Fig. 2A, B) and to finally visualize in real time anaphase spindle dynamics and chromosome segregation in an *in vitro* system (3, 4) reconstituted from sperm nuclei and extracts prepared from *Xenopus* eggs (Fig. 2C, D, E). 3-D images derived from a stack of optical sections have also proved very useful for determining the behavior of all of the chromosomes and their kinetochore regions within the spindle (Fig. 2F).

We gratefully acknowledge MBL for providing the H. L. Rand Fellowship to E.D.S., MBL and Nikon for providing the Nikon Fellowship to A. W. M. and for their generous loan of instruments, and Shinya Inoué and the Program in Architectural Dynamics for support and space for our *Xenopus* studies at the MBL. The instrument development and *Xenopus* studies are supported by NIH GM24364 to E.D.S. and GM 43987 to A.W.M.

Literature Cited

1. **Sawin, K. E., and T. J. Mitchison. 1992.** *J. Cell Biol.* **112:** 941–954.
2. **Mitchison, T. J., and E. D. Salmon. 1992.** *J. Cell Biol.* **119:** 569–582.
3. **Shamu, C. E., and A. W. Murray. 1992.** *J. Cell Biol.* **117:** 921–934.
4. **Hollaway, S. L., and A. W. Murray. 1993.** *Cell* **73:** 1393–1402.
5. **Waterman-Storer, C. M., J. W. Sanger, and J. M. Sanger. 1993.** *Cell Motil. Cytoskel.* **26:** 19–39.
6. **Cassimeris, L., S. Inoué, and E. D. Salmon. 1988.** *Cell Motil. Cytoskel.* **10:** 185–196.
7. **Chalfie, M., Y. Tu, G. Euskirchen, W. W. Ward, and D. C. Prasher. 1994.** *Science* **263:** 802–804.

Reference: *Biol. Bull.* **187:** 232–233. (October, 1994)

Through-Focal and Time-Lapse Stereoscopic Imaging of Dividing Cells and Developing Embryos in DIC and Polarization Microscopy

Shinya Inoué (Marine Biological Laboratory) and Theodore D. Inoué

Recent developments in confocal microscopy, and methods for computational deconvolution of serial optical sections, now permit three-dimensional (3-D) imaging of unfixed cells and developing embryos, generally in the fluorescence contrast mode (1). 3-D reconstruction is restricted to fluorescence contrast, partly because most confocal microscopes do not permit confocal imaging in other contrast modes, and partly because the 3-D point-spread function for fluorescence is relatively simple.

Although fluorescence microscopy is extremely effective at revealing specific chemical species and selected organelles, DIC and polarization microscopy can provide complementary spatial and fine-structural information, and at much greater speeds. However, the point-spread function in these latter modes of microscopy is extremely complex (2), and it is not obvious that 3-D images can be computationally reconstructed in these modes from serial optical sections.

Nevertheless, we reported earlier that very thin optical sections can be obtained in DIC, polarization, and phase contrast microscopy in the absence of confocal imaging by using well-corrected optics of high numerical aperature (NA) and video and

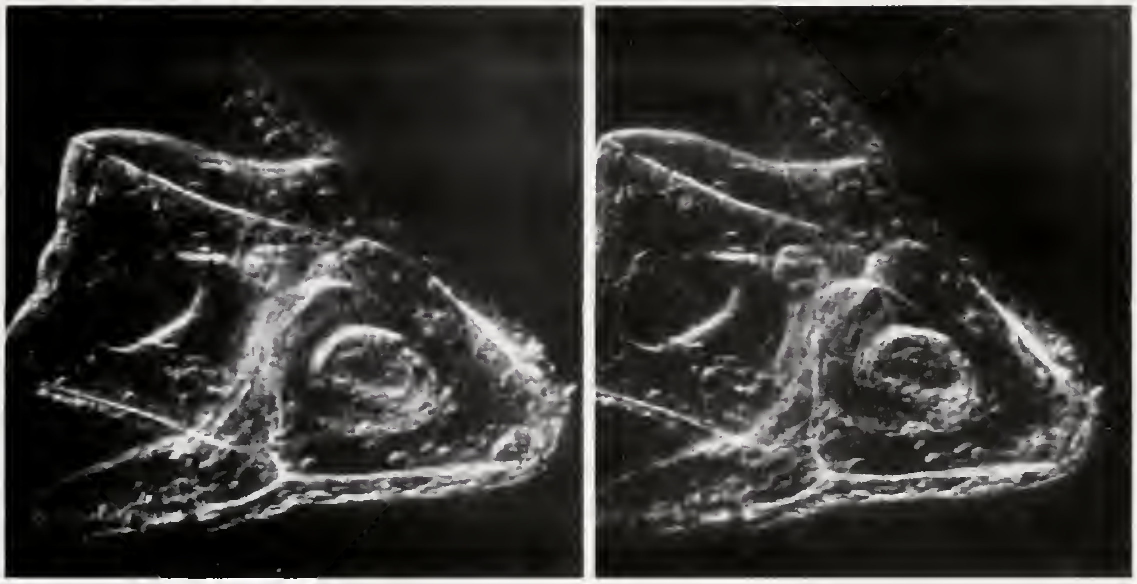

Figure 1. *Swimming pluteus larva of* Lytechinus variegatus *(sea urchin). The stereo pair is arranged for cross-eyed viewing. Each view was computed from a stack of ca. 100 optical sections which were acquired in DIC microscopy at 30 sections/s, then digitally processed to remove out-of-focus haze.*

digital contrast enhancement (3). We also described a method for very rapidly obtaining serial optical sections, repeatedly in time lapse, using video microscopy combined with synchronous computerized control of the objective and condenser fine-focus controls (4).

We now demonstrate, at these General Scientific Meetings, through-focal and three-dimensionally reconstructed stereoscopic images of a free-swimming, pluteus-stage sea urchin embryo and the mitotic spindle fibers within the two-cell stage of a dividing ctenophore egg. The former, generated from serial optical sections in DIC microscopy, shows details of the external morphology, including the presence of a scoop on the mouth, and internal organs of the pluteus, with unexpected clarity (Fig. 1). Stereo views of sequential slices, generated from limited sets of serial optical sections, bring out further details of the cellular organization, including the regular pavement-like arrangement of the circumoral epithelium and the shape of the mesenchyme cells that were masked by the overlapping complex structure in the whole embryo.

The spindle of the dividing ctenophore egg, reconstructed from serial optical sections in polarization microscopy, shows the 3-D organization of the birefringent chromosomal spindle fibers (kinetochore microtubule bundles) in rocking stereoscopic projection. The fibers appear unusually well differentiated from the background array of microtubules, which was presumably aided by the averaging algorithm in the computational reconstruction that we used to generate the 3-D projections from the haze-removed optical sections.

The ability to generate these clear 3-D views from optical sections, which were non-destructively acquired at the high speed of 30 through-focal serial sections per second in DIC and polarization microscopy, opens up new opportunities for physiological, embryological, and cytological studies of developing embryos and cells undergoing mitosis and other activities involving the dynamic reorganization of their fine-structural and macromolecular architecture. The practical method that permitted these 3-D reconstructions of the DIC and polarization optical images is reported elsewhere (5).

Support by grants R37 GM 31617-13 from NIH and DCB-8908169 from NSF to SI, and technical support by Robert A. Knudson of the MBL Instrument Development Laboratory and staff of the Universal Imaging Corporation are gratefully acknowledged.

Literature Cited

1. **Pawley, J. 1994.** *Handbook of Confocal Microscopy.* Plenum Press, New York.
2. **Galbraith, W. 1982.** *Microsc. Acta* **85:** 233–254.
3. **Inoué, S. 1988.** *Cell Motil. Cytoskel.* **10:** 13–17.
4. **Inoué, S., and T. D. Inoué. 1991.** *Biol. Bull.* **181:** 336–337.
5. **Inoué, S., and T. D. Inoué. 1994.** Abstract, Amer. Soc. Cell. Biol., *J. Cell Biol.*, in press.

Reference: *Biol. Bull.* **187**: 234–235. (October, 1994)

Study of Calcium Signaling in Cell Cleavage Using Confocal Microscopy

C. L. Meng (Dept. of Biology, Hong Kong University of Science and Technology, Hong Kong)
and D. C. Chang

Intracellular calcium is an important second messenger that is involved in many important cellular functions. Several recent studies have implicated Ca^{++} signaling in cell cleavage, particularly cytokinesis (1–4). Cytokinesis is an important part of the cell cycle; it also plays a key role in development. The spatial location and the timing of cytokinesis are both precisely regulated (2), but the regulatory mechanisms of cytokinesis are not well understood at present. The evidence implicating intracellular Ca^{++} in cytokinesis has, thus far, been indirect. The only relevant calcium images available, from medaka eggs, were obtained by the use of aequorin (3). Because of the limitations of spatial and temporal resolution, the changes in Ca^{++} level cannot yet be correlated with the onset of cytokinesis.

To shed some light on this problem, we decided to combine a number of recently developed imaging techniques to examine the variation of intracellular free Ca^{++} in zebrafish embryos during early cell cleavage. The major goal was to improve greatly the spatial and temporal resolution so that a more definitive Ca^{++} signal in association with cytokinesis could be characterized. Our approach was to micro-inject a Ca^{++} indicator probe, Calcium Green-1 conjugated to 10 kD dextran (from Molecular Probes, final concentration = 2–5 μM), into the embryo and then to use a laser-scanning confocal microscope (Bio-Rad) to measure the fluorescent signal; such signals can be converted into Ca^{++} concentrations with a standard calibration curve. This method has several advantages. First, because of the conjugation with dextran, our probe is not sequestered and is distributed only in the cytosol. Thus, the observed fluorescent signals reflect more faithfully the cytosolic free Ca^{++} concentration ($[Ca^{++}]_i$). Second, a relatively large dose of Calcium Green-1 can be injected into the zebrafish embryo without affecting its normal development. Thus, a high signal-to-noise ratio can be obtained. Also, the measurement can be done at a shorter time, thus providing better temporal resolution.

Third, using the confocal microscope, we can measure the variation of $[Ca^{++}]_i$ within a specific optical section; thus the spatial resolution can be greatly improved.

Using this method, we have examined the spatial and temporal variation of $[Ca^{++}]_i$ in the zebrafish embryo during the second and third cell cleavages. Our findings, based on 24 experiments, can be summarized as follows:

1. A localized elevation of $[Ca^{++}]_i$ was clearly observed along the equator of the dividing cell—the site of the constriction of the cleavage furrow (Fig. 1).
2. The rise of the free Ca^{++} level not only coincided with cytokinesis, it actually preceded, slightly, the initiation of furrow contraction (Fig. 1).
3. The magnitude of the $[Ca^{++}]_i$ rise in association with cytokinesis was highly significant; the elevated $[Ca^{++}]_i$ was at least fivefold that of the resting level (approximately 0.15 μM).

These results thus support the hypothesis that calcium signaling is involved in the triggering of cytokinesis, since the observed elevation of free Ca^{++} occurs not only in the right place, but also at the right time.

One might question whether, in this Ca^{++} imaging measurement, the observed elevation of $[Ca^{++}]_i$ could be an artifact

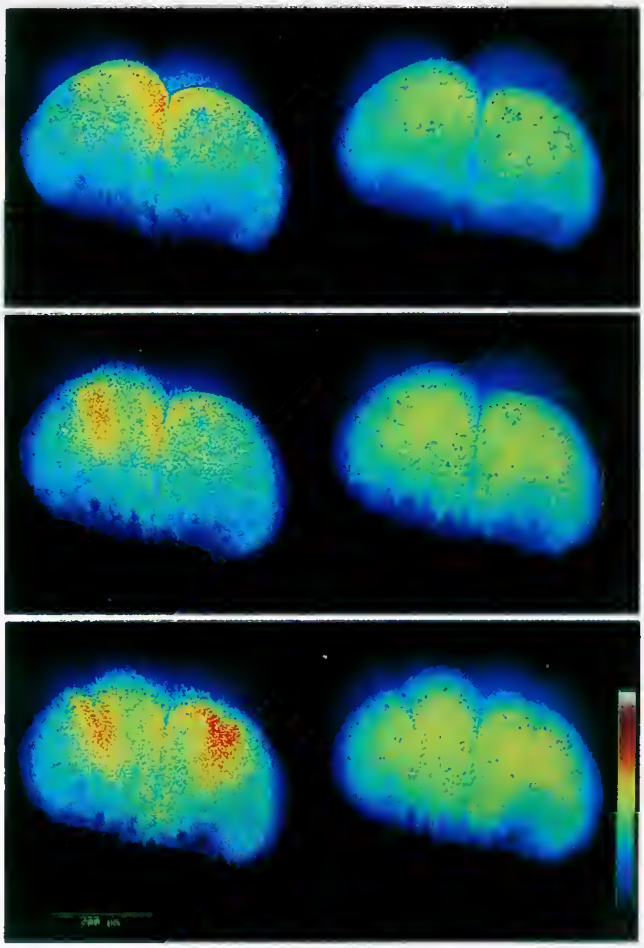

Figure 1. *Paired images of fluorescent signals from Calcium-Green-1 (left) and rhodamine (right), both of which were conjugated to 10 kD dextrans (from Molecular Probes). The two dyes were co-injected into the one-cell stage zebrafish embryo and then observed simultaneously using a confocal microscope operating under a two-channel mode. The intensity of the fluorescent signal is shown in pseudo-color. The rhodamine signal shows the distribution of the injected dyes, while the Calcium-Green signal shows the local concentration of free Ca^{++}. The three pairs of images were obtained at different times when the embryo was undergoing the third cell cleavage. (Top) Initial observation before the third cell cleavage began; (middle) 147 s later; (bottom) 322 s later.*

caused by an uneven distribution of the calcium-indicating dyes that somehow aggregated at the cleavage point. To test this possibility, we co-injected rhodamine that was conjugated to the same type of dextran macromolecules as the Calcium-Green into the embryo and used two laser lines to record simultaneously the fluorescent images of the two dyes. The paired images presented in Figure 1 (left: Calcium-Green, right: rhodamine) show that there was no spatial or temporal change in the rhodamine signal during cell cleavage, indicating that the observed changes in the Calcium-Green signal are a true reflection of $[\mathrm{Ca}^{++}]_i$ variations.

We further tested the possibility that cytokinesis could be blocked by lowering the intracellular level of free Ca^{++}. By injecting into the four-cell stage embryos a Ca^{++} buffer (a 1:1 mixture of free BAPTA and BAPTA conjugated to 70 kD dextran, in final concentration 5 m*M*), we were able to block cytokinesis in the injected cell but not the uninjected sister cells. This result is consistent with the notion that calcium signaling is involved in cytokinesis.

We are currently investigating the source of Ca^{++} ions that give rise to the cytokinesis signal. We have examined the effects of a number of pharmacological reagents that selectively inhibit various Ca receptors or channels. Our preliminary results indicated that the cytokinesis-associated elevation of $[\mathrm{Ca}^{++}]_i$ comes mainly from internal stores effected by an inositol-trisphosphate pathway (5).

We thank P. Xie for her technical assistance. This work was partially supported by grants from NSF, BRI, and RGC.

Literature Cited

1. **Hepler, P. K. 1992.** *Int. Rev. Cytol.* **138:** 239–268.
2. **Satterwhite, L. L., and T. D. Pollard. 1992.** *Curr. Opinion Cell Biol.* **4:** 43–52.
3. **Fluck, R. A., A. L. Miller, and L. F. Jaffe. 1991.** *J. Cell Biol.* **115:** 1259–1265.
4. **Miller, A. L., R. A. Fluck, J. A. McLaughlin, and L. F. Jaffe. 1993.** *J. Cell Sci.* **106:** 523–534.
5. **Berridge, M. 1993.** *Nature* **361:** 315–325.

Reference: *Biol. Bull.* **187:** 235–236. (October, 1994)

Video Light Microscopic Imaging of the Calcium Signal that Initiates Nuclear Envelope Breakdown in Sand Dollar (*Echinaracnius parma*) Cells

Robert B. Silver (Cornell University and Marine Biological Laboratory)

The details of the cellular mechanisms that initiate mitosis are still unresolved. Current thinking holds that transient elevations in the concentration of intracellular free calcium ion (Ca^{2+}_i, controlled by Ca^{2+}-regulatory endomembranes closely associated with the nucleus and later with the mitotic apparatus (MA), trigger specific mitotic events [*i.e.*, nuclear envelope breakdown (NEB), onset of anaphase (AO) and cytokinesis (*e.g.*, 1–4)]. This paper presents the first observation of a Ca^{2+}_i increase correlated with a specific structural event (NEB) during the cell cycle.

My working hypothesis is that Ca^{2+}-containing microdomains (5, 6) occur within the MA and the mitotic cell (2, 12–16), and that the Ca^{2+}_i concentration in these microdomains is regulated locally by the very ATP-dependent Ca^{2+} sequestering endomembranes that delimit these compartments. Moreover, the local regulation results in transient changes in Ca^{2+}_i concentration; discrete amounts of Ca^{2+} are released to the cytoplasm to effect a transient elevation of Ca^{2+}_i within a defined region of space ($< 1\ \mu\mathrm{m}^3$) and time (100 ms or less). This limited release of Ca^{2+}_i is called a quantum emission domain, or QED (5). A Ca^{2+}_i-QED is the smallest component of a complex signal: *i.e.*, a distinct spatial and temporal pattern of Ca^{2+}_i released to one or more cytoplasmic binding sites that initiates a particular Ca^{2+}-dependent process.

Transient elevations in Ca^{2+}_i concentration during the cell cycle were detected with a photon-counting video camera as bright observable blobs (BOBs; defined in 6) in second cleavage sand dollar (*Echinaracnius parma*) blastomeres cultured in Ca^{2+}-free Jamarin artificial seawater (Jamarin Laboratory, Inc., Osaka, Japan; 12, 13). The photon-counting camera used in this study was a dual microchannel plate intensified saticon device (C-2400-20 from Hamamatsu). When incident photons strike the faceplate of the intensifier, a cloud of electrons proportional to that number of photons is produced in the microchannels and presented to the faceplate of the saticon camera. The blastomeres were injected with 10 pl doses of semisynthetic aequorin (16) shortly after the first cytokinesis following fertilization, and observed by multispectral video microscopy (5–11) in the dark at 14°C. Two-cell embryos provide one experimental and one (sister) control cell; their activities would otherwise be identical. Moreover, because blastomeres in the second cell cycle are free of the effects of fertilization activation, they more closely resemble subsequent cell cycles. Sand dollar embryos are well suited to these experiments: they are nearly transparent, and they undergo the early cell cycles with near-perfect synchrony.

Large populations of BOBs arose from the perinuclear region 6 min before NEB (40-s duration). The resulting patterns were observed from one cell cycle to the next in a single cell, from cell to cell, and from batch to batch of eggs. As the cell is the only location of aequorin, and thus Ca^{2+}-dependent luminescence, the origin of the Ca^{2+} photons is intracellular; earlier work from this laboratory demonstrated that the pre-NEB Ca^{2+} signal originates from endomembranes, presumably portions of the endoplasmic reticulum (2, 13, 14). The timing and duration of

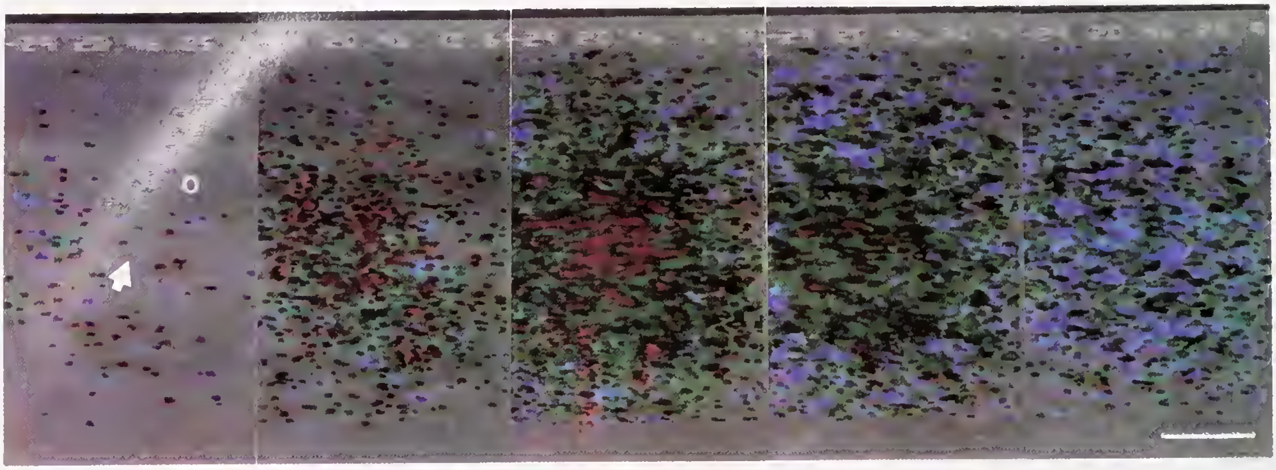

Figure 1. *A montage of the BOB pattern of the pre-NEB Ca^{2+}_i signal overlayed onto a differential interference contrast image of an aequorin-loaded dividing sand dollar* (Echinaracnius parma) *blastomere. Each panel shows one 33-ms video frame captured at 5-s intervals. With the tools used here, relative BOB age is depicted with pseudocolor, red for recent BOBs, progressing over 10 s to blue for older BOBs, shifting one color value per second, i.e., red to red-orange to orange . . . to blue. The large circle (○) is an oil droplet injected with the aequorin sensitive to Ca^{2+}_i at levels of 10^{-8} molar, the nucleus is indicated by the white arrow. Note the rapid onset and disappearance of the Ca^{2+}_i signal; it originates at the perinuclear region (arrow). Note also the high degree of symmetry of the signal and the absence of a spatial arc to this signal. The clock time of each frame is displayed at the top of each panel. The bar marker indicates 20 μm.*

these transient elevations in Ca^{2+}_i are consistent with the period of the cell's sensitivity to increased Ca^{2+} buffering; that is, when buffering is applied during this same time period it inhibits NEB (14, 15).

Analysis of the spatial and temporal pattern of the pre-NEB BOBs demonstrates that the Ca^{2+}_i signal arises from, and is roughly symmetric around, the nucleus. No lateral arc-like spatial translation of the BOB origins was observed; *i.e.*, there was no "wave" of the sort that often accompanies fertilization. Inhibition of the endoplasmic reticulum Ca^{2+}-pump with an affinity-purified anti-Ca^{2+}-pump IgG (13) rapidly elevated the Ca^{2+}_i concentration.

The discovery and resolution of discrete, rapid transient increases of Ca^{2+}_i within the overall Ca^{2+}_i elevation associated with NEB are suggestive of regulated, quantized pulses originating from endomembrane stores. Ca^{2+} buffering by the ATP-dependent endomembrane Ca^{2+}-pump is a necessary and highly efficient part of this regulatory system. Accuracy and precision in signaling is, of course, critical to the regulation of mitosis. This is a first step in deciphering the Ca^{2+}_i signals associated with the control of the Ca^{2+}-dependent steps of NEB, and supports the hypothesis presented above. The initial computational analyses of these BOB patterns are presented in an accompanying paper (6).

Grant support by NSF to R.B.S. is gratefully acknowledged. The author is also grateful to the reviewers and editor for their many helpful and well-considered suggestions in the final preparation of this manuscript.

Literature Cited

1. **Harris, P. 1971.** *Exp. Cell Res.* **94:** 409–425.
2. **Silver, R. B., R. D. Cole, and W. Z. Cande. 1980.** *Cell* **19:** 505–516.
3. **Kiehart, D. P. 1981.** *J. Cell Biol.* **88:** 604–617.
4. **Wolniak, S. M., P. K. Hepler, and W. T. Jackson. 1983.** *J. Cell. Biol.* **96:** 598–605.
5. **Llinás, R., M. Sugimori, and R. B. Silver. 1992.** *Science* **256:** 677–679.
6. **Silver, R. B., and S. Inoué. 1987.** *Biol. Bull.* **173:** 420–421.
7. **Silver, R. B., O. Shimomura, and S. Inoué. 1989a.** *J. Cell Biol.* **109:** 90a.
8. **Silver, R. B., O. Shimomura, and S. Inoué. 1989b.** *J. Cell Biol.* **109:** 90a.
9. **Llinás, R., M. Sugimori, and R. B. Silver. 1991.** *Biol. Bull.* **181:** 1–4.
10. **Llinás, R., M. Sugimori, and R. B. Silver. 1994.** Pp. 133–137 in *Molec. Cellular Mech. of Neurotransmitter Release*, L. Stjärne, P. Greengard, S. Grillner, J. Hökfelt and D. Ottoson, eds. Raven Press, New York.
11. **Silver, R. B. 1985.** *Biol. Bull.* **167:** 532.
12. **Silver, R. B. 1986.** *PNAS* **83:** 4302–4306.
13. **Silver, R. B. 1989.** *Dev. Biol.* **131:** 11–26.
14. **Silver, R. B. 1990.** *Ann. N. Y. Acad. Sci.* **582:** 207–221.
15. **Shimomura, O., S. Inouye, B. Musicki, and Y. Kishi. 1990.** *Biochem. J.* **270:** 309–322.
16. **Silver, R. B. 1986b.** *J. Cell Biol.* **103:** 140a.
17. **Silver, R. B., A. P. Reeves, M. Whitman, and B. Kelley. 1994.** *Biol. Bull.* **187:** 237–238.

Reference: *Biol. Bull.* **187:** 237–238. (October, 1994)

Analysis of Spatial and Temporal Patterns in the Ca^{2+} Signal that Signals Nuclear Envelope Breakdown in Sand Dollar (*Echinaracnius parma*) Cells

Robert B. Silver (Cornell University and Marine Biological Laboratory),
Anthony P. Reeves, Marcia Whitman, and Brian Kelley

Mitosis is a sequence of cytological events (1–3) resulting from interactions among many biochemical pathways operating either in series or parallel under the coordinated control of a cell cycle clock (5–7). Intracellular free Ca^{2+} (Ca^{2+}_i) is believed to play a central role in the regulation and timing of mitosis and in the assembly and functioning of the mitotic apparatus (MA), that control being mediated by endomembranes (4, 5, 8).

Our working hypothesis holds that local regulation of Ca^{2+}_i-dependent processes and changes in Ca^{2+}_i concentration therefore occur within microdomains that include or are bounded by ATP-dependent Ca^{2+}-sequestering membranes within the MA and mitotic cell (5–7, 9–11). A *microdomain* is an autonomous compartment of minimal spatio-temporal volume within which a signaled process can occur. A quantum emission domain (QED) is a quantal signal element within spatio-temporal and concentration space; the concept of a QED applied to Ca^{2+} signaling at the synaptic pre-terminal (12, 13) and later for relatively thick (*i.e.*, mitotic) cells (11). Within the model, and as observed in aequorin-loaded cells (9–11), transient changes in Ca^{2+}_i are expressed as QEDs of Ca^{2+}_i (Ca^{2+}_i-QEDs) from intracellular stores. To understand in detail the mechanism by which Ca^{2+} activates pathways essential for mitosis (*e.g.*, NEB, anaphase onset), we must identify the spatial and temporal patterns of Ca^{2+}_i-QEDs in mitotic cells (5, 6, 9, 10).

Ca^{2+}_i-QEDs were detected by multispectral video microscopy during the cell cycle in second cleavage sand dollar (*Echinaracnius parma*) blastomeres, that had been injected with semi-synthetic aequorin (14) shortly after the first post-fertilization cytokinesis. Two-cell embryos yield one experimental and one (sister) control cell whose activities would otherwise be identical (*e.g.*, 4, 5). Observations were performed in the dark to preclude stray light effects, and in a room maintained between 12° and 14°C for the health of the sand dollar embryos. Images were recorded on videotape. Analog video frames were digitized and prepared for subsequent computational analysis. The typical data set consisted of an isovolume of 640 pixels × 480 pixels × 800 frames, in which a pixel corresponded to 0.5 micrometer on a side, and each video frame corresponds to 33 ms. Observed events were classified into two categories based upon noise analysis: shot noise (events that lasted for one 33-ms video frame or one 16.7-ms video field), and bright observable blobs (BOBs) (events lasting two or more 33-ms video frames). BOBs typically lasted 67 to 100 ms (11). Each BOB in a data set was considered to be a potential point of origin, and near-neighbors were defined as BOBs that could be linked to the origin BOB or a preceding BOB by a set of parameters defining its position in space, its velocity (in pixel/frame), and its acceleration. Linkage was sought for a minimum of four BOBs along a trajectory defined by the set of parameters. Parameters were chosen to identify matches among BOBs along straight lines, "kinked" lines, and curves in which velocities ranged from 0 to 1 pixel per frame. Each of four or more BOBs along a trajectory was considered to be a Ca^{2+}_i-QED. Data and resultant analytical summaries can be displayed in tabular and graphical formats. Calibration of the aequorin signals was performed as previously described (12).

Ca^{2+}-dependent luminescence, seen as BOBs, arose from throughout the volume of the spherical (70 μm diameter) second cleavage cycle sand dollar blastomeres. Some observed events appear to originate outside the cell; in fact they are intracellular and are scattered and refracted by the cell and chamber. Analyses show that light subject to intracellular scattering, as well as events seen outside the cell due to 4π radiation from the cell acting as a self-luminous body, are random and unlikely to appear at a given site with any temporal regularity; such events did not meet the criteria for BOBs and were omitted from these analyses. Ca^{2+}_i-QEDs originating outside the plane of focus contributed little to the results presented here. Six minutes prior to nuclear envelope breakdown (NEB) a Ca^{2+}_i signal arises from the perinuclear region. This pre-NEB signal lasts for 40 s, consistent with earlier reports from this laboratory (*e.g.*, 5, 6, 9–11).

Computational analysis of pre-NEB Ca^{2+}_i-QEDs demonstrated a wide array of spatial and temporal attributes: (1) Ca^{2+}_i-QEDs occur within microdomains of 3 to 10 micrometers along a spatial axis and 900 to 3000 ms along the temporal axis (*e.g.*, 11, 12); (2) BOBs and Ca^{2+}_i-QEDs last between 16.7 and 100 ms, and the minimum lifetime may be shorter; (3) matches occurred among 40 to 45% of the BOB within data sets of 1000 or more BOBs; (4) the ratio of matches among observed data sets *versus* those among random data sets exceeds 75:1, for observed data sets of 400 to 1100 BOBs in an isovolume; (5) when acceleration among adjacent, co-linear Ca^{2+}_i-QEDs is factored into the analysis, no matches are seen with random data sets; (6) Fourier analyses of pre-NEB imagery show that different regions produce Ca^{2+}_i-QEDs with distinguishable power spectra (*i.e.*, different patterns of Ca^{2+}_i-QEDs); (7) near-neighbor analyses demonstrate that individual sets of Ca^{2+}_i-QEDs occur along linear tracks extending less than 15 micrometers; (8) the observed velocity (micrometers/s, *i.e.*, 0.5 micrometer pixels/33-ms frame) of individual Ca^{2+}_i-QEDs along linear tracks exceeds those predicted from random data sets; (9) the minimum refractory period for a given point in the cell emitting a Ca^{2+}_i-QED was forty 30-Hz video frames; (10) temporal filtration of video imagery to show only those Ca^{2+}_i-QEDs occurring within the above noted repeat period are principally located in the perinuclear region and along the linear tracks which criss-cross the perinuclear region; (11) in no case were spatial arcs of Ca^{2+}_i-QEDs found in either observed or random data sets. From these observations we conclude that (1) Ca^{2+}_i-QEDs are real, discrete events; (2) Ca^{2+}_i-QEDs occur within microdomains; (3) Ca^{2+}_i-QEDs associated with pre-NEB signaling occur principally along linear tracks whose trajectories cross the perinuclear region at various angles relative to one another; (4) individual $Ca^{2+}{}_i$-QEDs are separated in space and time by distances that correspond to velocities of 15 micrometers s^{-1}; and (5) no "waves" of $Ca^{2+}{}_i$-QEDs are components of the pre-NEB $Ca^{2+}{}_i$ signal. Given the regularity of observed spatial and temporal frequencies of BOBs along established trajectories, we suggest that precise regulation of the amplitude and frequency of $Ca^{2+}{}_i$-QEDs, and thus $[Ca^{2+}{}_i]$ is a necessary feature of the cell's regulation of mitosis.

Grant support by NSF to R.B.S. is gratefully acknowledged. The authors are also grateful to the reviewers and editor for their many helpful and well-considered suggestions in the final preparation of this manuscript.

Literature Cited

1. **Mazia, D. 1961.** Pp. 74–412 in *The Cell,* J. Brachet and A. E. Mirsky, eds. Academic Press, New York.
2. **Heilbrunn, L. V. 1956.** *The Dynamics of Living Cytoplasm.* Academic Press, New York.
3. **Inoué, S. 1981.** *J. Cell Biol.* **91:** 131s–147s.
4. **Silver, R. B. 1986a.** *PNAS* **83:** 4302–4306.
5. **Silver, R. B. 1989.** *Dev. Biol.* **131:** 11–26.
6. **Silver, R. B. 1990.** *Ann. N. Y. Acad. Sci.* **582:** 207–221.
7. **Silver, R. B., *et al.* 1994.** *Biol. Bull.* **187:** 242–244.
8. **Kiehart, D. P. 1981.** *J. Cell Biol.* **88:** 604–617.
9. **Silver, R. B., and S. Inoué. 1987.** *Biol. Bull.* **173:** 420–421.
10. **Silver, R. B., O. Shimomura, and S. Inoué. 1989.** *J. Cell Biol.* **109:** 90a.
11. **Silver, R. B. 1994.** *Biol. Bull.* **187:** 235–236.
12. **Llinás, R., M. Sugimori, and R. B. Silver. 1992.** *Science* **256:** 677–679.
13. **Llinás, R., M. Sugimori, and R. B. Silver. 1994.** Pp. 133–137 in *Molec. Cellular Mech. of Neurotransmitter Release,* L. Stjärne, Greengard, P., Grillner, S., Hökfelt, J., and Ottoson, D., eds. Raven Press, New York.
14. **Shimomura, O., S. Inouye, B. Musicki, and Y. Kishi. 1990.** *Biochem. J.* **270:** 309–322.

Reference: *Biol. Bull.* **187:** 238–239. (October, 1994)

Inhibitory Cell-Cell Interactions Control Development in the Embryos of *Cerebratulus lacteus*

Jonathan Q. Henry (University of Illinois, Department of Cell and Structural Biology, Urbana, IL 61801) and Mark Q. Martindale

Previous work by Hörstadius (1, 2) supported the contention that the cells of the early embryos of the nemertean *Cerebratulus lacteus* possess the ability to regulate their development when they are separated at the two- and four-cell stages. Hörstadius (1) claimed that all of the blastomeres isolated from the two- and four-celled embryo were able to form both a gut and an apical organ. Recent cell lineage studies reveal that all blastomeres of the four-cell embryo contribute equally to the formation of the gut and the apical tuft (3, and Henry and Martindale, in prep); thus the differentiation of these two cell fates by the isolated four-celled stage blastomeres must represent an inherent feature of their development. Hörstadius (1), therefore, did not actually demonstrate that these four cells are capable of displaying cellular regulation when raised in isolation. Here the term "regulation" is being used to denote the ability of isolated cells to generate missing structures that they would not normally produce in the intact embryo. Although pilidia larvae are fairly simple in their organization, they possess a number of other differentiated cell types, including an elaborate system of subepidermal muscle fibers. We have shown that only two of the four cells in the four-celled embryo (the left and right ventral blastomeres, LV and RV) contribute to the formation of the larval muscle fibers, while the other cells (left and right dorsal blastomeres, LD and RD) do not (Henry and Martindale, in prep). The basic lineage of these cells is diagrammed in Figure 1a, and the normal distribution of phallacidin-labeled larval muscle fibers is shown in Figure 1b.

To test whether embryonic cells of *C. lacteus* can regulate, we isolated the blastomeres from four-celled embryos and assayed for the development of larval muscle fibers, using Bodipy-phallacidin, a fluorescent marker for filamentous actin (Molecular Probes, Eugene, OR). Since one cannot distinguish between the identities of the four blastomeres at the time they are separated, the blastomeres were cultured as sets, and only cases in which all four of the isolated cells survived were scored. Twelve complete sets of isolated four-cell-stage blastomeres (48 quarter embryos) were successfully raised in separate culture wells in filtered seawater (FSW) for three days at 18–19°C. The complementary sets of "quarter larvae" were fixed in 10% formalin overnight at 4°C, washed in FSW, and stained with phallacidin.

In five sets, all four members formed well-differentiated muscle fibers. In another six sets, three of the four larvae contained well-differentiated muscle fiber cells, but the fourth member did not. In the twelfth set, only two of the quarter larvae formed muscle fiber cells. Without additional cell-specific markers, it is not possible to determine the exact dorsal or ventral fate of the few isolated cells that did not form muscle fibers. Of the 48 individual quarter larvae examined, all formed a gut and only 4 did not form an apical organ and tuft. The typical form of development displayed by the quarter larvae is shown in Figure 1c, where differentiated muscle fiber cells are clearly seen.

These results indicate that the two dorsal blastomeres (LD and RD), which normally do not contribute to the formation of muscle fibers, are able to form them when separated from the ventral cells (LV and RV). This finding indicates that the progeny of the ventral blastomeres normally inhibit the formation of larval muscle cells by descendants of the dorsal blastomeres in the intact embryo. Mounting evidence suggests that such inhibitory interactions control development in other organisms as well (4).

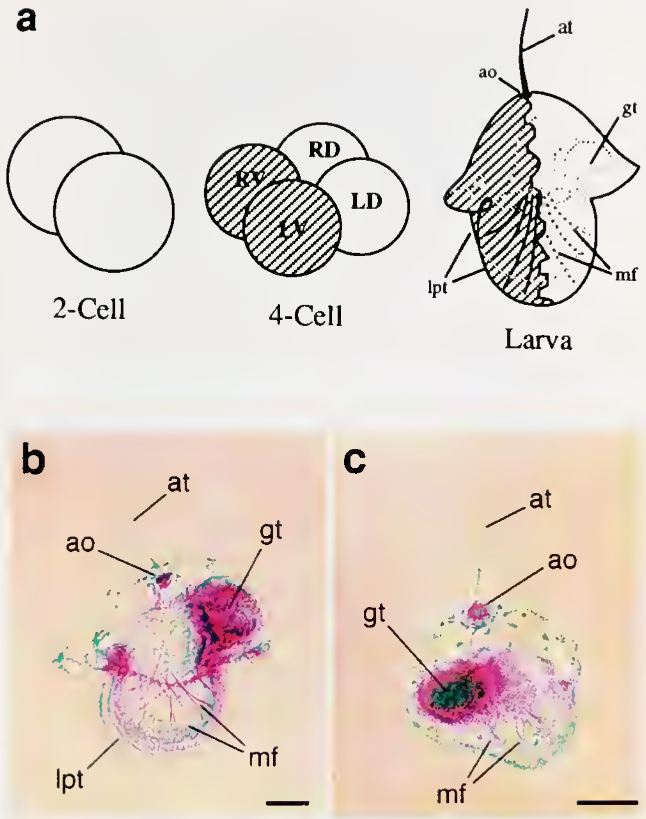

Figure 1. *(a) Diagram illustrating the basic early cell cleavage pattern and ultimate fates of the two ventral cells LV and RV (shaded) in forming the pilidium larva of* Cerebratulus lacteus. *The larva is illustrated from the left side. (LV and RV) left and right ventral blastomeres, (LD and RD) left and right dorsal blastomeres. LV and RD contribute to the formation of the ventral half of the larva and also generate the muscle fiber cells. (b) Fluorescence micrograph showing the distribution of red fluorescent Bodipy-phallacidin in the 3-day-old larva of* C. lacteus *(left lateral view). Bodipy-phallacidin label is associated with the apical organ, gut and the muscle fibers. (c) Fluorescence micrograph showing the distribution of red fluorescent Bodipy-phallacidin in a typical 3-day-old "quarter" larva of* C. lacteus *developed from one cell isolated from a four-celled embryo. Bodipy-phallacidin labeled muscle fibers are present. (ao) apical organ, (at) apical tuft, (lpt) lappet, (gt) gut, (mf) muscle fibers. Scale bar is approximately 50 μm.*

The authors thank the generous community of the Marine Biological Laboratory. J.Q.H. was supported as an MBL Associates' Fellow. M.Q.M. was supported by NSF and the Illinois chapter of the A.C.S.

Literature Cited

1. **Hörstadius, S. 1937.** *Biol. Bull.* **73:** 317–342.
2. **Hörstadius, S. 1973.** Pp. 164–174 in *Experimental Embryology of Marine and Fresh-water Invertebrates.* North Holland, Amsterdam.
3. **Henry, J. Q., and M. Q. Martindale. 1994.** *Dev. Genetics* **15:** 64–78.
4. **Henry, J. J., S. Amemiya, G. A. Wray, and R. A. Raff. 1989.** *Dev. Biol.* **136:** 140–153.

Reference: *Biol. Bull.* **187:** 239–240. (October, 1994)

Oscillations in Free $[Ca^{2+}]_i$ During Early Cell Division Cycles in *Xenopus laevis* Embryos

Brent Miller (Marine Biological Laboratory), Amrit Chauhan, Lionel F. Jaffe, and Andrew L. Miller

Two recent reports, both utilizing ultrasensitive recombinant aequorins (1), clearly demonstrate $[Ca^{2+}]_i$ oscillations in developing *Xenopus* embryos. Such oscillations also occur in embryos bathed in calcium-free medium, in artificially activated eggs, and in cleavage-blocked embryos. Taken together, these results suggest that such oscillations are associated with an autonomous, periodic, cytoplasmic activity that controls cell-cycle events. In the first of these reports, however, aequorin-generated light was collected only from the vegetal hemisphere of the developing embryo (2), whereas in the other, light was collected only from the animal hemisphere (3). This difference reflected the orientation of the photon-counting device in the two laboratories; moreover, because the *Xenopus* egg is opaque, these recordings could not represent the light output from the entire surface of the egg. Here we extend these findings by using a mirror device (Fig. 1A) to collect light from more of the egg surface. Kubota *et al.* (2), collecting light emission from the vegetal hemisphere (where there are no pigment granules), used both wild-type and albino embryos. Whereas Keating *et al.* (3), collecting light from the animal hemisphere, used only albino embryos, thus avoiding potential differences in light output resulting from pigment granule movement. As we collected light from both the vegetal and animal hemispheres via our mirror device, we also used only albino embryos.

By methods previously described, eggs were collected from frogs (3), and injected with about 10 nl of *f*-aequorin (4). Injected eggs were then immediately loaded into the device illustrated in Figure 1A.

The results illustrated in Figure 1B (a representative example; $n = 12$), confirm the earlier findings from the animal pole (3) and the vegetal pole (2). Thus, similar data from all three studies were recorded from albino eggs developing in a medium containing calcium. In our case the medium was artificial pond water (APW) made up as follows (in m*M*): 41 NaCl, 0.13 KCl, 0.069 NaH_2PO_4, 0.08 NaOH, 0.60 HEPES, 0.037 $CaCl_2$, and 0.013 $MgCl_2$. However, as Figure 1C (a representative example;

n = 5) illustrates, additional calcium spikes, superimposed on the overall oscillations, were consistently detected while eggs were developing in calcium-free medium (APW minus $CaCl_2$ + 1 m*M* EGTA). Recording from the animal hemisphere alone, Keating *et al.* (2) did not detect such transients from albinos developing in calcium-free medium. Kubota *et al.* (1) did not report any data from the vegetal hemisphere under these particular (*i.e.*, calcium-free) conditions. We suggest, therefore, that such superimposed spikes seen through the first few cell cycles represent early calcium-related developmental events specific to the vegetal hemisphere. The spatial nature and developmental significance of these calcium transients are currently under investigation.

We wish to thank Osamu Shimomura for the recombinant aequorin, and Andrew Murray and Kenneth Robinson for additional frogs. This work was supported by NSF grant BIR9211855 to A.L.M. and L.F.J., and an R.E.U. supplemental award to BIR9211855 to support B.J.M. and A.C.

Literature Cited

1. **Shimomura, O., S. Inouye, B. Musicki, and Y. Kishi. 1990.** *Biochem. J.* **270:** 309–312.
2. **Kubota, H. Y., Y. Yoshimoto, and Y. Hiramoto. 1993.** *Dev. Biol.* **160:** 512–518.
3. **Keating, T. J., J. R. Cork, and K. R. Robinson. 1994.** *J. Cell Sci.* (in press).
4. **Miller, A. L., E. Karplus, and L. F. Jaffe. 1994.** *Methods in Cell Biol.* **40:** 305–338.

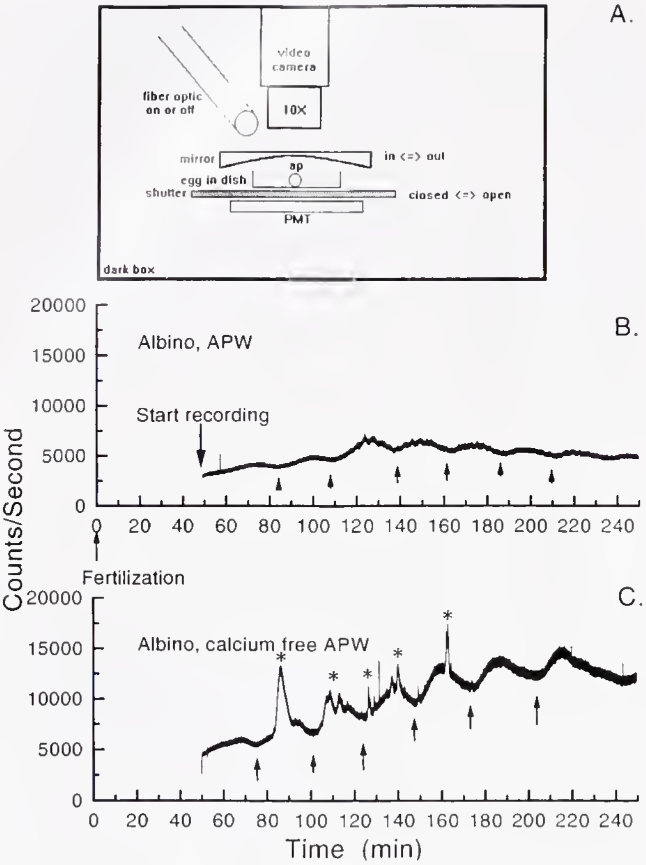

Figure 1. *(A) Schematic representation of the device used to collect the data (ap = animal pole of the egg). (B) Uninterrupted recording (i.e., no video images taken) of aequorin-generated light emission from an albino egg bathed in APW containing calcium. In cases where photon collection was interrupted and video images were taken in order to establish a temporal correlation between calcium oscillations and cleavage, it was clear that furrows appeared on the animal hemisphere at the bottom of the calcium oscillation (data not shown). The small arrowheads on both (B) and (C) indicate when furrows would be expected to appear on the animal hemispheres of the two embryos generating these traces. (C) Uninterrupted recording of an albino egg bathed in calcium-free APW. Asterisks mark the unexplained vegetal hemisphere calcium transients.*

Reference: *Biol. Bull.* **187:** 240–241. (October, 1994)

Mitosis, Cleavage, and Development of Highly Compressed Sea Urchin (*Lytechinus variegatus*) Zygotes

Fabrice Roegiers, Phong Tran, and Shinya Inoué (Marine Biological Laboratory)

The position of the mitotic spindle determines the cleavage plane of the cell undergoing mitosis. This in turn defines whether the cell will cleave equally or unequally. In the sea urchin, spindle position and orientation are important for formation of the micromeres, which occurs when the vegetal nucleus or spindle migrates to the vegetal cortex of the lower blastomeres at the eight-cell stage. Earlier studies have shown that flattening of the embryos at the two- and four-cell stages perturbs micromere formation in most embryos (1, 2). It is thought that the spindle is unable to move freely in flattened blastomeres and thus cannot reach its target site at the vegetal cortex. In the few cases where micromeres did form, this target zone appeared to lie in a plane perpendicular to the compression. In our study, we observed embryos compressed in an agarose sandwich with polarized light microscopy to visualize both spindle formation and orientation, and cytokinesis. By coupling this methodology to time-lapse video microscopy we were able to observe cleavage over long periods.

Eggs of *Lytechinus variegatus* were fertilized in 1 m*M* aminotriazole to prevent hardening of the fertilization envelope and were allowed to reach the two-cell stage. The fertilization envelope was then removed by filtration through a 74-μm Nytex filter and the embryos were placed in 70%/30% Ca^{2+}-free ASW/ASW (*a*rtificial *s*ea*w*ater). The embryos were then mechanically

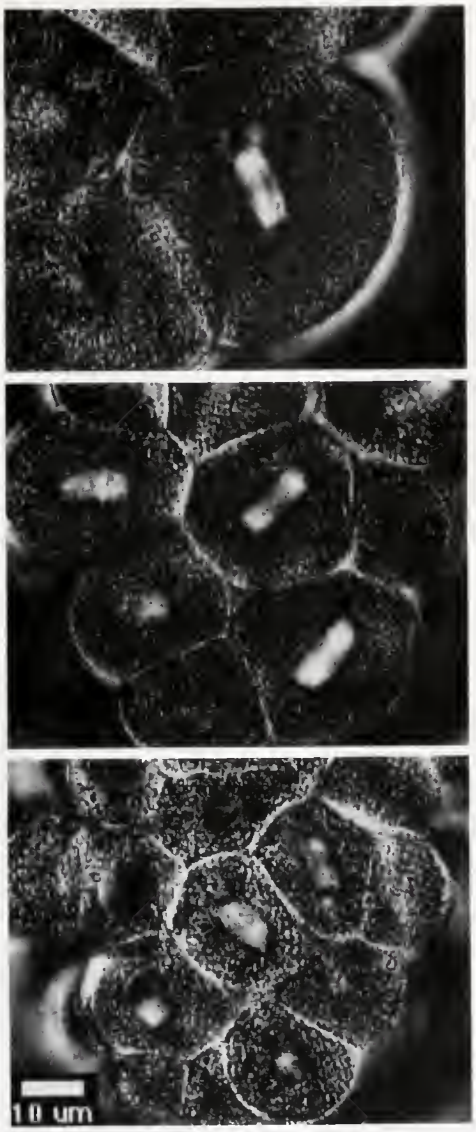

Figure 1. *Sequential computed images of a compressed* Lytechinus variegatus *zygote at 8-, 16-, and 32-cell stages. All spindles in side view, regardless of orientation, show up as white areas of high birefringence The metaphase plate coincides with the plane of cytokinesis. These images were generated using Oldenbourg's new pol-scope (5). Four images were taken at different compensator angles; from these a computed image with a pixel brightness proportional to the sample birefringence regardless of specimen orientation was rapidly and automatically calculated*

compressed between two thin sheets of agarose (3) or between a sheet of agarose and a coverslip. Compression down to 20 μm was achieved. These compressed embryos were then mounted in a micro-drop chamber for observation with either a polarized light microscope (4) or a novel pol-scope (5). Development was followed by time-lapse video. With the new pol-scope we were able to visualize spindles in any orientation in the plane of focus. This allowed us to predict the cleavage pattern of the embryos more precisely (Fig. 1).

In embryos that were compressed between two sheets of agarose, we observed that highly flattened embryos continued to cleave as a monolayer. Overnight these embryos reached several thousand cells and after 15 h of development, the cells had spread out over several fields of view. In one such embryo, we did observe the formation of micromeres at the 16- and 32-cell stages. These embryos showed no evidence of differentiated structures (ciliated cells, spicules, etc.).

Embryos compressed between coverslip and agarose sheet did not remain highly compressed. These embryos began forming a second layer of cells at the 5th cleavage (32 cell stage). In these embryos, epithelial differentiation, ciliogenesis, and perhaps even primordial spicule formation were observed.

These results show that highly compressed embryos can continue to divide despite a forced repositioning of the spindle. We have reason to believe that the commonly observed inability of eggs to proceed beyond one or two divisions when sandwiched between slide and coverslip is due to depletion of the oxygen supply; it is clearly not due to deformation from compression. In this connection, Ziegler has managed to grow compressed eggs to cleave up to the 64-cell stage by perfusing the slide constantly with fresh seawater (2).

We plan to use this technique, in combination with 4-D polarized light microscopy, to observe the behavior of spindles in compressed blastomeres in order to study the precise behavior of the spindle preceding a critical unequal cleavage and to explore the localized distribution of the vegetal pole determinant.

We would like to thank Ted Inoué for his assistance and advice, and R. Oldenbourg for the use of the new pol-scope. We would also like to thank Universal Imaging Corp. for a Physiology post-course fellowship to F.R. This work was supported by grants R37GM31617-13 from NIH and MCB-8908169 from NSF to S.I.

Literature Cited

1. **Dan, K., 1987.** *Dev. Growth Diff.* **29**(5): 503–515.
2. **Morgan, T. H. 1927.** *Experimental Embryology.* Columbia University Press. Pp. 468–472.
3. **Fukui, Y., S. Yumura, T. Yumura, and H. Mori. 1986.** *Methods Enzymol.* **134**: 573–580.
4. **Inoué, S. 1986.** *Video Microscopy.* Plenum Press. Pp. 493–497.
5. **Mei, G., and R. Oldenbourg. 1994.** *Proceedings of the Conference on Polarization Analysis and Measurement II, SPIE International Symposium* (in press).

Reference: *Biol. Bull.* **187**: 242–244. (October, 1994)

Leukotriene B_4, an Arachidonic Acid Metabolite, Regulates Intracellular Free Calcium Release in Eggs and Mitotic Cells of the Sand Dollar *(Echinaracnius parma)*

Robert B. Silver (Cornell University and Marine Biological Laboratory), Jeb B. Oblak, Gwendolyn S. Jeun, Jenny J. Sung, and Timothy C. Dutta

Regulation of intracellular free calcium ($Ca^{2+}{}_i$ concentration is a central feature in the control of Ca^{2+}-dependent cellular processes. This regulation, which sometimes occurs within microdomains, involves controlled movement across endomembranes [*e.g.*, nuclear envelope breakdown (NEB) (1–4); the plasma membrane (*e.g.*, synaptic transmission [5–7]); or a combination of both (8–10)]. It also involves ATP-dependent Ca^{2+} pumps and Ca^{2+} channels. Although similar in general function (*i.e.*, control of the passage of Ca^{2+} across a lipid membrane), such controls on the plasma and endomembranes differ in their specific mechanics. Endomembrane Ca^{2+} pumps differ from plasma membrane Ca^{2+} pumps in their primary structures, configurations, modifications, and kinetic properties (11, 12). Likewise, the Ca^{2+} channels of endomembranes and plasma membranes, upon which agonists act to evoke transient localized elevations of $Ca^{2+}{}_i$ ($Ca^{2+}{}_i$-QEDs; 5–7, 14, 37), appear to differ in characteristic fashions.

To date, two compounds are known as agonists that release Ca^{2+} from endomembrane stores: 1,4,5-inositol trisphosphate (1,4,5-IP_3) and cyclic ADP-ribose (8–10). Typically, processes that utilize these two agonists rely upon initial stimulation or activation at the plasma membrane.

NEB seems to be preceded by a Ca^{2+} transient derived from endomembrane stores rather than by external stimuli mediated across the plasma membrane (1–4, 13–16). Thus we reasoned that another agonist, generated locally and present for a very brief period of time, should be responsible for evoking $Ca^{2+}{}_i$ transients and thus triggering NEB or other processes signaled, initiated, coordinated, or controlled by intracellularly derived $Ca^{2+}{}_i$-QEDs. Arachidonic acid (AA) derivatives play a role in a wide variety of cellular processes (17, 18), including vascular contraction cycles (19), neutrophil activation (20–22), long-term potentiation and S-K^+ channels in hippocampal neurons (23, 24), activation of DNA synthesis (25), aggregation of marine sponge cells (26), and activation of tumor necrosis factor (27). Therefore we sought to determine whether AA metabolites generated at the endomembranes could serve as a suitable agonist in eggs and mitotic cells.

The potential role of AA or major AA-derived branch-point metabolites as agonists for release of Ca^{2+} from endomembrane stores of eggs and mitotic cells of sand dollar (*Echinaracnius parma*) was tested directly *in vitro* and *in vivo*. *In vitro* tests were performed on endomembrane fractions isolated from eggs or mitotic cells. Individual endomembrane fractions, resolved on sucrose gradients (28–30), were tested for their ability to achieve ATP-dependent Ca^{2+} uptake; we used a spectrophotometric assay for Ca^{2+} uptake and release by endomembrane fractions, with the metallochromic dye antipyrylazo III as the Ca^{2+} indicator (29, 30). Compounds were tested at final cuvette concentrations ranging from 10^{-9} to 10^{-5} *M* in log/2 steps. Under the conditions used here, the minimal effective concentration *in vitro* for LTB_4 was 10^{-7} *M*. Individual experiments were repeated between four and six times, with replicates of triplicate assays performed on each fraction tested.

Results from a typical experiment are presented in Table 1. Of the four endomembrane fractions resolved on sucrose density step gradients, only that fraction corresponding to heavy endoplasmic reticulum exhibited ATP-dependent Ca^{2+}-uptake activity (this work and 28–30), and also showed agonist-dependent Ca^{2+} release activity when challenged with 1,4,5-IP_3. Endomembranes that were loaded *in vivo* and that retained their Ca^{2+} were exposed to a pulse of candidate agonist at final cuvette concentrations of 10^{-5} to 10^{-8} molar, and the release of Ca^{2+} from those vesicles and reticula was assayed as a function of increase in optical absorbance (A_{710}–A_{790}) (29, 30). Among the tested compounds that elicited no release of Ca^{2+} from isolated endomembrane stores *in vitro* was AA, prostaglandins (G_2, H_2, E_2, $F_{2\alpha}$), thromboxane A_2, leukotriene A_4 (LTA_4), leukotriene C_4, leukotriene A_5, leukotriene C_5, leukotriene B_5, and oxidized leukotriene B_4 (LTB_4). Ca^{2+} release from endomembranes was elicited *in vitro* by LTB_4.

To test the efficacy of AA metabolites as agonists of Ca^{2+} release from endomembrane stores *in vivo*, candidate agonists were microinjected into aequorin-loaded (31) sand dollar (*Echinaracnius parma*) eggs or mitotic blastomeres, and the emission of Ca^{2+}-dependent photon signals was followed as previously described (5–7, 15, 16). Compounds were tested at tip concentration ranges between 10^{-9} and 10^{-3} *M*, with a final equilibrium dilution factor estimated at about 10^4. Aequorin preparations were generously provided by Dr. O. Shimomura (Marine Biological Laboratory) and his colleagues Drs. Inouye, Musicki, and Kishi. The microinjection method used in this study (2), originally developed by Hiramoto (32), relies upon an oil droplet injected with the aqueous sample. The candidate agonists tested were partially dried from ethanol stock solutions, diluted into dimethyl sulfoxide (DMSO), reconcentrated under dry N_2 gas and then diluted in injection buffer (Ca^{2+}-free phosphate buffered saline; 2, 30). To reduce the possibility that the samples would oxidize before being injected, they were kept in the dark and under dry N_2 gas until just before the pipette was loaded. Given the high degree of solubility in aqueous media of the AA metabolites and the rapidity of the microinjection procedure, it was assumed that the majority of the sample remained in the aqueous phase before injection. Control injections of injection buffer, DMSO diluted 10-fold in injection buffer, deionized H_2O, and vegetable oil elicited no detectable Ca^{2+}-dependent aequorin luminescence. Each condition was tested at least four times, in separate cells to assure reproducibility of the detected response (*e.g.*, 2).

The same group of substances tested *in vitro* (Table 1) was tested *in vivo*, with identical results. Again, of all the AA-derived candidate agonists, only LTB_4 elicited a release of Ca^{2+} from

Table I

Effects of arachidonate metabolites upon Ca^{2+} release from endomembrane subfractions

Agent	Pathway branch	Concentration of Ca^{2+} upon exposure to compound tested Gradient step[1] 0.25/1.0	1.0/1.3	1.3/1.5	1.5/2.0
Leucotriene B_4	5′-lipoxygenase	N.D.[2]	30 nM	N.D.	N.D.
Oxidized leucotriene B_4		N.D.	N.D.	N.D.	N.D.
Leucotriene C_4 (LtB_4 + G-SH)		N.D.	N.D.	N.D.	N.D.
Leucotriene B_5	Epoxygenase	N.D.	N.D.	N.D.	N.D.
Leucotriene C_5 (LtB_5 + G-SH)		N.D.	N.D.	N.D.	N.D.
Prostaglandin G_2	Cyclooxygenase	N.D.	N.D.	N.D.	N.D.
Prostaglandin H_2		N.D.	N.D.	N.D.	N.D.
Prostaglandin E_2		N.D.	N.D.	N.D.	N.D.
Prostaglandin $F_{2\alpha}$					
Thromboxane A_2	Thromboxane synthase	N.D.	N.D.	N.D.	N.D.
1,4,5-inositol trisphosphate, 10^{-6} *M*	Phospholipase C	N.D.	40 n*M*	N.D.	N.D.
ATP-dependent Ca^{2+} uptake, percent of total		0.0	100	0.0	0.0

[1] Molarity of sucrose at density interfaces. Endomembranes were fractionated on sucrose gradients, collected from sucrose interfaces, then assayed for release of Ca^{2+} as evoked by candidate agonists, as described in text. Assays were performed a minimum of four times, typically with membranes from 5 × 10^5/cells per individual assay. Data shown are for a typical experiment.

[2] N.D. = no release detected in any experiment, in a system sensitive to less than 3 n*M* Ca^{2+} in a 1-cm cuvette.

endomembrane stores—seen as a substantial increase in the level of photon emission from the injected cell upon injection of the candidate agonist. The total amount of light emitted, and thus the total amount of Ca^{2+} released, was proportional to the amount of LTB_4 or 1,4,5-IP_3 injected. Observations showed that these Ca^{2+}-dependent emissions spread radially from the point of injection at a rate of about 5 micrometers s^{-1} and ended at the inner surface of the plasma membrane. Eggs cultured in Ca^{2+}-free artificial seawater (the Jamarin and MBL recipes differ, but were indistinguishable with respect to their support of embryonic development), then injected with LTB_4 or 1,4,5-IP_3, also exhibited an elevation of their fertilization envelopes. Eggs injected with LTB_4 typically showed a more complete and native fertilization envelope elevation than those injected with 1,4,5-IP_3. Furthermore, blastomeres exhibited a dose-dependent response to AA pathway antagonists consistent with the notion that LTB_4 elicits the pre-NEB Ca^{2+} signal, and that products of the cyclooxygenase branch then regulate downstream steps in the mitotic process. Under these conditions, the minimal effective dose for LTB_4 was found to be at 10^{-8} *M* tip concentration, at which a very brief (2 to 3 s) response was noted.

In conclusion, LTB_4 among AA metabolites has the expected features of the specific agonist that evokes the release of Ca^{2+} from endomembrane stores to control Ca^{2+}_i-dependent processes within microdomains in eggs and mitotic cells. We speculate that specific branches of the AA pathway, activated sequentially in endomembranes, can control a cascade of Ca^{2+}-interdependent regulatory steps in mitotic cell division. In this scheme, phospholipase A_2 would act upon an endomembrane phospholipid to generate AA and a monoacylglycerol derivative. AA would then be converted by 5′-lipoxygenase to LTA_4. In the presence of adequate cytoplasmic concentrations of glutathione (G-SH), which provides the bulk of free cellular thiol groups (33), LTA_4 would be converted to LTC_4. Glutathione concentrations change in a cyclical nature during the cell cycle, being relatively abundant during interphase and markedly reduced at the onset of mitosis, *i.e.*, the so-called "Rapkine Cycle" (34–36). Thus, as a cell progresses towards prophase, and free glutathione levels become limiting, sufficient LTA_4 would become available to LTA_4 hydrolase to permit conversion to LTB_4. That LTB_4 would then be available to act upon an endomembrane Ca^{2+} release mechanism (*e.g.*, Ca^{2+} channel), yielding release of Ca^{2+} from that endomembrane store. LTB_4 rapidly and spontaneously oxidizes under physiological conditions to compounds not capable of eliciting Ca^{2+} release. In this way, a rapid, pulsed, and limited release of Ca^{2+} would be evoked from a discrete endomembrane store. Such a pulsed release of Ca^{2+} is consistent with the brief flashes of Ca^{2+}-dependent luminescence we observe in aequorin-loaded eggs and mitotic cells (*e.g.*, 3, 14–16, 37). This hypothesis can be readily extended to other Ca^{2+}_i-dependent cellular processes that do not *a priori* require stimulation at the level of the plasma membrane.

Grant support by NSF to R.B.S. is gratefully acknowledged. J.J.S. and T.C.D. gratefully acknowledge their NSF-REU support through the laboratory of R.B.S. G.S.J. was a recipient of a Woodruff Fellowship under the auspices of the Leadership Training Program fellowship through the College of Veterinary Medicine, Cornell University. The authors are also grateful to the reviewers and editor for their many helpful and well-considered suggestions made in the final preparation of this manuscript.

Literature Cited

1. **Silver, R. B. 1985.** *Biol. Bull.* **167:** 532.
2. **Silver, R. B. 1989.** *Dev. Biol.* **131:** 11–26.
3. **Silver, R. B., and S. Inoué. 1987.** *Biol. Bull.* **173:** 420–421.

4. **Silver, R. B. 1990.** *Ann. N Y Acad Sci.* **582:** 207–221.
5. **Llinás, R., M. Sugimori, and R. B. Silver. 1991.** *Biol. Bull.* **181:** 1–4.
6. **Llinás, R., M. Sugimori, and R. B. Silver. 1992.** *Science* **256:** 677–679.
7. **Llinás, R., M. Sugimori, and R. B. Silver. 1994.** Pp. 133–137 in *Molec. Cellular Mech. of Neurotransmitter Release.* L. Stjärne, Greengard, P., Grillner, S., Hökfelt, T., and Ottoson, D., eds. Raven Press, New York.
8. **Berridge, M. J. 1986.** *J Cell Sci. Suppl.* **4:** 137–153.
9. **Berridge, M. J. 1987.** *Biochim. Biophys. Acta* **907:** 33–45.
10. **Berridge, M. J., and R. F. Irvine. 1989.** *Nature* **341:** 197–205.
11. **Shull, G. E., and J. Greeb. 1988.** *J. Biol. Chem.* **263:** 15032–15040.
12. **Burk, S. E., J. Lytton, D. H. MacLennan, and G. E. Shull. 1989.** *J. Biol. Chem.* **264:** 18561–18568.
13. **Silver, R. B. 1986.** *J Cell Biol.* **103:** 140a.
14. **Silver, R. B. 1994.** *Biol. Bull.* **187:** 235–236.
15. **Silver, R. B., O. Shimomura, and S. Inoué. 1989a.** *J Cell Biol.* **109:** 90a.
16. **Silver, R. B., O. Shimomura, and S. Inoué. 1989b.** *J Cell Biol.* **109:** 90a.
17. **Samuelsson, B. 1983.** *Science* **220:** 568–575.
18. **Samuelsson, B., S.-E. Dahlén, J. Å. Lindgren, C. A. Rouzer, and C. N. Serhan. 1987.** *Science* **237:** 1171–1176.
19. **Van Diest, M. J., T. J. Verbeuren, and A. G. Herman. 1991.** *J. Pharmacol. Exp. Therapeutics* **256:** 194–203.
20. **Zhou, H. L., M. Chabot-Fletcher, J. J. Foley, H. M. Sarau, M. N. Tzimas, J. D. Winkler, and T. J. Trophy. 1993.** *Biochem. Pharmacol.* **46:** 139–148.
21. **Merritt, J. E., R. Jacob, and T. J. Hallam. 1989.** *J Biol. Chem.* **264:** 1522–1527.
22. **Lee, T. H., C. E. Horton, U. Kyan-Aung, D. Haskard, A. E. Crea, and B. W. Spur. 1989.** *Clin. Sci.* **77:** 195–203.
23. **Buttner, N., S. A. Siegelbaum, and A. Volterra. 1989.** *Nature* **342:** 553–555.
24. **O'Dell, T. J., R. D. Hawkins, E. R. Kandel, and O. Arancio. 1991.** *PNAS* **88:** 11285–11289.
25. **Palmberg, L., H.-E. Claesson, and J. Thyberg. 1987.** *J Cell Sci.* **88:** 151–159.
26. **Rich, A. M., G. Weissmann, C. Anderson, L. Vosshall, K. A. Haines, T. Humphreys, and P. Dunham. 1984.** *Biochem. Biophys. Res. Comm.* **121:** 863–870.
27. **Hayakawa, M., N. Ishida, K. Takeuchi, S. Shibamoto, T. Hori, N. Oku, F. Ito, and M. Tsujimoto. 1993.** *J. Biol. Chem* **268:** 11290–11295.
28. **Silver, R. B., R. D. Cole, and W. Z. Cande. 1980.** *Cell* **19:** 505–516.
29. **Silver, R. B. 1986.** *Meth. Enzymol.* **134:** 200–217.
30. **Silver, R. B. 1986.** *PNAS* **83:** 4302–4306.
31. **Shimomura, O., S. Inouye, B. Musicki, and Y. Kishi. 1990.** *Biochem. J* **270:** 309–322.
32. **Hiramoto, Y. 1974.** *Exp. Cell Res.* **87:** 403–406.
33. **Sies, H. 1989.** *Naturwissenshaften* **76:** 57–64.
34. **Rapkine, L. 1931.** *Ann. Physiol. Physiolchim. Biol.* **7:** 382.
35. **Rapkine, L. 1938.** *J. Chim. Phys.* **34:** 137.
36. **Mazia, D. 1961.** Pp. 77–412 in *The Cell,* Vol. III, J. Brachet and A. E. Mirsky, eds. Academic Press, New York.
37. **Silver, R. B., A. P. Reeves, M. Whitman, and B. Kelley, 1994.** *Biol. Bull.* **187:** 237–238.

Reference: *Biol. Bull.* **187:** 244–245. (October, 1994)

Muscle Fine Structure and Microtubule Birefringence Measured with a New Pol-Scope

Phong T. Tran, Shinya Inoué, Edward D. Salmon, and Rudolf Oldenbourg
(Marine Biological Laboratory)

The polarized light microscope has traditionally been an important tool for studying fine structure in living cells (1, 2). However, conventional design allows for retardance imaging only in a narrow range of orientations. One of us (RO) has improved upon conventional design by developing a new type of polarizing microscope (pol-scope), which can measure the retardance due to specimen anisotropy irrespective of orientation. The design of the new pol-scope is based on the traditional polarizing microscope but has two essential modifications: (a) the specimen is illuminated with nearly circularly polarized light, and (b) the traditional compensator is replaced by two liquid-crystal variable retarders. The liquid-crystal variable retarders form a "universal compensator" that is driven electrically, eliminating the need for any mechanical readjustment to the optical components. A video camera and computer-assisted image analysis provide measurements of specimen anisotropy for all points of the image constituting the field of view (3).

We used the pol-scope to measure the retardance of striated muscle for testing the reliability and imaging efficiency of the new pol-scope. Frog sartorious muscles were fixed with glutaraldehyde and osmium tetroxide solutions and embedded in resin, then sliced into thin sections and mounted in a matching index medium (Euparal) on a strain-free microscope slide. We imaged gold and purple sections which are about 180 nm and 360 nm thin, respectively. Figure 1a shows the birefringence of the same region of a thin muscle section measured at different angular orientations. Irrespective of orientation, we clearly observe the myofibrillar fine structures, consisting of isotropic Z lines, weakly birefringent I bands, and anisotropic A bands (Fig. 1b). We measured retardance of 0.22 ± 0.03 nm [$n = 7$] for the 180 nm muscle section, and retardance of 0.35 ± 0.02 nm [$n = 7$] for the 360 nm muscle section averaged over the length of the sarcomeres. These values are consistent with earlier measurements (4).

We also used the pol-scope to measure the retardance of microtubules. Phosphocellulose-purified brain tubulin was allowed to polymerize into long microtubules from the ends of isolated sea urchin axonemes. Figure 2 shows the computer-calculated birefringence distribution of microtubules and their associated axonemes. We can clearly detect the birefringence of microtubules from the ends of axonemes; but our current measurement setup cannot unambiguously differentiate between one microtubule and multiple microtubules bundled together. Nevertheless, the smallest measured retardance of the detectable microtubules is 0.32 ± 0.03 nm [n = 50]. This appears to be the retardance of single microtubules.

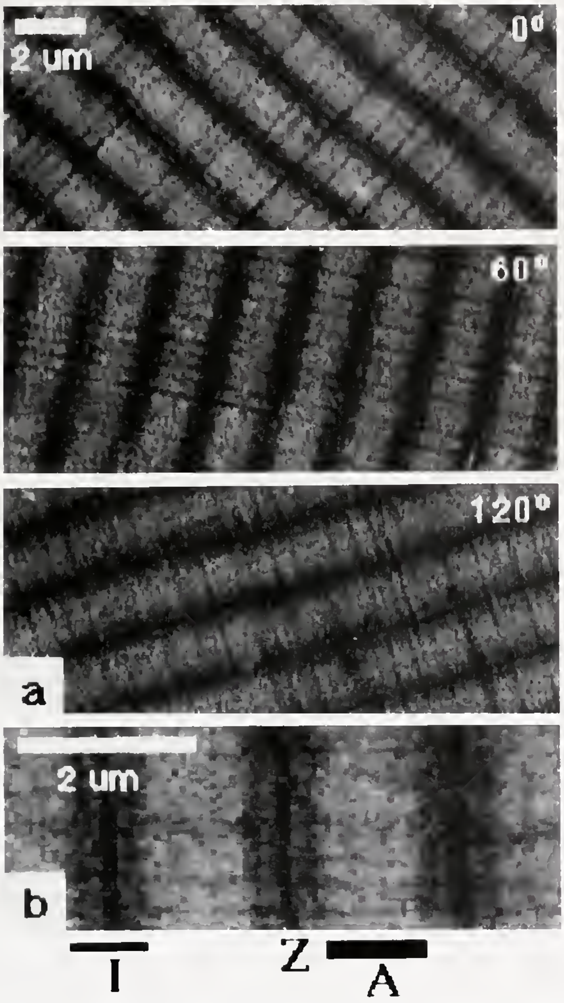

Figure 1. *Birefringence of frog sartorious muscle 360 nm thin section measured with the new pol-scope. (a) In the images shown here, the image brightness and contrast detail remain the same irrespective of specimen orientation; specimen rotated by angles indicated in top right corner. (b) Enlargement shows clearly the fine structures in sarcomeres in the myofibrils, consisting of I bands, Z lines, and A bands. The brightness depicted in the image is directly proportional to the retardance of the specimen, with 0.5 nm retardance in brightest pixels. The same optics used as described in legend to Fig. 2.*

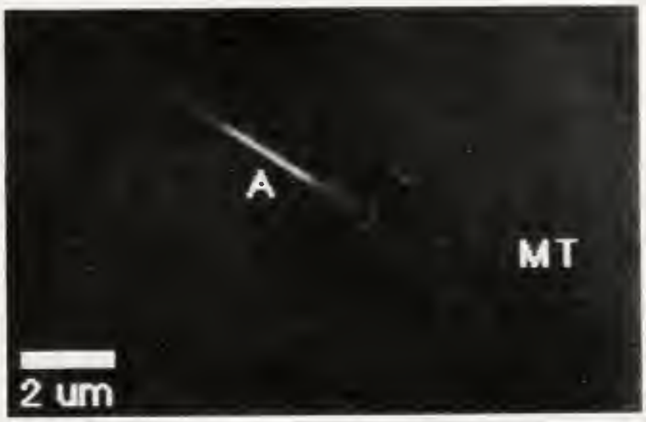

Figure 2. *Birefringence of microtubules (MT) polymerized off an axoneme (A). Both Figures 1 and 2 are computer-generated images whose pixel brightness is proportional to specimen retardance. The original data were collected with a Nikon Microphot-SA microscope equipped with 100-watt Hg arc lamp illumination; two liquid-crystal variable retarders (universal compensator) electronically controlled with variable voltages (10–40 volts); Nikon 1.4 NA condenser; Nikon PlanApo 60X DIC 1.4 NA objective; MTI CCD C72 video camera; Scion LG-3 image grabber; Macintosh Quadra 800; and processed using the custom-modified NIH Image program.*

Thus, the new pol-scope permits excellent imaging of cellular fine structures and precise measurement of their birefringence, with the added advantage of orientation-independent specimen placement. Its ability to visualize isotropic Z lines of the muscle sarcomeres confirms that the pol-scope is optically at least as good as or better than an excellent-quality conventional polarizing microscope equipped with polarization rectifiers.

We gratefully acknowledge the technical support of Dr. Guang Mei, and support by A. V. Wilson summer fellowship from the University of North Carolina to PTT, and NIH grants GM-49210 to RO, GM-31617 to SI, and GM-24364 to EDS.

Literature Cited

1. **Inoué, S. 1953.** *Chromosoma* **5:** 487–500.
2. **Schmidt, W. J. 1937.** *Die Doppelbrechung von Karyoplasma, Zytoplasma und Metaplasma. Protoplasma Monographien.* Vol. 11, Borntraeger, Berlin.
3. **Mei, G., and R. Oldenbourg. 1994.** *Proceedings of Conference on Polarization Analysis and Measurement II, SPIE International Symposium,* in press.
4. **Noll, D., and H. H. Weber. 1934.** *Pflüger's Archiv.* **235:** 234–246.

Reference: *Biol. Bull.* **187:** 246–247. (October, 1994)

Copper Induced Polymerization of Hemoglobin from the Ocean Pout, *Macrozoarces americanus*

Thomas A. Borgese (Lehman College, CUNY), Sharon Bourke, Bernarda Frias,
Donald Johnson, and John Harrington

Hemoglobins that polymerize are not uncommon among amphibians, reptiles, and elasmobranchs, but are rare among teleosts and humans. They are useful models for the study of protein structure, function, and molecular evolutionary relationships. The freshwater teleost *Hoplias malabarica* (1), the marine teleost *Lophius americanus* (2), and the clown fish, *Amphiprion* (3) are the only bony fishes reported to have hemoglobins that polymerize. *Hoplias* and *Lophius* polymerize by forming intermolecular disulfide bonds, while the polymerization mechanism for the clown fish is, as yet, unknown. Among humans, hemoglobins Ta-Li, Mississippi, and Porto Alegre (4, 5, 6) have a single mutation involving the substitution of a cysteine residue at different loci on the globin chain. We now report that the ocean pout has a single hemoglobin with six sulfhydryl groups per tetramer and polymerizes, *in vitro*, after oxidation with potassium ferricyanide ($K_3Fe(CN)_6$) or cupric chloride ($CuCl_2$).

Procedures for hemoglobin purification by DE-52 cellulose chromatography, molecular weight estimations by gel filtration on G-100 columns, and urea gel electrophoresis for globin subunit analysis have been described (2). Hemoglobin was incubated with a two- to threefold molar excess of $CuCl_2$ for 15 min in an ice bucket. The excess copper was removed by dialysis or by gel filtration from Sephadex G-25 columns equilibrated with 0.1 *M* $K\text{-}PO_4$ buffer, pH 7.4. Thereafter 20–40 mg of the hemoglobin was applied to and eluted from G-100 columns. One-ml fractions were collected and the absorbance of each measured at 540 nm. The approximate polymer molecular weight was estimated from the elution volume of the peak tube. Hemoglobin solutions (0.5–2.0 g/%) were also oxidized by adding 1–3 mg of potassium ferricyanide per ml of hemoglobin.

Iodoacetamide (IAA)-alkylated hemoglobin (15 μmoles/mg hemoglobin) was dialyzed overnight, centrifuged, and subsequently treated with $CuCl_2$.

In a separate experiment, a 60-fold molar excess of beta-mercaptoethanol (B-ME) was added to $CuCl_2$-treated hemoglobin, incubated for 1 h, and dialyzed for 3 h before G-100 chromatography. Untreated hemoglobin and hemoglobin treated with $CuCl_2$ alone served as controls and were dialyzed for the same period.

The gel filtration profile of known molecular weight proteins is shown in Figure 1A. The inset graph is a plot of the log of the molecular weight of each standard *versus* the elution volume of the peak tube. The linear relationship indicates that the peak tube elution volume provides a reasonable estimate of the protein molecular weight between 16,000 and 150,000 Da. (The molecular weight fractionation range for Sephadex G-100 is 4×10^3 and 1.5×10^5.)

The effect of $CuCl_2$ on pout hemoglobin is shown in Figure 1B. In the absence of the cation, the peak tube eluted at a volume comparable to human hemoglobin, suggesting a normal molecular weight for pout hemoglobin of approximately 60,000. The addition of $CuCl_2$ results in a polymer with a minimum molecular mass of 100 to 155 kDa, which corresponds to aggregates of, perhaps, two to three tetramers.

Cupric-chloride-induced polymer formation may be inhibited by prior incubation with IAA (Fig. 1C). Hemoglobin alkylated with IAA elutes at the same volume as normal pout and human hemoglobin, but in the absence of IAA, cupric-chloride-induced

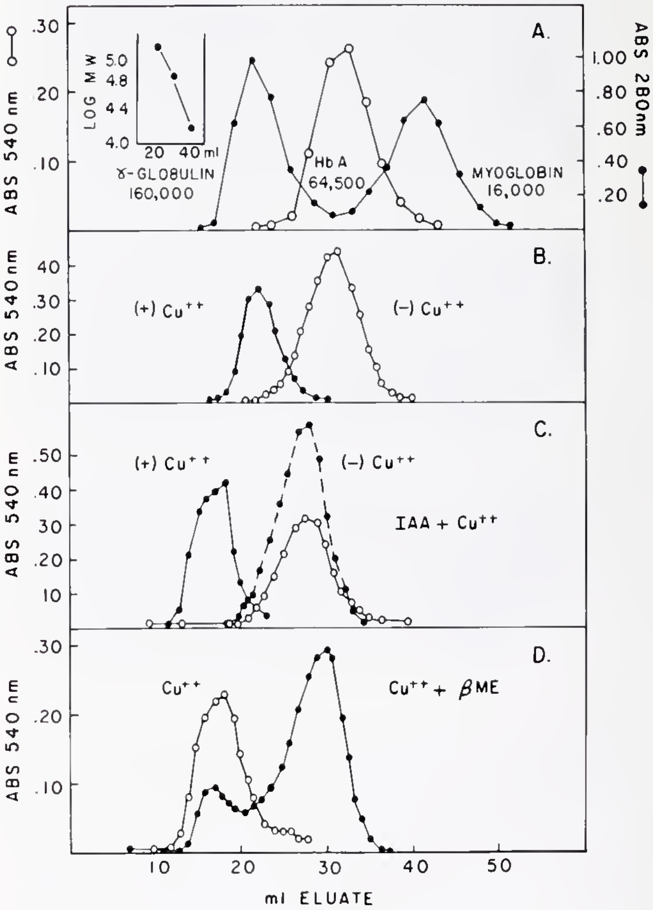

Figure 1. *Effect of copper on the polymerization of pout hemoglobin. (A) Sephadex G-100 columns (1 × 53 cm) calibrated with 5 mg each of known molecular weight standards and eluted with equilibration buffer, 0.1 M* $K\text{-}PO_4$*, pH 7.4. One-ml fractions collected and absorbance measured at 280 nm for gamma globulin and myoglobin and 540 nm for hemoglobin. Inset: Log of the standard's molecular weight plotted against its peak elution volume. (B) Elution profile of pout hemoglobin with and without* $CuCl_2$*. Hemoglobin to* $CuCl_2$ *ratio, 1:2. (C) Inhibitory effect of IAA on polymerization. Ten milligrams of hemoglobin are incubated with 150 μmoles of IAA prior to the addition of* $CuCl_2$*. (D) Partial reversal of* $CuCl_2$*-induced polymerization by a 60-fold molar excess of B-ME.*

polymerization occurs. The difference in the peak tube elution volumes for normal hemoglobin in Figure 1C relative to A and B is that different columns were poured, calibrated, and used for C and D.

Polymerization can be reversed by the addition of B-ME. In Figure 1D there is a partial but significant shift from the 160,000 molecular weight polymer to the normal 60,000 molecular weight species.

The results obtained with $CuCl_2$, including polymerization, inhibition with IAA, and reversal with B-ME, were indistinguishable from those obtained when $K_3Fe(CN)_6$ was used as the polymerizing agent.

Preliminary structural studies with urea gel electrophoresis indicate that pout hemoglobin is a tetramer consisting of two pairs of globin subunits.

In conclusion, pout hemoglobin has a molecular weight of about 60,000, approximately six sulfhydryl groups per tetramer, as measured by PCMB titration, and consists of two dissimilar subunits. It is polymerized, by $K_3Fe(CN)_6$ or $CuCl_2$, to polymers corresponding to about two to three tetramers. Polymerization is inhibited by IAA and reversed by B-ME, suggesting that polymerization may be due to the oxidation of cysteine sulfhydryl groups and the formation of intermolecular disulfide bonds.

This work has been supported by PSC-CUNY Grants #664308 and 665168 and NIGMS-NIH MARC Program Grant #5T34GM-08182.

Literature Cited

1. **Reischl, E. 1976.** *Comp. Biochem. Physiol.* **55B:** 255–257.
2. **Borgese, T. A., *et al.* 1988.** *Comp. Biochem. Physiol.* **91B:** 663–670.
3. **Leibovitz, L., *et al.* 1986.** *New England Chap. American Fisheries Soc. Univ. Mass., Amherst* (Abstract).
4. **Blackwell, R. Q., *et al.* 1971.** *BBA* **243:** 467–474.
5. **Adams, J. G., *et al.* 1987.** *Hemoglobin* **11:** 435–437.
6. **Tondo, C., *et al.* 1963.** *Am. J. Genetics* **15:** 265–279.

Reference: *Biol. Bull.* **187:** 247–248. (October, 1994)

Catalase Activity in Dogfish (*Mustelus canis*) Ocular Tissues

Seymour Zigman (University of Rochester School of Medicine, Rochester, NY) and Nancy S. Rafferty

Lens epithelium contains catalase, whose enzymatic activity is strongly inhibited by UV_A exposure (1, 2). This enzyme protects the lens from H_2O_2-related oxidative damage. A decrease in lens catalase activity would diminish its protective function. This would increase the lens' oxidative stress. The purpose of this work was to elucidate systems that protect the eye from oxidative stress.

The breakdown of H_2O_2 was measured with an O_2 electrode (Microelectrodes, Inc., MI-730), an oxygen meter (O M-7), and an XY recorder. The system was preset at 21% oxygen with H_2O. Beef liver catalase (Sigma) was the quantitative standard. Fresh ocular tissues or 50 μl of the $15{,}000 \times g$ supernates of homogenates were added to Ringer's medium containing 0.88 m*M* H_2O_2. The increase in O_2 with time was recorded. The same procedure was followed with $15{,}000 \times g$ supernatants of lens capsule epithelium that were exposed to radiation from a Woods lamp or sunlight through a Pyrex beaker. UV-A was the predominant radiant energy reaching the cells (*i.e.*, UV_A). The protection of catalase activity against UV damage was also tested by presoaking and irradiating samples in Ringer's medium containing 10 μg/ml of α-tocopherol or β-carotene.

Table 1

A. Catalase activities in dogfish ocular tissues

Tissue	Whole tissue % O_2 per minute per OD_{280}	15K g supernatant % O_2 per minute per OD_{280}
Retina	2.52 ± 16%*	2.78#
Iris	2.48 ± 20%	3.15
Cornea epithelium	1.36 ± 14%	2.23
Lens capsule epithelium	1.78 ± 12%	2.01
Aqueous humor	0.02 ± 50%	0.03

B. Effects on lens capsule epithelium catalase activity of Woods lamp UV

Whole tissue	% of control
Lens dark	100 ± 18%*
Lens UV-exposed	51 ± 20%
UV-exposed plus β-carotene (10 μg/ml)	51 ± 22%
UV-exposed plus α-tocopherol (10 μg/ml)	84 ± 15%

C. Effects on lens capsule epithelium catalase activity of sunlight

15K g supernatants	% of control
Dark	100#
UV-exposed	44
UV plus lens-soluble proteins	31
UV plus alpha crystallin	96

* Average of two experiments ± range; #One experiment in duplicate.
Note: Supernatant $O.D._{280} = 0.750$; alpha-crystallin $O.D._{280} = 1.0$.

Retina and iris had the most catalase activity; cornea epithelium and lens epithelium had 54–72% of the activity of these pigmented tissues. Aqueous humor had only trace activity (see Table 1A). UV_A exposure (75 J/cm^2) reduced the catalase activity of whole lens to about 50% of dark controls (Table 1B). Beta-carotene (10 μg/ml) was ineffective in protecting whole lens catalase activity, but α-tocopherol (10 μg/ml) was protective. Lens capsule epithelium $15{,}000 \times g$ supernates were also exposed to UV_A (25 J/cm^2); some samples contained total lens-soluble protein (TSP) or purified α-crystallin (which protects proteins against denaturation). Addition of TSP did not protect catalase activity, whereas Biogel A -50M purified α-crystallin did protect it (Table 1C).

The catalase activity of dogfish ocular tissues, especially the iris and retina, appears to detoxify ocular H_2O_2 efficiently. The epithelia of cornea and lens are less efficient in breaking down H_2O_2. It appears that α-tocopherol protects lens catalase activity from UV_A radiation, whereas β-carotene does not. In addition, α-crystallin protected lens catalase activity from UV_A-induced inhibition.

Support: National Eye Institute Grant EY 00459 (S.Z.); EY 00698 (N.S.R.) and Research to Prevent Blindness, Inc. Thanks to Bunnie R. Zigman for preparation of the manuscript.

Literature Cited

1. **Zigman, S., and N. S. Rafferty. 1993.** *Biol. Bull.* **185:** 328.
2. **Zigman, S., and N. S. Rafferty. 1994.** *Comp. Biochem. Physiol.* (in press).

Reference: *Biol. Bull.* **187:** 248–249. (October, 1994)

N^G-Monomethyl-L-Arginine Inhibits *Arbacia* Fertilization and Differentiation

Diane E. Heck, Jeffrey D. Laskin (UMDNJ—Robert Wood Johnson Medical School), Seymour Zigman, and Walter Troll

The amino acid L-arginine is crucial to a number of metabolic processes including not only protein synthesis, but also the urea cycle and polyamine metabolism (1). Recent studies also demonstrate that L-arginine metabolites are important mediators of cellular signal transduction (2, 3). Using eggs from the sea urchin *Arbacia punctulata,* we investigated the effects of a structural analog of L-arginine, N^G-monomethyl-L-arginine (NMMA), on the fertilization process. NMMA inhibits crucial metabolic processes involving arginine metabolism that are independent of protein synthesis, in particular, the activity of the L-arginine-dependent enzyme, NADPH diaphorase (4).

We have found that following fertilization, sea urchin eggs contain NADPH diaphorase activity, as measured by oxidation of nitroblue tetrazolium (2 m*M*), which was inhibited by NMMA. A characteristic of the fertilization process by sea urchin eggs is an oxidative burst. This is associated with the production of high levels of reactive oxygen intermediates, in particular, hydrogen peroxide. Current studies indicate that hydrogen peroxide is required for fertilization (5). At low concentrations of L-arginine, NADPH diaphorase generates superoxide anion as well as hydrogen peroxide. Using fluorescence image analysis in conjunction with the hydroperoxy-sensitive probe 2′,7′-dichlorofluorescin diacetate (DCFH-DA), we analyzed hydrogen peroxide production induced during the fertilization of sea urchin eggs (6). Eggs were immobilized on poly-L-lysine treated cell culture plates and incubated in seawater containing DCFH-DA (5 μM) in the presence and absence of amino acids. After 30 min the plates were washed three times in seawater, inoculated with sperm, and fluorescence intensity quantified with a Meridian ACAS 570 anchored cell analysis system equipped with a 5-watt argon laser; the excitation wavelength was set at 488 nm and emission monitored at 525 nm. During fertilization, untreated eggs readily produced hydrogen peroxide (Fig. 1, panel A). We found that when eggs are fertilized, there is an approximately 10-fold increase in hydrogen peroxide over 10 min. Eggs fertilized in the presence of 1 m*M* L-arginine (Fig. 1, panel B) also produced significant amounts of hydrogen peroxide during the fertilization process. But, in the presence of NMMA (3 m*M*), hydrogen peroxide production was markedly inhibited (90–95%), an effect that could be overcome by the presence of 1 m*M* L-arginine (Fig. 1, panels C and D, respectively). Both eggs and, in particular, sperm contained catalase, which may also regulate hydrogen peroxide production during development.

In further studies we have found that NMMA (0.1–3 m*M*) inhibits the fertilization and development process, as measured by the percentage of fertilized eggs undergoing cell division 1 h after fertilization, and the formation of rotating blastulas after 20 h. These effects were reversible by equimolar concentrations of L-arginine. Taken together, these data indicate that L-arginine is required for fertilization. In further studies it will be important to determine the precise site of action of NMMA in the fertilization process.

Research support was provided in part by NIH grants ES 03647 and ES 05022.

Literature Cited

1. **Stryer, L. 1975.** *Biochemistry.* W. H. Freeman and Co., San Francisco. Pp. 503–527.
2. **Rengasamy, A., and R. A. Johns. 1994.** *Biochem Pharmacol.* **48:** 423–425.
3. **Nathan, C., and Q. W. Xie. 1994.** *J. Biol. Chem.* **269:** 13725–13728.
4. **Bredt, B. S., and S. H. Snyder. 1990.** *PNAS* **87:** 682–685.
5. **Shapiro, B. M. 1991.** *Science* **252:** 533–536.
6. **Heck, D. E., D. L. Laskin, C. R. Gardner, and J. D. Laskin. 1992.** *J. Biol Chem.* **267:** 21277–21280.

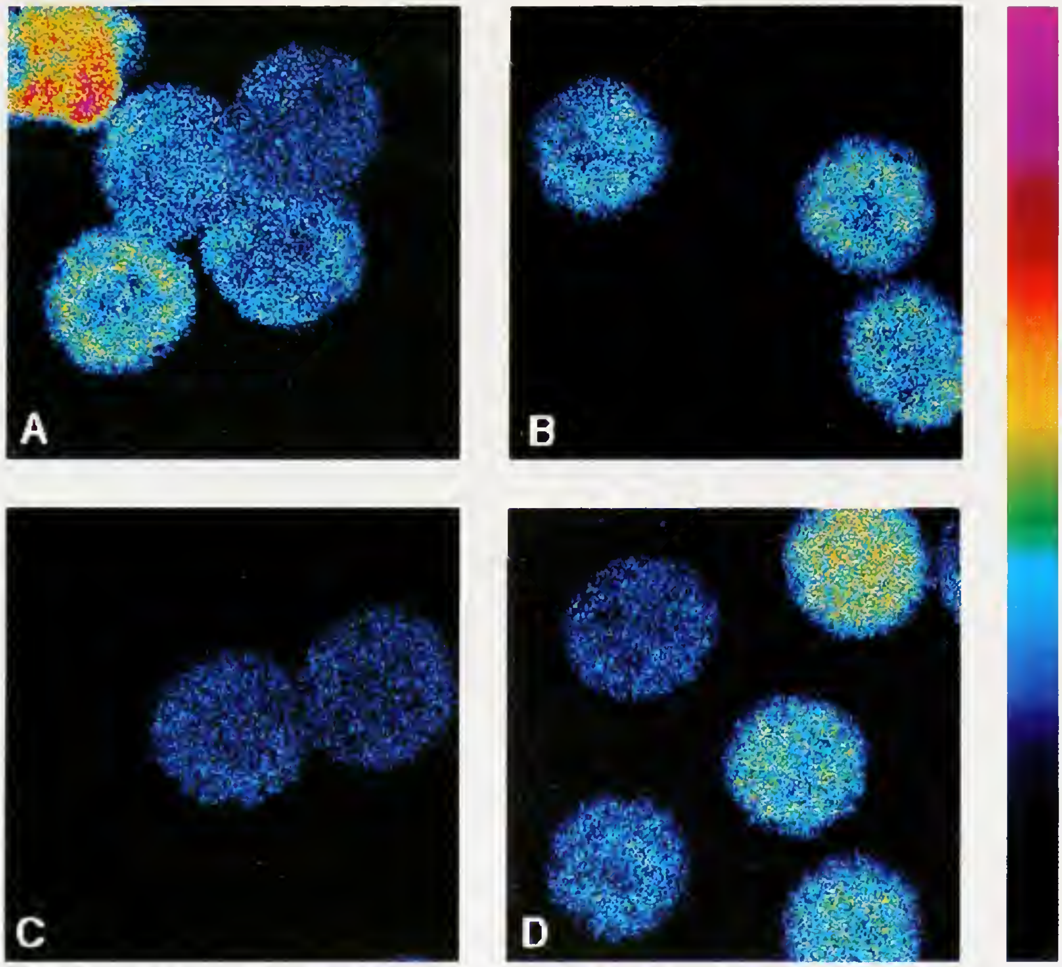

Figure 1. *Effects of N-monomethyl-L-arginine on hydrogen peroxide formation during the fertilization of sea urchin eggs. Eggs, immobilized on poly-L-lysine coated tissue culture plates, were incubated for 30 min with DCFH-DA (5 μM), incubated with sperm, and, after 10 min, analyzed with a Meridian ACAS anchored cell analysis system. Representative images are presented. Panel A, untreated fertilized eggs; panel B, eggs treated with 1 mM L-arginine; panel C, eggs treated with 1 mM NMMA; panel D, eggs treated with 1 mM NMMA in the presence of 1 mM L-arginine. The color bar represents increasing fluorescence on a four-decade log scale. Each panel shows a representative field from 12 different scans.*

Reference: *Biol. Bull.* **187:** 249–250. (October, 1994)

Enzymatic Hydrolysis of Tetriso as a Model for the Detoxication of the Neurotoxic Agent VX

Francis C. G. Hoskin (Marine Biological Laboratory) and John E. Walker

The enzymatic hydrolysis and thus detoxication of certain organophosphorus acid anhydrides, commonly termed "nerve gases," is now well documented (1). Some of these are P-F compounds; all are powerful acetylcholinesterase (AChE) inhibitors, which is the basis of their neurotoxicity. One such compound, Soman, is hydrolyzed by a particular organophosphorus acid anhydrolase (OPAA) found only in certain tissues of the cephalopods, notably squid nerve, from which the enzyme has been purified (1). A second generation of these highly toxic compounds is typified by the military agent VX (2). Now, with a decline in international confrontation, mild means of destruction are being sought for all of these agents (3). Although VX is both extremely hazardous and generally not available, a close analog, Tetriso, originally synthesized for use in neurophysiological experiments (4), is now revealing for the first time a detoxication pathway directly applicable to VX degradation.

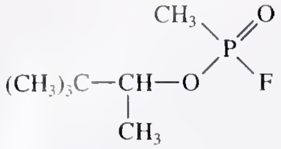

Soman

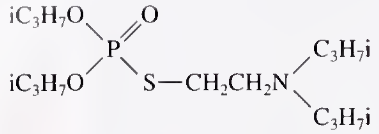

Tetriso

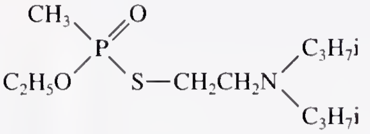

VX

The purification of an enzyme, organophosphorus hydrolase (OPH), derived from *Pseudomonas diminuta* through genetic manipulations and biochemical alterations, is the work of Wild and colleagues (5) who have also made the enzyme available to us. Briefly, this involves insertion of a *Pseudomonas* plasmid into *E. coli,* growth to late log or early stationary phase, and the resulting processing of a 38 kD protein to a 35 kD protein with OPH activity. (Lack of evidence about a natural substrate is an impediment in naming and numbering these enzymes.)

The degradation of Tetriso was measured in two ways. One was by the loss of AChE inhibitory potency (detoxication) by the original Ellman reaction, termed the "indirect" Ellman, as used by us (1). The second, termed the "direct" Ellman, is illustrated with Tetriso itself now serving directly as a substrate. Two spectrophotometer cuvettes contained, each, 2×10^{-4} *M* Tetriso in buffer, and the Ellman reagent dithionitrobenzoic acid (DTNB), all at pH 7. After recording at 412 nm for 5 min, OPH enzyme was added to the sample cuvette and recording was continued. The absorbance went from 0.000 to −0.003 during the 5 min, and linearly from 0.052 to 0.743 during the next 10 min. Readings were converted to μmoles Tetriso hydrolyzed per unit of time and quantity of enzyme.

When Tetriso was incubated with OPH in the "indirect" mode and detoxication was measured at 4 h, 0.01 ml OPH caused 96% detoxication, and 0.02 ml OPH caused 37% detoxication. Boiled enzyme showed no detoxication. The zero time measurement gave a second order rate constant for the inhibition of AChE (a necessary component in the "indirect" method) of 1.76×10^6 $l \cdot mole^{-1} \cdot min^{-1}$.

Tetriso was incubated with OPH in the "direct" mode over the substrate (*i.e.,* Tetriso) concentration range 7×10^{-5} to 10^{-2} *M*. The results of 14 determinations, processed by a computer program, gave a K_M of 6.7×10^{-3} *M* with a standard error of 0.2%.

The enzymatic hydrolysis of Tetriso was followed by the "direct" Ellman, and at predetermined times samples were removed from the cuvette, diluted, and subjected to the "indirect" measurement. The same experiments were carried out with the hydrolytic agent being an elevated pH of 11.5–12. The results suggest that while alkaline hydrolysis of Tetriso cleaves any one of the three ester bonds around the P atom of Tetriso (only one of which produces an Ellman sensitive product), enzymatic hydrolysis shows a selectivity for the P-S bond.

A small amount of VX was available to us from experiments conducted in the summer of 1979 (2). This had been held at −80° and still gave a second order AChE inhibition constant of 3.2×10^7 $l \cdot mole^{-1} \cdot min^{-1}$, in good agreement with the original value of $3\text{–}3.4 \times 10^7$ (2). Although there was only enough VX to permit a few experiments, we did determine that VX is detoxified and hydrolyzed by the *Pseudomonas diminuta*-derived OPH enzyme, but at about a fifth the rate found for Tetriso.

Neither Tetriso nor VX is hydrolyzed by the Soman hydrolyzing enzyme from squid (1).

The enzymatic degradation of Tetriso, the applicability of these findings to VX, and the development of a rapid assay for these reactions holds the promise of a mild means for the disposal of unwanted stockpiles of a dangerous compound.

Dr. H. Dupont Durst of Edgewood RD&E Center, Aberdeen Proving Ground, MD, and Dr. K. S. Rajan of Illinois Institute of Technology Research Institute, Chicago, IL, facilitated the support of this research. Ms. Diane M. Steeves of the U.S. Army RD&E Center, Natick, MA, provided computer assistance.

Literature Cited

1. **Hoskin, F. C. G. 1990.** Pp. 469–480 in *Squid as Experimental Animals.* D. L. Gilbert, W. J. Adelman, Jr., and J. M. Arnold, eds. Plenum Press.
2. **Farquharson, D. A., F. C. G. Hoskin, K. Hubbard, and R. D. Prusch. 1980.** *Bull. Environ. Contam. Toxicol.* **24:** 719–726.
3. **National Research Council. 1993.** Pp. 37–53 in *Alternative Technologies for the Destruction of Chemical Agents and Munitions.* J. P. Longwell, chmn. ISBN 0-309-04946-6. National Academy of Sciences.
4. **Hoskin, F. C. G., L. T. Kremzner, and P. Rosenberg. 1969.** *Biochem. Pharmacol.* **18:** 1727–1737.
5. **Dave, K. I., C. E. Miller, and J. R. Wild. 1993.** *Chem. Biol. Interact.* **87:** 55–68.

Reference: *Biol. Bull.* **187**: 251–252. (October, 1994)

Lead Toxicity in *Hermissenda crassicornis* Embryos and Cultured Neurons

Catherine T. Tamse, Peter J. S. Smith, Amine Aloulou, Herman T. Epstein, and Alan M. Kuzirian
(Marine Biological Laboratory)

Morphological abnormalities, behavioral deficits, and learning disabilities can be induced in mammals and other vertebrates by lead poisoning (1, 2). This study seeks to exploit *Hermissenda* as a non-mammalian biomedical and toxicological research model of heavy metal toxicity, particularly lead, and its effects on the extensively studied learning and behavioral patterns of this marine mollusc (3). We report the first results of a baseline study on how lead affects the development of *Hermissenda* embryos and the growth of cultured neurons.

Newly laid egg masses were collected from the *Hermissenda* Resource Facility, Marine Biological Laboratory (MBL), Woods Hole, Massachusetts, and processed for static, chronic toxicity tests for lead. The egg mass was cut into 5-mm strands and distributed individually into 50-ml conical tubes containing natural seawater. The average number of embryos in each strand was 1000. Three seawater regimes were used: ambient Lillie building seawater without EDTA (LSW); Lillie seawater with 0.25 mg/l (0.74 μM) EDTA (LESW), which we routinely use for *Hermissenda* culture; and ambient Marine Resources Center, MBL seawater (MSW). The following total lead acetate (PbAc) concentrations were used: 0.05, 0.1, 0.5, 1.0, 5.0, 7.0, 10.0 mg/l (0.09, 0.18, 0.9, 1.8, 9, 12.7, 18 μM, respectively), plus negative (no lead or EDTA added) and positive (no lead but with EDTA added) controls. Each test concentration was replicated, and the distribution was randomized. The tubes were incubated at 12°C and the embryonic development of 50 animals per treatment was recorded after 6 days lead exposure.

For the chronic *in vitro* neuronal exposure to PbAc, cell culture techniques developed for *Hermissenda* were followed (4). The central nervous system (CNS) of *Hermissenda* was dissected, digested in protease at 12°C, incubated overnight, and washed twice with 1.8% bovine serum albumin in artificial seawater (ASW), followed by a final ASW wash. The CNS was cut into four regions: left and right cerebropleural ganglia and left and right pedal ganglia. Neuronal cells were then dissociated, transferred to a poly-L-lysine-coated culture dish (35 × 10 mm) containing 3 ml of Leibovitz L-15 medium (5) supplemented with inorganic salts. Dishes were then left in a 12°C incubator until examined 24 h later, and daily thereafter, for growth morphology. Neurons 7–14 days into culture, with well-established neuritic morphology and stable growth, were exposed to PbAc. A 1 M stock solution of PbAc was added directly to the L-15 medium to obtain total concentrations of 0.5, 2.0, and 4.0 μg/ml (0.9, 3.6, 7.2 μM, respectively). Lead-exposed neurons were observed closely for the first 2–4 h for morphologic changes, and every 24 h thereafter. Cells were incubated in the L-15 medium–PbAc solution for 3–10 days.

The chronic toxicity tests clearly indicate that *Hermissenda* embryos are sensitive to lead, and that EDTA must be added routinely to LSW for their normal and synchronous development. This implies that the small amount of EDTA (0.74 μM) added to seawater from the Lillie building was sufficient to chelate an unknown heavy metal present in the seawater. Future tests involving lead studies will be conducted using MSW until more information is available about the apparent contaminant in LSW.

Toxicity effects observed were directly proportional to increasing concentrations of lead. The time course for embryonic development was lengthened and dominated by earlier developmental stages as the lead concentrations increased (0.5–1.0 mg/l). At higher concentrations (5.0–10.0 mg/l) added to ambient LSW, development was arrested at the morula stage with resultant embryonic mortalities. Although embryos in all seawater regimes reached the early veliger stage even after exposure to 0.5 mg/l PbAc and suffered no mortalities, their development was significantly slower than that of the controls with added EDTA. Lead added to both LESW and MSW had identical effects up to 0.5 mg/l lead levels.

Lead effects on cultured *Hermissenda* neurons seemed to be age-dependent as well as concentration-dependent. Some cells, 7 days into culture, responded as early as 5 min after exposure to 2 μg/ml PbAc with cytoplasmic material streaming out of the soma. After an hour, neurites of the remaining cells developed a granular appearance, and neurite structural breakdown was observed in some cells. Two days post-exposure, many dead neurons were observed, but other neurons still appeared intact. In older, more established cells (12–14 days into culture), a response was seen only after an hour post-exposure with organelles clustering at the junction of the soma and neurites. The development in the soma of a yellowish-brown pigment with lipid-like inclusions bodies, some nucleated, was observed more frequently 5–10 days post-exposure. At this stage, neurons still appeared intact but with neuritic disintegration at the distal edges. At the highest lead concentration tested (4.0 μg/ml), the eye and other neurons began to shrink within 30 min. By day 5 post-exposure, neurons were dead and mostly cellular debris remained. At 0.5 μg/ml PbAc, no changes were seen in exposed neurons even after 4 hours. The yellowish-brown pigmentation, unidentified bodies within the soma, and disintegration along the neurite branch were seen 3 days post-exposure at this concentration.

In summary, our preliminary findings indicate that lead at low concentrations delays embryonic development of *Hermissenda* and is embryotoxic at higher concentrations. Neurons in cell culture also show gross morphological changes. It appears that *Hermissenda* has excellent potential for use as a non-mammalian toxicological model. By integrating whole animal and cellular/neuronal studies on lead toxicity, we should also be able to study its effects on the adult animal's well-documented learning behavior and memory storage.

This research was funded in part by NCRR-NIH grant P40-RR03820 to A.M.K. and NIH P41-RR01395 grant to P.J.S.S. We also acknowledge the Institut National Agronomique Paris-Grignon for supporting A.A., and Dr. Neal Cornell for his helpful insights.

Literature Cited

1. **Kern, M., T. Audesirk, and G. Audesirk. 1993.** *Neurotoxicology* **14:** 319–327.
2. **Leland, H. V. and J. S. Kuwabara. 1985.** Chap. 13, pp. 374–415 in *Fundamentals of Aquatic Toxicology.*
3. **Alkon, D. L. 1989.** *Sci. Am.* **261:** 42–50.
4. **Tamse, C. T., A. M. Kuzirian, C. Collin, and P. J. S. Smith. 1994.** *In Vitro Cell. Dev. Biol.—Ani.* **30A:** 57.
5. **Leibovitz, A. 1963.** *Am. J. Hyg.* **78:** 173–180.

Reference: *Biol. Bull.* **187:** 252–253. (October, 1994)

***Hermissenda crassicornis* Larvae Metamorphose in Laboratory in Response to Artificial and Natural Inducers**

Conxita Avila, Adel Arigue, Catherine T. Tamse, and Alan M. Kuzirian (Marine Biological Laboratory)

Hermissenda crassicornis (Eschscholtz, 1831), an opisthobranch mollusc used as a model in neurobiological studies, is being cultured in our laboratory. A major aim in opisthobranch mariculture is to increase the rate and survival of metamorphic veliger larvae to juvenile slugs. Several authors have reported on the effects of natural and artificial substances that have induced opisthobranch larvae to metamorphose (1, 2, 3, and refs. in 3). Therefore, to improve the rate of metamorphosis in *Hermissenda,* we have tested the efficacy of the following putative inducers: L-glutamic acid, magnesium chloride, biofilms, and aqueous extracts of whole, or parts of, the hydroid *Tubularia crocea,* the natural inducer currently used in our laboratory (4).

Hermissenda larvae were obtained from our laboratory cultures. Competent larvae were obtained by standard culture methods (4). *Tubularia* was provided by the Marine Resources Department of the Marine Biological Laboratory. For each treatment listed in Table I, two replicate 50-ml tubes containing 30 larvae each (45 days old) were prepared with filtered seawater (FSW, mesh: 0.2 μm), EDTA (0.25 mg/l), and microalgae (as food) (4). The tubes were held in bottles and rotated in a roller-bottle system at 12°C. Negative controls received no additional treatment; positive controls had 3–4 polyps and stalks of *Tubularia* added. Whole or selected portions of *Tubularia* (amounts equal to the positive control) were homogenized in 3 ml of FSW to prepare aqueous extracts, that were added either full strength or diluted 50%. Biofilms were naturally grown on slides kept in running seawater for one month. Larvae were exposed to one of the treatments for 10 days. Subsequently, they were all changed to FSW (with EDTA and algae), plus *Tubularia* to (1) feed the metamorphosed juveniles, and (2) to test the metamorphic competency of those larvae that failed to respond to the initial treatment regime.

Each potential inducer, its concentration, and its metamorphic success rate are listed in Table I. The minimum latency before the onset of metamorphosis was 4 days. Some spontaneous metamorphosis did occur in the negative controls, at a higher than expected rate. Isolated *Tubularia* polyps did not induce

Table I

Responses of larvae of Hermissenda crassicornis *to natural and artificial putative inducers of metamorphosis*

Treatments	Maximum % of metamorphic success[f] 1st part[a] (days 0–10)	 2nd part[a] (days 11–19)
Negative control[b]	3.34	3.34
Positive control[b]	5	1.67
Polyps[c]	0	1.67
Stalks[c]	11.67	10
Tubularia extract[d]	0	0
Tub. extr. 50% dilution	0	0
Polyps extract	0	0
Pol. extr. 50% dilution	1.67	3.34
Stalks extract	0	0
St. extr. 50% dilution	1.67	0
Biofilms[e]	3.34	1.67
$MgCl_2$ (20 m*M*)	0	8.34
$MgCl_2$ (40 m*M*)	0	5
L-Glutamic acid (10^{-3} *M*)	3.34	6.7
L-Glutamic acid (10^{-4} *M*)	8.34	8.34
L-Glutamic acid (10^{-5} *M*)	3.34	6.7

[a] During the first part of the experiment (days 0–10), larvae were exposed to inducers; during the second part (days 11–19), larvae and juveniles were maintained in the absence of treatments, but with *Tubularia.*

[b] Negative controls contained FSW (mesh: 0.2 μm), EDTA (0.25 mg/l), and microalgae. Positive controls had 3–4 polyps and stalks of *Tubularia*/tube.

[c] Same amounts respectively as positive controls.

[d] Aqueous solutions were prepared by homogenizing 3–4 polyps and/or stalks of *Tubularia* in 3 ml of FSW.

[e] Biofilms consisted of natural floral/faunal growth on glass slides kept in running seawater for one month.

[f] Increased percentages listed in Part 2 include juvenile survival from Part 1; decreased numbers reflect juvenile death.

metamorphosis, but stalks alone did, giving a high percentage (10–12%) of metamorphic success compared with the normal success rates (5% in the positive control; see also ref. 2). A decrease in larval mortality due to predation by full-sized, mature polyps is the putative explanation for this result. Also, the small regenerating polyps on the stalks were easily eaten by juveniles, which increased their survival. Aqueous extracts of whole *Tubularia* failed to induce metamorphosis, even when diluted. Diluted extracts of polyps or stalks alone gave small yields. These results indicate either that a greater dilution is needed, or more likely, the chemical cue is not present in the aqueous extract. Biofilms, which induce metamorphosis in other molluscs (3, 5, and refs. therein), gave smaller results than the positive controls.

Magnesium chloride alone had no inducing activity (no juveniles were obtained during the first part of the experiment), but it clearly enhanced the induction by *Tubularia* added during the second part of the experiment (8.34% at 20 m*M*). This is comparable to the effect of potassium and other monovalent cations which have also been reported to be inducers for other molluscs (6, 7, 8, and refs. in 8). Glutamic acid gave high rates of induction in both the first and second portions of the experiment (maximum value of 8.34%) at an optimum concentration of 10^{-4} *M*. Glutamic acid has been reported to induce metamorphosis at 10^{-6} *M* in another nudibranch (9).

All juveniles from the treatments were healthy and behaved normally. These results will be applied to *Hermissenda* mariculture protocols to improve the rates of larval metamorphosis and the numbers of animals produced for researchers.

Financial support to C.A. (postdoctoral fellowships from the Catalan and Spanish Governments) and A.A. (Institut National Agronomique, Paris) is gratefully acknowledged. This research was supported by an NCRR-NIH grant (P40-RR03820) to A.M.K.

Literature Cited

1. **Bonar, D. B. 1976.** *Am. Zool.* **16:** 573–591.
2. **Harrigan, J. F., and D. L. Alkon. 1978.** *Biol. Bull.* **154:** 430–439.
3. **Pawlik, J. R. 1992.** *Oceanogr. Mar. Biol. Annu. Rev.* **30:** 273–335.
4. **Tamse, C. T., A. M. Kuzirian, and T. R. Capo. 1990.** *Amer. Malacol. Union Abstr.*, 56th Ann. Meeting, p. 61.
5. **Fitt, W. K., S. L. Coon, M. Walch, R. M. Weiner, R. R. Colwell, and D. B. Bonar. 1990.** *Mar. Biol.* **106:** 389–394.
6. **Yool, A. J., S. M. Grau, M. G. Hadfield, R. A. Jensen, D. A. Markell, and D. E. Morse. 1986.** *Biol. Bull.* **170:** 255–266.
7. **Eyster, L. S., and J. A. Pechenik. 1988.** *J. Exp. Mar. Biol. Ecol.* **118:** 269–279.
8. **Todd, C. T., M. G. Bentley, and J. N. Havenhand. 1991.** *J. Mar. Biol. Assoc. U. K.* **71:** 53–72.
9. **Bahamondes, I., and J. Tardy. 1988.** *Haliotis* **18:** 121–130.

Reference: *Biol. Bull.* **187:** 253–254. (October, 1994)

Ionic Fluxes During Wound Healing Following Segment Amputation in Sabellid Fanworms

Susan Douglas Hill (Department of Zoology, Michigan State University),
Alan M. Shipley, and Peter J. S. Smith

Sabellid fanworms (Annelida, Polychaeta) are well known for their ability to undergo extensive regeneration following segment amputation. A new head or tail can be regenerated at virtually any level of the body; thus, if a worm is transected into many fragments, many worms, with all body parts complete, result. The early signals of injury in regenerating animals are virtually unknown. Because the replacement of lost parts in fanworms is very precise and quite rapid, these animals may be good models with which to investigate events that initiate the regenerative process.

During limb regeneration in urodele amphibians, ionic currents, highest shortly after amputation and persisting until blastema formation, have been measured (1). More recently, ion fluxes have been measured in association with the sealing mechanisms of transected giant axons of squid and earthworms (2). We reported previously that ionic fluxes occur during wound closure and healing in sabellid fanworms. Using a one-dimensional vibrating probe system, we have measured a strong, transient, inward current immediately following segment amputation. This inward current was rapidly replaced by a persistent outward current that reached a peak about an hour after amputation (3).

We used the noninvasive two-dimensional vibrating probe assembly (4, 5) to investigate the currents associated with wound healing following amputation of anterior segments in sabellids. Portions consisting of 15 to 20 abdominal segments were isolated from each worm. Measurements were made at the anterior wound site. The configuration of an isolated fragment changes with time. Immediately following transection, tissue debris is lost from the injured somite. This is accompanied by a muscular contraction around the amputation site. The resulting wound area becomes quite concave, with the exception of the gut, which protrudes centrally. Because of the constriction of the body wall, the wound surface is reduced, becoming partially covered with old epidermis. Our goal was to determine the pattern of net ionic flux during wound closure and to investigate the relative contributions of different tissues following transection. Because of the complexity of the wound surface, we have measured voltage gradients in both horizontal and vertical planes.

The probe consists of an insulated wire electrode with an exposed tip of platinum black that responds, relative to a reference electrode, to voltage gradients produced by steady-state ion fluxes. Each probe was independently calibrated against a KCl-filled, current-passing, glass microelectrode. All measurements were made in Millipore-filtered seawater.

By 1 h after amputation, high outwardly directed currents were associated with the severed tissues (Fig. 1). Muscles of the body wall generated high currents. The cut wall of the gut pro-

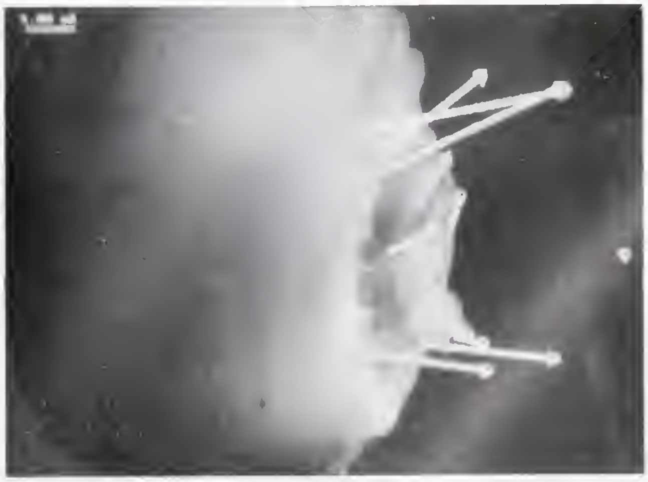

Figure 1. *Sabellid fanworm transected 1 h previously showing outwardly directed currents from cut surface. (Scale bar is 5 $\mu A/cm^2$)*

duced considerable flux. The ventral nerve cord is surrounded by muscle in sabellids. Currents associated with it could not be separated from those generated by the muscle masses. With time, as the body wall contracted, the surface area over which outward voltage gradients could be measured became more restricted. Inward currents were detected over the intact epidermis adjacent to the wound site.

The resulting current pattern is complex. Our results are consistent with the hypothesis that strong positive currents leave most or all of the severed tissues, resulting in a net outwardly directed flux from the wound site and that currents return through the adjacent epidermis and, at times, through the gut lumen.

This work was supported by NIH grant P41RR01395 to the National Vibrating Probe Facility, Marine Biological Laboratory, Woods Hole, MA.

Literature Cited

1. **Borgens, R. B., J. W. Vanable, Jr., and L. F. Jaffe. 1977.** *PNAS* **74:** 4528–4532.
2. **Krause, T. L., H. M. Fischman, M. L. Ballinger, and G. D. Bittner. 1994.** *J Neurosci.* (in press).
3. **Hill, S. D., A. M. Shipley, and P. J. S. Smith. 1993.** *Biol. Bull.* **185:** 303–304.
4. **Scheffey, C. 1988.** *Rev. Sci. Instrum.* **59:** 787–792.
5. **Jaffe, L. F., and R. Nuccitelli. 1974.** *J Cell Biol.* **63:** 614–628.

Reference: *Biol. Bull.* **187:** 254–255. (October, 1994)

Experimental Disinfection of Lobster Eggs Infected with *Leucothrix mucor*

Terrie J. Sadusky and Robert A. Bullis (Laboratory for Marine Animal Health, Marine Biological Laboratory, University of Pennsylvania)

The eggs of berried female lobsters delivered to the Massachusetts State Lobster Hatchery from offshore fishing vessels occasionally show signs of discoloration and swelling. Microscopic examination of eggs revealed active infections by the filamentous bacterium *Leucothrix mucor* (1), later confirmed by differential growth patterns on specialized media (2). Lobsters are presumably exposed to the pathogen during transport, when they are held with *Cancer* crabs under crowded, unrefrigerated conditions. Increased water temperature and high nutrient loading are known to promote the rapid growth of *Leucothrix* (3).

Microbial fouling can be detected in the egg mass through discoloration of the eggs, which swell and become opaque and change from dark green or gray to pink, orange, or yellow. In most cases, the initial infection occurs in the interior of the egg mass and then spreads outward in all directions.

To identify a reliable means of control, infected lobster eggs were removed by gentle teasing with forceps and collected in sterile seawater at room temperature (≈25°C). Infections were confirmed by microscopic examination at 5×. Three eggs were placed in each well of a 48-well culture plate and exposed to solutions of 0.1, 0.5, 1.0, 5.0, 10.0, and 50% chlorine bleach in sterile seawater for periods of up to 1 h. At 5-min intervals, eggs were removed and transferred to solid medium (2), then checked after 24 h for the presence of typical colonies. Unsterilized seawater and deionized water were added to solid medium as controls; both were supporting bacterial growth by 24 h. All solutions of chlorine suppressed growth at 24 h. The 0.1% bleach solution

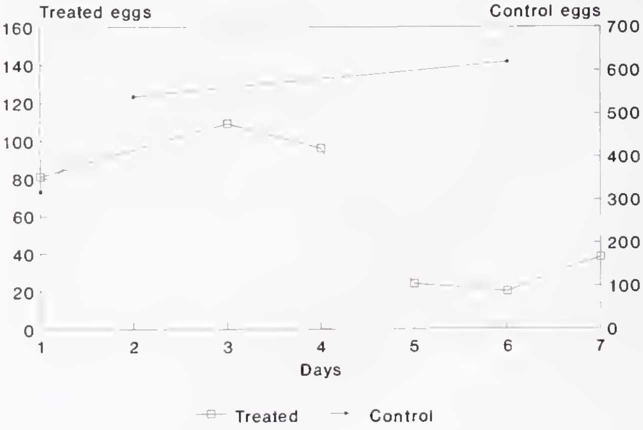

Figure 1. *The number of lobster eggs infected with* Leucothrix mucor *over time. All the eggs of control animals were dead by day 6. Treated animals continued to successfully hatch eggs for up to 10 days post treatment*

allowed a breakthrough in growth after 48 h, but the remaining cultures were still free of bacteria after 7 days.

A 5-min exposure to 5% bleach was selected for *in vivo* testing. The abdomens of three infected lobsters were exposed by manually suspending the animals in the solution. Lobsters with similarly sized infections served as controls. Figure 1 shows a typical response. The incidence of infection in untreated control animals continued unabated until the entire egg mass was destroyed by day 6. Infection was suppressed in treated animals for several days, after which the bacteria once again began to spread. Treated animals exhibited no signs of irritation at the treatment, and the uninfected eggs in all experiments hatched normal healthy spawn over the ensuing week.

Dilute chlorine solutions are effective in controlling the spread of *Leucothrix* infections in the lobster. We recommend that lobsters suspected of carrying *Leucothrix* infection be given an initial treatment upon their arrival at a holding facility, and a follow-up treatment at day 5. This appears to be a safe, cost-effective therapy.

The authors thank Michael J. Syslo of the Massachusetts State Lobster Hatchery and Research Station and Elizabeth Wadman for their assistance with this project.

Literature Cited

1. **Fisher, W. S., E. H. Nelson, J. F. Steenbergen, and D. V. Lightner. 1978.** Microbial diseases of cultured lobsters: a review. *Aquaculture* **14:** 115–140.
2. **Brock, T. D. 1989.** Pp. 2121–2124 in *Bergey's Manual of Systemic Bacteriology, V.3.*, J. T. Staley, ed. Williams & Wilkins, Baltimore.
3. **Johnson, P. W., J. M. Sieburth, A. Sastry, C. R. Arnold, and M. S. Doty. 1971.** *Limnol. Oceanogr.* **16:** 962–969.

Reference: *Biol. Bull.* **187:** 255–256. (October, 1994)

Microsporidian Spore Invasion Tubes as Revealed by Fluorescent Probes

Earl Weidner, S. B. Manale, S. K. Halonen, and J. W. Lynn (Department of Zoology and Physiology, Louisiana State University, Baton Rouge, LA)

Microsporidian protozoa are intracellular parasites common in arthropods and fish. The novel feature of these parasites is the extrusion apparatus of the spore stage. The central component of the apparatus is the polar filament, which consists of a membrane-bound paracrystal coil of protein (1). When the spore discharges, the polar filament converts into an invasion tube through which the spore injects a host cell to initiate an infection (2). In this investigation, we use video imaging to examine the extrusion of the spore invasion tube and also apply differential interference contrast optics (DIC), fluorescent probes, and standard electron microscopy. Diamidophenylindole (DAPI) and diethylaminobenzophenoxazine (Nile red) were selected to distinguish specific components within activated microsporidian spores: DAPI showed the position of the nucleus in discharging spore tubes; and Nile red provided an intense fluorescence, which enabled us to follow spore membrane movement during the formation of the tube.

Nile red fluorescence was intense during membrane discharge through invasion tubes, but this fluorescence was diminished once the membrane had emerged at the tip of the tube as a sac (Fig. 1A). Video analysis showed that at the onset of spore discharge the Nile red fluorescence was highest at the distal end of the emerging tube. Ultrastructural observations showed that these tubes had double-membrane cylinders at the distal ends. Fully extended discharged tubes appeared to have cylinders with only a single membrane. Those discharged spores with extruded sporoplasms had invasion tubes with no membranes.

The DNA fluorophore, DAPI, labeled the nuclear component of activated spores. Using DIC imaging with DAPI fluorescence, we observed nuclear movement in association with the reformation of the invasion tube and the emergence of the sporoplasm sac. Sporoplasm sacs did not appear at the tube ends until the latter had reached a maximum length of 70 μm, and the spore nucleus did not begin to traverse the tube until almost all of the

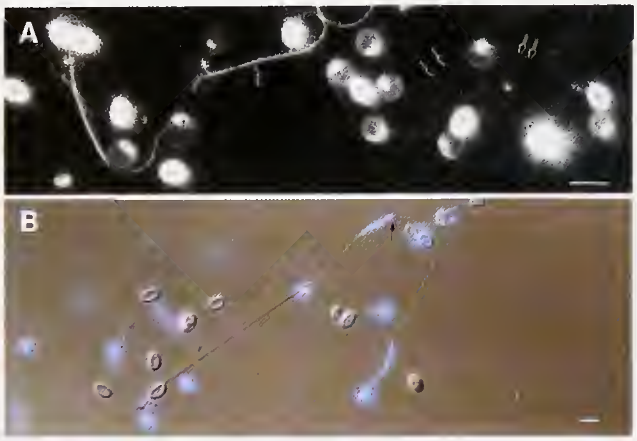

Figure 1. *Light optics showing discharging* Spraguea lophii *spores. (A) Nile red labeling of extruded sporoplasms (large spheres) and incompletely extruded invasion tubes (single arrow). The invasion tube with two arrows lacks fluorescence, probably because the membrane is absent. (B) DAPI with DIC imaging. The nuclear component, indicated by blue fluorescence, is confined to spores until most of the invasion tube has emerged. Note that in one invasion tube, the nucleus is at the end of the tube, but the sporoplasmic sac has not emerged (arrow); another invasion tube shows an emerged sporoplasm sac with the nucleus entering the sac. In a few instances, sporoplasm sacs were observed to have emerged fully at the ends of invasion tubes but with the nucleus still midway in the tube. Bar indicates 5 μm.*

discharged tube had emerged from the spore. In 1–2% of the discharged spores with extruded sporoplasm sacs, the nuclei were still within the invasion tubes (Fig. 1B).

The fluorescence data support a developing model that the membrane-bound polar filament of the discharging spore everts, with membrane sliding on membrane, as the inner cylinder delivers polar filament protein to the tube tip and the protein stabilizes into an outer polymer. When all of the invasion tube protein is assembled, the remaining membrane continues to slide out and contribute to the sporoplasmic sac at the end of the tube. The sporoplasm seems, characteristically, to enter the sporoplasmic sac milliseconds after the emergence of the sac membrane from the tube tip.

Literature Cited

1. **Weidner, E. 1976.** *J. Cell Biol.* **71:** 23–34.
2. **Unden, A. H. 1990.** *J. Theor. Biol.* **142:** 223–235.

Reference: *Biol. Bull.* **187:** 256. (October, 1994)

Neural Network with Embedded Oscillators

Vladimir Makarenko (Institute for Mathematical Problems of Biology,
Pushchino, Moscow Region, 142292, Russia)

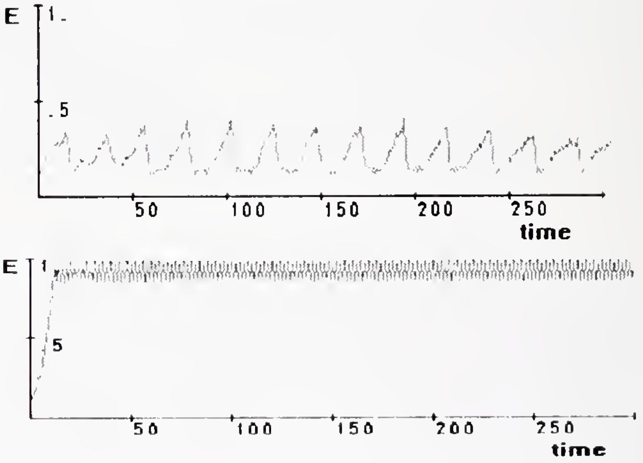

Figure 1. *Two main modes of activity in the network when connection strength is strong enough to excite surrounding neurons. Time is given in steps. E = fraction of excited neurons in the network. (Top) The weak periodicity produced by propagation of waves of excitation. The back slopes and minima correspond to the annihilation of the wave. Increase in the strength of connections leads to decrease of amplitude of oscillations. (Bottom) The fully synchronized mode corresponding to strong connections. There are no waves; the whole network is oscillating. Activity is presented by two stable antiphase configurations.*

In the present work I have focused on some aspects of the dynamics of a simulated neural network consisting of excitatory neurons with a small number of embedded endogenous oscillators. The main purpose was to see what kind of local and overall dynamics such a network could have if it contained no explicit inhibitory input. Networks with embedded pacemakers are quite common in biological neural systems, and also quite common are the difficulties that arise when electrophysiological data only are taken as the basis for understanding the dynamical processes in the network (1).

The model network consisted of 30 × 30 modulated neurons of the fire-and-integrate type. The neurons were placed in the nodes of a rectangular lattice with absorbing borders, and every neuron had equivalently strong interconnections with eight nearest neighbors. Five pacemakers, scattered over the network, worked synchronously; they were connected unidirectionally to eight nearest neurons.

Every simulation started with no neurons being excited except for the pacemakers. Around every pacemaker an induced wave of excitation appeared and propagated radially over the network. In general, the dynamics of the network were very complex, but depending on the strength of the interneural connections, the network had two main modes of behavior: periodic and fully synchronized. The weak periodicity of the overall activity was at least one order of magnitude greater than the period of the pacemakers (see Fig. 1a). The fully synchronized mode replaced the weakly periodic behavior as the strength of connections were increased. The connection strength required for the fully synchronized mode does not occur naturally in normal biological systems (Fig 1b). The particular feature that emerged was that the colliding waves were annihilated; thus the pacemakers supplied the network with a natural self-inhibition. This phenomenon was observed throughout the physiologically reasonable range of parameters.

In summary, the embedded oscillators caused the whole network to exhibit overall periodical activity; meanwhile the local activities in the different regions of the network were not correlated. Annihilation of the colliding waves is a phenomenon well studied in computer models of heart muscle (2) but not in model neural networks. Indeed, this could be the mechanism that protects the pacemakers from interferance and thus provides stability to the given mode of dynamics. In addition, the phenomenon imposes borders of "influence" on the particular pacemaker and self-inhibition in the network.

Supported by a fellowship from the James S. McDonnell Foundation.

Literature Cited

1. **Shepherd, G. M., ed. 1990.** *The Synaptic Organization of the Brain.* Oxford University Press, Oxford.
2. **Biktashev, V. N. 1991.** Propagation of autowaves in excitable media, preprint, Russian Academy of Sciences, Pushchino (in Russian).

Reference: *Biol. Bull.* **187**: 257–258. (October, 1994)

Operational Properties of Voltage-Clamped Electroreceptive Ampullary Organ Excised from *Raja*

Jin Lu (University of Texas Medical Branch at Galveston) and Harvey M. Fishman

The extraordinary ability of elasmobranch fishes to respond behaviorally to very weak electric fields (10 nV/cm) (1) is thought to be due to the properties of the electroreceptive organ, the ampulla of Lorenzini. We report here the operational voltage range of an isolated organ based on the afferent nerve activity for small voltage (microvolt) clamps of the ampullary epithelium and the stimulus amplitude range for a linear response of the ampullary epithelium.

An ampullary organ consisting of a 3-cm length of canal with ampulla, innervated by a 5-mm length of afferent nerve, was excised from live, anesthetized skates (*Raja erinacea* and *Raja ocellata*). The excised organ preparation was placed in a chamber and solutions similar to those described previously by Clusin and Bennett (2). Voltage control of the organ was implemented with an epithelial voltage-clamp system (3) connected to four chlorided-silver pellet electrodes. To voltage clamp the ampullary epithelium, we placed the tip of a long, tapered, electrolyte-filled pipette near the lumenal surface of the ampulla and used it to input the trans-ampullary voltage (referenced to the basal side) to the clamp system. All experiments were carried out at room temperature (20–22°C).

To determine the operational response of an isolated organ, the signal transfer characteristic from ampullary epithelium to afferent nerve (Fig. 1A) was determined during 0.5-s duration voltage clamps of the ampullary epithelium. The spike firing rate of the nerve relative to the resting rate (at holding potential of 0 mV), for lumen positive and negative voltage clamps, decreased and increased, respectively. The transfer characteristic curve was sigmoidal (Fig. 1A) with a change in spike rate discernible for clamp steps as small as 3 μV, in agreement with previous studies of organs in animals (4, 5) and of isolated organs (6); the spike rate for clamp steps that exceeded 100 μV was saturated. The sensitivity of an ampulla to trans-ampullary voltage also was reflected in the steep slope (1.05 Hz/μV ± 0.22 SD, $n = 3$) of the transfer curve at 0 mV.

To assess the linear range of ampullary responses, we used spectral analysis to determine the amplitude of harmonics generated in the trans-ampullary current in response to trans-organ voltage clamps to a 0.5-Hz sinusoidal waveform. Preparations gave linear responses (Fig. 1B; the rms value of all harmonics was <1% of the rms value of the fundamental) in the range from 7 to 200 μV rms. Significant nonlinearity (harmonic content of

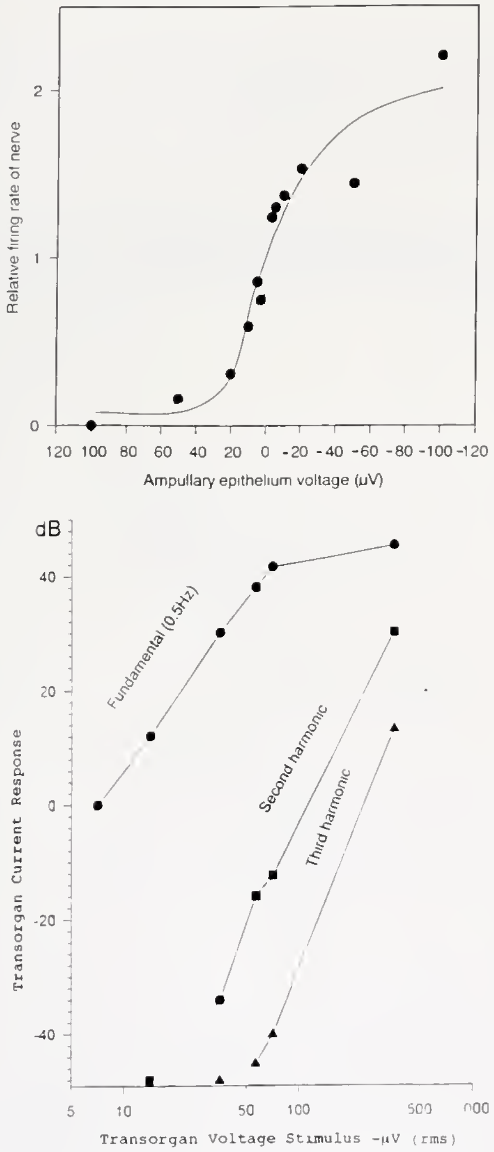

Figure 1. *(Top) Transfer characteristic of an isolated ampullary organ from skate. The firing rate of the afferent nerve innervating the preparation relative to the resting firing rate is plotted in response to trans-ampullary voltage clamps from 0 mV holding potential (HP). To minimize effects due to adaptation (4) and drift of electrodes, the nerve spike firing rate was determined during 0.5-s duration voltage clamps of the ampullary epithelium. The resting firing rate (30–40 Hz) for each data point was determined at the HP (0 mV) in the 0.5-s interval preceding the 0.5-s duration step clamp. Note that excitatory afferent nerve activity occurs for trans-ampullary voltage <0 (i.e., lumenal side of ampulla negative with respect to the basal side). The solid curve is a best fit to the data of a logistic function* $[-1.98/(1 + \exp(.26(V + 22)))^{11} + 2.1]$. *(Bottom) Harmonics generated by an isolated ampullary organ voltage clamped at an HP of 0 mV. Trans-organ current was recorded in response to various amplitudes of 0.5-Hz sinusoidal voltage superposed on the HP. The generation of significant harmonics (second and third) relative to the amplitude of the fundamental (0.5 Hz) is indicative of nonlinearity that became significant (10% of fundamental) above 500 µV. The total harmonic content relative to the fundamental in the response of this organ was <1% for stimuli <100 µV rms.*

10% or more) was observed for sinusoidal stimuli in excess of 500 μV rms.

Our voltage-clamp transfer data indicate that high sensitivity in the microvolt range is a property of an *isolated organ preparation*. Further, we find that the afferent nerve firing rate saturates for epithelial voltages that exceed 100 μV. Together with our harmonic analysis, these data suggest that the ampullary epithelium behaves as a linear transducer over the operating range of the afferent nerve.

Supported by ONR (N00014-90-J-1137) to H.M.F.

Literature Cited

1. **Kalmijn, A. J. 1982.** *Science* **218:** 916–918.
2. **Clusin, W. T., and M. V. L. Bennett. 1977.** *J Gen. Physiol.* **69:** 121.
3. **Fishman, H. M., and R. I. Macey. 1969.** *Biophys. J.* **9:** 127–139.
4. **Murray, R. W. 1962.** *J Exp. Biol.* **39:** 119.
5. **Bodznick, D., G. Hjelmstad, and M. V. L. Bennett. 1993.** *Jpn. J. Physiol* **43, Suppl 1:** S231–S237.
6. **Clusin, W. T., and M. V. L. Bennett 1979.** *J. Gen. Physiol.* **73:** 685–702.

Reference: *Biol. Bull.* **187:** 258–259. (October, 1994)

Directional Sensitivity of Saccular Afferents of the Toadfish to Linear Acceleration at Audio Frequencies

Richard R. Fay, Peggy L. Edds-Walton, and Stephen M. Highstein (Marine Biological Laboratory)

Hair cells are physiologically polarized and respond to deflection of their stereocilia in a directional manner (1). These cells are organized in various orientations on the otolithic endorgans of fishes. Otolithic endorgans respond to linear accelerations of the head with the otolith providing an inertial restraint for hair cell stereocilia. In many fishes, at least one of the otolithic endorgans, the saccule, also responds to acoustic particle motion (2). We investigated whether the saccule's response to particle motion could mediate the detection and localization of sound sources in the toadfish (*Opsanus tau*). Both male and female toadfish produce vocalizations in social contexts, and males produce courtship calls to attract females.

Rostral saccular afferents were recorded extracellularly during linear oscillations of the head at 50, 100, and 200 Hz. The animal's head was fixed in a rigid, water-filled dish, 23 cm in diameter and 8 cm high. The dish was accelerated by two orthogonal pairs of electrodynamic shakers in the horizontal plane, and one shaker oriented vertically. Computer-synthesized sinusoids activated the shaker channels with relative phases and amplitudes that were required to produce linear motion along six azimuthal axes spaced equally from 0 to 150°. Three orthogonally oriented accelerometers were used in the calibration of the dish's motion in azimuth and elevation prior to each experiment. Only male toadfish were used for the work reported here.

Because 95% of afferents phase-locked to sinusoidal motion, response magnitude (Z) was quantified as product of the square of the coefficient of synchronization and the number of spikes evoked. A "Z" of 20 was used to compare thresholds across stimulus angles [probability of random phase-locking <0.001 (3)]. For each axis of motion, the displacement threshold was plotted in polar coordinates (Fig. 1A). For all afferents studied in four animals ($n = 23$), the thresholds tended to fall on a line. The length of the vector orthogonal to the threshold line and passing through the origin defined the minimum threshold, and its angle defined the best azimuth. A threshold to vertical motion was used to estimate elevation. In polar coordinates, a linear threshold-function is equivalent to the circular (cosine) sensitivity-function characteristic of hair cells (1). The directionality observed in saccular afferents indicates that each innervates a single hair cell or a group of hair cells having similar directional orientations.

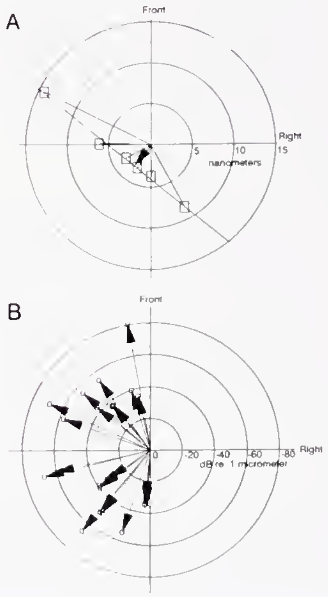

Figure 1. *(A) Illustration of directional and sensitivity determination for one afferent (11). In polar coordinates, the threshold (displacement corresponding to $Z = 20$) is plotted in the horizontal plane for six axes of motion at 100 Hz (open squares). The least-squares best fitting line through the thresholds accounts for 99% of the variance. The vector's length is the best threshold (3.3 nm), and its azimuth is 141° from straight ahead. (B) Maximum sensitivity vectors for 23 saccular afferents from left ears. The radial axis is in dB with respect to 1 μm. There is an essential 180° ambiguity for each vector due to the back-and-forth nature of the displacement stimuli; all vectors were plotted to the left arbitrarily.*

Thresholds were lowest at 100 Hz (0.1 to 35 nm). At 100 Hz, a displacement of 0.1 nm corresponds to the acoustic particle motion in the farfield accompanying the sound pressure at behavioral threshold for the toadfish (4). Best azimuths were widely distributed over 180° (Fig. 1B), and elevations were less than 50° above or below the horizontal plane.

Directionality and displacement sensitivity of saccular afferents in toadfish are similar to those in goldfish, except that all saccular afferents in goldfish have very similar azimuths (2). The wider variation in best azimuths among toadfish afferents probably arises from the relatively more diverse patterns of hair cell orientations within the toadfish saccule (5).

Our results indicate that toadfish could determine the axis of acoustic particle motion by analyzing the patterns of activity across populations of saccular neurons that are "labeled" according to their best directions.

Supported by Program Project Grant #1PO1DC018737 from NIH, NIDCD.

Literature Cited

1. **Flock, A. 1965.** *Acta Otolaryngol.* **Suppl. 199:** 1–90.
2. **Fay, R. R. 1984.** *Science* **225:** 951–953.
3. **Batschelet, E. 1981.** Pp. 54–58 in *Circular Statistics in Biology.* Academic Press Inc., New York.
4. **Fish, J., and G. Offutt. 1971.** *J. Acoust. Soc. Am.* **51:** 1318–1321.
5. **Edds-Walton, P. L., and A. N. Popper. 1995.** *Acta Zoologica* (in press).

Reference: *Biol. Bull.* **187:** 259–260. (October, 1994)

Time Course of Recovery from Adaptation by Hydroxyproline-Sensitive Lobster Olfactory Receptor Neurons

George Gomez and Jelle Atema (Boston University Marine Program, Marine Biological Laboratory)

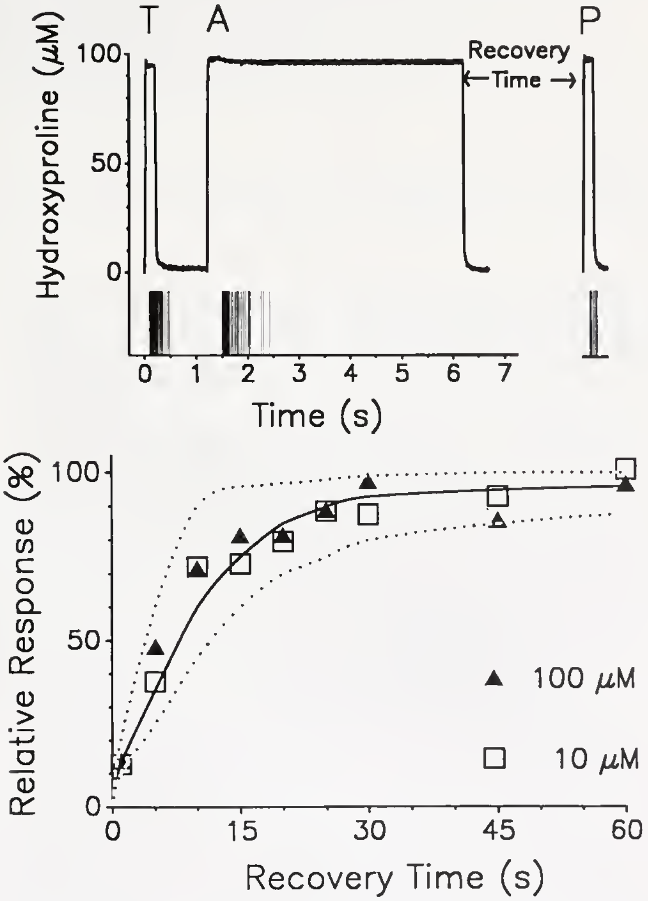

Figure 1. *(A—Top) Odor pulse series used in the experiment. Top portion of each graph shows an example of the on-line stimulus recording, while lower portion of each graph shows corresponding spike events from a single cell. T, 200-ms test pulse; A, 5-s adapting pulse; P, 200-ms probe pulse. Recovery times used for each cell were 1, 5, 10, 15, 20, 25, 30, 45, and 60 s. For this graph, the recovery time was 15 s. Each three-pulse series was presented at random and separated by at least 90 s. Within one cell, responses to the test pulse varied by 15% and showed no systematic decrease over the time of the experiment. All responses were phasic; the 100-ms time bin that had the maximum number of spikes usually started at the first to third spike of the response. (B—Bottom) To determine the time course of disadaptation of the cell population at both stimulus concentrations, averaged responses to the probe pulses (maximum number of spikes in 100 ms) were expressed as a percentage of the average of the immediately preceding test pulse response. Solid line shows an exponential curve fit that is identical for both concentrations. Although absolute response magnitudes to 100 µM pulses were greater than to 10 µM pulses, recovery time courses were identical. Dotted lines show the fastest and slowest recovery curves obtained from individual cells. Based on recovery rates of the single cells, we found no distinct subclasses of receptor cells.*

Natural turbulence breaks up odor released from a source into smaller and smaller patches. As patches travel away from the source, they form a spatial gradient of sizes and shapes that can be measured by chemoreceptor organs as temporal features of concentration pulses (1). The adaptation and disadaptation characteristics of chemoreceptor cells determine the temporal information that the animal can extract (1). Thus an understanding of these properties may help us understand how chemoreceptor cells mediate chemotaxis. The current study focused on the time course of disadaptation (recovery from adaptation) of chemoreceptor cells of the antennular lateral filament, an appendage known to mediate distance orientation in the lobster, *Homarus americanus.*

Details of the methods are found elsewhere (2, 3). Briefly, lateral antennules from intermolt lobsters were excised and situated in an olfactometer. We used precise focal stimulation techniques and monitored each stimulus presentation on-line with a high-resolution electrochemical probe to ensure stimulus replicability and odor pulse separation. Pulse series that were unacceptable (*i.e.*, pulse height varied by more than 10%) were discarded and repeated. Receptor cells were stimulated with odor steps of 10 and 100 μM hydroxyproline (Fig. 1A). The receptor cells were allowed to recover for at least 90 s between each stimulus series. Cell responses were quantified by the total number of spikes and by the maximum number of spikes in any 100-ms time period within a response.

Fifteen receptor cells survived the entire stimulus protocol and were used for data analysis. Cells responded to 10 and 100 μM test pulses with brief bursts of 12.4 ± 7.3 and 16.6 ± 6.6 spikes, respectively. Responses to the adapting pulse were phasic and terminated even when the odor was still present, indicating that the receptor cells completely adapted to the stimulus. After a 1 s recovery time, only 30% of the receptor cells responded to the probe pulse. When given a longer recovery time, individual receptor cells regained their sensitivity at different rates. After 30 s, all receptor cells recovered 90% of their original response; the magnitude of the probe pulse responses was not significantly different from the test pulse response magnitude ($P < 0.05$, paired t-test) for both stimulus concentrations used.

To assess the time course of recovery of the cell population, we compared the mean response values of the 15 cells for test and probe pulses (Fig. 1B). Responses fully recovered within 25 to 30 s; beyond 30 s, responses did not significantly increase. Surprisingly, the time course of recovery was the same for both stimulus concentrations.

Although full recovery took 30 s, cells regained 50% of their sensitivity within 9 s. Hydroxyproline-sensitive cells can follow 2 Hz pulse trains (3). It is the time course of recovery from adaptation that integrates odor events and sets the high frequency limit of the system for detection of the spectrum of odor concentration fluctuations that occurs in an odor plume.

This work was supported by NSF IBN 9222774 to J.A.; this study is part of the dissertation research of G.G.

Literature Cited

1. **Atema, J. 1987.** Pp. 303–316 in *Comparative Physiology: Life in Water and on Land*, P. Dejours, *et al.*, eds. IX-Liviana Press, Padova.
2. **Gomez, G., R. Voigt, and J. Atema. 1992.** *Biol. Bull.* **183:** 353–354.
3. **Gomez, G., R. Voigt, and J. Atema. 1994.** *J. Comp. Physiol. A* **174:** 803–811.

Reference: *Biol. Bull.* **187:** 260–261. (October, 1994)

Visual Responses in the Brain of *Limulus*

C. L. Passaglia, F. A. Dodge, and R. B. Barlow, Jr. (Syracuse University)

The lateral eye of the horseshoe crab *Limulus polyphemus* is one of the best understood visual structures in the animal kingdom. Studies of the lateral eye have provided us with the concepts of adapting quantal bumps in response to the absorption of a single photon (1, 2), lateral inhibition as a mechanism of edge enhancement (3), and circadian modulation of retinal function (4) as a component of visually guided behaviors (5). We know relatively little, however, about how the brain processes retinal input for the animal to see (6, 7).

Here we report on the first intracellular recordings from the lamina, the first level of synaptic processing of retinal signals in the brain. Glass micropipettes (3.0 M KCl, 40–80 MΩ) filled with 5% Neurobiotin in 1.0 M KCl (+0.5 nA for 5 min) (8) were advanced vertically into the surgically exposed brain *in situ*. Signals from the microelectrodes were fed to a bridge amplifier and monitored with a digital oscilloscope. Light stimuli were delivered to individual receptor units (ommatidia) in the retina with a 70-μm light pipe and to large regions of the eye with a fiber optic bundle.

We frequently impale as yet unidentified cellular compartments in the lamina that receive synaptic inputs from many optic nerve fibers and action potentials from a single optic nerve fiber. Illumination of a single ommatidium in the retina generally evokes slow depolarizing potentials (0–5 mV) in association with a single train of action potentials (20–60 mV) in the compartment, whereas illumination of the entire retina elicits slow hyperpolarizing potentials (5–15 mV) and a spike train of reduced rate (Fig. 1A). Resting potentials are in the range of −45 to −60 mV. Both discharge patterns resemble those of single optic nerve fibers (9), except that the spike size can change during a response and the spike duration can be up to four times longer (not shown).

Injections of Neurobiotin into the compartment have consistently labeled more than one fiber in the optic nerve (typically

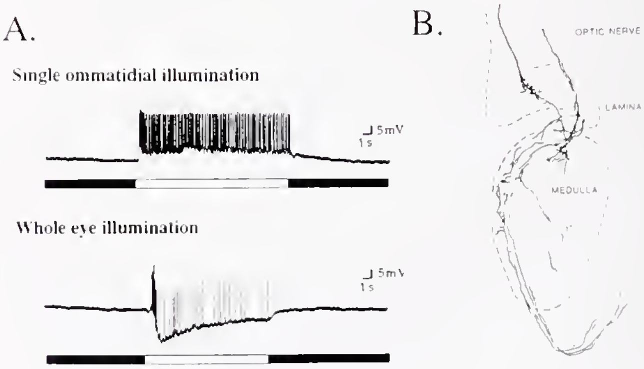

Figure 1. *(A) Recordings from a cell in the first synaptic layer of the brain (lamina). The compartment receives excitatory input from a single retinal cell and inhibitory inputs from many cells. The spike amplitude has been attenuated by the chart recorder during reproduction. (B) Camera lucida reconstruction of cell after Neurobiotin injection. Note retrograde labeling of more than one optic nerve fiber*

three), as well as processes in the lamina and medulla ($n = 10$, Fig. 1B). Previous anatomical studies with cobalt chloride showed that a single nerve fiber gives off a puff of processes in the lamina as it continues on into the medulla and other optic nuclei (10).

What is the cellular compartment we are recording from? The spike discharge and Neurobiotin staining patterns strongly suggest the axons of optic nerve fibers. However, such large slow potentials would not be expected in this compartment because the soma is located 4–5 cm away in the retina. Moreover, it is unclear why the spike size would change, spike duration would differ, and multiple axons would stain if this were the case. Hence, it appears that we are recording from synaptic compartments, presumably in the branches of optic nerve fibers, that receive action potentials from the main axon and slow potentials from other nerve fibers or cells in the brain. The differences in discharge patterns to single ommatidial and whole eye stimulation result from lateral inhibition in the retina, whereas the differences in slow potentials are a consequence of synaptic interactions in the lamina.

Neural processing in the lateral eye of the horseshoe crab is hidden from microelectrodes in the tangled web of the lateral plexus that interconnects neighboring ommatidia to mediate lateral inhibition. Neural processing in the lamina appears to use the same integrative mechanisms as the retina and may be more accessible to electrode studies. If so, we may gain an understanding of the synaptic interactions that occur across a parallel array of optic nerve fibers and their influence on the information sent to other regions of the brain.

Supported by NSF grant BNS9309539 and NIH grants MH49741 and EY00667.

Literature Cited

1. **Fuortes, M. G. F., and S. S. Yeandle. 1964.** *J. Gen. Physiol.* **47:** 443–463.
2. **Dodge, F. A., Jr., B. W. Knight, and J. Toyoda. 1968.** *Science* **160:** 88–90.
3. **Ratliff, F., and H. K. Hartline. 1974.** Pp. 245–661 in *Studies on Excitation and Inhibition in the Retina*, F. Ratliff, ed. The Rockefeller University Press, New York.
4. **Barlow, R. B., Jr. 1983.** *J Neurosci.* **3:** 856–870.
5. **Powers, M. K., R. B. Barlow, Jr., and L. Kass. 1991.** *Vis. Neurosci.* **7:** 179–189.
6. **Snodderly, D. M., Jr. 1971.** *J. Neurophysiol.* **34:** 588–611.
7. **Chamberlain, S. C., and R. B. Barlow, Jr. 1982.** *J Neurophysiol.* **48:** 505–519.
8. **Horikawa, K., and W. E. Armstrong. 1988.** *J. Neurosci. Meth.* **25:** 1–11.
9. **Hartline, H. K., and C. H. Graham. 1932.** *J. Cell. and Comp Physiol.* **1:** 227–295.
10. **Chamberlain, S. C., and R. B. Barlow, Jr. 1980.** *J. Comp. Neurol.* **192:** 387–400.

Reference: *Biol. Bull.* **187:** 261–262. (October, 1994)

Noise Components in *Limulus* Vision

F. A. Dodge, D. M. Porcello, S. A. Dodge, E. Kaplan, and R. B. Barlow, Jr.
(Marine Biological Laboratory)

As a horseshoe crab moves along the bottom of a shallow bay, its lateral eye continuously transmits a picture of its environment back to his brain. This "video picture" contains only about 40 × 25 pixels, is blurred by the wide acceptance angle of the ommatidium, and is distorted by the way the eye samples visual space nonuniformly. Within the eye, two neural inhibitory processes enhance contrast, but the net result of all the steps in neural encoding is often a very noisy image. In spite of the rather poor image quality, neural circuits in the *Limulus* brain can extract visual information to guide the animal's movements.

Unattached males during the mating season provide a particularly straightforward example of visually guided behavior; they generally turn and approach any object that is about the size of a mate. As first reported here last year (1), we can record the neural signals that the brain receives as the eye scans the same targets used in the behavioral experiments. Analysis of several such experiments has revealed that targets at a distance beyond that of the behavioral threshold elicit a perceptible modulation of spike rate (2). This result is fully consistent with theoretical computations of the expected responses (3). If the behavioral threshold cannot be explained by the sensitivity of the photoreceptors, perhaps our experimental paradigms have consistently underestimated the noise that the animal must contend with under natural conditions. We have therefore started to study how the statistical properties of the random fluctuations in spike rate depend on differing visual environments.

Two sources of noise that are intrinsic to the eye have been fully characterized; namely, the shot noise triggered by photon adsorption that is the excitatory input to the spike generator, and the summed inhibitory potential triggered by spikes in many neighbors. Because the unitary IPSP is longer than 0.5 s, it smooths nearly all fluctuations in its input and, in fact, makes only a minor contribution to the noise. The phototransduction noise can be quite large under dim ambient illumination, but decreases greatly as the eye adapts to higher illuminations. The power spectrum of this noise shows a relatively broad pass-band matching the dynamic transfer-function for sinusoidally modulated light (4). Phototransduction noise at illumination levels equivalent to the daylight field experiments (plus inhibitory synaptic noise) causes spike-rate fluctuations with a coefficient of variation (CV) of 7% or less.

As we move from the laboratory to the field experiments, we would expect to observe more noise caused by random fluctuations in light intensity. Some of the environmental noise is independent of the crab's motion. Figure 1 shows spike-rate recordings from three simultaneously active units; two (receptors 1 and 3) are probably adjacent receptors because they see the target at nearly the same time, and a third (receptor 2) looks at the sandy bottom below the target. For each spike train, we calculated the power spectrum of the spike-rate fluctuations over the 4-s span preceeding the response to the target. Each of these spectra shows a prominent quasiperiodic component at about 2 Hz and some harmonics. The noise here, CV = 16%, is more than twice that due to phototransduction alone. Cross-correlation of these records shows positive correlation of the noise for the two units that look in nearly the same direction, as would be expected for a common fluctuating source. The negative cross correlation of both of these with the other unit probably arises from the fortuitous condition that they are about half a cycle out of phase for the almost periodic component. Analyzing the video tape of this experiment, we immediately identified the source of this quasiperiodic noise as the rapidly moving bands of light concentrated by the cylindrical lens effect of waves (30-cm period, moving at 60 cm/s). These shimmering waves, little fish swimming in front of the target, and clumps of floating seaweed cause environmental fluctuations of light intensity that are independent of the animal's motion. It is hard to believe that such noise is statistically stationary, but both the magnitude and spectra remained similar over several hours of recording.

We would expect that a freely moving animal, scanning small-scale features of the environment, might generate even larger fluctuations in light intensity. We do not yet have any long recordings from a freely moving animal in the environment of the behavioral experiments. But, 20 years ago, E. Kaplan measured spike-rate fluctuations of a crab moving through weeds over the pebbly bottom of Great Harbor. He found CVs in the range of 30–120%, with spectra in which 95% of the power concentrated below 2 Hz (E. Kaplan, Rockefeller Univ., unpub.). Such large fluctuations generated by this visual "jungle" would obscure the response to a target, and this might be a partial explanation for why mating animals prefer sandy bays.

To see, *Limulus* must cope with external light noise in its environment, as well as with neural noise in its visual system. The animal minimizes endogenous photoreceptor noise at night via a circadian-clock (5); however, the phototransduction noise remains very large (6). But, during the day when the intrinsic noise is low, substantial environmental noise may require the animal to adjust in its brain the neural threshold for detecting an object.

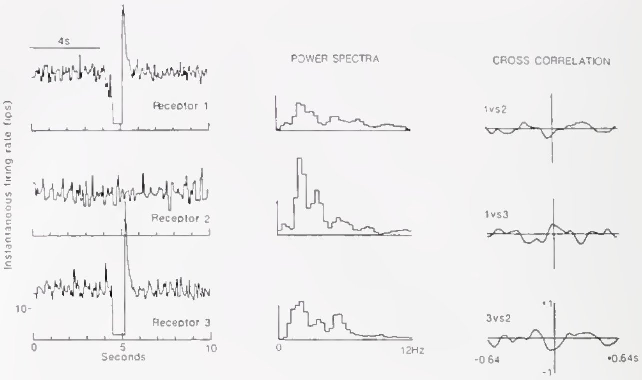

Figure 1. *Analysis of spike-rate fluctuations in each of three units recorded simultaneously in an experiment mimicking the stimulus conditions of the behavioral studies. The limulus was pulled along an underwater track past a black cylindrical target at 15 cm/s. The sample period for computing power spectra and cross correlations was 4 s long, prior to the response to the target. Power spectra with a bin width of 0.4 Hz were plotted on a common scale. Lagged product cross-correlations of all pairs of records were computed as labeled.*

Supported by NSF grant BNS9309539 and NIH grants MH49741 and EY00667.

Literature Cited

1. **Herzog, E. D., C. L. Passaglia, S. A. Dodge, N. D. Levine, and R. B. Barlow. 1993.** *Biol. Bull.* **185:** 307–308.
2. **Herzog, E. D. 1994.** Ph.D. Thesis, Syracuse University.
3. **Dodge, F. A. 1994.** *Invest. Ophthal. Vis. Sci.* **35:** 2131.
4. **Dodge, F. A., B. W. Knight, and J. Toyoda. 1968.** *Science* **160:** 88–90.
5. **Barlow, R. B., R. R. Birge, E. Kaplan, and J. Tallent. 1993.** *Nature* **366:** 64–66.
6. **Barlow, R. B., and E. Kaplan. 1977.** *J. Gen. Physiol.* **69:** 203–220.

Reference: *Biol. Bull.* 187: 262–263. (October, 1994)

The Effects of Quinine and Quinidine on Isolated Retinal Horizontal Cells

Robert Paul Malchow (University of Illinois College of Medicine), Haohua Qian, Laura M. Haugh-Scheidt, and Harris Ripps

Quinine and its stereoisomer quinidine have long been used as medicinal tonics to treat conditions as diverse as malaria, muscle cramps, and heart arrhythmias. These cinchona alkaloids also have potent effects on the nervous system in general and on the visual system in particular. High concentrations of these agents induce disorientation and blurred vision, and may even lead to acute blindness. We have used the whole-cell version of the patch-clamp technique to examine the effects of these alkaloids on enzymatically isolated retinal horizontal cells of the skate.

Consistent with previous work conducted on a variety of cell types, including cardiac myocytes and neurons, we found that quinine and quinidine block a number of voltage-gated conductances in the horizontal cells, including those selective for potassium, sodium, and calcium ions. However, these alkaloids also appeared to promote an *increase* in membrane conductance when the horizontal cells were held at potentials more positive than 0 mV. The outward current elicited under these conditions turned off rapidly upon repolarization of the cell to a holding potential of −70 mV. Tail-current analysis indicated that the alkaloid-induced current had a reversal potential very close to 0 mV. The outward current elicited by quinine and quinidine was blocked by 4 m*M* cobalt or a halothane-saturated Ringer solution, and was also reduced by acidification of the cells via the application of 25 m*M* acetate. Moreover, depolarization in the presence of quinine or quinidine permitted entry into the cells of extracellularly applied Lucifer yellow. In sum, the large, apparently nonselective nature of the conductance suggested by the tail current analysis, coupled with the block by halothane, cobalt, and acetate (agents known to suppress gap-junctional communication between cells), and the influx of extracellularly applied Lucifer yellow, have led us to suggest that the current elicited by these drugs results from the opening of hemi-gap junctional channels.

Several reports have indicated that large increases in internal calcium (*i.e.*, > 1 μ*M*) lead to the closure of gap junctions and a reduction in electrical communication between pairs of electrically coupled cells (1, 2). On the other hand, the results of recent studies suggest that gap junctions are permeant to calcium ions when intracellular calcium concentrations are below 1 μ*M* (3, 4). We have recently undertaken experiments to examine whether the conductance opened in the presence of the cinchona alkaloids is permeant to calcium. Using ratio imaging of the calcium-sensitive dye fura-2, we found that depolarizing horizontal cells in the presence of 200 μ*M* quinidine evoked a large increase in the level of intracellular calcium (Fig. 1); this increase occurred despite the presence of the calcium channel blocker nifedipine (100 μ*M*). Whether the increase in intracellular calcium results solely from the influx of extracellular calcium, or whether there is also a release of calcium from internal stores, are questions as yet unresolved. Nevertheless, our data raise the possibility that hemi-gap junctional channels are permeable to calcium ions.

This work was supported by grants (EYO6540, EYO9411, and EYO6516) from the National Eye Institute.

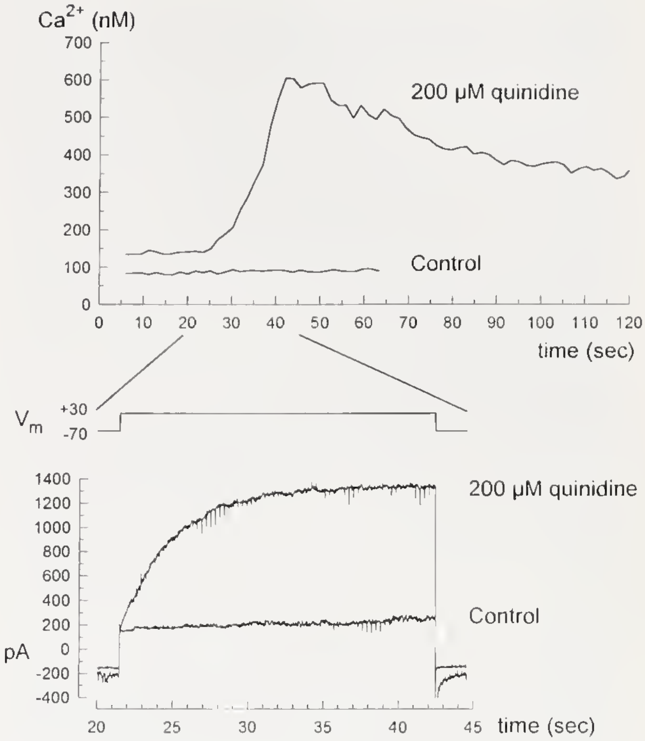

Figure 1. *Effect of quinidine on the level of intracellular calcium in a horizontal cell isolated from the skate retina. Bottom traces: Currents elicited from a skate horizontal cell in response to a 24-s voltage step to +30 mV from a holding potential of −70 mV. Measurements were made initially with the cell bathed in skate Ringer (control), and again after 1.5 min superfusion with 200 μM quinidine. The Ringer solution was supplemented with 100 μM nifedipine to block voltage-gated calcium conductances and a cocktail of compounds to reduce contributions from other voltage-gated conductances (5). Top traces: The internal calcium concentration from the same cell measured simultaneously. No increase in calcium was noted with the cell bathed in Ringer, while a large increase in calcium was detected when the quinine-induced current was activated. Two additional cells showed even greater increases in internal calcium (~ 2 μM) in the presence of quinidine; these cells also displayed small (< 200 nM) but significant rises in calcium when depolarized in control Ringer.*

Literature Cited

1. **Rose, B., and W. R. Lowenstein. 1975.** *Nature* **254:** 250–252.
2. **Spray, D. C., J. H. Stern, A. L. Harris, and M. V. L. Bennett. 1982.** *PNAS* **79:** 441–445.
3. **Saez, J. C., J. A. Conner, D. C. Spray, and M. V. L. Bennett. 1989.** *PNAS* **86:** 2708–2712.
4. **Christ, G. J., A. P. Moreno, A. Melman, and D. C. Spray. 1992.** *Am. J. Physiol.* **263:** C373–C383.
5. **Malchow, R. P., H. Qian, and H. Ripps. 1993.** *J Neurosci. Res.* **35:** 237–245.

Reference: *Biol. Bull.* **187:** 263–265. (October, 1994)

The GABA$_A$ Receptors of Müller (Glial) Cells in Skate Retina

Haohua Qian (Harvard University), Robert Paul Malchow, Richard L. Chappell, and Harris Ripps

The circuitry of the vertebrate retina is formed by interconnecting networks of neural pathways, and subtle alterations in synaptic transmission can exert profound effects on the activity of a given pathway. There is growing evidence that glial cells participate in this process through a variety of mechanisms, most notably via the uptake and metabolism of amino acid neuro-

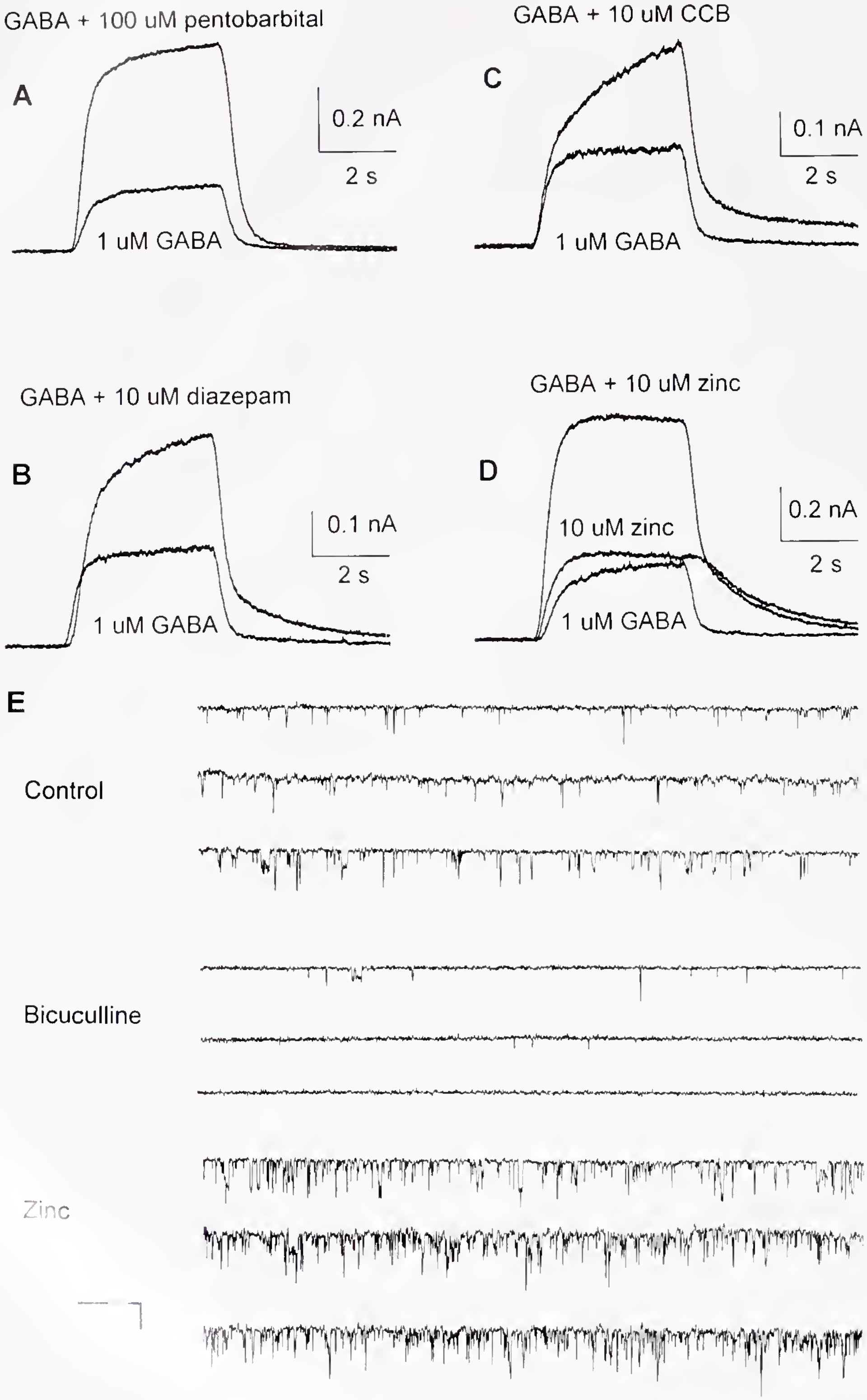

Figure 1. *Modulation of GABA responses from skate Müller cells voltage-clamped at 0 mV. (A) 100 μM pentobarbital, (B) 10 μM diazepam, (C) 10 μM n-butyl-β-carboline-3-carboxylate (CCB), and (D) 10 μM zinc enhanced the currents elicited by 1 μM GABA. Note that the application of zinc alone induced an outward current. Recordings (A)–(D) were obtained using the perforated-patch (amphotericin B) technique. (E) Cell-attached patch recordings from Müller cells voltage-clamped at −150 mV. Each trace is taken from a different cell. The upper three traces show spontaneous channel fluctuations recorded when the pipette contained a control solution consisting of 204 mM CsCl, 11 mM EGTA, 1 mM CaCl$_2$, 1 mM MgCl$_2$, 10 mM HEPES, and 360 mM urea, titrated to pH 7.6 with NaOH. The frequency of channel openings was greatly reduced by the addition of 100 μM bicuculline (middle three traces), and enhanced by the addition of 10 μM zinc*

transmitters, and by monitoring the ionic composition of the neuronal environment through the gating properties of ligand- and voltage-sensitive channels. γ-Aminobutyric acid (GABA), a principal inhibitory neurotransmitter in the CNS, is known to be involved in signal transmission in the vertebrate retina, and, as shown previously, the radial glia (Müller cells) of the skate retina are engaged in various ways in the regulation of GABA-mediated activity. For example, they take up GABA from the extracellular space (1) through the action of a sodium-dependent transporter (2), and they possess functional GABA$_A$ receptors that activate membrane chloride channels (3).

In the present study, we have attempted to characterize the GABA$_A$ receptor of enzymatically isolated Müller cells by using perforated (amphotericin B) patch recordings. The currents elicited by GABA were mimicked by the application of the GABA$_A$ agonist muscimol, suppressed in a dose-dependent fashion by the addition of the GABA$_A$ antagonist bicuculline or the chloride channel blocker picrotoxin, and potentiated by 100 μM pentobarbital (Fig. 1A) or 10 μM diazepam (Fig. 1B). The GABA$_B$ agonist baclofen failed to elicit a response. The dependence upon chloride, the block by bicuculline, the enhancement by diazepam and pentobarbital, the activation by muscimol, and the lack of effect of baclofen are consistent with the hypothesis that the GABA currents are mediated solely by GABA$_A$ receptors.

We now report pharmacological data suggesting that the modulatory sites on the GABA$_A$ receptors of skate Müller cells exhibit several unique features. First, the benzodiazepine inverse agonists methyl 6,7-dimethoxy-4-ethyl-β-carboline-3-carboxylate (DMCM) and *n*-butyl-β-carboline-3-carboxylate (CCB) enhanced the GABA-mediated responses (Fig. 1C); second, at low concentrations, zinc produced a similar enhancement of the responses to GABA (Fig. 1D). Interestingly, zinc itself induced a current comparable to that elicited by GABA: the reversal potential was the same as for the GABA current, the current was blocked by bicuculline, and the I-V relation was virtually indistinguishable from that produced by GABA. Moreover, cell-attached patch recordings (Fig. 1E) show that the spontaneous channel activity was blocked by bicuculline and increased by zinc. These findings suggest that zinc acts directly on the GABA$_A$ receptors of the Müller cells, and they raise the possibility that the subunit composition of the GABA receptor of the Müller cell differs from that of the neuronal GABA$_A$ receptors. It is noteworthy that zinc could be detected in skate photoreceptors by the Neo-Timm sulfide-silver method, and there is reason to think that it may be co-released with glutamate from the receptor terminals of the visual cells (4).

Supported by a Bernard Davis Fellowship (to H.Q.), and by grants (EY-09411, EY-00777, and EY-06516) from the National Eye Institute.

Literature Cited

1. **Ripps, H., and P. Witkovsky. 1985.** *Progr. Retinal Res.* **4:** 181–220.
2. **Qian, H., R. P. Malchow, and H. Ripps. 1993.** *Cell. Mol. Neurobiol.* **13:** 147–158.
3. **Malchow, R. P., H. Qian, and H. Ripps. 1989.** *PNAS* **86:** 4326–4330.
4. Wu, S., M. Qiao, J. L. Noebels, and X. L. Yang. *Vision Res.* **33:** 2611–2616.

Reference: *Biol. Bull.* **187:** 265–266. (October, 1994)

Effects of GABA on Outward Currents in *Hermissenda* Photoreceptors

Ebenezer Yamoah and Alan M. Kuzirian (Marine Biological Laboratory)

Exogenous application of γ-aminobutyric acid (GABA) on the photoreceptors of *Hermissenda* induces a brief hyperpolarization of their membrane potential (1). Similarly, both electrical and mechanical stimulation of the statocyst mimic the GABA-induced effects on the B photoreceptors, suggesting the involvement of GABA in the synaptic network between the vestibular organ and the photoreceptors (2). It has been proposed that the GABA-mediated network interaction may be crucial for the induction and perhaps maintenance of plasticity in *Hermissenda* photoreceptors (2). We have used immunohistochemical methods to identify GABA neurons in the vestibular organ and cells located at the base of the eye. In addition, we use whole-cell patch-clamp technique to detect the presence of GABA-induced outward currents in isolated photoreceptors of *Hermissenda*.

Nervous systems were removed and prefixed by the addition of two drops of 10% paraformaldehyde to 4 ml artificial seawater (ASW) for 10 min. The nervous systems were then fixed in fresh 4% paraformaldehyde in phosphate buffer saline (PBS) overnight at 4°C and permeabilized in 4% Triton X-100 in PBS for 4 h. The tissues were incubated for 48 h (4°C) in PBS containing a 1:100 dilution of a monoclonal antibody raised against GABA. The primary antibody was removed by washing (20 min in PBS), transferred into blocking solution for 15 min, and then incubated for 3 h in the dark, at room temperature, in a 1:60 dilution of secondary antibody labeled with fluorescein isothiocyanate (FITC). The preparation was washed, mounted with Poly-Aquamount (Polysciences) on slides and viewed with a Zeiss microscope equipped with epifluorescence.

Photoreceptors were isolated as previously described (3). Potassium currents were blocked with 5 m*M* 4-aminopyridine, 100 m*M* tetraethylammonium, and 10 m*M* BAPTA was used to dialyze the cells to block $I_{K,Ca}$. Inward voltage-dependent Na^+ and Ca^{2+} currents were reduced by substituting choline for Na^+ and by reducing the Ca^{2+} in ASW (1 m*M*). Outward Cl^- currents were recorded by substituting *N*-methyl glucamine chloride (NMG-Cl) (300 m*M*) and CsCl (100 m*M*) for internal KCl.

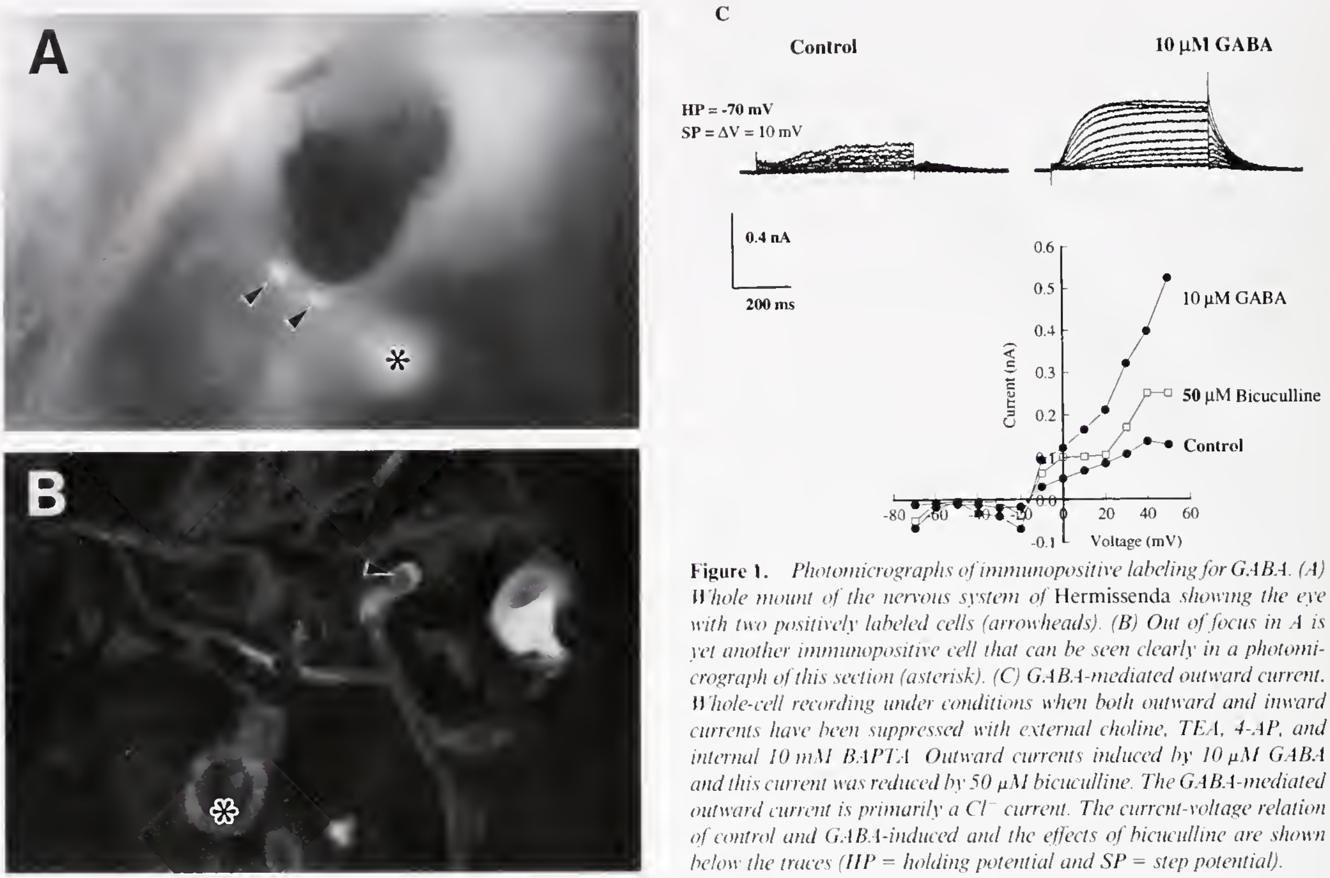

Figure 1. *Photomicrographs of immunopositive labeling for GABA. (A) Whole mount of the nervous system of* Hermissenda *showing the eye with two positively labeled cells (arrowheads). (B) Out of focus in A is yet another immunopositive cell that can be seen clearly in a photomicrograph of this section (asterisk). (C) GABA-mediated outward current. Whole-cell recording under conditions when both outward and inward currents have been suppressed with external choline, TEA, 4-AP, and internal 10 mM BAPTA. Outward currents induced by 10 µM GABA and this current was reduced by 50 µM bicuculline. The GABA-mediated outward current is primarily a Cl^- current. The current-voltage relation of control and GABA-induced and the effects of bicuculline are shown below the traces (HP = holding potential and SP = step potential).*

Possible inward and outward current contamination was prevented with ion substitution and pharmacological blockers as mentioned above.

Immunopositive cells were observed in the cerebropleural ganglia. Of interest was the consistent labeling of the statocyst organ and a neuron close to the arborization field of the vestibulovisual system of *Hermissenda.* Two cells at the base of the eye were also consistently labeled (Fig. 1A, B). Under electrophysiological conditions where voltage-gated currents were suppressed, minimal inward or outward currents were recorded. However, an outward current could be recorded following application of 10 *µM* GABA (Fig. 1C). The GABA-mediated outward current was blocked by bicuculline (100 *µM*), a known $GABA_A$ receptor blocker. The GABA-mediated current had two properties: first, the current magnitude and estimated reversal potential were altered depending on the external and internal Cl^- concentrations. Second, the current was reduced by 4,4′-diisothiocyanostilbene-2,2′-disulfonic acid (DIDS; 100 *µM*). These results indicate that the GABA-induced responses of the photoreceptors were mediated primarily by chloride ion. In addition, the Cl^- current was enhanced by an increase in external Ca^{2+}. This Cl^- current may contribute to the inhibitory, postsynaptic potential of the synaptic response of the hair cell.

E. Y. acknowledges the support of the Grass Foundation.

Literature Cited

1. **Matzel, L. D., and D. L. Alkon. 1991.** *Brain Res.* **554:** 77–84.
2. **Alkon, D. L., J. V. Sanchez-Andres, E. Ito, K. Oka, T. Yoshioka, and C. Collin. 1992.** *PNAS* 89: 11862–11866.
3. **Yamoah, E., and T. Crow. 1994.** *J Neurophysiol.* in press.

Reference: *Biol. Bull.* **187:** 267–268. (October, 1994)

Calcium and Voltage Sensitivity of Potassium Current Activation in Toadfish Semicircular Canal Hair Cells

Antoinette Steinacker and Conchita Zuazaga (Institute of Neurobiology, University of Puerto Rico, San Juan, PR 00901)

Sensory hair cells of the horizontal semicircular canal (HSCC) of the toadfish (*Opsanus tau*) exhibit two main types of rapidly activating potassium currents: a transient, or fast inactivating, current resembling an A current (IA), and a calcium activated potassium current (IKCa). Some cells show primarily IA or IKCa, while others exhibit both classes of current (1). Physiologically,

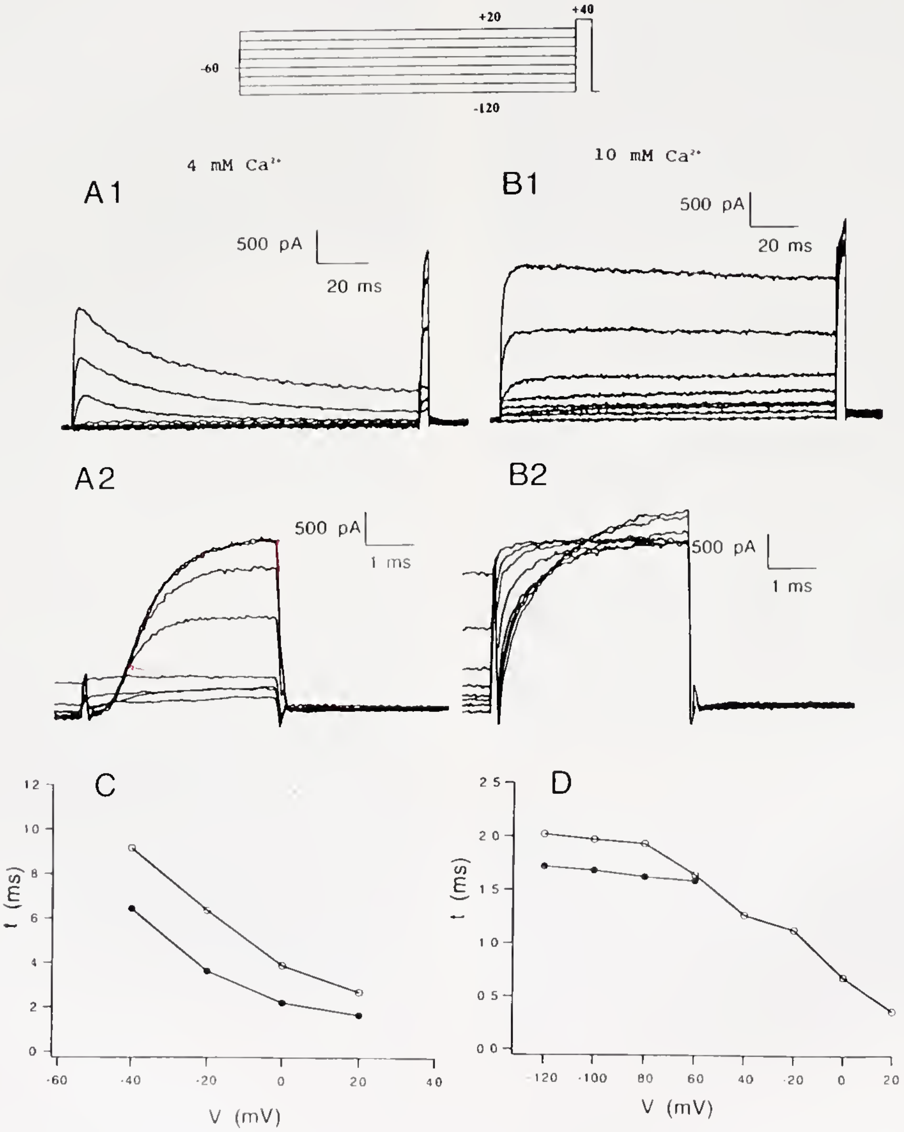

Figure 1. *Voltage and calcium sensitivity of potassium current activation. Voltage command protocol for all experiments in top panel. (A1) Activation of outward current in normal (4 mM Ca^{2+}) Ringer. (A2) Response to the test pulse in A1 on an expanded time scale. (B1) Activation of outward current as in A1, but with 10 mM Ca^{2+} in the bath. (B2) Response to the test pulse in B1 on a faster time scale. (C) Plot of 10–90% activation time (t) of outward current in response to prepulses (V) arising from a −60 mV holding potential. Filled circles are from data of A1 (4 mM Ca^{2+}); open circles are from data of B1 (10 mM Ca^{2+}). (D) Plot of 10–90% activation time of outward current in response to the test pulse, plotted against prepulse voltage. Open circles, 10 mM Ca^{2+}; filled circles, 4 mM Ca^{2+}.*

these outward potassium currents are activated in the basolateral surface of the hair cell by the transduction current at the apical pole. All sensory hair cells of all acoustico-lateralis systems studied exhibit an inward calcium current (ICa) that activates rapidly, preceding potassium current activation, and shows little inactivation (2–6). ICa is activated in the basolateral surface of the cell by the transduction current and by acetylcholine, an efferent transmitter on hair cells (7–10). The relative rates of activation of IKCa and IA in response to intracellular calcium concentration $[\mathrm{Ca}^{2+}]_i$, and voltage are data basic to an understanding of sensory transduction in the hair cell.

The calcium and voltage sensitivity of potassium current activation was studied with whole-cell patch-clamp methods (11) on hair cells isolated from the HSCC of the toadfish. The HSCC was chosen because the functional properties of HSCC afferents are well known (12, 13). Data were collected on-line using pCLAMP with a P/4 routine, and subsequent analysis was done with Igor (WaveMetrics Inc.). The bathing medium, maintained at 12°C, was teleost Ringer containing (in m*M*): NaCl (165), KCl (5), $\mathrm{CaCl_2}$ (4 or 10, see below), $\mathrm{MgCl_2}$ (1), and Hepes (10), all adjusted to pH 7.2 with NaOH. Quartz glass patch pipettes were filled with (in m*M*): KCl (165), $\mathrm{CaCl_2}$ (0.1), $\mathrm{MgCl_2}$ (1.5), Hepes $\mathrm{K^+}$ salt (5), EGTA (10), and $\mathrm{K^+}$ATP (2.5) all adjusted to pH 7.4 with KOH. Cells were held at −60 mV, close to the resting (zero current) potential of canal hair cells (A. Steinacker, unpub. data). The command voltage protocol was a 320-ms prepulse, from −120 mV to +20 mV in 20-mV increments, followed by a 4-ms test pulse to +40 mV (Fig. 1, top). This voltage protocol, with 320-ms or 1-s prepulses, was used with 33 HSCC hair cells.

Figure 1, A1, shows the response of an HSCC hair cell to the command protocol in normal (4 m*M* $\mathrm{Ca^{2+}}$) Ringer. From the outward potassium current profile of a rapidly inactivating current, this cell appears to express only IA. This is particularly clear when the response to the test pulse is shown on a faster time base (Fig. 1, A2). No significant current appears in response to the test pulse after prepulses more positive than −40 mV; this putative A current response to the test pulse is activated following a −60-mV prepulse, a value close to the resting potential of the hair cell.

The calcium concentration in the bath Ringer was increased to 10 m*M* to enhance the driving force for calcium and to mimic the increase in $[\mathrm{Ca}^{2+}]_i$ resulting from exposure to the efferent transmitter. The total outward current profile then shows an additional rapidly activating outward current (Fig. 1, B1). Note that the activation time for the additional current in Fig. 1, B1, is slower than that of the transient current when both are activated from the −60 mV holding potential (Fig. 1, A1 and C). The calcium current in hair cells is only minimally activated at −60 mV (3, 5, 6). The activation time constant of the outward current is greatly decreased by higher extracellular calcium (Fig. 1, B2 and D). This suggests that the decrease in activation time constant is the result of an increase in $[\mathrm{Ca}^{2+}]_i$ produced by the more positive prepulses. This current is designated an IKCa for the following reasons: it is evoked by the increase in $[\mathrm{Ca}^{2+}]_i$; it does not inactivate as an IA or delayed rectifier would (14); it reverses at the potassium equilibrium potential; and it is blocked by TEA (2–20 m*M*) (data not shown). In a recent study on A current inactivation of mutant Shaker potassium channels, no effect of increased external calcium on inactivation was seen (15). Indeed, increased calcium actually accelerates inactivation of potassium currents (16, 17). This induction of an additional current by an increase in $[\mathrm{Ca}^{2+}]_i$ may be of physiological significance in switching the operating mode of the cell in response to intense sensory stimulation or efferent transmitter action.

We thank M. E. Andreu-Sanchez for her help in data analysis. This work was supported by NSF 9120497 and NIMH MH 48190 and was carried out primarily at the Marine Biological Laboratory, Woods Hole, MA.

Literature Cited

1. **Steinacker, A., J. Monterrubio, R. Perez, and S. M. Highstein. 1992.** *Biol. Bull.* **183:** 346–347.
2. **Ohmori, H. 1984.** *J. Physiol.* **350:** 561–581.
3. **Art, J. J., and R. Fettiplace. 1987.** *J. Physiol.* **385:** 207–242.
4. **Hudspeth, A. J., and R. S. Lewis. 1988.** *J. Physiol.* **400:** 237–274.
5. **Fuchs, P. A., M. G. Evans, and B. W. Murrow. 1990.** *J. Physiol.* **429:** 553–568.
6. **Roberts, W., L. Robles, and A. J. Hudspeth. 1990.** *J. Neurosci.* **10:** 3664–3684.
7. **Shigemoto, T., and H. Ohmori. 1990.** *J. Physiol.* **420:** 127–148.
8. **Steinacker, A., and L. Perez. 1992.** *Ann. N. Y. Acad. Sci.* **656:** 27–48.
9. **Fuchs, P. A., and B. W. Murrow. 1992.** *J. Neurosci.* **12:** 800–809.
10. **Goodman, M. B., and J. J. Art. 1992.** *Soc. Neurosci. Abs.* **18:** 588.7.
11. **Hamill, O. P., A. Marty, E. Neher, B. Sakmann, and F. J. Sigworth. 1981.** *Pflugers Arch.* **391:** 85–100.
12. **Boyle, R., and S. M. Highstein. 1990.** *J. Neurosci.* **10:** 1557–1569.
13. **Boyle, R., J. P. Carey, and S. M. Highstein. 1991.** *J. Neurophys.* **66:** 1504–1521.
14. **Steinacker, A., and A. Romero. 1991.** *Brain Res.* **556:** 22–32.
15. **Lopez-Barneo, J., T. Hoshi, S. H. Heinemann, and R. W. Aldrich. 1993.** *Recept. Channels* **1:** 61–71.
16. **Alkon, D. L., J. J. Shoukimas, and E. Heldman. 1982.** *Biophys. J.* **40:** 245–250.
17. **Grissmer, S., and M. D. Cahalan. 1989.** *J. Gen. Physiol.* **93:** 609–630.

Reference: *Biol. Bull.* **187:** 269. (October, 1994)

Protein Synthesis in Nerve Endings from Squid Brain: Modulation by Calcium Ions

Juan Benech, Marianna Crispino, Jong Tai Chun, Barry B. Kaplan, and Antonio Giuditta (Department of General and Environmental Physiology, University of Naples, Italy)

We have previously shown that a system of protein synthesis is present in the squid giant axon (1, 2) and, more recently, in the nerve endings of the synaptosomal fraction prepared from squid optic lobe (3, 4). The latter demonstration rests on the different electrophoretic patterns displayed by synaptosomal translation products, including neurofilament (NF) proteins immunoabsorbed by a specific antibody, and by the translation products obtained from possible contaminants of the synaptosomal fractions, such as fragments of neuronal or glial cells, or axonal segments. As expected, the protein synthetic activity of the squid synaptosomal fraction is strongly inhibited by hypoosmotic treatment and by cycloheximide, but is not affected by RNase. These features are indicative of extramitochondrial polysomes enclosed by a plasma membrane. They confirm previous observations made on the same synaptosomal fraction (5), and in several synaptosomal preparations from mammals.

Polysomes purified from the synaptosomal and microsomal fractions of squid optic lobe actively synthesize proteins when supplemented with the supernatant fraction from a rabbit reticulocyte lysate. In preliminary analyses, the radiolabeled translation products of synaptosomal polysomes immunoabsorbed by a specific NF antibody display a prevalent 70S component, in agreement with the behavior of intact synaptosomes, but at variance with the pattern of the translation products of microsomal polysomes. The latter result confirms the segregation of specific mRNAs in the synaptosomal fraction as compared with the microsomal fraction.

The first evidence that the protein synthetic activity of squid brain synaptosomes is modulated by calcium ions was obtained by treatment of the synaptosomal fraction with the calcium ionophore A23187 (3). This treatment inhibited protein synthesis up to 80% when synaptosomes were incubated in artificial seawater (ASW) containing a normal concentration of calcium ions (11 m*M*). A comparable degree of inhibition was observed in the presence of ionomycin, a second calcium ionophore. However, inhibitory effects were also induced by both ionophores in calcium-free ASW supplemented with EGTA (1 m*M*). Strong inhibitory effects were also observed in the presence of either of two calmodulin blockers, trifluoperazine and W-7. This observation suggests that the complete lack of calcium ions or its functional inactivation are as deleterious to the protein synthetic activity of the synaptosomal fraction as calcium ion concentrations in the millimolar range. Presumably, the normal level of calcium prevailing in nerve endings (10 to 100 n*M*) is required to insure an optimal rate of protein synthesis.

A related observation concerns the strong inhibitory effect on synaptosomal protein synthesis elicited in normal ASW by EGTA (2 m*M*), but not by EDTA. This inhibition appeared to be readily reversible, and was prevented by the addition of funnel web spider toxin (FTX), but not by other calcium channel blockers, such as omega conotoxin or nifedipine. The latter findings suggest the involvement of the P calcium channel in the modulation of the rate of synaptosomal protein synthesis.

In conclusion, the data indicate that an extramitochondrial system of protein synthesis is present in the nerve endings of squid brain, and that the activity of this polysomal system is modulated by calcium ions. As calcium ions enter the axon terminals during nerve firing, they may regulate the rate of presynaptic protein synthesis depending on the increase in their local concentration and, ultimately, on the rate of firing. Determination of preterminal calcium levels by using suitable calcium indicators will be required to confirm this possibility.

We acknowledge the financial support of USPHS grant NS30715 and of grants provided by the European Community (CI1*-CT93-0037), CNR (PS Mezzogiorno), MURST and the University of Naples, Italy. J.B. is from IIBCE, Montevideo, Uruguay; M.C. and A.G. from the University of Naples, Italy; J.T.C. and B.B.K. from the University of Pittsburgh, PA.

Literature Cited

1. **Giuditta, A., *et al.* 1991.** *J. Neurosci. Res.* **28:** 18–28.
2. **Gioio, E. A., *et al.* 1994.** *J. Neurochem.* **63:** 13–18.
3. **Crispino, M., *et al.* 1993.** *Mol. Cell. Neurosci.* **4:** 366–374.
4. **Crispino, M., *et al.* 1993.** *J. Neurochem.* **61:** 1144–1146.
5. **Hernandez, A. G., *et al.* 1976.** *Acta Cient. Venez.* **27:** 120–123.

Reference: *Biol. Bull.* **187:** 270. (October, 1994)

Second Messenger Modulation of Steady-State Calcium Efflux in *Aplysia* Bag Cells

Ebenezer Yamoah and Peter J. S. Smith (National Vibrating Probe Facility,
Marine Biological Laboratory)

Second messengers modulate intracellular calcium (Ca_i^{2+}) level in two ways: by direct induction of Ca^{2+} release from intracellular Ca^{2+} stores (*e.g.*, inositol-triphosphate-induced Ca^{2+} release from intracellular stores) and by direct modulation of calcium conductances, or indirect modulation of other ionic conductances which results in transmembrane hyperpolarization. Membrane hyperpolarization activates calcium channels (T-type), which ultimately enhances Ca^{2+} influx (1). But Ca^{2+} channel modulation and Ca^{2+} release from stores forms a subset of the regulatory mechanism of Ca_i^{2+} homeostasis, which is an essential component of intracellular signaling. To prevent Ca_i^{2+} overload, the level of Ca_i^{2+} is regulated, for example, by the intracellular protein buffers, Ca^{2+}-ATPase, the Na^+-Ca^{2+}-exchanger, and passive Ca^{2+} leakage through the plasma membrane (2). We used the calcium sensitive vibrating probe technique (3) to examine the steady-state calcium efflux across the plasma membrane of *Aplysia* bag cells in culture and have assessed the extent to which second messengers influence this efflux.

Bag cells were cultured as previously described (4), but the bath Ca^{2+} was reduced to about 50–100 μM by replacement with Mg^{2+}. Cells remained viable in low-Ca^{2+} artificial seawater (ASW) for several days ($\approx$ 7 days). The following second messengers were used in this study: analogs of c-AMP (dibutyrl-c-AMP), c-GMP (dibutyrl-c-GMP), activators of protein kinase C, phorbol ester (TPA), and other compounds known to induce intracellular Ca^{2+} release, *e.g.*, caffeine. Whereas c-AMP and phorbol ester reduced the efflux, c-GMP enhanced it. Representative effects of 50 nM TPA and 2 mM bath application of dibutyrl-c-GMP are shown in Figure 1. Caffeine had no effect on the steady-state Ca^{2+} efflux on the bag cells.

The present observation of the effects of second messengers on steady-state Ca^{2+} efflux introduces a new dimension to the modulatory effect of second messengers on Ca_i^{2+} homeostasis. These results may be a direct consequence of the modulation of the activity of either the Ca^{2+}-ATPase or the Na^+-Ca^{2+} exchanger. But the indirect action of a second messenger, by either raising or reducing Ca_i^{2+} and thus the linked enhancement or reduction of the activity of the Ca^{2+}-pump or Na^+-Ca^{2+} exchanger, could also explain the present results. We are in the process of determining which of the known second messengers might have a direct effect on the mechanisms of steady-state Ca^{2+} efflux.

E.Y. acknowledges the support of the Grass Foundation.

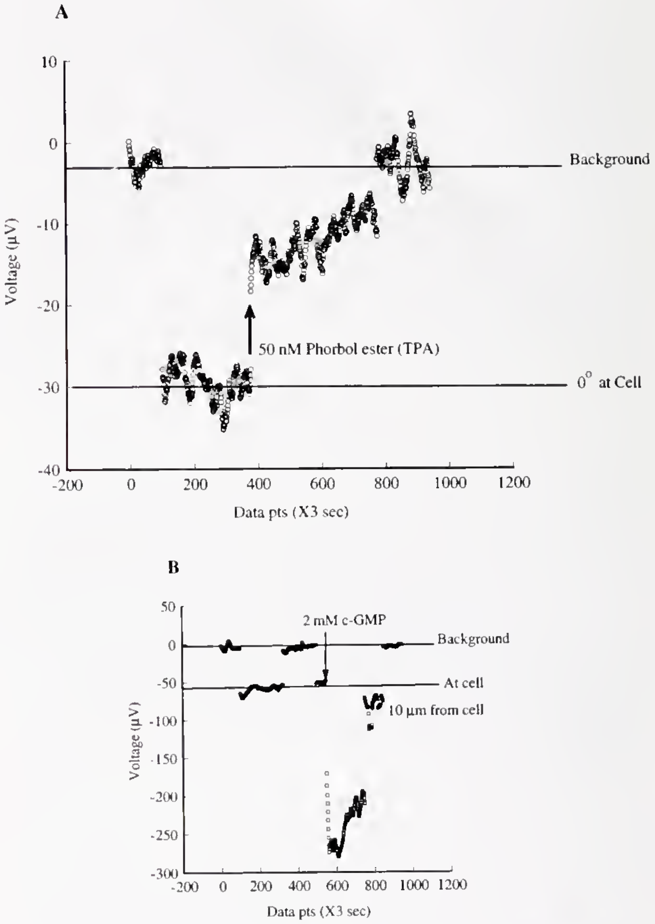

Figure 1. *(A) Effects of the PKC activator (TPA) on Ca^{2+} efflux. Deflection below the background (baseline) indicates Ca^{2+} efflux. TPA reduced the steady-state Ca^{2+} efflux over several minutes. (B) Effects of c-GMP analog. Shown here are repeated baseline recordings (recordings at about 300 µm from cell) and recording at cell. There was at least 3- to 4-fold increase in steady-state calcium upon bath application of 2 mM c-GMP-dibutyrl.*

Literature Cited

1. **Llinás, R. 1988.** *Science* **242:** 1654–1664.
2. **Carafoli, E. 1987.** *Annu. Rev. Biochem.* **56:** 395–433.
3. **Smith, P. J. S., R. H. Sanger, and L. F. Jaffe. 1994.** *Methods Cell Biol.* **40:** 115–134.
4. **Knox, R. J., E. A. Quattrocki, J. A. Connor, and L. K. Kaczmarek. 1992.** *Neuron* **8:** 883–889.

Reference: *Biol. Bull.* **187:** 271–272. (October, 1994)

Three-Dimensional Calibration of the Non-Invasive Ion Probe, NVP$_i$, of Steady Ionic Currents

Joseph G. Kunkel and Peter J. S. Smith (Marine Biological Laboratory)

A non-invasive approach has been developed and applied to measure the flux of specific ions that enter and exit cells or tissues (1, 2). The NVP$_i$ adds, to the ion measurement technology of specific ion electrodes, an oscillation of the electrode over a short distance, δr, typically 10 μm, which allows the estimation of the concentration gradient of the ion in the direction of oscillation. The NVP$_i$ has been calibrated previously in the single dimension of oscillation, but the fit of the observed to the expected μV difference was poor close to the source (2). Recent addition of two parameters—distance to infinite source, $\mathbf{r_0}$, and the electrode efficiency, **eff**— to the theoretical formula for predicting μV difference (2) allow the expected μV differences relative to the source to be modeled accurately over all radial distances from the source. The parameter $\mathbf{r_0}$ is needed because it is clear that the point of closest approach to the source is some distance, r_0, away from an infinite source. The parameter **eff** is needed to account for the inability of the microelectrodes to fully respond to the gradients being measured within the time constraints of the oscillation cycle. At 0.3 Hz, the electrode is able to make one measurement of a calcium gradient in one direction in about 3 s with an efficiency of 50%. If the oscillation is increased to 0.5 Hz, the efficiency drops to 30%.

After the development of routines for oscillating in three dimensions and collecting three-dimensional data (Fig. 1), the advantages of a method of 3-D calibration become a consideration. The most important technical advantage of a 3-D calibration is that it removes an obligation of the probe operator to position the probe precisely on the diffusional axis of the ion source, an exacting and time-consuming task in three dimensions. The theoretical advantage of the 3-D calibration is that it should conform to the law of conservation of charge moving through concentric shells about the source. The artificial diffusional source of ions provides a physical standard from which an observed dose-response curve and the efficiency of the probe can be estimated. The concentration of the ion of interest can be predicted knowing the radial distance from the source to the measurement point. Such a source has been used to create a calibration in a single dimension. A correct 1-D calibration is only obtained when measurements are made on a diffusional axis emanating from the source. Until now the 3-D version of the NVP$_i$ has been calibrated by using this artificial source and applying the 1-D predictive equation. However, a method incorporating all of the strengths of the 3-D approach would now be beneficial. A 3-D collection of data typically results in a 7 × 7 × 7 grid of 343 individual, equispaced, 3-D observation vectors, $dV_O = O_{ijk} = \{\mu Vx_i, \mu Vy_j, \mu Vz_k;\ i,j,k = 0 \ldots 6\}$, of μV-differences with element O_{303} at the nominal point of closest approach to the diffusional source which has geometric location $\{x_3, y_0, z_3\} = \{0,0,0\}$ (Fig. 1). If one gradient estimate were made for each dimension at each grid position at 0.3 Hz, the time to complete each 7 × 7 plane of data would be (3 × 7 × 7 × 3 s) = 7 min 21 s. The resultant planes of 49 dV$_O$s can be used to fit the unknown parameters of an expected μV-difference equation. The probe need not be placed on the actual axis of diffusion but merely close to it. The position of the axis of diffusion, $\mathbf{A_o} = \{x_A, 0, z_A\}$, in the 0-plane of closest approach {*i.e.*, at y = 0) becomes another parameter to be fit by the equation of linear concentration relation with the inverse of distance,

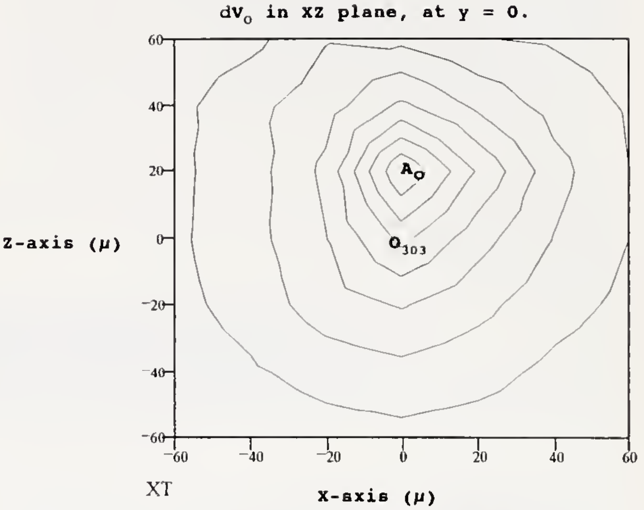

Figure 1. *Contour plot of 7×7 observed μV-differences, dV$_o$, at 20 μm intervals in the plane of closest approach to a 100 mM CaCl$_2$ source diffusing into a background concentration of 1 mM CaCl$_2$. The point of closest approach was at* $\boldsymbol{O_{303}}$ *but the estimated axis of ion diffusion in this plane is 20 μm away at* $\boldsymbol{A_o}$.

$$C_{x,y,z} = \mathbf{Cb} + \mathbf{K}/(\mathbf{r}_{xyz} + \mathbf{r_0}).$$

The equation for the expected value of μV-difference, $dV_E(r)$, to be measured at a radial distance, r, units along that concentration curve is now given by,

$$dV_E(r) = -10^3 \cdot \mathbf{S} \cdot \mathbf{eff} \cdot \mathbf{K} \cdot e^{-1} \cdot \frac{\delta r}{r^2 \cdot (\mathbf{Cb} + \mathbf{K}/(r + \delta r/2))}\ (\mu V),$$

where the effective radius from an observation point {x,y,z} to the infinite source, r, is given by

$$\mathbf{r} = \mathbf{r}_{xyz} + \mathbf{r_0}.$$

In the 3-dimensional case, r_{xyz}, is measured from the observation point to the diffusional axis, A$_o$, computed by

$$r_{xyz} = |\mathbf{O_{ijk}} - \mathbf{A_o}|.$$

The geometric coordinates of $\mathbf{A_o}$ are determined by finding the location of the maximum μV difference in the plane of closest approach (Fig. 1). The parameters of the above equations, other than $\mathbf{r_0}$ and **eff**, are discussed in detail elsewhere (2): briefly, **S** is the familiar Nernst coefficient for the ion of interest; **K** is the slope of the concentration equation for $C_{x,y,z}$; **e** is the base of natural logarithms. The unknown parameters are estimated by well-known methods of analytic geometry. First $\mathbf{r_0}$ is estimated by linearizing the equation for C_{xyz}, which then allows **K** to be estimated by linear regression. Finally **eff** is estimated by minimizing the Chi Square statistic on the observed *versus* the expected μV difference, Chi Square = $(dV_O - dV_E)^2/dV_E$.

These equations can then be applied to biological data collected in a few planes tangential to the source such that a point and a disc source of ions can be distinguished. Such sources are very often quite weak, so a simple one-dimensional transect away from a source does not yield much data.

Literature Cited

1. **Kühtreiber, W. M., and L. F. Jaffe. 1990.** *J. Cell Biol.* **110:** 1565–1573.
2. **Smith P. J. S., R. H. Sanger, and L. F. Jaffe. 1994.** *Meth. Cell Biol.* **40:** 115–134.

Reference: *Biol. Bull.* **187:** 272–273. (October, 1994)

Lobster Orientation in Turbulent Odor Plumes: Simultaneous Measurement of Tracking Behavior and Temporal Odor Patterns

Jennifer Basil and Jelle Atema (Boston University Marine Program, Marine Biological Laboratory)

Chemical cues play an important role in the food searching behavior of the lobster, *Homarus americanus.* Previous studies have shown that bilateral antennular chemoreception is necessary for search efficiency within a turbulent odor plume (1, 2). The manner in which lobsters orient within plumes indicates that there is directional information contained within turbulent odor plumes (3).

In addition, using chemical sensors (In Vivo Electrochemical System, IVEC) capable of measuring a tracer (dopamine) in seawater, Moore and Atema (4) measured the fine-scale, three-dimensional structure of plumes. Plumes showed spatial gradients of such features as pulse height, onset slope, and distribution, which could provide directional cues to orienting animals. The purpose of the present study was to implement techniques from which we could determine whether animals extract and use fine-scale features to successfully navigate to a distant odor source.

In the present experiment, behavioral and electrochemical measurements were made in a flow-through flume (250 × 90 × 20 cm). The food stimulus was gravity-fed through a Pasteur pipette positioned so that the nozzle released stimulus at the cross-sectional center of the tank, 9 cm off the bottom, at the upstream end of the flume. The lobster carried two IVEC electrodes mounted directly over the lateral antennules, and a submersible amplifier on its back. The backpack was connected, by a 2.5-m flexible cable, to a computer that ran the electrochemical software (IVEC). The overhead film record of the freely orienting lobster could be synchronized with the real-time concentration measurements.

Lobsters were fed twice weekly and were deprived of food for 3–10 days prior to each trial (3). Twenty-four hours before a trial, a lobster was fitted with a black plastic blindfold and allowed to habituate to the orientation arena. Food extracts (squid, clam, mussels) with tracer were used as stimuli (source tracer concentration = 40 m*M*).

The stimulus was introduced into the arena when a lobster settled into the downstream shelter. Localization was considered successful only if the lobster approached to within 15 cm of the pipette tip within 20 min after the start of stimulus introduction and did not walk along the side walls of the flume. Orientation paths were digitized at 1/s. Variables chosen to quantify tracking behavior included walking speed, turning angles, and headings.

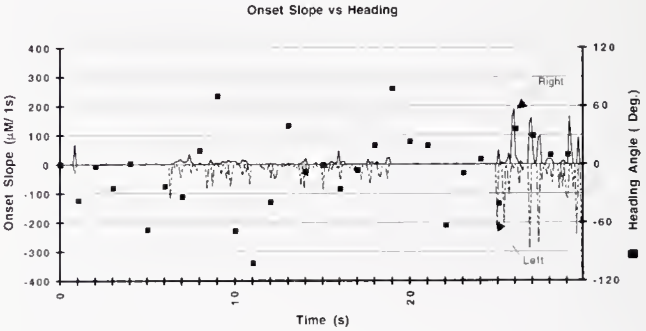

Figure 1. *Onset slope and heading angle, plotted together as a function of time (t = 0 s at start of orientation trial, t = 30 s when animal located source). Onset slope is plotted continuously at 10 Hz. Onset slope from electrode mounted over right antennule is top trace (solid line). Onset slope from left antennular area is plotted as the lower trace (dashed line). Large onset slopes are located close to the source, where heading angle improves.*

Backpacks did not affect orientation behavior. Figure 1 illustrates the onset slopes for odor tracer patches encountered by the left and right electrode (right electrode = positive values, left electrode = negative values), the slopes are plotted above the lobster's heading as it oriented towards the source (lobster hits source at 30 s). Positive headings indicate that the animal is moving to the right of the line connecting the starting point and the source. The odor patches, as encountered by the moving lobster, closely resemble those measured in previous studies (4). At points in the plume that are distant from the odor source, there were a greater number of patches of lower concentration and shallow onset slopes. Close to the source, the patches are of much higher concentration, and have steep onset slopes. As the steepness of the onset slopes increased, the headings of the orienting lobster improved (Fig. 1).

The events at t = 25 s give an indication of how a lobster might be using differential information at each antennule to make directional decisions. After a large signal is detected by the left electrode, the animal moves 30 degrees to the left. Subsequently, a large signal encountered by the right electrode is closely followed by rightward movement relative to the source. As the animal nears the source and the onset slopes remain greater on the left than on the right, the animal moves slowly to the left and ultimately reaches the source.

These experiments show that a number of odor patch variables change as the animal moves towards a distant odor source. Changes in these variables, onset slope in particular, appear to be correlated with changes in the animal's behavior, particularly heading angle, turning angle, and walking speed.

Supported by NSF IBN 9212650.

Literature Cited

1. **Devine, D. V., and J. Atema. 1982.** *Biol. Bull.* **163:** 144–153.
2. **Reeder, P., and B. Ache. 1980.** *Anim. Behav.* **28:** 831–839.
3. **Moore, P., N. Scholtz, and J. Atema. 1991.** *J. Chem. Ecol.* **17:** 1293–1307.
4. **Moore, P., and J. Atema. 1991.** *Biol. Bull.* **181:** 408–418.

Reference: *Biol. Bull.* **187:** 273. (October, 1994)

Lobster Orientation in Turbulent Odor Plumes: Electrical Recording of Bilateral Olfactory Sampling (Antennular "Flicking")

Ann E. Leonard, Rainer Voigt, and Jelle Atema (Boston University Marine Program, Marine Biological Laboratory)

Distance orientation to odor sources in the American lobster is mediated by the lateral flagella of the first antennae (lateral antennules) (1). Antennular flicking is closely associated with stimulus acquisition. The maximal flicking frequency is approximately 4 Hz (2). Each base of an antennule consists of three segments; the distal segment bears a lateral and a medial flagellum. Each segment has a depressor and a levator muscle (similar to the second antenna) (3); the antagonistic muscles in the distal segment control the flicking motion. In this study we extended techniques (2) to now measure extracellularly the bilateral electrical activity that occurs in the distal segment in association with each flick in a freely moving lobster.

We implanted Teflon-coated silver wire electrodes (O.D.: 75 μm bare, 112.5 μm coated; Medwire) in the distal segment of each antennule. A small hole was drilled through the exoskeleton in a dorsal-medial position over the depressor muscle. An electrode was inserted, then secured and sealed with cyanoacrylate (Zap-A-Gap and Zip Kicker). An indifferent electrode (Ag-AgCl wire) was attached to the lobster's carapace. The lobsters were allowed to recover from the implantation procedure until flicking motion indicated little impairment of each flick. The extracellular activity was differentially amplified with standard electrophysiological equipment and recorded on a VCR for later analysis. Simultaneous recording of neuronal activity on the audio channels and videotaping of the flicking motion allowed synchronization of the electrical response and flicking behavior. Visual/manual and computer-automated flick recognition were comparable, showing the reliability of the automated method (Fig. 1).

To quantify bilateral sampling behavior, a blindfolded lobster was placed in a small flume (125 × 18 × 20 cm) with a flow of 2 cm/s. Electrical records indicate independence of flicking of the left and right antennule. Often one side showed higher flick frequency than the other. When encountering a plume of odor (squid extract 10 mg/l and rhodamine dye), the flick frequency increased bilaterally from 1–2 Hz to 2–4 Hz.

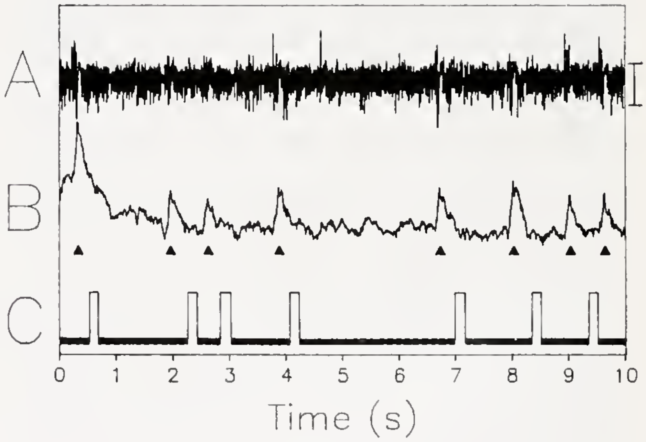

Figure 1. *(A) Recording of extracellular (probably neural) activity associated with antennular flicking (filter window: 1 Hz low, 1 kHz high; vertical scale: 25 μV). (B) Integrated responses of record in A (R-C Filter). Triangles indicate flicks selected automatically by computer program. (C) Event marker record of visual determination of antennular flicks lags about 0.2 s behind automated record, but shows same flick recognition by both methods.*

These results indicate reliable recording of bilateral flicking activity in freely moving lobsters. This technique will be used in correlating the rate of stimulus acquisition with the decision-making process of lobster chemotaxis.

Supported by NSF (IBN-9212650; JA) and a Howard Hughes fellowship (AEL).

Literature Cited

1. **Devine, D. V., and J. Atema. 1982.** *Biol. Bull.* **163:** 144–153.
2. **Berg, K., R. Voigt, and J. Atema. 1992.** *Biol. Bull.* **183:** 377–378.
3. **Bevengut, M., J. A. McTeague, and C. K. Govind.** *J. Crust. Biol.* **13:** 256–257.

Reference: *Biol. Bull.* **187:** 274–275. (October, 1994)

Food Detection and Preferences of the Nudibranch Mollusc *Hermissenda crassicornis:* Experiments in a Y-Maze

Elizabeth Tyndale, Conxita Avila, and Alan M. Kuzirian (Marine Biological Laboratory)

Hermissenda crassicornis (Eschscholtz, 1831), a nudibranch mollusc, is being reared in our laboratory as a biomedical research model for learning and memory studies. The aim of the present study was to determine whether *Hermissenda,* a generalist carnivore (1), is able to detect its prey chemotactically, and whether it displays a preference for certain foods. Previous studies on other nudibranchs demonstrated their ability to detect prey from a remote distance (2, 3).

Experiments were carried out in a 35 cm wide × 70 cm long × 12 cm deep Y-maze with a total equilibrated flow of 1500–2500 ml/min of ambient seawater (water depth: 3 cm each arm: 17 cm wide). A uniform, unidirectional flow was achieved with an upstream collimator made of soda straws. Dye tests confirmed the uniformity of the currents (*i.e.,* stimulus) across the full width of both arms of the maze.

The hydroid *Tubularia crocea,* the tunicate *Ciona intestinalis,* and the mussel *Mytilus edulis* were the foods tested. These species have all been used successfully in the past to feed *Hermissenda* in the laboratory (1, 4); *Ciona* was presented with the tunic removed, and mussels were presented without shells. Food was placed on one side of the Y-maze, with the other side remaining empty. For Y-maze experiments, *Tubularia* was presented whole; *Ciona* in three ways: whole, viscera only, and viscera cut into pieces; mussels were whole but without shells. In trials testing for a preference between stalks and polyps of *Tubularia,* the pieces of the hydroid were contained in 500-μm mesh bags, one on each side of the Y-maze.

Healthy *Hermissenda,* in groups of 3–6, were starved overnight before being tested. Individuals were selected at random from the starved group for each trial (1–3 non-consecutive trials/specimen). The nudibranch was placed on the centerline of the Y-maze, where it received stimuli from both sides (distance from the food barrier: 40 cm; 12–15 cm from the divider). The trial ended when *Hermissenda* was within 3 cm of the food barrier or after 30 min. The Y-maze was thoroughly cleaned between trials to remove the mucous trail of the previous specimen, and the maze was reconditioned by flushing for 10 min with ambient seawater between trials. Food was switched to the opposite side of the maze after 3–5 trials, and 33–56 trials were done with each food item. At least 50 *Hermissenda* individuals were used. About the same number of trials were done with the stimulus on the left and on the right; no significant bias was detected (χ^2). Results (number of times the side containing food was chosen *vs.* number of times the empty side was chosen) were compared by Chi-squared analysis.

Results of the Y-maze experiments are shown in Table I. In trials with *Tubularia,* when a choice was made, the nudibranchs went to the hydroid side in 72.5% of the trials (or 59% of the trials including no-choice data). When approaching *Tubularia,* a tendency for the pedal locomotion to accelerate in the last few centimeters was observed. The other foods gave much larger percentages of negative results (no choice made), whereas the results in which a choice was made were split about evenly between the presence and absence of food. When animals failed to make a choice, they crawled aimlessly or entered a quiescent state. For all foods tested, the average time for the nudibranchs to reach the finish line (when they made a choice) was between 6 and 16 min. Additional experiments with *Tubularia* were carried out at higher water temperatures; they also gave a large proportion (69%) of no-choice results. When stalks and polyps

Table I

Y-maze experiments with Hermissenda crassicornis *and various foods*

	Food chosen[a]	Blank chosen[a]	No choice[a]	n	χ^2
Tubularia (10–12°C; 17–19°C)[b]	59% (29)	22% (11)	18% (9)	49	8.10[c]
Tubularia (24°C)	31% (5)	0%	69% (11)	16	—
Ciona (whole) (20–23°C)	5% (2)	16% (6)	79% (30)	38	2.0
Ciona (viscera whole) (20–24°C)	11% (4)	8% (3)	81% (29)	36	0.14
Ciona (viscera pieces) (20–24°C)	17% (6)	9% (3)	74% (26)	35	1.0
Mytilus (22–24°C)	6% (2)	9% (3)	85% (28)	33	0.2
	Polyps chosen	Stalks chosen	No choice	n	χ^2
Tubularia (19–21°C) (polyps vs. stalks)	34% (19)	38% (21)	29% (16)	56	0.1

[a] Results are given in rounded percentages. (n) = Number of trials.

[b] The data from these sets of experiments, done at two temperature ranges, were combined because they were not statistically different (χ^2).

[c] Statistically significant ($P = 0.005$; d.f. = 1). Remaining χ^2 values were not significant.

of *Tubularia* were presented simultaneously, the nudibranchs went to the stalks as often as to the polyps (Table I).

This study demonstrates that *Hermissenda* can locate *Tubularia* by chemotaxis. Previous reports (5, 6) indicated that this nudibranch can locate dissolved food at a distance in the laboratory, but not solid food. In those studies, however, the nudibranchs were not tested with unidirectional water currents passing over food species. *Hermissenda* did not distinguish between hydroid polyps or stalks in the Y-maze, choosing equally between the two. Although they do eat the other tested foods in the laboratory, they were not strongly attracted to them in the Y-maze experiments. Entire *Ciona* may actually be repellent. This fact might be related to the presence, in *C. intestinalis*, of a cytotoxic steroidal hydroperoxide (7, 8). Feeding experiments done previously with adult *Hermissenda* showed that a diet of *Tubularia* sustained a higher growth rate than diets of *Ciona* viscera or mussels. These results reinforce the fact that the latter two foods are useful only as maintenance diets (9).

High percentages of negative trials (no choice expressed) in similar chemotactic experiments have been reported in the literature, putatively due to variability in the animal's physiological state and environmental conditions (3). In our experiments, negative results (no choice) increased in direct relationship to seawater temperature (Table I). A water temperature of 24°C greatly exceeds the normal temperature range for *Hermissenda*. Because *Tubularia* is also a natural inducer of larval metamorphosis, detection and selection of the hydroid as preferred prey can be ecologically critical to *Hermissenda*, by increasing the rate of larval and juvenile survival.

Financial support from the Woods Hole Marine Sciences Consortium to E.T. and the Catalan and Spanish Governments to C.A. are gratefully acknowledged. This research was supported by a grant to A.M.K. (N.C.R.R.-N.I.H.; P40-RR03820). Thanks are also due to Dr. J. Atema and Dr. R. Voigt for lending us the Y-maze for our experiments. Technical support of C.T. Tamse is also acknowledged.

Literature Cited

1. **Harrigan, J. F., and D. L. Alkon. 1978.** *Biol. Bull.* **154:** 430–439.
2. **Harris, L. G. 1971.** Pp. 77–90 in *Aspects of the Biology of Symbiosis*, T. C. Cheng, ed. University Park Press, London.
3. **Harris, L. G. 1973.** *Curr. Top. Comp. Pathobiol.* **2:** 213–315.
4. **Tamse, C. T., A. M. Kuzirian, and T. R. Capo. 1990.** *Am. Malacol. Union Abstr.*, 56th Ann. Meetings, p. 61.
5. **Agersborg, H. P. K. 1922.** *J Exp. Zool.* **36(4):** 423–444.
6. **Yarnall, J. L. 1972.** PhD Thesis. 126 pp.
7. **Guyot, M., D. Davoust, and C. Belaud. 1982.** *Tetrahedron Lett.* **23(18):** 1905–1906.
8. **Guyot, M., E. Morel, and C. Belaud. 1983.** *J. Chem. Res.* **5:** 188.
9. **Kuzirian, A. M., C. Tamse, and E. Yamoah. 1989.** *Am. Zool.* **29:** 333.

Reference: *Biol. Bull.* **187:** 275–276. (October, 1994)

Aggression-Reducing Courtship Signals in the Lobster, *Homarus americanus*

Paul Bushmann and Jelle Atema (Boston University Marine Program, Marine Biological Laboratory)

Shelters are very important for lobster social behavior. Males defend shelters (1), and dominant males in large "mating" shelters are more likely to mate (2). Females enter such occupied "mating" shelters and cohabit for about two weeks, during which time they molt and mate (3). Intermolt, transient matings have also been reported (4). The latter have been observed only in artificial laboratory conditions, but they do suggest multiple mating strategies.

This paper examines male and female entry of occupied shelters, and the postural and chemical signals used to communicate with the resident male. All experiments were carried out in a 3.7-m, Y-maze flume with a mating shelter in each arm. Seawater entered behind each shelter, flowed down each arm and through each shelter at 1.0 cm/s, and drained through a standpipe placed downstream at the other end of the flume. Two different dominant males were used throughout the experiment. A test began by placing one of the dominant males in one of the shelters, fitted with a transparent top. The other shelter was left empty. The test animal was placed behind a gate downstream near the standpipe. After 10 min the gate was removed and the animal allowed to move throughout the flume for 15 min. A camera over the flume, and another over the shelters, allowed observation of the visiting animal's movements in the flume and behaviors inside the shelter. Ten mature males and 15 mature females were tested. All experiments were conducted during the dark phase of a 14:10 light cycle. The flume was illuminated by dim incandescent bulbs, and the shelters by a red photographic safelight. Visiting animals were tested with and without an attached nephropore catheter, which collects urine, preventing its release into the water.

Of the 10 visiting males tested, 8 attempted to enter the occupied shelter. The resident male resisted, primarily by pushing with his claws. Occasional bouts of higher level aggression, such as claw lock (seizing an opponent with one claw), scissoring (rapidly crossing closed claws), and snapping (ripping an opponent with claws) were seen. Four of the five successful entering attempts required eviction of the resident. Blocking urine release had no significant effect upon resident male or visiting male behavior, or the visiting male's ability to evict the resident.

Females of all molt stages also attempted to enter the male-occupied shelter (13 of 15 tested), but the resident male's reaction was quite different. In all but two cases the females were allowed

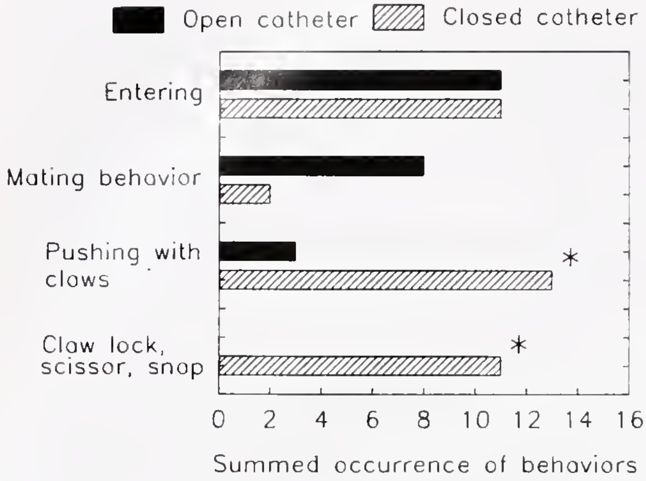

Figure 1. *Occurrence of shelter behaviors when visiting females were tested under open (urine released) or closed (no urine released) catheter conditions. Behaviors were scored once for each occurrence during a test. Counts were summed for the 15 females tested and differences between conditions were analyzed using the Wilcoxon signed rank test. Stars indicate significant differences. Upper star:* $z = -2.17$, $P < 0.05$. *Lower star:* $z = -2.20$, $P < 0.05$.

to enter, and no eviction of the resident occurred. Of those that entered, seven were mounted by the male, and two mated. The females that mated were intermolt, suggesting that intermolt matings may normally occur in shelters.

The resident male's distinct reactions to males and females suggest that females are communicating at least their sex. Both postural and chemical communication were observed. A female that had entered always assumed a submissive posture, often presenting her abdomen to the male. This resulted in the cessation of male pushing. These postures have been reported in premolt females at the beginning of cohabitation (2). They were observed here in both premolt and intermolt females and one male, suggesting their general utility as aggression-reducing signals. Visiting females released urine at a higher rate (40.5 μl/min) during the experiment than in isolation (10.5 μl/min), suggesting the involvement of female urine in shelter entering. Blocking visiting female urine release did not prevent entering, nor did it significantly affect the occurrence of mating behavior, but it did increase the occurrence and intensity of resident male aggression (Fig. 1).

Females of all molt stages can and do enter male shelters. They use both postural and chemical signals to accomplish this entry, and may mate with the resident male. In this way, a migrating female could obtain temporary protection and the use of a shelter. The male's benefit is less clear. If he cannot initially ascertain the reproductive state of the female, he may accept her even with a small chance of mating success.

Supported by NIH 2POINS25915-04A1 to J.A.

Literature Cited

1. **Karnofsky, E. B., J. Atema, and R. H. Elgin. 1989.** *Biol. Bull.* **176:** 239–246.
2. **Atema, J., S. Jacobson, E. Karnofsky, S. Oleszko-Szuts, and L. Stein. 1979.** *Mar. Behav. Physiol.* **6:** 277–296.
3. **Cowan, D. F., and J. Atema. 1990.** *Anim. Behav.* **39:** 1199–1206.
4. **Dunham, P. J., and D. Skinner-Jacobs. 1978.** *Mar Behav. Physiol.* **5:** 209–214.

Reference: *Biol. Bull.* **187:** 276–277. (October, 1994)

The Effect of Coastal Land Use on Inorganic Nutrient Concentrations in Groundwater Entering Estuaries of Waquoit Bay, Massachusetts

Kristin McDonnell, Michelle Rudy, Ivan Valiela, and Kenneth Foreman
(Boston University Marine Program, Marine Biological Laboratory)

Land use determines nutrient loading to estuaries by affecting the major sources of nutrients (*e.g.*, septic systems, fertilizer, or atmospheric deposition). In watersheds with unconsolidated sand sediments, groundwater is the primary transporter of nutrients to coastal estuaries (1). To investigate the effect of land use on nutrient concentrations in shallow estuarine systems, we measured inorganic nutrients in groundwater entering three estuaries of Waquoit Bay. The subwatersheds surrounding these estuaries vary in degree of urbanization, and we chose percentage of land covered by residential area as a convenient descriptor of land use. Percent residential area was estimated from a Geographical Information System map. Of the three subwatersheds, Childs River has the greatest residential area (27%), Quashnet River has a moderate amount (7%), and Sage Lot and Flat Ponds have the lowest percentage (3%).

Groundwater samples were collected at intervals of about 50–100 meters along the periphery of the three estuaries. All samples were analyzed for nitrate (NO_3^-) and ammonium (NH_4^+) on a Lachat autoanalyzer and for phosphate (PO_4^{3+}) by a manual method, adapted from Strickland and Parsons (2), for determining reactive PO_4^{3+}.

Mean NO_3^- concentration in groundwater was greatest at Childs River, lower at Quashnet River, and lowest at Sage Lot and Flat Ponds (Fig. 1, left panels); thus, NO_3^- concentrations paralleled the gradient in percent residential area. The presence of samples with high NO_3^- concentration (100–1000 μM) at

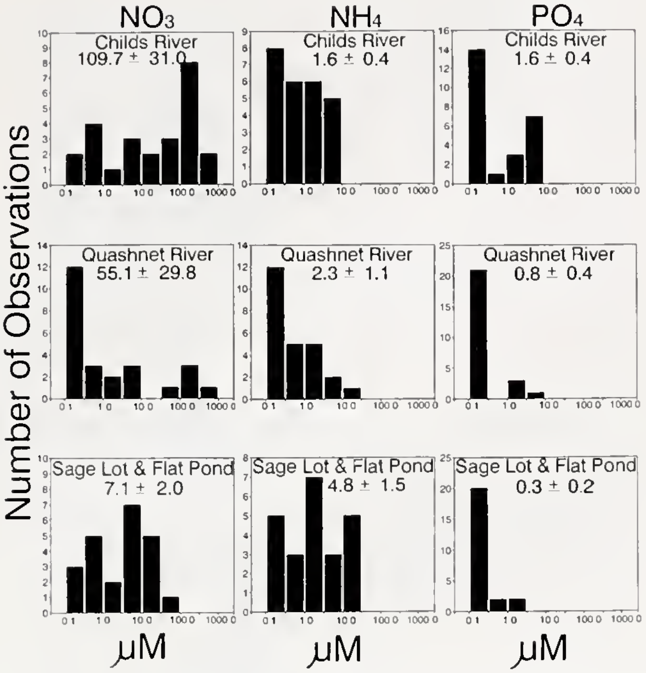

Figure 1. *Frequency distributions of inorganic nutrient concentrations in three estuaries of Waquoit Bay. All graphs show mean concentrations ± standard error. [Note: distributions do not include suspected anoxic samples (sulfurous or tinted samples).]*

Childs River and Quashnet River, combined with the absence of such spikes at Sage Lot and Flat Ponds, suggests input by plumes from septic tanks.

Mean NH_4^+ concentration in groundwater varied over a relatively small range across the three sites (Fig. 1, middle panels). NH_4^+ contributed less than 5% of the mean dissolved inorganic nitrogen (DIN) at Childs and Quashnet Rivers. Most of the inorganic nitrogen, therefore, enters these two estuaries in the form of NO_3^-. Nitrogen from septic tanks and soils enters the aquifer in reduced forms, such as NH_4^+ [untreated septic water contains up to 8000 μM NH_4^+ (J. McClelland, unpub. data)], which are oxidized to NO_3^- in the aquifer before reaching the estuary.

Mean PO_4^{3+} concentrations were relatively low and similar in the three estuaries (Fig. 1, right panels). One would not expect PO_4^{3+} to vary across the sites, despite a gradient in residential area, because PO_4^{3+} is readily adsorbed by soils.

Groundwater data from Waquoit Bay suggest that differences in land use can have a major effect on the concentrations of nitrogen entering a shallow estuary. To estimate the loading from groundwater to receiving estuaries and to estuarine systems, such as Waquoit Bay, concentration data such as those reported in this paper must be converted to flux by estimating actual water and nutrient transport. Calculated values of total system loading will be useful in deciding how to manage coastal estuaries threatened by eutrophication.

This work was supported by Waquoit Bay Land Margin Ecosystems Research and a Research Experience for Undergraduates grant. Special thanks to Lori Soucy for operating the autoanalyzer.

Literature Cited

1. **Valiela, I., *et al.* 1990.** *Biogeochemistry* **10:** 177–197.
2. **Strickland, J. D. H., and T. R. Parsons. 1960.** *Bull. Fish. Res. Board Can.* **125:** 1–185.

Reference: *Biol. Bull.* **187:** 277–278. (October, 1994)

From Watershed to Estuary: Assessment of Nutrient Loading, Retention, and Export from the Ipswich River Basin

Krista K. Ingram, Charles S. Hopkinson, Katherine Bowman, Robert Garritt, and Joe Vallino
(Marine Biological Laboratory)

High concentrations of dissolved nitrogen and phosphorus (80–150 μM N and 20–70 μM P) have been observed in small streams draining predominantly urban and agricultural watersheds within the Ipswich River drainage basin; at the same time, low nutrient concentrations in water are exported from the lower end of the river (< 20 μM N and 2 μM P) (Hopkinson, pers. obs.). To investigate this seeming paradox, transects were run along the entire 40-km length of the river to determine where nutrients were being removed, and a mass balance budget of nutrients was constructed for the entire drainage basin.

Concentrations of inorganic N and P were low along the entire length of the river, averaging 14 μM NO_3^--N, 1 μM NH_4^+-N, and 0.6 μM PO_4^{3-}-P. Concentrations were elevated at only 1 to 3 of the 20 stations investigated, and these were sites immediately adjacent to streams draining heavily populated residential areas or agricultural areas with livestock. Thus it appeared that high concentrations of nutrients entering the river were removed within 1–2 km downstream.

A nutrient mass balance budget for a 3-month growing season was constructed, including estimates of nutrient loading, uptake by wetland vegetation, and export from the watershed. Loading was estimated by combining information on land use for the 11 watersheds within the Ipswich River drainage basin with literature values for nutrient runoff from various types of land use and known point sources (1, 2, 3). Land use information was obtained using data from the Massachusetts Geographic Information System for 1985. In 1985, approximately 50% of the Ipswich watershed was classified as forest, 22% urban, 13% agri-

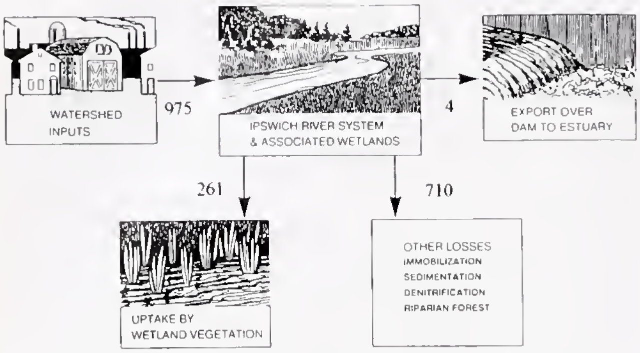
WATERSHED INPUTS
975
IPSWICH RIVER SYSTEM & ASSOCIATED WETLANDS
4
EXPORT OVER DAM TO ESTUARY
261
710
UPTAKE BY WETLAND VEGETATION
OTHER LOSSES
IMMOBILIZATION
SEDIMENTATION
DENITRIFICATION
RIPARIAN FOREST

Figure 1. *Annual budget of nitrogen loading, uptake, and export for the Ipswich River drainage basin. Units are in metric tonnes for a 3-month growing season during summer. (Drawn by Bob Golder.)*

culture, and 12% wetland. Estimates of 3-month loading for individual watersheds draining into the Ipswich River ranged from < 10 to 250 metric tonnes N and < 10 to 130 metric tonnes P.

Nutrient uptake by wetland vegetation along the Ipswich River was calculated from information on wetland area along the 11 reaches identified for the Ipswich River, observed species composition, and literature values for plant productivity and N and P content (4). Estimates of nutrient uptake for each reach ranged from 1 to 50 metric tonnes N and < 1 to 15 metric tonnes P. Variation between reaches was due solely to variations in wetland area.

The nutrient mass balance for the Ipswich River drainage basin indicated a large discrepancy between calculated nutrient loading and wetland plant uptake and measured export (Fig. 1). The total mass balance was constructed by summing values for each of the 11 watersheds. Of the 975 tonnes of nitrogen calculated to be entering the river, only 4 tonnes were measured leaving the river over the dam in Ipswich. Wetland vegetation was calculated to remove approximately 261 tonnes of N. This leaves 710 metric tonnes that could not be accounted for with this analysis. Additional removal mechanisms that are probably important include microbial immobilization, sedimentation, denitrification, and uptake by vegetation in the extensive riparian zone along the river.

These observations and calculations reveal the important role of river-basin processes in the removal of nutrients originating in agricultural and urban areas. In addition, the study indicates how increases in urbanization and decreases in wetland buffer communities can affect the chemical composition of riverine and estuarine systems.

This research was supported by supplemental funding to NSF grant (OCE-92-14461) from the NSF Research Experiences for Undergraduates program.

Literature Cited

1. **Dickerhoff-Delwiche, L., and D. Haith. 1983.** *Water Resources Bull.* **19:** 951–959.
2. **Omernik, J. 1976.** *U.S. Environmental Protection Agency* 600/3-76-014. 105 pp.
3. **Vollenweider, R. 1968.** *DAS/CSI/Rept 68.* 26 pp. Paris.
4. **Hopkinson, C. S., and J. P. Schubauer. 1984.** *Ecology* **65:** 961–969.

Reference: *Biol. Bull.* **187:** 278–279. (October, 1994)

Dissolved Organic Nitrogen in Groundwater Bordering Estuaries of Waquoit Bay, Massachusetts: Relations with Watershed Landscape Mosaics

Michelle Rudy, Kristin McDonnell, Ivan Valiela, and Kenneth Foreman
(Boston University Marine Program, Marine Biological Laboratory)

Anthropogenic activity generally increases inorganic nutrient content of groundwater (1), but factors influencing dissolved organic nitrogen (DON) are less well known. In this study we examine the effect of human activity as well as natural landscape configuration on concentrations of DON in groundwater.

In unconsolidated sandy soils like those that underlie the Waquoit Bay watershed, virtually all fresh water flows via groundwater transport (1). To assess the DON that potentially reaches three estuaries of Waquoit Bay, we collected fresh groundwater samples (salinity <0.5 ppt) from the periphery of each estuary. Particulate matter was excluded from our samples with a 0.45 μm pore-size filter. We analyzed groundwater samples for total nitrogen by the method of D'Elia *et al.* (2), and nitrate (NO_3^-) by Lachat autoanalyzer.

To assess the impact of urbanized areas on concentrations of DON in groundwater, we selected three watersheds that supported differing percent residential area (27% in Childs River, 7% in Quashnet River, and 3% in Sage Lot Pond) (3). Mean concentration of DON in groundwater samples was higher in watersheds with lower percentage of residential area (Fig. 1, left column). This pattern contrasts with the large increase in dissolved inorganic nitrogen (DIN) observed in Childs compared to Sage Lot Pond groundwater (4). In our most urbanized site, DON:DIN in groundwater was approximately 1:2. In our least urbanized site, the ratio of DON:DIN was 7:1.

DON concentration seems not to be related directly to urbanization, but rather to the mosaic of vegetation covering the surface of the land. For example, mean concentration of DON

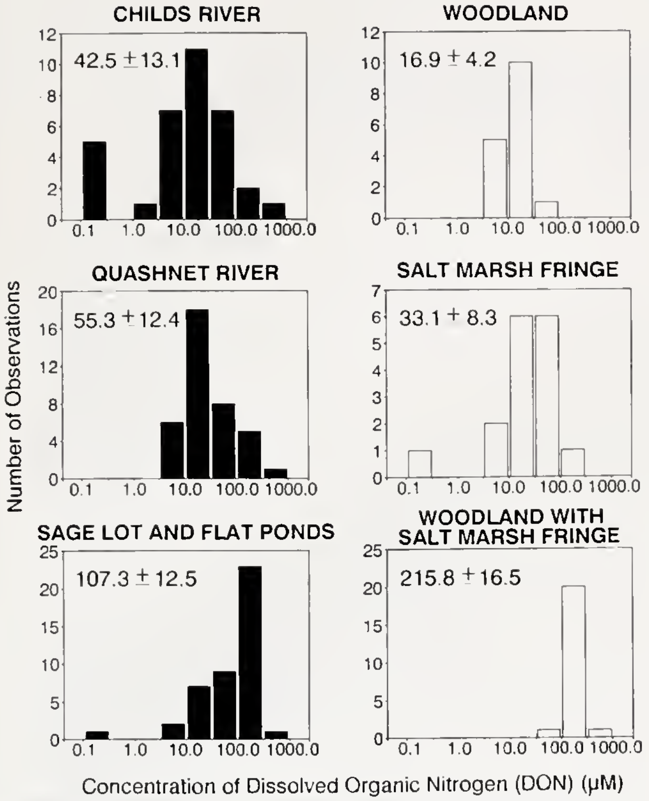

Figure 1. *Frequency distribution and mean ± standard error of dissolved organic nitrogen (DON) concentrations among areas of differing landscape configurations. Left column. DON in groundwater from watersheds with high (top), medium (middle), and low (bottom) cover of residential area. Right column. DON from groundwater in natural, unpopulated landscape units: areas with woodland but no bordering marsh (top), areas without forest bordering a marsh (middle), and the combination of woodland with bordering salt marsh (bottom).*

among the three watersheds increased in proportion to percent shoreline fringed with marsh ($r^2 = 0.999$). Salt marsh fringes evidently have some effect on DON content, but so do other vegetation covers, such as woodland.

To assess the relative importance of bordering salt marsh and woodland area on DON concentrations, we collected samples from unpopulated portions of the Sage Lot Pond and Quashnet River watersheds. Our collection sites included three categories of adjacent vegetation parcels: woodland areas; salt marsh areas fringed not by woodland but by sparse dune vegetation; and salt marsh areas fringed by woodland. Groundwater from a woodland edge with no salt marsh fringe showed an average of about 17 μM DON (Fig. 1, right top), while DON in groundwater bordering a salt marsh fringe without an adjacent forest showed nearly twice this concentration (Fig. 1, right middle). In areas where woodland was combined with a salt marsh fringe, the concentration of DON was 13 times greater than in woodland alone (Fig. 1, right bottom).

Humic matter leached from woodland soil appears to provide DON to groundwater, but its effect is small unless coupled to the influence of salt marshes. Marsh peat is of low hydraulic permeability (5), and thus it seems reasonable that its role is to slow the flow of groundwater entering the estuary. If flow is slow enough, aerobic microbial metabolism of terrestrially produced organic matter could lower O_2 content of groundwater. We found that 55% of groundwater samples from woodlands with salt marsh fringe were anoxic, judging by the sulfide odor. The other habitats we studied showed that only 13–15% of samples were anoxic. The reduced conditions could inhibit further microbial decay of organic matter (6) and lead to accumulation of DON.

Land use affects concentrations of dissolved organic and inorganic nitrogen in different ways. In heavily populated areas, septic tank leaching and fertilizer use increase inorganic nutrients in groundwater. In contrast, reduction of forests may lower the input of organic nitrogen to groundwater. On the other hand, destruction of salt marsh fringes may allow greater nutrient flow to estuaries.

We gratefully acknowledge Lori Soucy for her technical assistance. This study has been supported by the Research Experience for Undergraduates program.

Literature Cited

1. **Valiela, I., *et al.* 1990.** *Biogeochemistry* **10:** 177–197.
2. **D'Elia, C., *et al.* 1977.** *Limnol. Oceanogr.* **22:** 760–764.
3. Geographical Information System land use map of the Waquoit Bay watershed, 1985.
4. **McDonnell, K., *et al.* 1994.** *Biol. Bull.* **187:** 276–277.
5. **Dasberg, S., and S. Neuman 1977.** *J. Hydrol.* **32:** 219–239.
6. **Valiela, I. 1984.** P. 289 in *Marine Ecological Processes*, Springer-Verlag, New York.

Reference: *Biol. Bull.* **187:** 279–280. (October, 1994)

The Growth and Consumption of Macroalgae in Estuaries: The Role of Invertebrate Grazers Along a Nutrient Gradient in Waquoit Bay, Massachusetts

Ashton Horne, James McClelland, and Ivan Valiela (Boston University Marine Program, Marine Biological Laboratory)

The eutrophication of Waquoit Bay estuaries, which results from nutrient loading associated with urbanization, has altered the species composition of both floral and faunal assemblages (1). Certain species of macroalgae have replaced eelgrass beds as nutrient loads increased. The seaweed canopies of estuaries that experience different rates of nutrient loading contain dis-

Table I

Comparison of the growth and consumption rates of algae growing in estuaries of high and low nutrient loading rates

	Childs River (high nutrient)		Sage Lot Pond (low nutrient)	
Growth in the Absence of Grazers (gww)	Daily mean ± SE	% Increase	Daily mean ± SE	% Increase
Ulva	0.08 ± 0.01	16	0.03 ± 0.01	6
Enteromorpha	−0.04 ± 0.02	−8	0.02 ± 0.02	4
Cladophora	0.04 ± 0.01	8	0.02 ± 0.01	4
Gracilaria	0.06 ± 0.01	12	0.03 ± 0	6
Consumption by Grazers (gww)	Daily mean ± SE	% Daily growth consumed	Daily mean ± SE	% Daily growth consumed
Ulva	−0.01 ± 0.01	0	0.01 ± 0.01	33
Enteromorpha	0.03 ± 0.01	175	0.03 ± 0.02	150
Cladophora	0.03 ± 0.01	75	0 ± 0.01	0
Gracilaria	−0.03 ± 0.01	0	0.01 ± 0.01	33

tinctive suites of grazers (McClelland, unpub.). In this paper we examine whether these grazers play a role in controlling the abundance of different seaweed species.

We measured growth and consumption of four algae species (*Ulva, Enteromorpha, Cladophora,* and *Gracilaria*), by an amphipod, *Gammarus mucronatus,* in estuaries of high (Childs River) and low (Sage Lot Pond) nutrient loading. Three replicate sets of cages were installed in each estuary. Cages were constructed from 0.83-l translucent plastic boxes, screened on the sides and top with 500-μm mesh. Aluminum frames, anchored and buoyed, suspended the cages 20 cm above the algal mat to ensure adequate light intensity within the boxes. Each frame held eight cages, each containing 0.5 g of algae (two cages for each algal species). Half of the cages were designated for the assessment of grazing and contained eight amphipods in addition to the algae. *Gammarus* was used in all trials because it was the most abundant grazer gathered with the algae. The other four cages had no amphipods and were used to assess the growth of the algae during the experiment. Four 4-day trials were run during midsummer at intervals of about one week.

Biomass increase or decrease was measured after each trial to determine average rate of growth and consumption. The growth rates of algae in Childs River were greater than those in Sage Lot Pond (Table I, top), except for *Enteromorpha* in Childs River. Increased nutrient loading correlated with a doubling of growth rates for all algae except *Enteromorpha. Ulva* and *Gracilaria* grew fastest in both estuaries, followed by *Cladophora. Enteromorpha* did not grow at Sage Lot Pond and decreased in biomass at Childs River. This may have resulted because of accumulation of silt and epiphytes within the boxes, which reduced light intensity. *Enteromorpha,* which often floats near the surface where light intensity is greatest, seemed most susceptible to such reductions of light.

Consumption rates (Table I, bottom) were calculated by subtracting the total algal growth in the presence of grazers from the total growth without grazers. Grazing rates in Childs River and Sage Lot Pond were similar, so that nutrient loading did not directly alter grazing by the amphipod. However, because of the differences in growth rates, the impact of grazers was much greater at Sage Lot Pond. These results suggest that control of algae by grazers may be of greater significance in systems of low rather than high nutrient loading.

Literature Cited

1. **Valiela, I., *et al.* 1992.** *Estuaries* 15-4: 443–457.

Reference: *Biol. Bull.* **187**: 281. (October, 1994)

The Effect of Nutrient Loading on the Growth Rate of Two Species of Bivalves, *Mercenaria mercenaria* and *Mya arenaria*, in Estuaries of Waquoit Bay, Massachusetts

Anna Chalfoun, James McClelland, and Ivan Valiela (Boston University Marine Program, Marine Biological Laboratory)

Nutrient loading can accelerate primary production and hence affect consumers that depend on producers. This study investigated the effect of nutrient loading on the growth rate of two species of benthic suspension-feeding bivalves, soft-shelled clams (*Mya arenaria*) and quahogs (*Mercenaria mercenaria*). Such a link can be inferred from correlations between growth of *Mya* and concentrations of chlorophyll *a* and particulate organic matter (1). Three estuaries of Waquoit Bay (Childs River, Quashnet River, and Sage Lot Pond) differ in the extent to which they are urbanized, and thus provide a gradient of nutrient loading, with the highest loading at Childs River and the lowest at Sage Lot (2). Nutrient loading in Waquoit Bay is proportional to percent residential area; Childs River has 27% residential area, Quashnet 7%, and Sage Lot 3% (3).

Clams were placed in 11" by 7" by 4" plastic boxes covered with chicken wire, and half filled with sand. They were set out at three sites, of similar depth and salinity, in each of the three estuaries for eight weeks in midsummer. Boxes of each species were deployed at each site, and six clams were placed in each box. The clams were numbered, measured with calipers to the nearest 0.5 mm, and separated into three size classes to ensure that each box contained representative sizes.

Mya and *Mercenaria* growth rates were inversely correlated to size (Fig. 1); the larger the size, the slower the growth rate, as commonly found (4).

Growth rates increased with increased nutrient loading (Fig. 1, top). With *Mya*, all three size classes exhibited the highest growth rates in Childs River, and the lowest in Sage Lot Pond. Quashnet growth rate values were intermediate to the two extremes.

Mercenaria also showed faster growth in Childs River (Fig. 1, middle). Unlike growth of *Mya*, however, growth of *Mercenaria* was lowest in Quashnet River. Although chlorophyll *a* concentrations (a proxy for bivalve food availability) in Quashnet are intermediate (Fig. 1, bottom), water moves through Quashnet much faster than through the other two estuaries (Fig. 1, bottom). *Mercenaria* depends primarily on suspended phytoplankton for its diet, so faster water exchange may limit its efficiency in filtering particles and thus slow its growth. *Mya*, however, feeds on a mixed diet of resuspended detrital particles and plankton (D. Leavitt, pers. comm.), and so may not be as affected by the faster flow regime in Quashnet River.

Bivalve growth does respond to increases in nutrient loading, albeit indirectly through the effect of loading on primary producers. In addition, the hydrography of estuaries can affect growth rate, at least in the case of quahogs.

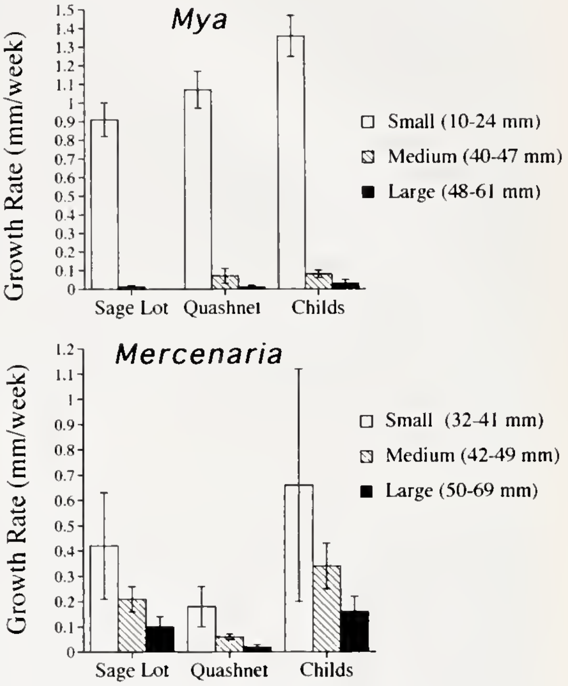

Chlorophyll a (µg/l)	10.1±4.8	12±3.6	14.7±4.0
Water Residence Time (Days)	2.2	0.3	1.1

Figure 1. *Growth rate (Mean and SE) of* Mya arenaria *(top) and* Mercenaria mercenaria *(middle) in three estuaries of Waquoit Bay with low (SL), medium (QR), and high (CR) nutrient loading. Mean chlorophyll* a *concentrations (data from K. Foreman, WBLMER) and water residence time (data from R. Geyer, WBLMER) for each estuary are provided at bottom of figure.*

This work was supported by the Research Experience for Undergraduates program.

Literature Cited

1. **Essink, K., and A. H. Bos. 1985.** *Netherlands J. Sea Res.* **19**: 45–51.
2. **Valiela, I., *et al.* 1992.** *Estuaries* **15**: 443–457.
3. **McDonnell, K., *et al.* 1994.** *Biol. Bull.* **187**: 276–277.
4. **Valiela, I. 1984.** *Marine Ecological Processes.* Springer-Verlag, New York. Pp. 192–200.

Reference: *Biol. Bull.* **187**: 282–283. (October, 1994)

Long-Term Changes of Macroinfaunal Assemblages in Experimentally Enriched Salt Marsh Tidal Creeks

Rafael Sardá (Centro de Estudios Avanzados de Blanes, CSIC, 17300-Blanes (Girona), Spain), Kenneth Foreman, and Ivan Valiela

We evaluated the long-term effects of resource enrichment on benthic community dynamics by manipulating nutrient supply in the field, allowing other factors such as climate and predation to vary naturally. Starting in 1974, we increased supply of food resources to a typical oligohaline deposit-feeding community (1) by experimental enrichment with fertilizer (2). For 20 years, experimental plots have been fertilized with 75 g m^{-2} $week^{-1}$ of a sewage-sludge-based fertilizer every two weeks from April to November. Sediment samples were collected at the beginning of the experiment, and again after 15 years, from benthic creeks that bisect each experimental plot. Macrofauna in these sediments were identified, counted, and measured.

Initially, fertilization increased the biomass of the benthic assemblage and stimulated growth of populations of opportunistic polychaetes in the creeks (3). After 15 years of nutrient addition, significant differences in both abundance ($F = 11.23$, $p < 0.01$) and biomass ($F = 11.45$, $p < 0.01$) were still found between fertilized and control creeks; however, biomass of the benthic assemblage in fertilized creeks was lower than it had been when first sampled in 1974. The decline in biomass within fertilized creeks is due to a shift in species dominance from opportunistic polychaetes to oligochaetes (the naidid *Paranais litoralis* and the tubificid *Monopylephorus evertus*).

The frequency distribution of monthly biomass classes is shown in Figure 1. The number of individuals per biomass class in fertilized creeks (open bars) exceeds that in control creeks (filled bars) during May-June and again in November-January. Macroinfauna responded to enrichment in spring and fall, but not in summer. The May-June response is due to blooms of the oligochaete *P. litoralis*. The November-January response is due to blooms of *M. evertus*. Caging experiments have demonstrated that the summer decrease was due to intense predation (4).

The coexistence of these two oligochaete populations can be explained by resource partitioning. Fertilization with sewage sludge increases primary production in these experimental plots. In spring, fertilizer addition increased the concentration of chlorophyll *a* in the creeks (5), and the population of *P. litoralis* grew using this resource. In fall, fertilizer addition increased the quality and quantity of *Spartina* detritus in the creeks, and the population of *M. evertus* grew using this high-quality detritus. Biomass peaks detected in fall and early winter were higher than those observed in spring because *M. evertus* is a larger species than *P. litoralis*.

Long-term enhancement of resource supply has modified the species composition of the creek fauna, leading to the dominance

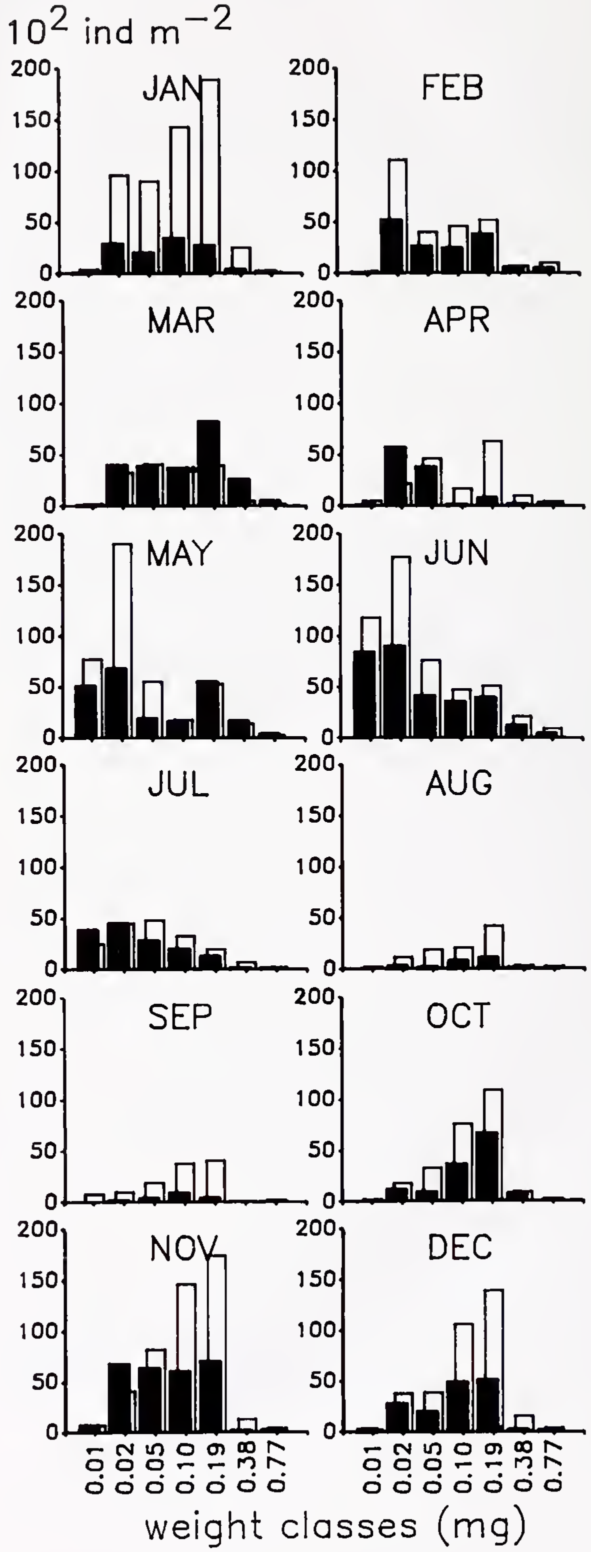

Figure 1. *Monthly frequency distribution of biomass classes in fertilized (open bars) and control (filled bars) creeks. Each month shows average biomass pooled from two years of sampling.*

of oligochaete species during two periods of the year. During these two periods, food limitation is a dominant factor regulating the community, whereas during summer, predation regulates macroinfaunal abundance and biomass (4).

We acknowledge Salt Pond Sanctuaries and Dorothea and the late Arnold Gifford for use of their land. This work was supported by grants from the National Science Foundation, Victoria Foundation, and the Pew Memorial Trust. A Fulbright Fellowship and an MBL Associates Fellowship supported Rafael Sardá during this work.

Literature Cited

1. **Sardá, R., K. Foreman, and I. Valiela.** In press. *Mar. Biol.*
2. **Valiela, I., and J. M. Teal. 1974.** Pp. 547–563 in *Ecology of Halophytes.* Academic Press, New York.
3. **Sardá, R., K. Foreman, and I. Valiela. 1992.** Pp. 85–91 in *Marine Eutrophication and Population Dynamics.* Olsen and Olsen, Fredensborg (DK).
4. **Wiltse, W. I., K. Foreman, J. M. Teal, and I. Valiela. 1984.** *J. Mar. Res.* **42:** 923–942.
5. **Foreman, K. 1989.** *PhD Dissertation.* Boston University.

Reference: *Biol. Bull.* **187:** 283–284. (October, 1994)

Effects of Algal Biomass on Benthic Nitrogen Flux in Nutrient-Loaded Estuaries of Waquoit Bay, Massachusetts

Peter Hurlbut (University of Massachusetts, Amherst), Charlene D'Avanzo, Deepti Sethi, and Kerry Guilfoyle

To test whether increased nitrogen loading from watersheds leads to increased rates of benthic regeneration, we measured rates of ammonium release in three estuaries of Waquoit Bay, Massachusetts (Childs River, Quashnet River, Sage Lot Pond), and a beach in Woods Hole by using benthic chambers. Childs River, Quashnet River, and Sage Lot Pond receive different amounts of nitrogen loading, from highest to lowest respectively, from their watersheds (1), and the Woods Hole beach receives little or no loading.

Dark benthic chambers were placed over bottom sediments of each estuary at similar depths. Algal biomass differed in the sites at which we carried out the ammonium release measurements. Water samples were taken from the head space of the chambers over a 4-h period, and ammonium concentrations were measured by the indolephenol method (2). Any high initial ammonium concentrations showed a disturbance of algae, and those chambers were not used.

Benthic ammonium release was nearly equal for Childs River, Quashnet River, and Sage Lot Pond. The average ammonium release in Childs River was 233.7 ± 108.2 μmol/m/h; for Quashnet River it was 249.3 ± 100.8 μmol/m^2/h; and for Sage Lot Pond the average was 209.3 ± 34.9 μmol/m^2/h. These values do not differ significantly, so different loading rates do not alter the rate of ammonium release.

It was the amount of seaweed biomass that increased with nutrient loading (Fig. 1). Where there was no seaweed, rates of NH_4^+ release for bare sediment in the three sites ranged between 100 and 200 μmol/m^2/h. This range is near average for coastal marine systems (3). In sites with higher algal biomass, however, ammonium flux rates are up to three times higher than reported rates. Algal biomass depends on nutrient loading (1), so NH_4^+ release rates are therefore indirectly related to loading from watersheds.

To evaluate the relative magnitude of the rates of NH_4^+ release, we compared them to loading rates from the watersheds. Average algal biomass for each system was obtained from unpublished data of Douglas Hersh. The average algal biomass for Childs River is 383 g/m^2, Quashnet River is 147 g/m^2, and Sage Lot Pond has an average aquatic vegetation biomass of 200 g/m^2. The ammonium flux rate, adjusted to algal biomass and to the area of each estuary (4), was also used to derive NH_4^+ release rates that could be compared to inputs. Regeneration rate of Childs River was highest (150 mg N/m^2/d); Quashnet River and Sage Lot Pond had lower rates (90 mg N/m^2/d and 110 mg N/

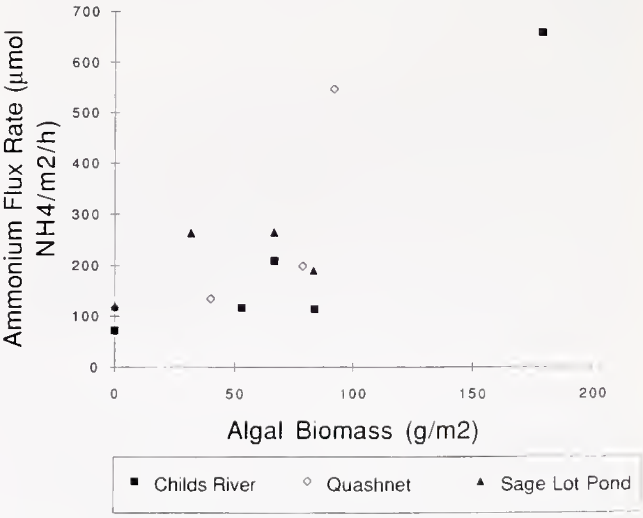

Figure 1. *Algal biomass versus ammonium flux rate. (Note: Woods Hole beach was added to Sage Lot Pond as a low-loading control site.)*

m^2/d, respectively). Childs River ammonium flux is about 23% of the total dissolved nitrogen input (670 mg N/m^2/d) for the same period. This percentage is slightly lower than has been found for nitrogen regeneration in Narragansett Bay, which accounts for 40% of nitrogen in the water column (3). Sage Lot Pond's dissolved nitrogen input (3.6 mg N/m^2/d) was 25 times lower than the flux rate of 90 mg N/m^2/d.

Literature Cited

1. **Valiela, I., *et al.* 1992.** *Estuaries* **15:** 443–457.
2. **Solorzano, L. 1969.** *Limnol. Oceanogr.* **12:** 799.
3. **Nixon, S. W. 1981.** Pp. 111–138 in *Estuaries and Nutrients.* B. J. Neilson and L. E. Krenin, eds. Humana Press, Clifton, NJ.
4. **Cambareri *et al.* 1992.** Pp. 1–24 in *Proceedings of Focus. Eastern Regional GroundWater Conference.*

Reference: *Biol. Bull.* **187:** 284–285. (October, 1994)

Daily Variation in Phytoplankton Production in Two Subestuaries of Waquoit Bay, Massachusetts

Jessica L. Boxhill, Lory Santiago Vázquez, Timothy R. Harrison, Kenneth Foreman, (Boston University Marine Program, Marine Biological Laboratory), and James N. Kremer

Much work has been devoted to documenting seasonal variation in primary phytoplankton production; however, few studies have examined variation on a daily basis. Moreover, the use of data collected once per month to estimate seasonal production has recently been criticized (1). We performed a time-intensive study of phytoplankton production in the Quashnet and Childs Rivers, two shallow coastal estuaries, subject to different rates of nutrient loading (2). We hypothesized that day-to-day phytoplankton production would be strongly correlated with irradiance levels, water temperature, and nutrient loading.

We made successive daily measurements of phytoplankton production and light extinction with depth over two 11- to 12-day intervals (22 June–3 July 1994 in Quashnet and 17–27 July in Childs). Surface and bottom water samples were collected in light and dark bottles (3) and incubated *in situ* between 1000 and 1400 h, the period of maximum irradiance. Concentrations of dissolved oxygen in the bottles were determined by the Winkler method and used to calculate an average hourly rate of gross primary production (GPP). Irradiance levels were recorded hourly by the WBNERR Meteorological Station, and water temperature was measured by an Endeco Model 6000 data logging sensor package, deployed in the water column. Figure 1A illustrates the variation in these physical conditions during the study.

Our data show that gross primary production was higher in the Childs River, and that it fluctuated daily in both estuaries ($\bar{X}$ = 0.92 mg O_2/l h, CV = 39%, $\bar{X}$ = 0.39 mg O_2/l h, CV = 62% for Quashnet) (Fig. 1B). To examine the sources of this variation, we compared rates of GPP in both estuaries to the average irradiance, during the 4-h incubation period (Fig. 1C). These data indicate that light has no effect on GPP in either estuary. The phytoplankton production was consistently higher in Childs than in Quashnet over the same range of irradiance. Light does not appear to be a limiting factor for GPP during

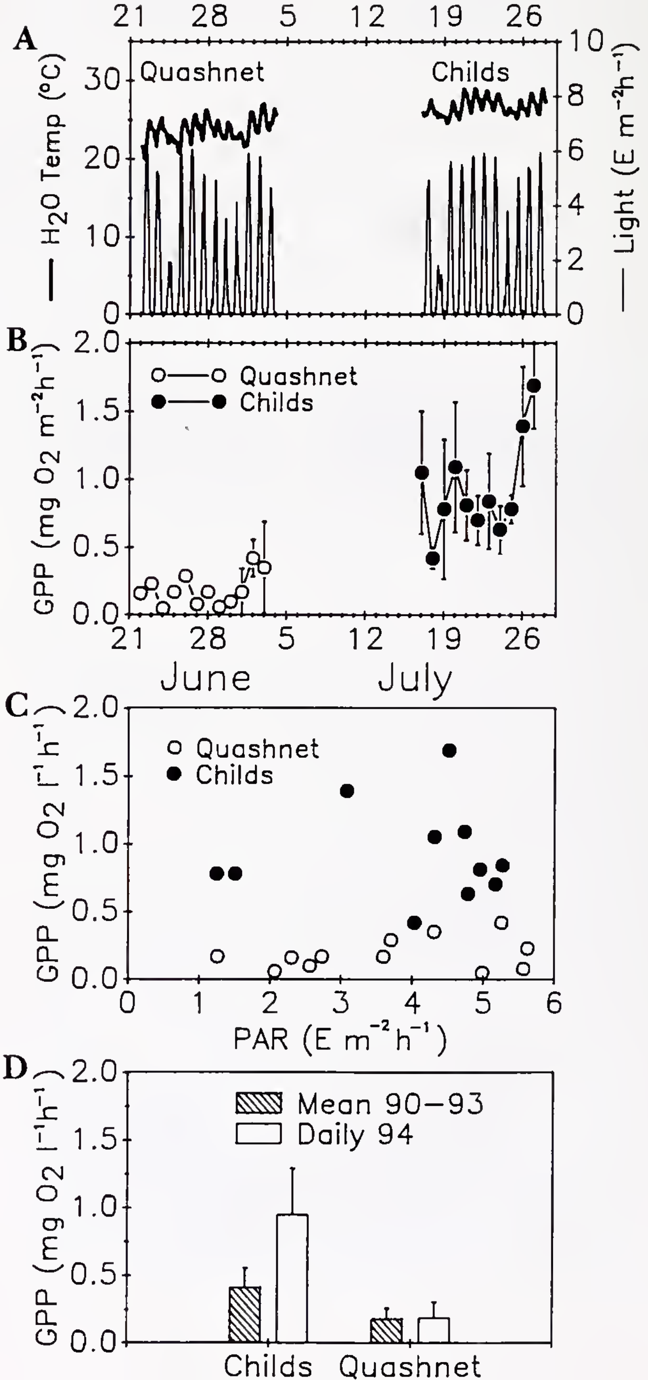

Figure 1. *(A) Water temperature (left axis, heavy line) and light (right axis, light line) during deployments in which primary production was measured in Quashnet and Childs Rivers; (B) mean ± range of rate of gross primary production (GPP) measured at two stations in the Quashnet River (open symbols) and two stations in the Childs River (solid symbols); (C) GPP plotted* vs. *photosynthetically available radiation (PAR) in both Quashnet (open symbols) and Childs (closed symbols) Rivers; (D) comparison of mean GPP ± 2 SE for measurements made daily during June (Quashnet) and July (Childs) in 1994 to mean ± 2 SE of measurements made monthly in the same month during 1990–93.*

summer, and it does not explain the difference in GPP between the two estuaries. Average light levels at mid-depth in the Quashnet and Childs were 693 μE/m^2 h and 319 μM E/m^2 h respectively. These values are at or above saturating irradiance for phytoplankton typically found in coastal waters (4). Similarly, we observed no relationship between water temperature and GPP. We did, however, find a trend in the GPP differences between the two estuaries. Phytoplankton production in the Childs River was significantly higher than in Quashnet, which may be explained by previously measured differences in nutrient loading and nutrient concentrations in freshwater input (2).

Figure 1D shows the relationship between the average time-intensive data (summer, 1994) and the average monthly data (June–July) for both estuaries over the period of 1990–1993. The mean GPP rates from our study do not appear significantly different from the prior three years for the same season. This suggests that daily variations in phytoplankton production may be comparable to the variation that occurs on an inter-annual time scale.

This work was supported by the Research Experience for Undergraduates program.

Literature Cited

1. **Taylor, C., and B. Howes. 1994.** *Mar. Ecol. Prog. Ser.* **108:** 193–203.
2. **Valiela, I., K. Foreman, M. LaMontagne, D. Hersh, J. Cost, C. D'Avanzo, M. Babione, P. Peckol, B. DeMeo-Anderson, C. Sham, J. Brawlely, and K. Lajtha. 1992.** *Estuaries* **154**(4): 43–457.
3. **Hall, C., and R. Moll. 1975.** Pp. 18–53 in *Primary Productivity of the Biosphere.* H. Lieth and R. H. Whitaker, eds. Springer-Verlag, New York.
4. **Ryther, J. 1956.** *Limnol. Oceanogr.* **1:** 61–70.

Reference: *Biol. Bull.* **187:** 285–286. (October, 1994)

The Effects of Wind Speed and Direction on Stratification and Phytoplankton Production in an Estuary of Waquoit Bay, Massachusetts

Lory Z. Santiago Vázquez, Jessica L. Boxhill, Timothy R. Harrison, James N. Kremer, and Kenneth Foreman (Boston University Marine Program, Marine Biological Laboratory)

Mixing between surface and bottom waters in partially stratified estuaries can alter water column productivity by changing the residence time and also by making regenerated nutrients available to plankton. Wind forcing, freshwater input, and the neap-spring tide cycle are important in structuring salinity profiles in shallow estuaries (1). We related the physical factors of wind speed and direction to water column stratification and phytoplankton production at Quashnet River, Waquoit Bay (Fig. 1A).

We measured physical factors and phytoplankton production continuously over a 12-day interval. Wind was measured by recording anemometers. Salinity and depth were measured by data-logging sensor packages (ENDECO models 1184 and 6000). Sensors were deployed near the surface and bottom of the water column. Phytoplankton production was measured daily by deployment of clear and dark bottles in which the change of oxygen was determined by the Winkler method (2).

Wind direction was initially from the southwest on 22–24 June, but wind velocities were low (Fig. 1B). Wind direction changed to the east on 24–25 June, then shifted again to the southwest on 25 June, and substantial southwest winds (3–6 m s^{-1}) continued to blow for 9 days (Fig. 1B). The wind speed declined, and wind direction shifted to the northeast near the end of the deployment on 3 July. Hence, the Quashnet River experienced a sustained period of wind forcing from the southwest along the main axis of the estuary (Fig. 1A) during our sampling interval. Such wind forcing may inhibit tidal exchange (3).

Bottom salinity stayed fairly constant throughout the deployment, at an average of 25 ppt (Fig. 1C). Surface salinity tended to decrease during 25 June–3 July when wind blew from the southwest, and increased when the wind shifted to the northeast. Stratification, expressed as the difference in salinities between surface and bottom waters, increased from 25 June–3 July (Fig. 1C).

Wind direction was more important in controlling mixing and stratification than wind speed. We did not observe any relationship between wind speed and delta salinity. When the wind blew from the northeast (downstream), stratification decreased, as bottom waters, which were more saline, replaced surface waters, which were rapidly flushed out of the estuary by both wind and gravitational forces in classic estuarine circulation. When the wind blew from the southwest (upstream), downstream transport was reduced, and fresh water accumulated in the surface waters, progressively increasing stratification (Fig. 1C).

The increase in stratification and retention of fresh water within the estuary provided us with an opportunity to examine the relationship between phytoplankton production and water residence time. We expected freshening of the surface water and increased stratification to result in increased gross production due to retention of both land-derived nutrients and plankton within the estuary. The mean rate of gross production over the sampling interval was 0.19 mg O_2 l^{-1} h. As a proxy for residence time, we plotted delta salinity against gross production (GPP). No substantial correlation was found between delta salinity and GPP (Fig. 1D). The lack of a clear relationship between strati-

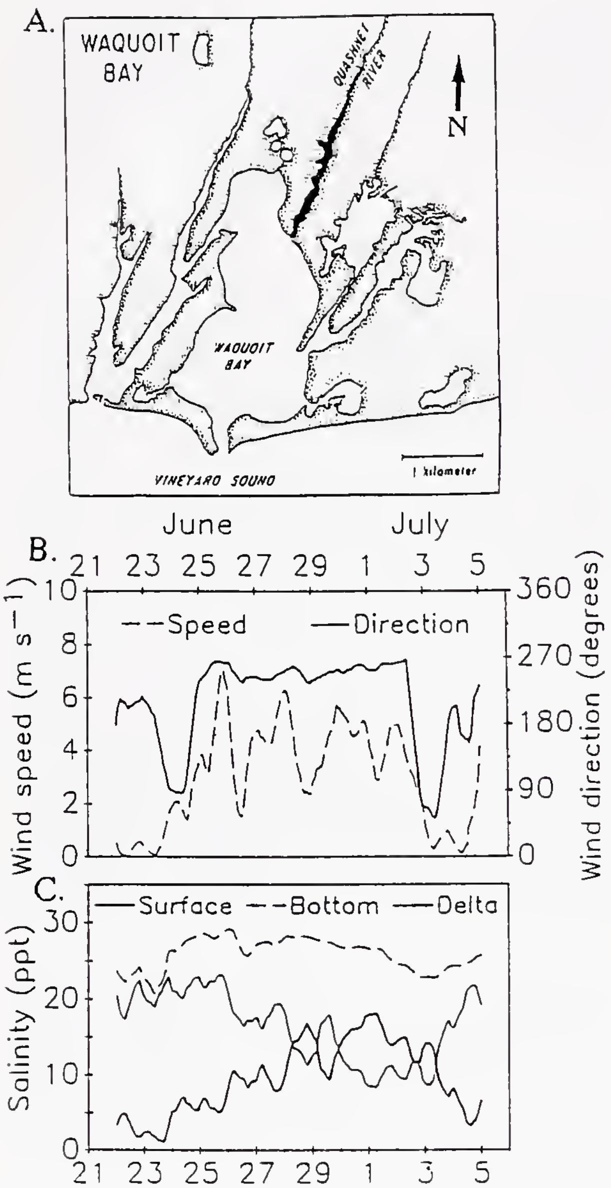

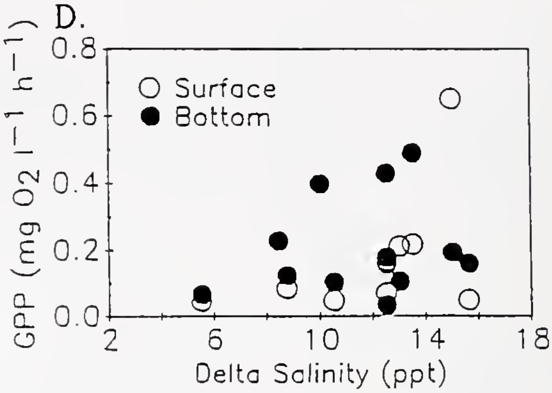

Figure 1. *(A) Location of Quashnet River, Waquoit Bay, Massachusetts. (B, C) Wind speed and direction, and salinity during this study. (D) Relationship between stratification and phytoplankton production.*

fication and productivity might be due to lags in the phytoplankton response, as well as to the opposing effects of mixing, which makes nutrients regenerated in the bottom available to plankton, and increased residence time, which allows plankton populations to build up within the estuary.

Literature Cited

1. **Kjerfve, B. 1989.** Pp. 47–48 in *Estuarine Ecology*, J. W. Day, C. A. S. Hall, W. M. Kemp, and A. Yanez-Arancibia, eds. John Wiley & Sons, New York.
2. **Hall, C., and R. Moll. 1975.** Pp. 18–53 in *Primary Productivity of the Biosphere*, H. Lieth and R. H. Whitaker, eds. Springer-Verlag, New York.
3. **Weisberg, R. H. 1976.** *J. Phys. Oceanogr.* **6:** 721–734.

Reference: *Biol. Bull.* **187**: 287–288. (October, 1994)

Comparison of Phytoplankton and Ecosystem Gross Production in the Quashnet River, an Estuary of Waquoit Bay, Massachusetts

Timothy R. Harrison, Jessica L. Boxhill, Lory Z. Santiago Vázquez, Kenneth Foreman, and James N. Kremer (Boston University Marine Program, Marine Biological Laboratory)

The Quashnet River is a shallow (av. depth 0.5 m) estuary of Waquoit Bay, Massachusetts, that supports a large biomass of benthic macroalgae, in addition to phytoplankton producers. To evaluate the factors controlling the relative contribution of phytoplankton production to total ecosystem production in the Quashnet River, we measured both gross phytoplankton production (GPP) and gross ecosystem production (GEP), along with a suite of physical factors, for 12 consecutive days. We related change in the ratio of GPP to GEP to photosynthetically available radiation (PAR), temperature, salinity, water column depth, and wind speed and direction.

Phytoplankton production was measured daily as the change of oxygen in light and dark bottles during 4- to 6-h incubations; the oxygen concentrations were measured by the Winkler Method (1). Ecosystem production was estimated from diel free water oxygen levels recorded by automated oxygen meters. ENDECO model 1184C and 6000 pulsed-sensor oxygen meters were used to measure the oxygen, temperature, depth, and salinity of the surface and bottom water, respectively. Wind speed and direction were measured with an Onset Tattletale 2-B computer linked to a Digitar #7902 anemometer.

The GEP and GPP fluctuated over time, going up or down in synchrony for most days (Fig. 1A). The average GPP was 1.32 g O_2 m^{-2} d^{-1} (SD = 0.65, SE = 0.20), and the average GEP was 3.79 g O_2 m^{-2} d^{-1} (SD = 1.17, SE = 0.353).

The proportion of GEP attributable to GPP has an average of 35% (SD = 13.4%, SE = 4%) (Fig. 1B). The GPP/GEP ratio ranges from 0.10 to 0.70. The ratio of GPP to GEP was higher (av. = 0.69, SD = 0.049) during the last 2 days of the deployment. This increase may have been due to progressive freshening of the surface water accompanied by increased irradiance.

Freshening of the surface waters implies increased residence time, which may allow phytoplankton populations to accumulate in the estuary. As Figure 1C shows, the Quashnet River became more stratified (expressed as delta salinity = bottom − surface salinity) and fresher over time.

Figure 1D shows the GPP/GEP ratio plotted against the ratio of the bottom-to-top salinity. These points are labeled with their corresponding PAR values, the dark squares being those points with PAR values >30 E m^{-2} d^{-1} and the light squares being points with PAR values ≤30 μE m^{-2} d^{-1}. The trends present in

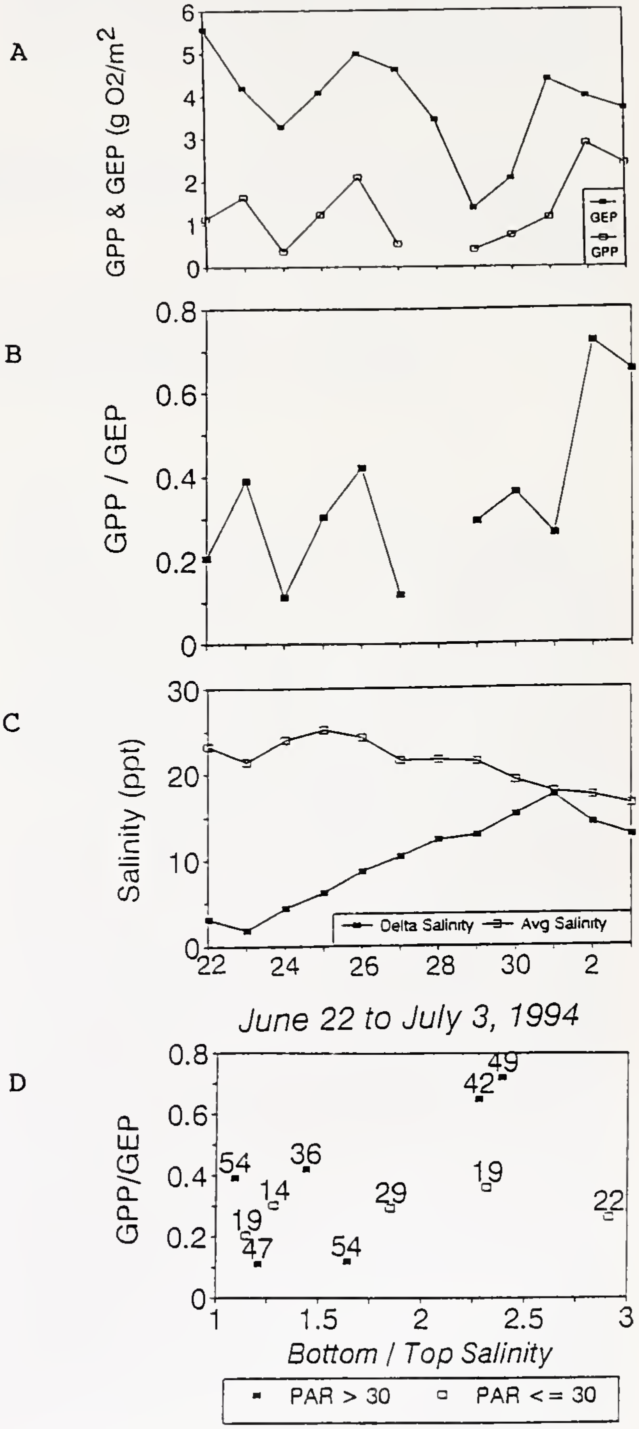

Figure 1. *(A) Gross production in whole ecosystem (GEP) and water column (GPP) in units of g O_2 m^{-2} d^{-1}; (B) ratio of GPP to GEP; (C) change in water column salinity over time; (D) ratio of GPP:GEP plotted against ratio of daily average bottom to surface salinity (numerical labels associated with each point indicate the daily PAR (E m^{-2} d^{-1}) during the day the measurements were made).*

Figure 1D include an increase in the GPP/GEP ratio with increased stratification and increased PAR (the dark squares tend to be higher than the light squares).

Other physical factors measured—temperature, depth, wind speed and direction—had no observable relationship with the GPP/GEP ratio.

In conclusion, GEP and GPP varied with time, increasing and decreasing in a similar fashion in response to a complex suite of physical factors. The ratio of GPP to GEP also varied with time. Although Figure 1D suggests an interesting relationship, there is still much variability unaccounted for. Further study of additional multi-day data sets using, for example, multivariate time-series analysis to assess effects of many interacting variables is certainly needed to evaluate lags in biological responses to physical forcing, and to further discern the relationship of GPP, GEP, and the GPP/GEP ratio to environmental factors.

This work was supported by the Research Experience for Undergraduates program.

Literature Cited

1. **Hall, C., and R. Moll. 1975.** Pp. 18–53 in *Primary Productivity of the Biosphere*. H. Lieth and R. H. Whitaker, eds. Springer-Verlag, New York.

Reference: *Biol. Bull.* **187:** 288–289. (October, 1994)

The Effects of Coupling Between the Oxic and Anoxic Layers of Sediment on Nutrient Release to Overlying Water

Eileen Monaghan (University of Massachusetts at Amherst) and Anne E. Giblin

The purpose of this experiment was to determine the effects of coupling between the oxic and anoxic portions of sediments on the flux of nutrients to overlying water. We hypothesize that interactions between the oxic and anoxic layers of sediment may reduce the amount of nutrients released from the sediment to the overlying water. Two mechanisms that reduce nutrient release are the trapping of phosphate by Fe(III) in the oxic layer (1) and nitrification/denitrification of nitrogen within the layers (2). We measured the impact of the coupling of oxic and anoxic layers on the release of nutrients from the sediment into the overlying water by experimentally separating the layers.

Sediment cores were taken from the Parker River Estuary, Massachusetts. The cores were 6.5 cm in diameter and 18 cm deep. The top 2 cm, considered the oxic layer of the sediment based on Eh data from other cores from the site, was sectioned from three cores and transferred to new core tubes. The next 10 cm of the sediment was then anaerobically transferred to additional new core tubes. The top 12 cm of three more cores was kept intact to serve as controls. Each core was covered with 500 ml of GF/F filtered water taken from the site and bubbled continuously: the oxic cores with air and the anoxic cores with nitrogen. The overlying water of all cores was sampled periodically over 10 days. Samples were analyzed for ammonium, nitrate, and phosphate.

The anoxic sections released the greatest amount of ammonium and phosphate into overlying water. The control cores released ammonium and phosphate at a rate intermediate between that of the oxic and anoxic sections. However, releases from the control cores were proportionately greater for ammonium than phosphate. No nitrate was detected above anoxic sediments, but towards the end of the experiment nitrate appeared in the overlying water of both the oxic and control cores. The drop in ammonium concentration that occurred with both the oxic and control cores was more than compensated for by an increase in nitrate, suggesting that nitrification occurred in the overlying water. The rate of release of total dissolved inorganic nitrogen (NH_4, NO_3, NO_2) present in the overlying water was similar for the anoxic and control cores throughout the experiment (Fig. 1).

If the release of nutrients into the overlying water from oxic sediment layers was independent of the release from anoxic sed-

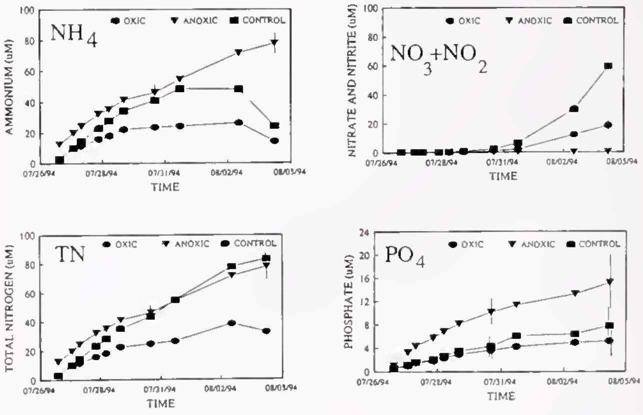

Figure 1. *Time course of ammonium, nitrate and nitrite, total nitrogen, and phosphate concentrations in the overlying water. Total nitrogen = ammonium + nitrate and nitrite. Nitrite was not measured separately. Vertical lines represent the standard error of the mean for triplicate samples.*

iment layers, releases from the intact sediment should equal the sum of nutrient release from the oxic and anoxic sections. However, as the data show, the release of nutrients from intact sediment is reduced by interactions between the two layers. At the end of the experiment, the control cores released only 38% of the phosphate and 77% of the total inorganic nitrogen that was released from the sum of the separated oxic and anoxic sections.

This research was supported by an LMER grant (NSF-OCE-9214461). Thanks to Ishi Buffam, Dave Giehtbrock, Chuck Hopkinson, Kathy Regan, and Amy Uhlenhopp for advice and assistance with sample analysis.

Literature Cited

1. **Caraco, N., J. J. Cole, and G. E. Likens. 1991.** Pp. 241–258 in *Comparative Analyses of Ecosystems.* Cole, Lovett, and Findlay, eds. Springer Verlag, New York.
2. **Klump, V. J., and C. S. Martens. 1983.** Pp. 411–457 in *Nitrogen in the Marine Environment.* Carpenter and Capone, eds. Academic Press, New York.

Reference: *Biol. Bull.* **187**: 289–290. (October, 1994)

Rate of Denitrification in Submerged Salt Marsh Sediments

Rachel Johnson, Michael LaMontagne, and Ivan Valiela (Boston University Marine Program, Marine Biological Laboratory)

Denitrification, a microbial process in which nitrate is converted to N_2 gas, may provide a significant nitrogen sink in salt marsh ecosystems. Salt marshes are located on a fringe between coastal watersheds and receiving estuaries, so that denitrification in marshes may lower nitrogen loading from the watershed to the receiving estuary.

To measure rates of denitrification in salt marshes, sediment cores were collected from marsh sites covered by *Spartina alterniflora* in Sage Lot Pond, an estuary of Waquoit Bay, Massachussetts. Cores were sampled five times over a period of increasing temperatures from 10 June to 1 August 1994. We also measured N_2 flux in another estuary of Waquoit Bay, Jehu Pond. After submerging the cores in seawater, denitrification was estimated by measuring N_2 concentrations over a 12–24 h period in the water overlying intact cores of salt marsh sediment (Fig. 1A). Water samples were analyzed for N_2 and O_2 content by the gas chromatography procedure developed by LaMontagne (unpub.).

Due to the scarcity of nitrate in salt marsh soils (1, 2, 3), NO_3^- for denitrification must be supplied by external sources or by nitrification, an oxygen-dependent microbial process that converts NH_4^+ to NO_3^-. To distinguish between N_2 degassing due to temperature changes and biological N_2 production, we created anoxic conditions in control cores to remove nitrification as an NO_3^- source. Submerged control sediments were degassed by bubbling overlying water with 22.1% He in N_2 gas and adding sodium bisulfite (0.03 g/l). Anoxic conditions were introduced 8–12 h prior to the start of the incubations.

Nitrogen fluxes from Sage Lot Pond marsh cores increased as temperature increased (Fig. 1B). This positive correlation found between rate of denitrification and temperature is con-

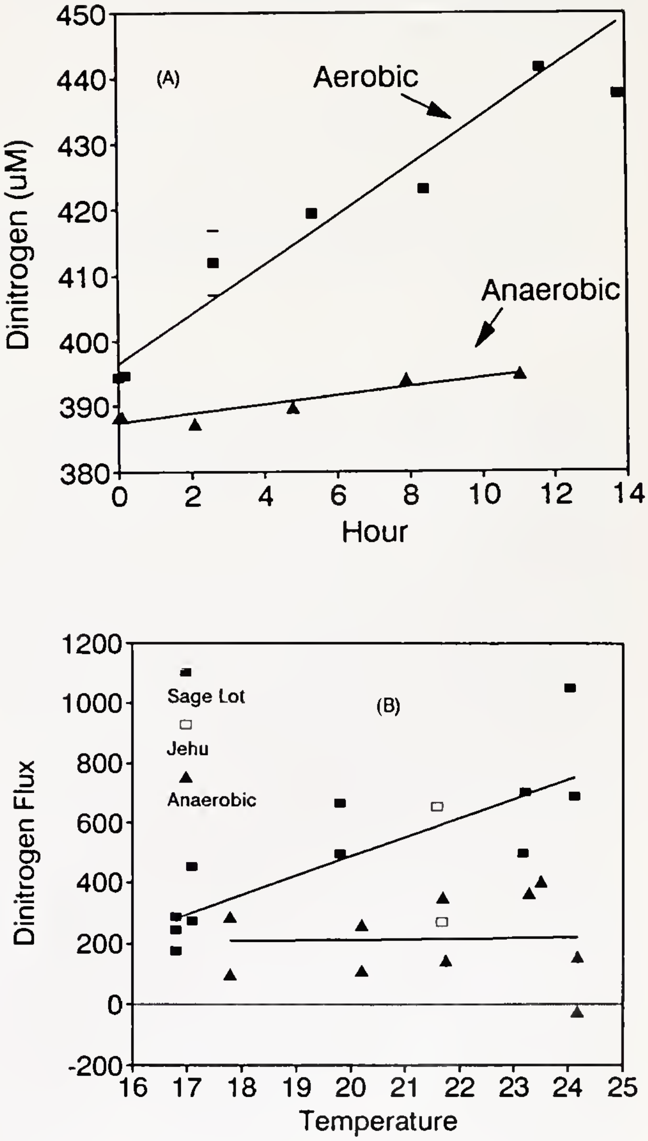

Figure 1. *Measurements of N_2 fluxes from salt marsh cores. (A) Typical flux measurement. N_2 changes are measured* versus *times under aerobic and anaerobic conditions. (B) N_2 flux, in μmol N_2 m^{-2} h^{-1}, versus temperature. Lines represent regressions between aerobic and anaerobic fluxes and temperature. The aerobic fluxes were significantly correlated with temperature ($p = 0.05$).*

sistent with previous findings (2, 3, 4). Fluxes in anaerobic controls did not change with temperature (Fig. 1B). Anaerobic fluxes were significantly lower than aerobic fluxes (Fig. 1). To calculate N_2 flux assignable to denitrification, the mean of the anaerobic flux rates was subtracted from that of N_2 fluxes. After subtraction of controls, denitrification ranged from −41 to 834 μmol N_2 m^2 h^{-1}.

Our rates are higher than those previously recorded for salt marsh sediments. Kaplan *et al.* (1) detected rates of 4–7 μmol N_2 m^{-2} h^{-1}; Aziz and Nedwell (4) measured rates between 4 and 5 μmol N_2 m^{-2} h^{-1}. Using the acetylene block technique, Van Raalte and Patriquin (5) found rates to be undetectable, while Koch *et al.* (6) reported rates ranging from 3 to 59 μmol N_2 m^{-2} h^{-1} in untreated sediment and 75 to 115 μmol N_2 m^{-2} h^{-1} in sediment incubated with nitrate-rich river water. Our direct measurements more closely match an ^{15}N estimate of annual denitrification or nitrogen removal of 140–200 mmol N_2 $m^{-2}y^{-1}$(7); however, the rates reported here are still relatively high. The correlation between denitrification and temperature indicates that significant nitrogen removal occurs only in summer. Extrapolating the average Sage Lot summer rates (280 μmol N_2 m^{-2} h^{-1}) to an annual removal yields 800 mmol N_2 m^{-2} y^{-1}. The difference between our values and those reported in the literature may be caused by differences in site or method, an issue that needs further study.

Literature Cited

1. **Kaplan, W., J. M. Teal, and I. Valiela. 1977.** *Microb. Ecol.* **3:** 193–204.
2. **Kaplan, W., I. Valiela, and J. M. Teal. 1979.** *Limnol. Oceanogr.* **24:** 726–734.
3. **George, U., and A. D. Antoine. 1982.** *Soil Biol. Biochem.* **14:** 117–125.
4. **Aziz, S. A., and D. B. Nedwell. 1986.** *Estuar. Coast. Shelf Sci.* **22:** 689–704.
5. **Van Raalte, C. D., and D. G. Patriquin. 1979.** *Mar. Biol.* **52:** 315–320.
6. **Koch, M. S., E. Maltby, G. A. Oliver, and S. A. Bakker. 1992.** *Estuar. Coast. Shelf Sci.* **34:** 471–485.
7. **White, D. 1994.** Ph. D. Thesis. Boston University, MA.

Reference: *Biol. Bull.* **187:** 290–291. (October, 1994)

Analysis of Acid Volatile Sulfide and Metals to Predict the Toxicity of Boston Harbor Sediments

Cristina Zago (Instituto per lo Studio della Dinamica delle Grandi Masse, ISDGM, Venice, Italy) and Anne E. Giblin

The bioavailability and toxicity of metals in sediments is related to the geochemical speciation and chemical activity of the metals in the interstitial water of the sediment. Di Toro *et al.* (1) conducted laboratory tests with marine and freshwater organisms to determine which factors controlled the toxicity of metals in sediments. Test results showed that the mortality of the animals was related to both the quantity of toxic heavy metals (Cu + Zn + Cd + Ni + Hg + Pb) and the acid volatile sulfide (AVS) released from acidified sediments. Metals extracted with the AVS are termed the *simultaneously extracted metals* (SEM). If the SEM/AVS ratio was greater than 1 or 2, the sediments were toxic; if the ratio was below 1, the sediments were not toxic regardless of the total metal concentration. Di Toro *et al.* (1) proposed that when the SEM/AVS ratio was less than 1, the toxic metals were all precipitated as insoluble metal sulfides and hence not biologically available.

We applied this technique to study the potential toxicity of sediments in Boston Harbor, Massachusetts. Samples were collected from two well-studied harbor sites (2, 3) that differ in their geochemical characteristics, total metal content, and benthic fauna. One station (T3) is located off Long Island in an area that received sewage sludge prior to January 1992. Large numbers of benthic amphipods and other organisms have been routinely observed at this site. The second site (T2) is on Governor Island Flats and is often devoid of macrofauna, although amphipods were observed there at the time of this study.

To achieve better mixing of the acid with the sediment, we modified the extraction technique (1) by adding the acid to the sediment and heating for 1 h.

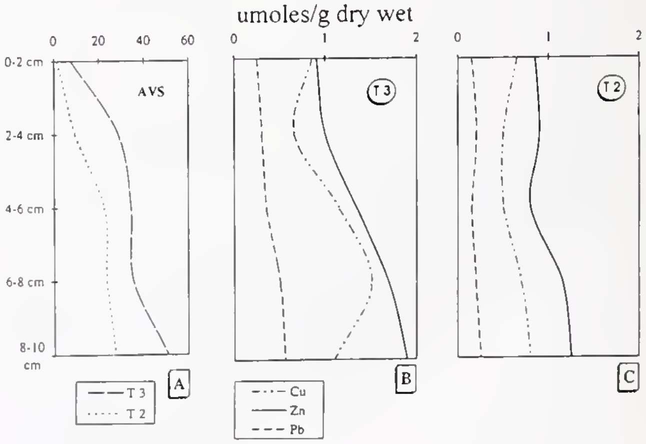

Figure 1. *Concentrations (μmoles/g dry weight of sediment) of acid volatile sulfide, Cu, Zn, and Pb in sediments from Boston Harbor. Sediments were sectioned in 2-cm intervals to a depth of 10 cm. (A) AVS profiles at stations T2 and T3. (B) Metal profiles at site T3. (C) Metal profiles at site T2.*

At both sites, AVS concentrations were low in surface sediments and increased with depth (Fig. 1A). Station T3 had higher concentrations of AVS and metals than T2 (Fig. 1A, B, C).

To test the toxicity of the sediments, we calculated the SEM/AVS ratio. We compared the sum of Cu, Pb, and Zn with the AVS concentration. Cd was not included because it was below our detection limits and therefore insignificant. Hg and Ni were not analyzed, but they are present in such low concentrations at these sites (4) that their omission should not affect our calculations. The (Cu + Zn + Pb)/AVS ratio was lower than 1 except in the 0–2 cm section from site T2, which had a value of 1.38.

These data would allow us to classify the sediments as nontoxic. This is consistent with our observations that infaunal animals were present. However, future studies should focus on site T2, where we have observed a large inter-annual variability in metal concentration, sediment texture, and animal abundance (unpub. data).

C. Zago was sponsored by an MBL Associate's Fellowship and by the Environmental Division of the Instituto per lo Studio della Dinamica delle Grandi Masse, National Research Council of Italy, Venice. Support for A.E.G. came from NOAA Sea Grant and from the Massachusetts Water Resources Authority.

Literature Cited

1. **Di Toro, D. M. 1992.** *Environ. Sci. Technol.* **26:** 96–101.
2. **Giblin, A. E., C. Hopkinson, and J. Tucker. 1993.** Massachusetts Water Resources Authority, Boston, MA. Tech. Rep. 93-2.
3. **Giblin, A. E., C. Hopkinson, J. Tucker, B. Nowicki, and J. R. Kelly. 1994.** Massachusetts Water Resources Authority, Boston, MA. Tech. Rep.
4. **Shea, D., and J. R. Kelly. 1991.** Massachusetts Water Resources Authority, Boston, MA. Tech. Rep. 92-4.

CONTENTS

A tribute to Professor Katsuma Dan on his 90th birthday 125

DEVELOPMENT AND REPRODUCTION

Gibson, Glenys D., and Fu-Shiang Chia
A metamorphic inducer in the opisthobranch *Haminaea callidegenita:* partial purification and biological activity 133

Temkin, M. H.
Gamete spawning and fertilization in the gymnolaemate bryozoan *Membranipora membranacea* . . . 143

FUNCTIONAL MORPHOLOGY

Williams, Terri A.
Locomotion in developing *Artermia* larvae: mechanical analysis of antennal propulsors based on large-scale physical models 156

Williams, Terri A.
A model of rowing propulsion and the ontogeny of locomotion in *Artemia* larvae 164

NEUROBIOLOGY

Nezlin, L. P., R. Elofsson, and D. A. Sakharov
Transmitter-specific subsets of sensory elements in the prosobranch osphradium 174

Chin, Gilbert J., Kemal Payza, David A. Price, Michael J. Greenberg, and Karen E. Doble
Characterization and solubilization of the FMRFamide receptor of squid 185

DellaCorte, Christian, Don S. Anderson, William O. McClure, and D. Lynn Kalinoski
Neurofilament-like immunoreactivity in the sea anemone *Condylactis gigantea* (Cnidaria: Anthozoa) 200

PHYSIOLOGY

Airriess, Chris N., and James J. Childress
Homeoviscous properties implicated by the interactive effects of pressure and temperature on the hydrothermal vent crab *Bythograea thermydron* 208

Yoon, K. S., Y. P. Chen, C. R. Lovell, D. E. Lincoln, L. W. Knapp, and S. A. Woodin
Localization of the choloroperoxidase of the capitellid polychaete *Notomastus lobatus* 215

Short Reports from the Marine Biological Laboratory's General Scientific Meetings 223

Volume 187 Number 3

THE BIOLOGICAL BULLETIN

Marine Biological Laboratory/
Woods Hole Oceanographic Institution
Library

DEC 1 9 1994

Woods Hole, MA 02543

DECEMBER, 1994

Published by the Marine Biological Laboratory

THE
BIOLOGICAL BULLETIN

ABK 7312

PUBLISHED BY
THE MARINE BIOLOGICAL LABORATORY

Marine Biological Laboratory/
Woods Hole Oceanographic Institution
Library

DEC 1 9 1994

Woods Hole, MA 02543

Associate Editors

PETER A. V. ANDERSON, The Whitney Laboratory, University of Florida
WILLIAM D. COHEN, Hunter College, City University of New York
DAVID EPEL, Hopkins Marine Station, Stanford University
J. MALCOLM SHICK, University of Maine, Orono

Editorial Board

THOMAS H. DIETZ, Louisiana State University
DAPHNE GAIL FAUTIN, University of Kansas
WILLIAM F. GILLY, Hopkins Marine Station, Stanford University
ROGER T. HANLON, Marine Biomedical Institute, University of Texas Medical Branch
CHARLES B. METZ, University of Miami
K. RANGA RAO, University of West Florida
BARUCH RINKEVICH, Israel Oceanographic & Limnological Research Ltd.
RICHARD STRATHMANN, Friday Harbor Laboratories, University of Washington
STEVEN VOGEL, Duke University
SARAH ANN WOODIN, University of South Carolina

Editor: MICHAEL J. GREENBERG, The Whitney Laboratory, University of Florida
Managing Editor: PAMELA L. CLAPP, Marine Biological Laboratory

DECEMBER, 1994

Printed and Issued by
LANCASTER PRESS, Inc.
3575 HEMPLAND ROAD
LANCASTER, PA

THE BIOLOGICAL BULLETIN

THE BIOLOGICAL BULLETIN is published six times a year by the Marine Biological Laboratory, MBL Street, Woods Hole, Massachusetts 02543.

Subscriptions and similar matter should be addressed to Subscription Manager, THE BIOLOGICAL BULLETIN, Marine Biological Laboratory, Woods Hole, Massachusetts 02543. Single numbers, $37.50. Subscription per volume (three issues), $90.00 ($180.00 per year for six issues).

Communications relative to manuscripts should be sent to Michael J. Greenberg, Editor-in-Chief, or Pamela L. Clapp, Managing Editor, at the Marine Biological Laboratory, Woods Hole, Massachusetts 02543. Telephone: (508) 548-3705, ext. 428. FAX: 508-540-6902. E-mail: pclapp@hoh.mbl.edu.

THE BIOLOGICAL BULLETIN is indexed in bibliographic services including *Index Medicus* and MEDLINE, *Chemical Abstracts*, and *Current Contents*.

Printed on acid free paper,
effective with Volume 180, Issue 1, 1991.

POSTMASTER: Send address changes to THE BIOLOGICAL BULLETIN, Marine Biological Laboratory, Woods Hole, MA 02543.

Copyright © 1994, by the Marine Biological Laboratory

Second-class postage paid at Woods Hole, MA, and additional mailing offices.
ISSN 0006-3185

INSTRUCTIONS TO AUTHORS

The Biological Bulletin accepts outstanding original research reports of general interest to biologists throughout the world. Papers are usually of intermediate length (10–40 manuscript pages). A limited number of solicited review papers may be accepted after formal review. A paper will usually appear within four months after its acceptance.

Very short, especially topical papers (less than 9 manuscript pages including tables, figures, and bibliography) will be published in a separate section entitled "Research Notes." A Research Note in *The Biological Bulletin* follows the format of similar notes in *Nature*. It should open with a summary paragraph of 150 to 200 words comprising the introduction and the conclusions. The rest of the text should continue on without subheadings, and there should be no more than 30 references. References should be referred to in the text by number, and listed in the Literature Cited section in the order that they appear in the text. Unlike references in *Nature*, references in the Research Notes section should conform in punctuation and arrangement to the style of recent issues of *The Biological Bulletin*. Materials and Methods should be incorporated into appropriate figure legends. See the article by Lohmann *et al.* (October 1990, Vol. **179**: 214–218) for sample style. A Research Note will usually appear within two months after its acceptance.

The Editorial Board requests that regular manuscripts conform to the requirements set below; those manuscripts that do not conform will be returned to authors for correction before review.

1. ***Manuscripts.*** Manuscripts, including figures, should be submitted in triplicate. (Xerox copies of photographs are not acceptable for review purposes.) The submission letter accompanying the manuscript should include a telephone number, a FAX number, and (if possible) an E-mail address for the corresponding author. The original manuscript must be typed in no smaller than 12 pitch or 10 point, using double spacing (*including* figure legends, footnotes, bibliography, etc.) on one side of 16- or 20-lb. bond paper, 8½ by 11 inches. Please, no right justification. Manuscripts should be proofread carefully and errors corrected legibly in black ink. Pages should be numbered consecutively. Margins on all sides should be at least 1 inch (2.5 cm). Manuscripts should conform to the *Council of Biology Editors Style Manual*, 5th Edition (Council of Biology Editors, 1983) and to American spelling. Unusual abbreviations should be kept to a minimum and should be spelled out on first reference as well as defined in a footnote on the title page. Manuscripts should be divided into the following components: Title page, Abstract (of no more than 200 words), Introduction, Materials and Methods, Results, Discussion, Acknowledgments, Literature Cited, Tables, and Figure Legends. In addition, authors should supply a list of words and phrases under which the article should be indexed.

2. ***Title page.*** The title page consists of a condensed title or running head of no more than 35 letters and spaces, the manuscript title, authors' names and appropriate addresses, and footnotes listing present addresses, acknowledgments or contribution numbers, and explanation of unusual abbreviations.

3. ***Figures.*** The dimensions of the printed page, 7 by 9 inches, should be kept in mind in preparing figures for publication. We recommend that figures be about 1½ times the linear dimensions of the final printing desired, and that the ratio of the largest to the smallest letter or number and of the thickest to the thinnest line not exceed 1:1.5. Explanatory matter generally should be included in legends, although axes should always be identified on the illustration itself. Figures should be prepared for reproduction as either line cuts or halftones. Figures to be reproduced as line cuts should be unmounted glossy photographic reproductions or drawn in black ink on white paper, good-quality tracing cloth or plastic, or blue-lined coordinate paper. Those to be reproduced as halftones should be mounted on board, with both designating numbers or letters and scale

bars affixed directly to the figures. All figures should be numbered in consecutive order, with no distinction between text and plate figures. The author's name and an arrow indicating orientation should appear on the reverse side of all figures.

4. ***Tables, footnotes, figure legends, etc.*** Authors should follow the style in a recent issue of *The Biological Bulletin* in preparing table headings, figure legends, and the like. Because of the high cost of setting tabular material in type, authors are asked to limit such material as much as possible. Tables, with their headings and footnotes, should be typed on separate sheets, numbered with consecutive Roman numerals, and placed after the Literature Cited. Figure legends should contain enough information to make the figure intelligible separate from the text. Legends should be typed double spaced, with consecutive Arabic numbers, on a separate sheet at the end of the paper. Footnotes should be limited to authors' current addresses, acknowledgments or contribution numbers, and explanation of unusual abbreviations. All such footnotes should appear on the title page. Footnotes are not normally permitted in the body of the text.

5. ***Literature cited.*** In the text, literature should be cited by the Harvard system, with papers by more than two authors cited as Jones *et al.*, 1980. Personal communications and material in preparation or in press should be cited in the text only, with author's initials and institutions, unless the material has been formally accepted and a volume number can be supplied. The list of references following the text should be headed Literature Cited, and must be typed double spaced on separate pages, conforming in punctuation and arrangement to the style of recent issues of *The Biological Bulletin*. Citations should include complete titles and inclusive pagination. Journal abbreviations should normally follow those of the U. S. A. Standards Institute (USASI), as adopted by BIOLOGICAL ABSTRACTS and CHEMICAL ABSTRACTS, with the minor differences set out below. The most generally useful list of biological journal titles is that published each year by BIOLOGICAL ABSTRACTS (BIOSIS List of Serials; the most recent issue). Foreign authors, and others who are accustomed to using THE WORLD LIST OF SCIENTIFIC PERIODICALS, may find a booklet published by the Biological Council of the U.K. (obtainable from the Institute of Biology, 41 Queen's Gate, London, S.W.7, England, U.K.) useful, since it sets out the WORLD LIST abbreviations for most biological journals with notes of the USASI abbreviations where these differ. CHEMICAL ABSTRACTS publishes quarterly supplements of additional abbreviations. The following points of reference style for THE BIOLOGICAL BULLETIN differ from USASI (or modified WORLD LIST) usage:

A. Journal abbreviations, and book titles, all underlined (for *italics*)

B. All components of abbreviations with initial capitals (not as European usage in WORLD LIST *e.g., J. Cell. Comp. Physiol.* NOT *J. cell. comp. Physiol.*)

C. *All* abbreviated components must be followed by a period, whole word components *must not* (*i.e., J. Cancer Res.*)

D. Space between all components (*e.g., J. Cell. Comp. Physiol.*, not *J.Cell.Comp.Physiol.*)

E. Unusual words in journal titles should be spelled out in full, rather than employing new abbreviations invented by the author. For example, use *Rit Vísindafjélags Islendinga* without abbreviation.

F. All single word journal titles in full (*e.g., Veliger, Ecology, Brain*).

G. The order of abbreviated components should be the same as the word order of the complete title (*i.e., Proc.* and *Trans.* placed where they appear, not transposed as in some BIOLOGICAL ABSTRACTS listings).

H. A few well-known international journals in their preferred forms rather than WORLD LIST or USASI usage (*e.g., Nature, Science, Evolution* NOT *Nature, Lond., Science, N.Y.; Evolution, Lancaster, Pa.*)

6. ***Reprints, page proofs, and charges.*** Authors receive their first 100 reprints (without covers) free of charge. Additional reprints may be ordered at time of publication and normally will be delivered about two to three months after the issue date. Authors (or delegates for foreign authors) will receive page proofs of articles shortly before publication. They will be charged the current cost of printers' time for corrections to these (other than corrections of printers' or editors' errors). Other than these charges for authors' alterations, *The Biological Bulletin* does not have page charges.

VOLUME CONTENTS

No. 1, August 1994

CELL BIOLOGY

Koppelhus, Uffe, Per Hellung-Larsen, and Vagn Leick
Physiological parameters affecting the chemosensory response of *Tetrahymena* 1

Koppelhus, Uffe, Per Hellung-Larsen, and Vagn Leick
An improved quantitative assay for chemokinesis in *Tetrahymena* 8

Read, A. T., R. R. Hessler, and C. K. Govind
Muscle and nerve terminal fine structure of a primitive crustacean, the cephalocarid *Hutchinsoniella macracantha* 16

ECOLOGY AND EVOLUTION

Metz, Edward C., Robert E. Kane, Hiroko Yanagimachi, and Stephen R. Palumbi
Fertilization between closely related sea urchins is blocked by incompatibilities during sperm-egg attachment and early stages of fusion 23

FUNCTIONAL MORPHOLOGY

Flammang, Patrick, Stephane DeMeulenaere, and Michel Jangoux
The role of podial secretions in adhesion in two species of sea stars (Echinodermata) 35

NEUROBIOLOGY AND BEHAVIOR

Anctil, Michel, and Jean-Pascal Carette
Glutamate immunoreactivity in non-neuronal cells of the sea anemone *Metridium senile* 48

Lucero, Mary T., Heraldo Farrington, and William F. Gilly
Quantification of L-dopa and dopamine in squid ink: implications for chemoreception 55

New, John G.
Electric organ discharge and electrosensory reafference in skates 64

PHYSIOLOGY

Dietz, Thomas H., Diondi Lessard, Harold Silverman, and John W. Lynn
Osmoregulation in *Dreissena polymorpha:* the importance of Na, Cl, K, and particularly Mg 76

Thuesen, Erik V., and James J. Childress
Oxygen consumption rates and metabolic enzyme activities of oceanic California medusae in relation to body size and habitat depth 84

SEX CHANGE IN INVERTEBRATES

Brook, Heather J., Timothy A. Rawlings, and Ronald W. Davies
Protogynous sex change in the intertidal isopod *Gnorimosphaeroma oregonense* (Crustacea: Isopoda) 99

Sewell, Mary A.
Small size, brooding, and protandry in the apodid sea cucumber *Leptosynapta clarki* 112

Annual Report of the Marine Biological Laboratory R1

No. 2, October 1994

A tribute to Professor Katsuma Dan on his 90th birthday 125

DEVELOPMENT AND REPRODUCTION

Gibson, Glenys D., and Fu-Shiang Chia
A metamorphic inducer in the opisthobranch *Haminaea callidegenita:* partial purification and biological activity 133

Temkin, M. H.
Gamete spawning and fertilization in the gymnolaemate bryozoan *Membranipora membranacea* . . . 143

FUNCTIONAL MORPHOLOGY

Williams, Terri A.
Locomotion in developing *Artermia* larvae: mechanical analysis of antennal propulsors based on large-scale physical models 156

Williams, Terri A.
A model of rowing propulsion and the ontogeny of locomotion in *Artemia* larvae 164

CONTENTS

NEUROBIOLOGY

Nezlin, L. P., R. Elofsson, and D. A. Sakharov
Transmitter-specific subsets of sensory elements in the prosobranch osphradium 174

Chin, Gilbert J., Kemal Payza, David A. Price, Michael J. Greenberg, and Karen E. Doble
Characterization and solubilization of the FMRFamide receptor of squid 185

DellaCorte, Christian, Don S. Anderson, William O. McClure, and D. Lynn Kalinoski
Neurofilament-like immunoreactivity in the sea anemone *Condylactis gigantea* (Cnidaria: Anthozoa) 200

PHYSIOLOGY

Airriess, Chris N., and James J. Childress
Homeoviscous properties implicated by the interactive effects of pressure and temperature on the hydrothermal vent crab *Bythograea thermydron* 208

Yoon, K. S., Y. P. Chen, C. R. Lovell, D. E. Lincoln, L. W. Knapp, and S. A. Woodin
Localization of the choloroperoxidase of the capitellid polychaete *Notomastus lobatus* 215

Short Reports from the Marine Biological Laboratory's General Scientific Meetings 223

No. 3, December 1994

RESEARCH NOTES

Silver, Robert B., Mutsuyuki Sugimori, Eric J. Lang, and Rodolfo Llinás
Time-resolved imaging of Ca^{2+}-dependent aequorin luminescence of microdomains and QEDs in synaptic preterminals 293

Sugimori, Mutsuyuki, Eric J. Lang, Robert B. Silver, and Rodolfo Llinás
High-resolution measurement of the time course of calcium concentration microdomains at squid presynaptic terminals 300

Johnson, Leland G., and Russell C. Babcock
Temperature and the larval ecology of the crown-of-thorns starfish, *Acanthaster planci* 304

DEVELOPMENT AND REPRODUCTION

Guo, Ximing, and Standish K. Allen, Jr.
Reproductive potential and genetics of triploid Pacific oysters, *Crassostrea gigas* (Thunberg) 309

ECOLOGY AND EVOLUTION

Lesser, Michael P., Jon D. Witman, and Kenneth P. Sebens
Effects of flow and seston availability on scope for growth of benthic suspension-feeding invertebrates from the Gulf of Maine 319

Parker, Terry, and Verena Tunnicliffe
Dispersal strategies of the biota on an oceanic seamount: implications for ecology and biogeography 336

Voris, Harold K., William B. Jeffries, and Sombat Poovachiranon
Patterns of distribution of two barnacle species on the mangrove crab, *Scylla serrata* 346

NEUROBIOLOGY AND BEHAVIOR

DellaCorte, Christian, William O. McClure, and D. Lynn Kalinoski
Identification of synaptophysin-like immunoreactivity in the sea anemone *Condylactis gigantea* (Cnidaria: Anthozoa) 355

Hanlon, Roger T., Malcolm J. Smale, and Warwick H. H. Sauer
An ethogram of body patterning behavior in the squid *Loligo vulgaris reynaudii* on spawning grounds in South Africa 363

Penn, Dustin, and H. Jane Brockmann
Nest-site selection in the horseshoe crab, *Limulus polyphemus* 373

PHYSIOLOGY

Reese, John E., and Charlotte P. Mangum
Subunit composition and O_2 binding of the crustacean hemocyanins: interspecific relationships 385

Shilling, Fraser M., and Donal T. Manahan
Energy metabolism and amino acid transport during early development of antarctic and temperate echinoderms 398

Index to Volume 187 408

Notice to Subscribers

The 1995 subscription rate for *The Biological Bulletin* will be $185 for the year (6 issues: $92.50 for 3 issues). Back and single issues are $37.50, and subject to availability. For additional information, please contact our subscription officer at the Marine Biological Laboratory, Woods Hole, MA 02543; tel: (508) 548-3705, ext. 402.

Reference: *Biol. Bull.* **187:** 293–299. (December, 1994)

Time-Resolved Imaging of Ca^{2+}-Dependent Aequorin Luminescence of Microdomains and QEDs in Synaptic Preterminals

ROBERT B. SILVER[1,3], MUTSUYUKI SUGIMORI[2,3], ERIC J. LANG[2,3],
AND RODOLFO LLINÁS[2,3]

[1]*Section and Department of Physiology, Cornell University, Ithaca, New York 14853-6401,*
[2]*Department of Physiology and Biophysics, New York University Medical Center, 550 First Avenue,*
New York, New York 10016, and [3]*Marine Biological Laboratory, Woods Hole, Massachusetts 02543*

Localized elevation of intracellular free calcium $[Ca^{2+}]_i$ concentration serves as the trigger for a wide variety of physiological processes, e.g., *neurotransmitter release at most chemical synapses (1–3). The details of the mechanisms that regulate these processes are still unresolved (3–6), but they must involve precise temporal sequences of molecular events initiated by a transient localized elevation of Ca^{2+} concentration* (i.e., *a Ca^{2+} microdomain [3, 7–15]). A microdomain is defined as an autonomous compartment of minimal spatio-temporal volume within which a signaled process can occur (8, 10, 12). A quantum emission domain (QED) is a quantal signal element (3, 16, 17). The concept of a QED was first applied to Ca^{2+} signaling at the synaptic preterminal (3, 4) and for large-diameter mitotic cells (16, 17).*

The concept of Ca^{2+} microdomains was tested by labeling preterminals of squid giant synapses with low-sensitivity aequorin (a photoprotein that emits a photon upon binding Ca^{2+} [18, 19]). That work confirmed earlier modeling efforts (10, 16) and showed that, upon depolarization, the $[Ca^{2+}]_i$ profile reaches 200–300 μM *within the microdomains, and that these $[Ca^{2+}]_i$ profiles are composed of groups of short-lived 0.5 μm diameter QEDs. In those records, obtained with 2:1 interlacing devices operating at the RS-170 standard, QEDs appeared as striped dots or chevrons rather than as solid dots, indicating that a QED lasted less than 16.6 ms (one video field), and thus establishing the need for higher sampling rates to better characterize the QED. In the present set of studies, we sought to extend our earlier work on calcium microdomains and QEDs with the goal of better understanding the lifetime of the QED and its relationship to the action potential. This is the first description of the methodology necessary to image the Ca^{2+} QED, and the techniques for obtaining, processing, and analyzing video information at high frame rates.*

Chevrons and dots in interpreting the duration of QEDs

QED patterns in aequorin-labeled synaptic preterminals were observed as discrete events following stimulation of single action potentials. These observations were initially performed at a video frame rate of 30 frames per second (fps), using cameras conforming to the RS-170 standard. Each video frame consisted of two interlaced video fields (*i.e.*, 2:1 interlace), each composed of the set of odd or even scan lines. A new field was captured every 16.7 ms, and each scan line lasted for 63.5 μs. Therefore, an event lasting 16.7 to 33 ms would be seen as a solid dot, while one lasting less than 16.7 ms would be observed as a set of horizontal stripes. Events of duration close to 16.7 ms might also appear as dots, depending upon the timing of the initiation of the event relative to the timing of the two video fields. If the event began close to the end of the first

---

Received 20 September 1994; accepted 5 October 1994.

Portions of this work were presented in preliminary form at the General Scientific Meetings at the Marine Biological Laboratory, Woods Hole, MA, on 16 August 1994.

Abbreviations: CCD = charge coupled device; dMCP = dual microchannel plate image intensifier; N.A. = numerical aperture; NTSC = National Television Standards Committee; QED = quantum emission domain; RS-170 = NTSC Resolution Standard 170: video frame resolution of 525 lines of horizontal resolution, 60 Hz video field sampling rate, 2:1 interlace of video fields within a single video frame, 33 ms per frame (16.66 ms per video field); used primarily for black and white video devices.

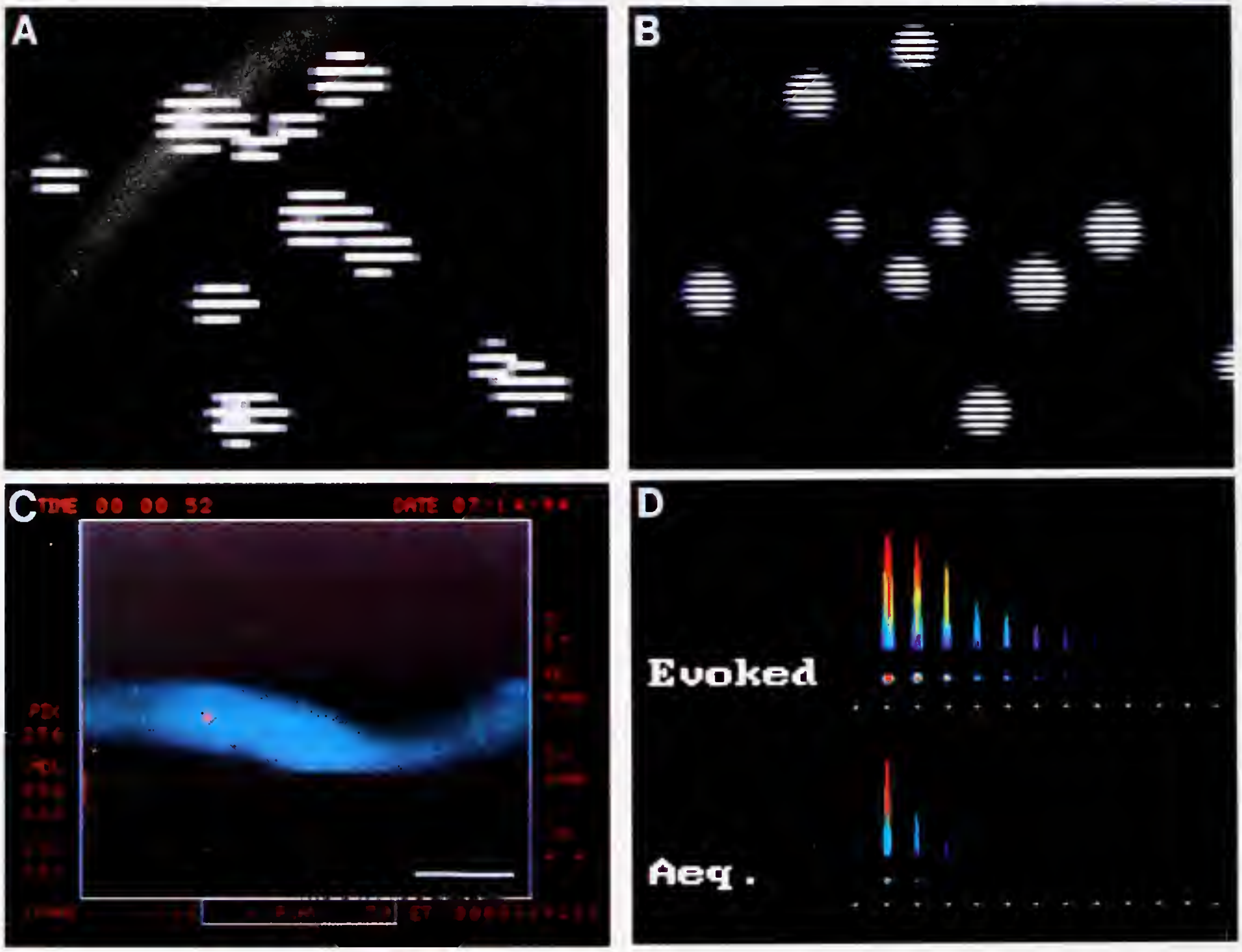

Figure 1. (A) Individual quantum emission domains (QEDs) activated by single action potentials at a preterminal appear as white chevrons when recorded at 30 frames per second (fps). A few of these QEDs show some filling between the stripes, indicating that those events began close to either the start or end of a single video field and overlapped to the preceding or following video field. The two QEDs seen in the lower right of this panel occurred in separate odd and even fields. (B) Individual QEDs activated by single presynaptic spikes appear as white chevrons recorded at 200 fps, indicating that the entire QED occurred within the 2.5-ms sampling period of the video field. Note that in this case, unlike that in panel A, all of the QEDs appear as chevrons, indicating that no observed QEDs overlapped two consecutive video fields. (C) The first 0.25-ms video frame recording of a single evoked QED (red) superimposed onto its point of origin in a synaptic preterminal (blue). The red characters surrounding the central image are typical of the display from the Kodak high-speed video camera. (D) The time course of an evoked QED, and one for a single QED emitted from aequorin expressed into calcium buffer, recorded at a video rate of 4000 fps. Spots of light from single video frames are displayed as a row of spots at the same horizontal level as the terms "Evoked" and "Aeq." The intensity profiles of each of the individual spots are seen directly above their respective spots. The spots and intensity profiles were printed in pseudocolor to aid in visualization; black and purple are 0 to low intensity, increasing through green, yellow, and orange to the highest values of red and white (8-bit gray-scale value of 255). These values are correlated with the luminance intensity incident to the faceplate of the dual microchannel plate (dMCP) intensifier. Small white points marking each individual video field appear below their respective spots. The scale marker in panel C represents 10 μm.

Standard methods were used to dissect stellate ganglia from small squid (*Loligo pealei*) and monitor synaptic transmission (3, 18). Video images were captured with a direct optical extension onto a dMCP Video Intensified Microscopy camera system (Hamamatsu Argus 100; Hamamatsu Photonics, Inc., Bridgewater, NJ) operated in photon-counting mode. Three different video cameras were used to detect clouds of electrons emanating from the dMCP. For video at 30 fps, a Hamamatsu saticon tube camera was used, operated under the RS-170 standard. Imagery from the saticon camera was recorded on an S-VHS videocassette recorder. An NAC HSV-400 (NAC, Inc., Japan) high-speed color video camera, S-VHS videocassette recorder, and Panasonic ST-1000 color video monitor (Matsushita Electric Industrial Co., Ltd., Fukuoka, Japan), all operated in B/W mode, were used for 200-fps imaging and recording. The NAC HSV-400 camera was fitted to the dMCP through a direct optical coupling. Care was taken to ensure that the output image of the dMCP video field or ended near to the start of the second video field, the event would be recorded as a partially filled chevron whose centroid coincided with the location of the point of origin for the event. Events that were very short compared with the video-field sampling rate would nearly always appear as chevrons. This principle applies to all 2:1 interlaced imaging devices, irrespective of video frame rate.

QED images at 30 video frames per second

Ca$^{2+}{}_i$-dependent aequorin luminescence was detected as discrete QEDs at the preterminal side of the synapse following presynaptic action potentials (Fig. 1A). Because QEDs were seen as chevrons, rather than solid spots, they must have had a lifetime of less than 16.7 ms; nearly all of the presynaptic QEDs observed after such action potentials appeared as chevrons. In several instances, chevron QEDs were seen to interlace. These were fortuitous observations, and would be expected for near-neighboring QEDs acting within microdomains. In several other instances, some of the QED signal extended to the following (or from the preceding) video field; that is, the blank space between the lines of the chevrons contained some record of a signal. We interpret these images to represent a short-lived event that occurred near the end (or beginning, respectively) of a given video field that contained the majority of the chevron QED photon emission.

QED images at 200 video frames per second

Because virtually all of the QEDs observed at 30 fps appeared on the video monitor as chevrons, better temporal resolution was clearly needed. To resolve individual QEDs in time, aequorin luminescence was videotaped at 200 fps (5-ms video frame, 2.5 ms per video field). Fig. 1B shows examples of QEDs recorded at a frame rate of 200 fps from a single evoked response. As at 30 fps, they appeared as chevrons, so their lifetime must be less than 2.5 ms. Moreover, fewer than 5% of the QEDs were seen as partially filled chevrons, indicating both that the event was less than the video frame rate and that no significant degree of overlap occurred in which QEDs "began" in one 1.25-ms video field and then extended into the next. These results indicate that a further increase in video sampling rate would be needed to resolve the images of individual QEDs.

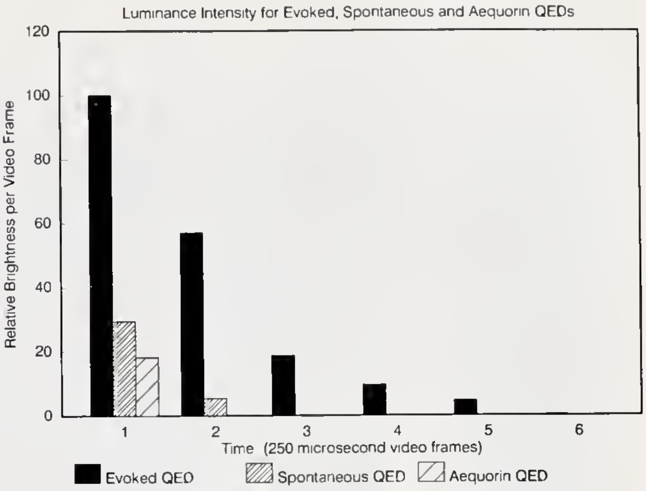

Figure 2. Luminance intensity for evoked, spontaneous, and aequorin QEDs corrected for phosphorescent afterglow. Values are means of the total luminance intensity for each of five QEDs for each category, and are expressed as relative to the brightness of the initial frame of an evoked QED. Evoked QEDs (solid black) lasted as long as five 0.25-ms video frames; mean spontaneous QEDs (thin double stripes) lasted only 0.5 ms; and aequorin QEDs (single diagonal crosshatches) were seen for only one 0.25-ms video frame.

To ensure that the imagery information was properly processed, the following assumptions and practices were adopted. The photon intensity information of the initial video frame recording a QED was considered to represent light from the photochemical reaction of Ca^{2+} and aequorin. The contribution of afterglow in the first video frame of each QED record was considered to be negligible for imagery at 4000 fps. Image information for each subsequent frame was considered to consist of a sum of the Ca^{2+}-dependent aequorin-based photon emission generated and integrated onto the detector faceplate during that video frame, and the afterglow attributable to the preceding video frame. The contribution of afterglow was determined with empirical values derived from the images for aequorin injected into Ca^{2+}-containing buffer as follows. The luminance intensity values for QED photon emissions from each 0.25-ms video frame were determined from digitized video records. Photon emission from the reaction of Ca^{2+} and aequorin was assumed to last 0.25 ms, or possibly less; so additional light detected by the CCD camera was considered to be due to afterglow of the dMCP. The ratio of the total intensity of the second frame divided by the preceding frame was taken as the proportion of the total luminance intensity of the first frame assignable as afterglow in the second frame.

---

was focused to the faceplate of the camera. Higher speed digital video imagery was obtained with a Kodak Ektapro high-speed video system (Hi-Spec Processor and SI camera) operated at various frame rates between 30 fps and 4000 fps. High frame rate recordings were performed with reduced frame size; *e.g.*, the center 64 × 256 pixel region of the field of view at 4000 fps. The Kodak SI camera and video processor combination was selected as the detector of choice behind the Hamamatsu dMCP, for its flexibility in video frame rates, the linear performance characteristics of the charge coupled device (CCD) used in this camera, and an added advantage that every image recorded by the CCD was a single, non-interlaced frame. Video imagery was recorded in S-VHS format on 3M ST 120 Master Broadcast Videocassettes (3M Corp., Minneapolis, MN). Hard-copy video prints were produced with a Kodak SV 6510 color video printer (Eastman Kodak, Inc., Rochester, NY).

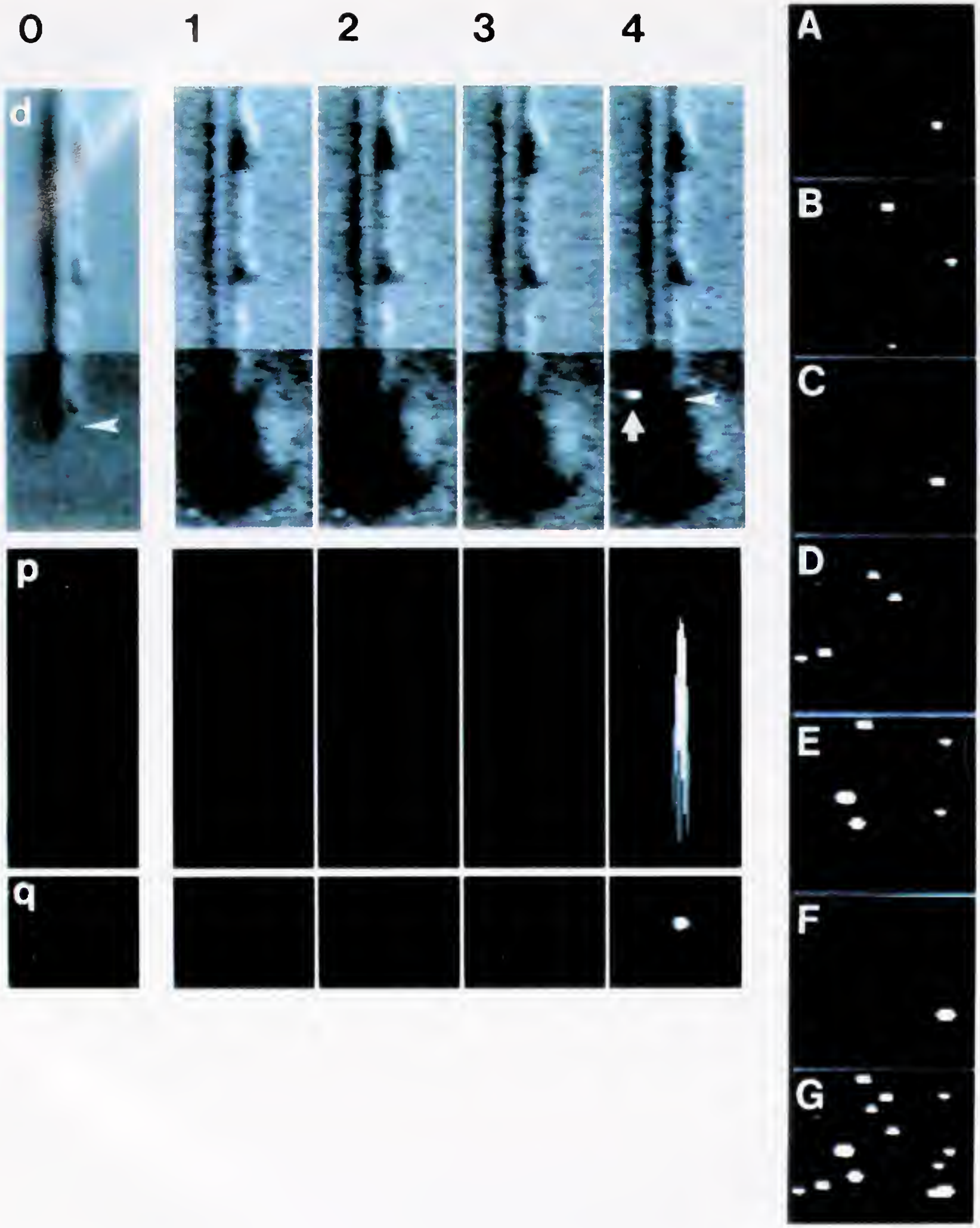

Figure 3. A recording of the time course of the calcium-dependent photon emission by aequorin. Columns 1 through 4 show images from single sequential 0.25-ms video frames from the 4000-fps video record. Column 0 shows an image obtained before the injection of aequorin. Row "d" shows the microinjection pipette using differential interference contrast (DIC) optics. Row "p" shows the linear intensity profile for each individual video frame corresponding to the DIC images in row "d" (above) and row "q" (below).

QED images at 4000 video frames per second

At 4000 fps, individual QEDs from within a stimulated preterminal were observed and recorded as sets of solid spots whose luminance intensity increased from background to maximum in the first frame and decreased in intensity with subsequent frames (Fig. 1C and D). Each QED record was preceded by a dark region (no light). The first frame of each QED showed a dramatic increase in luminance intensity, which resembled a symmetric dome of light distributed over an area less than 0.5 μm in diameter. Subsequent 0.25-ms video frames showed symmetrical domes with the same center as the first dome, but with less overall intensity. Each subsequent corrected frame decreased in intensity by a factor that seemed to follow an exponential decay curve (Fig. 2 and Table I).

Time-resolved imaging of aequorin luminescence in vitro

Any analysis of the QED images would require that we determine the time course for the aequorin reaction itself under the experimental conditions used. Published values for the lag time between the addition of Ca^{2+} to a solution of aequorin in a test tube and the emission of photons range between 2 and 10 ms (20, 21). That range is clearly too imprecise, so we sought a direct measurement using 4000-fps video, the imaging system being used for the experiments.

When aequorin was injected into Ca^{2+}-containing buffer, time-resolved Ca^{2+}-dependent aequorin luminescence could be detected with the dMCP-SI camera system operated at 4000 fps (Figs 1D and 3). Prior to the injection, the region around the tip of the micropipette appeared black; 0.75 ms after injection, bright spots of light appeared. Following the initial and rapid rise in luminescence, the signal diminished in intensity to background over a period of four or five 0.25-ms video frames. In six trials, 0.75 ms elapsed between the initial mixing of aequorin and Ca^{2+} buffer and the onset of photon emission. Thus, the intensity of Ca^{2+}-dependent aequorin luminescence was adequate to elicit a readily discernible signal from the dMCP-SI camera.

Shot noise

Shot noise was observed in recordings performed at all frame rates used in this study. In observations performed at 30 fps to 200 fps, shot noise appeared as a chevron. At 4000 fps, shot noise appeared as a bright spot lasting for one video frame (Fig. 1D). The intensity of these spots was typically less than 5% of the initial frame for a real QED.

Corrections of 4000 fps images for afterglow of faceplate phosphors

We applied arithmetic corrections to the raw QED images to compensate for the phosphorescent afterglow (22,

Row "q" shows the spots of light recorded as QEDs. Panel 1d corresponds to the same time period as shown in panels 1p and 1q; similarly 2d, 3d, and 4d correspond to 2p and 2q, 3p and 3q, and 4p and 4q, respectively. Panel 0d shows a 16-frame average of the oil- and aequorin-filled micropipette prior to injection of aequorin into the calcium buffer. Panels 0p and 0q show the corresponding intensity profile and QED record; *i.e.*, an absence of aequorin-mediated photon emission. The tip of the micropipette is noted with a horizontal, left-pointing arrowhead in this panel and panel 4d. Column 1 shows the first video frame following injection of aequorin into the calcium buffer. The micropipette in 1d is seen to be empty of the oil used to protect the aequorin from the calcium buffer prior to the injection. The oil droplet formed at the tip of the micropipette is seen as a sphere at the micropipette tip. Subsequent columns show the time course of the aequorin reaction, to the emission of the first QED (column 4).

Separately, panels A through F show an image integration of the first millisecond of QED emissions detected after injection of aequorin into calcium buffer for each of six separate experiments. The QED seen in panel C corresponds to the QED seen in panel 4d. Panel G shows an image integration of all of the QEDs detected in panels A through F. Note the high degree of spatial clustering of these initial QEDs recorded during one millisecond about the tip of the pipette.

To determine the lag time between the mixing of aequorin and Ca^{2+}, aequorin solutions were injected into Ca^{2+} buffers as previously described (3), and the reaction sequence was observed at 4000 fps. The method of injection of aequorin into the Ca^{2+} buffer was essentially identical to quantitative microinjections routinely performed (3, 19). For these experiments a multi-spectral video microscope was used (*e.g.*, 16, 17; developed by R. B. S.). The time of mixing was considered to have begun when the trailing meniscus of the first oil droplet was expressed from the tip of the pipette. Timing of the injection was coordinated with clock time of the video system. To assist in QED feature extraction and quantification, video images were processed, filtered, and analyzed with an Image1-AT (Universal Imaging Corp., West Chester, PA) running on a Dell 325 AT-bus computer, with macro programs written by one of us (R. B. S.). Ca^{2+},-dependent aequorin luminescence images of QEDs, seen as discrete spots on a dark background, were digitized and analyzed for each sequential video frame. The phosphorescent afterglow of the cameras and dMCP combinations contributes to the QED imagery (22, 23). The afterglow is due to the prolonged emission of energy from phosphors at the detector faceplate and is common to all phosphor-based image detectors. The afterglow and the contribution of shot noise to the imagery data are considered in the text and in Figure 2.

Table I

Mean luminance values and decay function attributes for individual evoked and spontaneous QEDs from synaptic preterminals and for aequorin QEDs produced in vitro

Event (*N*)	Video frame one mean intensity	Percent of frame one luminance intensity	Best curve fit[1]	Curve attributes a	Curve attributes b	R^2
Evoked (5)	22096	100.0	Exponential[2]	51502.3	−0.79	0.9909[3,4]
Spontaneous (5)	6491	29.4	Exponential[2]	36106.5	1.72	—[5]
Aequorin (5)	4027	18.2	Square pulse of 0.25 ms[6]			

[1] Solutions for best fit (highest value for R^2) were sought using linear, exponential, logarithmic and power curve fit models.

[2] The curve is described by the equation $y = ae^{bx}$.

[3] Curve calculated using values from five points: frames 1 through 5 having luminance intensity values greater than 0.

[4] Numerical analyses of the imagery data were performed within the Image 1-AT and Lotus 1-2-3 Version 3.0 environments using macro programs written by one of us (R.B.S.). Curve fit analyses were performed with an HP-41cv calculator (Hewlett-Packard, Corvallis, OR).

[5] No value is reported here because only two values could be used to solve the curve.

[6] Square pulse assumed given single frame lifetime following application of correction for phosphorescent afterglow.

23) of the dMCP faceplate (see figure legends). Quantitative data related to the corrected QEDs from the evoked and spontaneous responses from synaptic preterminals and from photon emission from aequorin injected into Ca^{2+} buffer are summarized in Table I.

Upon analysis, the processed image data showed that (a) the mean evoked response followed an exponential decay profile that was no longer than 1.25 ms; (b) in more than 90% of the observed cases, the maximum emission intensity was achieved in the first video frame; (c) in the first frame, the peak intensity for spontaneous events reached a value only 18.2% of that achieved for evoked responses; (d) as resolved at 4000 fps, the mean spontaneous response followed an exponential decay profile and lasted for no more than 0.5 ms; (e) evoked QEDs were about five times more intense than spontaneous QEDs; and (f) the aequorin response was a square pulse lasting at most 0.25 ms.

Discussion

Here we compare time-resolved video images of Ca^{2+}-dependent aequorin luminescence *in vitro* and in a synaptic preterminal, at frame rates from 30 to 4000 fps. Calcium microdomains and quantum emission domains (QEDs) in synaptic preterminals and QEDs emitted by aequorin reacting with calcium buffers *in vitro* with the photoprotein *n*-aequorin-J. These photon emissions were highly localized in time and space. Clues to the ultimate speed and duration of aequorin-mediated photon emissions in control and experimental systems came from the appearance of the spots of light viewed on the video monitors: namely the chevrons. Images obtained at 30 fps and 200 fps showed the QEDs as chevrons, rather than solid spots, indicating that QED lifetime was less than the duration of a single 200-fps video field (2.50 ms). Images at 4000 fps revealed the time course for calcium entry to the synaptic preterminal for both evoked and spontaneous events, as well as for the reaction of aequorin with calcium *in vitro*. Corrections for phosphorescent afterglow of the camera were developed and applied to the video records; they revealed that evoked and spontaneous events last a maximum of 1.25 and 0.5 ms, respectively; evoked QEDs had a fivefold greater intensity than spontaneous events. The reaction of aequorin with calcium *in vitro* occurred about 0.75 ms after the aequorin and calcium were mixed, and lasted 0.25 ms or less. The calcium concentration profiles are presented for evoked and spontaneous QEDs in synaptic preterminals *in vivo* and for aequorin reacting with calcium *in vitro*. The very rapid events reported here match earlier accounts of rapid, localized calcium currents at active zones during transmitter release.

In the application of a dMCP for photon-limited specimens, it is important to recall how the intensified image is produced and what the image represents (24): a cloud of electrons proportional to the number of photons produced in the microchannels and presented to the faceplate of the camera is used to produce the final image. The dMCP photocathode exhibits a 10% efficiency, and 60% of the output of that photocathode is sampled by the open area of the microchannels of the dMCP (24). Thus only 6% of the incident photons are available to be amplified by the dMCP. The 40×, 0.75 N.A. objective lens used in these studies is about 92% efficient at 465 nm, with a sampling cone angle of 38.8° (Ms. Becky Hohman, Carl Zeiss, Inc., pers. comm.); therefore, that objective lens can collect only 3.7% of the photons emitted from a single photon point source exhibiting 4π radiation. Thus, a system composed of that objective lens and dMCP exhibits a 0.022% efficiency for each 4π photon produced by the Ca^{2+}-dependent aequorin luminescence. For the observation system used in these experiments, the probability of detecting a photon emitted from a Ca^{2+}-aequorin complex acting as a point source is no greater than 2.22

$\times 10^{-3}$. This number is very small, but it represents a realistic estimate of the state of the art of optical components available for imaging single photon and photon-limited events.

When extending observations to high-speed video, the operational relationship between available light, detector sensitivity, and frame rate of the camera must be considered. Within the spectral sensitivity band of the detector, observed image intensity is dependent upon the number of photons interacting with the detector in a sampling period. This is a consideration long known to those using high-speed photographic emulsions at low light levels—for example, in photomicrography of fluorescent specimens. In practice, the faster the frame rate, the less light available per image frame: as the frame rate doubles, the light available for an image is halved. At 200 fps the light available per frame is roughly 7^{-1} of that available at 30 fps; at 4000 fps the light available per video frame is 132^{-1} of that available at 30 fps. At 4000 fps we are, at best, able to detect only 1.7×10^{-5} photons emitted from the specimen in a single 0.25-ms video frame.

This paper reports time-resolved images of Ca^{2+} entry to the synaptic preterminal for evoked and spontaneous events within microdomains. From the measurements of the reaction lag time and duration of the aequorin reaction *in vitro*, it also appears that high-speed video is an effective tool for the study of molecular reactions in solution. The implications of these observations for synaptic physiology are discussed in the accompanying paper (18).

Acknowledgments

We thank Drs. O. Shimomura, S. Inouye, B. Musicki, and Y. Kishi for the generous gifts of the custom aequorin preparations used in this study. Thanks are also extended to Mr. Paul W. DelGrego (Motion System Analysis Division, Eastman Kodak Co.) for his assistance with the digital high-speed video observations, and to Ms. Becky Hohman and Mr. Phil Presley (Carl Zeiss, Inc.) for information regarding the characteristics of the objective lens used for observations of photon emissions *in vivo*. This work supported by the N. I. H. (NS 13742 to R. L.), the U. S. Air Force (F49620-92-J-0363 to R. L.), and the N. S. F. (DCB-9005343 and DCB-9308024 to R. B. S.).

Literature Cited

1. **Katz, B. 1969.** *The Release of Neurotransmitter Substances.* The Sherrington Lectures X. Thomas, Springfield, IL.
2. **Llinás, R. R. 1977.** Pp. 139–160 in *Approaches to the Cell Biology of Neurons*, Vol. 2, C. W. M. Ferendelli and J. A. Ferendelli, eds. Soc. for Neurosciences, Bethesda, MD.
3. **Llinás, R., M. Sugimori, and R. B. Silver. 1992.** Microdomains of high calcium concentration in a presynaptic terminal. *Science* **256:** 677–679.
4. **Llinás, R., M. Sugimori, and R. B. Silver. 1991.** Imaging preterminal calcium concentration microdomains in the squid giant synapse. *Biol. Bull.* **181:** 316–317.
5. **Llinás, R., M. Sugimori, and R. B. Silver. 1993.** Presynaptic calcium concentration microdomains and transmitter release. *J. Physiol. (Paris)* **86:** 135–138.
6. **Llinás, R., M. Sugimori, and R. B. Silver. 1994.** Localization of calcium concentration microdomains at the active zone of the squid giant synapse. Pp. 133–137 in *Molecular and Cellular Mechanisms of Neurotransmitter Release*, L. Stjärne, P. Greengard, S. Grillner, J. Hökfelt and D. Ottoson, eds. Raven Press, New York.
7. **Llinás, R. R., I. Z. Steinberg, and K. Walton. 1981.** Relationship between presynaptic calcium current and postsynaptic action potential in squid giant synapse. *Biophys. J.* **33:** 323–351.
8. **Chad, J. E., and R. Ekert. 1984.** Calcium domains associated with individual channels can account for anomalous voltage relations of Ca-dependent responses. *Biophys. J.* **45:** 993–999.
9. **Simon, S. M., M. Sugimori, and R. R. Llinás. 1984.** Modeling the submembranous calcium-concentration changes and their relation to rate of presynaptic transmitter release in the squid giant synapse. *Biophys. J.* **45:** p264a.
10. **Simon, S. M., and R. R. Llinás. 1985.** Compartmentalization of the submembrane calcium activity during calcium influx and its significance in transmitter release. *Biophys. J.* **48:** 485–498.
11. **Fogelson, A. L., and R. S. Zucker. 1985.** Presynaptic calcium diffusion from various arrays of single channels. *Biophys. J.* **48:** 1003–1007.
12. **Zucker, R. S., and A. L. Fogelson. 1986.** Relationship between transmitter release and presynaptic calcium influx when calcium enters through discrete channels. *Proc. Natl. Acad. Sci. U.S.A.* **83:** 3032–3036.
13. **Llinás, R., I. Z. Steinberg, and K. Walton. 1981.** Presynaptic calcium currents in squid giant synapse. *Biophys. J.* **33:** 289–321.
14. **Pumplin, D. W., T. S. Reese, and R. Llinás. 1981.** Are the presynaptic membrane particles the calcium channels? *Proc. Natl. Acad. Sci. U.S.A.* **78:** 7210–7213.
15. **Pumplin, D. W., and T. S. Reese. 1978.** Membrane ultrastructure of the giant synapse of the squid *Loligo pealei*. *Neuroscience* **3:** 685–696.
16. **Silver, R. B. 1994.** Video light microscopic imaging of the calcium signal that initiates nuclear envelope breakdown in sand dollar (*Echinaracnius parma*) cells. *Biol. Bull.* **187:** 235–237.
17. **Silver, R. B., A. P. Reeves, M. Whitman, and B. Kelley. 1994.** Analysis of spatial and temporal patterns in the Ca^{2+} signal that signals nuclear envelope breakdown in sand dollar (*Echinaracnius parma*) cells. *Biol. Bull.* **187:** 237–238.
18. **Sugimori, M., E. J. Lang, R. B. Silver, and R. Llinás. 1994.** High-resolution measurement of the time course of calcium-concentration microdomains at squid presynaptic terminals. *Biol. Bull.* **187:** 300–303.
19. **Silver, R. B. 1989.** Nuclear envelope breakdown and mitosis in sand dollar embryos is inhibited by microinjection of calcium buffers in a calcium-reversible fashion and by antagonists of intracellular Ca^{2+}-channels. *Develop. Biol.* **131:** 11–26.
20. **Shimomura, O., B. Musicki, and Y. Kishi. 1989.** Semi-synthetic aequorins with improved sensitivity to Ca^{2+} ions. *Biochem. J.* **261:** 913–920.
21. **Shimomura, O., S. Inouye, B. Musicki, and Y. Kishi. 1990.** Recombinant aequorin and semi-synthetic recombinant aequorins. *Biochem. J.* **270:** 309–312.
22. **Inoué, S. 1986.** *Video Microscopy.* Plenum Press, New York. Pp. 149–262.
23. **Wayne, R. P. 1988.** *Principles and Applications of Photochemistry.* Oxford Science Publications, Oxford University Press, Oxford. Pp. 66–84.
24. **Hamamatsu Photonics K. K., Electron Tube Center. 1991.** *Image Intensifiers.* Shizuoka-ken, Japan.

Reference: *Biol. Bull.* **187**: 300–303. (December, 1994)

High-Resolution Measurement of the Time Course of Calcium-Concentration Microdomains at Squid Presynaptic Terminals

MUTSUYUKI SUGIMORI[1,3], ERIC J. LANG[1,3], ROBERT B. SILVER[2,3], AND RODOLFO LLINÁS[1,3]

[1]*Department of Physiology and Biophysics, New York University Medical Center, 550 First Avenue, New York, New York 10016,* [2]*Section and Department of Physiology, Cornell University, Ithaca, New York 14853-6401, and* [3]*Marine Biological Laboratory, Woods Hole, Massachusetts 02543*

Transmitter release is considered to be a secretory event triggered by localized calcium influx which, by binding to a low-affinity Ca^{2+} site at the presynaptic active zone, initiates vesicular exocytosis (1–7). In previous experiments with aequorin-loaded presynaptic terminals we visualized, upon tetanic presynaptic stimulation, small points of light produced by calcium concentration microdomains of about 300 μM (5). These microdomains had a diameter of about 0.5 μm (5) and covered 5–10% of the total presynaptic membrane with an average density of 8.4 μm^2 per 100 μm^2, corresponding closely to the size and distribution of the active zones in that junction (6, 7).

To understand in more detail the nature of these concentration microdomains, we obtained rapid video images (4000/s) after injecting the photoprotein n-aequorin-J into the presynaptic terminals of squid giant synapses. Using that experimental approach, we determined that microdomains evoked by presynaptic spike activation had a duration of about 800 μs. Spontaneous quantum emission domains (QEDs) observed at about the same locations as the microdomains were smaller in amplitude, shorter in duration, and less frequent.

These results illustrate the time course of the calcium concentration profiles responsible for transmitter release. Their extremely short duration compares closely with that of calcium current flow during a presynaptic action potential and indicates that, as theorized in the past (6–8), intracellular calcium concentration at the active zone remains high only for the duration of transmembrane calcium flow.

Received 20 September 1994; accepted 5 October 1994.

The spontaneous quantum emission domains (QEDs) observed prior to stimulation were imaged over an area corresponding to ≈20% of the total active zone of the preterminal studied. They occurred at a very low rate (10–15/s) and were generally located at the same sites as the evoked microdomains (Fig. 1B).

Calcium entry following tetanic stimulation of the presynaptic axon (500 ms or 1 s at 100 Hz) was characterized by the appearance of calcium microdomain sites that appeared to blink on and off during the tetanic stimulation (Fig. 1). The localization of the evoked microdomains in the presynaptic terminal is shown in Fig. 1A, and as previously reported (5), double-labeling of the presynaptic and postsynaptic fibers with fluorescent dyes demonstrated that QEDs are localized at the active zones (9).

These results suggest that the spontaneous and evoked light emissions probably correspond to spontaneous (10, 11) and voltage-evoked calcium channel openings, respectively. The low frequency of such light points indicates, however, that only a very small percentage of the total number of calcium entry events are being observed. Indeed, for spontaneous release given calculated levels of ≈35,000 quanta/s for the total active zone (10, 11), the area observed (20%) should generate ≈7000 QEDs/s rather than the 10–15 observed if we assume that one activated zone releases one QED. This number is based on the assumptions that (1) every spontaneous event is triggered by calcium entry at the active zone (which will overestimate the QEDs because some spontaneous transmitter release is calcium independent), and (2) each calcium entry event activates

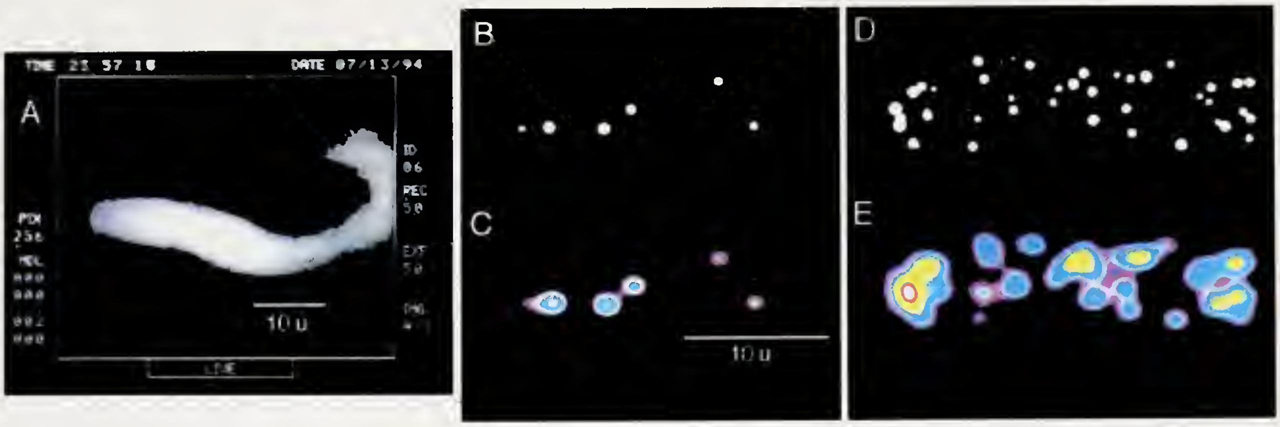

Figure 1. Fluorescence image and light emission from a squid synaptic preterminal injected with *n*-aequorin-J.

A hybrid synthetic aequorin, *n*-aequorin-J, with a sensitivity to [Ca^{2+}] on the order of 10^{-4} *M*, developed by Shimomura, Musicki, and Kishi (19) was used as an [Ca^{2+}]$_i$ indicator. This photoprotein was chosen because its low binding constant requires relatively large calcium concentrations to activate photon emission ($\approx$300–400 μM [10]), which is triggered with a short delay ($\approx$750 s [12]). In addition, it has the advantage of not substantially modifying the buffering properties of the intracellular milieu.

Presynaptic injection of this aequorin (5) in the squid (*Loligo pealii*) giant synapse (20), allowed the selective detection of high-calcium-concentration microdomains (5). The distribution of the injected aequorin inside the presynaptic terminal was determined by visualizing a fluorophore (rhodamine-labeled Dextran) that was injected with the photoprotein (5). The diffusion profile was visualized using a fluorescence microscope with a 40× water-immersion objective lens (N.A. 0.75). Aequorin luminescence was measured with a dMCP intensified camera operated in the photon-counting mode (12). The images were stored on conventional videotape (30 video frames/s), a fast-tape system (NAC HSV-400) with a 5-ms time resolution, or a digital system (Kodak HSC) with a 250-μs resolution (12). The synapses were dissected under flowing seawater, and during the experiments the preparation was bathed in artificial seawater containing 10 m*M* Ca^{2+}.

(A) Fluorescence image showing the preterminal on the larger of the post axons (not visible). (B) Spontaneous light emission recorded over 500 ms. (C) Same as in B, showing the light intensity (relative scale [12]) in pseudocolor. (D and E) Same as in B and C but taken over a 500-ms period of tetanic stimulation at 100 Hz.

aequorin (which also overestimates because such reactions—being dependent on concentration and time—are far from fully efficient).

The QED frequency for evoked release occurred at a rate of 250–500/s, with superimposed QEDs occurring at a rate of 3 to 5/s. QED frequency for evoked release was 20 to 30 times greater than the QED frequency for spontaneous activity (Fig. 1D and E). The QED frequency for the relative increase in evoked release was at about the level expected assuming a quantal content of 5 to 10 × 10^3 per action potential (3, 11). With 1 s of tetanic stimulation of 100 Hz, the quantal release would be near 0.5 to 1 × 10^6.

The experimental results indicate detection levels three orders of magnitude smaller than expected from such calculations. Two possible explanations for this very low yield are (1) that QEDs are generated only when calcium channel openings occur in particular spatial distribution (*e.g.*, clustering), *i.e.*, the so-called neighbor effect (8); (2) that our detection system sees only a small percentage of the photons emitted (12). Preliminary measurements suggest that only 0.22% of the light emitted is captured by the present system (12), which supports the view that the low observed QED yield is due to technical limitations in detection (12).

To compare the time course for evoked QEDs with that of the presynaptic calcium current triggered by a simulated action potential, these events were superimposed on the same time base (Fig. 2). The time course for I_{Ca} superimposes adequately on the time course of a microdomain evoked during the activation of similar presynaptic spikes (Fig. 2B). Note, however, that the light emission seems to outlast that of the transmembrane current. This is to be expected because high-level light emission does leave an afterglow in the photosensors (12). Indeed, as shown in Figure 2 panel C, the time course for the microdomain corrected for this distortion (12) matches quite closely the time course of the macroscopic I_{Ca}.

The results presented here demonstrate for the first time the true time course for the calcium microdomain at a chemical presynaptic terminal. These findings are in agreement with the time course for spike-evoked calcium currents (13) as well as with model results (8) for

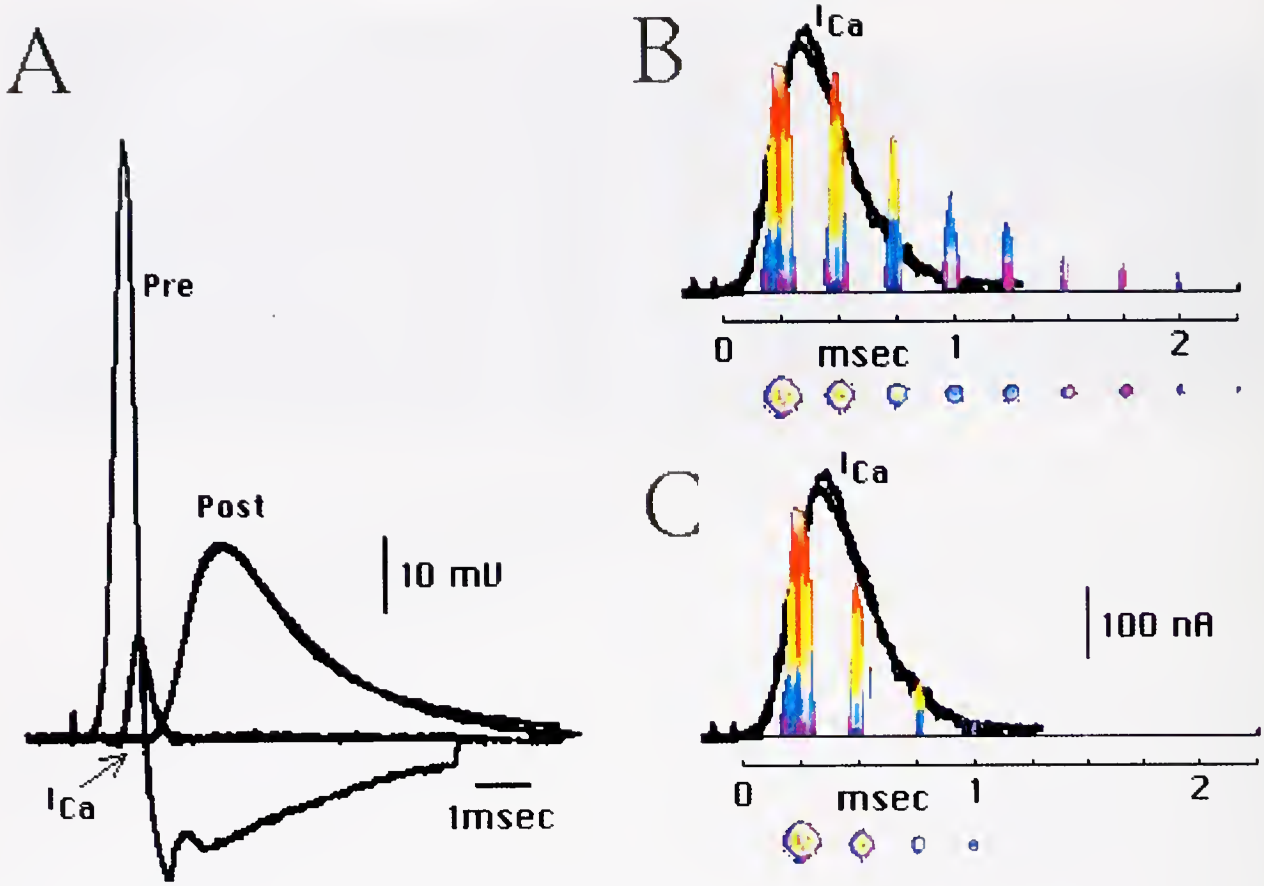

Figure 2. Time course for evoked calcium concentration microdomains. (A) Illustration of the time course for a presynaptic action potential (Pre) that simulates the voltage profile of a presynaptic spike recorded from the same fiber, before block of sodium and potassium channels (from 7); the calcium current (I_{Ca}) generated by the transient depolarization; and the postsynaptic response (Post) triggered by I_{Ca}. The presynaptic current (ICa—arrow), basically a tail current with an overall duration of $\approx$800 μs, and the postsynaptic potential obtained in previous experiments (7) are shown. (B and C) Superimposition of the time course for the calcium microdomain (amplitude on a relative scale) and the time course for the presynaptic calcium current. (B) Amplitude of raw light measurements taken every 250 μs. (C) Amplitudes after correction for afterglow. The area of the color circles under each time point relates to the amplitude of the light emission during that time bin.

the distribution and time course for transient calcium-concentration profiles, given by the equation for the analytical solution for three-dimensional calcium diffusion:

$$C(r,t) = \frac{2.0 \times 10^3 \text{ xJ}}{4.0 \times \pi \times \text{FAR} \times \text{Dca} \times r}\, erfc\left(\frac{4}{2.0\sqrt{\text{Dca} \times t}}\right)$$

where C (r, t) is the calcium concentration at time, t, and distance, r, from the channel; Dca is the diffusion coefficient for calcium; FAR is the Faraday constant; J is the flux per channel; and *erfc* is the complementary error function. This equation was used to calculate the calcium-concentration profile, which reaches a steady-state level of $\approx$300 μM at 500 Å from the channel pore in 1 μs and, following channel closure, decays to a level of 10 μM in a similar period for the same distance (8). Given the sensitivity level of *n*-aequorin-J, our results are, indeed, consistent with the model.

The time course reported here is different from that observed in other secretory systems such as the chromaffin cell (14), where the transient develops over 10 to 100 ms and where the calcium buffering properties may be quite different. However, our results are similar to the calcium concentration profile in individual frog-muscle sarcomeres following the activation of action potentials (14).

The overall duration of the microdomain is in agreement with the increased probability of release produced by a presynaptic spike. The calcium current produced by a presynaptic action potential has a peak at 0.3 ms and an overall duration of $\approx$0.8 ms (13), very much in agreement with measurements observed with the present technique.

The observations described in this paper constitute a direct demonstration of the time course for the calcium concentration microprofiles at a presynaptic terminal. This time course matches closely that of the release process (13) and the average opening time for P-type calcium channels (15) which may be responsible for the presynaptic calcium current in this terminal (16). The results further indicate that the temporal coherence for transmitter release is indeed produced by a well-matched relationship between the kinetic properties for the opening of calcium channels and the duration of the presynaptic action potential (13).

These results confirm our previous conclusion that synaptic neurotransmitter release is triggered by high-calcium-concentration microprofiles at the active zone that induce a rapid triggering of vesicle fusion lasting for the duration of the calcium profile (3, 17). Since the time course of the evoked microdomain is about three times as long and about fivefold larger than that produced by spontaneous QEDs, the evoked release may be triggered by the opening of many more calcium channels per active zone than the spontaneous events.

The number of calcium ions that are detected in an evoked microdomain may be estimated as follows. Consider that a presynaptic action potential generates an I_{Ca} of about 300 nA (10, 13), a current of 0.5 pA/channel, and that a single channel allows the flow of about 150 to 200 calcium ions (7, 18), then $\approx 6 \times 10^5$ channels are opened to release 5000 to 10,000 vesicles (4, 11) or $\approx$15,000 calcium ions/vesicle (13). [This is in contrast to the estimated minimum of 200 ions/vesicle (one calcium channel) for the ciliary ganglion (18)]. Given that the number of active zones in a presynaptic terminal is about 5000 to 10,000 (6), the number of channels open per action potential for each active zone is $\approx$100. If single channels allow the flow of 150 to 200 calcium ions (7, 18), an evoked microdomain, using *n*-aequorin-J and the present imaging technique, may represent an influx of calcium of about 15,000 ions.

Acknowledgments

We thank Drs. O. Shimomura, S. Inouye, B. Musicki, and Y. Kishi for the generous gift of the custom aequorin preparations used in this study. We are also grateful to Mr. P. W. DelGrego (Motion System Analysis Division, Eastman Kodak Co.) for assistance with the digital high-speed video observations. Work supported by the N.I.H. (NS13742 to R.L.), the U.S. Air Force (F49620-92-J-0363 to R.L.) and the N.S.F. (DCB-9005343 and DCB-9308024 to R.B.S.).

Literature Cited

1. **Augustine, G. J., E. M. Adler, and M. P. Charlton. 1991.** The calcium signal for transmitter secretion from presynaptic nerve terminals. *Annals NY Acad Sci.* **635:** 365–381.
2. **Katz, B. and R. Miledi. 1967.** A study of synaptic transmission in the absence of nerve impulses. *J Physiol. (Lond.)* **192:** 407–436.
3. **Llinás, R. 1977.** Calcium and transmitter release in squid synapse. Pp. 139–160 in *Society for Neuroscience Symposia,* Vol. 2, W. W. Cowan and J. A. Ferendelli, eds. Society for Neuroscience, Bethesda, MD.
4. **Llinás, R., I. Z. Steinberg, and K. Walton. 1981.** Relationship between presynaptic calcium current and postsynaptic potential in squid giant synapse. *Biophys J* **33:** 323–352.
5. **Llinás, R., M. Sugimori, and R. B. Silver. 1992.** Microdomains of high calcium concentration in a presynaptic terminal. *Science* **256:** 677–679.
6. **Pumplin, E. F., and T. S. Reese. 1978.** Membrane ultrastructure of the giant synapse of the squid *Loligo pealei. Neuroscience* **3:** 685–696.
7. **Pumplin, E. F., T. S. Reese, and R. Llinás. 1981.** Are the presynaptic membrane particles the calcium channels? *Proc. Natl. Acad. Sci. USA* **78:** 7210–7213.
8. **Simon, S. M. and R. Llinás. 1985.** Compartmentalization of the submembrane calcium activity during calcium influx and its significance in transmitter release. *Biophys. J.* **48:** 485–498.
9. **Llinás, R., M. Sugimori, and R. B. Silver. 1994.** Localization of calcium concentration microdomains at the active zone in the squid giant synapse. Pp. 133–136 in *Molecular and Cellular Mechanisms of Neurotransmitter Release.* L. Stjärne *et al.*, eds. Raven Press Ltd., New York.
10. **Lin, J.-W., M. Sugimori, R. Llinás, T. McGuinness, and P. Greengard. 1990.** Effects of synapsin I and calcium/calmodulin-dependent protein kinase II on spontaneous neurotransmitter release in the squid giant synapse. *Proc Natl Acad Sci USA* **87:** 8257–8261.
11. **Miledi, R. 1967.** Spontaneous synaptic potentials and quantal release of transmitter in the stellate ganglion of the squid. *J Physiol. (Lond.)* **192:** 379–406.
12. **Silver, R. B., M. Sugimori, E. J. Lang, and R. Llinás. 1994.** Time-resolved imaging of Ca^{2+}-dependent aequorin luminescence of microdomains and QEDs. *Biol. Bull.* **187:** 293–299.
13. **Llinás, R., M. Sugimori, and S. M. Simon. 1982.** Transmission by presynaptic spike-like depolarization in the squid giant synapse. *Proc. Natl. Acad. Sci. USA* **79:** 2415–2419.
14. **Monck, J. R., I. M. Robinson, A. L. Escobar, J. L. Vergara, and J. M. Fernandez. 1994.** Pulsed laser imaging of rapid Ca^{2+} gradients in excitable cells. *Biophys. J* **67:** 505–514.
15. **Usowicz, M. M., M. Sugimori, B. Cherksey, and R. Llinás. 1992.** P-type calcium channels in the somata and dendrites of adult cerebellar Purkinje cells. *Neuron* **9:** 1185–1199.
16. **Llinás, R., M. Sugimori, J. W. Lin, and B. Cherksey. 1989.** Blocking and isolation of calcium channel from neurons in mammals and cephalopods utilizing a toxin fraction (FTX) from funnel-web spider poison. *Proc. Natl. Acad. Sci. USA* **86:** 1689–1693.
17. **Llinás, R., I. Z. Steinberg, and K. Walton. 1981.** Presynaptic calcium currents in squid giant synapse. *Biophys. J.* **33:** 289–322.
18. **Stanley, E. F. 1993.** Single calcium channels and acetylcholine release at a presynaptic nerve terminal. *Neuron* **11:** 1007–1011.
19. **Shimomura, O., B. Musicki, and Y. Kishi. 1989.** Semi-synthetic aequorins with improved sensitivity to Ca^{2+} ions. *Biochem. J.* **261:** 913–920.
20. **Young, J. Z. 1939.** Fused neurons and synaptic contacts in the giant nerve fibers of cephalopods. *Phil. Trans. R. Soc Ser. B* **229:** 465–505.

Reference: *Biol. Bull.* **187:** 304–308. (December, 1994)

Temperature and the Larval Ecology of the Crown-of-Thorns Starfish, *Acanthaster planci*

LELAND G. JOHNSON[1] AND RUSSELL C. BABCOCK[2,*]

[1]*Department of Biology, Augustana College, Sioux Falls, South Dakota 57197, and* [2]*Australian Institute of Marine Science, Townsville, Queensland 4810, Australia*

The recently reported dramatic population increases (outbreaks) of the coral-eating crown-of-thorns starfish, Acanthaster planci, *which have damaged many reefs in the Indo-Pacific, are ending (1), but questions remain about the factors that affect* Acanthaster *distribution and densities. For example, the narrow temperature tolerance (26° or 27° to 30° or 31°C) reported for* Acanthaster's *larval development (2) is problematic because* Acanthaster *occurs where temperatures do not rise into this range (3, 4). We have further examined some temperature relationships in* Acanthaster's *early development. Cleavage proceeded normally over a range of about 10°C, but specific limiting temperatures depended upon the geographic source of the parents or their recent history of temperature exposure. Hatched, swimming gastrulae continued normal development to bipinnaria throughout a temperature range of 13°C. These results indicate that the narrow developmental temperature tolerances reported earlier for* Acanthaster *do not apply to all early developmental stages, and they add to the list of larval adaptations that can facilitate dispersal of* Acanthaster *larvae and propagation of outbreaks.*

Acanthaster planci is one of several Indo-Pacific asteroids that prey on coral polyps (5). Unlike other tropical starfish, however, *Acanthaster* undergoes occasional population outbreaks that have severely reduced coral cover on many reefs over the last 30 years. The causes of these outbreaks remain obscure despite much recent research (6–8). The outbreaks may be natural phenomena with a long history of occurrence (9), or they may be relatively recent in origin, brought about as a result of human activities (10). A combination of both explanations is also possible (11).

Two series of outbreaks of *Acanthaster planci* have been recorded on Australia's Great Barrier Reef (GBR) since the early 1960s, affecting reefs over approximately the central third of that system (12). Kenchington (13) hypothesized that outbreaks (termed primary) began somewhere to the north of Green Island (Fig. 1), and in turn initiated a cascade of additional outbreaks (termed secondary) that spread southward as a result of the advection of larvae by southward-flowing currents during the spawning season. Recent data from broadscale population surveys (1), genetic studies (14), and hydrodynamic models (15, 16) support Kenchington's hypothesis, though questions have been raised regarding some hydrodynamic models (17).

Population outbreaks of *Acanthaster* on the GBR have occurred over some 1000 km of reef (6 degrees of latitude). The main wave of outbreaks declined at around 20° S (18), which lies to the south of Davies Reef (Fig. 1); only a few smaller outbreaks are now being recorded at the far southern end of the system in the Swain complex (1). Lucas (2) has hypothesized that southern limits of *Acanthaster's* distribution may be dictated by larval temperature requirements. However, *Acanthaster* occurs in cooler waters near the limits of hard coral distribution (3, 4, 7). Temporally variable aggregations of *Acanthaster* at some Japanese sites appear to be derived entirely from settlement of larvae carried by currents from warmer water areas (19), but at other cooler water sites there are relatively stable *Acanthaster* populations. For example, there is evidence of increasing *Acanthaster* numbers at Lord Howe Island (Fig. 1) (20), although the mean surface water temperature there during January, the warmest month of the year, is about 24°C, which is below the reported range of developmental temperature tolerance. Population maintenance there conceivably could depend solely upon recruitment of larvae carried by currents from the GBR,

Received 3 January 1994; accepted 3 October 1994.

* Present Address: University of Auckland, Leigh Marine Laboratory, P. O. Box 349, Warkworth, New Zealand.

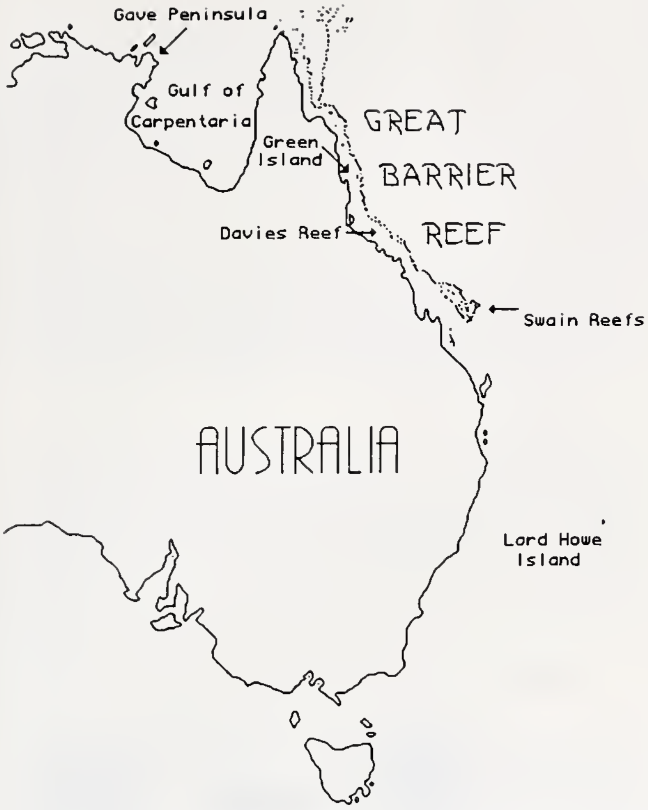

Figure 1. Map showing collection sites and other locations mentioned in the text.

but the Lord Howe Island population is genetically divergent from GBR populations (21), and gene flow into it from the GBR appears to be very limited, indicating a relatively isolated, locally reproducing population. Such evidence of successful reproduction under diverse environmental temperature regimes and genetic evidence for long-distance larval transport (14) suggest complexity in *Acanthaster's* developmental temperature relationships. We have investigated both the developmental temperature tolerances of offspring of geographically widely separated groups of *Acanthaster* and the effects of experimentally altering temperature exposures of adult, embryonic, and larval starfish.

Offspring of animals collected off the Gove Peninsula near Nhulunbuy and at Davies Reef in the GBR (Fig. 1) completed development to bipinnaria larvae equally well at 31°, 27°, and 24°C. At 22.3° and 21°C, Davies Reef embryos produced normal bipinnariae (Table I). At the same temperatures, some Gove embryos hatched, but they ceased development as abnormal early gastrulae.

Such geographic differences in developmental temperature tolerance may be due to genetic differentiation of separated populations, physiological acclimatization effects reflecting recent parental temperature exposure, or a combination of the two (22–24). We conducted a laboratory acclimation experiment to investigate a possible parental acclimatization effect in *Acanthaster.* A group of adults from Davies Reef was separated into two samples. One sample was held for 18 days at 31°C and the other at 25°C for 21 days. We observed differences between the offspring of 25°-acclimated animals and 31°-acclimated animals in tolerance to lower temperatures (Table I) and in early cleavage rates (Fig. 2), which in other echinoderms are proportional to overall developmental rates at least to the gastrula stage (25). The tolerance difference indicates an acclimatory translation of tolerance range, but more data at several temperatures would be needed to determine if the observed rate difference resulted from rotation of the rate: temperature curve.

We also examined possible parental effects due to seasonal change in water temperature in animals studied immediately after collection at Davies Reef in October (temperature at collection site: 25.5°C) and in November (temperature: 27°C). Offspring of the two groups differed in their tolerance to high temperature. In October-collected animals, development to early bipinnaria larvae proceeded normally between 21° and 27°C, but not at 32°C. However, offspring of November-collected animals developed into normal bipinnaria at 32°. This seasonal change resembles those reported for other echinoderms (26, 27).

Thus early developmental temperature tolerances in *Acanthaster* vary with recent parental temperature exposure as well as geographic source. However, our results do not distinguish the relative contributions made by

Table I

Development of embryos from each of four groups at low experimental temperatures

Group	Zygote to Bipinn. @ 22.3°C	Zygote to Bipinn. @ 21°C	Cleavage @ 18°C
DAVIES	+	+	none
GOVE	—	—	none
31°-ACCL	—	—	none
25°-ACCL	+	◇	abnormal

Bipinn. = bipinnaria larva; + indicates normal development to bipinnaria larvae; — indicates failure to develop to bipinnariae; ◇ indicates development of larvae with clumps of extra mesenchyme-like cells rarely observed in embryos developing at 31°, 27°, or 24°C. Gamete shedding was induced by 1-methyl adenine injection. Zygotes were transferred to rearing dishes at experimental temperatures within 5 min after fertilization at room temperature (24°C). Animals were collected off Nhulunbuy on the Gove Peninsula and at Davies Reef on 18 and 19 December 1991, and maintained in running seawater at approximately 27° until experiments began early in January 1992. Acclimation of samples of Davies Reef animals began on 3 January 1992, and continued at 31°C for 18 days and at 25°C for 21 days.

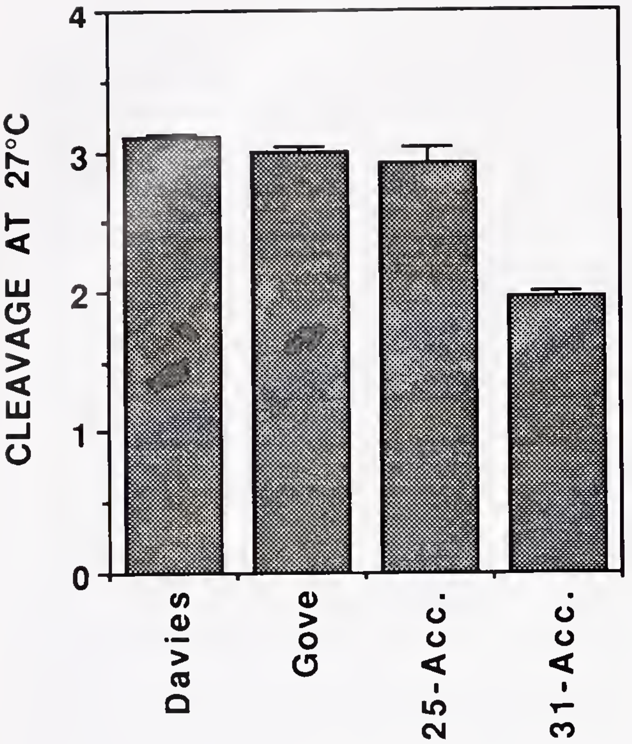

Figure 2. Cleavage rate comparisons at 27°C. For each group, four replicate cultures in 20-ml scintillation vials (mean no. of embryos per vial = 99) were fixed after 146 min. Embryos in each culture were counted and scored for cleavages completed. Bars represent means of individual culture means, with standard errors. Because ANOVA indicated a significant treatment effect, the Tukey test was applied. The mean for the 31°- acclimated group differs significantly from the other means (α = 0.05), which do not differ from one another.

population genetic differentiation and physiological acclimatization to the observed geographic variations.

Because of its importance for dispersal, the temperature tolerance of newly hatched swimming embryos was examined. Early gastrulae from cultures of Gove embryos were transferred to 21° and 18°C (temperatures at which Gove embryos cannot cleave normally). Transferred embryos continued to swim, completed gastrulation, and produced bipinnariae at both temperatures (Table II). This unexpectedly broad temperature tolerance in gastrula-stage embryos prompted additional transfer experiments. Newly hatched Davies Reef gastrulae transferred from 27° to 18.5°C developed into bipinnariae that appeared normal (Fig. 3). Even gastrulae transferred from 27° to 15°C and held there for 6 days continued to swim actively, slowly continued archenteron extension, and then quickly completed bipinnaria morphogenesis after transfer back to 27°C. However, these larvae contained clumps of extra mesenchyme-like cells.

In summary, data presented here support a modified concept of temperature tolerance during early *Acanthaster* development (Fig. 4), indicating that *Acanthaster's* distribution and abundance need not be as limited by developmental temperature as previously thought. Clearly, temperature relationships in later larval stages should be

Table II

Results of gastrula transfer experiments with Gove embryos

Transfer group	Days	Percent Bipinn. development
31° to 31° (Control)	2	93
31° to 21°	5	88
31° to 18°	17	81

Only swimming, newly hatched, early gastrulae were transferred. The numbers of days from transfer to final observation are given. Comparable results were obtained following transfers of embryos that developed from fertilization to hatching at 27°C.

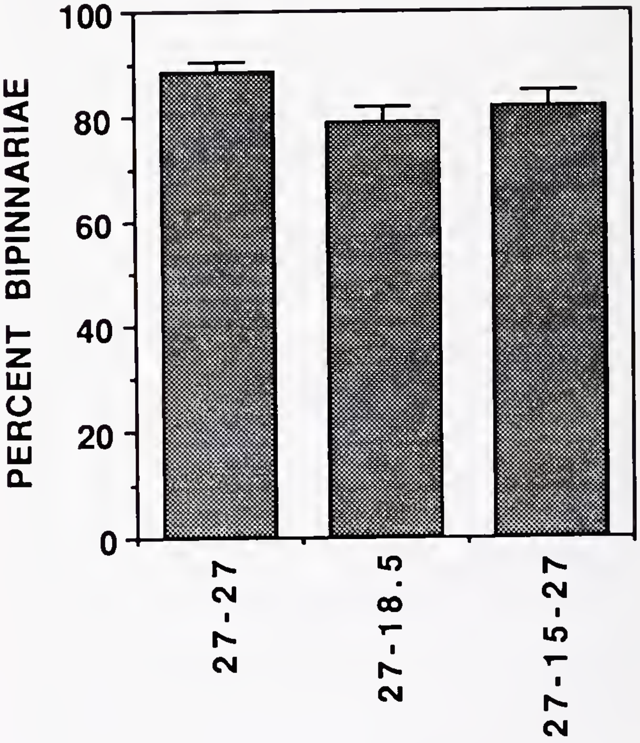

Figure 3. Gastrula transfer experiments with Davies Reef animals during December 1992. Early development proceeded at 27°C, and transfers were as described in Table II. Bars represent mean percentages, with standard errors, of bipinnaria development for 12 cultures (40 to 100 embryos in each) from two experiments. "27–27" represents controls; "27–18.5" represents transfer and continuing development at 18.5°C; and "27–15-27" represents gastrulae returned to 27°C after 6 days at 15°C. Bipinnariae in this latter group were normal in shape, but many contained clumps of extra mesenchyme-like cells. Embryos that were not returned from 15° to 27°C showed some archenteron extension, but eventually regressed and died.

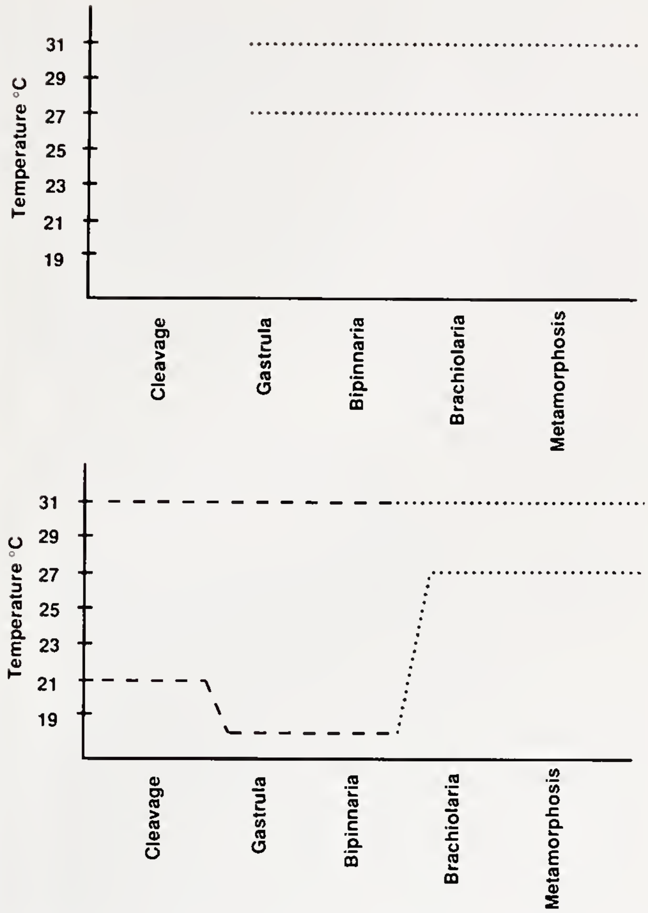

Figure 4. Conceptual models of crown-of-thorns starfish developmental temperature tolerances. The upper model is one inferred from data of Lucas (2) who transferred embryos at hatching and maintained cultures until settling and metamorphosis. The lower model retains the limited temperature tolerances (dotted lines) reported by Lucas for later larval stages, but incorporates the broader tolerances (dashed lines) of earlier developmental stages indicated by our data. Our data also indicate that actual limiting temperatures, but not necessarily size, of tolerance ranges vary with recent parental temperature exposure as well as geographic source.

reexamined, especially for populations at the extremes of *Acanthaster's* distribution. Further, the temperature tolerance of *Acanthaster* gastrulae adds to a list of traits that make *Acanthaster* larvae particularly well adapted for long-distance dispersal. Even larvae swept into cooler water could very slowly continue normal development during transport. This, along with the ability to develop at the low phytoplankton concentrations common in tropical waters (28, 29) and the negatively geotropic swimming behavior characteristic of *Acanthaster* gastrula (3), would allow transport to distant reef sites with conditions appropriate for later larval development and settling—processes that may be less resistant to environmental variation (2). Early larval hardiness may facilitate both the routine dispersal of larvae and the propagation of *Acanthaster* outbreaks.

Acknowledgments

This work was funded by the Great Barrier Reef Marine Park Authority through the Crown-of-Thorns Starfish Research Committee. We thank C. Cartwright, K. Hall, and D. Whitehead for technical assistance, P. Moran and C. Mundy for discussion and advice, J. Quam for map preparation, and C. Christie for collecting *Acanthaster* at Nhulunbuy.

Literature Cited

1. **Moran, P. J., G. De'ath, V. J. Baker, D. K. Bass, C. A. Christie, I. R. Miller, B. A. Miller-Smith, and A. A. Thompson. 1992.** Pattern of outbreaks of crown-of-thorns starfish (*Acanthaster planci* L.) along the Great Barrier reef. Pp. 555–568 in *Crown-of-Thorns Starfish on the Great Barrier Reef: Reproduction, Recruitment and Hydrodynamics*, C. Johnson, ed. *Aust. J. Mar. Freshwater Res.* **43(3).**
2. **Lucas, J. S. 1973.** Reproductive and larval biology of *Acanthaster planci* in great Barrier Reef waters. *Micronesica* **9:** 197–203.
3. **Yamaguchi, M. 1973.** Early life histories of coral reef asteroids, with special reference to *Acanthaster planci* (L.). Pp. 369–387 in *Biology and Geology of Coral Reefs, Vol. 2,* O. A. Jones and R. Endean, eds. Academic Press, New York.
4. **McKnight, D. G. 1978.** *Acanthaster planci* (Linnaeus) (Asteroidea: Echinodermata) at the Kermedec Islands. *N. Z. Oceanogr. Inst. Rec.* **4:** 17–19.
5. **Birkeland, C. 1989.** The influence of echinoderms on coral-reef communities. Pp. 1–79 in *Echinoderm Studies, Vol. 3,* M. Jangoux and J. M. Lawrence, eds. A. A. Balkema, Rotterdam.
6. **Zann, L. P., and P. J. Moran. 1988.** A coordinated research program on the *Acanthaster* phenomenon. Pp. 177–182 in *Proc. Sixth Int. Coral Reef Symp. Vol. 2.*
7. **Birkeland, C. and J. S. Lucas. 1990.** *Acanthaster planci: Major Management Problem of Coral Reefs.* CRC Press, Boca Raton, FL.
8. **Johnson, C., ed. 1992.** *Crown-of-Thorns Starfish on the Great Barrier Reef: Reproduction, Recruitment and Hydrodynamics. Aust. J. Mar. Freshwater Res.* **43(3).**
9. **Walbran, P. D., R. A. Henderson, A. J. T. Jull, and M. J. Head. 1989.** Evidence from sediments of long-term *Acanthaster planci* predation on corals of the Great Barrier reef. *Science* **245:** 847–850.
10. **Cameron, A. M., R. Endean, and L. M. DeVantier. 1991.** Predation on massive corals: Are devastating population outbreaks of *Acanthaster planci* novel events? *Mar. Ecol. Prog. Ser.* **75:** 251–258.
11. **Moran, P. J., and R. H. Bradbury. 1989.** The crown-of-thorns starfish controversy. *Search* **20:** 3–6.
12. **Reichelt, R. E., R. H. Bradbury, and P. J. Moran. 1990.** Distribution of *Acanthaster planci* outbreaks on the Great Barrier Reef between 1966 and 1989. *Coral Reefs* **9:** 97–103.
13. **Kenchington, R. A. 1977.** Growth and recruitment of *Acanthaster planci* (L.) on the Great Barrier Reef. *Biol. Conservation* **11:** 103–118.
14. **Benzie, J. A. H., and J. A. Stoddart. 1992.** Genetic structure of outbreaking and non-outbreaking crown-of-thorns starfish (*Acanthaster planci*) populations on the Great Barrier Reef. *Mar. Biol.* **112:** 119–130.
15. **James, M. K., and J. P. Scandol. 1992.** Larval dispersal simulations: correlation with the crown-of-thorns starfish outbreaks database. Pp. 569–582 in *Crown-of-Thorns Starfish on the Great Barrier Reef:*

Reproduction, Recruitment and Hydrodynamics. C. Johnson, ed. *Aust. J. Mar. Freshwater Res.* **43(3).**

16. **Scandol, J. P., and M. K. James. 1992.** Hydrodynamics and larval dispersal: a population model of *Acanthaster planci* on the Great Barrier Reef. Pp. 583–596 in *Crown-of-Thorns Starfish on the Great Barrier Reef: Reproduction, Recruitment and Hydrodynamics.* C. Johnson, ed. *Aust. J. Mar. Freshwater Res.* **43(3).**
17. **Wolanski, E. 1993.** Facts and numerical artefacts in modelling the dispersal of crown-of-thorns starfish larvae in the Great Barrier Reef. *Aust. J. Mar. Freshwater Res.* **44:** 427–436.
18. **Moran, P. J. 1986.** The *Acanthaster* phenomenon. *Oceanogr. Mar. Biol. Annu. Rev.* **24:** 379–480.
19. **Yamaguchi, M. 1987.** Occurrences and persistency of *Acanthaster planci* pseudo-population in relation to oceanographic conditions along the Pacific coast of Japan. *Galaxea* **6:** 277–288.
20. **DeVantier, L. M., and G. Deacon. 1990.** Distribution of *Acanthaster planci* at Lord Howe Island, the southern-most Indo-Pacific reef. *Coral Reefs* **9:** 145–148.
21. **Benzie, J. A. H., and J. A. Stoddart. 1992.** Genetic structure of crown-of-thorns starfish (*Acanthaster planci*) in Australia. *Mar. Biol.* **112:** 631–639.
22. **Moore, J. A. 1949.** Geographaphic variation of adaptive characters in *Rana pipiens* Schreber. *Evolution* **3:** 1–24.
23. **Tester, P. A. 1985.** Effects of parental acclimation temperature and egg-incubation temperature on egg-hatching time in *Acartia tonsa* (Copepoda: Calanoida). *Mar. Biol.* **89:** 45–53.
24. **Johnson, L. G. 1993.** Temperature tolerance, temperature stress, and animal development. Pp. 37–40 in *Proceedings of the Biostress Symposia.* N. H. Granholm, ed. South Dakota State Univ., Brookings.
25. **Fujisawa, H. 1989.** Differences in temperature dependence of early development of sea urchins with different growing seasons. *Biol. Bull.* **176:** 96–102.
26. **O'Connor, C., and J. C. Mulley. 1977.** Temperature effects on periodicity and embryology, with observations on the population genetics, of the aquacultural echinoid *Heliocidaris tuberculata. Aquaculture* **12:** 99–114.
27. **Horstadius, S. 1975.** A note on the effect of temperature on sea urchin eggs. *Exp. Mar. Biol. Ecol.* **18:** 239–242.
28. **Olson, R. R. 1987.** *In situ* culturing as a test of the larval starvation hypothesis for the crown-of-thorns starfish, *Acanthaster planci. Limnol. Oceanogr.* **32:** 895–904.
29. **Ayukai, T. 1994.** Ingestion of ultraplankton by the planktonic larvae of the crown-of-thorns starfish, *Acanthaster planci. Biol. Bull.* **186:** 90–100.

Reference: *Biol. Bull* **187**: 309–318. (December, 1994)

Reproductive Potential and Genetics of Triploid Pacific Oysters, *Crassostrea gigas* (Thunberg)

XIMING GUO[1] AND STANDISH K. ALLEN, JR.

Haskin Shellfish Research Laboratory, Institute of Marine and Coastal Sciences, Rutgers University, B8, Port Norris, New Jersey 08349

Abstract. The reproductive potential and genetics of triploidy were studied in the Pacific oyster. DNA content in sperm from triploids showed a single peak at 1.5c as determined by flow cytometry. In eggs from triploids, trivalents were the dominant form of synapsed chromosomes, although the degree of synapsis varied considerably within and among females. Some eggs went through complete synapsis and formed 10 trivalent chromosomes; most had a mixture of 11–13 trivalents, bivalents, and univalents. Factorial matings were produced from diploid (D) and triploid (T) parent oysters, creating four crosses: DD, DT, TD, and TT (female first).

Gametes from triploids were fully capable of fertilization. After fertilization, eggs from triploids went through two meioses and released two polar bodies as diploid eggs did. Karyological analyses showed that average ploidy of the resultant embryos was 2.0 n for DD, 2.46 n for DT, 2.52 n for TD, and 2.88 n for TT. Survival of fertilized eggs to metamorphosis and settlement was about 21% for DD, but considerably lower on other crosses: 0.0007% for DT, 0.0463% for TD, and 0.0085% for TT. Nine months after matings, all survivors from DT crosses were diploid. Survivors from TD crosses consisted of 33% diploids, 57% triploids, and 10% tetraploids. Survivors from the TT crosses consisted of 90% triploids, 4% diploids, and 6% mosaics. We hypothesize that differences in ploidy composition between DT and TD embryos and survivors were caused by pro-egg segregations that favor the retention, rather than loss, of extra chromosomes in the egg. The reproductive potential of triploids and evolutionary implications are discussed.

Introduction

Triploidy refers to the condition of a cell or organism having three sets of chromosomes. Such a condition in mammals is lethal. In many species of amphibians, fish, molluscs, and other invertebrates, triploids are fully viable and do not appear morphologically different from diploids. In a few species, such as certain gynogenetic fishes, triploidy is a natural mode of reproduction, but in most animals species, triploidy occurs infrequently and is considered a numerical mutation of chromosomes. However, triploidy can be easily induced in most lower animals by inhibiting the release of polar body II (Fankhauser, 1945; Thorgaard, 1983; Allen, 1986).

Triploids are commonly assumed to be sterile as a result of the extra set of chromosomes (Thorgaard, 1983). However, sterility in triploids is often incomplete and varies considerably among organisms. In plants, fertile triploids are common and are believed to have played a significant role in the evolution of plants (deWet, 1980). In salamanders, induced triploids were not completely sterile, and matings between triploids and diploids produced viable offspring (Fankhauser and Humphrey, 1950, 1954). In fish, induced triploids had severely reduced gonadal development in both sexes, although a small number of mature oocytes and sperm were observed (Lincoln, 1981a, b; Benfey and Sutterlin, 1984; Benfey, 1991; Gui *et al.*, 1991). No viable fish were obtained when triploid males were crossed with diploid females (Lincoln, 1981a; Lincoln and Scott, 1984). In invertebrates, triploid *Drosophila* produced viable offspring when mated with diploids (Morgan, 1925). In molluscs, triploids have been produced in a number of species, but so far most studies have been limited to the induction, growth, and gonadal development of triploids (Beaumont and Fairbrother, 1991). Although triploid molluscs generally show retarded gonadal

---

Received 26 January 1994; accepted 22 September 1994.

[1] Corresponding author.

development, the formation of apparently normal gametes was observed in both sexes of triploid Pacific oyster, *Crassostrea gigas* (Allen and Downing, 1990; Guo, 1991) and several other species. In the Pacific oyster, Allen (1987) made crosses between triploid males and diploid females and obtained viable offspring.

The reproductive potential and genetics of triploids is relevant to our understanding of animal evolution, particularly the increased attention on the evolutionary significance of polyploid animals (White, 1978; Schultz, 1980; Bogart, 1980). If triploidy occurs spontaneously in most species, what are the genetic consequences of triploidy? Is triploidy simply a genetic burden on the population, or is it a mutation that has vital importance for the evolutionary process? Our present knowledge about the biology and reproductive genetics of polyploid animals is limited, especially among marine invertebrates.

The reproductive potential and genetics of triploidy also has important practical implications. In the Pacific oyster, for example, triploids have been produced commercially for aquaculture since 1986 (Allen *et al.*, 1989). What impact may triploids have on the genetic structure of natural populations when released? Triploids have also been proposed as candidates for the testing of non-native species (Allen, 1993). If triploids are not completely sterile, are they likely to become established? This study was conducted to examine the reproductive potential and genetics of triploidy using the Pacific oyster as a model species.

Materials and Methods

To study the reproductive genetics of triploid Pacific oyster, matings were conducted within/between diploids (D) and triploids (T), producing four crosses: DD, DT, TD, and TT, with the female listed first. Triploids used in this study were two years old and had been induced by inhibiting the release of the second polar body in fertilized eggs (Allen *et al.*, 1989). Before making crosses, triploids were individually confirmed by flow cytometry. Gametes were obtained by dissecting gonads. Eggs were passed through an 85-μm screen to remove the large tissue debris and then rinsed on a 25-μm screen. Sperm was passed through a 15-μm screen to remove tissue debris. Fertilization and incubation were conducted at 25°C using filtered (2 μm) seawater. Embryos were cultured according to routine hatchery protocol (*e.g.*, Breese and Malouf, 1975).

Synapsis and meiotic segregation in eggs from triploids was analyzed in TD crosses. In all crosses, the ploidy of two-hour-old embryos was determined by chromosome counts, and the ploidy of 24-hour-old embryos and later survivors was determined by flow cytometry. Survival to D-stage (Day 1), Day 7, and Spat (Day 30) was recorded in each group. Each cross was repeated four to seven times using different pairs of oysters as parents.

Synapsis, meiotic segregation, and chromosome constitution were observed by aceto-orcein stain (Guo *et al.*, 1992). Briefly, eggs were fixed in acetic acid and methanol (1:3). A drop of fixed sample was loaded on a slide, mixed with 2–3 drops of orcein stain (0.5% orcein in 60% acetic acid), and covered with a cover glass. After staining for five minutes, the eggs were gently compressed by applying pressure to the cover glass, which was then sealed. For chromosome counts, 2–4 cell embryos were first treated with 0.005% colchicine for 15 min before they were fixed. Flow cytometry was conducted on a Partec II flow cytometer with a 4,6-diamidine-2-phenylindole (DAPI) stain (Allen, 1983; Guo *et al.*, 1993).

To make sure survivors were not contaminants, allozyme inheritance was analyzed with starch gel electrophoresis (Aebersold *et al.*, 1987; Hebert and Beaton, 1989). Allozymes examined included aspartate aminotransferase (AAT, EC 2.6.1.1.), dipeptidase (DAP, EC 3.4.-.-, Gly-leu as substrate), glucose-6-phosphate dehydrogenase (G6PDH, EC 1.1.1.49), glucose phosphate isomerase (GPI, EC 5.3.1.9), isocitrate dehydrogenase (IDH, EC 1.1.1.42), malate dehydrogenase (MDH, EC 1.1.1.37), mannose phosphate isomerase (MPI, EC 5.3.1.8), phosphoglucomutase (PGM, EC 2.7.5.1), superoxide dismutase (SOD, EC 1.15.1.1), tripeptidase (TAP, EC 3.4.-.-, Leu-gly-gly as substrate).

Results

Gametes from triploids

Seventy-seven triploid oysters were examined during this study, and gametes were observed in 60 (78%) of them. Based on the type of gametes observed, the 60 oysters consisted of 35 females (58%), 16 males (27%), and 9 hermaphrodites (15%). Nineteen of the triploid females that produced a large number of eggs were used for crosses.

Twenty-two crosses were made: six DD, seven DT, five TD, and four TT. Most of those crosses were not complete 2 × 2 factorials between diploids and triploids due to limitations of triploid parents. When only triploid females (or males) were found in a given day, they were used to make TD (or DT) crosses with DD controls. Later in the study, the lack of TT crosses was apparent, and seven TT crosses were made on the same day and combined into one mass culture.

Among the 19 females used in crosses, the number of eggs ranged from 19 thousand to 21.5 million, with a mean of 2.3 million and a median of about 1 million (Table 1). The numbers of eggs in the other 16 triploid females were deemed too few for making crosses and were not determined, but they were probably fewer than 19,000. Assuming that the 16 females not counted averaged about 15,000 eggs, the estimated fecundity of triploid females would be around 1.2 million eggs per female. Eggs in two

Table I

Fecundity of two-year-old triploid females of the Pacific oyster (median value in bold)

Female	Number of eggs $(\times 10^3)$
1	19.0
2	23.8
3	28.6
4	57.2
5	240.5
6	313.5
7	339.0
8	454.5
9	699.6
10	**968.0**
11	1,420.4
12	1,425.0
13	1,755.6
14	1,782.0
15	2,145.0
16	2,398.0
17	3,045.0
18	4,325.0
19	21,520.0
Mean	2,261.0

2-year-old diploids were counted during this study, and the egg numbers were 25 and 105 million per female, agreeing with the fecundity estimates of Quayle (1988) of 50–100 million. We conservatively estimate 50 million eggs as the average fecundity for diploid females of this age. Therefore, this study suggests that the relative fecundity of triploid females is about 2% of normal diploids.

Diameters of 10 eggs were measured for four diploids and six triploids. Within females there was little variation in egg diameter from both diploids and triploids, the coefficient of variation ranging from 1.8 to 3.3%. On the other hand, variation among diploid females and among triploid females was highly significant (ANOVA, *F*-test, $P < 0.0001$ for both diploids and triploids). Eggs from all triploids were significantly larger than those from diploids ($P < 0.0001$). Eggs from diploids had an average diameter of 53.0 μm, ranging from 50 to 55 μm. Eggs from triploids had an average diameter of 58.2 μm, with a range of 56 to 62 μm. On average, the diameter of eggs from triploids was 10% larger than eggs from diploids, which corresponds to a 33% increase in cell volume.

In the eggs, synapsed chromosomes became visible after germinal vesicle breakdown (15 to 30 min in 25°C seawater). Eggs from diploids had exactly 10 bivalents (synapsed homologous chromosomes) (Fig. 1A), with no detectable variation within or between females (Table II). On the contrary, synapsis in eggs from triploids was highly variable and chaotic. In some eggs, synapsis was complete with the formation of 10 trivalents (Fig. 1B). In others, synapsis was incomplete, showing a mixture of tri-, bi-, and univalents (Fig. 1C). Overall, trivalents were the dominant form of synapsed chromosomes. A few eggs exhibited "over-synapsis" and formed eight or nine chromosomes containing multivalents greater than three.

A precise count of valent formations was not possible, but total numbers of chromosomes (all forms) were determined. Among all eggs examined from triploids, the number of chromosomes ranged from 8 to 18, with an overall mean of 12. The average chromosome number among triploid females varied from 10.6 and 13.9 (Table II). Within females, chromosome number also varied considerably (Fig. 2). Of nine triploid females analyzed, two females had a modal chromosome number of 10 per egg (*e.g.*, Fig. 2, F1); three females had a modal chromosome number of 11 (*e.g.*, Fig. 2, F2); four had a modal number of 13 (*e.g.*, Fig. 2, F3). There was no correlation between the completeness of synapsis and fecundity ($r = 0.17$, $P = 0.76$, $n = 6$).

When analyzed by flow cytometry, sperm from triploid males had an average DNA content of 1.49c (1c = 1n = 10 chromosomes) (Table III). No haploid peaks were observed among triploid males in this study.

Fertilization and egg development

Gametes from triploids were fully capable of fertilization. On average, fertilization among crosses with triploid parents was slightly lower than that of DD crosses (Table IV). However, the range in all groups was approximately the same, suggesting that gametes from triploids had full potential for successful fertilization.

After fertilization, the development of eggs from triploids was examined in TD crosses. Like normal eggs, eggs from triploids resumed meiosis by gathering chromosomes within minutes post-fertilization (PF). Polar body I (PB1) was released in the majority of the eggs between 10 and 20 min PF. After PB1 release, meiosis in eggs from triploids continued with, on the average, 15 bivalents at metaphase (Fig. 1D). Anaphase II was reached in the majority of the eggs between 35 and 45 min PF (Fig. 1E). Polar body II (PB2) was released in the majority of the eggs by 50 min PF. In TD crosses, highly elongated maternal (15 on the average) and paternal (always 10) chromosomes reappeared in two separate groups around 60 min PF. They mixed and condensed into typical metaphase-shaped chromosomes for the first mitotic division (Fig. 1F). In some crosses, polar body releases and early cleavages among eggs from triploids were slightly slower and less synchronized than those in eggs from diploids. At 2 h PF, the majority of the TD embryos entered the 4-cell stage.

Chromosome numbers were determined for embryos in one DD, three DT, three TD, and four TT crosses.

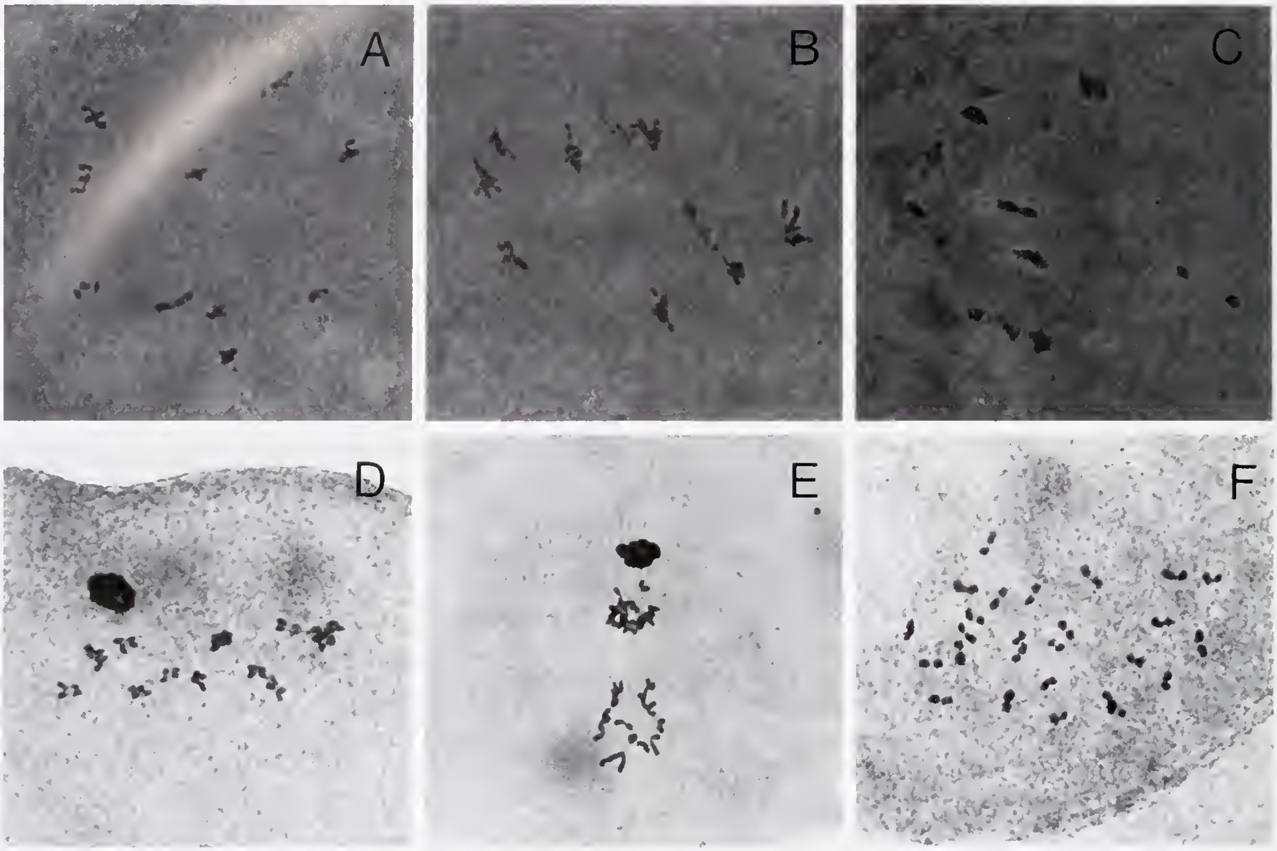

Figure 1. Synapsis and meiosis in eggs from triploid Pacific oysters: A—metaphase I eggs from diploids with 10 bivalents; B—complete synapsis in metaphase I eggs from triploids with 10 trivalents; C—incomplete synapsis in metaphase I eggs from triploids with a mixture of uni-, bi-, and trivalents; D—metaphase II in eggs from triploids; E—anaphase II in eggs from triploids; and F—metaphase of the first mitotic division of an embryo from a triploid (female) × diploid cross.

The orcein staining protocol used in this study was highly reliable for determining chromosome numbers in early embryos. Often more than half of the embryos had metaphases that could be clearly counted, and it was not unusual for embryos to have two countable metaphases. Most importantly, there is no artifactual chromosome loss. In the DD crosses, 49 of the 50 embryos analyzed had 20 chromosomes, and one had 30 chromosomes (Table V). In other crosses, the average chromosome numbers were 24.6 for DT, 25.2 for TD, and 28.8 for TT. TD embryos had a slightly greater mean chromosome number and coefficient of variation than DT crosses. The distribution of chromosome numbers among embryos in DT and TD crosses is shown in Figure 3. Comparatively, the distribution of chromosome numbers of DT embryos was closer to that expected from the random segregation of the third chromosome set than was the distribution of chromosome numbers in TD embryos. The latter had more embryos with 25+ chromosomes than DT crosses. Flow cytometric analysis of 24-hour-old embryos showed the same pattern, and the mean ploidy levels were 2.45 c for DT, 2.46 c for TD, and 2.90 c for TT crosses (Table III). Mean coefficient of variation of DNA content among the four groups was highest in the TD cross (Table III). Over time, the aneuploid peak in TD crosses split into two peaks: one close to 2 n and the other close to 3 n (Fig. 4). The peak splitting suggests that aneuploids closest to euploidy survive longer.

Survival

Survival of the fertilized eggs to D-stage was 65.8% for DD, 48.9% for DT, 31.7% for TD, and 39.5% for TT crosses (Table IV). Survival of fertilized eggs to Day 7 in crosses with triploid parents (0.50–7.9%) was obviously lower than that in DD crosses (39.8%). Surprisingly, TD crosses (7.9%) had much higher survival to Day 7 than DT crosses (0.52%). The same pattern of survival continued to 2 months PF: 20.6% for DD, 0.0007% for DT, 0.0463% for TD, and 0.0085 for TT crosses. When stan-

Table II

Total number of chromosomes (uni- and multivalents) in eggs from diploid and triploid Pacific oyster before fertilization

	Female	n	Mean	Difference*
2n	1	10	10.0	a
	2	15	10.0	a
			10.0	
3n	1	16	10.6	ab
	2	15	10.6	ab
	3	48	10.8	abc
	4	19	11.5	abcd
	5	12	12.2	bcde
	6	12	12.9	de
	7	44	13.2	e
	8	20	13.4	e
	9	10	13.9	e
			12.0	

* Different letters designate significant differences in means among females, as indicated by the Tukey HSD multiple comparison at a confidence level of 95%.

dardized by the survival of DD crosses, the survival of triploid crosses to two months was 0.0034% for DT, 0.2248% for TD, and 0.0413% for TT crosses.

At nine months PF, all experimental oysters died from an accidental crash of our rearing system. Tissues of some of the newly deceased oysters were saved, and their ploidy levels were analyzed by flow cytometry. All 30 oysters from one of the DD crosses were diploids. Twelve oysters from one of the DT crosses were also diploid. On the contrary, only one-third (32.5%) of the 40 TD oysters examined were diploid, and the other two-thirds were either triploid (57%) or tetraploid (10%). In the TT mass cultures which escaped the accidental crash, 48 oysters lived to one year of age. As analyzed by flow cytometry, the surviving TT oysters consisted of 90% triploids, 4% diploids, and 6% 2 n/3 n mosaics.

Allozyme patterns in DT survivors (all diploid) and all parents used in this study were analyzed. Out of the 11 allozymes analyzed, eight were successfully resolved, and five were polymorphic. No foreign alleles were detected, and we conclude survivors were not contaminants. Survivors from TD and TT groups were not analyzed, because the survivors were primarily polyploids that could not have been contaminants. However, we cannot rule out that the diploids found in either TD or TT crosses were the result of contamination from another stock or culture.

Discussion

Meiosis in triploids

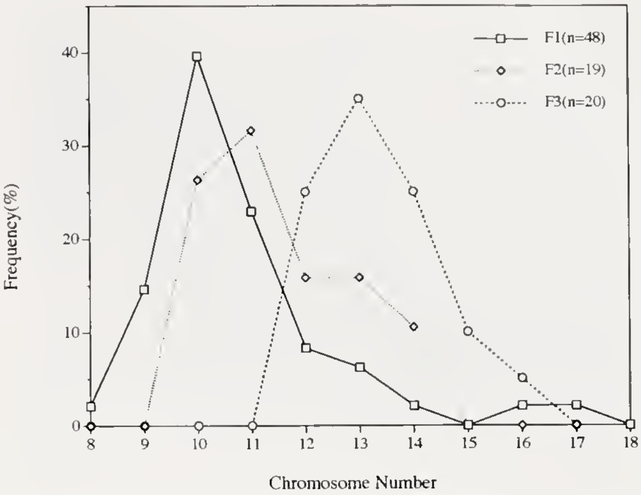

Figure 2. Distribution of chromosome numbers (uni, bi, tri, and multivalents) in Pacific oyster eggs from three different triploid females (F1–F3) prior to fertilization.

Trivalents were clearly the predominant form of synapsed chromosomes in eggs from triploid Pacific oysters, although incomplete synapsis was frequent with a mixture of tri-, bi-, and univalents. The formation of multivalents is common in polyploid plants and animals and has often been used as an indicator of recent polyploidization. Among 14 autotetraploid plants, for example, quadrivalent formation averaged 45%, ranging from 4 to 81% (Cauderon, 1986).

Completeness of synapsis varied considerably among females—variation that we cannot explain. Notably, there was no correlation between the degree of synapsis and fecundity, although our sample size was small ($n = 6$); further studies are needed to verify this observation. If

Table III

Relative DNA content measured by flow cytometry in parents and progeny of crosses within/between diploid (D) and triploid (T) Pacific oysters

Tissue	Group	n	Mean	SE	CV
Parent, somatic	2n	15	1.95	0.03	—
	3n	14	2.92	0.03	—
Parent, sperm	2n	15	1.00	*	—
	3n	11	1.49	0.01	—
Progeny, 24 h	DD	6	2.00	*	1.80
	DT	6	2.45	0.04	2.44
	TD	6	2.46	0.05	4.12
	TT	5	2.90	0.05	3.55

The first letter in the progeny group refers to the ploidy of the female. SE is standard error of mean DNA content in observations. CV is mean coefficient of variation of DNA histograms, where CV = 100* (standard deviation/mean).

* Used as standards.

Table IV

Percent survival of fertilized eggs to D-stage, to 7 days post fertilization (PF), and to spat (3 months PF) in crosses within/between diploid (D) and triploid (T) Pacific oyster; the first letter in the cross label refers to the female ploidy

Cross	Eggs ($\times 10^3$)	Fertilization (%)	D-stage (%)	7 days (%)	Spat (%)
DD					
1	1,811	61.5	84.7	—	—
2	381	95.2	97.8	32.2	18.7
3	103	9.6	22.2	19.5	—
5	1,574	50.3	40.6	40.6	27.1
8	1,400	94.9	63.9	43.5	23.3
9	1,748	94.6	85.6	63.4	13.3
		67.7	65.8	39.8	20.6
DT					
1	1,573	23.8	67.1	—	0.0043
3	1,027	13.7	100.0	0.13	—
4a	551	75.7	24.1	0.90	0
4b	103	77.9	18.0	1.27	0
5	3,148	40.9	26.9	0.10	0.0001
8	2,700	82.3	26.9	0.10	0
9	1,869	92.8	79.0	0.61	0
		58.2	48.9	0.52	0.0007
TD					
2b	622	33.6	26.2	9.14	0.0325
2c	149	66.7	17.5	4.45	0.1180
5a	996	16.9	28.0	19.30	0.0178
5b	115	20.7	29.8	6.20	0.0628
9	1,234	95.6	57.1	0.54	0.0005
		46.7	31.7	7.93	0.0463
TT					
6	878	9.0	40.8	0.40	0
7	11,974	—	16.1	0.83	0.0337
9a	1,164	89.3	80.4	0.67	0.0004
9b	700	31.8	20.7	0.11	0
		43.4	39.5	0.50	0.0085

fecundity is unrelated to completeness of synapsis in triploids, then low fecundity must be caused by factors other than synapsis, contrary to common belief. The inability to complete normal synapsis has been suggested as the cause for triploid sterility (or retarded gonadal development) in several species of fish (Thorgaard and Gall, 1979; Thorgaard, 1983, 1986; Benfey *et al.*, 1986). It is also difficult to argue that the low fecundity of triploid females is caused by aberrations in trivalent segregation. First, meiotic divisions remain arrested until after fertilization (Lu, 1986; Guo *et al.*, 1992). Second, triploid eggs seemed to complete meiosis normally.

For the most part, the extra set of chromosomes in triploids segregated randomly during meiosis. The sperm from triploid males had an average DNA content of 1.5 c, and no haploid sperm peaks were observed by flow cytometry. Allen (1987) observed that some triploid males produced haploid sperm; it is uncertain whether mosaic (2 n/3 n) triploids were involved. The random segregation of the extra chromosome set during meiosis was confirmed also by the fact that mean chromosome number of 2–4 cell embryos in both DT and TD embryos was about 2.5 n. There are no comparable studies on the ploidy of 2–4 cell embryos. Chromosome data in amphibians and plants were collected at late larvae or young plant stages and are therefore biased because of the likely differential mortality of aneuploids (Myers, 1944; Punyasingh, 1947; Fankhauser and Humphrey, 1950, 1954). On the other hand, the ploidy composition of survivors observed in this study agrees with findings from previous studies. In both plants and amphibians, polyploids were frequently observed from TD survivors, but rarely from DT survivors (Jones and Bamford, 1942; Fankhauser and Humphrey, 1950, 1954). In the Pacific oyster, the only study on DT crosses found that 149 of the 150 survivors analyzed were diploids (Allen, 1987), which supports our data.

Table V

Chromosome number in 2–4 cell embryos in experimental crosses within/between diploid (D) and triploid (T) Pacific oysters

Cross	n	Mean	CV
DD			
1	50	20.2*	7.0*
DT			
1	30	24.4	7.3
2	50	24.5	5.0
3	50	24.7	5.0
		24.6	5.8
TD			
1	17	25.0	7.6
2	46	25.0	10.2
3	71	25.5	11.6
		25.2	9.8
TT			
1	50	28.6	5.5
2	51	28.7	6.9
3	34	29.1	7.7
4	33	28.9	6.3
		28.8	6.6

CV = coefficient of variation 100* (standard deviation/mean chromosome count). The first letter in the cross label refers to the female ploidy.

* Mean > 20 and variance due to a single triploid. Otherwise DD mean = 20, CV = 0.0.

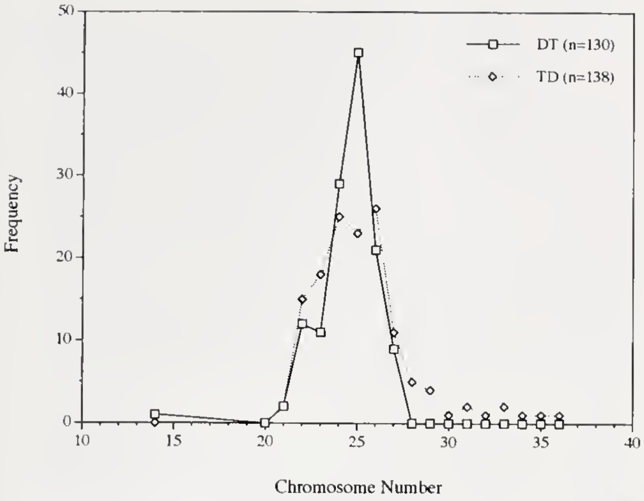

Figure 3. Distribution of number of chromosomes per cell in 2–4 cell diploid (female) × triploid (DT) and triploid (female) × diploid embryos (TD) of the Pacific oyster, showing some TD embryos had high chromosome numbers where DT did not.

Results of this study suggest that there are important differences between meiosis in triploid males and females. First, chromosome numbers in DT embryos are closer to the theoretical distribution than those in TD embryos, and TD embryos had more cells with 25+ chromosomes than DT embryos. Second, survivors from TD crosses were primarily polyploid, and survivors in DT crosses were primarily diploids. These observations suggest that meiosis in triploid females is more likely to make mistakes and produce gametes with chromosome gains rather than losses, compared with meiosis in triploid males. We hypothesize that in eggs from triploids, there is a general mechanism of *pro-egg segregation* which favors the retention, rather than loss, of chromosomes by the egg pronucleus.

In eggs, meiotic divisions are characterized by the formation of two polar bodies. We propose that segregation errors occur more often in the egg than in sperm; and when those errors occur, the egg tends to retain the errant chromosome(s) (either univalents or nondisjoined bivalents) rather than rejecting them into the polar body. In contrast, meiotic divisions in males produce four sperm, and therefore missegregated chromosomes are randomly distributed into daughter cells by default. The suppression of meiosis I and the formation of diploid gametes can be considered extreme cases of pro-egg segregation, which rarely occur in males. Pro-egg segregation would have a selective advantage because the gain of chromosomes is generally less harmful than their loss. Overall, the pro-egg segregation hypothesis predicts that meiotic segregation is random and more accurate in males than in females, and when missegregation occurs in the egg, there is a tendency for the egg to gain chromosomes rather than lose them.

Pro-egg segregation provides one explanation for the differences in DT and TD crosses observed in this study, and may be relevant to cytogenetic abnormalities in other taxa, such as human aneuploidy. Aneuploidy is a frequent form of chromosome abnormality in humans. There are two characteristics associated with human aneuploidy. First, there is a prevalence of trisomics (hyperploidy) over monosomics (hypoploidy) among spontaneous abortions and liveborns (Hecht and Hecht, 1987). Second, 90–95% of the trisomics receives the extra chromosome from the mother (Takaesu *et al.*, 1990; Antonarakis *et al.*, 1991,

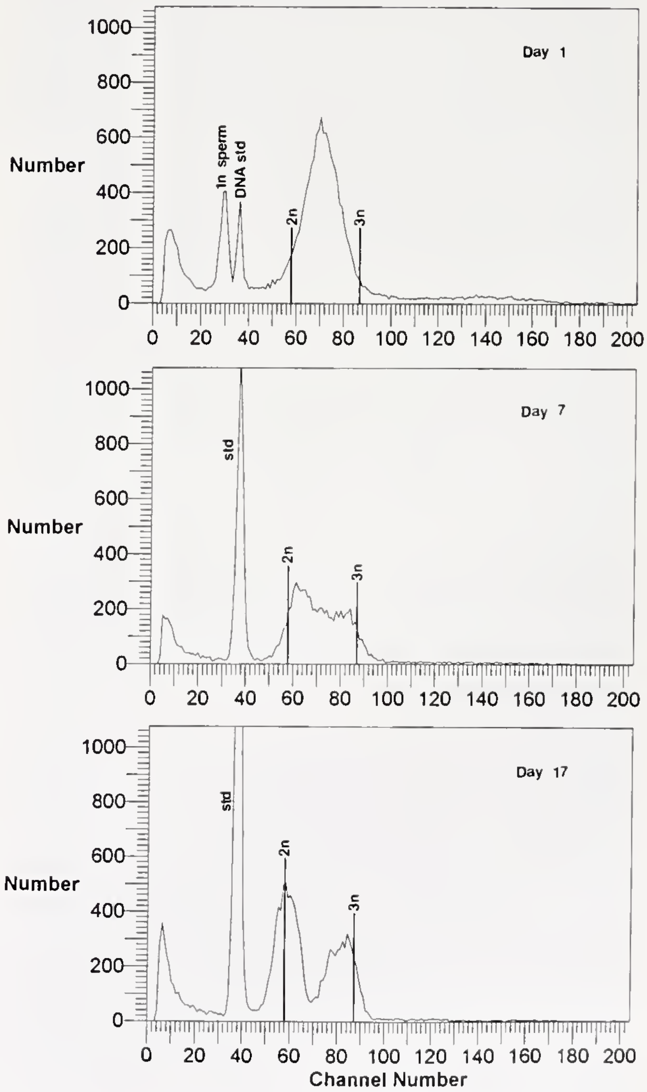

Figure 4. Relative DNA content measured by flow cytometry of dissociated cells of triploid (female) × diploid (TD) embryos of the Pacific oyster 24 h (top) and 17 days (bottom) days post fertilization, showing the loss of aneuploids and survival of larvae closer to euploid DNA contents of 2 n or 3 n.

1992), and there is a positive correlation between the frequency of trisomics and maternal age (Hecht and Hecht, 1987). The pro-egg segregation provides a possible explanation for these characteristics. An alternative explanation for the prevalence of trisomics among spontaneous abortions is the possibility that all monosomics die at an early stage before the recognition of pregnancy. Direct comparison of hypo-/hyperploidy ratio in mammalian sperm and oocytes has not been possible, because of the artifactual nature of hypoploid data. Unlike the orcein stain method used in this study, the standard air-dry procedure in mammalian cytogenetics is prone to chromosome loss. In fact, cytogenetic analyses in mammals often discard hypoploid data completely, and estimate the total aneuploidy frequency by doubling the hyperploidy frequency (Mailhes, 1987; Pellestor, 1991; Zenzes and Casper, 1992). (The assumption of hypo- and hyperploidy occurring at the same frequency would be invalid under the pro-egg segregation hypothesis.) Nevertheless, it has been well recognized that meiotic differences exist between human males and females. One of the hypotheses attributes the excessive non-disjunction in oocytes to the compromised microcirculation (Gaulden, 1992). Another hypothesis views that non-disjunction occurs randomly at all chromosome pairs in males, but not in females (Hecht and Hecht, 1987; Pellestor, 1991). Others have primarily focused on the positive correlation between trisomics and maternal age (Warburton, 1989; Eichenlaub-Ritter and Boll, 1989; Gaulden, 1989, 1992; Kloss and Nesse, 1992; Kratzer *et al.*, 1992; Zheng and Byers, 1992). The only one that is similar to the pro-egg segregation hypothesis is the chromosome competition hypothesis by Axelrod and Hamilton (1981). Recognizing the excess of hyperploids and their positive correlation with maternal age, Axelrod and Hamilton suggested that hyperploidy was due to competition among chromosomes to get into the oocyte rather than the polar body, as the mother approaches menopause.

There may be other mechanisms responsible for the apparent differences in meiosis between triploid females and males in this study. The formation of tetraploids in TD crosses, for example, could be caused by spontaneous suppression of meiosis I (Wilson, 1946; Fankhauser and Humphrey, 1950). In the Pacific oyster, blocking polar body I in TD zygotes indeed produced high proportions of tetraploids (Guo and Allen, 1994a). However, suppression of meiosis I, or even meiosis II, cannot explain the formation of a high proportion of diploid gametes in triploid females (corresponding to 3 n TD survivors).

Reproductive potential of triploids

This study clearly shows that triploid Pacific oysters are not completely sterile. Despite the fact that the majority of progeny from triploids were aneuploids, survivors were obtained from all crosses. This study also demonstrates that the majority of Pacific oyster aneuploids with intermediate chromosome numbers are inviable. Survivors that were classified as euploids in this study actually may be aneuploids because flow cytometry cannot detect small differences in DNA content without rigorous standardization. Viability of trisomics, hyper-triploids, hypo-, and hypertetraploids was demonstrated previously in the Pacific oyster (Guo and Allen, 1994a).

Because gametes from triploids were fully capable of fertilization, the reproductive potential of triploids primarily depends on their fecundity and survival of offspring. The relative fecundity of the triploid females was about 2% of diploid. Unfortunately, sperm production in triploid males was not determined in this study. Our observations seem to suggest that the relative fecundity (relative to diploids) of triploid males might be even lower than triploid females. Comparable fecundity data are not available in the literature, and most studies on the sterility of triploid animals are limited to histological observation of gonadal development (Beaumont and Fairbrother, 1991). In salamanders, triploid females produced half as many eggs as diploids (Fankhauser and Humphrey, 1950). In the clam (*Mulinia lateralis* Say), the relative fecundity of triploid females and males was about 59% and 80%, respectively, compared with diploids (Guo and Allen, 1994b). Among 500 triploids examined in the carp (*Carassius auratus*), one female was found to have a normally developed ovary filled with normal eggs (Gui *et al.*, 1991).

The results of our TT crosses are relevant to population control, as in the case where pure triploid populations are used in the culture or testing of a non-native species. Assuming that sperm is not the limiting factor (a conservative concession), the reproductive potential may be estimated as the product of reduced fecundity of triploids (0.02 of diploids) and survival of TT progeny relative to diploids (0.0085%/20.6%), or about 0.0008% of normal diploids in the first generation. For example, when diploids have 1 million chances to reproduce, triploids would have about 8. Furthermore 90% of TT survivors were triploid, although the chance of producing a diploid is not zero.

The other situation is a population mixed with diploids and triploids, as in the case where triploids (*e.g.*, Pacific oysters) are cultured in close proximity to a normal diploid population. Here, the fecundity of triploid males needs to be considered also. Assuming the triploid males also had a relative fecundity of 2%, triploids would have a reproductive potential of 0.0046% of normal diploids, *i.e.*, 46 in one million. The sperm production in triploid males may not be 2%, but since reproductive potential is primarily due to survival of TD, and not DT, crosses, our estimate would change little. In subsequent generations, the involvement of tetraploids—if fertile—may favor the production of triploids. Reproductive potential of tetraploids needs to be examined further.

These estimates of reproductive likelihood are preliminary, and many factors could affect the reproductive potential of triploids. For example, environmental factors could affect fecundity of triploids. We noticed that triploids from Washington State produced very few eggs, compared with ours reared in quarantine in New Jersey. More importantly, the reproductive potential estimated in laboratories probably overestimates that from natural situations. However, given adequate study, the reproductive potential of triploids is quantifiable.

Evolutionary implications

Reproduction in triploid Pacific oysters may have evolutionary implications. In plants, polyploid evolution has been described as a two-step process (deWet, 1980). The first step is the formation of triploids (often during hybridization); the second step—production of tetraploids from crosses between triploid females (3 n gametes) and diploid males (1 n gametes). Fankhauser and Humphrey (1950) duplicated these steps in the laboratory with the salamander, but their findings were largely neglected by evolutionary zoologists. Our finding of the same process in the Pacific oyster suggests that the triploid female × diploid male scenario may be a general phenomenon occurring in other animal groups. In special cases of fish and amphibians, the transition from triploid to tetraploid is accomplished by an endomitosis before meiosis (Schultz, 1980). However, endomitosis is rare and primarily limited to a group of all-female, gynogenetic fish (Cimino, 1973). Our data, along with those of Fankhauser and Humphrey (1950) plus data from plants, suggest that the triploid female × diploid male scenario may serve as a general mechanism for evolution by polyploidy in both animals and plants.

Another interesting finding of this study is that crosses within triploids produce primarily triploids, proving that triploids have some fertility and apparently can reproduce themselves genetically. The possibility of triploids mating with triploids exists in a hybridization zone where triploid hybrids are more viable than diploid hybrids. Those triploid hybrids may potentially mate with each other to reproduce themselves, or mate with diploids to produce fertile tetraploids. It has been documented in several species of fish that hybridization is only viable as triploids (Chevassus *et al.*, 1983; Scheerer and Thorgaard, 1983; Arai, 1984, 1986; Parson *et al.*, 1986; Yamano *et al.*, 1988).

Acknowledgments

We are grateful to Greg A. DeBrosse for care of brood stock, larval, and nursery cultures, and to Ann E. Arseniu for general lab assistance. This is New Jersey Agricultural Station Publication No. D-32100-1-94 and Contribution #94-03 of the Institute of Marine and Coastal Sciences, Rutgers University, supported by NOAA grant NA16FL0409-01 (91-ODR) to SKA and USDA/CSRS/OGPS 92-3703-7766 to SKA and XG.

Literature Cited

Aebersold, P. B., G. A. Winans, D. J. Teel, G. B. Milner, and F. M. Utter. 1987. *Manual for Starch Gel Electrophoresis: A Method for the Detection of Genetic Variation.* NOAA Technical Report NMFS 61, USA.

Allen, S. K., Jr. 1983. Flow cytometry: assaying experimental polyploid fish and shellfish. *Aquaculture* **33:** 317–328.

Allen, S. K., Jr. 1986. Genetic manipulations: critical review of methods and performances in shellfish. Pp. 127–143 in *Selection, Hybridization and Genetic Engineering in Aquaculture, Vol. II,* K. Tiews, ed. Heenemann Verlag, Berlin.

Allen, S. K., Jr. 1987. *Reproductive Sterility of Triploid Shellfish and Fish.* Ph.D. dissertation, University of Washington, Seattle, Washington.

Allen, S. K., Jr. 1993. Triploids for field study? The good, the bad, and the ugly. *J Shellfish Res.* **12:** 125 (abstract).

Allen, S. K., Jr., and S. L. Downing. 1990. Performance of triploid Pacific oysters, *Crassostrea gigas.* Gametogenesis. *Can. J. Fish. Aquat. Sci.* **47:** 1213–1222.

Allen, S. K., Jr., S. L. Downing, and K. K. Chew. 1989. *Hatchery Manual for Producing Triploid Oysters.* University of Washington Press, Seattle, Washington.

Antonarakis, S. E., and the Down Syndrome Collaborative Group. 1991. Parental origin of the extra chromosome in trisomy 21 as indicated by analysis of DNA polymorphism. *N. Engl. J. Med* **324:** 872–876.

Antonarakis, S. E., M. B. Petersen, M. G. McInnis, and P. A. Adelsberger. 1992. The meiotic stage of nondisjunction in trisomy 21: determination by using DNA polymorphisms. *Am. J. Hum. Genet.* **50:** 544–550.

Arai, K. 1984. Developmental genetic studies on salmonids: morphogenesis, isozyme phenotypes and chromosomes in hybrid embryos. *Mem. Fac. Fish. Hokkaido Univ.* **31**(1–2): 1–94.

Arai, K. 1986. Effects of allotriploidization on development of hybrids between female chum salmon and male brook trout. *Bull. Jpn. Soc. Sci. Fish.* **52**(5): 823–829.

Axelrod, R., and W. D. Hamilton. 1981. The evolution of cooperation. *Science* **211:** 1390–1396.

Benfey, T. J. 1991. The physiology of triploid salmonids in relation to aquaculture. *Can. Tech. Rep. of Fish. Aquat. Sci.* **1789:** 73–80.

Benfey, T. J., and A. M. Sutterlin. 1984. Growth and gonadal development in triploid landlocked Atlantic salmon (*Salmo salar*). *Can. J Fish. Aquat Sci.* **41:** 1387–1392.

Benfey, T. J., I. I. Solar, G. de Jong, and E. M. Donaldson. 1986. Flow-cytometric confirmation of aneuploidy in sperm from triploid rainbow trout. *Trans. Am. Fish. Soc.* **115:** 838–840.

Beaumont, A., and J. Fairbrother. 1991. Ploidy manipulation in molluscan shellfish: a review. *J. Shellfish Res.* **10**(1): 1–18.

Bogart, J. P. 1980. Evolutionary significance of polyploidy in amphibians and reptiles. Pp. 341–378 in *Polyploidy, Biological Relevance,* W. H. Lewis, ed. Plenum Press, New York.

Breese, W. P., and R. E. Malouf. 1975. *Hatchery Manual for the Pacific Oyster.* Oregon State University Sea Grant College Program, Publication no. ORESU-H-75002.

Cauderon, Y. 1986. Cytogenetics in breeding programs dealing with polyploidy, interspecific hybridization and introgression. Pp. 83–104 in *Genetic Manipulation in Plant Breeding.* W. Horn *et al.*, eds. Walter de Gruyter, New York.

Chevassus, B., R. Guyomard, D. Chourrout, and E. Quillet. 1983. Production of viable hybrids in salmonids by triploidization. *Genet. Sel. Evol* 15: 519–532.

Cimino, M. C. 1973. Meiosis in triploid all-female fish (*Poeciliopsis,* Poeciliidae). *Science* **175:** 1484.

deWet, J. M. J. 1980. Origins of polyploids. Pp. 3–15 in *Polyploidy, Biological Relevance,* W. H. Lewis, ed. Plenum Press, New York.

Eichenlaub-Ritter, U., and I. Boll. 1989. Nocodazole sensitivity, age-related aneuploidy, and alterations in the cell cycle during maturation of mouse oocytes. *Cytogenet. Cell Genet.* **52:** 170–176.

Fankhauser, G. 1945. The effects of changes in chromosome number on amphibian development. *Q Rev. Biol* **20:** 20–78.

Fankhauser, G., and R. R. Humphrey. 1950. Chromosome number and development of progeny of triploid axolotl females mated with diploid males. *J Exp. Zool.* **116:** 207–240.

Fankhauser, G., and R. R. Humphrey. 1954. Chromosome number and development of progeny of triploid axolotl males crosses with diploid females. *J Exp Zool.* **126:** 33–58.

Gaulden, M. E. 1989. A model that explains the varying frequency of aneuploid children with maternal age (J-shaped curve) as well as aneuploidy of paternal origin. Pp. 253–257 in *Mechanism of Chromosome Distribution and Aneuploidy,* M. A. Resnick and B. K. Vig, eds. Liss, New York.

Gaulden, M. E. 1992. Maternal age effect: the enigma of Down syndrome and other trisomic condition. *Mutation Res.* **296:** 69–88.

Gui, J. F., W. H. Xiao, L. Chen, S. C. Liang, and Y. G. Jiang. 1991. Gonadal development in artificial triploid transparent colored crucian carp. *ACTA Zool. Sinica* **37:** 297–304.

Guo, X. 1991. *Studies on Tetraploid Induction in the Pacific Oyster,* Crassostrea gigas *(Thunberg).* Ph.D. Dissertation, University of Washington, Seattle, Washington.

Guo, X., and S. K. Allen, Jr. 1994a. Viable tetraploids in the Pacific oyster (*Crassostrea gigas* Thunberg) produced by inhibiting polar body 1 in eggs from triploids. *Mol. Mar. Biol. Biotechnol.* **3**(1): 42–50.

Guo, X., and S. K. Allen, Jr. 1994b. Sex determination and polyploid gigantism in the dwarf surf-clam (*Mulinia lateralis* Say). *Genetics* 138:1–8.

Guo, X., W. K. Hershberger, K. Cooper, and K. K. Chew. 1992. Genetic consequences of blocking polar body I with cytochalasin B in fertilized eggs of the Pacific oyster, *Crassostrea gigas.* II. Segregation of chromosomes. *Biol Bull* **183:** 387–393.

Guo, X., W. K. Hershberger, K. Cooper, and K. K. Chew. 1993. Artificial gynogenesis with ultraviolet light-irradiated sperm in the Pacific oyster, *Crassostrea gigas.* I. Induction and survival. *Aquaculture* **113:** 201–214.

Hebert, P. D. N., and M. J. Beaton. 1989. *Methodologies for Allozyme Analysis Using Cellulose Acetate Electrophoresis.* Helena Lab, Beaumont, Texas. 32 pp.

Hecht, F., and B. K. Hecht. 1987. Aneuploidy in human: dimensions, demography, and dangers of abnormal numbers of chromosomes. Pp. 9–49 in *Aneuploidy. Part A Incidence and Etiology,* B. K. Vig and A. A. Sandberg, eds. Alan R. Liss, Inc., New York.

Jones, R. E., and R. Bamford. 1942. Chromosome number in the progeny of triploid Gladiolus with special reference to the contribution of the triploid. *Am J. Bot* **29:** 807–813.

Kloss, R. J., and R.,M. Nesse. 1992. Trisomy: chromosome competition or maternal stragegy *Ethol. Sociobiol.* **13:** 283–287.

Kratzer, P. G., M. S. Golbus, S. A. Schonberg, D. C. Heilbron, and R. N. Taylor. 1992. Cytogenetic evidence for enhanced selective miscarriage of trisomy 21 pregnancies with advancing maternal age. *Am. J. Med. Genet* **44:** 657–663.

Lincoln, R. F. 1981a. Sexual maturation in triploid male plaice (*Pleuronectes platessa*) and plaice × flounder (*Platichthys flesus*) hybrids. *J. Fish Biol.* **19:** 415–426.

Lincoln, R. F. 1981b. Sexual maturation in female triploid plaice, *Pleuronectes platessa,* and plaice × flounder, *Platichthys flesus,* hybrids. *J. Fish Biol.* **19:** 499–507.

Lincoln, R. F., and A. P. Scott. 1984. Sexual maturation in triploid rainbow trout, *Salmo gairdneri* Richardson. *J. Fish Biol.* **25:** 385–392.

Lu, J.-K. 1986. *The Combined Effects of Salinity and Temperature on Meiosis and Early Mitosis of the Pacific Oyster* (Crassostrea gigas) *Oocytes. M.S Thesis, University of Washington, Seattle.*

Mailhes, J. B. 1987. Incidence of aneuploidy in rodents. Pp. 67–101 in *Aneuploidy. Part A Incidence and Etiology,* B. K. Vig and A. A. Sandberg, eds. Alan R. Liss, Inc., New York.

Morgan, L. V. 1925. Polyploidy in *Drosophila melanogaster* with two attached X chromosomes. *Genetics* **10:** 148–178.

Myers, W. M. 1944. Cytological studies of a triploid perennial rye grass and its progeny. *J Hered* **35:** 17–23.

Parsons, J. E., R. A. Busch, G. H. Thorgaard, and P. Scheerer. 1986. Increased resistance of triploid rainbow trout × coho salmon hybrids to infectious hematopoeitic necrosis virus. *Aquaculture* **57:** 337–343.

Pellestor, F. 1991. Differential distribution of aneuploidy in human gametes according to their sex. *Human Reprod* **6**(9): 1252–1258.

Punyasingh, K. 1947. Chromosome number in crosses of diploid, triploid and tetraploid maize. *Genetics* **32:** 541–554.

Quayle, D. B. 1988. Pacific oyster culture in British Columbia. *Can. Bull. Fish Aquat. Sci.* **218:** 1–241.

Scheerer, P. D., and G. H. Thorgaard. 1983. Increased survival in salmonid hybrids by induced triploidy. *Can. J. Fish. Aquatic Sci.* **40:** 2040–2044.

Schultz, R. J. 1980. Role of polyploidy in the evolution of fishes. Pp. 313–340 in *Polyploidy, Biological Relevance,* W. H. Lewis, ed. Plenum Press, New York.

Takaesu, N., P. A. Jacobs, A. Cockwell, and R. D. Blackston. 1990. Nondisjunction of chromosome 21. *Am. J Med Genet* Suppl. 7: 175–181.

Thorgaard, G. H. 1983. Chromosome set manipulation and sex control in fish. Pp. 405–434 in *Fish Physiology,* vol. 9(B), W. S. Hoar, D. J. Randall, and E. M. Donaldson, eds. Academic Press, London.

Thorgaard, G. H. 1986. Ploidy manipulation and performance. *Aquaculture* **57:** 57–64.

Thorgaard, G. H., and G. A. E. Gall. 1979. Adult triploids in a rainbow trout family. *Genetics* **93:** 961–973.

Warburton, D. 1989. The effect of maternal age on the frequency of trisomy: change in meiosis or in utero selection? Pp. 165–181 in *Molecular and Cytogenetic Studies of Nondisjunction,* T. J. Hassold and C. J. Epstein, eds. Liss, New York.

White, M. J. D. 1978. *Modes of Speciation.* W. H. Freeman and Company, San Francisco. Pp. 261–285.

Wilson, G. B. 1946. Cytological studies in Musae. I. Meiosis in some triploid clones. *Genetics* **31:** 241–258.

Yamano, K., E. Yamaha, and F. Yamazaki. 1988. Increased viability of allotriploid pink salmon × Japanese char hybrids. *Nippon Suisan Gakkaishi* **54**(9): 1477–1481.

Zenzes, M. T., and R. F. Casper. 1992. Cytogenetics of human oocytes, zygotes, and embryos after in vitro fertilization. *Human Genet.* **88:** 367–375.

Zheng, C. J., and B. Byers. 1992. Oocyte selection: a new model for the maternal-age dependence of Down syndrome. *Human Genet.* **90:** 1–6.

Reference: *Biol. Bull.* **187**: 319–335. (December, 1994)

Effects of Flow and Seston Availability on Scope for Growth of Benthic Suspension-Feeding Invertebrates from the Gulf of Maine

MICHAEL P. LESSER[1,*], JON D. WITMAN[2,†], AND KENNETH P. SEBENS[2,‡]

[1]*Bigelow Laboratory for Ocean Sciences, McKown Point, West Boothbay Harbor, Maine 04575, and*
[2]*Marine Science Center, Northeastern University, East Point, Nahant, Massachusetts 01908*

Abstract. *Metridium senile*, the frilled sea anemone, and *Modiolus modiolus*, the northern horse mussel, are important members of benthic suspension-feeding assemblages at several rocky hard-bottom subtidal (30–35 m) sites in the Gulf of Maine. Measurements of food availability, rates of food capture, absorption efficiencies, and standard metabolic costs show that inshore populations of *Metridium senile* have a significantly lower scope for growth than offshore populations, despite higher mean concentrations of particulate organic matter inshore. Similar measurements and calculations for *Modiolus modiolus* reveal the opposite pattern. These differences persisted at both of these sites during two summers, 1989 and 1990, when differences in mean temperature were not physiologically significant. Thus temperature is precluded as the primary effect on metabolism and growth. We suggest that these physiological differences reflect a response to flow regime and food availability that appears to be manifested differently for *Metridium senile* and for *Modiolus modiolus*, a passive and an active suspension feeder, respectively. Results from a reciprocal transplant experiment, to measure growth rates, carried out over a one-year period support the calculated scope for growth during the season when maximum growth rates would be expected. The flux of seston appears to be an important factor affecting the organismal performance of the passive suspension feeder (*M. senile*), whereas the concentration of seston is more important for the active suspension feeder (*M. modiolus*).

Introduction

Throughout the rocky subtidal region of the Gulf of Maine (GOM), sessile suspension-feeding invertebrates are a dominant feature of benthic communities (Witman and Cooper, 1983; Sebens, 1985; Witman, 1985; Sebens, 1986; Witman, 1987; Ojeda and Dearborn, 1989). Within the GOM, the abundance of passive and active suspension-feeding invertebrates at a depth of 30–45 m coincides with the occurrence of a particulate maximum layer (PML) (Witman and Sebens, 1988; Townsend and Cammen, 1985), and includes a subsurface chlorophyll maximum (Townsend *et al.*, 1984; Morrison and Townsend, 1988).

Levels of phytoplankton biomass and productivity are higher in the coastal waters of the GOM than in the central open waters (Yentsch *et al.*, 1979; Yentsch and Garfield, 1981). Such regional differences in productivity could affect the dynamics of benthic suspension-feeding communities because of the linkage between the food resources of these communities and the hydrographic events occurring in the overlying water column. These hydrographic events do affect the production and transport of particulate food to the benthos (Graf *et al.*, 1982, 1983; Fréchette and Bourget, 1985a). Benthic-pelagic coupling has been demonstrated for intertidal (Fréchette and Bourget, 1985a) and deep-sea (Graf, 1989) secondary productivity and for successful settlement (Thresher *et al.*, 1989) or recruitment (Townsend and Cammen, 1988) of temperate marine fishes. Regional differences in the quantity of available seston occur between coastal and offshore waters of California where the scope for growth and the shell growth of mussels (*Mytilus edulis*) is food

---

Received 28 December 1992; accepted 18 July 1994.

[*] Present address: Department of Zoology, University of New Hampshire, Durham, NH 03824.

[†] Present address: Biology Department, Brown University, Providence, RI 02940.

[‡] Present address: Department of Zoology, University of Maryland, College Park, MD 20742.

limited offshore (Page and Ricard, 1990). The biomass and growth rates of suspension-feeding invertebrates depend on the quality (nitrogen content relative to carbon) as well as the quantity of seston (Stuart and Klumpp, 1984; Seiderer and Newell, 1985; Fielding and Davis, 1989; Page and Ricard, 1990; Grant and Crawford, 1991).

Food limitation in dense aggregations of suspension feeders on coral reefs (Glynn, 1973), in cryptic reef habitats (Buss and Jackson, 1981), and among intertidal and infaunal bivalves (Fréchette and Bourget, 1985b; Peterson and Black, 1987) supports the notion that particulate food resources and the distribution and abundance of benthic suspension feeders are related. Food availability is also coupled to current velocity, which ultimately determines the flux of material that can be captured and utilized (Sebens, 1984; Genin *et al.*, 1986). Variability in the near-bottom flow regime also affects the distribution and abundance of benthic suspension feeders through its influence on prey capture (Best, 1988; Patterson, 1991a, b), growth (Shick *et al.*, 1979; Sebens, 1981, 1984), metabolism (Patterson and Sebens, 1989), mode of reproduction and clonal structure of populations (Shick *et al.*, 1979), larval recruitment (Butman, 1986; Genin *et al.*, 1986), and dislodgment from the substratum (Witman, 1987).

We have examined, in two distinct sites, the effects of food availability and water flow on the physiological ecology of two members of a benthic suspension-feeding community. The two sites represent inshore and offshore oceanographic regimes in the GOM. The inshore site—Gull Rock Ledge (GRL), Monhegan Island—and the offshore site—Ammen Rock Pinnacle (ARP), Cashes Ledge—are being used to study the long-term dynamics of benthic communities at 30–35 m. Five-year records of bottom temperatures at these sites show remarkably similar seasonal temperature profiles (Witman, unpub.), which largely eliminates temperature-related effects on metabolism and secondary productivity as the primary determinants of the distribution and abundance of these communities. These two sites are, however, significantly different in annual new production (Townsend and Spinrad, 1986; Morrison and Townsend, 1988) and mean current velocities (Witman, unpub., Table 1).

Metridium senile, the frilled anemone, and *Modiolus modiolus*, the horse mussel, are important components of both the inshore and offshore rocky hard-bottom benthic communities (Witman and Sebens, 1988, 1990; Witman, unpub.). But the two species have different modes of suspension feeding and use different food resources. *Metridium senile* is a passive suspension feeder, while *M. modiolus* is an active suspension feeder; *M. senile* feeds primarily on crustacean and larval zooplankton (Sebens and Koehl, 1984), and *M. modiolus* feeds primarily on phytoplankton (Griffiths and Griffiths, 1987); yet both species can digest detritus (Seiderer and Newell, 1985; Zamer *et al.*, 1987). Although their distribution and abundance on subtidal hard bottoms is patchy, anemones and mussels have very different patterns of density at each site. *Modiolus modiolus* has higher densities at GRL than at ARP, whereas *M. senile* shows the opposite pattern, with higher mean densities at ARP than at GRL (Witman and Sebens, 1988; Witman, unpub.).

We hoped to discern the relative importance of particle flux *versus* seston concentration on scope for growth (SFG) of these two suspension feeders. Although competition for space or food has been invoked as a factor limiting the growth and survival of benthic suspension feeders (Buss and Jackson, 1981; Fréchette and Lefaivre, 1990), the plasticity in the physiological response of a species to different environments influences its growth and survival (Bayne and Widdows, 1978; MacDonald and Thompson, 1986; Zamer and Shick, 1987). Rather than measuring growth directly, the energy available for growth can be determined from an energy budget and used to infer long-term patterns of growth. SFG has provided a quantitative basis for comparing the bioenergetics of bivalve molluscs (Bayne and Widdows, 1978; Wilbur and Hilbish, 1989; Clarke and Griffiths, 1990; Grant and Cranford, 1991) and sea anemones (Zamer and Shick, 1987) exposed to different physical environments and food regimes. Such bioenergetic data should complement direct measurements of growth for benthic species occurring either onshore or offshore in the GOM. Here we report both long-term growth and physiological measurements for *Metridium senile* and *Modiolus modiolus*. These data reflect a response to flow regime and food availability that appears to be manifested differently in the two species.

Materials and Methods

Collection sites and experimental animals

Metridium senile and *Modiolus modiolus* were collected from 30–35 m depth at a coastal site, Gull Rock Ledge, Monhegan Island (43° 45.0′ N, 69° 17.5′ W), and an offshore site, Ammen Rock Pinnacle, Cashes Ledge (42° 51.25′ N, 68° 57.11′ W) in the GOM (Fig. 1). Mixed-gas scuba (NOAA Nitrox I and II) was used in June 1989 for work on *Metridium senile* and in August 1990 for work on *Modiolus modiolus*. Additional information was collected during these periods as described below, and in both years data collection from both sites was completed within one week of each other.

Seston flux and quality

The fluxes of total particulate matter (PM) and particulate organic matter (POM) at the level of the suspension-feeding community (10–20 cm off the bottom) were measured as follows. Scuba divers collected samples of sea-

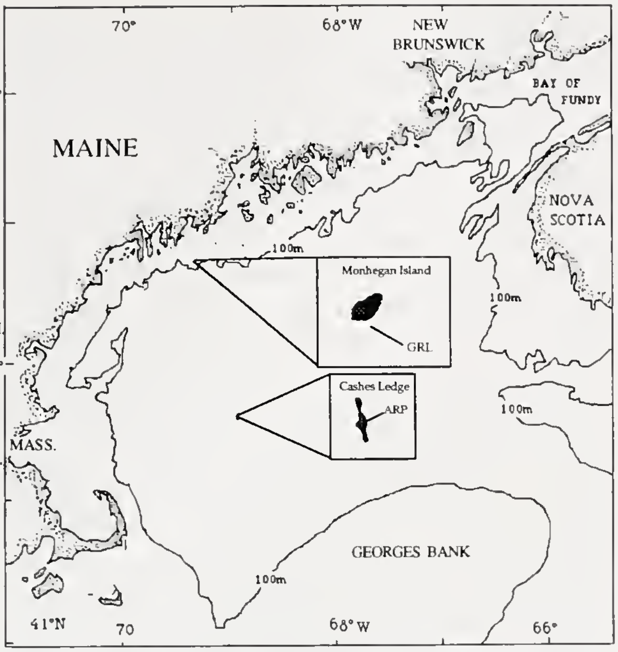

Figure 1. Map of the Gulf of Maine showing the location of the two sites—Gull Rock Ledge just off Monhegan Island and Ammen Rock Pinnacle on Cashes Ledge—where *Metridium senile* and *Modiolus modiolus* were collected. Dotted line represents 100-m depth contour.

water in 5-liter horizontal Niskin bottles. The divers held the bottles with one opening facing upstream into the ambient current. While remaining neutrally buoyant to avoid any resuspension of particulate matter from the benthos, they then triggered the bottles from the downstream side. Horizontal current velocity (cm s^{-1}) was measured simultaneously with electromagnetic current meters (InterOcean model S4) at the same location and time that the samples were collected. The recorded flow speeds were the averages of measurements of 1- to 5-min duration at 2 Hz (120 data points min^{-1}). The horizontal flux of particulate food moving past the suspension-feeding community was calculated as flux = velocity × POM (μg POM cm^{-2} s^{-1}). Replicate 0.5-l samples ($N = 10$) of benthic water from each site were filtered onto preweighed and baked (450°C) GF/F filters, frozen (−20°C), and returned to Bigelow Laboratory for Ocean Sciences for a determination of ash-free dry weight (AFDW = organic content) and carbon, hydrogen, and nitrogen (CHN) content. Filters for the calculation of PM and POM were washed with isotonic ammonium formate to remove salts. PM filters were then dried at 60°C for 24 h and weighed. Filters used for measuring POM were weighed and then combusted at 450°C for 6 h, and AFDW was calculated by difference. Filters for CHN analysis were kept under desiccation until just before analysis, and then freeze-dried again. Samples were combusted in a Control Equipment Corporation (Perkin Elmer) 240 XA elemental analyzer with an automatic sampler in an air-tight box to keep the samples dry, and acetanilide was used as a standard. No desiccation was provided while the samples were being processed. The values for particulate food fluxes, concentration of seston, and seston C:N ratios obtained at the two sites, GRL and ARP, were statistically compared with a Student's t test on arcsine or log-transformed data.

Biochemical composition of benthic invertebrates

Whole freeze-dried anemones and mussels ($N = 5$–7) were pulverized, and the powder from each individual anemone or mussel was subsequently subsampled in triplicate. The subsamples were each processed as described above to minimize the rehydration of the tissues. Still another set of samples of freeze-dried anemone and mussel tissues was combusted at 450°C as described above, and a CHN analysis was run on the remaining ash (= inorganic content). The CHN analyses of tissues and ash were used together to determine the proximate biochemical composition of tissues; the stoichiometric equations of Gnaiger and Bitterlich (1984) were applied as described by Zamer and Shick (1989). The tissue C:N ratios and proximate biochemical composition of tissues from animals collected at GRL and ARP were statistically compared with a Student's t test on arcsine or log-transformed data.

Scope for growth

The calculation of scope for growth (SFG) entailed the measurement of several parameters, specific for either mussels or anemones. Some of these measurements could not be made in the field. In particular, live anemones from GRL and ARP were returned to Bigelow Laboratory so that the maximum size of the tentacular crown in still water could be determined. This, in turn, allowed us to calculate the tentacular crown areas of individuals used in the measurement of respiration and ammonia flux. The regression of freeze-dried weight (X) on the maximum width of the tentacular crown (Y) (GRL: $Y = 2.44X^{0.332}$, $r^2 = 0.981$, $N = 7$, $P = 0.0001$; ARP: $Y = 2.38X^{0.289}$, $r^2 = 0.969$, $N = 6$, $P = 0.006$) was established for both populations as described for west coast populations of *M. senile* by Sebens (1981), and was used to calculate the maximum area of the tentacular crown.

These same anemones were also used to assess the effect of flow on the deformation and subsequent decrease in the size of the tentacular crown. This assessment was made in a recirculating flow tank (Vogel and LaBarbera, 1978) with the aid of close-up photographs, taken from above, of the anemone tentacular crown as it changed morphology under flow speeds up to 20 cm s^{-1}. The percent deformation under a specific flow regime was then applied to values for anemone tentacular crowns at GRL and ARP, allowing us to determine the maximum surface area available for prey capture. Filtering efficiency of the tentacular crown at different flow speeds was estimated from the model described for the soft-coral *Alcyonium siderium* by Patterson (1991a [Fig. 10], b [Fig. 3]). This model is also applicable to *M. senile* (Patterson, pers. comm.), and describes an inverse relationship between flow speed or Reynolds number and filtering efficiency by comparing the number of particles captured to the total number of particles that passed by the filtering element.

Anemones returned to the laboratory were fed a specific ration of food (*Artemia* sp. nauplii; <5% of anemone wet biomass) known to be in the size range of food captured by these anemones (Sebens and Koehl, 1984) and representative of the zooplankton that are known to make up a major portion of the diets of many carnivorous sea anemones (Shick, 1991), and of *M. senile* in particular (Sebens and Koehl, 1984). The absorption efficiency was determined at the measured temperature of the site, and only on animals that completely ingested the ration. All ejecta were collected with a syringe 24 h after feeding. Extraneous mucus was avoided, but collections of ejecta undoubtedly included mucus within the digested food bolus. The absorption efficiency of material ingested by anemones was determined by the ratio method of Conover (1966). This method assumes that only the organic component is significantly affected by the digestive process and compares changes in the proportion of organic matter in the food and feces. The organic content of food and feces was determined by vacuum filtering samples onto preweighed and combusted GF/F filters, and rinsing with isotonic ammonium formate to remove salts. The filters were then dried at 60°C for 24 h, weighed, and combusted at 450°C for 6 h. The AFDW of the food and feces was then calculated by difference, and the absorption efficiency of organic matter was calculated as described by Conover (1966).

The maximum amount of seston that could be caught by individual anemones at a specific flow speed was calculated as described by Best (1988), where the amount of seston caught is proportional to the volume of water processed (surface area of filter [= tentacular crown] × speed of flow) multiplied by the seston concentration and filtering efficiency. This value is equivalent to total energy consumption (C) in the balanced energy equation (see below), and is multiplied by the absorption efficiency in the calculation of total energy assimilated (A).

Logistic constraints in the field and in the laboratory precluded the measurement of clearance rate and absorption efficiency for *Modiolus modiolus*. But the literature on this mussel contains laboratory (algal monocultures, Winter, 1969, 1978) and field (natural seston, Navarro, 1990; Navarro and Thompson, 1994) measurements of the required values. Navarro (1990) studied *M. modiolus* from Newfoundland, and the mussels from this study had a smaller range of dry tissue weights (1.5–6.68 g). He observed only a slight, and insignificant, seasonal pattern for changes in clearance rate: those in the spring and summer remained consistently high and were not correlated with changes in temperature. Furthermore, the clearance rates Navarro (1990) calculated for August are not significantly different from our estimates calculated with the allometric equations of Winter (1969, 1978). Because the POM concentrations (0.38 to 1.36 mg l^{-1}; Navarro, 1990) and temperatures experienced by Newfoundland and GOM mussels are very similar, we used the August 1987 allometric equation from Navarro (1990, $Y = 0.91W^{0.53}$) on mussels employed in respiration and ammonia excretion experiments to calculate weight-specific clearance rates for GOM mussels feeding on natural seston. We then used these calculated clearance rates and covariance procedures (described below) to obtain a weighted clearance rate.

During their two-year study, Navarro (1990) and Navarro and Thompson (1994) used four different techniques (ash ratio, silicate ratio, organic carbon, and chloropigments) to measure absorption efficiency. Despite small, but significant, differences between methods (Navarro and Thompson, 1994), none of the four techniques showed significant seasonal variability or any effect of body size on the efficiencies of absorption for natural seston by *M. modiolus*. Both Winter (1978) and Navarro (1990) found that absorption efficiency was independent of body size. We applied the mean value of the pooled absorption efficiencies ($N = 188$, 76.2%) for natural seston for all seasons from Navarro (1990) to our samples at both sites.

The seston samples from GRL and ARP were analyzed for ash-free CHN content, and the percent organic carbon values of the seston were used, with the relationship described by Salonen *et al.* (1976) uncorrected for nitrogen, to calculate the energy content of the POM. The energetic value of the natural seston at the time of the experiments was used to determine the total energy ingested by the anemones and mussels at each site.

Respiration measurements

The respiration rates of anemones and mussels collected from onshore and offshore sites were measured after at least 24 h, and as long as 36 h, without food. Due to equipment shortages, respiration on all anemones could not be measured simultaneously after 24 h without food. A period of starvation was required to avoid, as much as possible, the costs associated with digestion or biosynthesis of macromolecules (*i.e.*, specific dynamic action). Specific dynamic action is very likely a consistent feature of both these suspension feeders in nature but, without any knowledge of their prior feeding history or the degree of specific dynamic action expressed, we chose to measure respiration and calculate SFG on post-absorptive animals. Data about the return of anemones to pre-prandial rates of respiration are scarce; however, in the case of *Anemonia viridis*, post-prandial rates of respiration were at, or below, pre-prandial rates from 24–36 h after a meal at 10°C (Shick, 1991, Fig. 3.9), while similar changes in *Aiptasia diaphana* were observed 12–24 h after a meal at 24°C (Shick, 1991, Fig. 3.9). Assuming that these symbiotic anemones are exhibiting typical times of returning to pre-prandial respiration rates, the times used here are consistent with those results. Indirect calorimetry was accomplished with oxygen electrodes (Nester Inc., non-oxygen-consuming) in fixed-volume, closed, Plexiglas respirometers at the ambient temperature (6–9°C) and salinity of collection; filtered (1.0 μm) seawater was used.

When *Modiolus modiolus* were collected in 1990, ambient temperatures at the two sites differed by less than 1°C (GRL, 9.2°C; ARP 8.6°C); but in 1989, when *M. senile* were collected, the differences were larger (GRL, 6.2°C; ARP 4.6°C). Therefore, to correct for these temperature effects, calculations of Q_{10} were made and applied to acute measurements, made on site, of respiration ($Q_{10} = 1.93$), and ammonium excretion ($Q_{10} = 2.12$) in freshly collected ARP anemones. The same set of anemones was used for measurements of respiration and ammonium excretion at about 4.6°C and 6.2°C. The values obtained were used in the formula $Q_{10} = (R_2/R_1)^{10/T_2-T_1}$; and the resulting Q_{10} value was used to correct for temperature effects according to the formula: $R_2 = R_1 \cdot Q_{10}^{(T_2-T_1/10)}$, where R = rate of process and T = temperature.

The unidirectional flows of the seawater within the chambers were relatively similar to *in situ* flows at each site (qualitatively determined by measuring particle speed visually), using a rheostat-controlled motor and a stirring wheel within the Plexiglas chamber. The different flow regimes within these chambers were sufficient to maintain maximum diffusion between the seawater and electrode and, therefore, sensitivity of the electrode to changes in oxygen concentration. The decline in oxygen concentration was begun 15 to 30 min after the animals were placed in the chambers under reduced lighting. Visual observations showed that *Metridium senile* was fully expanded during all respirometry runs, and *Modiolus modiolus* was actively pumping. Oxygen consumption was not measured below 70% of ambient; at this level the rate of uptake in oxyconforming species becomes dependent on external concentrations. Measurements of respiration were made over 1–4 h, depending on individual anemone or mussel biomass.

The oxygen consumption was either monitored continuously with a data logger equipped with an analog-to-digital converter, or manually recorded every 5 min and converted to rates of oxygen consumption (Table II) per individual. Rates were calculated from the slopes of oxygen consumption plotted against time. Blank controls with no animal, run before and after each experiment, were averaged and subtracted from the experimental rates. Rates of oxygen consumption for each animal were compared against its freeze-dried weight of tissue.

Ammonia excretion

Rates of ammonia excretion and respiration were determined at the same time and on the same animals. Seawater samples were taken from the respiration chamber before and after each respiration measurement. These samples were filtered (0.2 μm), frozen, and analyzed according to the phenol-hypochlorite method of Solorzano (1969). Rates of excretion were used with respiration measurements to calculate O:N (oxygen:nitrogen) ratios; that is, the atomic ratio of oxygen consumed and ammonia-nitrogen excreted. The O:N ratio can then be used to estimate the amount of protein catabolized relative to total carbohydrate and lipid, with low O:N ratios indicative of high protein catabolism. O:N ratios have been used as metabolic indicators and can provide information about the physiological state (*i.e.*, respiratory substrate being utilized) of the organism (Mayzaud and Conover, 1988; Szmant *et al.*, 1990).

The energy conversion factors for oxygen (0.45 J per μmol O_2) and ammonia (0.34 J per μmol NH^{4+}) were from Gnaiger (1983) and Elliot and Davison (1975) respectively. The respiration and excretion costs were directly measured on all anemones and mussels used in this study.

In analyzing the physiological measurements reported here, weight-specific rates were not compared. This is because physiological processes, especially respiration, scale allometrically; that is, they generally do not increase isometrically with volume or biomass (Patterson, 1992). Such data therefore violate the assumption of isometry required when measures of biomass are used to normalize the data. We have therefore used an analysis of covariance (ANCOVA) with dry weight as the covariate, and the individual slopes from each site used to weight all measurements within a site to an animal of standard size and tissue dry weight, whether anemone (grand mean = 2.53 g, range of 0.55 to 4.99 g [ARP], 0.58 to 6.22 g [GRL]) or mussel (grand mean = 7.61 g, range of 4.59 to 11.12 g [ARP], 1.67 to 15.24 g [GRL]) (Packard and Boardman, 1988). Regressions of dry weight upon the process of interest, from which the slopes were obtained for weighting purposes, are listed in Table II.

Calculating scope for growth

These weighted physiological responses of anemones and mussels were then converted to energy equivalents and used in the balanced energy equation to calculate

SFG, the energy available for growth and reproduction after maintenance costs are satisfied (Widdows and Johnson, 1988). Scope-for-growth calculations provide a rapid and quantitative method of assessing the physiological, and therefore energetic, status of an animal under different environmental conditions. The balanced energy equation is expressed as

$$C = P + R + U + F$$

where C = total consumption of food energy; P = somatic and gamete production; R = respiratory energy expenses; U = energy lost as waste or excreta; F = fecal energy loss. The absorbed ration, A, is the product of consumption, C, and the efficiency of absorption of energy from the food. Production can then be expressed as

$$P = A - (R + U)$$

and is estimated from the difference between the energy absorbed from food and the energy expenses of respiration and excretion, which is termed the SFG (Widdows and Johnson, 1988). Scope for growth and the individual measurements used to calculate SFG on GRL and ARP populations of *M. senile* and *M. modiolus* were tested statistically with a Student's *t* test at the 0.05 level of probability. SFG was calculated only for individual mussels and anemones for which respiration and ammonia excretion had been directly measured.

A condition index was also calculated for *Modiolus modiolus;* freeze-dried soft-tissue weight and dry shell weight were used to compare metabolism directed at shell with somatic growth, as described by Crosby and Gale [1990; CI = dry soft tissue wt. (g) × 1000/dry shell wt. (g)]. The condition index chosen is essentially a body component index, with higher values indicating energy directed towards tissue growth, and lower values indicating energy directed towards shell growth.

Reciprocal transplants and growth measurements

Metridium senile and *Modiolus modiolus* were transplanted from GRL at 30 m depth to the same depth offshore (ARP), and *vice versa,* in July 1989. The initial collection protocol consisted of removing mussels and anemones from their original habitat, avoiding the collection of anemone clonemates based on color, and measuring their size. For mussels, size was recorded as shell length in centimeters (range of 4.33 to 13.33 cm [ARP], 4.84 to 12.98 cm [GRL]) measured with Vernier calipers. For anemones, size was recorded as displacement volume (range of 3.0 to 55.0 ml [ARP], 2.0 to 50.0 ml [GRL]). For *M. senile,* regressions of volume displacement onto tissue dry weight were established for both sites by collecting anemones, forcing them to fully contract, blotting them dry, and measuring their displaced volume in a 1-l graduated cylinder filled with seawater. These animals were returned to the laboratory and dried to a constant weight at 60°C.

The transplantation proceeded as follows: Mussels and anemones were placed into one of three numbered compartments of a Vexar cage on a 80-kg base; the base measured 150 × 70 cm. Five replicate compartments were randomly assigned to each treatment and control, with treatments consisting of transplants from coastal to offshore habitats, and transplants from offshore to coastal habitats. Control groups of mussels and anemones were removed and returned to their original habitats in cage compartments. The complete experimental design at one site consisted of 50 replicate mussels and 40 replicate anemones for each treatment and control. Experimental and control animals were collected by scuba in August of 1990, and remeasured as described above. The growth data were analyzed with Ford-Walford plots and ANCOVA techniques. We also measured the total tissue dry weight of all individual *M. modiolus* so we could compare shell growth with somatic tissue growth.

Results

Current velocities, seston concentration, and seston quality

Mean current velocities were almost ninefold higher at ARP than at GRL in 1990 (Table 1) and are typical of those from other years (Witman and Sebens, 1988, unpub.). Both PM and POM concentrations were significantly greater (*t* test, $P < 0.05$) at GRL than at ARP in 1989 and 1990 (Table 1). When the flow and POM values are used to calculate mean flux of POM at both sites in 1990, we can see that ARP does exhibit higher fluxes of particulate food despite having lower concentrations of POM (Table 1). We used current velocities from 1990 to calculate the POM flux at GRL in 1989, assuming that the data for the two years would be similar. This assumption is supported by the consistently lower current velocities observed at GRL and other inshore sites in 1991, 1992, and 1993 (Witman, unpub., Table 1). Additionally, using the flow data from subsequent years or the mean of those years does not significantly change the differences in SFG or assimilated energy described below. Seston quality, as determined by the C:N ratio, was not significantly different within each year between sites (Table 1). The difference in seston quality between years may reflect the seasonal difference in C:N ratios due to an increase in the detrital component of the seston as nitrogen is removed by zooplankton and bacteria. All C:N ratios suggest that the POM consisted primarily of phytoplankton and bacteria rather than refractory organic material. Although no effort was made to fractionate the seston into its different components, zooplankton will also contribute to

Table I

Average flow speeds and seston quantity and quality for Gull Rock Ledge Island (GRL) and Ammen Rock Pinnacle (ARP) in 1989 and 1990

	1989			1990		
	GRL		ARP	GRL		ARP
Flow[1]	ND		18.3 ± 10.9 (N = 420)	2.9 ± 1.7 (N = 1847)		24.8 ± 12.5 (N = 798)
PM[2]	2.54 ± 1.41 (N = 10)	$P = 0.036$	1.49 ± 0.69 (N = 10)	5.54 ± 1.43 (N = 10)	$P = 0.001$	2.87 ± 1.86 (N = 10)
POM[3]	0.92 ± 0.51 (N = 10)	$P = 0.034$	0.54 ± 0.25 (N = 8)	2.0 ± 0.51 (N = 10)	$P = 0.001$	1.03 ± 0.67 (N = 10)
Flux[4]	2.67		9.88	5.80		25.54
C:N[5]	3.61 ± 1.09		4.16 ± 1.65	8.39 ± 3.26		6.76 ± 2.11

Flow speeds are 1–5 min averages of measurements of 1–5 min duration at 2 Hz, 120 data points min^{-1}. N = the total number of readings for the specific measurement. Mean flow speeds in 1991 for GRL (3.3 cm s^{-1}), 1992 (5.28 cm s^{-1}), and 1993 (2.64 cm s^{-1}) (Witman, unpub. data). ND = not determined.

[1] cm s^{-1} (mean ± SD).

[2] Total particulate matter, one-tailed t test (mg l^{-1} [mean ± SD]).

[3] Particulate organic matter, one-tailed t test (mg AFDW l^{-1} [mean ± SD]).

[4] μg POM cm^{-2} s^{-1}; 1989 GRL value determined using 1990 flow.

[5] μg/μg (mean ± SD, N = 5).

the total carbon and nitrogen pools in the seston. Calculated according to the equations of Salonen *et al.* (1976) the energy content (J mg^{-1}) of POM in 1989 was 8.8 for ARP and 7.3 for GRL, while in 1990 the POM values were 13.8 J mg^{-1} for ARP and 15.8 J mg^{-1} for GRL.

Scope for growth

The energetic conversions for the physiological responses and SFG of *Metridium senile* and *Modiolus modiolus* are presented in Figure 2. For most measured or calculated responses, except respiration (R) and energy assimilated (A), anemones from ARP had significantly higher rates when analyzed by ANCOVA (Table II) and weighted to an anemone of standard size (Table II, Fig. 2a). Scope for growth of ARP anemones was also significantly higher than for GRL anemones in June 1989 (Fig. 2a). Measured rates of respiration, and therefore maintenance costs, at ARP were consistently and significantly lower. Assessment of food, and therefore energy, consumption by anemones is complicated by the effects of flow on the flux of food, prey capture area, and capture or filter efficiency. Photographs of the tentacular crown show that for ARP anemones the surface area for prey capture decreased significantly ($P < 0.05$, $N = 5$ for each site on arcsine-transformed data)—to 50% of maximum on average—at the mean current velocity (18.29 cm s^{-1}), but for GRL anemones the prey capture area decreased by only 30% at ambient flows of 3.44 cm s^{-1}. According to the model of Patterson (1991a, b), the filtering efficiency is 40% for ARP anemones and 52% for GRL anemones. The calculated consumption (C) of total particulate matter (ARP, 13.91 ± 1.85 mg h^{-1}; GRL, 12.87 ± 2.81 mg h^{-1}), and POM (ARP, 5.04 ± 0.67 mg h^{-1}, GRL, 4.66 ± 1.02 mg h^{-1}), when converted to energy equivalents, was significantly different between sites (Fig. 2a, P = 0.019), but the total amount of assimilated energy (consumption times absorption efficiency = A) was not significantly different (P = 0.069, Fig. 2a), although the mean assimilated energy was higher in ARP anemones. The total particulate or POM rations available to ARP and GRL anemones averaged from 0.3 to 1.1% of the total body weight of anemones from either site. Our weighted estimates of absorption efficiency for ARP and GRL anemones were not significantly different from each other, although the mean absorption efficiency was higher in ARP anemones (Table II). An inverse relationship between the size of daily ration and absorption efficiency has been described for sea anemones (Shick, 1991, see Fig. 2.12 in this ref.). This relationship suggests that by providing *Artemia* sp. in amounts up to 5% of body weight as rations for determining absorption efficiency, we probably underestimated this factor.

Measurements on *Modiolus modiolus* reveal a pattern distinctly different from that exhibited by *Metridium senile*. Mussels from GRL consistently had a higher SFG than mussels from ARP in August 1990, and all components, except for costs associated with waste production (U), of the SFG calculation were significantly higher in GRL anemones (Fig. 2b). There were no significant differences in the weighted clearance rates (Table II) between ARP and GRL. Absorption efficiencies and clearance rates reported for *M. modiolus* in laboratory

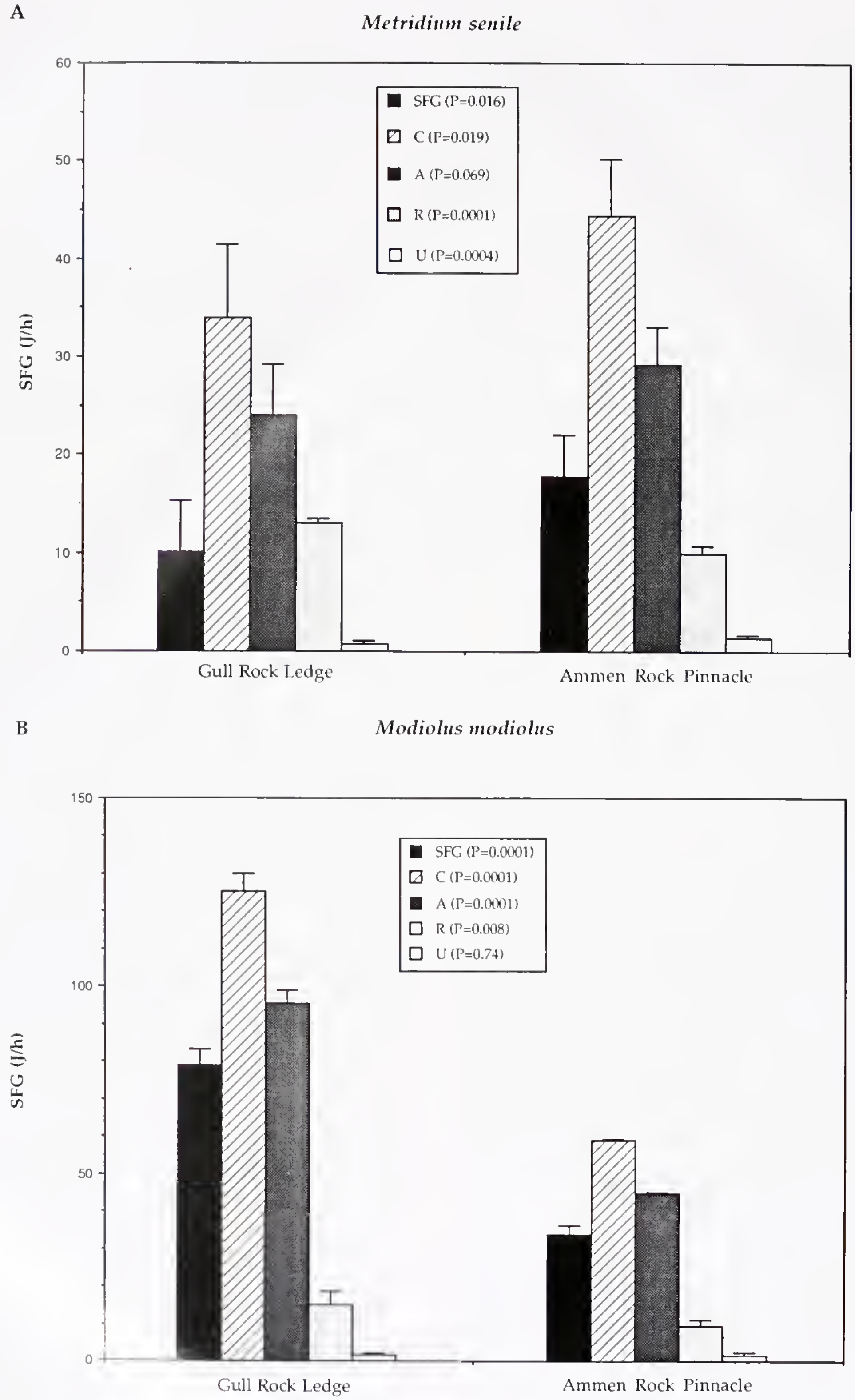

Figure 2. Calculated scope for growth (J h^{-1}) and measured or calculated components used in calculation (mean ± SD). C = total consumption of food energy; A = assimilated energy is the product of total consumption and absorption efficiency; R = respiratory energy costs; U = energy lost as excreta; P = production (or scope for growth). P = A − (R + U). (A) *Metridium senile*, (B) *Modiolus modiolus*. *P* values are the result of an unpaired, one-tailed *t* test comparing sites.

Table II

Measured and calculated physiological responses for Metridium senile *and* Modiolus modiolus

Function	Location	N	Rate	P value
Metridium senile				
Absorption efficiency (percentage ± SD)	ARP	6	68 ± 18	$P > 0.05$
		($Y = -0.184X - 0.176$, $N = 6$, $r^2 = 0.942$, $P < 0.001$)		
	GRL	7	58 ± 23	
		($Y = -0.139X - 0.392$, $N = 6$, $r^2 = 0.799$, $P < 0.025$)		
Respiration (μmol O_2 h^{-1} ± SD)	ARP	6	22.28 ± 1.51	$P = 0.0001$
		($Y = 7.202X + 3.98$, $N = 6$, $r^2 = 0.985$, $P = 0.0001$)		
	GRL	7	29.03 ± 0.86	
		($Y = 10.81X + 1.80$, $N = 7$, $r^2 = 0.999$, $P\,0.0001$)		
Ammonium excretion (μmol NH_4^+ h^{-1} ± SD)	ARP	6	7.47 ± 1.72	$P = 0.0001$
		($Y = 2.408X + 2.54$, $N = 6$, $r^2 = 0.864$, $P < 0.005$)		
	GRL	7	2.56 ± 1.05	
		($Y = 2.087X\quad 1.71$, $N = 7$, $r^2 = 0.937$, $P < 0.001$)		
Modiolus modiolus				
Clearance rate (l h^{-1})	ARP	5	4.2 ± 0.23	$P < 0.05$
		($Y = 0.408X + 1.03$, $N = 5$, $r^2 = 0.999$, $P = 0.0001$)		
	GRL	6	3.93 ± 0.5	
		($Y = 0.406X + 0.91$, $N = 6$, $r^2 = 0.996$, $P = 0.0001$)		
Absorption efficiency (percentage)	ARP	5	76.2 (Navarro, 1990)	
	GRL	6	76.2 (Navarro, 1990)	
Respiration (μmol O_2 h^{-1} ± SD)	ARP	5	21.26 ± 3.32	$P = 0.041$
		($Y = 4.063X - 9.63$, $N = 5$, $r^2 = 0.899$, $P < 0.01$)		
	GRL	6	33.48 ± 7.47	
		($Y = 3.652X + 5.71$, $N = 6$, $r^2 = 0.869$, $P < 0.005$)		
Ammonium excretion (μmol NH_4^+ h^{-1} ± SD)	ARP	5	4.72 ± 2.42	$P > 0.05$
		($Y = 1.658X - 7.90$, $N = 5$, $r^2 = 0.740$, $P < 0.05$)		
	GRL	6	5.08 ± 1.07	
		($Y = 0.571X + 0.74$, $N = 6$, $r^2 = 0.887$, $P < 0.005$)		

Regression formulas from which slopes were obtained are included. Results are weighted to a standard size anemone (2.53 g) or mussel (7.60 g) using an analysis of covariance (ANCOVA), with dry weight as the covariate, as described by Packard and Boardman (1988). Probability (P) values are from a Student's t test.

and field experiments (Winter, 1969, 1978; Navarro, 1990) suggest that these processes are largely invariant between populations. This lack of variation supports our application of literature values to ARP and GRL individuals. The higher SFG values appear to be correlated with differences in POM concentration and subsequent total energy intake for GRL mussels (Table I), rather than with flow regimes or flux of food—although flow itself may have a negative impact on active suspension feeders (see Discussion).

The tissue C:N ratios, the energetic content (*i.e.*, the specific enthalpy of combustion [kJ g^{-1} organic mass]), and the lipid, carbohydrate, or protein fractions from the biochemical composition of *M. modiolus* and *M. senile* were not significantly different ($P > 0.05$) between sites (Fig. 3; Table III). The lipid values for anemones and mussels must, however, be interpreted with caution. Although the samples remained desiccated until just before analysis, they could not be kept under continuous desiccation during the CHN analysis. This increases the likelihood of hygroscopic absorption of water and a corresponding increase in H content that would lead to higher lipid values. Higher lipid values would also contribute to the energy content of tissues, which for *M. senile* is slightly higher than values reported for other species of anemones (Shick, 1991).

Both the gross and net growth efficiencies (Table III) track with the calculated SFG; net growth efficiencies (K_2), calculated on an energetic basis, are higher in populations of anemones and mussels with higher SFG. The O:N ratio for *M. modiolus* was not significantly different between sites and indicates that protein is the primary catabolic substrate being utilized (O:N ranging from 3 to 16; Mayzaud and Conover, 1988). Although anemones are reported to rely heavily on protein as a catabolic substrate (Shick 1991), the O:N ratios for *M. senile* were significantly different between sites. The ratios indicate that metabolic requirements were fueled primarily by protein at ARP, but that lipid and car-

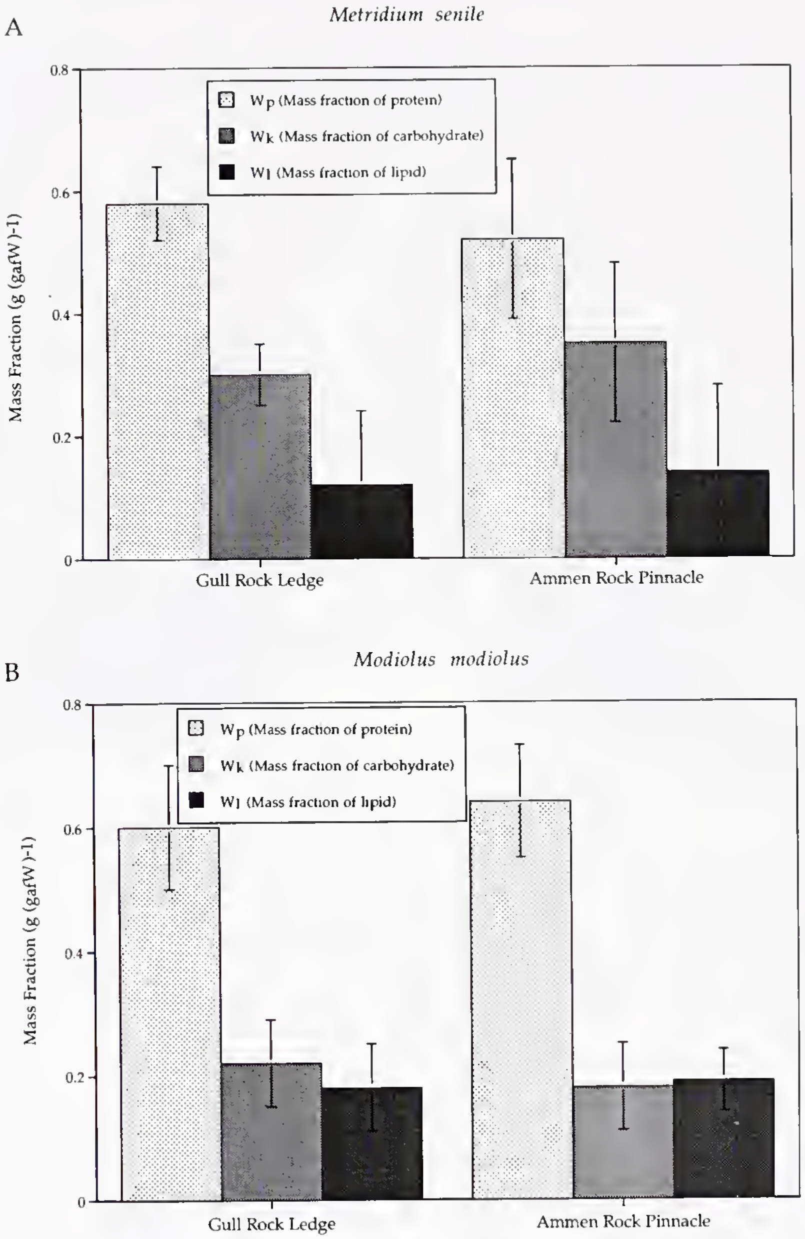

Figure 3. Proximate biochemical composition of *Metridium senile* (A), and *Modiolus modiolus* (B) for GRL and ARP sites. W_p = mass fraction of protein, W_k = mass fraction of carbohydrate, W_l = mass fraction of lipid. All results are mass fractions g $(g_{af}\ W)^{-1}$ ± SD as units.

bohydrate were the dominant respiratory substrates at GRL. If GRL anemones were feeding on resources that were enriched in lipid and carbohydrate, or were depending on stored forms of these constituents, this was not reflected in any significant differences in the biochemical composition of anemone tissues between the two sites. Lastly, the values of tissue C:N, seston C:N, and O:N that we observed for anemones and mussels suggest that the supply of nitrogen in the seston was adequate at both sites.

Reciprocal transplants and growth of anemones and mussels

All regressions for the transplant comparisons were significant (ANOVA, $P < 0.05$), with the number of samples for each comparison being the number of individuals recovered (minus losses due to storms and mortality) for which we could match numbered tags with individual identifying marks.

The relationship between volume displacement (Y) and dry tissue weight (X) was significant for samples of *Me-*

Table III

Growth efficiencies and metabolic and condition indices for Metridium senile *and* Modiolus modiolus *collected from onshore (Gull Rock Ledge [GRL]) and offshore (Ammen Rock Pinnacle [ARP]) sites in the Gulf of Maine*

	Metridium senile			*Modiolus modiolus*		
	GRL	ARP	*P* value	GRL	ARP	*P* value
K_1[1]	20 ± 10	39 ± 5	0.0009	63 ± 3	57 ± 4	0.02
K_2[2]	28 ± 15	60 ± 7	0.0004	82 ± 4	75 ± 5	0.02
O:N[3]	38 ± 22	7 ± 5	0.003	14 ± 6	15 ± 5	0.57
CI[4]	NA	NA	NA	146 ± 38	104 ± 32	0.035
C:N[5]	5.39 ± 0.63	6.22 ± 1.34	0.248	5.27 ± 0.88	5.19 ± 0.73	0.255
EC[6]	−23.91 ± 0.73	−23.78 ± 1.22	0.849	−25.26 ± 3.32	−24.38 ± 1.11	0.52

P values based on the results of a Students *t* test (unpaired, one-tailed for growth efficiencies; unpaired, two-tailed for O:N, CI, and EC; percentages, ratios, and indices are not normally distributed and were either arcsine or log transformed before analysis).

[1] Gross growth efficiency (Calculated SFG/Energy Consumed × 100%, mean ± SD; GRL, $N = 7$; ARP, $N = 6$).

[2] Net growth efficiency (Calculated SFG/Energy absorbed × 100%, mean ± SD, GRL, $N = 7$; ARP, $N = 6$).

[3] Atomic ratio of oxygen consumed and ammonia-N excreted (mean ± SD; GRL, $N = 7$; ARP, $N = 6$).

[4] Condition Index (Dry soft tissue wt (g) × 1000/dry shell wt (g), mean ± SD; GRL, $N = 6$; ARP, $N = 5$). NA = not applicable.

[5] C:N ratio (μg/μg, mean ± SD; ARP, $N = 6$; GRL, $N = 7$) of tissue samples.

[6] EC = energetic content (kJ g^{-1} organic mass; ARP, $N = 6$; GRL, $N = 7$) of tissue samples.

tridium senile from both GRL ($Y = 5.138X + 0.429$, ANOVA $P = 0.0001$, $N = 10$, $r^2 = 0.977$) and ARP ($Y = 3.75X + 5.151$, ANOVA $P = 0.0001$, $N = 13$, $r^2 = 0.804$). When the slopes were compared from the Ford-Walford plots, the results from the anemone transplant experiments showed no significant differences in growth rates of ARP and GRL controls (ANCOVA, $P > 0.05$). Because the slopes of the control anemones are statistically homogeneous, we can compare the y-intercepts, which were significantly different (ANCOVA, $P < 0.001$), indicating that the mean size of ARP control anemones was larger than that of the GRL control anemones (Fig. 4a). Anemones transplanted from GRL to ARP showed a significant increase in growth rates (ANCOVA, $P < 0.05$) compared to GRL controls (Fig. 4b), despite the low sample size ($N = 5$) for recovered transplants. Anemones transplanted from ARP to GRL showed no changes in growth rate compared to ARP controls (ANCOVA, $P > 0.05$), but a comparison of the y-intercepts again reveals a significant decrease in the mean size of ARP anemones transplanted to GRL (ANCOVA, $P < 0.001$) when compared to ARP controls (Fig. 4c).

Ford-Walford plots comparing changes in shell length for *Modiolus modiolus* for the two sites from 1989 to 1990 showed no significant differences between controls, or controls and transplanted mussels (ANCOVA, $P < 0.05$, data not shown), although the mean shell length of GRL control mussels was greater than that of ARP controls, mean shell length of mussels transplanted from ARP to GRL increased, and mussels transplanted from GRL to ARP actually decreased in shell length. The condition index for *M. modiolus* was significantly different for ARP and GRL mussels, with GRL mussels showing higher values (Table III). This indicates that a larger proportion of assimilated energy was being allocated into somatic growth consistent with the absence of any significant difference in shell length. Using the 1990 data we subsequently compared the relationships between shell length and dry tissue weight for the control and transplanted mussels. The slope of mean tissue weight as a function of shell length was significantly higher in control mussels from GRL than in control mussels from ARP (ANCOVA, $P < 0.05$, Fig. 5a); whereas this slope, in mussels transplanted from GRL to ARP, was significantly lower (ANCOVA, $P < 0.05$) than that in the GRL controls (Fig. 5b), suggesting a loss of tissue mass during the period of transplantation. Conversely, ARP mussels transplanted to GRL showed a significant increase in mean tissue weight as a function of shell length, suggesting again that more energy was directed into tissue growth in these mussels—a result consistent with the condition indices from the respective populations (ANCOVA, $P < 0.05$, Fig. 5c).

Discussion

Although these measurements of food, flow, and SFG in *Metridium senile* and *Modiolus modiolus* represent but a snapshot in time, we note that Navarro (1990), in a two-year study, found similar results for *M. modiolus* in Newfoundland; *i.e.*, he showed positive SFG in June and negative SFG in August for all size classes of mussels studied (1.0, 2.0, and 5.0 g). Our August results differ from those of Navarro (1990), reflecting, perhaps, differences in seston quality, and therefore energy content, or the quantity of seston at both of our sites, which was slightly higher than in Newfoundland. Seasonal decreases of SFG in other bivalve molluscs have been attributed to decreased seston concentrations (Griffiths and Griffiths, 1987), and intertidal bivalves usually show negative SFG as a result of the combined effects of decreased seston concentration and the tidally determined decrease in feeding time during the late summer (Griffiths and Griffiths, 1987). Our positive SFG results for August are not entirely unexpected because year-round positive SFG has been reported for blue mussels (*Mytilus edulis*) living in a subarctic environment with concentrations of particulate organic matter (Thompson, 1984) similar to the values reported in this study. Our conclusion that, for *Modiolus modiolus*, SFG is closely related to seston concentrations is also consistent with the different levels of productivity characteristically found at onshore and offshore sites. These differences in productivity are well known from successive years of oceanographic data collected in the Gulf of Maine (Townsend *et al.*, 1984; Townsend and Spinrad, 1986; Morrison and Townsend, 1988). Moreover, the more comprehensive work of Navarro (1990) is in agreement with our findings that total seston concentration is more important than seston flux in determining the SFG and biomass of horse mussels. Previous work on *Mytilus edulis* (Page and Ricard, 1990), in which secondary productivity of blue mussels was limited by offshore seston concentrations, also supports our conclusions.

The indirect measurements of growth on anemones and mussels, using an energetic approach, are corroborated by the direct measurements of growth from reciprocal transplants between the two study sites. The direct growth data show that, on average, anemones from ARP are larger than those from GRL, and that anemones transplanted from GRL to ARP grow faster. These data support the hypothesis that water flow, and thus the flux of seston, is important when considering the secondary productivity of these passive suspension feeders. Higher fluxes, however, do not always give positive results, as shown by the recent work of Eckman and Duggins (1993), in which benthic suspension feeders responded both positively and negatively as flow increased. For anemones, the flux of seston at each site appears to support different levels of secondary productivity, reflected in anemone numbers and biomass, at each site. Within each site, however, anemones maintain positive SFG into the summer, have similar biochemical compositions, and show tissue energy contents comparable to those of well-fed *Anthopleura elegantissima* (−23.4 kJ g^{-1} organic mass, Shick, 1991). It appears that, for these sites, flux of seston is an important variable regulating secondary productivity and physiological performance.

Significant differences in SFG between onshore and offshore mussels are not supported by the shell growth data, which are not significantly different between sites. The trend in mussel controls and transplants, however, suggests that shell growth may also be effected by differences in seston concentration. The mussel SFG data are supported by examining the changes in dry tissue weights in control and transplant mussels. Mussels have higher mean dry tissue weights at GRL, which has a higher concentration of seston. Moreover, mussels transplanted to GRL gain weight relative to ARP controls, and mussels transplanted to ARP lose weight. The most reasonable explanation for these changes is reflected in the SFG. The specific reasons for allocating more energy to somatic tissue growth than to shell growth are not discernible from this work; but the condition index we used provided another way of assessing the partitioning of energy in horse mussels from GRL (Table III). These growth data represent the integrated organismal response to environmental changes over a year-long period not included in this study. The use of scope for growth as an indicator of growth itself has been evaluated for the American oyster, *Crassostrea virginica* (Dame, 1972), and the blue mussel, *Mytilus edulis* (Bayne and Worrall, 1980). The two-year study by Bayne and Worrall (1980) revealed that physiological estimations of growth agreed well with direct measurements of tissue growth, as demonstrated in this study.

How are these physiological responses to differences in flow and seston availability reflected in the distribution and abundance of these benthic suspension feeders? Differences in population size distributions, due to changes in physical factors (*e.g.*, flow-induced biomechanical constraint on the size range of anemones), are probably of minor importance at these sites (Sebens, 1984, 1987; Shick *et al.*, 1979), but total numbers and biomass (= secondary production) for anemones and mussels in 1989 and 1990 are different, with anemone densities higher at ARP and mussel densities higher at GRL (Witman and Sebens, 1988; Witman, unpub.). We believe that this can be partially explained by the differential response demonstrated by anemones (passive suspension feeders) and mussels (active suspension feeders) to flow and seston concentration.

Flow regime alone, however, can influence the population structure of these animals by its effects on organismal performance. Flow-modulated rates of metabolism have been demonstrated in a number of marine organisms, including *M. senile*, that are dependent on direct gas exchange through their tissues (Patterson and Sebens, 1989; Patterson *et al.*, 1991; Lesser *et al.*, 1994), and certainly influence the rates of food capture by *Metridium senile*, a passive suspension feeder. Our results do not show any evidence of flow-modulated respiration rates in

M. senile (Fig. 2a). Higher growth efficiencies (K_2) in ARP anemones are the result, not only of higher consumption and assimilation, but also of the lower respiration rates observed in these anemones. The high flow regime at ARP would be expected to result in higher, flow-modulated metabolic rates (Patterson, 1992). Anemones reciprocally transplanted between ARP and GRL for one year exhibit an incomplete compensatory response, with respiration rates staying nearly the same as the control rates (Lesser, unpub.). This suggests either a genetic component constraining the phenotypic response of respiration rates between sites or an irreversible nongenetic adaptation (Zamer and Mangum, 1979). Anemones at ARP were found in large groups at high densities during the time of this study, and all of the field observations confirmed that anemones were fully expanded and not collapsing on the downstream side of the ambient flow. This could have been the result of the effects of neighbors on the flow regime or of the material properties of the anemones themselves. The issue of local selection of specific genotypes due to flow regime for low rates of respiration or enhanced materials properties remains to be assessed.

The effect of flow *per se,* or seston flux, on bivalve feeding and subsequent growth is poorly understood (Grizzle and Lutz, 1988). Within the range of flows measured at ARP and GRL at 30–35 m (Table 1) nonsiphonate bivalve molluscs generally show a negative effect of increasing water flow on filtration or clearance rate (Cahalan *et al.*, 1989; Wildish *et al.*, 1987; Grizzle *et al.*, 1992). Flow-induced inhibition of feeding cannot be ruled out for *M. modiolus* at ARP. In a recent study on *Mytilus edulis,* the blue mussel, a mytilid like *Modiolus modiolus,* the percent seston filtered decreased as flow increased up to 25 cm s^{-1}; flows greater than this did not further decrease feeding (Wildish and Miyares, 1990). Additionally, although the effect of food concentration on filtration rate in *M. modiolus* is not known for these particular populations, rates of filtration as a function of food concentration for this species (Winter, 1978) suggest that the concentrations of food measured at ARP and GRL are within the range in which maximum sustained rates of filtration would be expected without the production of pseudofeces.

For the sampling periods of this study, seston quality should not have been a determining factor: the POM concentration and seston C:N ratios indicate that the food source provided sufficient ingested ration with a low inorganic content for the mussels and anemones to be car-

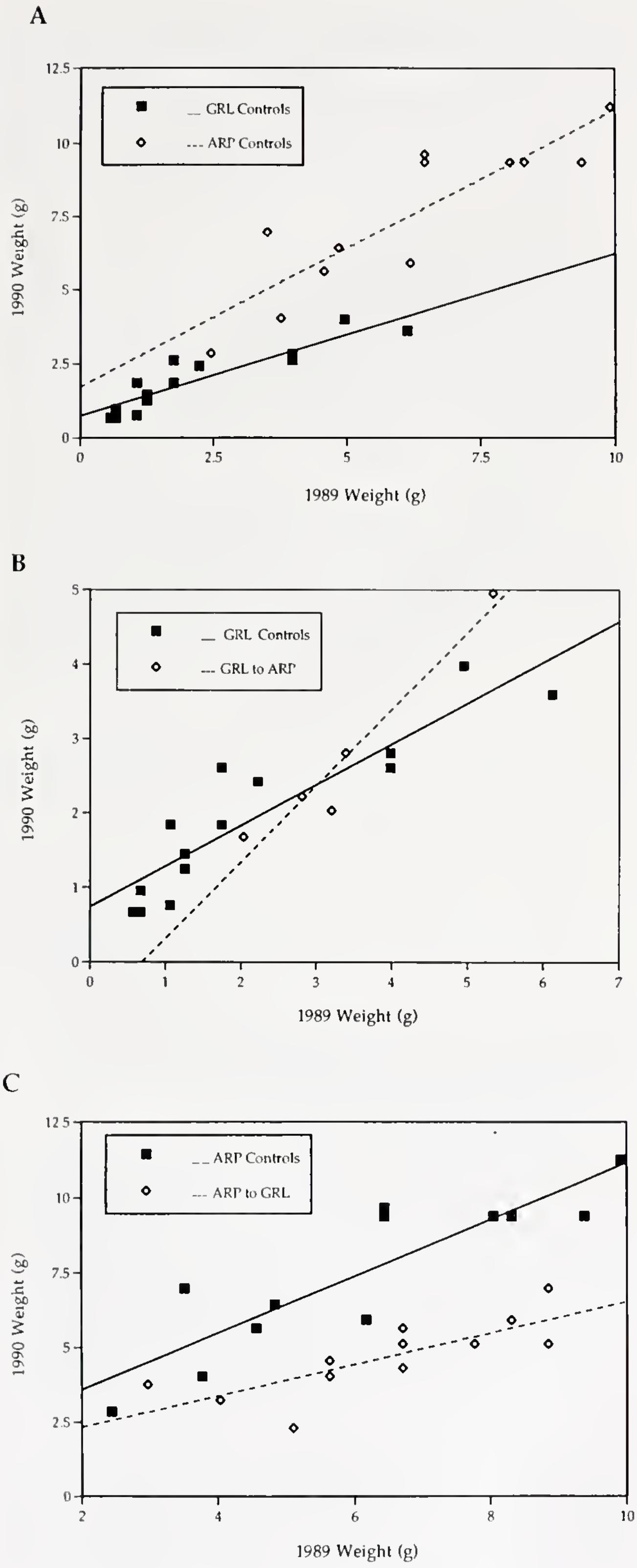

Figure 4. Results from the reciprocal transplant studies, Ford-Walford plots of 1989 and 1990 tissue dry weights. (A) *Metridium senile* caged controls; GRL = Monhegan Island, Gull Rock Ledge ($Y = 0.481X + 0.84$, $N = 15$, $r^2 = 0.797$, $P < 0.001$), ARP = Ammen Rock Pinnacle ($Y = 0.772X + 2.526$, $N = 13$, $r^2 = 0.618$, $P < 0.001$). (B) *Metridium senile* transplants; GRL controls as above, GRL to ARP caged transplants ($Y = 1.03X - 0.72$, $N = 5$, $r^2 = 0.938$, $P < 0.005$). (C) *Metridium senile* transplants; ARP controls as above, ARP to GRL caged transplants ($Y = 0.525X + 1.257$, $N = 14$, $r^2 = 0.62$, $P < 0.001$).

bon and nitrogen replete (Russell-Hunter, 1970). The protein content of horse mussel tissue is highest during the spring and summer, varies from 65–75%, and is dependent on seston food quality—specifically, the protein content of the seston (Navarro, 1990). In our study, the mass fraction of protein for both ARP and GRL mussels in the summer ranged from 60 to 65%, and the seston quality was high as in the study by Navarro (1990). For our mussel samples, the C:N ratio of tissue was low and not significantly different at the two sites, suggesting that food quality (in terms of carbon and nitrogen) was not decreasing in either population. Also, the energetic content of the mussel tissues at both sites was equivalent, and was slightly higher than that of Newfoundland mussels (Navarro, 1990); these results are consistent with high energetic values for the seston.

Differences in time-averaged seasonal levels of pelagic productivity are important features of these sites. But on shorter time scales, localized oceanographic features, such as island mixing at Gull Rock Ledge (Townsend *et al.*, 1983) or internal waves in the central Gulf of Maine (Lande and Yentsch, 1988; La Violette *et al.*, 1990), may bring the particulate maximum layer down to the depth of these suspension-feeding communities (Witman *et al.*, 1993) or resuspend particulate food and benthic phytoplankton into the water column, thus maintaining a positive SFG in both spring and summer.

Furthermore, both locations are likely to be influenced by local kelp beds. Duggins *et al.* (1989) demonstrated that kelp-derived organic carbon can further enhance the secondary productivity of sea anemones and mussels in nearshore benthic communities where phytoplankton production alone was believed to be limiting. These localized features may be important in maintaining a positive SFG over longer periods, but do not obscure the effects of regional differences in productivity.

Intertidal invertebrates exhibit compensatory responses to the decrease in food or energy arising from emersion and the resulting changes in temperature, gas exchange, metabolism, and duration of feeding (Newell, 1980; Shick *et al.*, 1988; Shick, 1991). The interspecific variation in these responses to a changing environment is correlated with the distribution and abundance of these sessile intertidal assemblages. Similar comprehensive work on the physiology of subtidal suspension-feeding invertebrates

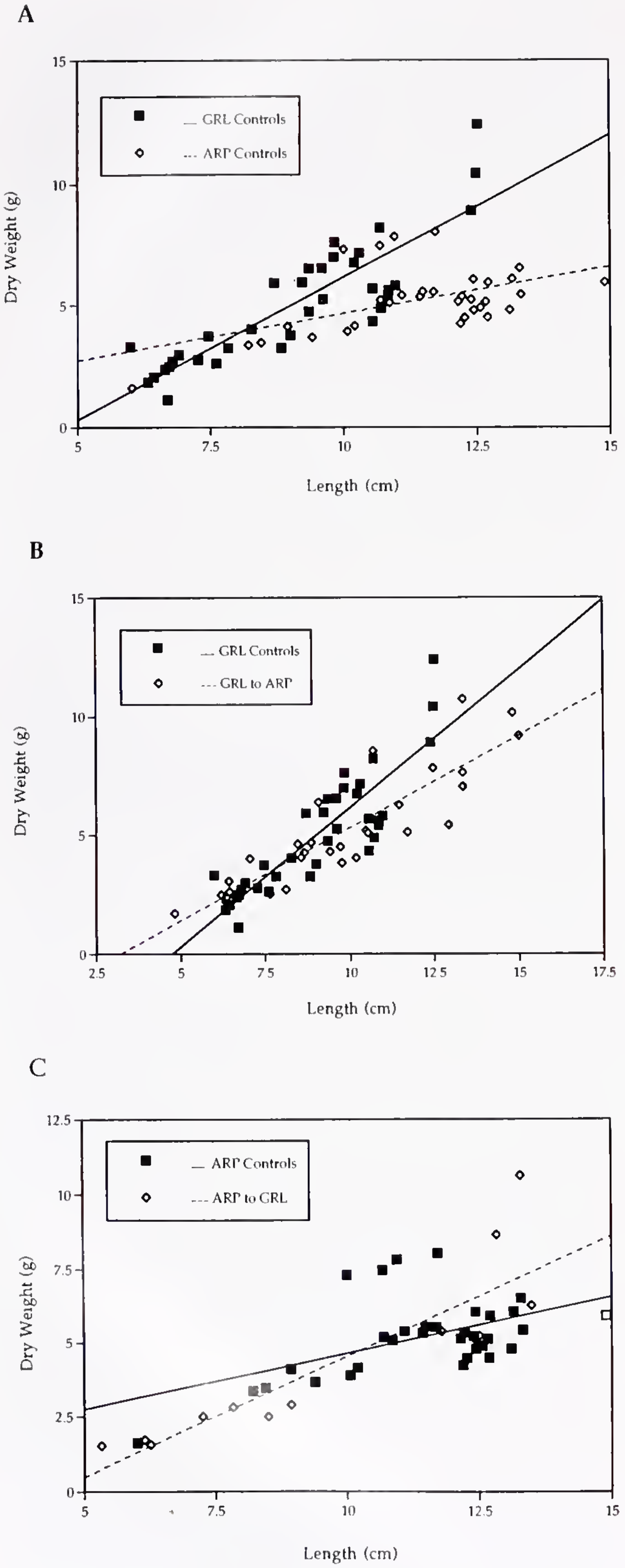

Figure 5. Results from the reciprocal transplant studies, allometric plots of 1990 shell lengths and 1990 dry somatic tissue. (A) *Modiolus modiolus* caged controls; GRL = Monhegan Island, Gull Rock Ledge ($Y = 1.13X - 5.226$, $N = 36$, $r^2 = 0.747$, $P < 0.001$), ARP = Ammen Rock Pinnacle ($Y = 0.377X + 0.875$, $N = 34$, $r^2 = 0.257$, $P < 0.005$). (B) *Modiolus modiolus* transplants; GRL controls as above, GRL to ARP caged transplants ($Y = 0.767X - 2.439$, $N = 31$, $r^2 = 0.765$, $P < 0.001$). (C) *Modiolus modiolus* transplants; ARP controls as above, ARP to GRL caged transplants ($Y = 0.814X - 3.592$, $N = 15$, $r^2 = 0.775$, $P < 0.001$).

under changing environmental conditions is lacking, except for scleractinian corals (Muscatine, 1990). We propose that for the suspension feeders examined in this study, their physiological ecology and differences in functional responses to flow and food availability are important features influencing their distribution and abundance.

Acknowledgments

We thank numerous divers from Northeastern University, Marine Science Center, and the NURC-UNCW Nitrox dive team, Steve Mastro, Ken Johns, and Lance Horn. We are grateful to Sandy Shumway and Larry Harris for constructive comments on earlier drafts of this manuscript, and we owe a special thank-you to Bill Zamer and Malcolm Shick for their extensive efforts to improve this manuscript. This work was supported by the National Oceanic and Atmospheric Administration—University of North Carolina (Wilmington), and by National Science Foundation grant OCE-8800640 to JDW. This is Bigelow Laboratory for Ocean Science contribution number 94004.

Literature Cited

Bayne, B. L., and J. Widdows. 1978. The physiological ecology of two populations of *Mytilus edulis* L. *Oecologia* **37:** 137–162.

Bayne, B. L., and C. M. Worrall. 1980. Growth and production of mussels, *Mytilus edulis* from two populations. *Mar. Ecol. Prog. Ser.* **3:** 317–328.

Best, B. A. 1988. Passive suspension feeding in a sea pen: effects of ambient flow on volume flow rate and filtering efficiency. *Biol. Bull.* **175:** 332–342.

Buss, L. B., and J. B. C. Jackson. 1981. Planktonic food availability and suspension-feeder abundance: evidence of *in situ* depletion. *J. Exp. Mar. Biol. Ecol* **49:** 151–161.

Butman, C. A. 1986. Larval settlement of soft-sediment invertebrates: some predictions based on an analysis of near-bottom velocity profiles. Pp. 487–513 in *Marine Interfaces: Ecohydrodynamics*, J. C. J. Nihoul, ed. Elsevier Oceanography Series 42, Amsterdam.

Cahalan, J. A., S. E. Siddall, and M. W. Luckenbach. 1989. Effects of flow velocity, food concentration and particle flux on growth rates of juvenile bay scallops *Argopecten irradians*. *J. Exp. Mar. Biol. Ecol.* **129:** 45–60.

Clarke, B. C., and C. L. Griffiths. 1990. Ecological energetics of mussels *Choromytilus meridionalis* under simulated rock pool conditions. *J. Exp. Mar. Biol. Ecol.* **137:** 63–77.

Conover, R. J. 1966. Assimilation of organic matter by zooplankton. *Limnol. Oceanogr.* **11:** 338–345.

Crosby, M. P., and L. D. Gale. 1990. A review and evaluation of bivalve condition index methodologies with a suggested standard method. *J. Shellfish Res.* **9:** 233–237.

Dame, R. F. 1972. The ecological energetics of growth, respiration and assimilation in the intertidal American oyster, *Crassostrea virginica*. *Mar. Biol.* **17:** 243–250.

Duggins, D. O., C. A. Simenstad, and J. A. Estes. 1989. Magnification of secondary production by kelp detritus in coastal marine ecosystems. *Science* **245:** 170–173.

Eckman, J. E., and D. O. Duggins. 1993. Effects of flow speed on growth of benthic suspension feeders. *Biol. Bull.* **185:** 28–41.

Elliott, J. M., and W. Davison. 1975. Energy equivalents of oxygen consumption in animal energetics. *Oecologia* **19:** 195–201.

Fielding, P. J., and C. L. Davis. 1989. Carbon and nitrogen resources available to kelp bed filter feeders in an upwelling environment. *Mar. Ecol. Prog. Ser.* **55:** 181–189.

Fréchette, M., and E. Bourget. 1985a. Energy flow between the pelagic and benthic zones: factors controlling particulate organic matter available to an intertidal mussel bed. *Can. J. Fish. Aquat. Sci.* **42:** 1158–1165.

Fréchette, M., and E. Bourget. 1985b. Food-limited growth of *Mytilus edulis* L. in relation to the benthic boundary layer. *Can. J. Fish. Aquat. Sci.* **42:** 1166–1170.

Fréchette, M., and D. Lefaivre. 1990. Discriminating between food and space limitation in benthic suspension feeders using self-thinning relationships. *Mar. Ecol. Prog. Ser.* **65:** 15–23.

Genin, A., P. K. Dayton, P. F. Lonsdale, and F. N. Spiess. 1986. Corals on seamount peaks provide evidence of current acceleration over deep-sea topography. *Nature* **322:** 59–61.

Glynn, P. W. 1973. Ecology of a Caribbean coral reef. The *Porites* reef flat biotype: Part II. Plankton community with evidence for depletion. *Mar. Biol.* **22:** 1–21.

Gnaiger, E. 1983. Calculation of energetic and biochemical equivalents of respiratory oxygen consumption. Pp. 337–345 in *Polarographic Oxygen Sensors: Aquatic and Physiological Applications*, E. Gnaiger and H. Forstner, eds. Springer-Verlag, Berlin and Heidelberg.

Gnaiger, E., and G. Bitterlich. 1984. Proximate biochemical composition and caloric content calculated from elemental CHN analysis: a stoichiometric concept. *Oecologia (Berlin)* **62:** 289–298.

Graf, G. 1989. Benthic-pelagic coupling in a deep-sea community. *Nature* **341:** 437–439.

Graf, G., W. Bengtsson, U. Diesner, R. Schulz, and H. Theede. 1982. Benthic response to sedimentation of a spring phytoplankton bloom: process and budget. *Mar. Biol.* **67:** 201–208.

Graf, G., R. Schulz, R. Peinert, and L.-A. Meyer-Reil. 1983. Benthic response to sedimentation events during autumn to spring at a shallow-water station in the western Kiel Bight. I. Analysis of processes on a community level. *Mar. Biol.* **77:** 235–246.

Grant, J., and P. J. Cranford. 1991. Carbon and nitrogen scope for growth as a function of diet in the sea scallop *Placopecten magellanicus*. *J. Mar. Biol. Ass. U. K.* **71:** 437–450.

Griffiths, C. L., and R. J. Griffiths. 1987. Bivalvia. Chapter 1 in *Animal Energetics*, Vol 2., T. J. Pandian and F. J. Vernberg, eds. Academic Press, New York.

Grizzle, R. E., and R. A. Lutz. 1988. A statistical model relating horizontal seston fluxes and bottom sediment characteristics to growth of *Mercenaria mercenaria*. *Mar. Biol.* **102:** 95–105.

Grizzle, R. E., R. Langan, and W. H. Howell. 1992. Growth responses of suspension-feeding bivalve molluscs to changes in water flow: differences between siphonate and nonsiphonate taxa. *J. Exp. Mar. Biol. Ecol.* **162:** 213–228.

Lande, R., and C. S. Yentsch. 1988. Internal waves, primary production and the compensation depth of marine phytoplankton. *J. Plank. Res.* **10:** 565–571.

Lesser, M. P., V. M. Weis, M. R. Patterson, and P. L. Jokiel. 1994. Effects of morphology and water motion on carbon delivery and productivity in the reef coral, *Pocillopora damicornis* (Linnaeus): diffusion barriers, inorganic carbon limitation, and biochemical plasticity. *J. Exp. Mar. Biol. Ecol.* **178:** 153–179.

La Violette, P. E., D. R. Johnson, and D. A. Brooks. 1990. Sun-glitter photographs of Georges Bank and the Gulf of Maine from the space shuttle. *Oceanography* **3:** 43–49.

MacDonald, B. A., and R. J. Thompson. 1986. Influence of temperature and food availability on the ecological energetics of the giant scallop *Placopecten magellanicus*. *Mar. Biol.* **93:** 37–48.

Mayzaud, P., and R. J. Conover. 1988. O:N atomic ratio as a tool to describe zooplankton metabolism. *Mar. Ecol. Prog. Ser.* **45:** 289–302.

Morrison, M., and D. W. Townsend. 1988. *Hydrography and Vertical Plankton Distributions in Relation to Submerged Rock Pinnacles in the Gulf of Maine: June, 1988.* Bigelow Laboratory for Ocean Sciences, Technical Report No. 66. 76 pp.

Muscatine, L. 1990. The role of symbiotic algae in carbon and energy flow in reef corals. Pp. 75–87 in *Ecosystems of the World, Coral Reefs,* Z. Dubinsky, ed. Elsevier, Amsterdam.

Navarro, J. 1990. *Influence of the Natural Food Supply on the Physiological Energetics and Biochemical Storage Cycles of the Horse Mussel,* Modiolus modiolus (*Linnaeus*). Ph.D. Dissertation, Department of Biology, Memorial University of Newfoundland. 127 pp.

Navarro, J., and R. J. Thompson. 1994. Comparison and evaluation of different techniques for measuring absorption efficiency in suspension feeders. *Limnol. Oceanogr.* **39:** 159–164.

Newell, R. C. 1980. The maintenance of energy balance in marine invertebrates exposed to changes in environmental temperature. Pp. 561–582 in *Animals and Environmental Fitness,* R. Gilles, ed. Pergamon Press, New York.

Ojeda, F. P., and J. H. Dearborn. 1989. Community structure of macroinvertebrates inhabiting the rocky subtidal zone in the Gulf of Maine: seasonal and bathymetric distribution. *Mar. Ecol. Prog. Ser.* **57:** 147–161.

Packard, G. C., and T. J. Boardman. 1988. The misuse of ratios, indices, and percentages in ecophysiological research. *Physiol. Zool.* **61:** 1–9.

Page, H. M., and Y. O. Ricard. 1990. Food availability as a limiting factor to mussel *Mytilus edulis* growth in California coastal waters. *Fish. Bull.* **88:** 677–686.

Patterson, M. R. 1991a. Passive suspension feeding by an octocoral in plankton patches: empirical test of a mathematical model. *Biol. Bull.* **180:** 81–92.

Patterson, M. R. 1991b. The effects of flow on polyp-level prey capture in an octocoral, *Alcyonium siderium. Biol. Bull.* **180:** 93–102.

Patterson, M. R. 1992. A mass transfer explanation of metabolic scaling relations in some aquatic invertebrates and algae. *Science* **255:** 1421–1423.

Patterson, M. R., and K. P. Sebens. 1989. Forced convection modulates gas exchange in cnidarians. *Proc. Natl. Acad. Sci. USA* **86:** 8833–8836.

Patterson, M. R., K. P. Sebens, and R. R. Olson. 1991. *In situ* measurements of flow effects on primary production and dark respiration in reef corals. *Limnol. Oceanogr.* **36:** 936–948.

Peterson, C. H., and R. Black. 1987. Resource depletion by active suspension feeders on tidal flats: influence of local density and tidal elevation. *Limnol. Oceanogr.* **32:** 143–166.

Russell-Hunter, W. D. 1970. *Aquatic Productivity: an Introduction to Some Basic Aspects of Biological Oceanography and Limnology.* Collier-MacMillan, London.

Salonen, K., J. Saevala, I. Hakala, and M. Viljanen. 1976. The relation of energy and organic carbon in aquatic invertebrates. *Limnol. Oceanogr.* **21:** 724–730.

Sebens, K. P. 1981. The allometry of feeding, energetics, and body size in three sea anemone species. *Biol. Bull.* **161:** 152–171.

Sebens, K. P. 1984. Water flow and coral colony size: interhabitat comparisons of the octocoral *Alcyonium siderium. Proc. Natl. Acad. Sci. USA* **81:** 5473–5477.

Sebens, K. P. 1985. The ecology of the rocky subtidal zone. *Am. Scientist.* 73: 548–557.

Sebens, K. P. 1986. Community ecology of vertical rock walls in the Gulf of Maine, USA: small-scale processes and alternate community states. Chapter 23 in *The Ecology of Rocky Coasts,* P. G. Moore and R. Seed, eds. Hodder and Stoughton Educational Press, Kent, England.

Sebens, K. P. 1987. The ecology of indeterminate growth in animals. *Annu. Rev. Ecol. Syst.* **18:** 371–407.

Sebens, K. P., and M. A. R. Koehl. 1984. Predation on zooplankton by the benthic anthozoans *Alcyonium siderium* (Alcyonacea) and *Metridium senile* (Actinaria) in the New England subtidal. *Mar. Biol.* **81:** 255–271.

Seiderer, L. J., and R. C. Newell. 1985. Relative significance of phytoplankton, bacteria and plant detritus as carbon and nitrogen resources for the kelp bed filter-feeder *Choromytilus meridionalis. Mar. Ecol. Prog. Ser.* **22:** 127–139.

Shick, J. M. 1991. *A Functional Biology of Sea Anemones.* Chapman and Hall, London. 395 pp.

Shick, J. M., R. J. Hoffman, and A. N. Lamb. 1979. Asexual reproduction, population structure, and genotype-environment interactions in sea anemones. *Am. Zool.* **19:** 699–713.

Shick, J. M., J. Widdows, and E. Gnaiger. 1988. Calorimetric studies of behavior, metabolism and energetics of sessile intertidal animals. *Am. Zool.* **28:** 161–181.

Solorzano, L. 1969. Determination of ammonia in natural waters by the phenol-hypochlorite method. *Limnol. Oceanogr.* **14:** 799–801.

Stuart, V., and D. W. Klumpp. 1984. Evidence for food-resource partitioning by kelp-bed filter feeders. *Mar. Ecol. Prog. Ser.* **16:** 27–37.

Szmant, A. M., L. M. Ferrer, and L. M. Fitzgerald. 1990. Nitrogen excretion and O:N ratios in reef corals: evidence for conservation of nitrogen. *Mar. Biol.* **104:** 119–127.

Thompson, R. J. 1984. The reproductive cycle and physiological ecology of the mussel *Mytilus edulis* in a subarctic, non-estuarine environment. *Mar. Biol.* **79:** 277–288.

Thresher, R. E., G. P. Harris, J. S. Gunn, and I. A. Clementson. 1989. Phytoplankton production pulses and episodic settlement of a temperate marine fish. *Nature* **341:** 641–643.

Townsend, D. W., and L. M. Cammen. 1985. A deep protozoan maximum in the Gulf of Maine. *Mar. Ecol. Prog. Ser.* **24:** 177–182.

Townsend, D. W., and L. M. Cammen. 1988. Potential importance of the timing of spring plankton blooms to benthic-pelagic coupling and recruitment of juvenile demersal fishes. *Biol. Oceanogr.* **5:** 215–229.

Townsend, D. W., and R. W. Spinrad. 1986. Early spring phytoplankton blooms in the Gulf of Maine. *Cont. Shelf Res.* **6:** 515–529.

Townsend, D. W., C. M. Yentsch, C. E. Parker, W. M. Balch, and E. D. True. 1983. An island mixing effect in the coastal Gulf of Maine. *Helgolander Meeresunters* **36:** 347–356.

Townsend, D. W., T. L. Cucci, and T. Berman. 1984. Subsurface chlorophyll maxima and the vertical distribution of zooplankton in the Gulf of Maine. *J. Plankton Res.* **6:** 793–802.

Vogel, S., and M. LaBarbera. 1978. Simple flow tanks for research and teaching. *BioScience* **10:** 638–643.

Widdows, J., and D. Johnson. 1988. Physiological energetics of *Mytilus edulis:* scope for growth. *Mar. Ecol. Prog. Ser.* **46:** 113–121.

Wilbur, A. E., and T. J. Hilbish. 1989. Physiological energetics of the ribbed mussel *Geukensia demissa* (Dillwyn) in response to increased temperature. *J. Exp. Mar. Biol. Ecol.* **131:** 161–170.

Wildish, D. J., and M. P. Miyares. 1990. Filtration rate of blue mussels as a function of flow velocity: preliminary experiments. *J. Exp. Mar. Biol. Ecol.* **142:** 213–219.

Wildish, D. J., D. D. Kristmanson, R. L. Hoar, A. M. DeCoste, S. McCormick, and A. W. White. 1987. Giant scallop feeding and growth responses to flow. *J. Exp. Mar. Biol. Ecol.* **113:** 207–220.

Winter, J. E. 1969. Über den Einfluß der Nahrungskonzentration und anderer Faktoren auf Filtrierleistung und Nahrungsausnutzung der Muscheln *Arctica islandica* und *Modiolus modiolus. Mar. Biol.* **4:** 87–135.

Winter, J. E. 1978. A review of the knowledge of suspension-feeding in lamellibranchiate bivalves, with special reference to artificial aquaculture systems. *Aquaculture* **13:** 1–33.

Witman, J. D., and R. A. Cooper. 1983. Disturbance and contrasting patterns of population structure in the brachiopod *Terebratulina septentrionalis* from two subtidal habitats. *J Exp. Mar Biol. Ecol.* **73:** 57–79.

Witman, J. D. 1985. Refuges, biological disturbance, and rocky subtidal community structure in New England. *Ecol. Monogr.* **55:** 421–445.

Witman, J. D. 1987. Subtidal coexistence: storms, grazing, mutualism, and the zonation of kelp and mussels. *Ecol. Monogr.* **57:** 167–187.

Witman, J. D., and K. P. Sebens. 1988. Benthic community structure at a subtidal rock pinnacle in the central Gulf of Maine. National Undersea Research Program Research Report, 88-3, pp. 67–104.

Witman, J. D., and K. P. Sebens. 1990. Distribution and ecology of sponges at a subtidal rock ledge in the central Gulf of Maine. Pp. 391–396 in *New Perspectives in Sponge Biology*. K. Rutzler, ed. Smithsonian Institution Press, Washington, DC.

Witman, J. D., J. J. Leichter, S. J. Genovese, and D. A. Brooks. 1993. Pulsed phytoplankton supply to the rocky subtidal zone: influence of internal waves. *Proc. Natl. Acad. Sci. USA* **90:** 1686–1690.

Yentsch, C. S., W. Skea, J. C. Laird, and T. S. Hopkins. 1979. Ocean color observations. Pp. 441–454 in *Apollo-Soyuz Test Project*, Summary Science Report, Vol. II, F. El-Baz and D. M. Warner, eds. NASA.

Yentsch, C. S., and N. Garfield. 1981. Principal areas of vertical mixing in the waters of the Gulf of Maine with reference to total productivity of the area. Pp. 303–312 in *Oceanography from Space*, J. F. R. Gower, ed. Plenum Press, New York.

Zamer, W. E., and C. P. Mangum. 1979. Irreversible nongenetic temperature adaptation of oxygen uptake in clones of the sea anemone *Haliplanella luciae* (Verrill). *Biol. Bull.* **157:** 536–547.

Zamer, W. E., and J. M. Shick. 1987. Physiological energetics of the intertidal sea anemone *Anthopleura elegantissima* II. Energy balance. *Mar. Biol.* **93:** 481–491.

Zamer, W. E., and J. M. Shick. 1989. Physiological energetics of the intertidal sea anemone *Anthopleura elegantissima*. III. Biochemical composition of body tissues, substrate-specific absorption, and carbon and nitrogen budgets. *Oecologia (Berlin)* **79:** 117–127.

Zamer, W. E., R. E. Robbins, and J. M. Shick. 1987. β-Glucuronidase activity and detritus utilization in the sea anemones *Metridium senile* and *Anthopleura elegantissima*. *Comp. Biochem. Physiol* **87B:** 303–308.

Reference: *Biol. Bull.* **187:** 336–345. (December, 1994)

Dispersal Strategies of the Biota on an Oceanic Seamount: Implications for Ecology and Biogeography

TERRY PARKER AND VERENA TUNNICLIFFE*

School of Earth and Ocean Sciences and Department of Biology, University of Victoria, Victoria, British Columbia, Canada V8W 2Y2

Abstract. Cobb Seamount lies at 46° 46′ N, 130° 48′ W in the northeast Pacific 510 km due west of the Oregon coast. The isolated seamount rises 3000 m in a current field flowing from west to east. The seamount supports dense populations of fish and benthos. Collections and submersible observations of the benthic community produced a list of 117 species representing 13 phyla. The organisms present can nearly all be found on the North American Pacific coast, but the diversity is low. This paper presents an analysis of the larval dispersal modes of the benthos at Cobb Seamount. This remote seamount is dominated by species with either a short-lived or no planktonic larval phase. The preponderance of such larval strategies and the observation of abundant drifting kelp near the seamount suggest that rafting of adults may be an effective dispersal mode. The presence of a recirculating flow in the form of a modified Taylor cap appears important for trapping short-lived larvae on the seamount. However, because the water mass is replaced about every 17 days, medium and long-lived larvae would not be retained. The interplay between local currents, available dispersal vectors, and life-history strategies cannot be overlooked in the interpretation of marine biogeographic patterns.

Introduction

The study of marine biogeography requires an appreciation of the dispersal capabilities of component species at various stages in their life histories. Recognition of vicariant events can reveal large-scale patterns, but differential dispersal capabilities among species modify those patterns. Investigations of species accumulation on the marine equivalent of islands—seamounts—test our ideas about mechanisms of biogeographic patterning. Seamounts have been considered as stepping stones, vicariant pathways, and points of endemic isolation (Hubbs, 1959; Briggs, 1974; Wilson and Kaufmann, 1987; Leal and Bouchet, 1991).

Marine invertebrates show various development patterns ranging from metamorphosed juveniles emerging directly from broods through yolk-supported (lecithotrophic) floating larvae to plankton-feeding (planktotrophic) larvae (see reviews by Mileikovsky, 1971; Grahame and Branch, 1985; Scheltema, 1986b). In some clades, taxa are constrained to a single developmental mode (Woollacott and Zimmer, 1978; Nielson, 1980); in others, life history strategies vary within a given family (Hadfield and Strathmann, 1990), genus (Johannesson, 1988), or even species (Levin, 1984). Planktonic larvae are considered the primary dispersal mechanism for benthic marine invertebrates (Mileikovsky, 1971; Jackson, 1986). Longer planktonic duration should allow for greater dispersal of larvae (Zinsmeister and Emerson, 1979; Scheltema 1986a, b). Prevailing theory predicts that species with long-lived planktonic larvae will have broader geographic ranges, whereas those with short-lived or brooded larvae will be geographically restricted (Mileikovsky, 1971; Hedgecock, 1986; Scheltema, 1986b, 1989) but better able to capitalize on favorable local environments (Jackson, 1986; Keogh and Chernoff, 1987).

Johannesson (1988) suggested that isolated islands and seamounts are more likely to be populated by species with limited larval dispersal abilities on the basis that a founder population can achieve reproductive success. Some observations of species with limited larval range in isolated marine habitats support this idea (Birkeland, 1971; Moore, 1977; Johannesson, 1988).

Received 17 December 1993; accepted 31 August 1994.

* Author to whom reprint requests should be addressed.

Cobb Seamount presents the opportunity to examine concepts of larval dispersal capabilities and biogeography. It lies far enough offshore to provide a habitat disjunct from coastal communities but close enough that larvae could be expected to gain access with some regularity. The seamount (46° 46′ N, 130° 47′ W) is located in the northeast Pacific, 510 km due west of the Oregon (USA) coast (Fig. 1). Early surveys (Budinger and Enbysk, 1960; Budinger, 1967) described a symmetrical seamount with several terraces and a central pinnacle measuring about 800 by 600 m. Our surveys record a shallowest depth of 24 m. Cobb was formed near the Juan de Fuca Ridge as part of the Cobb-Eickelberg Seamount chain (Davis and Karsten, 1986). Summit lavas were eruptive during the Pleistocene; samples date to 1.6 ± 0.3 million years ago (Dymond *et al.*, 1968). Farrow and Durant (1985) interpret submarine erosional features as stages in island subsidence and sea-level fluctuation. Beach characteristics are noted as deep as 310 m and may relate to the volcano's initial emergence. Low sea-level stands during the Wisconsin glacial period generated the large wave-cut terrace at 120–180 m.

Predominant flow is eastward at about 10 cm s^{-1} in the North Pacific Current which, in the vicinity of Cobb, splits into the northward Alaska Current and the southward California Current (Hickey, 1989). Well-defined surface currents from the coast offshore do not exist. Surface drifters released near Cobb move linearly from northwest to southeast and do not reflect deeper eddying or circulation (Dower *et al.*, 1992). A recent study documents the surface drift and flow around Cobb in more detail (Freeland, 1994). Early work by Birkeland (1971) reports dense assemblages of coastal species that include several brooders; many abundant inshore species are absent. In view of our diving experience on Cobb, we wondered how any population dependent on pelagic larvae could maintain itself: the open ocean surge is extreme and the persistent surface currents are likely to sweep propagules off the seamount.

Our study has three objectives: (1) to document the Cobb Seamount benthic community components, (2) to assess how these species may have arrived on the seamount, and (3) to examine the potential for development of stable populations in light of information from concurrent studies on the hydrodynamic processes around Cobb Seamount.

Materials and Methods

We examined the Cobb benthos during several cruises as part of a larger effort to characterize the oceanographic conditions around the seamount. The submersible support vessel *Pandora II* visited twice in the early 1980s and the Canadian Survey Ships *Parizeau* and *J. P. Tully* participated in an oceanographic program in the summers from 1990 to 1992. The Canadian submersible *Pisces IV* conducted six dives in July 1982 and one dive in 1983; four of these dives covered parts of the terrace or pinnacle, and the other three were deeper. Collection was possible with the manipulator, which retrieved some voucher specimens. Most dive information came from still-camera photographs and diver records from which only organisms that were clearly identifiable were used. Dredging was attempted during surface cruises of 1990 and 1991, but the recovery was poor on the rock outcrops. Best returns from the pinnacle came from examination of the epifauna on detached rock scallops (*Crassadoma gigantea*). The pinnacle top was nearly impossible to sample because of the wave surge during diving and the lack of loose aggregates for dredging. Some algal and epifloral samples were retrieved on fishing lines. The most complete collection and identification information came from the benthic assemblage on the upper terrace and pinnacle. For that reason, we limit our presentation and analysis to species recorded above 180 m depth.

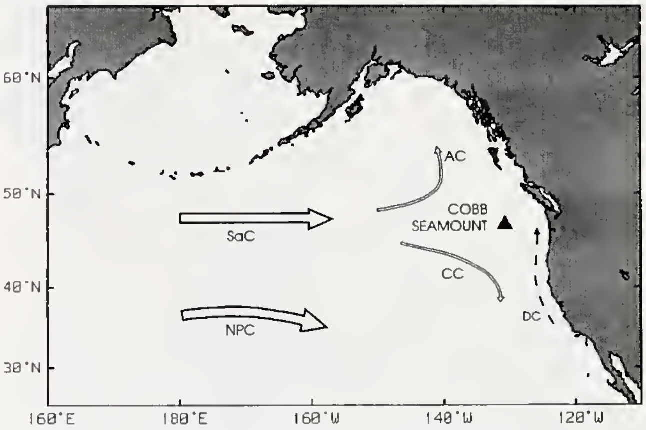

Figure 1. Location of Cobb Seamount in the northeast Pacific. Arrows indicate the major current patterns: SaC = Subarctic Current; AC = Alaska Current; NPC = North Pacific Current; CC = California Current; DC = the ephemeral Davidson Current.

To identify invertebrates from the 1990 and 1991 samples we used Kozloff (1987), with reference to Bernard (1972), Lambert (1981, 1986), and Laubitz (1970) for the Brachiopoda, Echinodermata, and caprellid amphipods respectively. We used Hatch (1947) for the tanaids and isopods, and Gabrielson *et al.* (1989) for the algae. Local authorities helped us with many identifications. We added additional species documented in Birkeland (1971) and a list of fish species compiled by D. Nelson (unpub. data) to produce the final species listing.

The literature provided information on propagule dispersal periods of the seamount species. Although our efforts focused on individual species, assumptions were made for species within groups known to have invariant dispersal modes. Species with crawl-away juveniles released from the adult or a benthic egg case form the "direct release" category. Species with pelagic larvae were categorized according to the length of time the larvae remain in the water column: less than 2 weeks = "short pelagic"; more than 2 but less than 8 weeks = "medium pelagic"; and more than 8 weeks = "long pelagic." Those species for which no information was available were left in an "unknown" category.

We constructed the expected distributions for larval dispersal modes of the benthic invertebrates from published information. Thorson (1961) presented the larval life spans of 195 species (no geographic range identified), which we redistributed in the time categories used in this paper. To add the category of nonpelagic development, we used the values of Thorson (1950) and Mileikovsky (1971); these numbers differ so we calculated the range of expected development types. Because many benthic invertebrates exhibit a latitudinal gradient in ratio of direct to pelagic developers (Thorson, 1950, 1961; Mileikovsky, 1971; Valentine and Jablonski, 1983), we used literature data only from Cobb's approximate latitude (38° N to 51° N). We restricted our final analysis to the benthic invertebrates because (1) a good body of theoretical and empirical work exists for comparison in this group, and (2) adult fish mobility may provide a source of migration unavailable to other organisms.

Results

The shallow Cobb community

The pinnacle top appears much as described by Birkeland (1971) who explored with scuba divers. The substratum is covered with coralline algae topped by patches of other algae (mostly *Desmarestia viridis*). Rock scallops (*Crassadoma gigantea*) with abundant epifauna inhabit cracks in the basalt. The sides of the pinnacle from 35 to 110 m support the densest aggregations of animals: little bare substratum is seen. A hummocky effect was created by the cementing scallops that are colonized by cnidarians (mostly *Corynactis californica*), tunicates, sponges, and bryozoans. Aggregations of the urchin *Strongylocentrotus franciscanus* are common at the shallower depths. Rockfish (*Sebastes* spp.) are very abundant in the water, with pelagic juveniles forming large schools.

The terrace at 125 to 300 m is mostly covered with white carbonate sediments through which some basalt outcrops protrude. Here echinoderms dominate the macrofauna. The crinoid *Florometra serratissima* and a variety of ophiuroids cover both sediments and outcrops. The asteroids *Pycnopodia helianthoides* and *Crossaster papposus* are common predators. Sediment samples recovered many gastropods and hermit crabs. Biomass on both pinnacle and terrace appears high. Comparison of the species list and photographs (from the University of Washington collection) of Birkeland (1971) with photographs and observations from 1982/83 and the samples of 1990/91 reveals little change in the composition of common and abundant species. There appear to have been outbreaks of the anenome *Metridium senile* and the sea urchin *Strongylocentrotus franciscanus*, but the overall species composition seems stable.

Table 1 lists the species known to occur at Cobb Seamount above 180 m. In total, 117 species from 13 phyla have been identified to date. Several species of nematodes, protozoa, and polychaetes remain unidentified and are not included. The fauna is depauperate compared to the coastal communities of the northeast Pacific. For example, a count of the benthic invertebrates (0 to 250 m) in a preliminary list of animals from the west coast of Vancouver Island (Austin, 1970) reaches 786 using only the phyla found on Cobb, where the equivalent number is 95.

Methods of propagule dispersal

For 26 of the 117 Cobb species (22.2%), dispersal data are unavailable or cannot be inferred; 26.5% release their juveniles directly onto the substratum; and 37.6% have propagules in the short pelagic category. Although this category includes species whose larvae spend up to 2 weeks in the plankton, the larvae of most of the species remain pelagic for a few days to just minutes. Species belonging to the medium and long pelagic larval dispersal groups each make up 6.8% of all Cobb species.

Figure 2A illustrates the distribution of propagule dispersal types recorded for the benthic invertebrates of Cobb Seamount. Among the 95 species, 31.6% are direct releasers and 32.6% belong to the short pelagic group. Medium and long pelagic larval dispersal groups make up 8.4% and 4.2% of all species respectively. Larval dispersal methods of 25.3% of Cobb invertebrate species remain unknown. Of the 12 species we classified as abundant (Table I), 8 have no planktonic larval phase, 2 are short pelagic, and 2 are long pelagic; no abundant species have a medium-length pelagic larval dispersal phase.

The calculated expected distribution of larval dispersal types for benthic marine invertebrates at the approximate latitude of Cobb Seamount is presented in Figure 2B. The ranges of values observed for this latitude are as follows: direct release, 26.0–36.5%; short pelagic, 9.5–11.1%; medium pelagic, 45.1–52.5%; long pelagic, 8.9–10.4%. No comparable "expected" data set exists for the Pacific northwest. We searched for information on polychaete reproduction from Strathmann (1987) and references therein because this group shows the whole range of reproductive strategies. For 46 coastal species, division of larval lifetimes were 13 direct, 8 short, 23 medium, and 2 long pelagic.

Table I

Systematic listing of species known to occur on Cobb Seamount, indicating relative abundance (for those identified from 1990 and 1991 collections), dispersal method, source of species identification, and references concerning dispersal method

Phylum	Class	Species	Abundance[†]	Dispersal Mode[‡]	Source of ID[§]	Reference[‖]
Chlorophyta	Ulvophyceae	*Pseudopringsheimia apiculata*	?	short pelagic*	B	(30)
Phaeophyta	Phaeophyceae	*Desmarestia viridis*	A	short pelagic*	C	(30)
		Ectocarpus corticulatus?	C	short pelagic*	C	(30)
Rhodophyta	Rhodophyceae	*Antithamnion kylnii*	C	short pelagic*	C	(30)
		Mastocarpus jardinii?	R	short pelagic*	C	(30)
		Polysiphonia pacifica	R	short pelagic*	C	(30)
		Polysiphonia urceolata	C	short pelagic*	C	(30)
		Ceramium sp.	R	short pelagic*	C	(30)
		Lithothamnion sp.	A	short pelagic*	O/B	(30)
		Lithophyllum sp.	?	short pelagic*	B	(30)
		Delesseria sp.	R	short pelagic*	C	(30)
		Porphyropsis sp.	R	short pelagic*	C	(30)
		unk. red blade	R	short pelagic*	C	(30)
Porifera	Desmospongiae	*Halichondria panicea*	C	short pelagic	W	(1)
Cnidaria	Hydrozoa	*Allopora verrilli*	A	direct release*	P/W	(23, 36)
	Anthozoa	*Desmophyllum cristigalli*	C	unknown	W	
		Cribrinopsis fernaldi	?	short pelagic	P/B	(34)
		Metridium senile	C	short pelagic	P	(3, 15, 23)
		Corynactis californica	A	direct release	P/C	(23)
		Urticina crassicornis	?	short pelagic	P	(4)
		Stomphia didemon	?	short pelagic	P	(33)
		Stylatula elongata	?	short pelagic	P	(23)
		Epizoanthus? sp.	?	unknown	P	
		colonial zoanthid?	R	unknown	C	
Annelida	Polychaeta	*Crucigera zygophora*	C	medium pelagic	C	(20, 36)
		Nothria conchylega	R	direct release	C	(31)
		Phyllochaetopterus prolifica	A	direct release	C	(23)
		Protula pacifica	R	short pelagic	C	(20)
		Phyllodoce maculata	?	medium pelagic	B	
		Trypanosyllis gemmipara	?	unknown	B	
		Nereis procera	?	short pelagic	B	(36)
		Eunice valens (=*E. kobiensis*)	?	direct release	B	(36)
		Serpula vermicularis	?	short pelagic	B	(23)
		Chitinopoma groenlandica	?	unknown	B	
		Euphrosine sp.	R	unknown	C	
		Lumbrineris inflata	A	short pelagic	C	(20, 36)
		cirratulid sp. 1	C	short pelagic*	C	(23, 36)
		spirorbid sp. 1	A	short pelagic*	C	(27)
		trichobranchid(?) sp. 1	R	unknown	C	
	Oligochaeta	oligochaete sp. 1	C	direct release	C	
Arthropoda	Amphipoda	*Caprella alaskana*	A	direct release*	C	(23)
		Caprella laeviuscula	C	direct release*	C	(23)
		gammaridean sp. 1	C	direct release*	C	(23, 25, 40)
		Proboloides? n. sp.	C	direct release*	C	(23, 25, 40)
		Micropleustes n. sp.	A	direct release*	C	(23, 25, 40)
		gammaridean sp. 4	C	direct release*	C	(23, 25, 40)
		Parapleustes n. sp.	A	direct release*	C	(23, 25, 40)
		gammaridean sp. 6	A	direct release*	C	(23, 25, 40)
		gammaridean sp. 7	R	direct release*	C	(23, 25, 40)
		Maera n. sp.	R	direct release*	C	(23, 25, 40)
	Copepoda	calanoid copepod	R	unknown	C	
		cyclopoid copepod	R	unknown	C	
		harpacticoid copepod	C	short pelagic*	C	(13)
	Isopoda	*Ianiropsis tridens*	C	direct release*	C	(23)
		Munna ubiquita	C	direct release*	C	(23)
		Munna chromatocephala	C	direct release*	C	(23)

Table I *(continued)*

Phylum	Class	Species	Abundance[†]	Dispersal Mode[‡]	Source of ID[§]	Reference[‖]
Arthropoda	Tanaidacaea	*Leptochelia* sp.	C	direct release*	C	(23)
		Paratanais sp.	C	direct release*	C	(23)
	Malacostraca	*Chorilia longipes*	C	medium pelagic*	C	(14)
		Oregonia gracilis	C	medium pelagic*	C	(14)
		Pagurus cavimanus	?	unknown	B	
Mollusca	Gastropoda	*Acmea instabilis*	R	unknown	W	
		Margarites marginatus	C	direct release	W	(36)
		Calliostoma annulatum	R	short pelagic	W	(10, 36)
		Calliostoma ligatum	C	short pelagic	C/W	(16)
		Homalopoma carpenteri	R	unknown	W	
		Diodora aspera	R	direct release	C	(39)
		Searlisia dira	C	direct release	W	(23)
		Ocenebra lurida	?	direct release	B	(8)
		Fusitriton oregonensis	?	unknown	B/O/C	
		Granulina margaritula	C	direct release	C	(26)
		Barleeia/Cingula	?	unknown	W	
		Bittium sp.	?	unknown	W	
		Battilaria/Antiplanes	?	unknown	W	
		Diorina albolineata	?	unknown	B	
		Archidoris montereyensis	?	short pelagic	B	(23)
		Archidoris odhneri	?	unknown	B	
	Bivalvia	*Crassodoma gigantea*	A	long pelagic	P/C	(23)
		Macoma balthica	R	medium pelagic	W	(6)
		Modiolus modiolus	R	medium pelagic	C	(5)
		Petricola pholadiformis	R	medium pelagic	C	(18)
		hiatellid sp.	R	long pelagic	C	(23)
		philobryid sp.	R	unknown	C	
		solemyid sp.	R	short pelagic*	C	(9)
Brachiopoda	Articulata	*Laqueus californianus*	?	short pelagic*	O/W/P	(37)
		Terebratulina sp.	?	short pelagic*	O/P	(37)
		Platidia hornii	C	short pelagic*	C	(29)
Bryozoa	Cyclostomata	*Bicrisia edwardsiana*	C	short pelagic*	C	(24, 41)
		Crisia occidentalis	C	short pelagic*	C	(24, 41)
		Filicrisia franciscana	C	short pelagic*	C	(24, 41)
	Cheilostomata	*Rhamphostomella spinigera*	?	short pelagic*	B	(41)
		Borgiola pustulosa	?	short pelagic*	B	(41)
		Bugula sp.	C	short pelagic*	C	(24, 41, 42)
		Lyrula sp.	C	short pelagic*	C	(41)
Sipuncula		*Phascolosoma agassizi*	C	short pelagic	C	(28, 36)
Echinodermata	Asteroidea	*Pycnopodia helianthiodes*	C	long pelagic	P	(7, 17, 23, 35)
		Crossaster papposus	C	medium pelagic	C/P	(17, 36)
		Henricia sanguinolenta	R	direct release	C	(17, 23, 32)
		Henricia leviuscula	C	direct release	C	(17, 23)
		Orthasterias koehleri	?	unknown	B	
		Leptasterias hexactis	R	direct release	C	(17, 23)
		Solaster sp.	?	unknown	O/P	
		Hippasterias spinosa	?	short pelagic	O	(17)
	Ophiuroidea	*Amphipholis squamata*	?	direct release	B	(38)
	Crinoidea	*Florometra serratissima*	A	short pelagic	P	(19, 22, 35)
	Echinoidea	*Strongylocentrotus franciscanus*	A	long pelagic	C	(23, 35, 36)
	Holothuroidea	*Parastichopus leukothele*	R	unknown	W	

Table I *(continued)*

Phylum	Class	Species	Abundance[†]	Dispersal Mode[‡]	Source of ID[§]	Reference[‖]
Chordata	Ascidiacea	*Ascidia ceratodes*	?	short pelagic*	P	(21)
	Chondricthyes	*Prionace glauca*	?	direct release	B	(12)
	Osteicthyes	cottid fish	R	unknown	C	
		Sebastes helvomaculatus	A	long pelagic	N	(2)
		Sebastes paucispinus	A	long pelagic	B/N	(2)
		Sebastes entomelas	A	long pelagic	B/N	(2)
		Sebastes ruberrimus	A	long pelagic	B/N	(2)
		Hemilepidotus spinosus	A	unknown	B/N	
		Embassichthys bathybius	C	unknown	N	
		Mola mola	?	unknown	B	

[†] Abundance Categories: A = abundant: two or more samples with several individuals; C = common: several individuals in one sample or two or more samples with at least 1 individual; R = rare: one or two individuals in only one sample; ? = abundance not estimated due to data source.

[‡] Dispersal Categories: Direct release: budding, fission, or benthic juveniles emerging from parent or benthic egg case; short pelagic: short-lived (<2 weeks) planktonic larvae, usually lecithotrophic; medium pelagic: usually planktotrophic larvae with a 2–8 week residence in the plankton; long pelagic: planktotrophic larvae with >8 week residence in the plankton.

[§] Source of species list: B = from Birkeland (1971); C = identified from collections made in 1990–1992; N = from an unpublished list compiled by Douglas Nelson (1983); O = from *Pisces* observations in early 1980s; P = identified from *Pisces* photographs; W = identified from our collection by W. C. Austin.

[‖] References: (1) Amano, 1986; (2) Boehlert & Yoklavich, 1984; (3) Chia, 1976; (4) Chia & Spaulding, 1972; (5) deSchweinitz & Lutz, 1976; (6) Gilbert, 1978; (7) Greer, 1962; (8) Griffith, 1967; (9) Gustafson, 1985; (10) Hadfield & Strathmann, 1990; (11) Hart, 1960; (12) Hart, 1973; (13) Hicks & Coull, 1983; (14) Hines, 1986; (15) Hoffmann, 1987; (16) Holyoak, 1988; (17) Lambert, 1981; (18) Mackie, 1984; (19) McEdward *et al.*, 1988; (20) D. McHugh, pers. comm.; (21) Millar, 1971; (22) Mladenov & Chia, 1983; (23) Morris *et al.*, 1980; (24) Nielsen, 1970; (25) Nielson, 1980; (26) T. Parker, pers. obs.; (27) Potswald, 1978; (28) Rice, 1967; (29) Rudwick, 1970; (30) Santelices, 1990; (31) Schroeder & Heimans, 1975; (32) Shield & Witman, 1993; (33) Seibert, 1973; (34) Seibert & Spaulding, 1976; (35) Strathmann, 1978; (36) Strathmann, 1987; (37) Valentine & Jablonski, 1983; (38) Walker & Lesser, 1989; (39) Webber, 1977; (40) Wildish, 1982; (41) Woollacott & Zimmer, 1978; (42) Woollacott *et al.*, 1989.

* Larval dispersal mode inferred from related species within groups showing a phylogenetic constraint on larval dispersal modes.

Discussion

Many authors emphasize the importance of larvae as dispersal mechanisms for marine invertebrates (*e.g.*, Zinsmeister and Emerson, 1979; Valentine and Jablonski, 1983; Scheltema, 1986a, b). "Good dispersers" dominate the molluscan faunas of oceanic islands (Scheltema and Williams, 1983). In this context, species with longer larval stages should dominate the Cobb benthos. What we find, conversely, is a poor representation by such species, suggesting that enhanced larval dispersability contributes little to population establishment or maintenance on this seamount. In fact, it appears that long-lived larvae may be a distinct disadvantage: only 15 of the 89 species for which we have good information had larvae pelagic for more than 2 weeks. Comparison with the expected proportion from equivalent latitudes (Fig. 2 and polychaete comparison data) underscores the depletion of these groups. The paucity of species with a medium-duration planktonic larval phase is quite intriguing. This group, which otherwise represents the largest proportion of species at this latitude, includes many species conspicuously absent from Cobb.

The proportion of species with direct development, while similar to the general observations for the latitude, is surprising on an isolated seamount. A study of gastropods on a series of Brazilian seamounts finds direct developers averaging only 7% of the fauna on each seamount (Leal and Bouchet, 1991). One can argue that once a founder group of such a species somehow arrives, it is liable to establish a population by self-recruitment. However, the large number of species with larvae pelagic for even less than 2 weeks still seems anomalous; on Cobb Seamount, tidal currents, surface currents at 10 cm s^{-1} (Freeland, 1994), and storm surges appear sufficient to sweep water-borne larvae far from a shallow substratum.

From the point of view of vicariance biogeography, species accumulation may represent relict distributions. Cobb Seamount was an emergent island during the last glaciation. While the coast south to 48° N was engulfed in an ice-sheet, Cobb represented an offshore refuge. That this island was colonized at this time is known. Sub-fossil debris of intertidal organisms such as bivalves and barnacles litters the 120-m terrace. Budinger (1967) dated one mussel shell at 6710 ± 330 years before present. This *Mytilus* species is no longer extant on the seamount because rising sea levels drowned the intertidal zone. We cannot know which of the remaining species have maintained populations since that time. Between Cobb Seamount and the coast lie a bare rock spreading ridge and a bathyal plain that form barriers to both vicariant path-

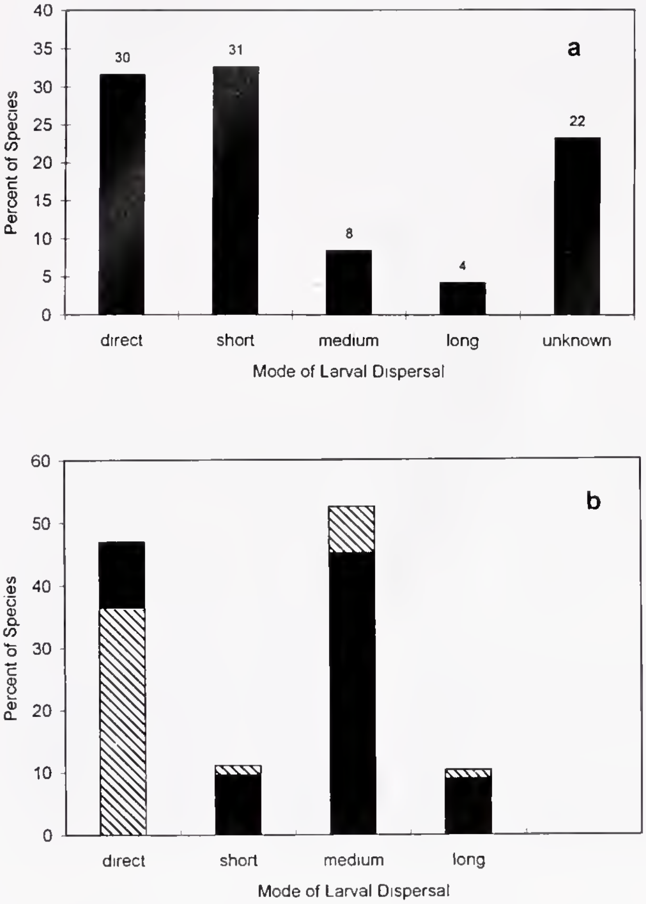

Figure 2. (a) Distribution of larval development modes for the invertebrate species of Cobb Seamount. This presentation represents 95 invertebrate species. Details are given in Table 1. Direct = species that have no pelagic stage; short = species with larvae pelagic for 2 weeks or less; medium = species with larvae that spend 2 to 8 weeks in the plankton; long = species with larvae that are pelagic for longer than 8 weeks. Above the columns are the numbers of invertebrates included. (b) Expected distributions of larval development modes for benthic invertebrates around the latitude of Cobb Seamount; values generated from Thorson (1950, 1961) and Mileikovsky (1961) as explained in the text. Because these authors give different values for the proportion of species that are direct releasers, we present a distribution with a maximum value for direct release (black) and one using a minimum value (pattern).

ways and individual adult migration. The nearest seamounts have summits below 500 m; only Union Seamount, 370 km north-north-west, is shallower.

We believe present dispersal does play a major role. All but four undescribed amphipod species are found on the North American coast; several have wider distributions. The seamount sits at the divergence of an eastward flow field; flow further east splits into the Alaskan and California Currents. Two seasonal currents, shallow Davidson and deep California Undercurrent, flow poleward from California hugging the coast (Hickey, 1989). Stray jets may extend offshore occasionally, but even a 15 cm s^{-1} current will take some 6 weeks to carry a larva from the coast. Medium- and short-duration larvae from surrounding continents are unlikely to survive the trip to Cobb. There are no other shallow seamounts nearby. The Alaskan gyre could bring long-lived larvae over thousands of kilometers from Alaska. Species with larvae of long planktonic duration may arrive from Alaska, the Pacific Northwest, California, or even Japan. The rock scallop *Crassadoma gigantea* was examined by protein electrophoresis for evidence of population differentiation between Cobb and British Columbia. Allozyme frequencies of several loci revealed no significant differences diagnostic of isolated populations (Dower and Tunnicliffe, unpub. data). This scallop releases pelagic larvae that are viable for several weeks. It is also noteworthy that, of the eight species with long pelagic dispersal, all but one have long adult lifespans (20 years or longer). Such populations have the potential to survive between infrequent recruitment events.

Johannesson (1988) predicts the result that we present: a paucity of species with longer pelagic larvae on Cobb Seamount. He proposes that successful colonization of isolated areas is enhanced by limited off-site advection of the founder population's progeny. His model emphasizes the role of dispersal agents in medium latitude oceans. He states, in fact, that presence of a species with a longer-lived larva on a place like Cobb Seamount is more problematic than that of a direct-developer.

Kelp is often observed floating near and over Cobb Seamount, although these macroalgae do not grow there. The large kelp forests of the west coast of North America support a rich, dense fauna. Because of considerable hydrodynamic drag, large kelps often break free (Koehl and Wainwright, 1977) and the associated epiphytic species may linger for over 100 days (Vàsquez, 1993). Floating kelp rafts move with the surface winds rather than with prevailing current; they can travel at averaged speeds of 5 to 10 cm s^{-1} and instantaneous speeds to 65 cm s^{-1} (Harrold and Lisin, 1989). Winds from the southwest could carry kelp from the California coast during the winter domination of the Aleutian low-pressure cell. Kelp rafts may provide a significant migration vector for metamorphosed invertebrates regardless of their larval development mode (Knox, 1954; Highsmith, 1985; Johannesson, 1988; Lane *et al.*, 1985; Sörlin, 1988; O'Foighil, 1989; Martel and Chia, 1991). Most epifaunal species listed in Table 1 can be found in kelp forests. Several, such as *Strongylocentrotus franciscanus, Acmaea instabilis,* and the *Calliostoma* species, are rarely found elsewhere. Given that rafts can deliver juveniles and adults to an isolated site, those species with brooded and short-lived larvae may be superior colonizers through subsequent local recruitment (Jackson, 1986; Keough and Chernoff, 1987) and adaptation (Behrens Yamada, 1989). In some cases, species with short or no planktonic larval periods have wider geographic ranges than those with longer larval periods (Levin, 1984; Johannesson, 1988; O'Foighil, 1989).

In both the early and late 1980s, we collected many of the species recorded by Birkeland (1971) in the 1960s. Persistent populations must propagate locally or have a constant recruitment. Direct-release species have little opportunity to spread further. Although we have not examined genetic characteristics in such species, population differentiation is demonstrated for two species of brooding crustaceans on two other isolated seamounts (Bucklin *et al.*, 1987; Wilson and Boehlert, 1993). Four of our direct-release amphipod species are new species or subspecies (Bousefield, pers. comm.). This feature argues for the persistence of isolated populations on Cobb Seamount.

A look at the local flow regime helps to explain the preponderance of species with larvae that are pelagic for 2 weeks or less. Dispersal in species with short-lived larvae is affected by water-flow patterns in a highly deterministic fashion (Olson, 1985; Bingham, 1992). Freeland (1994) has demonstrated the presence of a circulating flow around Cobb Seamount. He models the conditions necessary for formation of a "Taylor Proudman column" caused by the displacement of a stratified, linear current flow in the presence of the seamount (Hogg, 1973; Chapman and Haidvogel, 1992). Freeland (1994) describes anticyclonic flow around Cobb that is strongest near the base of the water column; it extends about 100 m upwards but does not penetrate to the surface. The lowest current meters identify an outflow in the bottom Ekman layer. Freeland estimates that the circulating water is replaced over about 17 days and forms a steady concentric inflow that would effectively trap larvae. He concludes that the recirculation is due primarily to a Taylor Proudman cap. Concentration of plankton over such topographic features has been recorded (Boden, 1952; Genin and Boehlert, 1985) and a recirculation mechanism implicated (Pingree and Maddock, 1985; Boehlert, 1988; Dower *et al.*, 1992). There is, therefore, a mechanism to retain larvae in our "short-lived" group near the seamount until resettlement and metamorphosis on the seamount can occur.

Recruitment to Cobb of many common species from the North American west coast is limited by their intermediate pelagic life span of 2 to 8 weeks. Fortuitous flow events such as eddies and jets that break away from the longshore flow (Hickey, 1989) may provide an occasional transport vehicle toward Cobb. Regardless of their means of arrival, populations established this way are liable to lose their own progeny as a result of the short residence time of water over their new domicile.

We found that classic theories of larval development strategy did not help us to predict the types of species that would accumulate on Cobb Seamount. Johannesson (1988), among others, questions the generality of the relative effectiveness of long-lived pelagic larvae as dispersal agents; our observations support his model. Species with long pelagic larval periods appear able to establish populations only if the species are long-lived as adults or the current supplying the larvae is consistent; there were few such species on Cobb. Most studies on teleplanic larvae are based in tropical/subtropical latitudes (Scheltema, 1971, 1986b; Zinsmeister and Emerson, 1979) where direct development and short-lived pelagic larvae are uncommon. In our case, the role of local flow around Cobb Seamount is likely the leading factor determining the success of species with different larval strategies. Although we have no direct evidence, the role of rafting deserves serious consideration. In considering biogeographic and life-history theories, the marine biologist is well served by an understanding of the regional history, physical dynamics, and biological characteristics of the system under study.

Acknowledgments

J. Dower, P. Finnigan, and K. Wilson helped at sea and in the lab. Drs. A. Austin, W. C. Austin, E. Bousfield, and P. Lambert helped identify species. We thank J. Dower for discussions on Cobb hydrography and dispersal potential; Dr. H. Freeland provided valuable insight on flow characteristics. Reviewer criticisms contributed to an improved manuscript. This project benefited greatly from the multidisciplinary Cobb Seamount Experiment. We appreciate the logistic support of Department of Fisheries and Oceans Canada vessels and financial support through DFO and NSERC Canada grant programs.

Literature Cited

Amano, S. 1986. Larval release in response to a light signal by the intertidal sponge *Halichondria panicea*. *Biol. Bull.* **171:** 371–378.

Austin, W. C. 1970. *A Preliminary List of Marine Invertebrates of the Barkley Sound Region (Bamfield Survey, Part V).* Bamfield Marine Station Report No. 3, Bamfield, Canada.

Behrens Yamada, S. D. 1989. Are direct developers more locally adapted than planktonic developers? *Mar. Biol.* **103:** 403–411.

Bernard, F. 1972. The living Brachiopoda of British Columbia. *Syesis* **5:** 73–82.

Bingham, B. L. 1992. Life histories in an epifaunal community: coupling of adult and larval processes. *Ecology* **73:** 224–229.

Birkeland, C. 1971. Biological observations on Cobb Seamount. *Northwest Sci.* **45:** 193–199.

Boden, B. P. 1952. Natural conservation of insular plankton. *Nature* **169:** 697–699.

Boehlert, G. W. 1988. Current-topography interactions at mid-ocean seamounts and the impact on pelagic ecosystems. *GeoJournal* **16:** 45–52.

Boehlert, G. W., and M. M. Yolakovich. 1984. Reproduction, embryonic energetics and the maternal-fetal relationship in the viviparous genus *Sebastes* (Pisces: Scorpaenidae). *Biol. Bull.* **167:** 354–370.

Briggs, J. C. 1974. Operation of zoogeographic barriers. *Syst. Zool.* **22:** 248–256.

Bucklin, A., R. R. Wilson, and K. L. Smith. 1987. Genetic differentiation of seamount and basin populations of the deep-sea amphipod *Eurythenes gryllus. Deep-Sea Res.* **34:** 1795–1810.

Budinger, T. F. 1967. Cobb Seamount. *Deep-Sea Res.* **14:** 191–201.

Budinger, T. F., and B. J. Enbysk. 1960. *Cobb Seamount, a Deep Sea Feature off the Washington Coast.* Dept. of Oceanogr. Univ. Wash. Tech. Rep. No. 60.

Chapman, D. C., and D. B. Haidvogel. 1992. Formation of Taylor caps over a tall isolated seamount in a stratified ocean. *Geophys. Astrophys. Fluid Dynamics* **64:** 31–65.

Chia, F.-S. 1976. Sea anemone reproduction: patterns and adaptive radiations. Pp. 261–277 in *Coelenterate Ecology and Behaviour* G. O. Mackie, ed. Plenum, New York.

Chia, F.-S., and J. G. Spaulding. 1972. Development and juvenile growth of the sea anemone *Tealia crassicornis. Biol. Bull.* **142:** 206–218.

Davis, E. E., and J. L. Karsten. 1986. On the cause of the asymmetric distribution of seamounts about the Juan de Fuca Ridge: ridge-crest migration over a heterogenous asthenophere. *Earth Planet. Sci. Let.* **79:** 385–396.

deSchweinitz, E. H., and R. A. Lutz. 1976. Larval development of the northern horse mussel *Modiolus modiolus* (L.) including a comparison with the larvae of *Mytilus edulis* (L.) as an aid in planktonic identification. *Biol. Bull.* **150:** 348–360.

Dower, J., H. Freeland, and S. K. Juniper. 1992. A strong biological response to oceanic flow past Cobb Seamount. *Deep-Sea Res.* **39:** 1139–1145.

Dymond, J. R., N. D. Watkins, and Y. R. Nayudu. 1968. Age of the Cobb Seamount. *J. Geophys. Res.* **73:** 3977–3979.

Farrow, G. E., and G. P. Durant. 1985. Carbonate-basaltic sediments from Cobb Seamount, northeast Pacific: zonation, bioerosion and petrology. *Mar. Geol.* **65:** 73–102.

Freeland, H. 1994. Ocean circulation at and near a shallow seamount. *Deep-Sea Res.* in press.

Gabrielson, P. W., R. F. Scagel, and T. B. Widdowson. 1989. *Keys to the Benthic Marine Algae and Seagrasses of British Columbia, Southeast Alaska, Washington and Oregon.* Univ. British Columbia Phycological Contribution #4. 187 pp.

Genin, A., and G. W. Boehlert. 1985. Dynamics of temperature and chlorophyll structures above a seamount: an oceanic experiment. *J. Mar. Res.* **43:** 907–924.

Gilbert, M. A. 1978. Aspects of the reproductive cycle in *Macoma balthica* (Bivalvia). *Nautilus* **92:** 21–24.

Grahame, J., and G. M. Branch. 1985. Reproductive patterns of marine invertebrates. *Oceanogr. Mar. Biol. Annu. Rev.* **23:** 373–398.

Greer, D. L. 1962. Studies on the embryology of *Pycnopodia helianthiodes* (Brandt) Stimpson. *Pac. Sci.* **16:** 280–285.

Griffith, L. M. 1967. *The Intertidal Univalves of British Columbia.* Handbook of British Columbia Provincial Museum 26. 101 pp.

Gustafson, R. G. 1985. *Development, Morphogenesis and Putative Symbiont Transmission in the Pericalymma Larva of* Solemya reidi *(Bivalvia, Cryptodonta. Solemyidae).* Ph.D. Thesis, University of Victoria, Victoria, BC.

Hadfield, M. G., and M. F. Strathmann. 1990. Heterostrophic shells and pelagic development in trochoideans: implications for classification, phylogeny and paleoecology. *J Molluscan Stud* **56:** 239–256.

Harrold, C., and S. Lisin. 1989. Radio-tracking rafts of giant kelp: local production and regional transport. *J Exp. Mar. Biol. Ecol.* **130:** 237–251.

Hart, J. 1960. Larval development of British Columbia brachyurans II: Majiidae, subfamily Oregoniinae. *Can. J Zool.* **38:** 539–546.

Hart, J. L. 1973. *Pacific Fishes of Canada.* Fisheries Research Board of Canada, Bulletin **180.**

Hatch, M. H. 1947. The Chelicera and Isopoda of Washington and adjacent regions. *Univ. Wash. Publ. Biol.* **10:** 155–274.

Hedgecock, D. 1986. Is gene flow from pelagic larval dispersal important in the adaptation and evolution of marine invertebrates? *Bull. Mar. Sci.* **39:** 550–564.

Hicks, G. R. F., and B. C. Coull. 1983. The ecology of marine meiobenthic harpacticoid copepods. *Oceanogr. Mar. Biol. Annu. Rev.* **21:** 67–175.

Hickey, B. M. 1989. Patterns and processes of circulation over the Washington continental shelf and slope. Ch. 2 in *Coastal Oceanography of Washington and Oregon.* M. R. Landry and B. M. Hickey, eds. Elsevier, Amsterdam.

Highsmith, R. 1985. Floating and algal rafting as potential dispersal mechanisms in brooding invertebrates. *Mar. Ecol. Prog. Ser.* **25:** 169–179.

Hines, A. H. 1986. Larval patterns in the life histories of brachyuran crabs (Crustacea, Decapoda, Brachyura). *Bull. Mar. Sci.* **39:** 444–466.

Hoffmann, R. J. 1987. Short-term stability of genetic structure in populations of the sea anemone *Metridium senile. Mar. Biol.* **93:** 499–507.

Hogg, N. G. 1973. On the stratified Taylor column. *J. Fluid Mech.* **58:** 517–537.

Holyoak, A. R. 1988. Spawning and larval development of the trochid gastropod *Calliostoma ligatum* (Gould, 1849). *Veliger* **30:** 369–371.

Hubbs, C. L. 1959. Initial discoveries of the fish faunas on the seamounts and offshore banks in the eastern Pacific. *Pac. Sci.* **13:** 311–316.

Jackson, J. B. C. 1986. Modes of dispersal of clonal benthic invertebrates: consequences for species distributions and genetic structure of local populations. *Bull. Mar. Sci.* **39:** 588–606.

Johannesson, K. 1988. The paradox of Rockall: Why is a brooding gastropod more widespread than one having a planktonic larval dispersal stage (*L. littorea*)? *Mar. Biol.* **99:** 507–513.

Keough, M. J., and H. Chernoff. 1987. Dispersal and population variation in the bryozoan *Bugula neritina. Ecology* **68:** 199–210.

Knox, G. A. 1954. Intertidal flora and fauna of the Chatham Islands. *Nature* **174:** 871–873.

Koehl, M. A. R., and S. A. Wainwright. 1977. Mechanical adaptations of a giant kelp. *Limnol. Oceanogr.* **22:** 1067–1071.

Kozloff, E. N. 1987. *Marine Invertebrates of the Pacific Northwest.* Univ. Washington Press, Seattle. 511 pp.

Lambert, P. 1981. *The Sea Stars of British Columbia.* Handbook of British Columbia Provincial Museum No. 39. 153 pp.

Lambert, P. 1986. Northeast Pacific holothurians of the genus *Parastichopus* with a description of a new species *Parastichopus leukothele* (Echinodermata). *Can. J. Zool.* **64:** 2266–2272.

Lane, D. J. W., A. R. Beaumont, and J. R. Hunter. 1985. Byssus drifting and the drifting threads of the young post-larval mussel *Mytilus edulis. Mar. Biol.* **84:** 301–308.

Laubitz, D. R. 1970. *Studies on the Caprellidae (Crustacea, Amphipoda) of the American North Pacific.* National Museum of Natural Sciences (Canada) Publications in Biological Oceanogr. 1.

Leal, J. H., and P. Bouchet. 1991. Distribution patterns and dispersal of prosobranch gastropods along a seamount chain in the Atlantic Ocean. *J Mar. Biol. Assoc. U. K.* **71:** 11–25.

Levin, L. 1984. Multiple patterns development in *Streblospio benedicti* Webster (Spionidae) from three coasts of North America. *Biol. Bull.* **166:** 494–508.

Mackie, G. L. 1984. Bivalves, in *The Mollusca: Volume 7, Reproduction.* A. S. Tompa, N. H. Verdonk and J. A. M. van den Biggelaar, eds. Academic Press, London.

Martel, A., and F.-S. Chia. 1991. Drifting and dispersal of small bivalves and gastropods with direct development. *J Exp. Mar. Biol. Ecol.* **150:** 131–147.

McEdward, L. R., S. F. Carson, and F.-S. Chia. 1988. Energetic content of eggs, larvae and juveniles of *Florometra serratissima* and the implications for the evolution of crinoid life histories. *Int. J. Invertebr. Reprod.* **13:** 9–22.

Mileikovsky, S. A. 1971. Types of larval development in marine bottom invertebrates, their distribution and ecological significance: a re-evaluation. *Mar. Biol.* **10:** 193–213.

Millar, R. H. 1971. The biology of ascidians. *Adv. Mar. Biol.* **9:** 1–100.

Mladenov, P. V., and F.-S. Chia. 1983. Development, settling behaviour, metamorphosis and pentacrinoid feeding and growth of the feather star *Florometra serratissima. Mar. Biol.* **73:** 309–323.

Moore, P. G., 1977. Additions to the littoral fauna of Rockall, with a description of *Araeolaimus penelope* sp. nov. (Nematoda: Axonolaimidae). *J. Mar. Biol. Ass. U. K.* **57:** 191–200.

Morris, R. H., D. P. Abbott, and E. C. Haderlie, eds. 1980. *Intertidal Invertebrates of California.* Stanford University Press, California.

Nielsen, C. 1970. On metamorphosis and ancestrula formation in cyclostomatous bryozoans. *Ophelia* **7:** 217–256.

Nielson, W. G. 1980. Reproductive patterns of gammaridean amphipods. *Sarsia* **65:** 61–71.

O'Foighil, D. 1989. Planktotrophic larval development is associated with restricted geographic range in *Lasaea*, a genus of brooding, hermaphroditic bivalves. *Mar. Biol.* **103:** 349–358.

Olson, R. R. 1985. The consequences of short-distance larval dispersal in a sessile marine invertebrate. *Ecology* **66:** 30–39.

Pingree, R. D., and L. Maddock. 1985. Rotary currents and residual circulation around banks and islands. *Deep-Sea Res.* **32:** 929–947.

Potswald, H. E. 1978. Metamorphosis in *Spirorbis* (Polychaeta). Pp. 127–143 in *Settlement and Metamorphosis of Marine Invertebrate Larvae.* F.-S. Chia and M. E. Rice, eds. Elsevier, New York.

Rice, M. E. 1967. A comparative study of the development of *Phascolosoma agassizii, Golfingia pugettensis* and *Themiste pyriodes* with a discussion of developmental patterns in the sipuncula. *Ophelia* **4:** 143–171.

Rudwick, M. J. S. 1970. *Living and Fossil Brachiopods.* Hutchinson and Co., London.

Santelices, B. 1990. Patterns of reproduction, dispersal and recruitment in seaweeds. *Oceanogr. Mar. Biol. Annu. Rev.* **28:** 177–276.

Schroeder, P. C., and C. O. Heimans. 1975. Pp. 1–213 in *Reproduction of Marine Invertebrates. Volume III Annelids and Echiurans.* A. C. Giese and J. S. Pearse, eds. Academic Press, New York.

Scheltema, R. S. 1971. The dispersal of larvae of shoal-water benthic invertebrate species over long distances by ocean currents. Pp. 7–28 in *Fourth Mar. Biol. Symp. Cambridge.* D. J. Crisp, ed. Cambridge Univ. Press, UK.

Scheltema, R. S. 1986a. Long distance dispersal by planktonic larvae of shoal-water benthic invertebrates among central Pacific Islands. *Bull. Mar. Sci.* **39:** 241–256.

Scheltema, R. S. 1986b. On dispersal and planktonic larvae of benthic invertebrates: an eclectic overview and summary of problems. *Bull. Mar. Sci.* **39:** 290–322.

Scheltema, R. S. 1989. Planktonic and non-planktonic development among prosobranch gastropods and its relationship to the geographic range of species. Pp. 183–188 in *Reproduction, Genetics and Distributions of Marine Organisms.* J. Ryland and P. Tyler, eds. Olsen & Olsen, Fredensborg, Denmark.

Scheltema, R. S., and I. P. Williams. 1983. Long-distance dispersal of planktonic larvae and the biogeography and evolution of some Polynesian and western Pacific mollusks. *Bull. Mar. Sci.* **33:** 545–565.

Shield, C. J., and J. D. Witman. 1993. The impact of *Henricia sanguinolenta* (O. F. Muller) (Echinodermata: Asteroidea) predation on the finger sponges *Isodictya* spp. *J. Exp. Mar. Biol. Ecol.* **166:** 107–133.

Seibert, A. E. 1973. A description of the sea anemone *Stomphia didemon* sp. nov. and its development. *Pac. Sci.* **27:** 363–376.

Seibert A. E., and J. G. Spaulding. 1976. The taxonomy, development and brooding behaviour of the anemone *Cribrinopsis fernaldi* sp. nov. *Biol. Bull.* **150:** 128–138.

Sörlin, T. 1988. Floating behaviour in the tellinid bivalve *Macoma balthica* (L.). *Oecologia* **77:** 273–277.

Strathmann, M. F. 1987. *Reproduction and Development of Marine Invertebrates of the Northern Pacific Coast.* Univ. Wash. Press., Seattle.

Strathmann, R. 1978. Length of pelagic period in echinoderms with feeding larvae from the Northwest Pacific. *J. Exp. Mar Biol. Ecol.* **34:** 23–27.

Thorson, G. 1950. Reproductive and larval ecology of marine bottom invertebrates. *Biol. Rev.* **25:** 1–45.

Thorson, G. 1961. Length of pelagic life in marine bottom invertebrates as related to larval transport by ocean currents. Pp. 455–474 in *Oceanography.* M. Sears, ed. A.A.A.S. Publ. 67, Washington, DC.

Valentine, J. W., and D. Jablonski. 1983. Larval adaptations and patterns of brachiopod diversity in space and time. *Evolution* **37:** 1050–1061.

Vásquez, J. A. 1993. Effects on the animal community of dislodgement of holdfasts of *Macrocystis pyrifera. Pac. Sci.* **47:** 180–184.

Walker, C. W., and M. P. Lesser. 1989. Nutrition and development of brooded embryos in the brittlestar *Amphipholis squamata:* Do endosymbiotic bacteria play a role? *Mar. Biol.* **103:** 519–530.

Webber, H. H. 1977. Gastropoda: Prosobranchia. Pp. 1–97 in *Reproduction of Marine Invertebrates. Volume IV, Molluscs: Gastropods and Cephalopods.* A. C. Giese and J. S. Pearse, eds. Academic Press, New York.

Wildish, N. J. 1982. Evolutionary ecology and reproduction in gammaridean Amphipoda. *Int. J. Invertebr. Reprod* **5:** 1–19.

Wilson, C. D., and G. W. Boehlert. 1993. Population biology of *Gnathophausia longispina* (Mysidacea: Lophogastrida) from a central North Pacific seamount. *Mar. Biol.* **113:** 537–543.

Wilson, R. R., and R. S. Kaufmann. 1987. Seamount biota and biogeography. Pp. 355–377 in *Seamounts Atolls and Islands.* B. H. Keating *et al.*, eds. Geophysical Monograph 43, American Geophysical Union, Washington, DC.

Woollacott, R. M., J. A. Pechenik, and K. M. Imbalazano. 1989. Effects of duration of larval swimming period on early colony development in *Bugula stolonifera* (Bryozoa: Cheilostomata). *Mar. Biol.* **102:** 57–63.

Woolacott, R. M., and R. L. Zimmer. 1978. Metamorphosis of cellularioid Bryozoans. Pp. 49–63 in *Settlement and Metamorphosis of Marine Invertebrate Larvae.* F.-S. Chia and M. E. Rice, eds. Elsevier, New York.

Zinsmeister, W. J., and W. K. Emerson. 1979. The role of passive dispersal in the distribution of hemipelagic invertebrates with examples from the tropical Pacific ocean. *Veliger* **22:** 32–40.

Reference: *Biol. Bull.* **187**: 346–354. (December, 1994)

Patterns of Distribution of Two Barnacle Species on the Mangrove Crab, *Scylla serrata*

HAROLD K. VORIS[1,*], WILLIAM B. JEFFRIES[2], AND SOMBAT POOVACHIRANON[3]

[1]*Department of Zoology, Field Museum of Natural History, Chicago, Illinois 60605;*
[2]*Department of Biology, Dickinson College, Carlisle, Pennsylvania; and*
[3]*Phuket Marine Biological Center, Phuket, Thailand*

Abstract. Two lepadomorph barnacle species, *Octolasmis angulata* and *O. cor*, were commonly found living together in the branchial chambers of the mangrove crab, *Scylla serrata*. Patterns of distribution are a reflection of cyprid choice at crab ecdysis. Among the 6648 barnacles observed, there were roughly twice as many *O. cor* as *O. angulata* (3670 to 1758). The remaining barnacles were indistinguishable as to species and included 1014 immatures, 168 cyprids, and 38 peduncles. The spatial distributions of both *O. angulata* and *O. cor* on the gills of *Scylla serrata* are nonrandom, uneven, and do not reflect available surface area. Both species are distributed differently on the hypobranchial (inside) and epibranchial (outside) surfaces of the gills. Both species are distributed differently on the gills of immature (<70 mm carapace width) and mature (>70 mm) crabs. Our data also show that the distribution patterns vary with different densities. Support is presented for the hypothesis that current flow through the gill chamber may be an important factor influencing site selection by cyprids.

Introduction

The goose barnacles of the genus *Octolasmis* that are under study here are members of the Lepadomorpha (Zevina, 1982), and they differ from other barnacles in several important ways. Most of the species in the genus *Octolasmis* are symbiotic on decapod Crustacea, particularly crabs and lobsters (Darwin, 1851; Walker, 1974; Jeffries *et al.*, 1992). The integument of these hosts is an ephemeral substrate for attached symbionts because at ecdysis they are shed with the discarded exoskeleton (Coker, 1902; Humes, 1941; Jeffries *et al.*, 1985). Colonization of newly molted crabs by octolasmid cyprids is highly pulsed because cyprids gather on the premolt crab and transfer from the old exuviae to the newly molted crab at the time of ecdysis (Jeffries *et al.*, 1989). Thus, cyprids colonizing crabs in this way may interact with other cyprids, but there is no chance of their encountering attached adult octolasmids on the recently molted crab.

Octolasmis cor (Aurivillius, 1892) and *Octolasmis angulata* (Aurivillius, 1894) are inhabitants of the gill chambers of numerous decapods found in the seas of South East Asia (Jeffries, *et al.*, 1982), and they are commonly found together in the gill chambers of the mangrove crab, *Scylla serrata* (Forskål, 1755). The two species are distinguishable on the basis of differences in labrum tooth counts; outline and size of the capitulum; size, shape, and arrangement of the calcareous plates; and fecundity (Jeffries *et al.*, 1991). The nauplius and cypris larvae of the two species are now being compared, and the initial results support the two-taxa hypothesis: *e.g.*, the cypris larvae of one species are larger than the other. To these observations we now add new information concerning their relative positions within the gill chambers.

Although the presence of diverse species within the gill chambers of crabs has been documented (Coker, 1902; Pearse, 1932, 1947; De Turk, 1940; Humes, 1941, 1942; Walker, 1974; Lang, 1976; Overstreet, 1983; Shields, 1992), this is the first precise comparison of the distribution of two related *Octolasmis* barnacle species in the gill chambers of a single host crab species, *S. serrata*. As a model system, it provides an excellent descriptive foundation for future experimental study of such aspects of symbiosis as site selection and competition for resources.

The purpose of this report is to describe and consider the spatial distributions of octolasmid barnacles in the gill

Received 20 December 1993; accepted 22 September 1994.

* To whom correspondence should be sent.

Table I

The distribution of 1758 O. angulata *over the inside (hypobranchial) and outside (epibranchial) surfaces of the gills in 225 gill chambers of 143* S. serrata *(top), and the distribution of 3670* O. cor *over the inside and outside surfaces of the gills in 346 gill chambers of 200* S. serrata *(bottom)*

Octolasmis angulata

	Inside of gills				Outside of gills				
Gill Number	Proximal	Medial	Distal	Totals	Proximal	Medial	Distal	Totals	In + Out Totals
1	2	1	0	3	0	1	14	15	18
2	0	0	2	2	6	6	4	16	18
3	8	47	17	72	15	6	2	23	95
4	19	54	11	84	64	28	0	92	176
5	82	48	10	140	151	68	9	228	368
6	130	116	19	265	41	45	2	88	353
7	152	324	38	514	7	13	1	21	535
8	88	94	5	187	0	3	0	3	190
TOTALS	481	684	102	1267	284	170	32	486	1753
ON RAKERS	5	0	0	5	0	0	0	0	5
				1272				486	1758

Octolasmis cor

	Inside of gills				Outside of gills				
Gill Number	Proximal	Medial	Distal	Totals	Proximal	Medial	Distal	Totals	In + Out Totals
1	30	27	3	60	0	0	0	0	60
2	2	2	4	8	6	6	2	14	22
3	133	289	20	442	0	1	0	1	443
4	540	575	14	1129	4	1	0	5	1134
5	292	441	18	751	16	7	0	23	774
6	375	393	21	789	0	3	0	3	792
7	133	218	17	368	0	0	1	1	369
8	22	42	6	70	0	1	0	1	71
TOTALS	1527	1987	103	3617	26	19	3	48	3665
ON RAKERS	5	0	0	5	0	0	0	0	5
				3622				48	3670

chambers of a natural population of the mangrove crab, *Scylla serrata*. In addition, both abiotic and biotic factors that influence the settlement patterns of two barnacle species, *Octolasmis angulata* and *O. cor*, are discussed.

Materials and Methods

We recently reported on the age of the mangrove crab, *Scylla serrata*, at colonization by *Octolasmis* spp. (Jeffries *et al.*, 1992), and the same specimens used in that study form the foundation for the current report. The sample of mangrove crabs, including 403 males and 453 females, and ranging in size from 10.9 to 132.3 mm carapace width (instars 5–18), was collected by hand and trap from a natural population in southern Thailand in 1990 and 1991. The crabs were examined for *Octolasmis* cyprids, juveniles, and adults. Adult barnacles were identified to species, whereas immatures could not be classified. The exact location of barnacle attachment [left or right gill chamber, gill number, inside (hypobranchial) or outside (epibranchial) gill surface, proximal, medial, or distal region of gill], and the length of the capitulum of each preserved barnacle were recorded by the methods previously employed (Jeffries *et al.*, 1982).

In this study we collected a sample of 856 crabs, among which 260 hosted a total of 6648 octolasmids. The barnacle population included 1758 *O. angulata*, 3670 *O. cor*, 1014 unknowns (all subadults), 38 peduncles only, and 168 cyprids.

Results

Analysis of O. angulata *distribution*

A total of 1758 *O. angulata* were observed on 143 *Scylla serrata*; 63 of these were female crabs, and 80 were males. All but 13 of the infested *S. serrata* also harbored one or more *O. cor* individuals. Each crab has two gill chambers, and not all of the 286 gill chambers of the 143 infested crabs held barnacles. In fact, 61 of the 143 crabs had one chamber that hosted no *O. angulata*. Thus, in this analysis the *O. angulata* distributed in 225 gill chambers of 143 crabs are being considered (Table I).

The distribution of *O. angulata* on the inside (hypobranchial) surface of gills 1 through 8 was compared to distributions that reflect gill length and gill surface area (Jeffries and Voris, 1983). The areas of the gills were estimated with the formula for the area of a right cone ($a = \pi rh$). The observed distribution is significantly different (Chi-square test, Mosteller and Rourke, 1973) from an expected distribution based on the length of the gills ($\chi^2 = 976.8$, df = 7, $P < .001$) and the area of the gill surface ($\chi^2 = 649.3$, df = 7, $P < .001$). For example, gills 4, 5, and 6 are of similar length, and yet gill 6 harbors more *O. angulata* than gills 4 and 5 combined.

By far, more of the *O. angulata* were attached to the inside (hypobranchial) surface of the gills (1267, 72%) than were attached to the outside (epibranchial) surface (486, 28%).

The distribution of *O. angulata* on the inside of gills 1 through 8 (gill totals, Table I) differs significantly from the distribution on the outside of gills 1 through 8 ($\chi^2 = 547.5$, df = 14, $P < .001$). For example, the inside surface of gill 7 has 40 percent (514) of all of the *O. angulata* found on the inside surface of the gills, whereas the outside surface of gill 7 has only 4.9% (21) of the *O. angulata* found on the outside (Fig. 1). Thus, the distribution of *O. angulata* on the inside gill surfaces is distinct from its distribution over the outside gill surfaces.

The distributions of *O. angulata* on the proximal, medial, and distal surfaces of the inside of gills 1 through 8 differ from one another for all three comparisons (proximal by medial, $\chi^2 = 84.0$, df = 14, $P < .001$; proximal by distal, $\chi^2 = 72.4$, df = 14, $P < .01$). Thus, the distribution of *O. angulata* over the inside surface of the proximal, medial, and distal regions of individual gills differs from gill to gill. This is also true for the distribution over the outside surfaces, although the numbers of barnacles are smaller (Table 1).

The totals of *O. angulata* on the inside surfaces of the proximal (481), medial (684), and distal (102) regions of gills 1 through 8 (Table 1) differ from the totals for the outside ($\chi^2 = 60.8$, df = 4, $P < .001$). For example, *O. angulata* are most common on the medial segments of the inside surfaces of gills (684, 54%), whereas they are most common on the proximal portion of the outside surface of gills (284, 58%).

Analysis of O. cor *distribution*

A total of 3670 *O. cor* were observed on 200 *Scylla serrata*, 93 females and 107 males. Of these, 127 harbored one or more *O. angulata*. Of the 200 crabs with *O. cor*, 54 crabs had one chamber that did not host any *O. cor*. In this analysis, therefore, the *O. cor* distributed in 346 gill chambers of 200 crabs are considered (Table 1).

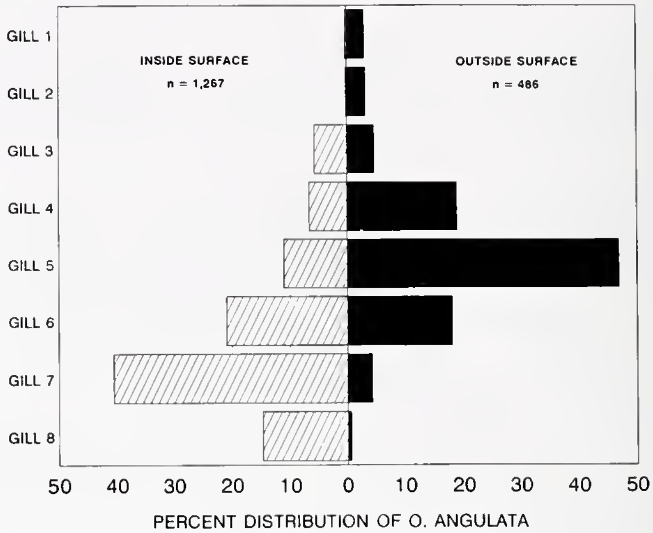

Figure 1. The percent distribution of 1267 *Octolasmis angulata* on the inside (hypobranchial) surfaces and 486 on the outside (epibranchial) surfaces of gills 1 through 8 in 225 gill chambers of 143 *Scylla serrata* is presented.

The spatial distribution results for *O. cor* are similar but not identical to those for *O. angulata*.

The distribution of *O. cor* on the inside surface of gills 1 through 8 (gill totals of *O. cor*) was compared to distributions that reflect gill length and gill surface area. In each case the observed distribution (Table I) was significantly different from an expected distribution based on gill length ($\chi^2 = 1888.9$, df = 7, $P < .001$) and area ($\chi^2 = 1643$, df = 7, $P < .001$). For example, gills 4, 5, and 6 are of similar lengths and yet gill 4 harbors roughly 30% more *O. cor* than either gill 5 or gill 6.

The vast majority (3617, or 98.6%) of the *O. cor* were attached to the inside surface of the gills rather than the outside surface (48, 1.3%).

The distribution of *O. cor* on the inside of gills 1 through 8 (gill totals) differs from that on the outside of gills 1 through 8 ($\chi^2 = 682.9$, df = 14, $P < .001$). For example, the inside surface of gill 4 has 31% (1129) of all the *O. cor* on the inside surface (Table I), whereas the outside surface of gill 4 has only 10% (5) of all the *O. cor* on the outside. *O. cor*, like *O. angulata*, colonizes the inside surfaces of the gills in a way distinct from its colonization of the outside gill surfaces.

The distributions of *O. cor* on the proximal, medial, and distal surfaces of the inside of gills 1 through 8 differ from one another for all three comparisons (proximal by medial, $\chi^2 = 57.2$, df = 14, $P < .001$; proximal by distal, $\chi^2 = 80.6$, df = 14, $P < .001$; distal by medial, $\chi^2 = 69.8$, df = 14, $P < .001$). Thus, the distribution of *O. cor* over the inside surfaces of the proximal, medial, and distal regions of individual gills differs from gill to gill. The number of *O. cor* on the outside surfaces is very small, so the distribution on these surfaces remains unclear (Table I).

The distribution of the totals for gills 1–8 of *O. cor* on the proximal (1527), medial (1987), and distal (103) surfaces of the inside of the gills (Table I) does not differ from the totals for the proximal, medial, and distal surfaces of the outside ($\chi^2 = 5.5$, df = 4, $P < .05$). This lack of difference is unlike our findings with *O. angulata* and may be due to small numbers of *O. cor* on the outside (Table I).

Comparison of O. angulata *and* O. cor *distributions*

The distributions of *O. angulata* and *O. cor* on the inside surfaces of gills 1 through 8 (gill totals) are significantly different from each other ($\chi^2 = 1103.4$, df = 14, $P < .001$). For example, gill 7 has the highest number (514) of *O. angulata* on the inside, whereas gill 4 has the highest number (1129) of *O. cor* on the inside (Table I). Figure 2 illustrates how differently *O. angulata* and *O. cor* are distributed on the inside surfaces of the gills.

Less than 2% of the *O. cor* were found on the outside gill surfaces, whereas 28% of the *O. angulata* were attached to the outside surfaces (Table I). Although these distributions were significantly different ($\chi^2 = 59.0$, df = 14, $P < .001$), the very low numbers of *O. cor* found on the outside make this comparison of questionable biological importance.

The distributions of *O. angulata* and *O. cor* on the proximal, medial, and distal segments of the inside surfaces of gills 1 through 8 (Table I) are different from one another ($\chi^2 = 64.8$, df = 4, $P < .001$). Both species have about 55% on the medial gill region but differ on the proximal and distal regions. A similar comparison for the barnacles distributed over the outside surfaces shows no significant difference ($\chi^2 = .41$, df = 4, $P < .05$).

Distribution of barnacles on crabs of different sizes

In an earlier study (Jeffries *et al.*, 1992), we divided the sample of crabs into two size categories: those with carapace widths below 70 mm (n=87), and those above 70 mm (n = 173). This size criterion was chosen because crabs larger than 70 mm are much more likely to be infested and have heavier infestations, and because the crab's sexual maturity probably begins at 70 mm (instar 14) (Jeffries *et al.*, 1992). This same carapace size (70 mm), was used to divide the crabs into two groups—larger and smaller—for the following comparisons of distributions.

For both species of barnacles, distribution on the inside of gills 1 through 8 (gill totals) of smaller crabs differs from the distribution on larger crabs (*O. angulata*: $\chi^2 = 26.2$, df = 14, $P < .02$; *O. cor*: $\chi^2 = 25.3$, df = 14, $P < .05$). For example, gill 7 bears 17% (11) of the *O. angulata* on the smaller crabs, whereas gill 7 bears 42% (503) of the *O. angulata* on the larger crabs (Table II). The distribution of *O. cor* on the inside of gills 1 through 8 (gill totals) on crabs of less than 70 mm carapace width also differs from the distribution on crabs larger than 70 mm.

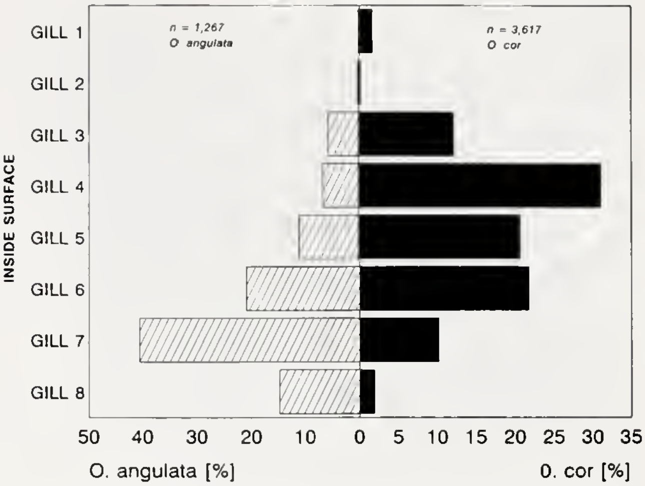

Figure 2. The percent distribution of 1267 *Octolasmis angulata* is compared with the percent distribution of 3617 *Octolasmis cor* on the inside (hypobranchial) surfaces of gills 1 through 8.

The distributions of *O. angulata* on the proximal, medial, and distal segments of the inside surfaces of gills 1 through 8 of smaller crabs were not significantly different from the distribution observed on larger crabs ($\chi^2 = .34$, df = 4, $P > .05$). This was also true for *O. cor* ($\chi^2 = 1.6$, df = 4, $P > .05$).

Table II also shows that smaller crabs (<70 mm) have fewer individual barnacles in their gill chambers than do the larger (>70 mm) crabs. Only two of the smaller crabs had more than 10 barnacles. Thus, crab size and barnacle density go hand-in-hand.

Effects of crowding on barnacle distributions

In analyzing barnacle numbers and barnacle distribution as a function of density, two points must be considered.

First, the "host unit" should be the gill chamber and not the individual crab. We think this because, as cyprids explore a given gill chamber, they can monitor directly only those conditions (whether biotic, *e.g.*, other cyprids or metamorphosed barnacles, or abiotic, *e.g.*, currents and oxygen concentrations) in that chamber. Of course, the two chambers of a crab are not wholly independent; for example, they have in common a crab of the same size,

Table II

The distribution of O. angulata *over the inside (hypobranchial) gill surfaces of 23* S. serrata *with carapace widths less than 70 mm and 120* S. serrata *greater than 70 mm (top), and the distribution of* O. cor *over the inside gill surfaces of 44* S. serrata *with carapace widths less than 70 mm and 156* S. serrata *greater than 70 mm (bottom)*

Octolasmis angulata

	Crabs < 70 mm; Inside of gills				Crabs > 70 mm; Inside of gills				
Gill Number	Proximal	Medial	Distal	Totals	Proximal	Medial	Distal	Totals	In + Out Totals
1	0	0	0	0	2	1	0	3	3
2	0	0	0	0	0	0	2	2	2
3	0	3	0	3	8	44	17	69	72
4	2	4	0	6	17	50	11	78	84
5	8	5	1	14	74	43	9	126	140
6	8	13	3	24	122	103	16	241	265
7	4	7	0	11	148	317	38	503	514
8	3	4	0	7	85	90	5	180	187
TOTALS	25	36	4	65	456	648	98	1202	1267
ON RAKERS	0	0	0	0	5	0	0	5	5
				65				1207	1272

Octolasmis cor

	Crabs < 70 mm; Inside of gills				Crabs > 70 mm; Inside of gills				
Gill Number	Proximal	Medial	Distal	Totals	Proximal	Medial	Distal	Totals	In + Out Totals
1	1	0	0	1	29	27	3	59	60
2	0	0	0	0	2	2	4	8	8
3	5	14	0	19	128	275	20	423	442
4	15	9	0	24	525	564	14	1103	1127
5	10	16	0	26	282	425	18	725	751
6	7	17	2	26	368	376	19	763	789
7	8	18	1	27	125	200	16	341	368
8	0	1	0	1	22	41	6	69	70
TOTALS	46	75	3	124	1481	1910	100	3491	3615
ON RAKERS	1	0	0	1	4	0	0	4	5
				125				3495	3620

general condition, health, and molt cycle stage, and a history of habitats visited.

Second, the density of barnacles in a chamber should be based on the sum of all barnacles found there. Thus, *O. angulata, O. cor,* unidentified specimens (mostly subadults), peduncles, and cyprids were all counted. The numbers of each of these categories for the 6648 barnacles observed are provided in the Materials and Methods section.

The first three columns of Table III present barnacle densities per chamber in increments of 10, the total number of chambers, and the total number of all barnacles per chamber. These data demonstrate that most chambers (292) had only 1 to 10 barnacles.

The remaining columns in Table III present the number of chambers and the number of barnacles, both *O. cor* and *O. angulata,* on the inside and outside gill surfaces. Both species are usually found exclusively on the inside gill surfaces when the barnacle density within the chamber is less than 20. This pattern continues to hold for *O. cor* at densities of 100 or more, but at densities above 20, *O. angulata* occurs on both the inside and outside gill surfaces (Fig. 3).

The above results are of limited significance because they do not allow discrimination between the two mitigating factors, crab size and barnacle density. Small crabs have fewer barnacles.

In an attempt to separate these two factors, a subset of crabs with similar carapace widths, between 70 and 90 mm, was considered; they were small- to medium-sized adults representing instars 14 to 16 (Ong, 1966). These crabs were separated into two groups: one group with from 1 to 20 barnacles per chamber (low density), and one group with from 21 to 98 barnacles (high density). All species and stages were counted.

The distributions of *O. angulata* over the inside surfaces of gills 1 through 8 (gill totals) of the low and high density groups were not significantly different from each other ($\chi^2 = 6.6$, df = 14, $P > .05$). Moreover, the distributions of the totals of *O. angulata* on the proximal, medial, and distal segments of the inside surfaces of gills 1 through 8 of both groups were also not significantly different ($\chi^2 = 2.1$, df = 4, $P > .05$).

The distributions of *O. cor* over the inside surfaces of gills 1 through 8 (gill totals) for the low density group and for the high density group (Table IV) are also not significantly different from each other ($\chi^2 = 21.2$, df = 14, $P > .05$). But the distributions of the totals of *O. cor* on the proximal, medial, and distal segments of the inside surfaces of gills 1 through 8 of the low density group and the high density group are significantly different ($\chi^2 = 13.8$, df = 4, $P < .01$). Thus, at higher densities there are more *O. cor* on the proximal portion of the gills and fewer (less than 1%) on the distal portion in comparison with the distribution observed in the low density chambers (Table IV).

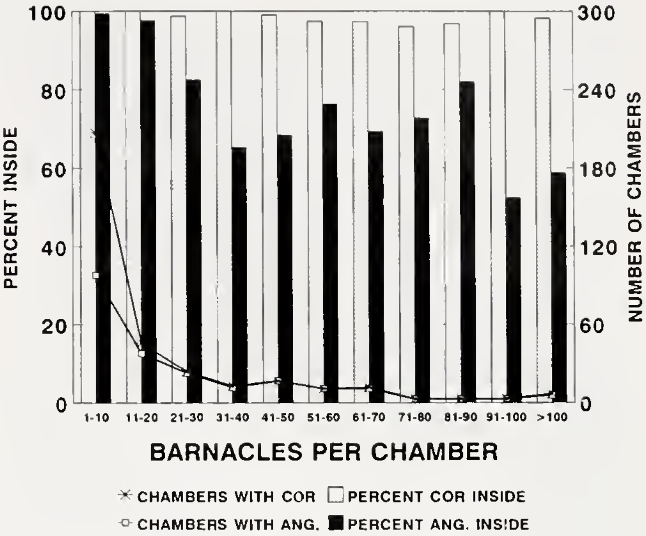

Figure 3. The percentages of *Octolasmis angulata* and *Octolasmis cor* on the inside (hypobranchial) surfaces of gills 1 through are shown for chambers with barnacle densities that increase by 10. On the second Y axis the number of chambers with *Octolasmis angulata* and *Octolasmis cor* is shown with connected symbols.

Discussion and Conclusions

The ability of barnacle cyprids to locate highly specific substrates (microhabitats) for colonization is well documented in the literature (Foster, 1987). Hui and Moyse (1987) have suggested that the cyprids of "parasitic or obligate commensal species . . . must be [attracted] to the host animal." Moyse (1971) reported that *Megatrema anglicum* is secondarily attracted to conspecifics after the host coral has been located.

Most species within the genus *Octolasmis* colonize a limited number of host species (usually decapods) and are typically very selective as to the site of attachment on the body of the host. Moreover, a symbiont may exploit only a subset of a host population, partitioning the population by factors such as age, sex, and environment. For example, cyprids of *O. angulata* and *O. cor* prefer adult hosts, and small juvenile crabs are rarely colonized (Jeffries *et al.*, 1992). *Callinectes sapidus* harbors *O. mülleri* in the Chesapeake Bay, from the mouth of the Rappahannock River south, but not to the north (van Engel, pers. comm.).

Our results demonstrate that the spatial distribution of *O. angulata* and *O. cor* on the gills of *Scylla serrata* is nonrandom and does not reflect available surface area as

Table III

The total numbers of O. cor *and* O. angulata *over the inside (hypobranchial) and outside (epibranchial) of* S. serrata *gill surfaces is given for gill chambers according to the range in density of all barnacles per chamber*

Range of density	Total number of chambers	Total number of barnacles	Number of chambers with *cor*	Total *cor* inside	Total *cor* outside	Number of chambers with *ang.*	Total *angulata* inside	Total *angulata* outside
1–10	292	985	207	522	0	98	157	1
11–20	49	739	46	478	0	38	123	3
21–30	24	594	24	378	5	23	94	20
31–40	14	506	13	240	0	12	96	51
41–50	17	765	17	418	4	17	180	83
51–60	11	602	11	298	8	11	145	45
61–70	12	791	12	427	12	11	113	50
71–80	3	225	3	120	5	3	48	18
81–90	3	259	3	148	5	3	50	11
91–100	3	285	3	138	0	3	77	70
>100	7	897	7	456	8	6	190	133
	435	6648	346	3623	47	225	1273	485

Table IV

The distribution of O. cor *on the inside (hypobranchial) surfaces of the gills 1 to 8 in 169 gill chambers of 99* S. serrata *with carapace widths of 70 to 90 mm*

Gill Number	Chambers with 1 to 20 octolasmids				Chambers with 21 to 98 octolasmids				In + out totals
	Proximal	Medial	Distal	Totals	Proximal	Medial	Distal	Totals	
1	0	1	0	1	0	3	0	3	4
2	0	1	2	3	0	1	0	1	4
3	24	52	6	82	9	32	2	43	125
4	95	97	5	197	68	62	0	130	327
5	46	112	2	160	38	57	0	95	255
6	61	112	7	180	36	34	0	70	250
7	39	78	10	127	12	31	0	43	170
8	3	16	1	20	7	8	2	17	37
TOTALS	268	469	33	770	170	228	4	402	1172
ON RAKERS	1	0	0	1	0	0	0	0	1
									1173

measured by gill length or gill area. These findings, although more detailed, are consistent with what has been reported for *O. mülleri* on *Callinectes sapidus* (Walker, 1974; Jeffries and Voris, 1983; Gannon, 1990) and for *O. angulata* and *O. cor* on *Scylla serrata* (Bullock, 1964; Arudpragasam, 1967; Venkateswaran and Fernando, 1982; Jeffries *et al.*, 1982, 1992).

In this study, we found that the distributions of *O. angulata* and *O. cor* on the inside and outside surfaces of the gills are distinct. The distributions over the proximal, medial, and distal surfaces (inside and outside gill surfaces) of individual gills also vary from gill to gill. Although Bullock (1964), Arudpragasam (1967), and Venkateswaran and Fernando (1982) all presented some numerical data on distributions, they did not make comparisons, and their categories are not directly comparable to ours.

If adult barnacle distributions mirror cyprid settlement patterns, then our results suggest that the cyprids of *O. angulata* and *O. cor* distribute themselves differently. Bullock (1964) did not address this point, but he did present tabular data on the distribution of four variants of *O. cor* removed from an unspecified number of *S. serrata*. For each variant he gave the distribution of the barnacles over gills 2 through 8 and over each of four gill regions. Using his sketches, we pooled his data and assumed that his varient "a" was *O. angulata* and his variants "b," "c," and "d" were *O. cor* (Jeffries *et al.*, 1991). The distributions of these two species over gills 2 through 8 are significantly different ($\chi^2 = 141.6$, df = 12, $P < .001$), thus corroborating our findings.

Both *O. angulata* and *O. cor* are distributed on the gills of smaller crabs (<70 mm carapace width) in a pattern that is distinct from that over the gill surfaces of larger crabs. Our data also reveal different patterns of distribution under different densities. Both *O. angulata* and *O. cor* are nearly always found on the inside gill surfaces when the density of all barnacles is less than 20 per chamber; this continues to hold for *O. cor* as densities increase to 100 or more per chamber. At densities above 20 per chamber, however, *O. angulata* appears on both the inside and outside gill surfaces.

The above conclusions are not independent, because they do not separate crab size from barnacle density. Recall that smaller crabs (<70 mm) have fewer individual barnacles in their gill chambers (see Fig. 3 on page 190 in Jeffries *et al.*, 1992).

A comparison of distributions on crabs of similar sizes, but containing different densities of barnacles, leads to different conclusions. The distributions of *O. angulata* on the inside gill surfaces of crabs of high and low densities do not differ. Thus, density did not affect how the cyprid of this species settled on the inside of the gills. But even among similar sized crabs, when barnacle densities were less than 20 per chamber, there were no *O. angulata* on the outside surface of the gills. Thus, density does seem to be a crucial factor in determining when *O. angulata* selects the outside surface of gills.

The distributions of *O. cor* on the inside gill surfaces of crabs of high and low densities do not differ over gills 1 through 8, but do differ over the proximal, medial, and distal portions. Thus, density does appear to have some effect on how the cyprids of *O. cor* are distributed on the inside surfaces of gills.

Determination of settlement sites

Adults of *O. angulata* and *O. cor* are permanently fixed to the substrate (gill lamellae) at the sites where their cyprids settled. Thus it is the cyprid larva that makes the key decision about where the adult barnacle will live.

Having established that the congeneric species *O. angulata* and *O. cor* live together in the gill chambers of the same host, *S. serrata*, the intriguing question is what factors direct the cyprids to select different settlement sites within the gill chambers. Site selection by *O. mülleri* cyprids on *Callinectes sapidus* (Jeffries and Voris, 1983) and the octolasmids on *Scylla* under study here is not random. Nor is site selection by cyprids governed by available space alone, whether the measurement is made by gill length or gill area. The high degree of similarity among the gills argues against the idea that substrate is an important factor for site selection within the gill chamber.

Several lines of reasoning support the hypothesis that current flow through the gill chamber (see Wolvekamp and Waterman, 1960; McMahon and Wilkens, 1983) is the single most important factor influencing site selection by octolasmid cyprids. First, the direction, path, and intensity of current flow govern the distribution of both food and oxygen within the gill chamber. Flow through the chamber also influences the disposal of respiratory and metabolic waste products and, by affecting sedimentation rates, influences fouling.

Water enters the crab hypobranchial chamber through openings at the bases of the thoracic appendages, and this occurs as a result of negative pressure created in the branchial chamber by the pumping action of the scaphognathites (Arudpragasm and Naylor, 1964a, b; Hughes *et al.*, 1969; McDonald, 1977; Taylor, 1982). Thus we assume that octolasmid cyprids entering *S. serrata* first encounter the inner sides and the proximal regions of the gills. This is likely the case as the cyprids converge on intermolt crabs. But at the molt of host mangrove crabs, when the major infestation by octolasmid cyprids takes place (Jeffries *et al.*, 1989), the scaphognathites are inactive for a time. With complete cessation of pumping, pressure in the branchial spaces immediately falls to zero (Hughes *et al.*, 1969), so factors other than current may be governing cyprid behavior during this period of quiescence. As the crab exoskeleton splits on the outer surface of each gill, proximal to distal along the afferent branchial blood vessel, the octolasmid cyprids would have access to the newly exposed gill.

Among symbiotic octolasmid barnacles, cyprid orientation is correlated with the direction of current on the gill surface of lobsters (Dinamani, 1964) and on sea snakes (Jeffries and Voris, 1979).

The orientation of the barnacle capitulum on the gills of lobsters has been studied by Dinamani (1964), and on the gills of *Scylla* by Bullock (1964). Although neither of these studies focused on cyprids or incorporated current flow measurements, both reported that the anterior-posterior orientation of the capitulum tends to parallel the major flow patterns in the chambers (Wolvekamp and Waterman, 1960; McMahon and Wilkens, 1983).

Our study suggests that, although current is likely an important factor influencing settlement patterns, it may not be the only factor. *O. angulata* and *O. cor* cyprids distribute themselves differently, and *O. angulata* distributes itself differently at low and high densities. Both of these behaviors might be explained by current flow, but other explanations, including historical and biotic factors, deserve consideration and testing. For example, *O. angulata* and *O. cor* may have different distributions because one species is a generalist, "averaging" optimal settlement sites over many host species, whereas the other is a specialist and is optimizing its distribution for a single host species, *Scylla serrata*. *O. angulata* may be the generalist with 17 known host species, whereas *O. cor*, known from 6 host species (Jeffries *et al.*, 1982), may be the more specialized of the two.

Although the density of adult barnacles may influence current flow within the gill chamber, the density of cyprids within the chamber just after molt would have negligible effect on current. Thus, *O. angulata* cyprids may assess overall cyprid densities (encounters) on the post-molt crab and distribute on the inside versus the outside accordingly.

Acknowledgments

We thank the staff of the Phuket Marine Biological Center for their logistical support and the use of their facilities. In particular, we are grateful to the Director, Mr. Udom Bhatia, for his generous cooperation. Special thanks are due to Mr. Boonchoy Kuoyratanakul, a fisherman, who collected most of the crabs, and Mr. Saengdee Chailert, who received crabs from fishermen for us. We thank Daryl Karns for valuable comments on earlier drafts of the manuscript. Support from the Dickinson College Faculty Research Fund and the Field Museum of Natural History made this investigation possible.

Literature Cited

Arudpragasam, K. D. 1967. Distribution and variation in form of the cirripede *Octolasmis cor* (Aurivillius, 1893) in relation to the respiratory current of its host *Scylla serrata*. *Ceylon J. Sci.* **7:** 105–115.

Arudpragasam, K. D., and E. Naylor. 1964a. Gill ventilation and the role of reversed respiratory currents in *Carcinus maenas* (L.). *J. Exp. Biol.* **41:** 299–307.

Arudpragasam, K. D., and E. Naylor. 1964b. Gill ventilation volumes, oxygen consumption and respiratory rhythms in *Carcinus maenas* (L.). *J. Exp. Biol.* **41:** 309–321.

Aurivillius, C. W. S. 1892. Neue Cirripeden aus dem Atlantischen, Indischen und Stillen Ocean. Ofversigt af Kungliga Svenska Vetenskapsakademiens Forhandlingar. **49:** 123–134.

Aurivillius, C. W. S. 1894. Studien Uber Cirripeden. I. Morphologie und Sysematik neuer oder wenig bekannter cirripeden. Kungliga Svenska Vetenskapsakademiens Handglingar. **26:** 1–89.

Bullock, J. A. 1964. Variation in the commensal cirriped, *Octolasmis cor* (Aur.), in relation to its position in the branchial chamber of *Scylla serrata* Forskål. *Fed. Museums J.* **IX:** 84–94.

Coker, R. E. 1902. Notes on a species of barnacle (*Dichelaspis*) parasitic on the gills of edible crabs. *U. S. Fish Comm. Bull.* **21**: 399–412.

Darwin, C. 1851. A monograph on the sub-class Cirripedia. 1. The Lepadidae: 1–400, 10 pls. (Ray Society, London).

De Turk, W. E., 1940. The parasites and commensals of some crabs of Beaufort, North Carolina. Ph.D. thesis, Duke University.

Dinamani, P. 1964. Variation in form, orientation and mode of attachment of the cirriped, *Octolasmis stella* (Ann.), symbiotic on the gills of lobster. *J. Animal Ecol.* **33**(2): 357–362.

Forskål, P. 1755. Descriptions Animalium, avium, amphibiorum, insectorum, vermium, quae in itinere orientali observavit. 19+xxxii + 64 pp. 1 map. Hafniae.

Foster, B. A. 1987. Barnacle ecology and adaptation. Pp. 113–133 in *Crustacean Issues 5, Barnacle Biology,* A. J. Southward, ed. A. A. Balkema, Rotterdam.

Gannon, A. T. 1990. Distribution of *Octolasmis muelleri,* an ectocommensal gill barnacle on the blue crab. *Bull. Mar. Sci.* **46**(1): 55–61.

Hughes, G. M., B. Knights, and C. A. Scammel. 1969. The distribution of PO_2 and hydrostatic pressure changes within the branchial chambers in relation to gill ventilation of the shore crab *Carcinus maenas* L. *J. Exp. Biol.* **51**: 203–220.

Hui, E., and J. Moyse. 1987. Settlement patterns and competition for space. Pp. 363–376 in *Crustacean Issues 5, Barnacle Biology,* A. J. Southward, ed. A. A. Balkema, Rotterdam.

Humes, A. G. 1941. Notes on *Octolasmis müelleri* (Coker), a barnacle commensal on crabs. *Trans. Amer. Micros. Soc.* **60**: 101–103.

Humes, A. G. 1942. The morphology, taxonomy, and bionomics of the nemertean genus *Carcinonemertes. Illinois Biol. Monogr.* **18** (4): 1–105.

Jeffries, W. B., and H. K. Voris. 1979. Observations on the relationship between *Octolasmis grayii* (Darwin, 1851) (Cirripedia, Thoracica) and certain marine snakes (Hydrophiidae). Crustaceana **37**(2):123–132.

Jeffries, W. B., and H. K. Voris. 1983. The distribution, size, and reproduction of the pedunculate barnacle, *Octolasmis müelleri* (Coker, 1902), on the blue crab, *Callinectes sapidus* (Rathbun, 1896). *Fieldiana NS* **16**: 1–10.

Jeffries, W. B., and H. K. Voris, and C. M. Yang. 1982. Diversity and distribution of the pedunculate barnacle *Octolasmis* in the seas adjacent to Singapore. *J. Crustacean Biol.* **2**(4): 562–569.

Jeffries, W. B., H. K. Voris, and C. M. Yang. 1985. Growth of *Octolasmis cor* (Aurivillius, 1892) on the gills of *Scylla serrata* (Forskål, 1755). *Biol. Bull.* **169**: 291–296.

Jeffries, W. B., H. K. Voris, and C. M. Yang. 1989. A new mechanism of host colonization: pedunculate barnacles of the genus *Octolasmis* on the mangrove crab *Scylla serrata. Ophelia* **31**(1): **51–58**.

Jeffries, W. B., H. K. Voris, and C. M. Yang. 1991. Species recognition among the pedunculate barnacles (Cirripedia: Thoracica) on the mangrove crab, *Scylla serrata.* Raffles *Bull. Zool.* **40**(1): 83–92.

Jeffries, W. B., H. K. Voris, and S. Poovachiranon. 1992. Age of the mangrove crab, *Scylla serrata,* at colonization by stalked barnacles of the genus *Octolasmis. Biol. Bull.* **182**: 188–194.

Lang, W. H. 1976. The larval development and metamorphosis of the pedunculate barnacle *Octolasmis müelleri* (Coker, 1902) reared in the laboratory. *Biol. Bull.* **150**: 255–267.

McDonald, D. G. 1977. Respiratory physiology of the crab *Cancer magister.* Ph.D. Thesis, University of Calgary, Calgary, Alberta, Canada.

McMahon, B. R., and J. L. Wilkens. 1983. Ventilation, perfusion, and oxygen uptake. Pp. 289–372 in *The Biology of the Crustacea, Vol 5.,* L. H. Mantel, ed. Academic Press, New York.

Mosteller, F., and R. E. K. Rourke. 1973. *Study Statistics, Nonparametrics and Order Statistics.* Addison-Wesley Publishing Co., Reading, MA. 395 pp.

Moyse, J. 1971. Settlement and growth pattern of the parasitic barnacle, *Pyrgoma anglicum.* Pp. 125–141 in *Fourth European Marine Biology Symposium,* D. J. Crisp, ed. Cambridge University Press, Cambridge.

Ong, K. S. 1966. Observations on the post-larval life history of *Scylla serrata* Forskål, reared in the laboratory. *Malaysian Agricultural J.* **45**(4): *429–443.*

Overstreet, R. M. 1983. Metazoan symbionts of crustaceans. Pp. 155–250 in *The Biology of the Crustacea, vol 6,* A. J. Provenzano, ed. Academic Press, New York.

Pearse, A. S. 1932. Observations on the parasites and commensals found associated with crustaceans and fishes at Dry Tortugas, Florida. *Carnegie Institution of Washington Publication No.* **435**: 103–115.

Pearse, A. S. 1947. On the occurrence of ectoconsortes on marine animals at Beaufort, N. C. *J. Parasitol.* **33**: 453–458.

Shields, J. D. 1992. Parasites and symbionts of the crab *Portunus pelagicus* from Moreton Bay, Eastern Australia. *J. Crustacean Biol.* **12**(1): 94–100.

Taylor, E. W. 1982. Control and co-ordination of ventilation and circulation in crustaceans: responses to hypoxia and exercise. *J. Exp. Biol.* **100**: 289–319.

Venkateswaran, K., and S. A. Fernando. 1982. Distribution and variation in form of the epizoic cirriped *Octolasmis cor* (Aurivillius, 1893). *Indian J. Mar. Sci.* **11**: 243–246.

Walker, G. 1974. The occurrence, distribution and attachment of the pedunculate barnacle *Octolasmis müelleri* (Coker) on the gills of crabs, particularly the blue crab, *Callinectes sapidus* Rathbun. *Biol. Bull.* **147**: 678–689.

Wolvekamp, H. P., and T. H. Waterman. 1960. Respiration. Pp. 35–100 in *The Physiology of Crustacea 1,* T. H. Waterman, ed. Academic Press, New York.

Zevina, G. B. 1982. Cirripede crustaceans of the suborder Lepadomorpha (Cirripedia, Thoracica) of the World Ocean. Part 2, *Fauna SSSR* **133**: 1–224.

Reference: *Biol. Bull.* **187**: 355–362. (December, 1994)

Identification of Synaptophysin-Like Immunoreactivity in the Sea Anemone *Condylactis gigantea* (Cnidaria: Anthozoa)

CHRISTIAN DELLACORTE[1,*], WILLIAM O. MCCLURE[1], AND D. LYNN KALINOSKI[2]

[1]*Department of Neurobiology, University of Southern California, Los Angeles, California 90089-2520, and* [2]*Monell Chemical Senses Center, Philadelphia, Pennsylvania 19104*

Abstract. Synaptophysin is a membrane protein of synaptic vesicles that serves as an antigenic marker for nervous and endocrine systems in mammals. Monoclonal antisera generated against synaptophysin were used for immunocytochemical staining in tissues of the tentacles of the sea anemone *Condylactis gigantea* (Cnidaria: Anthozoa). Specific staining, visible at the light and electron microscope levels, was found in the tentacle. Proteins were extracted from the tissues and solubilized. Using SDS-polyacrylamide gel electrophoresis and Western blotting, we identified proteins with apparent molecular weights of 38,000, 78,000, and 114,000. The data suggest the tissues of this anthozoan contain synaptophysin-like proteins with molecular properties similar to those of mammalian neurons.

Introduction

Neural communication is accomplished at the synapse, a highly specialized structure where a nerve cell comes into apposition with its target. Synaptic vesicles, multimolecular neurotransmitter "packets" within neurons, are well-known storage compartments that sequester peptide and nonpeptide transmitter molecules used during the intercellular signaling process (Kelly, 1993). The release of neurotransmitter is a highly regulated, plastic event that can be fine-tuned by the neuron through a series of changes in intracellular levels of seconds messengers and related protein phosphorylation events. The modulatory effects take place at many sites including the pre- and postsynaptic terminals and the synaptic vesicles (Kelly, 1993). In the last few years progress has been made in investigating the molecular composition of mammalian synaptic vesicles and, in particular, in elucidating their membrane composition. Results suggest vesicles contain highly specific groups of abundant membrane proteins that participate in transmitter release. These groups include proteins thought to control the mobilization of vesicles (Sudhof *et al.*, 1989; De Camilli *et al.*, 1990), those involved in intracellular "trafficking" and docking (Schiavo *et al.*, 1992), and those involved in the formation of fusion pores between secretory vesicles and the plasma membrane (Jessell and Kandel, 1993).

Synaptophysin (p38) is a major integral membrane protein found in clear, small synaptic vesicles (SSVs) present in the mammalian spinal cord and retina, at neuromuscular junctions, and in the adrenal medulla (Wiedenmann and Franke, 1985). The protein, thought to be involved in the formation of transient fusion pores, shares structural features with gap junction channels (Buckley *et al.*, 1987; Thomas *et al.*, 1988; Sudhof and Jahn, 1991). Also known as synaptophysin I, one of two isoforms abundant in the brain, it represents up to 0.3% of the total protein in the cerebral cortex or 7% of synaptic vesicle protein (Knaus *et al.*, 1986; Jahn *et al.*, 1987; Wiedenmann and Franke, 1985). Synaptophysin has been isolated from several sources, sequenced, and found to be highly conserved (Leube *et al.*, 1987; Sudhof *et al.*, 1987; Johnston *et al.*, 1989; Cowan *et al.*, 1990).

Examination of neural transmission and neuroendocrine function in some lower organisms has not kept pace with that in more advanced organisms. The simplest metazoans known to possess a nervous system are those of

---

Received 13 January 1994; accepted 26 September 1994.

[*] Current address: Monell Chemical Senses Center, 3500 Market Street, Philadelphia, PA 19104.

the phylum Cnidaria whose members include the familiar hydra, jellyfish, sea anemones, and corals. The nervous system in these organisms has been described functionally and structurally as a diffuse nerve net (Bullock and Horridge, 1965). Yet some studies have shown condensation of neural components that form "giant axons" or a neural plexus (Mackie, 1973, 1990; Van Marle, 1977; Spencer and Arkett, 1984). Elements of these nervous systems are known to include defined sensory cells and motor cells and their processes. The molecular structure of the neural elements, however, is largely unknown. Our work involves the use of immunocytochemical techniques, as well as protein isolation and light and electron microscopy, to study protein components of the nervous system in the subtropical sea anemone *Condylactis gigantea* (Cnidaria: Anthozoa). Results of our studies suggest that the tissues of this anthozoan contain proteins with synaptophysin-like molecular properties similar to those found in the nervous and endocrine systems of mammals.

Materials and Methods

Animals

Specimens of *C. gigantea* were obtained from a supplier in Los Angeles, California, and were kept in aquaria in aerated, filtered, recirculating natural seawater (24°C) obtained from the Catalina Marine Science Center (Santa Catalina Island, California). Animals acquired from local suppliers in Philadelphia, Pennsylvania, were kept in aquaria in aerated, filtered artificial seawater and were used within a few days of purchase. Specimens were maintained on a 12/12 photoperiod and fed a diet of *Artemia* nauplii, small pieces of squid, or both three times a week. Water was changed at 2-week intervals.

Anesthetic and tentacle removal

Animals were anesthetized by immersion in seawater containing succinylcholine chloride (67 μg/ml, Sigma Chemical Co., St. Louis, Missouri). Relaxed tentacles of the anesthetized animals were about the length of normal tentacles, but somewhat smaller in diameter. Tentacles were clamped with a hemostat at the junction of the oral disk and excised proximal to the clamp.

Light microscopic immunocytochemistry

Excised tentacles were placed in 2% paraformaldehyde in phosphate-buffered saline (PBS; 0.1 *M* sodium phosphate buffer, 0.9% NaCl), pH 6.5, for 2 h at room temperature before postfixation for 8 h at 4°C in 2% paraformaldehyde in PBS, pH 11 (Berod *et al.*, 1981). Samples were rinsed three times in PBS, pH 7.4, prior to cryoprotection by immersion for 12–24 h each in 10%, 20%, and 30% sucrose in PBS, pH 7.4, at 4°C. Tissue was placed in Tissue-Tek (Miles Inc., Elkhart, Indiana) and frozen in isopentane at liquid nitrogen temperatures. Twenty-micrometer sections were made on a Microm 500 M Cryostat (Zeiss Inc., Thornwood, New York) at −20°C and thaw-mounted on slides. Endogenous peroxidases were inactivated in 0.3% hydrogen peroxide in PBS for 20 min after a rinse in PBS for 15 min. After three successive 15-min rinses in PBS and a 1-h immersion in PBS containing 0.3% Triton X-100 and 10% normal serum (Vector Laboratories, Burlingame, California), all specimens were incubated at 4°C in mouse monoclonal primary antisera directed against (1) synaptophysin (SY38; Boehringer Mannheim Corp., Indianapolis, Indiana) at a 1:5 dilution of stock (10 μg/ml) for 48 h; or (2) synaptophysin (C7.2; Jahn *et al.*, 1985) at a 1:10,000 dilution of stock for 24 h. Three successive 15-min rinses in PBS were followed by incubation with a biotinylated goat–anti-mouse immunoglobulin, several PBS rinses, and incubation in an avidin–horseradish peroxidase complex (Vector Laboratories, Burlingame, California) following manufacturer's instructions. Tissues were incubated in a chromagen solution composed of equal volumes of 0.1% hydrogen peroxide and 0.5% 3,3′-diaminobenzidine tetrahydrochloride (DAB, Sigma Chemical Co., St. Louis, Missouri) in PBS.

Control procedures for immunostaining included replacement of the primary antibody with goat normal serum and deletion of the secondary antibody.

SDS-PAGE and Western blotting

To demonstrate the existence of synaptophysin in the sea anemone *C. gigantea*, we isolated the constituent proteins. To minimize protein contamination, food was withheld from anemones for 3 days before extraction. Whole anemones were cleaned of debris and weighed. Specimens were chilled for 15 min at −70°C before being quickly chopped into 1-cm^3 pieces and placed in SEDTA (20 m*M* Na-ACES buffer, 0.3 *M* sucrose, 2 m*M* EDTA, pH 7.4) for 15 min with intermittent gentle hand agitation to remove mucus. Minced tissue was transferred and homogenized in TME medium [10 m*M* tris(hydroxymethyl)-aminomethane (Tris) HCl, 3 m*M* $MgCl_2$, 2 m*M* K_2-ethylene glycol-bis(β-aminoethyl ether)-*N,N,N′,N′*-tetraacetic acid (EGTA), pH 8.2] in the presence of protease inhibitors (10 μg/ml leupeptin, 76.8 n*M* aprotinin, 0.7 μ*M* pepstatin, 0.83 m*M* benzamide, 0.23 m*M* phenylmethanesulfonyl fluoride, and 1 m*M* iodoacetamide) at 4°C. The homogenate was centrifuged at 800 × *g* (SS34 rotor) for 10 min at 0°C to remove insoluble debris. The supernatant was transferred and centrifuged at 9000 × *g* for

2 h at 0°C. The supernatant was reserved and stored at −70°C. Pelleted material was resuspended in TME containing 2% SDS, briefly homogenized, and centrifuged at 9000 × *g* for 2 h at 0°C. The supernatant was either used immediately or stored at −70°C. Protein content was determined by the method of Bradford (1976). Control procedures consisted of extraction of rat brain as described above.

Proteins were electrophoresed in 12.5% SDS-polyacrylamide gels by the method of Laemmli (1970) and transferred to nitrocellulose sheets. Western blotting was performed by the method of Towbin *et al.* (1979). In brief, blots were processed through incubations with blocking solution (5% skim milk in PBS) for 12 h at 4°C, then immunostained with one of the following at 4°C with gentle agitation: (1) monoclonal antibodies raised against synaptophysin (SY38; Boehringer Mannheim Corp., Indianapolis, Indiana) for 1 h at a 1:150 dilution; (2) monoclonal anti-synaptophysin (C7.2) for 3 h at a 1:2000 dilution; (3) rabbit polyclonal anti-synaptophysin (G95) for 3 h at a 1:1000 dilution; or (4) rabbit polyclonal anti-p29 for 5 h at a 1:1000 dilution. Incubations were followed by biotinylated goat-anti-mouse or goat–anti-rabbit immunoglobulin, several PBS rinses and incubation in an avidin–horseradish peroxidase complex (Vector Laboratories, Burlingame, California) following manufacturer's instructions. Conjugates were visualized using a 4-chloro-1-naphthol/peroxidase substrate system (Kirkegaard & Perry, Gaithersburg, Maryland).

Electron microscopic immunocytochemistry

Portions of tentacles were transferred to 4.0% paraformaldehyde/0.5% glutaraldehyde in 0.1 *M* PBS, pH 6.5, for 1 h at room temperature and were transferred to 4.0% paraformaldehyde/0.5% glutaraldehyde in PBS, pH 11, for 8 h at 4°C before washing in PBS, pH 7.4, and dehydration in a graded ethanol series. Samples were infiltrated and embedded in EM-BED-812 (Electron Microscopy Sciences, Ft. Washington, Pennsylvania) according to manufacturer's directions. Silver to gold sections were placed on nickel grids (Ted Pella Inc., Redding, California). Grids were floated on small amounts of reagent at room temperature as follows: (1) 1 h on 0.1 *M* PBS, pH 7.4; (2) 10 min on a saturated solution of sodium metaperiodate, followed by 30 min on several changes of PBS; (3) 1 h on 10% normal serum (Vector Laboratories, Burlingame, California), (4) three successive 30-min rinses on PBS; and (5) 4 h on monoclonal antiserum to synaptophysin (SY38; 1:200). Three successive 30-min rinses on PBS preceded floating the grids on a 1:40 dilution of gold-conjugated IgG (Janssen Life Sciences Products, Piscataway, New Jersey) for 1 h, and two successive 20-min distilled water rinses.

Grids were postfixed for 15 min on a drop of 2% glutaraldehyde and poststained in lead citrate and uranyl acetate, followed by two successive 15-min rinses on distilled water. Specimens were examined and photographed in a JEOL 100CXII electron microscope (JEOL USA, Inc., Peabody, Maine).

Controls consisted of replacement of the primary antiserum with nonimmune serum.

Results

Light microscopic immunocytochemistry

To demonstrate the presence of a synaptophysin-like protein in the tissues of this species, sections of tentacle were examined after application of a monoclonal synaptophysin I antiserum (SY38; Boehringer Mannheim Corp., Indianapolis, Indiana). SY38 has been shown to react with synaptophysin-containing presynaptic vesicles of cerebral and spinal neurons in a variety of species (Wiedenmann and Franke, 1985). The antibody does not recognize synaptophysin II (synaptoporin; Knaus *et al.*, 1990). Figure 1 shows a cross section of tentacle. A fine punctate pattern of immunoreactivity is located in the tissues at the center of the tentacle (Fig. 1A, B, C), an area in and around the mesoglea that is known to contain a dense plexus of nerve cell bodies and processes (Van Marle, 1977; C. DellaCorte, unpub. obs.). Immunolabeling was also assessed using the anti-synaptophysin I antibody C7.2, which recognizes a site in the cytoplasmic tail of the synaptic vesicle protein (Jahn *et al.*, 1985). The extent of immunolabeling and pattern of distribution within the tentacle did not significantly differ from that seen with SY38 (not shown). The staining pattern described was not seen when control IgGs were substituted.

Electron microscopic immunocytochemistry

Labeling was found at the surface of SSVs within the processes of the neural plexus (Fig. 2). Immunogold labeling was exclusive to the SSVs although not all vesicles within the same region showed reaction product. The distribution of the gold particles around SSVs was not homogenous; some regions contained more labeling than others, exhibiting a semi-"corona-like" decoration. Corona decoration of synaptic vesicles has been reported (De Camilli *et al.*, 1983; Wiedenmann and Franke, 1985). No appreciable amount of gold particles was observed over non-neural tissues, although some diffuse background staining was present. As with the sections processed for light microscopy, the specificity of labeling was assessed with controls. Sections adjacent to those immunolabeled with synaptophysin were re-

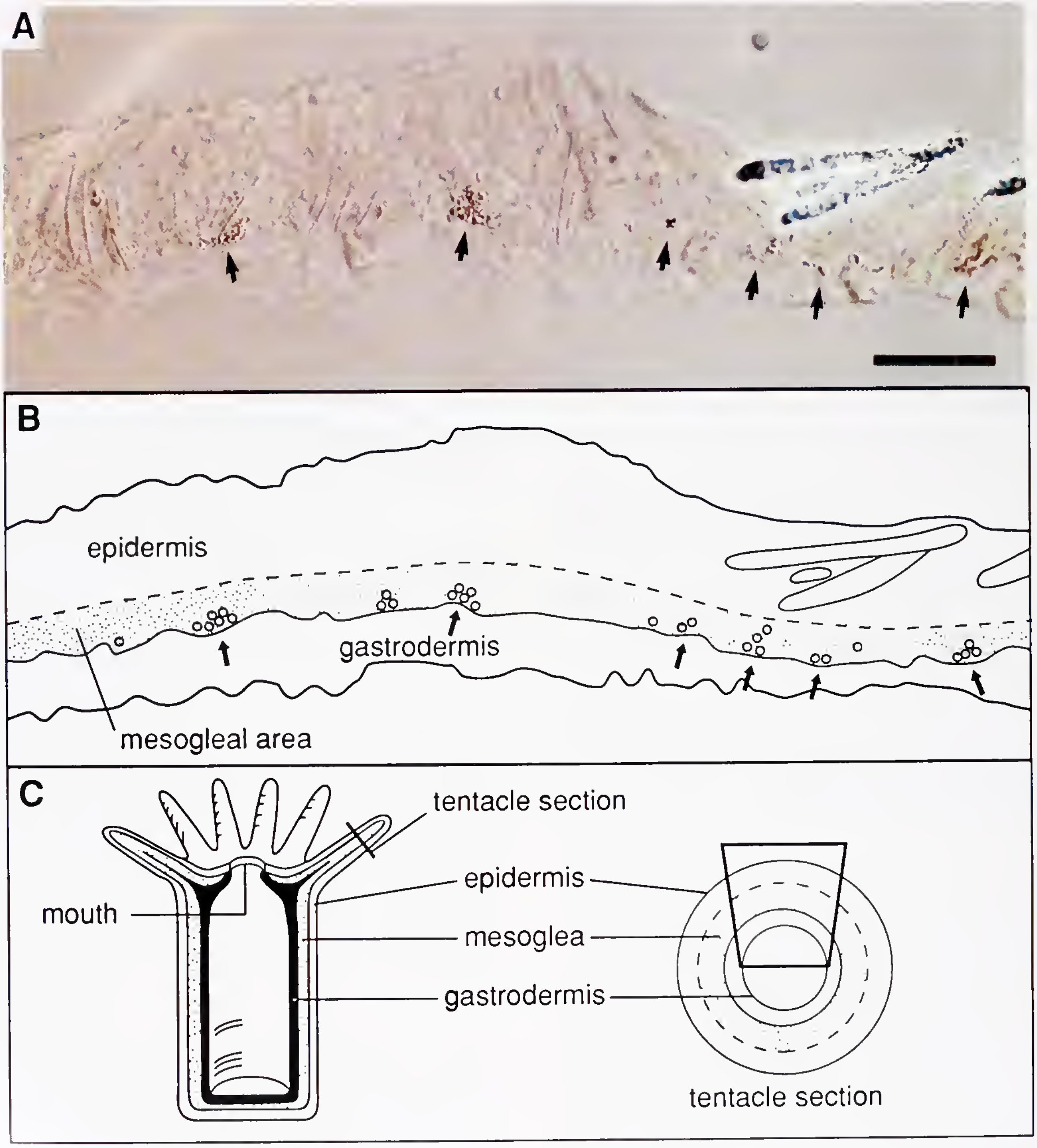
A
B
epidermis
gastrodermis
mesogleal area
C
tentacle section
mouth
epidermis
mesoglea
gastrodermis
tentacle section

Figure 1. (A) Light microscopy. Cross section of the tentacle of *Condylactis gigantea* immunolabeled with monoclonal anti-synaptophysin (SY38). The epidermal neural plexus consists of a layer, mid-tentacle, between the overlying epidermis and the basal gastrodermis. The section reveals specific, punctate-like labeling within and adjacent to the area of the neural plexus. The scale bar is 20 μm. (B) The epithelial layers of the tentacle are defined in this schematic representation. (C) The arrangement of the tissue within a cross section of tentacle.

acted with nonimmune serum. The labeling described above was absent, or showed only sparse and randomly scattered distribution of gold particles, demonstrating very low background.

Gel electrophoresis and Western blotting

To further demonstrate the presence of synaptophysin-like moieties in this species of anthozoan, we isolated the

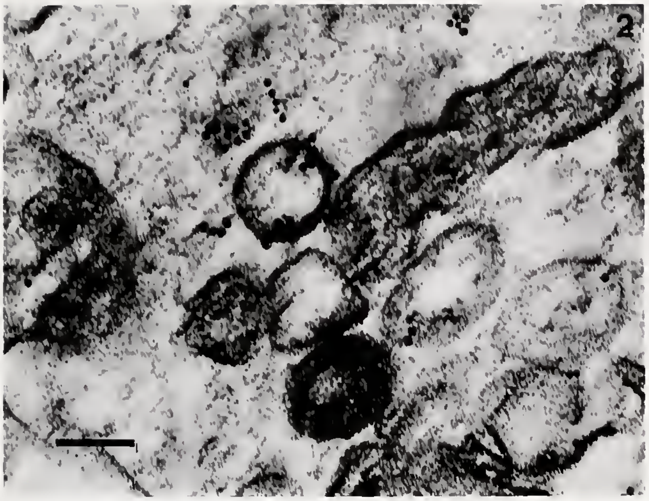

Figure 2. Electron microscopy. Cross section of the tentacle of *Condylactis gigantea* showing immunogold labeling of anti-synaptophysin (SY38). A semi-corona-like reaction product is seen at the surface of a clear-cored synaptic-like vesicle within a neurite in the neural plexus. The scale bar is 0.067 μm.

constituent proteins. When the proteins were visualized with SY38, bands with apparent molecular weights of 78,000 and 114,000 daltons were specifically labeled in both freshly extracted and stored protein fractions (Fig. 3, lanes 4 and 5). The 78,000-dalton protein appeared to predominate after storage, however (Fig. 3, lane 5). The molecular weight of these proteins does not differ considerably from synaptophysin dimers and trimers found in other species (Rehm *et al.*, 1986; Thomas *et al.*, 1988).

In addition, immunoreactivity was assessed with the anti-synaptophysin antibodies G95 (not shown) and C7.2 (Fig. 4). Patterns of synaptophysin-like immunoreactivity at MW_r 78,000 and 114,000 daltons were seen in freshly prepared extracts from *C. gigantea* (lane 4). Similar patterns were also seen in the extracts from rat brain (lane 3). In addition, immunoblotting labeled a 38-kD molecular weight fraction from the extract of *C. gigantea* that had been stored for 1 month at −70°C.

The protein fraction from *C. gigantea* was reacted with a monoclonal antibody to p29, an integral membrane protein present in small clear synaptic vesicles of neurons and endocrine cells. Antibodies to p29 have been shown to cross-react with synaptophysin I (Baumert *et al.*, 1990). Our results show a band with an apparent molecular weight of 29,000 daltons in extracts of tissue from rat brain (Fig. 5). Faint labeling at 38,000 daltons was seen in the protein sample from *C. gigantea* that had been stored (lane 5). A more robust banding pattern was found at 78,000 and 114,000 daltons in both the freshly extracted and the stored protein fractions (lanes 4 and 5). Immunolabeling of a 38-kD band in the rat extract was revealed at 1:150 to 1:200 antibody titers (not shown) (Baumert *et al.*, 1990).

Discussion

Many synaptic vesicle proteins, including synaptophysin, exist in multiple isoforms. At present, two forms of synaptophysin have been identified: synaptophysin I (Jahn *et al.*, 1985; Wiedenmann and Franke, 1985) and synaptophysin II/synaptophorin (Knaus *et al.*, 1990; Bixby, 1992). The properties of synaptophysin I, the focus of our study, have been extensively investigated and show that the glycoprotein contains four membrane-spanning domains, with cytoplasmic amino and carboxy termini (Johnston *et al.*, 1989). The highly immunogenic tail region encompasses 10 copies of a tyrosine-rich repeat (Sudhof *et al.*, 1987). A high degree of homology between synaptophysin I and II suggests that the two forms have similar transmembrane organization, although they share little sequence similarity in the region of the carboxyl-terminal tail (Knaus *et al.*, 1990; Bixby, 1992).

Immunocytochemical light microscopy results show that synaptophysin antibodies recognize an antigenic de-

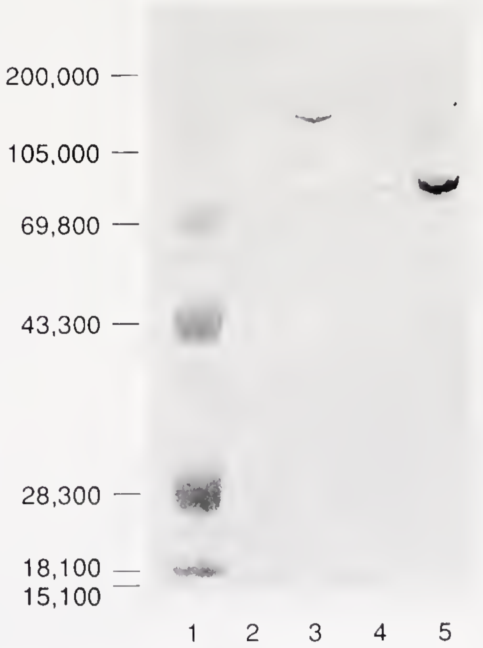

Figure 3. Western blotting. *Condylactis gigantea* synaptophysin-like proteins were visualized using a monoclonal synaptophysin antibody (SY38). Two prominent, high molecular weight protein bands are seen in the membrane fraction of the rat. A faint band is also seen at 38 kD. Bands of MW_r 78 kD and 114 kD were specifically labeled in the protein extract from *C. gigantea.* Lane 1: Molecular weight standards (MW_r); Lane 2: rat brain cytosolic fraction, 15 μg/lane; Lane 3: rat brain membrane fraction, 15 μg/lane; Lane 3: freshly prepared fraction of anemone membrane, 15 μg/lane; Lane 4: anemone membrane fraction stored at −70°C for 1 month, 15 μg/lane.

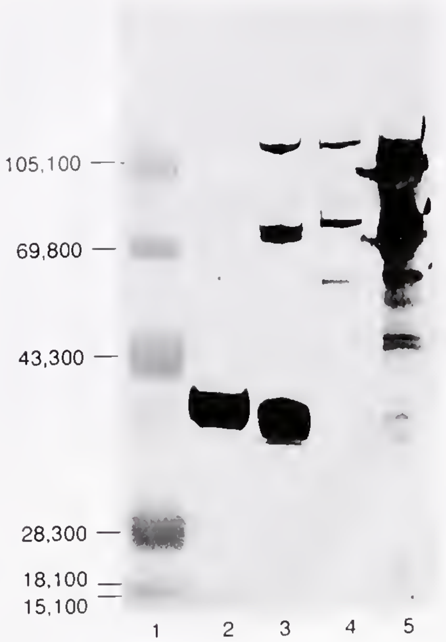

Figure 4. Western blotting. Immunolabeling with antisynaptophysin (C7.2) reveals protein bands at MW$_r$ 78 kD and 114 kD in the freshly made extract from the sea anemone *Condylactis gigantea*, while the stored extract presents another, faint band, at 38 kD. Lane 1: Molecular weight standards (MW$_r$); Lane 2: rat brain cytosolic fraction, 15 μg/lane; Lane 3: rat brain membrane fraction, 15 μg/lane; Lane 4: freshly prepared anemone membrane, 15 μg/lane; Lane 5: anemone membrane fraction stored at −70°C for 1 month, 15 μg/lane.

terminant in the tentacles of *C. gigantea*. In this anthozoan, the epidermal neural plexus forms a discrete layer that is sandwiched between the overlying surface layer of epithelial cells and the epidermal musculature that abuts the mesoglea (C. DellaCorte, unpublished results). As such, it is located almost in the center of the tentacle wall. The positioning of the immunostained product co-localizes with the neural plexus. Electron microscopy shows some antigenic surfaces to be small, clear-cored vesicles within the processes of the neural plexus. Large, dense-cored vesicles did not appear to be labeled. The pattern of labeling (*i.e.*, the overall punctate appearance in light microscopy and the semi-corona-like pattern seen at the surface of putative synaptic vesicles in electron microscopy) are in agreement with those seen in other studies (Bock and Helle, 1977; Navone *et al.*, 1986; Obata *et al.*, 1986; Alder *et al.*, 1992).

Although the synaptophysin molecule has a deduced molecular weight of 38,000 daltons, it has been suggested that the 76,000-dalton dimeric structure may be the native form (Jahn *et al.*, 1985; Wiedenmann and Franke, 1985; Navone *et al.*, 1986; Rehm *et al.*, 1986). Higher molecular weight homo-multimer complexes are known to form (Wiedenmann and Franke, 1985; Rehm *et al.*, 1986; Jahn *et al.*, 1987; Thomas *et al.*, 1988; Johnston and Sudhof, 1990). Dimers, trimers, and tetramers have been identified following chemical cross-linking studies (Rehm *et al.*, 1986; Thomas *et al.*, 1988; Fykse *et al.*, 1993). Disulfide cross-links also form spontaneously in nontreated extracts (Johnston and Sudhof, 1990; Fykse *et al.*, 1993) and upon storage (Rehm *et al.*, 1986; Thomas *et al.*, 1988). The apparent molecular weights of the synaptophysin-like proteins isolated from the tissues of the sea anemone *Condylactis gigantea* are within the parameters defined by these studies.

The variation in immunoblotting patterns between the SY38 and C7.2 antibodies in our study was initially surprising. Yet similar patterns have been noted. Studies by Wiedemann and Franke (1985) and Rehm *et al.* (1986) reported a lack of synaptophysin immunoreactivity in endocrine cells and a phylogenetic distribution restricted to mammals. Navone and co-workers (1986), however, suggested that these results may have resulted from a limited epitope specificity of SY 38. Their research, using several anti-synaptophysin antibodies including C7.2,

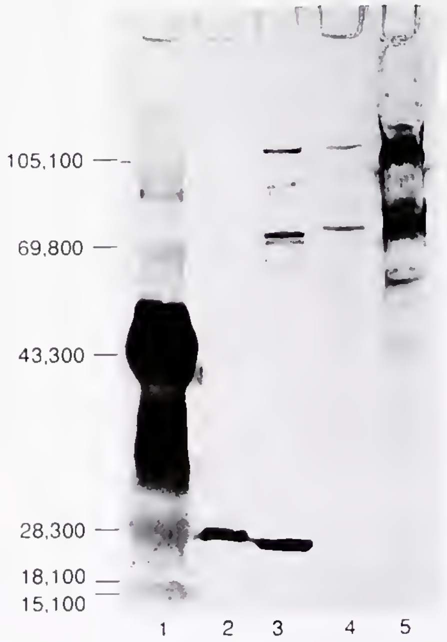

Figure 5. Western blotting. The putative synaptophysin-containing fraction from *Condylactis gigantea* was immunoblotted with monoclonal antibodies to p29. A band with an apparent molecular weight of 29 kD is seen in extracts of tissue from rat brain. In the extract from *C. gigantea* tissues, faint cross-reactive immunolabeling is seen at 38 kD, with more robust banding patterns at 78 kD and 114,000 kD. Lane 1: Molecular weight standards (MW$_r$); Lane 2: rat brain cytosolic fraction, 15 μg/lane; Lane 3: rat brain membrane fraction, 15 μg/lane; Lane 4: freshly prepared anemone membrane, 15 μg/lane; Lane 5: anemone membrane fraction stored at −70°C for 1 month, 15 μg/lane.

showed the presence of synaptophysin immunolocalization in many vertebrate classes down to amphibia, although not all species were found to display reactivity to every antibody. Furthermore, synaptophysin labeling was found in a variety of neuroendocrine cells.

The protein-containing extract from *C. gigantea* was further characterized by immunoblotting with antibodies directed against p29. The immunogenic tail of synaptophysin is a characteristic shared by the synaptic vesicle protein p29, an integral nonglycosylated protein. Studies demonstrate that this structural relationship between p29 and synaptophysin may result in patterns of antibody cross-reactivity (Baumert *et al.*, 1990) such as that seen in this study with *C. gigantea.*

The data from our study suggest that synaptophysin-like proteins with molecular weights similar to those found in mammalian neural and endocrine systems exist in the sea anemone *C. gigantea.* It will be enlightening to determine the sequence and structure of these proteins and compare them with those from other studies. Comparisons may provide insight into the functional constraints of protein sequences during evolution. Furthermore, characterization of the synaptophysin-like protein by the application of modern techniques on evolutionarily divergent species such as these may be helpful in identifying functionally significant regions of these important molecules.

Acknowledgments

We thank Dr. Reinhard Jahn of Yale University for making available several of the antibodies used in this study. Support was provided by a Biomedical Research Support Grant from the University Park Campus of the University of Southern California, by a grant from the Los Angeles chapter of the ARCS (Achievement Rewards for College Scientists) Foundation through the Hancock Institute for Marine Studies at the University of Southern California and, in part, by NIH DG001228 to D.L.K.

Literature Cited

Alder, J., B. Lu, F. Valtorta, P. Greengard, and M.-M. Poo. 1992. Calcium-dependent transmitter secretion reconstituted in *Xenopus* oocytes: requirement for synaptophysin. *Science* **257:** 657–661.

Baumert, M., K. Takei, J. Hartinger, P. M. Burger, G. Fischer von Mollard, P. R. Maycox, P. De Camilli, and R. Jahn. 1990. P29: a novel tyrosine-phosphorylated membrane protein present in small clear vesicles of neurons and endocrine cells. *J Cell Biol.* **110:** 1285–1294.

Berod, A., B. K. Hartman, and J. F. Pujol. 1981. Importance of fixation in immunohistochemistry: Use of formaldehyde solutions at variable pH for the localization of tyrosine hydroxylase. *J Histochem. Cytochem.* **29:** 844–850.

Bixby, J. L. 1992. Identification of an alternatively spliced avian member of the synaptophysin gene family. *Mol. Brain Res.* **13:** 339–348.

Bock, E., and K. B. Helle. 1977. Localization of synaptin on synaptic vesicle membranes, synaptosomal plasma membranes and chromaffin granule membranes. *FEBS Lett.* **82:** 175–178.

Bradford, M. M. 1976. A rapid and sensitive method for the quantitation of microgram quantities of protein utilizing the principle of protein-dye binding. *Anal. Biochem.* **72:** 248–254.

Buckley, K. M., E. Floor, and R. B. Kelly. 1987. Cloning and sequence analysis of cDNA encoding p38, a major synaptic vesicle protein. *J. Cell Biol.* **105:** 2447–2456.

Bullock, T. H., and G. A. Horridge, eds. 1965. Coelenterata and Ctenophora. Pp. 459–534 in *Structure and Function in the Nervous Systems of Invertebrates.* Vol 1. W. H. Freeman Press, San Francisco.

Cowan, D., M. Linial, and R. H. Scheller. 1990. Torpedo synaptophysin: evolution of a synaptic vesicle protein. *Brain Res.* **509:** 1–7.

De Camilli, P., S. M. Harris, Jr., W. B. Huttner, and P. Greengard. 1983. Synapsin I (Protein I), a nerve terminal-specific phosphoprotein. II. Its specific association with synaptic vesicles demonstrated by immunocytochemistry in agarose-embedded synaptosomes. *J. Cell Biol.* **96:** 1355–1373.

De Camilli, P., F. Benfenati, F. Valtorta, and P. Greengard. 1990. The synapsins. *Ann. Rev. Cell Biol.* **6:** 433–460.

Fykse, E. M., K. Takei, C. Walch-Solimena, M. Geppert, R. Jahn, P. De Camilli, and T. C. Sudhof. 1993. Relative properties and localizations of synaptic vesicle protein isoforms: the case of the synaptophysins. *J. Neurosci.* **13:** 4997–5007.

Jahn, R., W. Schiebler, C. Ouimet, and P. Greengard. 1985. A 38,000-dalton membrane protein (p38) present in synaptic vesicles. *Proc. Natl. Acad Sci. USA* **82:** 4237–4141.

Jahn, R., F. Navone, P. Greengard, and P. I. De Camilli. 1987. Biochemical and immunocytochemical characterization of p38, an integral membrane glycoprotein of small synaptic vesicles. *Ann. N.Y. Acad Sci.* **493:** 497–499.

Jessell, T. M., and E. R. Kandel. 1993. Synaptic transmission: a bidirectional and self-modifiable form of cell-cell communication. *Cell* **72**/*Neuron* **10:** 1–30.

Johnston, P. A., and T. C. Sudhof. 1990. The multisubunit structure of synaptophysin. Relationship between disulfide bonding and homo-oligomerization. *J. Biol. Chem.* **265:** 8869–8873.

Johnston, P. A., R. Jahn, and T. C. Sudhof. 1989. Transmembrane topography and evolutionary conservation of synaptophysin. *J. Biol. Chem.* **264:** 1268–1273.

Kelly, R. B. 1993. Storage and release of neurotransmitters. *Cell* **72**/*Neuron* **10:** 3–53.

Knaus, P., H. Betz, and H. Rehm. 1986. Expression of synaptophysin during postnatal development of the mouse brain. *J Neurochem.* **47:** 1302–1304.

Knaus, P., B. Marqueze-Pouey, H. Scherer, and H. Betz. 1990. Synaptoporin, a novel putative channel protein of synaptic vesicles. *Neuron* **5:** 453–462.

Laemmli, U. K. 1970. Cleavage of structural proteins during assembly of the head of bacteriophage T4. *Nature* **227:** 680–685.

Leube, R. E., P. Kaiser, A. Seiter, R. Zimbelmann, W. W. Franke, H. Rehm, P. Knaus, P. Prior, H. Betz, H. Reinke, K. Beyreuther, and B. Weidenmann. 1987. Synaptophysin: molecular organization and mRNA expression as determined from cloned cDNA. *EMBO J.* **6:** 3261–3268.

Mackie, G. O. 1973. Report on giant nerve fibers in *Nanomia Publ. Seto Marine Labs.* **20:** 745–756.

Mackie, G. O. 1990. Evolution of cnidarian giant axons. Pp. 395–407 in *Evolution of the First Nervous Systems.* P.A.V. Anderson, ed. Plenum Press, New York.

Navone, F., R. Jahn, G. Di Gioia, H. Studenbrok, P. Greengard, and P. De Camilli. 1986. Protein p38: an integral membrane protein specific for small vesicles of neurons and neuroendocrine cells. *J. Cell Biol.* **103:** 2511–2527.

Obata, K., H. Nishiye, S. Fujita, T. Shirao, H. Inoue, and K. Uchizono. 1986. Identification of a synaptic vesicle-specific 38,000 dalton protein by monoclonal antibodies. *Brain Res.* **375:** 37–48.

Rehm, H., B. Wiedenmann, and H. Betz. 1986. Molecular characterization of synaptophysin, a major calcium-binding protein of the synaptic vesicle membrane. *EMBO J* **5:** 535–541.

Schiavo, G., F. Benfenati, B. Poulain, R. Rossetto, P. Polverino de Laureto, B. R. DasGupta, and C. Montecucco. 1992. Tetanus and botulinum-B neurotoxins block neurotransmitter release by proteolytic cleavage of synaptobrevin. *Nature* **359:** 832–835.

Spencer, A. N., and S. A. Arkett. 1984. Radial symmetry and the organization of central neurones in a hydrozoan jellyfish. *J. Exp. Biol* **110:** 69–90.

Sudhof, T. C., and R. Jahn. 1991. Proteins of synaptic vesicles involved in exocytosis and membrane recycline. *Neuron* **6:** 665¾77.

Sudhof, T. C., F. Lottspeich, P. Greengard, E. Mehl, and R. Jahn. 1987. A synaptic vesicle protein with a novel cytoplasmic domain and four transmembrane regions. *Science* **238:** 1142–1144.

Sudhof, T. C., A. J. Czernik, H.-T. Kao, K. Takei, P. A. Johnston, A. Horiuchi, S. D. Kanazir, M. A. Wagner, M. S. Perin, P. De Camilli, and P. Greengard. 1989. Synapsins: mosaics of shared and individual domains in a family of synaptic vesicle phosphoproteins. *Science* **245:** 1474–1480.

Thomas, L., K. Hartung, D. Langosch, H. Rehm, E. Banberg, W. W. Franke, and H. Betz. 1988. Identification of synaptophysin as a hexameric channel protein of the synaptic vesicle membrane. *Science* **242:** 1050–1053.

Towbin, H., T. Staehelin, and J. Gordon. 1979. Electrophoretic transfer of proteins from polyacrylamide gels to nitrocellulose sheets: procedure and some applications. *Proc. Natl. Acad. Sci. USA* **76:** 4350–4354.

Van Marle, J. 1977. Contribution to the knowledge of the nervous system in the tentacles of some Coelenterates. *Bydragen tot de Dierkunde.* **46:** 219–260.

Wiedenmann, B., and W. W. Franke. 1985. Identification and localization of synaptophysin, an integral membrane glycoprotein of MW 38,000 characteristic of presynaptic vesicles. *Cell* **41:** 1017–1028.

Reference: *Biol. Bull.* **187:** 363–372. (December, 1994)

An Ethogram of Body Patterning Behavior in the Squid *Loligo vulgaris reynaudii* on Spawning Grounds in South Africa

ROGER T. HANLON[1], MALCOLM J. SMALE[2], AND WARWICK H. H. SAUER[2]

[1]Marine Biomedical Institute, University of Texas Medical Branch, Galveston, Texas 77555–1163, and [2]Port Elizabeth Museum, P.O. Box 13147, Humewood 6013, South Africa

Abstract. Squids are capable of a high degree of visual signaling, most of which is expressed through the neurally controlled chromatophore organs in the skin. An accurate catalog (or ethogram) of these signals is an essential prerequisite to quantified behavioral analyses and experimentation. Body patterns such as those described here may also be useful for distinguishing between morphologically identical species or subspecies of commercial importance. The natural behavior of *Loligo vulgaris reynaudii* on spawning grounds was filmed by divers, and the body patterning repertoire was described in detail; 23 chromatic components, 4 postural components, and 9 locomotor components of body patterning were observed and correlated with different types of behaviors. Most of the chromatic components were expressed during intraspecific behaviors (*e.g.,* agonistic behavior among males, courtship, mating) and, to a lesser extent, during interspecific interactions with fishes. Several of the most basic types of body patterns are described, the most distinctive of which are Lateral Display and White Flashing used between males in agonistic contests. This species is comparable to other *Loligo* spp. in its complexity of body patterning behavior.

Introduction

Cephalopods have evolved a chromatophore system unique in the animal kingdom: because the pigmented cells in the skin are under neuromuscular control, skin color and pattern can change rapidly, resulting in a high diversity of appearances in individual animals. Much of the behavior of cephalopods is expressed through these pattern and color changes of the body, which convey visual signals to conspecifics, predators, and prey (*e.g.,* Moynihan and Rodaniche, 1982; Hanlon and Messenger, in press). These "body patterns" are made up of *chromatic* (*i.e.,* color), *textural, postural,* and *locomotor* components (*cf.,* Packard and Sanders, 1971; Packard and Hochberg, 1977; Hanlon, 1982; Hanlon and Messenger, 1988). Chromatic components are discrete neural entities, just as postural, locomotor, and textural components are. That is, the expression of Dark head and arms, for example, represents the selective neural excitation of motor neurons in the CNS that control the expansion of all chromatophores on the head and arms. A wide variety of body patterns can be exhibited by each individual of each species; patterns are not only species-specific, some are also sex-specific.

Our aim in this paper is to describe an ethogram for the commercially important squid *Loligo vulgaris reynaudii.* An ethogram is a catalog and description of behaviors and is used as the basis for studying behavior. In cephalopods, the development of a system of names for the components of body patterning, combined with careful illustration and description of each one, is mandatory for at least three types of studies: (a) accurate and quantitative analyses of behavior (*e.g.,* Moynihan and Rodaniche, 1982; DiMarco and Hanlon, in prep.; Hanlon and Messenger, unpub.), (b) developing taxonomic keys to species identification (Hanlon, 1988; Roper and Hochberg, 1988), and (c) comparing conserved characters of chromatic expression that can aid phylogenetic studies (*e.g.,* Moynihan, 1985; Hanlon, 1988; Burghardt and Gittleman, 1990).

Loligo vulgaris reynaudii (D'Orbigny) attains average adult sizes of 23 cm mantle length for females and 32 cm

Received 3 February 1994; accepted 22 September 1994.

for males, and is an important commercial species in South Africa, with up to 10,000 tons caught annually by hand jigging (Augustyn, 1990, 1991; Sauer *et al.*, 1992). This paper is part of a broader study of the biology and life history of the species; the long-term goal is to acquire adequate information to manage the fishery properly (Augustyn *et al.*, 1992, 1994). Previous studies included preliminary behavioral observations from video footage taken by a small, remotely operated vehicle (ROV). One of these studies (Sauer *et al.*, 1992) revealed glimpses of rather complex signaling related to spawning behavior, which led to the present investigation.

Materials and Methods

Behavior can be observed directly and at close range because squids habituate to divers within a few minutes; a close approach is facilitated if the divers move slowly or are immobile. During 33 dives throughout daylight hours, nearly 11 hours of squid behavior were observed from 11 November to 1 December 1993 on spawning grounds in depths of 17–30 m. The study area was between Port Alfred in the east (33°36′87 S, 26°55′51 E) and the Tsitsikamma Coastal National Park in the west (34°01′81 S, 23°56′43 E), or about 700 km east of Cape Town. Over 4 of the 11 hours of behavior were recorded with a Sony TR81 Hi-band 8-mm video camera in an underwater housing. An additional 1.3 hours of videotape from previous years were also reviewed (filmed by W. Sauer and G. Fridgeon from 1989 to 1992 in the same areas). Drawings from the video images were made with the software program CorelDRAW for DOS.

Video sampling (Martin and Bateson, 1993) was accomplished as follows. During the early dives, sampling was *ad libitum* with continuous recording because we sought preliminary data that would reveal the variety of behaviors observable with hand-held cameras; approximately half our recordings were *ad libitum*. After analyzing these tapes on board ship, we switched to behavior sampling, in which a group was watched and only particular behaviors were recorded (*e.g.*, agonistic bouts, mating, fish interactions, *etc.*); about a third of the recordings were such behavior samples. The remaining recordings involved focal sampling, in which we followed and taped an individual squid (*e.g.*, a lone male, a paired female, a sneaker male, *etc.*) or a dyad (*e.g.*, a courting pair and any competing males). Analyses involved many replays of the recordings by all coauthors, so that each type of information sought could be obtained (*e.g.*, one replay for observing components, one for describing them, one for counting them, one for describing mating, *etc.*). The time spent on total analysis thus totaled several hundred person-hours.

Terminology

A **Body Pattern** is the overall appearance of the cephalopod at any moment, and it is made up of one or more of the following **Components**: chromatic (*i.e.*, color), textural, postural, and locomotor. Textural components refer to skin papillation in cuttlefishes and octopuses, but squids do not have this ability. For convention, components are capitalized in the first word only, while body patterns are capitalized at the beginning of each word. Names of components and of body patterns follow existing cephalopod literature (reviewed by Hanlon and Messenger, in press). Emphasis was given to naming components and body patterns as morphological descriptors to avoid behavioral or functional connotations. Following the tradition in ichthyology and herpetology (Robins *et al.*, 1991), the terms "stripe," "line," or "streak" mean longitudinal chromatic components that parallel the body axis, whereas "bar" or "band" mean transverse or vertical components.

Results and Discussion

Table 1 lists the components and body patterns of *Loligo vulgaris reynaudii.* The chromatic components are illustrated in Figure 1. Unless stated otherwise, all components and body patterns were shown by both sexes.

The body patterns and components listed in this ethogram constitute a subset of all squid behaviors, and they reflect only the types of behaviors we sampled for and the behaviors that happened to occur on those dives on those days in the immediate vicinity of the egg beds. Although numerical quantification is not appropriate for this study, we list in parentheses, in Table 1, the number of times (n) that we counted a body pattern or component on video tapes to give the reader an impression of how common some of them are.

Light chromatic components

Only three were observed, and each is common to all *Loligo* spp. **Clear** is characterized by retraction of all chromatophores, rendering the animal whitish or translucent. This component can act alone as a body pattern, and it is the most common pattern in calm, undisturbed squids. Two iridescent components, both thought to aid in crypsis, were also observed: **Dorsal mantle collar iridophores** and **Dorsal mantle splotches**; these are not illustrated but can be seen in color plates in Hanlon (1982).

Males show the **Accentuated testis** component. Accentuation of this white organ is accomplished by expansion of most mantle chromatophores while simultaneously there is selective retraction (*i.e.*, lack of neural excitation) of the chromatophores over and even beyond the border of the testis. Males of other loliginid squids also have this capability (Hanlon, 1982, 1988; Moynihan, 1985), which is thought to be an expression of "maleness," although this has not been demonstrated. *Loligo vulgaris reynaudii* shows the component to other males and to females.

The white **Accentuated oviducal gland** of females is similar in appearance to the Accentuated testis of males, but is different in shape, position, and frequency of expression. On rare occasions, females show a white area directly over the eggs in the most posterior dorsal mantle.

Dark chromatic components

Loligo vulgaris reynaudii has three color classes of chromatophores: yellow, red, and brown. **All dark** is characterized by expansion of all chromatophores, resulting in a reddish-brown overall color. This component, which also acts independently as a body pattern, is an expression of alarm or disturbance in the squid. For example, close unexpected approaches of fishes (even small nonpredatory ones) cause brief expression of All dark, but the pattern is also used intraspecifically during agonistic encounters, and even between males and females, when one or the other is startled (Hanlon, 1982; Hanlon *et al.*, 1983; this study). There is a distinctive unilateral variation in which one side of the entire arms, head, and mantle (but usually not the fins) becomes dark, illustrating a striking bilateral asymmetry. Another variation of All dark is **Dark fins**, giving the impression that the posterior half of the mantle is darkened. Conversely, **Dark head and arms** shows the opposite effect, and there is a variation of this in which only the arms are darkened; these components are seen during intraspecific agonistic encounters. Dark head and arms is also exhibited by *Loligo opalescens*, but in that species it is seen during mating (Hurley, 1977). Occasionally, males show **Dark tentacle or arm tips** but the significance of this component is unknown; on occasion when Raised arm (see below) is used during agonistic contests, males darken the arm tip. **Shaded eye** aids in crypsis by covering the bright iridescent sclera of the eyeballs and is common among loliginid squids.

The only transversely oriented component is **Bands** (called Rings in previous literature), which are common in loliginids and are associated either with (a) crypsis through disruptive coloration (as in *Loligo pealei;* Stevenson, 1934) or with (b) secondary defense, in which a squid approached closely by a predator (or possibly a large object like an ROV with shining lights) shows disruptive coloration, often with some distinctive arm posture (Sauer and Smale, 1993). This component functions alone as a body pattern, but has rarely been seen thus far, and no comments are yet appropriate.

Dark striped components. Loligo vulgaris reynaudii shows five striped chromatic components. **Dark dorsal stripe** is common to *Loligo* spp. and is seen in calm squids; the stripe varies in width from a few millimeters to one-third of the mantle width. It is thought to aid in crypsis through countershading when viewed laterally and through disruptive coloration when viewed from above, by covering some of the bright organs such as the testis, oviducal glands, and ink sac (Hanlon, 1982, 1988; Hanlon and Messenger, in press).

The next four striped components are used during intraspecific agonistic encounters. **Fin stripe** occurs when squids appear to be mildly alarmed during agonistic contests; also, the component is observed commonly on squids that have been jigged and brought into the boat (a highly unnatural situation to which no function can be ascribed, although this is presumably an extreme form of stress and alarm). **Mantle margin stripe** is very common among *Loligo* spp. and is usually shown posteriorly as a dark red line below the fin insertion. However, it is occasionally shown as a longitudinal dark red line from the fin insertion forward to the mantle collar. It is also a mild reaction to disturbance or alarm from intraspecific encounters. **Arm stripe** is seen in similar situations, but is quite uncommon; either the first or third pair of arms is darkened. **Ventral mantle stripe** is analogous to the "Mid-ventral ridge" of *Loligo plei* (Hanlon, 1982) except that there is not the extrusion of skin that produces the ridge in *Loligo plei*. The function is unknown in *L. vulgaris reynaudii* or in *Loligo forbesi* (Porteiro *et al.*, 1990), except that in the present observations males showed this component often while swimming alongside a mate. It can be seen only from below, but this may be important because males often swim slightly above their female mate. The possibility that the stripe helps disrupt the body shape when viewed from below (by predators) should not be discounted.

Dark spotted components. These three components are expressed during alarm or threat situations, mainly intraspecifically, and are often shown unilaterally on the side towards the other squid. **Arm spots** are small and can occur either on the base of the second or third arms, whereas the **Infraocular spot** occurs roughly between the eye and the Arm spots. Both are sometimes expressed simultaneously. There is considerable variation in the expression of the "spot," as illustrated. **Fin spots** are about 5 mm in diameter in large adults and are distributed as illustrated; they are expressed commonly during agonistic contests between males.

Dark components associated with reproduction. In addition to Accentuated testis and Accentuated oviducal gland, four other components are related to sexual behavior.

Table I

Body patterns and their components in the squid Loligo vulgaris reynaudii *(f = female, m = male); (n) is the number of times each component was observed on video. Compare Figure 1*

Chromatic components			
Dark:	n =	Light:	n =
1. All dark	(87)	1. Clear	(356)
2. Dark dorsal stripe	(76)	2. Dorsal mantle collar iridophores	(50)
3. Ventral mantle stripe	(25)	3. Dorsal mantle splotches	(>50)
4. Mantle margin stripe	(136)	4. Accentuated oviducal gland (f only)	(149)
5. Fin stripe	(34)	5. Accentuated testis (m only)	(46)
6. Arm stripe	(83)		
7. Fin spots	(52)		
8. Arm spots	(75)		
9. Infraocular spot	(57)		
10. Dark fins	(56)		
11. Bands	(2)		
12. Shaded eye	(41)		
13. Dark head and arms	(98)		
14. Dark tentacle or arm tips	(30)		
15. Lateral mantle streaks (m predominantly)	(84)		
16. Red accessory nidamental gland (f only)	(2)		
17. Shaded oviducal gland (f only)	(9)		
18. Lateral blush (f only)	(34)		
Postural components:		**Locomotor components:**	
1. Raised arm	(48)	1. Inking	(6)
2. Downward V curl	(2)	2. Jetting	(>100)
3. Splayed arms	(42)	3. Parallel positioning	(>25)
4. Egg holding (f only)	(22)	4. Fin beating (m only)	(>10)
		5. Jockeying and Parrying	(23)
		6. Head-to-head mating	(0)
		7. Male parallel mating (m only)	(10)
		8. Male "sneak" mating (m only)	(10)
		9. Mate guarding (m only)	(>100)
Body Patterns			
Chronic patterns: (minutes-hours)		Acute patterns: (seconds)	
1. Clear	(356)	1. White Flashing (m)	(>182)
2. Dorsal Stripe	(76)	2. Dark Flashing	(32)
		3. Accentuated Oviducal Gland (f)	(149)
		4. Accentuated Testis (m)	(46)
		5. Bands	(2)
		6. Blanch-Ink-Jet Maneuver	(3)
		7. Lateral Display (m)	(>30)

Three are shown only by females. Females can mask Accentuated oviducal gland with the component **Shaded oviducal gland**; this is particularly effective when the squid is in the otherwise Clear body pattern because, as noted often by divers and from video recordings, it decreased conspicuousness of the very white oviducal gland. The **Red accessory nidamental gland** is large and bright in this species and can be seen through the mantle, either from below or laterally. Thus it must be considered a potential signal in communication, even though it is internal. Its primary anatomical function is unknown, but it may be a sign of female sexual maturity since it turns red only upon attainment of full maturation (Drew, 1911; Hanlon, 1982). Finally, females show a **Lateral blush** component that may be analogous to similar components in other loliginids, for example, the Lateral blush of *Loligo plei* (see Hanlon, 1982), the Pied pattern of females of the Caribbean reef squid *Sepioteuthis sepioidea* (see Moynihan and Rodaniche, 1982) and the Lateral mantle spot in female *Lolliguncula brevis* (see Dubas *et al.*, 1986).

Lateral mantle streaks are basically male-only streaks of chromatophores, each streak from 2–24 mm long and surrounded by a clear area of about 1–2 mm that is completely devoid of chromatophores, thus rendering the

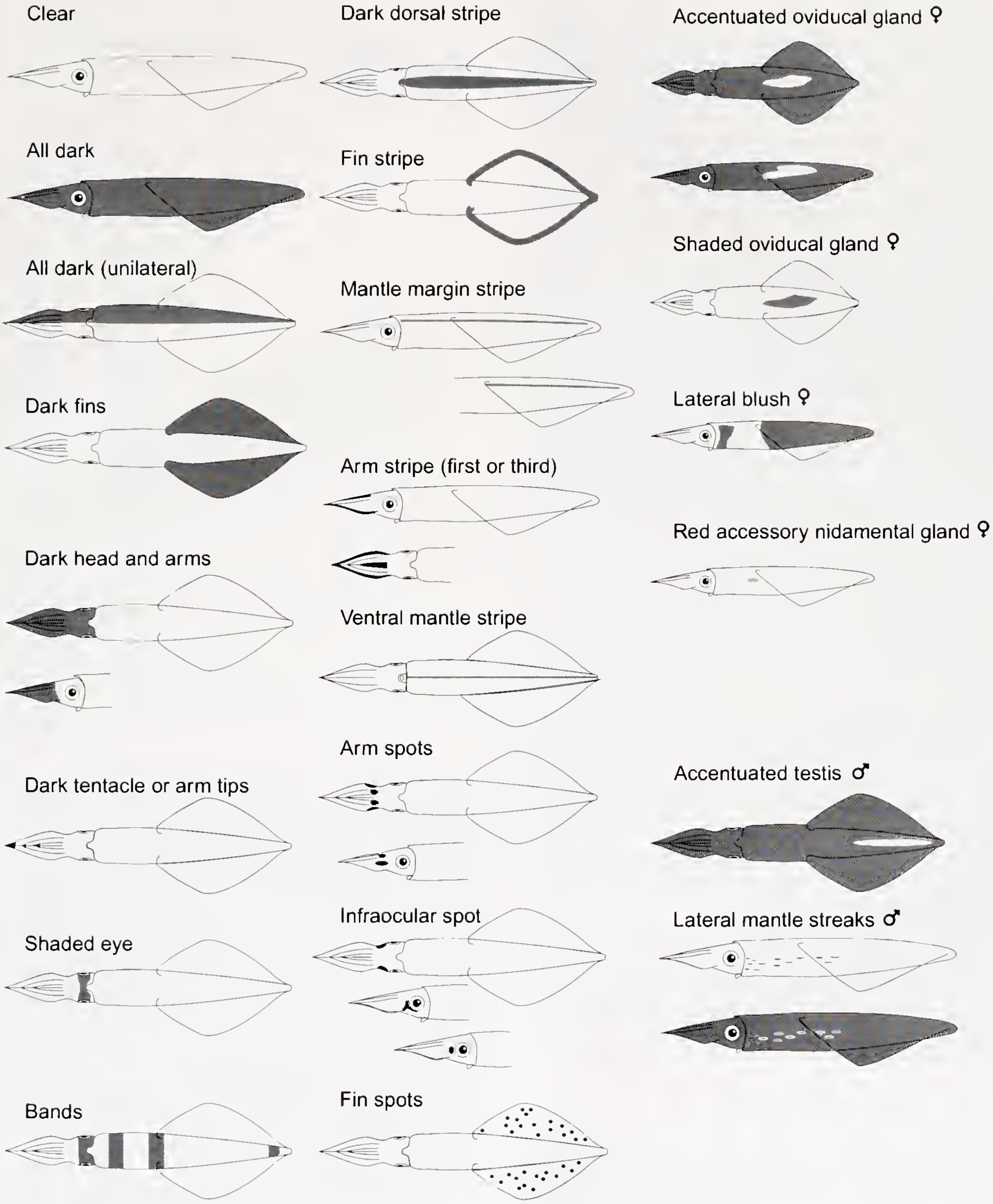
Clear
All dark
All dark (unilateral)
Dark fins
Dark head and arms
Dark tentacle or arm tips
Shaded eye
Bands
Dark dorsal stripe
Fin stripe
Mantle margin stripe
Arm stripe (first or third)
Ventral mantle stripe
Arm spots
Infraocular spot
Fin spots
Accentuated oviducal gland ♀
Shaded oviducal gland ♀
Lateral blush ♀
Red accessory nidamental gland ♀
Accentuated testis ♂
Lateral mantle streaks ♂

Figure 1. Neural expression of the chromatic components of body patterning in the squid *Loligo vulgaris reynaudii.*

streaks more obvious relative to surrounding chromatophores. A sample of the number and distribution of these streaks is given in Table II. Large mature males have 8–17 streaks, whereas mature females have only 1–3 streaks, but in females they occur only in the largest animals and are very small and almost certainly insignificant for visual signaling, being so small and indistinct. In all cases, most of the streaks are located anteriorly (see Fig. 1). In a typically sized streak of ~16 mm long in a male, there are about 320 chromatophores, whereas in a typical streak of 4 mm length in a female there are only 29 chromatophores. The morphological arrangement of chromatophores in the streaks differs from that on the rest of the animal. The arrangement is similar to the "Yellow-Brown Discoid Unit" in *Loligo plei* (Hanlon, 1982); that is, there are only two color classes of chromatophores instead of the customary three. The streaks are similar in appearance to the Lateral flame component in *Loligo plei* and *Loligo pealei* (Hanlon, 1982; Hanlon *et al.*, 1983) and to the Lateral mantle streaks in *Loligo vulgaris vulgaris* and *Loligo forbesi* (Hanlon, 1988). However, there seems to be a major difference in the way they are used behaviorally, because in *Loligo vulgaris reynaudii* they are not used during the Lateral Display (see below), whereas in *Loligo plei* they are a major component during Lateral Displays (Hanlon, 1982; DiMarco and Hanlon, unpub.).

Taxonomically it may be important that the streaks in male *Loligo vulgaris reynaudii* are shorter than those in male *Loligo forbesi*, even on a proportional scale. For example, *Loligo vulgaris reynaudii* in the range of 14–38 cm mantle length had streaks 4–13 mm long, whereas *Loligo forbesi* in the same size range had streaks 10–30 mm long (from Table 3 in Hanlon, 1988). Furthermore, female *Loligo vulgaris reynaudii* have only one or a few inconspicuous streaks, whereas female *Loligo forbesi* have 8–12 streaks on each side of the mantle, each about 14 mm long; these latter streaks were easily visible in the skin unlike those of *Loligo vulgaris reynaudii*. This may be a distinguishing character in both sexes and should be checked carefully in *Loligo vulgaris vulgaris* as a possible diagnostic character with which to separate *Loligo vulgaris vulgaris* from *Loligo forbesi* in their widely overlapping ranges off European coastlines.

Table II

Number and length of the chromatic component Lateral mantle streaks on the mantle of the squid Loligo vulgaris reynaudii. *Measurements in mm*

		Mantle length	No. streaks per side		Mean streak length and (range)	
			Left	Right	Left	Right
Males:	1	138	11	9	3.9 (2–6)	4 (3–5)
	2	142	9	9	3.6 (2–5)	4 (2–6)
	3	170	11	9	4.8 (4–7)	4.2 (3–6)
	4	196	8	9	6.5 (3–9)	5.9 (4–8)
	5	212	8	8	6 (5–7)	5.4 (4–8)
	6	215	14	8	5.8 (3–11)	7 (5–10)
	7	220	6	5	5.8 (4–8)	6.8 (5–8)
	8	265	12	12	7.3 (3–14)	7.6 (4–15)
	9	270	10	12	7.8 (4–11)	12 (6–8)
	10	305	10	13	8.7 (4–13)	7.8 (2–12)
	11	310	8	8	8.8 (6–12)	8.1 (6–10)
	12	320	8	9	10.6 (7–19)	9.5 (5–19)
	13	335	12	9	10.7 (5–18)	12.4 (7–19)
	14	355	13	17	10.5 (7–16)	11.5 (5–24)
	15	385	12	10	12.6 (5–18)	12.1 (6–20)
Females:	1	175	1	1	5 (5)	3 (3)
	2	177	1	1	4 (4)	3 (3)
	3	190	2	1	5 (4–6)	7.5 (7.5)
	4	195	2	1	4.5 (3–6)	6 (6)
	5	198	1	1	5 (5)	6 (6)
	6	201	1	1	3 (3)	6 (6)
	7	205	1	3	3 (3)	6.3 (4–8)
	8	215	1	2	6 (6)	5 (5)
	9	225	2	3	3.5 (2–5)	4 (3–5)

Postural and locomotor components

Inking is the expulsion of ink mixed with mucus. It takes two basic forms: (a) relatively small puffs either in the form of a pseudomorph that resembles the size and shape of an escaping squid, or more commonly just a general blackened spot; or (b) large and dense clouds of ink. **Jetting** refers to rapid body movement by expulsion of water from the funnel (*i.e.*, jet propulsion), usually only about 1 m in distance and usually backwards. There is considerable Jetting combined with Inking on the spawning grounds (especially among females) at the conclusion of mating, at the conclusion of laying an egg strand (Smale *et al.*, in press), or when small fishes (*e.g.*, *Pagellus bellottii natalensis* and *Spondyliosoma emarginatum*) nip at them in the water column (Sauer and Smale, 1993). Thus, it is used as a secondary defense in the form of Deimatic behavior; *i.e.*, behavior that threatens, startles, frightens, or bluffs a predator (McFarland, 1982; Hanlon and Messenger, in press).

Several components are used only by males during agonistic encounters. **Raised arm** is a unilateral raising of one of the first pair of arms, on the side towards the approaching squid; sometimes the tip is darkened. This component is seen during similar circumstances in *Loligo pealei* (Arnold, 1962), but not in other loliginids. **Downward V curl** is downward curling of the arms, which are parted equally and bilaterally into groups; it is common in most loliginids when they are alarmed (Moynihan, 1985). **Splayed arms** is a highly conspicuous posture in which all eight arms and the two tentacles are spread radially, with a bias laterally. It is common during agonistic contests between males and may function in mate guarding. **Parallel positioning** is simply positioning parallel and laterally to another squid, with the arms in the same direction on each animal. **Fin beating** occurs during Parallel positioning and represents escalation of an agonistic encounter, because there is a transition from visual signaling to physical contact (DiMarco and Hanlon, unpub.; Hanlon and Messenger, in press); physical contact is mild and no obvious harm is done. **Jockeying** (from dictionary "to move by skillful maneuvering . . . to act trickily") is another component of agonistic encounters in which one male (the "intruder") attempts to maneuver over or under the "owner" male it is fighting and to get nearer the female. Conversely, **Parrying** (from dictionary "to ward off . . . to turn aside . . . by a defensive movement") refers to the swimming maneuvers used by the owner male to counter the approach efforts of the intruder male. Both maneuvers involve swimming finesse and influence the outcome of agonistic contests.

Several other components are associated with mating and egg laying. *Loligo vulgaris reynaudii* mates in three ways. **Head-to-head mating** is when the male and female face each other and entangle the arms; it is common in loliginids and is best illustrated by Drew (1911). This component is thought to be the only way in which males place spermatophores in a female's bursa copulatrix, which is a pouch for storing sperm. Head-to-head mating was not observed directly in our study, but most *Loligo vulgaris reynaudii* females already had spermatophores in the bursa. **Male parallel mating** occurs when the male swims beneath the female and grasps her with his arms and passes spermatophores to the mantle cavity near the oviduct; this is also common in loliginids and is illustrated in Drew (1911). **Male "sneak" mating,** newly discovered in this study, occurs when small "sneaker" or "satellite" males jet in very quickly and grasp females near the base of the first or second arms (*i.e.*, always from above), presumably to place spermatophores amidst the arms, where single egg strands are held and fertilized regardless of the mating method. The posture **Egg holding** is seen after the female has drawn the single egg strand out of the mantle. The first two pairs of arms are compressed dorsally, holding the eggs in some distinctive way, perhaps to fertilize them with sperm drawn from the bursa copulatrix. Alternatively, the eggs could already be fertilized from spermatophores placed near the oviduct during male-parallel mating, or sperm from sneaker males could fertilize some ova; none of this is yet understood. **Mate guarding** occurs when the male of a temporary mating pair accompanies the female to the egg mop (a collection of egg strands on the substrate) and remains a few centimeters above her until she deposits an egg strand into the mop. This is also common among loliginids (*e.g.*, Hurley, 1977; Griswold and Prezioso, 1981; Hanlon and Messenger, in press).

Body patterns

Chronic patterns last for minutes or hours. When squids are calm they are usually in the **Clear** body pattern or Clear with **Dorsal stripe.** These are cases in which a single chromatic component acts as a body pattern.

Acute patterns last seconds or, rarely, a minute or two. **White Flashing** is a male-only pattern that is used during agonistic contests between males. It can be differentiated from Clear by three factors: (1) it is shown only for a few seconds; (2) the whiteness appears brighter than Clear, probably due to reflective iridophores also being expressed, in addition to chromatophores being retracted (*n.b.*, iridophores are cells that produce structural or reflected color as opposed to pigmentary color; they have recently been shown to be controlled actively by the animal, Hanlon *et al.*, 1990); and (3) it is intermittent and can even appear somewhat pulsating. **Dark Flashing** is the brief appearance of the dark chromatic component All dark, usually 2-3 times in succession over a few seconds. It is shown by both sexes: during agonistic contests between males, by females when fighting males approach too closely, and by females when they jet away from the eggs after depositing an egg strand. **Bands** have rarely been seen (see comments above). **Accentuated Oviducal Gland** and **Accentuated Testis** are shown briefly by females and males, respectively, during courtship or during agonistic contests in males. There are other occasions in which single dark components are shown alone, but these were rare in our observations and cannot be described in any detail.

The **Blanch-Ink-Jet Maneuver** may be universal in squids inhabiting the photic zone: the animal blanches Clear and jets away quickly in the backwards direction while ejecting ink in a pseudomorph that remains in the same approximate position from which the squid started the maneuver. The pseudomorph resembles the size and shape of the dark squid that was just there. This is a secondary defense against predation (when, for instance, crypsis fails) and represents a typical escape response to attacking predators (Hanlon and Messenger, in press). Such behavior is called protean behavior because the variable and erratic escape response upsets target prediction by the attacking predator (Driver and Humphries, 1988).

Lateral Display is a complex behavior performed only by males in agonistic contests. It is somewhat stereotyped, but there is variability in the details and in the order in which components are shown. It begins with Parallel positioning by two males and then includes various visual signals of Arm spots, Fin spots, Infraocular spot, and Mantle margin stripe, accompanied by the postural components Raised arm or Splayed arms. There are then dynamic interactions that include White Flashing and Dark Flashing, and the contest can escalate to Fin beating followed by Jockeying by the intruder to get near the female, while the "owner" male Parries to keep the intruder away from her.

Can body patterning ethograms help distinguish subspecies?

The subspecies *Loligo vulgaris reynaudii* and *Loligo vulgaris vulgaris* are separated mainly by club sucker dentition and protein electrophoresis (Augustyn and Grant, 1988), and the subspecies seem to overlap in the region of West-Central Africa. We do not know whether their body patterns (and thus their behaviors) are distinct. Unfortunately, *Loligo vulgaris vulgaris* has only been studied briefly in the laboratory (Hanlon, 1988) so no comparison is possible. Therefore, we would appreciate information from biologists working with *L. v. vulgaris* off the Mediterranean or the Atlantic coasts from Europe to northwestern Africa (see distribution in Worms, 1983) about spawning locations that are comparable to that of *Loligo vulgaris reynaudii* in South Africa.

The data available for these two subspecies suggest that the chromatic component Mantle spots, seen in *Loligo vulgaris vulgaris* by Hanlon (1988), is unique to that subspecies. We would almost certainly have seen Mantle spots in our observations of *L. v. reynaudii*, since we commonly saw Fin spots, which are common in both subspecies. Conversely, the chromatic components Arm spots, Dark fins, Bands, Dark head and arms, Dark tentacle or arm tips, Accentuated testis, Accentuated oviducal gland, and Shaded oviducal gland of *Loligo vulgaris reynaudii* have not been reported in *Loligo vulgaris vulgaris* and should be searched for specifically in future work. Furthermore, the specific arrangement and length of the Lateral mantle streaks (see *Dark chromatic components* above and Table I) should be compared carefully, because this component appears to be important in reproductive behavior, which is likely to be different in the two subspecies.

Loligo vulgaris vulgaris overlaps extensively with *Loligo forbesi* around European coastlines; thus a comparison of the chromatic components listed here with those listed by Porteiro *et al.* (1990) for *Loligo forbesi* might help to distinguish *Loligo vulgaris vulgaris* from *Loligo forbesi*. This is of major importance to fisheries biologists, who currently have no way to distinguish the two species with confidence either in the laboratory (with preserved specimens) or on board ship (with freshly caught animals). Making decisions for catch quotas and recruitment processes is impossible without certain identification of the species involved.

A similar study on *Loligo pealei* on its spawning grounds near Cape Cod in the Northeastern USA would provide additional information on the visual signaling capability of that species, which, in addition to being commercially important (Summers, 1983), is used in biomedical and neuroscience research (Gilbert *et al.*, 1990).

Behavioral diversity among loliginid squids

The chromatic components of body patterns are particularly important because (1) they are discrete physiological entities under direct control by the CNS; (2) they are the primary components of the visual signal (*cf.*, Packard and Hochberg, 1977; Hanlon, 1982); and (3) they are specific to the organism, *i.e.*, they are genetically determined. As a general index of behavioral diversity, the number of chromatic components can be compared among various *Loligo* spp. (Hanlon and Messenger, in press): *Loligo vulgaris reynaudii* 23 (S. Africa), *Loligo plei* 20 (Caribbean), *Loligo forbesi* 17 (Europe), *Loligo vulgaris vulgaris* 16 (Europe), *Loligo pealei* 14 (northeastern USA), *Loligo opalescens* 13 (western USA). Not all species have been studied in comparable detail, but from familiarity with each species (RTH) this listing is basically correct insofar as the first two species show slightly richer repertoires of chromatic expression. Other genera in the Family Loliginidae such as *Lolliguncula* and *Alloteuthis* are substantially less rich, having only 12–13 chromatic components; furthermore, they have only two color classes of chromatophores (yellow and brown), compared to three (yellow, red, and brown) for *Loligo* and *Sepioteuthis* (Lipinski, 1985; Dubas *et al.*, 1986; Hanlon and Messenger, in press). In contrast, the loliginid *Sepioteuthis sepioidea* has 23 chromatic components and can project many rich combinations of these into numerous body patterns, producing far more diverse body patterning behaviors than any squid known (Moynihan and Rodaniche, 1982).

Conclusions

Nearly all of the components described in this study—29 of 36 (Table I)—were involved in intraspecific behavior. It is predictable that many ritualized intraspecific visual signals will be found in squids because they are social animals with a complex mating system in which males compete for females, and both sexes are polygamous. Agonistic contests in male squids seem always to involve some variations of a Lateral Display, which is a form of "visual battle" used to establish or maintain dominance; this dominance presumably confers an advantage to males for temporary pairing and "preferred mating access" to females (DiMarco and Hanlon, unpub.; Hanlon and Messenger, in press).

None of the 36 components of patterning were completely unique to *Loligo vulgaris reynaudii* compared to other loliginid squids. We know of an analog for every component (*cf.*, Hanlon, 1982, 1988; Moynihan, 1985; Porteiro *et al.*, 1990; Hanlon and Messenger, in press), although of course there will be detailed variations of each component that are species-specific. The more important differences between species are in the ways the components are combined into body patterns and used in different behaviors. The durations, frequencies, and sequences of components shown during different displays (*e.g.*, the Lateral Display during agonistic contests) will certainly be different in *Loligo vulgaris reynaudii* and in any other loliginid (*e.g.*, *Loligo plei*; DiMarco and Hanlon, unpub.). White Flashing has not been seen in other squids, although a similar behavior—called Lateral Silver—has been described in the loliginid *Sepioteuthis sepioidea;* it is a unilateral signal to repel rival males only in the latest stages of courtship (Moynihan and Rodaniche, 1982).

Our ethogram of body patterning behavior is reasonably complete for intraspecific components of body patterning. The direct observations amidst hundreds (sometimes thousands) of highly active squids on their spawning grounds provided more variety and the opportunity to see a wider range of behaviors than is possible in the laboratory. Furthermore, many of the intraspecific behaviors are highly stereotyped and were seen repeatedly. A greater amount of focal or behavioral sampling would certainly have yielded some new behaviors and should be attempted in the future. In addition, the behavior of *Loligo vulgaris reynaudii* should be recorded (1) during other stages of the life cycle, and (2) during dusk and dawn, as well as at night (using light intensifiers) so that other components and body patterns used for crypsis or predator evasion can be observed. Only 7 of 36 components were noted during behaviors other than intraspecific: Clear, Dorsal mantle collar iridophores, Dorsal mantle splotches, Bands, Shaded eye, Inking, and Jetting. Younger squids are generally found farther offshore, and the probability of observing them is lower (Augustyn, 1991). The hand-held video technique is preferable to using ROVs at night because the bright lights on the vehicle are unnatural and the ROVs are not nearly as maneuverable as a diver-held camera.

We cannot overemphasize the importance of studying behavior in the natural environment despite its difficulties. In the marine environment around southernmost South Africa, the cold rough waters and the relatively deep diving (usually about 25 m) resulted in short dives (about 30–40 min) that limited observations even when the water was somewhat clear and the squids were most active; on many dives subsequent to these, no squids were found or visibility was close to zero. Nevertheless, this is a good location for behavioral studies when conditions permit because squids are rather concentrated along the coast. Video was absolutely imperative because it maximized data acquisition and proved far superior to underwater note taking and still photography as a means of recording and analyzing the body patterns accurately. The zoom capability of the video allowed a variety of sampling techniques: scan, focal, behavior, or *ad libitum*. Many details and pleasant surprises emerged from the tapes during analysis. For example, previous studies with the stationary ROV (Sauer *et al.*, 1992) revealed only seven chromatic components of patterning, whereas the present study, with diver-controlled video, revealed 23 chromatic components. This is because divers could scan the scene, anticipate behavioral sequences, and use focal or behavior sampling to follow either (a) mating pairs, (b) large lone males, or (c) small lone "sneaker" males, all of which were engaging in different types of behavior.

The chromatic components are taxonomic characters useful for distinguishing at the species (*e.g.*, Hanlon, 1988; Roper and Hochberg, 1988) and possibly the subspecies level (this paper). Because the chromatic components are genetically coded physiological entities, they are as appropriate as any morphological character. In particular, the taxonomy of the Family Loliginidae is confused, especially at the generic level. *Loligo* spp. are so similar in general appearance—especially after preservation—that these physiological chromatic components in the living animals may be better diagnostic characters than the traditional morphological ones. For the future, combining traditional morphological data with body patterning and behavioral data and eventually with molecular data (Kuncio and Hanlon, 1991; Brierley *et al.*, 1993) will certainly be required to resolve these taxonomic questions.

Acknowledgments

We thank Captain Peers Pittard and his crew on the squid fishing vessel *Langusta* for tolerating our presence on board, and we thank Murray Ralfe and John Francis for executing Figure 1. Travel funds for RTH were kindly provided by the South African Squid Management Industrial Association, and per diem costs were provided by the MSRDP fund of the Marine Biomedical Institute, The University of Texas Medical Branch. Part of this research budget was provided by the Sea Fisheries Research Institute in Cape Town, the Port Elizabeth Museum, and the Foundation for Research and Development. We gratefully acknowledge use of the research "ski boat" *Calmar* sponsored by the Small Business Development Corporation (SA) and a Land Rover and petrol for both by Caltex Oil SA.

Literature Cited

Arnold, J. M. 1962. Mating behavior and social structure in *Loligo pealii*. *Biol. Bull.* **123**: 53–57.

Augustyn, C. J. 1990. Biological studies on the chokker squid *Loligo vulgaris reynaudii* (Cephalopoda; Myopsida) on spawning grounds off the South-East coast of South Africa. *S. Afr. J. Mar Sci.* **9:** 11–26.

Augustyn, C. J. 1991. The biomass and ecology of chokka squid *Loligo vulgaris reynaudii* off the west coast of South Africa. *S. Afr. J. Zool.* **26:** 164–181.

Augustyn, C. J., and W. Grant. 1988. Biochemical and morphological systematics of *Loligo vulgaris vulgaris* Lamarck and *Loligo vulgaris renaudii* D'Orbigny nov., comb. (Cephalopoda: Myopsida). *Malacologia* **29:** 215–233.

Augustyn, C. J., M. R. Lipinski, and W. H. H. Sauer. 1992. Can the *Loligo* squid fishery be managed effectively? A synthesis of research on *Loligo vulgaris renaudii. S Afr. J. Mar Sci.* **12:** 903–918.

Augustyn, C. J., M. R. Lipinski, W. H. H. Sauer, M. J. Roberts, and B. A. Mitchell-Innes. 1994. Chokka squid on the Agulhas Bank: life history and ecology. *S. Afr. J. Sci.* **90:** 143–154.

Brierley, A. S., J. P. Thorpe, M. R. Clarke, and H. R. Martins. 1993. A preliminary biochemical genetic investigation of the population structure of *Loligo forbesi* Steenstrup, 1856 from the British Isles and the Azores. Pp. 61–69 in *Recent Advances in Fisheries Biology.* Okutani, T., R. K. O'Dor, and T. Kubodera, eds. Tokai University Press, Tokyo.

Burghardt, G. M., and J. L. Gittleman. 1990. Comparative behavior and phylogenetic analyses: new wine, old bottles. Pp. 192–225 in *Interpretation and Explanation in the Study of Animal Behavior. Volume II: Explanation, Evolution, and Adaptation,* M. Bekoff and D. Jamieson, eds. Westview Press, San Francisco.

Drew, G. A. 1911. Sexual activities of the squid, *Loligo pealii* (Les.). *J. Morphol., Wistar Inst. of Anatomy and Biology* **22:** 327–359.

Driver, P. M., and D. A. Humphries. 1988. *Protean Behavior. The Biology of Unpredictability.* Clarendon Press, Oxford.

Dubas, F., R. T. Hanlon, G. P. Ferguson, and H. M. Pinsker. 1986. Localization and stimulation of chromatophore motoneurons in the brain of the squid, *Lolliguncula brevis. J. Exp. Biol.* **121:** 1–25.

Gilbert, D. L., W. J. Adelmann, Jr., and J. M. Arnold, eds. 1990. *Squid as Experimental Animals.* Plenum Press, New York. 516 pp.

Griswold, C. A., and J. Prezioso. 1981. *In situ* observations on reproductive behavior of the long-finned squid, *Loligo pealei. Fish. Bull.* **78:** 945–947.

Hanlon, R. T. 1982. The functional organization of chromatophores and iridescent cells in the body patterning of *Loligo plei* (Cephalopoda: Myopsida). *Malacologia* **23:** 89–119.

Hanlon, R. T. 1988. Behavioral and body patterning characters useful in taxonomy and field identification of cephalopods. *Malacologia* **29:** 247–264.

Hanlon, R. T., and J. B. Messenger. 1988. Adaptive coloration in young cuttlefish (*Sepia officinalis* L.): the morphology and development of body patterns and their relation to behaviour. *Phil. Trans. R. Soc. Lond. B.* **320:** 437–487.

Hanlon, R. T., and J. B. Messenger. (in press). *Cephalopod Behaviour.* Cambridge University Press, Cambridge, U. K.

Hanlon, R. T., K. M. Cooper, B. U. Budelmann, and T. C. Pappas. 1990. Physiological color change in squid iridophores. I. Behavior, morphology and pharmacology in *Lolliguncula brevis. Cell Tissue Res.* **259:** 3–14.

Hanlon, R. T., R. F. Hixon, and W. H. Hulet. 1983. Survival, growth, and behavior of the loliginid squids, *Loligo plei, Loligo pealei* and *Lolliguncula brevis* (Mollusca: Cephalopoda) in closed sea water systems. *Biol. Bull.* **165:** 637–685.

Hurley, A. C. 1977. Mating behavior of the squid *Loligo opalescens. Mar. Behav. Physiol.* **4:** 195–203.

Kuncio, G. S., and R. T. Hanlon. 1991. Analysis of cephalopod evolution and systematics using ribosomal RNA sequence data. *Bull. Mar. Sci.* **49:** 665. (Abstract)

Lipinski, M. R. 1985. Laboratory survival of *Alloteuthis subulata* (Cephalopoda: Loliginidae) from the Plymouth area. *J. Mar. Biol. Assoc. U. K.* **65:** 845–855.

Martin, P., and P. Bateson. 1993. *Measuring Behavior. An Introductory Guide.* 2nd Edition. Cambridge University Press, Cambridge, U. K. 222 pp.

McFarland, D. 1982. *The Oxford Companion to Animal Behaviour.* Oxford University Press, Oxford, U. K.

Moynihan, M. 1985. *Communication and Noncommunication by Cephalopods.* Indiana University Press, Bloomington. 141 pp.

Moynihan, M., and A. F. Rodaniche. 1982. *The Behavior and Natural History of the Caribbean Reef Squid* Sepioteuthis sepioidea. *With a Consideration of Social, Signal and Defensive Patterns for Difficult and Dangerous Environments.* Advances in Ethology No. 25. Verlag Paul Parey, Berlin and Hamburg. 150 pp.

Packard, A., and F. G. Hochberg. 1977. Skin patterning in *Octopus* and other genera. *Symp. Zool. Soc. Lond.* **38:** 191–231.

Packard, A., and G. D. Sanders. 1971. Body patterns of *Octopus vulgaris* and maturation of the response to disturbance. *Anim. Behav.* **19:** 780–790.

Porteiro, F. M., H. R. Martins, and R. T. Hanlon. 1990. Some observations on the behaviour of adult squids, *Loligo forbesi,* in captivity. *J. Mar. Biol. Assoc. U. K.* **70:** 459–472.

Robins, C. R., R. M. Bailey, C. E. Bond, J. R. Brooker, E. A. Lachner, R. N. Lea, and W. B. Scott. 1991. Common and scientific names of fishes from the United States and Canada. *American Fisheries Society,* Special Publication 20, Fifth Edition.

Roper, C. F. E., and F. G. Hochberg. 1988. Behavior and systematics of cephalopods from Lizard Island, Australia, based on color and body patterns. *Malacologia* **29:** 153–193.

Sauer, W. H. H., and M. J. Smale. 1993. Spawning behaviour of *Loligo vulgaris reynaudii* in shallow coastal waters of the South-Eastern Cape, South Africa. Pp. 489–498 in *Recent Advances in Fisheries Biology,* T. Okutani, R. K. O'Dor, and T. Kubodera, eds. Tokai University Press, Tokyo.

Sauer, W. H. H., M. J. Smale, and M. R. Lipinski. 1992. The location of spawning grounds, spawning and schooling behaviour of the squid *Loligo vulgaris reynaudii* (Cephalopoda: Myopsida) off the Eastern Cape Coast, South Africa. *Mar. Biol.* **114:** 97–107.

Smale, M. J., W. H. H. Sauer, and R. T. Hanlon (in press). Ambush predation on spawning squids *Loligo vulgaris reynaudii* by benthic pajama sharks *Poroderma africanum* off South Africa. *J. Mar. Biol. Ass. U. K.*

Stevenson, J. A. 1934. On the behaviour of the long-finned squid (*Loligo pealii,* (Lesueur)). *Can. Field-Nat.* **48:** 4–7.

Summers, W. C. 1983. *Loligo pealei.* Pp. 115–142 in *Cephalopod Life Cycles, Vol. I,* P. R. Boyle, ed. Academic Press, London.

Worms, J. 1983. *Loligo vulgaris.* Pp. 143–157 in *Cephalopod Life Cycles, Vol. I* P. R. Boyle, ed. Academic Press, London.

Reference: *Biol. Bull.* **187**: 373–384. (December, 1994)

Nest-Site Selection in the Horseshoe Crab, *Limulus polyphemus*

DUSTIN PENN AND H. JANE BROCKMANN

Department of Zoology, University of Florida, Gainesville, Florida 32611

Abstract. Like a number of other species, horseshoe crabs lay their eggs on beaches in the intertidal zone. The elevation of the beach on which they nest differs among populations. We examined two factors that potentially affect egg survival at different beach elevations: erosion and rate of development. We found no evidence that eggs buried at different elevations incur different risks of erosion by wave action. However, the optimal beach elevation for egg development differed between our two study sites, Florida and Delaware, and the difference was related to beach morphology. Rate of development increased with oxygen concentration, redox potential, and temperature, and all three of these factors changed with elevation. The nests in the lower beach failed to develop, especially in Florida, where the beach was fine-grained and poorly drained. The nests in the upper beach were prone to dessication, especially in Delaware, where the beach was course-grained and well-drained. This means that differences between sites in the optimal location for egg development coincided with horseshoe crab preferences in nest-site selection. We suggest that horseshoe crabs synchronize their nesting with the tides that reach the aerobic sediments on the beach, resulting in nesting patterns that differ with differences in tidal regimes and beach morphology.

Introduction

Horseshoe crabs (*Limulus polyphemus*) synchronize their spawning with flood tides, especially the highest (spring) tides associated with lunar syzygies (Lockwood, 1870; Rudloe, 1980; Cohen and Brockmann, 1983; Barlow *et al.*, 1986). Although they deposit their eggs in sediments found on the mid to upper beach, nesting elevation varies among populations (Shuster, 1982). For example, horseshoe crabs in Florida (Rudloe, 1980; Cohen and Brockmann, 1983) and Massachusetts (Cavanaugh, 1975; Barlow *et al.*, 1986; Badgerow and Sydlik, 1989) nest in a narrow band in the upper middle quarter of the beach, whereas crabs in the Delaware Bay nest in a wide band over most of the wave-swept section of the beach (Shuster, 1982; Shuster and Botton, 1985; Botton *et al.*, 1992). The adaptive significance of nest-site preferences of horseshoe crabs is unclear, but it has been suggested that they nest at beach elevations where environmental conditions are most conducive to egg development (Lockwood, 1870; Shuster, 1982; Badgerow and Sydlik, 1989). Another possibility is that horseshoe crabs nest at elevations that minimize the loss of eggs due to beach erosion. In this paper we examine these hypotheses and the costs and benefits of the nest-site preferences of horseshoe crabs.

Horseshoe crabs spawn during the spring and early summer on certain beaches along the Atlantic and Gulf coasts of the United States, and in the Yucatan, Mexico (Shuster, 1982). At high tide females bury themselves in the sediments near the water's edge and lay a series of discrete egg clusters, each containing thousands of eggs (Brockmann, 1990). These eggs are fertilized by sperm released by an attached male and by one or more satellite males that typically congregate around the nesting couple (Rudloe, 1980; Brockmann, 1990; Brockmann and Penn, 1992; Brockmann *et al.*, 1994). The eggs develop in sediments 5 to 20 cm (mean 11.5 ± 2.8 SD cm) below the beach surface (Rudloe, 1979; Brockmann, 1990). After 2 to 4 weeks and four embryonic molts, the embryos hatch into "trilobite" larvae (Kingsley, 1892, 1893; Patten, 1896; Sekiguchi *et al.*, 1982; Sekiguchi, 1988). The nonfeeding larvae remain in the sand in distinct aggregations for several additional weeks, until they enter the ocean by moving toward the beach surface when tidal inundation occurs again (Rudloe, 1979). Within 2 weeks, the free-swimming trilobite larvae molt into juveniles that live in the near-shore sand flats (Sekiguchi *et al.*, 1982).

Received 17 September 1993; accepted 28 September 1994.

The preference that horseshoe crabs show for nesting in the upper elevations of the beach is puzzling because it is associated with several costs. (1) Individuals risk stranding on nesting beaches, which results in physiological stress or death from desiccation or predation (Botton and Loveland, 1989; Penn and Brockmann, in press). Stranding is riskier at higher beach elevations for two reasons: subsequent tides are less likely to "rescue" stranded crabs; and beach slope, which is necessary for orienting to the sea (Botton and Loveland, 1987; pers. obs.), diminishes in the upper beach. (2) Eggs located higher on the beach are likely to incur greater extremes of temperature and moisture and therefore may risk desiccation (Middaugh *et al.*, 1983). (3) Nesting on the beach requires that horseshoe crabs synchronize spawning with high tides, but this synchronization leaves individuals fewer opportunities to reproduce and increases competition for mates and nesting sites (Ims, 1990).

These costs suggest that there is some compensating benefit to the choice of spawning sites by horseshoe crabs. One possible explanation is that horseshoe crabs nest at elevations that optimize egg development (Lockwood, 1870; Badgerow and Sydlik, 1989). Shuster (1982) suggested that the development of *Limulus* eggs depends on a combination of temperature, moisture, and oxygen gradients on the beach, which vary according to local tidal amplitude. Sea turtles nest high on the beach because hatching success is increased by burying eggs in well-aerated sediments (Hays and Speakman, 1993; Horrocks and Scott, 1991). A second possible advantage is that wave action may be less likely to expose or wash away horseshoe crab eggs at certain beach elevations. Some intertidally spawning fishes, such as grunion, deposit their eggs in the upper intertidal to avoid beach erosion in the lower beach (Thompson, 1919; Taylor, 1984). To test hypotheses, we quantified the nesting locations of two populations of horseshoe crabs, Florida and Delaware, and conducted experiments that evaluated the effect of environmental variables and erosion on egg development and survival. The results of these experiments provide evidence for the adaptiveness of nest-site selection and spawning synchrony in horseshoe crabs.

Materials and Methods

Study sites

We studied horseshoe crabs at two locations in the United States: Florida (25 May to 5 June 1990 and 27 March to 31 April 1991) and Delaware (13 to 23 July 1990 and 11 May to 15 June 1991). The Florida (FL) site was a low-energy sandy beach on the south shore of Seahorse Key, a small island in the Gulf of Mexico, 4 km from Cedar Key (29°06′ N, 83°04′ W), Levy County. The Delaware site (DE) was a low-energy beach of mixed sand and gravel located just inside the mouth of the Delaware Bay at the Cape Henlopen State Park (38°47′ N, 75°06′ W).

Beach measurements

To quantify beach elevation, we measured the oblique distance from a zero point on the beach to locations higher on the beach ("Beach Distance"). The zero point was the bottom of the beach where the mud flat ended and the beach began; *i.e.*, the slope and sediment composition changed abruptly. Beach distance was more practical to measure than elevation and the variations in beach slope, 2–5°, were insufficient to affect our measurements. We quantified the location at which eggs were laid by placing wire flagging stakes on either side of the female during nesting. We marked each egg cluster that the female laid by putting these flags across the female's hinge each time she moved forward in the sand; this procedure minimized the possibility of eggs from other females contaminating the egg clusters (Brockmann, 1990). At low tide we measured the distance from the bottom of the beach to the center of each set of flags ("Nesting Distance"). We also measured the water depth in which females nested and their distances to the water's edge. We quantified the timing of nesting by counting the number of nesting couples on the beach on three tides for 3 hours before and after the MHT in FL (1989) and DE (1991). "Tidal Distance" was quantified by measuring the extent of tidal inundation on the beach, using wooden stakes that were driven into the beach at 2-m intervals (measured as beach distances). We used tidal data recorded by the National Oceanic and Atmospheric Administration (at Cedar Key, FL, and Lewes, DE) to calculate mean high tide line (MHTL) for each. NOAA tide heights and our tidal distance measurements were highly correlated (FL $r = 0.92$; DE $r = 0.93$), which enabled us to interpolate the MHTL (±95% CI) in tidal distance for April in FL and May in DE, 1991.

Egg development

To test the hypothesis that egg development was affected by beach elevation, we reburied newly laid eggs at three different beach distances and examined the eggs after 10 days (1990). After marking nests, we excavated and collected the freshly laid eggs at low tide from 25 (FL) and 22 (DE) different nests, broke up the clusters, separated the eggs from the sediments, and measured their volume (Brockmann, 1990). To separate the eggs we used a sieve (1 mm mesh) in FL, but the mixed sand-gravel beach in DE required that we elutriate the eggs from the sediments. We reburied 60 (FL) and 90 (DE) egg clusters ("Egg Batches") 8 cm below the sand surface at three different beach distances (3, 5, and 8 m) at 20 (FL) and 30 (DE) locations along 1 km of beach, marking their location with flagging stakes. To prevent egg loss or contamination from other nests, half of the batches were placed in "cages" (2 mm nylon mesh bags sealed with Velcro). After 10 days we excavated the egg batches and quantified their development in two ways. First, we estimated the percent of developed eggs by visually inspecting the developmental stages of a 1-ml sample of eggs under a dissecting microscope, separating undeveloped eggs from embryos (*i.e.*, those with limb buds which occur during stage 13; Sekiguchi *et al.*, 1982), and counting the number to obtain a "Percent Eggs Developed" within each batch. Second, we measured the increase in the volume of egg batches ("Egg Batch Volume") due to developmental swelling (*i.e.*, the 1.7-mm *Limulus* eggs become 3.6-mm embryos before hatching). For example, volume of egg batches (due to developmental swelling) increased significantly with developmental rate (developmental index) ($r^2 = 0.65$, $F_{1,8} = 10.6$, $P = 0.01$). Changes in volume were calculated by dividing the volume at 10 days by the initial volume of an egg batch (V_2/V_1) because the initial volume of the egg batches varied (20–50 ml). Variation in initial volume of egg batches did not significantly affect developmental rate ($\beta = 0.25$, $T = 1.9$, $P = 0.06$).

To test the hypothesis that egg development was affected by environmental variables that changed with beach elevation, we collected freshly laid eggs from 13 (FL) and 23 (DE) nests and reburied the caged egg batches at 8 (FL) and 7 (DE) different predetermined beach distances for 12 days (1991). In DE we anchored the cages with flagging stakes so they would not be exposed by other nesting crabs. To quantify the average development of each egg batch after 12 days, we used a "Developmental Index" (D.I.). This index provided more resolution than "percent developed" used in 1990 because it weights development by the time required to reach each stage under standard conditions. Samples from each egg batch were divided into four categories based on developmental stages: eggs (stages 1–17), embryos (stages 18–19), late embryos (stages 20–21), and larvae (Sekiguchi *et al.*, 1982). After counting the number of individuals in each category, we multiplied this number by the number of days required to reach that stage in the laboratory (stage × days) (Brown and Clapper, 1981). We calculated an overall D.I. for each batch by taking the sum of the stage × days for all developmental stages divided by the total number of individuals. For example, the D.I. for one batch that had 5 eggs, 14 early embryos, 198 late embryos, and 0 larvae is $\sum[\text{stage} \times \text{days}] = [5\ (0) + 14\ (15) + 198\ (21) + 0\ (26)]/217 = 20$, which means that the batch contains a large proportion of late embryos. We used stepwise multiple regressions to determine the environmental factors that best predicted developmental rate.

We measured six environmental variables near the developing egg batches. (1) Temperature was measured *in situ* with a thermistor probe inserted 10 cm below the surface, and measurements were taken three (DE) or five (FL) times for each egg batch (means used in analyses). (2) Moisture content (%H_2O) was measured by collecting sediment samples near each egg batch (in sealed plastic containers), weighing (within 2 h), drying (oven baked at 105°C), and reweighing (%H_2O = [(wet weight − dry weight)/wet weight] × 100). (3) Salinity of the interstitial water (10 cm from surface) was measured in FL with a refractometer. (4) Interstitial oxygen concentration ($[O_2]$) could not be measured directly because %H_2O varies at different beach distances. Instead we used a portable YSI oxygen meter to measure the dissolved $[O_2]$ in 120 ml of seawater inside a plastic bag that we buried in the sediments near the egg batches. Dissolved $[O_2]$ within the bags equilibrates with the surrounding $[O_2]$ sediments because polyethylene is permeable to oxygen (Fremling and Evans, 1963). Two (FL) or three (DE) measurements per bag were taken (mean used in analyses). We also collected sediments (50 ml) near each egg batch, added seawater (50 ml) to each sample, and then directly measured the $[O_2]$ 1 h later at 30°C ("Sediment Analysis"). (5) Redox potential (Eh) was also measured inside the bags using a Fisher 955 pH/mV meter with a naked platinum electrode (Corning 476080 Redox Combination Electrode) because [Eh] is a more reliable indicator of oxygen availability than $[O_2]$ measurements (McLachlan, 1978). [Eh] also indicates ion imbalances in sediments due to microbial activity (ZoBell, 1946; Bånger and Niemistö, 1978). (6) Sediment data were taken because the grain size determines the drainage and interstitial oxygen content of beaches (Eagle, 1983). Sediments were collected in FL and the mean grain size (M_z) and the variation, or sorting coefficient ($\sigma_1\phi$), was measured by sieving (at 1ϕ intervals in the range -2 to $5\ \phi$). The units are on the phi (ϕ) scale, where $\phi = -\log_2 S$ and S is the grain size in mm (Boggs, 1987). The results were compared with descriptions of sediments from DE (Maurmeyer, 1978).

Because *Limulus* embryos can postpone development under anaerobic conditions (Palumbi and Johnson, 1982), we determined whether undeveloped eggs were still viable by transferring them to aerobic conditions in the laboratory. Eggs from each egg batch were reared in petri dishes (100 eggs per dish) with filtered seawater (periodically changed) in a FormaScientific incubator (under a 14 h daylight schedule at 30°C day, 26°C nighttime temperature; Brown and Clapper, 1981). In DE we noted the number of individuals within egg batches that were obviously dead (decayed and crumbly) after 12 days on the beach and compared the relative mortality of eggs at different beach distances.

Egg loss due to erosion

To test the hypothesis that beach elevation affects erosion of eggs from the sand, we measured the net amount of sand lost (erosion) or deposited at different beach distances (1991). We hammered forty 1-m wooden stakes into the sand (the same stakes we used for measuring tidal distance). After the tide receded, we recorded the change in beach level ("erosion/deposition") that occurred since the previous tide. In FL we recorded the change in sand erosion/deposition at four beach distances ($n = 7$) using the mean from 11 high tides. In DE, we recorded the mean erosion/deposition at five beach distances ($n = 5$) from five tides. We looked for evidence of egg loss by comparing the change in volume between matched pairs of caged and uncaged egg batches from the egg development experiment (1990). Reduced volume in uncaged egg batches relative to caged ones would provide evidence for egg loss due to erosion. We also used egg-sized, colored glass beads to minimize the effects of predation (FL 1991). We made 30 "bead batches" (3-g batches), and buried them at three different beach distances, 8 cm below the surface ($n = 10$). To monitor the erosion during the experiment, we buried each batch near an erosion stake (using the mean erosion/deposition for analyses). After 17 days, the depth of the bead batches (the distance from the surface) was remeasured, and, after allowing them to dry, each batch was reweighed to estimate bead loss.

Data analyses

Before performing statistical tests, we examined the residual plots to validate the assumptions of the tests and used arcsine transformations on percentage data (to normalize variances). We used higher-level regression models (such as quadratic versus linear) only if there was a significant increase in the variation explained by adding an additional term to the model ($\alpha = 0.05$). We used multiple regressions to evaluate the significance of various factors and stepwise regression procedures to select the model when colinearity occurred. We used "Statview" (Abacus concepts, 1989a) and "SuperANOVA" (Abacus Concepts, 1989b) statistical software. Data are reported as mean ± standard deviation, unless otherwise stated.

Results

Differences in nest-site location, tidal synchrony, and beach characteristics

Horseshoe crabs in DE nested higher and over a wider range of beach than those in FL (Fig. 1); the mean nesting distance and the variance were significantly greater in DE than in FL (Table I). In DE 95% of the crabs nested over 61% of the beach, whereas in FL 95% of the horseshoe crabs nested over 40% of the beach. The mean nesting distances were not significantly different from the mean high tide line (MHTL) in FL or DE (*t*-test, $P > 0.1$) and the nesting distances increased slightly with increasing tidal distance (FL: $r^2 = 0.25$, $F_{1,142} = 433$, $P = 0.0001$). The crabs nested in or just below the swash zone and neither the distance from the water's edge nor the water depth (*t*-test, $T_{179} = 1.1$, $P = 0.29$) of nesting crabs differed significantly between FL and DE populations (Table I).

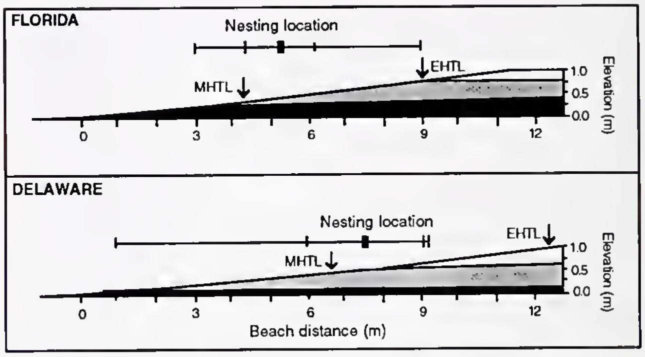

Figure 1. A comparison of the location on the beaches where horseshoe crabs nest in Florida and Delaware. "Nesting location" is the beach distance (mean ± SD and range) where nesting occurs. MHTL is the mean high tide line and EHTL is the extreme high tide line. The moisture gradients on the beaches are shown as the saturated zone (■), moist zone (□), and drying zone (□).

The DE and FL populations exhibited different patterns of lunar and tidal synchrony (Table I). (1) In FL the crabs spawned only during spring tides. In DE the largest populations emerged during spring tides, but they continued to spawn during neap tides. (2) Spawning crabs were more abundant during the higher of the two daily tides in DE and FL. We noted one exception in DE when tidal inequality was reversing; *i.e.*, during lunar quadrature, the crabs were more abundant on the lower tide of the day in DE (see also Barlow *et al.*, 1986). In FL the highest tides were usually during the day, whereas in DE they were usually at night (1990; Table I). (3) In FL the largest numbers of horseshoe crabs nested around the time of the MHT (see also Cohen and Brockmann, 1983), but in DE they nested after MHT, *i.e.*, during the receding tide (Fig. 2).

The FL and DE beaches differed in a number of important respects (Table I). First, the extent of tidal inundation was greater in DE than in FL. Second, although both beaches can be classified as low energy, the FL beach was of a much finer grain size than the DE beach. Third, associated with these two variables was the fact that the saturated zone and the drying zones were higher on the beach in FL than in DE; *i.e.*, the finer grained sediments of the FL beach held water better than the coarser grained sediments of DE. Fourth, FL and DE beaches differed in the beach distances at which there was available oxygen (Table I).

Egg development

FL and DE differed in the pattern of egg development with beach distance. In FL, egg batches placed at the high-

Table I

Nest-site selection by horseshoe crabs, the development of their eggs, and characteristics of the beach at various elevations at two sites, Florida and Delaware

	Florida	Delaware
Nesting Behavior		
Location of Nesting Crabs		
Mean nesting distance	5.1 ± 0.9 m (n = 434)	7.4 ± 1.9 m (n = 1396)
Range of nesting distance	3 to 9 m (n = 433)	1 to 9 m (n = 1395)
Mean distance from water's edge	68 ± 68 cm (n = 37)	85 ± 70 cm (n = 145)
Mean water depth	8 ± 9 cm (n = 37)	7 ± 8 cm (n = 144)
Nest depth	11.5 ± 2.8 cm (n = 382)	9.3 ± 3.9 cm (n = 112)
Spawning Synchrony		
Lunar	spring tides	spring and neap tides
Tidal	both daily tides (n = 13)	higher tide (n = 13) which usually occurs at night
Timing of maximum crab density	around high tide	after high tide
Egg Development (Percent Developed, 1991)		
Beach Distance		
11–12 m	^{Y}	73
9–10 m	^{Y}	74
7–8 m	81	97
5–6 m	70	95
3–4 m	40	76
0–2 m	0	39
Beach Characteristics		
Tides		
Tidal amplitude[†]	1.0 ± 0.5 m	2.0 ± 1.0 m
Mean high tide line	4.3 ± 0.6 m	6.7 ± 0.05 m
Extreme high tide line beach distance	9.0 m	12.5 m
Diurnal equality	nearly equal	unequal
Beach slope	2 to 5°	2 to 5°
Beach Sediments		
Percent gravel	0.0	0.1 to 82.0*
Percent sand	100	18.0 to 99.9*
Mean grain sizes (M_Z)	medium sand (0.31 mm, 1.67ϕ)	very coarse sand (1 mm, 0.008ϕ)*
Moisture Gradient (at different beach distances)		
Drying zone (<5%)	>8 m	≥4 m
Moist zone (5–17%)	3–8 m	1–3 m
Saturated zone (>18%)	<3 m	≤0 m
Oxygen/Eh Gradient (at different beach distances)		
High (>2.5 ppm and +Eh)	>5 m	>3 m
Medium (1–2 ppm and +Eh)	3–8 m	1–3 m
Low (<1 ppm and −Eh)	<3 m	≤0 m

[†] The predicted mean spring (and neap) tidal amplitudes (NOAA); ^{Y} Elevations above EHTL were not sampled; *Delaware data from Maurmeyer, 1978 (mean of four samples from the Breakwater Harbor beach face).

est location on the beach (8 m) were well-developed after 10 (1990; Table II) and 12 days (1991; Table I), whereas those placed at the lowest beach distances showed no signs of development and 26% were black, crumbly, and putrid smelling (1990; n = 14). Developmental rate (Fig. 3a) and egg-batch volume (Fig. 3b) increased significantly with beach distance. In DE the developmental rate of egg batches did not vary significantly with beach distance in 1990 (Table II), but in 1991 (Table I) developmental rate was maximal in the mid-section of the beach. Developmental rate increased with beach distance up to 8 m, and then decreased (Fig. 3c), and egg-batch volume increased with beach distance up to 4 m, and then decreased (Fig. 3d). The greatest egg mortality occurred below 4 m and above 8 m (r^2 = 0.15, P = 0.04).

Oxygen concentration, redox potential, temperature, and moisture content varied significantly with beach distance in both FL and DE (Fig. 4). In FL developmental rate increased with all variables except salinity, which was invariably 26 ppt (n = 10), and these variables were

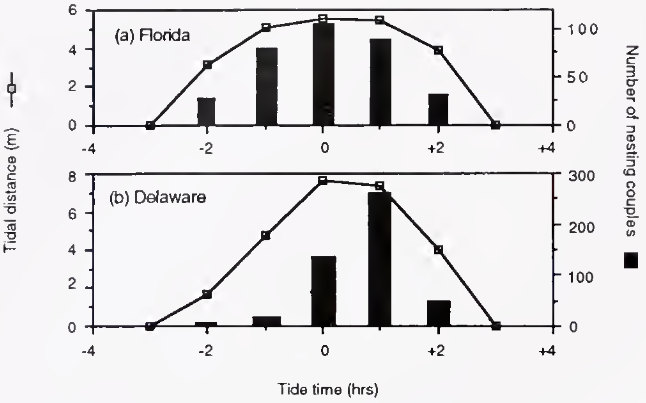

Figure 2. The time of maximum horseshoe crab spawning compared with the time of maximum high tide at (a) Seahorse Key, Florida (1989) and (b) Cape Henlopen, Delaware (1991). The bars indicate the mean number of nesting couples over three days and the points indicate the mean tidal distance recorded during three flood tides. "Tide time" indicates the hours before (−) and after (+) the maximum high tide (adapted from Burger *et al.*, 1977). Tidal synchrony was significantly different between the two populations ($\chi^2 = 945$, df = 4, $P < 0.001$).

intercorrelated with each other (Table III). A stepwise regression analysis found that $[O_2]$ was the variable that best predicted the developmental index in FL ($r^2 = 0.53$, $F_{1,22} = 25.2$, $P = 0.0001$), whereas the best predictor of D.I. in DE was $\%H_2O$ ($r^2 = 0.67$, $F_{2,23} = 23.6$, $P = 0.0001$).

The $[O_2]$ in the sediment samples (sediment analysis) increased significantly with beach distance ($r^2 = 0.45$, $F_{1,22} = 18$, $P = 0.0001$) in FL. Sand color below the surface was lighter at higher beach distances (ANOVA, $F_{1,158} = 143$, $P = 0.0001$) and was black or grey from 0 to 3 m, indicating anaerobic conditions (Eagle, 1983). Developmental rate (D.I.) of eggs in the incubator increased significantly with beach distance ($r^2 = 0.33$, $F_{1,34} = 16.7$, $P = 0.0003$) and eggs that had been buried in the lower beach (below 3 m) never hatched. Unlike FL, the sediments beneath the surface in DE were rarely grey or black, and most eggs in the lower beach showed some signs of development.

Egg loss due to erosion

In FL sand was eroded from the lower part of the beach and deposited at higher beach distances (Fig. 5). However, in the artificial egg experiment, bead loss occurred only at the highest beach distance (ANCOVA, $F_{1,28} = 7.92$, $P = 0.009$). No significant associations were found between bead loss ($P = 0.75$) or final bead depth ($P = 0.70$) and sand erosion. In the egg-loss experiment, volume (V_2/V_1) did not differ between caged and uncaged treatments (Wilcoxon Signed-Ranks, $z = 0.77$, $n = 13$, $P = 0.22$). In DE sand was eroded only at the highest beach distance ($r^2 = 0.23$, $F_{1,22} = 6.9$, $P = 0.02$) and this was negligible (*i.e.*, < 5 cm) (Fig. 5). Egg batch volume (V_2/V_1) did not differ between caged and uncaged treatments ($F_{1,74} = 2.7$, $P = 0.12$).

Discussion

Nest-site selection and egg development

Horseshoe crabs nested at beach elevations where egg development was maximized. They nested just above the mean high tide line, avoiding the lower and upper elevations where egg development was impaired. Our results show that variation in egg development with elevation is due to chemical and thermal gradients on the beach. The sediments in the upper beach were warmer and drier than the lower beach, which explains why eggs buried above the mean tide line were more likely to desiccate than eggs buried lower on the beach. The sediments in the lower beach contained insufficient interstitial oxygen concentrations for egg development to occur. The color and odor of the lower beach indicated the presence of hydrogen sulfide and explains why the eggs became black and crumbly. The inability of eggs to survive in anoxic sediments supports the suggestion that nesting horseshoe crabs avoid beaches with anoxic peat beds because they impair embryonic development (Botton *et al.*, 1988). Horseshoe crabs may avoid anaerobic conditions (anoxic sediments, peat beds, and sewer outflows; Rudloe, 1971) by using oxygen-sensitive elements in their book gills (Crabtree and Page, 1974) and prosoma (Thompson and Page, 1975). It has also been suggested that horseshoe crabs have H_2S receptors (Botton *et al.*, 1988).

Horseshoe crabs in Delaware nest over a wider range of the beach than in Florida, probably because the range of elevations conducive to development is wider in Delaware. The differences in egg development between the two sites can be explained by differences in oxygen and moisture gradients on the beaches. In Florida the interstitial oxygen concentration increased slowly with distance (not reaching $[O_2] > 1$ ppm and +Eh until 3 m), whereas oxygen concentration increased sharply with beach distance in Delaware ($[O_2] > 1$ ppm and Eh > +80 above 1 m section of the beach) (Figs. 4a, e). Also the redox potentials in the lower beach in Delaware (+140 to −30 mV) were never as low as in Florida (−50 to −250 mV) (Figs. 4b, f). This means that the Delaware crabs can nest lower on the beach without adversely affecting the development of their eggs.

The differences in interstitial oxygen (and redox gradients) and moisture gradients between the Florida and Delaware sites can ultimately be attributed to differences in beach morphology (Table I). Sediment grain size determines the drainage of a beach, which greatly affects the interstitial oxygen content (Gordon, 1960; Brafield, 1964; Eagle, 1983). The Florida sediments were fine to medium

FLORIDA

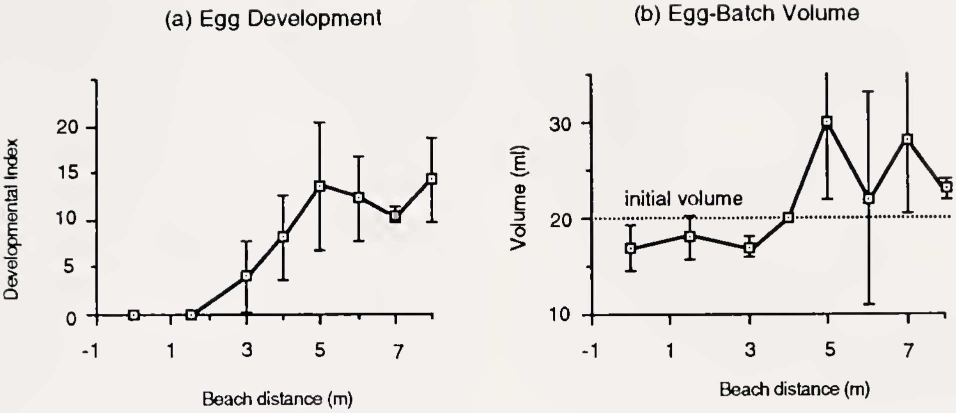

DELAWARE

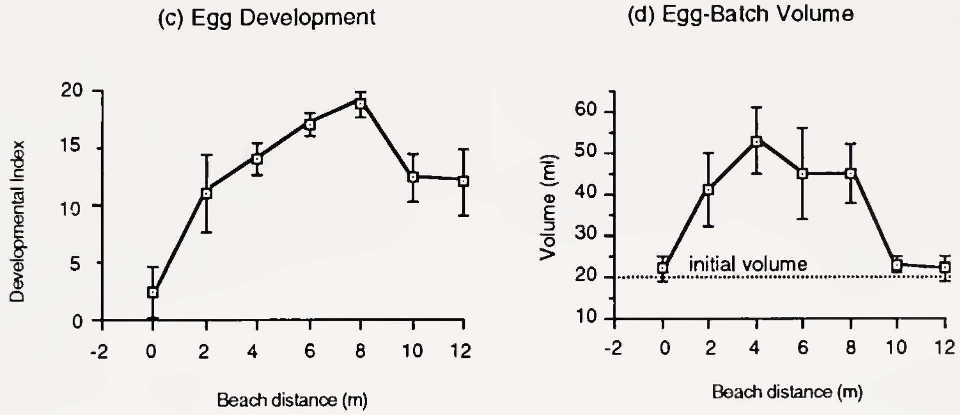

Figure 3. Development of *Limulus* eggs, embryos and larvae (mean ± SE) at different beach distances in Florida (a and b) and Delaware (c and d). Development, as measured by the developmental index, varied with beach distance in (a) Florida ($r^2 = 0.35$, $F_{1,21} = 11.3$, $n = 3$, $P = 0.003$) and in (c) Delaware ($r^2 = 0.44$, $F_{2,42} = 16$, $n = 7$, $P = 0.0001$). Egg batch volume due to developmental swelling also varied with beach distance in (b) Florida ($r^2 = 0.12$, $F_{1,21} = 2.9$, $P = 0.10$) and (d) Delaware ($r^2 = 0.32$, $F_{2,42} = 9.7$, $P = 0.0003$).

grained and had poor drainage (*e.g.*, the moisture content decreased gradually, not dropping to 5% until 7 m), whereas the Delaware sediments were coarse grained with relatively high drainage (*e.g.*, the interstitial water dropped sharply, falling below 5% at 4 m) (Figs. 4d, and h). Thus, even though the tidal amplitudes were greater in Delaware, the water content of the beach was lower than in Florida. Fine-grained sediments, such as in Florida, also have greater surface areas for microbial growth. This further depletes interstitial oxygen, increases hydrogen sulfide, and lowers redox levels (Eagle, 1983; Boaden, 1985). Variation in beach geochemistry may also explain why the crabs in Florida nested up to the EHTL but well below this mark in Delaware (Fig. 1). In Delaware the eggs in the highest part of the beach were usually desiccated. Water retention was so poor in Delaware that water concentration was the best predictor of egg development on the beach. Increased risk of desiccation on higher parts of the beach may explain why crabs in Massachusetts shift their nesting sites to lower beach distances during the summer (Barlow *et al.*, 1986).

Nesting synchrony

Nesting synchrony varied significantly between the two populations. In the Delaware Bay, horseshoe crabs often spawn during neap tides, as reported for Massachusetts (Cavanaugh, 1975; Barlow *et al.*, 1986; pers. obs.). However, crabs in Florida almost never spawn during neap tides (Rudloe, 1980; Cohen and Brockmann, 1983; pers. obs.). Our results from the egg-development experiments suggest an adaptive explanation for differences in spawning synchrony between these populations. The aerobic sediments occur at higher elevations in Florida than in

Table II

The development of Limulus *eggs placed at different locations on the beach*

	Florida		Delaware	
Beach distance	% Developed	*n*	% Developed	*n*
Upper beach (8 m)	67 ± 32	23	61 ± 33	30
Middle beach (5 m)	5 ± 2	21	65 ± 30	29
Lower beach (3 m)	0	14	59 ± 33	27

Results from the 1990 development experiment. Egg development (percent eggs developed $\bar{x} \pm$ SD) increased with beach distance in Florida (ANOVA, $F_{2,55} = 82$, $P = 0.0001$), but not in DE ($F_{2,78} = 0.39$, $P = 0.68$). Overall, egg development was significantly greater in DE than in FL ($F_{1,142} = 886$, $P = 0.0001$).

Delaware, and neap tides are lower in Florida than in Delaware (Table I; tidal amplitude decreases with latitude in the eastern U.S.). In Florida the flood tides rarely reach the aerobic zone of the beach (Fig. 6), which explains why horseshoe crabs there do not nest during neap tides.

Nesting synchrony corresponds to local tidal patterns in yet another way. In Florida the two daily flood tides were nearly equal in height and the crabs spawned on both (Rudloe, 1980; Cohen and Brockmann, 1983). However, in northern latitudes, the two daily tides were disproportionate in size (indeed, the largest neap tides are higher than the lower spring tides) and northern horseshoe crabs preferred the higher of the two tides (Barlow *et al.*, 1986; pers. obs.), which occurred at night during the spring and early summer. Only the higher of the two tides at this latitude reached the aerobic zone of the beach (Fig. 6). Knowing the local tidal rhythms and the location of the aerobic zone on the beach may enable one to predict the location and timing of horseshoe crab spawning.

Another similarity in spawning synchrony between Delaware and Massachusetts populations, which differed from Florida, is that the crabs in both locations largely spawned one hour after the maximum high tide (Howard *et al.*, 1984). There are several possible explanations for nesting during the receding tide. (1) The mixed sand and gravel sediments in Delaware may make nest excavation relatively difficult (*e.g.*, the carapaces of females are often eroded in Delaware Bay). The crabs may reduce nesting effort by nesting during the receding tide when the sediments seem to be softer (pers. obs.). (2) Because the scour phase occurs on the incoming tide (whereas the deposition phase occurs on receding tides) (Strahler, 1966), nesting on the receding tide might minimize egg loss due to erosion. However, we had little erosion of eggs at any locality so this seems unlikely. (3) Nesting on the receding tide might minimize egg loss caused by disturbance from other nesting crabs, which appears to be the major source of egg loss in Delaware Bay (Barash, 1993; pers. obs.).

Nest-site selection and egg loss due to erosion

We found no evidence that nests at lower elevations were more likely to be washed away by erosion in Florida or Delaware. Our measurements indicated that erosion was insufficient to uncover horseshoe crab nests buried 5 to 20 cm below the sand surface (Brockmann, 1990). Measurements of erosion recorded during the incoming "scouring phase" of the tide, however, reveal that the lower beach is more dynamic than the upper beach (Strahler, 1966). Still, in the artificial egg experiment, more beads were lost in the upper beach (where wave action appeared to be the greatest). However, bead loss may have been due to nesting crabs uncovering beads, rather than erosion, because bead-depth and erosion did not vary with bead loss. Such differential excavation of beads by nesting crabs was not controlled in the experiment because the densities of spawning crabs were relatively low in Florida, and because caged controls interfere with erosion (Quammen, 1981). Despite the negative effect here, it must be noted that our experiments did not incur any storms at either locality, and substantial beach erosion occurs during severe storms (pers. obs.).

Nest-site selection and egg loss due to predation

Horseshoe crabs are generally thought to nest on beaches to minimize egg loss from aquatic predators such as fish (Rudloe, 1980; Cohen and Brockmann, 1983; Botton and Loveland, 1989). Eggs and larvae have been found in several fishes in Delaware Bay (Shuster, 1982). We observed small schools of striped killifish (*Fundulus majalis*) burrowing into nests that were located just below the sand surface in Florida, but only on four occasions in 1991. We found no differences in egg loss when we compared caged and uncaged eggs at any beach elevation in Florida or Delaware (Penn, 1992). We suspect that fish feed mainly on eggs uncovered by nesting crabs and wave action (Shuster, 1960), and on trilobite larvae that are moving into the sea at high tide (Rudloe, 1979). Even if aquatic egg predation is a negligible selective pressure on nest-site selection in horseshoe crabs today, aquatic egg predators may have provided the initial selective pressures for intertidal spawning in ancestral merostomes. Intertidal spawning may have preadapted the early chelicerates for the initial animal invasion of land (Størmer, 1977; Little, 1983).

The heaviest predation on horseshoe crab eggs is undoubtedly from shorebirds (Mallory and Schneider, 1979; Botton, 1984; Castro *et al.*, 1989; Castro and Myers, 1993; Botton *et al.*, 1994). Although shorebirds might be expected to feed on nests located higher on the beach, they often forage along the water's edge following the tide line (Recher, 1966; Recher and Recher, 1969; Burger *et al.*, 1977; Evans, 1988; pers. obs.) apparently capitalizing on

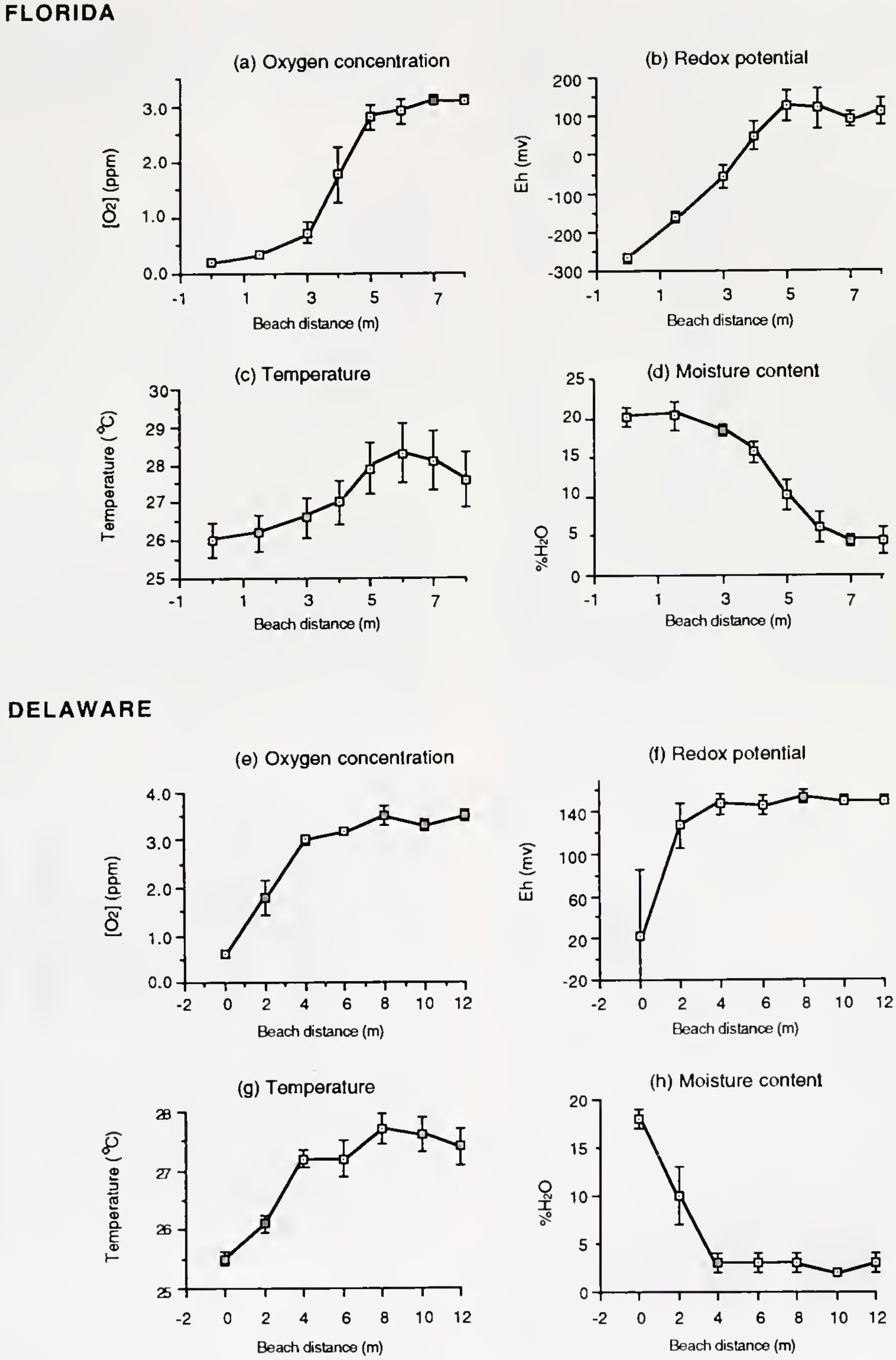

Figure 4. The conditions of the sediments at different beach distances (1991; mean ± SE, $n = 3$) in Florida: (a) interstitial oxygen concentration ($r^2 = 0.78$; $F_{1,22} = 78$; $P = 0.0001$), (b) redox potential ($r^2 = 0.79$; $F_{1,19} = 70$; $P = 0.0001$), (c) temperature ($r^2 = 0.64$; $F_{1,22} = 39$; $P = 0.0001$), (d) moisture content ($r^2 = 0.80$; $F_{1,22} = 87$; $P = 0.0001$); and Delaware: (e) interstitial oxygen concentration ($r^2 = 0.82$; $F_{2,46} = 102$; $P = 0.0001$), (f) redox potential ($r^2 = 0.36$; $F_{2,39} = 11$; $P = 0.0002$), (g) temperature ($r^2 = 0.61$; $F_{2,46} = 35$; $P = 0.0001$), and (h) moisture content ($r^2 = 0.83$; $F_{2,27} = 67$; $P = 0.0001$).

Table III

The effects of four environmental factors in beach sediments on the development of Limulus *eggs (D.I.) at the FL and DE sites (1991)*

Parameter	Florida r^2	Florida Significance test	Delaware r^2	Delaware Significance test
$[O_2]$	0.53	$F_{1,22} = 25.2$; $P = 0.0001$	0.42	$F_{2,42} = 15$; $P = 0.0001$
Eh	0.32	$F_{1,19} = 8.8$; $P = 0.0008$	0.31	$F_{2,35} = 7.7$; $P = 0.002$
Temperature	0.44	$F_{1,22} = 17.6$; $P = 0.0004$	0.32	$F_{2,42} = 10.7$; $P = 0.0002$
$\%H_2O$	0.41	$F_{1,22} = 15.2$; $P = 0.0001$	0.67	$F_{2,23} = 23.6$; $P = 0.0001$
$[O_2]$ and Eh	0.68	$F_{1,19} = 40$; $P = 0.0001$	0.33	$F_{1,40} = 19.6$; $P = 0.0001$
$[O_2]$ and temperature	0.76	$F_{1,22} = 70$; $P = 0.0001$	0.56	$F_{1,47} = 64$; $P = 0.0001$
$[O_2]$ and $\%H_2O$	0.80	$F_{1,22} = 86.3$; $P = 0.0001$	0.92	$F_{1,26} = 251$; $P = 0.0001$
Temperature and Eh	0.49	$F_{1,19} = 18.1$; $P = 0.0004$	0.26	$F_{1,40} = 14$; $P = 0.0006$
Temperature and $\%H_2O$	0.84	$F_{1,22} = 119$; $P = 0.0001$	0.58	$F_{1,20} = 30.2$; $P = 0.0001$
Eh and $\%H_2O$	0.45	$F_{1,19} = 16$; $P = 0.0008$	0.43	$F_{1,21} = 16$; $P = 0.0007$

Note: A polynomial regression was used on the Delaware data and nonsignificant effects were not included.

the softer substrate at the water's edge. Because the tides rarely reach them, higher nests may actually be safer from the probing bills of shorebird predators than lower nests. Such "bottom-up" predation has been found in several species of shorebirds (Prater, 1972; Ambrose, 1986; Peterson, 1991). Our observations in Florida suggest that most horseshoe crabs nest above the elevation where sanderlings (*Calidris alba*) and willets (*Catoptrophorus semipalmatus*) forage (Penn, 1992). This would favor avoiding nesting in the lower beach. In Delaware laughing gulls (*Larus atricilla*) and numerous shorebirds fed on *Limulus* eggs. However, rather than probing below the surface, the birds fed on the copious eggs on the beach

(a) FLORIDA

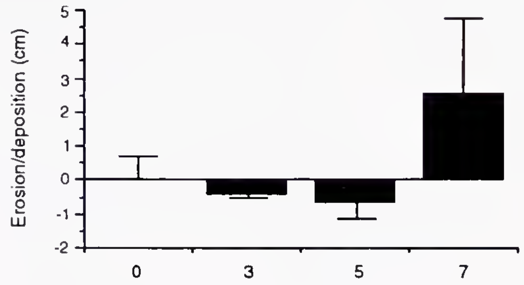

(b) DELAWARE

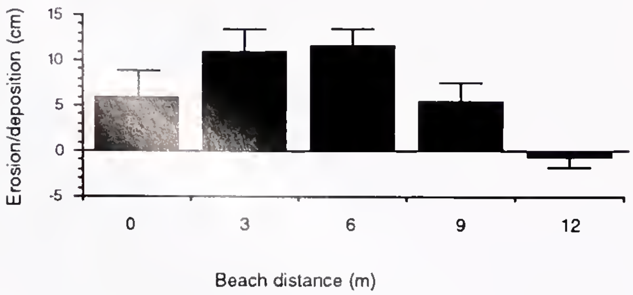

Figure 5. Changes in beach level from erosion and deposition of sediments at different beach distances in (a) Florida and (b) Delaware. Deposition occurred at the highest beach distance in Florida ($r^2 = 0.32$; $F_{1,26} = 12$; $P = 0.002$), whereas erosion occurred at the highest beach distance in (b) Delaware ($r^2 = 0.23$; $F_{1,22} = 7$; $P = 0.02$).

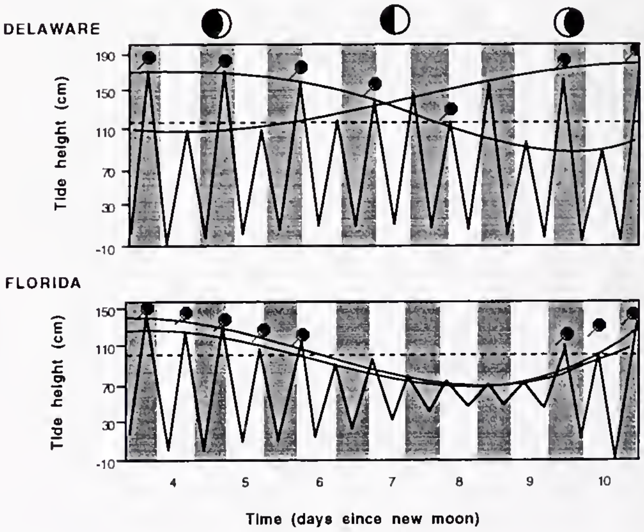

Figure 6. A model of spawning synchrony of horseshoe crabs with tidal rhythms in Delaware and Florida. Tidal amplitude (/\/) decreases during lunar quadrature (neap tides) and increases during lunar syzygy (spring tides). Tidal inequality of daily tides (sinusoidal lines) is greatest during spring tides, especially in Delaware. Horseshoe crabs in Delaware synchronize their spawning with the higher of the two daily tides (which usually occurs at night), which enables them to reach the aerobic sediments on the beach (dashed lines). Horseshoe crabs in Florida do not spawn during neap tides, when the tides fail to reach the aerobic elevations. However, during spring tides they spawn during both daily tides as there is little tidal inequality.

surface uncovered by nesting crabs (Barash, 1993; Botton *et al.*, 1994). Thus, it seems unlikely that nest-site selection is an adaptation to protect eggs from shorebirds in Delaware.

Conclusions

Horseshoe crabs nest just above the mean high tide line where the development of their eggs is maximized. Beach sediments lower on the beach contain inadequate interstitial oxygen concentrations (and probably high H_2S), whereas sediments higher on the beach are too dry for egg development. Differences in nest-site preferences between the Florida and Delaware horseshoe crabs correspond to differences in the location where eggs successfully develop, which is ultimately due to differences in geochemistry on these beaches. Although beach geochemistry and local tidal rhythms provide a partial explanation for the geographic variation in nest-site preferences and nesting synchrony among horseshoe crabs, they do not explain all of the variation in nesting behavior. Other factors, such as predation and intraspecific competition for nesting sites, are likely to affect nest-site selection in *Limulus*.

Acknowledgments

This paper is dedicated to Melanie Meador Penn (1962–1994) who provided us with much assistance with this and our other horseshoe crab studies. We also thank our other diligent field assistants, K. Abplanalp, A. Alonso, B. Biederman, M. Marquez, D. Weaver, R. Shammami, and L. Niko. We are grateful to Drs. C. Shuster, C. Lanciani, and L. McEdward and to two anonymous reviewers for their comments on earlier drafts of this manuscript. We sincerely thank Frances Stone for the egg cages and Drs. E. Maurmeyer, C. Oyen, and F. Nordlie for their advice and assistance. We especially thank Michael Penn and Ginger Penn for their support and encouragement. We thank Mike Kennedy and the Cape Henlopen State Park. This research was supported by NSF OCE90-06392, Sigma Xi Grants-In-Aid of Research, the University of Delaware College of Marine Sciences, the University of Florida Foundation, the Department of Zoology and the Seahorse Key Marine Laboratory under a special permit from the Lower Suwanee National Wildlife Refuge.

Literature Cited

Abacus Concepts. 1989a. *StatView.* Abacus Concepts, Inc., Berkeley.

Abacus Concepts. 1989b. *SuperANOVA.* Abacus Concepts, Inc., Berkeley.

Ambrose, W. G., Jr. 1986. Estimate of removal rate of *Nereis virens* (Polychaeta: Nereidae) from an intertidal mudflat by gulls (*Larus* spp.). *Mar. Biol.* **90:** 243–247.

Badgerow, J. P., and M. A. Sydlik. 1989. Nest site selection in horseshoe crabs (*Limulus polyphemus*) using a Cape Cod Beach. *Am. Zool.* **29:** 36A.

Bånger, L. E., and L. Niemistö. 1978. An evaluation of the use of redox measurements for characterizing recent sediments. *Estuarine Coastal Mar. Sci.* **6:** 127–134.

Barash, L. 1993. Mass appeal. *National Wildl.* **31:** 14–19.

Barlow, R. B., Jr., M. K. Powers, H. Howard, and L. Kass. 1986. Migration of *Limulus* for mating: relation to lunar phase, tide height, and sunlight. *Biol. Bull.* **171:** 310–329.

Boaden, P. 1985. *An Introduction to Coastal Ecology.* Blackie, Glasgow.

Boggs, S., Jr. 1987. *Principles of Sedimentary and Stratigraphy.* Merrill, Columbus.

Botton, M. L. 1984. Effects of laughing gull and shorebird predation on the intertidal fauna at Cape May, New Jersey. *Estuarine Coastal Shelf Sci.* **18:** 209–220.

Botton, M. L., and R. E. Loveland. 1987. Orientation of the horseshoe crab, *Limulus polyphemus*, on a sandy beach. *Biol. Bull.* **173:** 289–298.

Botton, M. L., and R. E. Loveland. 1989. Reproductive risk: high mortality associated with spawning by horseshoe crabs (*Limulus polyphemus*) in Delaware Bay, USA. *Mar. Biol.* **101:** 143–151.

Botton, M. L., R. E. Loveland, and T. R. Jacobsen. 1988. Beach erosion and geochemical factors: influence on spawning success of horseshoe crabs (*Limulus polyphemus*) in Delaware Bay. *Mar. Biol.* **99:** 325–332.

Botton, M. L., R. E. Loveland, and T. R. Jacobsen. 1992. Overwintering by trilobite larvae of the horseshoe crab *Limulus polyphemus* on a sandy beach of Delaware Bay (New Jersey, USA). *Mar. Ecol. Progr. Ser.* **88:** 289–292.

Botton, M. L., R. E. Loveland, and T. R. Jacobsen. 1994. Site selection by migrating shorebirds in Delaware Bay, and its relationship to beach characteristics and abundance of horseshoe crab (*Limulus polyphemus*) eggs. *Auk* **111**(3): 605–616.

Brafield, A. E. 1964. The oxygen content of interstitial water in sandy shores. *J. Anim. Ecol.* **33:** 97–116.

Brockmann, H. J. 1990. Mating behavior of horseshoe crabs, *Limulus polyphemus*. *Behaviour* **114:** 206–220.

Brockmann, H. J., T. Colson, and W. Potts. In press. Sperm competition in horseshoe crabs (*Limulus polyphemus*). *Behav. Ecol. Sociobiol.*

Brockmann, H. J., and D. Penn. 1992. Male mating tactics in the horseshoe crab, *Limulus polyphemus*. *Anim. Behav.* **44:** 653–665.

Brown, G. G., and D. L. Clapper. 1981. Procedures for maintaining adults, collecting gametes, and culturing embryos and juveniles of the horseshoe crab, *Limulus polyphemus* L. Pp. 268–290 in *Laboratory Animal Management, Marine Invertebrates*, R. Hinegardner, J. Atz, R. Fay, M. Fingerman, R. Josephson, and N. Meinkoth, eds. National Academy Press, Washington.

Burger, J., M. A. Howe, D. C. Hahn, and J. Chase. 1977. Effects of tide cycles on habitat selection and habitat partitioning by migrating shorebirds. *Auk* **94:** 743–758.

Castro, G., J. P. Myers, and A. R. Place. 1989. Assimilation efficiency of sanderlings (*Calidris alba*) feeding on horseshoe crab (*Limulus polyphemus*) eggs. *Physiol. Zool.* **62:** 716–731.

Castro, G. and J. P. Myers. 1993. Shorebird predation on eggs of horseshoe crabs during spring stopover on Delaware Bay. *Auk.* **110**(4): 927–930.

Cavanaugh, C. M. 1975. Observations on mating behavior in *Limulus polyphemus*. *Biol. Bull.* **149:** 422.

Cohen, J. A. and H. J. Brockmann. 1983. Breeding activity and mate selection in the horseshoe crab, *Limulus polyphemus*. *Bull. Mar. Sci.* **33:** 274–281.

Crabtree, R. L. and C. H. Page. 1974. Oxygen-sensitive elements in the book gills of *Limulus polyphemus*. *J. Exp. Biol.* **62:** 545–554.

Eagle, G. A. 1983. The chemistry of sandy beach ecosystems: a review. Pp. 203–325 in *Sandy Beaches as Ecosystems*. A. McLachlan and B. Erasumus, eds. Dr. Junk, Boston.

Evans, P. R. 1988. Predation of intertidal fauna by shorebirds in relation to time of the day, tide and year. Pp. 65–78 in *Behavioral Adaptation to Intertidal Life*, G. Chelazzi and M. Vannini, eds. Plenum Press, New York.

Fremling, C. R., and J. J. Evans. 1963. A method for determining the dissolved-oxygen concentration near the mud-water interface. *Limnol. Oceanogr.* 8: 363–364.

Gordon, M. S. 1960. Anaerobiosis in marine sandy beaches. *Science* **132:** 616–617.

Hays, G. C., and J. R. Speakman. 1993. Nest placement by loggerhead turtles, *Caretta caretta*. *Anim. Behav.* **45:** 47–53.

Horrocks, J. A., and N. McA. Scott. 1991. Nest site location and nest success in the hawksbill turtle *Eretmochelys imbricata* in Barbados, West Indies. *Mar. Ecol. Prog. Ser.* **69:** 1–8.

Howard, H. A., R. W. Fiordalice, M. D. Camara, L. Kass, M. K. Powers, and R. B. Barlow, Jr. 1984. Mating behavior of *Limulus:* relation to lunar phase, tide height, and sunlight. *Biol. Bull.* **167:** 527.

Ims, R. A. 1990. The ecology and evolution of reproductive synchrony. *Trends Ecol. Evol.* **5:** 135–140.

Kingsley, J. S. 1892. The embryology of *Limulus*. *J. Morphol.* **7:** 35–68.

Kingsley, J. S. 1893. The embryology of *Limulus*—part II. *J. Morphol.* **8:** 195–268.

Little, C. 1983. *The Colonization of Land: Origins and Adaptations of Terrestrial Animals.* Cambridge University Press, New York.

Lockwood, S. 1870. The horse foot crab. *Am. Nat.* **4:** 257–274.

Mallory, E. P., and D. C. Schneider. 1979. Agonistic behavior in short-billed dowitchers feeding on a patchy resource. *Wilson Bull.* **91:** 271–278.

Maurmeyer, E. 1978. *Geomorphology and Evolution of Transgressive Estuarine Washover Barriers along the Western Shore of Delaware Bay.* Ph.D. Thesis, University of Delaware.

McLachlan, A. 1978. A quantitative analysis of the meiofauna and the chemistry of the redox potential discontinuity zone in a sheltered sandy beach. *Estuarine Coastal Mar. Sci.* **7:** 275–290.

Middaugh, D. P., H. W. Kohl, and L. E. Burnett. 1983. Concurrent measurement of intertidal environmental variables and embryo survival for the California grunion, *Leuresthes tenuis*, and Atlantic silverside, *Menidia menidia* (Pisces: Atherinidae). *Calif. Fish Game* **69:** 89–96.

Palumbi, S. R., and B. A. Johnson. 1982. A note on the influence of life-history stage on metabolic adaptation: the responses of *Limulus* eggs and larvae to hypoxia. Pp. 115–124 in *Physiology and Biology of Horseshoe Crabs: Studies on Normal and Environmentally Stressed Animals*, J. Bonaventura, C. Bonaventura, and S. Tesh, eds. Alan R. Liss, Inc., New York.

Patten, W. 1896. Variations in the development of *Limulus polyphemus*. *J. Morphol.* **12:** 17–148.

Penn, D. 1992. *The Adaptive Significance of Nest-Site Selection and Spawning Synchronization in Horseshoe Crabs (Limulus polyphemus).* M.S. Thesis, University of Florida.

Penn, D., and H. J. Brockmann. In press. Age-biased stranding and righting in horseshoe crabs, *Limulus polyphemus*. *Anim. Behav.*

Peterson, C. H. 1991. Intertidal zonation of marine invertebrates in sand and mud. *Am. Sci.* **79:** 236–249.

Prater, A. J. 1972. The food and feeding habits of knot (*Calidris canutus* L.) in Morecambe Bay. *J. Appl. Ecol.* **9:** 179–194.

Quammen, M. L. 1981. Use of exclosures in studies of predation by shorebirds on intertidal mudflats. *Auk* **98:** 812–817.

Recher, H. F. 1966. Some aspects of the ecology of migrant shorebirds. *Ecology* **47:** 393–407.

Recher, H. F., and J. A. Recher. 1969. Some aspects of the ecology of migrant shorebirds. II. Aggression. *Wilson Bull.* **81:** 140–154.

Rudloe, A. 1979. Locomotor and light responses of larvae of the horseshoe crab, *Limulus polyphemus* (L.). *Biol. Bull.* **157:** 494–505.

Rudloe, A. 1980. The breeding behavior and patterns of movement of horseshoe crabs, *Limulus polyphemus*, in the vicinity of breeding beaches in Apalachee Bay, Florida. *Estuaries* **3:** 177–183.

Rudloe, J. 1971. *The Erotic Ocean.* World Publishers, New York.

Sekiguchi, K., ed. 1988. *Biology of Horseshoe Crabs.* Science House Co., Ltd., Tokyo.

Sekiguchi, K., Y. Yamamichi, and J. D. Costlow. 1982. Horseshoe crab developmental studies I. Normal embryonic development of *Limulus polyphemus* compared with *Tachypleus tridentatus*. Pp. 53–73 in *Physiology and Biology of Horseshoe Crabs: Studies on Normal and Environmentally Stressed Animals*, J. Bonaventura, C. Bonaventura, and S. Tesh, eds. Alan R. Liss, Inc., New York.

Shuster, C. N., Jr. 1960. Horseshoe "crabs"—in former years, during the month of May, these animals dominated Delaware Bay shores. *Estuarine Bull.* **5:** 3–9.

Shuster, C. N., Jr. 1982. A pictorial review of the natural history and ecology of the horseshoe crab *Limulus polyphemus*, with reference to other Limulidae. Pp. 1–52 in *Physiology and Biology of Horseshoe Crabs: Studies on Normal and Environmentally Stressed Animals*, J. Bonaventura, C. Bonaventura, and S. Tesh, eds. Alan R. Liss, Inc., New York.

Shuster, C. N., Jr., and M. L. Botton. 1985. A contribution to the population biology of horseshoe crabs, *Limulus polyphemus* (L.) in Delaware Bay. *Estuaries* **8:** 363–572.

Strahler, A. N. 1966. Tidal cycle of changes in an equilibrium beach, Sandy Hook, New Jersey. *J. Geol.* **74:** 247–268.

Størmer, L. 1977. Athropod invasion of land during Silurian and Devonian times. *Science* **192:** 1362–1364.

Taylor, M. H. 1984. Lunar synchronization of fish reproduction. *Trans. Am. Fish. Soc.* **113:** 484–493.

Thompson, C., and C. Page. 1975. Nervous control of respiration: oxygen-sensitive elements in the prosoma of *Limulus polyphemus*. *J. Exp. Biol.* **60:** 631–639.

Thompson, W. F. 1919. The spawning of the grunion. *Fish Bull.* **3:** 2–29.

ZoBell, C. E. 1946. Studies on redox potential of marine sediments. *Bull. Am. Assoc. Petroleum Geol.* **30:** 477–513.

Reference: *Biol. Bull.* **187**: 385–397. (December, 1994)

Subunit Composition and O_2 Binding of the Crustacean Hemocyanins: Interspecific Relationships

JOHN E. REESE AND CHARLOTTE P. MANGUM*

Department of Biology, College of William & Mary, Williamsburg, Virginia 23187-8795

Abstract. The monomeric subunit composition and oxygen binding properties of hemocyanins were examined in 9 taxonomic groups of 43 crustacean species and 1 hybrid. In native polyacrylamide electrophoresis the banding pattern was highly species specific, even in closely related congeners. In less closely related taxa, there was little apparent relationship between phylogenetic affinity and banding pattern.

Within a taxonomic group, pH dependence was the most highly conserved and O_2 affinity was the most diverse of the O_2 binding properties investigated. In congeneric but not sibling species, O_2 affinity was more highly correlated with an environmental variable such as temperature than with phylogenetic affinity. Only in very closely related groups found in similar environments were different O_2 binding properties correlated with differences in particular electrophoretic bands.

Introduction

Crustacean hemocyanins (Hcs) exist *in vivo* as hexamers (1 × 6 monomers) and multiples of hexamers, most often a pair (2 × 6-mers). Although the polypeptide composition of both artificial and natural 1 × 6-mers can be homogeneous, the native blood in a species contains more than one, and up to a dozen or more different, monomeric chains (reviewed by Markl, 1986, and Markl and Decker, 1992; see also Callicott and Mangum, 1993; Mangum and Greaves, unpub. data). This condition, which is known as monomeric subunit heterogeneity, is a necessary prerequisite to differences in polypeptide chain composition between individuals of a species, which is known as monomeric subunit polymorphism.

Using electrophoretic heterogeneity and immunological relatedness in combination, Markl (1986) described distinct patterns of monomeric subunit composition in different arthropod families, both crustacean and arachnid. He formulated three discrete immunological categories of chains, designated alphas, betas, and gammas. When separated by native polyacrylamide gel electrophoresis (PAGE), members of each category exhibit migration rates that are characteristic of their category.

Subunit composition can influence intrinsic O_2-binding properties. Artificial components such as isolated monomers (Jeffrey and Treacy, 1980) or homohexamers of them (Johnson *et al.*, 1987) differ in O_2 binding. More important in the present context, the respiratory properties of natural Hcs with different subunit compositions can differ within a polymorphic species or between sibling species. In addition, the differences can be attributed to particular chains and, in one case, their effects on oligomerization (Mangum and Rainer, 1988; Mangum *et al.*, 1991; Mangum, 1993a, b, 1994). On the other hand, not all different Hc morphs, either within or between species, have appreciably different functional properties (Mangum, 1993a, b).

Markl's (1986) investigations were designed to elucidate broad phylogenetic relationships of Hcs representing taxonomic categories ranging from families to subphyla. Because his sample was composed of, at most, a few species per family, the patterns he described may or may not be characteristic of the families. Few interspecific comparisons of PAGE banding patterns, much less respiratory properties, have been made under common experimental conditions. In addition, the level of evolutionary divergence at which subunit composition and respiratory properties begin to differ is not known.

Here we present PAGE and O_2-binding data for nine taxonomic sets of crustaceans, primarily decapods, of various degrees of relatedness. The taxonomic sets differ

Received 2 December 1991; accepted 3 October 1994.

---

* Author to whom correspondence should be addressed.

in their composition. The separation ranges from a natural hybrid and its sibling parental species, to sibling species, to nonsibling and also sympatric congeners, to different genera, to closely related families.

Materials and Methods

The species investigated are listed in Table I. Most representatives were collected and bled by the present authors. *Pagurus impressus, P. lacustris,* and *Uca virens* were purchased from a commercial supplier and then bled by us. The Pacific coast species of *Cancer,* the two species of *Chaceon* and *Menippe,* and the *Menippe* hybrid were bled by colleagues and the fresh material was shipped to us within 24 h. *Callinectes arcuatus, C. toxotes, Portunus spinnemanus, Panopeus lacustris, Cataleptodius floridanus, Uca inversa,* and the two species of *Gnathophausia* were bled by colleagues and the material was shipped to us frozen.

Blood samples

Blood was taken from the infrabranchial sinuses into a hypodermic syringe and allowed to clot in a tissue grinder. Blood from all available individuals of a species (see Table III for the actual numbers) was pooled. The pool was then homogenized and centrifuged, and the clot was discarded. A small aliquot of serum was frozen for PAGE, and O_2 binding of the remainder was determined immediately.

Most of the O_2-binding measurements were performed within 1–2 days of bleeding, on material that had not been frozen. Because freezing can lower cooperativity (Morris, 1988), we have chosen not to report cooperativity values for most of the Hcs that had been frozen. We report values for *Callinectes arcuatus* and *C. toxotes,* however, because an investigation of *Callinectes sapidus* Hc revealed no effect of similarly brief periods of freezing (Mangum *et al.,* 1991).

Electrophoresis

The frozen material was thawed, and its Hc concentration was estimated by absorbance of dissociated subunits at the active site (338 nm). It was then diluted to about 5 mg ml^{-1} with a buffer (0.05 mol l^{-1} Tris + 0.05 mol l^{-1} EDTA, pH 8.9) that dissociates native oligomers into their constituent monomers. The Hc monomers were then separated by native PAGE; the gels, reagents, and other conditions were those detailed by Hames and Rickwood (1985). This is the most sensitive procedure available for separating the monomers of these proteins; for comparison with alternative methods, please see Markl *et al.* (1979), Brenowitz *et al.* (1981), and Stöcker *et al.* (1988).

In most cases, the best separation was obtained on 12.5% gels. Higher and lower gel concentrations were also employed when we encountered dense bands that suggested more than one chain with similar migration rates. Three or more amounts of Hc were first examined to determine the optimal level for each species; the level chosen was similar within a taxonomic set, but it differed between sets. The Hcs from each set were subsequently analyzed on the same gel.

Most gels were stained with Coomassie Blue alone. After the banding pattern for a species was ascertained, a gel was prepared for the detection of Cu in the bands. The presence of Cu was examined by noting the quenching of fluorescence generated by bathocuproine sulfonate (Bruyninckx *et al.,* 1978). In the present investigation, EDTA was omitted from the dissociating buffer (N.B. Terwilliger, pers. comm.). Due to the lower sensitivity of the bathocuproine sulfonate procedure, the Hc concentration was raised by a factor of 6. The positions of the Cu-positive bands were marked and the gels were then stained with Coomassie Blue to verify their correspondence to those previously noted with Coomassie Blue alone.

The number of bands in a species was ascertained by visual inspection of the gels on a light table. In most species, the relative amounts of material in each band were estimated from densitometric scans. A few species were investigated in a laboratory in which no densitometer was available. Gels were initially scanned with a Gelman integrating densitometer. Although the width of the scan produced by this instrument is not adjustable, it gave the best resolution of the individual peaks. It expresses the area of each peak as an integram (a number of spikes that varies directly with peak area), which permits calculation of the percentage of the total material. These calculations (in Table II) include only the Cu-positive material. To aid in the examination of gel photographs, additional scans were made with a Shimadzu densitometer. The widths of these scans were precisely compressed so that the peaks were aligned with their corresponding bands on the gel. Photographs of the gels and their corresponding scans can be found in Reese (1989).

O_2 binding

Hcs were stripped of organic modulators by 12 h dialysis with Spectrapor high-speed membranes, against a physiological saline. Where possible, the saline was based on the ionic composition of a blood representative of a taxonomic set. If no information on ionic composition was available, seawater was used. The dialyzed Hcs were then diluted to the optimal absorbance range with 0.05 mol l^{-1} Tris-buffered saline, and the pH was adjusted with HCl and NaOH.

Table I

The classification, geographic distribution and habitats of the species

Species	Habitat	Geographic Range
Order Decapoda		
Infraorder Anomura		
Family Diogenidae		
Clibinarius vittatus (Bosc)	subtidal, 0 to 22 m	Virginia to Brazil
Family Paguridae		
Pagurus impressus (Benedict)	subtidal, 1 to 33 m	North Carolina to Florida
Pagurus longicarpus Say	intertidal to 200 m	Massachusetts to Florida
Pagurus pollicaris (Say)	subtidal to 200 m	New Brunswick to Florida
Infraorder Brachyura		
Family Cancridae		
Cancer antennarius Stimpson	0 to 20 m	British Columbia to Baja California
Cancer anthonyii Rathbun	0 to 20 m	Monterey Bay to Gulf of Baja California
Cancer borealis Stimpson	intertidal to 800 m	Nova Scotia to Florida
Cancer irroratus Say	subtidal, 0 to 575 m	Labrador to Florida
Cancer magister (Dana)	shallow subtidal	Aleutians to Monterey Bay
Cancer productus (Randall)	shallow subtidal	Kodiak to Baja California
Family Geryonidae		
Chaceon fenneri (Manning & Holthius)	300 m +	Gulf of Mexico
Chaceon quinquedens (Smith)	300 to 700 m +	Gulf of Mexico
Family Grapsidae		
Sesarma cinereum (Bosc)	semiterrestrial	Maryland to Mexico
Sesarma reticulatum (Say)	semiterrestrial	Massachusetts to Florida
Family Majidae		
Libinia dubia H. Milne-Edwards	subtidal, 0 to 46 m	Massachusetts to Cuba
Libinia emarginata (Leach)	subtidal, 0 to 49 m	Novia Scotia to Gulf of Mexico
Family Ocypodidae		
Ocypode quadrata (Fabricius)	semiterrestrial	Rhode Island to Brazil
Uca crenulata coloradensis (Lockington)	semiterrestrial	Gulf of Baja California
Uca inversa Hoffman	semiterrestrial	Indian Ocean and Arabian Sea from Natal to Pakistan
Uca musica musica Rathbun	semiterrestrial	Baja California to San Blas
Uca princeps monilifera Crane	semiterrestrial	Gulf of Baja California
Uca pugilator (Bosc)	semiterrestrial	Massachusetts to Florida
Uca pugnax (Smith)	semiterrestrial	Massachusetts to Florida
Uca minax (Le Conte)	semiterrestrial	Massachusetts to Florida
Uca virens (Salmon & Atsaides)	semiterrestrial	Florida to Mexico
Family Portunidae		
Ovalipes ocellatus (Herbst)	subtidal, 0 to 95 m	Northumberland Straits to Georgia
Portunus gibbesii (Stimpson)	subtidal, 0 to 393 m	Ma. to Gulf of Mexico; French Guiana
Portunus spinimanus (Latreille)	subtidal, 0 to 91 m	New Jersey to Brazil
Callinectes arcuatus Ordway	subtidal, 0 to 28 m	Southern California to Peru
Callinectes bellicosus Stimpson	subtidal, 0 to 18 m	San Diego to Matzatlan
Callinectes ornatus Ordway	subtidal, 0 to 75 m	Virginia to Brazil
Callinectes sapidus Rathbun	subtidal, 0 to 90 m	Nova Scotia to Argentina
Callinectes similis Williams	subtidal, 0 to 392 m	Delaware Bay to Colombia
Callinectes toxotes Ordway	subtidal, 0 to 27 m	Baja California to Peru
Family Xanthidae		
Menippe adina Williams & Felder	shallow subtidal	Northern and western Gulf of Mexico
Menippe mercenaria (Say)	subtidal, 0 to 54 m	North Carolina to Mexico; Jamaica
Hybrid		Northwestern Florida
Panopeus herbstii H. Milne-Edwards	intertidal, to 22 m	Massachusetts to Brazil
Panopeus obesus (Smith)	intertidal	North Carolina to Florida
Panopeus lacustris Desbonne	intertidal to shallow subtidal	Bermuda, southern Florida to Brazil
Eurypanopeus depressus (Smith)	intertidal to 48 m	Massachusetts to tropics
Cataleptodius floridanus (Gibbes)	intertidal	Bermuda, southern Florida to Brazil
Order Mysidacea		
Gnathophausia gigas (Willemoes-suhm)	mesopelagic	North Pacific Ocean
Gnathophausia ingens (Dorhn)	mesopelagic	North Pacific Ocean

O_2 binding of all but a few Hcs was determined tonometrically at atmospheric pressure (Burnett, 1979), with precision mixed, humidified gases passed through tonometers in a rapidly shaken water bath (± <0.5°C); absorbance was determined with a Milton Roy Spectronic 501 spectrophotometer. The remaining Hcs, designated as such in Figure 2 and Table III, were examined with the cell respiration procedure (Mangum and Lykkeboe, 1979). In both cases P_{50} and n_{50} were estimated from Hill plots, using linear regions of the data in the region of 50% oxygenation. Bohr plots (log P_{50} *vs.* pH) were described by regression lines, and 95% confidence intervals were constructed around the lines and their slopes. Many of the data sets differ significantly throughout the pH range examined; a smaller number are statistically indistinguishable throughout the range examined. These relationships are clear from the Bohr plots. Many, however, differ significantly in only a portion of the pH range, which is indicated in the Results section. Cooperativity values were compared by using a Student's *t* test.

In vivo respiratory variables

Blood was taken anaerobically into a hypodermic syringe from the pericardial and infrabranchial sinuses, and pH and PO_2 were measured with a Radiometer BMS1 Blood Gas System. Because the samples were often small, the suction line was disconnected from the pH capillary electrode, and a syringe was used instead to position the material.

Results

Hc subunit composition

We have attempted to accurately represent the species investigated by choosing high-frequency phenotypes for those known to be polymorphic (Mangum, 1990, 1993a; Callicott and Mangum, 1993; Mangum and Greaves, unpub. data; C. P. Mangum and K. T. White, unpub. data). As discussed below, in no case known thus far can a morph of one species be confused with a morph in another. We note that one species (*Cancer productus*) is polymorphic (Wache *et al.*, 1988), but the polymorphism has not been characterized. In all likelihood, other members of our sample will also prove to be polymorphic.

Figures 1A and B summarize the banding patterns found in each species and allow direct comparison of the electrophoretic behavior of the monomers composing most of the Hcs in our sample. A few species were investigated after these gels were prepared; they are shown in Fig. 1C. All bands were assigned numbers in order from the top (anode) to the bottom (cathode) of the gel, with no implication that the same number in different species reflects co-migration. The relative amounts of the Cu-containing bands in each species are given in Table II.

1. *Anomuran hermit crabs: Diogenidae and Paguridae.* The Hc of the diogenid *Clibinarius vittatus* consistently exhibited two electrophoretic bands in apparently equal quantities. Visual inspection of the gels clearly revealed a light area in the middle and a corresponding constriction at the edges of the single dark band in Fig. 1A (lane 1); however, the separation does not show in this photograph. Regardless, the pattern differed unambiguously from that of the three pagurid Hcs, each of which had additional bands (Fig. 1, lanes 2–4). Most bands in the pagurids were more cathodic than those in *C. vittatus.* Each pagurid species clearly contained at least one band that did not co-migrate with a band found in the others. Although several of the bands in *C. vittatus, P. pollicarus,* and *P. longicarpus* did co-migrate, the proportions of the co-migrants differ considerably (Table II).

2. *Brachyurans: Cancridae.* The subunit compositions of the *Cancer* Hcs did not resemble one another very closely (Fig. 1B, lanes 1–6). Thus, it is unlikely that a morph of *C. productus* will prove to resemble that of any other species. *C. borealis* and *irroratus* Hcs each separated into three different bands, whereas *anthonyi* and *productus* Hcs separated into four, and *antennarius* and *magister* Hcs separated into five bands (see also Larsen *et al.*, 1981). Each Hc exhibited electrophoretically unique bands.

As in *Cancer pagurus* (Markl, 1986), the bands in the present sample of cancrids fell into three more or less distinct groups: an anodic group, an intermediate group, and a cathodic group. They may correspond to Markl's (1986) immunological categories, in the order beta, alpha, gamma. Within each group, some of the bands migrated at identical rates, and the migration rates of others differed only slightly. In all cases, however, the proportions of the co-migrants are considerably different (Table II).

3. *Grapsidae. Sesarma cinereum* Hc separated into two bands, whereas *S. reticulatum* Hc separated into three (Fig. 1A, lanes 13–14). Only band 2 in each species co-migrated.

4. *Majidae.* The Hcs of *Libinia dubia* and *emarginata* each exhibited four bands (Fig. 1B, lanes 9–10). In both species the most cathodic band predominated. Moreover, the position of this predominant band was quite different in each species, although some of the minor bands co-migrated.

5. *Ocypodidae. Ocypode quadrata* Hc (Fig. 1A, lane 19) contained four distinct bands (see also Markl, 1986; Johnson, 1987), none of which co-migrated with any bands found in the genus *Uca* (Figs. 1A, lanes 15–18, and Fig. 1C, lanes 5–7). The present material from *U. pugilator, U. pugnax,* and *U. virens* all contained four Cu-positive bands that migrated similarly but not exactly. The relative amounts of material are quite distinct in each species (Table II). Despite repeated attempts and with dif-

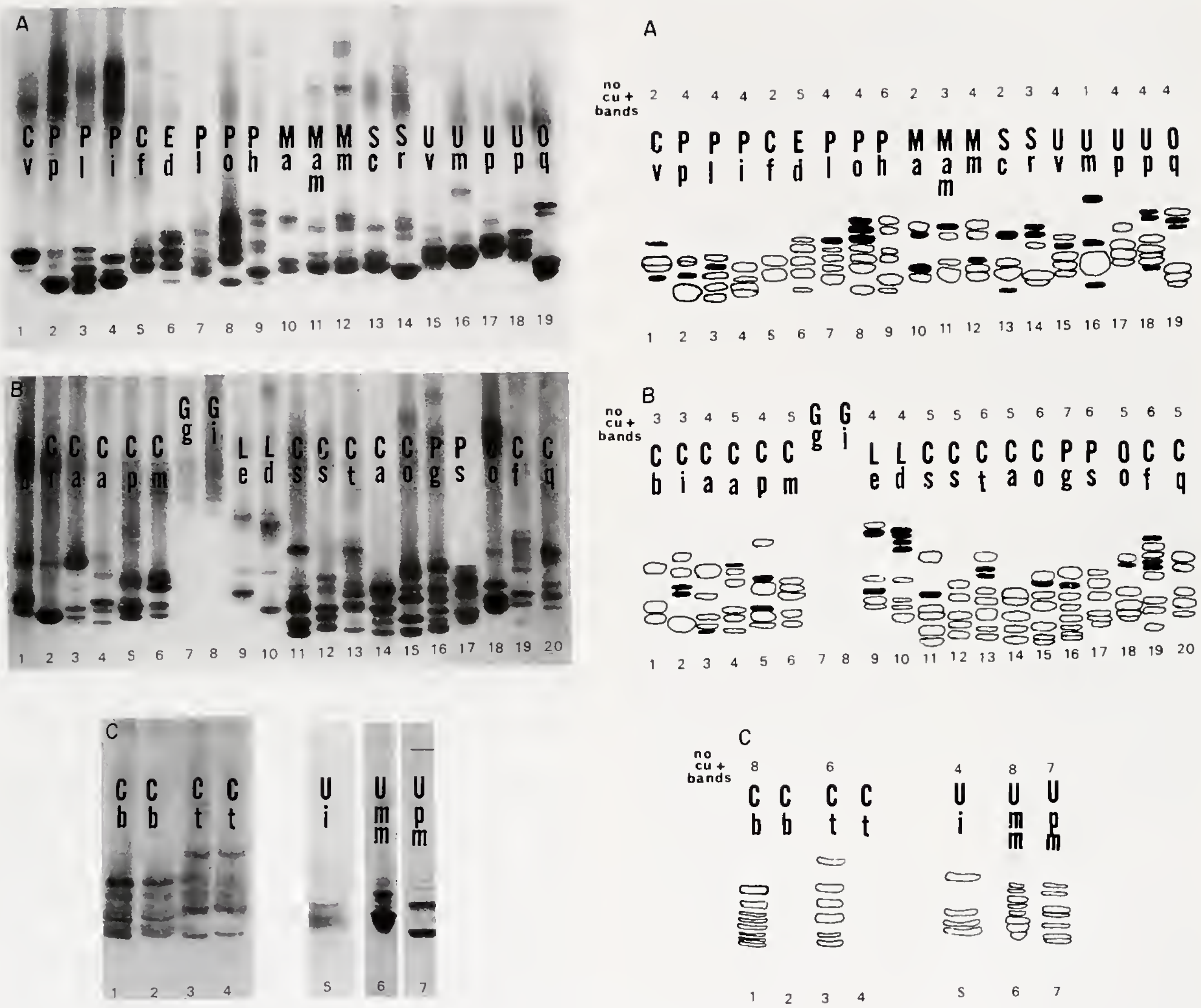

Figure 1. Native PAGE banding patterns of dissociated hemocyanins examined in the present investigation. Left: Photographs of gels summarizing the nine taxonomic clusters. Lane nos. at bottom. Right: Diagrammatic representations of photographs. Lane nos. at bottom. Number of Cu-positive (Cu +) bands at top. Cu-negative bands are blackened.

Panel A, from left to right beginning with lane 1: [1] *Clibinarius vittatus*, [2] *Pagurus pollicaris*, [3] *P. longicarpus*, [4] *P. impressus*, [5] *Cataleptodius floridanus*, [6] *Eurypanopeus depressus*, [7] *Panopeus lacustris*, [8] *P. obesus*, [9] *P. herbstii*, [10] *Menippe adina*, [11] *Menippe adina–mercenaria* hybrid, [12] *M. mercenaria*, [13] *Sesarma cinereum*, [14] *S. reticulatum*, [15] *Uca virens*, [16] *U. minax*, [17] *U. pugnax*, [18] *U. pugilator*, [19] *Ocypode quadrata*.

Panel B, left to right: [1] *Cancer borealis*, [2] *C. irroratus*, [3] *C. anthonyi*, [4] *C. antennarius*, [5] *C. productus*, [6] *C. magister*, [7] *Gnathophausia gigas*, [8] *G. ingens*, [9] *Libinia emarginata*, [10] *L. dubia*, [11] *Callinectes sapidus*, [12] *C. similis*, [13] *C. toxotes*, [14] *C. arcuatus*, [15] *C. ornatus*, [16] *Portunus gibbesii*, [17] *P. spinnemanus*, [18] *Ovalipes ocellatus*, [19] *Chaceon fenneri*, [20] *C. quinquedens*.

Panel C, left to right: *Callinectes bellicosus* (high conc.), *C. bellicosus* (low conc.), *C. toxotes* (high), *C. toxotes* (low), *Uca inversa*, *U. musica musica*, *U. princeps monilifera*.

ferent gel concentrations, we were unable to demonstrate more than one Cu-positive band in *U. minax* Hc, although several additional bands that were not Cu-positive clearly appeared on the gels.

Hcs from *U. musica musica*, *U. princeps monilifera*, and *U. inversa* were electrophoresed on the same gel with material from *U. pugilator* (Mangum, 1993a; Callicott and Mangum, 1993) to ascertain relative positions of the bands. *U. musica musica* Hc separated into eight bands, *U. princeps monilifera* Hc separated into seven bands, and *U. inversa* Hc separated into four bands (Fig. 1C, lanes 5–7). The major bands were diagnostic of each

Table II

Relative amounts (%) of electrophoretic bands

Species (abb; #)[*]	Subunit Number 1	2	3	4	5	6	7
Infraorder Anomura							
Clibinarius vittatus (Cv, A1)	*ca* 50[†]	*ca.* 50[†]					
Pagurus impressus (Pi, A4)	24	14	31	31			
Pagurus longicarpus (Pl, A3)	9	24	37	30			
Pagurus pollicaris (Pp, A2)	12	11	39	39			
Infraorder Brachyura							
Cancer antennarius (Ca, B4)	3	4	48	31	14		
Cancer anthonyi (Ca, B3)	64	4	17	15			
Cancer borealis (Cb, B1)	26	39	35				
Cancer irroratus (Ci, B2)	18	22	60				
Cancer magister (Cm, B6)	13	26	40	12	9		
Cancer productus (Cp, B5)	11	19	46	24			
Family Grapsidae							
Sesarma cinereum (Sc, A13)	40	60					
Sesarma reticulatum (Sr, A14)	18	41	41				
Family Majidae							
Libinia dubia (Ld, B10)	17	16	19	48			
Libinia emarginata (Le, B9)	11	23	20	27			
Family Ocypodidae							
Ocypode quadrata (Oq, A19)	20	42	16	22			
Uca pugilator (Up, B18)	25	25	18	32			
Uca pugnax (Up, B17)	26	31	36	7			
Uca minax (Um, B16)	100						
Uca virens (Uv, B15)	5	33	44	18			
Family Portunidae							
Ovalipes ocellatus (Oc, B18)	12	32	31	21	4		
Portunus gibbesii (Pg, B16)	11	11	7	10	11	23	27
Portunus spinnemanus (Ps, B17)	9	22	14	14	26	15	
Callinectes arcuatus (Ca, B14)	33	15	28	13	11		
Callinectes ornatus (Co, B15)	13	8	21	25	19	14	
Callinectes sapidus (Cs, B11)	10	25	18	29	0	18	
Callinectes similis (Cs, B12)	16	6	32	23	23		
Callinectes toxotes (Ct, B13)	21	1	22	36	4	16	
Family Xanthidae							
Menippe adina (Ma, A10)	34	66					
Menippe mercenaria (Mm, A12)	16	16	38	30			
Hybrid (Mam, A11)	14	15	71				
Panopeus herbstii (Ph, A9)	14	19	11	13	31	1	
Panopeus obesus (Po, A8)	13	30	26	31			
Panopeus lacustris (Pl, A7)	13	34	25	28			
Eurypanopeus depressus (Ed, A6)	10	24	35	25	6		
Cataleptodius floridanus (Cf, A5)	50	50					
Family Geryonidae							
Chaceon fenneri (Cf, B19)	24	5	6	43	19	3	
Chaceon quinquedens (Cq, B20)	55	13	5	22	5		

[*] Species abbreviation and lane number used in Fig. 1.

[†] Estimated by eye.

species of *Uca*, although some of the minor bands comigrated.

6. *Portunidae.* The subunit composition of *Callinectes sapidus* Hc is polymorphic (Mangum and Rainer, 1988; Mangum, 1990; Mangum *et al.*, 1991), as well as heterogeneous (Mason *et al.*, 1983; Johnson *et al.*, 1984; Stöcker *et al.*, 1988). The highly variable band 5 was not found in the material examined here; for comparison with Fig. 1B, lane 11, see scans in deFur *et al.* (1990). The degree of heterogeneity found earlier in *C. sapidus* appears to be characteristic of the portunid Hcs (Fig. 1B, lanes 11–15). The subunit patterns were distinct in each of the three genera examined. *Ovalipes ocellatus* Hc (Fig. 1B, lane 18) separated into five bands, one of which was anodic to any in *Portunus* (Fig. 1B, lanes 16–17). *Callinectes sapidus* (Fig. 1B, lane 11) and *C. toxotes* (Fig. 1B, lane 13 and 1C, lanes 3–4) Hcs had even more anodic (and also co-migratory) bands. A number of the bands in *P. gibbesii* co-migrated with those of *P. spinnemanus* (Fig. 1B, lanes 16 and 17), although the relative amounts of these bands are quite different (Table II). Other bands were qualitatively distinct as well. Similarly, several bands among the *Callinectes* congeners co-migrated (Fig. 1B, lanes 11–15). *C. bellicosus* and *C. toxotes* are of particular interest (see Discussion); although four bands co-migrated, each Hc exhibited diagnostic bands, and the proportions of most co-migrants differ (Table II), which is also true of the other members of the genus. At least one band in *Portunus gibbesii* (Fig. 1B, lane 16) co-migrated with one in *Callinectes ornatus* (lane 15).

7. *Xanthidae.* The Hcs from the mud crabs were clearly distinctive (Fig. 1A, lanes 7–9). *P. herbstii* Hc separated into at least six bands, whereas *P. obesus* and *lacustris* Hcs each separated into four. Several bands co-migrated. As in the other families, however, the relative amounts of the co-migrants are not at all similar (Table II), and many bands were unique to a particular species.

Eurypanopeus depressus Hc (Fig. 1A, lane 6) contained at least five bands, four of which co-migrated with bands found in the three species of *Panopeus;* one band, however, was clearly unique to *E. depressus. Cataleptodius floridanus* (Fig. 1A, lane 5) Hc contained only two Cu-positive bands, both of which co-migrated with, and occur in concentrations similar to, bands in *E. depressus.* In *C. floridanus,* however, there was no sign of co-migrants with the remaining three *E. depressus* bands.

The sample of *Menippe adina* Hc contained only two bands that were clearly positive for Cu, whereas the Hc of its sibling *M. mercenaria* contained four (Fig. 1A, lanes 10–12). Both bands of *M. adina* Hc co-migrated with *M. mercenaria* bands. The relative amounts differ, though not dramatically. The number of bands expressed in the hybrid is intermediate between the number found in the two parents. Each hybrid band co-migrated with a *mercenaria* band, but only the most cathodic one co-migrated with an *adina* band.

8. *Geryonidae. Chaceon fenneri* Hc separated into six different bands, whereas *C. quinquedens* Hc separated into only five (Fig. 1B, lanes 19–20). None clearly co-migrated, and the relative amounts are distinct (Table II).

9. *Order Mysidacea.* The long-frozen bloods from the two species of *Gnathophausia* contained unusually high levels of material that was not positive for Cu, and a low concentration of Hc. Although the multiplicity of bands was clear, their resolution was so poor (Fig. 1B, lanes

7–8) that we chose not to characterize the banding patterns further. The gels are included in Fig. 1B to call attention to the distinctive behavior. The Hc bands migrated at a much slower rate than any of the other Hcs, all from decapods. Investigation of better preserved material would be of interest.

O_2 binding

Bohr plots of the data for each species are shown in Figure 2. Values for the Bohr factor, obtained as the slopes of the regression lines in Figure 2, are given in Table III, along with estimates of cooperativity.

1. *Diogenidae and Paguridae.* O_2 affinity of the four anomuran Hcs (Fig. 2; Table III, lines 1–4) differs significantly throughout most of the pH range examined, although the difference between *P. impressus* and *P. pollicarus* Hcs disappears at low pH. The Bohr factor for *Clibinarius vittatus* Hc differs considerably from those for *P. longicarpus* and *P. pollicarus* Hcs, which also differ significantly from one another (Table III, lines 1–4). Although the estimate of cooperativity for *C. vittatus* Hc is distinctive as well, the values for the three pagurids do not differ significantly from one another (Table III, lines 2–4).

2. *Geryonidae, Majidae, Grapsidae, and Mysidacea.* The Hcs of the two members of each congeneric pair of crabs had O_2 affinities that differ significantly from one another throughout the pH range examined (Fig. 2). The two mysid Hcs also differ, but only at high pH. We report these values, despite the poor condition of the material, primarily because they closely resemble the results for fresh (as well as previously frozen) material from *G. ingens* (Sanders and Childress, 1990). Only in the grapsids do values for cooperativity and pH dependence differ significantly (Table III, lines 11–12, 13–14, 39–40, and 41–42).

3. *Ocypodidae.* In *Ocypode quadrata*, O_2-affinity differed significantly from that in the *Uca* species, either above pH 7.2 (*pugilator* and *princeps monilifera*) or throughout the pH range examined (all other species). In the genus *Uca*, Hc O_2 affinities were generally distinctive but often become indistinguishable at high pH. Of particular interest (see Discussion) is a difference between *Uca pugnax* and *virens* below pH 7.4.

Bohr factors are fairly diverse (Table III, lines 15–21). If the values are arranged in series, each differs from all others except the next higher or lower one. The cooperativity figures fall into two significantly different groups: (1) the three lowest (*U. minax, pugnax,* and *virens*) and (2) the four highest (other) values.

4. *Cancridae.* Hc O_2 affinities were more alike in this than in any other genus. In 23 of the 30 possible interspecific comparisons between the six cancrid Hcs, the O_2 affinity data are indistinguishable. In no case do the values differ significantly throughout the pH range investigated. In addition, the few significant differences are small from a physiological point of view. All Bohr factors are statistically indistinguishable except those for *C. magister* and *irroratus* Hcs (Table III, lines 5–10). The cooperativity values, however, differ significantly in all comparisons except that of *C. productus* with either *magister* or *irroratus*.

5. *Portunidae.* In the following comparisons, the O_2 affinity data are statistically indistinguishable throughout the pH range examined: (1) *Callinectes similis* and *sapidus*, (2) *C. arcuatus* and *toxotes*, and (3) *C. ornatus, Ovalipes ocellatus,* and *Portunus spinnemanus.* O_2 affinity of *O. ocellatus* Hc differs from *P. gibbesii* Hc only above pH 7.4; in the remaining comparisons O_2 affinity differs significantly, either throughout the pH range or at all but the two pH extremes.

Bohr factors (Table III, lines 22–30) for the two most pH-sensitive Hcs (*C. arcuatus* and *toxotes*) differ significantly from those for the two least pH-sensitive Hcs (*P. spinnemanus* and *C. ornatus*); the Bohr factors for *C. arcuatus* and *toxotes* also differ significantly from the value for *C. sapidus*. The remaining values are not significantly different. Most of the cooperativity values are statistically homogeneous, even though *Callinectes arcuatus* and *toxotes* Hcs had been frozen and the others had not. The values for *C. ornatus* and *similis* Hcs, which do not differ from one another, are both significantly larger than the rest.

6. *Xanthidae.* The O_2 affinity values for *Cataleptodius floridanus* and *Eurypanopeus depressus* Hcs are statistically indistinguishable throughout the pH range examined, as are those for the two species of *Menippe*. *C. floridanus* Hc differed significantly from that for *M. mercenaria* except at high pH, and the *Menippe* hybrid Hc differed from the two parent species except at low pH. The difference between *Panopeus herbstii* and *obesus* Hc O_2 affinities becomes insignificant at pH 8.

Many of the Bohr factors (Table III, lines 31–38) do not differ significantly, the exceptions being (1) *P. lacustris* Hc, which is different from any other, (2) *P. herbstii* Hc, which differs from *E. depressus* and the three *Menippe* Hcs, and (3) the *Menippe* hybrid Hc, which differs from *M. adina*. The cooperativity values for *M. adina* and the *Menippe* hybrid Hcs do not differ significantly from one another. Both differ from *M. mercenaria* Hc, although the differences are small. The cooperativity value for *P. obesus* Hc is significantly greater than that for *E. depressus* Hc, again by a small margin: neither differs from *P. herbstii* Hc.

Blood PO_2 and pH

The information required to assess the physiological importance of different O_2 binding properties is available

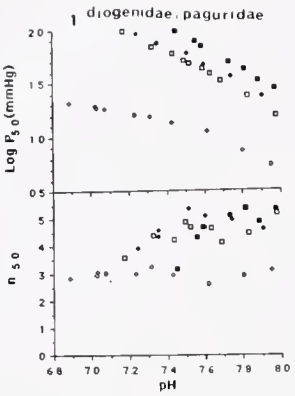
1
diogenidae, paguridae
Log P50 (mmHg)
n50
2.0
1.5
1.0
0.5
5
4
3
2
1
0
6.8 7.0 7.2 7.4 7.6 7.8 8.0
pH

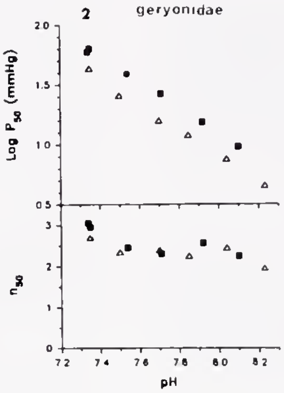
2
geryonidae
Log P50 (mmHg)
n50
2.0
1.5
1.0
0.5
3
2
1
0
7.2 7.4 7.6 7.8 8.0 8.2
pH

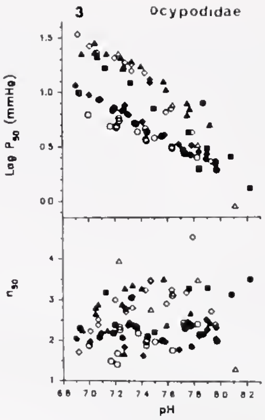
3
ocypodidae
Log P50 (mmHg)
n50
1.5
1.0
0.5
0.0
4
3
2
1
6.8 7.0 7.2 7.4 7.6 7.8 8.0 8.2
pH

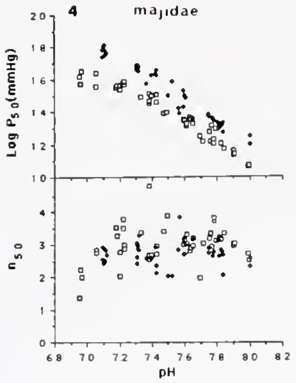
4
majidae
Log P50 (mmHg)
n50
2.0
1.8
1.6
1.4
1.2
1.0
4
3
2
1
0
6.8 7.0 7.2 7.4 7.6 7.8 8.0 8.2
pH

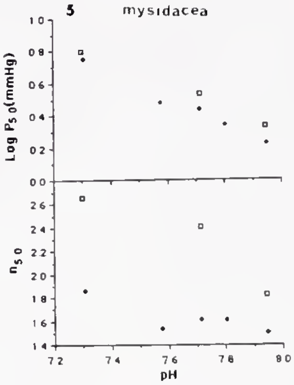
5
mysidacea
Log P50 (mmHg)
n50
1.0
0.8
0.6
0.4
0.2
0.0
2.6
2.4
2.2
2.0
1.8
1.6
1.4
7.2 7.4 7.6 7.8 8.0
pH

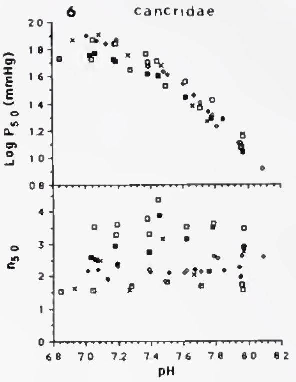
6
cancridae
Log P50 (mmHg)
n50
2.0
1.8
1.6
1.4
1.2
1.0
0.8
4
3
2
1
0
6.8 7.0 7.2 7.4 7.6 7.8 8.0 8.2
pH

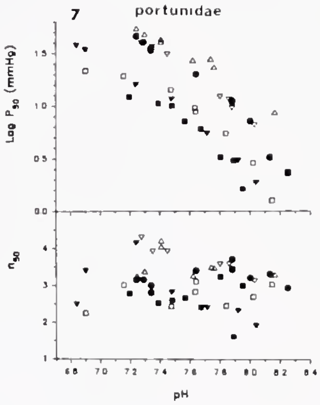
7
portunidae
Log P50 (mmHg)
n50
1.5
1.0
0.5
0.0
4
3
2
1
6.8 7.0 7.2 7.4 7.6 7.8 8.0 8.2 8.4
pH

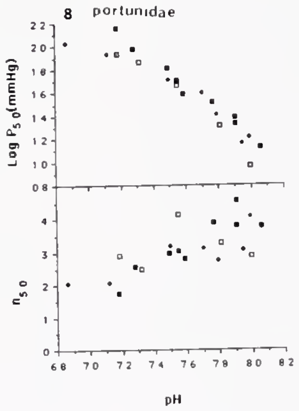
8
portunidae
Log P50 (mmHg)
n50
2.2
2.0
1.8
1.6
1.4
1.2
1.0
0.8
4
3
2
1
0
6.8 7.0 7.2 7.4 7.6 7.8 8.0 8.2
pH

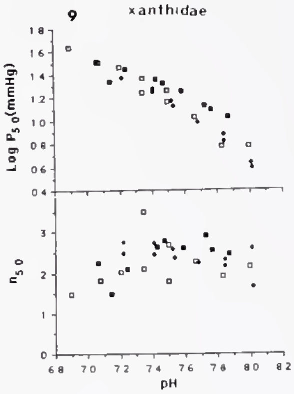
9
xanthidae
Log P50 (mmHg)
n50
1.8
1.6
1.4
1.2
1.0
0.8
0.6
0.4
3
2
1
0
6.8 7.0 7.2 7.4 7.6 7.8 8.0 8.2
pH

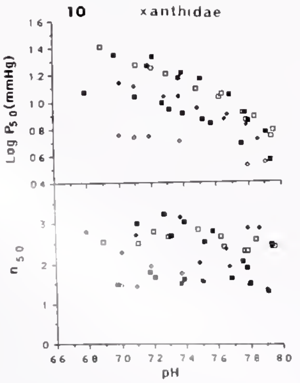
10
xanthidae
Log P50 (mmHg)
n50
1.6
1.4
1.2
1.0
0.8
0.6
0.4
3
2
1
0
6.6 6.8 7.0 7.2 7.4 7.6 7.8 8.0
pH

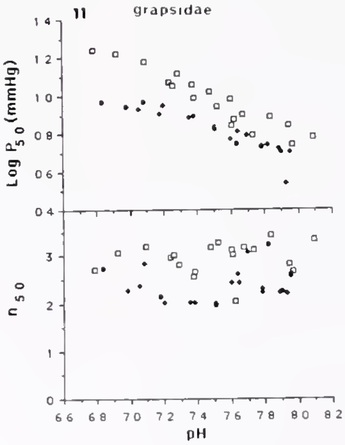
11
grapsidae
Log P50 (mmHg)
n50
1.4
1.2
1.0
0.8
0.6
0.4
3
2
1
0
6.6 6.8 7.0 7.2 7.4 7.6 7.8 8.0 8.2
pH

in the literature for either a single member of the taxonomic sets examined here or more than one member, but not under common environmental conditions.

In Table IV, data obtained under conditions very similar to those of the O_2 binding measurements are shown for several of the mud and fiddler crabs in our sample. In all cases the predicted oxygenation at the gill appears to be essentially complete even though experimental temperatures were fairly high. Although the predicted deoxygenation at the tissues is appreciable in most of the species, the venous reserve is high in both *Uca minax* and *U. pugnax*, perhaps because these very active runners were held in small aquaria that constrained locomotion.

Discussion

Subunit composition

The clearest findings of the survey of electrophoretic separation of crustacean Hc subunits are (1) The PAGE banding patterns are highly species specific, and (2) above the level of sibling species, the PAGE banding patterns are not especially characteristic of a taxon.

The specificity is best illustrated by following interspecific examples in which morphological differences are small, suggesting that divergence of the Hc O_2 transport system may occur quite early in speciation. As a first example, *Callinectes bellicosus* is regarded as difficult to distinguish from *C. toxotes* (Brusca, 1990). Their essentially non-overlapping but contiguous geographic ranges (Table I) raise the possibility that they are siblings; several bands in these two species co-migrated. *C. similis* is exceptionally difficult to distinguish from *C. ornatus* (Ruppert and Fox, 1988), although in this case the geographic ranges do overlap. In both cases, the differences in subunit composition are unambiguous, qualitative, and far greater than the differences between the Hc morphs found within *Callinectes sapidus* (deFur *et al.*, 1990; Mangum, 1994).

As a second example, Williams (1983) has shown that *Panopeus herbstii* (*sensu lato* Rathbun) is in fact a complex of no less than six cryptic species, which can be distinguished by careful morphological examination as well as ecological preference (Reames and Williams, 1983; Williams, 1983). Sullivan *et al.* (1983) reported that at least four of the six differ in Hc subunit composition (the other two were not examined). Our data for *P. herbstii sensu stricto* H. Milne Edwards, *obesus*, and *lacustris* strongly support this conclusion. Sullivan *et al.* (1983) briefly mentioned the existence of intraspecific polymorphism in *P. herbstii*. Although we have not yet completed our own investigation of this species, data for hundreds of individuals from the same locality and others as well

Figure 2. O_2 binding of hemocyanins examined here. 20°C, tonometric method, unless specified otherwise.

Panel 1: Diogenidae and Paguridae. *Clibinarius vittatus* (◇), *Pagurus impressus* (⊡), *P. pollicaris* (◆), *P. longicarpus* (■). 0.05 mol l^{-1} Tris-buffered saline containing 460 mmol l^{-1} NaCl, 11 mmol l^{-1} KCl, 13 mmol l^{-1} $CaCl_2$, 20 mmol l^{-1} $MgCl_2$, 29 mmol l^{-1} $NaSO_4$ and 3 mmol l^{-1} $NaHCO_3$.

Panel 2: Geryonidae. *Chaceon fenneri* (■), *C. quinquedens* (△). 0.05 mol l^{-1} Tris-buffered saline containing 455 mmol l^{-1} NaCl, 11 mmol l^{-1} KCl, 13 mmol l^{-1} $CaCl_2$, 18 mmol l^{-1} $MgCl_2$, 22 mmol l^{-1} Na_2SO_4 and 3 mmol l^{-1} $NaHCO_3$.

Panel 3: Ocypodidae. *Uca crenulata coloradensis* (■), *U. minax* (○), *U. princeps monilifera* (△), *U. pugilator* (◇), *U. pugnax* (◆), *U. virens* (●), *Ocypode quadrata* (▲). The data for *U. crenulata coloradensis* and *princeps monilifera* were collected with the cell respiration method. 0.05 mol l^{-1} Tris-buffered saline containing 383 mmol l^{-1} NaCl, 11 mmol l^{-1} KCl, 11 mmol l^{-1} $CaCl_2$, 45 mmol l^{-1} $MgCl_2$, 40 mmol l^{-1} Na_2SO_4 and 3 mmol l^{-1} $NaHCO_3$.

Panel 4: Majidae. *Libinia dubia* (⊡), *L. emarginata* (◆). 0.05 mol l^{-1} Tris-buffered saline containing 350 mmol l^{-1} NaCl, 8 mmol l^{-1} KCl, 10 mmol l^{-1} $CaCl_2$, 42 mmol l^{-1} $MgSO_4$ and 3 mmol l^{-1} $NaHCO_3$.

Panel 5: Mycidacea. *Gnathophausia gigas* (⊡), *G. ingens* (◆). Buffered saline as in panel 2.

Panel 6: Cancridae. *Cancer antennarius* (□), *C. anthonyi* (■), *C. borealis* (⊡), *C. irroratus* (◆), *C. productus* (X). 0.05 mol l^{-1} Tris-buffered saline containing 441 mmol l^{-1} NaCl, 15 mmol l^{-1} KCl, 11 mmol l^{-1} $CaCl_2$, 40 mmol l^{-1} $MgCl_2$, 10 mmol l^{-1} Na_2SO_4 and 3 mmol l^{-1} $NaHCO_3$.

Panel 7: Portunidae. *Callinectes arcuatus* (□), *C. bellicosus* (■), *C. ornatus* (▽), *C. sapidus* (●), *C. similis* (△), *C. toxotes* (▼). Data collected at 25°C with the cell respiration method. Buffered saline as in panel 2.

Panel 8: Portunidae. *Ovalipes ocellatus* (⊡), *Portunus spinnemanus* (◆), *P. gibbesii* (■). Buffered saline as in panel 2.

Panel 9: Xanthidae. *Menippe adina* (◆), *M. mercenaria* (⊡), *M. adina–mercenaria* hybrid (■). 0.05 mol l^{-1} Tris-buffered saline containing 350 mmol l^{-1} NaCl, 7 mmol l^{-1} KCl, 11 mmol l^{-1} $CaCl_2$, 33 mmol l^{-1} $MgCl_2$, 20 mmol l^{-1} Na_2SO_4 and 3 mmol l^{-1} $NaHCO_3$.

Panel 10: Xanthidae. *Cataleptodius floridanus* (■), *Eurypanopeus depressus* (⊡), *Panopeus herbstii* (◆), *P. lacustris* (◇), *P. obesus* (◘). Buffered saline as in panel 9.

Panel 11: Grapsidae. *Sesarma cinereum* (⊡), *S. reticulatum* (◆). 0.05 mol l^{-1} Tris-buffered saline containing 383 mol l^{-1} NaCl, 11 mmol l^{-1} KCl, 16 mmol l^{-1} $CaCl_2$, 45 mmol l^{-1} $MgCl_2$, 40 mmol l^{-1} Na_2SO_4 and 3 mmol l^{-1} $NaHCO_3$.

(K. T. White and C. P. Mangum, unpub. obs.) confirm this inference. Once again, none of the morphs could be confused with a pattern reported here for another species in the Xanthidae.

Table III

Bohr factors and cooperativity values

Species	Number of individuals (n)	Bohr Factor $\Delta \log p_{50}/\Delta pH$ (±95% CI)	Cooperativity n_{50} ($\bar{x}$ ± SE)
Order Decapoda			
Infraorder Anomura			
Family Diogenidae			
1. *Clibinarius vittatus*	7	−0.54 ± 0.10	2.96 ± 0.02
Family Paguridae			
2. *Pagurus impressus*	6	−0.98 ± 0.07	4.51 ± 0.04
3. *Pagurus longicarpus*	47	−1.06 ± 0.06	4.71 ± 0.11
4. *Pagurus pollicaris*	5	−0.88 ± 0.10	4.71 ± 0.07
Infraorder Brachyura			
Family Cancridae			
5. *Cancer antennarius*	12	−0.76 ± 0.17	3.61 ± 0.04
6. *Cancer anthonyii*	12	−0.74 ± 0.16	2.95 ± 0.05
7. *Cancer borealis*	6	−0.61 ± 0.11	2.08 ± 0.02
8. *Cancer irroratus*	6	−0.83 ± 0.13	2.12 ± 0.01
9. *Cancer magister*	4	−1.05 ± 0.11	2.36 ± 0.03
10. *Cancer productus*	1	−0.77 ± 0.24	2.25 ± 0.08
Family Grapsidae			
11. *Sesarma cinereum*	42	−0.43 ± 0.07	3.17 ± 0.07
12. *Sesarma reticulatum*	22	−0.30 ± 0.06	2.28 ± 0.07
Family Majidae			
13. *Libinia dubia*	24	−0.60 ± 0.04	2.85 ± 0.07
14. *Libinia emarginata*	15	−0.64 ± 0.04	2.70 ± 0.06
Family Ocypodidae			
15. *Ocypode quadrata*	9	−0.83 ± 0.12	2.66 ± 0.12
16. *Uca crenulata coloradensis*	7	−0.97 ± 0.13	3.08 ± 0.16
17. *Uca minax*	11	−0.50 ± 0.09	2.18 ± 0.06
18. *Uca princeps monilifera*	5	−1.60 ± 0.35	2.93 ± 0.25
19. *Uca pugilator*	102	−1.17 ± 0.16	2.82 ± 0.13
20. *Uca pugnax*	65	−0.63 ± 0.06	2.20 ± 0.18
21. *Uca virens*	24	−0.70 ± 0.05	2.18 ± 0.05
Family Portunidae			
22. *Ovalipes ocellatus*	4	−1.19 ± 0.30	3.14 ± 0.12
23. *Portunus gibbesii*	6	−1.09 ± 0.14	3.23 ± 0.09
24. *Portunus spinimanus*	2	−0.77 ± 0.29	2.91 ± 0.12
25. *Callinectes arcuatus**	12	−1.51 ± 0.34	2.73 ± 0.11
26. *Callinectes bellicosus**	10	−0.97 ± 0.34	2.45 ± 0.10
27. *Callinectes ornatus**	10	−0.82 ± 0.16	3.68 ± 0.22
28. *Callinectes sapidus**	6	−0.98 ± 0.10	3.18 ± 0.08
29. *Callinectes similis**	5	−1.03 ± 0.18	3.54 ± 0.20
30. *Callinectes toxotes**	12	−1.38 ± 0.14	2.64 ± 0.27
Family Xanthidae			
31. *Menippe adina*	6	−0.96 ± 0.11	2.39 ± 0.03
32. *Menippe mercenaria*	2	−0.85 ± 0.14	2.17 ± 0.06
33. Hybrid	2	−0.63 ± 0.09	2.41 ± 0.05
34. *Panopeus herbstii*	30	−0.45 ± 0.14	2.61 ± 0.05
35. *Panopeus obesus*	12	−0.45 ± 0.14	2.74 ± 0.04
36. *Panopeus lacustris*	7	−0.32 ± 0.07	
37. *Eurypanopeus depressus*	29	−0.61 ± 0.07	2.55 ± 0.01
38. *Cataleptodius floridanus*	18	−0.63 ± 0.15	
Family Geryonidae			
39. *Chaceon fenneri*	10	−1.06 ± 0.07	2.64 ± 0.12
40. *Chaceon quinquedens*	10	−1.08 ± 0.10	2.35 ± 0.10
Order Mysidacea			
41. *Gnathophausia gigas*	3	−0.72 ± 0.15	
42. *Gnathophausia ingens*	2	−0.80 ± 0.15	

* 25°C, cell respiration method.

Additional evidence in support of the specificity of PAGE banding of Hc monomers has been obtained for sibling species of the lobster genus *Homarus* and their hybrids (Mangum, 1993b) and for several other sibling species, including stone crabs of the genus *Menippe* investigated here (C. P. Mangum, unpub. data).

Of the sibling species in the present sample, the difference between only one pair remains tentative. The status of *Uca virens* (Salmon and Astiades) remains unresolved. It is variously regarded as a synonym of *U. rapax*, a subspecies of *U. pugnax*, or a separate and valid species (reviewed by Barnwell and Thurman, 1984; Salmon and Kettler, 1987). The most cathodic band in the present material from *U. virens* and *pugnax* differs greatly in quantity and slightly in migration rate. Although more recent findings make it clear that the morphs found within *Uca pugnax* do not include a phenotype that could be confused with those found in a sample of *U. rapax/virens* from the northern Gulf of Mexico (C. P. Mangum, unpub. data), we have not yet compared *Uca rapax* and *U. virens* in depth.

At higher taxonomic levels, only a few general features are common to a set. One is the considerable monomeric heterogeneity found in the portunid genera *Callinectes* and *Portunus*. Another is the sorting of bands into three electrophoretic categories with characteristic migration rates in the genus *Cancer*, as originally reported by Markl (1986).

Native PAGE banding patterns, however, are not especially characteristic of a genus, much less a family. In the six species of *Cancer*, electrophoretic patterns differ as much from one another as do those in different families. In this example, the dissimilarities may entail the distance of the interspecific relationships. One would expect the patterns to be most similar in recently separated species with wholly allopatric geographic ranges, such as *Homarus americanus* and *gammarus* (Mangum, 1993b). In contrast, the cancrids in the present sample are either separated by a continent or they are sympatric, suggesting far more phylogenetic distance between species. Similarly, the sympatric species of *Sesarma* and *Libinia*, in each of which the Hc phenotype is quite different from that of its congener, are not very closely related to one another (D. L. Felder, pers. comm.). In distantly related species, such as *Portunus gibbesii* and *Callinectes ornatus*, co-migratory bands may well prove to represent unlike polypeptides that happen to be similar in net charge.

Respiratory properties

The clearest findings to emerge from the survey of the O_2-binding properties examined are that within a taxo-

Table IV

In vivo *respiratory variables (23°C)*

Species	Medium	PaO_2	PvO_2	PaH	PvH	Hc_aO_2	Hc_vO_2
		(Torr)				(%)	
Family Ocypodidae							
Uca minax	water	88 ± 9 (4)	17 ± 1 (4)	7.55 ± 0.05 (5)	7.55 ± 0.03 (7)	100	88
Uca pugilator	(24 h)	63 ± 4 (7)	20 (2)	7.48 ± 0.03 (16)	7.40 ± 0.05 (10)	99	63
Uca pugnax		95 ± 10 (6)	10 ± 3 (4)	7.53 ± 0.07 (8)	7.43 ± 0.08 (8)	100	73
Uca minax	air	63 ± 6 (64)	12 ± 1 (5)	7.43 ± 0.08 (4)	7.35 ± 0.04 (8)	100	73
Uca pugilator	(24 h)	72 ± 13 (4)	16 ± 2 (4)	7.42 ± 0.02 (4)	7.39 ± 0.03 (10)	100	49
Uca pugnax		72 ± 5 (6)	10 ± 2 (5)	7.56 ± 0.05 (6)	7.45 ± 0.04 (11)	100	73
Family Xanthidae							
Eurypanopeus depressus	water	101 ± 8 (6)	16 ± 2 (3)	7.44 ± 0.05 (6)	7.27 ± 0.20 (5)	100	49
Panopeus herbstii		77 ± 6 (14)	18 ± 2 (10)		7.38*	99	61
Panopeus obesus		135 (2)	9 ± 2 (3)	7.55 ± 0.08 (2)	7.56 ± 0.05 (4)	100	75

a = postbranchial, v = prebranchial. Mean ± SE (*n*)

* From Mangum (1973).

nomic set, (1) O_2 affinity varies the most in closely related species; (2) cooperativity also varies but not as often; and (3) the pH dependence of O_2 affinity is the most highly conserved.

Although most of the Hcs in the present sample have O_2 affinities that are species specific, there are numerous exceptions. The portunid Hcs, which are always composed of a large number of different subunits, can have very different O_2 affinities, but O_2 affinities can also be identical. Moreover, the cancrids, which have quite diverse subunit patterns, have the least different O_2 affinities.

The comparison of sibling and cryptic species is also of interest here. The difference in O_2-binding properties of Hcs from the cryptors *Panopeus herbstii* and *P. obesus* suggests divergence at the physiological level. These differences are also adaptive in terms of the magnitude of O_2 transport. *P. herbstii,* with its higher prebranchial blood PO_2, has the lower Hc O_2 affinity; *P. obesus,* with its lower prebranchial blood PO_2, has the higher Hc O_2 affinity. The result is that deoxygenation at the tissues differs less than it would if O_2 affinity were the same.

Cooperativity is distinctive in only one taxonomic set, the pagurids, in which it is unusually high. Otherwise, the values are typical of the crustacean Hcs. Many of the differences within a taxonomic set, though significant, are small. Within the Cancridae, however, the range is fairly large. It would be interesting to learn whether this diversity is related to the notable heterogeneity and interspecific diversity of subunit composition.

Bohr factors are the most highly conserved of the respiratory properties examined here. In general, they appear to be at least somewhat characteristic of a taxonomic set. For example, in the two grapsids the pH sensitivity of O_2 affinity is unusually small for crustaceans, and in the two majids it is only moderate. The greater pH dependence of the portunid, cancrid, and pagurid Hcs is typical of crustacean Hcs. But this generalization is not entirely reliable, as indicated by the diversity within the *Panopeus* species complex.

Relationship between subunit composition and respiratory properties

Finally, the survey of 44 crustacean Hcs failed to reveal a simple relationship between intrinsic respiratory properties and either qualitative or quantitative aspects of electrophoretic subunit composition. Instead, it suggested that respiratory properties are strongly selected by factors of immediate relevance to the particular species, and that the response is constrained very little, if at all, by monomeric subunit composition.

For example, in *Callinectes* two pairs of congeneric Hcs have identical O_2-binding properties but very different subunit compositions. In *C. sapidus* and *similis*—sympatric species that are easily distinguished morphologically—O_2 binding properties are indistinguishable, and yet only one of six bands co-migrated. Moreover, the diagnostic bands in *C. sapidus* included nos. 3 and 6, which are known to influence O_2 affinity (Mangum and Rainer, 1988; deFur *et al.,* 1990; Mangum *et al.,* 1991). The differences in oxygenation properties of *Uca minax, U. pugnax,* and *U. virens* Hcs are also small, in spite of quite different subunit compositions. At more distant levels of taxonomic separation, the Hcs of the xanthids *Eurypanopeus depressus* and *Cataleptodius floridanus* were as different as any in subunit composition but as similar as any in O_2 binding. On the other hand, different subunit compositions may be responsible for functional differences between sibling species such as the stone crabs investigated here and the lobsters examined earlier (Mangum, 1993b).

In general, O_2 affinity appeared to be more closely related to thermal properties of the environment than to subunit composition. The family Cancridae, for example, with its similar O_2 affinities and dissimilar subunit patterns, is essentially a boreal to temperate zone family, with its species found in offshore, colder waters of the latter; O_2 affinity was uniformly low. In contrast, *Callinectes,* with its widely differing O_2 affinities, is believed to be a genus that is of tropical origin and is rapidly speciating northwards; O_2 affinity was lower in the more northern and higher in the more southern species. The decreasing O_2 affinity with increasing latitude in some of the species of *Panopeus* and *Uca* also supports this hypothesis. Although the low O_2 affinities in the southeastern Atlantic coast species of *Chaceon* might appear to be exceptional, in fact both inhabit offshore, cold waters. In addition, the species with the lower Hc O_2 affinity is found at the greater depths and thus at the lower temperature. In these examples, O_2 affinities differ less at mean environmental temperatures than they would if P_{50} values were identical (see also Mangum, 1982; Mauro and Mangum, 1982). Moreover, the existence of very similar respiratory properties in quite distantly related species indicates selection for common functional properties, which can be brought about by very different Hc monomers.

We do not intend to suggest that environmental temperature is the sole selection pressure on intrinsic O_2 affinity, or even that the environment is the sole determinant. A thermal interpretation is not consistent with the geographic ranges of the two species of grapsids or the three temperate zone species of *Uca.* According to Fotheringham and Brunenmeister (1975), the grapsid *Sesarma reticulatum,* which had the higher Hc O_2 affinity, carries on gas exchange in the (perhaps hypoxic) water filling a deep burrow, whereas *S. cinereum,* with its lower O_2 affinity, is basically an air-breather with a larger gill surface area than its congener. The difference between *Uca pugilator* and *U. pugnax,* however, is fairly large despite similar branchial surface areas (Pearse, 1950) and geographic ranges. In this case burrow PO_2 may differentiate the sand (*U. pugilator*) and the mud (*U. pugnax*) fiddler crabs.

Acknowledgments

Supported by NSF DCB 88-16172 (Physiological Processes). We thank the numerous colleagues who sent us material, K. A. Callicott for measurements of blood PO_2 and pH, and M. Brenowitz for many helpful suggestions on the manuscript.

Literature Cited

Barnwell, F. H., and C. L. Thurman. 1984. Taxonomy and biogeography of the fiddler crabs (Ocypodidae: Genus *Uca*) of the Atlantic and Gulf coasts of eastern North America. *Zool. J. Linn Soc.* **81:** 23–87.

Brenowitz, M., C. Bonaventura, J. Bonaventura, and E. Gianazza. 1981. Subunit composition of a high molecular weight oligomer: *Limulus polyphemus* hemocyanin. *Arch. Biochem. Biophys.* **210:** 748–761.

Brusca, R. C. 1990. *Common Intertidal Invertebrates of the Gulf of California.* Univ. Ariz. Press, Tucson.

Bruyninckx, W. J., S. Gutteridge, and H. S. Mason. 1978. Detection of copper on polyacrylamide gels. *Anal. Biochem.* **89:** 174–177.

Burnett, L. E. 1979. The effects of environmental oxygen levels on the respiratory function of hemocyanin in the crabs, *Libinia emarginata* and *Ocypode quadrata. J. Exp. Zool.* **210:** 289–300.

Callicott, K. A., and C. P. Mangum. 1993. Phenotypic variation and lability of the subunit composition of the hemocyanin of *Uca pugilator. J. Exp. Mar. Biol. Ecol.* **165:** 143–160.

deFur, P. L., C. P. Mangum, and J. E. Reese. 1990. Respiratory responses of the blue crab *Callinectes sapidus* to long term hypoxia. *Biol. Bull.* **178:** 46–54.

Fotheringham, N., and S. Brunenmeister. 1975. *Common Marine Invertebrates of the Northwestern Gulf Coast.* Gulf Publ. Co., Houston.

Hames, B. D., and D. Rickwood. 1985. *Gel Electrophoresis of Proteins.* IRL Press, Oxford.

Jeffrey, P. D., and G. B. Treacy. 1980. Hemocyanin from the Australian freshwater crayfish *Cherax destructor.* Oxygen binding studies of major components. *Biochemistry* **19:** 5428–5433.

Johnson, B. A. 1987. Structure and function of the hemocyanin from a semi-terrestrial crab, *Ocypode quadrata. J. Comp. Physiol.* **157:** 501–509.

Johnson, B., C. Bonaventura, and J. Bonaventura. 1984. Allosteric modulation of *Callinectes sapidus* hemocyanin by binding of L-lactate. *Biochemistry* **23:** 872–878.

Johnson, B. A., J. Bonaventura, and C. Bonaventura. 1987. Determination of L-lactate binding stoichiometry and differences in allosteric interactions of structurally distinct homohexamers from *Panulirus interruptus* hemocyanin. *Biochem. Biophys. Acta* **916:** 376–380.

Larsen, B. A., N. B. Terwilliger, and R. C. Terwilliger. 1981. Subunit heterogeneity of *Cancer magister* hemocyanin. *Biochem. Biophys. Acta* **667:** 294–302.

Mangum, C. P. 1973. Evaluation of the function properties of invertebrate hemoglobins. *Neth. J. Sea Res.* **7:** 303–315.

Mangum, C. P. 1982. On the relationship between P_{50} and the mode of gas exchange in tropical crustaceans. *Pac. Sci.* **36:** 403–410.

Mangum, C. P. 1990. Inducible O_2 carriers in the crustaceans. Pp. 92–103 in *Animal Nutrition and Transport Processes,* J.-P Truchot and B. Lalou, eds. Karger, Basel.

Mangum, C. P. 1993a. Structural and functional polymorphism of the hemocyanin O_2 transport system of the sand fiddler crab *Uca pugilator J. Exp. Mar. Ecol.* **165:** 133–142.

Mangum, C. P. 1993b. Hemocyanin subunit composition and oxygen binding in two species of the lobster genus *Homarus* and their hybrids. *Biol. Bull.* **184:** 105–113.

Mangum, C. P. 1994. Subunit composition of hemocyanins of *Callinectes sapidus:* phenotypes from naturally hypoxic waters, and isolated oligomers. *Comp. Biochem. Physiol.* (in press).

Mangum, C. P., and G. Lykkeboe. 1979. The influence of inorganic ions and pH on the oxygenation properties of the blood in the gastropod mollusc *Busycon canaliculatum. J. Exp. Zool.* **207:** 417–430.

Mangum, C. P., and J. S. Rainer. 1988. The relationship between subunit composition and O_2 binding of blue crab hemocyanin. *Biol. Bull.* **174:** 77–82.

Mangum, C. P., J. Greaves, and J. S. Rainer. 1991. Oligomer composition and oxygen binding of the hemocyanin of the blue crab *Callinectes sapidus. Biol. Bull.* **181:** 453–458.

Markl, J. 1986. Evolution and function of structurally diverse subunits in the respiratory protein hemocyanin from arthropods. *Biol. Bull.* **171:** 90–115.

Markl, J., and H. Decker. 1992. Molecular structure of the arthropod hemocyanins. Pp. 325–376 in *Blood and Tissue Oxygen Carriers*, C. P. Mangum, ed. Springer-Verlag, Heidelberg.

Markl, J., A. Hofer, G. Bauer, A. Markl, B. Kempter, M. Brenzinger, and B. Linzen. 1979. Subunit heterogeneity in arthropod hemocyanins: II. Crustacea. *J. Comp. Physiol.* **133:** 167–175.

Mason, R. P., C. P. Mangum, and G. Godette. 1983. The influence of inorganic ions and acclimation salinity on hemocyanin-oxygen binding in the blue crab *Callinectes sapidus. Biol. Bull.* **164:** 104–123.

Mauro, N. A., and C. P. Mangum. 1982. The role of the blood in the temperature dependance of oxidative metabolism in decapod crustaceans. II. Interspecific adaptations to latitudinal change. *J. Exp. Zool.* **219:** 189–196.

Morris, S. 1988. Effects of freezing on the function and association state of crustacean haemocyanins. *J. Exp. Biol.* **138:** 535–539.

Pearse, A. S. 1950. *The Emigrations of Animals from the Sea.* Sherwood Press, Dryden, N.Y.

Reames, R. C., and A. B. Williams. 1983. Mud crabs of the *Panopeus herbstii* H. M. Edw., S. L., complex in Alabama, U. S. A. *Fish. Bull.* **81:** 885–890.

Reese, J. E. 1989. Structure and function of crustacean hemocyanin. M. A. Thesis. College of William and Mary, Williamsburg, Virginia, 75 pp.

Ruppert, E. E., and R. S. Fox. 1988. *Seashore Animals of the Southeast.* Univ. So. Carolina Press, Columbia, S.C.

Salmon, M., and M. K. Kettler. 1987. The importance of behavioral and biochemical differences between fiddler crab taxa, with special reference to *Uca rapax* (Smith) and *U. virens* (Salmon and Atsaides). *Contr. Mar. Sci.* **30:** 63–76.

Sanders, N. K., and J. J. Childress. 1990. Adaptations to the deep sea oxygen minimum layer: oxygen binding by the hemocyanin of the bathypelagic mysid *Gnathophausia ingens. Biol. Bull.* **178:** 286–294.

Stöcker, W., U. Raeder, M. M. C. Bijholt, T. Wichertjes, E. F. J. van Bruggen, and J. Markl. 1988. The quaternary structure of four crustacean two-hexameric hemocyanins: immunocorrelation, stoichiometry, reassembly, and topology of individual subunits. *J. Comp. Physiol.* **B158:** 271–289.

Sullivan, B., K. Miller, K. Singleton, A. G. Scheer, and A. B. Williams. 1983. Electrophoretic analysis of hemocyanin from four species of mud crabs, genus *Panopeus*, with observations of the ecology of *P. obesus. Fish. Bull.* **81:** 883–885.

Wache, S., N. B. Terwilliger, and R. C. Terwilliger. 1988. Hemocyanin structure changes during early development of the crab *Cancer productus. J. Exp. Zool.* **247:** 23–32.

Williams, A. B. 1983. The mud crab, *Panopeus herbstii* (S. L.). Partition into six species (Decapoda: Xanthidae). *Fish. Bull.* **81:** 863–882.

Reference: *Biol. Bull.* **187:** 398–407. (December, 1994)

Energy Metabolism and Amino Acid Transport During Early Development of Antarctic and Temperate Echinoderms

FRASER M. SHILLING[1] AND DONAL T. MANAHAN[2]

Department of Biological Sciences, University of Southern California, Los Angeles, California 90089-0371

Abstract. The rates of oxygen consumption by embryos of antarctic echinoderms (*Acodontaster hodgsoni, Odontaster validus, Psilaster charcoti,* and *Sterechinus neumayeri*) were compared to the biomass (ash-free dry organic weight) of the egg of each species. These species could survive for months to years (range: 10 months to 5 years) by relying solely on the reserves present in the egg. However, certain species did not use any of the egg's reserves during early development. Embryonic stages of *O. validus* (a species with planktotrophic larvae) did not decrease in lipid, protein, or total biomass during the first 35 days of development. During the first 42 days of development, embryos of *A. hodgsoni* (a species with lecithotrophic development) used protein as an energy source. For both species lipid composed 40 to 50% of egg biomass, but was not used as an energy reserve. Larvae of *O. validus* have a high-affinity transport system for amino acids dissolved in seawater ($K_t = 1.3\ \mu M$ for alanine). The rate of alanine transport from a low concentration (50 n*M*) could supply 32% of the larva's metabolic needs. This is a 10-fold higher input to metabolism than was determined (3% at 50 n*M*) for larvae of a temperate asteroid, *Asterina miniata*. Larvae of antarctic echinoderms live in an environment where the food supply is low for most of the year. Relative to their metabolic rates, antarctic larvae have larger energy stores and planktotrophic larvae have higher nutrient transport capacities when compared to larvae from temperate regions. These physiological differences allow antarctic larvae to survive for long periods without particulate food.

Introduction

Many species of marine invertebrates in Antarctica have lecithotrophic (nonfeeding) stages of development (Pearse *et al.*, 1991). For antarctic species that have planktotrophic (particle-feeding) larvae, the strategies for survival in a low-food environment remain unknown. For example, *Odontaster validus* is a very abundant echinoderm (asteroid) in McMurdo Sound, Antarctica, and has a planktotrophic larval stage (Pearse, 1969). The adults spawn in austral winter (June–September: Pearse *et al.*, 1991) and larvae are present for several months in a water column that has very low concentrations of phytoplankton (*ca.* 0.01 μg chlorophyll *a* l^{-1}, Rivkin, 1991). Yet, when cultured *in situ* in the water column, larvae of this species survive for weeks to months (Olson *et al.*, 1987) prior to the phytoplankton bloom of austral summer (December–January, Rivkin, 1991).

The present study was undertaken to determine the physiological bases for the survival of antarctic echinoderm larvae living under low-food conditions. It has been suggested that, in the near-absence of algae, larvae of antarctic echinoderms could be using other sources of food, such as bacteria or organic material dissolved in seawater (Rivkin *et al.*, 1986). In addition, larvae could be endowed with large amounts of energy reserves from the egg. This would permit survival in a nutrient-poor water column if the larvae have lower metabolic rates (*cf.* temperate larval forms) and correspondingly lower rates of utilization of energy reserves. In the present study, egg mass and metabolic rates were measured for four species of antarctic echinoderms to allow for a calculation of life span in the absence of any exogenous food source. Embryos of *Acodontaster hodgsoni* (a species with lecithotrophic development) and *O. validus* were also cultured through em-

Received 4 June 1993; accepted 26 September 1994.

[1] Current address: Vollum Institute for Advanced Biomedical Research, Oregon Health Sciences University, L-474, Portland, OR 97201.

[2] Address for correspondence.

bryogenesis to determine actual rates of utilization of biomass (ash-free dry organic weight) and energy reserves (lipid and protein content). To assess the possible role of dissolved organic material as a source of nutrition for larvae, the mass-specific rates of amino acid transport from seawater were compared with the mass-specific metabolic rates of larvae. These physiological processes (amino acid transport and metabolic rate) were measured for larvae of *O. validus* and compared to the measurements made for similar larvae of a temperate asteroid (*Asterina miniata*).

Materials and Methods

Culturing of embryos and larvae

Adult echinoderms were collected using scuba from several locations in McMurdo Sound, Antarctica, during austral spring (asteroids: *Acodontaster hodgsoni, Odontaster validus, Perknaster fuscus, Psilaster charcoti;* and the echinoid, *Sterechinus neumayeri*). Prior to spawning, adults were maintained in ambient seawater (on sea tables) for up to 2 weeks in the aquarium at McMurdo Station. Gametes were obtained from adult asteroids by intracoelomic injection of 1 m*M* 1-methyladenine. Gametes from sea urchins were obtained by intracoelomic injection of 0.5 *M* KCl. Fertilized eggs of the antarctic species were suspended in 200-l vessels (Nalgene) of filtered seawater (0.2 μm pore-size). Eggs (and later the embryos and larvae) were kept in suspension by mixing the cultures with vertically moving Plexiglas paddles driven by electric motors set at slow speeds (5–10 rpm). Low concentrations of individuals were maintained in the culture vessels (*e.g., O. validus* was cultured at 2–3 individuals ml^{-1} and *A. hodgsoni* at 0.1 individuals ml^{-1}). The temperature of the cultures was maintained by immersing the 200-l culture vessels in tanks of flowing ambient seawater (mean temperature of −1.2°C). The culture seawater was replaced every 4 to 5 days with newly filtered seawater, at which time the vessels were cleaned by acid-washing. For *O. validus,* one batch of eggs (a total of 1.5 million eggs obtained from several females) was divided equally among three replicate 200-l culture vessels to ensure sufficient numbers of individuals in each vessel for measurements of biomass, biochemical composition, and metabolic rates. Embryos and larvae of the temperate species (*Asterina miniata*) were cultured in California at 14°C. Gametes of this species were obtained from ripe adults purchased from Marinus Inc., Long Beach, California.

Biochemical composition of antarctic eggs (4 species) and changes in biomass during early development of A. hodgsoni *and* O. validus

Prior to sampling, all of the embryos or larvae from a single culture were slowly siphoned from the culture vessel and concentrated onto a nylon screen (80 μm, mesh size) that was partially immersed in ambient seawater. At each change of seawater, three to six samples were taken for the measurement of biomass (ash-free dry organic weight) and an additional three samples were taken for biochemical composition (lipid and protein content). Salts were removed from the samples using serial washes of an ammonium formate solution (methods described previously by Jaeckle and Manahan, 1989). Protein content was measured with the Bradford assay (1976). Trichloroacetic acid-insoluble protein was dissolved by heating (60°C) the protein pellet in 1 *M* NaOH (aq.). This method results in a close (7%) approximation of the absolute amount of protein, as determined by measuring with high-performance liquid chromatography the total amino acid content of acid-hydrolyzed protein homogenates of larvae (Manahan *et al.,* unpub. obs.). Lipid was measured according to Mann and Gallager (1985). Carbohydrate content was not measured in our studies because carbohydrate is a low percentage (2–4%) of the total organic material in eggs of antarctic echinoderms (McClintock and Pearse, 1986), as has been reported for eggs and larvae of other species of marine invertebrate (Holland, 1978).

Metabolic rates of embryos and larvae

Rates of oxygen consumption were measured using Strathkelvin (Glasgow, U.K.) polarographic oxygen sensors (Model 1302) that were connected to oxygen meters (Model 781). The output (as volts) from each meter was recorded by an IBM computer using a software package for data acquisition and analysis (Datacan, Sable Systems Inc., Los Angeles, California). Two or three respiration chambers (Strathkelvin, Model RC 200) were used simultaneously and two to six independent measurements of respiration were made using different groups of embryos or larvae at the same stage of development.

Rates of oxygen consumption were measured for the antarctic species at either −1.4°C or −2.0°C (see Results for corresponding temperature and experiment). Oxygen consumption was measured on the same day that samples were taken for biomass and biochemical composition, or when rates of alanine transport were determined. Prior to any series of measurements on a given day, the respiration chamber and the membrane of the oxygen sensor were washed with 75% ethanol to minimize bacterial activity, and then rinsed four times with filtered seawater. At temperatures of −1.4 or −2.0°C, the oxygen sensors took an average of 2–3 h to stabilize when filtered seawater (with no animals added) was present in the respiration chamber. To obtain reliable data for the antarctic species, all respiration rates were determined only when at least 2 h had elapsed after the animals were placed into the respiration chamber. Rates of oxygen consumption for

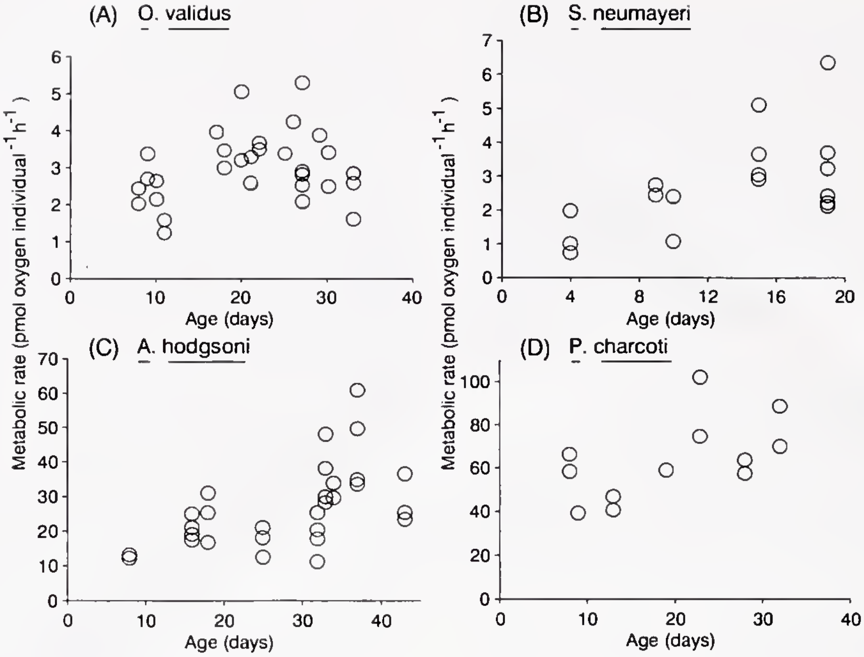

Figure 1. Rates of oxygen consumption by the developing stages of antarctic echinoderms. (A) *Odontaster validus;* (B) *Sterechinus neumayeri;* (C) *Acodontaster hodgsoni;* and (D) *Psilaster charcoti.* Each data point represents a single determination of metabolic rate over a period of 1–2 h.

larvae of the temperate species (*A. miniata*) were determined at 12°C using the same respiration apparatus as was used for the antarctic species. At these higher temperatures the oxygen sensors needed only 30 min to stabilize, allowing measurements to be made over the subsequent 30–60 min.

The volume of each of the respiration chambers (Model RC 200) was calibrated with an Eppendorf pipettor and set at 50 μl for all the antarctic species and 100 μl for the temperate species. At the end of each measurement, the animals were removed from the respiration chamber and counted. The number of animals used in the chamber depended upon the species. For the antarctic echinoderms, the number of individuals used ranged from 5 to 20 for the larger species (*A. hodgsoni* and *P. charcoti*) and from 33 to 221 for the smaller species (*O. validus* and *S. neumayeri*). For *A. miniata,* 29 to 93 larvae were used per chamber. The rate of oxygen depletion per individual was calculated by determining the rate of respiration of all the embryos or larvae in the chamber and dividing that rate by the number of individuals present. Rates of oxygen consumption with no animals present were determined as controls for each set of measurements and were subtracted from the rates where animals were present. For each set of measurements two control measurements were done, one immediately before and one after those measurements made with animals present. For all measurements (n = 97), the changes in oxygen tension in the absence of animals (controls) ranged from 5 to 25% of those rates with animals present (experimental). Data were used only if they had a signal-to-noise ratio of at least 3-to-1; *i.e.*, the rate with larvae was at least 3-fold greater than the rate without larvae (controls).

Calibration and accuracy of polarographic oxygen sensors at low temperatures

The voltage output from each oxygen sensor was calibrated to the concentration of oxygen in seawater (at the experimental temperatures) by immersing the sensor in a BOD (biological oxygen demand) bottle containing 300 ml of seawater. The voltage readings from the oxygen sensors were recorded and the amount of oxygen present in the BOD bottle was measured by Winkler's titration (Parsons *et al.*, 1984).

The measured metabolic rates of the antarctic embryos and larvae were low (see Fig. 1) and often near the limit of detection of the polarographic oxygen sensors (signal-to-noise ratio of 3:1). The following procedure was used to check that the low rate of oxygen depletion that was observed was not an artifact of any abnormal functioning of the sensors at the cold temperature of antarctic seawater. The biological depletion of oxygen at −2.0°C was mimicked by bubbling helium into seawater. Up to 50% of the oxygen was removed from seawater that had been placed in a series of seven BOD bottles. The voltage reading was recorded from the oxygen sensor placed in each BOD bottle containing reduced oxygen and the actual amount of oxygen present in each seawater sample was then measured chemically with Winkler's titration. The decrease in the oxygen content of seawater measured with the sensors was not significantly different from the decrease as measured independently by Winkler's titration (least-squares linear regression analysis, variance ratio of slope = 0.35^{ns}, $n = 7$).

Measurement of alanine transport rates by antarctic and temperate larvae

Time course experiments were done at a range of different alanine concentrations to determine the kinetics of amino acid transport by larvae of *O. validus* (at −2.0°C) and *A. miniata* (at 12.0°C) (methods previously described by Manahan *et al.*, 1989). Radioactive alanine (^{3}H-alanine, 84 Ci mmol^{-1}, New England Nuclear) was added (2 or 5 μCi) to 10 ml of seawater in the presence of a range of concentrations (0.1–100 μM) of nonradioactive alanine (Sigma Chemical Co.). Aliquots (500 μl) containing larvae (*O. validus:* 222 ml^{-1}; *A. miniata:* 322 ml^{-1}) were taken from the 10-ml vial every 2 min for 20 min. The transport rate of alanine at a given concentration was calculated (as pmol alanine larva^{-1} h^{-1}) using (1) the measured rate of accumulation of radioactivity (as disintegrations per minute after quench correction), (2) the specific activity of the radiolabel, and (3) the number of larvae per sample. The rate of alanine transport per larva as a function of increasing alanine concentration was plotted to determine the affinity (K_t) and maximum capacity (J_{max}) of the amino acid transporter in antarctic and temperate larvae.

Results

Metabolic rates during early development

During early development of *O. validus*, from the blastula (8 days) to late gastrula stage (27 days), there was an increase in metabolic rate (Fig. 1A) measured at −1.4°C. The significance of this increase was determined using analysis of variance for the data during that 19-day period (variance ratio, VR = 6.80*, $F_{0.05[1,23]} = 4.28$). The data for early bipinnaria (after 27 days) were not used in this analysis of early development because the increase in respiration rate did not continue once the larval stage was reached. For *S. neumayeri* (Fig. 1B), there was an increase in metabolic rate (VR = 8.28*, $F_{0.05[1,15]} = 4.54$) from the unhatched blastula (4 days) to the gastrula stage (19 days). The larval stage of *A. hodgsoni* (a bilobed bipinnaria, Bosch and Pearse, 1990) had developed by 36 days. From the early embryo (8 days) to the larval stage (36 days) there was an increase (VR = 14.41***, $F_{0.05[1,24]} = 4.26$) in metabolic rate (Fig. 1C). However for *P. charcoti*, a species with lecithotrophic development, no significant change was measured in metabolic rate during the period of development studied (to 32 days) (Fig. 1D, VR = 4.56^{ns}, $F_{0.05[1,10]} = 4.96$). The lack of statistical significance may be an effect of a smaller sample size for this species.

The metabolic rates of the bipinnaria larvae used for the comparison of metabolic rates and amino acid transport rates were 27.5 ± 1.51 pmol O_2 larva^{-1} h^{-1} ($n = 6$) for 5-day-old larvae of *A. miniata* (measured at 12°C) and 2.22 ± 0.69 pmol larva^{-1} h^{-1} (n = 4) for 42-day-old larvae of *O. validus* (−2°C). These different ages of larvae for the two species represent the same stage of development (early bipinnaria) because of the slower development rate of *O. validus* relative to *A. miniata*. Errors given here and throughout this paper (unless otherwise stated) are one standard error of the mean (±1 SEM).

Scaling of metabolic rates with biomass during early development of antarctic echinoderms

The scaling of metabolic rate to ash-free dry organic weight (biomass) for embryos of *S. neumayeri, O. validus, A. hodgsoni*, and *P. charcoti* is shown in Figure 2A. When the log of metabolic rate (mean of all values for each species from Fig. 1) was plotted against the log of biomass (mean for each species), a slope of 0.66 ± 0.213 (95% confidence limit) was calculated. These metabolic data can be described by the power function:

$$\text{Metabolic rate} = 3.14\ M^{0.66}$$

where metabolic rate is given as pmol O_2 individual^{-1} h^{-1} and mass (M) has units of μg ash-free dry organic weight.

Volume to biomass relationship, and lipid and protein content of eggs of antarctic echinoderms

The slope of the line describing the relationship of egg biomass to egg volume is 0.917 (Fig. 2B). The egg diameters for the five species used in this comparison were obtained from the following reports: *S. neumayeri* from Bosch *et al.* (1987), and *A. hodgsoni, O. validus, P. fuscus*, and *P. charcoti* from Bosch and Pearse (1990). Values for biomass and egg diameters used to construct Figure 2B are given in Table IA for four of the five species (egg volumes based on a sphere). The data point for the eggs of *P. fuscus* is based on the following values: biomass = 87.9 ± 1.07 μg, diameter = 1200 μm, volume = 904.7 × 10^{-3} mm^3.

The percent of the ash-free dry organic weight of eggs that was composed of lipid and protein was calculated for four asteroid species (Fig. 2C). Eggs of *O. validus* had equal proportions of lipid and protein, whereas eggs of the three other species (all have lecithotrophic development) had a greater proportion of biomass as lipid. The percent recovery of dry organic weight as lipid and protein ranged from 65% (*P. charcoti*) to 89% (*P. fuscus*)—*i.e.*, 11 to 35% of total dry organic weight was not accounted for by the lipid and protein content of the eggs.

Changes in biomass, lipid, and protein content during early development of O. validus *and* A. hodgsoni

Embryos of *O. validus* in the three replicate cultures had similar changes in biomass, lipid, and protein content from the egg (0 days) to early bipinnaria larva (35 days) (Fig. 3A). As stated earlier, one batch of eggs obtained from several females was used to start all three of the 200-l cultures. Biomass increased significantly (ANOVA, VR = 83.13***, $F_{0.05[1,21]}$ = 4.32) from the egg (0 days) to the early gastrula stage (pooled data for 9, 10, and 12 day-old) and thereafter remained fairly constant (*i.e.*, no significant difference between gastrula and early larval stage at d 35, VR = 2.24^{ns}, $F_{0.05[1,32]}$ = 4.12). The equation for the fitted curve through all the biomass data points is given in the figure legend. Linear regression analyses were used to determine the rates of lipid and protein utilization during early development of *O. validus* (regression lines excluded for graphical simplicity, Fig. 3A). Lipid and protein content did not change significantly (determined by ANOVA) from the egg to early larva ($VR_{protein}$ = 0.22^{ns}, VR_{lipid} = 0.09^{ns}, *n* = 22).

For the first 42 days of development of *A. hodgsoni*, lipid content did not change (Fig. 3B, VR = 0.01^{ns}, *n* = 25). Both protein content and biomass did, however, decrease during this period. Protein decreased at a rate of 25.7 ± 8.8 ng individual^{-1} day^{-1} (VR = 8.60**, $F_{0.05[1,21]}$ = 4.32). Biomass decreased at a rate of 52.4 ± 14.3 ng individual^{-1} d^{-1} (VR = 13.49**, $F_{0.05[1,23]}$ = 4.28).

Transport of alanine from seawater by larvae of A. miniata *and* O. validus

The larvae of *A. miniata* had a maximal transport capacity (J_{max}) for alanine of 17.15 pmol μg^{-1} h^{-1} (at 12°C), whereas the J_{max} for alanine by larvae of *O. validus* was 6.51 pmol μg^{-1} h^{-1} (at −2°C) (Fig. 4A). The affinities (values of K_t) of the alanine transport systems in larvae of both species were similar (see slopes, Fig. 4B), at 1.9 μM for *A. miniata* and 1.3 μM for *O. validus*.

Discussion

Lifespan of embryos and larvae

Antarctic echinoderm larvae have to survive periods of many months in a nutrient-poor water column (Olson *et al.*, 1987; Pearse *et al.*, 1991; Rivkin, 1991). Survival under such conditions should be difficult, especially for those species with larval forms that require food to complete development (*e.g.*, *O. validus* and *S. neumayeri*). An estimate of larval life span under starvation conditions can be obtained by calculating how long the maternal endowment of energy reserves initially present in the egg could supply the metabolic demand (rates of respiration) of embryos and larvae. Starvation conditions are defined here as the absence of any dietary inputs, either in particulate form or as dissolved organic material. The energy available as biomass in the eggs of species with planktotrophic and lecithotrophic modes of development was compared to the metabolic rates of those same species during early development (Table 1). The time it would take to deplete

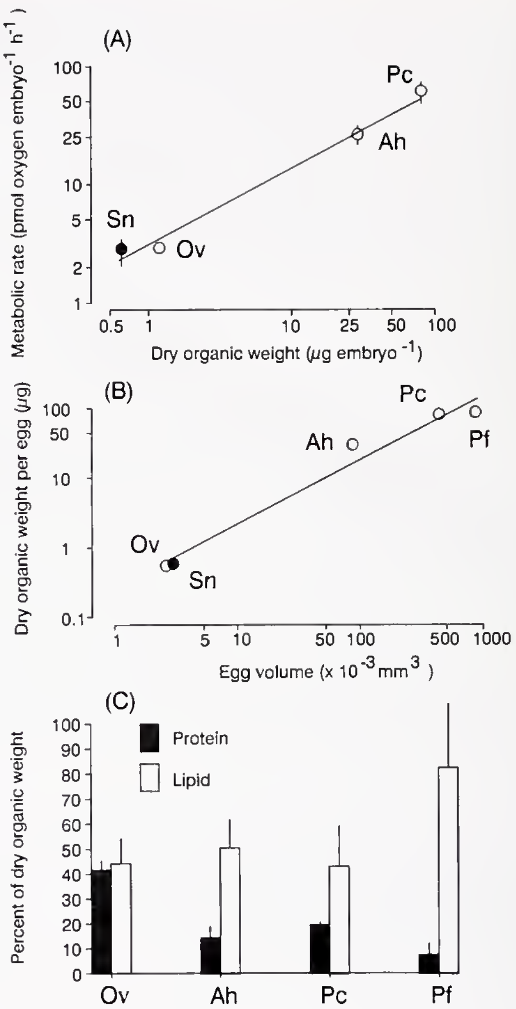

Figure 2. Metabolic scaling, relationship of egg volume to biomass (ash-free dry organic weight), and lipid and protein content of eggs of antarctic echinoderms. Ah, *Acodontaster hodgsoni;* Ov, *Odontaster validus;* Pc, *Psilaster charcoti;* Pf, *Perknaster fuscus;* Sn, *Sterechinus neumayeri* (echinoid, closed circles). (A) Change in metabolic rate as a function of embryos' biomass, error bars represent 95% confidence limits of the mean, where no error bars are shown errors fell within graphical representation of data point. (B) Relationship of egg biomass to egg volume. (C) Lipid and protein content of eggs as percent of biomass with 95% confidence limits.

Table I

Calculation of the duration of larval life span: (A) for the antarctic echinoderms Acodontaster hodgsoni, Odontaster validus, Psilaster charcoti, *and* Sterechinus neumayeri. *(B) For temperate echinoderms* Asterina miniata *and* Strongylocentrotus purpuratus

(A) Antarctic species:

Species	*O. validus*	*S. neumayeri*	*A. hodgsoni*	*P. charcoti*
Egg size[1] (μm)	170	179	550	950
Egg biomass[2] (μg ± SEM)	0.63 ± 0.018	0.69 ± 0.032	30.1 ± 0.06	81.3 ± 1.91
Metabolic rate[3] (pmol O_2 ind.$^{-1}$ h^{-1})	2.94 ± 0.18	2.90 ± 0.33	26.1 ± 2.26	63.9 ± 5.09
Biomass depletion[4] (ng ind.$^{-1}$ day^{-1})	1.08	1.06	9.55	23.4
Time to deplete 50% of egg biomass (months)	9.8	10.8	52.5	58.0

(B) Temperate species:

Species	*A. miniata*	*S. purpuratus*
Egg size[1] (μm)	180	70
Egg biomass[2] (μg ± SEM)	0.70 ± 0.01	0.07
Metabolic rate (pmol O_2 ind.$^{-1}$ h^{-1})	27.5 ± 1.51	12.7
Biomass depletion[4] (ng ind.$^{-1}$ day^{-1})	10.1	4.65
Time to deplete 50% of egg biomass (months)	1.16	0.25

[1] Egg diameters from Bosch *et al.*, 1987; Bosch and Pearse, 1990; Strathmann, 1987.

[2] Biomass measured as ash-free dry organic weight, data from this study or from Shilling and Manahan, 1990.

[3] Metabolic rate, data from this study (mean ± SEM) or from Shilling and Manahan (*op. cit.*).

[4] Biomass depletion, ng of dry organic weight (individual)$^{-1}$ (day)$^{-1}$. Each rate of aerobically catabolized biomass was calculated using the mean of the oxyenthalpic equivalents of lipid and protein [484.0 kJ (mol O_2)$^{-1}$] and the specific enthalpy of combustion of lipid and protein (31.75 kJ g^{-1}) (values from Gnaiger, 1983).

50% of the eggs' biomass was calculated. For the antarctic species studied that had the smallest egg biomass (0.63 μg, *O. validus*), 50% of the egg's biomass could provide sufficient energy to meet metabolic demand (2.94 pmol O_2 individual^{-1} h^{-1}) for 9.8 months (Table IA). For *P. charcoti*, an antarctic species that had the largest egg biomass (81.3 μg) in this comparison, a similar calculation revealed that the lecithotrophic larvae of this species could survive for a remarkably long time under starvation conditions—58 months (4.8 years).

The long survival times of antarctic larval forms are in marked contrast to those of temperate species of echinoderm. Larvae of *A. miniata*, starting from a similar egg size to *O. validus*, have an 8.4-fold shorter potential life span (Table IB). Larvae of the sea urchin *Strongylocentrotus purpuratus* would deplete 50% of the egg's biomass in only 8 days. In summary, the potential life spans of larvae of the antarctic species are in the range of months to years, while those of the temperate species are much shorter at days to weeks. This comparison of life spans of antarctic and temperate echinoderm larvae suggests that antarctic larval forms living in an environment that is episodic with respect to food availability have a "wait-and-see" strategy of being able to withstand starvation conditions for periods of months to years. This strategy is not available to temperate larval forms and tropical larval forms when developing at temperatures characteristic of their respective habitats, at least for echinoderms. The tropical species do not have correspondingly larger egg sizes (Emlet *et al.*, 1987) when compared to eggs of antarctic echinoderms (Fig. 2B; see also McClintock and Pearse, 1986; Bosch *et al.*, 1987; Bosch and Pearse, 1990) or temperate species (McEdward and Chia, 1991).

Transport of dissolved amino acids and relationship of transport capacity to metabolic rate

The above calculations of life span show one possible physiological mechanism for survival of antarctic echinoderm larvae under low-food conditions. A comparison of nutrient uptake rates and metabolic rates of antarctic and temperate larval forms revealed a second possibility: antarctic larvae have a high nutrient uptake capacity relative to metabolic rate when compared to a temperate larval form (Table II). The bipinnaria larvae of the antarctic and temperate species of asteroid chosen for this physiological comparison develop from eggs of similar sizes (*O. validus*, 0.63 ± 0.018 μg; *A. miniata*, 0.697 ± 0.007 μg). At the appropriate temperature for each species (−2.0 and 12.0°C) the larvae of these two species had a 20.6-fold difference in mass-specific metabolic rates (2.22 *cf.* 45.75 pmol O_2 μg^{-1} h^{-1}). However, the mass-specific capacity for alanine transport (J_{max}) was only 2.6-fold higher for the temperate species (6.51

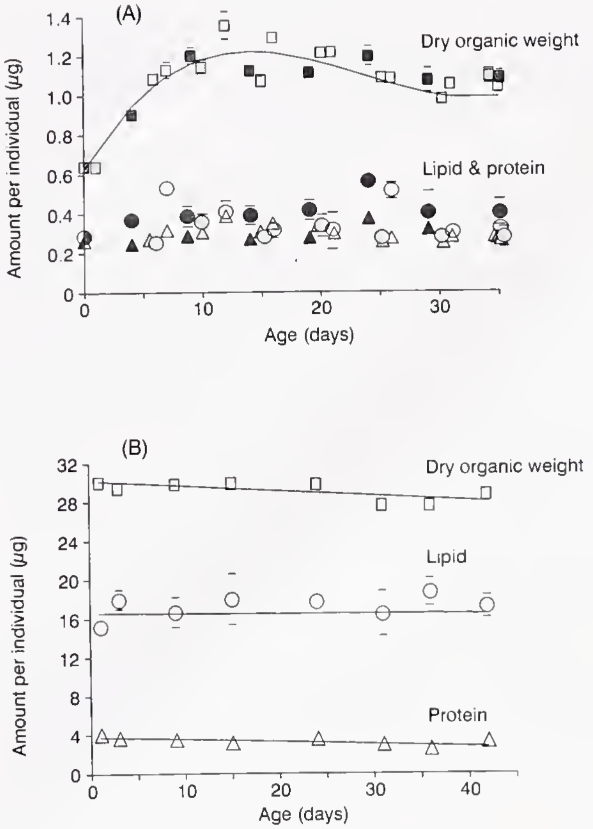

Figure 3. Changes in dry organic weight, lipid, and protein content of embryos of (A) *Odontaster validus* and (B) *Acodontaster hodgsoni.* Squares, ash-free dry organic weight (biomass); circles, lipid; triangles, protein. For all graphs error bars represent one standard error of mean (SEM), where bars are not shown the error fell within graphical representation of data point. (A) Open, stippled, and solid symbols represent three different cultures reared from the same batch of eggs. Curve was fitted through all biomass data points (n = 122, including replicates) using the equation: $Y = (0.6236) + (0.0976X) + (-0.00495X^2) + (0.00007X^3)$, where Y is ash-free dry organic weight (µg) and X is time (days). (B) Lines represent slopes calculated from least-square regression analyses.

cf. 17.15 pmol alanine $\mu g^{-1}\ h^{-1}$). Both species had a high affinity for amino acid transport (K_t = 1.3 or 1.9 µ*M*). Alanine was chosen for these studies because it is transported by developing marine invertebrates at a rate that is close to the average when a mixture of amino acids is present (Manahan, 1989).

The consequence for the antarctic species of having a higher-capacity transport system relative to metabolic rate, compared to the temperate species, is that the former could gain substantial metabolic benefit from the transport of amino acids present at low concentrations. The amino acid concentrations in waters of McMurdo Sound, Antarctica, were measured with high-performance liquid chromatography from austral winter (August) to austral summer (January) (Welborn and Manahan, 1991). Total amino acid concentrations in the water column prior to the phytoplankton bloom in December were low, ranging from below the limit of detection of the analysis to *ca.* 100 n*M*. If larvae of *O. validus* were in an environment with 50 n*M* alanine, the rate of alanine transport could supply 32% of the larva's metabolic rate (Table II). In contrast, larvae of the temperate species could supply only 3% of their metabolic rate at 50 n*M* alanine (*A. miniata,* Table II). A contribution of ⅓ of metabolic rate for a marine invertebrate is a very high metabolic input from transport of dissolved amino acids alone at a concentration of only 50 n*M* (see reviews by Stephens, 1988; Wright, 1988; Wright and Manahan, 1989; Manahan, 1990). For the temperate species to supply ⅓ of metabolic rate, larvae of *A. miniata* would require a 15.8-fold higher substrate concentration of 788 n*M*. At the maximal transport capacity (J_{max}) of alanine, larvae of *A. miniata* accounted for *ca.* 100% of metabolic needs (Table II). Similar matching of nutrient maximum transport rates with metabolic needs has been found during larval development of the mollusc *Crassostrea gigas* (Manahan *et al.,* 1989) and in vertebrate intestines (Ferraris and Diamond, 1989; Buddington and Diamond, 1989). In contrast, the antarctic larvae (*O. validus*) have a much higher ratio of nutrient transport to metabolic rate (Table II), with the moles

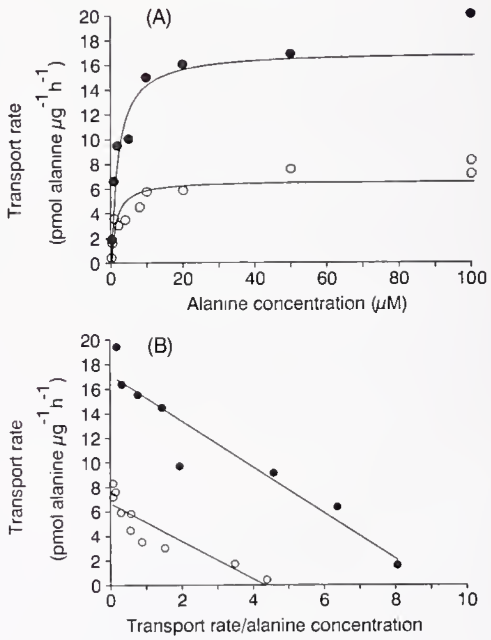

Figure 4. Kinetics of alanine transport by bipinnaria-stage larvae of *Asterina miniata* (12°C, closed circles) and *Odontaster validus* (−2°C, open circles). Values for biomass of larvae given in Table II. Each point represents the transport rate obtained from a separate time course experiment based on 10 samples. The Michaelis-Menten equation was used to plot the saturation curves in (A) using values for K_t and J_{max} for each species (see text) obtained from linear regression analysis of Eadie-Hofstee plots (B).

Table II

Mass-specific metabolic rates and mass-specific rates of alanine transport for bipinnaria larvae of Odontaster validus *(42-day-old) and* Asterina miniata *(5-day-old)*

	O. validus (−2°C)	*A. miniata* (12°C)
Metabolic rate[1]		
(pmol oxygen μg^{-1} h^{-1})	2.22	45.75
(pmol Ala-equivalents μg^{-1} h^{-1})	0.74	15.25
Transport rate[2] (pmol alanine μg^{-1} h^{-1})		
maximum transport rate (J_{max})	6.51	17.15
transport rate at 50 n*M* alanine	0.24	0.45
Percent of metabolic rate as alanine equivalents supplied by transport from 50 n*M*	32.4%	3.0%
Ratio of maximum transport rate (J_{max}) of alanine to metabolic rate as alanine equivalents	8.8	1.1

[1] Mass (ash-free dry organic weight) of *O. validus* was 1.0 μg; *A. miniata* was 0.6 μg. Alanine equivalents of oxygen consumption based on stoichiometry that complete combustion of 1 mole alanine requires 3 moles O_2. Errors for metabolic rates given in "Results."

[2] Calculated with Michaelis-Menten equation using values of K_t and J_{max} for alanine transport by each species (see Fig. 4B for graphical estimates of errors).

of alanine transported at J_{max} accounting for 8.8-times metabolic needs.

Comparisons with previous research

Except for one species *(P. fuscus),* the linear relationship of ash-free dry organic weight of eggs as a function of egg volume (Fig. 2B) is consistent with previously published values of egg diameters of antarctic echinoderms (Bosch *et al.,* 1987; Bosch and Pearse, 1990). McClintock and Pearse (1986) report a dry weight of 2640 μg (5.9% ash) for an egg of *P. fuscus* (1200 μm diameter), compared with our measurement of egg biomass at 87.9 μg dry organic weight. McClintock and Pearse (1986) used a different technique to obtain eggs than the one we used. In their study, full-grown oocytes were separated from the ovary, dried, and weighed. Freely spawned oocytes were used in our study. Perhaps this difference might have resulted in what we suggest was an overestimate by McClintock and Pearse (1986) of the egg weight for *P. fuscus* relative to eggs from other species of antarctic echinoderms (see Fig. 2B, value of *P. fuscus* at 87.9 μg, *cf.* that data point if weight was 2640 μg even allowing for a 5.9% ash weight).

Olson *et al.* (1987) measured the metabolic rates of bipinnaria-stage larvae of *O. validus* and reported values of 1–2 nl O_2 larva^{-1} h^{-1} over a temperature range of −1.0 to −1.86°C. This metabolic rate is equivalent to 67 pmol O_2 larva^{-1} h^{-1} (equal to 1.5 nl O_2 at STP), which is 2.4-fold greater (per larva) than the metabolic rate of the temperate species *A. miniata* measured at 12°C (Table IB: 27.5 ± 1.51 pmol O_2 larva^{-1} h^{-1}). The data of Olson *et al.* (1987) would lead to the suggestion that the antarctic larvae are "cold-adapted" (*cf.* studies with antarctic fish: Torres and Somero, 1988; Crockett and Sidell, 1990). However, our data do not support that conclusion. On a mass-specific basis, the metabolic rate value of Olson *et al.* is 30-fold greater (based on a 1-μg larva) than the value we measured for bipinnaria of *O. validus* (Table II). Our measurement of metabolic rate for this species is consistent with the measurements for the other three antarctic species (Fig. 2A). Together the metabolic rates for the antarctic species give a metabolic power equation (metabolic rate = $3.14\ M^{0.66}$) consistent with the ⅔ mass exponent as argued by Heusner (1991) to be the relationship between mass and metabolic rate, although a slope of 0.75 (Schmidt-Nielsen, 1984) would fall within the 95% confidence limits of our measurement (0.66 ± 0.213). A major difference in methodology between our study and that of Olson *et al.* is that in the present study the polarographic oxygen sensors (POS) were allowed to equilibrate for 2–3 h in the respiration chamber (with larvae present) prior to taking any measurements, as opposed to 30 min in the study by Olson *et al.* (1987). We found that a 2–3 hour equilibration time was necessary for the rate of oxygen consumption by the POS to be less than the low rates of oxygen consumption of the antarctic embryos and larvae. This may be the cause of the discrepancy between our values and the higher values of Olson *et al.* (1987).

Changes in organic weight and biochemical composition during early development

Previous studies have shown statistically significant increases in dry organic weight during embryogenesis of echinoderms and molluscs (Jaeckle and Manahan, 1989; Shilling and Manahan, 1990; Jaeckle and Manahan, 1992; Shilling and Bosch, 1994). Identical techniques (described in Jaeckle and Manahan, 1989) were used in the present study to measure the surprisingly large increase in organic weight for stages of *O. validus* lacking a digestive system (day 0 to 10, Fig. 3A). There was no corresponding increase in lipid or protein content of *O. validus* during the period of biomass increase. The biomass increase of *O. validus* is probably not due to a gain in carbohydrate, as marine invertebrate eggs and embryos do not contain much of this energy reserve (Holland, 1978; McClintock and Pearse, 1986; Jaeckle and Manahan, 1989; Shilling and Manahan, 1990). An alternative explanation for the observed increase in biomass of *O. validus* is that the increase is an artifact of the measurement techniques used and that the values for biomass are too small for stages less than 5 days old (Fig. 3A). The observed differences between stages might be due to differences in drying procedures. This possibility can be eliminated, however, because all samples from the three different cultures were kept frozen until they were all analyzed (dried and ashed) at the same time. The possibility of growth during early development of antarctic echinoderms deserves consideration and further testing because at this time we can offer no physiological mechanism that might explain the observed large biomass increase of stages of *O. validus* lacking a digestive system. Pending further studies, we stress the simpler interpretation of these data: *none* of the metabolic needs during the early development of *O. validus* can be explained through the catabolism of biomass initially present in the egg.

The possibility of growth for stages lacking a digestive system may be specific to only certain species of antarctic echinoderms. A species that has a lecithotrophic mode of development *(A. hodgsoni)* had no increase in biomass during the first 42 days of development (Fig. 3B). It is noteworthy that lipid content did not decrease during this time, a finding consistent with the data showing no decrease in lipid content during 35 days of development of *O. validus* (Fig. 3A). Although lipid is a major reserve in eggs and larvae of marine invertebrates (Holland, 1978), it is not used during the early development of these antarctic species even though the lipid content is high in eggs of species with lecithotrophic development (McClintock and Pearse, 1986; Fig. 2C of this study). For these two species of antarctic echinoderm, we find no evidence for the widely held view that lipid is the major energy reserve used during development.

In conclusion, developing antarctic echinoderms can survive for months to years by relying solely on the energy reserves present in the egg. In the episodic food-environment of the southern ocean, the larvae could survive long periods of starvation.

Acknowledgments

We are most grateful to Dr. Isidro Bosch for his assistance in collecting the antarctic echinoderms in McMurdo Sound, and for his assistance with larval culturing. We thank Dr. Richard Rivkin for his advice and help during the "Winfly" period on the ice. Our thanks also go to Dr. John Pearse for discussions about conducting this research. Antarctic Support Associates, The U.S. Navy (VXE-6), and The National Science Foundation provided logistic and scientific support in Antarctica. This research was supported by NSF grant 88-20130. One of us (DTM) would like to dedicate this paper to his deceased father, the late Mr. C. A. Manahan.

Literature Cited

Bosch, I., and J. S. Pearse. 1990. Developmental types of shallow-water asteroids of McMurdo Sound, Antarctica. *Mar. Biol.* **104:** 41–46.

Bosch, I., K. A. Beauchamp, M. E. Steele, and J. S. Pearse. 1987. Development, metamorphosis, and seasonal abundance of embryos and larvae of the antarctic sea urchin *Sterechinus neumayeri*. *Biol. Bull.* **173:** 126–135.

Bradford, M. M. 1976. A rapid and sensitive method for the quantitation of microgram quantities of protein utilizing the principle of protein-dye binding. *Anal. Biochem.* **72:** 248–254.

Buddington, R. K., and J. M. Diamond. 1989. Ontogenetic development of intestinal nutrient transporters. *Ann. Rev. Physiol.* **51:** 601–619.

Crockett, E. L., and B. D. Sidell. 1990. Some pathways of energy metabolism are cold adapted in antarctic fishes. *Physiol. Zool.* **63:** 472–488.

Emlet, R. E., L. R. McEdward, and R. R. Strathmann. 1987. Echinoderm larval ecology viewed from the egg. Pp. 55–136 in *Echinoderm Studies*, Vol. 2, M. Jangoux and J. M. Lawrence, eds. A. A. Balkema, Rotterdam.

Ferraris, R. P., and J. M. Diamond. 1989. Specific regulation of intestinal nutrient transporters by their dietary substrates. *Ann. Rev. Physiol.* **51:** 125–141.

Gnaiger, E. 1983. Calculation of energetic and biochemical equivalents of respiratory oxygen consumption. Pp. 337–345 in *Polarographic Oxygen Sensors: Aquatic and Physiological Applications*, E. Gnaiger and H. Forstner, eds. Springer-Verlag, New York.

Heusner, A. A. 1991. Size and power in mammals. *J. Exp. Biol.* **160:** 25–54.

Holland, D. L. 1978. Lipid reserves and energy metabolism in the larvae of benthic marine invertebrates. Pp. 85–123 in *Biochemical and Biophysical Perspectives in Marine Biology*, Vol. 4, D. C. Malins and J. R. Sargent, eds. Academic Press, London.

Jaeckle, W. B., and D. T. Manahan. 1989. Growth and energy imbalance during the development of a lecithotrophic molluscan larva *(Haliotis rufescens)*. *Biol. Bull.* **177:** 237–246.

Jaeckle, W. B., and D. T. Manahan. 1992. Experimental manipulations of the organic chemistry of seawater: implications for studies of energy budgets in marine invertebrate larvae. *J. Exp. Mar. Biol. Ecol.* **156:** 273–284.

Manahan, D. T. 1989. Amino acid fluxes to and from seawater in axenic veliger larvae of a bivalve *(Crassostrea gigas)*. *Mar. Ecol. Prog. Ser.* **53:** 247–255.

Manahan, D. T., S. Nourizadeh, and W. B. Jaeckle. 1989. Ontogenic changes in the rates of amino acid transport by marine invertebrate larvae (Echinodermata, Echiura, Mollusca). *Biol. Bull.* **176:** 161–168.

Manahan, D. T. 1990. Adaptations by invertebrate larvae for nutrient acquisition from seawater. *Am. Zool.* **30:** 147–160.

Mann, R., and S. M. Gallager. 1985. Physiological and biochemical energetics of larvae of *Teredo navalis* L. and *Bankia gouldi* (Bartsch) (Bivalvia: Teredinidae). *J. Exp. Mar. Biol. Ecol.* **85:** 211–228.

McClintock, J. B., and J. S. Pearse. 1986. Organic and energetic content of eggs and juveniles of antarctic echinoids and asteroids with lecithotrophic development. *Comp. Biochem. Physiol.* **85A:** 341–345.

McEdward, L. R., and F.-S. Chia. 1991. Size and energy content of eggs from echinoderms with pelagic lecithotrophic development. *J. Exp. Mar. Biol. Ecol.* **147:** 95–102.

Olson, R. R., I. Bosch, and J. S. Pearse. 1987. The antarctic larval food limitation hypothesis examined for the asteroid *Odontaster validus. Limnol. Oceanogr.* **32:** 686–690.

Parsons, T. R., Y. Maita, and C. A. Lailli. 1984. *A Manual of Chemical and Biological Methods for Seawater Analysis,* Pergamon Press, Oxford.

Pearse, J. S. 1969. Slow developing demersal embryos and larvae of the antarctic sea star *Odontaster validus. Mar. Biol.* **3:** 110–116.

Pearse, J. S., J. B. McClintock, and I. Bosch. 1991. Reproduction of antarctic benthic marine invertebrates. *Am. Zool.* **31:** 65–80.

Rivkin, R. R. 1991. Seasonal patterns of planktonic production in McMurdo Sound, Antarctica. *Am. Zool.* **31:** 5–16.

Rivkin, R. R., I. Bosch, J. S. Pearse, and E. J. Lessard. 1986. Bacterivory: a novel feeding mode for asteroid larvae. *Science* **223:** 1311–1314.

Schmidt-Nielsen, K. 1984. *Scaling: Why Is Animal Size So Important?* Cambridge University Press, Cambridge.

Shilling, F. M., and D. T. Manahan. 1990. Energetics of early development for the sea urchins *Strongylocentrotus purpuratus* and *Lytechinus pictus* and the crustacean *Artemia* sp. *Mar. Biol.* **106:** 119–127.

Shilling, F. M., and I. Bosch. 1994. 'Pre-feeding' embryos of antarctic and temperate echinoderms use dissolved organic material for growth and metabolic needs. *Mar. Ecol. Prog. Ser.* **109:** 173–181.

Stephens, G. C. 1988. Epidermal amino acid transport by marine invertebrates. *Biochim. Biophys. Acta.* **947:** 113–138.

Strathmann, M. F. 1987. *Reproduction and Development of Marine Invertebrates of the Northern Pacific Coast: Data and Methods for the Study of Eggs, Embryos, and Larvae.* University of Washington Press, Seattle and London. 670 pp.

Torres, J. J., and G. N. Somero. 1988. Metabolism, enzymic activities and cold adaptation in Antarctic mesopelagic fishes. *Mar. Biol.* **98:** 169–180.

Welborn, J. R., and D. T. Manahan. 1991. Seasonal changes in concentrations of amino acids and sugars in seawaters of McMurdo Sound, Antarctica: uptake of amino acids by asteroid larvae. *Antarctic J. U.S* **26:** 160–162.

Wright, S. H. 1988. Nutrient transport across the integument of marine invertebrates. Pp. 173–218 in *Advances in Comparative and Environmental Physiology,* Vol. 2, R. Gilles, ed. Springer-Verlag, Berlin.

Wright, S. H., and D. T. Manahan. 1989. Integumental nutrient uptake by aquatic organisms. *Ann. Rev. Physiol.* **51:** 585–600.

INDEX

A

A metamorphic inducer in the opisthobranch *Haminaea callidegenita:* partial purification and biological activity, 133
A model of rowing propulsion and the ontogeny of locomotion in *Artemia* larvae, 164
α_2-macroglobulin, 229
Acanthaster larval ecology, 304
Adhesion, 35
Aequorin, 293, 300
Aggression-reducing courtship signals in the lobster, *Homarus americanus,* 275
Airriess, Chris N., and James J. Childress, Homeoviscous properties implicated by the interactive effects of pressure and temperature on the hydrothermal vent crab *Bythograea thermydron,* 208
Allen, Standish K., Jr., see Ximing Guo, 309
Aloulou, Amine, see Catherine T. Tamse, 251
Amino acids, 48, 398
Ammonium regeneration, 283
An ethogram of body patterning behavior in the squid *Loligo vulgaris reynaudii* on spawning grounds in South Africa, 363
An improved quantitative assay for chemokinesis in *Tetrahymena,* 8
Analysis of acid volatile sulfide and metals to predict the toxicity of Boston Harbor sediments, 290
Analysis of spatial and temporal patterns in the Ca^{2+} signal that signals nuclear envelope breakdown in sand dollar (*Echinaracnius parma*) cells, 237
Anctil, Michel, and Jean-Pascal Carette, Glutamate immunoreactivity in non-neuronal cells of the sea anemone *Metridium senile,* 48
Anderson, Don S., see Christian DellaCorte, 200
Aneuploidy, 309
Annihilation, 256
Annual Report of the Marine Biological Laboratory, R1
Antarctica, 398
Antennular flicking, 273
Anthozoa, 200, 355
Arachidonic acid, 242
Arginine, 248
Arigue, Adel, see Conxita Avila, 252
Armstrong, Peter B., Sandra Misquith, Subita Srimal, Ralph Melchior, and James P. Quigley, Identification of limulin as a major cytolytic protein in the plasma of the American horseshoe crab, *Limulus polyphemus,* 227
Armstrong, Peter B., see Ralph Melchior, 228; James Quigley, 229
Artemia, 156, 164
Artificial and natural inducers, 252
Assay, 1, 8
Asteroid larvae, 304
Atema, Jelle, see Ann E. Leonard, 273; George Gomez, 259; Jennifer Basil, 272; Paul Bushmann, 275
Avila, Conxita, Adel Arigue, Catherine T. Tamse, and Alan Kuzirian, *Hermissenda crassicornis* larvae metamorphose in the laboratory in response to artificial and natural inducers, 252
Avila, Conxita, see Elizabeth Tyndale, 274

B

Babcock, Russell C., see Leland G. Johnson, 304
Bag cells, 270
Barlow, R. B., Jr., see C. L. Passaglia, 260; F. A. Dodge, 261
Barnacle settlement patterns, 346
Basil, Jennifer, and Jelle Atema, Lobster orientation in turbulent odor plumes: simultaneous measurement of tracking behavior and temporal odor patterns, 272
Behavior, 272, 275, 363
Benech, Juan, Marianna Crispino, Jong Tai Chun, Barry B. Kaplan, and Antonio Giuditta, Protein synthesis in nerve endings from squid brain: modulation by calcium ions, 269
Benthic
  invertebrates, 319
  nitrogen cycling, 288
  nitrogen flux, 283
Biogeography, 336
Bivalve, 76, 281
Body pattern, 363
Borgese, Thomas A., Sharon Bourke, Bernarda Frias, Donald Johnson, and John Harrington, Copper induced polymerization of hemoglobin from the ocean pout, *Macrozoarces americanus,* 246
Bourke, Sharon, see Thomas A. Borgese, 246
Bowman, Katherine, see Krista K. Ingram, 277
Boxhill, Jessica L., Lory Santiago Vásquez, Timothy R. Harrison, Kenneth Foreman, and James N. Kremer, Daily variation in phytoplankton production in two subestuaries of Waquoit Bay, Massachusetts, 284
Boxhill, Jessica L., see Lory Z. Santiago Vásquez, 285; Timothy R. Harrison, 287
Brockmann, H. Jane, see Dustin Penn, 373
Brooding, 112
Brook, Heather J., Timothy A. Rawlings, and Ronald W. Davies, Protogynous sex change in the intertidal isopod *Gnorimosphaeroma oregonense* (Crustacea: Isopoda), 99
Bryozoa, 143
Bullis, Robert A., see Terrie J. Sadusky, 254
Bushmann, Paul, and Jelle Atema, Aggression-reducing courtship signals in the lobster, *Homarus americanus,* 275
Bythograea thermydron, 208

C

C-Reactive protein, 299
Ca^{2+} microdomains, 293
Calcium, 235, 237, 242, 267, 270
  concentration, 300
  signaling, 234
Calcium and voltage sensitivity of potassium current activation in toadfish semicircular canal hair cells, 267
Carette, Jean-Pascal, see Michel Anctil, 48
Catalase, 247

Catalase activity in dogfish (*Mustelus canis*) ocular tissues, 247
Cell
  cycle, 231
  division, 240
Cell-cell interactions, 238
Cephalocarid, 16
Cephalopod, 55, 363
CHALFOUN, ANNA, JAMES MCCLELLAND, and IVAN VALIELA, The effect of nutrient loading on the growth rate of two species of bivalves, *Mercenaria mercenaria* and *Mya arenaria*, in estuaries of Waquoit Bay, Massachusetts, 281
CHANG, D. C., see C. L. Meng, 234
CHAPPELL, RICHARD L., see Haohua Qian, 263
Characterization and solubilization of the FMRFamide receptor of squid, 185
CHAUHAN, AMRIT, see Brent Miller, 239
Chemical signals, 275
Chemokinesis, 1, 8
Chemoreception, 55, 259
Chemotaxis, 8, 274
CHEN, Y. P., see K. S. Yoon, 208
CHIA, FU-SHIANG, see Glenys D. Gibson, 133
CHILDRESS, JAMES J., see Chris N. Airriess, 208; Erik V. Thuesen, 84
CHIN, GILBERT J., KEMAL PAYZA, DAVID A. PRICE, MICHAEL J. GREENBERG, and KAREN E. DOBLE, Characterization and solubilization of the FMRFamide receptor of squid, 185
Chloroperoxidase, 208
Chromatophore pattern, 363
Chromosome synapsis and segregation, 309
CHUN, JONG TAI, see Juan Benech, 269
Citrate synthase, 84
Cl, 76
  current, 265
Clearance of proteases from the circulation of the American horseshoe crab, *Limulus polyphemus:* a possible function for α_2-macroglobulin, 228
Cnidaria, 48, 84, 200, 355
Coastal land use, 276, 278
Cobb, 336
Comparison of phytoplankton and ecosystem gross production in the Quashnet River, an estuary of Waquoit Bay, Massachusetts, 287
Copper induced polymerization of hemoglobin from the ocean pout, *Macrozoarces americanus*, 246
Crassostrea gigas, 309
CRISPINO, MARIANNA, see Juan Benech, 269
Crown-of-thorns starfish, 304
Crustacean, 259, 385
Cytokinesis, 234

D

D'AVANZO, CHARLENE, see Peter Hurlbut, 283
Daily variation, 284
Daily variation in phytoplankton production in two subestuaries of Waquoit Bay, Massachusetts, 284
DAVIES, RONALD W., see Heather J. Brook, 99
Deep sea, 84
DELLACORTE, CHRISTIAN, DON S. ANDERSON, WILLIAM O. MCCLURE, and D. LYNN KALINOSKI, Neurofilament-like immunoreactivity in the sea anemone *Condylactis gigantea* (Cnidaria: Anthozoa), 200
DELLACORTE, CHRISTIAN, WILLIAM O. MCCLURE, and D. LYNN KALINOSKI, Identification of synaptophysin-like immunoreactivity in the sea anemone *Condylactis gigantea* (Cnidaria: Anthozoa), 355
DEMEULENAERE, STEPHANE, see Patrick Flammang, 35
Denitrification, 289
Detoxication, 249
Development, 239
Developmental temperature tolerance, 304
DIETZ, THOMAS H., DIONDI LESSARD, HAROLD SILVERMAN, and JOHN W. LYNN, Osmoregulation in *Dreissena polymorpha:* the importance of Na, Cl, K, and particularly Mg, 76
Directional sensitivity of saccular afferents of the toadfish to linear acceleration at audio frequencies, 258
Disinfection, 254
Dispersal strategies of the biota on an oceanic seamount: implications for ecology and biogeography, 336
Dissolved organic nitrogen, 278
Dissolved organic nitrogen in ground water bordering estuaries of Waquoit Bay, Massachusetts: relations with watershed landscape mosaics, 278
Distribution of barnacles, 346
DOBLE, KAREN E., see Gilbert J. Chin, 185
DODGE, F. A., D. M. PORCELLO, S. A. DODGE, E. KAPLAN, and R. B. BARLOW, JR., Noise components in *Limulus* vision, 261
DODGE, F. A., see C. L. Passaglia, 260; F. A. Dodge, 261
Dopamine, 55
Dorso-ventral axis specification, 238
Drag, 156
Dreissena, 76
DUTTA, TIMOTHY C., see Robert B. Silver, 242

E

Echinodermata, 35
Ecosystem production, 287
EDDS-WALTON, PEGGY L., see Richard R. Fay, 258
Effects of algal biomass on benthic nitrogen flux in nutrient-loaded estuaries of Waquoit Bay, Massachusetts, 283
Effects of flow and seston availability on scope for growth of benthic suspension-feeding invertebrates from the Gulf of Maine, 319
Effects of GABA on outward currents in *Hermissenda* photoreceptors, 265
Egg activation, 143
Elasmobranch, 64
Electric organ, 64
Electric organ discharge and electrosensory reafference in skates, 64
Electrical recordings, 273
Electron microscopy, 16
Electrophysiology, 271, 300
Electroreception, 64, 257
ELOFSSON, R., see L. P. Nezlin, 174
Energy, 398
Energy metabolism and amino acid transport during early development of Antarctic temperate echinoderms, 398
Enzymatic hydrolysis of Tetriso as a model for the detoxication of the neurotoxic agent VX, 249
Enzymes, 84
EPSTEIN, HERMAN T., see Catherine T. Tamse, 251
Estuary, 287
Eutrophication, 277, 282, 285
Experimental disinfection of lobster eggs infected with *Leucothrix mucor*, 254

F

FARRINGTON, HERALDO, see Mary T. Lucero, 55
FAY, RICHARD R., PEGGY L. EDDS-WALTON, and STEPHEN M. HIGHSTEIN, Directional sensitivity of saccular afferents of the toadfish to linear acceleration at audio frequencies, 258
Fertilization, 23, 143, 248
Fertilization between closely related sea urchins is blocked by incompatibilities during sperm-egg attachment and early stages of fusion, 23
FISHMAN, HARVEY M., see Jin Lu, 257
FLAMMANG, PATRICK, STEPHANE DEMEULENAERE, and MICHEL JANGOUX, The role of podial secretions in adhesion in two species of sea stars (Echinodermata), 35
Flow, 319
Food detection and preferences of the nudibranch mollusc *Hermissenda crassicornis:* experiments in a Y-maze, 274
Force coefficients, 156

Foreman, Kenneth, see Jessica L. Boxhill, 284; Kristin McDonnell, 276; Lory Z. Santiago Vásquez, 285; Michelle Rudy, 278; Rafael Sardá, 282; Timothy R. Harrison, 287
Free calcium oscillations 239
Frias, Bernarda, see Thomas A. Borgese, 246
From watershed to estuary: assessment of nutrient loading, retention, and export from the Ipswich River Basin, 277
Functional morphology, 35

G

GABA, 263, 265
Gamete spawning, 143
Gamete spawning and fertilization in the gymnolaemate bryozoan *Membranipora membranacea*, 143
Gap junctions, 262
Garritt, Robert, see Krista K. Ingram, 277
Giant synapse, 300
Giblin, Anne E., see Cristina Zago, 290; Eileen Monaghan, 288
Gibson, Glenys D., and Fu-Shiang Chia, A metamorphic inducer in the opisthobranch *Haminaea callidegenita:* partial purification and biological activity, 133
Gilly, William F., see Mary T. Lucero, 55
Giuditta, Antonio, see Juan Benech, 269
Glutamate, 48
Glutamate immunoreactivity in non-neuronal cells of the sea anemone *Metridium senile*, 48
Gomez, George, and Jelle Atema, Time course of recovery from adaptation by hydroxyproline-sensitive lobster olfactory receptor neurons, 259
Govind, C. K., see A. T. Read, 16
Greenberg, Michael J., see Gilbert J. Chin, 185
Gross primary production, 284
Groundwater, 276, 278
Growth, 281
Guilfoyle, Kerry, see Peter Hurlbut, 283
Gulf of Maine (GOM), 319
Guo, Ximing, and Standish K. Allen, Jr., Reproductive potential and genetics of triploid Pacific oysters, *Crassostrea gigas* (Thunberg), 309

H

Hair cells, 267
Halonen, S. K., see Earl Weidner, 25
Haminaea, 133
Hanlon, Roger T., Malcolm J. Smale, and Warwick H. H. Sauer, An ethogram of body patterning behavior in the squid *Loligo vulgaris reynaudii* on spawning grounds in South Africa, 363
Harmonic analysis, 257
Harrington, John, see Thomas A. Borgese, 246
Harrison, Timothy R., Jessica L. Boxhill, Lory Z. Santiago Vásquez, Kenneth Foreman, and James N. Kremer, Comparison of phytoplankton and ecosystem gross production in the Quashnet River, an estuary of Waquoit Bay, Massachusetts, 287
Harrison, Timothy R., see Jessica L. Boxhill, 284; Lory Z. Santiago Vásquez, 285
Haugh-Scheidt, Laura M., see Robert Paul Malchow, 262
Hearing, 258
Heart rate, 208
Heavy metals, 290
Heck, Diane E., Jeffrey D. Laskin, Seymour Zigman, and Walter Troll, N^G-monomethyl-L-arginine inhibits *Arbacia* fertilization and differentiation, 248
Hellung-Larsen, Per, see Uffe Koppelhus, 1, 8
Hemocyanin, 385
Hemoglobin, 246
Hemolysis, 227
Henry, Jonathan Q., and Mark Q. Martindale, Inhibitory cell-cell interactions control development in the embryos of *Cerebratulus lacteus*, 238
Hermissenda, 251, 252, 274
Hermissenda crassicornis larvae metamorphose in the laboratory in response to artificial and natural inducers, 252
Hessler, R. R., see A. T. Read, 16
High resolution multimode digital imaging system for mitosis studies *in vivo* and *in vitro*, 231
High-resolution measurement of the time course of calcium concentration microdomains at squid presynaptic terminals, 300
Highstein, Stephen M., see Richard R. Fay, 258
Hill, Susan Douglas, Alan M. Shipley, and Peter J. S. Smith, Ionic fluxes during wound healing following segment amputation in sabellid fanworms, 253
Holothurian, 112
Homeoviscous, 208
Homeoviscous properties implicated by the interactive effects of pressure and temperature on the hydrothermal vent crab *Bythograea thermydron*, 208
Hopkinson, Charles S., see Krista K. Ingram, 277
Horne, Ashton, James McClelland, and Ivan Valiela, The growth and consumption of macroalgae in estuaries: the role of invertebrate grazers along a nutrient gradient in Waquoit Bay, Massachusetts, 279
Horseshoe crab, 373
Hoskin, Francis C. G., and John E. Walker, Enzymatic hydrolysis of Tetriso as a model for the detoxication of the neurotoxic agent VX, 249
HPLC, 55
Hurlbut, Peter, Charlene D'Avanzo, Deepti Sethi, and Kerry Guilfoyle, Effects of algal biomass on benthic nitrogen flux in nutrient-loaded estuaries of Waquoit Bay, Massachusetts, 283
Hutchinsoniella macracantha, 16
Hybridization and genomic evolution, 309
Hydrodynamics, 164
Hydrothermal vent crab, 208

I

Identification of limulin as a major cytolytic protein in the plasma of the American horseshoe crab, *Limulus polyphemus*, 227
Identification of synaptophysin-like immunoreactivity in the sea anemone *Condylactis gigantea* (Cnidaria: Anthozoa), 355
Image analysis, 293
Immunoreactivity, 200, 355
Indirect immunofluorescence, 208
Ingram, Krista K., Charles S. Hopkinson, Katherine Bowman, Robert Garritt, and Joe Vallino, From watershed to estuary: assessment of nutrient loading, retention, and export from the Ipswich River Basin, 277
Inhibitory cell-cell interactions control development in the embryos of *Cerebratulus lacteus*, 238
Inorganic nutrients, 276
Inoué, Shinya, and Theodore D. Inoué, Through-focal and time-lapse stereoscopic images of dividing cells and developing embryos in DIC and polarization microscopy, 232
Inoué, Shinya, see Fabrice Roegiers, 240; Phong T. Tran, 244
Inoué, Theodore D., see E. D. Salmon, 231; Shinya Inoué, 232
Intermediate filaments, 200
Intertidal, 99
Invertebrate, 185, 319
  grazers, 279
Ion regulation, 76
Ionic current, 253
Ionic fluxes during wound healing following segment amputation in sabellid fanworms, 253
Isopod, 99

J

Jaffe, Lionel F., see Brent Miller, 239
Jangoux, Michel, see Patrick Flammang, 35
Jeffries, William B., see Harold K. Voris, 346

Jeun, Gwendolyn S., see Robert B. Silver, 242

Johnson, Donald, see Thomas A. Borgese, 246

Johnson, Leland G., and Russell C. Babcock, Temperature and the larval ecology of the crown-of-thorns starfish, *Acanthaster planci*, 304

Johnson, Rachel, Michael LaMontagne, and Ivan Valiela, Rate of denitrification in submerged salt marsh sediments, 289

K

K, 76

Kalinoski, D. Lynn, see Christian DellaCorte, 200, 355

Kane, Robert E., see Edward C. Metz, 23

Kaplan, Barry B., see Juan Benech, 269

Kaplan, E., see F. A. Dodge, 261

Kelley, Brian, see Robert B. Silver, 237

Knapp, L. W., see K. S. Yoon, 208

Koppelhus, Uffe, Per Hellung-Larsen, and Vagn Leick, An improved quantitative assay for chemokinesis in *Tetrahymena*, 8

Koppelhus, Uffe, Per Hellung-Larsen, and Vagn Leick, Physiological parameters affecting the chemosensory response of *Tetrahymena*, 1

Kremer, James N., see Jessica L. Boxhill, 284

Kremer, James N., see Lory Z. Santiago Vásquez, 285; Timothy R. Harrison, 287

Kunkel, Joseph G., and Peter J. S. Smith, Three-dimensional calibration of the non-invasive ion probe, NVP$_i$, of steady ionic currents, 271

Kuzirian, Alan M., see Catherine T. Tamse, 251; Conxita Avila, 252; Ebenezer Yamoah, 265; Elizabeth Tyndale, 274

L

L-dopa, 55

Lactate dehydrogenase, 84

Lamina, 260

LaMontagne, Michael, see Rachel Johnson, 289

Lang, Eric J., see Mutsuyuki Sugimori, 300

Lang, Eric J., see Robert B. Silver, 293

Larva, 398

Larval dispersal, 336

Laskin, Jeffery D., see Diane E. Heck, 248

Lateral inhibition, 260

Lead toxicity, 251

Lead toxicity in *Hermissenda crassicornis* embryos and cultured neurons, 251

Leick, Vagn, see Uffe Koppelhus, 1, 8

Leonard, Ann E., Rainer Voigt, and Jelle Atema, Lobster orientation in turbulent odor plumes: electrical recording of bilateral olfactory sampling (antennular "flicking"), 273

Lessard, Diondi, see Thomas H. Dietz, 76

Lesser, Michael P., Jon D. Witman, and Kenneth P. Sebens, Effects of flow and seston availability on scope for growth of benthic suspension-feeding invertebrates from the Gulf of Maine, 319

Leucothrix mucor, 254

Leukotriene, 242

Leukotriene B$_4$, an arachidonic acid metabolite, regulates intracellular free calcium release in eggs and mitotic cells of the sand dollar (*Echinaracnius parma*), 242

Limulin, 227, 229

Limulus polyphemus, 227, 288, 299, 373

Lincoln, D. E., see K. S. Yoon, 208

Liquid crystal, 244

Llinás, Rodolfo, see Mutsuyuki Sugimori, 300; Robert B. Silver, 293

Lobster, 254, 259, 272, 273, 275
  eggs, 254

Lobster orientation in turbulent odor plumes: electrical recording of bilateral olfactory sampling (antennular "flicking"), 273

Lobster orientation in turbulent odor plumes: simultaneous measurement of tracking behavior and temporal odor patterns, 272

Localization, 208

Localization of the choloroperoxidase of the capitellid polychaete *Notomastus lobatus*, 215

Locomotion, 156, 164

Locomotion in developing *Artermia* larvae: mechanical analysis of antennal propulsors based on large-scale physical models, 156

Loligo, 185, 293, 300, 363

Long-term changes of macroinfaunal assemblages in experimentally enriched salt march tidal creeks, 282

Lovell, C. R., see K. S. Yoon, 208

Lu, Jin, and Harvey M. Fishman, Operational properties of voltage-clamped electroreceptive ampullary organ excised from *Raja*, 257

Lucero, Mary T., Heraldo Farrington, and William F. Gilly, Quantification of L-dopa and dopamine in squid ink: implications for chemoreception, 55

Lynn, J. W., see Earl Weidner, 25; Thomas H. Dietz, 76

M

Macroalgae, 279

Macroinfaunal assemblages, 282

Macrozoarces americanus, 246

Makarenko, Vladimir, Neural network with embedded oscillators, 256

Malchow, Robert Paul, Haohua Qian, Laura M. Haugh-Scheidt, and Harris Ripps, The effects of quinine and quinidine on isolated retinal horizontal cells, 262

Malchow, Robert Paul, see Haohua Qian, 263

Manahan, Donal T., see Fraser M. Shilling, 398

Manale, S. B., see Earl Weidner, 255

Mangrove crab, 346

Mangum, Charlotte P., see John E. Reese, 385

Map2, 200

Martindale, Mark Q., see Jonathan Q. Henry, 238

Mating, 275

McClelland, James, see Anna Chalfoun, 281; Ashton Horne, 278

McClure, William O., see Christian DellaCorte, 200, 355

McDonnell, Kristin, Michelle Rudy, Ivan Valiela, and Kenneth Foreman, The effect of coastal land use on inorganic nutrient concentrations in groundwater entering estuaries of Waquoit Bay, Massachusetts, 276

McDonnell, Kristin, see Michelle Rudy, 278

Medusae, 84

Meiosis, 309

Melchior, Ralph, James P. Quigley, and Peter B. Armstrong, Clearance of proteases from the circulation of the American horseshoe crab, *Limulus polyphemus*: a possible function for α_2-macroglobulin, 228

Melchior, Ralph, see Peter B. Armstrong, 227

Meng, C. L., and D. C. Chang, Study of calcium signaling in cell cleavage using confocal microscopy, 234

Metabolism, 398

Metamorphic inducer, 133

Metamorphosis, 252

Method, 1, 8

Metridium, 48

Metz, Edward C., Robert E. Kane, Hiroko Yanagimachi, and Stephen R. Palumbi, Fertilization between closely related sea urchins is blocked by incompatibilities during sperm-egg attachment and early stages of fusion, 23

Mg, 76

Microdomains, 237, 300

Microscopy, 232, 244

Microsporidian invasion tubes, 255

Microsporidian spore invasion tubes as revealed by fluorescent probes, 255

Microtubules, 231

Miller, Andrew L., see Brent Miller, 239

Miller, Brent, Amrit Chauhan, Lionel F. Jaffe, and Andrew L. Miller, Oscillations in free [Ca^{2+}]$_i$ during early cell division cycles in *Xenopus laevis* embryos, 239

Misquith, Sandra, see James Quigley, 229; Peter B. Armstrong, 227

Mitosis, 231, 235, 237
Mitosis, cleavage, and development of highly compressed sea urchin (*Lytechinus variegatus*) zygotes, 240
Mollusc, 185
  larvae, 252
MONAGHAN, EILEEN, and ANNE E. GIBLIN, The effects of coupling between the oxic and anoxic layers of sediment on nutrient release to overlying water, 288
Motor nerve terminal, 16
Multivalent formation, 309
MURRAY, A. W., see E. D. Salmon, 231
Muscle and nerve terminal fine structure of a primitive crustacean, the cephalocarid *Hutchinsoniella macracantha*, 16
Muscle cell development, 238
Muscle fine structure and microtubule birefringence measured with a new pol-scope, 244
Myofibril, 16

N

Na, 76
Nematocysts, 48
Nerve endings, 269
Nest-site selection in horseshoe crabs, *Limulus polyphemus*, 373
Nesting, 373
Neural network, 256
Neural network with embedded oscillators, 256
Neurobiotin staining, 260
Neurofilament, 200
Neurofilament-like immunoreactivity in the sea anemone *Condylactis gigantea* (Cnidaria: Anthozoa), 200
Neurons, 251
Neuropeptide, 185
Neurotransmitters, 174
NEW, JOHN G., Electric organ discharge and electrosensory reafference in skates, 64
NEZLIN, L. P., R. ELOFSSON, and D. A. SAKHAROV, Transmitter-specific subsets of sensory elements in the prosobranch osphradium, 174
N^G-monomethyl-L-arginine inhibits *Arbacia* fertilization and differentiation, 248
Noise components in *Limulus* vision, 261
Non-invasive ion probe, 271
Nudibranch prey preferences, 274
Nutrient
  loading, 277, 279, 281, 283
  release, 288
  uptake, 277

O

O_2 binding, 385
OBLAK, JEB B., see Robert B. Silver, 242
Ocean pout, 246
Octolasmis, 346
Ocular tissues, 247
OLDENBOURG, RUDOLF, see Phong T. Tran, 244
Ontogeny, 164
Operational properties of voltage-clamped electroreceptive ampullary organ excised from *Raja*, 257
Opisthobranch, 133
Optical sectioning, 232
Organophosphorus, 249
Orientation, 272
Oscillations, 256
Oscillations in free $[Ca^{2+}]_i$ during early cell division cycles in *Xenopus laevis* embryos, 239
Osmoregulation, 76
Osmoregulation in *Dreissena polymorpha*: the importance of Na, Cl, K, and particularly Mg, 76
Osphradium, 174
Oxic and anoxic sediment layers, 288
Oxidation, 247
Oxygen affinity, 385
Oxygen consumption rates and metabolic enzyme activities of oceanic California medusae in relation to body size and habitat depth, 84

P

PALUMBI, STEPHEN R., see Edward C. Metz, 23
Parker River Estuary, 288
PARKER, TERRY, and VERENA TUNNICLIFFE, Dispersal strategies of the biota on an oceanic seamount: implications for ecology and biogeography, 336
PASSAGLIA, C. L., F. A. DODGE, and R. B. BARLOW, JR., Visual responses in the brain of *Limulus*, 260
Patterns of distribution of two barnacle species on the mangrove crab, *Scylla serrata*, 346
PAYZA, KEMAL, see Gilbert J. Chin, 185
PENN, DUSTIN, and H. JANE BROCKMANN, Nest-site selection in horseshoe crabs, *Limulus polyphemus*, 373
Phosphorescent afterglow, 293
Photoreceptors, 265
Physiological parameters, 1
Physiological parameters affecting the chemosensory response of *Tetrahymena*, 1
Phytoplankton, 284, 285, 287
Polarization, 244
Polarization microscopy, 240
Polychaete, 208, 215, 253
Polymerization, 246
Polyploidy, 309
POOACHIRANON, SOMBAT, see Harold K. Voris, 346
PORCELLO, D. M., see F. A. Dodge, 261
Potassium current, 267
Preliminary investigation of the molecular basis for the functional differences between the two pentraxins limulin and C-reactive protein from the plasma of the American horseshoe crab, *Limulus polyphemus*, 229
Pressure, 208
PRICE, DAVID A., see Gilbert J. Chin, 185
Prosobranch molluscs, 174
Protandry, 112
Protease clearance, 228
Protein synthesis, 269
Protein synthesis in nerve endings from squid brain: modulation by calcium ions, 269
Protogynous sex change in the intertidal isopod *Gnorimosphaeroma oregonense* (Crustacea: Isopoda), 99
Protogyny, 99
Pseudomonas diminuta, 249

Q

QIAN, HAOHUA, ROBERT PAUL MALCHOW, RICHARD L. CHAPPELL, and HARRIS RIPPS, The GABAA receptors of Müller (glial) cells in skate retina, 263
QIAN, HAOHUA, see Robert Paul Malchow, 262
Quantification of L-dopa and dopamine in squid ink: implications for chemoreception, 55
Quantum emission domain, 293
QUIGLEY, JAMES P., see Peter B. Armstrong, 227; Ralph Melchior, 228
QUIGLEY, JAMES, SANDRA MISQUITH, AVADHESHA SUROLIA, SUBITA SRIMAL, and PETER ARMSTONG, Preliminary investigation of the molecular basis for the functional differences between the two pentraxins limulin and C-reactive protein from the plasma of the American horseshoe crab, *Limulus polyphemus*, 229
Quinine, 262

R

RAFFERTY, NANCY S., see Seymour Zigman, 247
Rate of denitrification in submerged salt march sediments, 289

Rawlings, Timothy A., see Heather J. Brook, 99

Read, A. T., R. R. Hessler, and C. K. Govind, Muscle and nerve terminal fine structure of a primitive crustacean, the cephalocarid *Hutchinsoniella macracantha,* 16

Reafference, 64

Reese, John E., and Charlotte P. Mangum, Subunit composition and O_2 binding of the crustacean hemocyanins: interspecific relationships, 385

Reeves, Anthony P., see Robert B. Silver, 237

Reproduction, 373

Reproductive isolation, 23

Reproductive potential and genetics of triploid Pacific oysters, *Crassostrea gigas* (Thunberg), 309

Respiration, 84

Retina, 262

Retinal Müller cells, 263

Ripps, Harris, see Haohua Qian, 263; Robert Paul Malchow, 262

Roegiers, Fabrice, Phong Tran, and Shinya Inoué, Mitosis, cleavage, and development of highly compressed sea urchin (*Lytechinus variegatus*) zygotes, 240

Rudy, Michelle, Kristin McDonnell, Ivan Valiela, and Kenneth Foreman, Dissolved organic nitrogen in groundwater bordering estuaries of Waquoit Bay, Massachusetts: relations with watershed landscape mosaics, 278

Rudy, Michelle, see Kristin McDonnell, 276

S

Saccule, 258

Sadusky, Terrie J., and Robert A. Bullis, Experimental disinfection of lobster eggs infected with *Leucothrix mucor,* 254

Sakharov, D. A., see L. P. Nezlin, 174

Salmon, E. D., T. Inoué, A. Sesai, and A. W. Murray, High resolution multimode digital imaging system for mitosis studies *in vivo* and *in vitro,* 231

Salmon, Edward D., see Phong T. Tran, 244

Salt marsh, 282, 289

Sand dollar, 235, 242

Santiago Vásquez, Lory Z., see Jessica L. Boxhill, 284; Timothy R. Harrison, 287

Santiago Vásquez, Lory Z., Jessica L. Boxhill, Timothy R. Harrison, James N. Kremer, and Kenneth Foreman, The effects of wind speed and direction on stratification and phytoplankton production in an estuary of Waquoit Bay, Massachusetts, 285

Sarcoplasmic reticulum, 16

Sardá, Rafael, Kenneth Foreman, and Ivan Valiela, Long-term changes of macroinfaunal assemblages in experimentally enriched salt marsh tidal creeks, 282

Sauer, Warwick H. H., see Roger T. Hanlon, 363

Scaling, 164

Scope for growth (SFG), 319

Scylla, 346

Sea anemone, 48

Sea urchin, 23, 248

Sealing, 84

Seamounts, 336

Sebens, Kenneth P., see Michael P. Lesser, 319

Second messenger, 270

Second messenger modulation of steady-state calcium efflux in *Aplysia* bag cells, 270

Sediment, 290

Sensory neurons, 174

Sesai, A., see E. D. Salmon, 231

Seston, 319

Sethi, Deepti, see Peter Hurlbut, 283

Sewell, Mary A., Small size, brooding, and protandry in the apodid sea cucumber *Leptosynapta clarki,* 112

Sex change, 99

Shilling, Fraser M., and Donal T. Manahan, Energy metabolism and amino acid transport during early development of Antarctic temperate echinoderms, 398

Shipley, Alan M., see Susan Douglas Hill, 253

Signaling, 363

Silver, Robert B., Anthony P. Reeves, Marcia Whitman, and Brian Kelley, Analysis of spatial and temporal patterns in the Ca^{2+} signal that signals nuclear envelope breakdown in sand dollar (*Echinaracnius parma*) cells, 237

Silver, Robert B., Jeb B. Oblak, Gwendolyn S. Jeun, Jenny J. Sung, and Timothy C. Dutta, Leukotriene B_4, an arachidonic acid metabolite, regulates intracellular free calcium release in eggs and mitotic cells of the sand dollar (*Echinaracnius parma*), 242

Silver, Robert B., Mutsuyuki Sugimori, Eric J. Lang, and Rodolfo Llinás, Time-resolved imaging of Ca^{2+}-dependent aequorin luminescence of microdomains and QEDs in synaptic preterminals, 293

Silver, Robert B., see Mutsuyuki Sugimori, 300

Silver, Robert B., Video light microscopic imaging of the calcium signal that initiates nuclear envelope breakdown in sand dollar (*Echinaracnius parma*) cells, 235

Silverman, Harold, see Thomas H. Dietz, 76

Skate, 64

Smale, Malcolm J., see Roger T. Hanlon, 363

Small size, brooding, and protandry in the apodid sea cucumber *Leptosynapta clarki,* 112

Smith, Peter J. S., see Catherine T. Tamse, 251; Ebenezer Yamoah, 270; Joseph Kunkel, 271; Susan Douglas Hill, 253

Spartina alterniflora, 289

Speciation, 23

Specific ion electrode, 271

Spectral analysis, 261

Sperm transfer, 143

Sperm-egg recognition, 23

Spindle, 240

Squid, 185, 293, 300, 363
  brain, 269
  ink, 55

Srimal, Subita, see James Quigley, 229; Peter B. Armstrong, 227

Steinacker, Antoinette, and Conchita Zuazaga, Calcium and voltage sensitivity of potassium current activation in toadfish semicircular canal hair cells, 267

Sterility, 309

Stratification affecting production, 285

Study of calcium signaling in cell cleavage using confocal microscopy, 234

Subunit composition, 385

Subunit composition and O_2 binding of the crustacean hemocyanins: interspecific relationships, 385

Sugimori, Mutsuyuki, Eric J. Lang, Robert B. Silver, and Rodolfo Llinás, High-resolution measurement of the time course of calcium concentration microdomains at squid presynaptic terminals, 300

Sugimori, Mutsuyuki, see Robert B. Silver, 293

Sung, Jenny J., see Robert B. Silver, 242

Surolia, Avadhesha, see James Quigley, 229

Synaptic transmission, 300

Synaptophysin, 355

Synchrony, 373

T

Tamse, Catherine T., Peter J. S. Smith, Amine Aloulou, Herman T. Epstein, and Alan M. Kuzirian, Lead toxicity in *Hermissenda crassicornis* embryos and cultured neurons, 251

Tamse, Catherine T., see Conxita Avila, 252

Tau, 200

Temkin, M. H., Gamete spawning and fertilization in the gymnolaemate bryozoan *Membranipora membranacea,* 143

Temperature, 208

Temperature and *Acanthaster* development, 304

Temperature and the larval ecology of the crown-of-thorns starfish, *Acanthaster planci,* 304

Temporal filter properties, 259

Tetrahymena, 1, 8

The effect of coastal land use on inorganic nutrient concentrations in groundwater entering estuaries of Waquoit Bay, Massachusetts, 276

The effect of nutrient loading on the growth rate of two species of bivalves, *Mercenaria mercenaria* and *Mya arenaria*, in estuaries of Waquoit Bay, Massachusetts, 281

The effects of coupling between the oxic and anoxic layers of sediment on nutrient release to overlying water, 288

The effects of quinine and quinidine on isolated retinal horizontal cells, 262

The effects of wind speed and direction on stratification and phytoplankton production in an estuary of Waquoit Bay, Massachusetts, 285

The GABAA receptors of Müller (glial) cells in skate retina, 263

The growth and consumption of macroalgae in estuaries: the role of invertebrate grazers along a nutrient gradient in Waquoit Bay, Massachusetts, 279

The role of podial secretions in adhesion in two species of sea stars (Echinodermata), 35

Three-dimensional imaging, 232

Through-focal and time-lapse stereoscopic images of dividing cells and developing embryos in DIC and polarization microscopy, 232

Thuesen, Erik V., and James J. Childress, Oxygen consumption rates and metabolic enzyme activities of oceanic California medusae in relation to body size and habitat depth, 84

Time course of recovery from adaptation by hydroxyproline-sensitive lobster olfactory receptor neurons, 259

Time-intensive study, 284

Toadfish, 258

Toxicity, 290

Tran, Phong, see Fabrice Roegiers, 240

Tran, Phong T., Shinya Inoué, Edward D. Salmon, and Rudolf Oldenbourg, Muscle fine structure and microtubule birefringence measured with a new pol-scope, 244

Transmitter-specific subsets of sensory elements in the prosobranch osphradium, 174

Transport, 398

Triploidy, 309

Troll, Walter, see Diane E. Heck, 248

Tube feet, 35

Tunnicliffe, Verena, see Terry Parker, 336

Tyndale, Elizabeth, Conxita Avila, and Alan M. Kuzirian, Food detection and preferences of the nudibranch mollusc *Hermissenda crassicornis:* experiments in a Y-maze, 274

U

Underwater vision, 261

V

Valiela, Ivan, see Anna Chalfoun, 281; Ashton Horne, 278; Kristin McDonnell, 276; Michelle Rudy, 278; Rachel Johnson, 289; Rafael Sardá, 282

Vallino, Joe, see Krista K. Ingram, 277

Video light microscopic imaging of the calcium signal that initiates nuclear envelope breakdown in sand dollar (*Echinaracnius parma*) cells, 235

Video microscopy, 293

Visual responses in the brain of *Limulus*, 260

Visually guided behavior, 261

Viviparity, 112

Voigt, Rainer, see Ann E. Leonard, 273

Voltage-clamped ampullary organ, 257

Voris, Harold K., William B. Jeffries, and Sombat Poovachiranon, Patterns of distribution of two barnacle species on the mangrove crab, *Scylla serrata*, 346

W

Walker, John E., see Francis C. G. Hoskin, 249

Watershed, 277

Weidner, Earl, S. B. Manale, S. K. Halonen, and J. W. Lynn, Microsporidian spore invasion tubes as revealed by fluorescent probes, 255

Whitman, Marcia, see Robert B. Silver, 237

Williams, Terri A., A model of rowing propulsion and the ontogeny of locomotion in *Artemia* larvae, 164

Williams, Terri A., Locomotion in developing *Artermia* larvae: mechanical analysis of antennal propulsors based on large-scale physical models, 156

Witman, Jon D., see Michael P. Lesser, 319

Woodin, S. A., see K. S. Yoon, 208

Wound healing and regeneration, 253

X

Xenopus, 239

Y

Y-maze, 274

Yamoah, Ebenezer, and Alan M. Kuzirian, Effects of GABA on outward currents in *Hermissenda* photoreceptors, 265

Yamoah, Ebenezer, and Peter J. S. Smith, Second messenger modulation of steady-state calcium efflux in *Aplysia* bag cells, 270

Yanagimachi, Hiroko, see Edward C. Metz, 23

Yoon, K. S., Y. P. Chen, C. R. Lovell, D. E. Lincoln, L. W. Knapp, and S. A. Woodin, Localization of the choloroperoxidase of the capitellid polychaete *Notomastus lobatus*, 215

Z

Zago, Cristina, and Anne E. Giblin, Analysis of acid volatile sulfide and metals to predict the toxicity of Boston Harbor sediments, 290

Zebra mussel, 76

Zebrafish, 234

Zigman, Seymour, and Nancy S. Rafferty, Catalase activity in dogfish (*Mustelus canis*) ocular tissues, 247

Zigman, Seymour, see Diane E. Heck, 248

Zinc, 263

Zuazaga, Conchita, see Antoinette Steinacker, 267

CONTENTS

RESEARCH NOTES

Silver, Robert B., Mutsuyuki Sugimori, Eric J. Lang, and Rodolfo Llinás
Time-resolved imaging of Ca^{2+}-dependent aequorin luminescence of microdomains and QEDs in synaptic preterminals 293

Sugimori, Mutsuyuki, Eric J. Lang, Robert B. Silver, and Rodolfo Llinás
High-resolution measurement of the time course of calcium concentration microdomains at squid presynaptic terminals 300

Johnson, Leland G., and Russell C. Babcock
Temperature and the larval ecology of the crown-of-thorns starfish, *Acanthaster planci* 304

DEVELOPMENT AND REPRODUCTION

Guo, Ximing, and Standish K. Allen, Jr.
Reproductive potential and genetics of triploid Pacific oysters, *Crassostrea gigas* (Thunberg) 309

ECOLOGY AND EVOLUTION

Lesser, Michael P., Jon D. Witman, and Kenneth P. Sebens
Effects of flow and seston availability on scope for growth of benthic suspension-feeding invertebrates from the Gulf of Maine 319

Parker, Terry, and Verena Tunnicliffe
Dispersal strategies of the biota on an oceanic seamount: implications for ecology and biogeography 336

Voris, Harold K., William B. Jeffries, and Sombat Poovachiranon
Patterns of distribution of two barnacle species on the mangrove crab, *Scylla serrata* 346

NEUROBIOLOGY AND BEHAVIOR

DellaCorte, Christian, William O. McClure, and D. Lynn Kalinoski
Identification of synaptophysin-like immunoreactivity in the sea anemone *Condylactis gigantea* (Cnidaria: Anthozoa) 355

Hanlon, Roger T., Malcolm J. Smale, and Warwick H. H. Sauer
An ethogram of body patterning behavior in the squid *Loligo vulgaris reynaudii* on spawning grounds in South Africa 363

Penn, Dustin, and H. Jane Brockmann
Nest-site selection in the horseshoe crab, *Limulus polyphemus* 373

PHYSIOLOGY

Reese, John E., and Charlotte P. Mangum
Subunit composition and O_2 binding of the crustacean hemocyanins: interspecific relationships 385

Shilling, Fraser M., and Donal T. Manahan
Energy metabolism and amino acid transport during early development of antarctic and temperate echinoderms 398

Index to Volume 187 408

MBL/WHOI LIBRARY
WH 1B2R 4